

Copper(I)-catalyzed 1,3-Halogen Migration

By

Ryan Van Hoveln

A dissertation submitted in partial fulfillment of
the requirements for the degree of

Doctor of Philosophy

(Chemistry)

At the

UNIVERSITY OF WISCONSIN – MADISON

2015

Date of final oral examination: 07/10/2015

The dissertation is approved by the following members of the final oral committee:

Jennifer M. Schomaker, Associate Professor, Chemistry

Steven D. Burke, Professor, Chemistry

Shannon S. Stahl, Professor, Chemistry

Randall H. Goldsmith, Assistant Professor, Chemistry

Richard P. Hsung, Professor, Pharmacy

Abstract

Copper(I)-catalyzed 1,3-Halogen Migration

Ryan Van Hoveln

Under the Supervision of Jennifer M. Schomaker

At the University of Wisconsin – Madison

An ongoing challenge in modern catalysis is to identify and understand new modes of reactivity promoted by earth-abundant and inexpensive first-row transition metals. Herein, we describe a new Cu(I)-catalyzed 1,3-halogen migration reaction which effectively recycles an activating group by transferring bromine from a sp^2 to a benzylic carbon with concomitant borylation of the Ar-Br bond. Both racemic and enantioselective variants of this transformation have been developed. Computational modelling aids in understanding the outcome of the asymmetric reaction and the benzyl bromide can be displaced with a variety of nucleophiles to produce a wide array of enantioenriched functionalized products. An extensive mechanistic study, which includes a combination of experimental and computational experiments, indicated this reaction does not involve any oxidation state changes at copper; rather, migration occurs through a series of formal sigmatropic shifts. Insight provided from these studies will be used to expand the utility of aryl copper species in synthesis and develop new ligands for enantioselective copper-catalyzed halogenation. Finally, the development of a nickel catalyzed hydroboration is discussed, including the synthesis of new heteroleptic nickel complexes.

Acknowledgments

As I begin to write this section, I realize that a few pages are truly not enough to thank everyone who needs to be thanked. How can I thank everyone? A Ph.D. is such a collaborative effort, not just scientifically, but emotionally and spiritually, that I'm not sure I can name everyone who helped along the way. So, here is my feeble attempt to show my gratitude.

Good science never happens in a vacuum, and so I would like to thank the Schomaker group, both past and current members, for their many conversations, encouragement, and support over the years. In particular, I would like to thank Steve Schmid and David Grigg who worked with me on the projects described in this dissertation. They have contributed ample helpful insight and experimental work. I would also like to thank the many undergrads who have worked with me during my time in graduate school: Carl Buttke, Gabe Le Gros, Eric Touney and Allen Moltzan.

The Department of Chemistry at the University of Wisconsin – Madison is a remarkable place to conduct research. This is in no small part due to the faculty and staff. I would like to thank Desiree Bates (Computational Chemistry), Charlie Fry (NMR), Heike Hofstetter (NMR), Monika Ivancic (NMR), Martha Vestling (Mass. Spec.), and Ilia Guzei (X-ray Crystallography). In particular, I would like to thank Desiree and Charlie. Desiree spent countless hours teaching me computational chemistry (which was no small task considering I knew nothing before working with her) and eventually became a good and supportive friend. I am grateful for Charlie's willingness to indulge my outlandish ideas and find creative solutions to some of my more difficult problems (and always having fun along the way). I would also like to show my appreciation towards the faculty in the department, who have always been willing to offer their advice, insight, and instruction during the course of my graduate research, especially Profs. Steve Burke, Shannon Stahl, Randy Goldsmith, and Richard Hsung, who kindly agreed to sit on my final committee.

Over the course of my academic career, there have been a number of people who have been particularly influential. First, I would like to thank Mr. Hummel who was my chemistry teacher in high school. He always pushed us beyond what we thought we were capable of and as a result we discovered what we were actually capable of. In retrospect, it should have been during his class that I discovered I had an aptitude for chemistry. Next, I would like to thank Dr. Robert Gayhart, my general chemistry professor, for encouraging me to pursue chemistry

seriously. Finally, I would like to thank Dr. Brad Andersh, my undergraduate mentor, who shaped so much of life trajectory. He was the first to spark my interest in organic chemistry, advised me in undergraduate research, and suggested that I consider academia as a career (good advice which I did not take seriously until years later).

Throughout my graduate career, there are an immense number of people who did not help me scientifically, per se, but were absolutely essential to my success. First among these are my parents and my sister. They have always been behind me whether I was excited about everything or in the dark places of grad school. I would also like to thank my small group, who have been immensely supportive and always willing to go out of their way to take care of me when I desperately needed it. In particular, Mary Van Vleet, Cale Weatherly, Ben Parrot, Carrie Francis, and Matt Russ went above and beyond the call of duty. I cannot express how grateful I am to all of you for always being there. Lastly, I would like to thank my officemates, Alicia Phelps, Nick Dolan, and Julie Alderson. Your good humor and willingness to be fodder for venting have been my first line of defense throughout grad school.

Last, but certainly not least, I would like to thank the most important person behind this manuscript, my graduate advisor, Jen Schomaker. Thank you for always encouraging me to try new things, being supportive when I ventured into unfamiliar territory, and being excited about my research (especially when I was not). It has been an honor working with you over the last four years of my life and I hope that I can have the same capacity for enthusiasm and wellspring of ideas for my mentees.

Table of Contents

Abstract.....	i
Acknowledgments	ii
List of Abbreviations	ix
List of Figures, Tables, and Schemes	xv
Chapter 1: Introduction to Formal Dyotropic Rearrangements in Organometallic Transformations	1
1.1 Introduction to Dyotropic Rearrangements.....	2
1.2. Stoichiometric Organometallic Dyotropic Rearrangements	3
1.2.1 1,2-Rearrangements	4
1.2.2 1,3-rearrangements.....	6
1.2.3 1,4-Rearrangements	7
1.3. Examples of Organometallic Dyotropic Rearrangements in Catalysis	9
1.3.1 1,4-Rearrangements	9
1.4. Conclusions and Outlook.....	15
1.5 Bibliography	16
Chapter 2: Cu(I)-catalyzed Recycling of a Halogen Activating Groups via 1,3-Halogen Migration	20
2.1 Introduction to Activating Group Recycling.....	21
2.1.1 Recent Examples of Activating Group Recycling.....	22
2.2 Optimization of Copper(I)-catalyzed 1,3-Halogen Migration	22
2.3 Scope of 1,3-Halogen Migration.....	24
2.4 Conclusions.....	25
2.5 Experimental Details.....	26

2.5.1 Synthesis of Styrene Starting Materials	26
2.5.2 Procedure for the 1,3-Halogen Migration	32
2.6 Bibliography	38
Chapter 3: Formal Asymmetric Hydrobromination of Styrenes via Copper(I)-Catalyzed 1,3-Halogen Migration ...	40
3.1 Introduction to Asymmetric Halogenation Reactions	41
3.2 Optimization of Asymmetric 1,3-Halogen Migration.....	41
3.3 Scope of Asymmetric 1,3-Halogen Migration	43
3.4 A Predictive Model for Determining Reaction Yield	43
3.4.1 Developing the Predictive Model.....	44
3.4.2 Testing the Predictive Model	45
3.5 Demonstration of Activating Group Recycling	46
3.6 Conclusions.....	47
3.7 Experimental Details.....	47
3.7.1 Synthesis of Styrene Starting Materials	47
3.7.2 Procedure for the Asymmetric 1,3-Halogen Migration.....	54
3.7.3 Developing the Predictive Model.....	60
3.7.4 Displacement of the Benzyl Bromide with Nucleophiles	69
3.8 Bibliography	73
Chapter 4: Mechanistic Studies of Copper(I)-Catalyzed 1,3-Halogen Migration.....	76
4.1 Introduction.....	77
4.2 Control Experiments	78
4.3 Crossover Experiment.....	79
4.4 Non-Linear Effects Study of the Dependence of Product ee on Ligand ee.....	80

4.5 Kinetics Studies of 1,3-Halogen Migration	81
4.5.1 Hammett Analysis of 1,3-Halogen Migration	82
4.5.2 Kinetic Isotope Effect on 1,3-Halogen Migration	83
4.5.3 Conclusions from Kinetics Studies	83
4.6 Stoichiometric NMR Experiments to Elucidate Organocopper Intermediates	84
4.6.1 Stoichiometric Experiments with Phosphine-supported Copper Species	84
4.6.2 Stoichiometric Experiments with NHC-supported Copper Species	84
4.6.3 Diffusion-NMR Study of NHC-Copper Hydrides	85
4.7 Preliminary Mechanistic Proposal	85
4.8 Determining the Substrate and Catalyst Parameters that Dictate Selectivity between Migration and Hydroboration	86
4.8.1 Computational Investigation of the Impact of Steric Bulk on Hydroboration	86
4.8.2 Experimental Investigation of the Factors Impacting the Selectivity of Migration	87
4.9 Experimental Investigation of the Migration Step: Transfer of Stereochemistry	88
4.9.1 Comparison of the Enantioselectivity between Hydroboration and Migration under Asymmetric Conditions	88
4.9.2 Use of Deuterium Labeling to Determine Transfer of Stereochemistry during the Migration Step	89
4.10 Computational Investigation of Possible Migration Pathways	90
4.10.1 Oxidative Insertion/Reduction Elimination Pathways	90
4.10.2 Pathways Involving One Electron Changes at Copper	91
4.10.3 A Dearomative Pathway Involving No Oxidation State Changes at Copper	92
4.11 Determination of the Enantio-Determining Step in Asymmetric 1,3-Halogen Migration	93
4.12 Overall Reaction Profile: Comparison between Phosphine and NHC Supported Copper Hydrides	94

4.13 Testing the Mechanistic Hypothesis: 1,5-Halogen Migration.....	95
4.14 Conclusions.....	96
4.15 Experimental Details.....	96
4.15.1 Preparation of Substrates.....	96
4.15.2 Control Experiment.....	101
4.15.3 Crossover Experiment.....	101
4.15.4 Non-Linear Effects Study.....	103
4.15.5 Kinetics and Hammett Studies.....	105
4.15.6 Stoichiometric NMR Experiments.....	111
4.15.7 Factors Impacting Selectivity.....	126
4.15.8 Transfer of Stereochemistry Experiments.....	128
4.15.9 Stoichiometric and Catalytic 1,5-Halogen Migration.....	132
4.15.10 Computational Details.....	138
4.16 Bibliography.....	139
Chapter 5: Nickel-Catalyzed Hydroboration of Styrenes.....	144
5.1 Introduction to Nickel-catalyzed Borylations.....	145
5.2 Optimization of Nickel-catalyzed Hydroboration.....	145
5.3 Substrate Scope of Hydroboration.....	146
5.4 Impact of Steric Bulk of the Catalyst on Selectivity.....	147
5.5 Proposed Mechanism.....	148
5.6 Conclusions.....	149
5.7 Experimental Details.....	149
5.7.1 Preparation of Novel Nickel Complexes.....	149

5.7.2 General Procedure for the Hydroboration of Styrenes.	151
5.7.3 Effect of Sterics on Hydroboration.	155
5.8 Bibliography	161
Appendix A: NMR Spectra	163
Appendix B: Optimized Geometries.....	331
B.1 Optimized Geometries for the Predictive Model.....	332
B.2 Optimized Geometries for the Calculated Pathway	363
Appendix C: Crystallographic Details and Structures	412
C.1 Determination of absolute configuration for asymmetric 1,3-halogen migration	413
C.2. IPr(Cy ₃ P)NiCl ₂	420
C.3 IMes(Cy ₃ P)NiCl ₂	475
C.4. IPr*(Cy ₃ P)NiCl ₂	489
Appendix D: HPLC Chromatograms.....	527

List of Abbreviations

<i>(R,R)</i> -iPr-BPE	(+)-1,2-Bis((2 <i>R</i> ,5 <i>R</i>)-2,5-diisopropylphospholano)ethane
<i>(S,S)</i> -Me-BPE	(+)-1,2-Bis((2 <i>S</i> ,5 <i>S</i>)-2,5-dimethylphospholano)ethane
<i>(S,S)</i> -Ph-BPE	(+)-1,2-Bis((2 <i>S</i> ,5 <i>S</i>)-2,5-diphenylphospholano)ethane
Å	angstrom(s)
Ac	acetyl
AcOH	acetic acid
aq	aqueous
Ar	aryl
ASAP	atmospheric solids analysis probe
ATRP	atom transfer radical polymerization
B3LYP	Becke 3-Parameter, Lee-Yang-Parr density functional method
Bcat	catecholborane
Bn	benzyl
Bpin	4,4,5,5-tetramethyl-1,3,2-dioxaborolane
br d	broad doublet
br s	broad singlet
Bu	normal-butyl
C	Celsius
cat.	Catalyst
cod	cyclooctadiene
COSY	correlation spectroscopy
Cp	cyclopentadienyl
Cp*	pentamethylcyclopentadienyl

Cy	cyclohexyl
d	doublet
dcype	1,2-bis(dicyclohexylphosphino)ethane
dd	double of doublets
ddd	doublet of doublet of doublets
dEtpe	1,2-bis(diethylphosphino)ethane
DFT	density functional theory
dMepe	1,2-bis(dimethylphosphino)ethane
DMF	N,N-dimethylformamide
DMP	Dess-Martin periodinane
DMSO	dimethyl sulfoxide
DOSY	diffusion NMR spectroscopy
DPEphos	(Oxydi-2,1-phenylene)bis(diphenylphosphine)
dppb	1,4-bis(diphenylphosphino)butane
dppbz	1,2-bis(diphenylphosphino)benzene
dppe	1,2-bis(diphenylphosphino)ethane
dppf	1,1'-bis(diphenylphosphino)ferrocene
dppm	1,1-bis(diphenylphosphino)methane
dppp	1,3-bis(diphenylphosphino)propane
dq	doublet of quartets
<i>dr</i>	diastereomeric ratio
dt	doublet of triplets
d'Bupe	1,2-bis(di- <i>tert</i> -butylphosphino)ethane
<i>ee</i>	enantiomeric excess
EI	electron ionization

equiv	equivalent
<i>er</i>	enantiomeric ratio
ESI	electrospray ionization
Et	ethyl
Et ₂ O	diethyl ether
Et ₃ P	triethylphosphine
EtO	ethoxy
EtOAc	ethyl acetate
EtOH	ethanol
g	gram
h	heptet
h	hour
HMBC	heteronuclear multiple bond correlation
HRMS	high resolution mass spectrometry
HSQC	heteronuclear single quantum coherence
Hz	hertz
IMes	1,3-Bis(2,4,6-trimethylphenyl)-1,3-dihydro-2 <i>H</i> -imidazol-2-ylidene
IMesHCl	1,3-Bis(2,4,6-trimethylphenyl)imidazolium chloride
IPr	1,3-Bis(2,6-diisopropylphenyl)-1,3-dihydro-2 <i>H</i> -imidazol-2-ylidene
IPrHCl	1,3-Bis(2,6-diisopropylphenyl)imidazolium chloride
iPrO	isopropoxy
<i>J</i>	spin-spin coupling constant in hertz
kcal	kilocalorie
KOtBu	potassium tert-butoxide
LDA	lithium diisopropyl amide

M	molar
m	multiplet
M06	Minnesota 06 functional
Me	methyl
MeOH	methanol
MeS	thiomethoxy
mg	milligram
MHz	megahertz
min	minute
mL	milliliter
mM	millimolar
mmHg	millimeters of mercury
mmol	millimole
mol	moles
mp	melting point
Ms	methanesulfonyl
MS	molecular sieves
NaOtBu	sodium <i>tert</i> -butoxide
NBO	Natural Bond Orbital Theory
NBS	N-bromosuccinimide
nBu ₃ P	tributylphosphine
n-BuLi	normal-butyllithium
NHC	N-heterocyclic carbene
NMR	nuclear magnetic resonance spectroscopy
NPA	Natural Population Analysis

OAc	acetate
OBz	benzoate
OMe	methoxy
PCy ₃	tricyclohexylphosphine
Ph	phenyl
phen	1,10-phenanthroline
Piv	trimethylacetyl
PMe ₃	trimethylphosphine
PMHS	Poly(methylhydrosiloxane)
PPh ₃	triphenylphosphine
ppm	parts per million
Pr	normal-propyl
pTSA	<i>p</i> -Toluenesulfonic acid monohydrate
pyr	pyridine
q	quartet
qd	quartet of doublets
Rf	retention factor
rt	room temperature
s	singlet
SMD	solute molecular density
TBS	tert-butyltrimethylsilyl
tBu	<i>tert</i> -butyl
tBu ₂ MeP	di- <i>tert</i> -butylmethylphosphine
tBu ₃ P	tri- <i>tert</i> -butylphosphine
td	triplet of doublets

THF	tetrahydrofuran
THF-d ₈	Octadeuterotetrahydrofuran
TLC	thin layer chromatography
TPA	triphenylacetyl
TsOH	<i>p</i> -Toluenesulfonic acid monohydrate
tt	triplet of triplets
Xantphos	4,5-Bis(diphenylphosphino)-9,9-dimethylxanthene
δ	chemical shift in ppm
μL	microliter
μmol	micromole

List of Figures, Tables, and Schemes

Figure 1.1 Classical Type I and Type II dyotropic rearrangements.....	2
Scheme 1.1. Dyotropic rearrangement of a cuprate.....	4
Scheme 1.2. Dyotropic rearrangement of dimethylcuprate.....	4
Scheme 1.3. Net C-F oxidative insertion <i>via</i> a dyotropic rearrangement.....	5
Scheme 1.4. Light-induced dyotropic rearrangement of a Fischer carbene.....	6
Scheme 1.5. Stepwise 1,3-dyotropic rearrangement via a silyl cation.....	7
Scheme 1.6. 1,3-dyotropic rearrangement of an Ir(Cp*) complex.....	7
Scheme 1.7. Stepwise 1,4-dyotropic rearrangement of an aryl rhenium via a proposed radical pathway.....	8
Scheme 1.8. Alkenyl to aryl 1,4-rearrangements with rhodium, iridium, and ruthenium.....	9
Scheme 1.9. Common mechanistic pathway for 1,4-rearrangements.....	9
Scheme 1.10. Catalytic 1,4-dyotropic rearrangements in biaryl systems involving Pd.....	10
Scheme 1.11. Catalytic 1,4-dyotropic rearrangement to activate α -aryl protons with Pd.....	11
Scheme 1.12. Seminal 1,4-dyotropic rearrangement alkylating an aromatic with Rh.....	12
Scheme 1.13. Seminal 1,4-dyotropic rearrangement hydroarylation with Rh.....	13
Scheme 1.14. Multiple functionalizations via Rh catalysis.....	13
Scheme 1.15. Co-catalyzed addition of arylzinc to alkynes with 1,4-rearrangement to reform an arylzinc.....	14
Scheme 1.16. Formal 1,3-rearrangement via sequential 1,4-rearrangements.....	15
Scheme 2.1. New mode of arene functionalization vs. traditional cross-coupling approach.....	21
Scheme 2.2. Examples of activating group recycling.....	22
Table 2.1. Initial ligand screen.....	23
Table 2.2. Optimization of the reaction conditions.....	24
Table 2.3. Substrate scope of 1,3-halogen migration.....	25
Scheme 3.1. Burns catalytic enantioselective dihalogenation.....	41

Table 3.1. Optimization of the ligand for 1,3-halogen migration.....	42
Table 3.2. Optimization of reaction conditions.....	42
Table 3.3. Initial scope of asymmetric 1,3-halogen migration.....	43
Figure 3.1. Factors impacting product yield.....	44
Table 3.4. Training set of substrates for the predictive model.....	45
Table 3.5. Testing the predictive power of the model.....	46
Scheme 3.2. Recycling of the benzyl bromide.....	47
Scheme 4.1. Cu(I)-catalyzed hydroboration vs. halogen migration.....	78
Scheme 4.2. Cross-over experiments <i>via</i> ^{79/81} Br isotopic labeling.....	80
Figure 4.1. Dependence of product <i>ee</i> on ligand <i>ee</i>	81
Figure 4.2. Time course of 1,3-halogen migration and rate dependence on catalyst loading.....	82
Figure 4.3. Hammett plot of Cu(I)-catalyzed 1,3-halogen migration.....	83
Scheme 4.3. Pre-equilibrium step forming π -olefin complex and rate-determining step.....	84
Scheme 4.4. Preliminary mechanistic proposal.....	86
Figure 4.4. Impact of steric bulk on hydroboration.....	87
Table 4.1. Factors impacting the product distribution in the 1,3-halogen migration.....	88
Figure 4.5. Comparing enantioinduction for hydroboration and migration.....	89
Scheme 4.5. Transfer of stereochemical information during the 1,3-halogen migration.....	90
Figure 4.6. Proposed oxidative addition pathways proceeding through a Cu(I)/Cu(III) cycle.....	91
Figure 4.7. Pathways invoking potential Cu(II) intermediates.....	92
Figure 4.8. Proposed Cu-catalyzed 1,3-halogen migration pathway invoking a dearomatized intermediate.....	93
Figure 4.9. Transition state structures for the enantiodetermining step.....	94
Scheme 4.5. Complete catalytic cycle for the Cu-catalyzed 1,3-halogen migration/borylation.....	95
Figure 4.10. Long range atom transfer <i>via</i> copper(I)-catalyzed halogen migration.....	96
Table 5.1. Optimization of Ni-catalyzed hydroboration.....	146
Table 5.2. Comparison of nickel complex reactivity.....	146

Table 5.3. Substrate scope.....	147
Table 5.4. Effect of steric bulk on selectivity.....	148
Scheme 5.1. Proposed catalytic cycle.....	149

Chapter 1: Introduction to Formal Dyotropic Rearrangements in Organometallic Transformations

Reproduced with permission from Croisant, M. F.; Van Hoveln, R.; Schomaker, J. M. *Eur. J. Org. Chem.* **2015**,

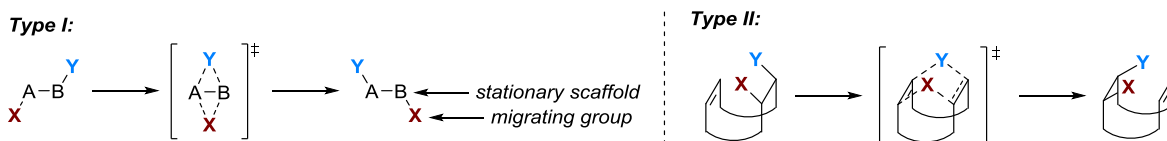
DOI: 10.1002/ejoc.201500561. Copyright 2015 WILEY-VCH Verlag GmbH & Co.

1.1 Introduction to Dyotropic Rearrangements

Over the last several decades, transition metal-catalyzed transformations have cemented their place as a bedrock of synthetic organic methodology and are utilized in a number of important industrial processes.¹ This wide range of utility is due in large part to the relatively small number of general mechanistic steps that give rise to diverse C-C and carbon-heteroatom bond-forming reactions.² These steps, which typically consist of oxidative addition, transmetalation and reductive elimination, are usually highly predictable, making new reactivity fairly easy to engineer.³ In the last several years, significant effort has been directed towards developing our understanding of conventional mechanistic pathways.⁴ However, the continued identification and elucidation of the mechanisms of unusual modes of reactivity is important for the development of new transformations, particularly in the area of base metal catalysis. One such transformation with the potential to provide considerable flexibility in organometallic catalysis is the dyotropic rearrangement. Presently, the application of dyotropic rearrangements to organometallic reactions has not been well-studied, with the exception of the few systems that will be the subject of this chapter.

Traditionally, dyotropic rearrangements fall into two broad categories, referred to as Type I and Type II (Figure 1.1).⁵ Type I dyotropic rearrangements consist of 1,2-shifts in which two migrating groups interchange positions along a stationary scaffold. This process occurs in a concerted fashion, resulting in an inversion of configuration for both migrating groups due to the anti-conformation of the transition state. On the other hand, Type II dyotropic rearrangements involve migration of two groups to new binding sites; however, the groups do not interchange positions. Over time, these general definitions have been expanded considerably to include not only concerted reactions, but those that proceed via step-wise, metal-catalyzed or photochemical pathways.

Figure 1.1 Classical Type I and Type II dyotropic rearrangements.



Type I dyotropic rearrangements vary widely in terms of the nature of the migrating group (halogen interchange, oxygen migration, alkyl shifts), the stationary scaffold (C-C versus C-N, differences in the steric hindrance and the electron density) and the effects of substituents on the reaction outcome. To what extent these factors contribute to the activation energy barriers for Type I dyotropic rearrangements is a topic of particular

interest to synthetic and computational chemists and several insights have recently been reported. Notable examples have been described by Fernández and Cossío in their studies to determine substituent effects on the dyotropic rearrangements of a series of cyclic and acyclic 1,2-dibromoalkanes.⁶ Density functional theory (DFT) calculations predict that π -donating substituents facilitate stabilization of the four-membered transition state of the dyotropic rearrangement. Expanding this understanding to rearrangements involving metals could lead to new modes of catalysis, where multiple sites in a substrate can be functionalized without dissociation of the catalyst from the substrate. Both stoichiometric and catalytic examples describing formal dyotropic rearrangements involving metals have been reported, although the majority of these reactions result in a single functionalization of the substrate at a position distal to the activating group and are rarely used to carry out multiple functionalizations of the same molecule. However, the ability to functionalize multiple sites would enable rapid increases in complexity from simple starting materials and lead to more efficient synthetic strategies.

While the nomenclature and definitions for dyotropic rearrangements of organic molecules have been well-established for quite some time, the terminology is ill-defined when a metal is one of the migrating groups or is part of the stationary scaffold. While the use of the term ‘dyotropic’ has permeated the organometallic community to some extent, dyotropic rearrangements involving metals have also been referred to as “metallate rearrangements,” “metal migrations,” “metal transpositions,” “diatropic rearrangements” (likely a misspelling of ‘dyotropic’), “tandem metal shifts,” or simply “shifts.” To complicate matters further, this nomenclature is conflated with rearrangements that do not fit well within the general definition of a dyotropic rearrangement, resulting in terminology overlap for a broad range of transformations. For the sake of simplicity, and to maintain some alignment with the original definition, we will refer to dyotropic rearrangements as any rearrangement in which two groups are interchanged by the breaking and reforming two σ bonds, presumably in an intramolecular fashion, regardless of whether the mechanism is concerted or not. In this chapter, a wide range of stoichiometric and catalytic examples of Type I organometallic dyotropic rearrangements will be discussed. Where applicable, the various mechanistic pathways of these transformations will also be reviewed.

1.2. Stoichiometric Organometallic Dyotropic Rearrangements

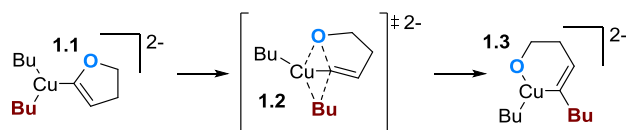
Stoichiometric dyotropic rearrangements have been studied extensively. While many such examples focus on mechanistic aspects of the rearrangement, these reactions also show significant potential for development into

synthetically useful catalytic transformations. As metals are capable of adopting a variety of bonding modes, these dyotropic rearrangements are not limited to 1,2-shifts; migrations can occur over as many as four atoms or groups.

1.2.1 1,2-Rearrangements

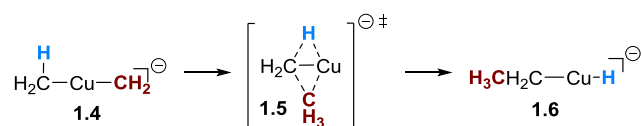
A 1990 review by Barber has described numerous examples of copper species undergoing 1,2-dyotropic rearrangements to produce trisubstituted alkenes from 1-hetero-1-alkenyl metallates (Scheme 1.1).⁷ Dialkyl cuprates bound to an alkene bearing a heteroatom, as exemplified by **1.1**, are known to undergo 1,2-rearrangements in which an R group on copper is transferred to the alkenyl carbon and the heteroatom migrates to copper. Cuprate **1.3** can then be protonated to form a homoallylic alcohol containing a highly substituted alkene. Boron, aluminum, zirconium, nickel, and zinc have also been shown to participate in this type of rearrangement process.^{7,8} Such transformations have been applied to the synthesis of natural products, including lacrimin A and phalluside-1, as well as the synthesis of various alkenylpolyol chains.⁹

Scheme 1.1. Dyotropic rearrangement of a cuprate.



A 2010 study by O'Hair offers another unique example of a 1,2-dyotropic rearrangement that takes place from an organo-cuprate precursor.¹⁰ Gas-phase collision-induced dissociation experiments to determine the fragmentation reactivity of dimethylcuprate showed that the dominant pathway was homolytic cleavage to produce methyl radical and the radical anion $[\text{CH}_3\text{Cu}]^\cdot$. However, another pathway involved the elimination of ethylene from $[\text{Me}_2\text{Cu}]^-$ to produce a dihydride anion $[\text{HCuH}]^-$. This reaction was proposed to occur via a dyotropic rearrangement of $[\text{Me}_2\text{Cu}]^-$ to yield the mono-hydridocuprate species **1.6** (Scheme 1.2), which subsequently undergoes β -hydride elimination to produce $[\text{HCuH}]^-$ and ethylene. When one of the methyl groups was deuterated, the $[\text{DCuH}]^-$ ion was observed, providing further support for this proposed fragmentation.

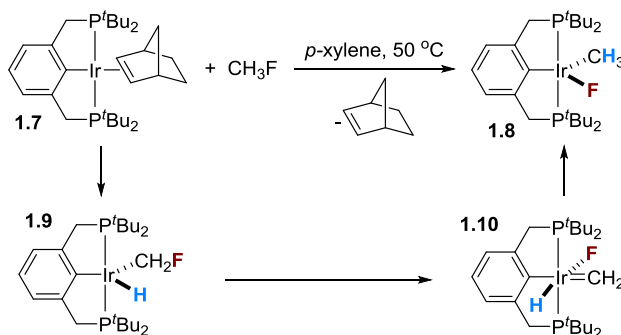
Scheme 1.2. Dyotropic rearrangement of dimethylcuprate.



These types of dyotropic rearrangements are unusual, as the metal is typically not part of the stationary scaffold, but tends to migrate. Additionally, most organometallic dyotropic rearrangements reported thus far involve early transition metals. However, in recent years, a number of research groups, including our own, have been harnessing the ability of later transition metals to participate in dyotropic rearrangements in order to develop practical catalytic transformations, particularly in the context of 1,3-rearrangements (*vide infra*).

A rare example of fluorine participating in a 1,2-dyotropic rearrangement has also been reported by Goldman (Scheme 1.3).¹¹ In this process, a C-H bond of fluoromethane or a benzyl fluoride is activated by iridium to form intermediate **1.9**, after which two subsequent migrations occur. An α -fluoride abstraction first produces methyldiene intermediate **1.10**, followed by migration of the hydride on iridium back to the carbon to form the observed product **1.8**. The net result is an oxidative addition of a C(sp³)-F bond to an iridium complex via a non-concerted 1,2-dyotropic rearrangement and the proposed mechanism is supported by both DFT and NMR studies. As the high bond strength of C-F bonds often precludes direct oxidative addition, this reaction pathway involving C-H activation acts as a means to indirectly facilitate C(sp³)-F oxidative addition and provides insight into other ways in which the catalytic formation of C(sp³)-F bonds may be achieved.

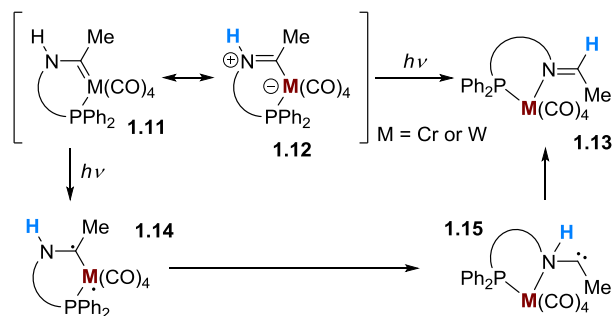
Scheme 1.3. Net C-F oxidative insertion *via* a dyotropic rearrangement.



Dyotropic rearrangements may also be promoted photochemically.^{5a,12} Cossío and Sierra reported that irradiation of a chromium or tungsten Fischer carbene complex resulted in the clean conversion of the carbene to an imine (Scheme 1.4).¹² It is unlikely that this reaction proceeds in a concerted fashion; rather, the proposed mechanism likely involves photoexcitation of the carbene complex to a triplet diradical **1.14**. The metal then migrates from carbon to nitrogen to generate the carbene **1.15**. Hydrogen migration from the nitrogen to the carbene carbon of **1.15** yields the final product **1.13**. The proposed mechanism has been studied computationally for both

chromium and tungsten, and the energetic pathways are nearly the same for both metals. This is surprising, as first row transition metals typically do not exhibit similar reactivity to their 2nd and 3rd-row counterparts, and in cases where they do, the energetic difference is typically substantial. However, this rearrangement seems limited to substrates in which hydrogen is bound to the nitrogen. Other groups on nitrogen, even methyl groups, undergo either carbonylation or ring contraction with extrusion of the carbene.¹²

Scheme 1.4. Light-induced dyotropic rearrangement of a Fischer carbene.

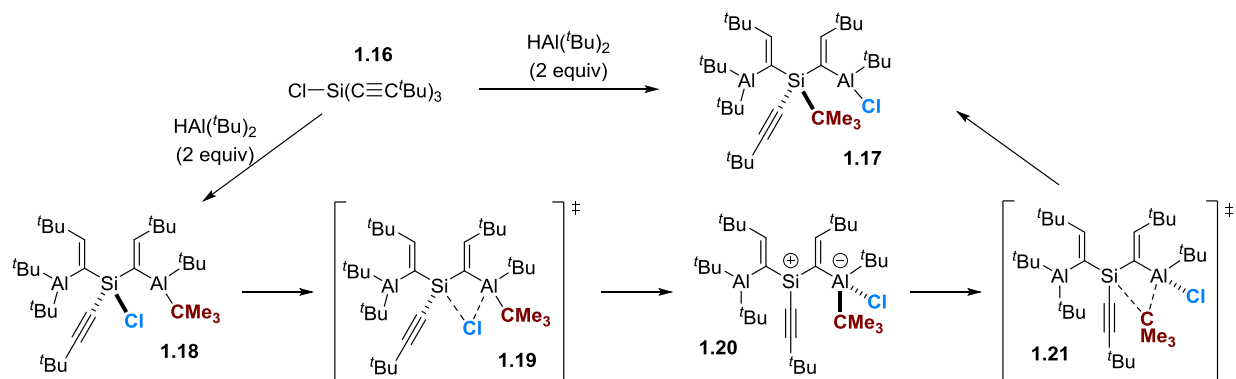


1.2.2 1,3-rearrangements

Since metals have long bond lengths and can adopt a number of binding modes, dyotropic rearrangements involving metals are not necessarily limited to vicinal rearrangements and can occur across several atoms. In general, dyotropic rearrangements involving metals tend to be even-numbered rearrangements (1,2- and 1,4-migrations) rather than odd-numbered (such as 1,3-migrations).^{5a}

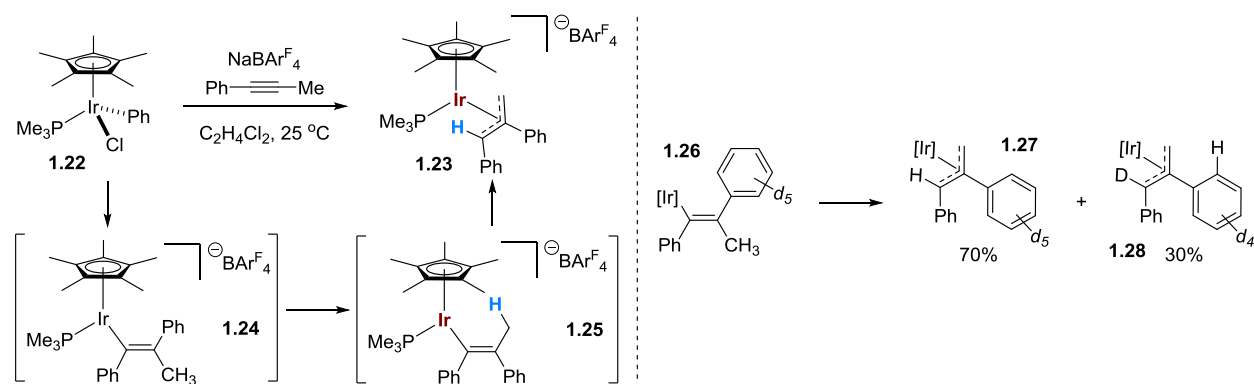
One example of a stoichiometric 1,3-dyotropic rearrangement involves the interchange of groups between a silicon and an aluminum center.¹³ In this rearrangement, a chlorine and a tert-butyl group interchange positions by a stepwise mechanism involving a silyl cation **1.20** (Scheme 1.5). Interestingly, this is another example where the metal remains part of the stationary scaffold, rather than migrating during the dyotropic rearrangement.

Scheme 1.5. Stepwise 1,3-dyotropic rearrangement via a silyl cation.



A 1,3-dyotropic rearrangement has been observed in a Cp*Ir complex (Scheme 1.6).¹⁴ The aryl-Ir complex **1.22** undergoes carbometallation of the π -bond of methylphenylacetylene to form vinyl-Ir complex **1.24**. A double bond isomerization then occurs, giving the proper conformation for the allylic proton and Ir to interchange positions yield an η^3 π -allyl Ir complex **1.23**. While this pathway proceeds through multiple mechanisms, the major pathway is direct 1,3-rearrangement *via* an oxidative insertion/reductive elimination process. The other pathway involves successive 1,4-rearrangements that give rise to the same product (*vide infra* for 1,4-rearrangements of Cp*Ir complexes). Deuterium labeling experiments support this mechanistic proposal; deuteration of the aromatic ring would be expected to yield subsequent incorporation into the allyl carbon, indicating successive 1,4-rearrangements. However, only 30% of product **1.28** was observed, indicating the major mechanistic pathway is direct 1,3-rearrangement (Scheme 1.6, right).

Scheme 1.6. 1,3-dyotropic rearrangement of an Ir(Cp*) complex.

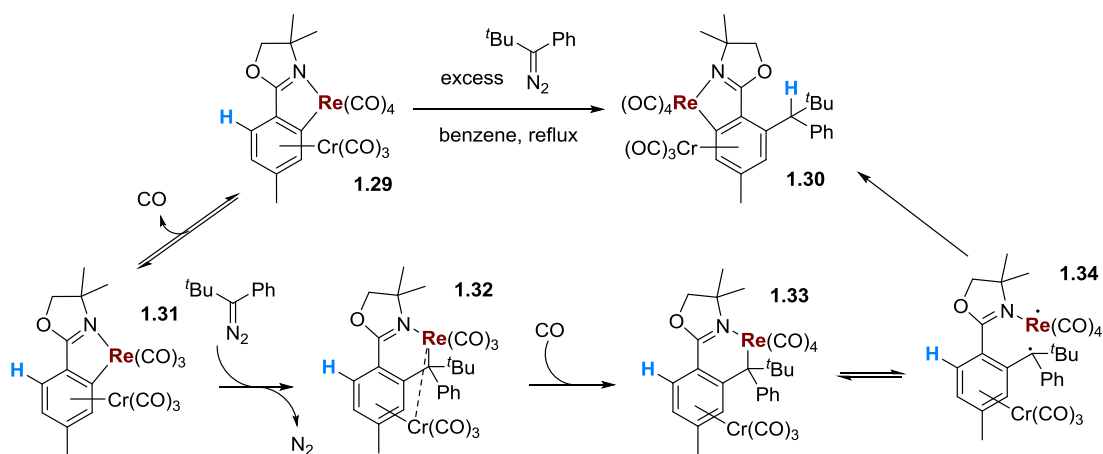


1.2.3 1,4-Rearrangements

The most common and widely employed dyotropic reactions that involve metals consist of 1,4-rearrangements. A number of examples have been reported in the literature that encompass a variety of metals, including rhodium, iridium, and ruthenium.¹⁵ In almost all cases, the metal interchanges positions with a hydrogen.

A recent example of a 1,4-dyotropic rearrangement involves rhenium as the migrating group (Scheme 1.7).^{15d} The reaction is believed to proceed via a radical, stepwise mechanism; however, it is not clear whether this transformation is intermolecular or intramolecular. The starting complex **1.29** is an aryl-Re complex supported by an oxazoline. Dissociation of a carbonyl ligand is followed by insertion of an in situ generated carbene into the C-Re bond to generate a benzyl Re complex **1.32**. This complex then undergoes a series of hydrogen atom abstractions and radical recombinations to transfer the hydrogen to the benzyl carbon that was initially bound to the Re, eventually producing a new aryl-Re species **1.30**, where the metal is bound to the carbon previously occupied by the hydrogen. Isolation of trace decarbonylated and benzyl Re side products provide evidence for the proposed decarbonylation/re-carbonylation mechanism, as opposed to direct ortho-insertion of the carbene. Notably, this mechanism is a rare example of a non-photochemical, formal dyotropic rearrangement thought to proceed via a radical mechanism.

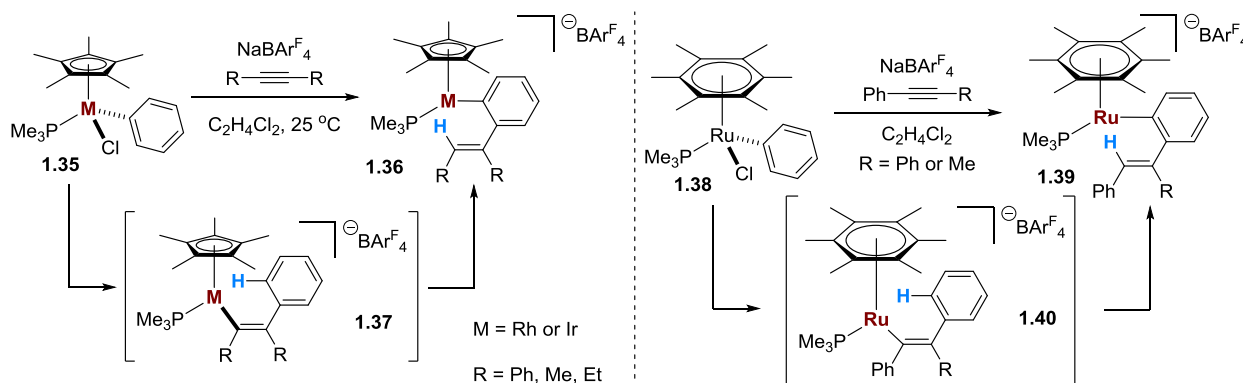
Scheme 1.7. Stepwise 1,4-dyotropic rearrangement of an aryl rhenium via a proposed radical pathway.



Many examples of formal 1,4-dyotropic rearrangements occur in metal-arene complexes involving metals such as Rh, Ir, and Ru (Scheme 1.8).^{15a-c} In all cases, a metal-aryl bond adds across the π -bond of an alkyne. The resulting vinyl-metal complex **1.37** can then activate a C-H bond on the aromatic ring to promote a 1,4-rearrangement, where the metal and aryl proton interchange positions to yield the aryl-metal bond of **1.36**. Since

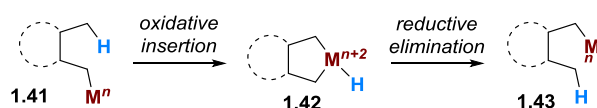
1,4-rearrangements occur more frequently in catalysis compared to other formal dyotropic rearrangements, such transformations have been extensively studied in the context of long-range C-H activation in both stoichiometric and catalytic regimes (*vide infra*).

Scheme 1.8. Alkenyl to aryl 1,4-rearrangements with rhodium, iridium, and ruthenium.



The typical mechanisms proposed for dyotropic 1,4-rearrangement involve oxidative insertion/reductive elimination pathways (Scheme 1.9). Oxidative insertion of the metal into the C-H bond results in a five-membered metallacycle **1.42**, which then undergoes reductive elimination to afford the rearranged organometallic complex. This pathway is invoked in catalytic examples of 1,4-dyotropic rearrangements as well, and should be considered the mechanism of choice for these types of rearrangements unless otherwise noted.

Scheme 1.9. Common mechanistic pathway for 1,4-rearrangements.



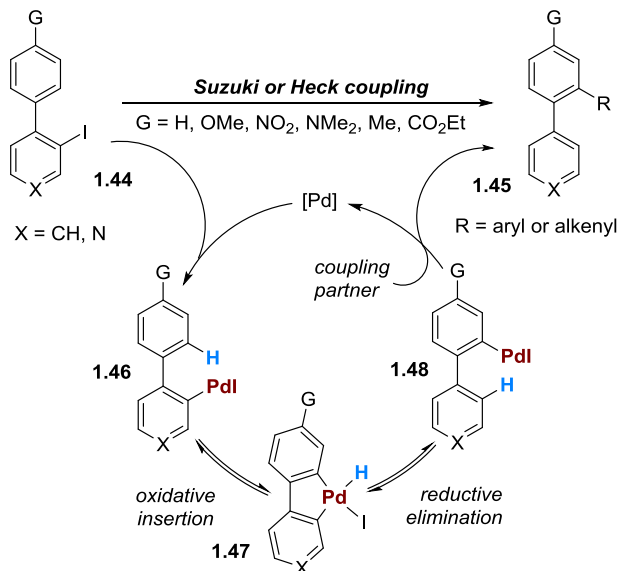
1.3. Examples of Organometallic Dyotropic Rearrangements in Catalysis

There are many examples of organometallic dyotropic rearrangements which occur during the course of a catalytic transformation; however, most of these are related to 1,4-rearrangements promoted by Pd and Rh as a strategy for the long-range activation of C-H bonds.¹⁶ Examples of other metals participating in 1,n-rearrangements are rare; nonetheless, there exists great potential for identifying new examples of this type of reactivity catalyzed by a wider array of transition metals.

1.3.1 1,4-Rearrangements

Dyotropic rearrangements occurring during catalysis involving 1,4-migrations are commonplace and are dominated by palladium and rhodium. Biaryl substrates are particularly popular scaffolds for carrying out palladium-mediated 1,4-rearrangements (Scheme 1.10).¹⁷ In these systems, palladium inserts into an ortho C-X bond (X = Cl, Br, I) to yield **1.46**, which is followed by the activation of an ortho C-H bond on the adjacent aryl ring to give **1.48**. The net result is the migration of the palladium to the other aryl ring; this organometallic intermediate can be intercepted using standard Suzuki or Heck couplings. A rare example of platinum participating in a similar 1,4-rearrangement has also been reported.^{17c}

Scheme 1.10. Catalytic 1,4-dyotropic rearrangements in biaryl systems involving Pd .

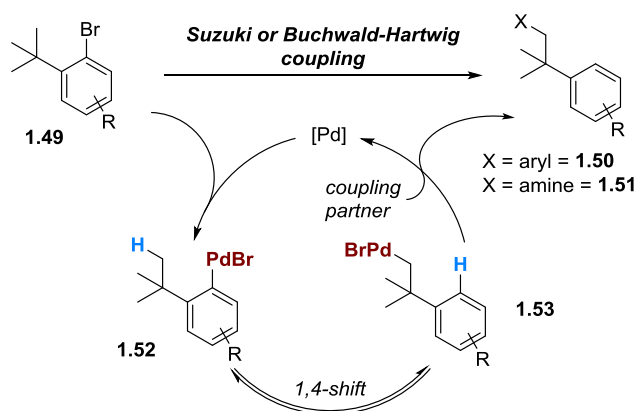


Since the palladium is bound to either aryl ring during the course of the reaction, presumably coupling could occur at either of the ortho sites in Scheme 1.10. The intramolecular nature of this 1,4-palladium rearrangement reduces the barrier for C-H activation, as there is no entropic penalty. Thus, the rearrangement is reversible and the two species **1.46** and **1.48** are in equilibrium. Whether coupling occurs at the original site of palladium insertion or at the migration site on the adjacent ring reflects the equilibrium position of the palladium between the two sites, and correlations have been drawn between this site preference and relative C-H acidity. Biaryl systems containing electron-withdrawing substituents distal from the site of initial oxidative insertion (labeled “G” in Scheme 1.10) were found to undergo coupling at the migratory site with moderate selectivity (up to 77:23 in

the case of $G = \text{NO}_2$).^{18b} The substitution of electron-donating groups at this position (as well as weaker electron-withdrawing groups like CO_2Et) essentially rendered the coupling unselective.

The dyotropic 1,4-palladium rearrangement has also been used to activate C-H bonds β to an aromatic ring. For example, Buchwald has described two different functionalizations of unactivated sp^3 C-H bonds (Scheme 1.11).¹⁸ Both reactions initially follow identical catalytic cycles, where the palladium inserts into an ortho bromide and is followed by the oxidative insertion/reductive elimination mechanism shown in Scheme 1.9 to form the alkyl palladium **1.53**. This alkyl palladium can then participate in either Suzuki or Buchwald-Hartwig couplings to yield **1.50** or **1.51**, respectively. In the case of the amination reaction, the steric bulk of the aryl halide substrate plays an important role in suppressing the competing C-N cross-coupling event. In some substrates, a cyclobutane by-product results from reductive elimination of the palladacycle.^{19,20a} Additionally, if β -protons are present on the alkyl substituent, β -hydride elimination can be problematic.²⁰

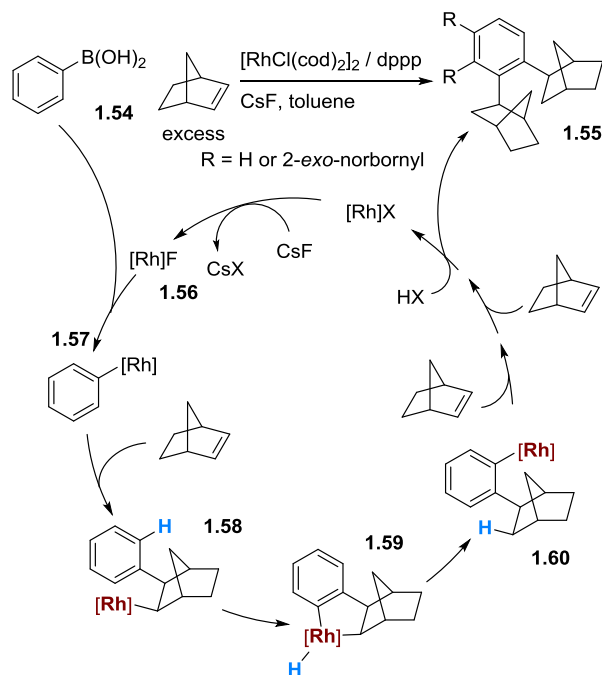
Scheme 1.11. Catalytic 1,4-dyotropic rearrangement to activate β -aryl protons with Pd.



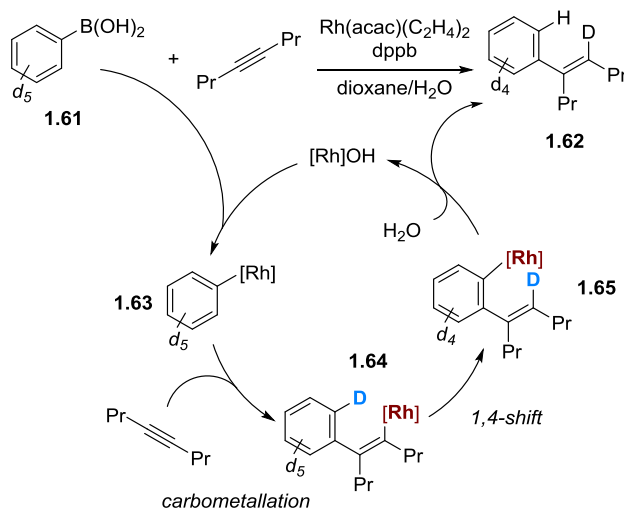
The other transition metal that commonly promotes 1,4-rearrangements is Rh. Seminal reports of Rh-catalyzed dyotropic reactions first appeared in the early 2000s. One such example details the reaction of arylboronic acids with norbornene to yield products containing varying degrees of substitution on the aromatic ring (Scheme 1.12).²¹ The proposed mechanism proceeds through an exo addition of $\text{Ph}[\text{Rh}]$ across the π -bond of norbornene to yield **1.58**, followed by a 1,4-metal migration *via* the 5-membered rhodacycle **1.59**. This process can be repeated multiple times, leading to the formation of di-, tri-, and tetrasubstituted products and the product distribution can be readily controlled by varying the equivalents of norbornene. A more recent report expanded on these initial results

to produce the corresponding acylated norbornanes.²² This process is also the mechanistic basis of the Catellani reaction which uses Pd as the catalyst.²³

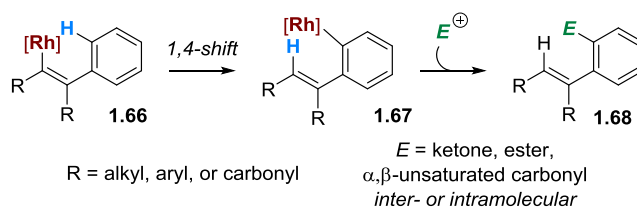
Scheme 1.12. Seminal 1,4-dyotropic rearrangement alkylating an aromatic with Rh.



The Hayashi group has also reported a Rh-catalyzed hydroarylation of alkynes (Scheme 1.13) that proceeds through a 1,4-metal migration.²⁴ The reaction of 4-octyne with phenylboronic acid was found to produce the corresponding alkene product **1.62** with syn-selectivity. It was originally thought that the hydrogen of the newly-formed sp^2 C-H bond was being incorporated from the solvent, but deuterium labeling experiments did not support this hypothesis. When the reaction was performed in dioxane/ H_2O with deuterated phenylboronic acid, deuterium incorporation at the vinyl position was observed in excess of 93%. Correspondingly, when the reaction was performed using non-deuterated phenylboronic acid in a mixture of dioxane/ D_2O , a 98% incorporation of deuterium at the ortho position of the aryl ring was observed in the product.

Scheme 1.13. Seminal 1,4-dyotropic rearrangement hydroarylation with Rh.

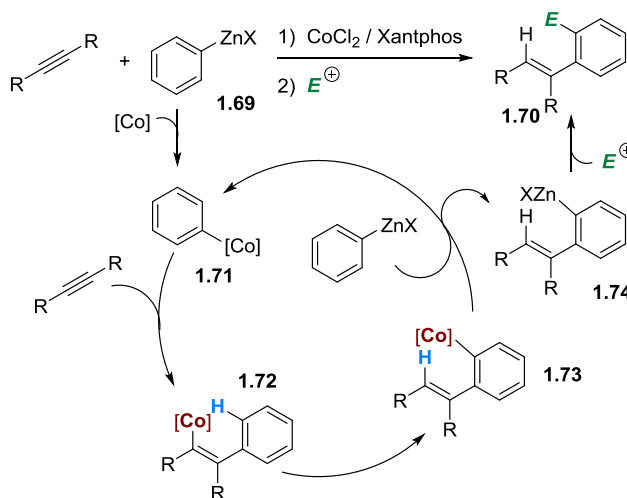
Following these seminal reports, 1,4-rhodium rearrangements have been observed in a number of transformations that include cyclizations,^{25,26} ring expansions,²⁷ and nucleophilic additions. In fact, a variety of nucleophilic addition reactions featuring 1,4-rhodium rearrangements have been reported that facilitate such transformations as intramolecular acylation,²⁸ spirocycle formation,²⁹ and conjugate addition (Scheme 1.14).³⁰ A general mechanism is illustrated in Scheme 1.14 and involves a vinyl rhodium species **1.66** which undergoes 1,4-rhodium rearrangement to place the metal at the ortho position of the aryl ring **1.67**. The Ar-Rh species then reacts with an electrophile, such as an ester or the β -position of an α,β -unsaturated ketone, to yield the final product **1.68**. A rare example of iridium undergoing similar rearrangements has also been reported.³¹

Scheme 1.14. Multiple functionalizations via Rh catalysis.

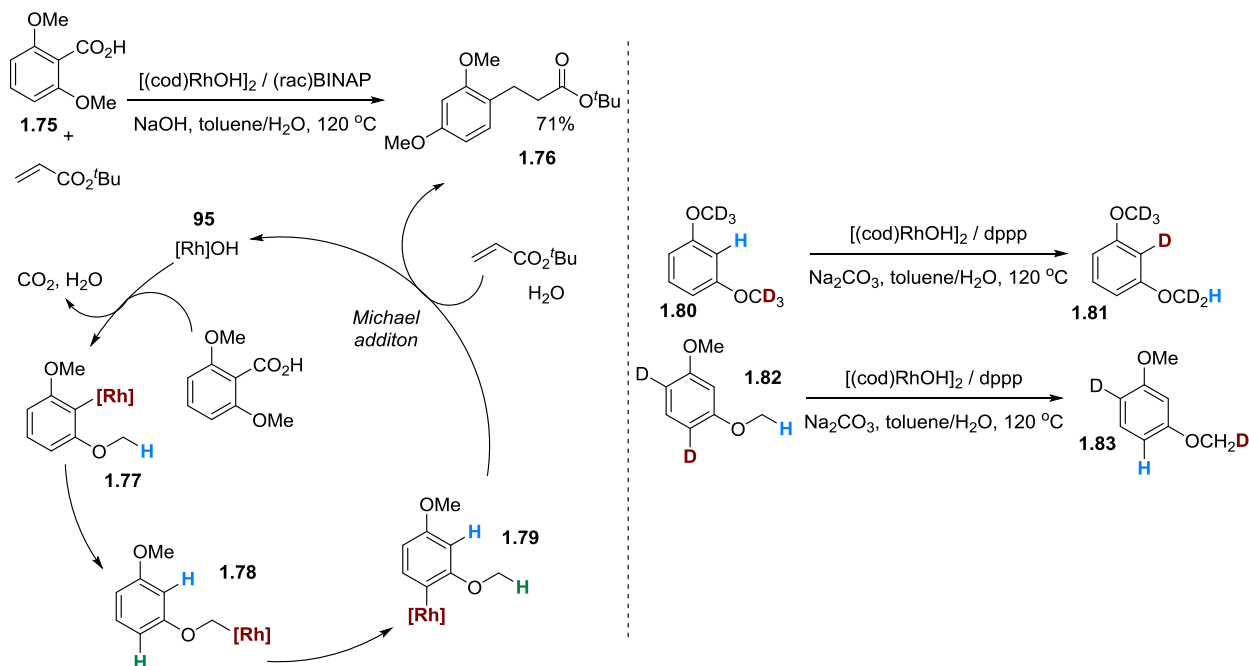
Most instances of metal 1,4-rearrangements occurring via addition of an aryl-metal across the π -bond of an alkyne, followed by subsequent rearrangement to a new aryl-metal species, involve rhodium or iridium (and a few other 2nd- or 3rd-row transition metals).^{25,31} However, the base metal cobalt is also capable of participating in 1,4-rearrangements.³² As illustrated in Scheme 1.15, transmetalation of an aryl-zinc species to cobalt forms an aryl-

cobalt **1.71** that adds across the π -bond of the alkyne. Intermediate **1.72** undergoes a 1,4-rearrangement to form **1.73**, followed by transmetalation with another equivalent of aryl-zinc to form the new aryl-zinc **1.74** and regenerate the catalyst. In the presence of an added electrophile, the aryl-zinc forms a highly functionalized aromatic product. While the mechanism of this rearrangement has not been studied, it is likely to proceed via a different mechanism than the oxidative insertion/reductive elimination pathways exhibited by 2nd and 3rd-row transition metals.

Scheme 1.15. Co-catalyzed addition of arylzinc to alkynes with 1,4-rearrangement to reform an arylzinc.



Successive 1,4-dyotropic-like rearrangements can give rise to formal 1,3-rearrangements.³³ Scheme 1.16 illustrates the Rh-catalyzed decarboxylation of an ortho methoxy benzoic acid to yield an ArRh species **1.77**. A 1,4-rearrangement of **1.77** with one of the ethereal protons is followed by a successive 1,4-rearrangement to place the Rh back on the aromatic ring. The result is a formal 1,3-rearrangement process, where Rh ends up at a carbon meta to its starting position. The proposed mechanism is supported by deuterium labeling of both the methyl ether and the aromatic ring (Scheme 1.16, right). When the methyl group is labeled, the deuterium is incorporated into the aromatic at the position where rhodium was initially bound. When the aromatic ring is labeled, the deuterium is incorporated into the methyl group. While this is an indirect strategy for achieving 1,3-rearrangements, until recently, catalytic examples of direct 1,3-rearrangement were not known. We are currently investigating a unique copper-catalyzed 1,3-dyotropic rearrangement achieved by coupling substituted 2-bromostyrenes with pinacol borane (HBpin) using a copper(I)-hydride as the catalyst (see chapters 2-4).

Scheme 1.16. Formal 1,3-rearrangement via sequential 1,4-rearrangements.

1.4. Conclusions and Outlook

This chapter presents a number of examples of stoichiometric and catalytic organometallic reactions that involve formal Type I dyotropic rearrangements, which we have defined as any rearrangement involving the interchange of two groups *via* the breaking and reforming of two σ bonds. These reactions vary widely in terms of the overall transformation that is taking place, the number of atoms across which the migrating groups interchange, the metal involved, and whether the metal acts as the migrating group or as part of the stationary scaffold. The mechanisms of interchange also vary substantially. While many of these reactions proceed through oxidative insertion/reductive elimination mechanisms, others involve no oxidation state change at the metal or proceed *via* a radical mechanism. A few such rearrangements proceed in a concerted fashion; however, most occur by a stepwise mechanism. Additionally, the driving force behind most of these reactions is not clear.

In spite of the recent growth in transition metal catalyzed reactions that proceed through dyotropic rearrangements, there is much potential for further development. For instance, while there are several examples of 1,4-rearrangements in which a metal interchanges positions with a hydrogen, there are fewer examples of 1,2- and 1,3-rearrangements or examples of groups other than hydrogen participating in the migration. Additionally, the factors that promote these unusual rearrangements are, for the most part, still unclear. A clearer mechanistic

understanding of formal dyotropic rearrangements would lead to the development of new and synthetically useful transformations.

1.5 Bibliography

1. *Applications of Transition Metal Catalysis in Drug Discovery and Development: An Industrial Perspective* (Eds.: M. L. Crawley, B. M. Trost), Wiley, Hoboken, **2012**.
2. a) Cai, X. H.; Xie, B. *Synthesis-Stuttgart* **2015**, *47*, 737-759; b) Wasa, M.; Engle, K. M.; Yu, J.-Q. *Isr. J. Chem.* **2010**, *50*, 605-616. c) Kuhl, N.; Schroeder, N.; Glorius, F. *Adv. Synth. Catal.* **2014**, *356*, 1443-1460. d) Fischer, C.; Koenig, B. *Beilstein J. Org. Chem.* **2011**, *7*, 59-74. e) Lennox, A. J. J.; Lloyd-Jones, G. C. *Chem. Soc. Rev.* **2014**, *43*, 412-443.
3. a) *Handbook of Organopalladium Chemistry for Organic Synthesis* (Eds.: E. Negishi, A. de Meijere), Wiley, New York, **2002**; b) *Metal-Catalyzed Cross-Coupling Reactions, Second Edition* (Eds.: A. de Meijere, F. Diederich), Wiley-VCH, Weinheim, **2008**.
4. a) Sambiagio, C.; Marsden, S. P.; Blacker, A. J.; McGowan, P. C. *Chem. Soc. Rev.* **2014**, *43*, 3525-3550. b) Engelin, C. J.; Fristrup, P. *Molecules* **2011**, *16*, 951-969. c) Karak, M.; Barbosa, L. C. A.; Hargaden, G. C. *RSC Adv.* **2014**, *4*, 53442-53466.
5. a) Fernandez, I.; Cossio, F. P.; Sierra, M. A. *Chem. Rev.* **2009**, *109*, 6687-6711. b) Reetz, M. T. *Angew. Chem. Int. Ed.* **1972**, *11*, 129-130; *Angew. Chem. Int. Ed.* **1972**, *11*, 130-131. c) Gridnev, I. D. *Coord. Chem. Rev.* **2008**, *252*, 1798-1818. d) Davis, R. L.; Tantillo, D. J. *J. Org. Chem.* **2010**, *75*, 1693-1700. e) Gutierrez, O.; Tantillo, D. J. *J. Org. Chem.* **2012**, *77*, 8845-8850. f) Reetz, M. T. *Adv. Organomet. Chem.* **1977**, *16*, 33-65.
6. a) Fernandez, I.; Bickelhaupt, F. M.; Cossio, F. P. *Chem. Eur. J.* **2012**, *18*, 12395-12403. b) Fernandez, I.; Sierra, M. A.; Cossio, F. P. *Chem. Eur. J.* **2006**, *12*, 6323-6330.
7. Kocienski, P.; Barber, C. *Pure Appl. Chem.* **1990**, *62*, 1933-1940.
8. a) Denichoux, A.; Debien, L.; Cyldinsky, M.; Kaci, M.; Chemla, F.; Ferreira, F.; Perez-Luna, A. *J. Org. Chem.* **2013**, *78*, 134-145. b) Erker, G.; Petrenz, R. *J. Chem. Soc., Chem. Commun.* **1989**, 345-346. c) Ward, A. S.; Mintz, E. A.; Kramer, M. P. *Organometallics* **1988**, *7*, 8-12.

9. a) Gais, H.-J.; Rao, C. V.; Loo, R. *Chem. Eur. J.* **2008**, *14*, 6510-6528. b) Black, F. J.; Kocienski, P. J. *Org. Biomol. Chem.* **2010**, *8*, 1188-1193. c) Jarowicki, K.; Kocienski, P.; Komsta, Z.; Wojtasiewicz, A. *Synthesis-Stuttgart* **2012**, *44*, 946-952.
10. a) Rijs, N. J.; Yates, B. F.; O'Hair, R. A. J. *Chem. Eur. J.* **2010**, *16*, 2674-2678. b) Rijs, N. J.; O'Hair, R. A. *J. Organometallics* **2010**, *29*, 2282-2291.
11. Choi, J.; Wang, D. Y.; Kundu, S.; Choliy, Y.; Emge, T. J.; Krogh-Jespersen, K.; Goldman, A. S. *Science* **2011**, *332*, 1545-1548.
12. a) Fernandez, I.; Sierra, M. A.; Jose Mancheno, M.; Gomez-Gallego, M.; Cossio, F. P. *Eur. J. Inorg. Chem.* **2008**, 2454-2462. b) Sierra, M. A.; Fernandez, I.; Mancheno, M. J.; Gomez-Gallego, M.; Torres, M. R.; Cossio, F. P.; Arrieta, A.; Lecea, B.; Poveda, A.; Jimenez-Barbero, J. *J. Am. Chem. Soc.* **2003**, *125*, 9572-9573. c) Fernandez, I.; Sierra, M. A.; Gomez-Gallego, M.; Mancheno, M. J.; Cossio, F. P. *Angew. Chem. Int. Ed.* **2006**, *45*, 125-128.
13. Uhl, W.; Bohnemann, J.; Layh, M.; Wuerthwein, E.-U. *Chem. Eur. J.* **2014**, *20*, 8771-8781.
14. Ikeda, Y.; Takano, K.; Kodama, S.; Ishii, Y. *Organometallics* **2014**, *33*, 3998-4004.
15. a) Ikeda, Y.; Takano, K.; Waragai, M.; Kodama, S.; Tsuchida, N.; Takano, K.; Ishii, Y. *Organometallics* **2014**, *33*, 2142-2145. b) Takano, K.; Ikeda, Y.; Kodama, S.; Ishii, Y. *Chem. Commun.* **2015**, *51*, 4981-4984. c) Ikeda, Y.; Takano, K.; Kodama, S.; Ishii, Y. *Chem. Commun.* **2013**, *49*, 11104-11106. d) Werle, C.; Le Goff, X.-F.; Djukic, J.-P. *J. Organomet. Chem.* **2014**, *751*, 754-759. e) Keen, A. L.; Doster, M.; Johnson, S. A. *J. Am. Chem. Soc.* **2007**, *129*, 810-819.
16. For examples of 1,4-rearrangements with palladium and rhodium, see also: a) Ma, S. M.; Gu, Z. H. *Angew. Chem. Int. Ed.* **2005**, *44*, 7512-7517. b) Zhao, J.; Campo, M.; Larock, R. C. *Angew. Chem. Int. Ed.* **2005**, *44*, 1873-1875. c) Tobisu, M.; Hyodo, I.; Onoe, M.; Chatani, N. *Chem. Commun.* **2008**, 6013-6015. d) Wang, L.; Pan, Y.; Jiang, X.; Hu, H. *Tetrahedron Lett.* **1999**, *41*, 725-727. e) Matsuda, T.; Suda, Y.; Takahashi, A. *Chem. Commun.* **2012**, *48*, 2988-2990. f) Piou, T.; Bunescu, A.; Wang, Q.; Neuville, L.; Zhu, J. *Angew. Chem. Int. Ed.* **2013**, *52*, 12385-12389. g) Kesharwani, T.; Verma, A. K.; Emrich, D.; Ward, J. A.; Larock, R. C. *Org. Lett.* **2009**, *11*, 2591-2593.
17. For biaryl palladium examples, see also: a) Karig, G.; Moon, M. T.; Thasana, N.; Gallagher, T. *Org. Lett.* **2002**, *4*, 3115-3118. b) Campo, M. A.; Zhang, H.; Yao, T.; Ibdah, A.; McCulla, R. D.; Huang, Q.; Zhao, J.;

- Jenks, W. S.; Larock, R. C. *J. Am. Chem. Soc.* **2007**, *129*, 6298-6307. c) Singh, A.; Sharp, P. R. *J. Am. Chem. Soc.* **2006**, *128*, 5998-5999. d) Masselot, D.; Charmant, J. P. H.; Gallagher, T. *J. Am. Chem. Soc.* **2006**, *128*, 694-695. e) Campo, M. A.; Larock, R. C. *J. Am. Chem. Soc.* **2002**, *124*, 14326-14327.
18. a) Barder, T. E.; Walker, S. D.; Martinelli, J. R.; Buchwald, S. L. *J. Am. Chem. Soc.* **2005**, *127*, 4685-4696. b) Pan, J.; Su, M.; Buchwald, S. L. *Angew. Chem. Int. Ed.* **2011**, *50*, 8647-8651.
19. Dyker, G. *Angew. Chem. Int. Ed.* **1994**, *33*, 103-105.
20. For examples where beta-hydride elimination is observed, see also: a) Baudoin, O.; Herrbach, A.; Gueritte, F. *Angew. Chem. Int. Ed.* **2003**, *42*, 5736-5740. b) Hitce, J.; Retailleau, P.; Baudoin, O. *Chem. Eur. J.* **2007**, *13*, 792-799.
21. Oguma, K.; Miura, M.; Satoh, T.; Nomura, M. *J. Am. Chem. Soc.* **2000**, *122*, 10464-10465.
22. Oguma, K.; Miura, M.; Satoh, T.; Nomura, M. *J. Organomet. Chem.* **2002**, *648*, 297-301.
23. Catellani, M.; Frignani, F.; Rangoni, A. *Angew. Chem. Int. Ed.* **1997**, *1-2*, 119-122.
24. Hayashi, T.; Inoue, K.; Taniguchi, N.; Ogasawara, M. *J. Am. Chem. Soc.* **2001**, *123*, 9918-9919.
25. For examples of 1,4-rhodium rearrangements in cyclizations, see also: a) Shintani, R.; Hayashi, T. *Org. Lett.* **2005**, *7*, 2071-2073. b) Shintani, R.; Okamoto, K.; Hayashi, T. *J. Am. Chem. Soc.* **2005**, *127*, 2872-2873. c) Shintani, R.; Takatsu, K.; Hayashi, T. *Angew. Chem. Int. Ed.* **2007**, *46*, 3735-3737. d) Shintani, R.; Takatsu, K.; Katoh, T.; Nishimura, T.; Hayashi, T. *Angew. Chem. Int. Ed.* **2008**, *47*, 1447-1449.
26. 1,4-palladium shifts have also been observed in cyclizations. See also: a) Dyker, G. *Angew. Chem. Int. Ed. in Engl.* **1992**, *31*, 1023-1025; *J. Org. Chem.* **1993**, *58*, 6426-6428; *Chem. Ber.* **1994**, *127*, 739-742. b) Zhao, J.; Yue, D.; Campo, M. A.; Larock, R. C. *J. Am. Chem. Soc.* **2007**, *129*, 5288-5295. c) Lee, H. J.; Kim, K. H.; Kim, S. H.; Kim, J. N. *Tetrahedron Lett.* **2013**, *54*, 170-175. d) Zhao, J.; Larock, R. C. *J. Org. Chem.* **2006**, *71*, 5340-5348. e) Huang, Q. H.; Fazio, A.; Dai, G. X.; Campo, M. A.; Larock, R. C. *J. Am. Chem. Soc.* **2004**, *126*, 7460-7461. f) Campo, M. A.; Huang, Q. H.; Yao, T. L.; Tian, Q. P.; Larock, R. C. *J. Am. Chem. Soc.* **2003**, *125*, 11506-11507. g) Tian, Q. P.; Larock, R. C. *Org. Lett.* **2000**, *2*, 3329-3332. h) Larock, R. C.; Tian, Q. P. *J. Org. Chem.* **2001**, *66*, 7372-7379.
27. For examples of 1,4-rhodium shifts in ring expansions, see also: a) Matsuda, T.; Shigeno, M.; Murakami, M. *J. Am. Chem. Soc.* **2007**, *129*, 12086-12087. b) Lambert, J.; Hergenroeder, R.; Suter, D.; Deckert, V.

- Angew. Chem. Int. Ed.* **2009**, *48*, 6343-6345. c) Shigeno, M.; Yamamoto, T.; Murakami, M. *Chem. Eur. J.* **2009**, *15*, 12929-12931. d) Seiser, T.; Cramer, N. *Angew. Chem. Int. Ed.* **2010**, *49*, 10163-10167.
28. Miura, T.; Sasaki, T.; Nakazawa, H.; Murakami, M. *J. Am. Chem. Soc.* **2005**, *127*, 1390-1391.
29. Shintani, R.; Isobe, S.; Takeda, M.; Hayashi, T. *Angew. Chem. Int. Ed.* **2010**, *49*, 3795-3798.
30. a) Sasaki, K.; Hayashi, T. *Tetrahedron-Asymmetry* **2012**, *23*, 373-380. b) Sasaki, K.; Nishimura, T.; Shintani, R.; Kantchev, E. A. B.; Hayashi, T. *Chem. Sci.* **2012**, *3*, 1278-1283.
31. Partridge, B. M.; Gonzalez, J. S.; Lam, H. W. *Angew. Chem. Int. Ed.* **2014**, *53*, 6523-6527.
32. a) Tan, B.-H.; Dong, J.; Yoshikai, N. *Angew. Chem. Int. Ed.* **2012**, *51*, 9610-9614. b) Wu, B.; Yoshikai, N. *Angew. Chem. Int. Ed.* **2013**, *52*, 10496-10499.
33. Zhang, J.; Liu, J.-F.; Ugrinov, A.; Pillai, A. F. X.; Sun, Z.-M.; Zhao, P. *J. Am. Chem. Soc.* **2013**, *135*, 17270-17273.

Chapter 2: Cu(I)-catalyzed Recycling of a Halogen Activating Groups via 1,3-Halogen Migration

Reproduced with permission from Grigg, R. D.; Van Hoveln, R.; Schomaker, J. *J. Am. Chem. Soc.* **2012**, *134*,

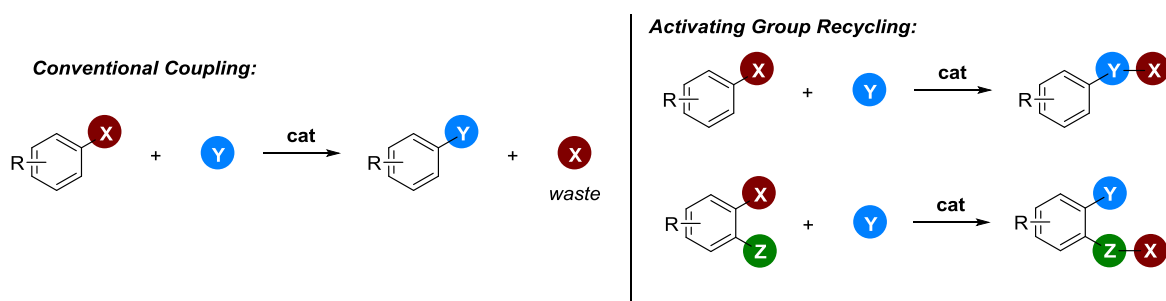
16131-16134. Copyright 2012 American Chemical Society.

2.1 Introduction to Activating Group Recycling

The ability to functionalize aromatic rings is an important tool in a synthetic organic chemist's repertoire.¹ Typically, activating groups such as aryl halides or pseudohalides are used to provide reliable regioselectivity (Scheme 2.1, left). However, using an activating group means these transformations have less-than-ideal atom economy, as only one new bond is formed at the expense of the activating group which is lost as waste. Furthermore, installation of the activating group can require multiple steps, making it a valuable functional group in terms of labor and cost. Direct C-H functionalization eliminates the need for pre-activation, yet the stoichiometric or super-stoichiometric additives necessary for many of these reactions means that this approach can also be wasteful.² Although important advances have been made towards more practical and general directing groups for C-H functionalization,³ the use of halide or pseudohalide activating groups remains the most convenient and commonly-used route to aryl functionalization. A more attractive use of activating groups might be to "recycle" the halide by reincorporating it into the product so that it could be used in further functionalizations.⁴

Conventional arene functionalization utilizes a range of transition metal catalysts and coupling partners to transform aryl-X bonds into new carbon-carbon or carbon-heteroatom bonds, as represented by C-Y in Scheme 2.1. Generally, activating group recycling falls into two broad types (Scheme 2.1, right). The first category is when the coupling partner, Y, is formally inserted into the aryl-X bond. Thus, the activating group is retained for further functionalization. The other broad category is when the activating group is transferred to an adjacent functional group during the course of the reaction. In this case, the C-X bond is transformed into a C-Y bond with concomitant formation of a new Z-X bond. In both cases, there is no net loss of functionality. In other words, a functional group is not sacrificed for a new bond, but rather the final product retains the functionality of both coupling partners.

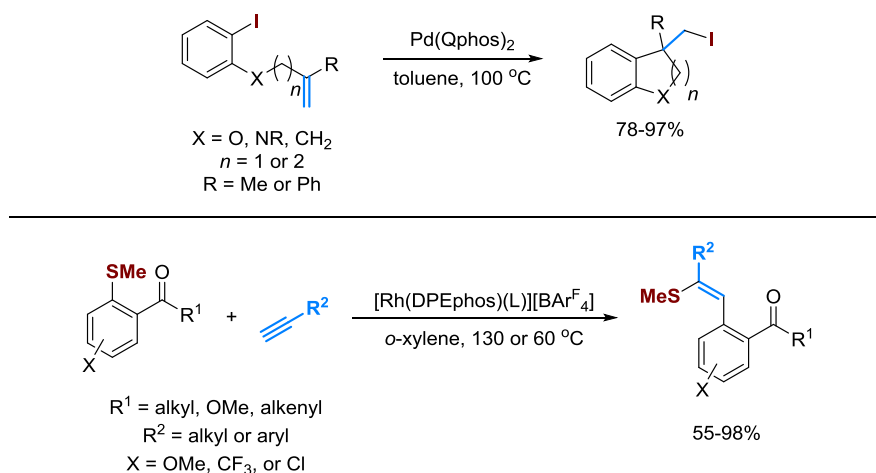
Scheme 2.1. New mode of arene functionalization vs. traditional cross-coupling approach.



2.1.1 Recent Examples of Activating Group Recycling

Lautens and Willis have pioneered the area of activating group recycling. In 2011, Lautens reported an intramolecular palladium-catalyzed carbo-iodination/cyclization (Scheme 2.2, top).^{4a} In this reaction, presumably, the Pd undergoes oxidative insertion into the carbon-iodide bond, then, after carbopalladation of the alkene, undergoes reductive elimination to regenerate the catalyst and produce the product. For this reaction, it was important that the alkene did not have any β -hydrogens to prevent β -hydride elimination. In 2012, Willis reported an intermolecular rhodium-catalyzed carbothiolation of alkynes (Scheme 2.2, bottom).^{4b} The mechanism of this transformation follows one rather similar to Lautens' carboiodination.

Scheme 2.2. Examples of activating group recycling.



Both of these examples are the first type of activating group recycling in which the coupling partner is formally inserted into the aryl-activating group bond. In the Lautens example, the alkene is inserted into the carbon-iodine bond and in the Willis example, the alkyne is inserted into the aryl-sulfur bond. The work described herein reports a methodology in which the second type of activating group recycling is used; the activating group is transferred to a neighboring functional group.

2.2 Optimization of Copper(I)-catalyzed 1,3-Halogen Migration

This work arose from our attempts to prepare **2.3** from **2.1** using a reported CuCl/dppbz catalyst (Table 2.1, entry 1).⁵ While none of the desired hydroboration was noted, due mainly to polymerization of the styrene, we observed small amounts of an unexpected byproduct **2.2**, in which the halogen had undergone a 1,3-migration. Curious as to

whether **2.2** might be obtained exclusively, we undertook an investigation of several mono- and bidentate ligands for CuCl (Table 2.1).

Table 2.1. Initial ligand screen.

9 mol% CuCl
9 mol% ligand
18 mol% KO^tBu
THF, 40 °C, 18 h

		2.1			2.2			2.3		
entry	ligand	2.1	2.2	2.3	entry	ligand	2.1	2.2	2.3	
1	dppbz	<10%	<10%	0%	7	dppb	68%	0%	0%	
2	PPh ₃	50%	0%	0%	8	dppf	0%	0%	0%	
3	PCy ₃	60%	0%	29%	9	phen	94%	0%	0%	
4	dppm	51%	0%	41%	10	Xantphos	1%	0%	72%	
5	dppe	30%	0%	0%	11	DPEphos	42%	0%	0%	
6	dppp	19%	0%	0%	12	dCype	0%	70%	0%	

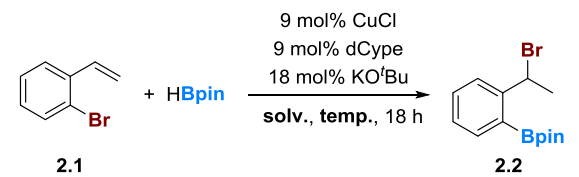
Xantphos

dCype

NMR yield determined using 1,1,1,2-tetrachloroethane as the internal standard

These preliminary studies revealed that neither monodentate phosphine ligands (Table 2.1, entries 2, 3) or electron-poor bidentate ligands (entries 4-8) were capable of promoting the desired reaction. Often, mass balance of the reaction was quite low due to polymerization of the starting material. Phenanthroline (entry 9) gave only recovered starting material. Interestingly, the *trans*-spanning Xantphos ligand (entry 10) gave exclusively the hydroboration product **2.3** in 72% yield, while a similar DPEphos ligand (entry 11) gave no **2.2** or **2.3**. Finally, we found that the electron-rich and bulky bidentate phosphine ligand, bis(dicyclohexylphosphino)ethane (dCype, entry 12), exclusively promoted the desired 1,3-halogen migration.⁶

Further reaction optimization was undertaken using the dCype ligand (Table 2.2). Etheral solvents such as THF and dioxane (entries 1 and 2) proved superior to toluene, CH₂Cl₂, Et₂O, CH₃CN and CHCl₃ (entries 3-7). Lowering the temperature to 40 °C (entry 8) did not increase the yield of the desired product compared to entry 1, but did improve the mass balance. Finally, scaling the reaction to 5.0 mmol (entry 9) reproducibly increased the yield to 94% of **2.2**.

Table 2.2. Optimization of the reaction conditions.


entry	solvent	temperature	2.1	2.2
1	THF	70	2%	73%
2	dioxane	70	0%	68%
3	toluene	70	0%	41%
4	CH ₂ Cl ₂	70	6%	54%
5	Et ₂ O	70	3%	40%
6	CH ₃ CN	70	2%	0%
7	CHCl ₃	70	12%	0%
8	THF	40	27%	60%
9	THF	40	0%	94%

NMR yields determined by using 1,1,1,2-tetrachloroethane as an internal standard.

2.3 Scope of 1,3-Halogen Migration

The scope of the reaction was explored (Table 2.3). In general, 1,3-bromine migration was favored throughout a variety of substrates (migration products **numbered in dark red**). However, placing electron-withdrawing halogen groups *meta* to the olefin (entries 2 and 3) diminished the 1,3-halogen migration and resulted in significant hydroboration (hydroboration products **numbered in blue**). Other groups at this position favored migration. Curiously, if a bromine (entry 8) was placed *para* to the olefin, no reaction occurred. Neutral and electron-donating substituents F, Ph, ^tBu and OMe (entries 9-12) *para* to the olefin yielded predominantly the 1,3-halogen migration products. For the latter three cases, the benzyl bromide products were too sensitive for purification and thus trapped with propargyl alcohol prior to isolation. Consistent with prior observations,^{5a} the 4-methoxy substrate (entry 12) reacted slowly. Finally, substitution on the β carbon of the styrene (entry 13) was tolerated in the 1,3-halogen migration, as *trans*-β-methylstyrene **2.16** gave **2.28** in 75% yield. Although 2-chlorostyrene did not undergo halogen migration, it was found that 2-iodostyrene did produce the migration product in 59% yield, although only 79% conversion was observed. The sensitive benzyl iodide had to be trapped with propargyl alcohol. Reactivity

was also examined for 2-bromo-3-methylstyrene and 2-bromo-6-methylstyrene. For these highly sterically-encumbered substrates, minimal conversion was observed.

Table 2.3. Substrate scope of 1,3-halogen migration.

9 mol% CuCl
9 mol% dCype
18 mol% KO^tBu
THF, 40 °C, 18 h

entry	substrate	% yield		entry	substrate	% yield	
1		94% 2.2	0% 2.3	7		87% 2.22	0% 2.34
2		57% 2.17	31% 2.29	8		0% 2.23	0% 2.35
3		49% 2.18	28% 2.30	9		89% 2.24	0% 2.36
4		73% 2.19	0% 2.31	10		66% 2.25^a	12% 2.37
5		69% 2.20^a	0% 2.32	11		65% 2.26^a	0% 2.38
6		67% 2.21	0% 2.33	12		36% 2.27^a	0% 2.39
				13		75% 2.28	0% 2.40

^a The product was trapped with propargyl alcohol prior to isolation.

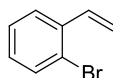
2.4 Conclusions

In conclusion, Cu(I) promotes a cascade 1,3-halogen migration/borylation/functionalization that proceeds under mild conditions to reincorporate the bromine activating group. This methodology provides a complement to the activating group methodologies currently reported in the literature insofar as all other methods formally insert the coupling partner into the aryl-activating group bond, whereas this methodology transfers the activating group to a neighboring functional group. This work provides a first generation catalyst system for 1,3-halogen migration that

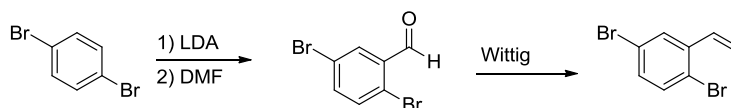
will be expanded on to include asymmetric halogen transfer, mechanistic study and expanding the coupling partners to a wide range of electrophiles (see Chapters 3 and 4).

2.5 Experimental Details

2.5.1 Synthesis of Styrene Starting Materials

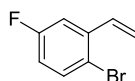


Compound 2.1. To a vigorously stirred slurry of methyltriphenylphosphonium iodide (20.0 g, 49.4 mmol, 1.15 equiv) in 400 mL of THF at 0 °C was added 24.0 mL of *n*BuLi (2.0 M, 48 mmol, 1.12 equiv). The reaction is allowed to stir for approximately 15 min and then 2-bromobenzaldehyde (5.0 mL, 42.8 mmol) was added dropwise. After an additional 15 min, the ice bath was removed and the reaction was allowed to stir for 2 h. The reaction was extracted with EtOAc (200 mL) and water (200 mL). The aqueous layer was washed with one 200 mL portion of EtOAc and 50 mL of silica gel was added to the combined organics. The mixture was concentrated *in vacuo* to yield a slurry which was poured on top of a pad of silica gel and eluted with 500 mL of hexanes. The hexanes were concentrated *in vacuo* and the resulting yellow oil purified by column chromatography using 100% hexanes as an eluent. The styrene was isolated as a clear, colorless oil in 60% yield. The characterization data was consistent with that obtained from a commercially available sample.

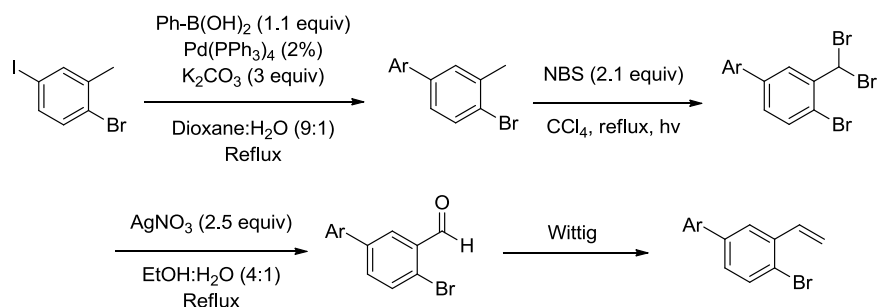


Compound 2.4.⁷ To a flame-dried, three-neck, 500 mL round bottom flask equipped with two septa and an addition funnel was added 150 mL THF and diisopropylamine (16.0 mL, 113.4 mmol, 1.13 equiv) under an atmosphere of nitrogen. The flask was cooled to 0 °C in an ice bath and *n*BuLi (44 mL, 2.5M, 110 mmol, 1.10 equiv) was slowly added. The flask was cooled to -84 °C using an EtOAc/*N*₂ slurry. If the temperature rose much higher than -80 °C, the reaction darkened in color and yielded an intractable mixture of products. The 1,4-dibromobenzene (24.0 g, 100.3 mmol) was dissolved in 100 mL THF and added *via* an addition funnel over a period of 5 min. The reaction mixture was allowed to stir for 45 min while a temperature of -84 °C was carefully maintained. Dimethylformamide (13.0 mL, 167.9 mmol, 1.67 equiv) was then added and the cold bath was removed. After 3 h, 150 mL of 1 M HCl and 100 mL of diethyl ether was added and the phases separated. The aqueous layer was extracted with 2 x 100 mL

portions of ether, the combined organics dried with Na_2SO_4 and concentrated *in vacuo*. The solid residue was recrystallized from hexanes/EtOAc and the filtrate concentrated to yield a second crop crystals. The product was isolated as long, pale yellow crystals in 42% overall yield. The desired **2.4** was prepared this aldehyde according to the same procedure described for the preparation of **2.1**. The product was isolated as a clear, colorless oil and the characterization data was consistent with literature values.⁸



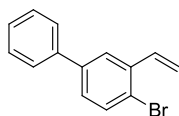
Compound 2.5. The desired product was prepared from 2-bromo-5-fluorobenzaldehyde in a fashion similar to that employed for the synthesis of **2.1**. The product was isolated as a clear, colorless oil and the characterization data was consistent with literature values.⁹



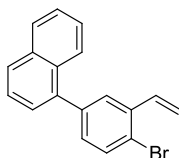
Preparation of styrenes 2.6, 2.7, and 2.8. In the representative procedure, the 2-bromo-5-iodotoluene (5.94 g, 20.0 mmol, 1.0 equiv) was placed in a 100 mL roundbottom flask containing the desired aryl boronic acid (21.0 mmol, 1.05 equiv), K_2CO_3 (8.30 g, 60.0 mmol, 3 equiv), and $\text{Pd}(\text{PPh}_3)_4$ (0.69 g, 0.60 mmol, 0.03 equiv). The flask was placed under a N_2 atmosphere and 50 mL of N_2 -sparged dioxane:water (9:1) was added. The solution was allowed to reflux overnight. After cooling, the reaction mixture was carefully quenched with saturated NaHCO_3 and extracted with three portions of EtOAc. Concentration and purification of the residue by column chromatography (hexanes eluent) afforded the biphenyl, which was immediately used in the bromination, as described below.

The biphenyl was treated with N-bromosuccinimide (NBS, 2.1 equiv) in CCl_4 . The reaction was allowed to reflux under heating by a UV lamp for 3 h, or until TLC indicated consumption of the NBS. The solution was cooled, filtered to remove the by-product succinimide and the filtrate concentrated to a crude oil. The oil was immediately dissolved in EtOH, treated with AgNO_3 (2.5 equiv) in H_2O (4:1 EtOH: H_2O) and the resulting slurry allowed to

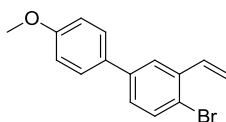
reflux for 1 h. The suspension was filtered through a pad of celite, concentrated to half volume and diluted with water/EtOAc. The organic phase was separated and the aqueous extracted with EtOAc (3 x 20 mL). The combined organics were washed with brine (50 mL), dried with MgSO₄ and concentrated to a crude solid. This material could be purified by either column chromatography or by recrystallization from hexanes. The desired aldehydes were generally isolated in 50-60% yield over the 2 steps, and were used immediately in the Wittig olefination, as described for the synthesis of **2.1**. In this fashion, the styrenes **2.6**, **2.7**, and **2.8** were prepared from 2-bromo-4-phenylbenzaldehyde as clear, colorless oils.



Compound 2.6. The product was isolated in 83% yield as a clear, colorless oil. ¹H NMR (300 MHz, CDCl₃) δ 7.74 (d, *J* = 2.3 Hz, 1H), 7.54-7.63 (m, 3H), 7.30-7.48 (m, 4H), 7.10 (dd, *J* = 17.5, 11.0 Hz, 1H), 5.77 (dd, *J* = 17.5, 1.0 Hz, 1H), 5.40 (dd, *J* = 11.0, 1.0 Hz, 1H). ¹³C NMR (75 MHz, CDCl₃) δ 140.7, 140.0, 137.7, 135.8, 133.2, 128.9, 127.8, 127.7, 127.0, 125.5, 122.6, 116.9. HRMS (EI) *m/z* calculated for C₁₄H₁₁Br [M]⁺ 258.0039, found 258.0037.



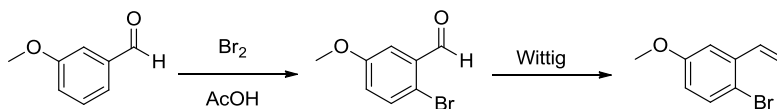
Compound 2.7. The product was isolated in 80% yield as a clear, colorless oil. ¹H NMR (300 MHz, CDCl₃) δ 7.82-7.93 (m, 3H), 7.67 (s, 1H), 7.66 (d, *J* = 5.5 Hz, 1H), 7.38-7.55 (m, 4H), 7.24 (dd, *J* = 8.1, 2.2 Hz, 1H), 7.14 (dd, *J* = 17.4, 10.9 Hz, 1H), 5.71 (dd, *J* = 17.4, 0.9 Hz, 1H), 5.38 (dd, *J* = 10.9, 0.9 Hz, 1H). ¹³C NMR (75 MHz, CDCl₃) δ 140.2, 138.9, 137.3, 135.6, 133.8, 132.7, 131.4, 130.7, 128.4, 128.3, 128.1, 126.8, 126.3, 125.9, 125.7, 125.3, 122.6, 117.0. HRMS (EI) *m/z* calculated for C₁₈H₁₃Br [M]⁺ 308.0196, found 308.0188.



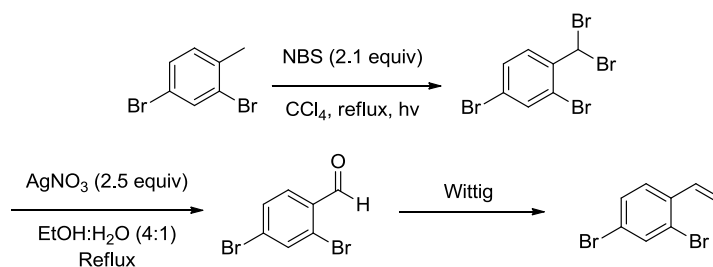
Compound 2.8. The compound was isolated in 91% yield as a clear, colorless oil. ¹H NMR (300 MHz, CDCl₃) δ 7.70 (d, *J* = 2.3 Hz, 1H), 7.57 (d, *J* = 8.4 Hz, 1H), 7.51 (d, *J* = 8.5 Hz, 2H), 7.29 (dd, *J* = 8.4, 2.3 Hz, 1H), 7.09 (dd, *J* = 17.5, 11.0 Hz, 1H), 6.98 (d, *J* = 8.5 Hz, 2H), 5.76 (d, *J* = 17.5 Hz, 1H), 5.40 (d, *J* = 11.0 Hz, 1H), 3.85 (s, 3H). ¹³C

NMR (75 MHz, CDCl_3) δ 159.4, 140.3, 137.6, 135.9, 133.1, 132.5, 128.0, 127.5, 125.0, 121.9, 116.8, 114.3, 55.4.

HRMS (EI) m/z calculated for $\text{C}_{15}\text{H}_{13}\text{BrO}$ $[\text{M}]^+$ 288.0145, found 288.0152.

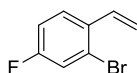


Compound 2.9.¹⁰ To a 250 mL roundbottom flask cooled in an ice bath was added 35 mL of acetic acid and *m*-anisaldehyde (5.0 mL, 41 mmol). Bromine (6.0 mL, 116.4 mmol, 2.8 equiv) in 11 mL acetic acid was added dropwise. After 15 min, the ice bath was removed and the reaction was allowed to stir for 16 h at rt. The reaction mixture was then poured into 250 mL of ice water, the resulting solid filtered off and filtrate washed with dichloromethane (3 x 50 mL). The solid was dissolved in the combined organics and the solution washed with saturated sodium bisulfite (2 x 100 mL). The organic layer was concentrated *in vacuo* to yield a pale yellow solid that was used without further purification. ^1H NMR (300 MHz, CDCl_3) δ 10.32 (s, 1H), 7.53 (d, J = 8.9 Hz, 1H), 7.42 (d, J = 3.2 Hz, 1H), 7.04 (dd, J = 8.9, 3.2 Hz, 1H), 3.85 (s, 3H). The styrene was then prepared from the aldehyde in a fashion similar to that described for the synthesis of **2.1**. The product was purified by vacuum distillation to yield a clear, colorless oil. ^1H NMR (300 MHz, CDCl_3) δ 7.43 (d, J = 8.6 Hz, 1H), 7.08 (d, J = 3.1 Hz, 1H), 7.02 (dd, J = 17.5, 10.9 Hz, 1H), 6.71 (dd, J = 8.9, 2.9 Hz, 1H), 5.69 (dd, J = 17.4, 1.0 Hz, 1H), 5.36 (dd, J = 10.9, 0.9 Hz, 1H), 3.81 (s, 3H). ^{13}C NMR (75 MHz, CDCl_3) δ 141.17, 120.34, 118.05, 115.59, 98.92, 97.45, 96.50, 94.11, 59.66, 59.24, 58.82, 37.65. HRMS (EI) for $\text{C}_9\text{H}_9\text{BrO}$ m/z calculated $[\text{M}]^+$ 211.9832, found 211.9836.

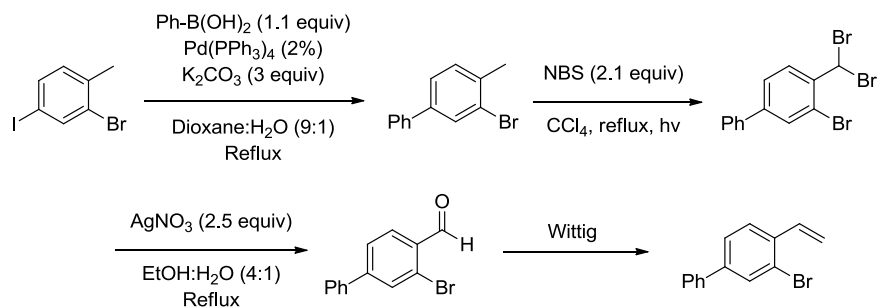


Compound 2.10. A solution of 2,4-dibromotoluene (3.75 g, 15.0 mmol) in 50 mL of CCl_4 was treated with NBS (5.61 g, 31.5 mmol, 2.1 equiv). The reaction was allowed to reflux under a UV lamp for 2 h, cooled and the resulting mixture filtered to remove succinimide. The filtrate was concentrated to a crude oil, which was immediately dissolved in 40 mL EtOH and treated with AgNO_3 (6.37 g, 37.5 mmol, 2.5 equiv) in 10 mL H_2O . The slurry was heated to reflux for 2 h, the resulting suspension filtered through a celite pad, concentrated to half

volume, and diluted with water and EtOAc. The organic phase was separated and the aqueous extracted with EtOAc (3 x 20 mL). The combined organics were washed with brine (50 mL), dried with MgSO₄ and concentrated to a crude solid, which could be purified by recrystallization from hexanes. The aldehyde was isolated in 70% yield over the 2 steps, and was used immediately for the subsequent Wittig olefination. The styrene **2.10** was prepared from the above 2,4-dibromobenzaldehyde in a fashion similar to that described for the synthesis of **2.1**. The product was isolated as a clear, colorless oil in 80% yield. ¹H NMR (300 MHz, CDCl₃) δ 7.71 (m, 1H), 7.40 (m, 2H), 6.97 (dd, *J* = 17.4, 11.0 Hz, 1H), 5.69 (dd, *J* = 17.4, 0.9 Hz, 1H), 5.38 (dd, *J* = 11.0, 0.9 Hz, 1H). ¹³C NMR (75 MHz, CDCl₃) δ 136.5, 135.1, 134.8, 130.7, 127.8, 124.0, 121.7, 117.3. HRMS (EI) *m/z* calculated for C₈H₆Br₂ [M]⁺ 259.8831, found 259.8842.

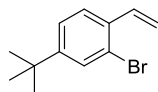


Compound 2.11. The styrene **2.11** was prepared from 2-bromo-4-fluorobenzaldehyde in a similar fashion to that described for the synthesis of **2.1**. The product was isolated as a clear, colorless oil. ¹H NMR (300.1 MHz, CDCl₃) δ 7.52 (dd, *J* = 8.7, 6.3 Hz, 1H), 7.30 (dd, *J* = 8.4, 2.4 Hz, 1H), 7.02 (td, *J* = 8.4, 3.0 Hz, 1H), 6.99 (dd, *J* = 17.4, 11.4 Hz, 1H), 5.64 (d, *J* = 17.8 Hz, 1H), 5.35 (d, *J* = 11.0 Hz, 1H). ¹³C NMR (75 MHz, CDCl₃) δ 246.0, 235.7, 233.4, 223.4, 218.2, 163.6, 160.3, 134.9, 134.0, 133.94, 127.9, 127.8, 123.7, 123.6, 120.2, 119.9, 116.6, 115.1, 114.9. HRMS (EI) C₈H₆BrF *m/z* calculated [M]⁺ 199.9632, found 199.9634.

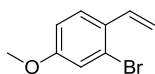


Compound 2.13. The aldehyde precursor was prepared by combining 2-bromo-4-iodotoluene (2.00 g, 6.74 mmol) in a 100 mL roundbottom flask with phenyl boronic acid (0.863 g, 7.08 mmol, 1.05 equiv), K₂CO₃ (2.79g, 20.2 mmol, 3.0 equiv) and Pd(PPh₃)₄ (0.23 g, 0.20 mmol, 0.03 equiv). The flask was placed under a N₂ atmosphere and 25 mL of N₂-sparged dioxane:water (9:1) was added. The solution was allowed to reflux overnight. After cooling, the reaction mixture was quenched with saturated NaHCO₃ and extracted with three portions of EtOAc. Removal of

the volatiles and purification of the residue by column chromatography (hexanes eluent) afforded the biphenyl in 76% yield, which was immediately used in the bromination. The biphenyl was treated with NBS (1.92 g, 10.8 mmol, 2.1 equiv) in 40 mL CCl_4 . The reaction was allowed to reflux under a UV lamp for 3 h, the solution cooled and the resulting succinimide removed by filtration. The filtrate was concentrated to a crude oil, which was immediately dissolved in 60 mL EtOH and treated with AgNO_3 (1.87 g, 11 mmol, 2.15 equiv) in 15 mL H_2O . The resulting slurry was refluxed for 1 h, the suspension filtered through a pad of celite, concentrated to half volume and diluted with water and EtOAc. The organic phase was separated and the aqueous extracted with EtOAc (3 x 20 mL). The combined organics were washed with brine (50 mL), dried with MgSO_4 and concentrated to a crude solid, which could be purified by recrystallization from hexanes. The aldehyde was isolated in 61% yield over the 2 steps, and was used immediately in the Wittig olefination. The styrene **2.13** was prepared from the 2-bromo-4-phenylbenzaldehyde in a fashion similar to that described for the synthesis of **2.1**. The product was isolated as a clear, colorless oil in 74% yield. ^1H NMR (300 MHz, CDCl_3) δ 7.79 (d, $J = 1.9$ Hz, 1H), 7.30-7.64 (m, 7H), 7.08 (dd, $J = 17.4, 10.9$ Hz, 1H), 5.74 (dd, $J = 17.4, 1.0$ Hz, 1H), 5.38 (dd, $J = 10.9, 1.0$ Hz, 1H). ^{13}C NMR (75 MHz, CDCl_3) δ 142.1, 139.2, 136.1, 135.3, 131.3, 128.9, 127.9, 126.9, 126.9, 126.1, 124.0, 116.6. HRMS (EI) m/z calculated for $\text{C}_{14}\text{H}_{11}\text{Br}$ $[\text{M}]^+$ 258.0039, found 258.0036.

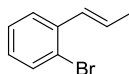


Compound 2.14. The styrene **2.14** was prepared from 2-bromo-4-*tert*-butyltoluene in a fashion similar to that described for the synthesis of **2.10**. The styrene was isolated as a clear colorless oil. ^1H NMR (300 MHz, CDCl_3) δ 7.54 (d, $J = 2.1$ Hz, 1H), 7.47 (d, $J = 8.2$ Hz, 1H), 7.28 (dd, $J = 8.2, 1.8$ Hz, 1H), 7.02 (dd, $J = 17.4, 10.9$ Hz, 1H), 5.65 (d, $J = 17.4$ Hz, 1H), 5.30 (d, $J = 10.9$ Hz, 1H), 1.29 (s, 9H). ^{13}C NMR (75 MHz, CDCl_3) δ 152.92, 135.75, 134.75, 130.00, 126.51, 124.91, 123.77, 116.08, 34.82, 31.32. HRMS (EI) m/z calculated for $\text{C}_{10}\text{H}_{15}\text{Br}$ $[\text{M}]^+$ 238.0352, found 238.0354.



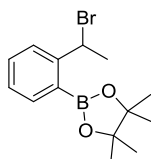
Compound 2.15. The styrene was prepared from 2-bromo-4-methoxybenzaldehyde¹¹ in a fashion similar to that described for the synthesis of **2.1**. The product was isolated as a clear, colorless oil in 86% yield. ^1H NMR (300 MHz, CDCl_3) δ 7.47 (d, $J = 8.7$ Hz, 1H), 7.09 (d, $J = 2.6$ Hz, 1H), 6.98 (dd, $J = 17.5, 11.0$ Hz, 1H), 6.84 (dd, $J = 8.7,$

2.6 Hz, 1H), 5.58 (dd, $J = 17.5, 1.1$ Hz, 1H), 5.24 (dd, $J = 11.0, 1.1$ Hz, 1H), 3.79 (s, 3H). ^{13}C NMR (75 MHz, CDCl_3) δ 159.6, 135.1, 130.0, 127.2, 123.9, 117.5, 114.5, 114.1, 55.5. HRMS (EI) m/z calculated for $\text{C}_9\text{H}_9\text{BrO} [\text{M}]^+$ 211.9832, found 211.9831.



(*E*)- β -methyl-2-bromostyrene 2.16.¹² To a round bottom flask charged with 80 mL of hexanes was added 3-pentanone (4.5 mL, 42.5 mmol, 1.0 equiv). To the stirred solution was added boron trifluoride diethyl etherate (5.5 mL, 43.4 mmol, 1.0 equiv) and then 2-bromobenzaldehyde (4.5 mL, 38.6 mmol). The reaction was refluxed for 1 h, cooled and quenched with 80 mL of water. The organic and aqueous layers were separated and the aqueous phase extracted with 80 mL of hexane. The combined organic layers were dried over Na_2SO_4 and concentrated *in vacuo*. The resulting black tar was purified by column chromatography using 100% hexanes as the eluent. The product was isolated as a clear, colorless oil in 30% yield. The characterization data was consistent with literature values.¹³

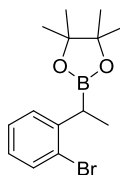
2.5.2 Procedure for the 1,3-Halogen Migration Reaction



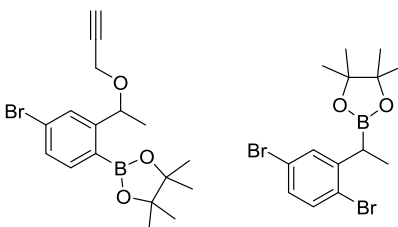
Compound 2.2. In a glovebox, CuCl (44.5 mg, 0.45 mmol, 0.09 equiv), 1,2-bis(dicyclohexylphosphino)ethane (190 mg, 0.45 mmol, 0.09 equiv) and potassium *tert*-butoxide (101 mg, 0.90 mmol, 0.18 equiv) were added to a 50 mL roundbottom flask. The flask was charged with 10 mL of dry, degassed THF, fitted with a septum and removed from the glovebox. The mixture was allowed to stir at ambient temperature for approximately 10 min. A portion of 4,4,5,5-tetramethyl-1,3,2-dioxaborolane (0.87 mL, 6.0 mmol, 1.2 equiv) was added and the reaction was allowed to stir for an additional 10 min. An aliquot of 2-bromostyrene (0.63 mL, 4.97 mmol) was added to the reaction and the flask moved to an oil bath preset to 40 °C. The mixture was stirred for 18 h, cooled, filtered through a pad of celite and washed with 50 mL of diethyl ether. The filtrate was concentrated *in vacuo* and the organic residue was purified by column chromatography using an isocratic 10:1 hexanes:EtOAc mobile phase. The product was isolated in 94% yield as a clear, colorless, viscous oil. ^1H NMR (300.1 MHz, CDCl_3) δ 7.78 (dd, $J = 7.4, 1.5$ Hz, 1H), 7.68 (d, $J = 7.9$ Hz, 1H), 7.44 (td, $J = 7.4, 1.0$ Hz, 1H), 7.24 (td, $J = 7.2, 1.0$ Hz, 1H), 6.26 (q, $J = 7.1$ Hz, 1H), 2.02 (d, $J = 7.0$

Hz, 3H), 1.36 (s, 6H), 1.34 (s, 6H). ^{13}C NMR (75.5 MHz, CDCl_3) δ 149.6, 136.0, 131.6, 127.4, 126.6, 84.0, 48.7, 27.2, 25.2, 24.9. HRMS (ESI) m/z calculated for $\text{C}_{14}\text{H}_{20}\text{BO}_2$ $[\text{M} - \text{Br}]^+$ 230.1588, found 230.1579.

The following compounds were prepared in the same fashion as **2.1**, with exceptions noted as necessary.

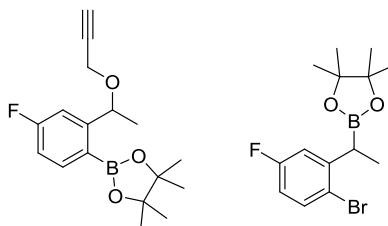


Compound 2.3. Compound **2.3** was prepared in the same fashion as described for the preparation of **2.2** except Xantphos was employed as the ligand in place of 1,2-bis(dicyclohexanephosphino)ethane. An integrated ^1H NMR yield of 72% was obtained using 1,1,1,2-tetrachloroethane as an internal standard. ^1H NMR (300 MHz, CDCl_3) δ 7.50 (d, $J = 8.0$ Hz, 1H), 7.30 – 7.19 (m, 2H), 7.00 (ddd, $J = 8.0, 6.0, 3.0$ Hz, 1H), 2.79 (q, $J = 7.5$ Hz, 1H), 1.34 (d, $J = 7.6$ Hz, 3H), 1.24 (s, 12H). ^{13}C NMR (75 MHz, CDCl_3) δ 144.70, 132.72, 128.95, 127.69, 126.89, 125.08, 83.66, 24.87, 15.95. HRMS (EI) m/z calculated $[\text{M} + \text{NH}_4]^+$ 327.1115, found 327.1129.



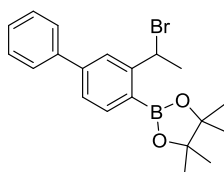
Compound 2.17 and 2.29. Compound **2.17** was prepared in the same fashion as **2.2**, but after complete borylation, the benzyl bromide was trapped with propargyl alcohol for characterization. The reaction was cooled to ambient temperature and propargyl alcohol (1.2 equiv), 18-crown-6 (0.20 equiv), and K_2CO_3 (1.5 equiv) was added. The solution was heated to 45 $^\circ\text{C}$ and allowed to stir overnight before filtration, concentration, and chromatography. The product was obtained in 57% yield as a clear, colorless, viscous oil. ^1H NMR (300 MHz, CDCl_3) δ 7.66 (d, $J = 2.0$ Hz, 1H), 7.60 (d, $J = 8.1$ Hz, 1H), 7.38 (dd, $J = 8.1, 2.0$ Hz, 1H), 5.31 (q, $J = 6.3$ Hz, 1H), 4.10 (dd, $J = 15.6, 2.5$ Hz, 1H), 3.91 (dd, $J = 15.6, 2.4$ Hz, 1H), 2.39 (t, $J = 2.4$ Hz, 1H), 1.42 (d, $J = 6.2$ Hz, 3H), 1.34 (s, 12H). ^{13}C NMR (75 MHz, CDCl_3) δ 152.11, 137.27, 129.94, 128.34, 126.53, 84.10, 80.37, 75.15, 74.09, 56.11, 25.03, 24.72. HRMS (EI) m/z calculated for $\text{C}_{14}\text{H}_{23}\text{BBr}_2\text{NO}$: $[\text{M} + \text{NH}_4]^+$ 364.0955, found 364.0945.

Compound **2.29** was isolated in 31% yield as a clear, colorless, viscous oil. ^1H NMR (300 MHz, CDCl_3) δ 7.37 (d, J = 1.0 Hz, 1H), 7.35 (d, J = 7.0 Hz, 1H), 7.12 (dd, J = 8.4, 2.4 Hz, 1H), 2.72 (q, J = 7.5 Hz, 1H), 1.33 (d, J = 7.5 Hz, 3H), 1.24 (s, 12H). ^{13}C NMR (75 MHz, CDCl_3) δ 146.92, 133.92, 131.78, 129.85, 123.66, 121.62, 83.82, 24.90, 24.80, 15.54. HRMS (EI) m/z calculated for $\text{C}_{14}\text{H}_{19}\text{BBr}_2\text{O}_2$: $[\text{M}]^+$ 386.9876, found 386.9856.

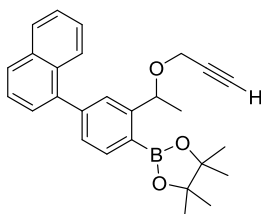


Compound 2.18 and 2.30. The product **2.18** prepared as product **2.2**, but after complete borylation, the benzyl bromide was trapped with propargyl alcohol for characterization. The reaction was cooled to ambient temperature and propargyl alcohol (1.2 equiv), 18-crown-6 (0.20 equiv), and K_2CO_3 (1.5 equiv) was added. The solution was heated to 45 °C and allowed to stir overnight before filtration, concentration, and chromatography. Compound **2.18** was obtained in 49% yield as a clear, colorless, viscous oil. ^1H NMR (300 MHz, CDCl_3) δ 7.76 (dd, J = 8.3, 6.5 Hz, 1H), 7.23 (dd, J = 10.6, 2.6 Hz, 1H), 6.94 (td, J = 8.4, 2.6 Hz, 1H), 5.38 (qd, J = 6.4, 1.6 Hz, 1H), 4.09 (dd, J = 15.6, 2.4 Hz, 1H), 3.92 (dd, J = 15.6, 2.4 Hz, 1H), 2.39 (t, J = 2.4 Hz, 1H), 1.42 (d, J = 6.4 Hz, 3H), 1.34 (s, 12H). ^{13}C NMR (75 MHz,) δ 167.19, 163.88, 153.60, 153.51, 138.25, 138.14, 114.01, 113.74, 112.25, 111.97, 83.96, 80.42, 75.12, 74.01, 56.09, 25.05, 25.02, 24.71. HRMS (EI) m/z calculated for $\text{C}_{16}\text{H}_{19}\text{BFO}_3$: $[\text{M} - \text{CH}_3]^+$ 288.1443, found 288.1435.

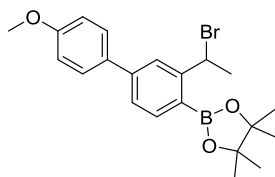
Compound **2.30** was isolated in 28% yield as a clear, colorless, viscous oil. ^1H NMR (300 MHz, CDCl_3) δ 7.44 (dd, J = 8.7, 5.6 Hz, 1H), 6.99 (dd, J = 10.1, 3.1 Hz, 1H), 6.73 (td, J = 8.3, 3.1 Hz, 1H), 2.76 (q, J = 7.5 Hz, 1H), 1.33 (d, J = 7.5 Hz, 3H), 1.24 (s, 12H). ^{13}C NMR (75 MHz, CDCl_3) δ 164.03, 160.77, 146.97, 133.57, 133.46, 118.97, 116.02, 115.71, 114.03, 113.73, 83.81, 24.89, 24.81, 15.60. HRMS (EI) m/z calculated for $\text{C}_{14}\text{H}_{19}\text{BBrFO}_2$: $[\text{M}]^+$ 328.0640, found 328.0626.



Compound 2.19. The product was obtained in 73% yield as a clear, colorless, viscous oil. ^1H NMR (300 MHz, CDCl_3) δ 7.91 (d, $J = 1.5$ Hz, 1H), 7.85 (d, $J = 7.8$ Hz, 1H), 7.62 (d, $J = 8.4$ Hz, 2H), 7.41-7.50 (m, 3H), 7.36 (t, $J = 7.2$ Hz, 1H), 6.30 (q, $J = 6.9$ Hz, 1H), 2.07 (d, $J = 6.9$ Hz, 3H), 1.38 (s, 6H), 1.36 (s, 6H). ^{13}C NMR (75 MHz, CDCl_3) δ 150.0, 144.2, 140.7, 136.5, 128.8, 127.7, 127.3, 125.9, 125.4, 83.9, 48.5, 27.2, 25.0, 24.7. HRMS (ESI) m/z calculated for $\text{C}_{20}\text{H}_{28}\text{BBrNO}_2$ $[\text{M} + \text{NH}_4]^+$ 403.1428, found 403.1435.

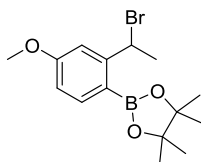


Compound 2.20. The typical product was trapped with propargyl alcohol prior to isolation due to the sensitivity of the benzyl bromide. Upon completion of 1,3-halogen migration as indicated by TLC, propargyl alcohol (1.2 equiv), 18-crown-6 (0.2 equiv), and K_2CO_3 (1.2 equiv) were added to the reaction mixture. The resulting suspension was stirred at 60°C for 6 h, filtered through a pad of celite and washed with diethyl ether. The filtrate was concentrated *in vacuo* and the organic residue was purified by column chromatography using an isocratic 10:1 hexanes:EtOAc solvent system. The product was isolated in 69% yield as a white solid. ^1H NMR (300 MHz, CDCl_3) δ 7.82-7.92 (m, 4H), 7.67 (d, $J = 1.5$ Hz, 1H), 7.40-7.55 (m, 5H), 5.43 (q, $J = 6.4$ Hz, 1H), 4.14 (dd, $J = 15.6, 2.4$ Hz, 1H), 3.99 (dd, $J = 15.6, 2.4$ Hz, 1H), 2.36 (t, $J = 2.4$ Hz, 1H), 1.52 (d, $J = 6.4$ Hz, 3H), 1.39 (s, 12H). ^{13}C NMR (75 MHz, CDCl_3) δ 149.6, 143.6, 140.1, 135.4, 133.8, 131.4, 128.4, 128.3, 127.8, 126.9, 126.7, 126.1, 125.9, 125.7, 125.3, 83.8, 80.5, 75.6, 73.6, 55.8, 24.9, 24.7. HRMS (ESI) m/z calculated for $\text{C}_{27}\text{H}_{33}\text{BNO}_3$ $[\text{M} + \text{NH}_4]^+$ 429.2585, found 429.2587.

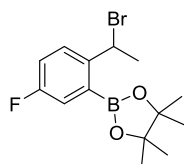


Compound 2.21. The product was obtained in 67% yield as a clear, colorless, viscous oil. ^1H NMR (300 MHz, CDCl_3) δ 7.87 (d, $J = 1.6$ Hz, 1H), 7.82 (d, $J = 7.8$ Hz, 1H), 7.57 (d, $J = 8.9$ Hz, 2H), 7.44 (dd, $J = 7.8, 1.6$ Hz, 1H), 6.99 (d, $J = 8.9$ Hz, 2H), 6.30 (q, $J = 6.9$ Hz, 1H), 3.85 (s, 3H), 2.07 (d, $J = 6.9$ Hz, 3H), 1.38 (s, 6H), 1.36 (s, 6H).

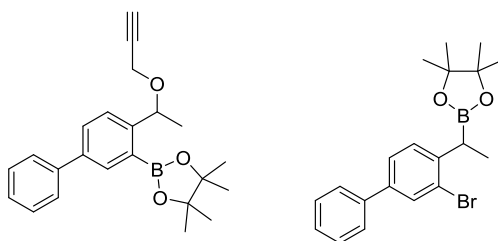
^{13}C NMR (75 MHz, CDCl_3) δ 159.5, 150.0, 143.8, 136.5, 133.2, 128.3, 125.5, 124.9, 114.2, 83.8, 55.4, 48.7, 27.2, 25.0, 24.7. HRMS (ESI) m/z calculated for $\text{C}_{21}\text{H}_{30}\text{BBrNO}_3$ $[\text{M}+\text{NH}_4]^+$ 433.1533, found 433.1519.



Compound 2.22. The product was obtained in 89% yield as a clear, colorless, viscous oil. ^1H NMR (300 MHz, CDCl_3) δ 7.74 (d, $J = 8.3$ Hz, 1H), 7.21 (d, $J = 2.5$ Hz, 1H), 6.77 (dd, $J = 8.5, 2.5$ Hz, 1H), 6.26 (q, $J = 6.9$ Hz, 1H), 3.80 (s, 3H), 1.99 (d, $J = 7.0$ Hz, 3H), 1.33 (s, 6H), 1.32 (s, 6H). ^{13}C NMR (75 MHz, CDCl_3) δ 162.3, 151.8, 138.0, 112.7, 112.6, 83.6, 55.2, 48.4, 27.3, 25.0, 24.7. HRMS (ESI) m/z calculated for $\text{C}_{15}\text{H}_{26}\text{BBrNO}_3$ $[\text{M} + \text{NH}_4]^+$ 357.1220, found 357.1228.



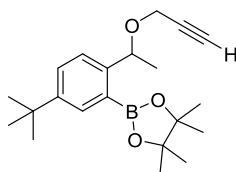
Compound 2.24. The product was obtained in 89% yield as a clear, colorless, viscous oil. ^1H NMR (300 MHz, CDCl_3) δ 7.65 (dd, $J = 8.7, 5.0$ Hz, 1H), 7.44 (dd, $J = 9.3, 2.9$ Hz, 1H), 7.11 (td, $J = 8.2, 3.2$ Hz, 1H), 6.44 (q, $J = 6.9$ Hz, 1H), 2.00 (d, $J = 6.9$ Hz, 3H), 1.37 (s, 6H), 1.35 (s, 6H). ^{13}C NMR (75 MHz, CDCl_3) δ 163.3, 160.1, 145.5, 145.5, 128.8, 128.7, 122.2, 121.9, 118.6, 118.3, 84.4, 47.8, 27.3, 25.1, 24.8. HRMS (EI) m/z calculated for $\text{C}_{14}\text{H}_{19}\text{BFO}_2$: $[\text{M} - \text{Br}]^+$ 249.1457, found 249.1457.



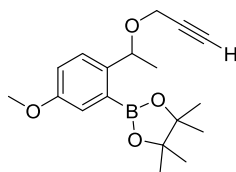
Compounds 2.25 and 2.37. Compound **2.25** was obtained as compound **2.2**, but after complete borylation, the benzyl bromide was trapped with propargyl alcohol for characterization. The reaction was cooled to ambient temperature and propargyl alcohol (1.2 equiv), 18-crown-6 (0.20 equiv), and K_2CO_3 (1.5 equiv) was added. The

solution was heated to 45 °C and allowed to stir overnight before filtration, concentration, and chromatography. **2.25** was obtained in 66% yield as a white solid. ^1H NMR (300 MHz, CDCl_3) δ 7.97 (d, $J = 1.9$ Hz, 1H), 7.67 (dd, $J = 8.1, 2.1$ Hz, 1H), 7.56-7.63 (m, 3H), 7.42 (t, $J = 7.4$ Hz, 2H), 7.32 (tt, $J = 7.4, 1.3$ Hz, 1H), 5.37 (q, $J = 6.4$ Hz, 1H), 4.03 (ABX quartet, $J = 15.6, 2.5$ Hz, 2H), 2.38 (t, $J = 2.5$ Hz, 1H), 1.49 (d, $J = 6.4$ Hz, 3H), 1.36 (s, 12H). ^{13}C NMR (75 MHz, CDCl_3) δ 148.4, 140.9, 139.4, 134.1, 129.9, 128.6, 127.1, 125.5, 83.8, 80.5, 75, 73.6, 55.8, 24.8, 24.6. HRMS (ESI) m/z calculated for $\text{C}_{23}\text{H}_{31}\text{BNO}_3$ $[\text{M}+\text{NH}_4]^+$ 379.2428, found 379.2426.

The undesired hydroboration product **2.37** was isolated in 12% yield as a colorless oil. ^1H NMR (400 MHz, CDCl_3) δ 7.76 (d, $J = 1.9$ Hz, 1H), 7.55 (d, $J = 7.3$ Hz, 2H), 7.47 (dd, $J = 8.0, 1.9$ Hz, 1H), 7.42 (t, $J = 7.3$ Hz, 2H), 7.30-7.35 (m, 2H), 2.82 (q, $J = 7.5$ Hz, 1H), 1.38 (d, $J = 7.5$ Hz, 3H), 1.26 (s, 12H). ^{13}C NMR: (100.6 MHz, CDCl_3) δ 143.4, 139.8, 139.7, 131.0, 128.9, 128.8, 127.4, 126.9, 126.2, 125.2, 83.5, 24.7, 24.7, 15.8. HRMS (ESI) m/z calculated for $\text{C}_{20}\text{H}_{28}\text{BBrNO}_2$ $[\text{M} + \text{NH}_4]^+$ 403.1428, found 403.1420.

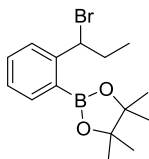


Compound 2.26. The product was obtained using the same method as reported for **2.26** and was isolated in 65% yield as a clear, colorless, viscous oil. ^1H NMR (300 MHz, CDCl_3) δ 7.72 (d, $J = 2.1$ Hz, 1H), 7.48 (dd, $J = 8.3, 2.2$ Hz, 1H), 7.42 (d, $J = 8.3$ Hz, 1H), 5.30 (q, $J = 6.4$ Hz, 1H), 4.06 (dd, $J = 15.5, 2.4$ Hz, 1H), 3.88 (dd, $J = 15.6, 2.4$ Hz, 1H), 2.36 (t, $J = 2.4$ Hz, 1H), 1.45 (d, $J = 6.4$ Hz, 3H), 1.35 (s, 12H), 1.33 (s, 9H). ^{13}C NMR (75 MHz, CDCl_3) δ 149.2, 146.5, 131.9, 128.5, 125.0, 83.8, 80.8, 75.6, 73.7, 55.8, 34.6, 31.6, 25.1, 24.8. HRMS (EI) for $\text{C}_{21}\text{H}_{35}\text{BO}_3$ m/z calculated $[\text{M}+\text{NH}_4]^+$ 359.2741, found 359.2753.



Compound 2.27. Toluene was utilized as the solvent instead of THF. The hydroboration was conducted for 5 h, as extended times did not improve conversion and led to elimination of the sensitive benzyl bromide prior to the nucleophilic trapping as in **2.27**. The product was isolated in 36% yield as a colorless oil. ^1H NMR (400 MHz,

CDCl₃) δ 7.43 (d, *J* = 8.6 Hz, 1H), 7.24 (d, *J* = 2.7 Hz, 1H), 6.99 (dd, *J* = 8.6, 2.7 Hz, 1H), 5.26 (q, *J* = 6.5 Hz, 1H), 4.03 (dd, *J* = 15.3, 2.4 Hz, 1H), 3.88 (dd, *J* = 15.3, 2.4 Hz, 1H), 3.82 (s, 3H), 2.36 (t, *J* = 2.4 Hz, 1H), 1.43 (d, *J* = 6.5 Hz, 3H), 1.35 (s, 12H). ¹³C NMR (100 MHz, CDCl₃) δ 158.1, 141.4, 126.5, 119.4, 117.4, 83.8, 80.6, 75.1, 73.4, 55.5, 55.3, 24.8, 24.6. HRMS (ESI) *m/z* calculated for C₁₈H₂₅BNaO₄ [M+Na]⁺ 338.1775, found 338.1779.



Compound 2.16. The product was obtained in 75% yield as a clear, colorless, viscous oil. ¹H NMR (300 MHz, CDCl₃) δ 7.77 (dd, *J* = 7.5, 1.6 Hz, 1H), 7.66 (dd, *J* = 7.9, 1.1 Hz, 1H), 7.46 (td, *J* = 7.6, 1.6 Hz, 1H), 7.25 (td, *J* = 7.4, 1.2 Hz, 1H), 5.99 (dd, *J* = 8.0, 6.6 Hz, 1H), 2.34 – 2.19 (m, 1H), 2.19 – 2.05 (m, 1H), 1.36 (s, 6H), 1.35 (s, 6H), 0.99 (t, *J* = 7.2 Hz, 3H). ¹³C NMR (75 MHz, CDCl₃) δ 148.64, 135.91, 131.67, 127.65, 127.23, 84.03, 56.49, 34.20, 25.07, 25.01, 13.10. HRMS (EI) *m/z* calculated for C₁₅H₂₂BO₂: [M - Br]⁺ 245.1708, found 245.1704.

2.6 Bibliography

1. a) Negishi, E.-i.; de Meijere, A. Ed. *Handbook of Organopalladium Chemistry for Organic Synthesis*; Wiley: New York, **2002**. b) de Meijere, A.; Diederich, F. Ed. *Metal-Catalyzed Cross-Coupling Reactions*, 2nd ed. Wiley-VCH: Weinheim, **2004**.
2. Selected reviews of C-H functionalization: a) Mkhaliid, I.A.; Barnard, J.H.; Marder, T.B.; Murphy, J.M.; Hartwig, J.F. *Chem. Rev.* **2010**, *110*, 890. b) Lyons, T.W.; Sanford, M.S. *Chem. Rev.* **2010**, *110*, 1147. c) Engle, K.M.; Mei, T.-S.; Wasa, M.; Yu, J.-Q. *Acc. Chem. Res.* **2012**, *45*, 788. d) Neufeldt, S.R.; Sanford, M.S. *Acc. Chem. Res.* **2012**, *45*, 936. e) Song, G.; Wang, F.; Li, X. *Chem. Soc. Rev.* **2012**, *41*, 3651. f) Ackermann, L. *Chem. Rev.* **2011**, *111*, 1315. g) Davies, H.M.L.; Morton, D. *Chem. Soc. Rev.* **2011**, *40*, 1857. h) Wendlandt, A.E.; Suess, A.M.; Stahl, S.S. *Angew. Chem. Int. Ed.* **2011**, *50*, 11062.
3. a) Bedford, R.B.; Coles, S.J.; Hursthouse, M.B.; Limmert, M.E. *Angew. Chem. Int. Ed.* **2003**, *42*, 112. b) Ihara, H.; Suginome, M. *J. Am. Chem. Soc.* **2009**, *131*, 7502. c) Robbins, D.W.; Boebel, T.A.; Hartwig, J.F. *J. Am. Chem. Soc.* **2010**, *132*, 4068. (d) Dai, H.-X.; Stepan, A.F.; Plummer, M.F.; Zhang, Y.-H.; Yu, J.-Q. *J. Am. Chem. Soc.* **2011**, *133*, 7222. (e) Huang, C.; Chattopadhyay, B.; Grevorgyan, V. *J. Am. Chem. Soc.* **2011**, *133*, 12406. (f) Gulevich, A.V.; Melkonyan, F.S.; Sarkar, D.; Grevorgyan, V. *J. Am. Chem. Soc.* **2012**, *134*, 5528.

4. Recent examples of activating group recycling: a) Newman, S.G.; Lautens, M. *J. Am. Chem. Soc.* **2011**, *133*, 1778. b) Hooper, J.F.; Chaplin, A.B.; González-Rodríguez, C.; Thompson, A.L.; Weller, A.S.; Willis, M.C. *J. Am. Chem. Soc.* **2012**, *134*, 2906.
5. a) Noh, D.; Chea, H.; Ju, J.; Yun, J. *Angew. Chem. Int. Ed.* **2009**, *48*, 6062. b) Noh, D.; Yoon, S.K.; Won, J.; Lee, J.Y.; Yun, J. *Chem. Asian J.* **2011**, *6*, 1967. c) Won, J.; Noh, D.; Yun, J.; Lee, J.Y. *J. Phys. Chem. A* **2010**, *114*, 12112.
6. Shiroodi, R.K.; Dudnik, A.S.; Gevorgyan, V. *J. Am. Chem. Soc.* **2012**, *134*, 6928 and references therein.
7. Luliński, S.; Serwatowski, J.; Szczerbińska, M. *Eur. J. Org. Chem.* **2008**, 1797.
8. Zhang, Z.; Zhang, L.; Guan, X.; Shen, Z.; Chen, X.; Xing, G.; Fan, X.; Zhou, Q. *Liq. Cryst.* **2010**, *37*, 69.
9. Wu, X.; Nilsson, P.; Larhed, M. *J. Org. Chem.* **2005**, *70*, 346.
10. Sánchez-Larios, E.; Holmes, J.M.; Daschner, C.L.; Gravel M. *Org. Lett.* **2010**, *12*, 5772.
11. Moorthy, J.N.; Samanta, S. *J. Org. Chem.* **2007**, *72*, 9786.
12. Kabalka, G.W.; Tejedor, D.; Li, N.-S.; Malladi, R.R.; Trotman, S. *Tetrahedron* **1998**, *54*, 15525.
13. Padwa, A.; Rieker, W.F.; Rosenthal, R.J. *J. Am. Chem. Soc.* **1985**, *107*, 1710.

Chapter 3: Formal Asymmetric Hydrobromination of Styrenes *via* Copper(I)-Catalyzed 1,3-Halogen Migration

Reproduced with permission from Van Hoveln, R.; Schmid, S. C.; Tretbar, M.; Buttke, C. T.; Schomaker, J. M.

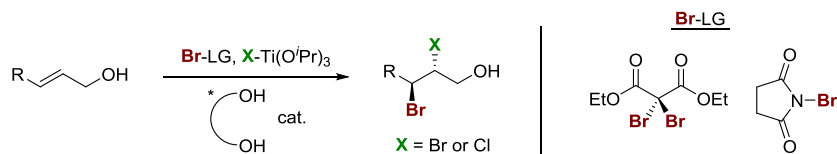
Chem. Sci. **2014**, *5*, 4763-4767. Copyright 2014 Royal Society of Chemistry.

3.1 Introduction to Asymmetric Halogenation Reactions

The enantioselective halogenation of olefins remains a challenging goal in organic synthesis.¹ However, recent strides have been made in asymmetric α -halogenation of carbonyls,² olefin aminohalogenations,³ semi-pinacol rearrangements⁴ and halocyclizations.⁵ To the best of our knowledge, catalytic, enantioselective hydrohalogenations of olefins have not been reported.⁶

Notably, Burns recently reported the enantioselective dihalogenation of allylic alcohols (Scheme 3.1).^{6b,c} The strategy Burns employed was to divide the electrophilic and nucleophilic halogen sources into two separate species. The catalytic chiral alcohol binds to the Ti to generate a chiral bromide source and then the electrophilic halogen source binds to Ti as well, activating both halogens. The allylic alcohol acts as a directing group for the catalyst to the olefin. Loadings of the chiral alcohol tend to be high, (10-30%) and in several cases the alcohol is used stoichiometrically in order to achieve acceptable enantioselectivity. Additionally, this method produces significant stoichiometric waste. However, given the dearth of general methods for catalytic enantioselective dihalogenation, this represents a significant advancement.

Scheme 3.1. Burns catalytic enantioselective dihalogenation.



Since Cu-catalyzed 1,3-halogen migration⁷ represents a formal styrene hydrobromination with an arene borylation, we envisioned adapting this methodology (with a chiral ligand) to achieve catalytic enantioselective hydrobromination. This would convert readily available halostyrenes into compounds bearing two differentiated functional groups that can be further transformed at each site in an orthogonal manner. Experimental efforts, in combination with density functional theory (DFT) calculations, have provided: 1) a highly enantioselective hydrohalogenation method for a variety of substituted halostyrenes, and 2) a predictive reactivity profile for determining the yield for a broader range of substrates.

3.2 Optimization of Asymmetric 1,3-Halogen Migration

Studies were initiated by exploring a series of chiral bidentate phosphine ligands with CuCl (Table 3.1). While three ligands (entries 2, 4 and 14) gave *er*'s greater than 80:20 at 50 °C, (*S,S*)-Ph-BPE (entry 14) gave the best

combination of yield and *er* while producing none of the benzyl boronic ester **3.3**, prompting its use in further investigations.

Table 3.1. Optimization of the ligand for 1,3-halogen migration.

3.1 $\xrightarrow[1.2 \text{ equiv HBpin}]{5 \text{ mol\% CuCl/L}^*, 10 \text{ mol\% KOtBu}}$ **3.2**: X = Br, Y = Bpin
3.3: X = Bpin, Y = Br

(*R*)-T-BINAP Ar = 4-MeC₆H₄,
(*R*)-DM-BINAP Ar = 3,5-diMeC

entry	ligand	3.1	3.2	3.3	<i>er</i>
1	(<i>R</i>)-T-BINAP	23	17	0	77:23
2	(<i>R</i>)-DM-BINAP	18	33	0	83:17
3	SEGPPOS	12	29	0	65:35
4	DTBM-SegPhos	15	8	0	81:19
5	(<i>S</i>)-TunePhos	8	46	0	29:71
6	Tangphos	22	17	31	n.d.
7	DIPAMP	20	17	0	53:47
8	(<i>R,R</i>)-Me-DuPhos	8	23	0	61:39
9	(<i>S,S</i>)-iPr-DuPhos	23	0	0	n.d.
10	(<i>R</i>)-BenzP*	36	21	0	36:64
11	(<i>S</i>)-Josiphos SL-J003-1	0	82	0	68:32
12	(<i>S,S</i>)-Me-BPE	19	0	0	n.d.
13	(<i>R,R</i>)-iPr-BPE	13	17	0	45:55
14	(<i>S,S</i>)-Ph-BPE	14	34	0	89:11

(*S*)-Josiphos SL-J003-1

(*S,S*)-R-BPE

Further reaction optimization probed the reaction dependence on temperature, concentration and base (Table 3.2). While the yield decreased at ambient temperature, the *er* improved compared to running the reaction at 50 °C (entry 1). Decreasing the concentration from 0.5 M to 0.1 M significantly improved the mass balance by decreasing the rate of atom transfer radical polymerization (ATRP) (entry 2), a major side reaction.⁸ Higher catalyst loadings did not increase conversion, but switching the base from KO^tBu to NaO^tBu increased the yield to 75% at the expense of *er* (entries 3, 4). The best results were obtained by lowering the reaction temperature to 0 °C in the presence of NaO^tBu as the base (entry 5). Under these conditions, the enantioenriched benzyl bromide **3.2** was produced in 73% yield and 98:2 *er*.

Table 3.2. Optimization of reaction conditions.

3.1 $\xrightarrow[\text{toluene, temp}]{\text{CuCl}/(S,S)\text{-Ph-BPE, MOtBu, HBpin}}$ **3.2**

entry	temp (°C)	MO ^t Bu	loading [conc]	3.1	3.2	<i>er</i>
1	25	KOtBu	5% 0.5 M	16	46	93:7
2	25	KOtBu	5% 0.1 M	52	34	91:9
3	25	KOtBu	10% 0.1 M	41	38	92:8
4	25	NaOtBu	10% 0.1 M	13	75	87:13
5	0	NaOtBu	10% 0.1 M	<10	73	98:2

NMR yields determined using 1,1,1,2-tetrachloroethane as the internal standard.

3.3 Scope of Asymmetric 1,3-Halogen Migration

Significant optimization efforts yielded reaction conditions which gave generally high *er*, but variable yields (Table 3.3). Changing the OMe group to a bulkier O^{*i*}Pr group resulted in a lower yield but excellent *er* (entry 2). Substitution of the Br with I diminished the *er* to 83:17 (entry 3) due to the sensitive nature of the benzyl iodide product. The parent 2-bromostyrene still exhibited good *er* (entry 4), but the yield was significantly lower compared to the 94% obtained using the dCype catalyst system, presumably due to ATRP competition.⁹ Substitution at the β -carbon of the styrene, as well as a fluorine at C5, were tolerated (entries 5 and 6), moreover the *er* values were still respectable. Notably, the fluorinated substrate (entry 6) did not produce any of the benzyl boronic ester side product that was observed with the dCype ligand.

Table 3.3. Initial scope of asymmetric 1,3-halogen migration

Reaction scheme: Substituted styrene (3.1, 3.4-3.8) + HBpin $\xrightarrow[\text{toluene, 0 }^\circ\text{C, 18h}]{10 \text{ mol\% CuCl, 10 mol\% (S,S)-Ph-BPE, 20 mol\% NaOtBu}}$ 1,3-dibromostyrene (3.2, 3.9-3.13)

entry	substrate	yield	<i>er</i>	entry	substrate	yield	<i>er</i>
1		73% 3.2	98:2	4		28% 3.11	92:8 ^b
2		53% 3.9	>99:1	5		40% 3.12	95:5 ^c
3		71% ^a 3.10	83:17	6		38% 3.13	92:8

^a Trapped with LiSePh before isolation. ^b *er* determined after trapping with 2-naphthalenethiol. ^c *er* determined after trapping with LiSePh.

3.4 A Predictive Model for Determining Reaction Yield

Often, qualitative observations concerning either the electronics or sterics of a particular system are used to rationalize reaction outcome.⁹ However, our system did not appear to follow an obvious pattern based on a qualitative analysis of electronic factors. To obtain a better understanding of the factors controlling the reactivity, DFT calculations were carried out. Rather than modelling an overall reaction coordinate, three major features of the substrates were modelled with the goal of developing a straightforward, empirical equation capable of correlating

substrate parameters with reaction yield for a range of substituted *o*-bromostyrenes in the asymmetric 1,3-halogen migration.¹⁰

3.4.1 Developing the Predictive Model

We hypothesized that greater electron density at the bromine-bearing carbon (carbon labelled γ , Figure 3.1) would promote the 1,3-halogen migration reaction. The major ATRP side reaction was proposed to be favored by factors that promote or stabilize the formation of a benzyl radical (represented by $\Delta\Delta E$). Finally, the steric bulk of the (*S,S*)-Ph-BPE catalyst is greater than that of the dCype ligand used in our racemic studies which might lower the yield; thus, a steric factor (the volume of the substrate relative to 2-bromostyrene) was also included in the computational studies (represented by χ). Ten substrates were used as the “training set” to generate equation 1 (Table 4). For the 10 substrates used to create equation 1, the calculated yield matched the experimental yield to within $\pm 10\%$, though many matched much more closely. Given that NMR yields have an error of $\sim 10\%$ ¹¹ and the simplicity of our analysis, we felt that this was an exceptionally close fit to establish a trend. The close fit also indicates that the parameters we chose are indeed the major factors impacting yield. For the substrates used in generating equation 1, χ and $\Delta\Delta E$ contributed nearly equally, whereas γ contributed approximately twice that of either χ or $\Delta\Delta E$. In Table 3.4, factors that would improve yield relative to the unsubstituted styrene are shown in **green** whereas factors that would be detrimental to the yield are shown in **red**. Each of these factors were parameterized from optimized structures (B3LYP/6-311++G(2d,p))^{12,13} using Gaussian 09¹⁴ and NBO¹⁵ (see the section 3.7.3 for details).

Figure 3.1. Factors impacting product yield.

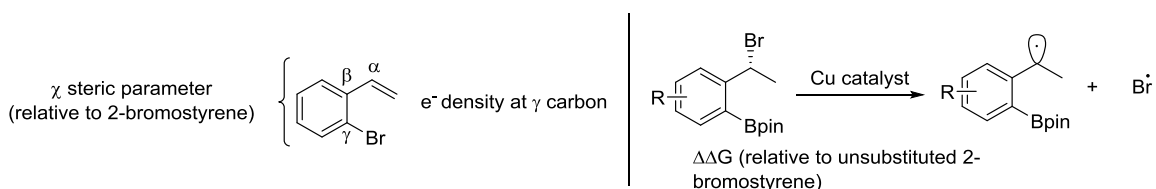
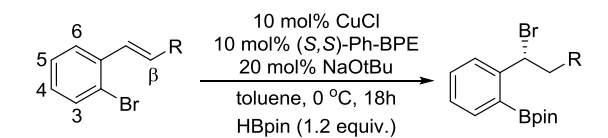


Table 3.4. Training set of substrates for the predictive model.


Entry	Substrate	Calc. Yield	Exp. Yield	γ	$\Delta\Delta G$	χ
1	H	34	35	-0.069	0.00	0.00
2	5-OMe	65	73	-0.095	0.21	22.2
3	5-F	46	37	-0.087	-0.59	10.3
4	5-O ^t Pr	56	54	-0.097	0.37	55.8
5	5- ^t Bu	24	25	-0.075	0.16	48.9
6	4- ^t Bu	13	4	-0.069	0.04	50.5
7	4-Ph	0.4	7	-0.072	-0.84	57.0
8	5-pyrrolyl	23	24	-0.081	-0.42	50.2
9	4-F	12	14	-0.057	-0.12	9.01
10	β -Me	39	40	-0.071	0.34	9.06

NMR yields determined using 1,1,1,2-tetrachloroethane as the internal standard.

$$\text{Predicted yield} = -1415\gamma + 16.2(\Delta\Delta E) - 0.432\chi - 63.2 \quad (1)$$

This straightforward equation indicates that relative to 2-bromostyrene (Table 4, entry 1), increasing the electron density at the γ carbon results in increased yield (entry 2). However, if the $\Delta\Delta E$ of benzyl radical formation is negative compared to 2-bromostyrene (entry 3), the yield is adversely affected. Finally, the presence of even remote, large R groups (entry 4) is also detrimental to the yield.

3.4.2 Testing the Predictive Model

The predictive power of equation 1 was then tested on a variety of 2-bromostyrene substrates that were not used to generate equation 1 (Table 3.5). Equation 1 predicted a poor yield when a -SMe group is placed *para* to the Br as in **3.14**. This was indeed the case because sulfur does not participate in conjugation with an aromatic ring as well as oxygen, making the γ carbon relatively electron poor (Table 3.5, entry 1). Addition of a weakly donating group in the C5 position did not result in a significant improvement in yield (entry 2). Installation of an OEt group at the C5 position was predicted to give **3.22** in 58% yield, which was nearly identical to the observed yield of 57% (entry 3). Although substitution on the alkene resulted in slightly lower yields than expected, the observed and calculated yields were reasonably comparable (entry 4). Placement of functional groups adjacent to the bromine (entries 5-6) might be expected to reduce the predictive power of equation 1, since none of the substrates used to create the equation have steric bulk *ortho* to a reactive site. Indeed, even though equation 1 predicted that placing OMe at C3 of **3.18** would result in a quantitative yield, the actual yield of **3.24** (entry 5) was only 50%. However, the model

was useful for ascertaining the relative success of the 1,3-migration, as installing a F at C3 resulted in a good yield for the asymmetric 1,3-halogen migration (entry 6).

Table 3.5. Testing the predictive power of the model.

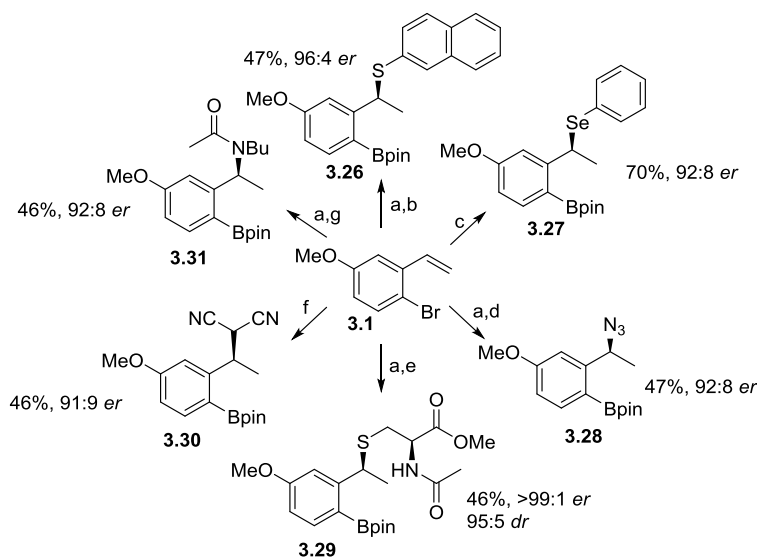
entry	substrate	calc. yield	yield	er	entry	substrate	calc. yield	yield	er				
1		3.14	10%	13% ^a	3.20	n.d.	4		3.17	63%	50% ^b	3.23	97:3 ^d
2		3.15	36%	30% ^b	3.21	92:8 ^c	5		3.18	quant.	50% ^b	3.24	87:13
3		3.16	58%	57% ^b	3.22	95:5 ^d	6		3.19	quant.	65% ^a	3.25	91:9 ^d

^a NMR yields determined using 1,1,1,2-tetrachloroethane as the internal standard. ^b Isolated yield. ^c *er* determined after trapping with LiSePh. ^d *er* determined after trapping with 2-naphthalenethiol.

Establishing the relationship between various substrate parameters and reaction yield was a useful endeavor. The model enabled us to consider substrates that we would have not otherwise tried (Table 3.5, entries 5-6), since *ortho*-substituted substrates performed poorly when using the achiral catalyst, we would not have considered them for the enantioselective catalyst, thus the model broadened the range of potential substrates. Additionally, this multifaceted approach demonstrates the need to assess several reaction parameters acting in concert, rather than focusing on one parameter in a simple, qualitative approach.

3.5 Demonstration of Activating Group Recycling

Recycling of the benzyl bromide was demonstrated by transforming **3.1** into a variety of benzyl-substituted aryl boronic esters, often in one pot (Scheme 3.2). Asymmetric 1,3-halogen migration, followed by displacement of the bromide with sulfur nucleophiles (**3.26**, **3.29**), showed essentially no degradation in the *er*, while selenium, nitrogen, and carbon nucleophiles (**3.27-3.28**, **3.30-3.31**) resulted in slight loss in enantioenrichment. The use of chiral nucleophiles, such as the cysteine leading to **3.29**, did not lead to significant epimerization at the benzyl carbon (95:5 *dr*) and lead to a product with >99:1 *er*. A derivative of **3.26** allowed us to establish the absolute stereochemistry by X-ray crystallography (see Appendix B.1 for details).

Scheme 3.2. Recycling of the benzyl bromide.

(a) Standard asymmetric halogen migration conditions and then the solvent was removed. (b) 1.5 equiv 2-naphthalenethiol, 2.5 equiv K_2CO_3 , DMF, 1 h, RT. (c) Standard asymmetric halogen migration conditions and then 3 equiv of LiSePh in THF was added. (d) 3.0 equiv NaN_3 , DMSO, 40 °C, 1 h. (e) 1.5 equiv *N*-acetyl cysteine methyl ester, 2.5 equiv K_2CO_3 , DMSO, 40 °C, 3 h. (f) Standard asymmetric conditions and then 3.0 equiv lithium malononitrile in THF. (g) 3 equiv butylamine, 5 equiv K_2CO_3 , DMF, 40 °C, 1 h then 5 equiv Ac_2O , 40 °C, 1h.

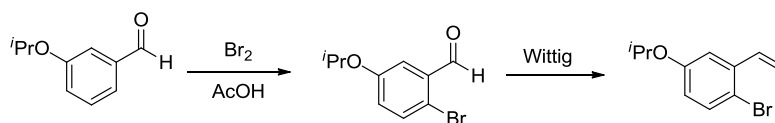
3.6 Conclusions

A Cu(I) catalyst supported by a (*S,S*)-Ph-BPE ligand promotes an asymmetric cascade 1,3-halogen migration/borylation reaction which proceeds under mild conditions and results in a formal enantioselective addition of HBr across a carbon-carbon double bond. In-depth experimental and computational studies have allowed us to successfully correlate yields with features of both the substrate and the product, including electron density at the bromine-bearing carbon, the steric bulk of the substrate and the propensity of the product to form promiscuous radicals. The enantiodetermining step will be discussed in Chapter 4. Current work focuses on catalyst design to tolerate a wide range of substrates while still maintaining good enantioinduction.

3.7 Experimental Details

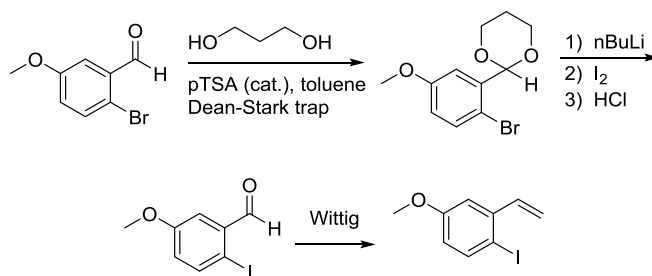
3.7.1 Synthesis of Styrene Starting Materials

Starting materials **3.1**, **3.11**, **3.7**, and **3.8** were synthesized as describe in Section 2.5.1



Compound 3.4. Acetic acid (12 mL), 3-isopropoxybenzaldehyde (1.6 mL, 10.1 mmol, 1.0 equiv), and bromine (1.5 mL, 29.3 mmol, 2.9 equiv) were added to a 50 mL round bottom flask and allowed to stir at ambient temperature for 2 h. The reaction was transferred to a separatory funnel, diluted with CH_2Cl_2 and the organic layer washed 3x with water, 1x with saturated NaHSO_3 and 1x with 1 M KOH. The organic layer was dried over Na_2SO_4 and concentrated *in vacuo*. The product 2-bromo-5-isopropoxybenzaldehyde was isolated in 94% yield and used without further purification.

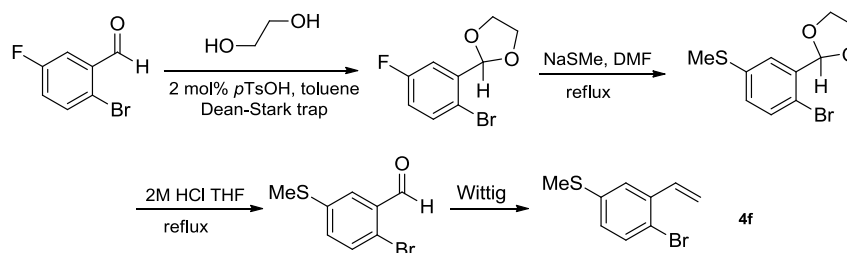
THF (40 mL) was added to a flame dried 200 mL round bottom flask under N_2 in an ice bath containing methyltriphenylphosphonium iodide (3.44 g, 8.5 mmol, 1.2 equiv). A solution of *n*BuLi (4.0 mL of a 2.27 M solution, 9.1 mmol, 1.32 equiv) was added in a dropwise fashion to the slurry and the reaction mixture allowed to stir for 30 min at 0 °C. An aliquot of 2-bromo-5-isopropoxybenzaldehyde (1.2 mL, 6.9 mmol, 1.0 equiv) was added slowly and the reaction mixture allowed to stir at rt for 3 h. Silica gel was added and the volatiles removed under reduced pressure. The resulting powder was loaded onto a plug of silica and flushed with ~200 mL of hexanes. The hexanes were removed *in vacuo* and the residue was purified by column chromatography using hexanes/EtOAc as the eluent. A gradient was employed using 0-2% in 0.5% increments. The 2-bromo-5-isopropoxystyrene **3.4** was isolated as a clear, colorless oil in 50% yield. ^1H NMR (500 MHz, CDCl_3) δ 7.41 (d, $J = 8.8$ Hz, 1H), 7.07 (d, $J = 3.0$ Hz, 1H), 7.00 (dd, $J = 17.4, 10.9$ Hz, 1H), 6.69 (dd, $J = 8.8, 3.0$ Hz, 1H), 5.67 (d, $J = 17.4$ Hz, 1H), 5.35 (d, $J = 10.9$ Hz, 1H), 4.53 (hept, $J = 6.3$ Hz, 1H), 1.33 (d, $J = 6.1$ Hz, 6H). ^{13}C NMR (126 MHz, CDCl_3) δ 157.24, 138.21, 135.87, 133.37, 116.91, 116.59, 114.24, 114.05, 70.27, 21.95. HRMS (EI) m/z calculated for $\text{C}_{11}\text{H}_{13}\text{BrO}$ $[\text{M}]^+$ 240.0146, found 240.0145.



Compound 3.5. A 200 mL flask fitted with a Dean-Stark trap and reflux condenser was charged with 2-bromo-5-methoxybenzaldehyde (6.20 g, 28.8 mmol, 1.0 equiv), 1,3-propanediol (2.1 mL, 29.1 mmol, 1.01 equiv), *p*-toluenesulfonic acid (0.52 g, 2.7 mmol, 0.1 equiv) and 50 mL of toluene. The reaction mixture was heated to reflux

for 1 h and cooled to rt. The mixture was washed with saturated NaHCO_3 , the aqueous layer extracted 2x with portions of CH_2Cl_2 and the combined organic layers were dried with Na_2SO_4 and concentrated *in vacuo*. The acetal was isolated in quantitative yield and used without further purification.

A flame-dried 500 mL round bottom flask under N_2 was charged with THF (60 mL) and 2-bromo-5-methoxybenzaldehyde trimethylene glycol acetal (3.5 mL, 18.2 mmol, 1.0 equiv). The flask was placed in an acetone/ CO_2 bath and *n*BuLi (9.0 mL of a 2.5 M solution, 22.5 mmol, 1.2 equiv) was added slowly. The reaction mixture was allowed to stir at $-78\text{ }^\circ\text{C}$ for 1 h and I_2 (10.15 g, 40.0 mmol, 2.2 equiv) added in a single portion. The reaction was allowed to warm slowly to rt and stirred overnight. A solution of 1 M HCl (~150 mL) was added to the flask and the reaction mixture refluxed under N_2 for 1 h. The cooled mixture was poured into a separatory funnel and diluted with CH_2Cl_2 . The aqueous layer was extracted 1x with CH_2Cl_2 and the combined organic layers were washed with saturated NaHSO_3 . The organic layer was dried with Na_2SO_4 and concentrated *in vacuo*. The crude material was of sufficient purity for subsequent reactions or could be purified by column chromatography with hexanes/EtOAc as the eluent. A 0-10% gradient of EtOAc was used in 2% increments. The product 2-iodo-5-methoxybenzaldehyde was isolated in 61% yield as a yellow solid. The aldehyde was used as the substrate for a Wittig olefination to prepare the styrene **3.5** in a fashion similar to that described for the synthesis of **3.4**. The 2-iodo-5-methoxystyrene was purified by column chromatography using hexanes/EtOAc as the eluent. A gradient was employed using 0-2% EtOAc in 0.5% increments. The styrene **3.5** was isolated as a clear, colorless oil in 47% yield. ^1H NMR (500 MHz, CDCl_3) δ 7.69 (d, $J = 8.7$ Hz, 1H), 7.07 (d, $J = 3.1$ Hz, 1H), 6.86 (dd, $J = 17.2, 10.8$ Hz, 1H), 6.59 (dd, $J = 8.7, 3.1$ Hz, 1H), 5.62 (dd, $J = 17.3, 1.0$ Hz, 1H), 5.32 (dd, $J = 10.9, 1.0$ Hz, 1H), 3.81 (s, 3H). ^{13}C NMR (126 MHz, CDCl_3) δ 160.02, 141.52, 140.56, 139.82, 116.86, 115.72, 111.94, 88.39, 55.39. HRMS (EI) m/z calculated for $\text{C}_9\text{H}_9\text{IO}$ $[\text{M}]^+$ 259.9693, found 259.9694.



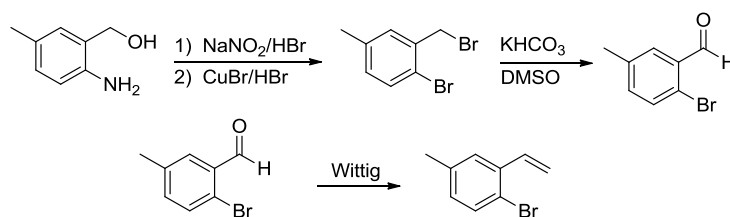
Compound 3.14. A 50 mL, two-neck round bottom flask equipped with a Dean-Stark apparatus was charged with 2.0 g (8.1 mmol, 1.0 equiv) 2-bromo-5-fluorobenzaldehyde dissolved in 12 mL toluene. Then 40.0 mg (0.195 mmol,

2 mol %) para-toluenesulfonic acid and 710 μl (786 mg, 12.7 mmol, 1.3 equiv) ethylene glycol was added. The reaction mixture was refluxed for 18 h. After cooling to room temperature, 10 mL of saturated NaHCO_3 was added and the mixture extracted three times with 25 mL portions of diethyl ether. The combined organic phases were dried over Na_2SO_4 , filtered and evaporated under reduced pressure. The acetal was purified by column chromatography ($R_f = 0.45$, hexane/EtOAc [9:1]) and isolated in 90 % (2.4 g) yield as a colorless liquid. ^1H NMR (500 MHz, CDCl_3) δ 7.52 (dd, $J = 8.7$ Hz, 5.1 Hz, 1H), 7.33 (dd, $J = 9.2$ Hz, 3.1 Hz, 1H), 6.96 (ddd, $J = 11.0$ Hz, 8.3 Hz, 3.1 Hz, 1H), 6.04 (d, $J = 0.8$ Hz, 1H), 4.22-4.03 (m, 4H). ^{13}C NMR (126 MHz, CDCl_3) δ 162.0, 138.7, 134.3, 117.7, 116.8, 115.1, 102.0, 65.6. HRMS (EI) m/z calculated for $\text{C}_9\text{H}_8\text{O}_2\text{BrF}$ [$\text{M} + \text{H}$] $^+$ 245.9687, found 245.9687.

A 100 mL one-neck flask equipped with a condenser was charged with 625.0 mg (8.9 mmol, 1.1 equiv) of sodium thiomethoxide dissolved in 15 mL anhydrous DMF. An aliquot of 2.0 g (8.1 mmol, 1.0 equiv) of 2-(2-bromo-5-fluorophenyl)-1,3-dioxolane was added to this solution and the reaction mixture was stirred overnight (18 h) at 100 $^\circ\text{C}$. The cooled reaction mixture was treated with 40 mL brine and extracted 4x with 50 mL portions of diethyl ether. The combined organic phases were dried over Na_2SO_4 and evaporated under reduced pressure. Column purification ($R_f = 0.37$, hexane/EtOAc [10:1]) gave 40 % (0.9 g) of 2-(2-bromo-5-(methylthio)phenyl)-1,3-dioxolane as a colorless oil. ^1H -NMR (500 MHz, CDCl_3) δ 7.48 (d, $J = 2.2$ Hz, 1H), 7.46 (d, $J = 8.4$ Hz, 1H), 7.26 (s, 1H), 7.10 (dd, $J = 8.4$, 2.3 Hz, 1H), 4.16 (dd, $J = 8.8$ Hz, 5.1 Hz, 2H), 4.07 (dd, $J = 8.7$ Hz, 5.1 Hz, 2H), 2.47 (d, $J = 7.4$ Hz, 3H). ^{13}C -NMR (125 MHz, CDCl_3) δ 138.41, 136.86, 133.17, 128.48, 125.68, 119.02, 102.35, 65.49, 15.87. HRMS (EI) m/z calculated for $\text{C}_{10}\text{H}_{11}\text{O}_2\text{BrS}$ [$\text{M} + \text{H}$] $^+$ 273.9658, found 273.9666.

A 50 mL one-neck round bottom flask was charged with 885.0 mg (3.2 mmol, 1.0 equiv) of 2-(2-bromo-5-(methylthio)phenyl)-1,3-dioxolane dissolved in 18 mL of THF. The solution was treated with 6 mL (12.1 mmol, 3.75 equiv) of 2 M hydrochloric acid and refluxed for 1.5 h. The reaction was monitored by SiO_2 -TLC ($R_f = 0.53$, hexane/EtOAc [10:1]) until no starting material was detected. The reaction was quenched with 25 mL water and the mixture extracted twice with 25 mL portions of ethyl acetate. The combined organic phases were dried over Na_2SO_4 and concentrated under evaporation to give 93% yield (689.0 mg) of the aldehyde as a colorless oil. The crude aldehyde was used in the subsequent Wittig reaction without further purification. ^1H -NMR (400 MHz, CDCl_3) δ = 10.33 (s, 1H), 7.73 (d, $J = 2.5$ Hz, 1H), 7.53 (d, $J = 8.4$ Hz, 1H), 7.31 (dd, $J = 8.4$ Hz, 2.5 Hz, 1H), 2.51 (s, 3H). HRMS (EI) m/z calculated for $\text{C}_8\text{H}_7\text{OBrS}$ [$\text{M} + \text{H}$] $^+$ 229.9396, found 229.9391.

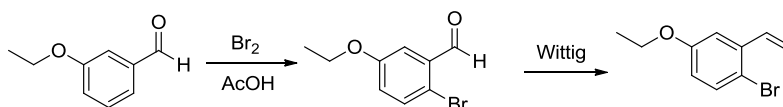
The aldehyde was employed in a Wittig olefination to prepare the styrene **3.14** in a fashion similar to that described for the synthesis of **3.4**. The 2-bromo-5-thiomethoxystyrene **4f** was purified by column chromatography using 10:1 hexanes/EtOAc as the eluent. The styrene **3.14** was isolated as a clear, colorless oil in 70% yield. $^1\text{H-NMR}$ (300 MHz, CDCl_3) δ 7.45 (d, $J = 8.4$ Hz), 7.41 (d, $J = 2.4$ Hz), 7.08 – 6.94 (m), 7.08 – 6.93 (m), 5.70 (dd, $J = 17.4, 0.9$ Hz), 5.38 (dd, $J = 11.0, 0.9$ Hz), 2.49 (s). $^{13}\text{C-NMR}$ (100 MHz, CDCl_3) δ 138.1, 137.8, 135.5, 133.1, 127.3, 124.8, 120.0, 117.2. HRMS (EI) m/z calculated for $\text{C}_9\text{H}_{11}\text{BrS}$ $[\text{M} + \text{H}]^+$ 227.9603, found 227.9601.



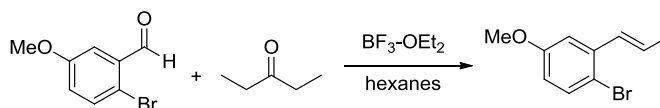
Compound 3.15. The 2-amino-5-methylbenzyl alcohol (3.04 g, 22.2 mmol, 1.0 equiv) was dissolved in 20 mL of concentrated HBr and the mixture cooled to $0\text{ }^\circ\text{C}$. NaNO_2 (1.58 g, 23.0 mmol, 1.04 equiv) dissolved in 10 mL of H_2O was added dropwise. The solution was allowed to stir at rt for 1 h. Meanwhile, a 100 mL round bottom flask equipped with a reflux condenser was charged with CuBr (1.68 g, 11.7 mmol, 0.53 equiv) was dissolved in 5 mL of conc. HBr and heated to $140\text{ }^\circ\text{C}$. The diazonium salt solution was added dropwise to the refluxing CuBr solution over 15-20 min. The heat was removed and the reaction was allowed to cool to rt slowly and stirred overnight. The reaction mixture was poured into CH_2Cl_2 . The aqueous layer was extracted 3x with portions of CH_2Cl_2 and the combined organic layers were dried over Na_2SO_4 and concentrated *in vacuo*. The crude material was purified by column chromatography with hexanes as the eluent to give 2-bromo-5-methyl benzyl bromide in 41% yield as a clear, colorless oil.

A 100 mL round bottom flask was charged with 2-bromo-5-methylbenzyl bromide (2.56 g, 9.69 mmol, 1.0 equiv) dissolved in 40 mL dry DMSO and KHCO_3 (4.91 g, 49.1 mmol, 5.1 equiv). The reaction mixture was heated under nitrogen at $80\text{ }^\circ\text{C}$ overnight. The reaction mixture was allowed to cool to rt and then poured into water/ CH_2Cl_2 . The organic layer was washed two additional times with portions of water. The combined organic layers were dried over Na_2SO_4 and concentrated *in vacuo*. The 2-bromo-5-methylbenzaldehyde was purified with column chromatography using hexanes/ EtOAc as the eluent. A gradient was employed using 0-8% EtOAc in 2% increments. The aldehyde was isolated as a clear colorless oil in 71% yield.

The aldehyde was used as the substrate for a Wittig olefination to prepare the styrene **3.15** in a fashion similar to that described for the synthesis of **3.4**. The 2-bromo-5-methylstyrene was purified by column chromatography using hexanes as the eluent. The styrene **3.15** was isolated as a clear, colorless oil in 68% yield. ^1H NMR (500 MHz, CDCl_3) δ 7.41 (d, $J = 8.1$ Hz, 1H), 7.36 (d, $J = 1.4$ Hz, 1H), 7.03 (dd, $J = 17.5, 10.9$ Hz, 1H), 6.93 (dd, $J = 8.1, 2.2$ Hz, 1H), 5.68 (d, $J = 17.4$ Hz, 1H), 5.33 (d, $J = 10.9$ Hz, 1H), 2.31 (s, 3H). ^{13}C NMR (126 MHz, CDCl_3) δ 137.25, 137.00, 135.83, 132.54, 130.03, 127.37, 120.32, 116.32, 20.96. HRMS (EI) m/z calculated for $\text{C}_9\text{H}_9\text{Br}$ $[\text{M}]^+$ 195.9883, found 195.9883.

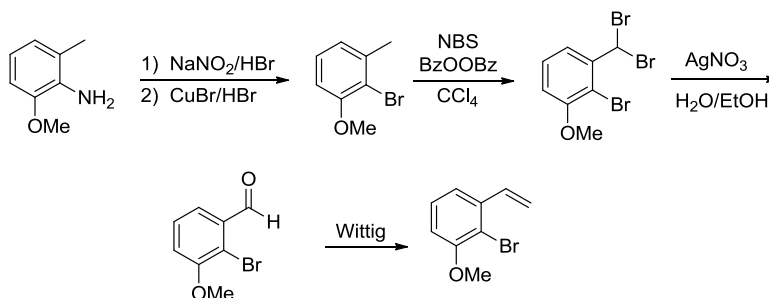


Compound 3.16. Compound **3.16** was synthesized and purified in a fashion similar to that described for **3.4**. The 2-bromo-5-ethoxybenzaldehyde was isolated as a clear colorless oil in 91% yield and the styrene **3.16** was isolated as a clear colorless oil in 45% yield. ^1H NMR (500 MHz, CDCl_3) δ 7.41 (d, $J = 8.8$ Hz, 1H), 7.07 (d, $J = 3.0$ Hz, 1H), 7.01 (dd, $J = 17.4, 10.9$ Hz, 1H), 6.69 (dd, $J = 8.8, 3.0$ Hz, 1H), 5.68 (dd, $J = 17.4, 1.0$ Hz, 1H), 5.35 (dd, $J = 10.9, 1.0$ Hz, 1H), 4.03 (q, $J = 7.0$ Hz, 2H), 1.42 (t, $J = 7.0$ Hz, 3H). ^{13}C NMR (126 MHz, CDCl_3) δ 158.32, 138.12, 135.89, 133.36, 116.63, 115.71, 114.14, 112.60, 63.73, 14.77. HRMS (EI) m/z calculated for $\text{C}_{10}\text{H}_{11}\text{BrO}$ $[\text{M}]^+$ 225.9988, found 225.9992.



Compound 3.17. A flame-dried 250 mL round bottom flask equipped with a reflux condenser under an atmosphere of N_2 was charged with 80 mL of hexanes and 2-pentanone (4.5 mL, 42.5 mmol, 0.98 equiv). Boron trifluoride diethyl etherate (5.5 mL, 44.6 mmol, 1.02 equiv) was added slowly, followed by 2-bromo-5-methoxybenzaldehyde (9.36 g, 43.5 mmol, 1.0 equiv). The reaction was allowed to reflux for 1 h and then carefully quenched with water. The aqueous phase was extracted twice with hexanes and the combined organic layers were dried with Na_2SO_4 and concentrated *in vacuo*. The crude material was purified using column chromatography with hexanes as the initial eluent. A mobile phase consisting of 99.5% hexanes/0.5% EtOAc was then employed until the material had fully eluted. The 2-bromo-5-methoxy-*trans*- β -methylstyrene **3.17** was isolated as a clear, colorless oil in 27% yield. ^1H NMR (500 MHz, CDCl_3) δ 7.40 (d, $J = 8.7$ Hz, 1H), 7.00 (d, $J = 3.0$ Hz, 1H), 6.68 (dq, $J = 15.7, 1.8$ Hz, 1H), 6.65

(dd, $J = 8.8, 3.1$ Hz, 1H), 6.18 (dq, $J = 15.6, 6.7$ Hz, 1H), 3.79 (s, 3H), 1.92 (dd, $J = 6.7, 1.8$ Hz, 3H). ^{13}C NMR (126 MHz, CDCl_3) δ 158.89, 138.39, 133.28, 129.94, 128.97, 114.30, 113.76, 111.91, 55.43, 18.64. HRMS (EI) m/z calculated for $\text{C}_{10}\text{H}_{11}\text{BrO} [\text{M}]^+$ 225.9988, found 225.9990.

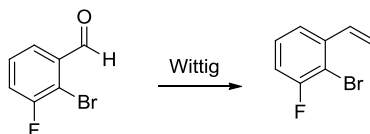


Compound 3.18. The 2-bromo-3-methoxytoluene was prepared in similar fashion as described for the synthesis of **3.15**. The crude material was purified by column chromatography with hexanes/EtOAc as the eluent. A gradient was employed using 0-3% EtOAc in 1% increments. The 2-bromo-3-methoxytoluene was isolated as a clear colorless oil which solidified upon standing in 47% yield.

A 500 mL round bottom flask was charged with 2-bromo-3-methoxytoluene (1.7 mL, 11.7 mmol, 1.0 equiv), NBS (5.32 g, 29.9 mmol, 2.56 equiv) and benzoyl peroxide (0.28 g, 1.15 mmol, 0.098 equiv) in 50 mL of carbon tetrachloride. The reaction was refluxed for 3 h under irradiation with a 300 W lamp. The reaction mixture was then filtered through pad of Celite and washed with CH_2Cl_2 . The solvent was removed *in vacuo* and the residue dissolved in 50 mL 4:1 EtOH:H₂O. AgNO_3 (5.12 g, 30.1 mmol, 2.57 equiv) was added to the ethanol solution and the reaction mixture was refluxed for 1 h. The reaction was filtered through a pad of Celite and washed with EtOAc. The volume of the filtrate was reduced to about 20 mL and then added to a mixture of water and EtOAc. The aqueous layer was extracted 2x with portions of EtOAc and the combined organic layers were dried over Na_2SO_4 and concentrated *in vacuo*. The crude material was purified by column chromatography with hexanes/EtOAc as the eluent. A gradient was employed using 0-8% EtOAc in 2% increments. The 2-bromo-3-methoxybenzaldehyde was isolated a white solid in 82% yield over two steps.

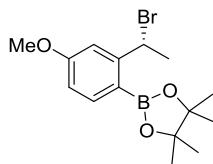
The aldehyde was employed as the substrate for a Wittig olefination to prepare the styrene **4j** in a fashion similar to that described for the synthesis of **3.4**. The 2-bromo-3-methoxystyrene was purified by column chromatography using hexanes/EtOAc as the eluent. A gradient was employed using 0-1% EtOAc in 0.5% increments. The styrene **4j** was isolated as a white solid in 64% yield. ^1H NMR (500 MHz, CDCl_3) δ 7.24 (t, $J = 7.9$ Hz, 1H), 7.17 (d, $J =$

6.5 Hz, 1H), 7.12 (dd, $J = 17.5, 11.0$ Hz, 1H), 6.82 (d, $J = 7.8$ Hz, 1H), 5.70 (dd, $J = 17.4, 1.3$ Hz, 1H), 5.37 (dd, $J = 11.0, 1.2$ Hz, 1H), 3.90 (s, 3H). ^{13}C NMR (126 MHz, CDCl_3) δ 156.03, 139.20, 136.09, 127.78, 118.98, 116.99, 113.21, 110.74, 56.41. HRMS (EI) m/z calculated for $\text{C}_9\text{H}_9\text{BrO} [\text{M}]^+$ 211.9832, found 211.9835.



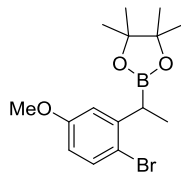
Compound 3.19. The 2-bromo-3-fluorobenzaldehyde was used as the substrate for a Wittig olefination to prepare the styrene **3.19** in a fashion similar to that described for the synthesis of **3.4**. The 2-bromo-3-fluorostyrene was purified by column chromatography using hexanes as the eluent. The styrene **3.19** was isolated as a clear colorless oil in 36% yield. ^1H NMR (500 MHz, CDCl_3) δ 7.34 (d, $J = 7.9$ Hz, 1H), 7.24 (td, $J = 8.0, 5.5$ Hz, 1H), 7.06 (dd, $J = 17.7, 11.0$ Hz, 1H), 7.03 (td, $J = 8.5, 1.8$ Hz, 1H), 5.74 (dd, $J = 17.4, 0.9$ Hz, 1H), 5.42 (d, $J = 11.0$ Hz, 1H). ^{13}C NMR (126 MHz, CDCl_3) δ 160.20, 158.24, 139.75, 134.86, 134.83, 128.18, 128.12, 121.95, 121.93, 117.88, 115.19, 115.01, 110.59, 110.42. HRMS (EI) m/z calculated for $\text{C}_8\text{H}_6\text{BrF} [\text{M}]^+$ 199.9632, found 199.9633.

3.7.2 Procedure for the Asymmetric 1,3-Halogen Migration Reaction

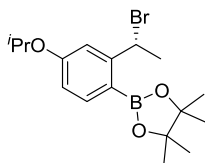


Compound 3.2. In a glovebox, CuCl (10.0 mg, 0.101 mmol, 0.10 equiv), NaO^tBu (20.0 mg, 0.208 mmol, 0.21 equiv), (*S,S*)-Ph-BPE (51.0 mg, 0.101 mmol, 0.10 equiv) and 10 mL of dry, degassed toluene were added to a dry, 25 mL round bottom flask. The flask was fitted with a septum, removed from the glovebox and the reaction mixture stirred for 10 min. HBpin (0.18 mL, 1.24 mmol, 1.20 equiv) was added in one aliquot and the reaction was transferred to a cryo-bath set to $0\text{ }^\circ\text{C}$ and stirred for a further 10 min. The 2-bromo-5-methoxy-styrene (0.16 mL, 1.03 mmol, 1.0 equiv) was added and reaction was allowed to stir for 18 h at $0\text{ }^\circ\text{C}$. The mixture was filtered through a pad of Celite and the solids washed with Et_2O (3x10 mL). The volatiles were removed *in vacuo* and the residue purified by column chromatography using 8% EtOAc in hexanes as the eluent. The product **3.2** was isolated as a clear, colorless, viscous liquid in 72% yield and 96% *ee*. $[\alpha]_{\text{D}}^{24} -0.325$ ($c = 0.039$ g/mL, CH_2Cl_2 , $l = 4.5$ cm) All spectroscopic data were with those described in 2.5.2.

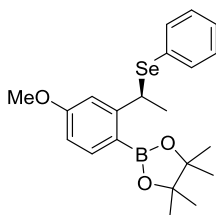
The following compounds were prepared in the same fashion as **3.2**, with exceptions noted as necessary.



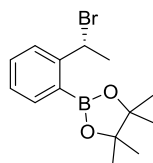
Compound 3.3. Compound **3.3** was prepared in the same fashion as described for the preparation of **3.2**, except Xantphos was employed as the ligand in place of (*S,S*)-Ph-BPE and the reaction was conducted at 40 °C. An integrated ^1H NMR yield of 69% was obtained using 1,1,1,2-tetrachloroethane as an internal standard. ^1H NMR (300 MHz, CDCl_3) δ 7.39 (d, $J = 8.7$ Hz, 1H), 6.83 (d, $J = 3.0$ Hz, 1H), 6.57 (dd, $J = 8.7, 3.0$ Hz, 1H), 3.77 (s, 3H), 2.73 (q, $J = 7.5$ Hz, 1H), 1.33 (d, $J = 7.5$ Hz, 3H), 1.24 (s, 12H). ^{13}C NMR (75 MHz, CDCl_3) δ 159.23, 145.80, 133.09, 115.66, 115.15, 112.26, 83.69, 55.50, 24.96, 24.90, 15.94. HRMS (ESI) m/z calculated for $\text{C}_{15}\text{H}_{26}\text{BrNO}$ $[\text{M}+\text{NH}_4]^+$ 357.1220, found 357.1217.



Compound 3.9. Compound **3.9** was prepared in the same fashion as described for compound **3.2**. The product was purified by column chromatography using 5% EtOAc in hexanes as the eluent. The product was isolated as a clear, colorless, viscous liquid in 53% yield and >99% ee. ^1H NMR (400 MHz, CDCl_3) δ 7.71 (d, $J = 8.3$ Hz, 1H), 7.19 (d, $J = 2.2$ Hz, 1H), 6.76 (dd, $J = 8.3, 2.3$ Hz, 1H), 6.24 (q, $J = 6.8$ Hz, 1H), 4.63 (hept, $J = 6.0$ Hz, 1H), 1.99 (d, $J = 6.9$ Hz, 3H), 1.35 (s, 6H), 1.33 (s, 6H). ^{13}C NMR (101 MHz, CDCl_3) δ 160.58, 151.72, 137.86, 114.41, 114.01, 83.53, 69.56, 48.53, 27.24, 25.01, 24.71, 21.98. HRMS (ESI) m/z calculated for $\text{C}_{17}\text{H}_{30}\text{BrBNO}_3$ $[\text{M}+\text{NH}_4]^+$ 385.1533, found 385.1533.

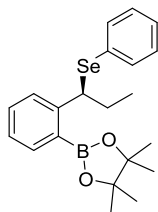


Compound 3.10. Compound **3.10** was prepared in the same fashion as described for compound **3.2** except the benzyl iodide was trapped with lithium phenylselenoate prior to isolation. Selenium (0.2199 g, 2.78 mmol, 2.81 equiv.) was added to a flame-dried conical flask under nitrogen and diluted with THF to prepare a 1 M solution. Phenyllithium (1.7 mL of a 1.78 M solution, 3.03 mmol, 3.06 equiv.) was added to the selenium/THF mixture and the LiSePh solution allowed to form at ambient temperature for 30 min. The solution was transferred to the flask containing the benzyl bromide and the reaction mixture was allowed to stir at ambient temperature for 2 h. The mixture was filtered through a pad of Celite and the solids washed with Et₂O (3x10mL). The filtrate was concentrated *in vacuo* and the residue was purified by column chromatography using hexanes/EtOAc as the eluent in a 0-8% gradient in 2% increments. Compound **3.10** was isolated as a pale yellow, viscous oil in 71% yield. ¹H NMR (500 MHz, CDCl₃) δ 7.72 (d, *J* = 8.3 Hz, 1H), 7.46 (dd, *J* = 8.1, 1.6 Hz, 2H), 7.25 – 7.17 (m, 3H), 6.88 (d, *J* = 2.4 Hz, 1H), 6.72 (dd, *J* = 8.3, 2.5 Hz, 1H), 5.55 (q, *J* = 7.0 Hz, 1H), 3.78 (s, 3H), 1.71 (d, *J* = 6.9 Hz, 3H), 1.32 (s, 12H). ¹³C NMR (126 MHz, CDCl₃) δ 161.86, 152.36, 137.93, 134.80, 130.38, 128.56, 127.28, 112.24, 111.33, 83.37, 55.06, 39.69, 24.91, 24.82, 22.36. HRMS (ESI) *m/z* calculated for C₂₁H₂₈BO₃Se [M+H]⁺ 432.1584, found 432.1588.

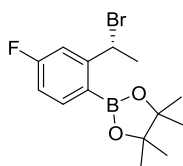


Compound 3.11. Compound **3.11** was prepared in the same manner as compound **3.2**. The crude material was purified by column chromatography using hexanes as the initial eluent. The eluent was then switched to 10% EtOAc/hexanes. The product was isolated as clear colorless, viscous oil in 28% yield. All spectroscopic data were with those described in 2.5.2.

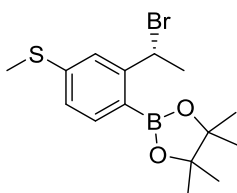
To determine enantiomeric excess, the product was trapped with 2-thionaphthalene as described for the sulfide of compound **3.26**. The sulfide was isolated in 84% *ee*. ¹H NMR (500 MHz, CDCl₃) δ 7.80 – 7.73 (m, 3H), 7.70 – 7.64 (m, 2H), 7.57 (dd, *J* = 7.7, 1.1 Hz, 1H), 7.46 – 7.36 (m, 4H), 7.21 (td, *J* = 7.4, 1.1 Hz, 1H), 5.57 (q, *J* = 6.9 Hz, 1H), 1.64 (d, *J* = 6.9 Hz, 3H), 1.33 (s, 6H), 1.32 (s, 6H). ¹³C NMR (126 MHz, CDCl₃) δ 149.41, 135.95, 133.66, 133.65, 131.98, 131.23, 129.33, 129.00, 127.85, 127.61, 127.23, 126.27, 126.22, 125.63, 83.72, 44.41, 24.90, 24.86, 22.47.



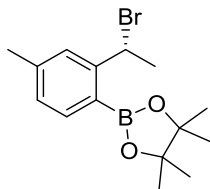
Compound 3.12. Compound **3.12** was prepared and purified in the same manner as compound **3.10**. The product was isolated as a pale yellow, viscous oil in 40% yield and 89% *ee*. ^1H NMR (500 MHz, CDCl_3) δ 7.73 (d, $J = 7.5$ Hz, 1H), 7.43 (d, $J = 6.9$ Hz, 2H), 7.36 (d, $J = 3.5$ Hz, 2H), 7.23 – 7.14 (m, 4H), 5.32 (dd, $J = 8.6, 6.7$ Hz, 1H), 2.09 – 2.00 (m, 2H), 1.33 (s, 6H), 1.32 (s, 6H), 0.86 (t, $J = 7.3$ Hz, 6H). ^{13}C NMR (126 MHz, CDCl_3) δ 148.96, 135.81, 134.72, 131.06, 130.42, 128.50, 127.13, 126.85, 125.77, 83.58, 47.40, 29.92, 24.95, 24.79, 13.07. HRMS (ESI) m/z calculated for $\text{C}_{21}\text{H}_{28}\text{BSeO}_2$ $[\text{M}+\text{H}]^+$ 399.1369, found 399.1374.



Compound 3.13. Compound **3.13** was prepared in the same fashion as described for compound **3.2**. The product was purified by column chromatography using 5% EtOAc in hexanes as the eluent. The product was isolated as a clear, colorless, viscous liquid in 38% yield and 81% *ee*. $[\alpha]_{\text{D}}^{24}$ -0.030 ($c = 0.018$ g/mL, CH_2Cl_2 , $l = 4.5$ cm) All spectroscopic data were with those described in 2.5.2.

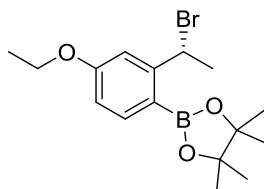


Compound 3.20. Compound **3.20** was prepared in the same fashion as described for compound **3.2**. An integrated ^1H NMR yield of 13% was obtained using 1,1,1,2-tetrachloroethane as an internal standard. ^1H NMR (500 MHz, CDCl_3) δ 7.68 (d, $J = 7.9$ Hz, 1H), 7.53 (d, $J = 1.8$ Hz, 1H), 7.10 (dd, $J = 8.0, 1.9$ Hz, 1H), 6.21 (q, $J = 6.9$ Hz, 1H), 2.51 (s, 3H), 2.00 (d, $J = 6.9$ Hz, 3H), 1.36 (s, 6H), 1.34 (s, 6H). ^{13}C NMR (126 MHz, CDCl_3) δ 150.00, 142.97, 136.37, 124.36, 123.99, 83.81, 48.17, 27.12, 24.98, 24.87, 24.84, 24.72, 24.70, 24.64, 15.07. HRMS (ESI) m/z calculated for $\text{C}_{15}\text{H}_{26}\text{BrBNO}_2\text{S}$ $[\text{M}+\text{NH}_4]^+$ 373.1070, found 373.1060.



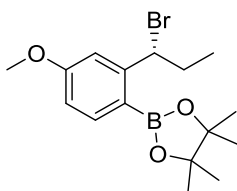
Compound 3.21. Compound **3.21** was prepared in the same fashion as described for compound **3.2**. The crude material was purified by column chromatography using hexanes as the initial eluent. The eluent was then switched to 10% EtOAc/hexanes. The product was isolated as a clear, colorless, viscous oil in 30% yield. ^1H NMR (500 MHz, CDCl_3) δ 7.67 (d, $J = 7.6$ Hz, 1H), 7.49 (s, 1H), 7.08 (d, $J = 7.6$ Hz, 1H), 6.25 (q, $J = 6.9$ Hz, 1H), 2.37 (s, 3H), 2.01 (d, $J = 6.9$ Hz, 3H), 1.36 (s, 6H), 1.34 (s, 6H). ^{13}C NMR (126 MHz, CDCl_3) δ 149.48, 141.66, 136.05, 128.18, 127.18, 83.69, 48.80, 27.08, 24.98, 24.86, 24.68, 21.72. HRMS (ESI) m/z calculated for $\text{C}_{15}\text{H}_{26}\text{BBrNO}_2$ $[\text{M}+\text{NH}_4]^+$ 341.1271, found 341.1272.

To determine enantiomeric excess, the product was trapped with lithium phenylselenoate as described for compound **3.10**. The selenide was isolated in 85% *ee*. $[\alpha]_{\text{D}}^{24} -0.077$ ($c = 0.025$ g/mL, CH_2Cl_2 , $l = 4.5$ cm) ^1H NMR (500 MHz, CDCl_3) δ 7.66 (d, $J = 7.6$ Hz, 1H), 7.45 (dd, $J = 7.9, 1.5$ Hz, 2H), 7.25 – 7.18 (m, 3H), 7.16 (s, 1H), 7.01 (d, $J = 7.5$ Hz, 1H), 5.54 (q, $J = 7.0$ Hz, 1H), 2.31 (s, 3H), 1.72 (d, $J = 7.0$ Hz, 3H), 1.33 (s, 6H), 1.32 (s, 6H). ^{13}C NMR (126 MHz, CDCl_3) δ 149.89, 141.07, 136.17, 134.68, 130.67, 128.55, 127.22, 127.07, 126.84, 83.49, 39.91, 24.90, 24.86, 22.40, 21.69. HRMS (EI) m/z calculated for $\text{C}_{21}\text{H}_{27}\text{BO}_2\text{Se}$ $[\text{M}]^+$ 416.1645, found 416.1642.



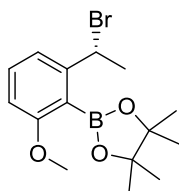
Compound 3.22. Compound **3.22** was prepared and purified in the same manner as compound **3.2**. The product was isolated as a clear, colorless, viscous oil in 57% yield. ^1H NMR (500 MHz, CDCl_3) δ 7.72 (d, $J = 8.3$ Hz, 1H), 7.21 (d, $J = 2.4$ Hz, 1H), 6.77 (dd, $J = 8.4, 2.4$ Hz, 1H), 6.25 (q, $J = 6.8$ Hz, 1H), 4.13 – 4.03 (m, 2H), 1.99 (d, $J = 6.8$ Hz, 3H), 1.43 (t, $J = 7.0$ Hz, 3H), 1.35 (s, 6H), 1.34 (s, 6H). ^{13}C NMR (126 MHz, CDCl_3) δ 161.57, 151.65, 137.87, 113.20, 112.98, 83.54, 63.33, 48.48, 27.17, 24.99, 24.68, 14.74. HRMS (ESI) m/z calculated for $\text{C}_{16}\text{H}_{28}\text{BBrNO}_3$ $[\text{M}+\text{NH}_4]^+$ 371.1377, found 371.1369.

To determine enantiomeric excess, the product was trapped with 2-thionaphthalene as described for the sulfide of compound **3.26**. The sulfide was isolated in 89% *ee*. ^1H NMR (500 MHz, CDCl_3) δ 7.78 – 7.71 (m, 3H), 7.67 (d, J = 8.7 Hz, 2H), 7.45 – 7.38 (m, 3H), 7.13 (d, J = 2.4 Hz, 1H), 6.73 (dd, J = 8.3, 2.5 Hz, 1H), 5.61 (q, J = 6.9 Hz, 1H), 4.08 – 3.97 (m, 2H), 1.61 (d, J = 6.9 Hz, 3H), 1.38 (t, J = 7.0 Hz, 3H), 1.31 (s, 12H). ^{13}C NMR (126 MHz, CDCl_3) δ 161.56, 151.93, 137.94, 133.86, 133.65, 131.90, 128.93, 128.77, 127.80, 127.58, 127.17, 126.18, 125.53, 112.77, 112.17, 83.39, 63.20, 44.15, 24.86, 24.84, 22.71, 14.73. HRMS (EI) m/z calculated for $\text{C}_{26}\text{H}_{32}\text{BO}_3\text{S}$ $[\text{M}+\text{H}]^+$ 434.2197, found 434.2195.

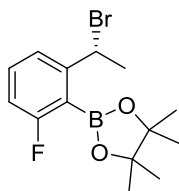


Compound 3.23. Compound **3.23** was prepared and purified in the same manner as compound **3.2**. The product was isolated as a clear, colorless, viscous oil in 50% yield. ^1H NMR (500 MHz, CDCl_3) δ 7.73 (d, J = 8.4 Hz, 1H), 7.19 (d, J = 2.4 Hz, 1H), 6.79 (dd, J = 8.4, 2.5 Hz, 1H), 6.00 (dd, J = 7.8, 6.7 Hz, 1H), 3.84 (s, 3H), 2.29 – 2.03 (m, 2H), 1.34 (s, 6H), 1.33 (s, 6H), 0.99 (t, J = 7.2 Hz, 3H). ^{13}C NMR (126 MHz, CDCl_3) δ 162.21, 150.73, 137.73, 113.37, 112.70, 83.56, 56.15, 55.17, 34.21, 24.87, 24.84, 12.86. HRMS (ESI) m/z calculated for $\text{C}_{16}\text{H}_{28}\text{BBrNO}_3$ $[\text{M}+\text{NH}_4]^+$ 371.1377, found 371.1373.

To determine enantiomeric excess, the product was trapped with 2-thionaphthalene as described for the sulfide of compound **3.26**. The sulfide was isolated in 93% *ee*. ^1H NMR (500 MHz, CDCl_3) δ 7.77 – 7.70 (m, 3H), 7.67 – 7.62 (m, 2H), 7.46 – 7.35 (m, 3H), 7.15 (d, J = 2.5 Hz, 1H), 6.73 (dd, J = 8.4, 2.5 Hz, 1H), 5.44 (dd, J = 8.6, 6.0 Hz, 1H), 3.78 (s, 3H), 2.05 – 1.86 (m, 2H), 1.32 (s, 6H), 1.31 (s, 6H), 0.91 (t, J = 7.4 Hz, 3H). ^{13}C NMR (126 MHz, CDCl_3) δ 162.24, 151.16, 137.74, 133.97, 133.63, 131.80, 128.77, 128.76, 127.73, 127.55, 127.12, 126.12, 125.44, 112.35, 111.81, 83.38, 55.05, 50.69, 30.62, 24.95, 24.79, 12.18. HRMS (EI) m/z calculated for $\text{C}_{26}\text{H}_{32}\text{BO}_3\text{S}$ $[\text{M}+\text{H}]^+$ 434.2197, found 434.2193.



Compound 3.24. Compound **3.24** was prepared and purified in the same manner as compound **3.2**. The product was isolated as a clear, colorless, viscous oil in 50% yield and 70% *ee*. ^1H NMR (500 MHz, CDCl_3) δ 7.32 (t, J = 8.0 Hz, 1H), 7.19 (d, J = 7.8 Hz, 1H), 6.74 (d, J = 8.3 Hz, 0H), 5.36 (q, J = 6.9 Hz, 1H), 3.78 (s, 3H), 2.03 (d, J = 6.9 Hz, 3H), 1.42 (s, 6H), 1.41 (s, 6H). ^{13}C NMR (126 MHz, CDCl_3) δ 162.50, 148.01, 131.09, 118.45, 109.57, 84.15, 55.72, 48.81, 26.98, 24.88, 24.73. HRMS (ESI) m/z calculated for $\text{C}_{15}\text{H}_{26}\text{BBrNO}_3$ $[\text{M}+\text{NH}_4]^+$ 357.1120, found 357.1208.



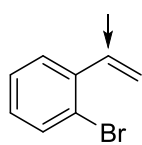
Compound 3.19. Compound **3.19** was prepared in the same fashion as described for compound **3.2**. An integrated ^1H NMR yield of 65% was obtained using 1,1,1,2-tetrachloroethane as an internal standard. The crude material was purified by column chromatography using hexanes as the initial eluent. The eluent was then switched to 10% EtOAc/hexanes. The product was isolated as a clear, colorless, viscous oil in 41% yield. ^1H NMR (500 MHz, CDCl_3) δ 7.43 – 7.33 (m, 2H), 6.93 (ddd, J = 8.9, 7.5, 1.7 Hz, 1H), 5.76 (q, J = 6.9 Hz, 1H), 2.04 (d, J = 6.9 Hz, 3H), 1.43 (s, 6H), 1.40 (s, 6H). ^{13}C NMR (126 MHz, CDCl_3) δ 166.94, 164.98, 149.87, 149.81, 132.12, 132.05, 121.77, 121.74, 114.76, 114.56, 84.36, 47.47, 47.45, 26.53, 24.92, 24.76. HRMS (ESI) m/z calculated for $\text{C}_{14}\text{H}_{23}\text{BBrFNO}_2$ $[\text{M}+\text{NH}_4]^+$ 345.1021, found 345.1020.

To determine enantiomeric excess, the product was trapped with 2-thionaphthalene as described for the sulfide of compound **3.26**. The sulfide was isolated in 81% *ee*. ^1H NMR (500 MHz, CDCl_3) δ 7.80 – 7.76 (m, 2H), 7.75 – 7.68 (m, 2H), 7.49 – 7.41 (m, 2H), 7.37 (dd, J = 8.5, 1.8 Hz, 1H), 7.33 – 7.25 (m, 2H), 6.90 (ddd, J = 9.0, 7.5, 1.7 Hz, 1H), 5.04 (q, J = 7.0 Hz, 1H), 1.68 (d, J = 7.0 Hz, 3H), 1.41 (s, 6H), 1.40 (s, 6H). ^{13}C NMR (126 MHz, CDCl_3) δ 166.20 (d, J = 245 Hz), 150.12 (d, J = 7.5 Hz), 133.64, 132.71, 132.06, 131.71 (d, J = 9.3 Hz), 129.52, 128.85, 128.03, 127.61, 127.30, 126.30, 125.81, 122.02 (d, J = 2.7 Hz), 113.66 (d, J = 24.5 Hz), 84.23, 45.53 (d, J = 1.9 Hz), 24.9 (d, J = 16 Hz), 22.54. HRMS (ESI) m/z calculated for $\text{C}_{24}\text{H}_{30}\text{BFNO}_2\text{S}$ $[\text{M}+\text{NH}_4]^+$ 408.1840, found 408.1834.

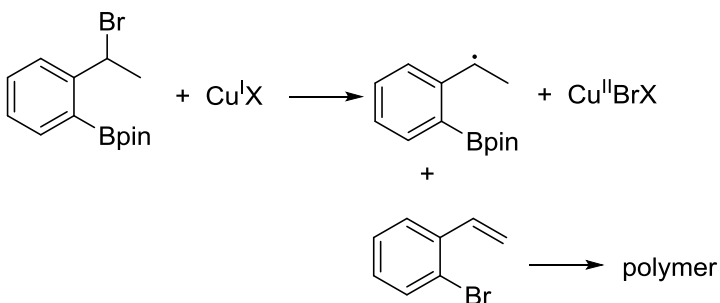
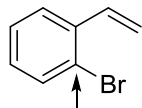
3.7.3 Developing the Predictive Model

The tables below summarize the computational data used to create and test the trend. The geometries and absolute energies can be found below the summary tables. All structures were optimized in Gaussian 09 using B3LYP/6-311++G(2d,p) and the vibrational frequencies were checked to make sure the structure was at a minimum on the potential energy surface. A Natural Population Analysis was performed at the same level of theory and basis set. The volume was calculated using the volume(tight) key word.

Electron Density at the Olefin: To quantify the electron density at the olefin, we used the NPA charge at the α carbon of the olefin (indicated as ' α ' in Figure 3.1, Table 3.6, Table 3.7 below) for a number of substituted styrenes. We believe that this is a reasonable assumption as this is the carbon that binds to the copper in the course of the reaction. The atomic charges at the β carbons of the various olefins did not appear to trend with the observed reactivity. In addition, the average electron density at the two carbons of the olefins were nearly the same for all the substrates that were initially optimized (H, 5-OMe, 5-F). Thus, this parameter does not appear to greatly impact the yield.



Electron Density at the Carbon Bearing Bromine: A more electron-rich sp^2 bromine-bearing carbon appeared to correlate with increased yield in the 1,3-halogen migration reaction, presumably because this facilitates the transposition of the bromine to the benzylic carbon. The importance of the electron density at this carbon is perhaps not surprising, as we hypothesize this carbon eventually binds to the copper catalyst during the course of the 1,3-halogen migration. To quantify the electron density at this carbon, we used the NPA charge (indicated as ' γ ' in Figure 3.1, Table 3.4, Table 3.6, Table 3.7) at the carbon bearing the bromine atom. Interestingly, it appears that this parameter has the largest impact on the yield of the reaction (except when the substrate is severely sterically congested).



Propensity to form Radicals: Atom Transfer Radical Polymerization (ATRP) is a major side reaction in this chemistry. It is well-known that a copper(I) salt can abstract the halide of a benzyl halide, resulting in a Cu(II) salt and a benzyl radical. The presence

of this radical can initiate the polymerization of the remaining styrene substrate, simultaneously deactivating the

catalyst and destroying the starting material. As would be expected, disfavoring this reaction is a prerequisite for high yields in the 1,3-halogen migration reaction. To quantify this empirical observation, the energy of the benzyl bromide (indicated as 'bn br e' in Table 3.6 and Table 3.7 below), the energy of the benzyl radical (denoted as 'rad e'), and the energy of the radical bromine (labeled as 'br rad e') was calculated. The ΔE (in kcal/mol) was calculated based upon these energies using the following formula: $[(\text{rad e} + \text{br rad e}) - \text{bn br e}] * 627.509$. The $\Delta\Delta E$ relative to the substituted product was calculated by subtracting the ΔE for the substituted product from the ΔE for all of the substituted products ($\Delta\Delta E$, in Figure 3.1, Table 3.4, Table 3.6, Table 3.7). The $\Delta\Delta E$ is the parameter used in generating an equation for the trend.

Sterics: Given the size of the Ph-BPE ligand, sterics are expected to play a significant role in the outcome of the reaction. However, sterics are traditionally difficult to parameterize. A values were initially investigated, as they are readily available for many groups. However, A values did not accurately reflect the steric effects that were present in many of our substrates. Fundamentally, A values quantify the steric interactions between a specific group and a proton, thus ignoring many of the potential steric interactions for many larger groups. A viable solution was to use the volumes of the groups bound to the aromatic ring as the steric parameter. The volumes of all substrates were calculated (in cm^3/mol) (molar V , in Table 3.6 and Table 3.7 below) and the volume of 2-bromostyrene was subtracted from volume of the substituted styrene (indicated as ' χ ' in Table 3.6 and Table 3.7 below). This χ value was used as the steric parameter when generating the equation. There is an important assumption concerning this steric parameter that should be kept in mind in analyzing data from our equation. The steric parameter does not take into account where the steric bulk is located; thus, for substrates where the steric bulk is closer to the reactive site, the yield would be expected to be lower as the steric interactions would be exacerbated. For substrates containing long chains attached to the aromatic, the calculated volume would be quite large, but only the first few carbons in the chain actually play a major role in affecting the yield. In these cases, the actual yield would probably be higher than that predicted by the model.

Creating the Trend Equation: The trend was modelled in Excel using the Solver add-on (See Figure 3.2). An initial equation was introduced into Excel that multiplied each of the parameters described above by a coefficient cell. The sums were then added together to generate a value that was designated as the predicted yield (denoted by 'pred. yield' in Table 3.6, Table 3.7 and Figure 3.2). A second equation was generated that calculated the difference

between the predicted yield and the actual NMR yield ('dif' in Table 3.6, Table 3.7 and Figure 3.2). Solver was then allowed to change the coefficient cells such that the average of the differences was close to zero and none of the differences was greater than +/- 10%. The following equation resulted from these calculations:

$$\text{pred. yield} = -0.547(\chi) + 227(\alpha) + -1220(\gamma) + 18.5(\Delta\Delta E)$$

This equation was created in a double blind fashion. Ten substrates were used to generate the equation (see Table 3.6: Substrates in Model). An additional four substrates were randomly excluded in the development of the initial equation. These substrates were used as a preliminary test of the accuracy of the equation (Table 3.7: Control group). All of the substrates outside the model were predicted within 12% yield. As many of the yields for the 1,3-halogen migration were measured by integrations of ^1H NMRs using an internal standard, a method that can give errors up to 10%, we felt this level of accuracy was sufficient for these initial studies.

Figure 3.2: Solver Parameters

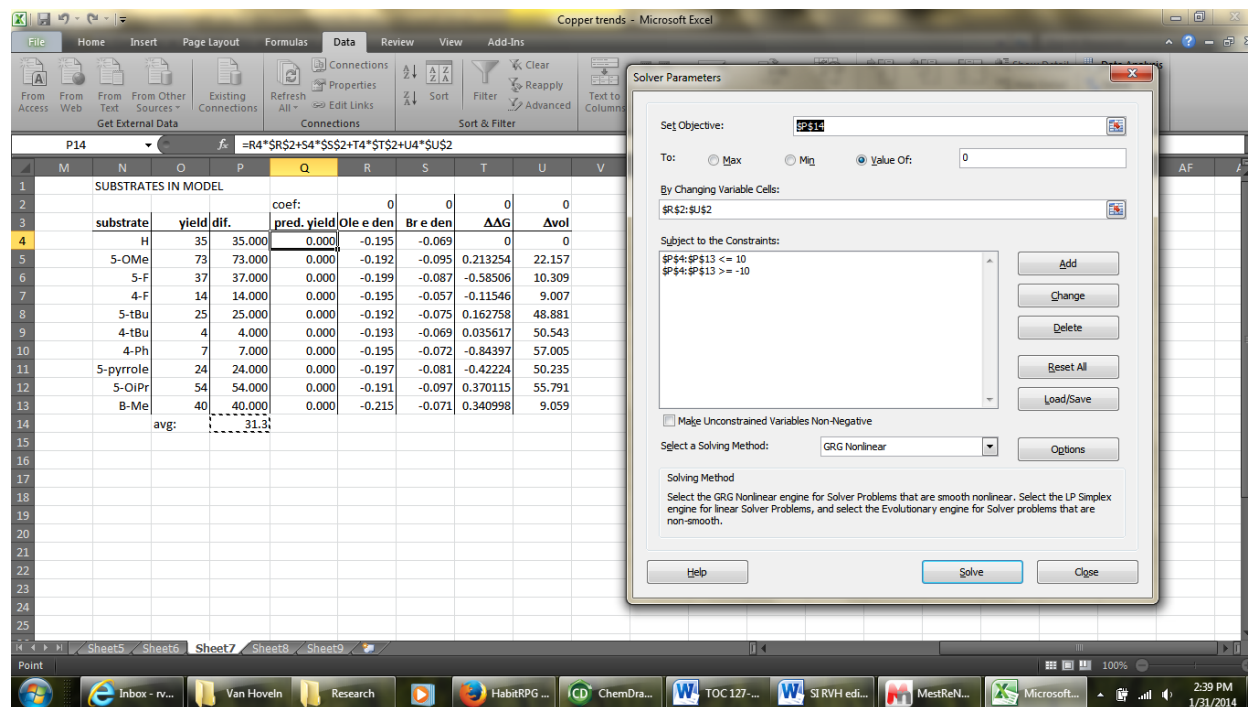


TABLE 3.6: SUBSTRATES IN MODEL

substrate	yield	pred. yield	coef:		α	γ	Bn rad. E.	Br rad. E.	rad. E.	ΔE	$\Delta\Delta E$	Molar Volume	χ
			abs. diff.	227.1366									
H	35	40.2	5.2		-0.195	-0.069	-3295.32	-2574.1	-721.14	54.975	0.000	111.428	0
5-OMe	73	64.5	8.5		-0.192	-0.095	-3409.89	-2574.1	-835.70	55.188	0.213	133.585	22.157
5-F	37	44.8	7.8		-0.199	-0.087	-3394.60	-2574.1	-820.41	54.390	-0.585	121.737	10.309
4-F	14	18.4	4.4		-0.195	-0.057	-3394.60	-2574.1	-820.41	54.859	-0.115	120.435	9.007
5-tBu	25	24.4	0.6		-0.192	-0.075	-3452.62	-2574.1	-878.44	55.138	0.163	160.309	48.881
4-tBu	4	13.6	9.6		-0.193	-0.069	-3452.62	-2574.1	-878.44	55.010	0.036	161.971	50.543
4-Ph	7	-3.0	10.0		-0.195	-0.072	-3526.44	-2574.1	-952.26	54.131	-0.844	168.433	57.005
5-pyrrole	24	19.1	4.9		-0.197	-0.081	-3504.35	-2574.1	-930.17	54.553	-0.422	161.663	50.235
5-OiPr	54	51.6	2.4		-0.191	-0.097	-3488.54	-2574.1	-914.36	55.345	0.370	167.219	55.791
β -Me	40	39.4	0.6		-0.215	-0.071	-3334.65	-2574.1	-760.46	55.316	0.341	120.487	9.059

TABLE 3.7: CONTROL GROUP

substrate	pred. yield	abs. diff.	coef:		Bn rad. E.	Br rad. E.	rad. E.	ΔE	$\Delta\Delta E$	Molar Volume	χ
			227.1366	-1223.84							
5-OBz	7.5	0.5	-0.197	-0.086	-3715.05	-2574.1	-1140.9	54.252	-0.723	183.864	72.436
5-OTBS	9.7	11.3	-0.194	-0.095	-3897.32	-2574.1	-1323.1	55.236	0.261	234.378	122.95
5-Br	24.1	8.1	-0.199	-0.076	-5868.86	-2574.1	-3294.7	54.438	-0.537	136.627	25.199
6-F	21.3	12.3	-0.214	-0.057	-3394.59	-2574.1	-820.41	54.945	-0.030	110.091	-1.337

Refining the Equation: A regression analysis was performed on the parameters from Table 3.6, the results of which are shown in Figure 3.3. A strong linear correlation was observed ($R^2 = 0.93$), however the parameter that accounted for the electron density at the olefin had an error that was significantly higher than the coefficient itself. As such, this parameter was removed and another regression analysis was performed (Figure 3.4). Interestingly, the linear correlation was still present and the standard error for all other parameters decreased. The new equation without that does not take into account the electron density at the olefin is:

$$\text{predicted yield} = -0.4321(\chi) - 1415(\gamma) + 16.22(\Delta\Delta E) - 63.16$$

The predicted yield was compared to actual yields and no one substrate deviated more than 10% (Table 3.8). Entries 1-10 represent the substrates whose parameters were used in the regression analysis and entries 11-14 represent the control group.

Figure 3.3: Regression Analysis of Parameters.

SUMMARY OUTPUT							
<i>Regression Statistics</i>							
Multiple R		0.964933457					
R Square		0.931096576					
Adjusted R Square		0.875973837					
Standard Error		7.520459316					
Observations		10					
<i>ANOVA</i>							
		<i>df</i>	<i>SS</i>	<i>MS</i>	<i>F</i>	<i>Significance F</i>	
Regression		4	3821.313458	955.3283646	16.8913336	0.004147168	
Residual		5	282.7865416	56.55730833			
Total		9	4104.1				
		<i>Coefficients</i>	<i>Standard Error</i>	<i>t Stat</i>	<i>P-value</i>	<i>Lower 95%</i>	<i>Upper 95%</i>
Intercept		-56.7390577	85.33091292	-0.664929692	0.53553131	-276.0891524	162.6110371
ΔV		-0.43592512	0.12532782	-3.478278946	0.01769139	-0.758090537	-0.1137597
Ole e den.		31.13904421	406.6093897	0.076582206	0.94192587	-1014.083667	1076.361755
Br e den.		-1412.29484	213.5100907	-6.614651484	0.00118822	-1961.139999	-863.449678
$\Delta\Delta G$		16.2529797	6.356456066	2.556924728	0.05083622	-0.086810806	32.5927702

Figure 3.4: Regression Analysis without Olefin Electron Density.

The screenshot shows an Excel spreadsheet with the following data:

SUMMARY OUTPUT								
Regression Statistics								
Multiple R		0.964891577						
R Square		0.931015755						
Adjusted R Square		0.896523632						
Standard Error		6.869233835						
Observations		10						
ANOVA								
		df	SS	MS	F	Significance F		
Regression		3	3820.981759	1273.660586	26.992127	0.00069928		
Residual		6	283.1182409	47.18637348				
Total		9	4104.1					
		Coefficients	Standard Error	t Stat	P-value	Lower 95%	Upper 95%	Lower 95.0%
Intercept		-63.1591141	14.54363994	-4.342730866	0.00486084	-98.74611897	-27.5721091	-98.746119
ΔV		-0.43209705	0.10497585	-4.116156699	0.00624309	-0.688963702	-0.1752304	-0.6889637
Br e den		-1414.65301	192.9825803	-7.330469953	0.00032937	-1886.86437	-942.441644	-1886.86437
$\Delta\Delta G$		16.22634303	5.79732752	2.798935022	0.03120772	2.040793615	30.41189244	2.040793615

Table 3.8: Predicted vs. Actual Yield using Refined Equation.

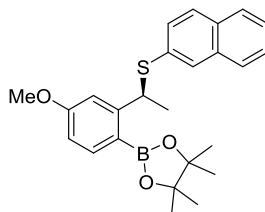
entry	substrate	pred. yield	actual yield	dif.
1	H	34.45	35	0.55
2	5-OMe	65.12	73	7.88
3	5-F	45.97	37	-8.97
4	4-F	11.71	14	2.29
5	5-tBu	24.46	25	0.54
6	4-tBu	13.19	4	-9.19
7	4-Ph	0.37	7	6.63
8	5-pyrrole	22.87	24	1.13
9	5-OiPr	55.96	54	-1.96
10	β -Me	38.90	40	1.10
11	5-OBz	15.48	8	-7.48
12	5-OTBS	22.34	21	-1.35
13	5-Br	24.75	16	-8.75
14	6-F	17.57	9	-8.57

Employing the Trend: A number of different substrates were optimized as potential candidates to be used in this methodology. Table 3.9 represents a summary of those substrates and their comparison of predicted vs. actual yield.

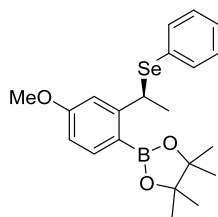
Table 3.9: Substrates Chosen for Testing the Predictive Model.

Substrate	int. = -63.16		coef: -1415							16.22	-0.4321	
	yield	pred. yield	dif.	γ	Bn rad. E	Br rad. E	rad. E	ΔE	$\Delta\Delta E$	Molar Volume	χ	
5-SMe	13	10.44	2.56	-0.066	-3732.87	-2574.1	-1158.68	55.01623	0.041478	158.733	47.305	
5-Me	30	36.51	-6.51	-0.075	-3334.65	-2574.1	-760.466	55.14445	0.169697	132.922	21.494	
5-OEt	57	57.6	-0.6	-0.09408	-3449.21	-2574.1	-875.025	55.42837	0.453615	157.01	45.582	
5-OMe- β -Me	50	62.66	-12.66	-0.09651	-3449.21	-2574.1	-875.022	55.18017	0.205421	143.922	32.494	
3-OMe	50	110.4	-60.4	-0.118	-3409.88	-2574.1	-835.69	55.89818	0.923425	130.751	19.323	
3-F	65	153.9	-88.9	-0.153	-3394.59	-2574.1	-820.405	55.01914	0.044386	111.626	0.198	

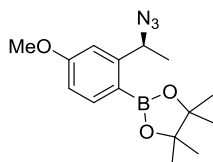
3.7.4 Displacement of the Benzyl Bromide with Nucleophiles



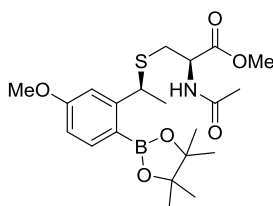
Compound 3.26. A solution of crude migration product **3.2** (21.7 mg, 0.06125 mmol, 1.0 equiv) in 300 μ L DMF was treated with 2-naphthalenethiol (15.3 mg, 0.096 mmol, 1.57 equiv) and K_2CO_3 (22.0 mg, 0.159 mmol, 2.60 equiv). The yellow mixture was stirred at rt until judged complete by TLC (generally 1 h). The reaction was quenched by the addition of EtOAc (10 mL) and water (10 mL), the layers partitioned and the aqueous layer extracted with EtOAc (3x 10 mL). The organic layers were combined, washed with brine (10 mL), dried over Na_2SO_4 and concentrated *in vacuo*. The residue was purified by column chromatography (0 – 75% gradient, CH_2Cl_2 /hexanes, 15% increments) and isolated as a clear oil (22.8 mg, 85%). 1H NMR (300 MHz, $CDCl_3$) δ 7.71 (m, 5H), 7.42 (m, 3H), 7.14 (d, $J = 2.5$ Hz, 1H), 6.74 (dd, $J = 8.3, 2.5$ Hz, 1H), 5.61 (q, $J = 6.9$ Hz, 1H), 3.78 (s, 3H), 1.62 (d, $J = 6.9$ Hz, 1H), 1.31 (s, 12H). ^{13}C NMR (75 MHz, $CDCl_3$) δ 162.43, 152.26, 138.20, 134.06, 133.90, 132.17, 129.24, 129.04, 128.06, 127.82, 127.41, 126.43, 125.79, 112.45, 111.97, 83.65, 55.30, 44.42, 25.10, 25.08, 22.97. HRMS (EI) m/z calculated for $C_{25}H_{30}BO_3S$ $[M+H]^+$ calculated 420.2040, found 420.2050.



Compound 3.27. Compound **3.27** was prepared from compound **1** in the same fashion as Compound **3.10**. The product was isolated in 70% yield and 83% *ee* in one pot and over two steps. $[\alpha]_D^{24}$ -0.199 (c = 0.075 g/mL, CH_2Cl_2 , $l = 4.5$ cm)

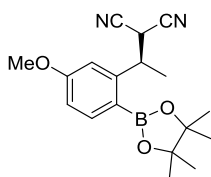


Compound 3.28. In a glovebox, a dry 25 mL round bottom flask was charged with CuCl (10 mg, 0.101 mmol, 10%), NaOtBu (20 mg, 0.208 mmol, 20%), (*S,S*)-Ph-BPE (51 mg, 0.101, 10%) and dry, degassed toluene (10 mL). The flask was equipped with a septum and removed from the glovebox and the reaction was allowed to stir for 10 min. HBpin (0.18 mL, 1.24 mmol, 1.20 equiv) was added in one aliquot and the reaction was transferred to a cryo-bath set to 0 °C and stirred for a further 10 min and then 2-bromo-5-methoxystyrene (0.16 mL, 1.03 mmol, 1.0 equiv) was added. The reaction was allowed to stir for 18 hours at 0 °C. The reaction was filtered through a pad of celite and washed with Et₂O (2x10 mL). The solvent was removed *in vacuo*. The crude material was dissolved in 2 mL dry DMSO and then NaN₃ (0.1997 g; 3.07 mmol, 2.98 equiv) was added and the reaction was allowed to stir at 40 °C for 1 hour. The reaction was poured into water and diethyl ether and then filtered through a pad of silica. The organic layer was then dried with Na₂SO₄ and concentrated *in vacuo*. The residue was purified by column chromatography using hexanes/CH₂Cl₂ as the eluent. A gradient was employed using 0-50% in 10% increments. Compound **3.28** was isolated in 47% yield and 85% *ee*. $[\alpha]_D^{24}$ -0.955 (*c* = 0.060 g/mL, CH₂Cl₂, *l* = 4.5 cm) ¹H NMR (500 MHz, CDCl₃) δ 7.79 (d, *J* = 8.4 Hz, 1H), 7.02 (d, *J* = 2.5 Hz, 1H), 6.81 (dd, *J* = 8.3, 2.5 Hz, 1H), 5.56 (q, *J* = 6.7 Hz, 1H), 3.84 (s, 3H), 1.47 (d, *J* = 6.7 Hz, 3H), 1.34 (s, 6H), 1.33 (s, 6H). ¹³C NMR (126 MHz, CDCl₃) δ 162.36, 150.09, 138.20, 112.27, 111.03, 83.57, 58.88, 55.17, 24.89, 24.78, 22.44. HRMS (ESI) *m/z* calculated for C₁₅H₂₆BN₄O₃ [M+NH₄]⁺ 320.2129, found 320.2117.



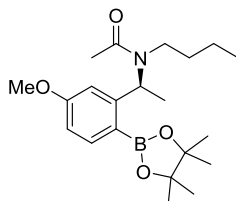
Compound 3.29. In a glovebox, A dry 25 ml round bottom flask was charged with (10 mg, 0.101 mmol, 10%), NaOtBu (20 mg, 0.208 mmol, 20%), (*S,S*)-Ph-BPE (51 mg, 0.101, 10%) and dry, degassed toluene (10 mL). The flask was fitted with a septum, removed from the glovebox and mixture was allowed to stir for 10 min. HBpin (0.18 mL, 1.24 mmol, 1.20 equiv) was added in one aliquot and the reaction was transferred to a cryo-bath set to 0 °C and stirred for a further 10 min and then 2-bromo-5-methoxystyrene (0.16 mL, 1.03 mmol, 1.0 equiv) was added. The reaction was allowed to stir for 18 hours at 0 °C. The reaction was filtered through a pad of celite and washed with Et₂O (2x10 mL). The solvent was removed *in vacuo*. The crude material was dissolved in 5 mL dry DMSO and then *N*-acetyl cysteine methyl ester (0.2383 g; 1.34 mmol, 1.30 equiv) and K₂CO₃ (0.3328 g, 2.41 mmol, 2.34 equiv)

was added and the reaction was allowed to stir at 40 °C for 3 hours. The reaction was poured into water and diethyl ether. The organic layer was washed once with water and then dried with Na₂SO₄ and concentrated *in vacuo*. The residue was purified by column chromatography using hexanes/EtOAc as the eluent. A gradient was employed using 10-50% in 10% increments. Compound **3.29** was isolated in 46% yield, >99% *ee*, and 95:5 d.r. [α]_D²⁴ -1.363 (c = 0.062 g/mL, CH₂Cl₂, *l* = 4.5 cm) ¹H NMR (500 MHz, CDCl₃) δ 7.72 (d, *J* = 8.3 Hz, 1H), 7.10 (d, *J* = 2.5 Hz, 1H), 6.76 (dd, *J* = 8.3, 2.5 Hz, 1H), 6.11 (d, *J* = 7.5 Hz, 1H), 4.96 (q, *J* = 7.0 Hz, 1H), 4.71 (td, *J* = 7.1, 4.3 Hz, 1H), 3.83 (s, 3H), 3.64 (s, 3H), 2.83 (dd, *J* = 13.3, 4.3 Hz, 1H), 2.70 (dd, *J* = 13.3, 6.7 Hz, 1H), 1.98 (s, 3H), 1.50 (d, *J* = 7.0 Hz, 3H), 1.35 (s, 6H), 1.34 (s, 6H). ¹³C NMR (126 MHz, CDCl₃) δ 171.30, 169.80, 162.20, 152.38, 137.66, 112.32, 111.63, 83.62, 55.10, 52.39, 51.58, 41.50, 32.71, 24.92, 24.72, 23.03, 22.95. HRMS (EI) *m/z* calculated for C₂₁H₃₃BNO₆S [M+H]⁺ 437.2153, found 437.2153.



Compound 3.30. In a glovebox, a dry 25 mL round bottom flask was charged with CuCl (10 mg, 0.101 mmol, 10%), NaOtBu (20 mg, 0.208 mmol, 20%), (*S,S*)-Ph-BPE (51 mg, 0.101, 10%) and dry, degassed toluene (10 mL). The flask was equipped with a septum and removed from the glovebox and the reaction was allowed to stir for 10 min. HBpin (0.18 mL, 1.24 mmol, 1.20 equiv) was added in one aliquot and the reaction was transferred to a cryo-bath set to 0 °C and stirred for a further 10 min and then 2-bromo-5-methoxystyrene (0.16 mL, 1.03 mmol, 1.0 equiv) was added. The reaction was allowed to stir for 18 hours at 0 °C and then allowed to warm to ambient temperature. A solution of lithium malononitrile was prepared by treating diisopropylamine (0.42 mL, 3.00 mmol, 2.91 equiv) with *n*BuLi (1.2 mL of a 2.5 M solution, 3.00 mmol, 2.91 equiv) in 12 mL of dry THF. The lithium diisopropylamide was allowed to stir at 0 °C for 15 min and then malononitrile (0.19 mL, 3.02 mmol, 2.93 equiv) was added. The solution was allowed to stir for a further 15 min at 0 °C and then it added to the reaction flask. The reaction was allowed to stir for 18 hours at ambient temperature. The reaction was filtered through a pad of celite and washed with Et₂O (2x10 mL). The solvent was removed *in vacuo*. The residue was purified by column chromatography using hexanes/EtOAc as the eluent. A gradient was employed using 0-10% in 2% increments. Compound **3.30** was isolated in 46% yield and 80% *ee*. ¹H NMR (500 MHz, CDCl₃) δ 7.83 (d, *J* = 8.3 Hz, 1H),

6.96 (d, $J = 2.4$ Hz, 1H), 6.84 (dd, $J = 8.4, 2.4$ Hz, 1H), 4.27 (qd, $J = 7.1, 4.1$ Hz, 1H), 4.20 (d, $J = 4.2$ Hz, 1H), 1.65 (d, $J = 7.1$ Hz, 3H), 1.36 (s, 6H), 1.36 (s, 6H). ^{13}C NMR (126 MHz, CDCl_3) δ 162.44, 146.94, 139.10, 112.98, 112.93, 112.22, 111.71, 84.06, 55.23, 38.41, 31.63, 24.95, 24.79, 15.53. HRMS (EI) m/z calculated for $\text{C}_{18}\text{H}_{27}\text{BN}_3\text{O}_3$ $[\text{M}+\text{NH}_4]^+$ 343.2177, found 343.2165.



Compound 3.31. In a glovebox, A dry 25 ml round bottom flask was charged with (5 mg, 0.0506 mmol, 10%), NaOtBu (10 mg, 0.104 mmol, 20%), (*S,S*)-Ph-BPE (26 mg, 0.0513, 10%) and dry, degassed toluene (5 mL). The flask was fitted with a septum, removed from the glovebox and mixture was allowed to stir for 10 min. HBpin (0.10 mL, 0.689 mmol, 1.34 equiv) was added in one aliquot and the reaction was transferred to a cryo-bath set to 0 °C and stirred for a further 10 min and then 2-bromo-5-methoxystyrene (0.08 mL, 0.514 mmol, 1.0 equiv) was added. The reaction was allowed to stir for 18 hours at 0 °C. The reaction was filtered through a pad of celite and washed with Et_2O (2x10 mL). The solvent was removed *in vacuo*. The crude material was dissolved in 2.5 mL dry DMF and then *n*-butylamine (0.15 mL, 1.52 mmol, 2.96 equiv) and K_2CO_3 (0.3249 g, 2.35 mmol, 4.55 equiv) was added and the reaction was allowed to stir for 1 hour. Then, acetic anhydride (0.24 mL, 2.54 mmol, 4.94 equiv) was added and the reaction was allowed to stir for another hour. The reaction was poured into water and diethyl ether. The organic layer was washed once with water and then dried with Na_2SO_4 and concentrated *in vacuo*. The residue was purified by column chromatography using hexanes/EtOAc as the eluent. A gradient was employed using 10-50% in 10% increments. Compound **3.31** was isolated as a mixture of rotamers in a 3:1 ratio in 46% yield and 85% *ee*. $[\alpha]_{\text{D}}^{24}$ -0.114 ($c = 0.036$ g/mL, CH_2Cl_2 , $l = 4.5$ cm) ^1H NMR (500 MHz, CDCl_3) δ 7.83 (d, $J = 8.2$ Hz, 1H), 6.85 (d, $J = 2.4$ Hz, 1H), 6.79 (dd, $J = 8.3, 2.5$ Hz, 1H), 5.67 (q, $J = 6.9$ Hz, 1H), 3.83 (s, 3H), 3.36 (ddd, $J = 13.3, 10.9, 5.0$ Hz, 1H), 3.12 (ddd, $J = 13.2, 10.7, 5.2$ Hz, 1H), 2.16 (s, 3H), 1.65 (broad s, 2H), 1.53 (d, $J = 6.7$ Hz, 3H), 1.32 (d, $J = 1.3$ Hz, 12H), 1.16 (hex, $J = 7.2$ Hz, 2H), 0.77 (t, $J = 7.3$ Hz, 3H). ^{13}C NMR (126 MHz, CDCl_3) δ 171.69, 162.25, 150.55, 138.75, 112.69, 110.78, 83.56, 75.03, 55.16, 55.05, 43.09, 31.55, 24.87, 24.86, 24.75, 24.71, 24.68, 22.35, 20.39, 20.37, 13.69. HRMS (EI) m/z calculated for $\text{C}_{21}\text{H}_{35}\text{BNO}_4$ $[\text{M}+\text{H}]^+$ 375.2690, found 375.2694.

3.8 Bibliography

1. For recent reviews on enantioselective halogenations see: (a) Castellanos, A.; Fletcher, S. P. *Chem. Eur. J.* **2011**, *17*, 5766-5776. (b) Hennecke, U. *Chem. Asian J.* **2012**, *7*, 456-465. (c) Denmark, S. E.; Kuester, W. E.; Burk, M. T. *Angew. Chem. Int. Ed.* **2012**, *51*, 10938-10953. (d) Smith, A. M. R.; Hii, K. K. *Chem. Rev.* **2011**, *111*, 1637-1656.
2. (a) Oestreich, M. *Angew. Chem. Int. Ed.* **2005**, *44*, 2324-2327. (b) Zheng, W.; Zhang, Z.; Kaplan, M. J.; Antilla, J. C. *J. Am. Chem. Soc.* **2011**, *133*, 3339-3341. (c) Wack, H.; Taggi, A. E.; Hafez, A. M.; Drury, W. J.; Lectka, T. *J. Am. Chem. Soc.* **2001**, *123*, 1531-1532. (d) Shibata, N.; Kohno, J.; Takai, K.; Ishimaru, T.; Nakamura, S.; Toru, T.; Kanemansa, S. *Angew. Chem. Int. Ed.* **2005**, *117*, 4276-4279. (e) Douglas, J.; Ling, K. B.; Concellon, C.; Churchill, G.; Slawin, A. M. Z.; Smith, A. D. *Eur. J. Org. Chem.* **2010**, *30*, 5863-5869. (f) Reynolds, N. T.; Rovis, T. *J. Am. Chem. Soc.* **2005**, *127*, 16406-16407. (g) Vora, H. U.; Rovis, T. *J. Am. Chem. Soc.* **2010**, *132*, 2860-2861.
3. (a) Cai, Y.; Liu, X.; Hui, Y.; Jiang, J.; Wang, W.; Chen, W.; Lin, L.; Feng, X. *Angew. Chem. Int. Ed.* **2010**, *49*, 6160-6164. (b) Xu, X.; Kotti, R. S. S.; Cannon, J. F.; Headley, A. D.; Li, G. *Org. Lett.* **2004**, *6*, 4881-4884. (c) Alix, A.; Lalli, C.; Retailleau, P.; Masson, G. *J. Am. Chem. Soc.* **2012**, *134*, 10389-10392.
4. (a) Li, H.; Zhang, F.-M.; Tu, Y.-Q.; Zhang, Q.-W.; Chen, Z.-M.; Chen, Z.-H.; Li, J. *Chem. Sci.* **2011**, *2*, 1839-1841. (b) Chen, Z.-M.; Zhang, Q.-W.; Chen, Z.-H.; Li, H.; Tu, Y.-Q.; Zhang, F.-M.; Tian, J.-M. *J. Am. Chem. Soc.* **2011**, *133*, 8818-8821.
5. (a) Jaganathan, A.; Staples, R. J.; Borhan, B. *J. Am. Chem. Soc.* **2013**, *135*, 14806-14813. (b) Yousefi, R.; Ashtekar, K. D.; Whitehead, D. C.; Jackson, J. E.; Borhan, B. *J. Am. Chem. Soc.* **2013**, *135*, 14524-14527. (c) Zhang, W.; Zheng, S.; Liu, N.; Werness, J. B.; Guzei, I. A.; Tang, W. *J. Am. Chem. Soc.* **2010**, *132*, 3664-3665. (d) Zhang, W.; Liu, N.; Schienebeck, C. M.; Decloux, K.; Zheng, S.; Werness, J. B.; Tang, W. *Chem. Eur. J.* **2012**, *18*, 7296-7305. (e) Chen, G.; Ma, S. *Angew. Chem. Int. Ed.* **2010**, *49*, 8306-8308. (f) Ikeuchi, K.; Ido, S.; Yoshimura, S.; Asakawa, T.; Inai, M.; Hamashima, Y.; Kan, T. *Org. Lett.* **2012**, *14*, 6016-6019.
6. For a recent example of catalytic enantioselective dichlorination of allylic alcohols see: (a) Nicolaou, K. C.; Simmons, L. N.; Ying, Y.; Heretsch, P. M.; Chen, J. S. *J. Am. Chem. Soc.* **2011**, *133*, 8134-8137. To the best of our knowledge, there are only three reports of enantioselective dibromination: (b) Hu, D. X.; Shibuya, G. M.;

- Burns, N. Z. *J. Am. Chem. Soc.* **2013**, *135*, 12960-12963. (c) Hu, D. X.; Seidl, F. J.; Bucher, C.; Burns, N. Z. *J. Am. Chem. Soc.* **2015**, *137*, 3795-3798. (d) El-Qisairi, A. K.; Qaseer, H. A.; Katsigras, G.; Lorenzi, P.; Trivedi, U.; Tracz, S.; Hartman, A.; Miller, J. A.; Henry, P. M. *Org. Lett.* **2003**, *5*, 439-441.
7. For examples of copper-catalyzed 1,3-migration see: (a) Alcaide, B.; Almendros, P.; Alonso, J. M.; Cembellin, S.; Fernandez, I.; Martinez del Campo, T.; Torres, M. R. *Chem. Commun.* **2013**, *49*, 7779-7781. (b) Yang, Y.; Buchwald, S. L. *Angew. Chem. Int. Ed.* **2014**, *53*, 8677-8681.
 8. (a) Matyjaszewski, K.; Xia, J. *Chem. Rev.* **2001**, *101*, 2921-2990. (b) Wang, J.-S.; Matyjaszewski, K. *Macromolecules*, **1995**, *28*, 7901-7910.
 9. Hammett parameters are often invoked to rationalize an electronic trend; for a helpful review of Hammett parameters see: (a) Hansch, C.; Leo, A.; Taft, R. W. *Chem. Rev.* 1991, **91**, 165-195. For a useful resource on A values, see: (b) E. L. Eliel, *Stereochemistry of Organic Compounds*, Wiley, New York, **1994**.
 10. Gormisky, P. E.; White, M. C. *J. Am. Chem. Soc.* **2013**, *135*, 14052-14055.
 11. Reich, H. J. Integration of Proton NMR Spectra, <http://www.chem.wisc.edu/areas/reich/nmr/05-hmr-01-integration.htm>, (accessed July 2014)
 12. Becke, A. D. *J. Chem. Phys.* **1993**, *98*, 5648-5652.
 13. (a) McLean, A. D.; Chandler, G. S. *J. Chem. Phys.* **1980**, *72*, 5639-5648. (b) Raghavachari, K.; Binkley, J. S.; Seeger, R.; Pople, J. A. *J. Chem. Phys.* **1980**, *72*, 650-654. (c) Binning, R. C.; Curtiss, L. A. *J. Comp. Chem.* **1990**, *11*, 1206-1216. (d) McGarth, M. P.; Radom, L. *J. Chem. Phys.* **1991**, *94*, 511-516. (e) Curtiss, L. A.; McGarth, M. P.; Blaudeau, J.-P.; Davis, N. E.; Binning Jr., R. C.; Radom, L. *J. Chem. Phys.* **1995**, *103*, 6104-6113.
 14. Gaussian 09, Revision D.01, M. J. Frisch, G. W. Trucks, H. B. Schlegel, G. E. Scuseria, M. A. Robb, J. R. Cheeseman, G. Scalmani, V. Barone, B. Mennucci, G. A. Petersson, H. Nakatsuji, M. Caricato, X. Li, H. P. Hratchian, A. F. Izmaylov, J. Bloino, G. Zheng, J. L. Sonnenberg, M. Hada, M. Ehara, K. Toyota, R. Fukuda, J. Hasegawa, M. Ishida, T. Nakajima, Y. Honda, O. Kitao, H. Nakai, T. Vreven, J. A. Montgomery, Jr., J. E. Peralta, F. Ogliaro, M. Bearpark, J. J. Heyd, E. Brothers, K. N. Kudin, V. N. Staroverov, T. Keith, R. Kobayashi, J. Normand, K. Raghavachari, A. Rendell, J. C. Burant, S. S. Iyengar, J. Tomasi, M. Cossi, N. Rega, J. M. Millam, M. Klene, J. E. Knox, J. B. Cross, V. Bakken, C. Adamo, J. Jaramillo, R. Gomperts, R. E. Stratmann, O. Yazyev, A. J. Austin, R. Cammi, C. Pomelli, J. W. Ochterski, R. L. Martin, K. Morokuma, V. G.

Zakrzewski, G. A. Voth, P. Salvador, J. J. Dannenberg, S. Dapprich, A. D. Daniels, O. Farkas, J. B. Foresman, J. V. Ortiz, J. Cioslowski, and D. J. Fox, Gaussian, Inc., Wallingford CT, **2013**.

15. NBO 6.0. E. D. Glendening, J. K. Badenhoop, A. E. Reed, J. E. Carpenter, J. A. Bohmann, C. M. Morales, C. R. Landis, and F. Weinhold (Theoretical Chemistry Institute, University of Wisconsin, Madison, WI, **2013**); <http://nbo6.chem.wisc.edu/>

Chapter 4: Mechanistic Studies of Copper(I)-Catalyzed 1,3-Halogen Migration

Reproduced with permission from Van Hoveln, R.; Hudson, B. M.; Wedler, H. B.; Bates, D. M.; Le Gros, G.; Tantillo, D. J.; Schomaker, J. M. *J. Am. Chem. Soc.* **2015**, *137*, 5346–5354. Copyright 2015 American Chemical Society.

4.1 Introduction

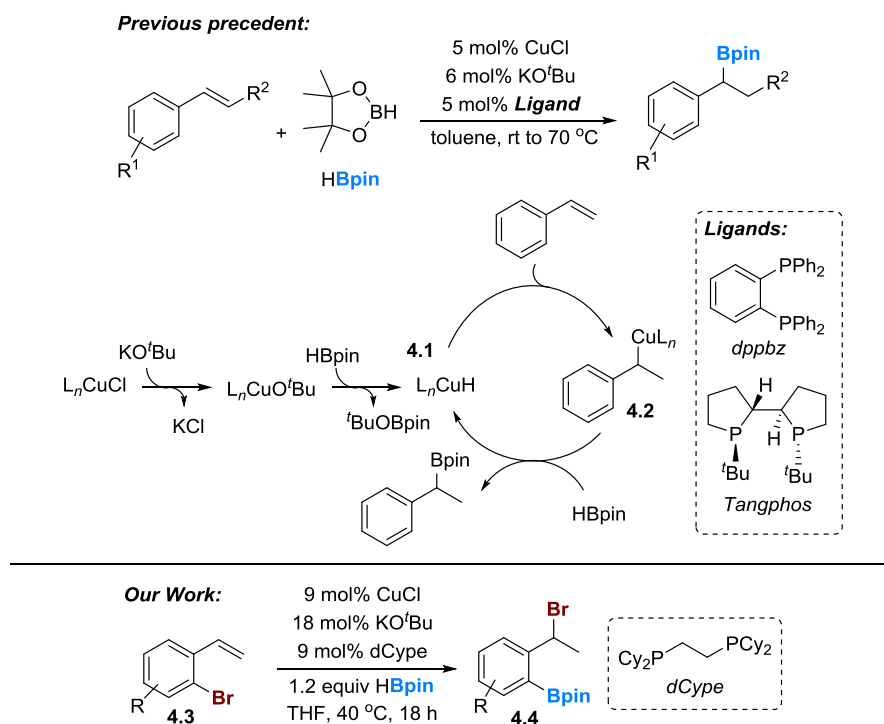
The field of base metal catalysis is a vibrant area of research and offers many potential advantages over more widely-utilized precious metal catalysts. Not only are earth-abundant, first-row transition metals significantly less expensive and better from an environmental perspective, their differing electronic structures compared to 2nd and 3rd row metals provides promise for uncovering new reactivities that proceed through novel mechanistic pathways. While the mechanisms of precious metal-catalyzed reactions have been studied extensively, the emphasis on better mechanistic understandings of reactions catalyzed by base metals is more recent.¹ Key to the further development of our 1,3-halogen migration chemistry into synthetically useful, Cu-catalyzed carbon-carbon and carbon-heteroatom bond-forming methodologies is an understanding of the mechanistic details of this new reactivity.

The functionalization of arenes *via* cross-coupling is arguably one of the most important and versatile reactions in organic synthesis.² The majority of these reactions use aryl or vinyl halides with an organometallic coupling partner, such as a boronic acid or ester (Suzuki), organozinc (Negishi), organostannanes (Stille), organosilane (Hiyama) or Grignard reagents (Kumada).^{2,3} While the majority of cross-coupling reactions are catalyzed by palladium, there has been much interest recently in promoting these types of transformations using first-row transition metals, including nickel, iron and copper.² However, there are challenges associated with promoting the typical mechanistic pathway invoked for cross-coupling, which involves the oxidative addition of the metal into the aryl halide or pseudohalide bond, transmetalation of the coupling partner to the metal and a final reductive elimination to yield the product.² Typically, first-row transition metals prefer one-electron oxidation state changes, as in the oft-invoked Cu(I)/Cu(II) and Fe(II)/Fe(III) mechanistic cycles.⁴ This renders oxidative addition more challenging with earth-abundant metals, often requiring the use of less convenient pseudohalides, high temperatures, long reaction times or a combination of forcing conditions.^{5,6} Furthermore, one-electron chemistry can complicate the reaction pathways, making both spectroscopic and mechanistic analyses difficult.⁴ While great strides have been made by several groups to promote Pd-like mechanistic pathways with first-row metals,^{5,6} an alternative approach is developing Cu-catalyzed reactions that invoke unusual mechanistic pathways involving no oxidation state changes at the metal center.

Our work in this area began when we attempted to synthesize a benzyl boronic ester *via* a Cu-catalyzed hydroboration of 2-bromostyrene using a method recently reported by the Yun group (Scheme 4.1, top).⁷ In Yun's

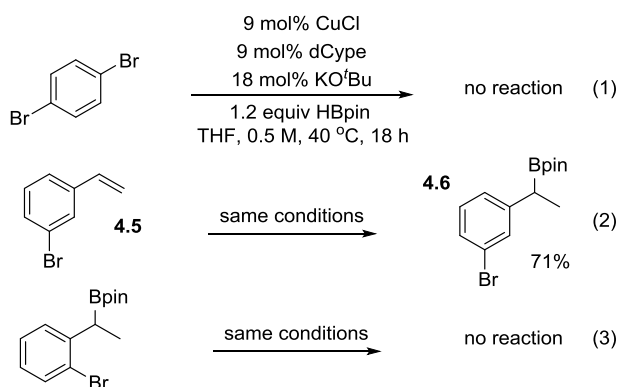
proposed mechanism, a phosphine-supported copper-hydride **4.1** which is generated *in situ*, adds to the styrene in a Markovnikov fashion. A subsequent σ -bond metathesis of the benzyl copper species **4.2** with pinacol borane (HBpin) regenerates the catalyst and forms the product. However, when 2-bromostyrene **4.3** was utilized with this protocol, very little of the desired product was formed; instead we observed small amounts (< 10%) of what was eventually identified as **4.4** (Scheme 4.1, bottom). We were intrigued by this unusual and poorly understood transformation and wanted to undertake a thorough mechanistic study to gain insight as to the features of both the catalyst and the substrate that promote this pathway.⁸ With this mechanistic understanding in hand, we expected to be able to expand the scope and utility of copper-catalyzed arene and benzyl functionalization chemistries. The efforts described in this chapter have allowed us to: 1) establish a reasonable energy profile for the 1,3-halogen migration *via* density functional theory (DFT) studies, 2) identify the enantiodetermining step in the asymmetric version of this reaction (see chapter 3), and 3) identify intermediates in this reaction that can be used to develop a wide range of synthetically useful transformations.

Scheme 4.1. Cu(I)-catalyzed hydroboration vs. halogen migration.



4.2 Control Experiments

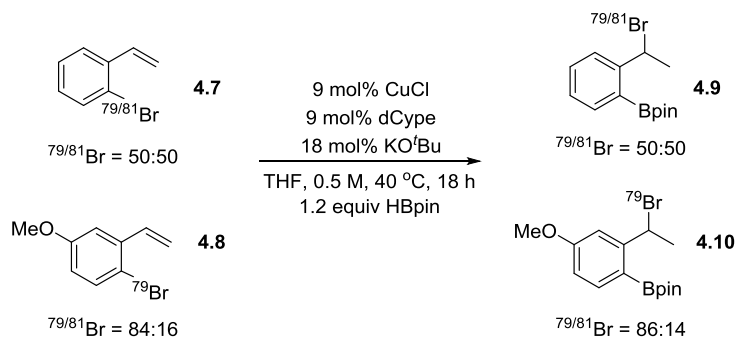
To rule out the possibility that the reaction proceeds *via* direct borylation of the aryl halide, followed by bromination of the styrene, 1,4-dibromobenzene was subjected to the reaction conditions (eq 1). No reaction was observed, indicating that the olefin is necessary for reactivity. When 3-bromostyrene **4.5** was subjected to the reaction conditions, only hydroboration occurred, showing that the olefin's location relative to the bromine is also important (eq 2). This result suggests that the 1,3-halogen migration is an intramolecular reaction. Finally, subjecting the hydroboration product to the reaction conditions resulted in no further reaction (eq 3); thus, the benzyl boronic ester can be ruled out as a potential intermediate in this transformation.



4.3 Crossover Experiment

Crossover experiments using an isotopically enriched styrene **4.8** (Scheme 4.2) indicated that the halogen migration was most likely either an intramolecular or rapid dissociation and recombination pathway. In this experiment, isotopically enriched styrene **4.8** and styrene **4.7** at natural abundance were subjected to the reaction conditions in the same flask after confirming that styrenes **4.8** and **4.7** reacted at comparable rates. Since the product **4.9**, which arises from styrene **4.7**, was at natural abundance and no incorporation of the ⁷⁹Br was detected, we can infer that this reaction is likely proceeds through an intramolecular mechanism. The product **4.10** also had the same isotopic enriched (within experimental error) as the corresponding starting material **4.8**. This supports our hypothesis from the control experiments that this transformation is intramolecular.

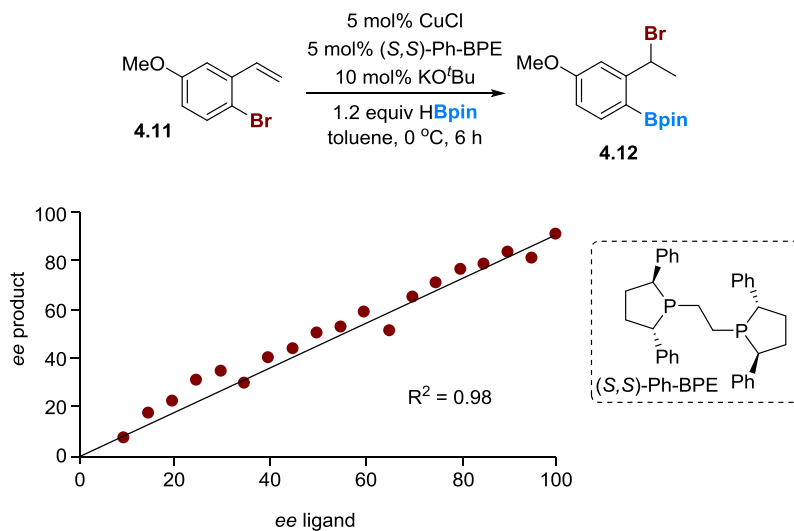
Scheme 4.2. Cross-over experiments *via* $^{79/81}\text{Br}$ isotopic labeling.



4.4 Non-Linear Effects Study of the Dependence of Product *ee* on Ligand *ee*

Initial studies to better understand the nature of the copper catalyst were undertaken. Although we suspected that the phosphine-supported copper(I) hydride was the active catalyst, these species are known to form dimers and other higher-order oligomers and aggregates, which could complicate the mechanistic picture.⁹ Fortunately, we have recently developed an asymmetric version of the 1,3-halogen migration reaction, which permitted a non-linear effects study to gain insight into the nuclearity of the catalyst (Figure 4.1). If catalytically important dimers or oligomers were present, they could form diastereomeric mixtures, which could have different energies. This could create ‘reservoirs’ for the minor enantiomer of the copper complex, which would cause deviation from linearity between ligand *ee* and product *ee*. The absence of non-linear effects supports the assumption that the active catalyst in solution is monomeric in nature and argues against the presence of off-cycle organocopper dimers or higher order aggregates.^{10,11}

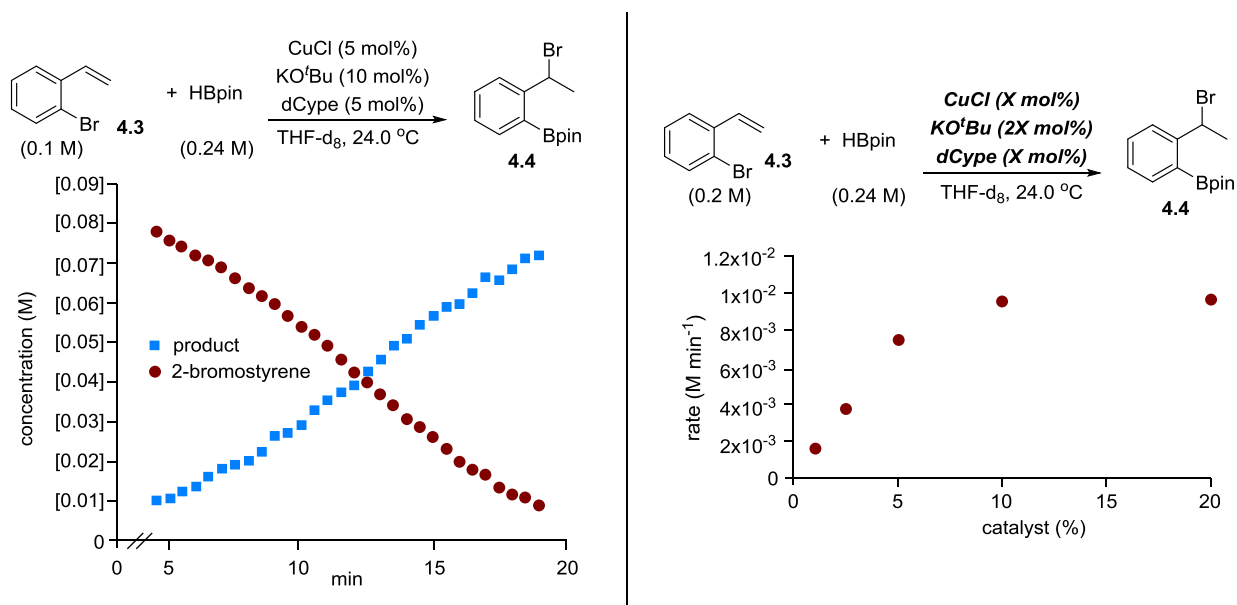
Figure 4.1. Dependence of product *ee* on ligand *ee*.



4.5 Kinetics Studies of 1,3-Halogen Migration

An investigation of the kinetics of the 1,3-halogen migration reaction using dCype as the ligand showed that there is no rate dependence on either 2-bromostyrene or HBpin and that the reaction is first order in catalyst at low catalyst concentrations (Figure 4.2). At higher catalyst loadings, the reaction displayed saturation behavior, presumably due to the decreased solubility of the metal complex at higher concentrations as the reaction is opaque at higher concentrations of catalyst.

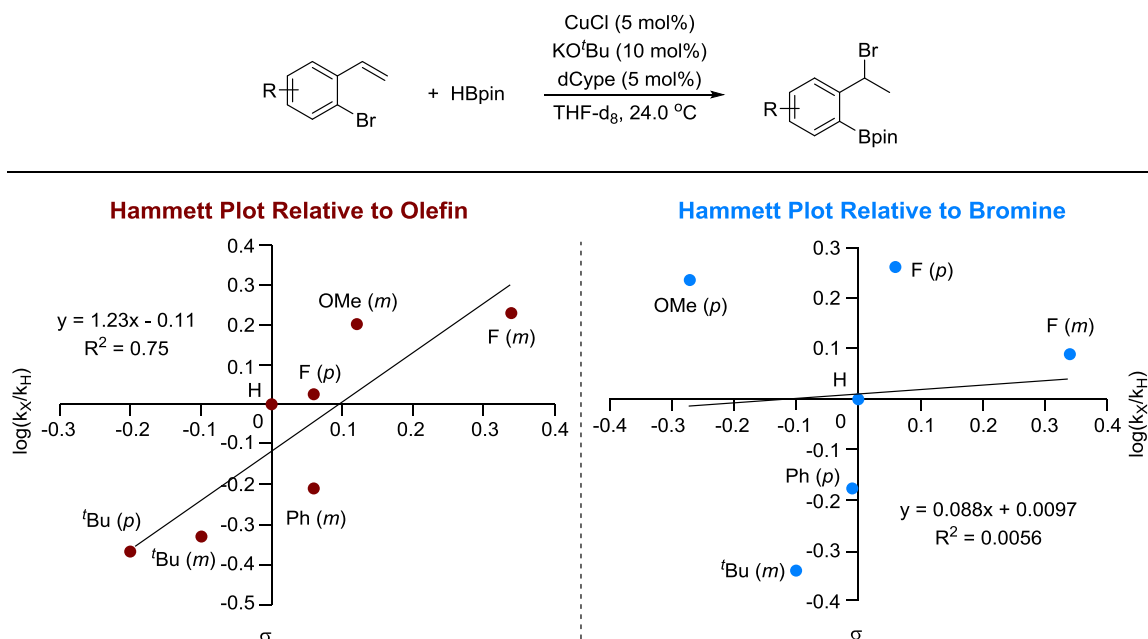
Figure 4.2. Time course of 1,3-halogen migration and rate dependence on catalyst loading.



4.5.1 Hammett Analysis of 1,3-Halogen Migration

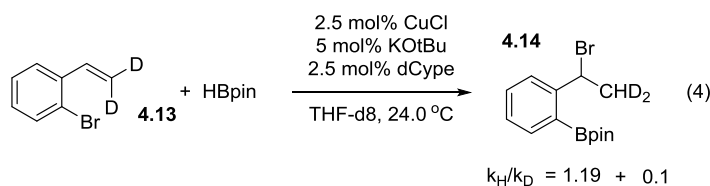
The rates of several substituted 2-bromostyrenes were investigated to establish the effect of electronics on 1,3-halogen migration (Figure 4.3). Since there are two functional groups that could be involved in the rate-determining step (the olefin and the bromine), the Hammett analysis was carried out twice with the same set of rate data, once relative to the olefin (left) and once relative to the bromine (right). The reaction shows some rate dependence on the electronics of the olefin. This Hammett plot shows that there is moderate negative charge build-up at the olefin in the rate-determining step. However, the weak correlation is indicative of other factors playing a role in the rate of the reaction. Based off of our findings with the asymmetric reaction (see chapter 3), we can conclude that this reaction is highly sensitive to the sterics of the substrate. Large groups such as *tert*-butyl and phenyl would slow the rate of the reaction more than their electronic factors would indicate. This is one potential factor contributing to the lack of high linearity in the Hammett plot. Regardless, it appears as though the olefin is involved in the rate-determine step. When the same analysis was used relative to bromine, no correlation was observed, indicating the bromine is not involved in the rate-determining step.

Figure 4.3. Hammett plot of Cu(I)-catalyzed 1,3-halogen migration.



4.5.2 Kinetic Isotope Effect on 1,3-Halogen Migration

Deuteration of the terminal position of the olefin resulted in a secondary kinetic isotope effect (KIE) of 1.19 (eq 4).¹² This indicates that the terminal carbon of the styrene is undergoing a hybridization change in the rate-determining step, despite the fact that the overall reaction is zero-order in styrene. This is in accord with our Hammett analysis.

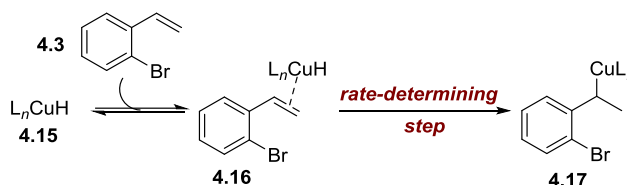


4.5.3 Conclusions from Kinetics Studies

To explain the kinetics data, which superficially seems contradictory, we hypothesize that the active catalyst is the ligand-supported copper hydride (Scheme 4.3); however, interaction of the Cu-H with the styrene forms a π -olefin complex.¹³ Since the styrene is in high concentration relative to the copper-hydride, the concentration of this intermediate is dictated by the concentration of the CuH. The copper hydride then adds across the olefin in the rate-

determining step. This proposed pre-equilibrium accounts for the zero-order rate dependence on the styrene, but still allows it to be involved in the rate-determining step.¹⁴

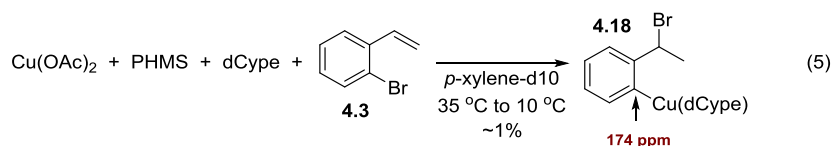
Scheme 4.3. Pre-equilibrium step forming π -olefin complex and rate-determining step.



4.6 Stoichiometric NMR Experiments to Elucidate Organocopper Intermediates

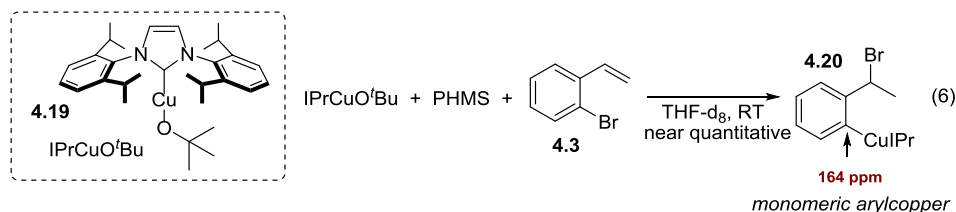
4.6.1 Stoichiometric Experiments with Phosphine-supported Copper Species

In an effort to elucidate possible intermediates spectroscopically, stoichiometric studies were undertaken. The phosphine-supported copper hydride was generated *in situ* by treating $Cu(OAc)_2$ and dCype with polymethylhydrosiloxane (PMHS) and then 1 equiv of 2-bromostyrene was added. Upon warming, approximately 1% of what appears to be arylcopper **4.18** (eq. 5) formed quickly. At cooler temperatures, the intermediate was stable long enough to acquire a variety of spectra. In spite of the fact that only a small percentage formed, nearly all of the carbons and protons from the aryl skeleton could be assigned. Notably, the aryl carbon bearing copper has a chemical shift of 174 ppm. While this is an unusual chemical shift for aryl carbons, it is typical for aryl carbons bearing copper(I).^{15,11h} For more details and all spectra, see section 4.15.6.



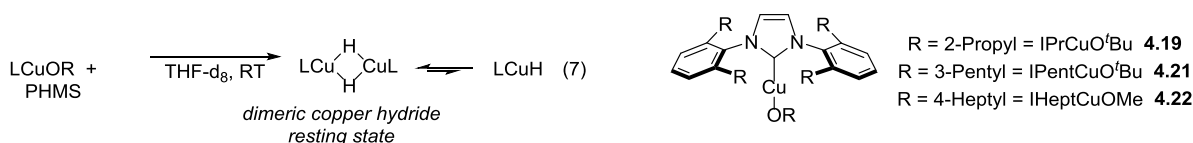
4.6.2 Stoichiometric Experiments with NHC-supported Copper Species

When the ligand is switched from a phosphine to the *N*-heterocyclic carbene (NHC) ligand IPr, the aryl copper forms near quantitatively (based on consumption of 2-bromostyrene) (eq 6). The general features of the spectra matched fairly closely to that of the phosphine ligated aryl copper. Notably, since this organocopper was in higher concentration, diffusion-NMR experiments could be carried out, which indicate that the arylcopper is a monomer.



4.6.3 Diffusion-NMR Study of NHC-Copper Hydrides

Since the NHC ligated copper complexes were ideal for studying this reactivity by NMR, a series of copper-hydrides were generated *in situ* to study their nuclearity. All three copper-hydrides were found to be dimers in solution, which is consistent with the crystal structure of IPrCuH. We believe that these dimeric copper hydrides are in equilibrium with their monomeric counterparts, since the organocopper intermediates seem to be monomeric in nature. However, this seems to be in conflict with our non-linear effects study (see section 4.4). There are a number of possible explanations for this. First, since the non-linear effects study used phosphine ligands and diffusion NMR experiments used NHC ligands, these two systems may not be able to be fairly compared. Second, the diastereomeric dimers with the chiral ligand may all be similar in energy, in which case no non-linear effect would be observed. Unfortunately, the phosphine ligated copper complexes tend to form complex mixtures in solution, which precludes simple study by NMR.

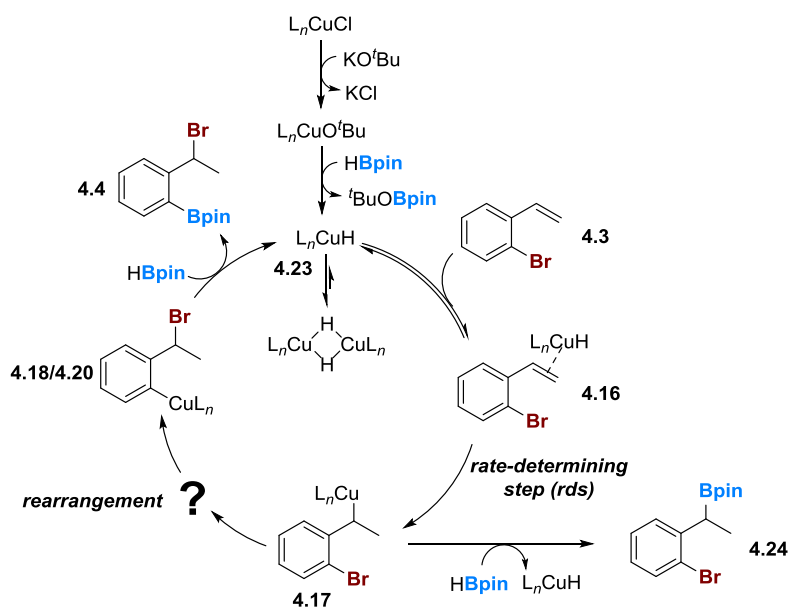


4.7 Preliminary Mechanistic Proposal

Based on these preliminary studies, a partial mechanism was proposed (Scheme 4.4). The copper hydride **4.23** adds to the olefin in a regioselective manner to give the benzyl copper intermediate **4.17**. This species then undergoes a formal 1,3-rearrangement to generate an aryl copper **4.18**, followed by σ -bond metathesis with HBpin to form the benzyl bromide product and regenerate the catalyst.¹⁶ The competing pathway involves direct metathesis of the benzyl copper **4.17** with HBpin to afford the unobserved benzyl boronic ester **4.24** originally reported by Yun.⁷ This proposed mechanistic pathway raises two important questions that need to be answered. First, it is unclear what parameters in both the substrate and the catalyst contribute to the tendency of the benzyl copper **4.17** to undergo rearrangement, as opposed to immediate borylation. Second, the nature of the migration of

the benzyl copper **4.17** to the aryl copper species **4.18** needs to be understood, especially as it relates to transfer of chiral information in the enantioselective version of the 1,3-halogen migration.

Scheme 4.4. Preliminary mechanistic proposal.



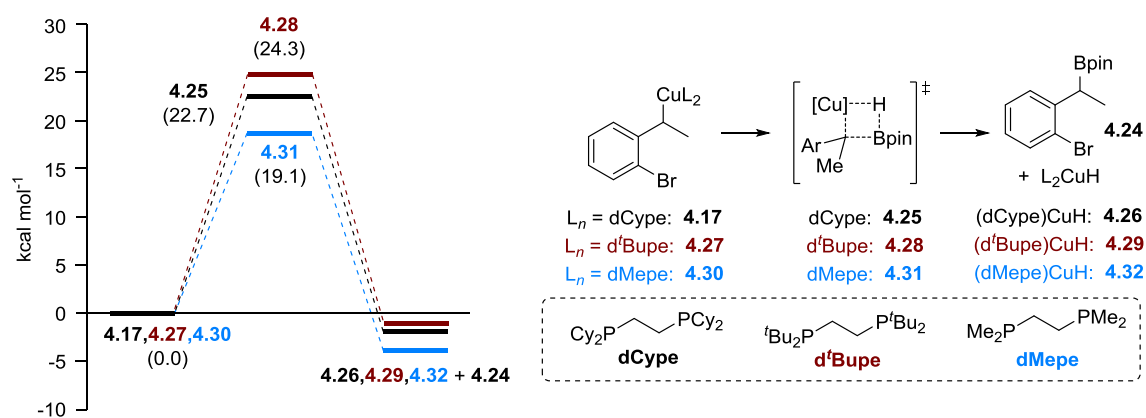
4.8 Determining the Substrate and Catalyst Parameters that Dictate Selectivity between Migration and Hydroboration

4.8.1 Computational Investigation of the Impact of Steric Bulk on Hydroboration

To answer the question as to why migration occurs only with certain ligands, while other ligands give the benzyl boronic ester, a blend of experimental and computational studies were carried out. All structures throughout our studies were optimized with Gaussian 09¹⁷ using the M06¹⁸ functional with a 6-311G* basis set for H, B, C, O, P, and Br¹⁹ and a LANL2TZ+ basis set for copper.²⁰ An SMD continuum model was used with THF as the solvent (except where noted).²¹ All minima were checked for absence of imaginary vibrational modes and all transition states were checked for one imaginary vibrational mode and confirmed with intrinsic reaction coordinate (IRC) calculations.²² The barriers of the σ -bond metathesis leading to the benzyl boronic esters were calculated for the dCype, dMepe (1,2-bis(dimethylphosphino)ethane), and d^tBupe (1,2-bis(di-*tert*-butylphosphino)ethane) ligands. The barrier for the dCype ligand (**4.25**) was much higher than that of the dMepe ligand (**4.31**) (Figure 4.4). Since the dCype ligand prefers migration, the barrier for hydroboration can provide an upper limit for the energy required for migration, whereas the hydroboration using the dMepe ligand may provide the lower limit. Thus, the barrier for

migration is most likely between 22.7 and 19.1 kcal mol⁻¹. Presumably, this difference in barriers can be attributed to steric bulk. Indeed, the barrier for hydroboration using d^tBuPe (**4.28**) was the highest of the three, predicting that a more sterically bulky ligand should favor migration to a greater extent for substrates that currently give mixtures of products. This design principle will be tested in future investigations of new ligands for 1,3-halogen migration.

Figure 4.4. Impact of steric bulk on hydroboration.



Free energies shown are in kcal mol⁻¹ relative to **4.17**, **4.27**, and **4.30** computed at SMD(THF)-M06/6-311G(d):LANL2TZ+ (Cu).

4.8.2 Experimental Investigation of the Factors Impacting the Selectivity of Migration

To examine the role the steric and electronic features of both the substrate and the ligand play in controlling the distribution of products between migration and hydroboration, a series of ligands were investigated with a variety of substrates (Table 4.1). In the case of 2-bromostyrene itself (entries 1-4), as predicted by our calculations (Figure 4.4), the smaller dMePe and dEtpe (1,2-bis(diethylphosphino)ethane) ligands switched the reactivity from exclusively migration to exclusively hydroboration (entries 2-3). The larger 1,2-bis[(2*S*,5*S*)-2,5-diphenylphospholano]ethane ((*S,S*)-Ph-BPE) ligand (entry 4), used as a surrogate for d^tBuPe, still gave exclusively the migration product, albeit in much lower yield than dCype (entry 1). As the substrate becomes more electron-poor, the hydroboration product is increasingly favored with dCype, indicating that the rate of halogen migration slows with electron-poor aromatics (entries 5 and 7). However, the bulkier (*S,S*)-Ph-BPE ligand still favored the migration product with these bromostyrenes, showing that greater steric bulk does promote the migration (entries 6 and 8). We were curious if increasing the electron density of the 2-bromostyrene might enable less bulky ligands to catalyze the 1,3-halogen migration (entries 9-14); however, this did not appear to be the case when only one electron donating group was present on the arene (entries 9-11). Nonetheless, the combination of a bulky, electron-rich

catalyst and an electron-rich aromatic gave near-quantitative yields of the migration product. Increasing the electron density of the substrate even further resulted in some migration product (entries 13-14). From these results, we can conclude that increasing the electron density of the aromatic ring favors migration to a greater extent, while decreasing electron density disfavors migration. Additionally, increasing the steric bulk of the ligand disfavors hydroboration, while small ligands favor hydroboration.

Table 4.1. Factors impacting the product distribution in the 1,3-halogen migration.

NMR yields using 1,1,1,2-tetrachloroethane as an internal standard

Entry	R =	Ligand	Migration	Hydroboration
1	H	dCype	94	0
2	H	4.3 dMepe	0	4.4 91
3	H	dEtpe	0	98
4	H	Ph-BPE	37	0
5	5-F	dCype	49	4.34 28
6	5-F	4.33 Ph-BPE	21	4.35 0
7	5-CF ₃	dCype	28	31
8	5-CF ₃	4.36 Ph-BPE	14	4.37 6
9	5-OMe	dCype	87	0
10	5-OMe	4.11 dMepe	0	4.12 52
11	5-OMe	dEtpe	0	100
12	3,5-OMe	dCype	98	0
13	3,5-OMe	4.40 dMepe	16	4.41 40
14	3,5-OMe	dEtpe	17	32

dMepe

dEtpe

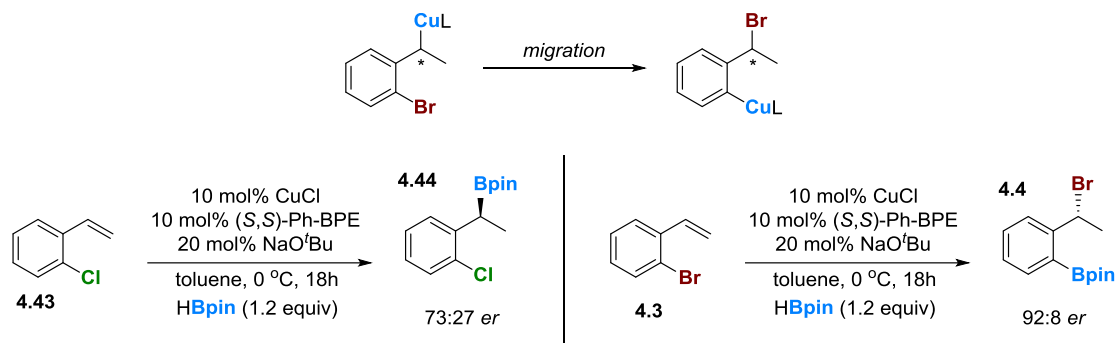
(S,S)-Ph-BPE

4.9 Experimental Investigation of the Migration Step: Transfer of Stereochemistry

4.9.1 Comparison of the Enantioselectivity between Hydroboration and Migration under Asymmetric Conditions

The second question concerning the mechanism involves the nature of the migration event that transforms the benzyl copper to the aryl copper species. The development of an asymmetric method provided a unique opportunity to explore how stereochemical information is relayed throughout the course of the reaction. In the initial hydrocupration, a stereocenter is created in the benzyl copper. The aryl copper also has a stereocenter. If a substrate is used that does not undergo migration, then the absolute stereochemistry of the benzyl copper could be determined and compared to the enantioselectivity of the migration product. Using 2-chlorostyrene **4.43**, which is sterically and electronically similar to 2-bromostyrene, we found that the enantioselectivity of the resulting benzyl boronic ester is significantly different than that of the corresponding migration product **4.4**. Not only are the absolute stereochemistries opposite, the enantioinduction is quite different. This implies that the stereochemistry of the initial benzyl copper is lost during the course of the migration and that the stereochemistry is reset in the final product.

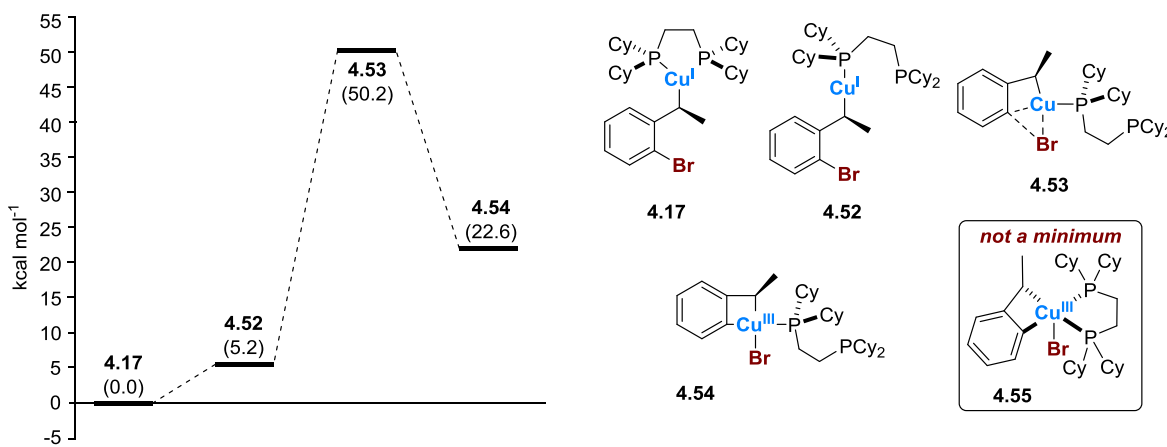
Figure 4.5. Comparing enantioinduction for hydroboration and migration



4.9.2 Use of Deuterium Labeling to Determine Transfer of Stereochemistry during the Migration Step

To better understand the nature of the 1,3-halogen migration and how stereochemistry is transferred throughout the reaction, a deuterated dihydronaphthalene substrate **4.45** was designed (Scheme 4.5) to determine if the stereochemistry set during the initial hydrocupration step was retained, inverted or ablated during the 1,3-halogen migration event. Since the hydrocupration of a π -bond is preceded to occur in a *syn* fashion to give **4.47**,²⁶ the stereochemistry of the bromine relative to the deuterium in the product **4.46** should indicate whether migration occurs with retention or inversion of stereochemistry. In the case of retention, the product **4.49** should display an *anti* relationship between the bromine and deuterium. If inversion is taking place, then product **4.51** should display a *syn* relationship between these same two groups. Interestingly, the product obtained from this experiment was a 1:1 mixture of diastereomers, indicating the presence of a stereoablative step in the migration process, consistent with the investigation of enantioselective transfer of stereochemistry.

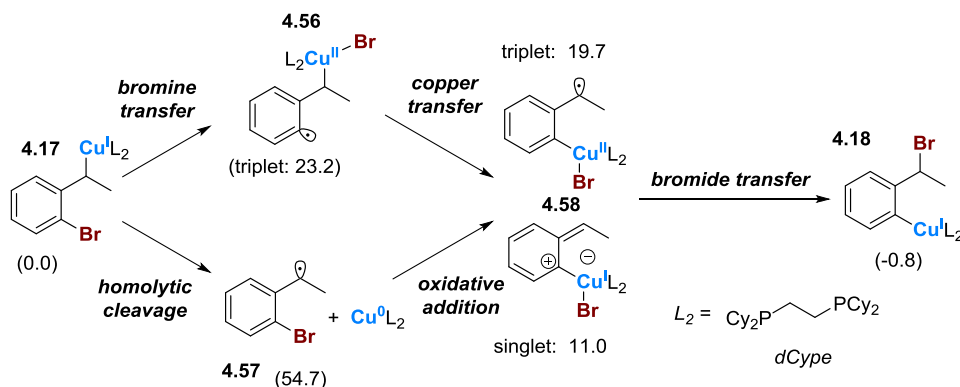
Figure 4.6. Proposed oxidative addition pathways proceeding through a Cu(I)/Cu(III) cycle.



4.10.2 Pathways Involving One Electron Changes at Copper

Since a Cu(I)/Cu(III) pathway seemed unlikely, we considered a pathway that would take advantage of a facile Cu(I)/Cu(II) oxidation state change (Figure 4.7). In this pathway, bromine abstraction by copper would form an aryl radical/Cu(II) species, **4.56**. Homolytic cleavage of the benzyl carbon-copper bond, followed by rapid recombination with the aryl radical, would produce a relatively stable benzyl radical intermediate **4.58**. From this intermediate, the bromine could potentially undergo a 1,4-shift to form an aryl Cu(I) species **4.18**. Unfortunately, the aryl radical **4.56** was high in energy, making the formation of this intermediate unlikely. Another possible pathway that could lead to the benzyl radical/aryl copper species **4.58** involves homolytic cleavage of the benzyl carbon-copper bond of **4.17** to produce a benzyl radical and a phosphine-supported Cu(0) intermediate **4.57**, followed by oxidative addition of the metal into the aryl carbon-bromine bond. This pathway proved to be even higher in energy than the Cu(I)/Cu(II) pathway and was not considered further.

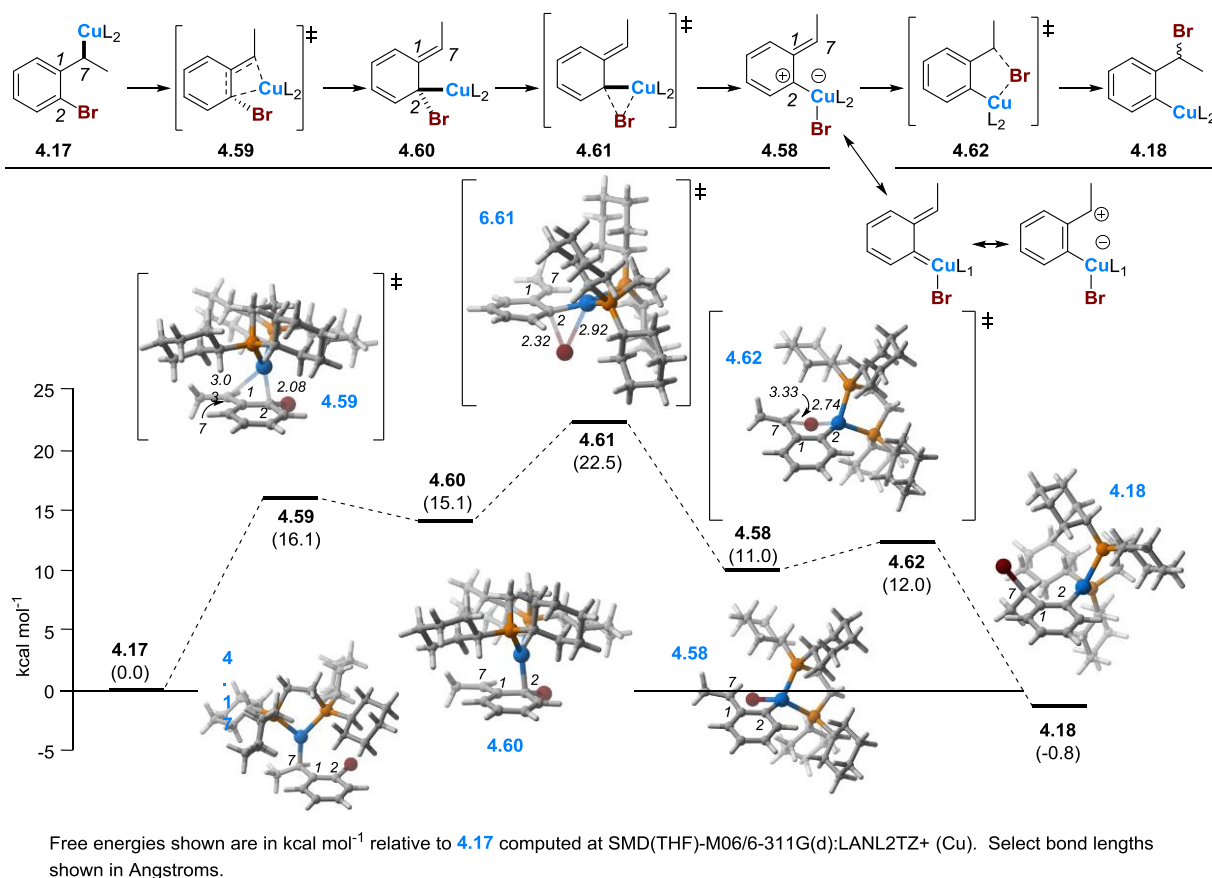
Figure 4.7. Pathways invoking potential Cu(II) intermediates.



4.10.3 A Dearomative Pathway Involving No Oxidation State Changes at Copper

We next investigated a dearomatization pathway that did not involve changes in the oxidation state at copper (Figure 4).^{8b,25} The proposed mechanism consists of a three-step process. Initially, **4.17** proceeds through a dearomative η^3 Cu(I) transition state leading to non-aromatic **4.60**, where both bromine and Cu(I) are bound to the same carbon. The carbon bearing the bromine, C2, can be thought of as the ‘nucleophile’ in the dearomatizing step, whereas the copper can be thought of as the electrophile. According to this model, increasing the electron density at this carbon should favor migration; this has been borne out in studies where the electronics of the substrate have been varied (see Table 4.1). In **4.60**, the Cu(I) occupies the pseudoaxial position of the tetrahedral carbon while the bromine is in the equatorial position, making bromine and the benzyl carbon, C7, nearly coplanar. Since the bromine needs to add to the π -system at C7, it must come from either above or below C7, not in the C7-C2-Br plane. Thus, this geometry does not allow for the correct trajectory for bromine migration to the benzylic position without a conformational change. However, calculations revealed a 1,2-Br shift onto the Cu(I) atom that proceeds through a low-barrier transition state structure to restore aromaticity in **4.62**. In this intermediate, the bromine and the benzylic carbon are no longer co-planar, allowing the bromine to be oriented in a manner that would permit transfer to the benzylic position. A final 1,4-Br shift from Cu(I) to the benzylic position results in the aryl copper **4.18**. It should be noted that **4.62** allows for free rotation to take place around the C2-Cu(I) bond; thus, Br could be delivered to either face of the benzylic carbon. This energetically viable dearomative pathway accounts for the stereoablative step; furthermore, this pathway is consistent with the electronic effects of the substrate that impact selectivity between migration and hydroboration (see Table 4.1).

Figure 4.8. Proposed Cu-catalyzed 1,3-halogen migration pathway invoking a dearomatized intermediate.

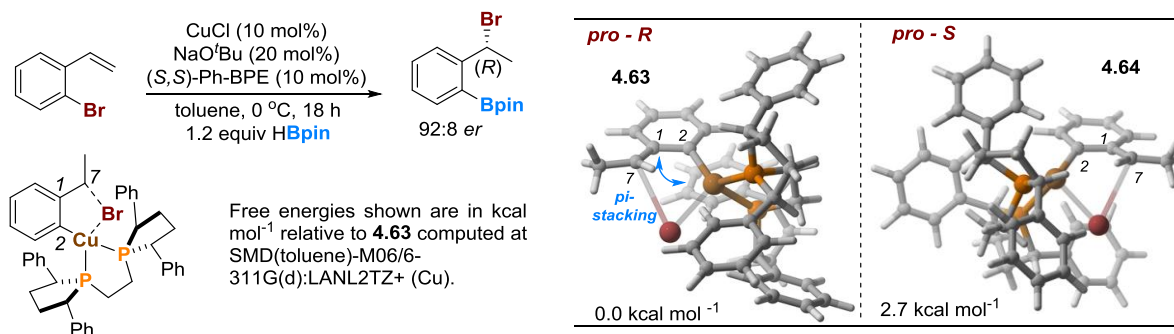


4.11 Determination of the Enantio-Determining Step in Asymmetric 1,3-Halogen Migration

With our current understanding of the mechanism in hand, we wanted to return to the asymmetric 1,3-halogen migration to investigate the nature of the enantiodetermining step.^{7a,26} If we assume the dearomatization pathway described in Figure 4.8 is the operative mechanism, the step that sets the stereochemistry of the final benzyl bromide product is the 1,4-bromide shift from the copper of **4.62** to the benzyl carbon of **4.18**. When the transition state structures that lead to both the (*R*) and the (*S*) products were optimized with the (*S,S*)-Ph-BPE ligand, the transition state structure that leads to the (*S*) enantiomer (**4.65**) was slightly higher in energy, which corresponds to our observed stereochemistry (Figure 4.9). While the energy difference is relatively small, the expected energy difference given the *er* for this substrate (92:8) and the reaction conditions is ~1.4 kcal mol⁻¹.²⁷ In transition state **4.64** that leads to the observed stereochemistry, the geometry is reinforced by a π -stacking interaction between the substrate and one of the phenyl rings on the ligand. In transition state **4.65**, which leads to the minor enantiomer, the

phenyl ring of the ligand is pushed away from the substrate and, consequently, does not have any favorable π -stacking interactions.

Figure 4.9. Transition state structures for the enantiodetermining step.

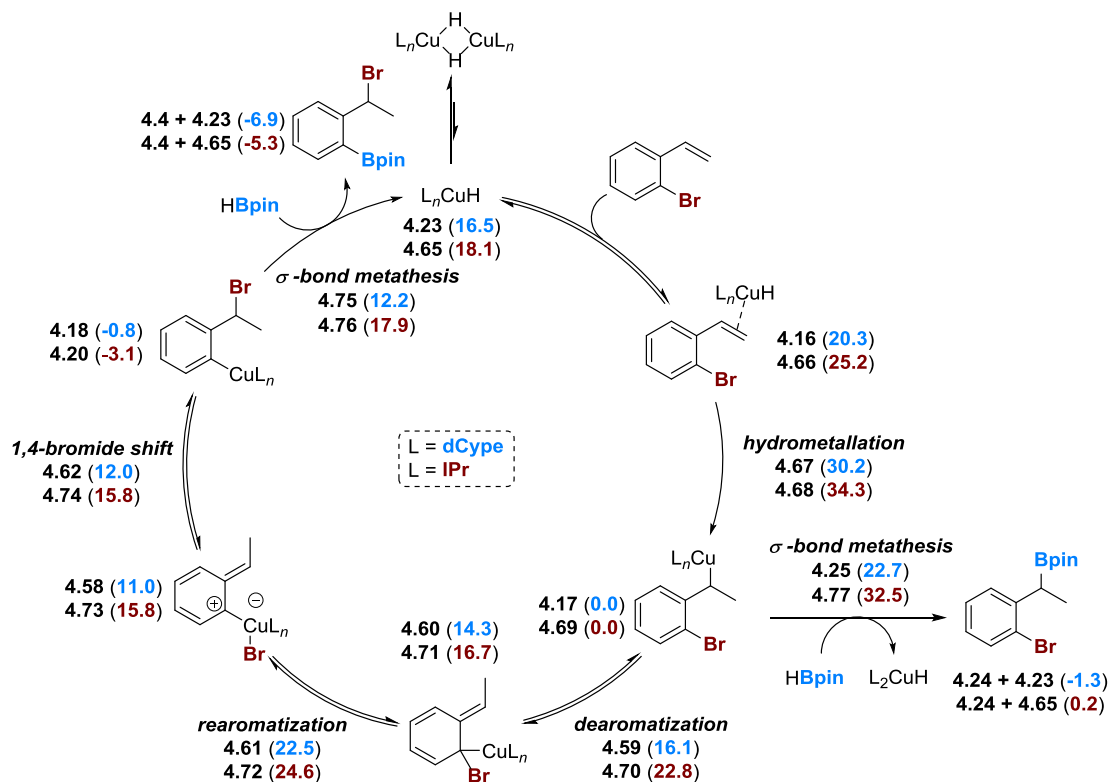


4.12 Overall Reaction Profile: Comparison between Phosphine and NHC Supported Copper Hydrides.

The full proposed mechanism is illustrated in Scheme 4.5, which compares the energetics of the **dCype** ligand (energies shown in **blue**) and the **IPr** ligand (energies shown in **dark red**). A phosphine supported copper hydride **4.23** is the active catalyst that forms a π -olefin complex **4.16** with 2-bromostyrene. This complex undergoes hydrometallation to form a benzyl copper **4.17**. Notably, the hydrometallation transition state is the highest in energy, making this step the rate-determining step, which fits well with our kinetics studies (see Figure 4.2). The benzyl copper **4.17** then either reacts with HBpin to form the undesired hydroboration product or undergoes a 1,3-copper shift that dearomatizes the ring. As the hydroboration pathway is higher in energy than the dearomatization pathway, or any subsequent transition state, the benzyl copper **4.17** prefers to undergo migration in the presence of the appropriate ligand. The dearomatized intermediate **4.59** quickly rearomatizes in a 1,2-bromide shift to form **4.61**. This intermediate then transfers bromine from copper to the benzyl carbon, which in the presence of chiral ligand, constitutes the enantiodetermining step. The aryl copper **4.18** then reacts with HBpin to form the product and regenerate the copper-hydride catalyst. In general, the energies throughout the reaction coordinate for the IPr ligand are only a few kcal/mol higher than the energies for dCype. The notable exception is the hydroboration of the benzyl copper, where the difference between transition state **4.25** and **4.77** is nearly 10 kcal/mol. In the case of the 16 electron phosphine benzyl copper complex, the copper is less Lewis acidic than the 14 electron IPr benzyl copper

complex. This means that there is more electron density on the benzyl carbon of the phosphine complex, making it more reactive towards HBpin and, therefore, has the lower transition state energy for hydroboration.

Scheme 4.5. Complete catalytic cycle for the Cu-catalyzed 1,3-halogen migration/borylation.



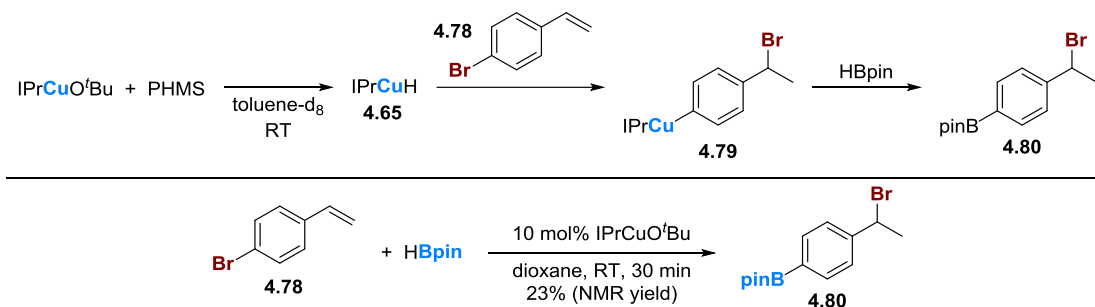
The mechanistic proposal described herein is somewhat unusual. It does not represent the most direct pathway to products, and it involves uncommon steps. For example, the conversion of **4.17** to **4.18** can be considered to be a formal dyotropic rearrangement. Dyotropic rearrangements—migrations of two groups, often past each other so that they exchange positions—have a long history.²⁸ The dyotropic rearrangement described herein is only formal in nature, i.e., it is stepwise rather than concerted. While other examples of stepwise dyotropic processes are known,^{28,29} ours is unusual in terms of the different pathways travelled by the two migrating groups: While the copper migrates directly to its new position, the bromine follows a more convoluted route.

4.13 Testing the Mechanistic Hypothesis: 1,5-Halogen Migration

If the mechanism for 1,3-halogen migration is indeed proceeding through a dearomative pathway, then a similar catalyst system should be able to activate halogens at positions other than just the 2-position. When 4-bromostyrene

is subjected to the stoichiometric conditions with IPrCuOtBu, a small amount (~30%) of aryl copper forms which is the result of 1,5-migration. Under catalytic conditions, the 1,5-migration product forms, albeit in low yield. This preliminary result opens the possibility for long-range atom transfer *via* copper catalysis.

Figure 4.10. Long range atom transfer *via* copper(I)-catalyzed halogen migration.



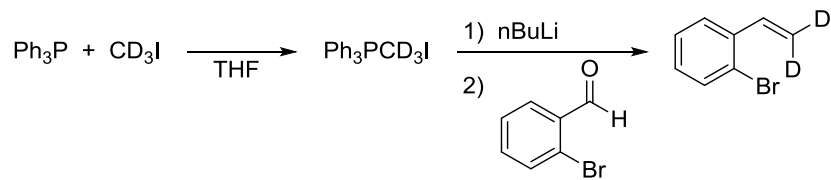
4.14 Conclusions

In conclusion, we have reported computational and experimental studies to elucidate the mechanism of an unusual transformation in which an aryl bromide is reincorporated into the product *via* a dearomative 1,3-shift. These in-depth studies have revealed that organocopper intermediates are probably monomeric in nature and that the rate determining step is hydrometallation. Additionally, we have shown that this transformation is unlikely to involve oxidation state changes at the metal center, but rather favors a dearomative 1,3-shift that does not require copper to change its oxidation state. In the enantioselective 1,3-halogen migration, the enantio-determining step is a 1,4-bromide shift from copper to the benzyl carbon. Current studies are focused on using 1,3-halogen migration as a strategy to enable a broad range of aromatic functionalizations. Additionally, insights gained from this study will be used in the design of improved catalysts for asymmetric 1,3-halogen migration.

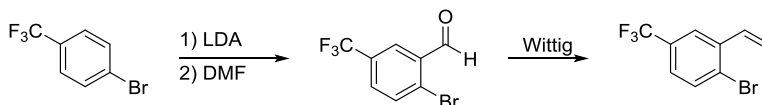
4.15 Experimental Details

4.15.1 Preparation of Substrates

Substrates 2-bromostyrene (Table 1, entries 1-4), 2-bromo-5-methoxystyrene (entries 9-11), and 2-bromo-5-fluorostyrene (entries 5-6) were prepared according to procedures reported in Chapter 2.



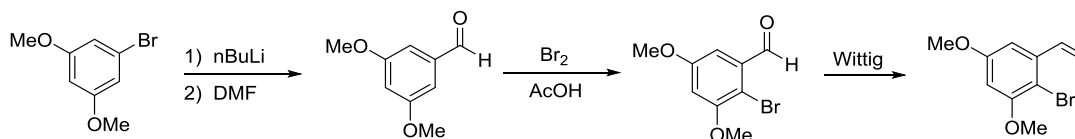
Compound 4.13. A flame-dried 250 mL flask was charged with iodomethane- d_3 (0.93 mL, 14.9 mmol, 1.16 equiv), triphenylphosphine (3.96 g, 15.1 mmol, 1.18 equiv) and 70 mL of dry THF and equipped with a reflux condenser under an atmosphere of nitrogen. The reaction was refluxed for 6 h and then cooled in an ice bath. To the slurry was added nBuLi (6.0 mL of a 2.5 M solution in hexanes, 15 mmol, 1.17 equiv) in a dropwise fashion. The reaction was allowed to stir for 30 min and then 2-bromobenzaldehyde (1.5 mL, 12.8 mmol, 1.0 equiv) was added slowly. The reaction was allowed to stir at ambient temperature for 1 h and then quenched by adding silica gel. The mixture was concentrated *in vacuo* to a slurry. The slurry was poured onto the top of a pad of silica and then washed with ~500 mL of hexanes. The hexanes were removed *in vacuo* and the crude product was purified by column chromatography using hexanes as the eluant. The styrene was isolated as a clear, colorless oil in 18% yield. ^1H NMR (500 MHz, CDCl_3) δ 7.55 (dd, $J = 8.0, 1.4$ Hz, 2H), 7.28 (td, $J = 7.8, 0.8$ Hz, 1H), 7.11 (td, $J = 7.8, 1.7$ Hz, 1H), 7.05 (broad s, 1H). ^{13}C NMR (126 MHz, CDCl_3) δ 137.5, 135.6, 132.9, 129.1, 127.5, 126.8, 123.6, 116.1 (m). HRMS (EI) m/z calculated for $\text{C}_8\text{H}_5\text{D}_2\text{Br}$ $[\text{M}]^+$ 183.9852, found 183.9855.



Compound 4.36.³⁰ A 250 mL three-neck round bottom flask was flame-dried, equipped with an addition funnel was placed under an atmosphere of nitrogen and charged with 50 mL of THF. A portion of 10 mL of THF was placed in the addition funnel and the flask was placed in an acetone/ CO_2 bath. Diisopropylamine (8.5 mL, 60.6 mmol, 1.21 equiv) was added to the flask and then nBuLi (26.0 mL of a 2.38 M solution in hexanes, 61.9 mmol, 1.24 equiv) was added dropwise. The reaction was allowed to stir at -78°C for 20 min. then a solution of 4-trifluoromethylbromobenzene (7.0 mL, 50.0 mmol, 1.0 equiv) in THF was added dropwise over 10 min. Once the addition was complete, the reaction was allowed to stir for 30 min at -78°C . A portion of dry DMF (11.0 mL, 142 mmol, 2.84 equiv) was added in one aliquot. After 5 min, the acetone/dry ice bath was removed and the reaction was allowed to warm to ambient temperature. After 1 h, 100 mL of 1 M HCl was added and the reaction was allowed to stir for 5 min. The mixture was extracted with CH_2Cl_2 three times and the combined organic layers were dried with

Na_2SO_4 and concentrated *in vacuo*. The product was purified by column chromatography using hexanes/EtOAc as the eluant. A gradient was employed using 0-10% EtOAc in 2% increments. The aldehyde was isolated as a yellow oil in 74% yield.

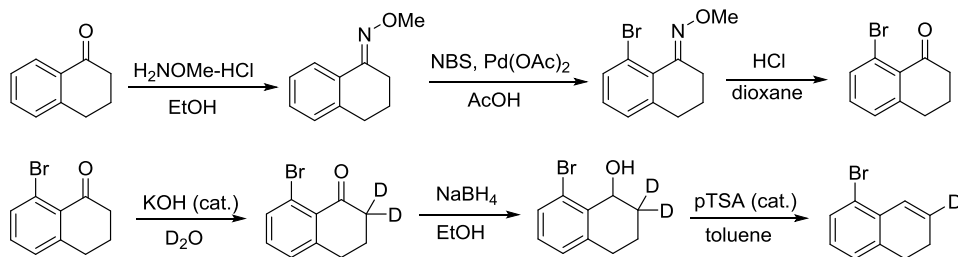
A flame-dried 500 mL round bottom flask was charged with triphenylmethylphosphonium iodide (9.64 g, 23.8 mmol, 1.20 equiv) and 200 mL of THF under an atmosphere of nitrogen and placed in an ice bath. To the slurry was added nBuLi (9.5 mL of a 2.38 M solution in hexanes, 22.6 mmol, 1.14 equiv) dropwise. The reaction was allowed to stir for 30 min and then 2-bromo-5-trifluoromethylbenzaldehyde (3.0 mL, 19.9 mmol, 1.0 equiv) was added slowly. The reaction was allowed to stir at ambient temperature for 1 h and then quenched by adding silica gel. The mixture was concentrated *in vacuo* to a slurry. The slurry was poured onto the top of a pad of silica and washed with ~500 mL of hexanes. The hexanes were removed *in vacuo* and the crude product was purified by column chromatography using hexanes as the eluant. The styrene was isolated as a clear, colorless oil in 46% yield. ^1H NMR (500 MHz, CDCl_3) δ 7.77 (d, J = 2.5 Hz, 1H), 7.68 (d, J = 8.3 Hz, 1H), 7.36 (dd, J = 8.4, 2.3 Hz, 1H), 7.06 (dd, J = 17.4, 11.0 Hz, 1H), 5.78 (d, J = 17.4 Hz, 1H), 5.48 (d, J = 11.0 Hz, 1H). ^{13}C NMR (126 MHz, CDCl_3) δ 138.3, 134.8, 133.5, 130.1 (q, J = 32.8 Hz), 127.1 (q, J = 1.7 Hz), 125.4 (q, J = 3.7 Hz), 123.8 (q, J = 272.4 Hz), 123.6 (q, J = 3.9 Hz). HRMS (EI) m/z calculated for $\text{C}_9\text{H}_6\text{BrF}_3$ $[\text{M}]^+$ 249.9600, found 249.9606.



Compound 4.40. A flame-dried 250 mL flask was charged with 3,5-dimethoxybromobenzene (5.00 g, 23.0 mmol, 1.0 equiv) and 150 mL of dry THF under an atmosphere of nitrogen. The flask was transferred to an acetone/dry ice bath and allowed to stir for 10 min. An aliquot of nBuLi (13.5 mL of a 2.08 M solution in hexanes, 28.1 mmol, 1.22 equiv) was added slowly. The reaction was allowed to stir for 20 min and then DMF (5.5 mL, 71.0 mmol, 3.09 equiv) was added in one aliquot. The reaction was allowed to stir for 20 min and then allowed to warm to ambient temperature. A portion of 100 mL 1 M HCl was added and the mixture was allowed to stir for 5 min. The aqueous mixture was extracted three times with CH_2Cl_2 and the combined organic layers were dried with Na_2SO_4 and concentrated *in vacuo*. The crude material was purified by column chromatography using hexanes/EtOAc as the eluant. A gradient was employed using 0-30% EtOAc in 6% increments. The 3,5-dimethoxybenzaldehyde was isolated as a pale yellow solid in 78% yield.

A 100 mL round bottom flask was charged with 20 mL acetic acid, 3,5-dimethoxybenzaldehyde (3.00 g, 18.1 mmol, 1.0 equiv), and bromine (0.83 mL, 16.2 mmol, 0.90 equiv). The reaction was allowed to stir for 10 min and then poured into water/CH₂Cl₂. The organic layer was washed three times with water, once with saturated NaHSO₃ and once with 1 M KOH. The organic layer was dried with Na₂SO₄ and concentrated *in vacuo*. The solid crude product was placed in a Büchner funnel and washed with a small amount of cold methanol to remove the remaining starting material. The yellow solid was isolated in 71% yield and used without further purification.

The aldehyde was used in the subsequent Wittig olefination to prepare 2-bromo-3,5-dimethoxystyrene in a fashion similar to that described for the synthesis of 2-bromo-β,β-dideuterostyrene. The 2-bromo-3,5-dimethoxystyrene was purified by column chromatography using hexanes/CH₂Cl₂ as the eluant. A gradient was employed using 0-30% CH₂Cl₂ in 6% increments. The 2-bromo-3,5-dimethoxystyrene was isolated as a thick, clear oil in 29% yield. ¹H NMR (500 MHz, CDCl₃) δ 7.11 (dd, *J* = 17.3, 10.9 Hz, 1H), 6.70 (d, *J* = 2.7 Hz, 1H), 6.43 (d, *J* = 2.8 Hz, 1H), 5.68 (dd, *J* = 17.4, 1.1 Hz, 1H), 5.37 (dd, *J* = 10.8, 1.1 Hz, 1H), 3.87 (s, 3H), 3.83 (s, 3H). ¹³C NMR (126 MHz, CDCl₃) δ 159.6, 156.7, 139.1, 136.3, 116.9, 104.5, 102.8, 99.2, 56.4, 55.5. HRMS (EI) *m/z* calculated for C₁₀H₁₁BrO₂ [M]⁺ 241.9937, found 241.9934.



Compound 4.46.³¹ A 250 mL round bottom flask was charged with tetralone (6.5 mL, 48.9 mmol, 1.0 equiv) and methoxyamine hydrochloride (6.55 g, 78.4 mmol, 1.60 equiv) in 100 mL ethanol. The reaction was refluxed for 1.5 h, allowed to cool to ambient temperature and poured into water/CH₂Cl₂. The water layer was extracted 2x with CH₂Cl₂. The combined organic layers were dried with Na₂SO₄ and concentrated *in vacuo*. The crude product was used without further purification.

A 500 mL round bottom flask was charged with tetralone O-methyl oxime (used directly from previous reaction), palladium acetate (0.559 g, 2.49 mmol, 5 mol%) and NBS (8.97 g, 50.4 mmol, ~1 equiv) in 350 mL of acetic acid. The reaction was refluxed under an atmosphere of nitrogen for 1.5 h. The reaction was allowed to cool to ambient

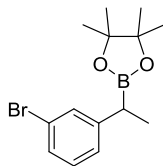
temperature and then poured into water and CH_2Cl_2 . The organic layer was washed with water and then a portion of 1 M KOH. The organic layer was dried with Na_2SO_4 and concentrated *in vacuo*. The crude product was used without further purification.

A 500 mL round bottom flask was charged with the crude bromotetralone O-methyloxime, 200 mL of 6 M HCl and 120 mL of dioxane. The reaction was refluxed for 2.5 h, allowed to cool to ambient temperature and poured into CH_2Cl_2 /water. The layers were separated, the aqueous layer extracted twice with CH_2Cl_2 , the combined organic layers dried with Na_2SO_4 and then concentrated *in vacuo*. The crude material was used without further purification.

A 250 mL round bottom flask was charged with 100 mL D_2O , bromotetralone (used directly from previous reaction), KOH (0.298 g, 5.31 mmol, 10 mol%), and 18-crown-6 (0.622 g, 2.35 mmol, 5 mol%). The reaction was refluxed for 1 h, allowed to cool to ambient temperature and poured into CH_2Cl_2 . The aqueous layer was extracted twice with CH_2Cl_2 and the combined organic layers were dried with Na_2SO_4 and concentrated *in vacuo*. The crude material was used without further purification.

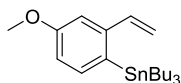
A 250 mL round bottom flask was charged with deuterated bromotetralone (used directly from previous reaction) and NaBH_4 (3.681 g, 97.3 mmol, ~2 equiv) in 100 mL of EtOH. The reaction was allowed to stir at 0 °C for 30 min. Saturated NH_4Cl was added until the effervescence ceased. The reaction was then poured into water and CH_2Cl_2 and the aqueous layer was extracted twice with CH_2Cl_2 . The combined organic layers were dried with Na_2SO_4 and concentrated *in vacuo*. The crude material was used without further purification. A 100 mL round bottom flask was charged with the deuterated bromotetralol (used directly from the previous reaction) and *para*-toluenesulfonic acid (0.977 g, 5.14 mmol, ~10 mol%) in 50 mL of toluene. The flask was equipped with a Dean-Stark trap and a reflux condenser and the reaction refluxed for 30 min. The reaction was cooled to ambient temperature and poured into saturated NaHCO_3 , the aqueous layer extracted with EtOAc, the combined organic layers dried with Na_2SO_4 and concentrated *in vacuo*. The product was purified by column chromatography using hexanes as the eluant. The deuterated bromodihydronaphthalene was isolated as a clear, colorless oil in 47% yield over the six steps. ^1H NMR (500 MHz, CDCl_3) δ 7.37 (d, $J = 7.8$ Hz, 1H), 7.03 (d, $J = 7.5$ Hz, 1H), 6.95 (t, $J = 7.7$ Hz, 1H), 6.83 (broad s, 1H), 2.78 (t, $J = 8.2$ Hz, 2H), 2.29 (t, $J = 8.3$ Hz, 2H). ^{13}C NMR (126 MHz, CDCl_3) δ 138.0, 133.0, 130.7, 130.6 (1,1,1-triplet, $J = 24.6$ Hz), 127.8, 126.7, 126.2, 121.9, 28.2, 22.7. HRMS (EI) m/z calculated for $\text{C}_{10}\text{H}_8\text{DBr} [\text{M}]^+$ 208.9945, found 208.9946.

4.15.2 Control Experiment

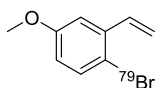


Compound 4.6. Compound **4.6** was prepared using the same procedure described for compound **2.2** (see section 2.5.2). The product was isolated in 71% yield as a clear, colorless, viscous oil. Characterization data was consistent with literature values.³²

4.15.3 Crossover Experiment



The stannane was prepared according to a previously published literature procedure and the spectral data were consistent with those previously reported.⁵



Compound 4.8. Following a modified literature procedure,⁶ the stannane (1.00 g, 2.36 mmol, 1.0 equiv) was dissolved in 40 mL of 14:1 THF/H₂O. A portion of NH₄⁷⁹Br (250 mg, 2.55 mmol, 1.08 equiv, 90% ⁷⁹Br) was added. This was immediately followed by 1.2 mL of peracetic acid (32% solution in acetic acid, 2.5 equiv). The solution was stirred for 20 min prior to dilution with water and diethyl ether (40 mL each). The phases were separated and the organics were extracted with ether (3 x 20 mL). The combined organic phases were washed with saturated NaHCO₃ (30 mL), followed by washing with a sodium bisulfite solution. The organic solution was dried over MgSO₄, filtered, concentrated, and immediately chromatographed on silica gel (hexane eluent) to yield the product in 61% yield. The NMR data were consistent with the data reported for **4.8** (see chapter 2). Mass spectrometry indicated that the product possessed a ⁷⁹Br:⁸¹Br ratio of 84:16. HRMS (ESI) *m/z* calculated for C₉H₉BrO [M]⁺ 211.9832, found 211.9831.

Experimental details for the crossover experiment. In a glovebox, CuCl (9 mg, 0.09 mmol, 0.09 equiv), 1,2-bis(dicyclohexanephosphino)ethane (38 mg, 0.09 mmol, 0.09 equiv) and potassium *tert*-butoxide (20 mg, 0.19

mmol, 0.18 equiv) were added to a 25 mL roundbottom flask. The flask was charged with 4 mL of dry, degassed THF, fitted with a septum and removed from the glovebox. The reaction mixture was allowed to stir at ambient temperature for approximately 10 min. A portion of 4,4,5,5-tetramethyl-1,3,2-dioxaborolane (0.175 mL, 1.20 mmol, 1.20 equiv) was added and the reaction was allowed to stir for an additional 10 min. Compound **4.3** (91.5mg, 0.500 mmol, 0.5 equiv) and **4.7** (106 mg, 0.500 mmol, 0.5 equiv) dissolved in 1 mL of THF were injected into the mixture. The flask was moved to an oil bath preset to 40 °C and the reaction was allowed to stir overnight. The mixture was cooled, filtered through a pad of celite and washed with 20 mL of diethyl ether. The solution was concentrated and the crude residue analyzed by mass spectrometry. The product **4.9** was determined to possess a 50:50 distribution of bromine isotopes (see **Figure 1**). The product **4.10** was found to possess an 86:14 distribution of ^{79}Br : ^{81}Br isotopes (see **Figure 2**), similar to the ratio reported for the substrate **4.8**.

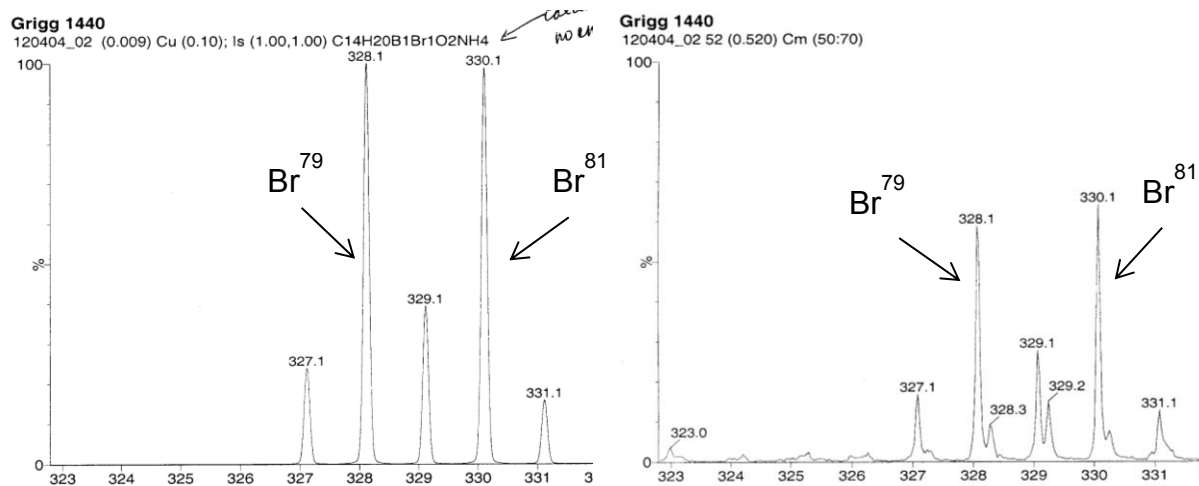


Figure 1: Mass Spectrum of Product **4.9**. Figure at left shows calculated molecular ion signals for compound with natural isotope distribution. The figure on the right shows the experimentally-obtained signals.

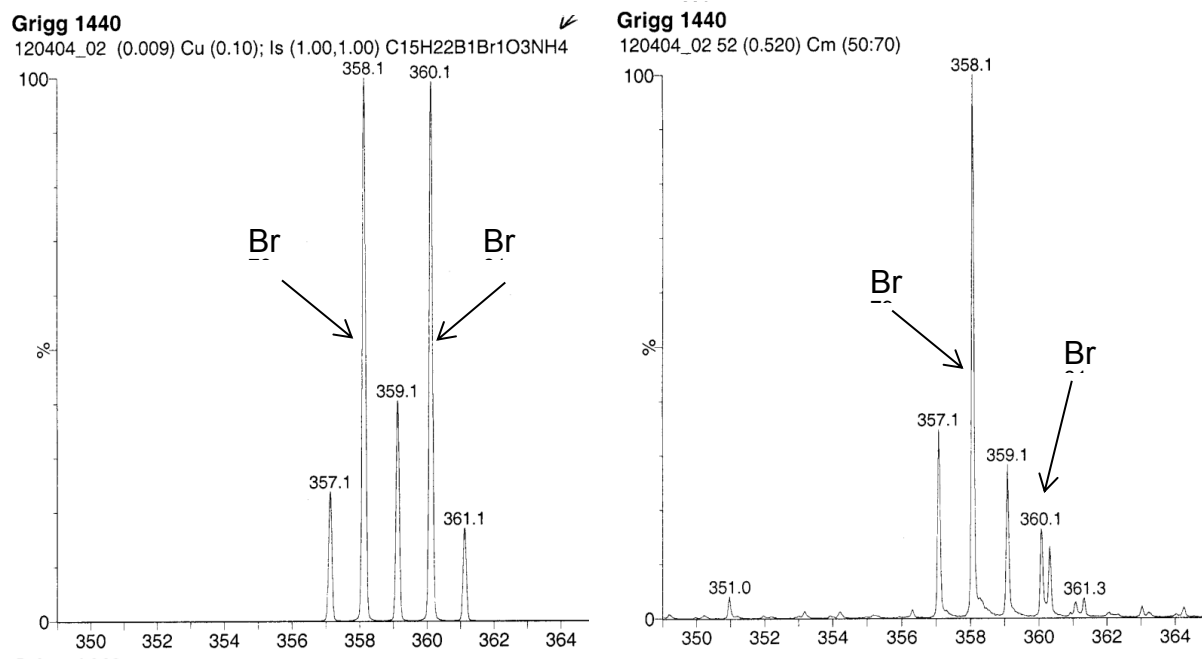
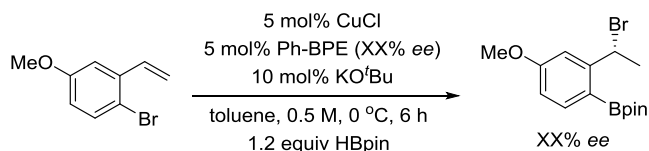


Figure 2: Mass Spectrum of Product **4.10**. Figure at left shows calculated molecular ion signals for compound with natural isotope distribution. The figure on the right shows the experimentally-obtained signals.

4.15.4 Non-Linear Effects Study



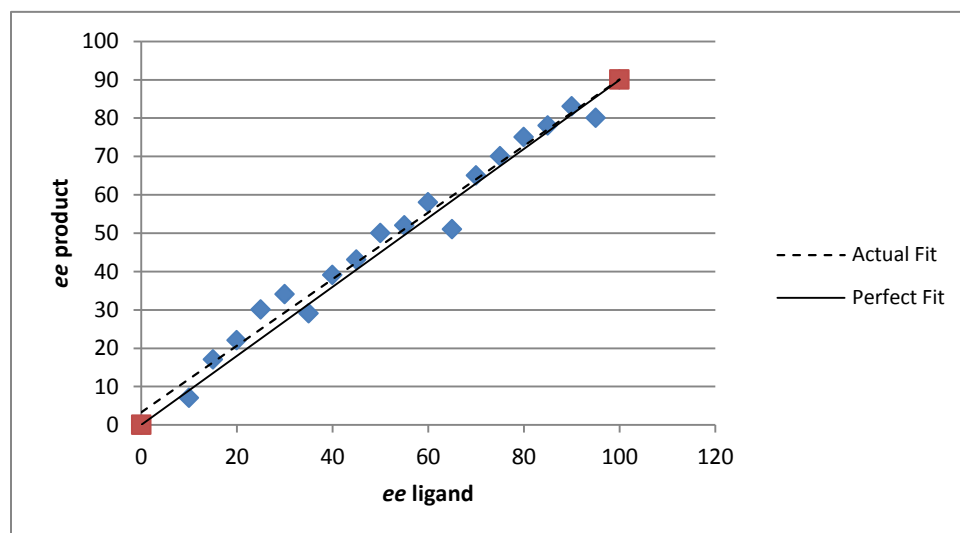
In a glovebox, a scintillation vial was charged with a solution of (*S,S*)-Ph-BPE (56 mg) in 4.0 mL of toluene (0.027 M). Another scintillation vial was charged with a solution of (*R,R*)-Ph-BPE (18 mg) in 1.3 mL of toluene (0.027 M). A mixture of CuCl (15 mg) and KO^tBu (34 mg) was thoroughly ground together to form a homogenous, fine powder. A 1.5 mL vial was charged with 1.6 mg of the CuCl/KO^tBu mixture (5 mol% CuCl, 10 mol% KO^tBu) and the ligand solutions (5 mol% total ligand loading) so that the total volume was 250 μ L; for exact amounts, see Table 1). The vial was equipped with a screw cap that had a septum and the reaction was removed from the glovebox. The reaction was allowed to stir for 10 min and then HBpin (22 μ L, 0.15 mmol, 1.2 equiv) was added in one aliquot. The reaction was transferred to an ice bath and 2-bromo-5-methoxystyrene (19 μ L, 0.125 mmol, 1.0 equiv) was added. The reaction was allowed to stir at 0 $^{\circ}$ C for 6 h and then passed through a plug of silica gel using diethyl ether as the eluant. The volatiles were removed *in vacuo* and the crude material was used for chiral HPLC analysis

without further purification (in general, rigorous purification of enantioenriched benzyl bromides resulted in the degradation of *ee*). Chromatograms were acquired on a Shimadzu Prominence HPLC equipped with a Chiracel AD-H column. Flow rate: 1.00 mL/min.; Oven temp: 40.0 °C; Solvent: isocratic 1.00% *i*PrOH in hexanes; Detector: UV @ 254 nm and 225 nm. $t_R = 4.15$ min, $t_S = 5.03$ min, $t_{SM} = 4.56$ min.

Table 1: Tabulation of non-linear effects

entry	<i>S</i> soln. (μL)	<i>R</i> soln. (μL)	ligand <i>ee</i>	product <i>ee</i>
1	250	0	100	90
2	244	6.0	95	80
3	238	12	90	83
4	231	19	85	78
5	225	26	80	75
6	219	31	75	70
7	213	37	70	65
8	206	44	65	51
9	200	50	60	58
10	194	56	55	52
11	188	62	50	50
12	181	69	45	43
13	175	75	40	39
14	169	81	35	29
15	163	87	30	34
16	156	94	25	30
17	150	100	20	22
18	144	106	15	17
19	138	112	10	7

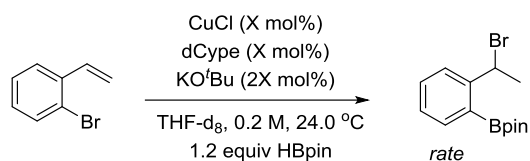
Figure 1: Graph of non-linear effects with trend lines



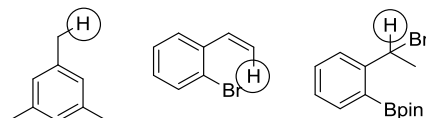
Perfect Linear Fit Equation: $y = 0.9x$

Actual Linear Fit Equation: $y = 0.868x + 3.305$; $R^2 = 0.9801$

4.15.5 Kinetics and Hammett Studies



In a glovebox, CuCl, KOtBu, dCype and dry, degassed THF- d_8 (see Table 2 for exact amounts at different catalyst loadings) were added to a dry NMR tube. A rubber septum was placed on the tube and the tube was removed from the glovebox. Mesitylene (10 μ L) was added to the NMR tube as an internal standard and the tube was sonicated for 10 min. Pinacol borane (HBpin, see Table 2) was added in one aliquot and the NMR tube was inverted once. The 2-bromostyrene (see Table 2) was immediately added and the tube was inverted once, a stopwatch was started, and the tube was placed in the spectrometer. The sample was locked and shimmed and then a pulse program was used that acquired a one-scan spectrum every 30 sec. The time from the injection of the 2-bromostyrene to the first scan was typically 1-4 min. The sample was spun at frequency of 20 Hz and the probe temperature was held steady at 24.0 $^{\circ}$ C. Typically, a sample from a previous run was used to set receiver gain, lock and shim so that minimal shim time on the new sample was required. For all runs, the circled protons were integrated.



The reaction showed first-order rate dependence on catalyst concentration displaying saturation between 5 mol% and 10 mol% catalyst loading (Fig. 2, 3; Table 3). This rate dependence is likely due to catalyst solubility, as not all of the pre-catalyst went into solution (visually).

Table 2: Amounts of reagents for different catalyst loadings

cat. loading	CuCl (mg)	KOtBu (mg)	dCype (mg)	THF- d_8 (mL)	substrate (μ L)	HBpin (μ L)
1%	2.0 mL of a stock solution of CuCl (1.3 mg), KOtBu (2.9 mg) and dCype (5.5 mg) in 6.5 THF- d_8 was used.				50	70
2.5%	1.2	2.8	5.5	2.50	63	87

5%	1.2	2.8	5.5	1.25	31	44
10%	2.5	5.6	11	1.25	31	44
20%	5	11	21	1.25	31	44

Figure 2: Time courses with different catalyst loadings

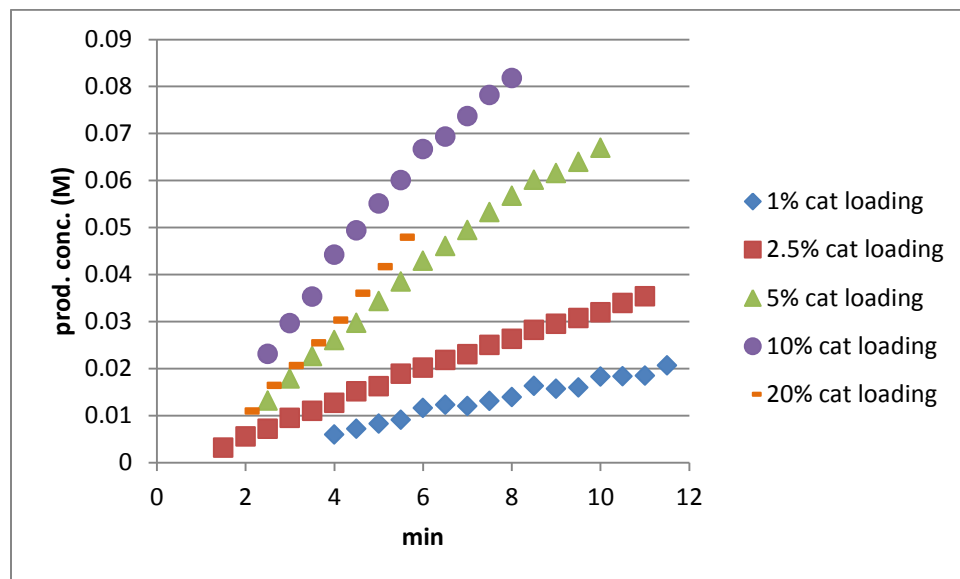
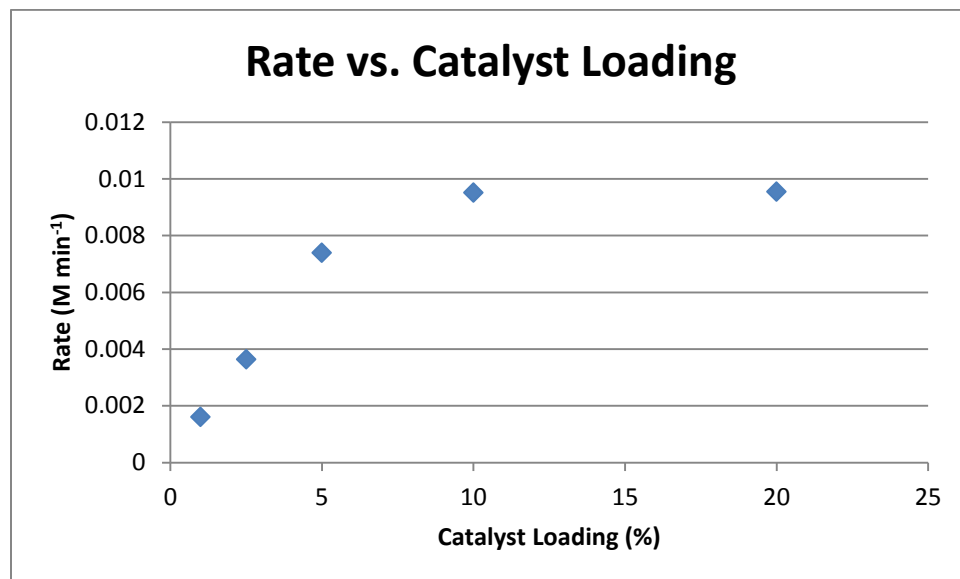


Table 3: Summary of kinetics studies with different catalyst loadings

catalystloading	initial rates	average	standard deviation
1%	0.001518	0.001604	8.38547E-05
1%	0.00161		
1%	0.001685		
2.50%	0.003248	0.003633	0.000405858
2.50%	0.003342		
2.50%	0.003838		
2.50%	0.004102		
5%	0.006305	0.007388	0.000483438
5%	0.006985		
5%	0.007241		
5%	0.009021		
10%	0.008738	0.009506	0.00107051
10%	0.00905		
10%	0.010729		

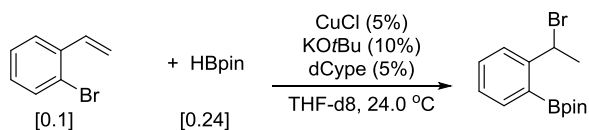
20%	0.008699	0.009539	0.000737983
20%	0.00921		
20%	0.009863		
20%	0.010385		

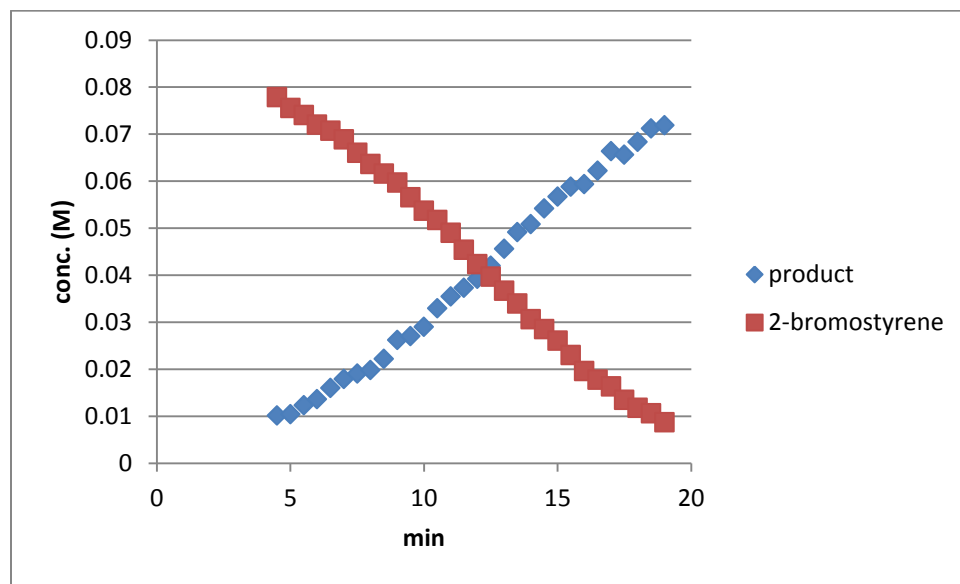
Figure 3: Rate vs. catalyst loading



Over the course of the entire reaction, the rate of the reaction did not change as both the concentration of the 2-bromostyrene and HBpin changed (Figure 4). From this observation, it was determined that the reaction rate is not dependent on either 2-bromostyrene or HBpin. However, most time courses showed dramatic changes in rate over time as catalyst death occurred,⁶ eventually halting the reaction altogether. Deuterating the substrate at the terminal position of the styrene resulted in a small normal KIE of 1.19 ± 0.1 (Figure 5, Table 4).

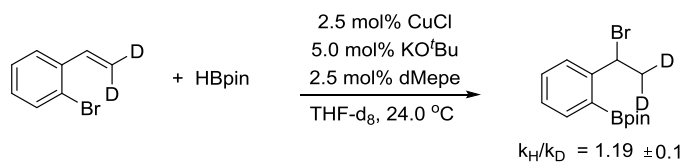
Figure 4: Time course over entire reaction





To determine if there was a change in rate if the terminal position of the styrene was deuterated, the reaction was run using 2-bromo- β,β -dideuterostyrene. The same procedure was used as described above except 13 μL of 2-bromo- β,β -dideuterostyrene (0.099 mmol, 1.0 equiv), 17 μL HBpin (0.117 mmol, 1.18 equiv), and 0.5 mL of a stock solution of 1.5 mg CuCl, 3.4 mg KO^tBu, and 6.3 mg dCype in 3.0 mL of THF- d_8 was used (2.5 mol% catalyst loading). ^1H NMR (500 MHz, CDCl_3) δ 7.77 (dd, $J = 7.4, 1.5$ Hz, 1H), 7.68 (dd, $J = 7.9, 1.1$ Hz, 1H), 7.46 (td, $J = 7.7, 1.5$ Hz, 1H), 7.26 (td, $J = 7.3, 1.1$ Hz, 1H), 6.24 (d, $J = 6.8$ Hz, 1H), 1.99 (broad-d, $J = 7.0$ Hz, 1H), 1.37 (s, 6H), 1.36 (s, 6H). ^{13}C NMR (126 MHz, CDCl_3) δ 149.4, 135.9, 131.5, 127.2, 126.4, 83.9, 48.5, 26.5 (1:2:3:2:1-pentet, $J = 19.9$ Hz), 25.0, 24.7. HRMS (ESI) m/z calculated for $\text{C}_{14}\text{H}_{22}\text{D}_2\text{BBrNO}_2$ $[\text{M}+\text{NH}_4]^+$ 330.1206, found 330.1215.

Figure 5: Time courses of unlabeled vs. deuterated substrate



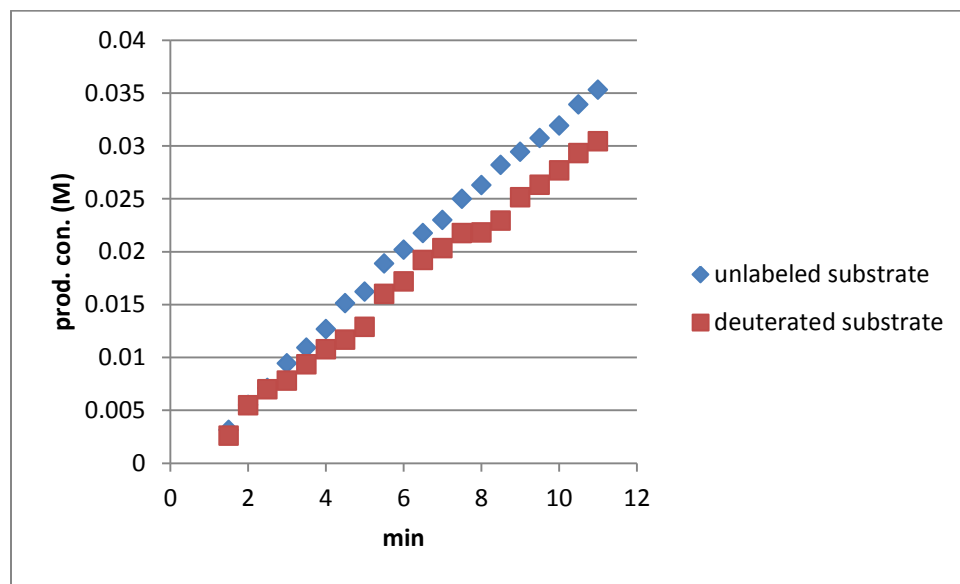
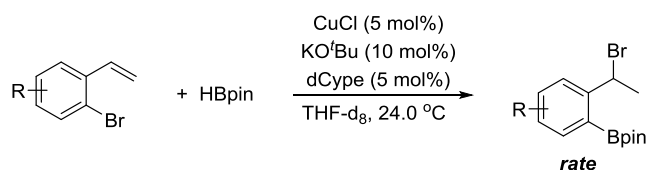


Table 4: Summary of KIE studies

substrate	initial rate	average	standard deviation	k_H/k_D	error
deuterated	0.003202	0.00304	0.000175	1.194901	0.105191
deuterated	0.003063				
deuterated	0.002855				
unlabeled	0.003248	0.003633	0.000406		
unlabeled	0.003342				
unlabeled	0.003838				
unlabeled	0.004102				



Hammett Plot: In a glovebox, CuCl (2.5 mg; 25 μ mol; 10 mol%), KOtBu (5.6 mg; 50 μ mol; 20 mol%), dCypc (11 mg; 25 μ mol; 10 mol%) and 0.5 mL of dry, degassed THF- d_8 were added to a dry NMR tube. A rubber septum was placed on the tube and the tube was removed from the glovebox. Mesitylene (10 μ L) was added to the NMR tube as an internal standard and the tube was sonicated for 10 min. Pinacol borane (HBpin; 44 mL; 303 μ mol; 1.2 equiv) was added in one aliquot and the NMR tube was inverted once. The substituted 2-bromostyrene (250 μ mol; 1.0

equiv) was immediately added and the tube was inverted once, a stopwatch was started, and the tube was placed in the spectrometer. The sample was locked and shimmed and then a pulse program was used that acquired a one-scan spectrum every 30 sec. The time from the injection of the substituted 2-bromostyrene to the first scan was typically 1-4 min. The sample was spun at frequency of 20 Hz and the probe temperature was held steady at 24.0 °C.

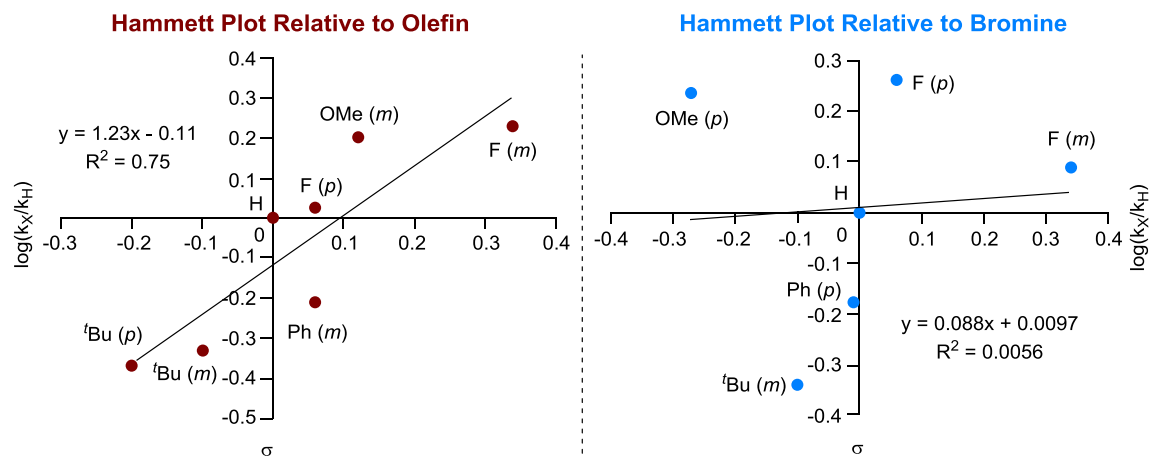


Table 1. Rates relative to olefin.

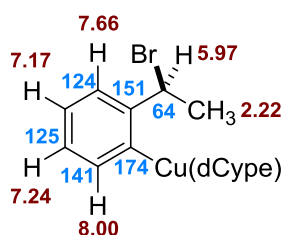
substrate	rate			avg	σ	Log(kx/kH)	Std. deviation
H	0.142581	0.122147	0.127437	0.130721	0	0	0.010606
F(p)	0.142233	0.149076	0.123546	0.138285	0.06	0.02443	0.013215
OMe(m)	0.208929	0.208847	0.316725	0.244834	0.12	0.272525	0.06226
F(m)	0.248845	0.194979		0.221912	0.34	0.229835	0.038089
Ph(m)	0.073473	0.088566		0.081019	0.06	-0.20776	0.010672
tBu(p)	0.06741	0.044133		0.055771	-0.2	-0.36993	0.016459
tBu(m)	0.078785	0.042979		0.060882	-0.1	-0.33186	0.025319

Table 2. Rates relative to bromine.

substrate	Avg. rate	σ	log(kx/kH)
H	0.122147	0	0
F(m)	0.149076	0.34	0.086527
OMe(p)	0.208847	-0.27	0.232947
F(p)	0.221912	0.06	0.2593
Ph(p)	0.081019	-0.01	-0.17829
tBu(m)	0.055771	-0.1	-0.34047

4.15.6 Stoichiometric NMR Experiments

In a glovebox, a dry NMR tube was charged with $\text{Cu}(\text{OAc})_2$ (4.5 mg, 24.8 μmol , 1.0 equiv), dCype (11 mg, 26.0 μmol , 1.05 equiv) and 0.5 mL of *p*-xylene- d_{10} . The NMR tube was equipped with a septum and removed from the glovebox where the septum was wrapped with parafilm. The NMR tube was shaken, then PHMS (3.0 μL , 50.2 μmol , 2.03 equiv) and then shaken again. Just before placing in the spectrometer, 2-bromostyrene (3.1 μL , 24.7 μmol , 1.0 equiv) was injected and then the NMR tube was warmed in 40-45 $^\circ\text{C}$ water for 1.5-2 minutes. The NMR tube was then placed in an NMR spectrometer where the probe had been pre-cooled to 10 $^\circ\text{C}$. At this temperature, the aryl copper species was stable for 1.5-2 hours before significant degradation occurred.



All spectra were acquired on a 750 MHz NMR.

Spectra

^1H -NMR

1D-TOCSY selecting proton at 5.97 ppm (stacked with ^1H)

1D-TOCSY selecting proton at 8.00 ppm (stacked with ^1H , various mix times ranging from 15ms-120ms)

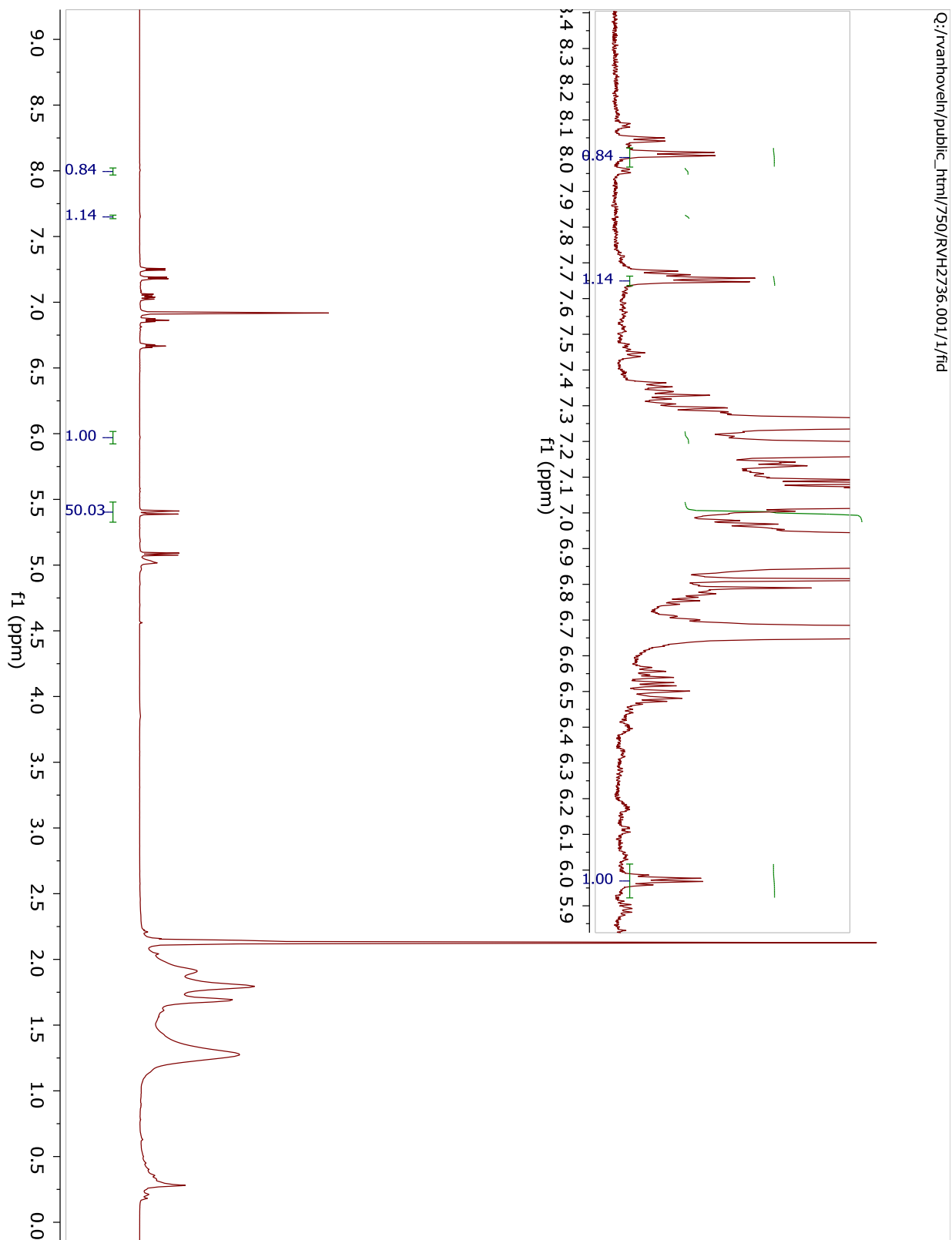
1D-NOESY selecting proton at 5.97 ppm (stacked with ^1H)

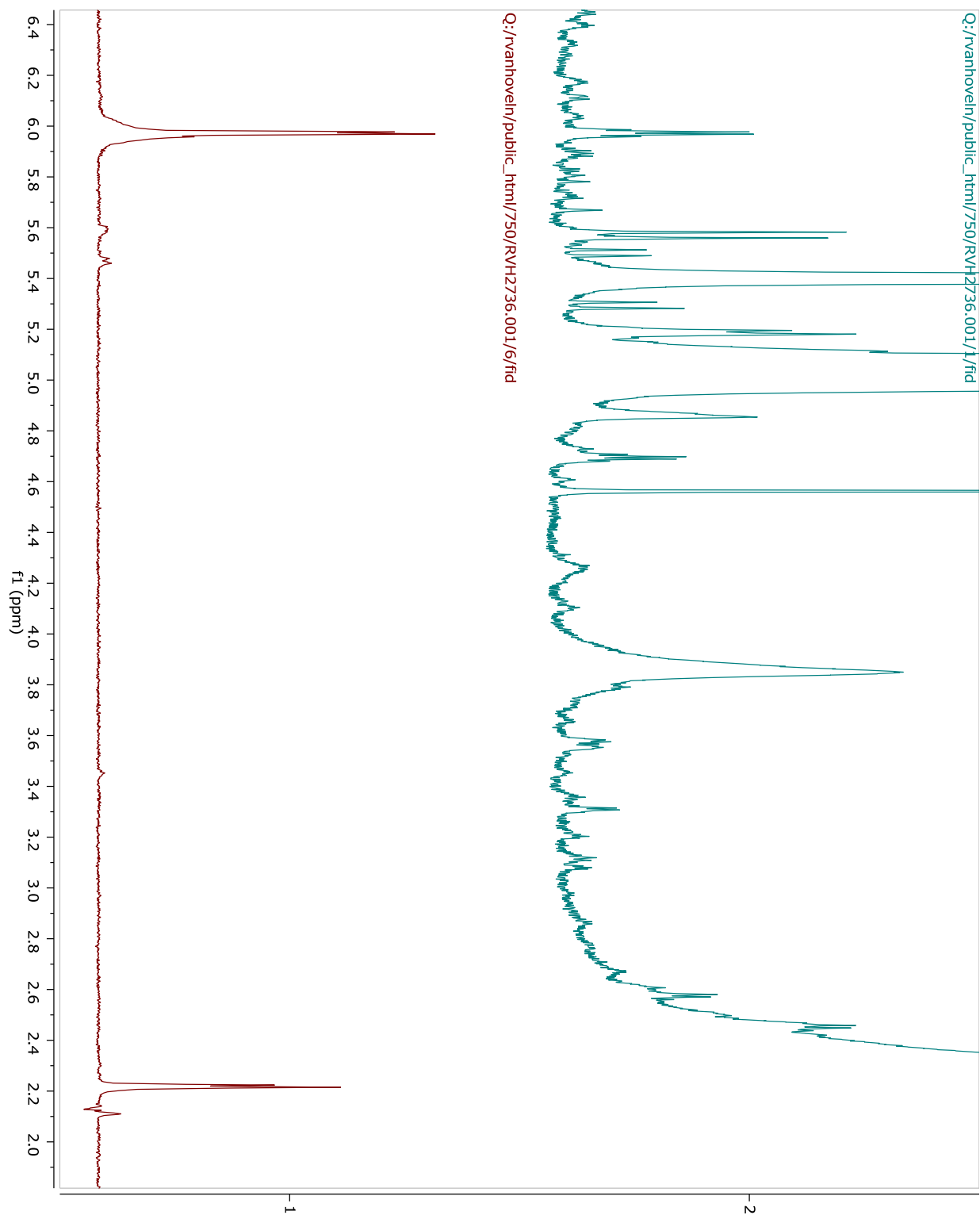
HMBC with ^1H trace

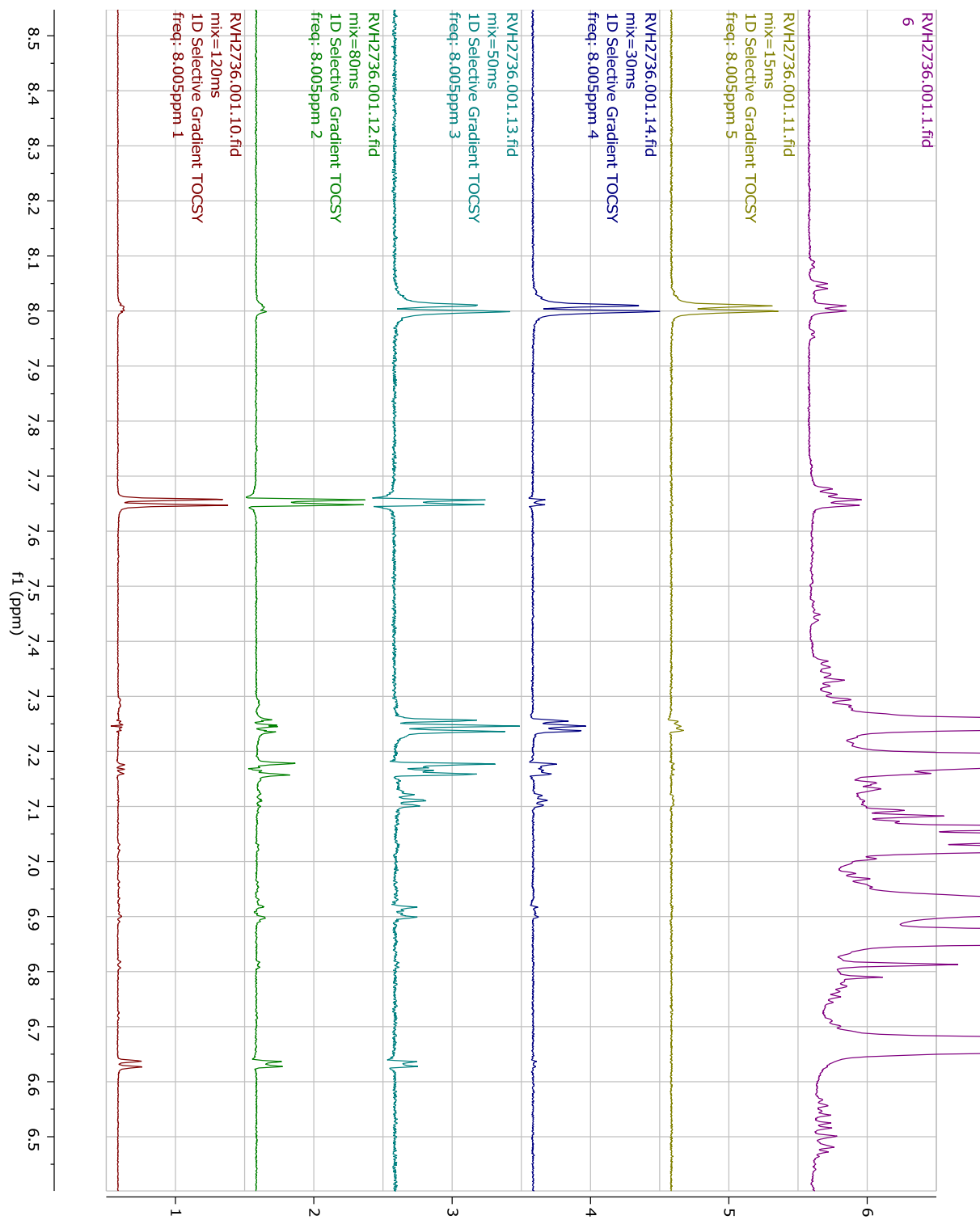
HMBC with 1D-TOCSY trace

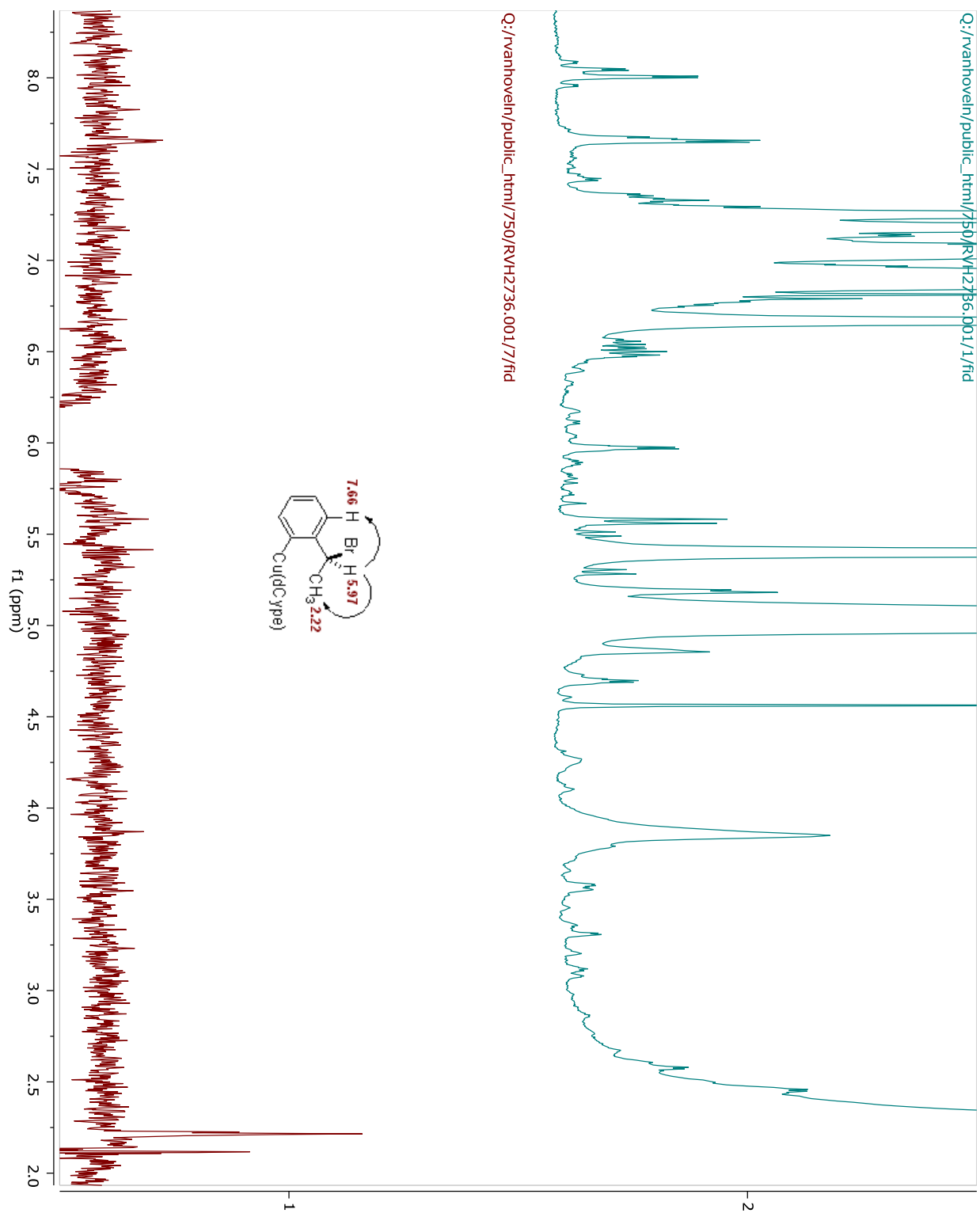
HSQC with ^1H trace

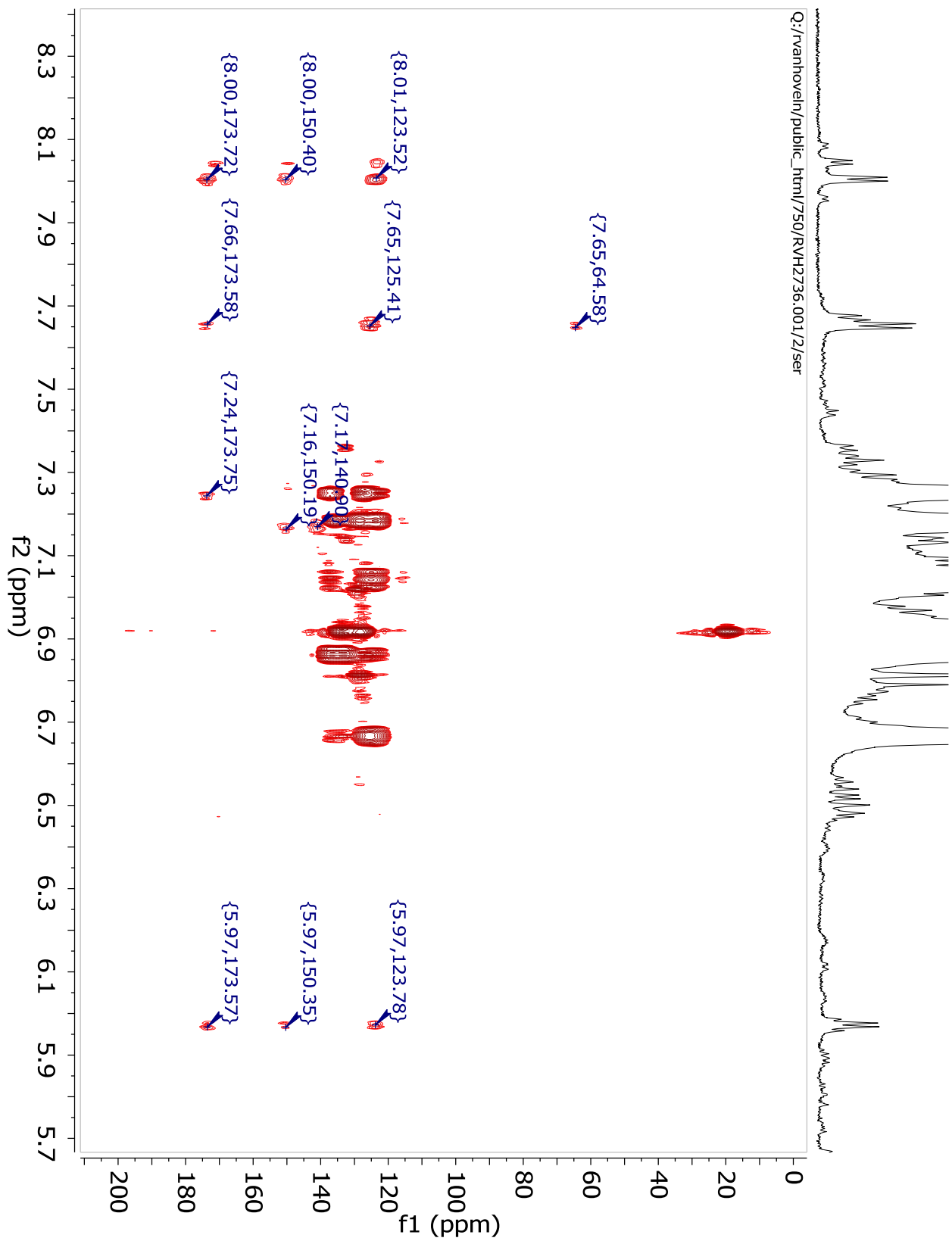
HSQC with 1D-TOCSY trace

$^1\text{H-NMR}$ of aryl copper

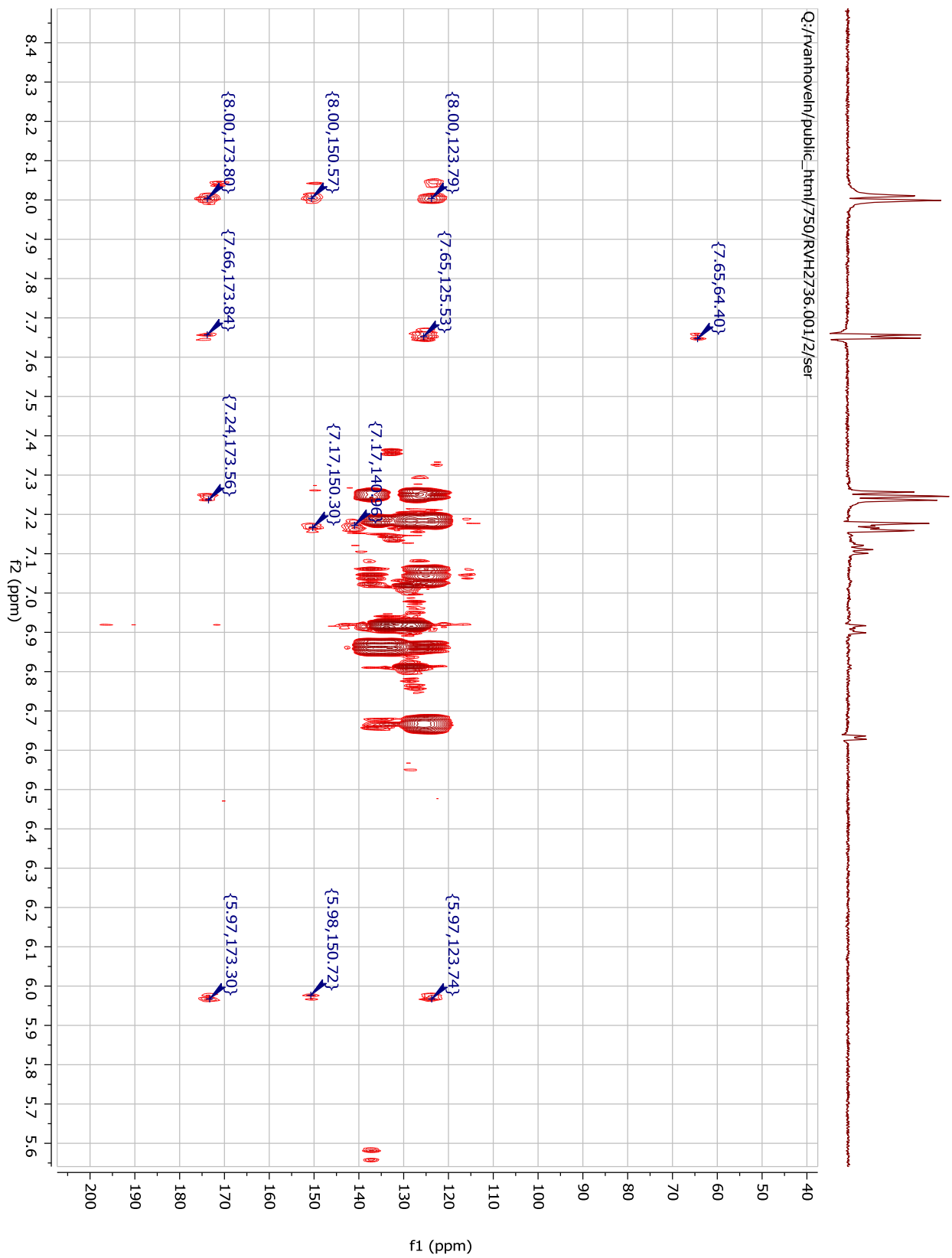
1D-TOCSY selecting proton at 5.97 ppm (stacked with $^1\text{H-NMR}$)

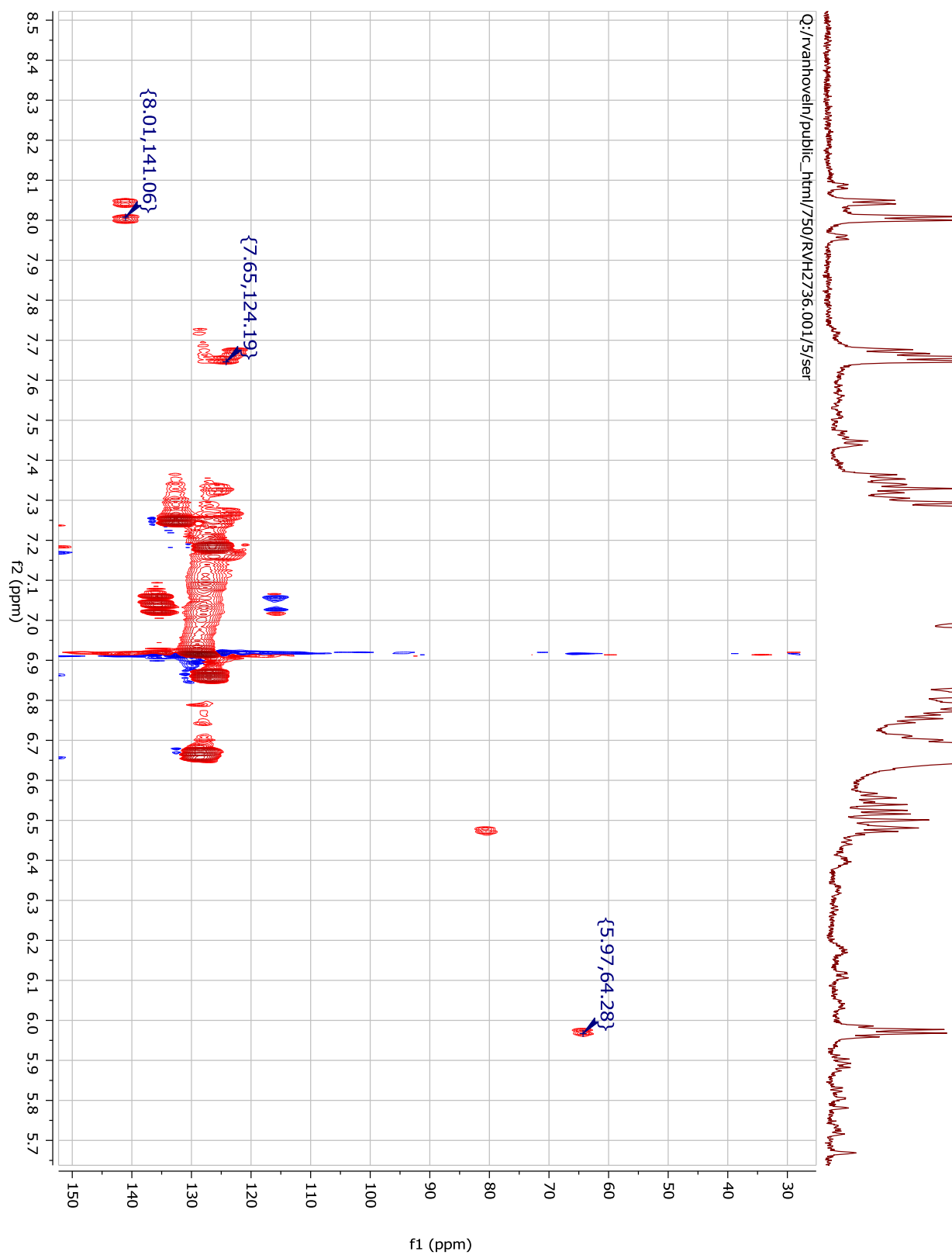
1D-TOCSY selecting proton at 8.00 ppm (stacked with ^1H , various mix times)

1D-NOESY selecting proton at 5.97 ppm (stacked with ^1H)

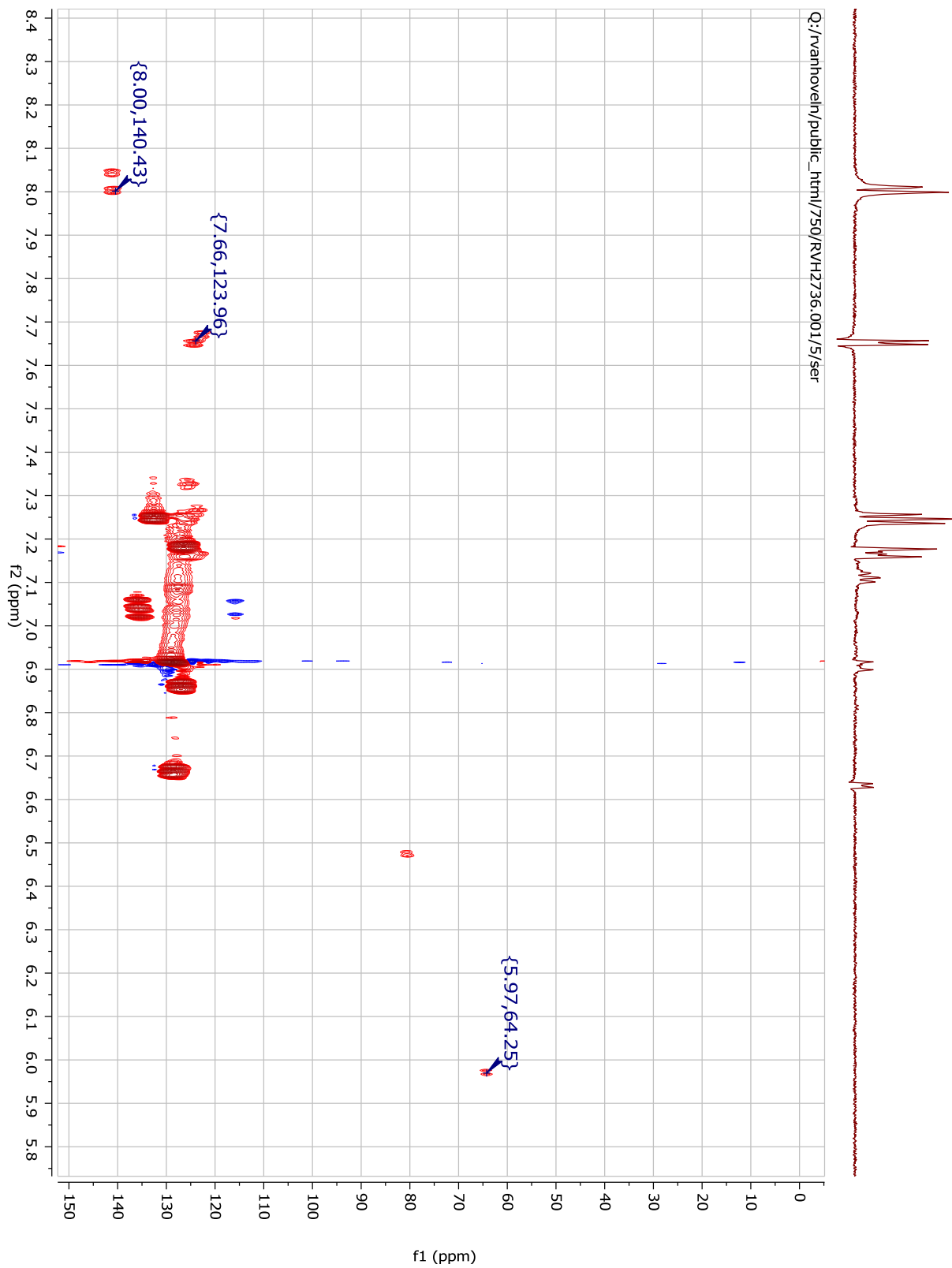
HMBC with ^1H trace

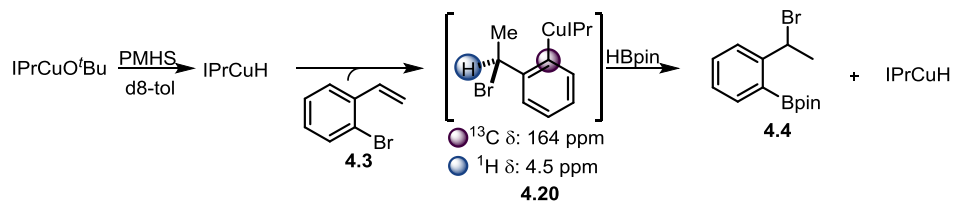
HMBC with 1D-TOCSY trace



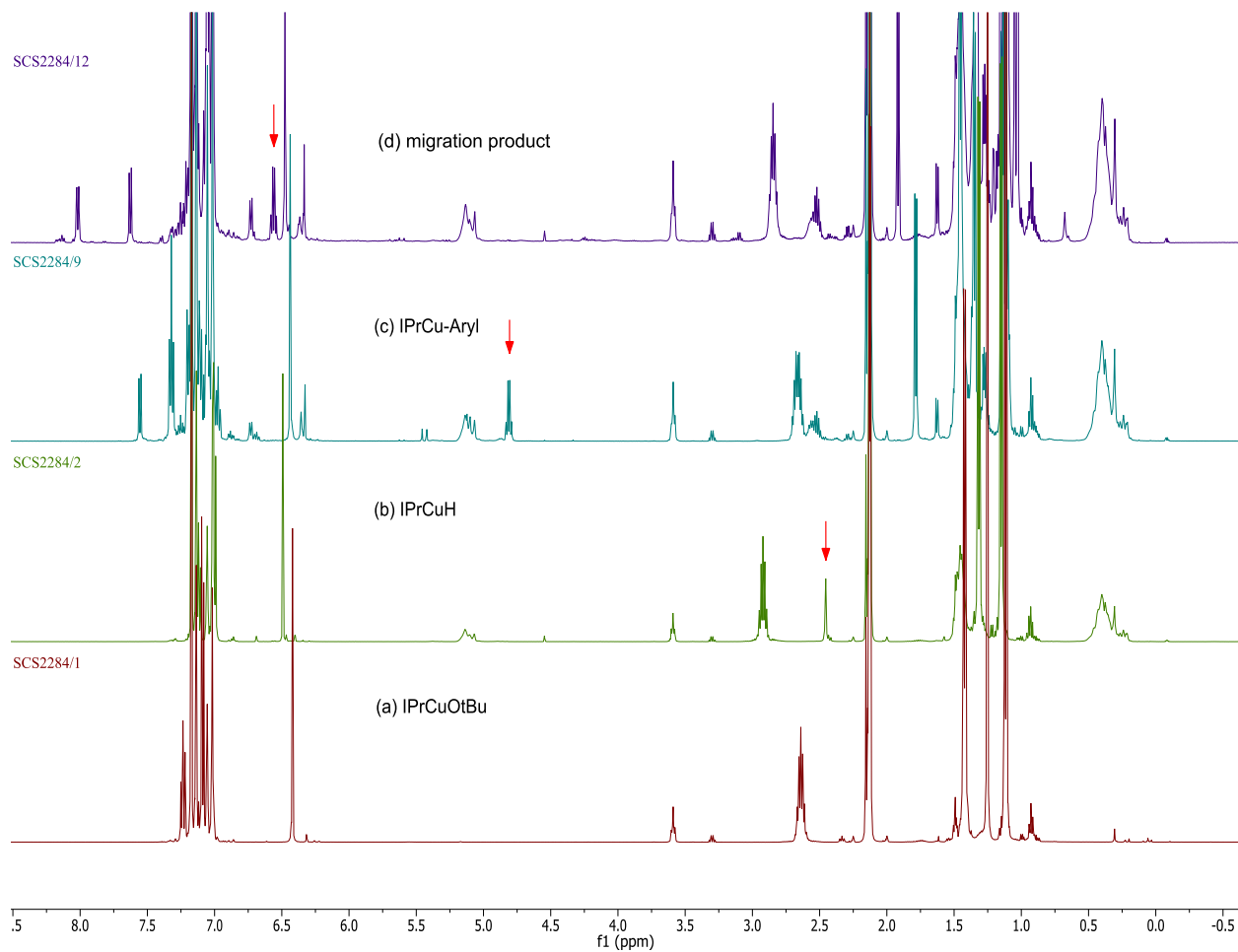
HSQC with ^1H trace

HSQC with 1D-TOCSY trace

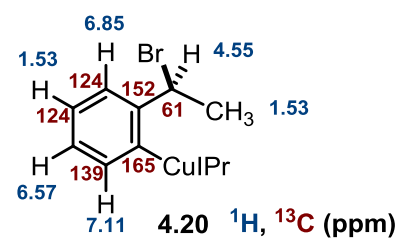




In the glovebox, IPrCuO^tBu (13.1 mg, 0.025 mmols) was weighed into an NMR tube and suspended in d_8 -toluene (0.5 mL). The tube was capped with a septum and removed from the glovebox. PMHS (1.8 μL , 0.03 mmols) was added *via* syringe giving a bright yellow solution that became homogenous after several rounds of inverting the NMR tube. An ^1H NMR spectrum was acquired on IPrCuH to ensure its complete formation. After acquisition, **4.3** (3.2 μL , 0.025 mmols) was added. After several seconds, a color change from bright yellow to clear was observed and the sample reinserted into the spectrometer. Complete conversion of IPrCuH to aryl-copper(I) **4.20** was observed and the complex was characterized by ^1H NMR and HMBC. It should be noted the ^{13}C shift of the ipso-copper aryl carbon, 164.6 ppm, closely matches that seen by Herron (166.1 ppm).¹⁵ Following characterization of **4.20**, HBpin (7.3 μL , 0.05 mmols) was added and product **4.4** was formed and the colored IPrCuH regenerated.

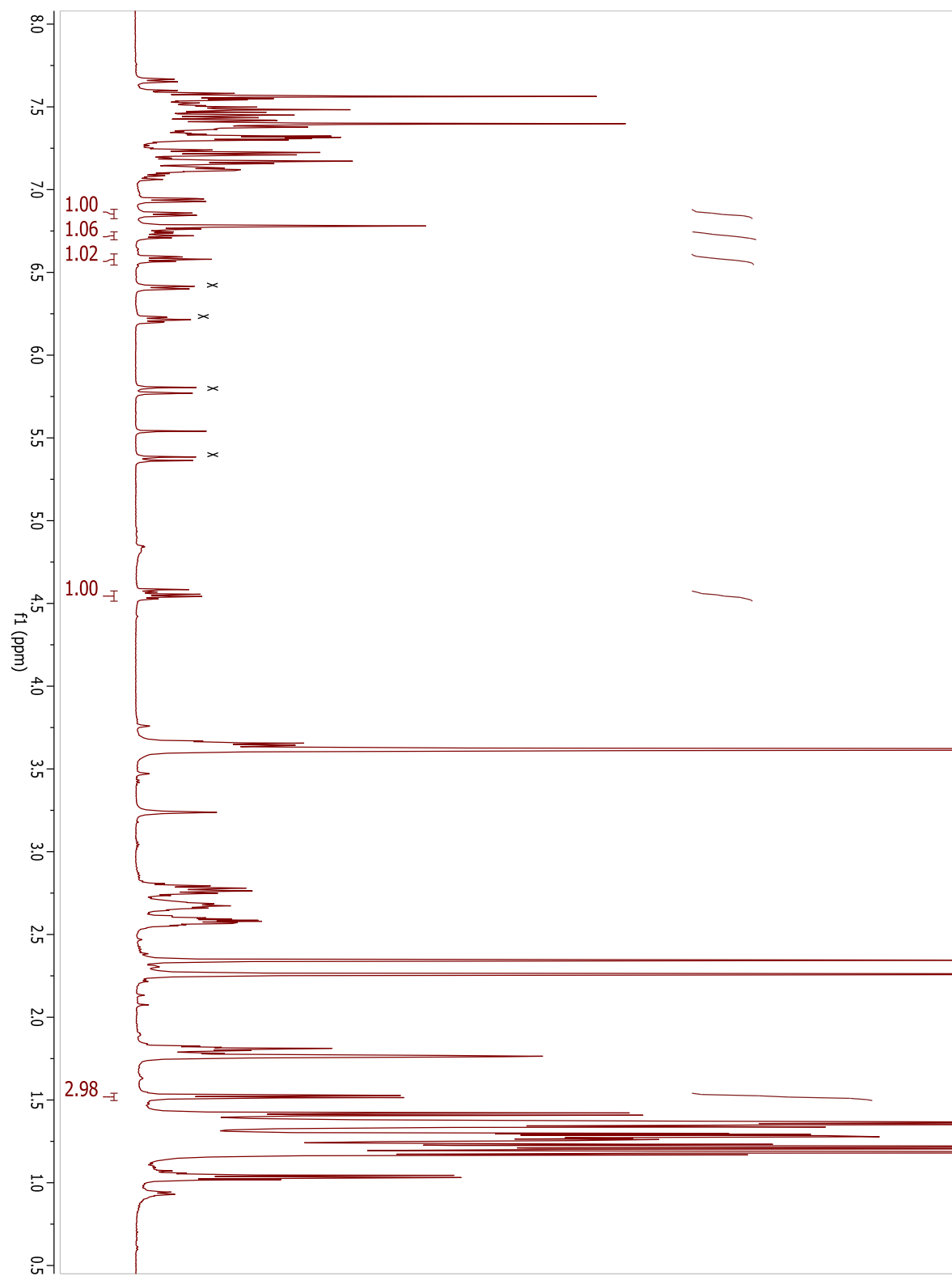


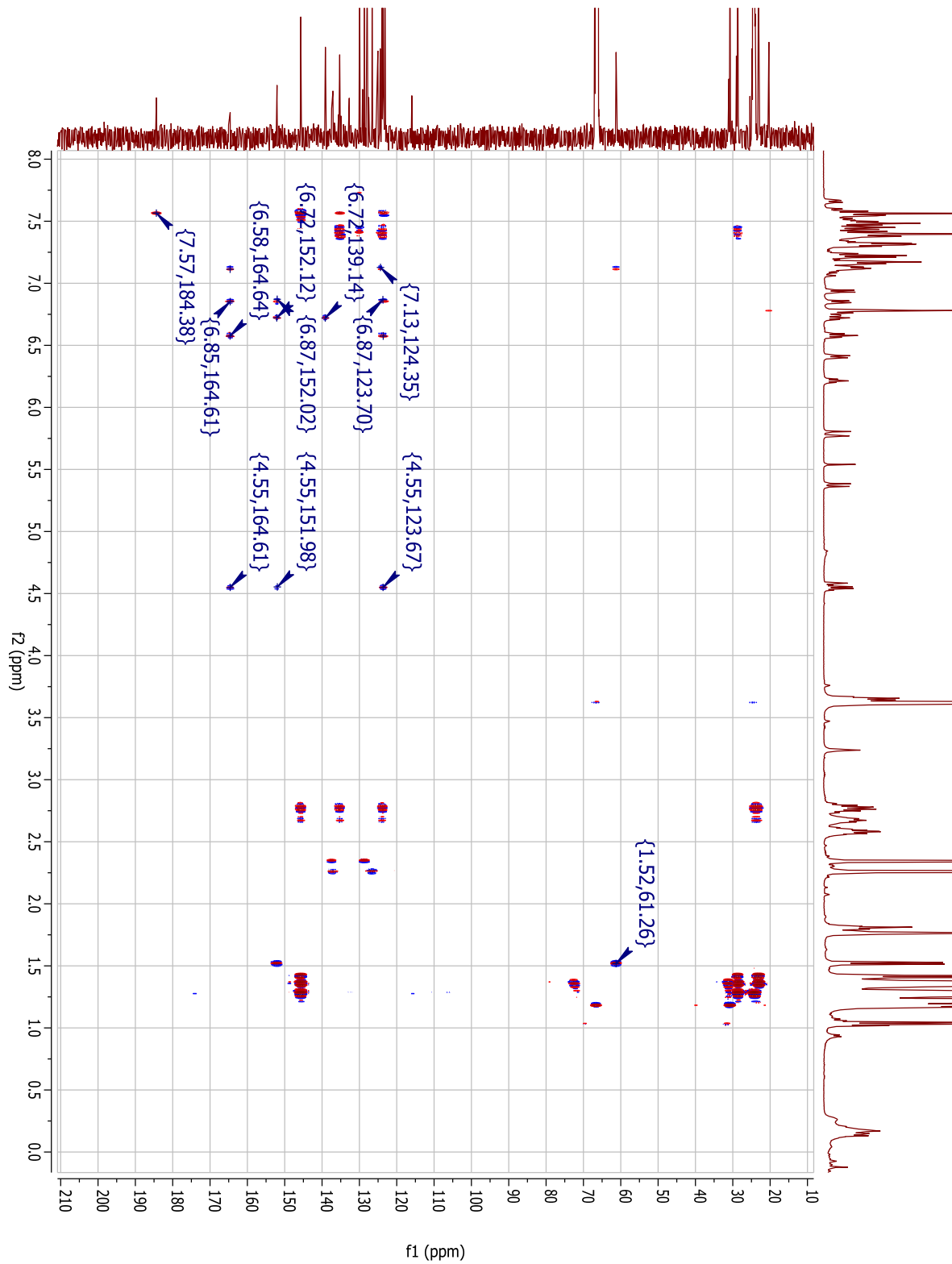
(a) IPrCuOtBu in d_8 -toluene. (b) IPrCuH formed on addition of PMHS, closely resembling the literature spectra in THF.¹ (c) IPrCu-Aryl **4.20** formed on addition of **4.3** to IPrCuH (quartet at 4.73 ppm). (d) Migration product observed on addition of HBpin to **4.4**.



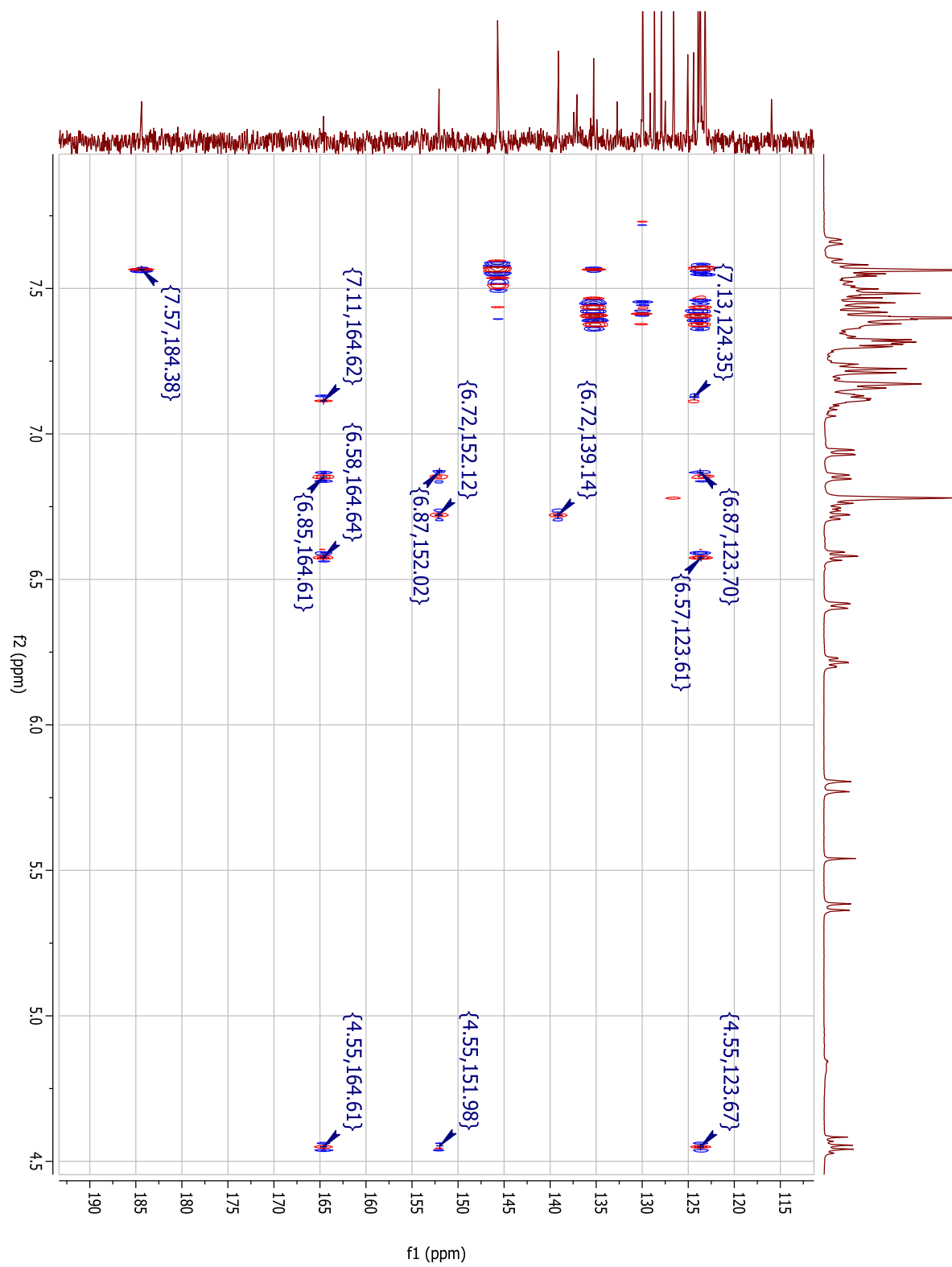
^1H NMR

-HMBC traces

¹H NMR (d8-THF) (x = excess 2-bromostyrene)

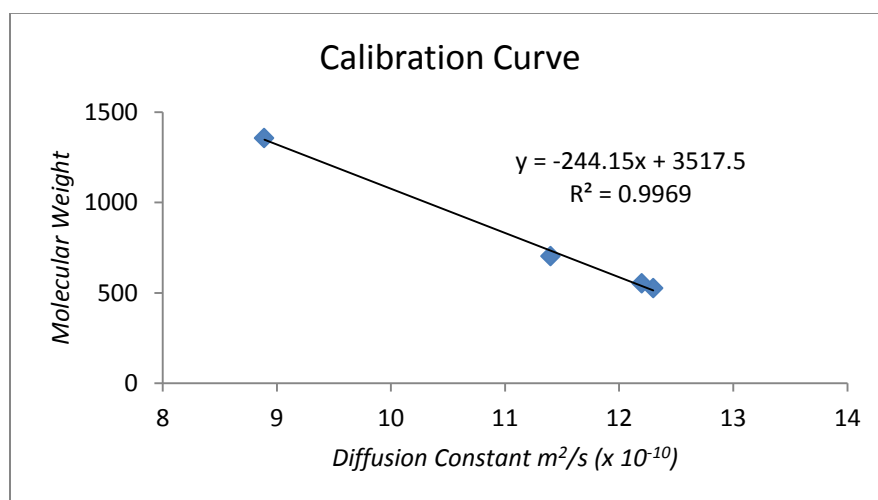
HMBC (d8-THF) with ^1H and ^{13}C traces.

HMBC (d8-THF) – Blowup of Aromatic Region



More insight into the nature of the NHC-Cu-H species in solution was obtained using pulse gradient spin echo (PGSE) NMR. The PGSE experiment measures the translational motion of molecules and weakly associated complexes through a solution, permitting the extraction of diffusion coefficients for individual compounds.³³ As these coefficients are inversely related to the hydrodynamic volume of the complexes, they can be used to probe monomer-dimer equilibria in solution and yield information about the relative molecular weights of species that cannot be isolated in the solid state.^{33,34} In our studies, $\text{Rh}_2(\text{TPA})_4$ (TPA = triphenylacetate), IPrCuOtBu , $(\text{dCype})\text{NiCl}_2$, and $\text{PdCl}_2(\text{PPh}_3)_2$ were used as reference compounds.

Complex	diffusion constant $\text{m}^2/\text{s} (\times 10^{-10})$	Molecular Weight
$\text{Rh}_2(\text{TPA})_4$	8.89	1355.14
IPrCuOtBu	12.3	525.26
$(\text{dCype})\text{NiCl}_2$	12.2	552.21
$\text{PdCl}_2(\text{PPh}_3)_2$	11.4	701.9



The NHC-Cu-hydrides were formed with PMHS *in situ* as described above and their diffusion constants measured:

Complex	diffusion constant $\text{m}^2/\text{s} (\times 10^{-10})$	Calc. Molecular Weight	Expected Monomer Weight	Expected Dimer Weight
IPrCuH	9.82	1119.9	453.15	906.3
IPentCuH-1	9.13	1288.4	565.47	1130.74
IPentCuH-2	8.49	1444.7		
IHeptCuH-1	8.5	1442.2	677.59	1355.18
IHeptCuH-2	7.9	1588.7		

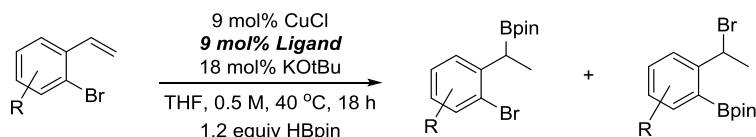
Following the measurement of the diffusion constants, the molecular weights were calculated from the calibration curve above. All 3 NHC-Cu-hydrides, IPr, IPent, and IHept showed much larger diffusion constants than expected for monomeric species, consistent with their presence as dimers in solution. We attribute the fact that the

calculated molecular weights for IPrCuH, IPentCuH, and IHeptCuH eclipse the expected dimer weights to solvation by THF. Additionally, IPentCuH and IHeptCuH had two separate species in solution which we postulate are differently solvated dimer complexes in solution although DOSY is not accurate enough to assign their exact structures with confidence.

We also measured the diffusion constant of aryl copper **4.20** (*vide infra*):

Complex	diffusion constant m^2/s ($\times 10^{-10}$)	Calc. Molecular Weight	Expected Monomer Weight	Expected Dimer Weight
IPrCuAr (3.1)	11.4	734.19	636.19	1272.38

4.15.7 Factors Impacting Selectivity

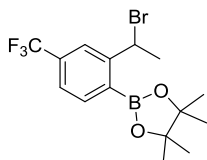


In a glovebox, CuCl (2.5 mg, 0.025 mmol, 10 mol%), KO^tBu (5.6 mg, 0.050 mmol, 20 mol%), the ligand (see Table 5 for exact amount, 0.025 mmol, 10 mol%) and 0.5 mL of dry, degassed THF were added to a dry round bottom flask. A rubber septum was placed on the flask and the flask was removed from the glovebox. Pinacol borane (HBpin, 0.05 mL, 0.35 mmol, 1.4 equiv) was added in one aliquot and then a 2-bromostyrene (see Table 2, 0.25 mmol, 1.0 equiv) was added. The reaction was transferred to a sand bath set to 40 °C and stirred for at least 30 min (typically, overnight). The reaction was quenched by filtering through a pad of celite eluted with diethyl ether. The solvent was removed *in vacuo* and the NMR yield was determined by using 1,1,1,2-tetrachloroethane as an internal standard (see Table 5).

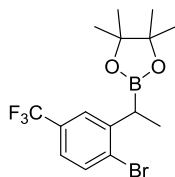
Table 5: Effects of ligand sterics and substrate electronics

entry	Ligand	Substrate	Ligand Amt. (mg or μ L)	Substrate amt. (μ L)	Hydroboration (%)	Migration (%)
1	dCype	H	11 mg	40	0	94
2	dMepe	H	4.0 μ L	40	91	0
3	dEtpe	H	6 μ L	40	98	0
4	Ph-BPE	H	13 mg	40	0	37
5	dCype	5-F	11 mg	40	28	49
6	Ph-BPE	5-F	13 mg	40	0	21
7	dCype	5-CF ₃	11 mg	40	31	28
8	Ph-BPE	5-CF ₃	13 mg	40	6	14

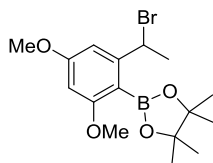
9	dCype	5-OMe	11 mg	40	0	87
10	dMepe	5-OMe	4.0 μ L	40	52	0
11	dEtpe	5-OMe	6 μ L	40	100	0
12	dCype	3,5-OMe	11 mg	50	0	98
13	dMepe	3,5-OMe	4.0 μ L	50	40	16
14	dEtpe	3,5-OMe	6 μ L	50	32	17



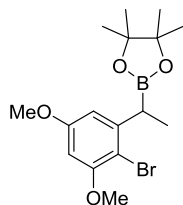
Compound 4.37. ^1H NMR (500 MHz, CDCl_3) δ 7.93–7.86 (m, 2H), 7.49 (dd, $J = 7.9, 0.9$ Hz, 1H), 6.22 (q, $J = 6.9$ Hz, 1H), 2.03 (d, $J = 6.9$ Hz, 3H), 1.39 (s, 6H), 1.37 (s, 6H). ^{13}C NMR (126 MHz, CDCl_3) δ 150.3, 136.4, 133.2 (q, $J = 32.3$ Hz), 123.9 (q, $J = 272.6$ Hz), 123.7 (q, $J = 3.7$ Hz), 123.1 (q, $J = 3.8$ Hz), 84.4, 46.9, 26.8, 25.0, 24. HRMS (EI) m/z calculated for $\text{C}_{15}\text{H}_{19}\text{BBrF}_3\text{O}_2$ $[\text{M}]^+$ 378.0611, found 378.0608.



Compound 4.38. ^1H NMR (500 MHz, CDCl_3) δ 7.63 (d, $J = 8.2$ Hz, 1H), 7.50 (d, $J = 2.2$ Hz, 1H), 7.26 (dd, $J = 8.3, 2.2$ Hz, 1H), 2.82 (q, $J = 7.5$ Hz, 1H), 1.37 (d, $J = 7.5$ Hz, 3H), 1.24 (s, 12H). ^{13}C NMR (126 MHz, CDCl_3) δ 145.7, 133.0, 129.8 (q, $J = 32.4$ Hz), 128.7 (q, $J = 1.6$ Hz), 125.5 (q, $J = 3.8$ Hz), 124.1 (q, $J = 272.2$ Hz), 123.4 (q, $J = 3.8$ Hz), 83.7, 24.7, 24.6, 15.5. HRMS (EI) m/z calculated for $\text{C}_{15}\text{H}_{19}\text{BBrF}_3\text{O}_2$ $[\text{M}]^+$ 377.0645, found 377.0646.

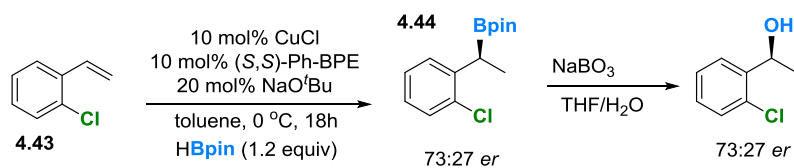


Compound 4.41. ^1H NMR (500 MHz, CDCl_3) δ 6.73 (d, $J = 2.0$ Hz, 1H), 6.31 (d, $J = 2.0$ Hz, 1H), 5.45 (q, $J = 6.8$ Hz, 1H), 3.83 (s, 3H), 3.76 (s, 3H), 2.00 (d, $J = 6.8$ Hz, 3H), 1.40 (s, 6H), 1.39 (s, 6H). ^{13}C NMR (126 MHz, CDCl_3) δ 164.2, 162.3, 149.5, 103.2, 97.5, 83.8, 55.7, 55.3, 48.8, 27.1, 24.9, 24.7. HRMS (ESI) m/z calculated for $\text{C}_{16}\text{H}_{25}\text{BBrO}_4$ $[\text{M}+\text{H}]^+$ 371.1027, found 371.1032.



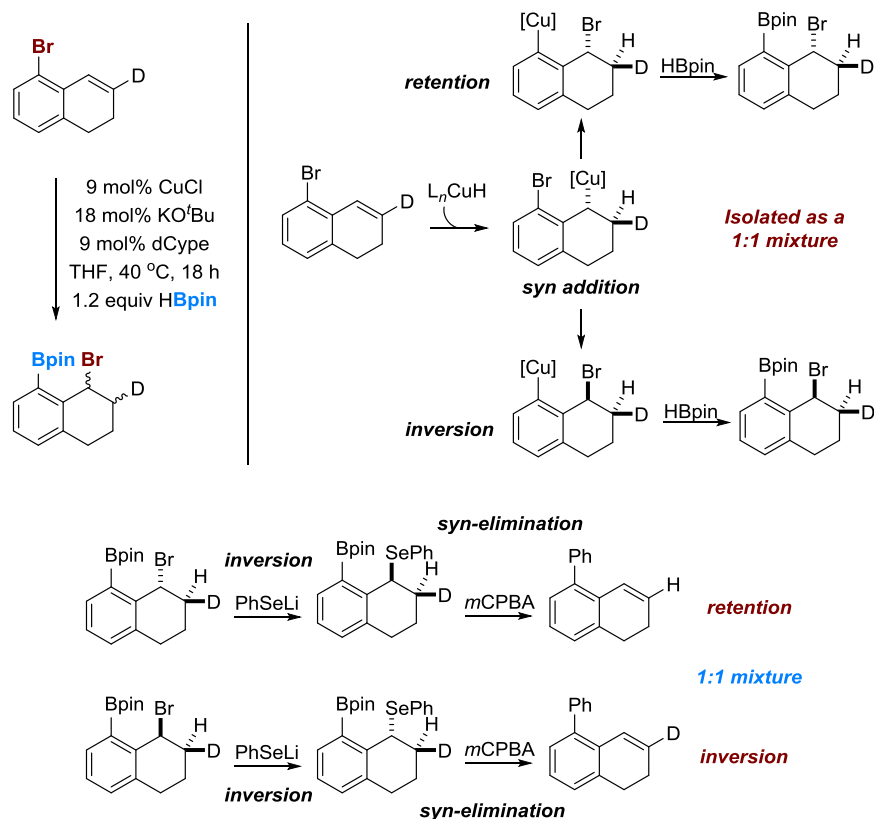
Compound 4.42. ^1H NMR (500 MHz, CDCl_3) δ 6.49 (d, $J = 2.7$ Hz, 1H), 6.35 (d, $J = 2.7$ Hz, 1H), 3.88 (s, 3H), 3.82 (s, 3H), 2.83 (q, $J = 7.5$ Hz, 1H), 1.35 (d, $J = 7.7$ Hz, 3H), 1.27 (s, 12H). ^{13}C NMR (126 MHz, CDCl_3) δ 159.5, 156.4, 146.6, 105.6, 105.1, 96.8, 83.5, 56.2, 55.4, 24.8, 24.7, 15.7. HRMS (EI) m/z calculated for $\text{C}_{16}\text{H}_{25}\text{BBrO}_4$ $[\text{M}+\text{H}]^+$ 370.1061, found 370.1057.

4.15.8 Transfer of Stereochemistry Experiments



In a glovebox, CuCl (2.5 mg; 25 μmol ; 10 mol%), NaOtBu (5 mg; 50 μmol ; 20 mol%), (*S,S*)-Ph-BPE (13 mg; 25 μmol ; 10 mol%) and 2.0 mL of toluene were added to a dry 10 mL round bottom flask. The flask was fitted with a septum, removed from the glovebox, and the mixture was allowed to stir for 10 minutes. HBpin (44 μL ; 0.303 mmol; 1.2 equiv) was added in one aliquot and then 2-chlorostyrene (34 μL ; 0.25 mmol; 1.0 equiv) was added. The reaction was allowed to stir for 18 hours at 0 $^\circ\text{C}$. The reaction was filtered through a pad of celite and washed with Et_2O (2x10 mL). The solvent was removed *in vacuo*. The crude benzyl boronic ester was used without further purification.

The crude boronic ester was dissolved in 5 mL of 1:1 THF: H_2O and sodium perborate (0.383 g; 2.5 mmol; 5 equiv) was added and then the reaction was stirred vigorously. The reaction was diluted with CH_2Cl_2 and washed with several times with water. The solvent was dried with Na_2SO_4 and concentrated. The crude material was purified with column chromatography using isocratic 20% EtOAc in hexanes. The *S* enantiomer of the benzyl alcohol was isolated in 73:27 *er* (see appendix D for chromatograms).



To better understand the nature of the 1,3-halogen migration, an experiment was designed to explore how stereochemical information in the reaction is transferred from the benzyl copper to the aryl copper species, and eventually to the final product. A deuterated dihydronaphthalene substrate was designed to determine if the stereochemistry set during the initial hydrocupration step was retained, inverted or ablated during the 1,3-halogen migration event. Since the hydrocupration of a π -bond occurs in a *syn* fashion to give a benzyl copper, the stereochemistry of the bromine relative to the deuterium in the final product should indicate whether migration occurs with retention or inversion of stereochemistry. In the case of retention, the product should display an *anti* relationship between the two protons on adjacent carbons. If inversion is taking place, then the product should display a *syn* relationship between these same two protons. The benzyl bromide could not be isolated, as it degraded during attempted purification by column chromatography. Even so, NMRs of the two diastereomers of the product would be nearly identical, and therefore not diagnostic. An alternative strategy involved displacement of the benzyl bromide with lithium phenylselenoate, which proceeds with excellent inversion of stereochemistry (see chapter 3). Selenoxide eliminations are known to proceed through a *syn* elimination.³⁵ Thus, if migration occurs through inversion of stereochemistry, then deuterium should be incorporated into the final product. If migration occurs

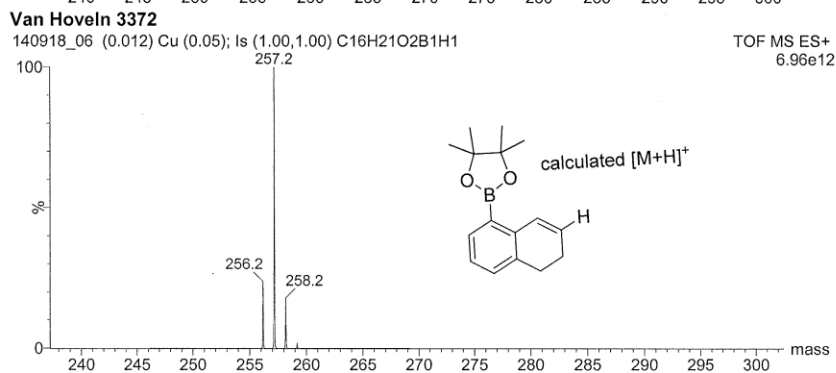
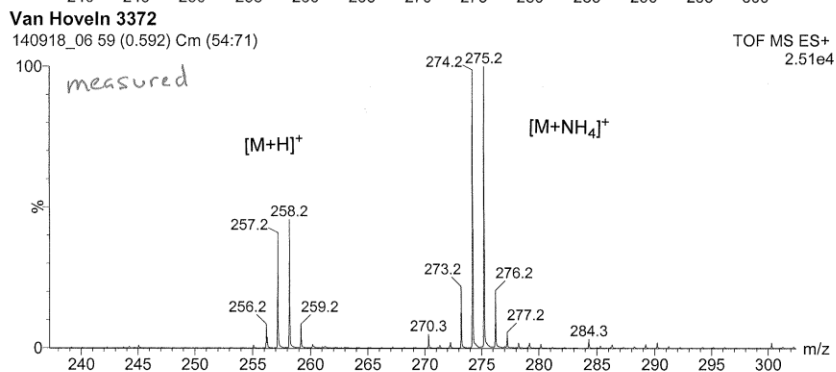
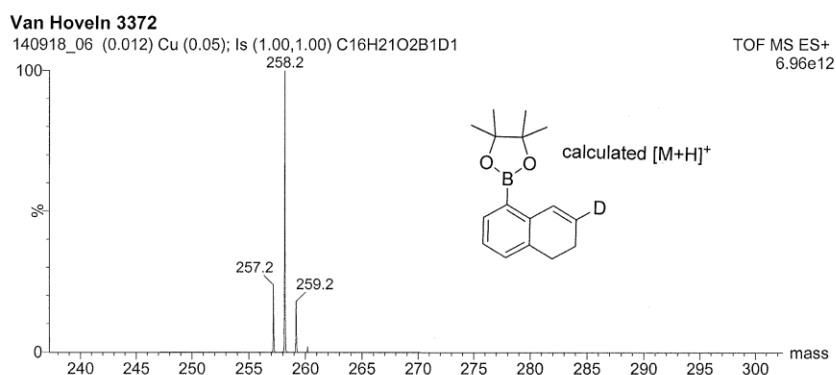
through retention of stereochemistry, then the final product should contain exclusively protons. Interestingly, the olefin that was isolated was nearly 50:50 proto:deutero, as supported by both the mass spec and NMR data, indicating the presence of a stereo-ablative step in the migration process.

8-[2-(4,4,5,5-tetramethyl-1,3,2-dioxaborolane)]-1-(phenylselenyl)(2-D)-1,2,3,4-tetrahydronaphthalene. In a glovebox, a dry 25 mL round bottom flask was charged with CuCl (50 mg, 0.51 mmol, 10 mol%), KO^tBu (112 mg, 1.0 mmol, 20 mol%), and dCype (211 mg, 0.50 mmol, 10 mol%) in 10 mL of THF and allowed to stir for 10 min. HBpin (0.87 mL, 6.00 mmol, 1.21 equiv) was added in one aliquot and the reaction was stirred for a few minutes, followed by addition of the deuterated bromodihydronaphthalene (0.72 mL, 4.94 mmol, 1.0 equiv). The reaction was allowed to stir for 3 h at 40 °C. Meanwhile, lithium phenylselenoate was prepared by treating selenium metal (0.394 g, 4.99 mmol, 1.01 equiv) in 5 mL of THF with phenyllithium (2.8 mL of a 1.8 M solution in dibutylether, 5.04 mmol, 1.01 equiv) and allowing it to stir for 30 min. The LiSePh solution was then transferred to the round bottom flask containing the 1,3-halogen migration reaction mixture, and allowed to stir at ambient temperature for 3 h. The reaction mixture was filtered through a pad of celite, washed with Et₂O (2x10 mL) and the solvent removed *in vacuo*. The crude material was purified by column chromatography using hexanes/CH₂Cl₂ as the eluant. A gradient was employed using 0-50% CH₂Cl₂ in 10% increments. The purified product was isolated as a pale yellow, viscous oil in 47% yield. ¹H NMR (500 MHz, CDCl₃) δ 7.60–7.53 (m, 3H), 7.30–7.08 (m, 3H), 7.13–7.09 (m, 2H), 5.78 (s, 1H), 2.90–2.73 (m, 2H), 2.41–2.22 (m, 1H), 2.06–1.92 (m, 1H), 1.79–1.66 (m, 1H), 1.33 (s, 6H), 1.32 (s, 6H). ¹³C NMR (126 MHz, CDCl₃) δ 141.0, 136.9, 133.4, 132.8, 132.1, 131.9, 128.8, 126.6, 126.0, 83.7, 42.9, 29.6, 27.8 (1,1,1-triplet, *J* = 19.6 Hz), 25.1, 24.6, 18.5. HRMS (EI) *m/z* calculated for C₂₂H₃₀DBSeO₂ [M+NH₄]⁺ 433.1675, found 433.1670.

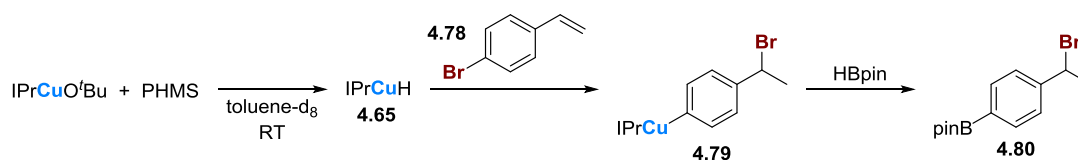
8-[2-(4,4,5,5-tetramethyl-1,3,2-dioxaborolane)]-2-deutero-3,4-dihydronaphthalene.³⁶

It was necessary to run the reaction at cold temperatures, using *m*CPBA as the oxidant to prevent competing oxidation of the boronic ester and olefin. The phenylselenide from above (0.206 g, 0.50 mmol, 1.0 equiv) was dissolved in ~1.5 mL of CH₂Cl₂ in a vial. The vial was placed in an acetone/CO₂ bath and then *m*CPBA (0.125 g, 0.72 mmol, 1.45 equiv) in ~1 mL of CH₂Cl₂ was added to the vial slowly. The reaction was allowed to stir for 15 min at -78 °C and then poured into 30 mL of 50:50 CH₂Cl₂:Et₃N. The organic was washed with water and the aqueous layer was extracted once with CH₂Cl₂. The combined organic layers were dried with Na₂SO₄ and

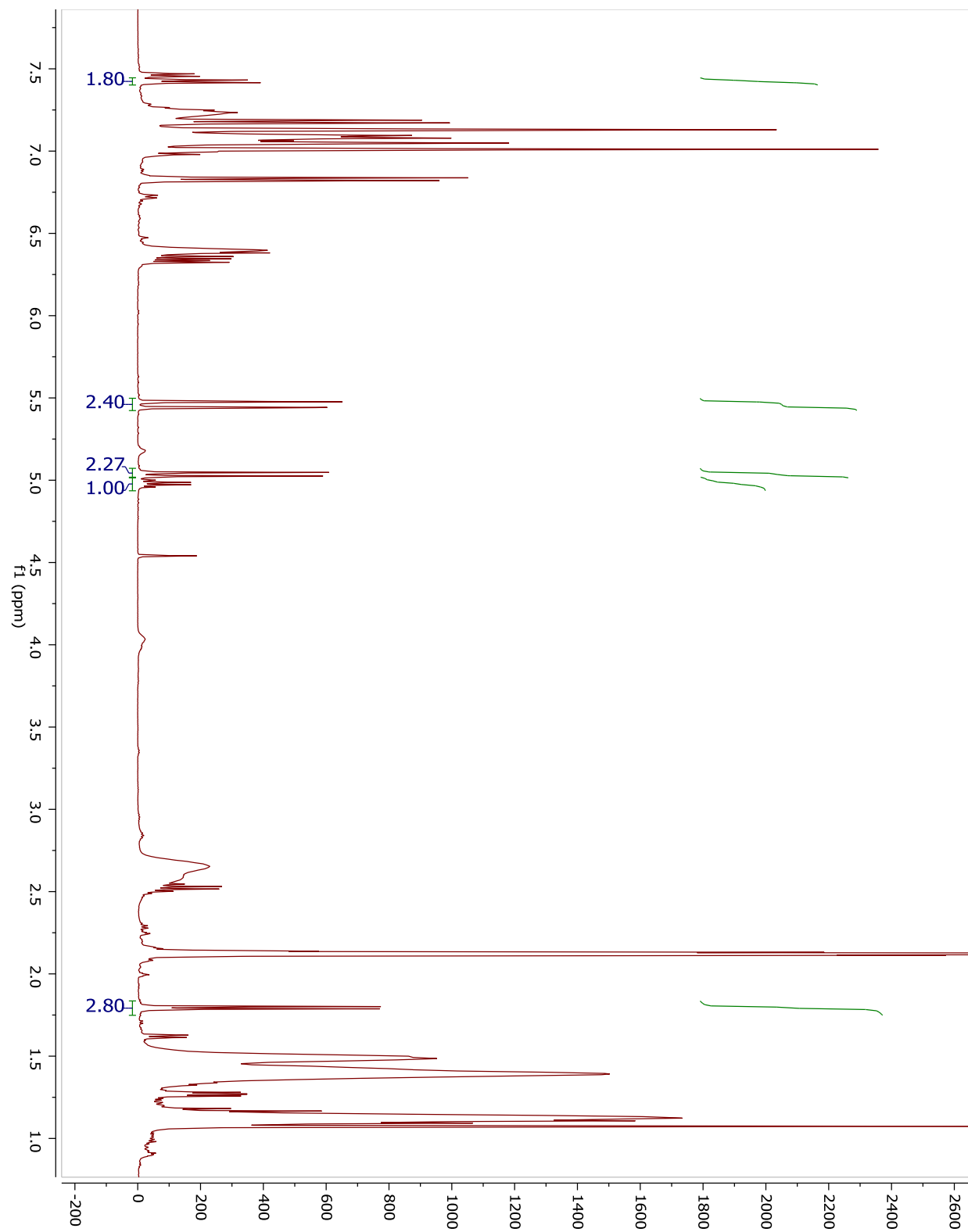
concentrated *in vacuo*. The crude product was purified by column chromatography using hexanes/CH₂Cl₂ as the eluant. A gradient was employed using 0-50% CH₂Cl₂ in 10% increments. The product was isolated in 73% yield. ¹H NMR (500 MHz, CDCl₃) δ 7.64 (dd, *J* = 7.5, 1.5 Hz, 1H), 7.33 – 7.28 (m, 1H), 7.17 (dd, *J* = 7.4, 0.9 Hz, 1H), 7.10 (t, *J* = 7.4 Hz, 1H), 6.10 (dt, *J* = 9.8, 4.4 Hz, 0.5H), 2.78 (t, *J* = 8.2 Hz, 2H), 2.36 – 2.21 (m, 2H), 1.35 (s, 12H). ¹³C NMR (126 MHz, CDCl₃) δ 139.6, 135.4, 134.2, 130.4, 129.3, 129.0 (1,1,1-triplet, *J* = 24.3 Hz), 128.2, 128.0, 125.9, 83.5, 28.3, 24.9, 22.8, 22.7. HRMS (ESI) *m/z* calculated for C₁₆H₂₄BNO₂ [M+NH₄]⁺ 273.2009, found 273.2012.



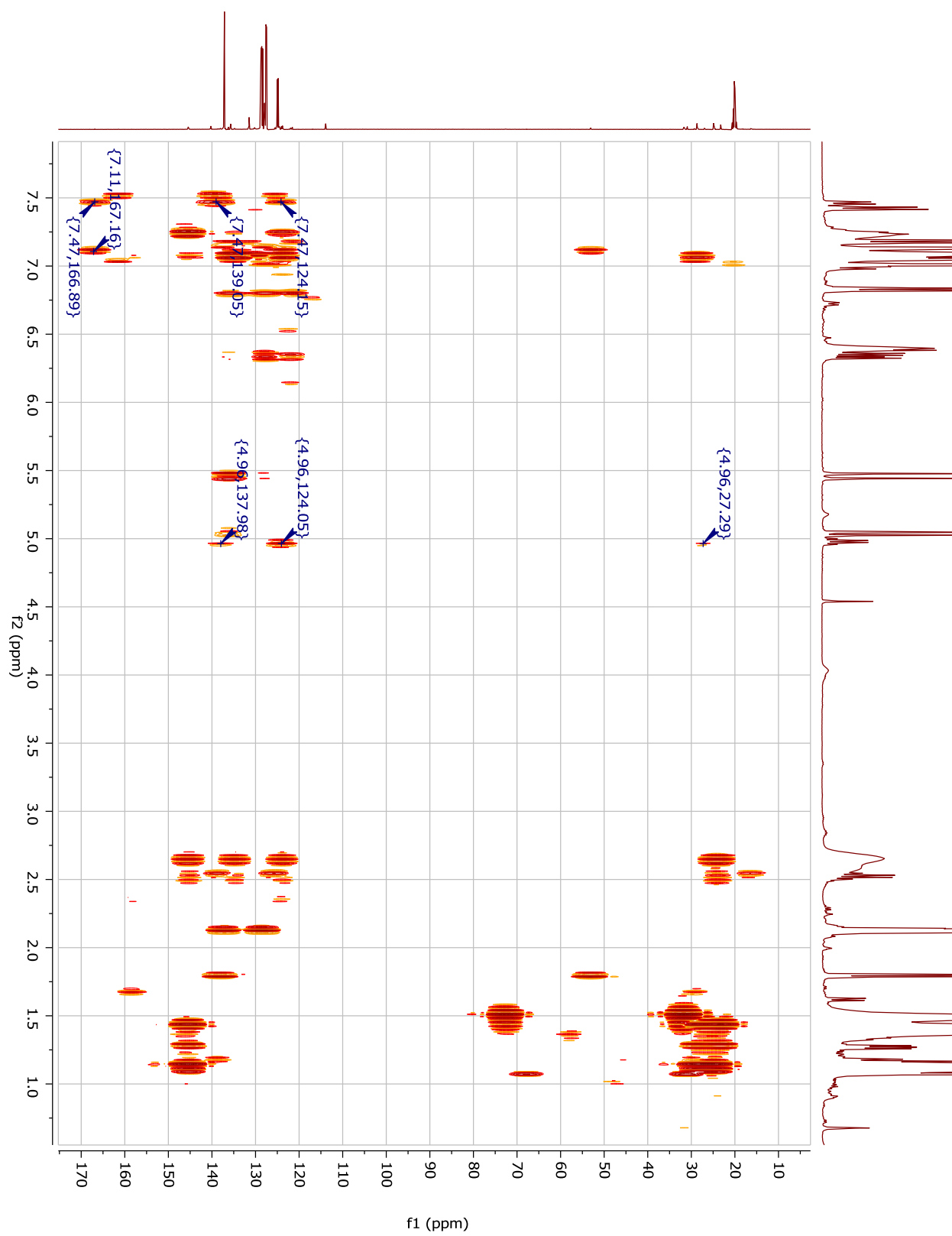
4.15.9 Stoichiometric and Catalytic 1,5-Halogen Migration



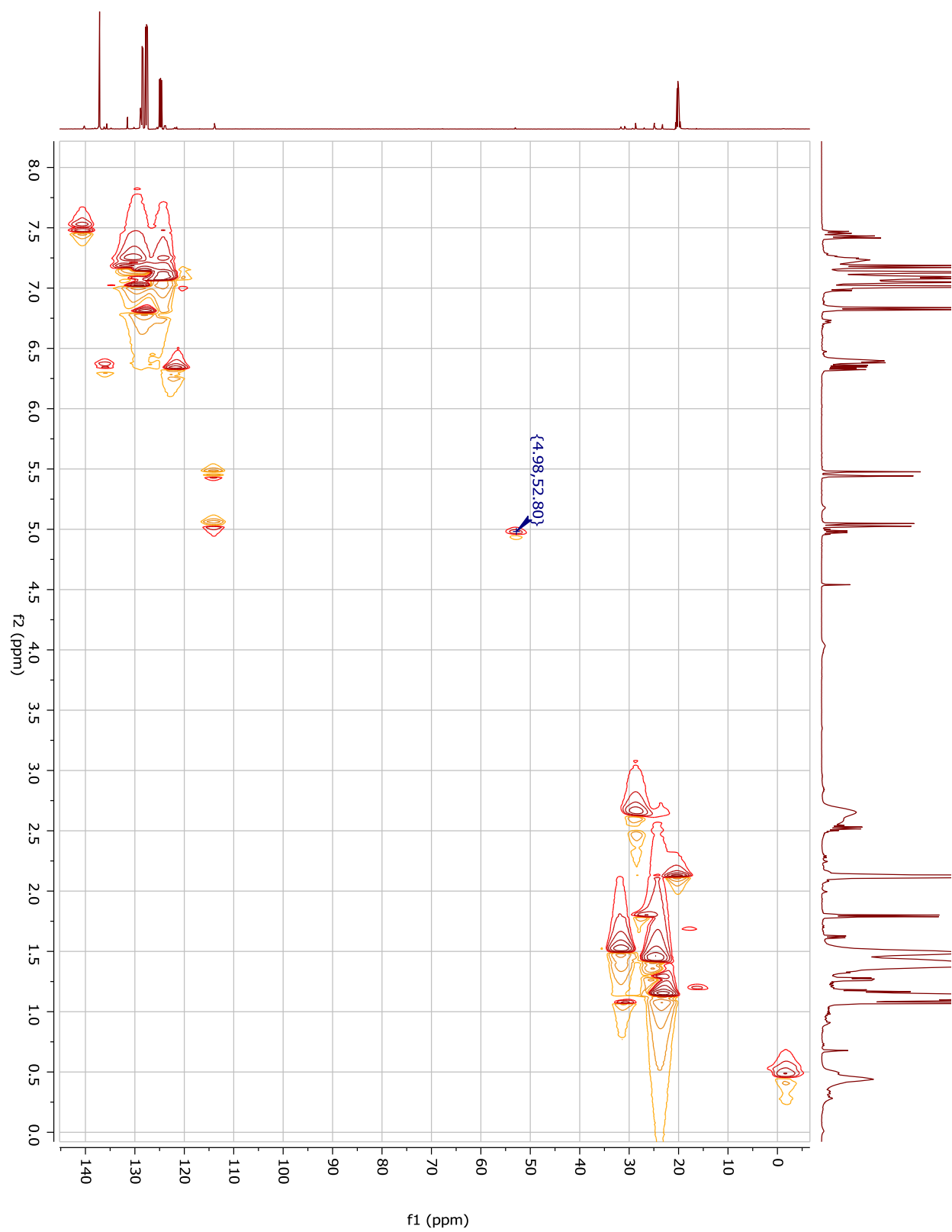
In the glovebox, IPrCuO^tBu (13.1 mg, 0.025 mmols) was weighed into an NMR tube and suspended in d8-toluene (0.5 mL). The tube was capped with a septum and removed from the glovebox. PMHS (1.8 μL , 0.03 mmols) was added *via* syringe giving a bright yellow solution that became homogenous after several rounds of inverting the NMR tube. An ^1H NMR spectrum was acquired on IPrCuH to ensure its complete formation. After acquisition, **4.78** (3.2 μL , 0.025 mmols) was added. The sample reinserted into the spectrometer. Approximately 30% conversion of 4-bromostyrene to aryl-copper(I) **4.79** was observed and the complex was characterized by ^1H NMR, HSQC, and HMBC. It should be noted the ^{13}C shift of the ipso-copper aryl carbon, 167 ppm, closely matches that seen by Herron (166.1 ppm).¹⁵ Following characterization of **4.79**, HBpin (7.3 μL , 0.05 mmols) was added and product **4.80** was formed and the colored IPrCuH regenerated.

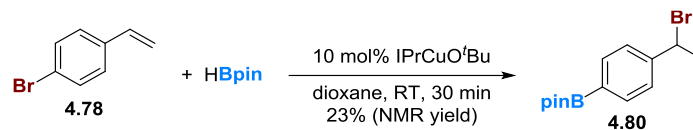
^1H of 4.79

HMBC of 4.79

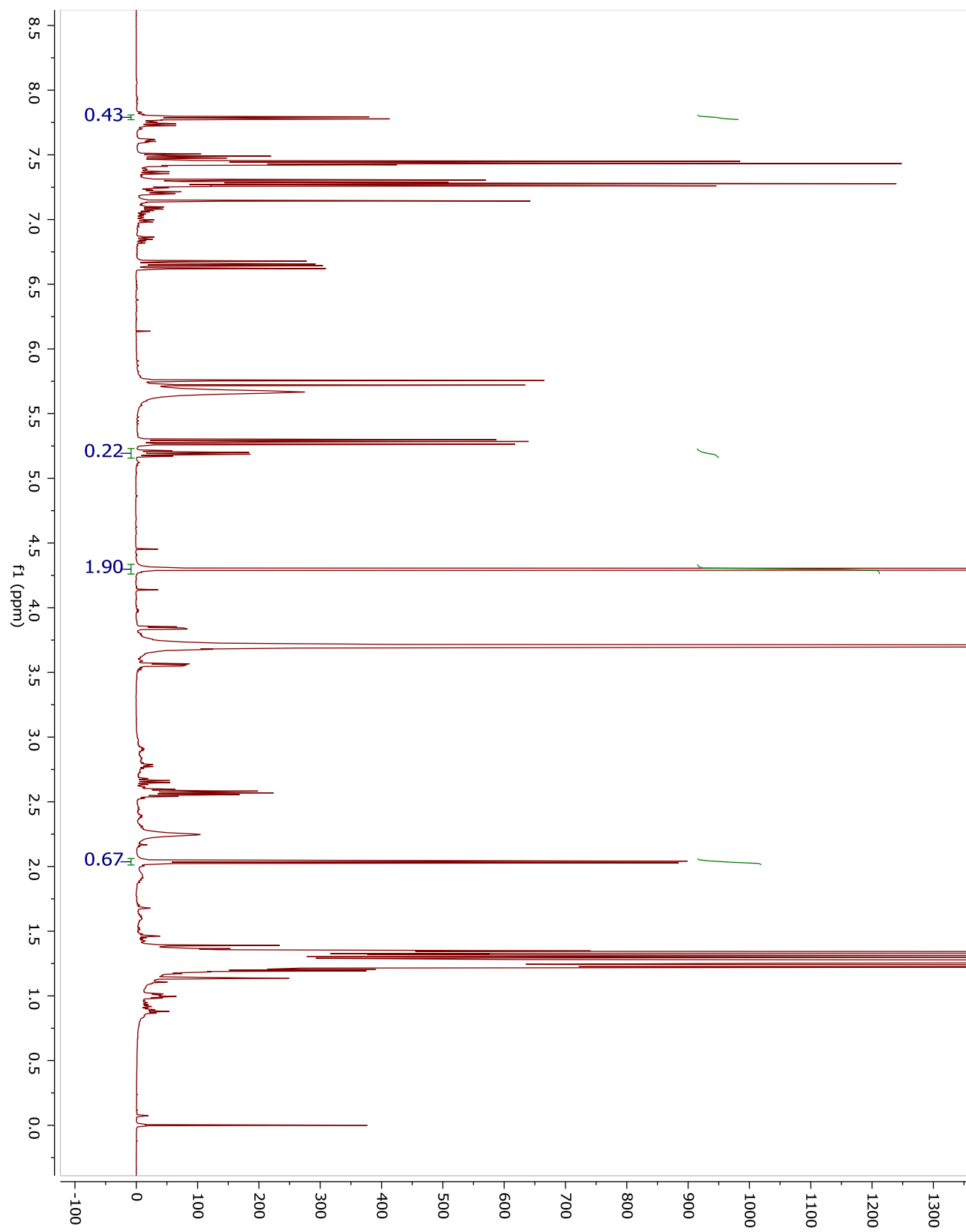


HSQC of 4.79



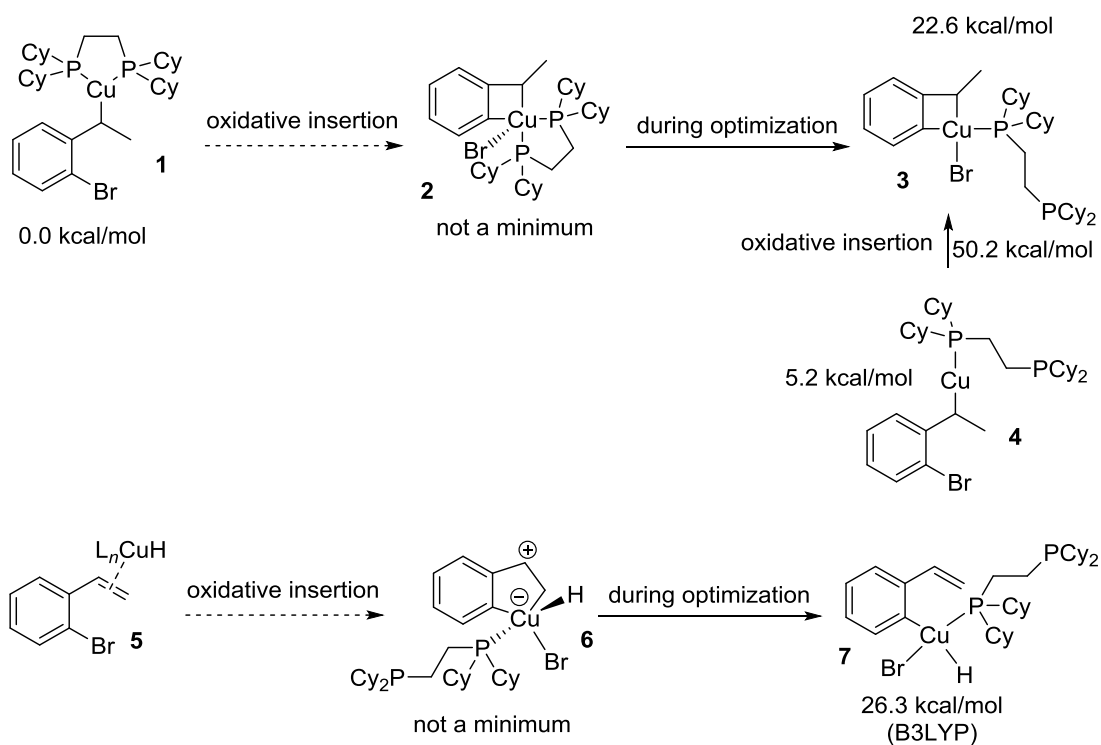


In a glovebox, IPrCuOtBu (5.3 mg; 10 μ mol; 10 mol%) and 0.5 mL of dioxanes were added to a dry vial. The vial was fitted with a septum and removed from the glovebox. HBpin (40 μ L; 280 μ mol; 2.8 equiv) was added in one aliquot and then the 4-bromostyrene (13 μ L; 100 μ mol; 1.0 equiv) was added. The reaction was allowed to stir for 30 min. at 60 $^{\circ}$ C. The reaction was filtered through a plug of silica and washed with CH₂Cl₂. The solvent was removed *in vacuo*. The crude material was dissolved in CDCl₃ and 10 μ L of 1,1,1,2-tetrachloroethane was added. The product and starting material peaks were integrated against the standard. The standard was integrated such that integrations of one proton peaks would represent yield. The product **4.80** was integrated to 23% yield.



4.15.10 Computational Details

All structures throughout these were optimized with Gaussian 09¹ using the M06² functional with a 6-311G* basis set for H, B, C, N, O, P, and Br and a LANL2TZ+ basis set with an electric core potential designed for copper. An SMD continuum solvent model was used with THF as the solvent. All minima were checked for absence of imaginary vibrational modes and all transition states were checked for one imaginary vibrational mode and confirmed by visual inspection and IRC calculations. Molecular and Natural Bond Orbitals were calculated by using the NBO keyword in Gaussian. Structural drawings were generated with CYLview. Molecular orbitals were visualized with Guassview.



Three oxidative insertion pathways were ultimately considered: 1) oxidative insertion from the benzyl copper **1**, 2) oxidative insertion from the π -acid complex **5**, 3) oxidative insertion of the copper-hydride. The pentacoordinate complex **2** that results from oxidative insertion from the benzyl copper always dissociated a phosphine ligand during the optimization. The tetracoordinate oxidative insertion product **3** was energetically feasible, but the transition state energy leading to this intermediate was far too high. The oxidative insertion intermediate from the π -acid complex **5** always broke a carbon-copper bond to form the intermediate that results from direct oxidative insertion of copper-hydride into the aryl-bromine bond (**7**). The direct oxidative insertion intermediate was also too high in energy

(relative to the benzyl copper); thus, it is reasonable to expect that the transition state energy would also be too high in energy.

4.16 Bibliography

- 1) For selected references, see: (a) Ritleng, V.; Sirlin, C.; Pfeffer, M. *Chem. Rev.* **2002**, *102*, 1731. (b) Lyons, T. W.; Sanford, M. S. *Chem. Rev.* **2010**, *110*, 1147. (c) Diederich, F.; Stang, P. J., Eds. *Metal-catalyzed Cross-coupling Reactions* Wiley-VCH: Weinheim, **1998**. (d) Phapale, V. B.; Cárdenas, D. *Chem. Soc. Rev.* **2009**, *38*, 1598. (e) McDonald, R. I.; Liu, G.; Stahl, S. S. *Chem. Rev.* **2011**, *111*, 2981. (f) Farina, V. *Adv. Syn. Catal.* **2004**, *346*, 1553. (g) Jana, R.; Pathak, T.P.; Sigman, M. S. *Chem. Rev.* **2011**, *111*, 1417. (h) Xu, L.-M.; Li, B.-J.; Yang, Z.; Shi, Z.-J. *Chem. Soc. Rev.* **2010**, *39*, 712.
- 2) (a) Negishi, E.-I.; de Meijere, A., Eds. *Handbook of Organopalladium chemistry for Organic Synthesis*; Wiley: New York, **2002**. (b) de Meijere, A., Diederich, F., Eds. *Metal-Catalyzed Cross-Coupling Reactions*, 2nd ed.; Wiley-VCH: Weinheim, **2004**.
- 3) (a) Tamaru, Y.; Ed. *Modern Organonickel Chemistry*; Wiley: Weinheim, **2005**. (b) Krause, N.; Ed. *Modern Organocopper Chemistry*; Wiley: Weinheim, **2002**. (c) Rosen, B.M.; Quasdorf, K. W.; Wilson, D. A.; Zhang, N.; Resmerita, A.; Garg, N. K.; Percec, V. *Chem. Rev.* **2011**, *111*, 1346. (d) Alonso, D. A.; Najera, C. in *Science of Synthesis*; de Meijere, A., Ed.; Thieme: New York, Stuttgart, **2009**; Vol. 47a, pp 439-479. (e) Jana, R.; Pathak, T. P.; Sigman, M. S. *Chem. Rev.* **2011**, *111*, 1417. (f) Li, B.; Xu, L.; Wu, Z.; Guan, B.; Sun, C.; Wang, B.; Shi, Z. *J. Am. Chem. Soc.* **2009**, *131*, 14656. (g) Han, F.-S. *Chem. Soc. Rev.* **2013**, *42*, 5270.
- 4) (a) Wendlandt, A. E.; Suess, A. M.; Stahl, S. S. *Angew. Chem. Int. Ed.* **2011**, *50*, 11063-11087. (b) Beletskaya, I. P.; Cheprakov, A. V. *Coord. Chem. Rev.* **2004**, *248*, 2337-2364. (c) Sperotto, E.; van Klink, G. P. M.; van Koten, G.; de Vries, J. G. *Dalton Trans.* **2010**, *39*, 10338-10351. (d) Sherry, B. D.; Fürstner, A. *Acc. Chem. Res.* **2008**, *41*, 1500-1511. (e) Czaplik, W. M.; Mayer, M.; Cvengros, J.; Jacobi, A. *Chem. Sus. Chem.* **2009**, *2*, 396-417.
- 5) (a) Watson, M. P.; Jacobsen, E. N. *J. Am. Chem. Soc.* **2008**, *130*, 12504-12505. (b) Mao, J.; Guo, J.; Fang, F.; Ji, S.-J. *Tetrahedron*, **2008**, *64*, 3905-3911. (c) Li, J.-H.; Li, J.-L.; Wang, D.-P.; Pi, S.-F.; Xie, Y.-X.;

- Zhang, M.-B.; Hu, X.-C. *J. Org. Chem.* **2007**, *72*, 2053-2057. (d) Evinder, G.; Batey, R. A. *J. Org. Chem.* **2006**, *71*, 1802-1808.
- 6) (a) Ehle, A. R.; Zhou, Q.; Watson, M. P. *Org. Lett.* **2012**, *14*, 1202-1205. (b) Guan, B.-T.; Wang, Y.; Li, B.-J.; Yu, D.-G.; Shi, Z.-J. *J. Am. Chem. Soc.* **2008**, *130*, 14468-14470. (c) Quasdorf, K. W.; Antoft-Finch, A.; Liu, P.; Silberstein, A. L.; Komaromi, A.; Blackburn, T.; Ramgren, S. D.; Houk, K. N.; Snieckus, V.; Garg, N. K. *J. Am. Chem. Soc.* **2011**, *133*, 6352-6363.
- 7) (a) Noh, D.; Chea, H.; Ju, J.; Yun, J. *Angew. Chem. Int. Ed.* **2009**, *48*, 6062. (b) Won, J.; Noh, D.; Yun, J.; Lee, J. Y. *J. Phys. Chem. A* **2010**, *114*, 12112.
- 8) For other examples of copper-catalyzed 1,3-migration, see: (a) Alcaide, B.; Almendros, P.; Alonso, J. M.; Cembellin, S.; Fernandez, I.; Martinez del Campo, T.; Torres, M. R. *Chem. Comm.* **2013**, *49*, 7779-7781. (b) Yang, Y.; Buchwald, S. L. *Angew. Chem. Int. Ed.* **2014**, *53*, 8677-8681.
- 9) (a) Bezman, S. A.; Churchill, M. R.; Osborn, J. A.; Wormald, J. *J. Am. Chem. Soc.* **1971**, *93*, 2063-2065. (b) Mankad, N. P.; Laitar, D. S.; Sadighi, J. P. *Organometallics* **2004**, *23*, 3369-3371. (c) Lemmen, T. H.; Foltling, K.; Huffman, J. C.; Caulton, K. G. *J. Am. Chem. Soc.* **1985**, *107*, 7774-7775.
- 10) (a) Christian Girard and Henri B. Kagan. *Angew. Chem. Int. Ed.* **1998**, *37*, 2922 – 2959. (b) Blackmond, D. G. *Acc. Chem. Res.* **2000**, *33*, 402-411.
- 11) For examples of monomeric organocopper complexes see: (a) Russo, V.; Herron, J. R.; Ball, Z. T. *Org. Lett.* **2010**, *12*, 220-223. (b) Laitar, D. S.; Tsui, E. Y.; Sadighi, J. P. *Organometallics*, **2006**, *25*, 2405-2408. (c) Mankad, N. P.; Laitar, D. S.; Sadighi, J. P. *Organometallics*, **2004**, *23*, 3369-3371. (d) Mankad, N. P.; Gray, T. G.; Laitar, D. S.; Sadighi, J. P. *Organometallics*, **2004**, *23*, 1191-1193. (e) Hope, H.; Olmstead, M. M.; Power, P. P.; Sandell, J.; Xu, X. *J. Am. Chem. Soc.* **1985**, *107*, 4337-4338. (f) Rucker, R. P.; Whittaker, A. M.; Dang, H.; Lalic, G. *J. Am. Chem. Soc.* **2012**, *134*, 6571-6574. (g) Laitar, D. S.; Tsui, E. Y.; Sadighi, J. P. *J. Am. Chem. Soc.* **2006**, *128*, 11036-11037. (h) Gurung, S. K.; Thapa, S.; Kafle, A.; Dickie, D. A.; Giri, R. *Org. Lett.* **2014**, *16*, 1264-1267.
- 12) Anslyn, E. V.; Dougherty, D. A. *Modern Physical Organic Chemistry*; University Science Books: Sausalito, CA, **2006**; pp 428-430.
- 13) Yamamoto, Y. *J. Org. Chem.* **2007**, *72*, 7817-7831.

- 14) (a) Goering, H. L.; Kantner, S. S.; Seitz, E. P. *J. Org. Chem.* **1985**, *50*, 5495-5499. (b) House, H. O.; Wilkins, J. M. *J. Org. Chem.* **1978**, *43*, 2443-2454.
- 15) Herron, J. R.; Ball, Z. T. *J. Am. Chem. Soc.* **2008**, *130*, 16486-16487.
- 16) Van Hoveln, R. J.; Schmid, S. C.; Schomaker, J. M. *Org. Biomol. Chem.* **2014**, *12*, 7655.
- 17) Gaussian 09, Revision D.01, M. J. Frisch, G. W. Trucks, H. B. Schlegel, G. E. Scuseria, M. A. Robb, J. R. Cheeseman, G. Scalmani, V. Barone, B. Mennucci, G. A. Petersson, H. Nakatsuji, M. Caricato, X. Li, H. P. Hratchian, A. F. Izmaylov, J. Bloino, G. Zheng, J. L. Sonnenberg, M. Hada, M. Ehara, K. Toyota, R. Fukuda, J. Hasegawa, M. Ishida, T. Nakajima, Y. Honda, O. Kitao, H. Nakai, T. Vreven, J. A. Montgomery, Jr., J. E. Peralta, F. Ogliaro, M. Bearpark, J. J. Heyd, E. Brothers, K. N. Kudin, V. N. Staroverov, T. Keith, R. Kobayashi, J. Normand, K. Raghavachari, A. Rendell, J. C. Burant, S. S. Iyengar, J. Tomasi, M. Cossi, N. Rega, J. M. Millam, M. Klene, J. E. Knox, J. B. Cross, V. Bakken, C. Adamo, J. Jaramillo, R. Gomperts, R. E. Stratmann, O. Yazyev, A. J. Austin, R. Cammi, C. Pomelli, J. W. Ochterski, R. L. Martin, K. Morokuma, V. G. Zakrzewski, G. A. Voth, P. Salvador, J. J. Dannenberg, S. Dapprich, A. D. Daniels, O. Farkas, J. B. Foresman, J. V. Ortiz, J. Cioslowski, and D. J. Fox, Gaussian, Inc., Wallingford CT, **2013**.
- 18) (a) Zhao, Y.; Truhlar, D. G. *Theor. Chem. Account* **2008**, *120*, 215-241. (b) Karton, A.; Tarnopolsky, A.; Lamere, J.-F.; Schatz, G. C.; Martin, J. M. L. *J. Phys. Chem. A* **2008**, *112*, 12868-12886. (c) Zhao, Y.; Truhlar, D. G. *J. Chem. Phys.* **2006**, *125*, 194101-194118. (d) Zhao, Y.; Truhlar, D. G. *J. Phys. Chem. A* **2006**, *110*, 13126-13130.
- 19) (a) Hay, P. J.; Wadt, W. R. *J. Chem. Phys.* **1985**, *82*, 270-283. (b) Yang, Y.; Weaver, M. N.; Merz Jr., K. M. *J. Phys. Chem. A* **2009**, *113*, 9843-9851. (c) Su, M.-D.; Chu, S.-Y. *J. Am. Chem. Soc.* **1997**, *119*, 10178-10185. (d) Vigalok, A.; Uzan, O.; Shimon, J. W.; Ben-David, Y.; Martin, J. M. L.; Milstein, D. *J. Am. Chem. Soc.* **1998**, *120*, 12539-12544. (e) Kadyrov, R.; Börner, A.; Selke, R. *Eur. J. Inorg. Chem.* **1999**, 705-711. (f) Su, M.-D.; Chu, S.-Y. *Chem. Eur. J.* **1999**, *5*, 198-207. (g) Yu, Z.-X.; Wender, P. A.; Houk, K. N. *J. Am. Chem. Soc.* **2004**, *126*, 9154-9155. (h) Luo, X.; Tang, D.; Li, M. *THEOCHEM* **2005**, *714*, 61-72. (i) Luo, X.; Tang, D.; Li, M. *Int. J. Quantum Chem.* **2005**, *105*, 108-123. (j) Ardura, D.; López, R.; Sordo, T. L. *J. Org. Chem.* **2006**, *71*, 7315-7321. (k) Alagona, G.; Chio, C.; Rocchiccioli, S. *J. Mol. Model.* **2007**, *13*, 823-837. (l) Yu, Z.-X.; Cheong, P. H.-Y.; Liu, P.; Legault, C. Y.; Wender, P. A.; Houk,

- K. N. *J. Am. Chem. Soc.* **2008**, *130*, 2378-2379. (m) Siebert, M. R.; Yudin, A. K.; Tantillo, D. J. *Eur. J. Org. Chem.* **2011**, *3*, 553-561.
- 20) (a) Hay, P. J.; Wadt, W. R. *J. Chem. Phys.* **1985**, *82*, 270. (b) Hay, P. J.; Wadt, W. R. *J. Chem. Phys.* **1985**, *82*, 284. (c) Hay, P. J.; Wadt, W. R. *J. Chem. Phys.* **1985**, *82*, 299.
- 21) Marenich, A. V.; Cramer, C. J.; Truhlar, D. G. *J. Phys. Chem. B.* **2009**, *113*, 6378-6396.
- 22) (a) Gonzalez, C. S.; Schlegel, H. B. *J. Phys. Chem.* **1990**, *94*, 5523. (b) Fukui, K. *Acc. Chem. Res.* **1981**, *14*, 363-368. (c) Maeda, S.; Harabuchi, Y.; Ono, Y.; Taketsugu, T.; Morokuma, K. *Int. J. Quantum Chem.* **2014**, *115*, 258-269.
- 23) (a) Deutsch, C.; Krause, N.; Lipshutz, B. H. *Chem. Rev.* **2008**, *108*, 2916-2927. (b) Semba, K.; Fujihara, T.; Terao, J.; Tsuji, Y. *Chem. Eur. J.* **2012**, *18*, 4179-4184. (c) Reeker, H.; Norrby, P.-O.; Krause, N. *Organometallics*, **2012**, *31*, 8024-8030.
- 24) Selected examples of Cu(III) species from C–X oxidative addition: (a) Maiti, D.; Sarjeant, A. A. N.; Itoh, S.; Karlin, K. D. *J. Am. Chem. Soc.* **2008**, *130*, 5644-5645. (b) Casitas, A.; King, A. E.; Parella, T.; Costas, M.; Stahl, S. S.; Ribas, X. *Chem. Sci.* **2010**, *1*, 326-330.
- 25) Hartwig, J. F. *Organotransition Metal Chemistry*, University Science Books: Sausalito, CA, **2010**, pp 301-317.
- 26) (a) Zhu, S.; MacMillan, D. W. C. *J. Am. Chem. Soc.* **2012**, *134*, 10815-10818. (b) Dattelbaum, A. M.; Martin, J. D. *Inorg. Chem.* **1999**, *38*, 6200-6205.
- 27) For other examples of CuH asymmetric transformations, see: (a) Zhu, S.; Niljianskul, N.; Buchwald, S. L. *J. Am. Chem. Soc.* **2013**, *135*, 15746-15749. (b) Appella, D. H.; Moritani, Y.; Shintani, R.; Ferreira, E. M.; Buchwald, S. L. *J. Am. Chem. Soc.* **1999**, *121*, 9473-9474. (c) Jurkauskas, V.; Buchwald, S. L. *J. Am. Chem. Soc.* **2002**, *124*, 2892-2893.
- 28) Walsh, P. J.; Kozlowski, M. C. *Fundamentals of Asymmetric Catalysis*; University Science Books: Sausalito, CA, **2009**.
- 29) (a) Reetz, M. T. *Angew. Chem., Int. Ed.* **1972**, *11*, 129-130. (b) Reetz, M. T. *Angew. Chem. Int. Ed.* **1972**, *11*, 130-131. (c) Reetz, M. T. *Tetrahedron* **1973**, *29*, 2189-2194. (d) Reetz, M. T. *Adv. Organomet. Chem.* **1977**, *16*, 33-65. (e) Hoffmann, R.; Williams, J. E., Jr. *Helv. Chim. Acta* **1972**, *55*, 67-75. (f) Buenker, R. J.; Peyerimhoff, S. D.; Allen, L. C.; Whitten, J. L. *J. Chem. Phys.* **1966**, *45*, 2835-2847. (g) Gutierrez, O.;

- Tantillo, D. J. *J. Org. Chem.* **2012**, *77*, 8845-8850. (h) Braddock, D. C.; Roy, D.; Lenoir, D.; Moore, E.; Rzepa, H. S.; Wu, J. I.-C.; Schleyer, P. v. R. *Chem. Commun.* **2012**, *48*, 8943-8945. (i) Fernández, I.; Cossío, F.P.; Sierra, M.A. *Chem. Rev.* **2009**, *109*, 6687-6711.
- 30) Luliński, S.; Serwatowski, J.; Szczerbińska, M. *Eur. J. Org. Chem.* **2008**, 1797.
- 31) Ohwada, T.; Tani, N.; Sakamaki, Y.; Kabasawa, Y.; Otani, Y.; Kawahata, M.; Yamaguchi, K. *Proc. Natl. Acad. Sci. U.S.A.* **2013**, *110*, 4206-4211.
- 32) Harrowven, D.C.; Curran, D.C.; Kostiuk, S.L.; Wallis-Guy, I.L.; Whiting, S.; Stenning, K.J.; Tang, B.; Packard, E.; Nanson, L. *Chem. Commun.* **2010**, *46*, 6335.
- 33) Price, W.S. *Concepts Magn. Reson.* **1997**, *9*, 299.
- 34) (a) Casey, C.P.; Johnson, J.B.; Singer, S.W.; Cui, Q. *J. Am. Chem. Soc.* **2005**, *127*, 3100. (b) Valentini, M.; Pregosin, P.S.; Rügger, H. *Organometallics* **2000**, *19*, 2551.
- 35) Sharpless, K. B.; Young, M. W.; Lauer, R. F. *Tetrahedron Lett.* **1973**, *22*, 1979-1982.
- 36) Callant, P.; Ongena, R.; Vandewalle, M. *Tetrahedron*, **1981**, *37*, 2085-2089.

Chapter 5: Nickel-Catalyzed Hydroboration of Styrenes

5.1 Introduction to Nickel-catalyzed Borylations.

First-row transition metal catalysis has many advantages over second and third-row transition metal catalysis. Namely, first-row transition metals are significantly less expensive, generally less toxic, and more sustainable. While significant effort has been made to use first-row transition metals to carry out many of the transformations currently catalyzed by lower transition metals, success towards this goal has been somewhat limited by the differing electronic structures of first-row transition metals compared to their second and third row counterparts.¹

One transformation in particular that has received much attention over the last several years is metal-catalyzed borylations since boronic esters can be used in a wide array of carbon-carbon and carbon-heteroatom bond-forming transformations. Traditionally, precious metals such as rhodium, iridium, and platinum have been used to perform a wide range of different borylations.² In recent years, nickel has shown great promise in catalyzing several different borylations including coupling to aryl and alkyl halides to make boronic esters,³ diboration,⁴ and 1,4-hydroboration.⁵ There are only two reports where nickel is used to catalyze the hydroboration of simple olefins. Srebnik showed two examples where $\text{CpNiPPh}_3(\text{Cl})$ catalyzed the hydroboration of olefins, but only one non-symmetrical example with excellent selectivity to form the linear boronic ester.⁶ The other report uses nickel metal to catalyze the hydroboration of a few olefins, but with limited selectivity.⁷ However, there are no methods featuring nickel-catalyzed hydroboration of olefins to form the branched boronic ester. Herein, we report the synthesis of benzyl boronic esters via nickel-catalyzed hydroboration of styrenes.

5.2 Optimization of Nickel-catalyzed Hydroboration

We began our investigation of nickel-catalyzed hydroboration with the easily accessible nickel complexes $(\text{Cy}_3\text{P})_2\text{NiCl}_2$ and $\text{Ni}(\text{cod})_2$ (Table 5.1). Encouragingly, in the presence of pinacol borane (HBpin) and a tert-butoxide additive, both of these complexes produced the desired product in good to excellent yield (entries 1 and 2). However, $\text{Ni}(\text{cod})_2$ exhibited limited reactivity with other styrenes (Table 5.2). Switching to pre-catalyst $(\text{Cy}_3\text{P})_2\text{NiCl}_2$ still produced variable results for different substrates, but exhibited more consistent reactivity than the $\text{Ni}(0)$ pre-catalyst. With this in mind, a series of bis-phosphine complexes were synthesized in the hopes of increasing reactivity further. Increasing the sterics of the catalyst complex reduced the yield (Table 5.1, entries 3 and 4) while reducing the sterics of the complex shut down reactivity altogether (entries 5 and 6). A novel heteroleptic carbene/phosphine nickel complex, $\text{IPr}(\text{Cy}_3\text{P})\text{NiCl}_2$, was synthesized using a method similar to that of

Matsubara.⁸ This heteroleptic complex restored reactivity (entry 7). Furthermore, IPr(Cy₃P)NiCl₂ produced the most consistent and reproducible results with other styrenes (Table 5.2). Further optimization of the carbene showed that IMes(Cy₃P)NiCl₂ was the best pre-catalyst (Table 5.1, entry 8). However, the bis-NHC complex did not produce any of the desired product (entry 9). These results are consistent with previous findings as heteroleptic nickel complexes have displayed significantly improved reactivity for coupling over either bis-phosphine or bis-NHC nickel complexes.⁸

These easily accessible heteroleptic complexes reap orthogonal benefits from each of the ligands. The NHC ligand provides enhanced stability through strong sigma donation to the metal center while the phosphine ligand can provide increased reactivity through its hemilability. These features are design principles that will be explored in future studies of heteroleptic nickel complexes to achieve a wide range of synthetically useful transformations.

Table 5.1. Optimization of Ni-catalyzed hydroboration.

entry	Ni complex	yield
1	(Cy ₃ P) ₂ NiCl ₂	73%
2	Ni(cod) ₂	99%
3	(^t Bu ₃ P) ₂ NiCl ₂	10%
4	(^t Bu ₂ MeP) ₂ NiCl ₂	23%
5	(ⁿ Bu ₃ P) ₂ NiCl ₂	0%
6	(Et ₃ P) ₂ NiCl ₂	0%
7	IPr(Cy ₃ P)NiCl ₂	77%
8	IMes(Cy ₃ P)NiCl ₂	99%
9	(IMes) ₂ NiCl ₂	0%

IPr

IMes

NMR yields determined using 1,1,1,2-tetrachloroethane as an internal standard.

Table 5.2. Comparison of nickel complex reactivity.

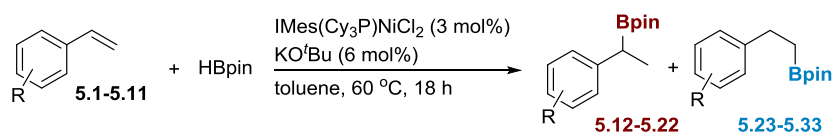
R	Ni(cod) ₂	(Cy ₃ P) ₂ NiCl ₂	IPr(Cy ₃ P)NiCl ₂
H	99%	73%	77%
<i>o</i> -Me	27%	43%	72%
<i>p</i> -OMe	0%	10%	50%(6%)
<i>o</i> -CF ₃	58%	53%	55%

NMR yields determined using 1,1,1,2-tetrachloroethane as an internal standard.
(Yield of linear product shown in parentheses.)

5.3 Substrate Scope of Hydroboration

Using the $\text{IMes}(\text{Cy}_3\text{P})\text{NiCl}_2$ pre-catalyst, the substrate scope was explored (Table 5.3). The product yield did not seem to be dramatically affected by the electronics of the substrate as electron-rich styrenes (entries 2-4) and electron-deficient styrenes (entries 5-7) performed comparably. Although, the catalyst loading had to be increased with 4-OMe styrene to achieve good conversion (entry 4). Additionally, the reaction was tolerant of substitution on the olefin (entry 8) as well as polyaromatics (entries 9-11). The reaction also did not seem to be affected by steric bulk near the reactive site in spite of a large catalyst complex (entries 2, 3, and 6). In all cases, selectivity for the branched boronic ester was strongly preferred over the linear boronic ester; in most cases, no linear product was observed. Notably, halogenated aromatics did not perform well in this reaction.

Table 5.3. Substrate scope.



entry	substrate	yield ^a (NMR) ^b 5.12-2.22	(NMR yield) ^b 5.23-5.33	entry	substrate	yield ^a (NMR) ^b 5.12-2.22	(NMR yield) ^b 5.23-5.33
1		74%(99%)	---	7		80%(68%)	(5%)
2		66%	---	8		73%	---
3		73%	---	9		67%	---
4		86% ^c (76%)	(3%)	10		82%	---
5		70%	---	11		89%	(trace)
6		62%	---				

^aIsolated yield on a 1.0 mmol scale. ^bNMR yields shown in parentheses determined using 1,1,1,2-tetrachloroethane as an internal standard on a 0.25 mmol scale. ^c6 mol% catalyst used

5.4 Impact of Steric Bulk of the Catalyst on Selectivity

Interestingly, for 4-OMe styrene, both the $\text{IPr}(\text{Cy}_3\text{P})\text{NiCl}_2$ and $\text{IMes}(\text{Cy}_3\text{P})\text{NiCl}_2$ pre-catalysts gave a mixture of branched and linear boronic esters. While both strongly favored the branched boronic ester, the selectivity of the IMes complex (25:1 branched:linear) was much better than that of the IPr complex (8.3:1 branched:linear). Since

IPr is sterically bulkier than IMes, we wondered if the selectivity could be manipulated by changing the sterics of the catalyst. As such, we synthesized the sterically demanding nickel complex, $\text{IPr}^*(\text{Cy}_3\text{P})\text{NiCl}_2$, and used it as the pre-catalyst for the hydroboration of selected styrenes (Table 5.4). Surprisingly, this catalyst performed well and provided good conversion of the starting material, in spite of the increased steric bulk. For all styrenes, a significant amount of the linear product was observed. While these are un-optimized results, they indicate that the product distribution can be controlled by judicious choice of the NHC ligand.

Table 5.4. Effect of steric bulk on selectivity.

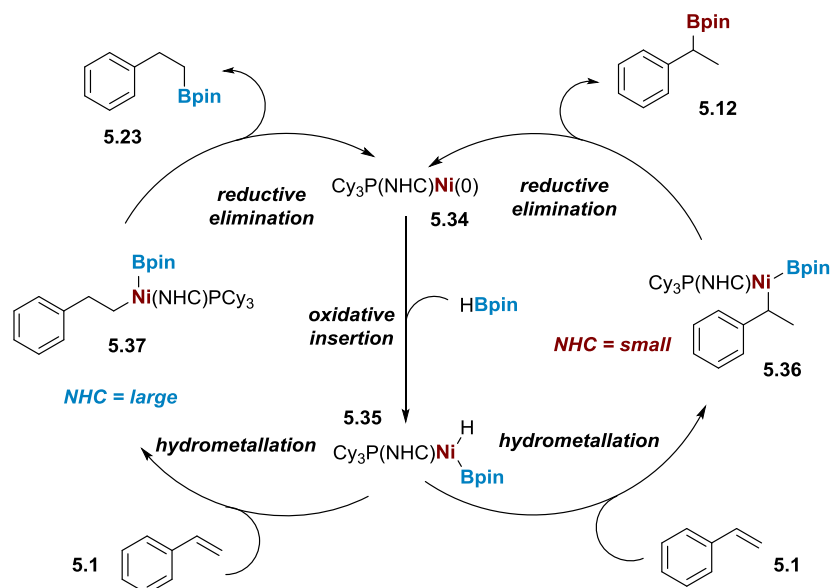
entry	substrate	SM	branched	linear
1	H	0%	48%	33%
2	4-OMe	20%	36%	27%
3	4-CF ₃	5%	39%	35%
4	4-Ph	17%	40%	31%

NMR yields determined using 1,1,1,2-tetrachloroethane as an internal standard.

5.5 Proposed Mechanism

A possible mechanism for nickel-catalyzed hydroboration is shown in Scheme 5.1. Given that a Ni(0) precatalyst can catalyze this reaction, we propose that the heteroleptic Ni(II) precatalyst is reduced by HBpin to generate the active Ni(0) catalyst **5.34**. Then, the Ni undergoes oxidative insertion into the B-H bond to form a nickel borohydride **5.35**. The metal hydride can then add to the olefin in one of two ways. The preferred route is addition to produce benzyl nickel **5.36**, which is stabilized by conjugation with the π -system of the aromatic ring. However, if the catalyst is sufficiently bulky, as in the case where IPr* is the carbene ligand, this intermediate can be disfavored by steric repulsion between the aromatic ring and the ligand. In this case, the Ni can add to the β carbon of the olefin to form intermediate **5.37**. From either nickel intermediate, reductive elimination produces the respective product and regenerates the Ni(0) catalyst. Presumably, an even bulkier NHC ligand could disfavor the benzyl nickel species further; however, reactivity may suffer given the bulk of the nickel complex.

Scheme 5.1. Proposed catalytic cycle.



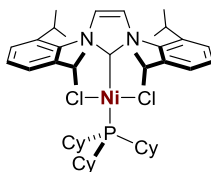
5.6 Conclusions

In conclusion, we have shown that nickel can effectively catalyze the hydroboration of styrenes. Use of new, heteroleptic carbene/phosphine nickel complexes enables excellent selectivity for the branched hydroboration product over the linear product as well as good yields overall. However, increasing the steric bulk of the NHC ligand can increase the amount of the linear product that is observed. Future studies will focus on the use of these novel nickel complexes to carry out a range of transformations.

5.7 Experimental Details

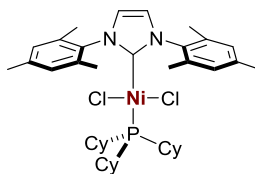
5.7.1 Preparation of Novel Nickel Complexes

Bis-phosphine nickel complexes were synthesized according to a previously reported procedure.⁹ Heteroleptic complexes were prepared using a modified procedure.⁸



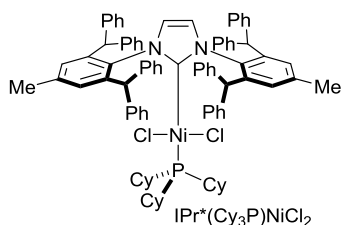
IPr(Cy₃P)NiCl₂. In a glovebox, a 100 mL round bottom flask was charged with 1,3-Bis(2,6-diisopropylphenyl)imidazolium chloride (1.276 g; 3.00 mmol; 1.0 equiv), KOtBu (0.404 g; 3.60 mmol; 1.2 equiv)

and 10 mL THF. The reaction was allowed to stir for 2.5 hours and then filtered through a pad of celite with a small amount of THF into a Schlenk flask containing $(\text{Cy}_3\text{P})_2\text{NiCl}_2$ (2.072 g; 3.00 mmol; 1.0 equiv). The reaction was stirred overnight in the glovebox. The reaction was removed from the glovebox and transferred to a round bottom flask and the solvent was removed *in vacuo*. The resulting red solid was washed with hexanes and then filtered. The filtrate was evaporated to dryness and the red solid was dissolved in a minimal amount of toluene, layered on top of nitromethane, and allowed to slowly diffuse overnight. The resulting crystals of $\text{IPr}(\text{Cy}_3\text{P})\text{NiCl}_2$ were isolated in 30% yield and were suitable for catalysis and X-ray crystallography. ^1H NMR (500 MHz, CDCl_3) δ 7.56 (t, $J = 7.8$ Hz, 2H), 7.43 (d, $J = 7.7$ Hz, 4H), 6.99 (s, 2H), 3.09 (h, $J = 6.8$ Hz, 4H), 1.78 – 1.55 (m, 20H), 1.54 – 1.43 (m, 8H), 1.41 (d, $J = 6.6$ Hz, 12H), 1.32 – 1.10 (m, 5H), 1.07 (d, $J = 7.0$ Hz, 12H). ^{13}C NMR (126 MHz, CDCl_3) δ 166.8 (d, $J = 123.4$ Hz), 147.5, 135.9, 129.7, 123.9 (d, $J = 3.8$ Hz), 123.5, 30.9 (d, $J = 17.4$ Hz), 29.1, 28.7, 27.7 (d, $J = 10.0$ Hz), 26.6, 26.5, 22.6. ^{31}P NMR (202 MHz, CDCl_3) δ 5.78.



IMes(Cy₃P)NiCl₂. In a glovebox, a 100 mL round bottom flask was charged with 1,3-Bis(2,4,6-trimethylphenyl)imidazolium chloride (3.086 g; 9.00 mmol; 1.0 equiv), KOtBu (1.215 g; 10.8 mmol; 1.2 equiv) and 30 mL THF. The reaction was allowed to stir for 30 min. and then filtered through a pad of celite with a small amount of THF into a Schlenk flask containing $(\text{Cy}_3\text{P})_2\text{NiCl}_2$ (6.215 g; 9.00 mmol; 1.0 equiv). The reaction was stirred overnight in the glovebox. The reaction was removed from the glovebox, filtered and washed with THF. The filtrate was concentrated *in vacuo*. The resulting red solid was with hexanes and then filtered. The orange solid that was isolated was the bis-NHC complex, $\text{IMes}_2\text{NiCl}_2$, in 53% yield (relative to the imidazolium salt). The complex was pure enough for catalysis. The filtrate was evaporated to dryness and the red solid was dissolved in a minimal amount of toluene, layered on top of nitromethane, and allowed to slowly diffuse overnight. The resulting crystals of $\text{IMes}(\text{Cy}_3\text{P})\text{NiCl}_2$ were isolated in 8% yield and were suitable for catalysis and X-ray crystallography. ^1H NMR (500 MHz, CDCl_3) δ 7.12 (s, 4H), 6.92 (s, 2H), 2.43 (s, 6H), 2.37 (s, 12H), 1.81 – 1.62 (m, 18H), 1.61 – 1.48 (m, 6H), 1.31 – 1.13 (m, 3H), 1.13 – 0.96 (m, 6H). ^{13}C NMR (126 MHz, CDCl_3) δ 165.2 (d, $J = 121.3$ Hz), 138.4,

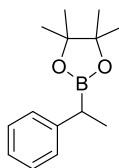
136.7, 136.1, 128.8, 122.8 (d, $J = 3.4$ Hz), 30.5 (d, $J = 17.6$ Hz), 29.3, 27.7 (d, $J = 10.0$ Hz), 26.7, 21.2, 19.4. ^{31}P NMR (202 MHz, CDCl_3) δ 7.03.



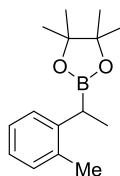
$\text{IPr}^*(\text{Cy}_3\text{P})\text{NiCl}_2$. IPr^*HCl was prepared as previously reported.¹⁰ In a glovebox, a 100 mL round bottom flask was charged with IPr^*HCl (1.84 g; 2.00 mmol; 1.0 equiv), KOtBu (0.269 g; 2.40 mmol; 1.2 equiv) and 10 mL THF. The reaction was allowed to stir for 45 min. and then filtered through a pad of celite with a small amount of THF into a Schlenk flask containing $(\text{Cy}_3\text{P})_2\text{NiCl}_2$ (1.90 g; 2.75 mmol; 1.4 equiv). The reaction was stirred overnight in the glovebox. The reaction was removed from the glovebox and transferred to a round bottom flask and the solvent was removed *in vacuo*. The resulting red solid was washed with hexanes and then filtered. The filtrate was evaporated to dryness and the red solid was dissolved in a minimal amount of toluene, layered on top of nitromethane, and allowed to slowly diffuse overnight. The resulting solid of $\text{IPr}^*(\text{Cy}_3\text{P})\text{NiCl}_2$ was isolated in 9.5% yield and were suitable for catalysis. The solid could then be crystallized by dissolving in a minimal amount of *p*-xylene, layered on top of nitromethane, and allowed to slowly diffuse overnight. The resulting crystals were suitable for X-ray crystallography. ^1H NMR (500 MHz, CDCl_3) δ 7.47 (d, $J = 7.6$ Hz, 8H), 7.23 (t, $J = 7.5$ Hz, 8H), 7.18 (t, $J = 7.2$ Hz, 4H), 7.05 – 6.95 (m, 12H), 6.89 (s, 4H), 6.68 (d, $J = 7.0$ Hz, 8H), 5.91 (s, 4H), 4.10 (s, 2H), 2.30 (s, 6H), 1.95 – 1.77 (m, 9H), 1.66 – 1.54 (m, 15H), 1.21 – 1.03 (m, 9H). ^{13}C NMR (126 MHz, CDCl_3) δ 166.3 (d, $J = 122.7$ Hz), 145.6, 143.9, 143.8, 137.9, 135.5, 131.1, 129.6, 129.5, 127.7, 125.9, 125.9, 122.1, 122.1, 51.2, 31.2 (d, $J = 17.1$ Hz), 29.3, 27.8 (d, $J = 10.0$ Hz), 26.4, 21.9. ^{31}P NMR (202 MHz, CDCl_3) δ 7.90.

5.7.2 General Procedure for the Hydroboration of Styrenes.

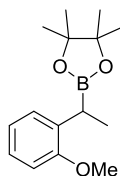
All styrenes were purified by distillation or column chromatography before use.



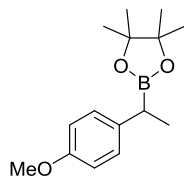
Compound 5.12. In a glovebox, a 10 mL round bottom flask was charged with IMes(Cy₃P)NiCl₂ (21 mg; 0.03 mmol; 3 mol%), KOtBu (6.7 mg; 0.06 mmol; 6 mol%), and 2 mL of toluene. The flask was fitted a septum, removed from the glovebox and the mixture was allowed to stir for 10 minutes. Then, HBpin (0.18 mL; 1.24 mmol; 1.2 equiv) and then styrene (0.12 mL; 1.04 mmol; 1.0 equiv) was added. The reaction was allowed to stir overnight at 60 °C. The reaction was filtered through a plug of silica and washed with 10% EtOAc in hexanes and concentrated. The crude material was purified by column chromatography using isocratic 5% EtOAc in hexanes. NOTE: product decomposition occurs on silica, so the product should elute in 10 minutes or less. Compound **5.12** was isolated in 74% yield as a clear, colorless, viscous oil. ¹H NMR (500 MHz, CDCl₃) δ 7.26 (t, *J* = 7.5 Hz, 2H), 7.22 (d, *J* = 7.5 Hz, 2H), 7.13 (t, *J* = 7.2 Hz, 1H), 2.43 (q, *J* = 7.5 Hz, 1H), 1.33 (d, *J* = 7.5 Hz, 3H), 1.21 (s, 6H), 1.20 (s, 6H). ¹³C NMR (126 MHz, CDCl₃) δ 145.0, 128.3, 127.8, 125.0, 83.3, 24.6, 17.0. HRMS (ESI) *m/z* calculated for C₁₄H₂₅BNO₂ [M+NH₄]⁺ 249.2010, found 249.2013.



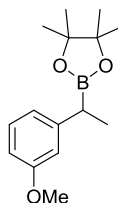
Compound 5.13. Compound **5.13** was prepared and purified in the same fashion as compound **5.12**. Compound **5.13** was isolated in 66% yield. ¹H NMR (500 MHz, CDCl₃) δ 7.20 (d, *J* = 7.7 Hz, 1H), 7.16 – 7.08 (m, 2H), 7.04 (t, *J* = 7.4 Hz, 1H), 2.58 (q, *J* = 7.5 Hz, 1H), 2.31 (s, 3H), 1.32 (d, *J* = 7.4 Hz, 3H), 1.22 (s, 6H), 1.20 (s, 6H). ¹³C NMR (126 MHz, CDCl₃) δ 143.4, 135.6, 123.0, 127.1, 126.0, 125.0, 83.2, 24.7, 19.9, 16.4. HRMS (ESI) *m/z* calculated for C₁₅H₂₈BNO₂ [M+NH₄]⁺ 263.2166, found 263.2163.



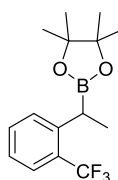
Compound 5.14. Compound **5.14** was prepared and purified in the same fashion as compound **5.12**. Compound **5.14** was isolated in 73% yield. ¹H NMR (500 MHz, CDCl₃) δ 7.18 – 7.11 (m, 2H), 6.89 (t, *J* = 7.4 Hz, 1H), 6.80 (d, *J* = 8.0 Hz, 1H), 3.80 (s, 3H), 2.45 (q, *J* = 7.5 Hz, 1H), 1.28 (d, *J* = 7.6 Hz, 3H), 1.23 (s, 6H), 1.22 (s, 6H). ¹³C NMR (126 MHz, CDCl₃) δ 156.8, 133.9, 128.4, 126.2, 120.7, 109.7, 83.0, 54.9, 24.7, 15.1. HRMS (ESI) *m/z* calculated for C₁₅H₂₇BNO₃ [M+NH₄]⁺ 279.2115, found 279.2115.



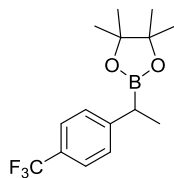
Compound 5.15. Compound **5.15** was prepared and purified in the same fashion as compound **5.12** except the amount of IMe(Cy₃P)NiCl₂ and KOtBu were doubled. Compound **5.15** was isolated in 86% yield. ¹H NMR (500 MHz, CDCl₃) δ 7.13 (d, *J* = 8.7 Hz, 2H), 6.81 (d, *J* = 8.6 Hz, 2H), 3.77 (s, 3H), 2.37 (q, *J* = 7.5 Hz, 1H), 1.29 (d, *J* = 7.5 Hz, 3H), 1.21 (s, 6H), 1.20 (s, 6H). ¹³C NMR (126 MHz, CDCl₃) δ 157.2, 137.0, 128.61, 113.8, 83.2, 55.2, 24.6, 17.4. HRMS (ESI) *m/z* calculated for C₁₅H₂₇BNO₃ [M+NH₄]⁺ 279.2115, found 279.2116.



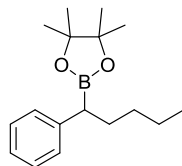
Compound 5.16. Compound **5.16** was prepared and purified in the same fashion as compound **5.12**. Compound **5.16** was isolated in 70% yield. ¹H NMR (500 MHz, CDCl₃) δ 7.17 (t, *J* = 7.9 Hz, 1H), 6.81 (d, *J* = 7.7 Hz, 1H), 6.78 (t, *J* = 2.5 Hz, 1H), 6.68 (dd, *J* = 8.2, 2.6 Hz, 1H), 3.79 (s, 3H), 2.41 (q, *J* = 7.5 Hz, 1H), 1.32 (d, *J* = 7.5 Hz, 3H), 1.21 (s, 6H), 1.20 (s, 6H). ¹³C NMR (126 MHz, CDCl₃) δ 159.6, 146.6, 129.2, 120.3, 113.5, 110.5, 83.3, 55.1, 24.6, 17.0. HRMS (ESI) *m/z* calculated for C₁₅H₂₄BO₃ [M+H]⁺ 262.1850, found 262.1853.



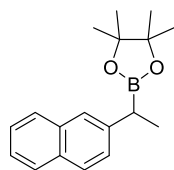
Compound 5.17. Compound **5.17** was prepared and purified in the same fashion as compound **5.12**. Compound **5.17** was isolated in 62% yield. ¹H NMR (500 MHz, CDCl₃) δ 7.58 (d, *J* = 7.9 Hz, 1H), 7.46 (t, *J* = 7.6 Hz, 1H), 7.41 (d, *J* = 7.8 Hz, 1H), 7.22 (t, *J* = 7.6 Hz, 1H), 2.84 (q, *J* = 7.5 Hz, 1H), 1.35 (d, *J* = 7.4 Hz, 3H), 1.21 (s, 6H), 1.21 (s, 6H). ¹³C NMR (126 MHz, CDCl₃) δ 144.6, 131.6, 129.6, 128.0 (q, *J* = 29.0 Hz), 125.7 (q, *J* = 5.9 Hz), 124.7 (q, *J* = 273.8 Hz), 124.9, 83.4, 24.6, 17.7. HRMS (ASAP) *m/z* calculated for C₁₅H₂₀BF₃O₂ [M]⁺ 299.1540, found 299.1543.



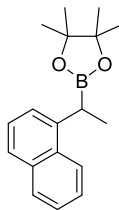
Compound 5.18. Compound **5.18** was prepared and purified in the same fashion as compound **5.12**. Compound **5.18** was isolated in 80% yield. ^1H NMR (500 MHz, CDCl_3) δ 7.51 (d, $J = 8.0$ Hz, 2H), 7.32 (d, $J = 8.0$ Hz, 2H), 2.50 (q, $J = 7.5$ Hz, 1H), 1.34 (d, $J = 7.5$ Hz, 3H), 1.21 (s, 6H), 1.20 (s, 6H). ^{13}C NMR (126 MHz, CDCl_3) δ 149.3, 128.0, 127.4 (q, $J = 32.5$ Hz), 125.2 (q, $J = 3.8$ Hz), 124.5 (q, $J = 271.6$ Hz), 83.6, 24.6, 24.6, 16.7. HRMS (ASAP) m/z calculated for $\text{C}_{15}\text{H}_{20}\text{BF}_3\text{O}_2$ $[\text{M}]^+$ 299.1540, found 299.1539.



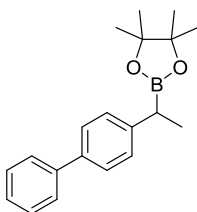
Compound 5.19. Compound **5.19** was prepared and purified in the same fashion as compound **5.12**. Compound **5.19** was isolated in 73% yield. ^1H NMR (500 MHz, CDCl_3) δ 7.25 – 7.18 (m, 4H), 7.12 (t, $J = 7.1$ Hz, 1H), 2.29 (t, $J = 7.9$ Hz, 1H), 1.84 (dq, $J = 14.8, 7.8$ Hz, 1H), 1.64 (dq, $J = 14.7, 7.6$ Hz, 1H), 1.35 – 1.21 (m, 4H), 1.20 (s, 6H), 1.18 (s, 6H), 0.86 (t, $J = 7.1$ Hz, 3H). ^{13}C NMR (126 MHz, CDCl_3) δ 143.5, 128.4, 128.2, 125.0, 83.20, 32.3, 31.6, 24.6, 22.7, 14.0. HRMS (ESI) m/z calculated for $\text{C}_{17}\text{H}_{31}\text{BNO}_2$ $[\text{M}+\text{NH}_4]^+$ 291.2479, found 291.2478.



Compound 5.20. Compound **5.20** was prepared and purified in the same fashion as compound **5.12**. Compound **5.20** was isolated in 67% yield. ^1H NMR (500 MHz, CDCl_3) δ 7.84 – 7.72 (m, 3H), 7.64 (s, 1H), 7.48 – 7.34 (m, 3H), 2.61 (q, $J = 7.5$ Hz, 1H), 1.42 (d, $J = 7.5$ Hz, 3H), 1.21 (s, 6H), 1.20 (s, 6H). ^{13}C NMR (126 MHz, CDCl_3) δ 142.6, 133.8, 131.7, 127.6, 127.5, 127.4, 127.2, 125.6, 125.2, 124.7, 83.4, 24.6, 16.8. HRMS (ASAP) m/z calculated for $\text{C}_{18}\text{H}_{23}\text{BO}_2$ $[\text{M}]^+$ 281.1822, found 281.1818.

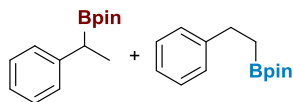


Compound 5.21. Compound **5.21** was prepared and purified in the same fashion as compound **5.12**. Compound **5.21** was isolated in 82% yield. ^1H NMR (500 MHz, CDCl_3) δ 8.10 (d, $J = 8.2$ Hz, 1H), 7.83 (d, $J = 7.8$ Hz, 1H), 7.66 (d, $J = 7.9$ Hz, 1H), 7.50 – 7.35 (m, 4H), 3.11 (q, $J = 7.5$ Hz, 1H), 1.49 (d, $J = 7.4$ Hz, 3H), 1.20 (s, 6H), 1.19 (s, 6H). ^{13}C NMR (126 MHz, CDCl_3) δ 141.4, 133.9, 132.0, 128.7, 125.8, 125.3, 125.2, 124.2, 124.0, 83.4, 24.7, 24.5, 16.4. HRMS (ESI) m/z calculated for $\text{C}_{18}\text{H}_{27}\text{BNO}_2$ $[\text{M}+\text{NH}_4]^+$ 299.2166, found 299.2165.



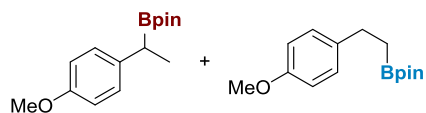
Compound 5.22. Compound **5.22** was prepared and purified in the same fashion as compound **5.12**. Compound **5.22** was isolated in 89% yield. ^1H NMR (500 MHz, CDCl_3) δ 7.58 (d, $J = 7.6$ Hz, 2H), 7.50 (d, $J = 8.0$ Hz, 2H), 7.41 (t, $J = 7.6$ Hz, 2H), 7.33 – 7.27 (m, 3H), 2.48 (q, $J = 7.5$ Hz, 1H), 1.36 (d, $J = 7.5$ Hz, 3H), 1.23 (s, 6H), 1.22 (s, 6H). ^{13}C NMR (126 MHz, CDCl_3) δ 144.2, 141.2, 137.9, 128.6, 128.2, 127.0, 126.9, 126.8, 83.4, 24.6, 17.1. HRMS (ESI) m/z calculated for $\text{C}_{20}\text{H}_{29}\text{BNO}_2$ $[\text{M}+\text{NH}_4]^+$ 325.2322, found 325.2317.

5.7.3 Effect of Sterics on Hydroboration.

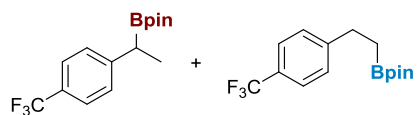


In a glovebox, a 5 mL vial was charged with $\text{IPr}^*(\text{Cy}_3\text{P})\text{NiCl}_2$ (9.9 mg; 7.5 μmol ; 3 mol%), KOtBu (1.7 mg; 15 μmol ; 6 mol%), and 0.5 mL of toluene. The vial was fitted a septum, removed from the glovebox and the mixture was allowed to stir for 10 minutes. Then, HBpin (44 μL ; 0.303 mmol; 1.2 equiv) and then styrene (29 μL ; 0.252 mmol; 1.0 equiv) was added. The reaction was allowed to stir overnight at 60 $^\circ\text{C}$. The reaction was filtered through a plug of silica and washed with 10% EtOAc in hexanes and concentrated. The crude material was dissolved in CDCl_3 and 10 μL of 1,1,1,2-tetrachloroethane was added. The product and starting material peaks were integrated

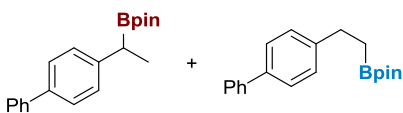
against the standard. The standard was integrated such that integrations of one proton peaks would represent yield. 48% branched; 33% linear; 0% SM.



The mixture of branched and linear products were synthesized as described above. 36% branched; 27% linear; 20% SM.

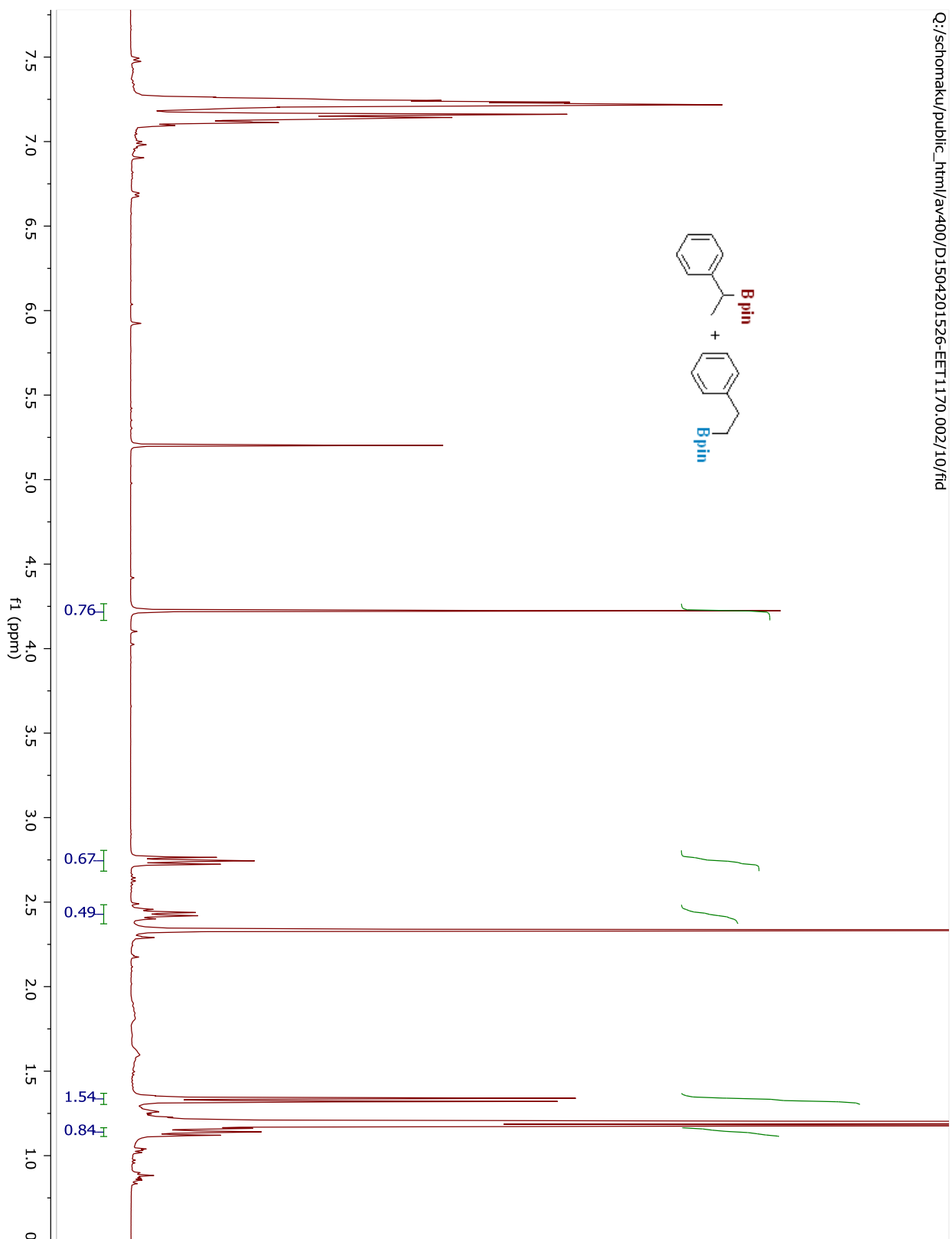


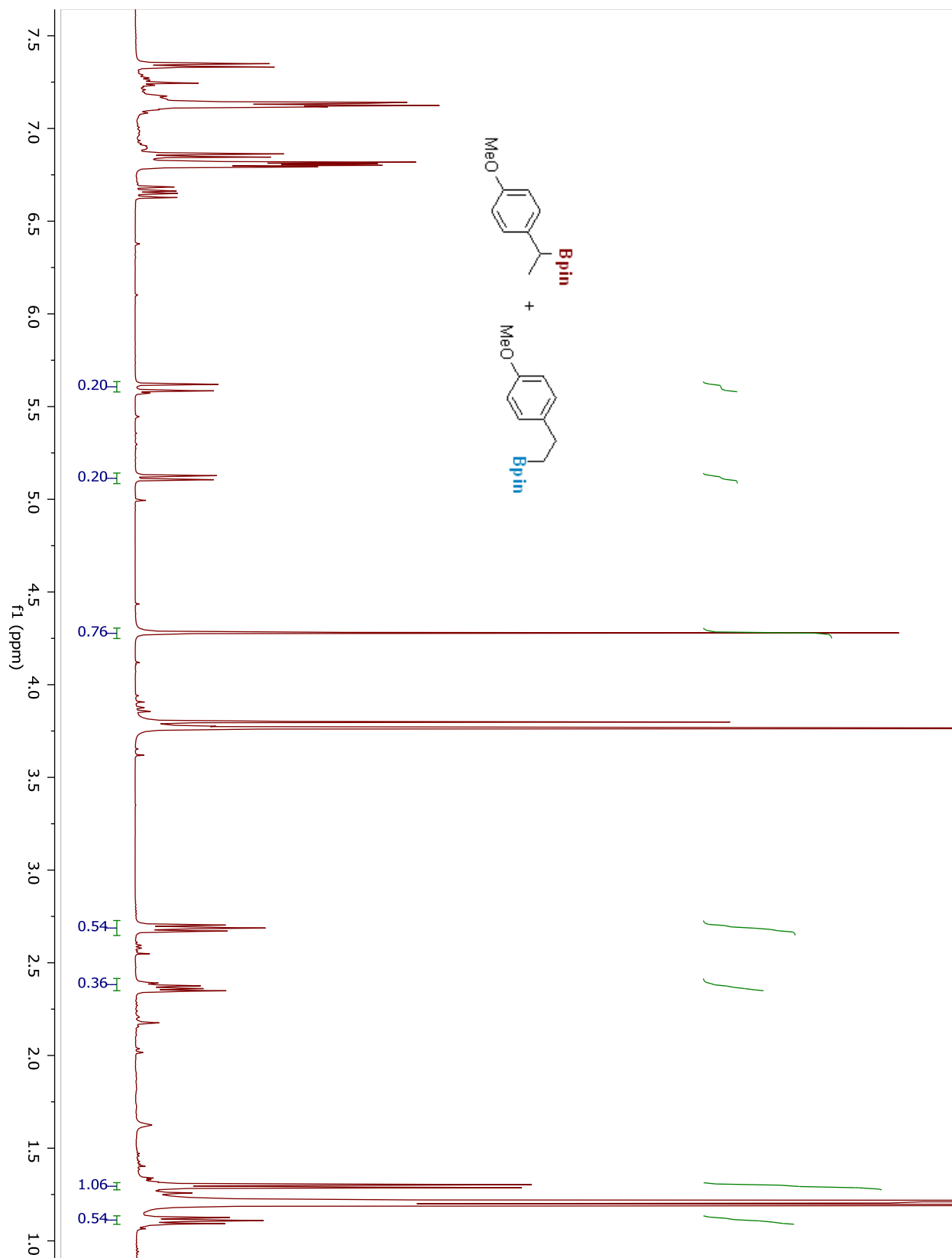
The mixture of branched and linear products were synthesized as described above. 39% branched; 35% linear; 5% SM.

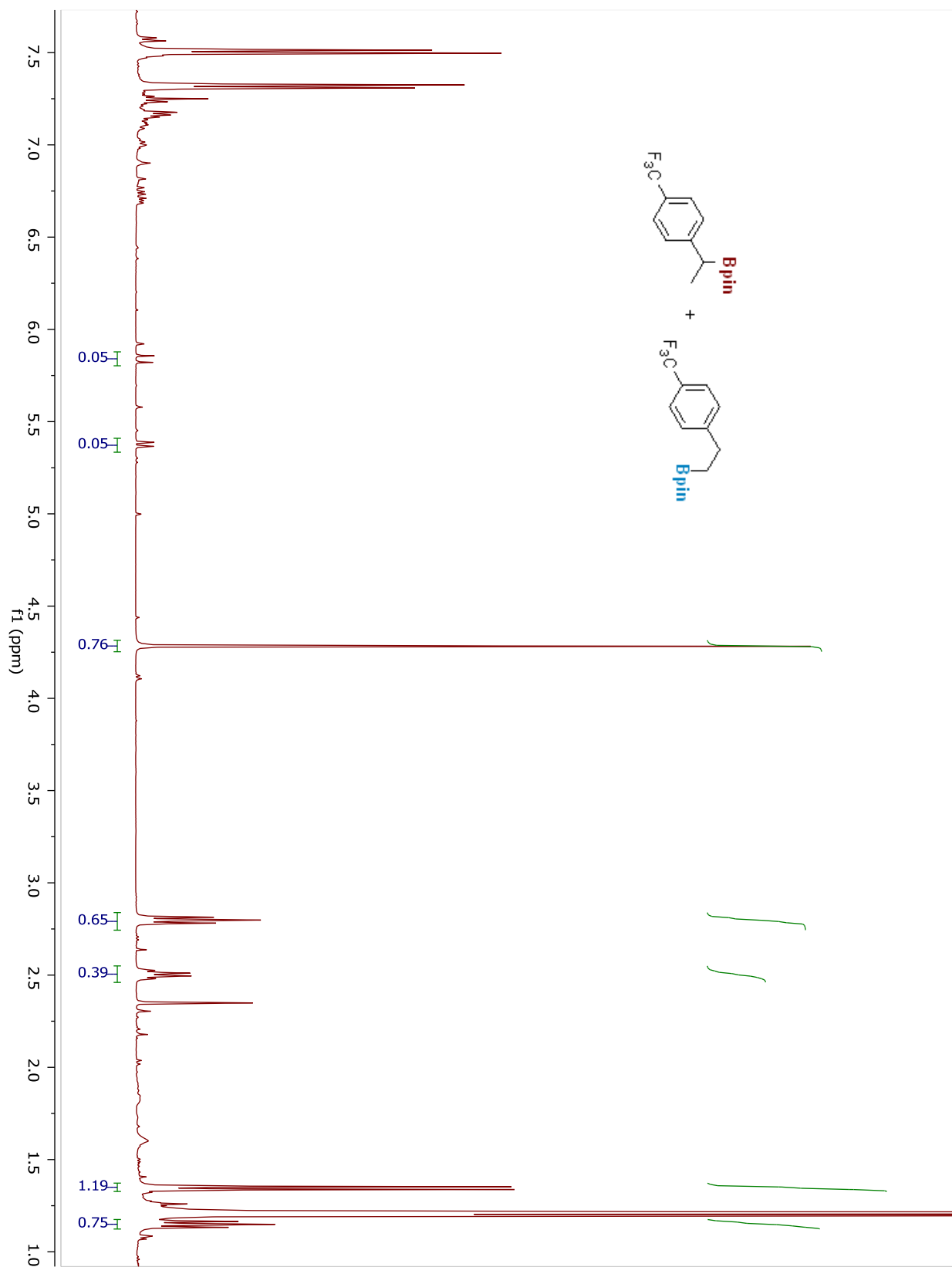


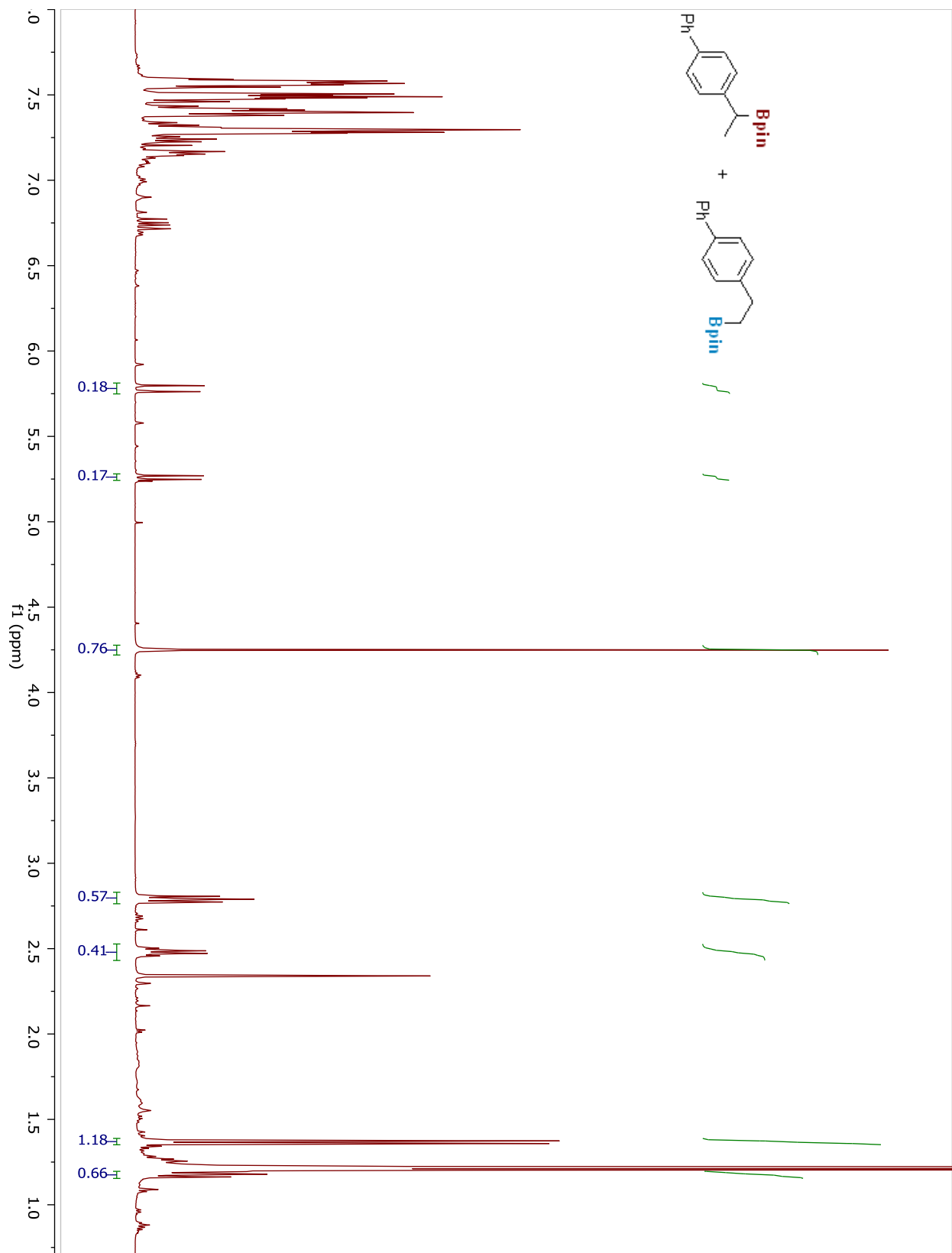
The mixture of branched and linear products were synthesized as described above. 41% branched; 31% linear; 17% SM.

Q:/schomaku/public_html/av400/D1504201526-EET1170.002/10/fid









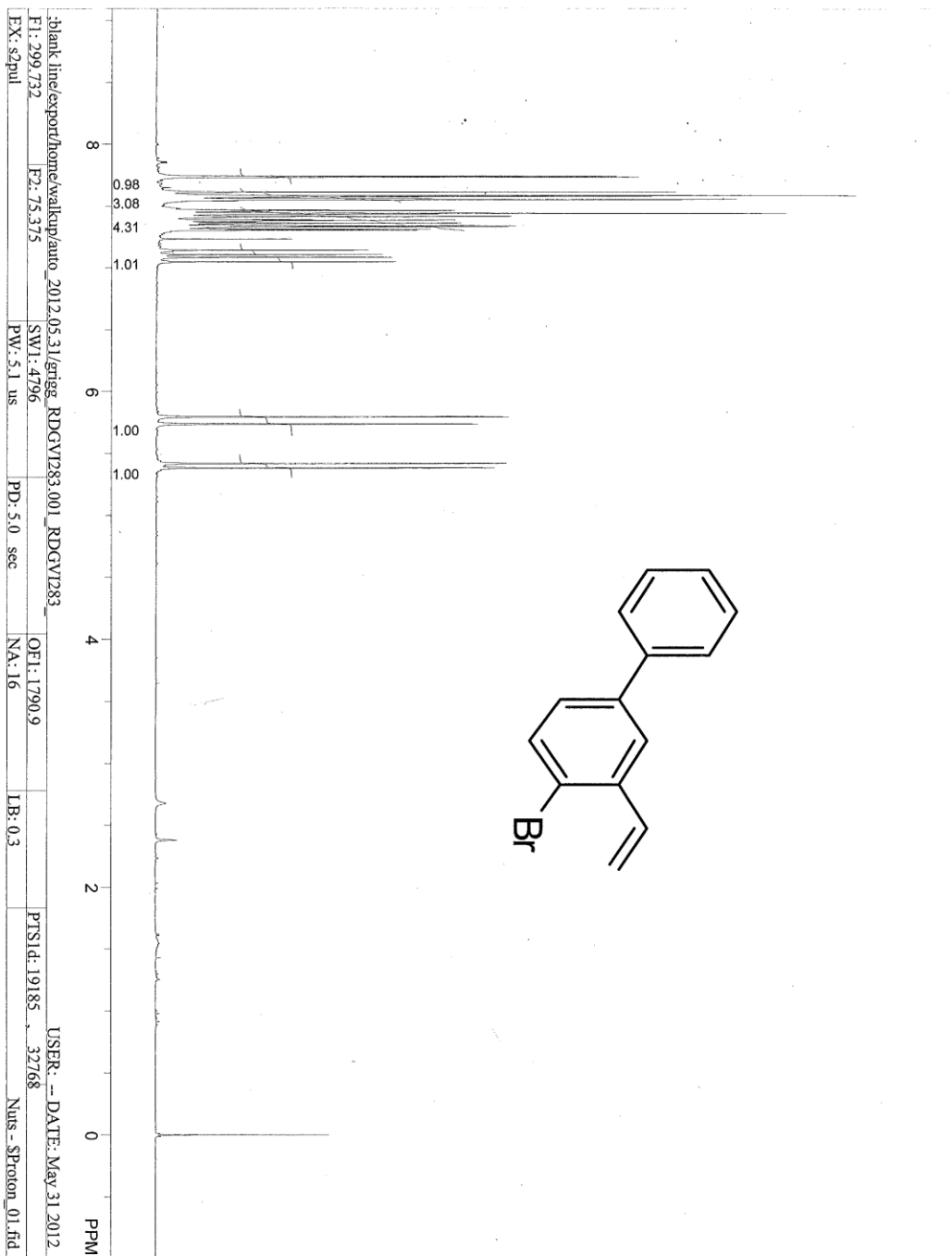
5.8 Bibliography

- (a) Ritleng, V.; Sirlin, C.; Pfeffer, M. *Chem. Rev.* **2002**, *102*, 1731. (b) Lyons, T. W.; Sanford, M. S. *Chem. Rev.* **2010**, *110*, 1147. (c) Diederich, F.; Stang, P. J., Eds. *Metal-catalyzed Cross-coupling Reactions* Wiley-VCH: Weinheim, **1998**. (d) Phapale, V. B.; Cárdenas, D. *Chem. Soc. Rev.* **2009**, *38*, 1598. (e) McDonald, R. I.; Liu, G.; Stahl, S. S. *Chem. Rev.* **2011**, *111*, 2981. (f) Farina, V. *Adv. Syn. Catal.* **2004**, *346*, 1553. (g) Jana, R.; Pathak, T.P.; Sigman, M. S. *Chem. Rev.* **2011**, *111*, 1417. (h) Xu, L.-M.; Li, B.-J.; Yang, Z.; Shi, Z.-J. *Chem. Soc. Rev.* **2010**, *39*, 712. (i) Tamaru, Y.; Ed. *Modern Organonickel Chemistry*; Wiley: Weinheim, **2005**. (j) Krause, N.; Ed. *Modern Organocopper Chemistry*; Wiley: Weinheim, **2002**. (k) Rosen, B.M.; Quasdorf, K. W.; Wilson, D. A.; Zhang, N.; Resmerita, A.; Garg, N. K.; Percec, V. *Chem. Rev.* **2011**, *111*, 1346. (l) Alonso, D. A.; Najera, C. in *Science of Synthesis*; de Meijere, A., Ed.; Thieme: New York, Stuttgart, **2009**; Vol. 47a, pp 439-479. (m) Jana, R.; Pathak, T. P.; Sigman, M. S. *Chem. Rev.* **2011**, *111*, 1417. (n) Li, B.; Xu, L.; Wu, Z.; Guan, B.; Sun, C.; Wang, B.; Shi, Z. *J. Am. Chem. Soc.* **2009**, *131*, 14656. (o) Han, F.-S. *Chem. Soc. Rev.* **2013**, *42*, 5270.
- (a) Li, Q.; Liskey, C. W.; Hartwig, J. F. *J. Am. Chem. Soc.* **2014**, *136*, 8755–8765. (b) Cho, S. H.; Hartwig, J. F. *Chem. Sci.* **2014**, *5*, 694-698. (c) Larsen, M. A.; Hartwig, J. F. *J. Am. Chem. Soc.* **2014**, *136*, 4287-4299. (d) Liskey, C. W.; Hartwig, J. F. *Synthesis* **2013**, *45*, 1837–1842. (e) Mlynarski, S. N.; Schuster, C. H.; Morken, J. P. *Nature*. **2014**, *505*, 386. (f) Coombs, J. R.; Haeffner, F.; Kliman, L. T.; Morken, J. P. *J. Am. Chem. Soc.* **2013**, *135*, 11222.
- For examples of coupling to make boronic esters, see: (a) Sogabe, Y.; Namikoshi, T.; Watanabe, S.; Murata, M. *Synthesis* **2012**, *44*, 1233-1236. (b) Zhang, P.; Roundtree, I. A.; Morken, J. P. *Org. Lett.* **2012**, *14*, 1416-1419. (c) Yi, J.; Liu, J.-H.; Liang, J.; Dai, J.-J.; Yang, C.-T.; Fu, Y.; Liu, L. *Adv. Synth. Catal.* **2012**, *354*, 1685-1691. (d) Tobisu, M.; Nakamura, K.; Chatani, N. *J. Am. Chem. Soc.* **2014**, *136*, 5587-5590. (e) Furukawa, T.; Tobisu, M.; Chatani, N. *Chem. Commun.* **2015**, *51*, 6508-6511. (f) Huang, K.; Yu, D.-G.; Zheng, S.-F.; Wu, Z.-H.; Shi, Z.-J. *Chem. Eur. J.* **2011**, *17*, 786-791. (g) Molander, G. A.; Cavalcanti, L. N.; Garcia-Garcia, C. *J. Org. Chem.* **2013**, *78*, 6427-6439. (h) Zhang, H.; Hagihara, S.; Itami, K. *Chem. Lett.* **2015**, *44*, 779-781.

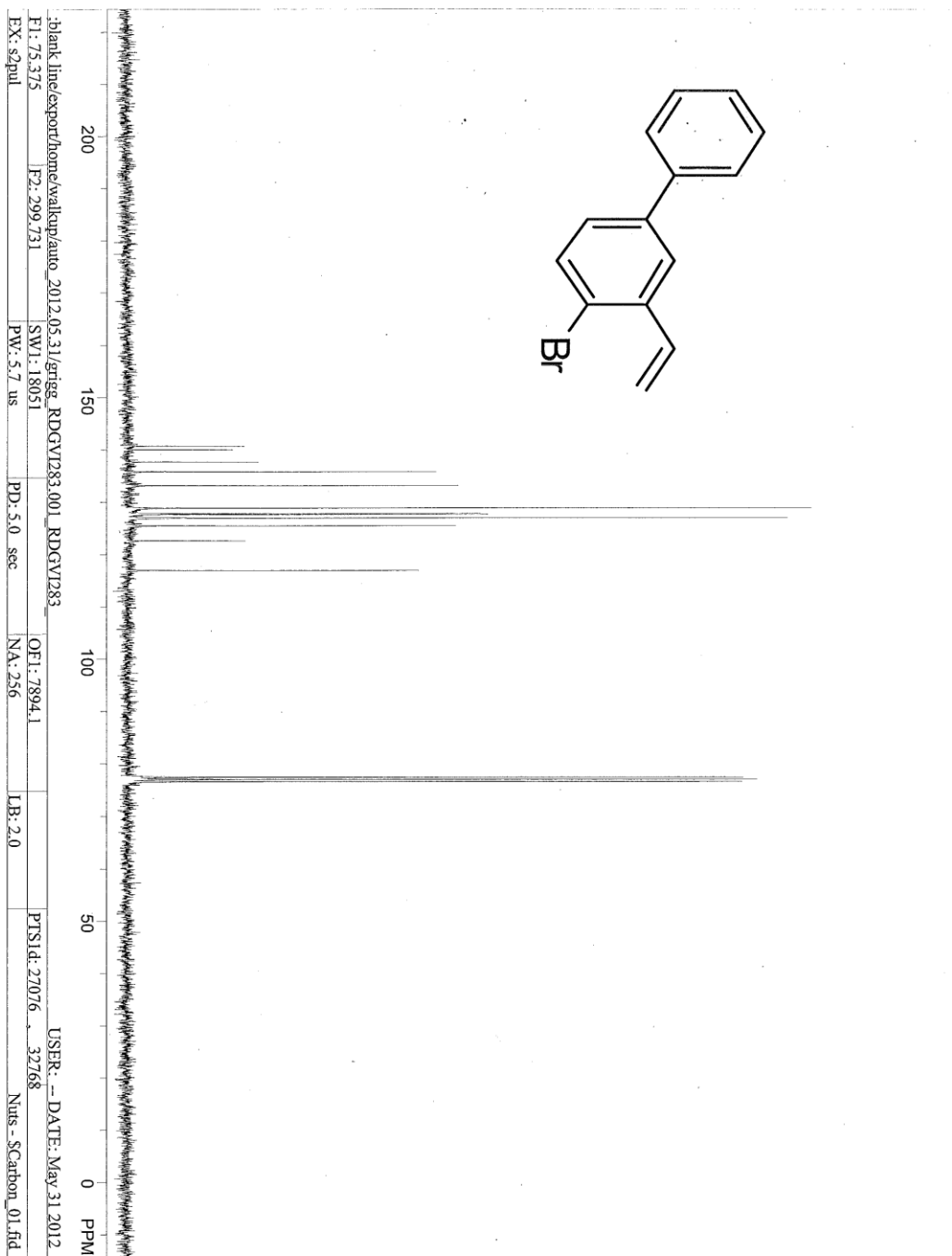
4. For examples of diboration, see: (a) Cho, H. Y.; Yu, Z.; Morken, J. P. *Org. Lett.* **2011**, *13*, 5267-5269. (b) Ely, R. J.; Morken, J. P. *Org. Lett.* **2010**, *12*, 4348-4351. (c) Cho, H. Y.; Morken, J. P. *J. Am. Chem. Soc.* **2008**, *130*, 16140-16141. (d) Cho, H. Y.; Morken, J. P. *J. Am. Chem. Soc.* **2010**, *132*, 7576-7577.
5. For examples of 1,4-hydroboration, see: (a) Ely, R. J.; Yu, Z.; Morken, J. P. *Tetrahedron Lett.* **2015**, *56*, 3402-3405. (b) Crotti, S.; Bertolini, F.; Macchia, F.; Pineschi, M. *Org. Lett.* **2009**, *11*, 3762-3765. (c)
6. Pereria, S.; Srebnik, M. *Tetrahedron Lett.* **1996**, *37*, 3283-3286.
7. Kabalka, G. W.; Narayana, C.; Reddy, N. K. *Synth. Commun.* **1994**, *24*, 1019-1023.
8. Matsubara, K.; Ueno, K.; Shibata, Y. *Organometallics* **2006**, *25*, 3422-3427.
9. Quasdorf, K. W.; Tian, X.; Garg, N. K., *J. Am. Chem. Soc.* **2008**, *130*, 14422.
10. Berthon-Gelloz, G.; Siegler, M. A.; Spek, A. L.; Tinant, B.; Reek, J. N. H.; Marko, I. E. *Dalton Trans.* **2010**, *39*, 1444-1446.

Appendix A: NMR Spectra

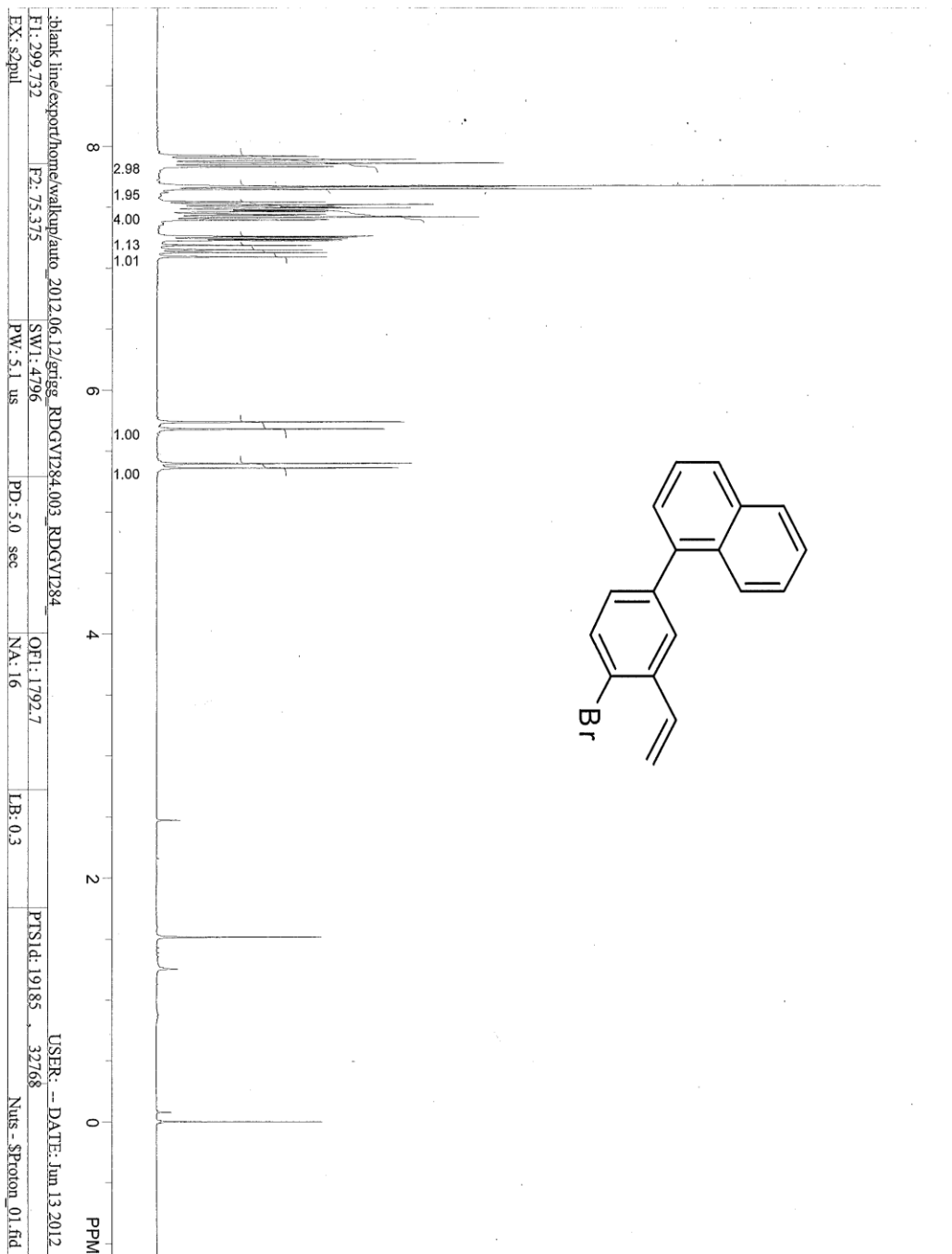
Compound 2.6.



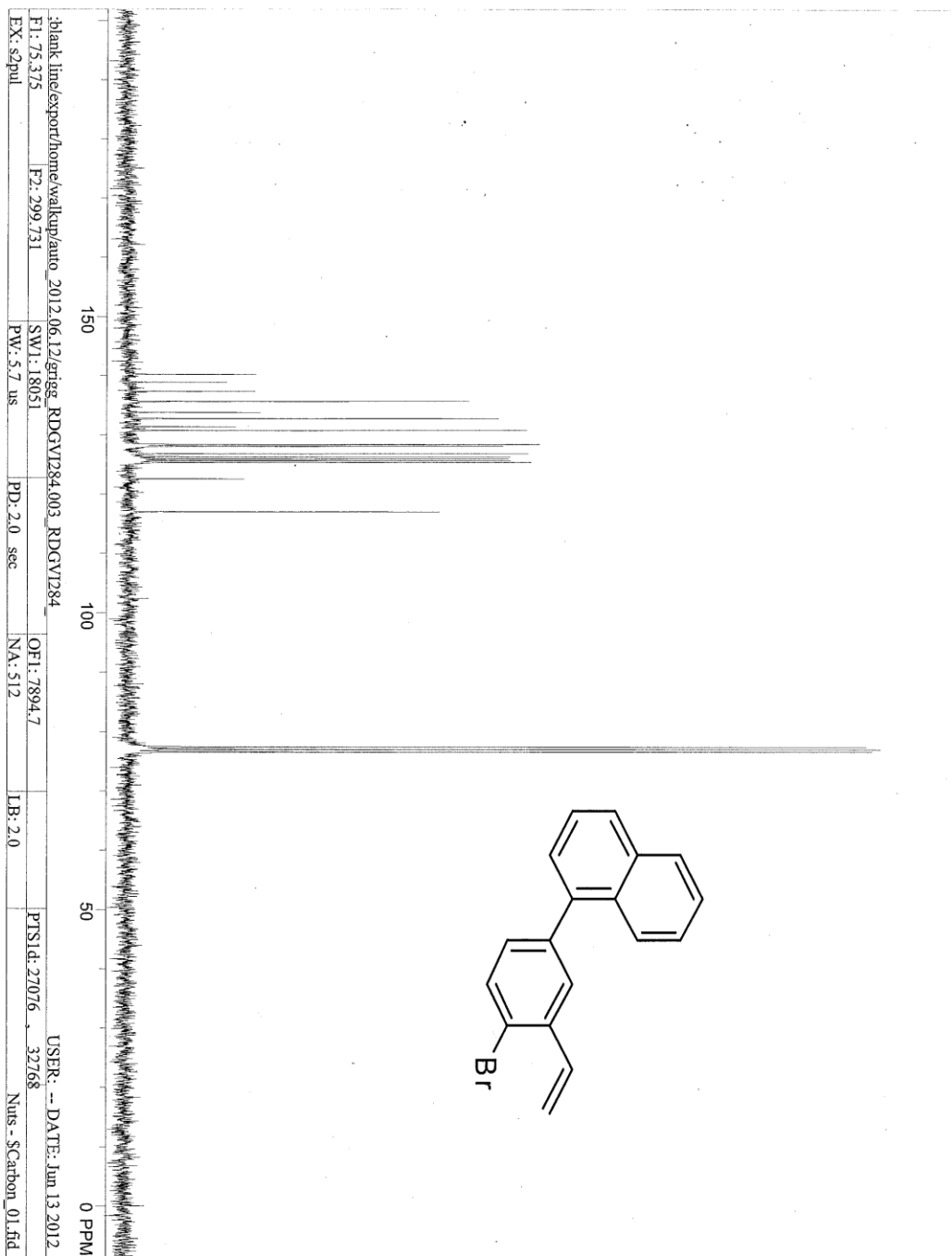
Compound 2.6.



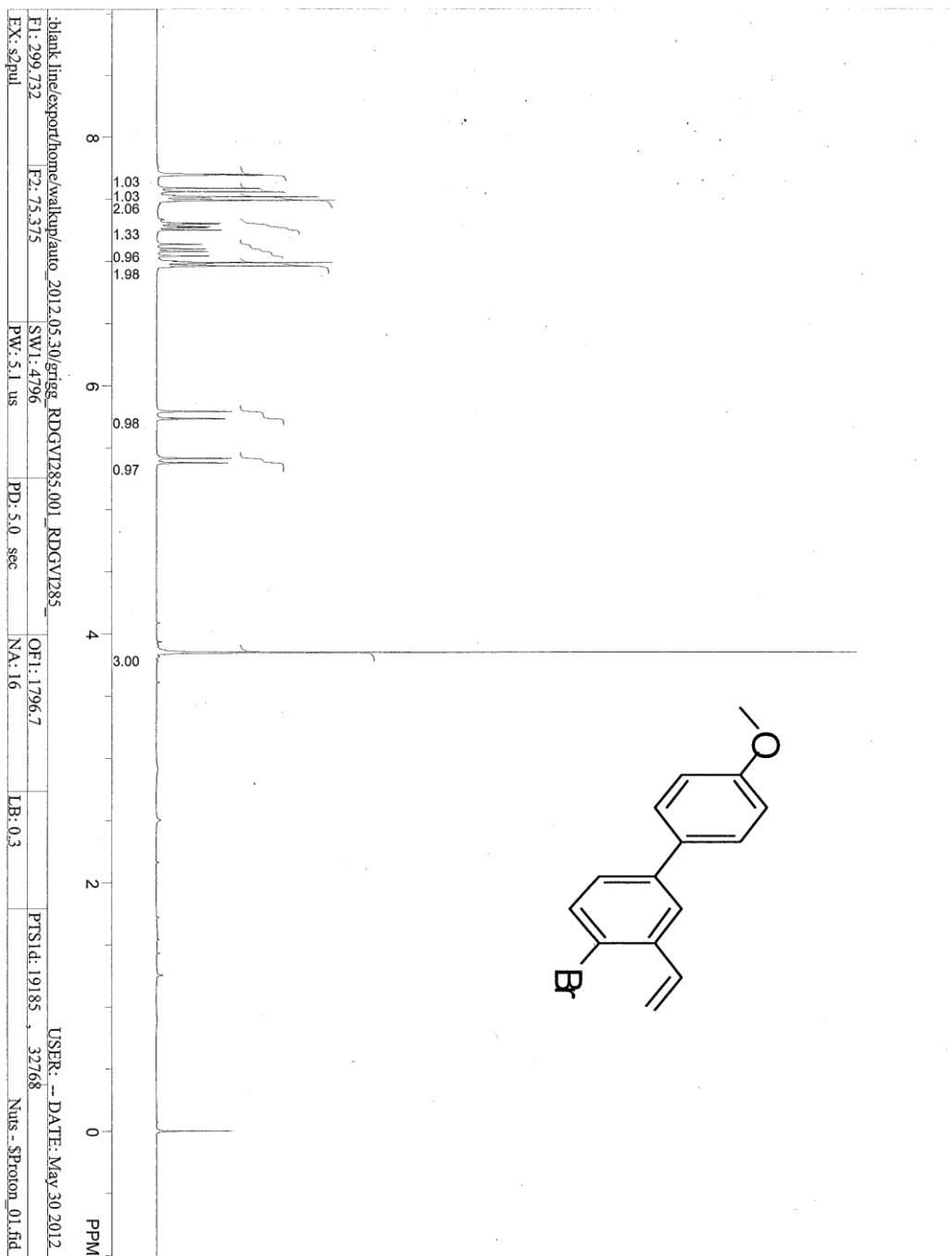
Compound 2.7.



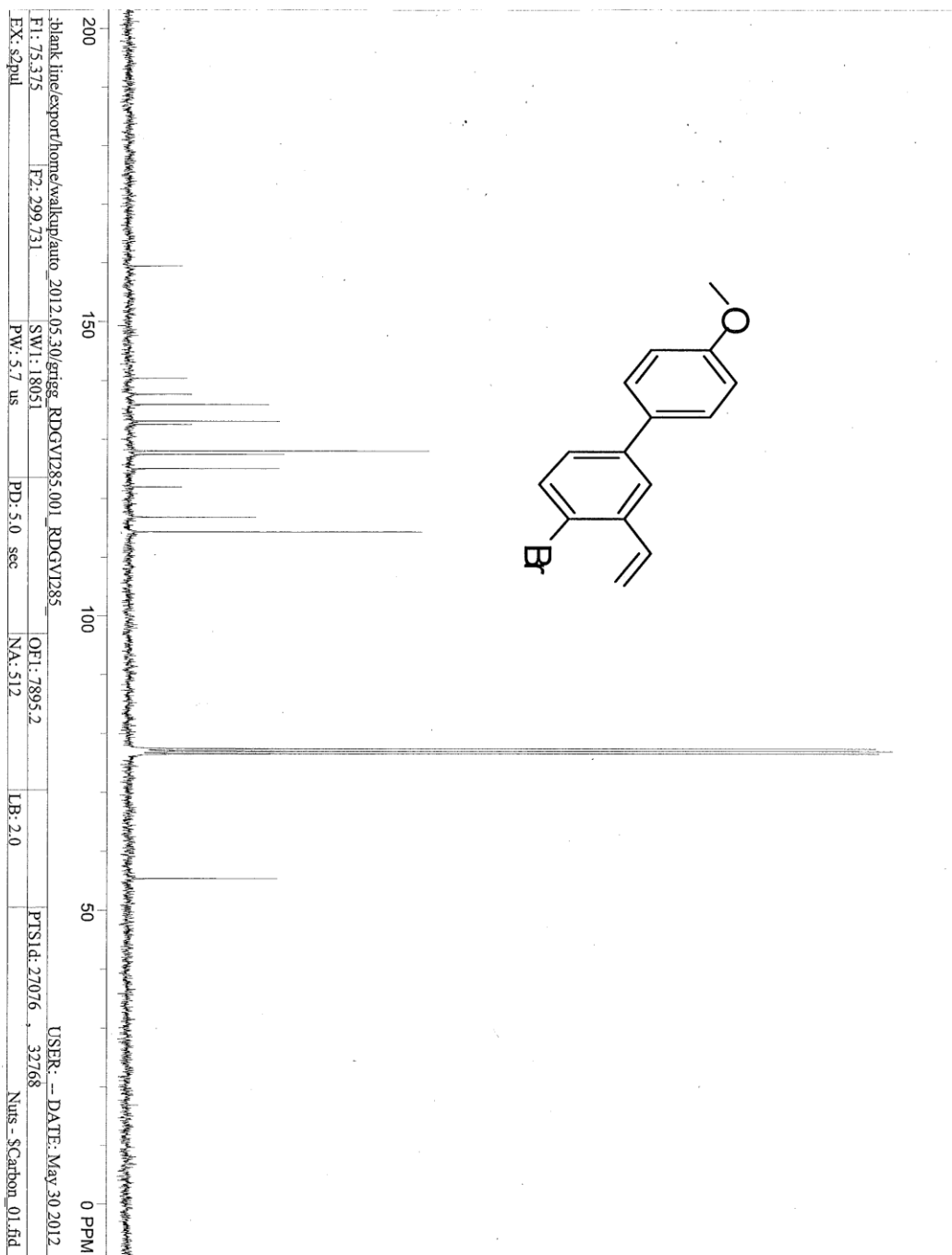
Compound 2.7.



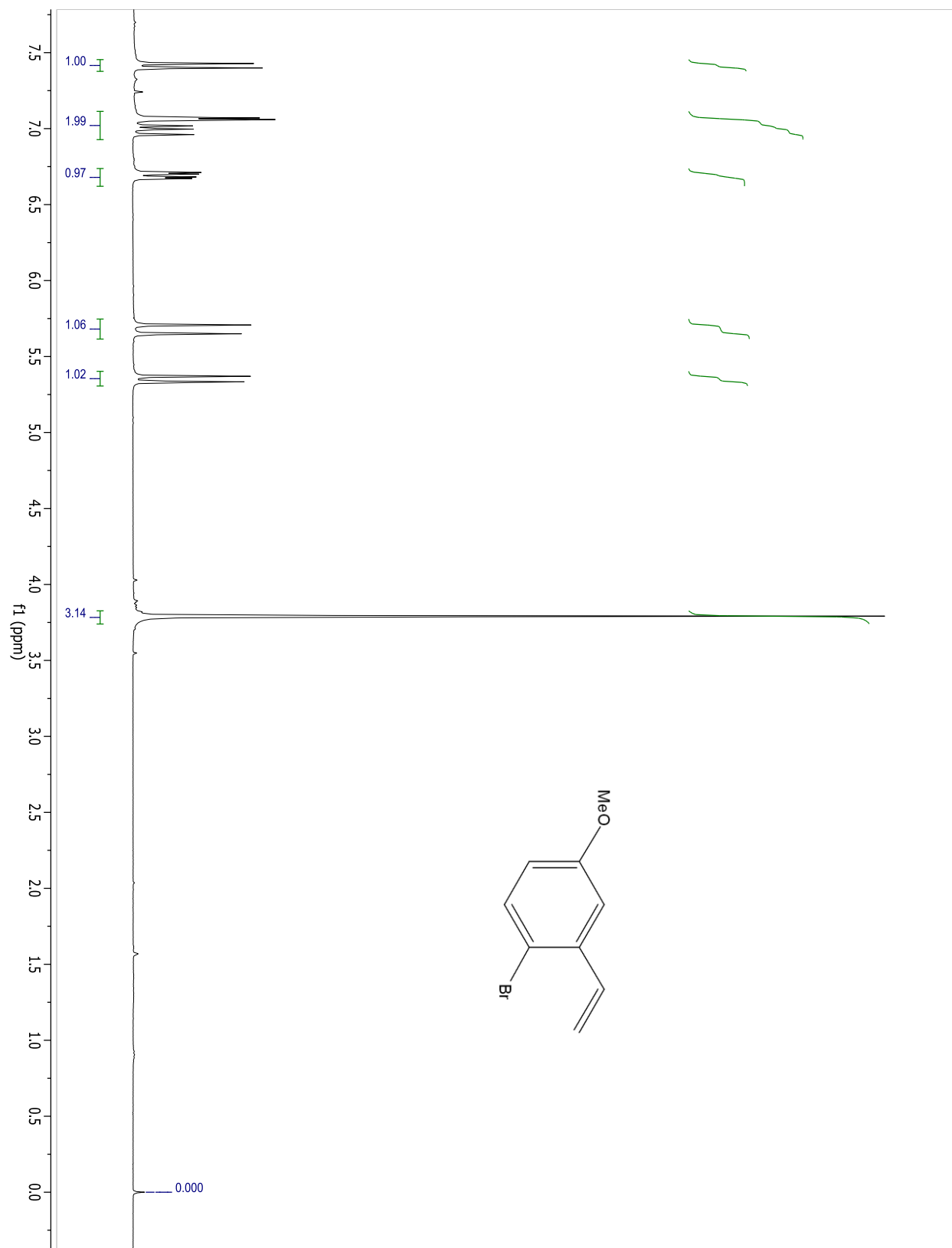
Compound 2.8.



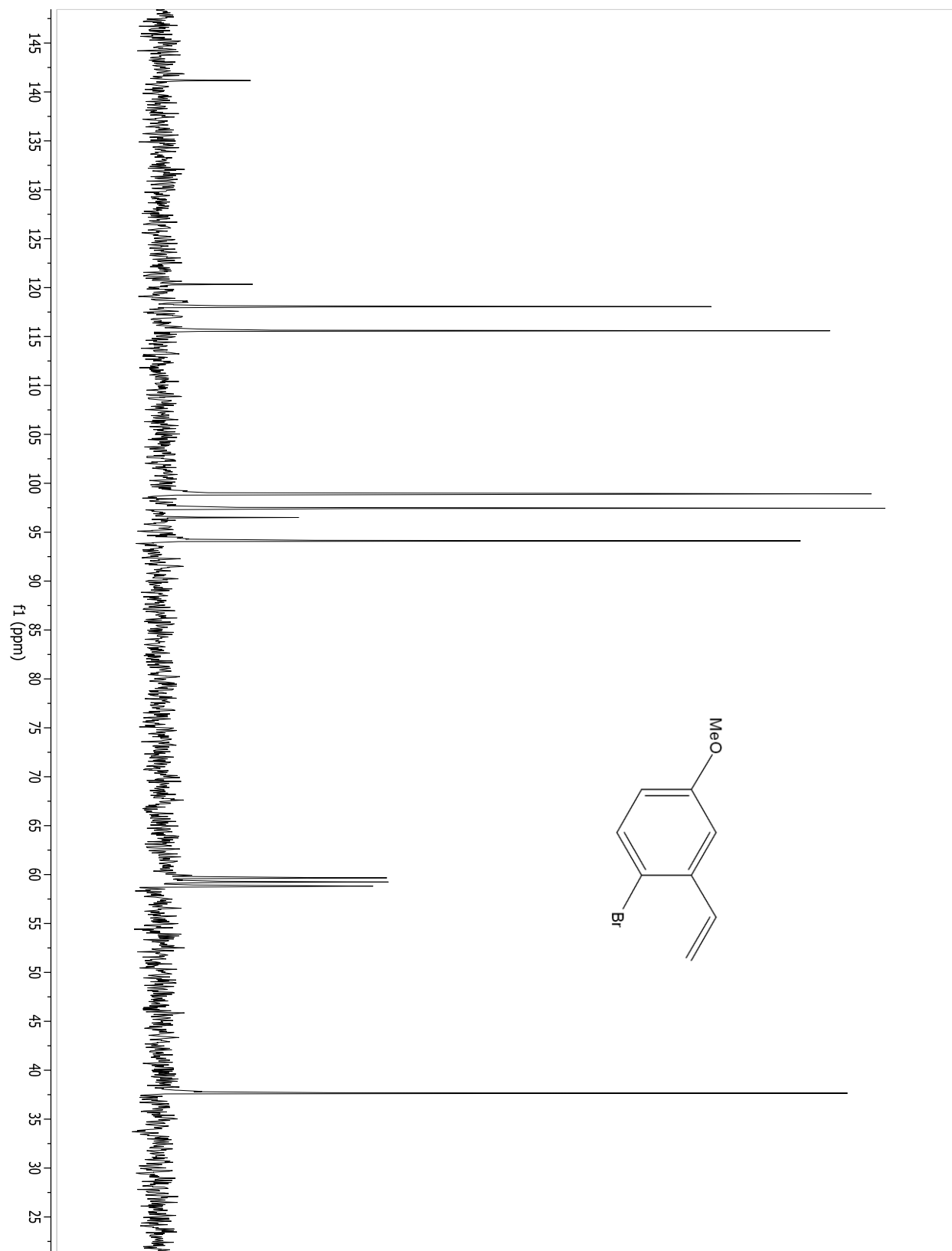
Compound 2.8.



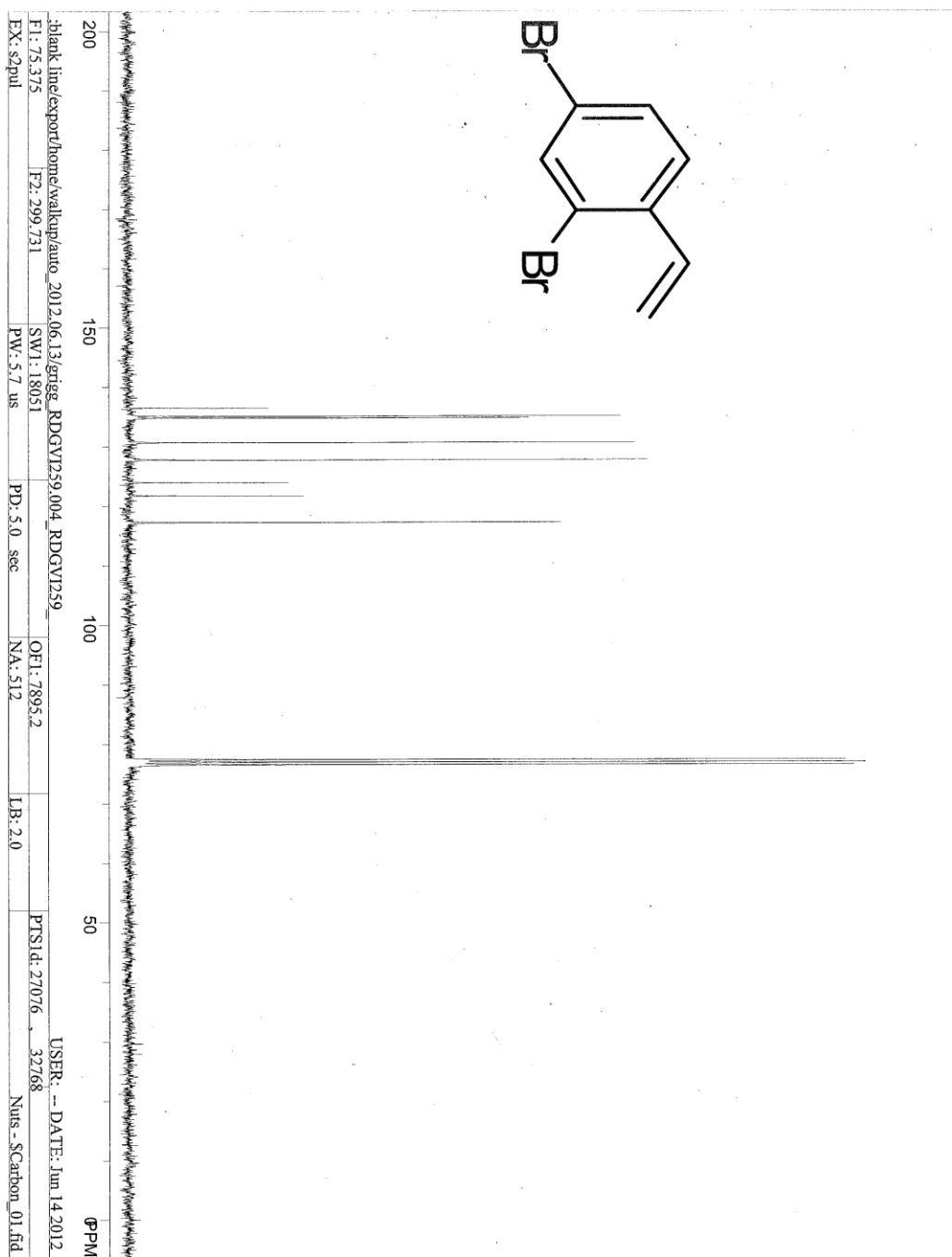
Compound 2.9.



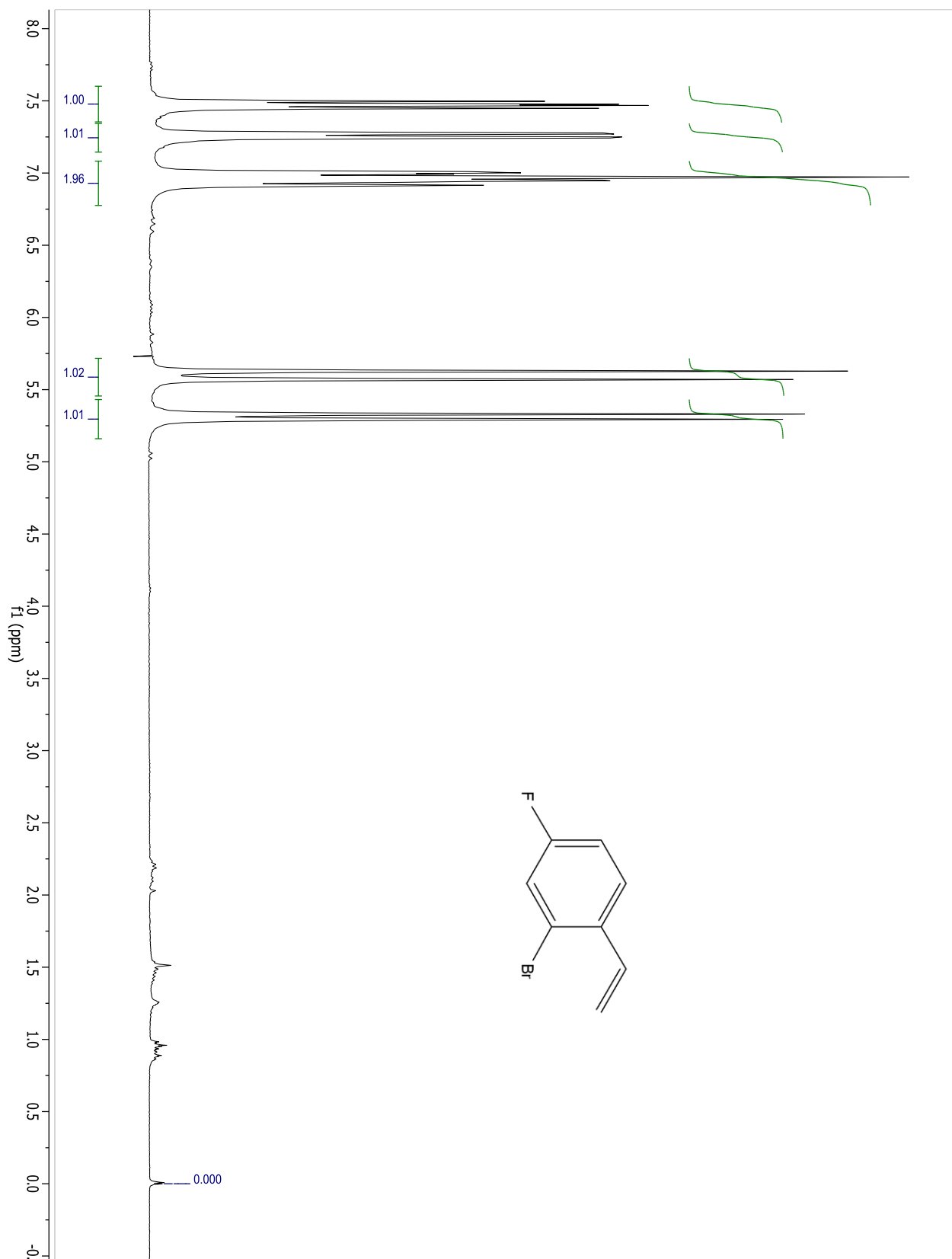
Compound 2.9.



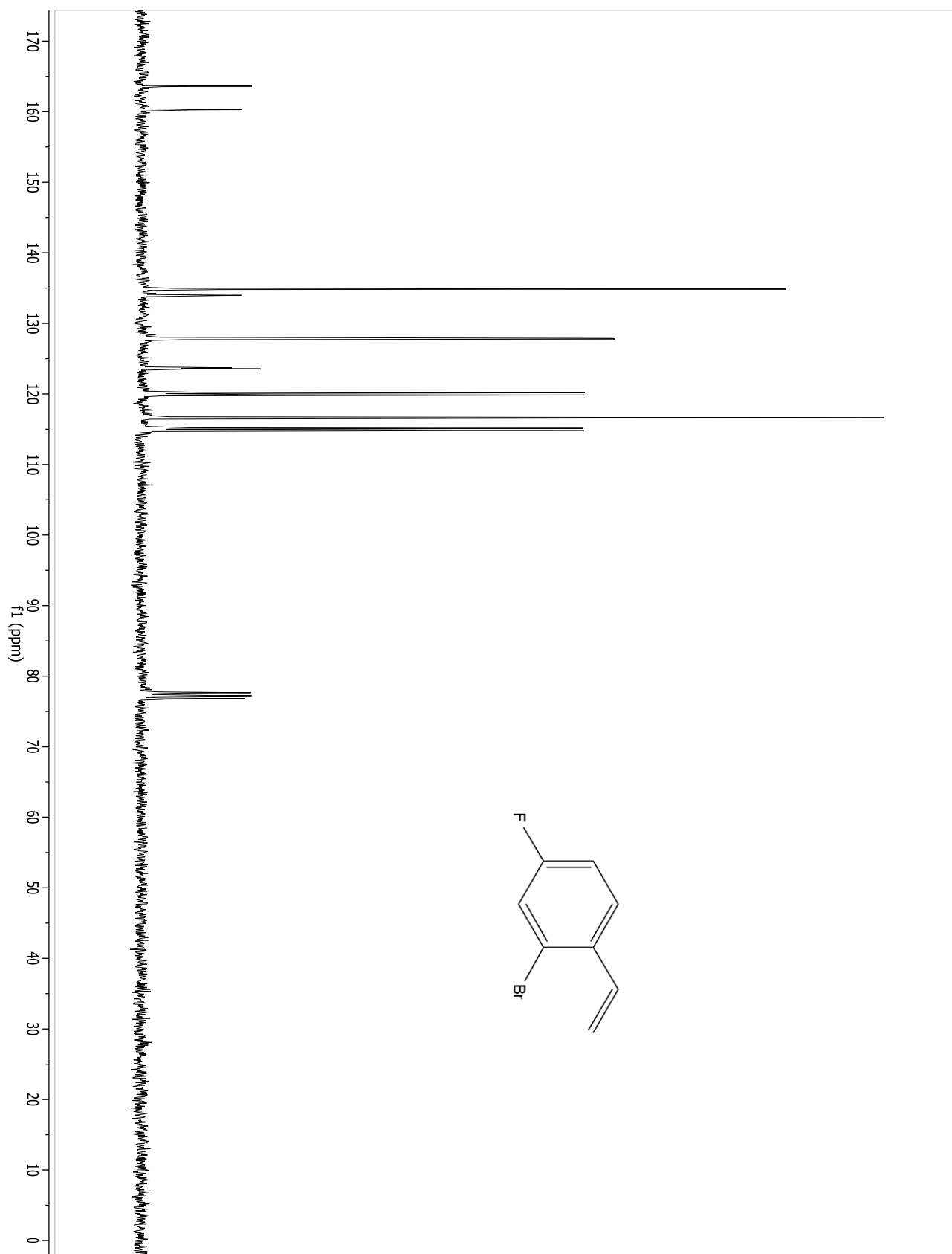
Compound 2.10.



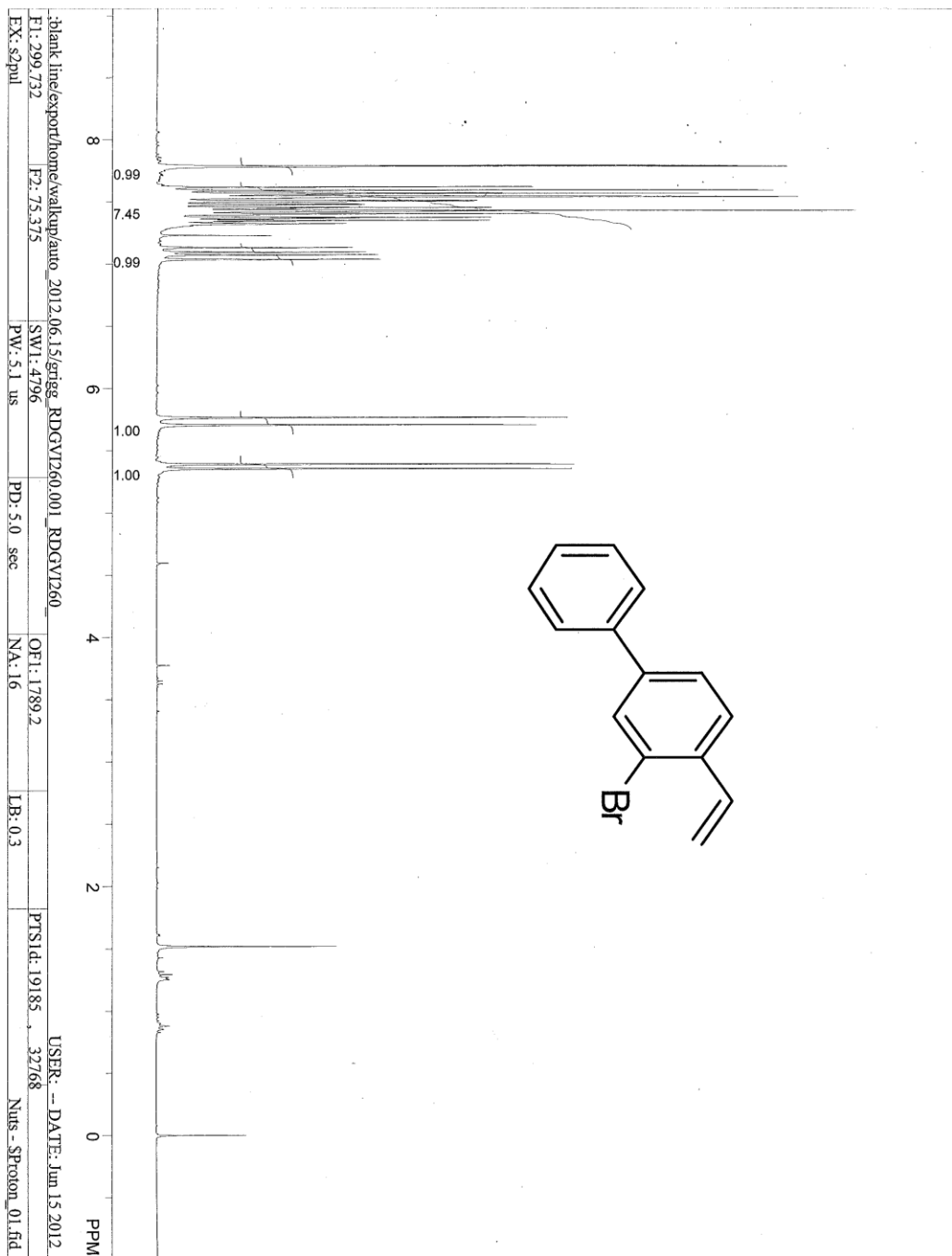
Compound 2.11.



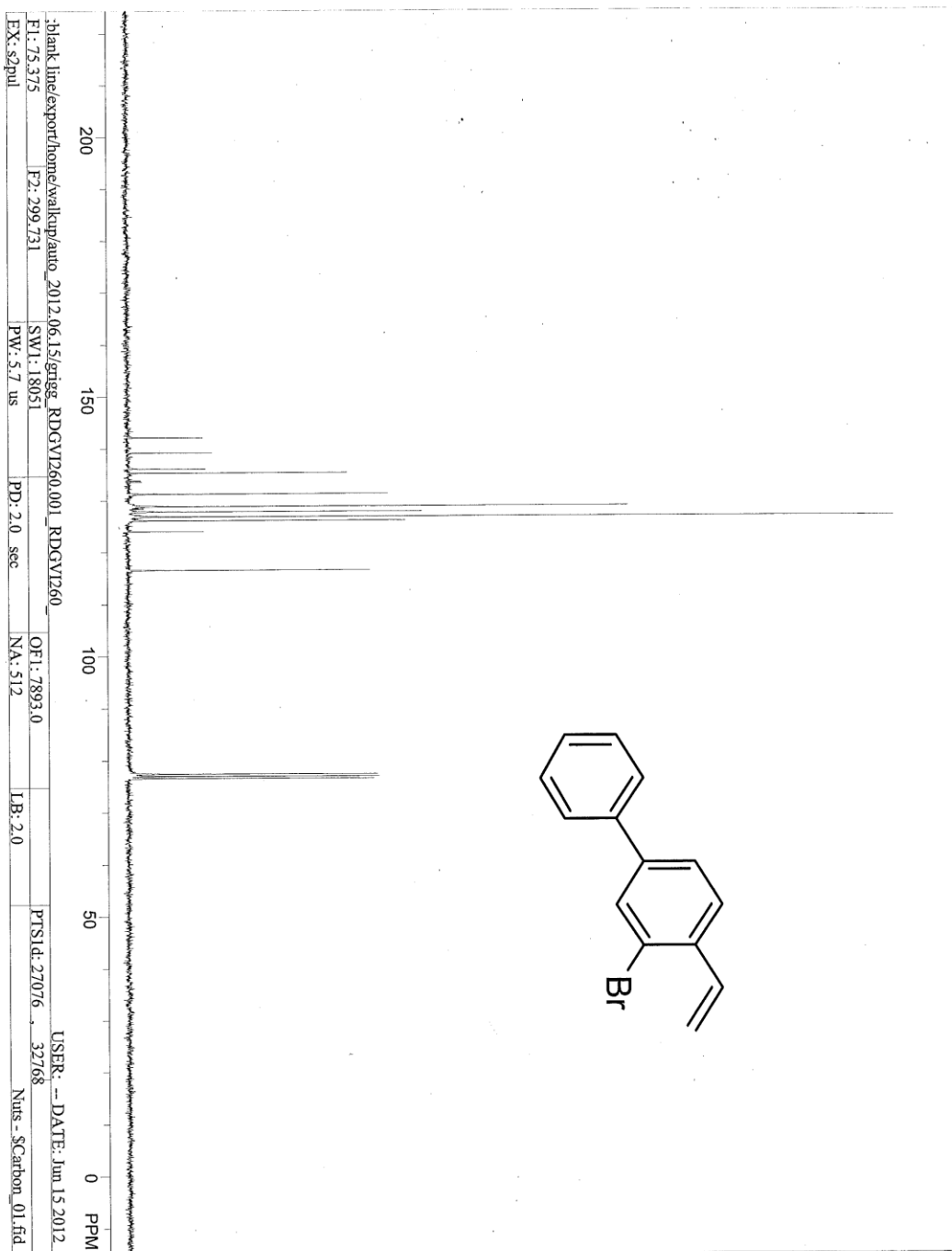
Compound 2.11.



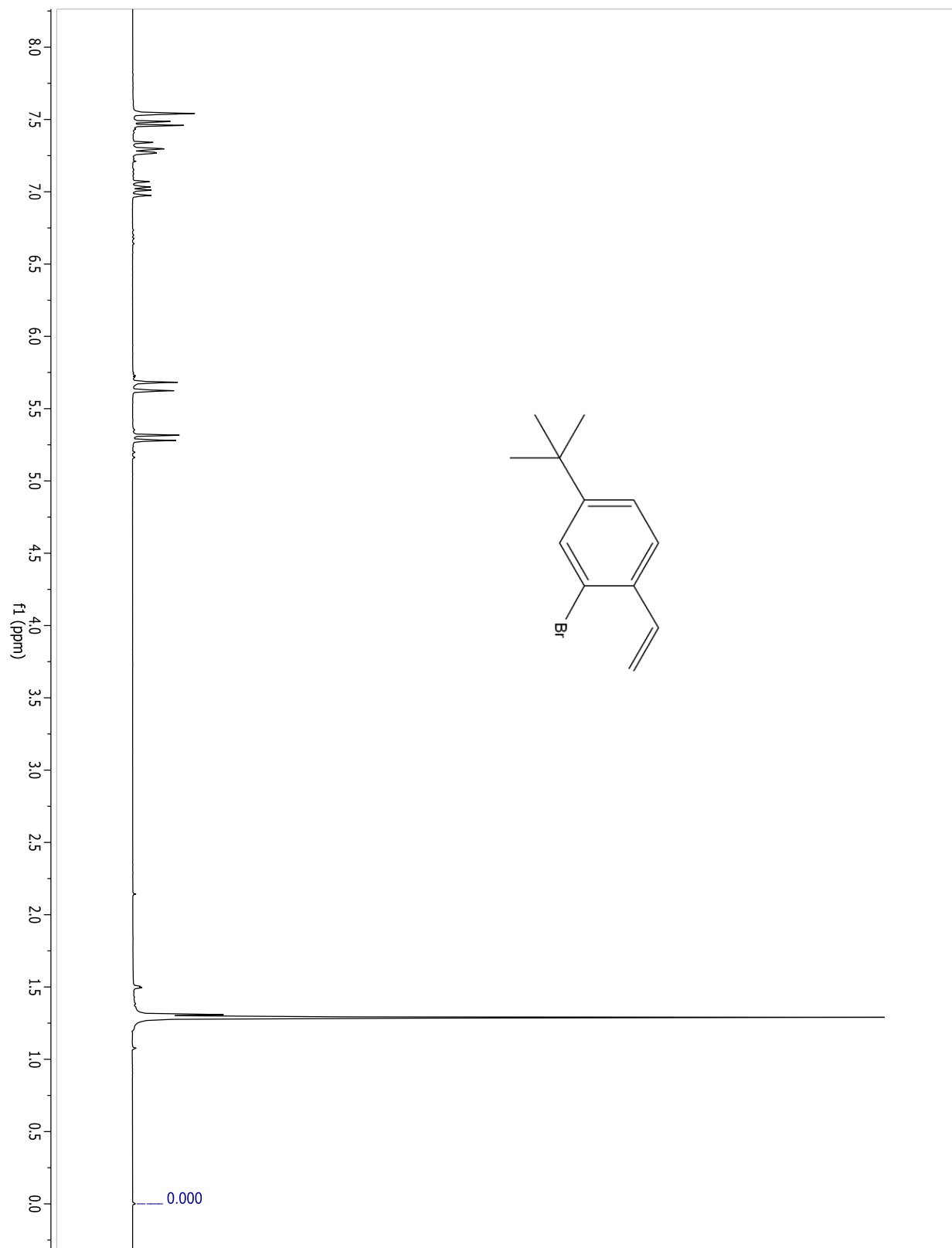
Compound 2.13.



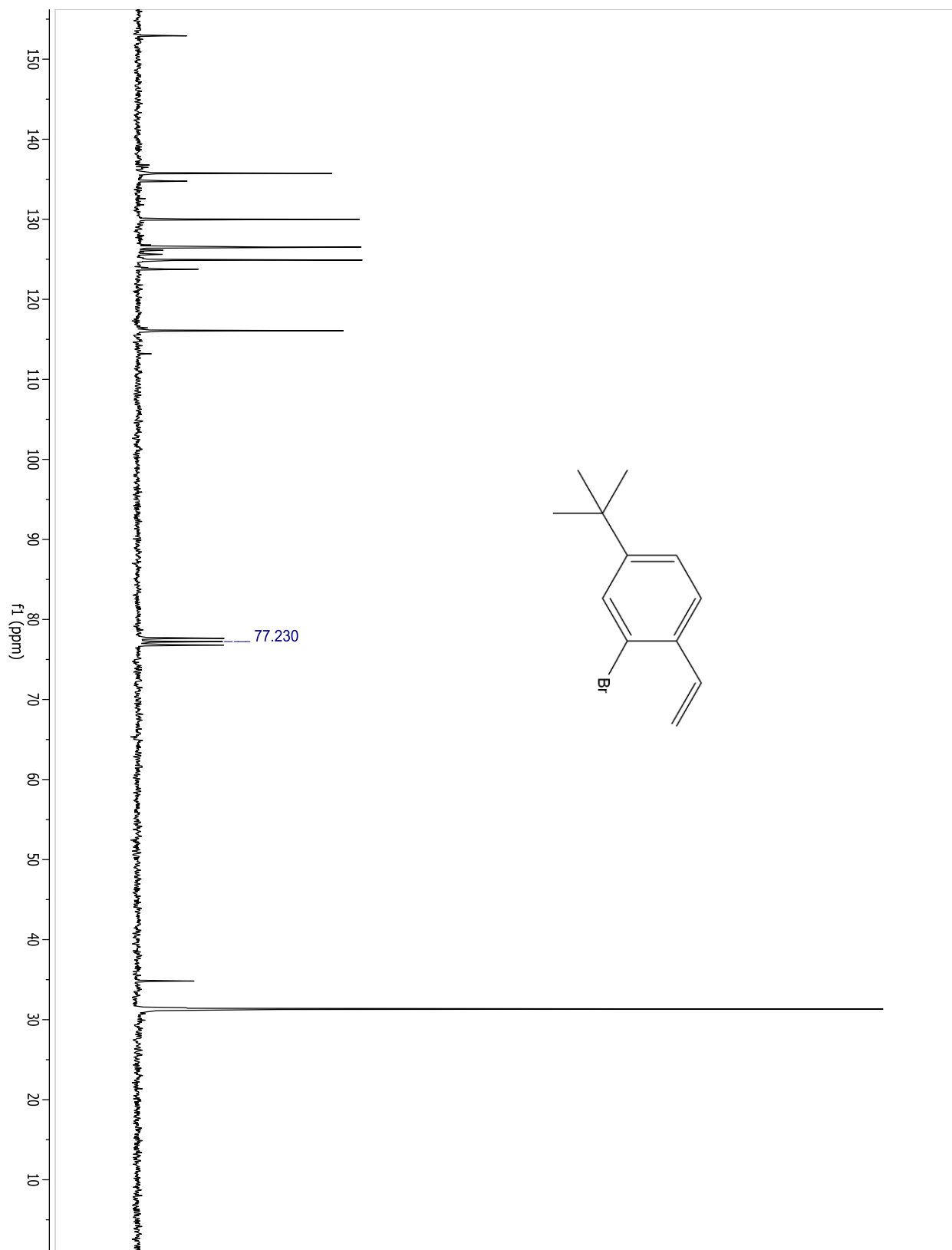
Compound 2.13.



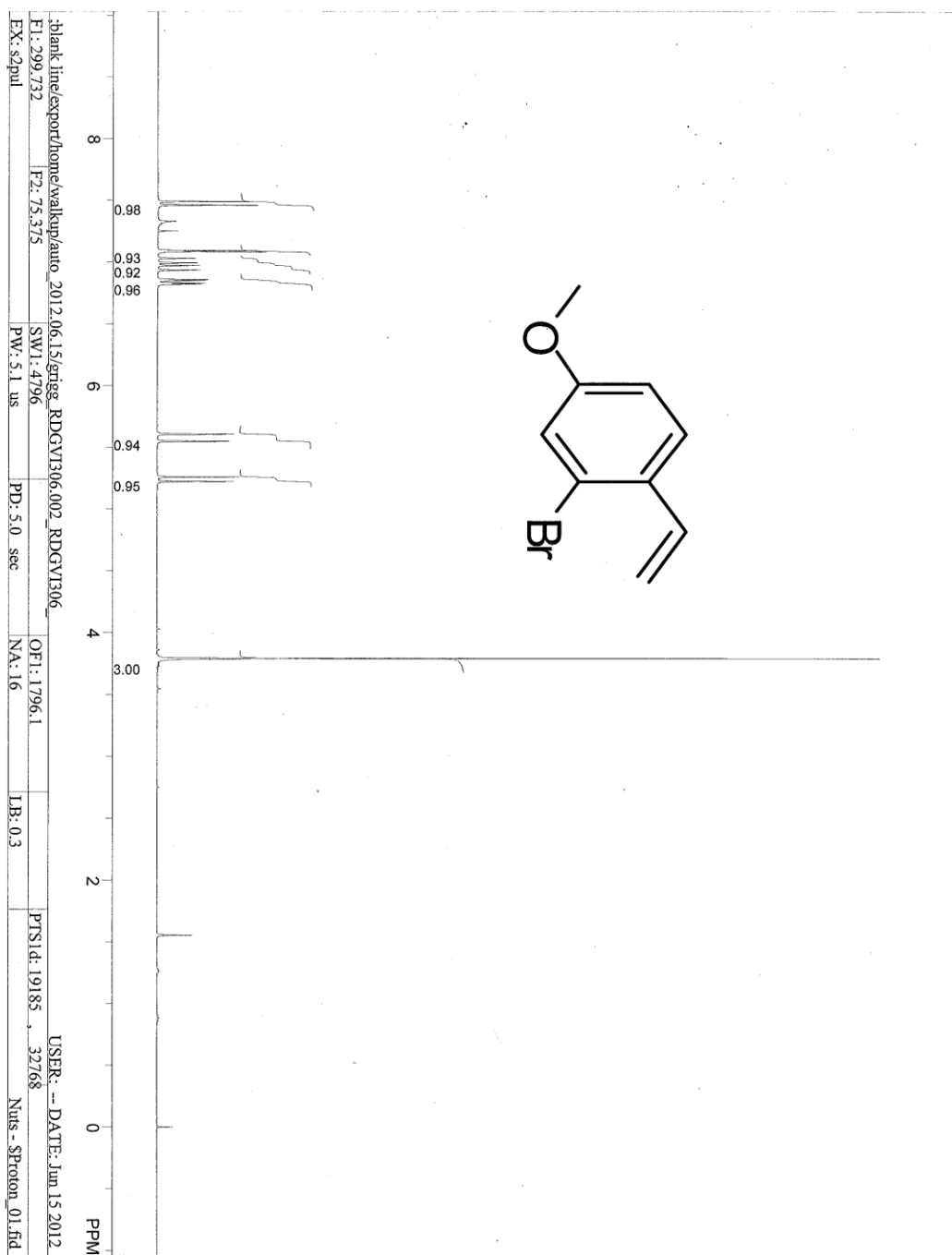
Compound 2.14.



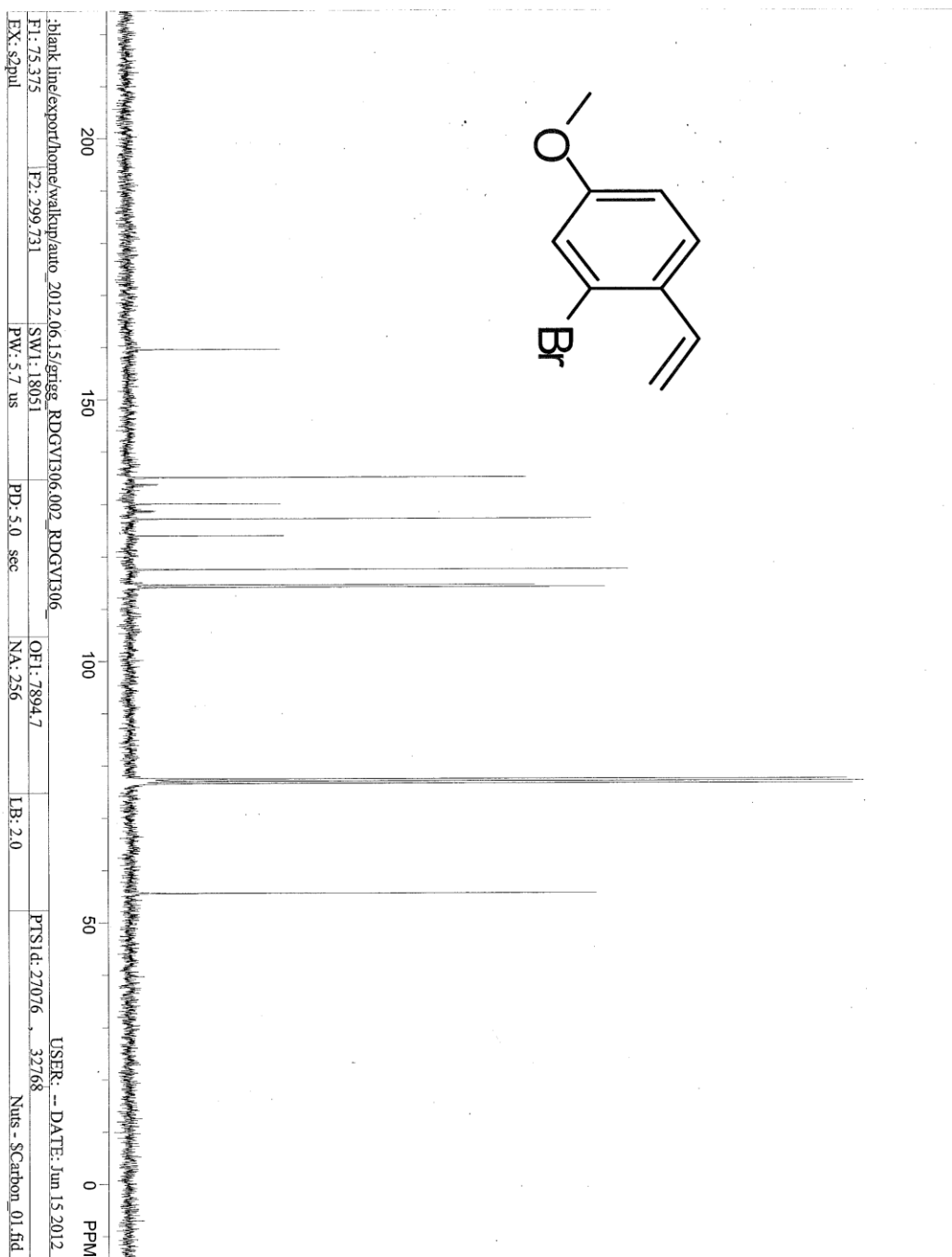
Compound 2.14.



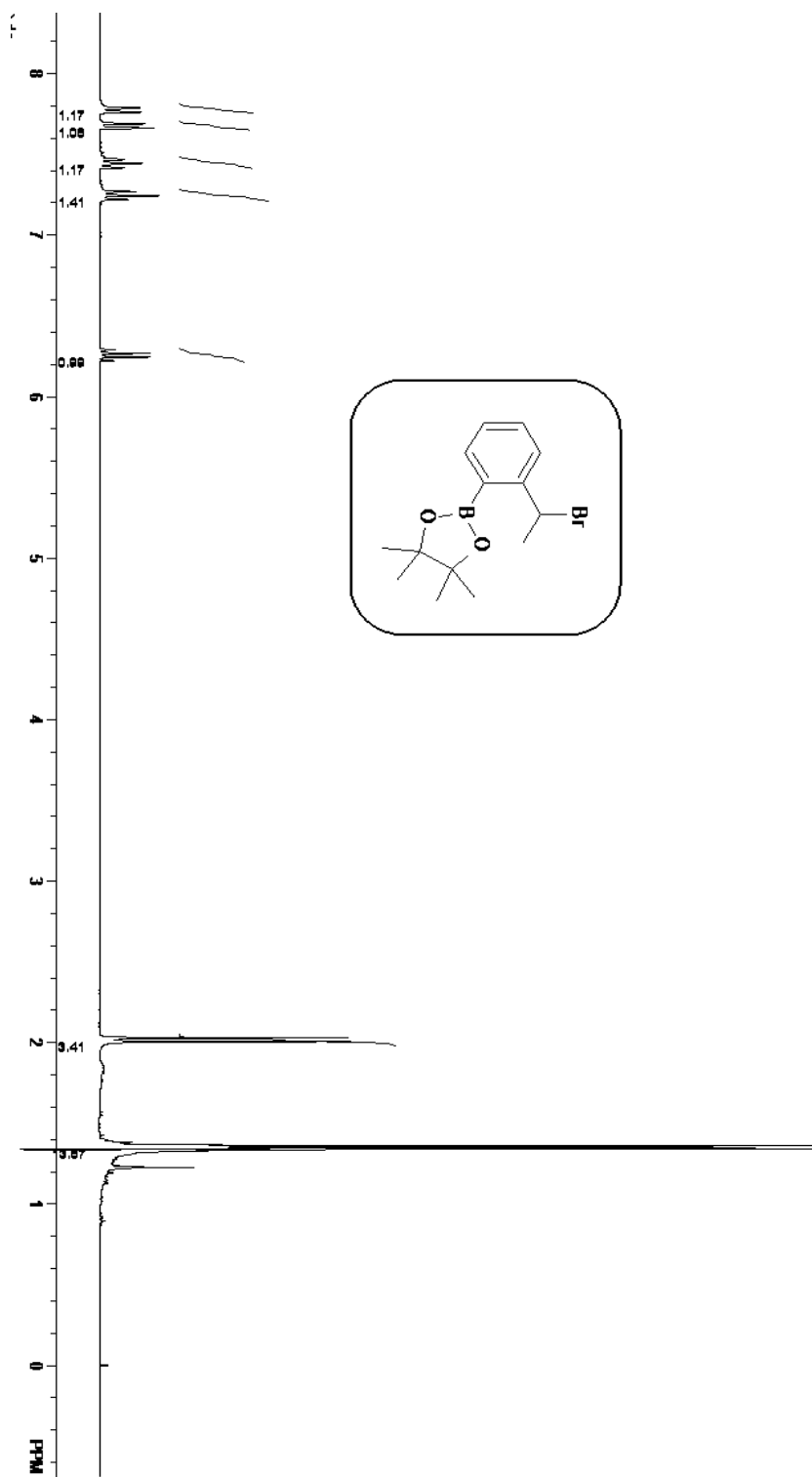
Compound 2.15.



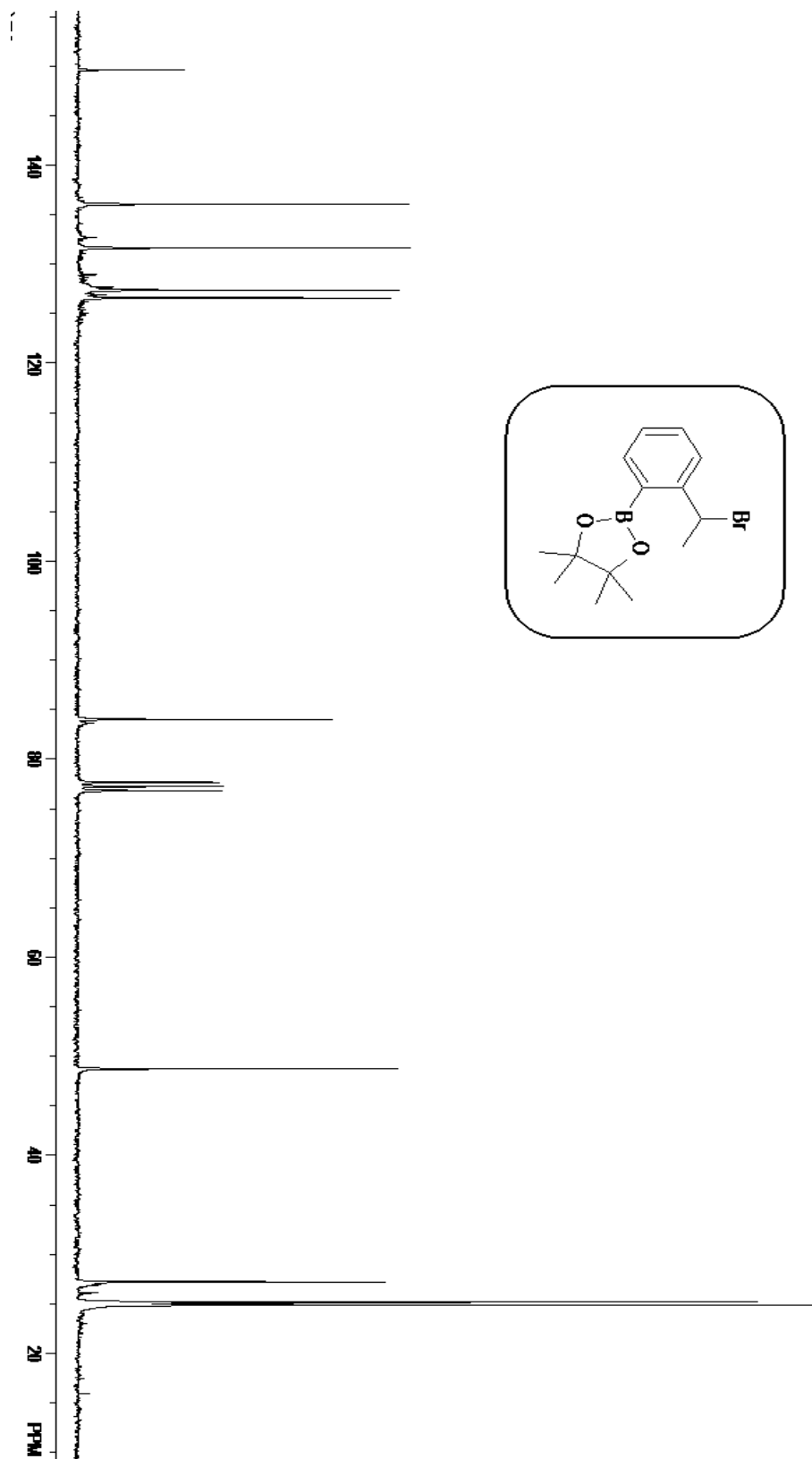
Compound 2.15.



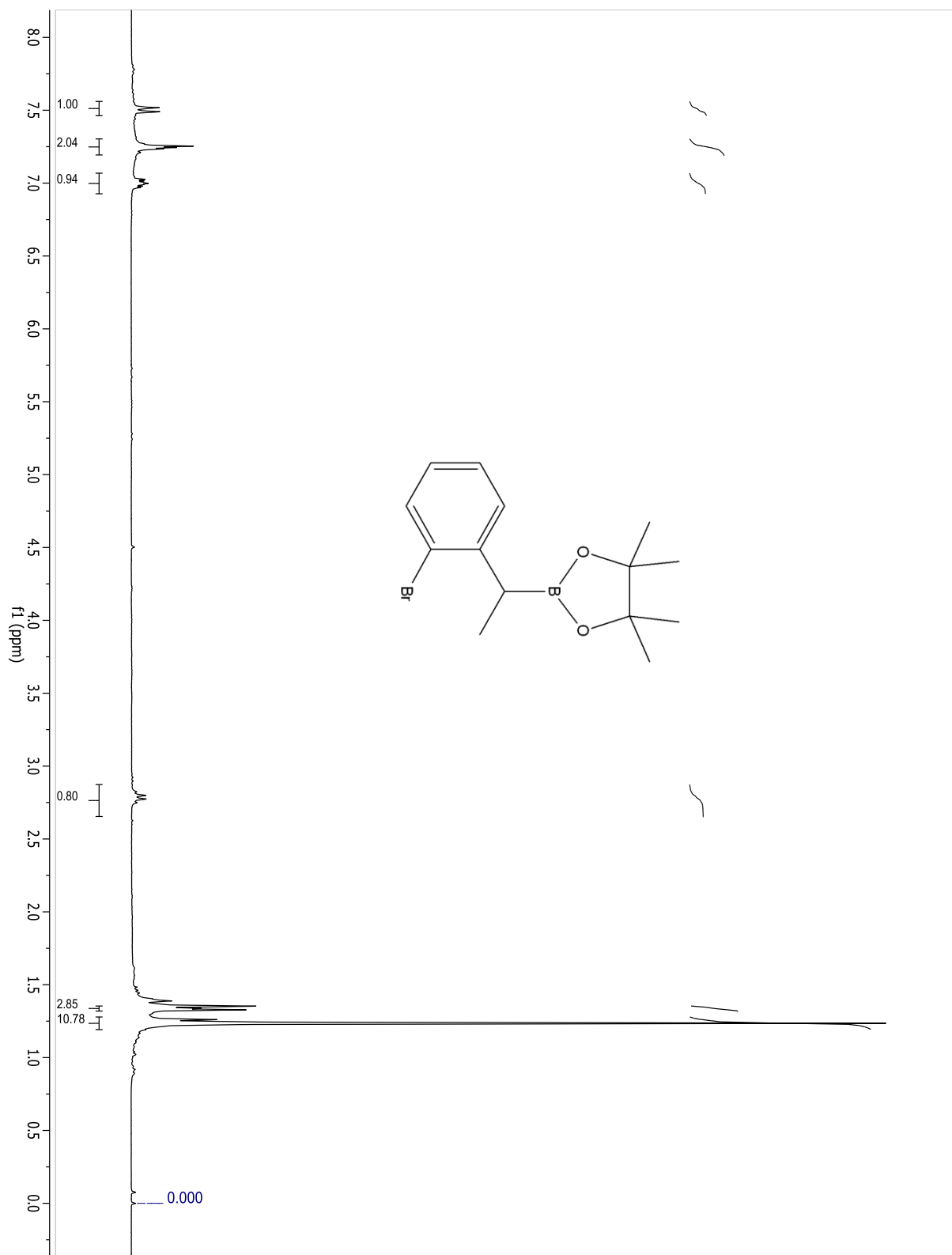
Compound 2.2.



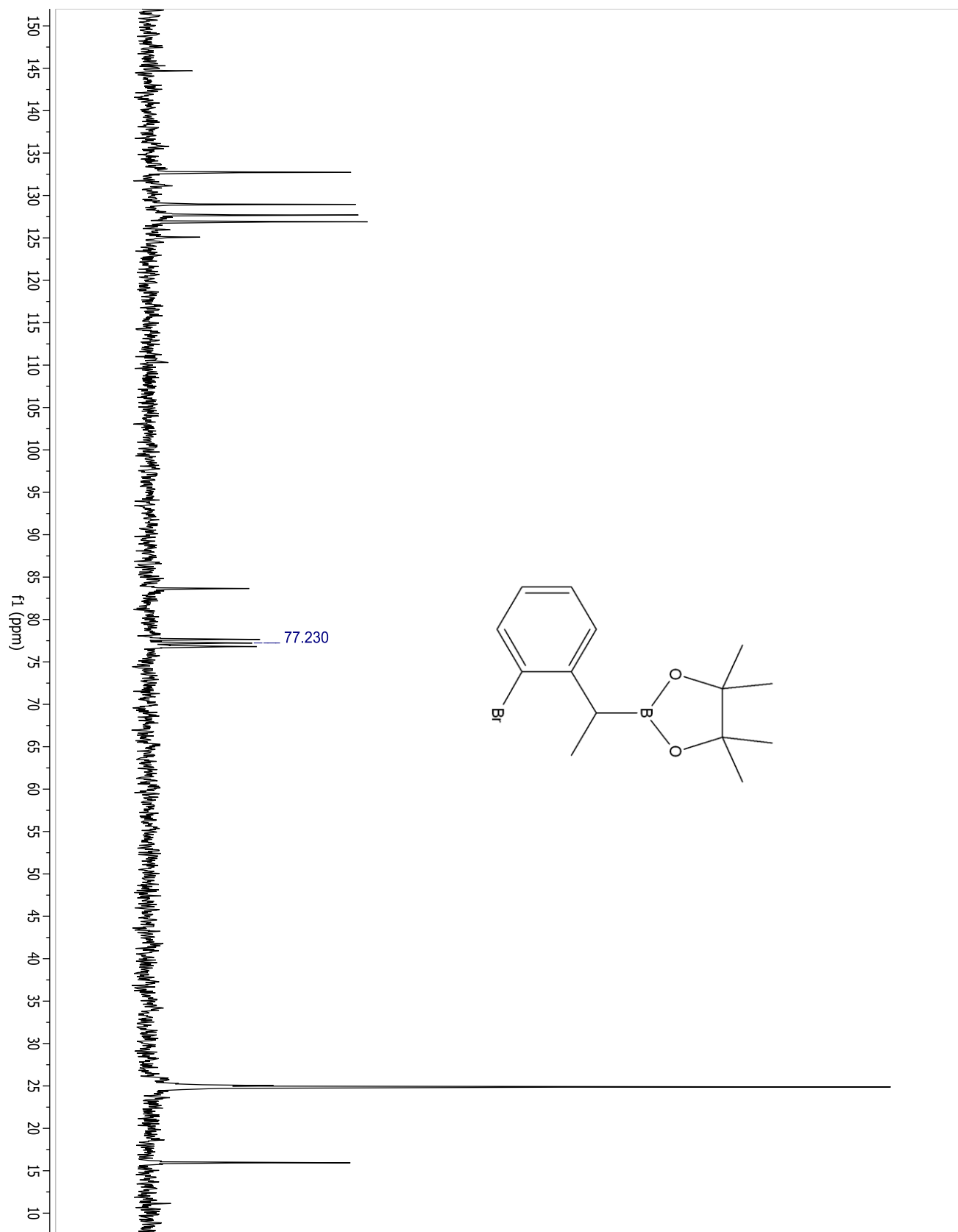
Compound 2.2.



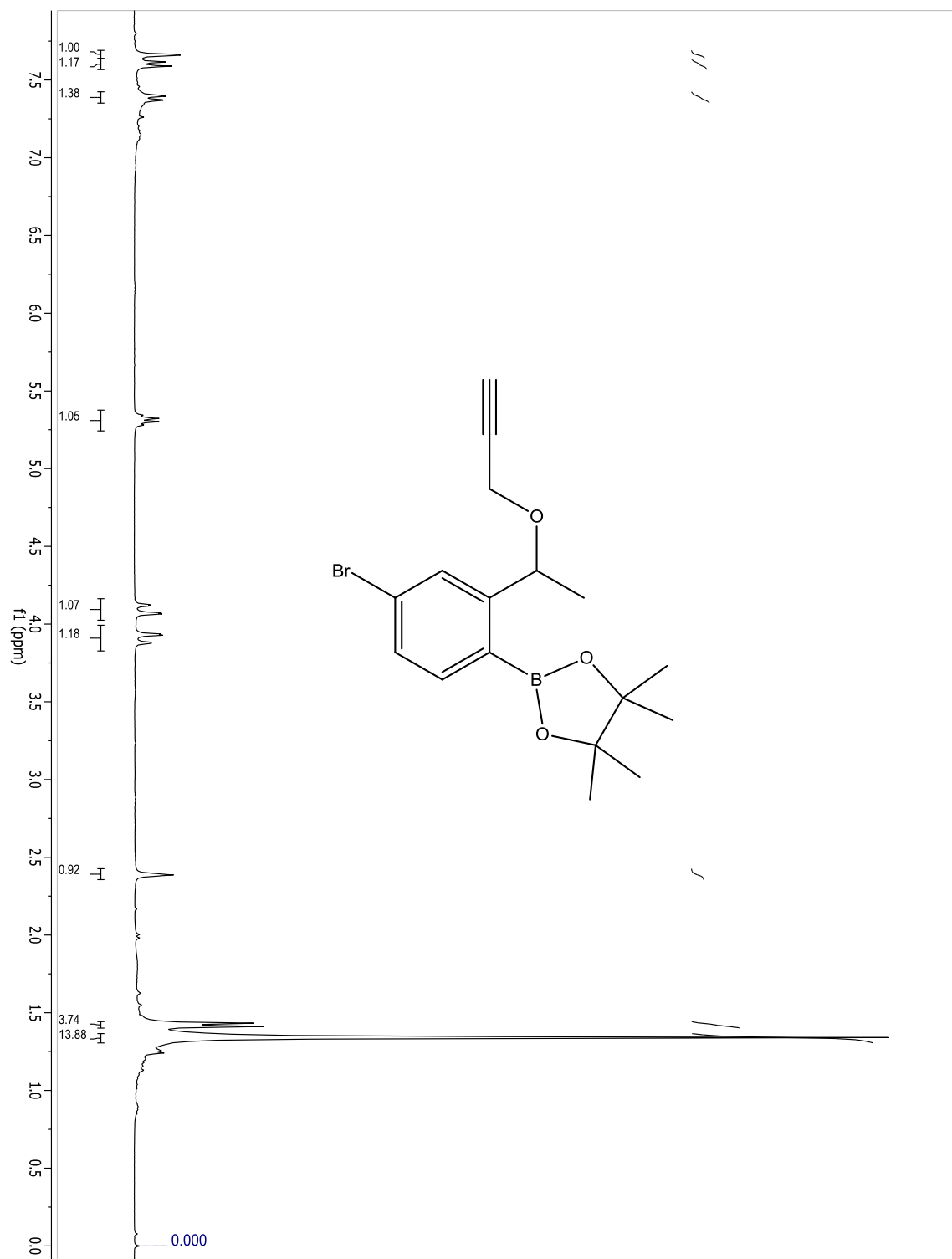
Compound 2.3.



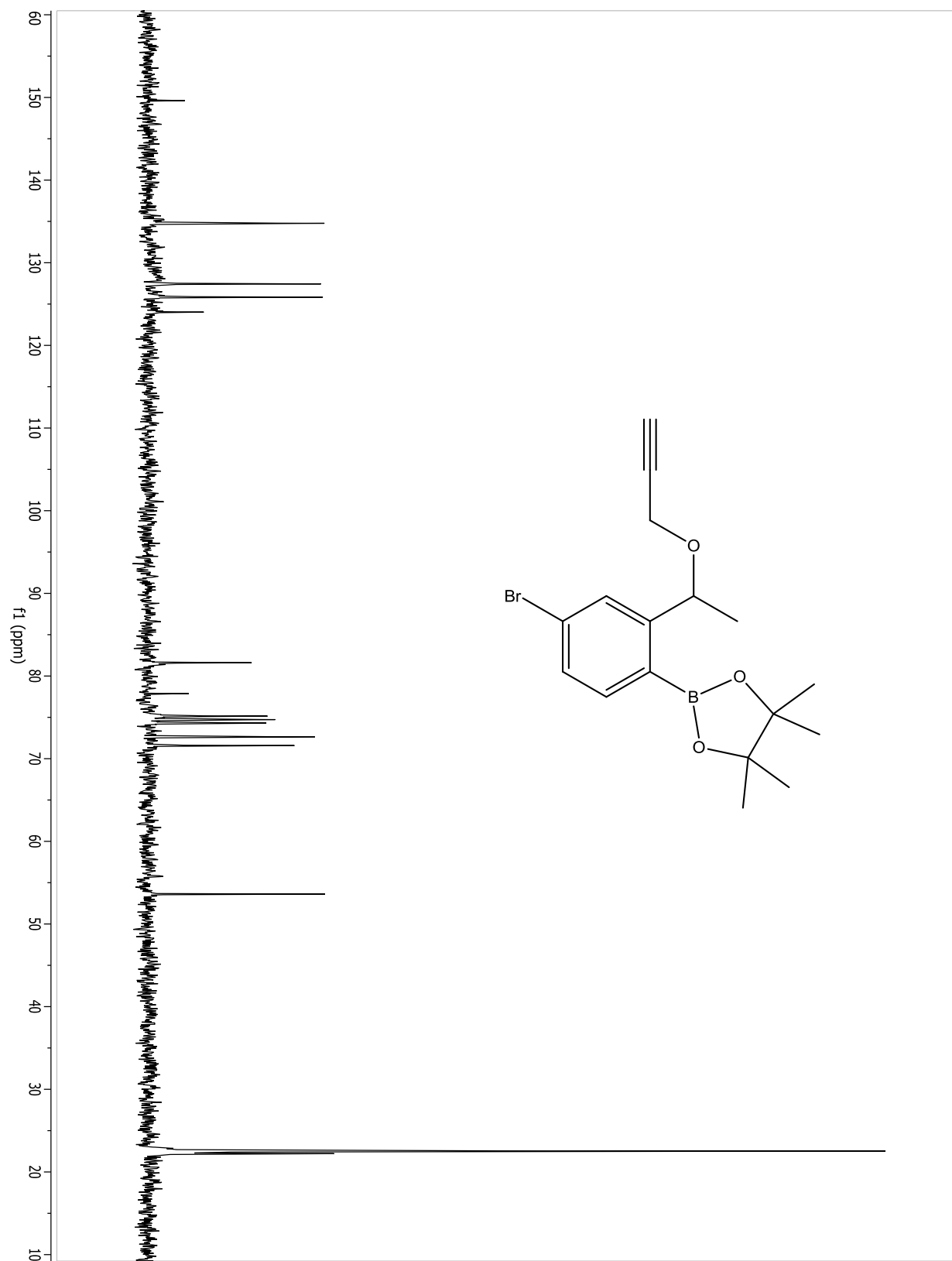
Compound 2.3.



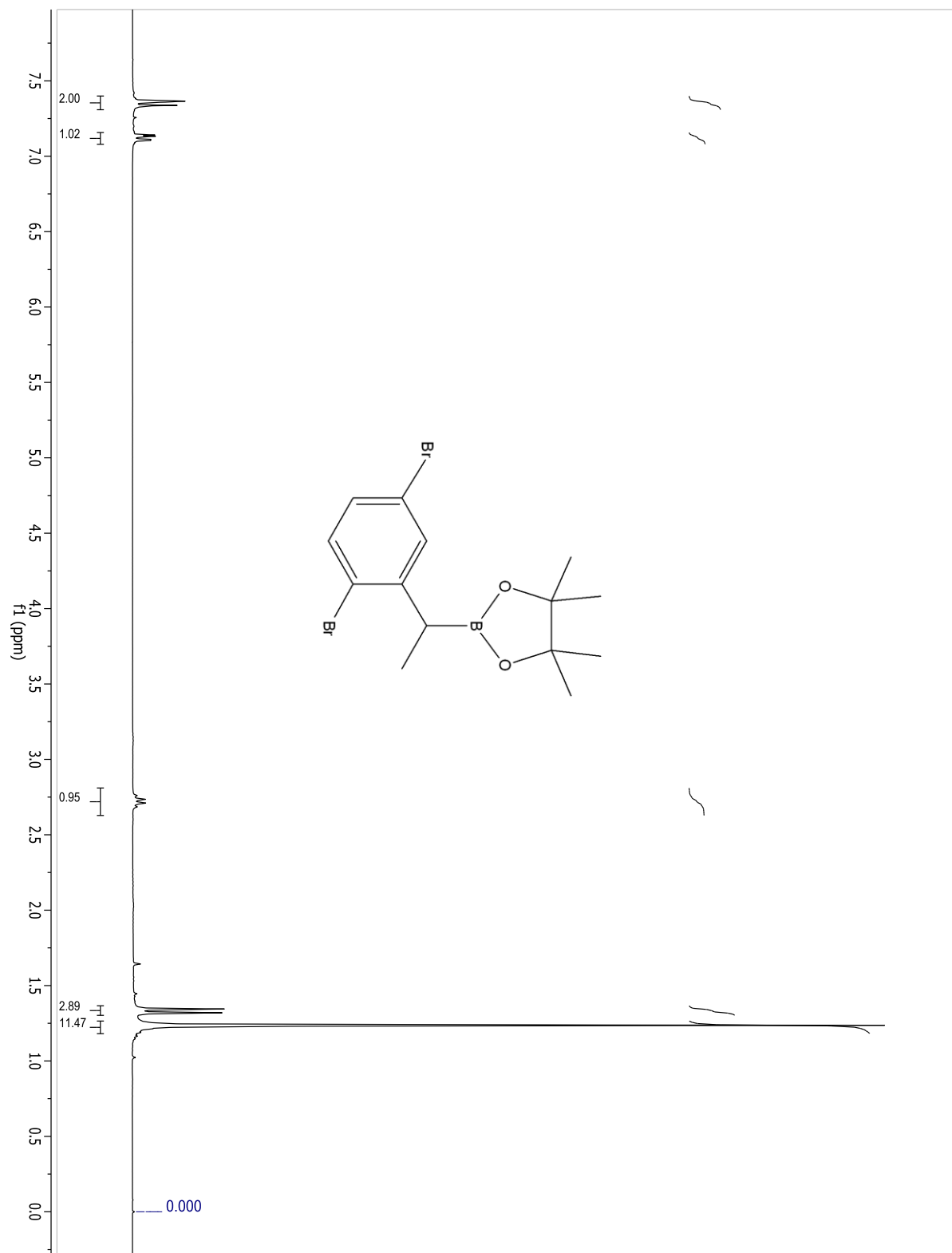
Compound 2.17.



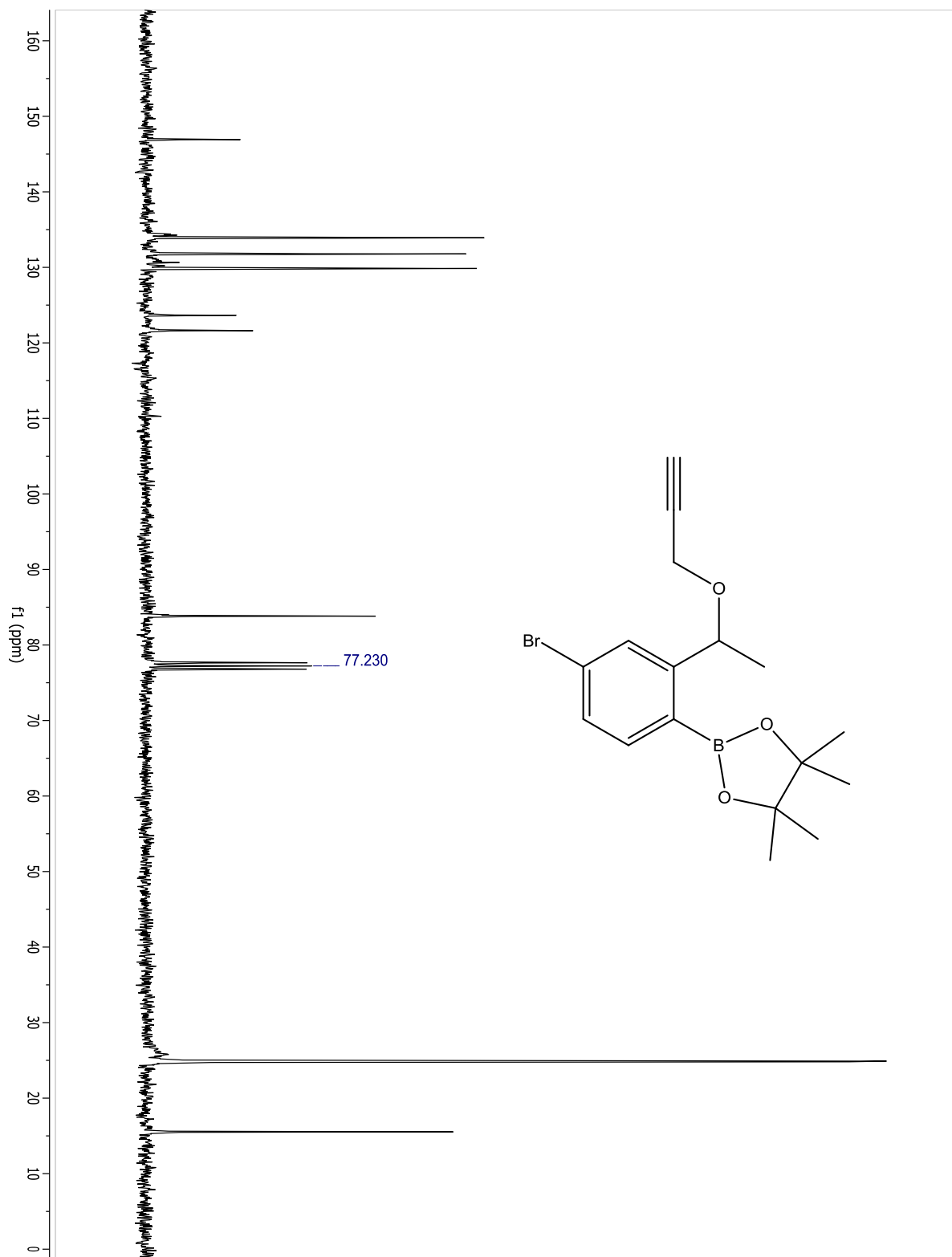
Compound 2.17.



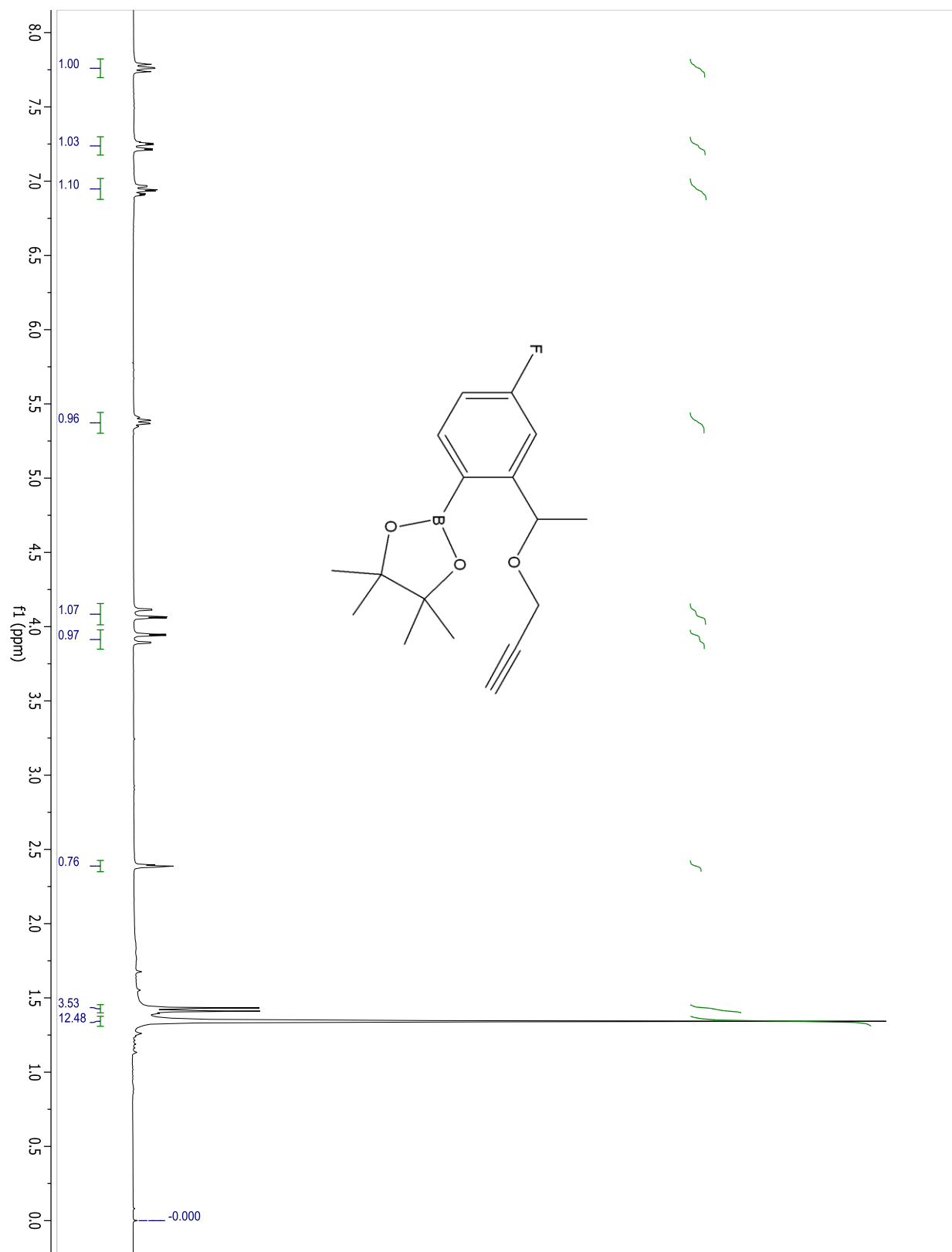
Compound 2.29.



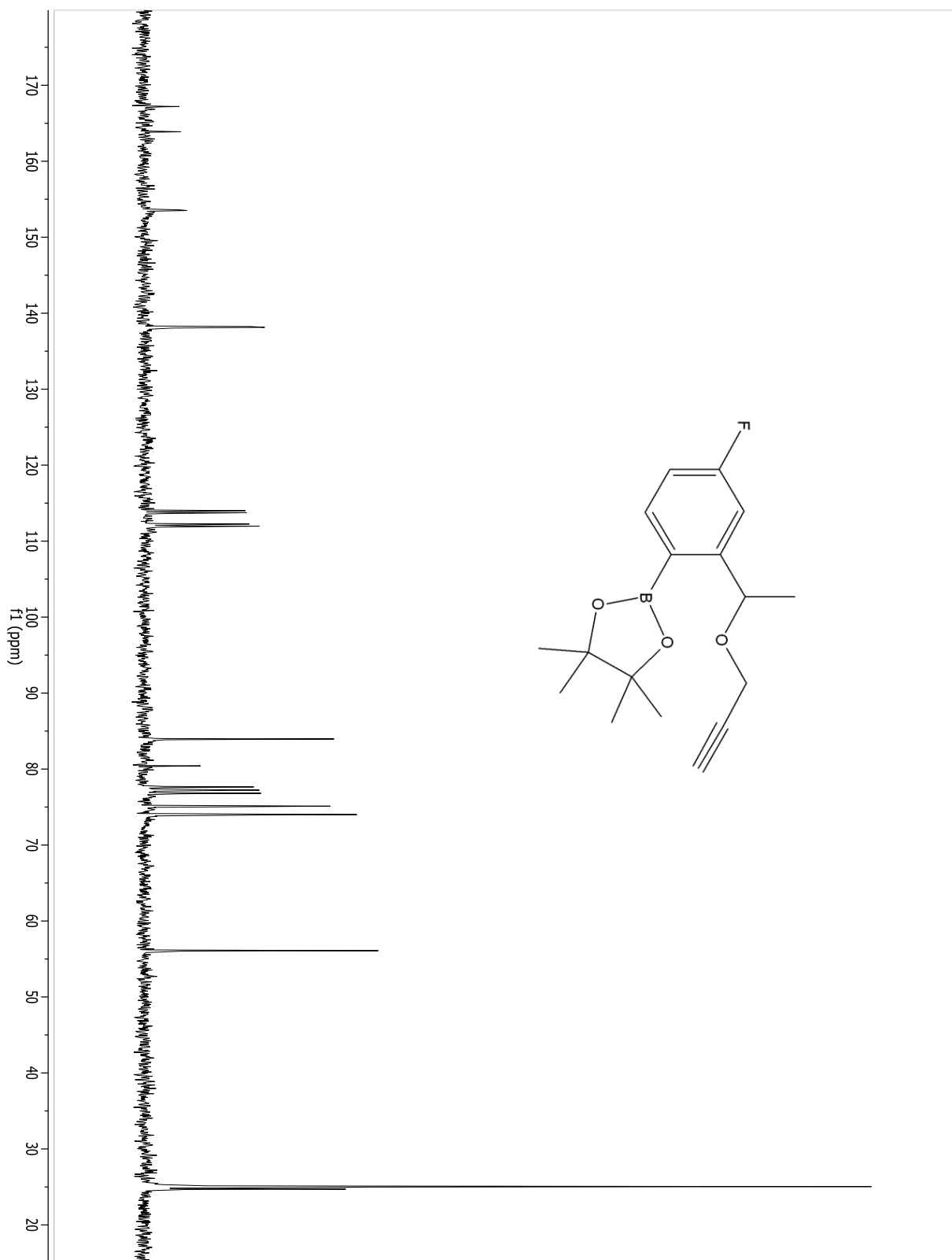
Compound 2.29.



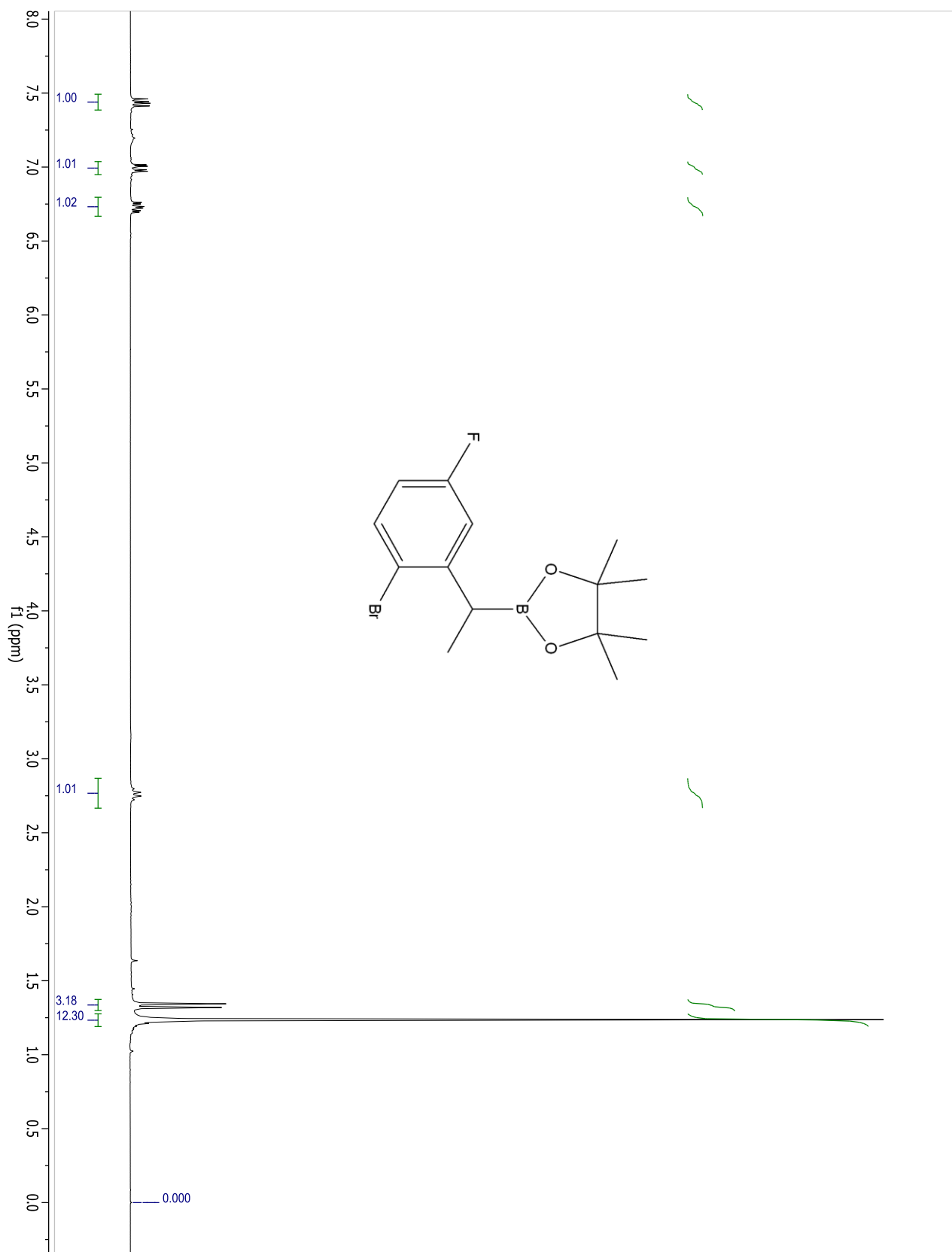
Compound 2.18.



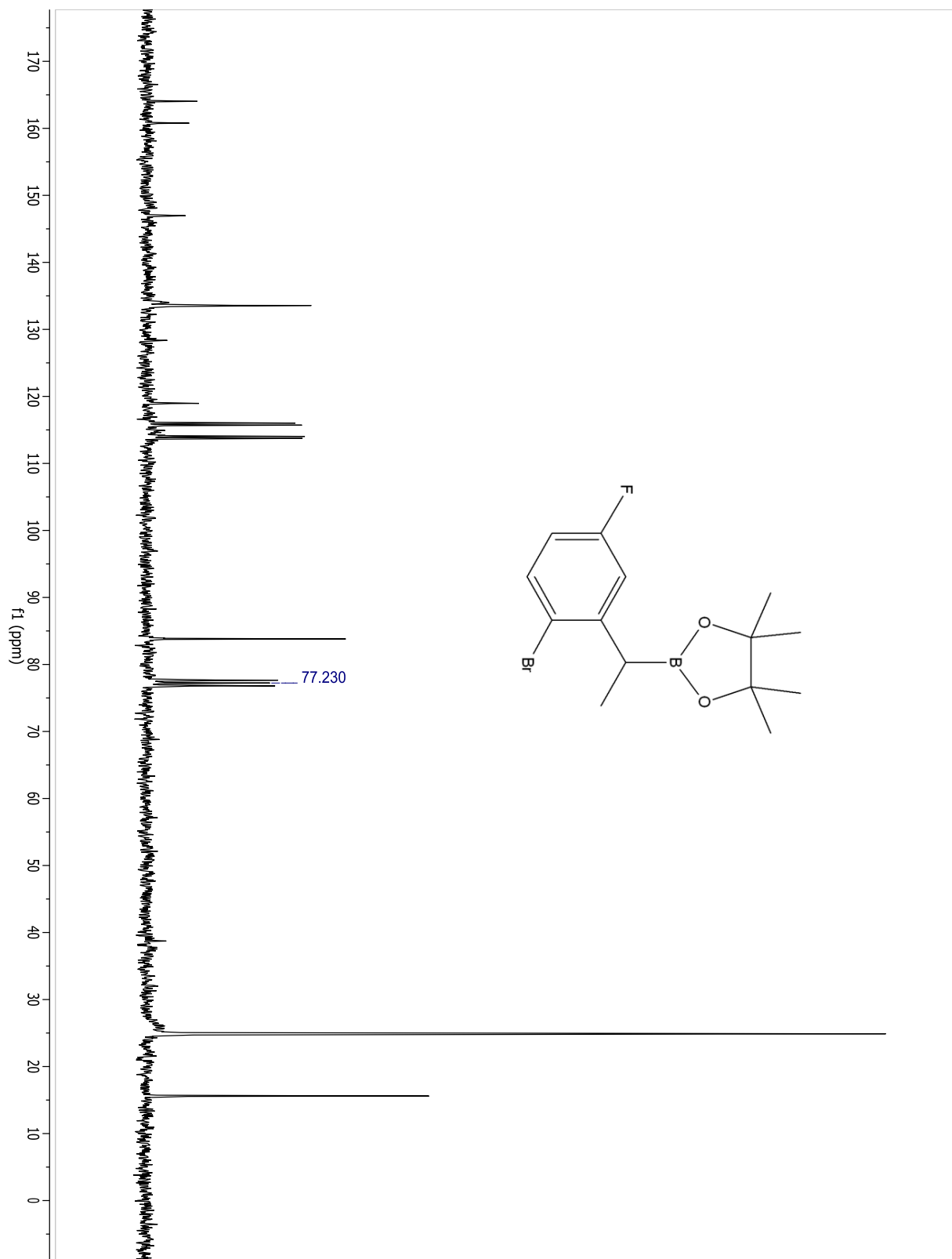
Compound 2.18.



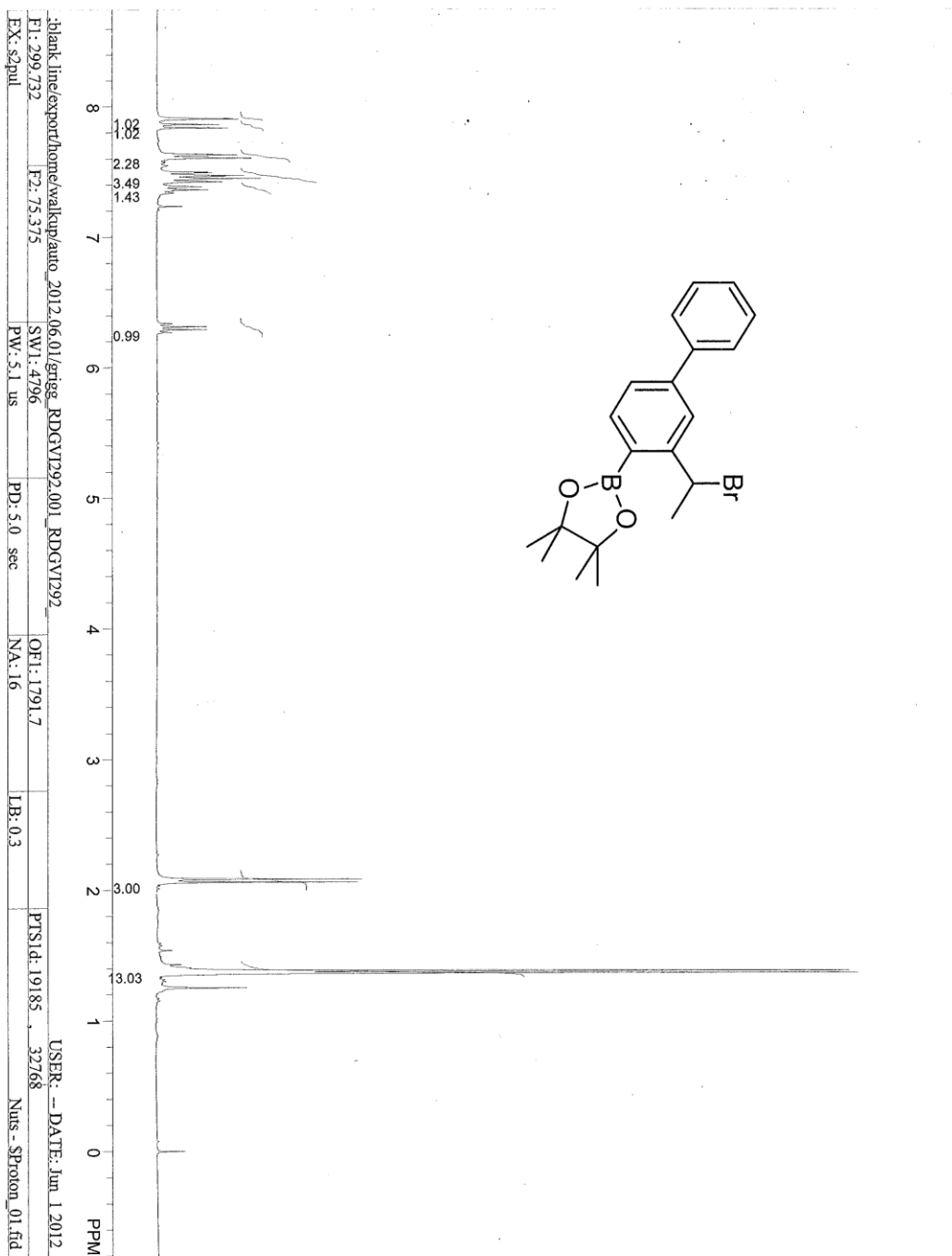
Compound 2.30.



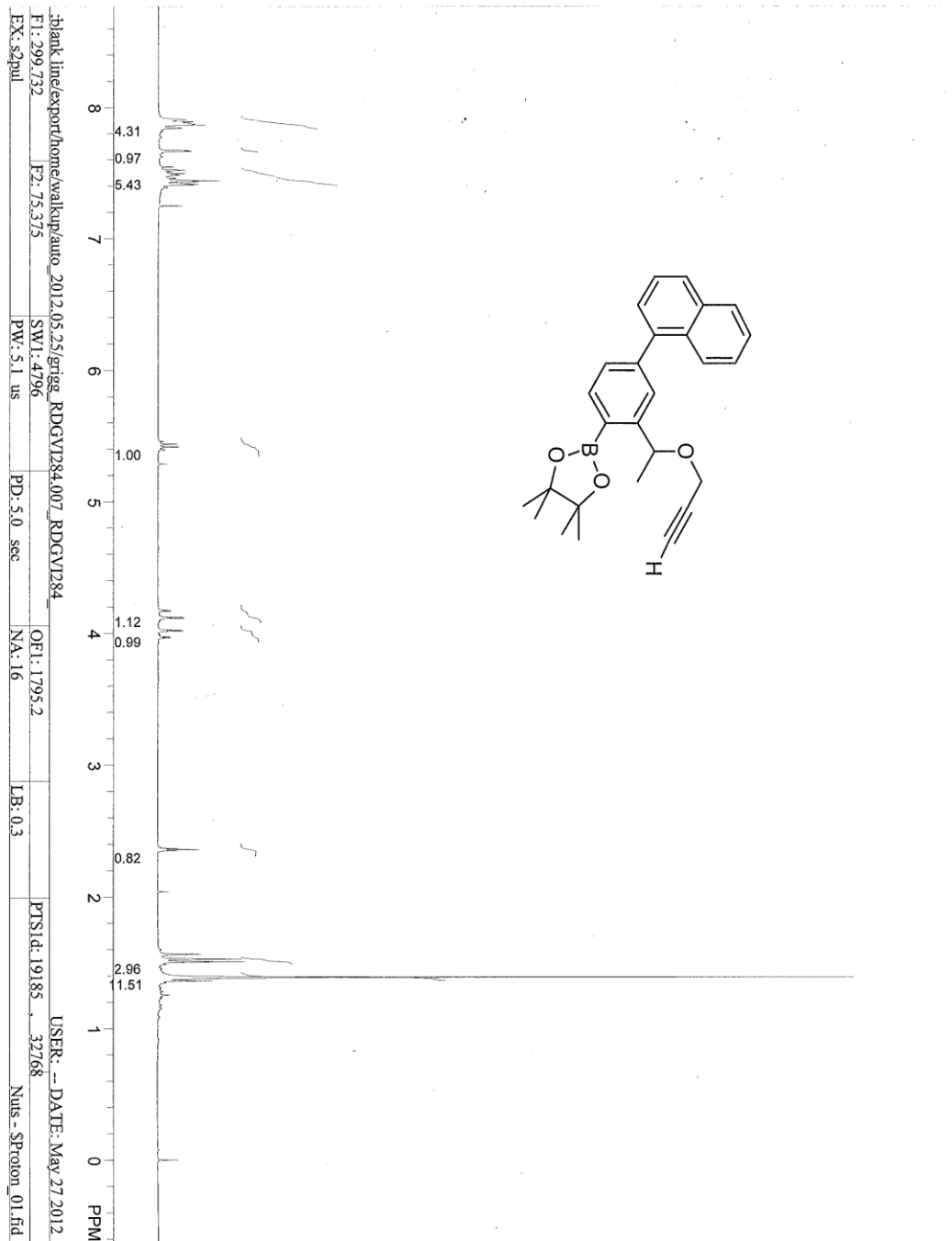
Compound 2.30.



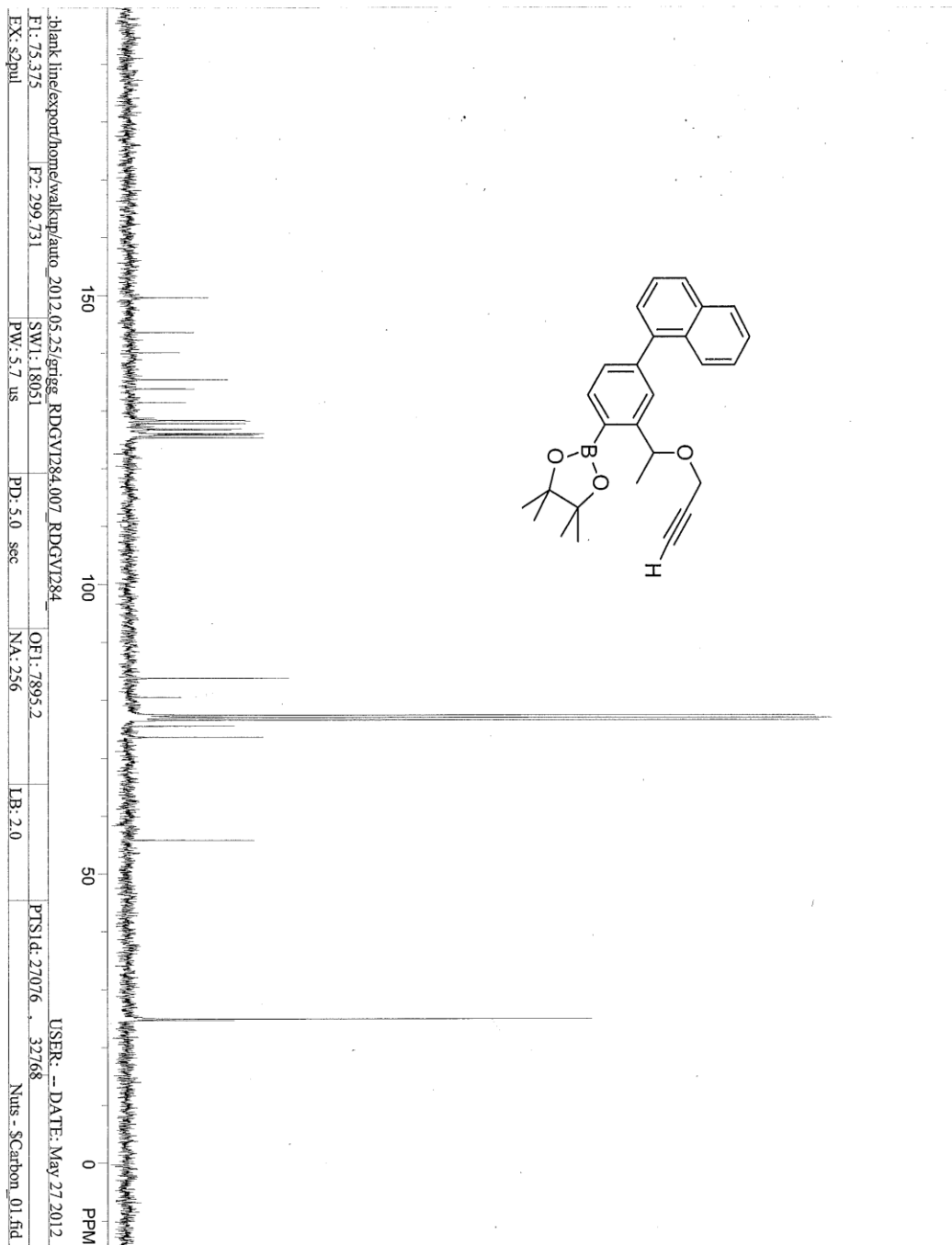
Compound 2.19.



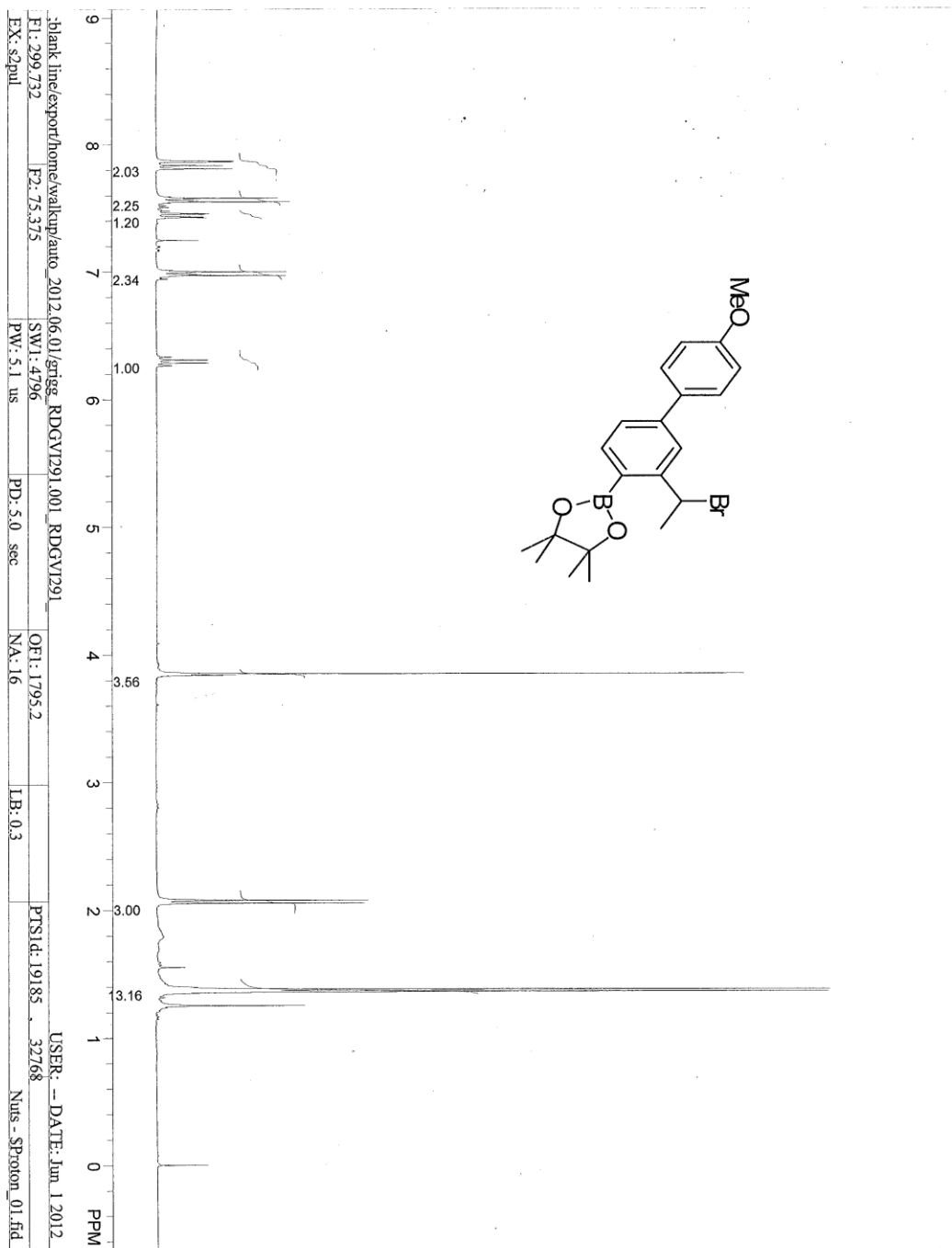
Compound 2.20.



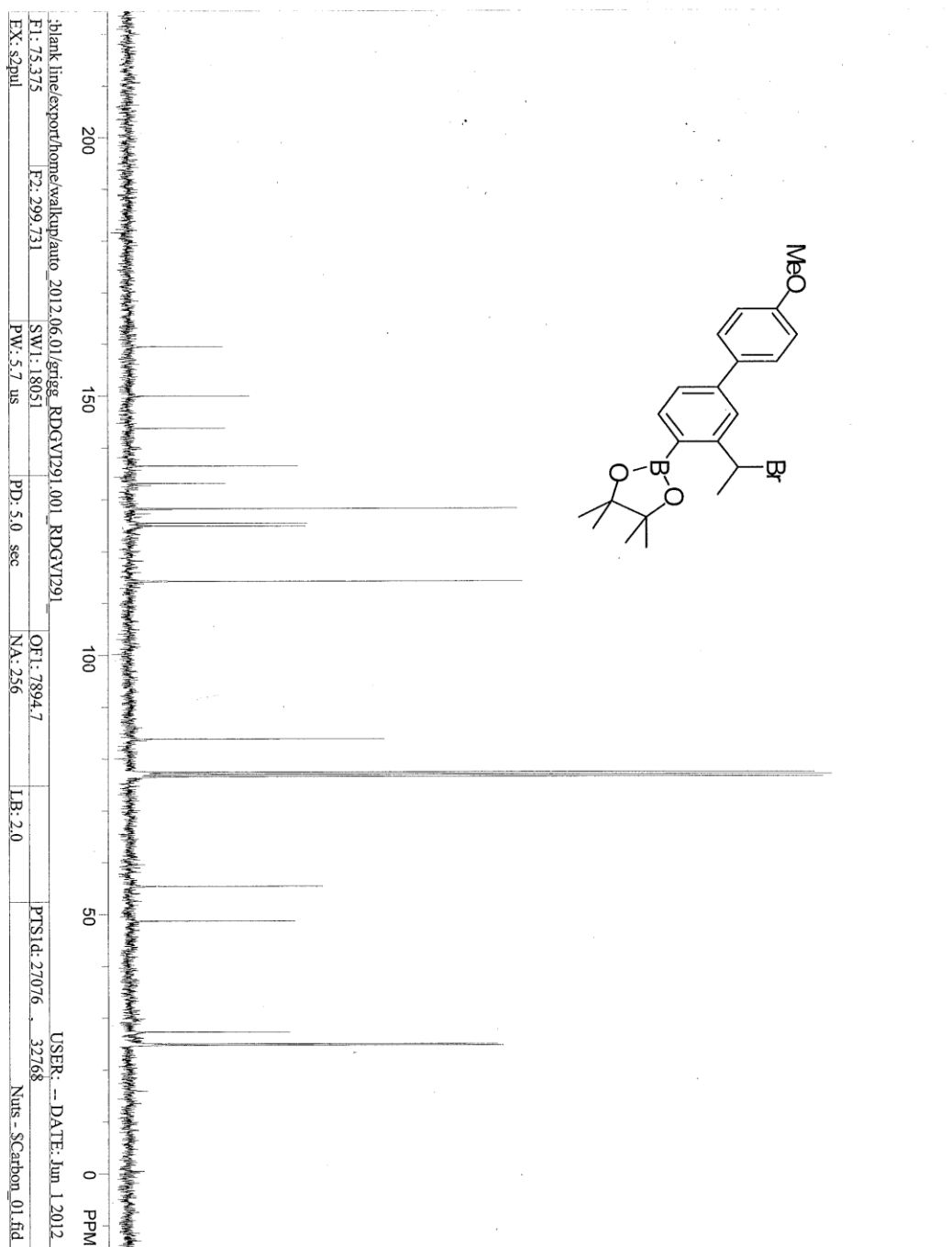
Compound 2.20.



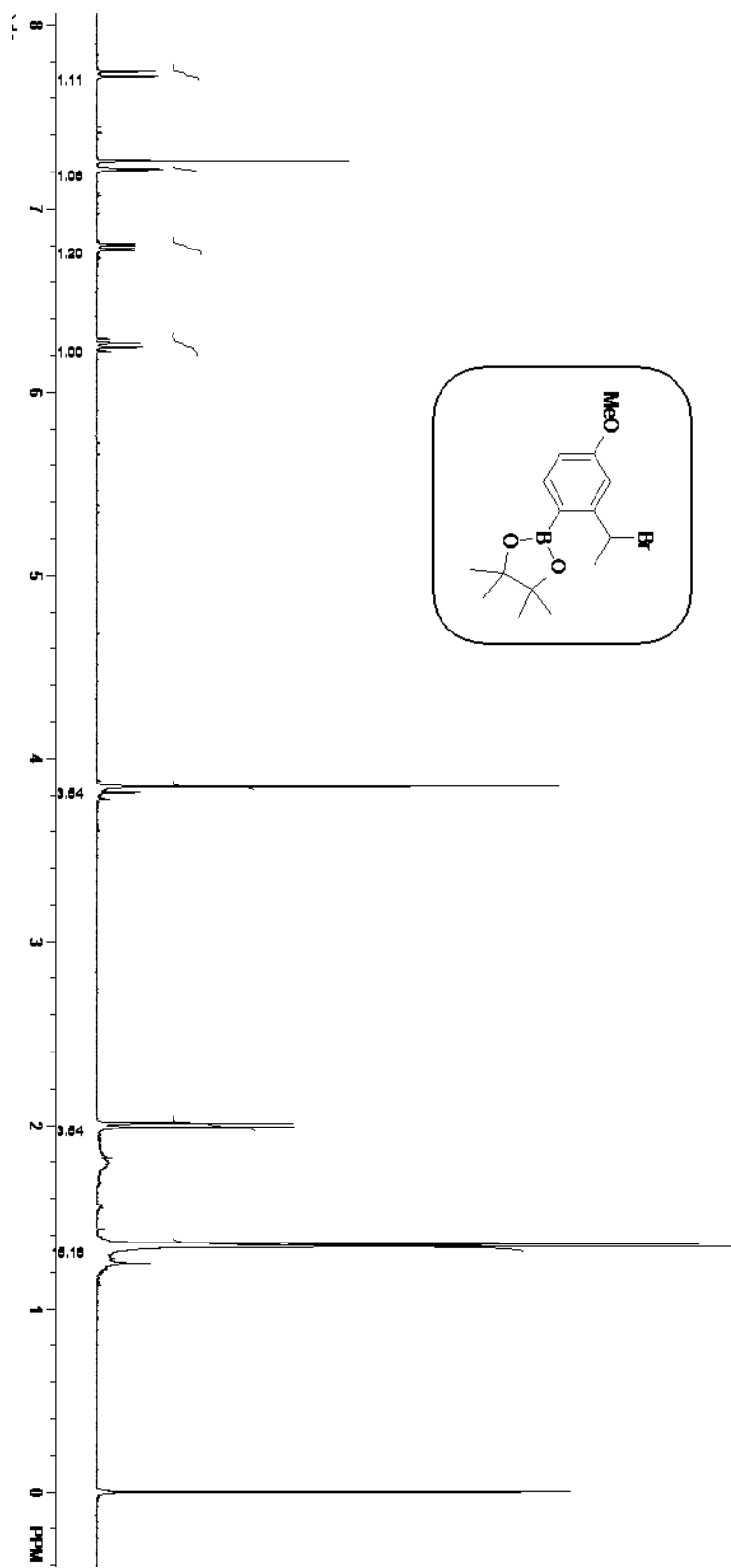
Compound 2.21.



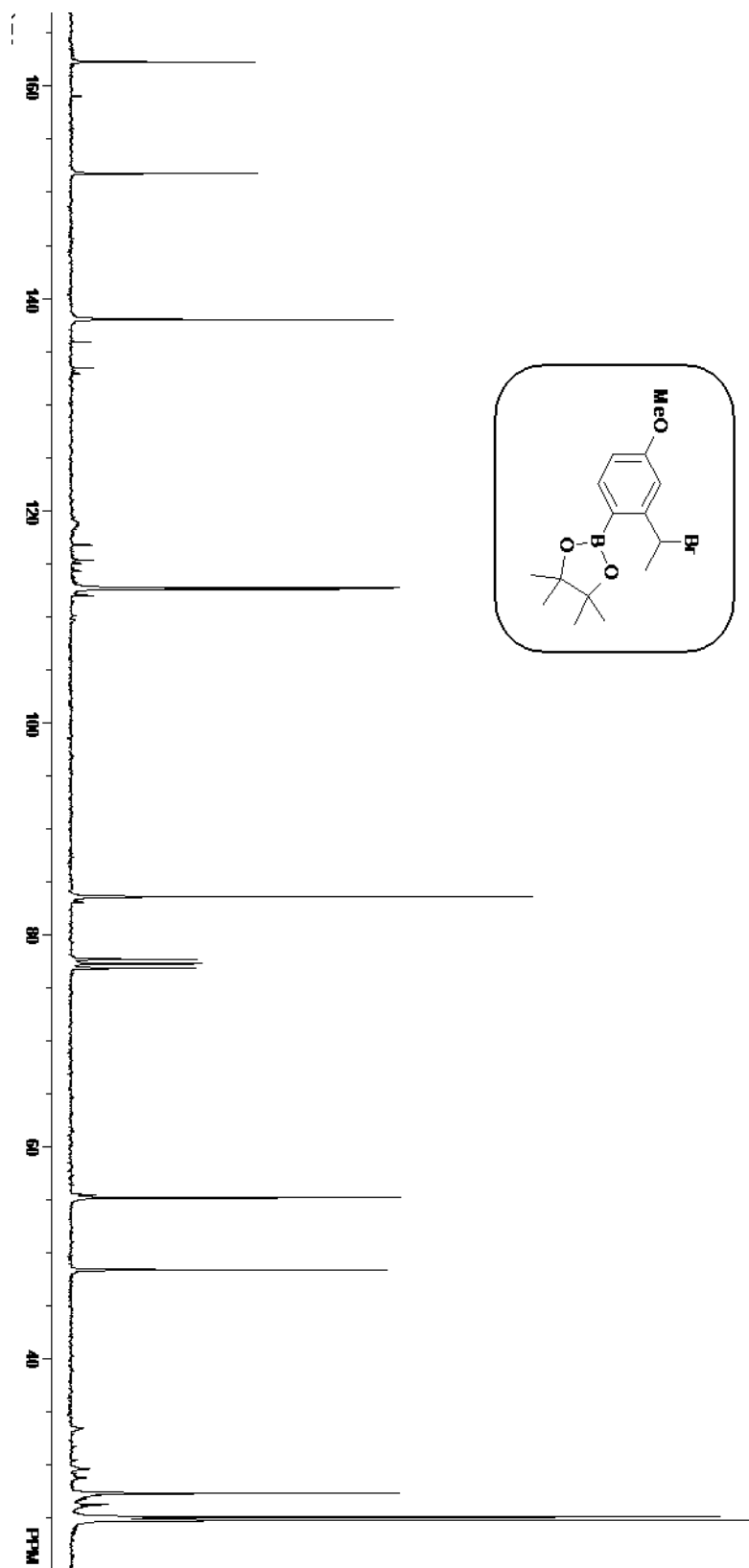
Compound 2.21.



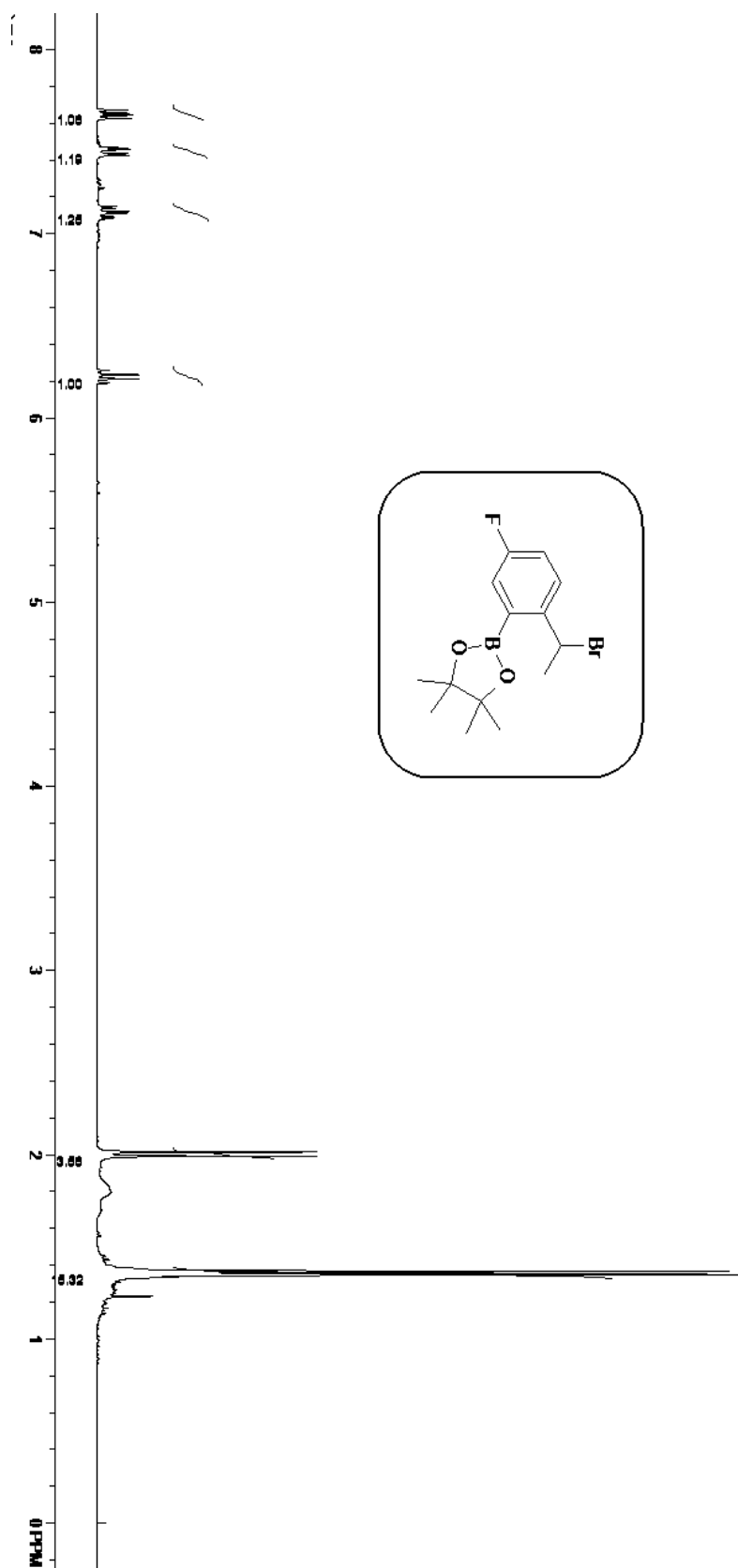
Compound 2.22.



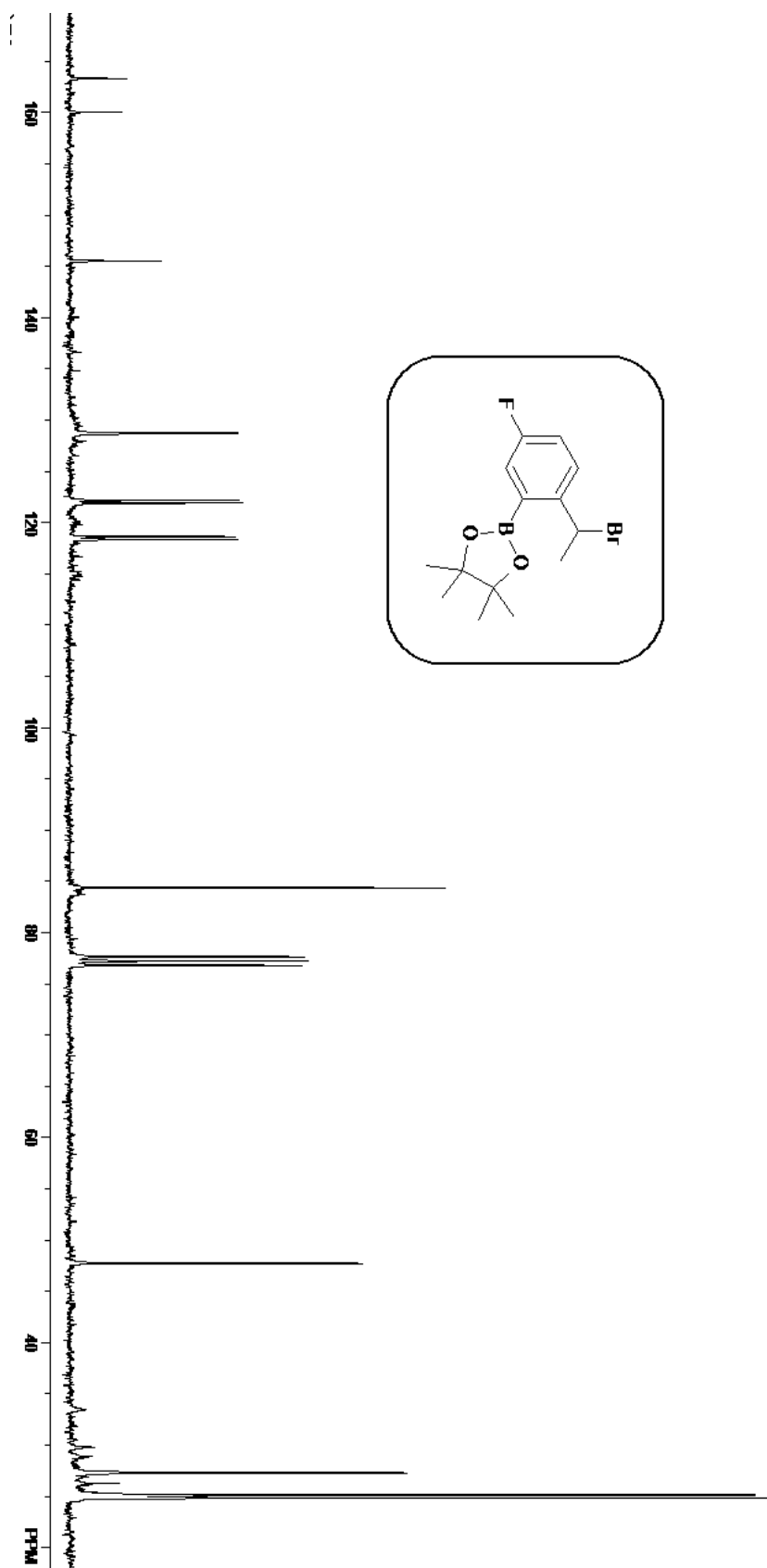
Compound 2.20.



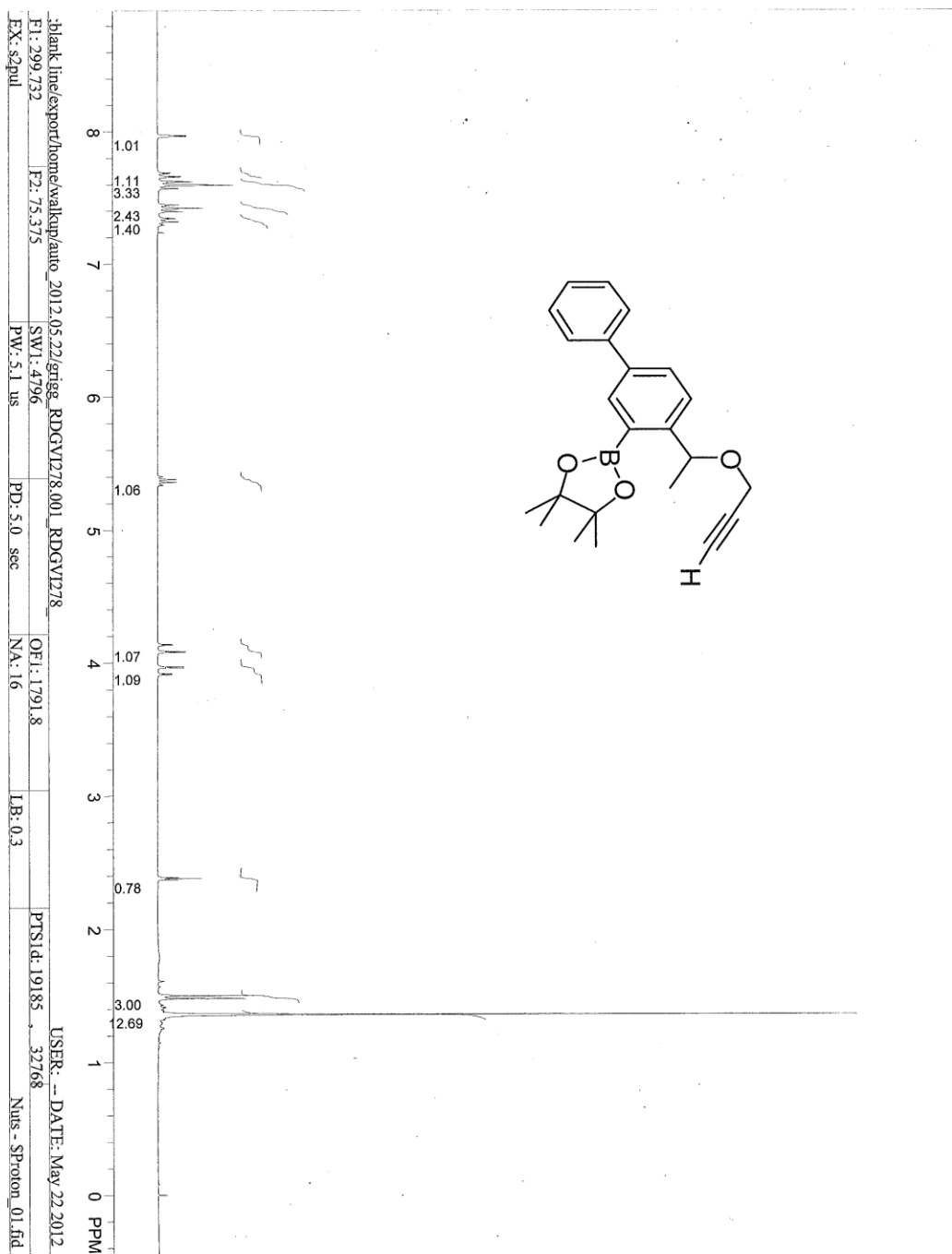
Compound 2.24.



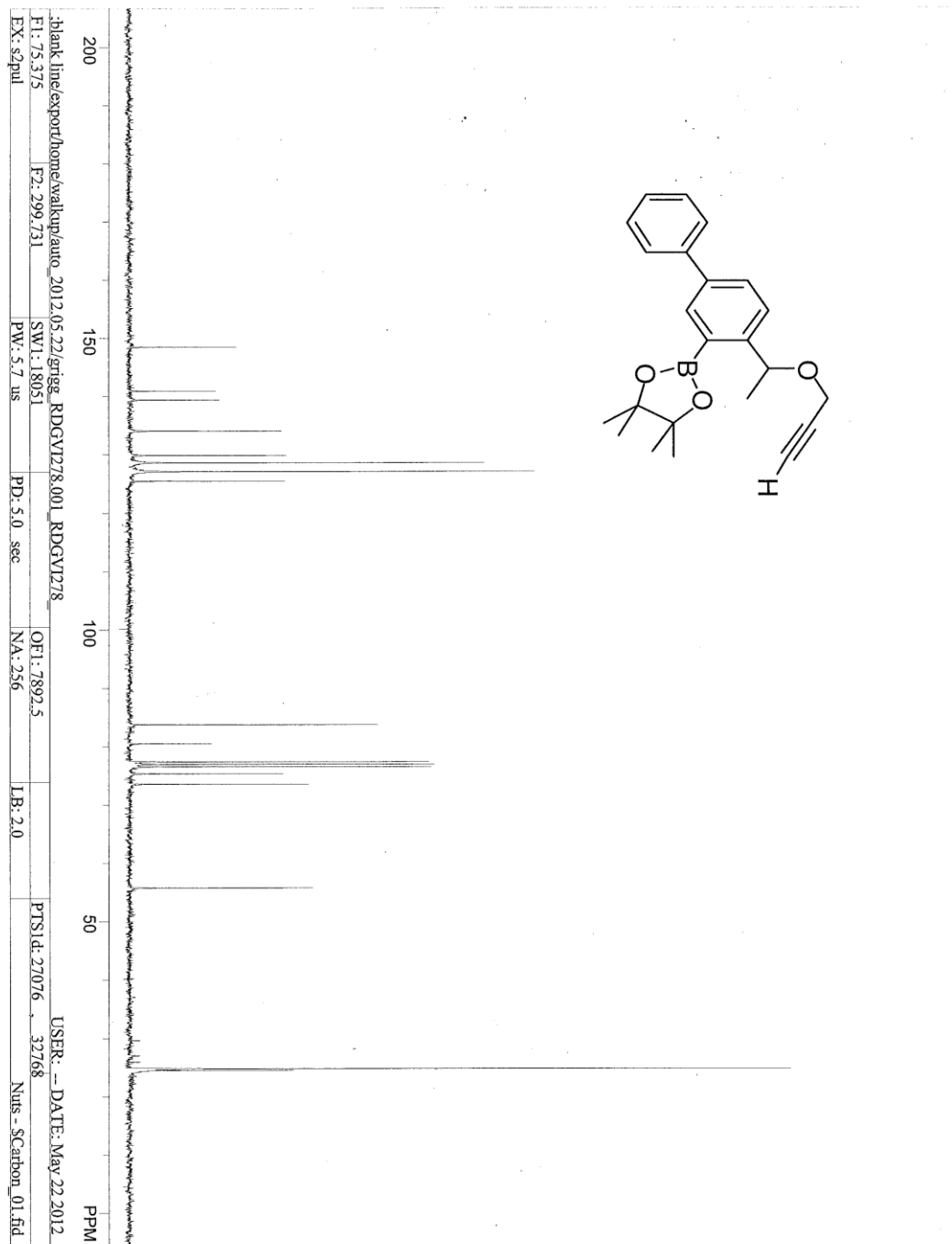
Compound 2.24.



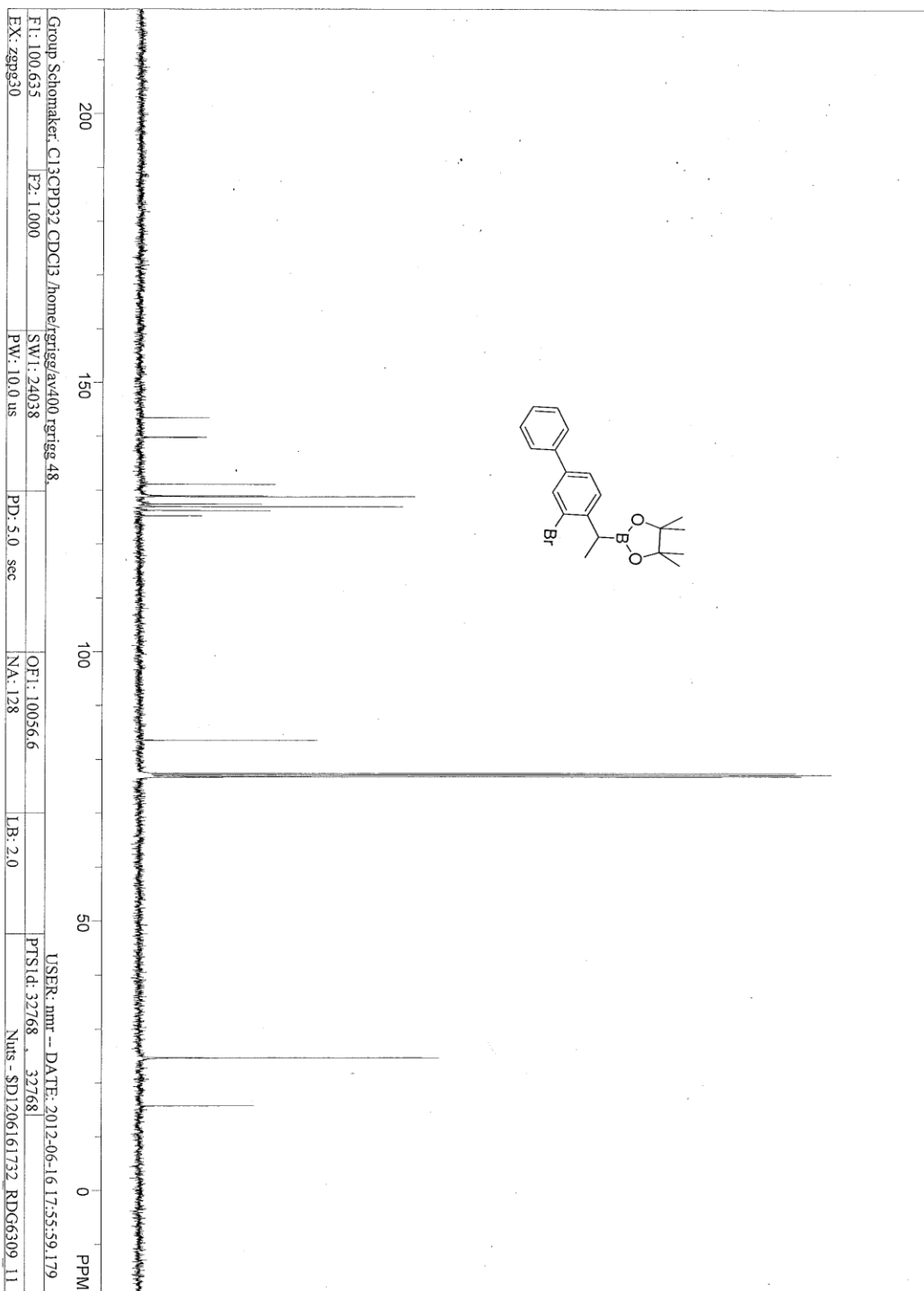
Compound 2.25.



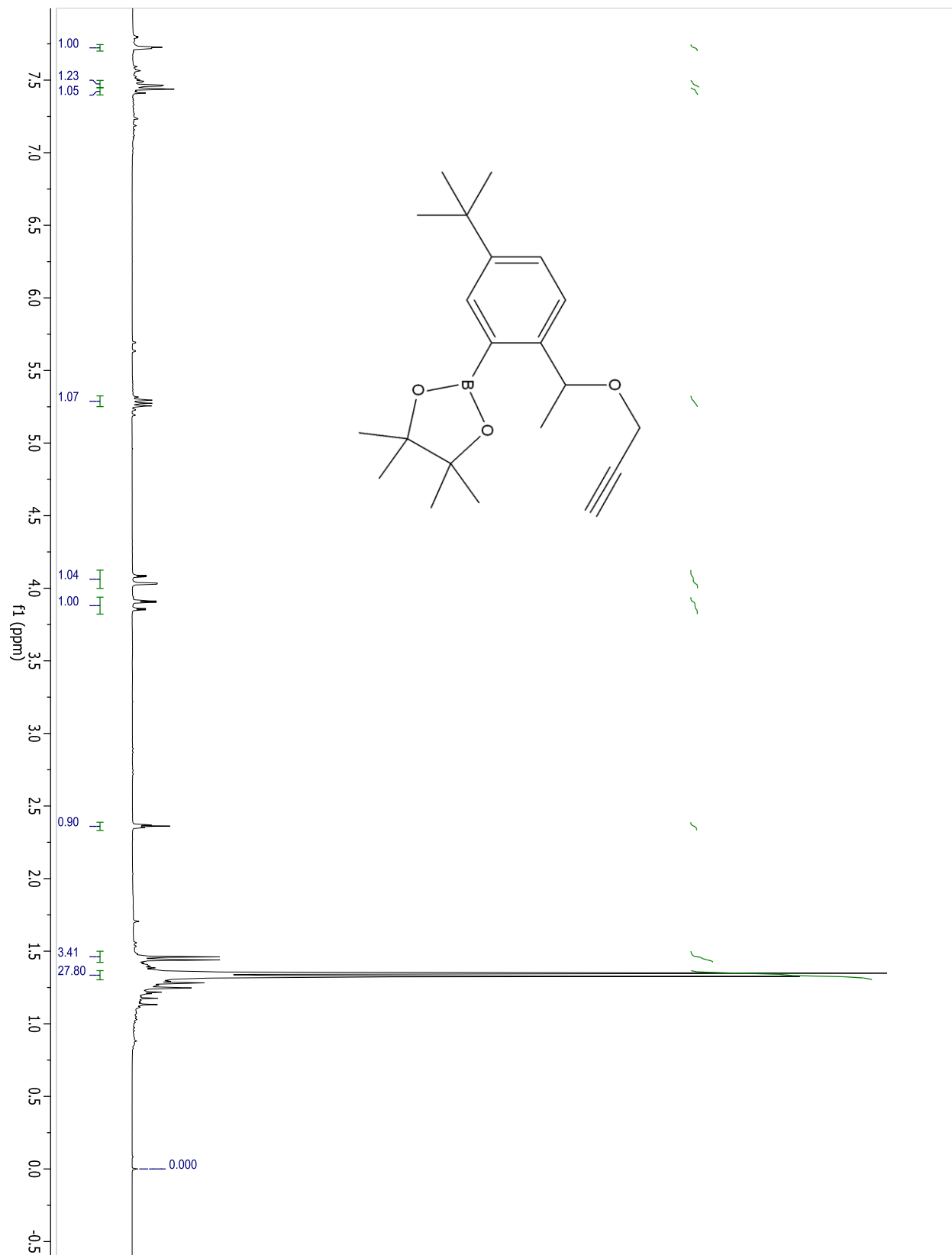
Compound 2.25.



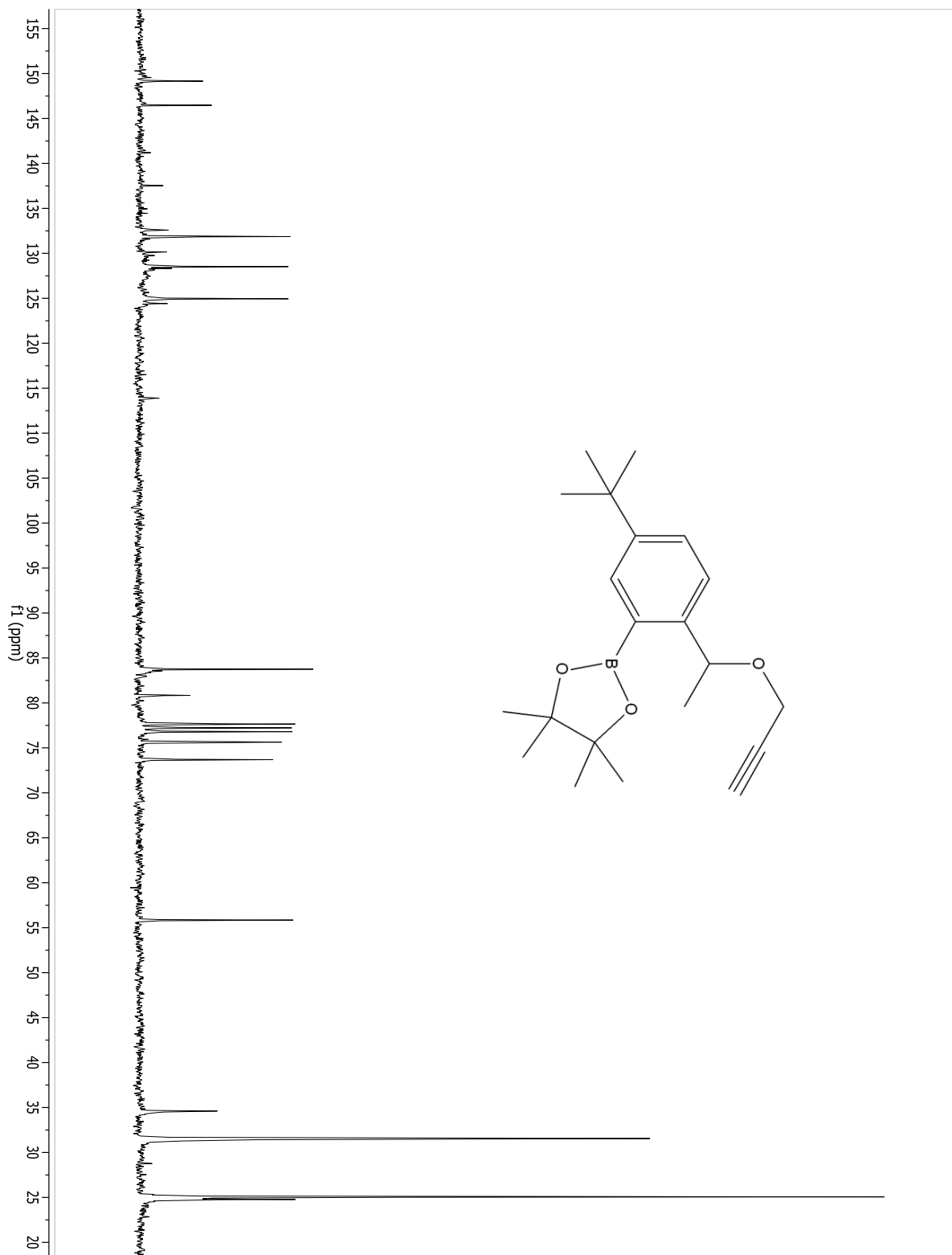
Compound 2.37.



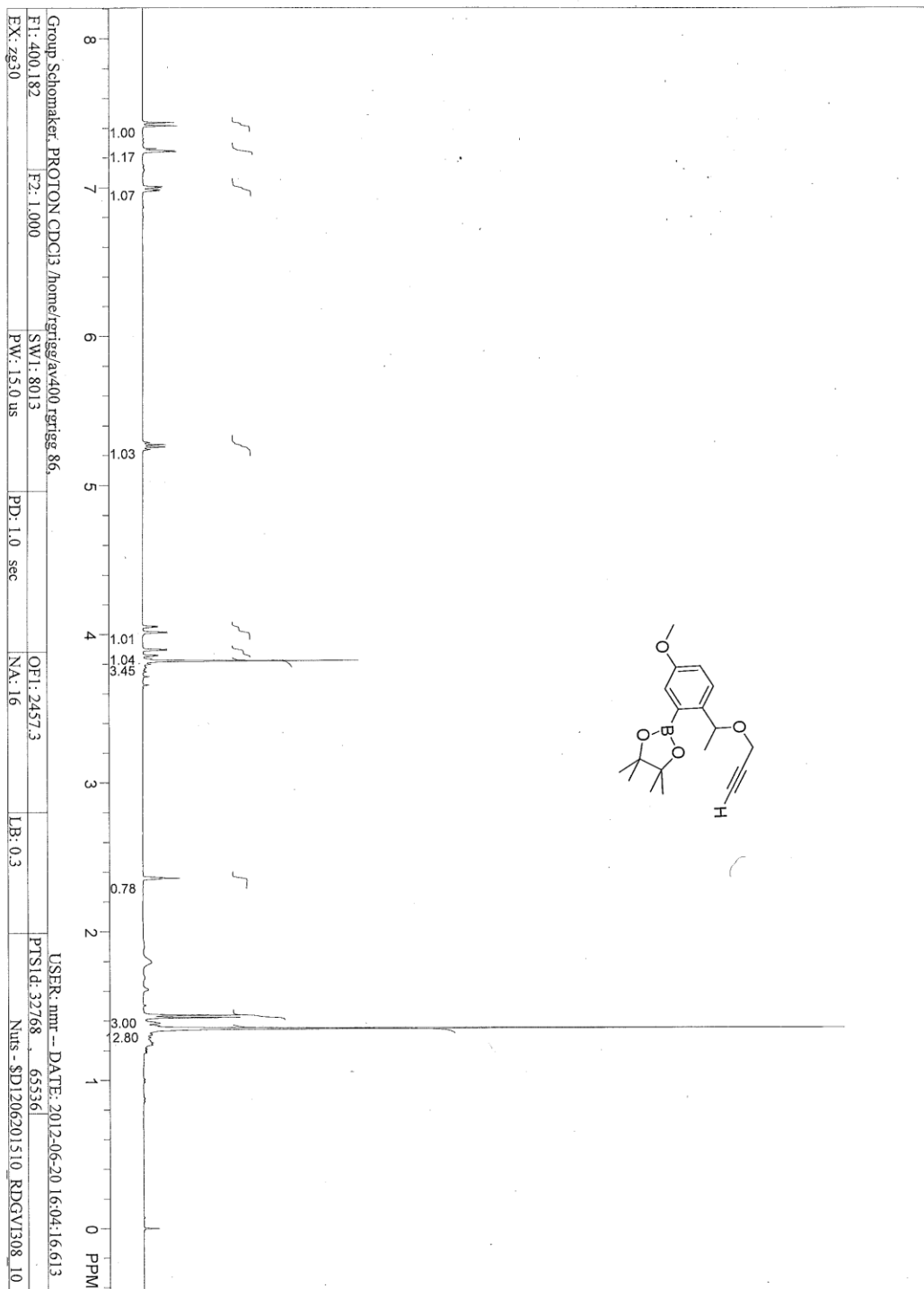
Compound 2.26.



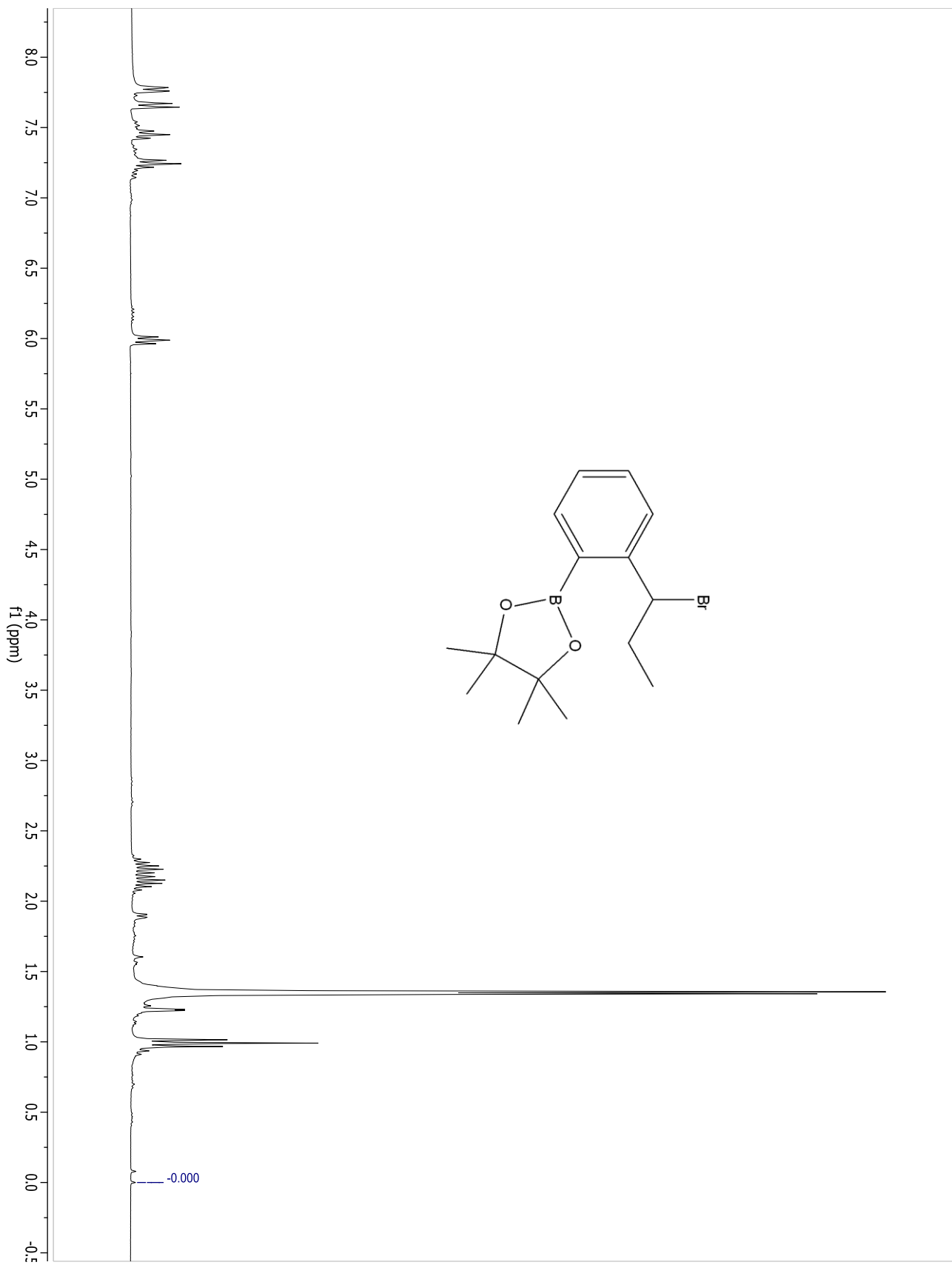
Compound 2.26.



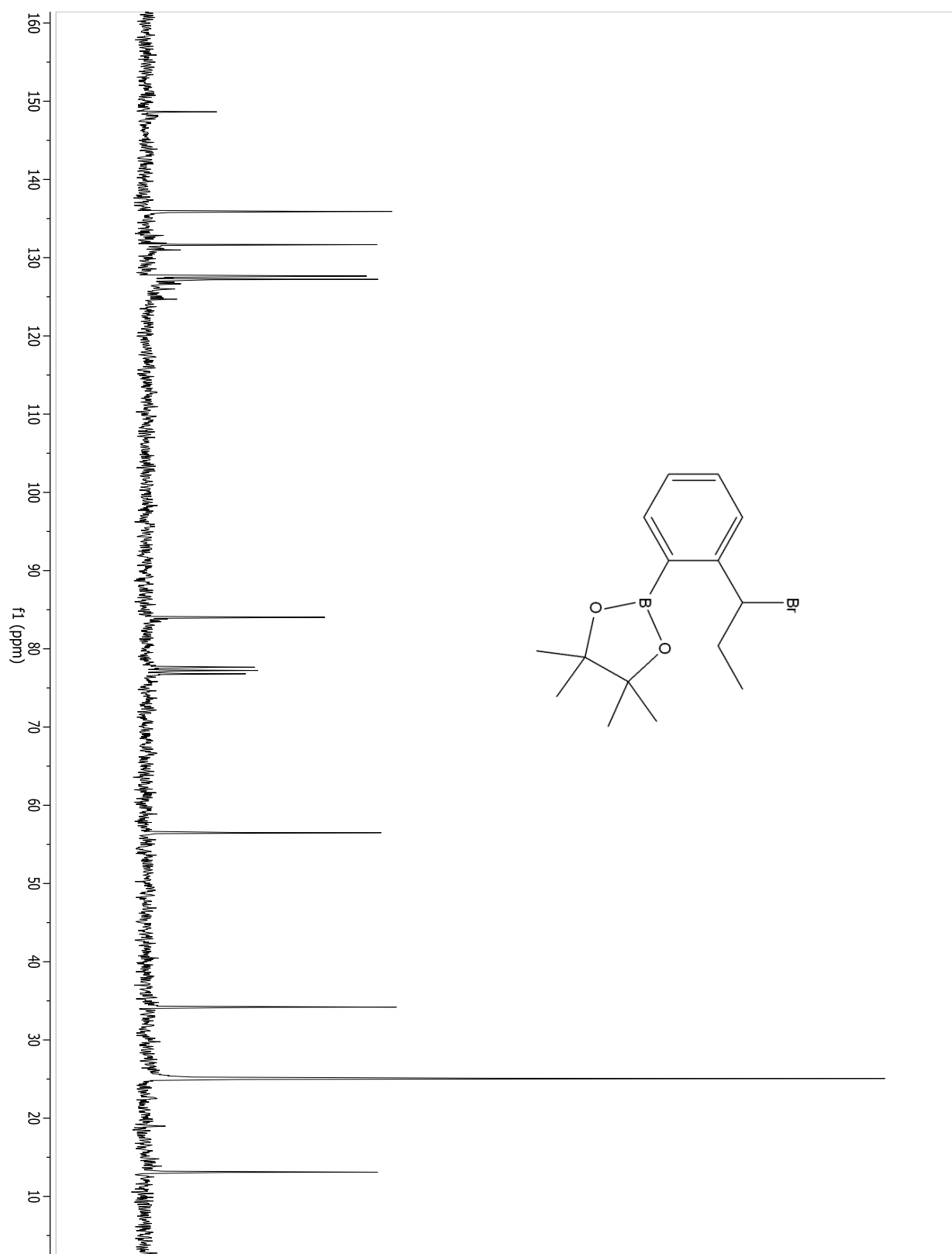
Compound 2.27.



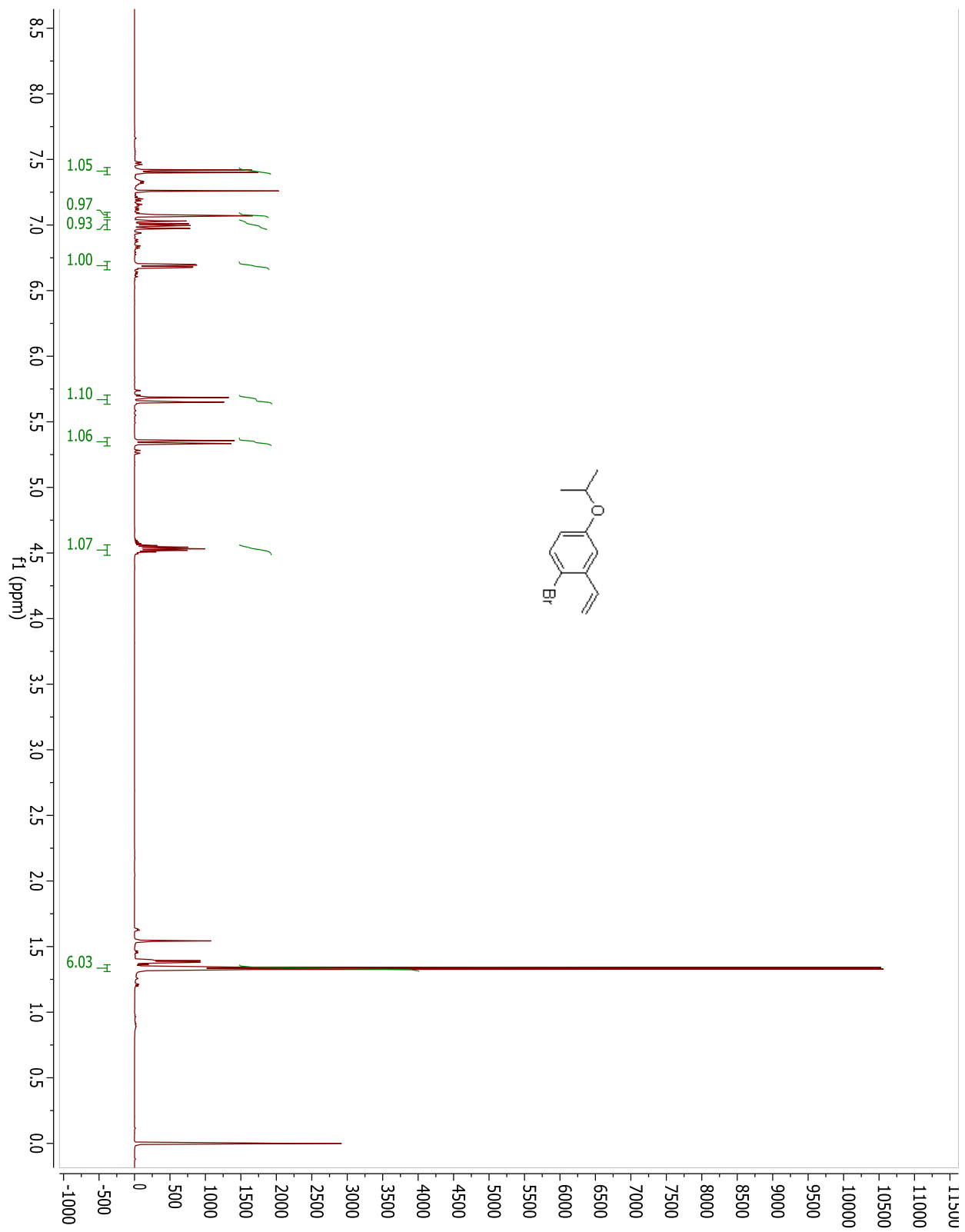
Compound 2.28.



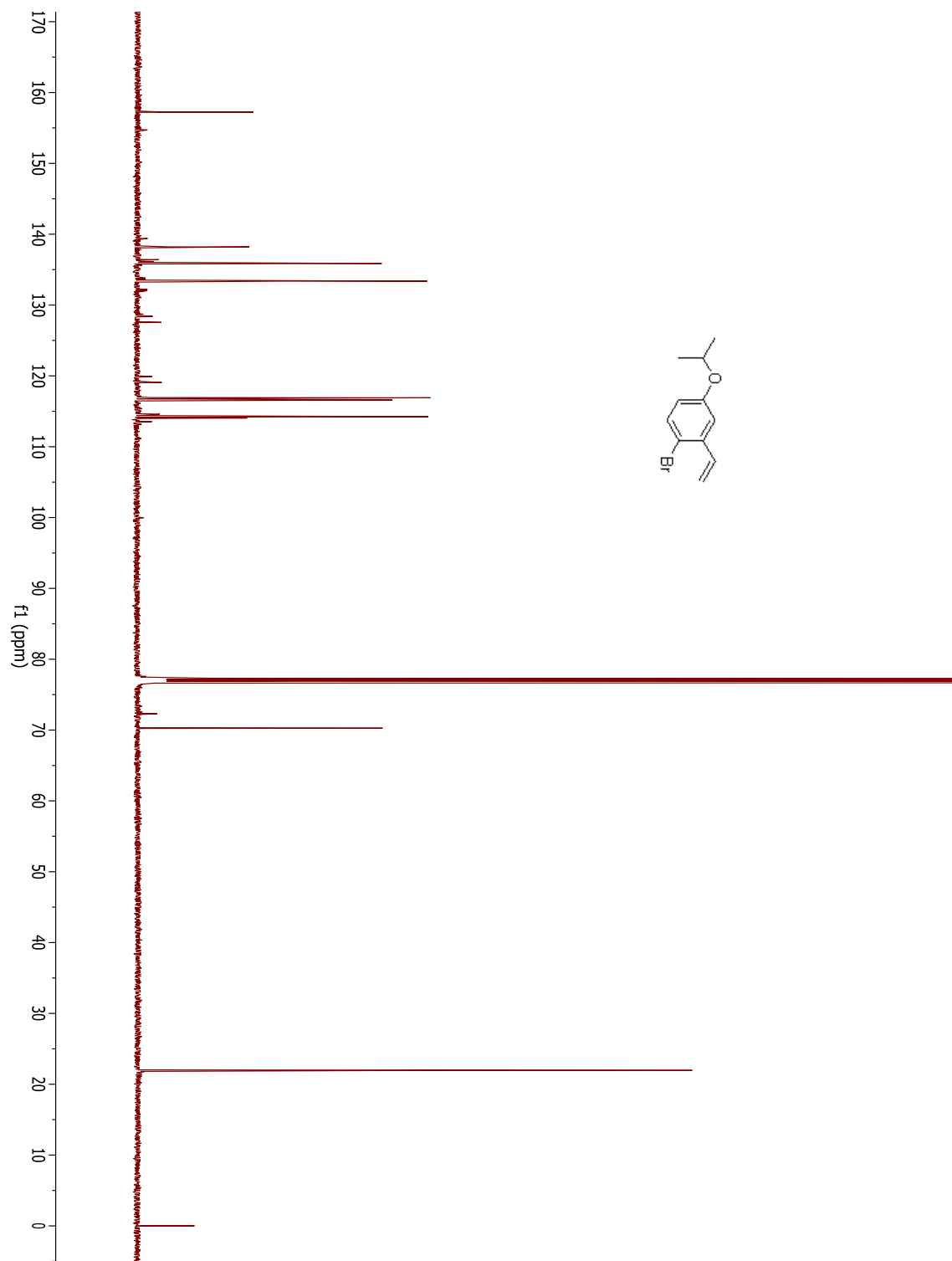
Compound 2.28.



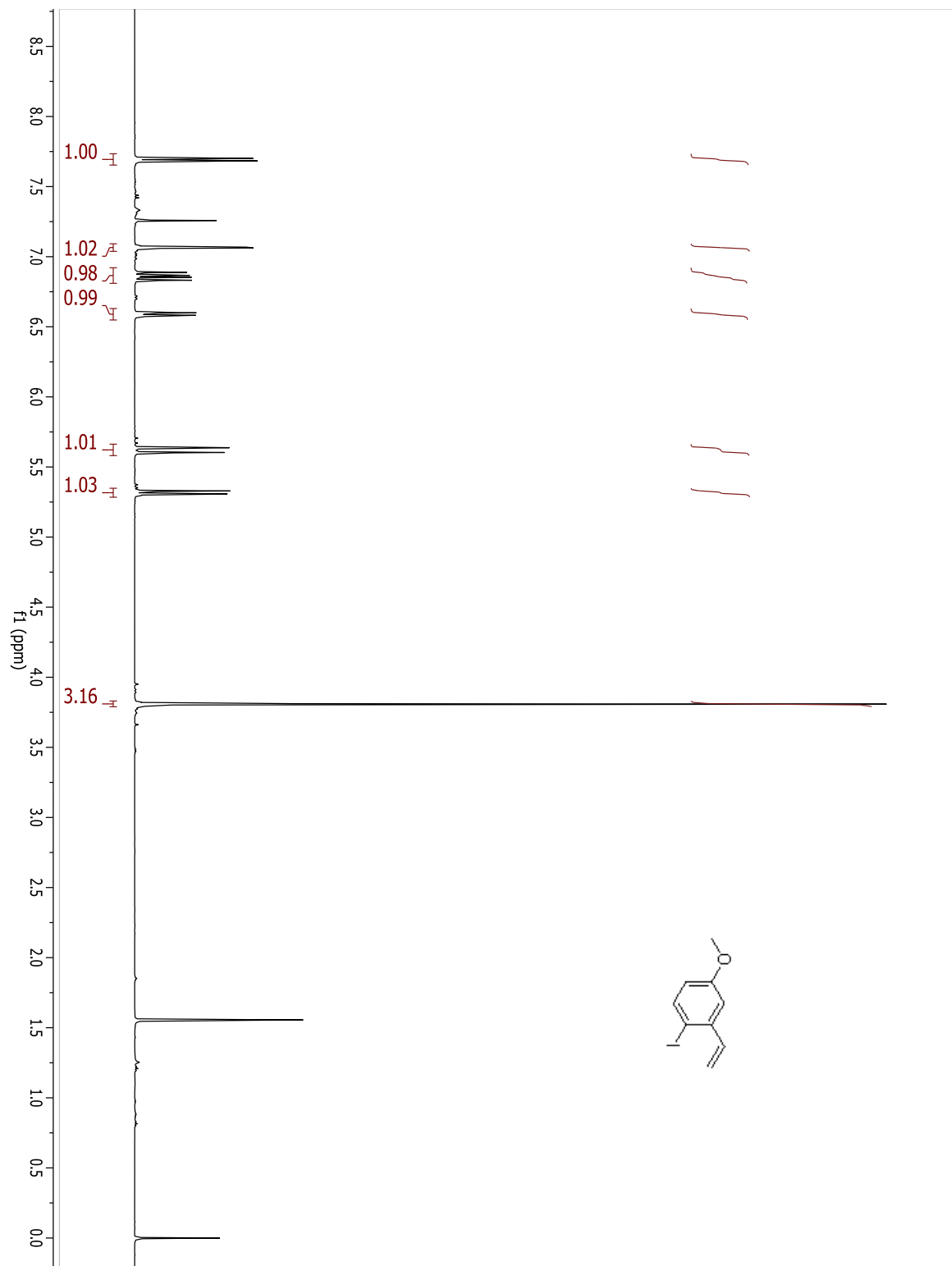
Compound 3.4.



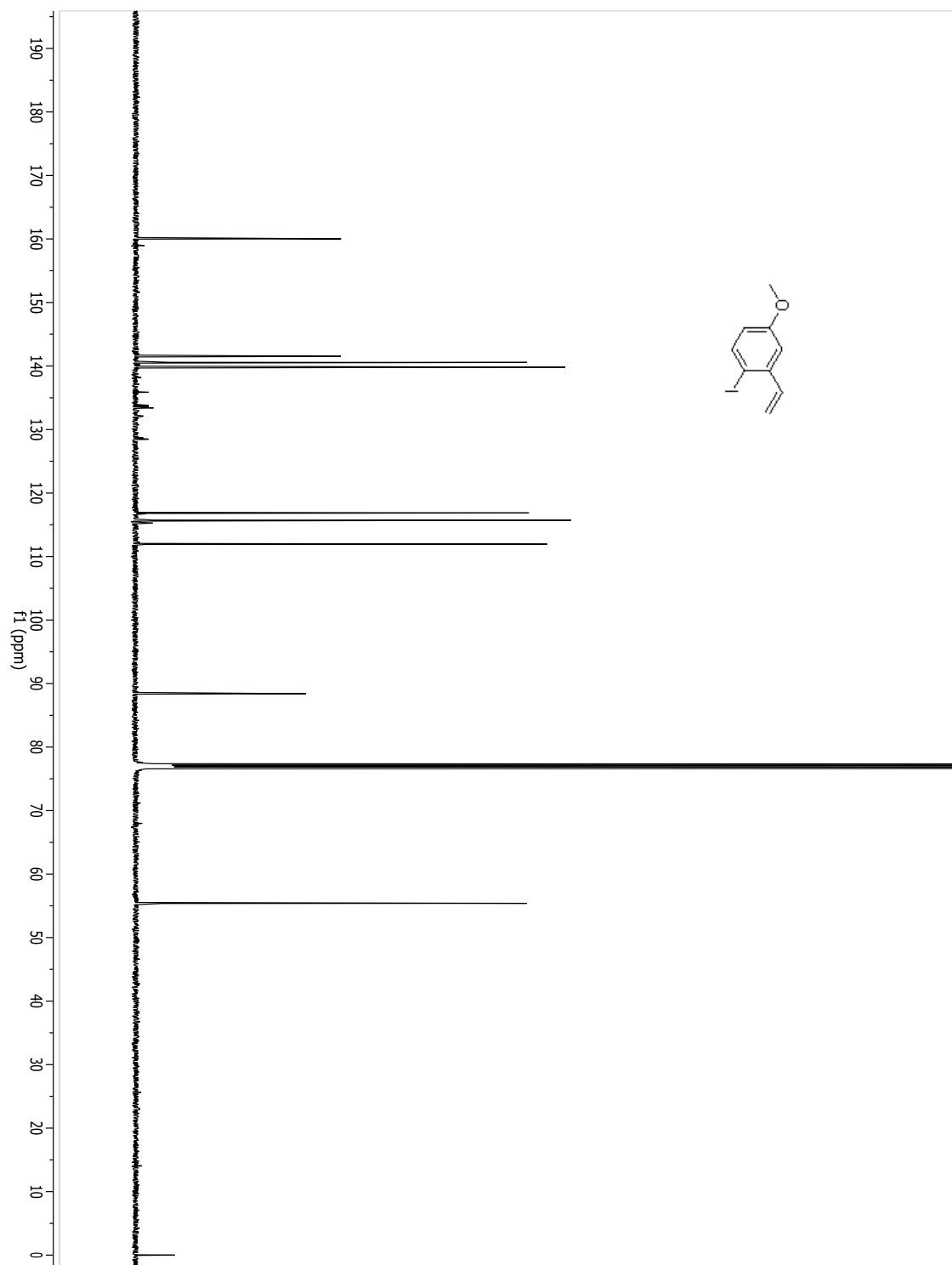
Compound 3.4.



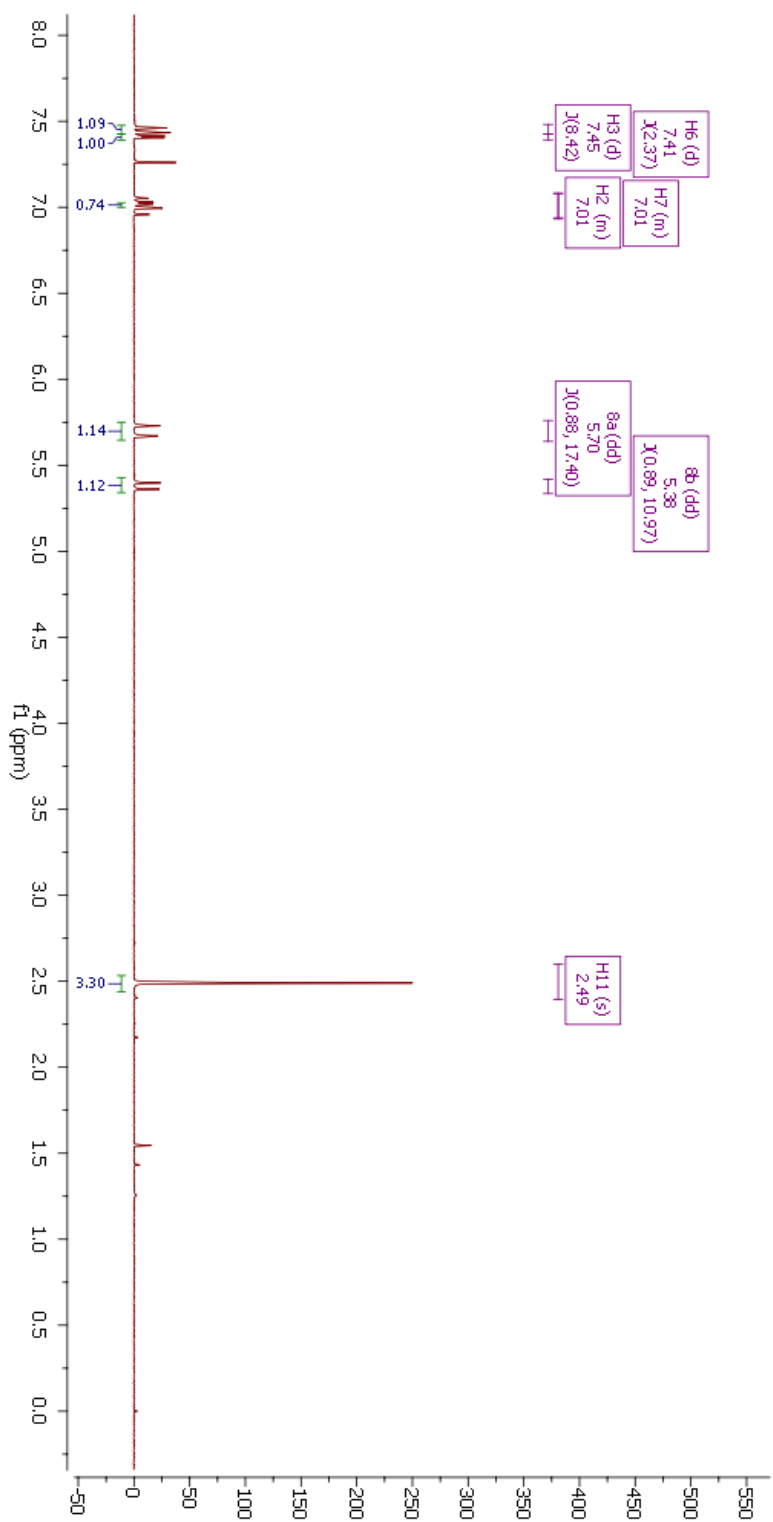
Compound 3.5.



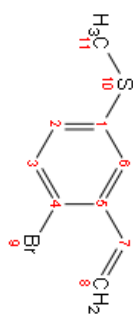
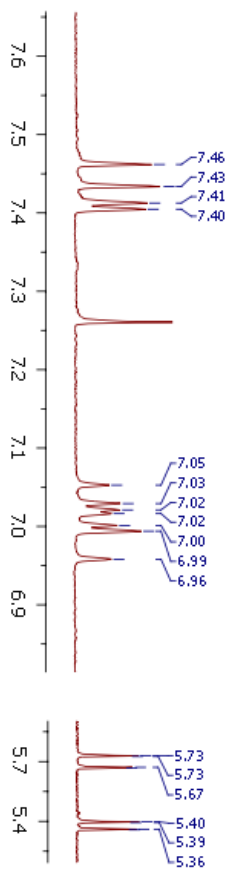
Compound 3.5.



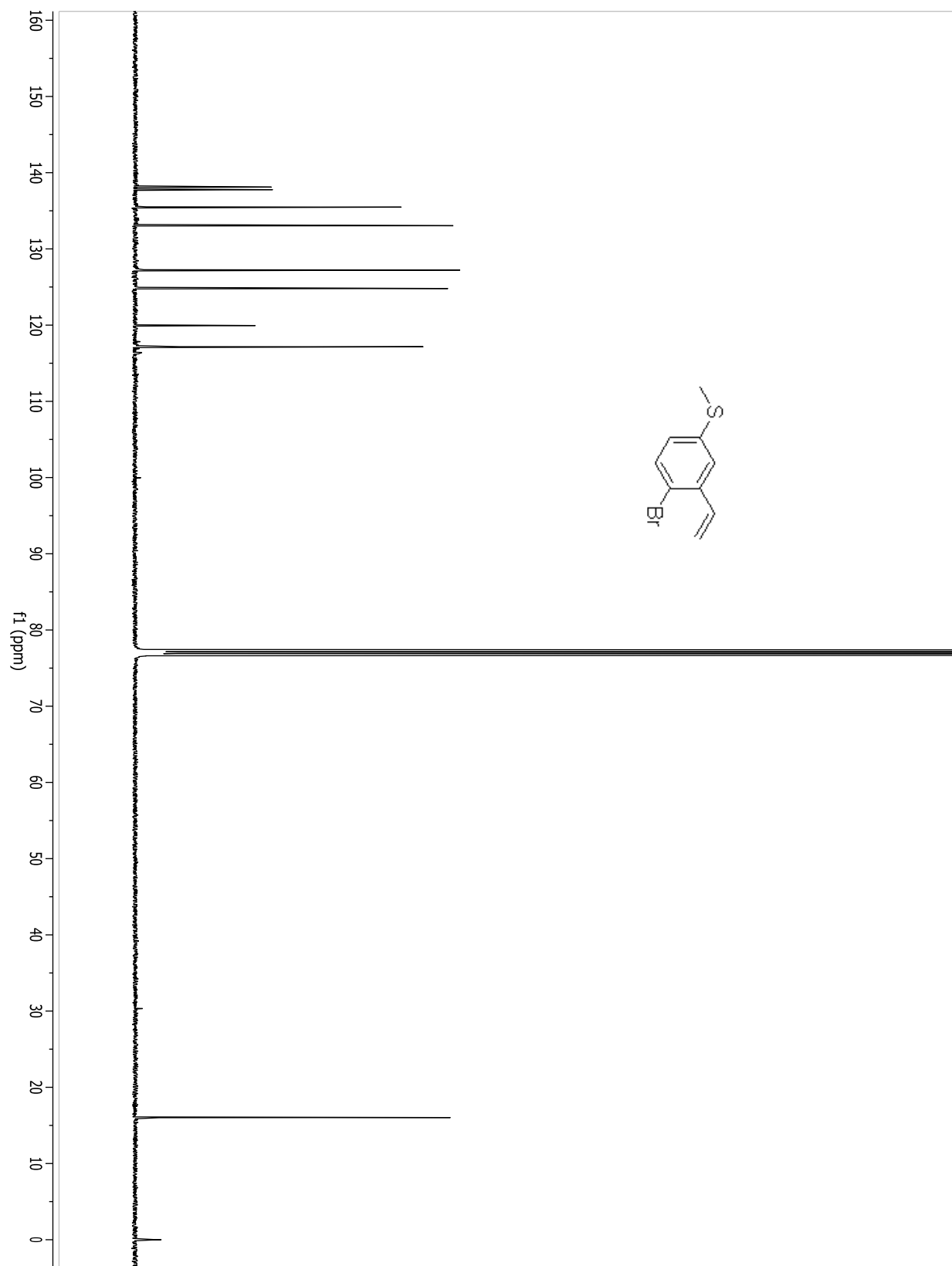
Compound 3.14.



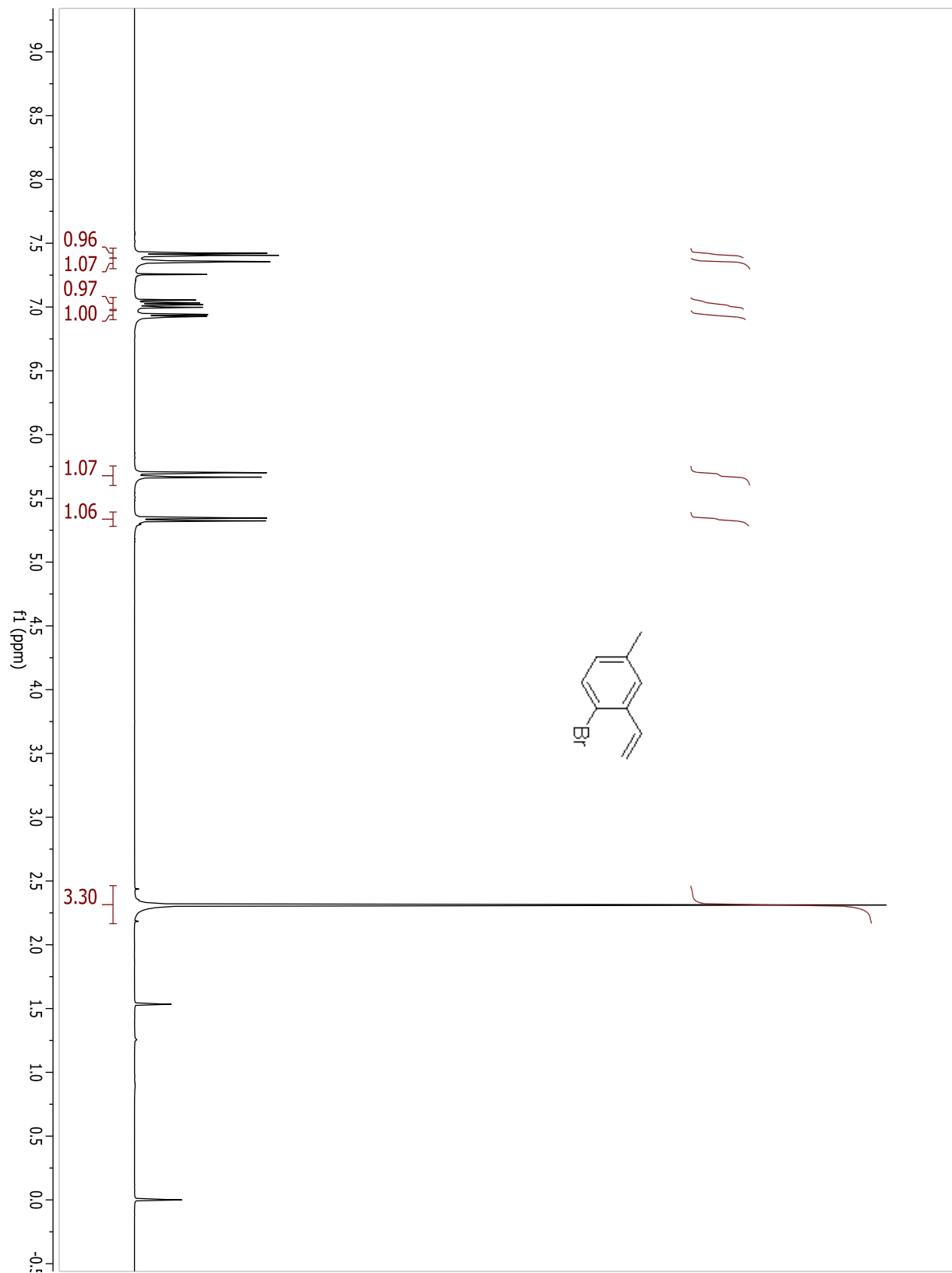
PD-MT104F6-10_1H



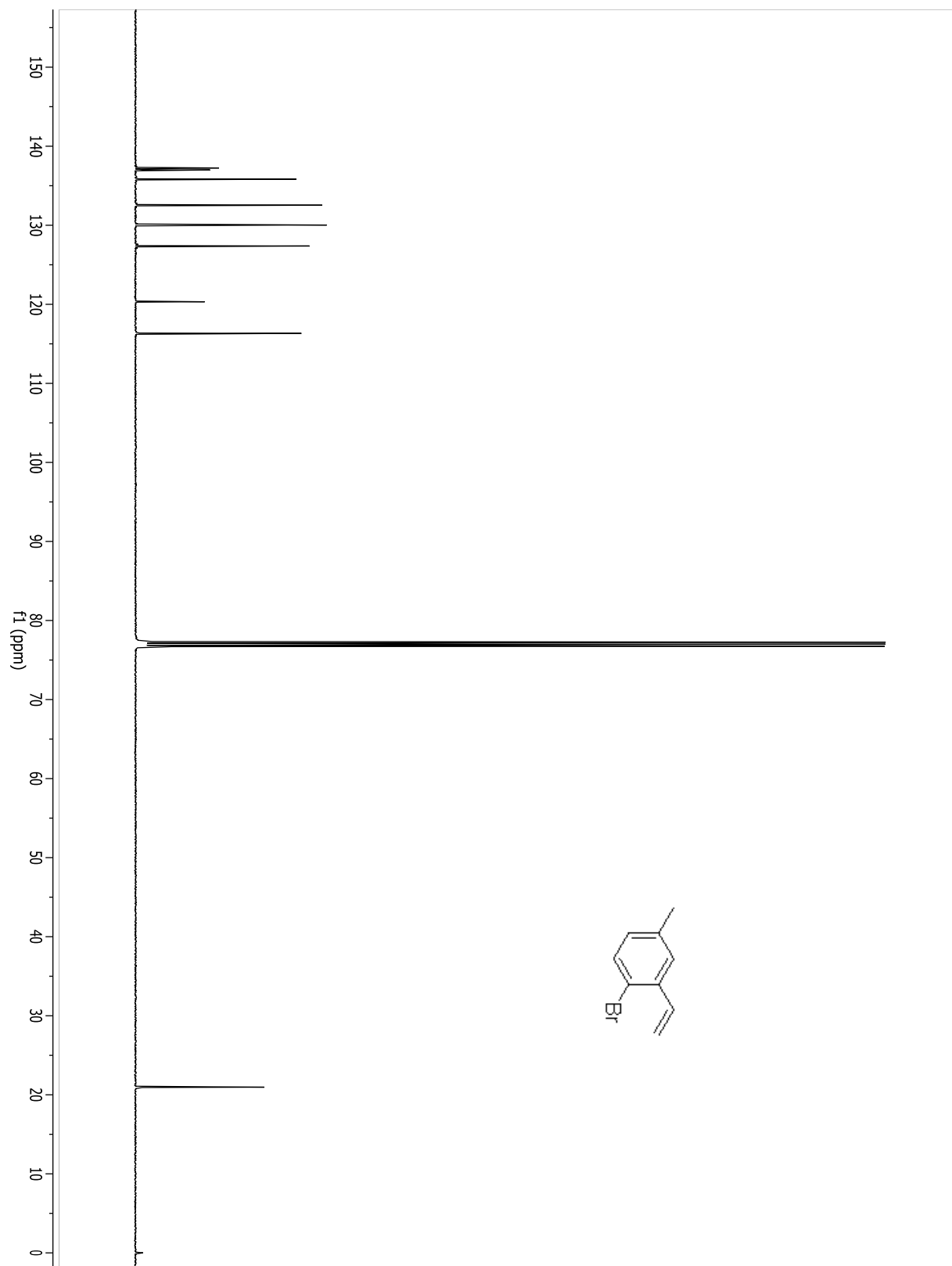
Compound 3.14.



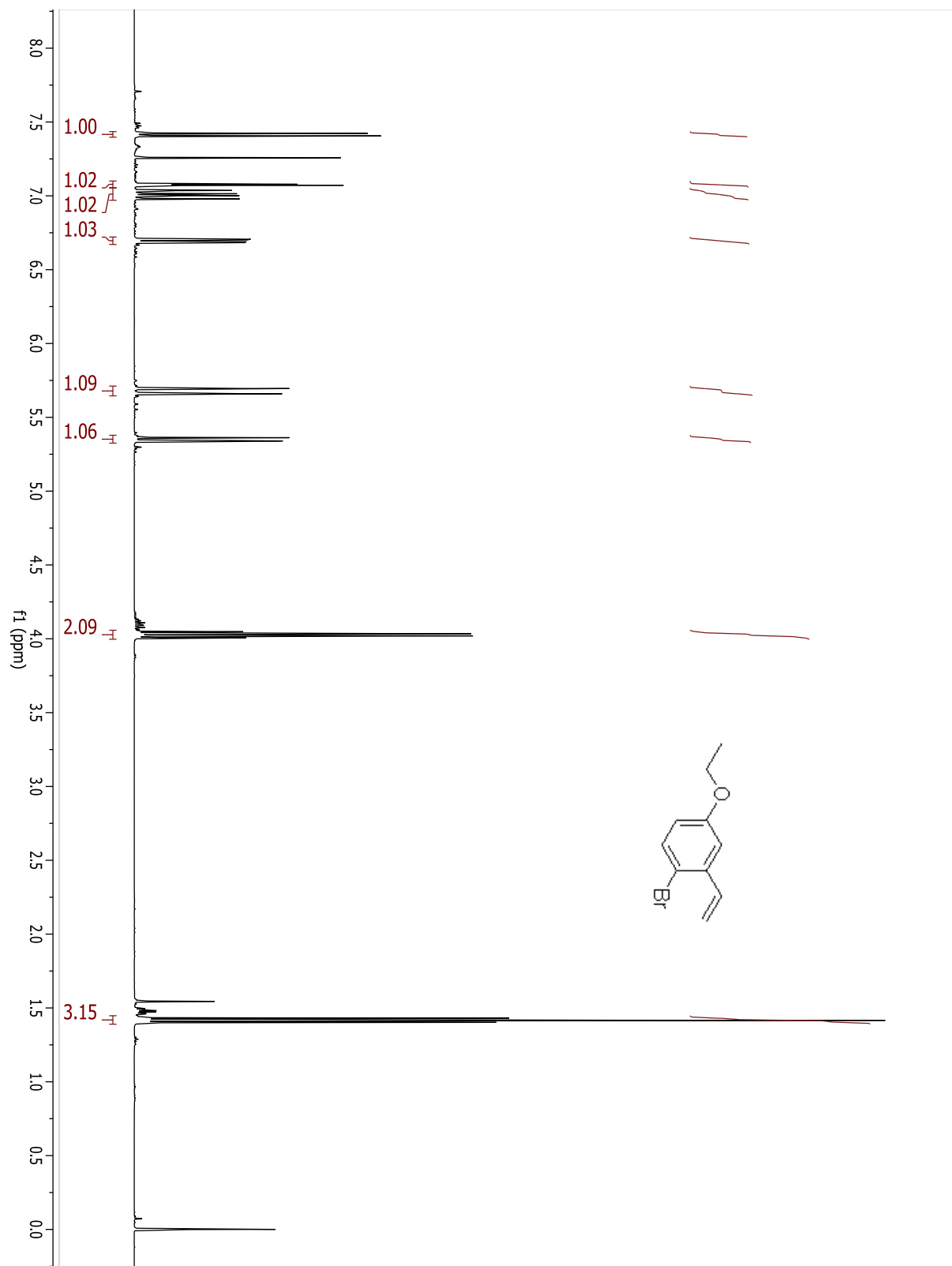
Compound 3.15.



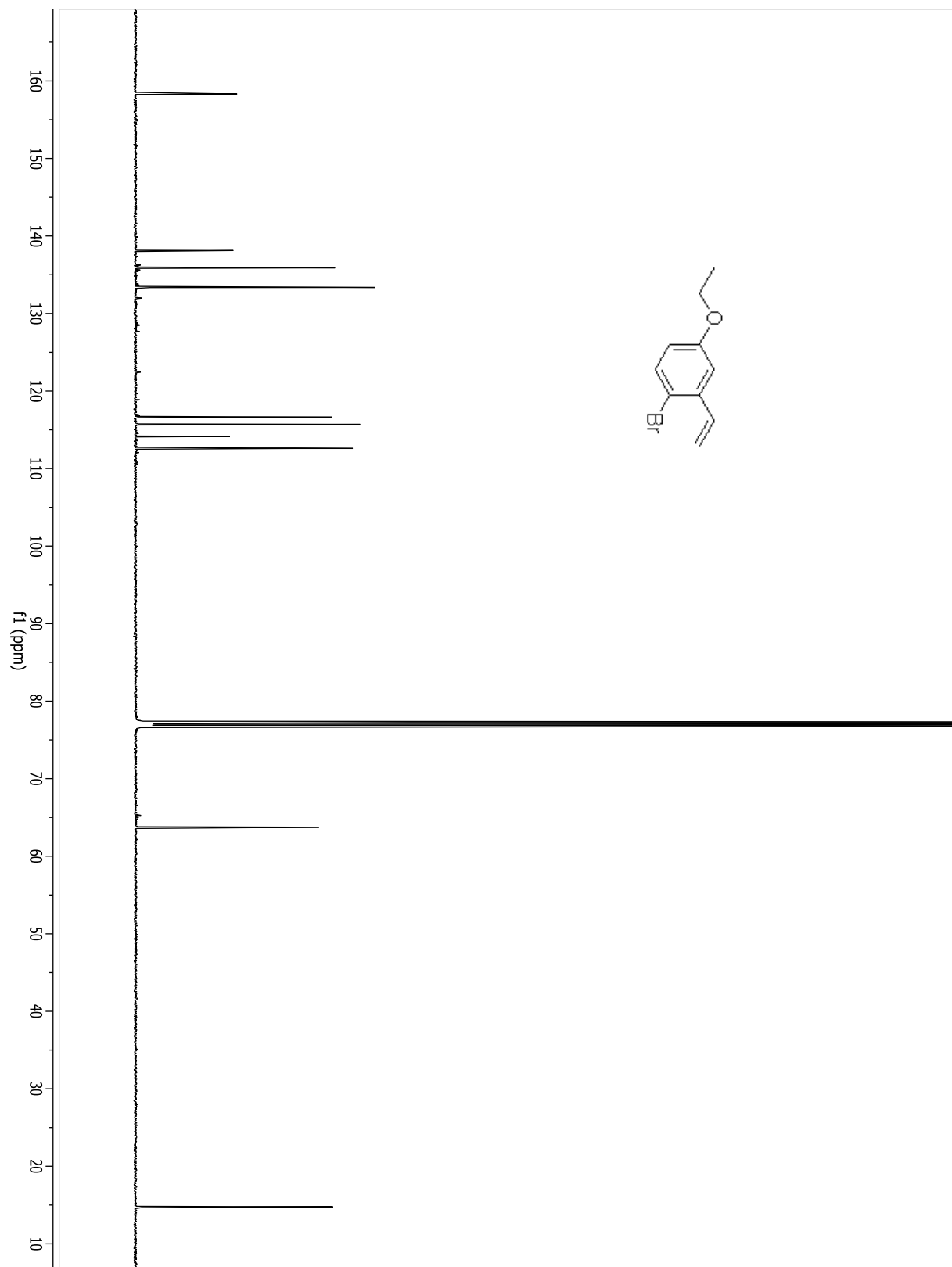
Compound 3.15.



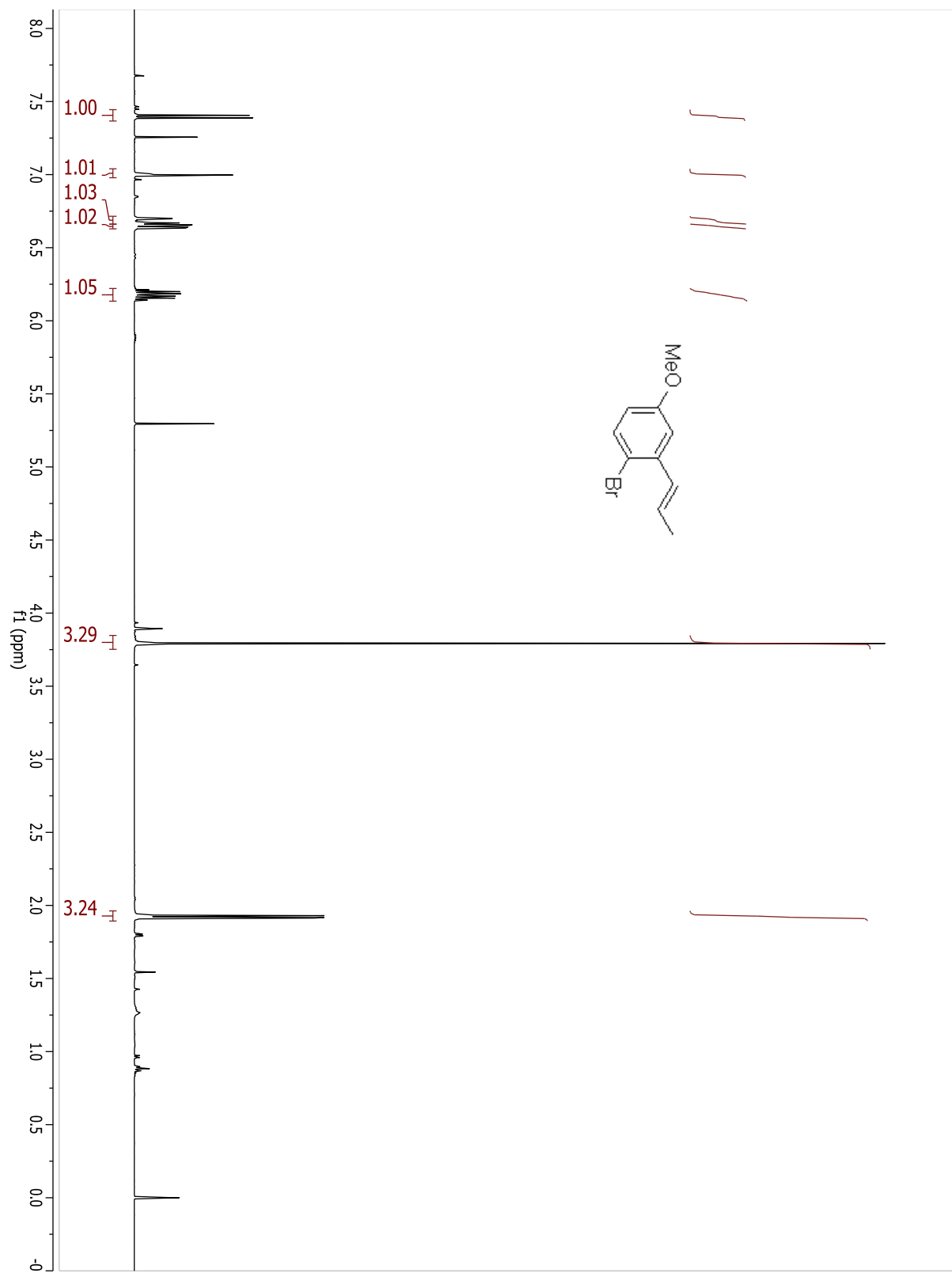
Compound 3.16.



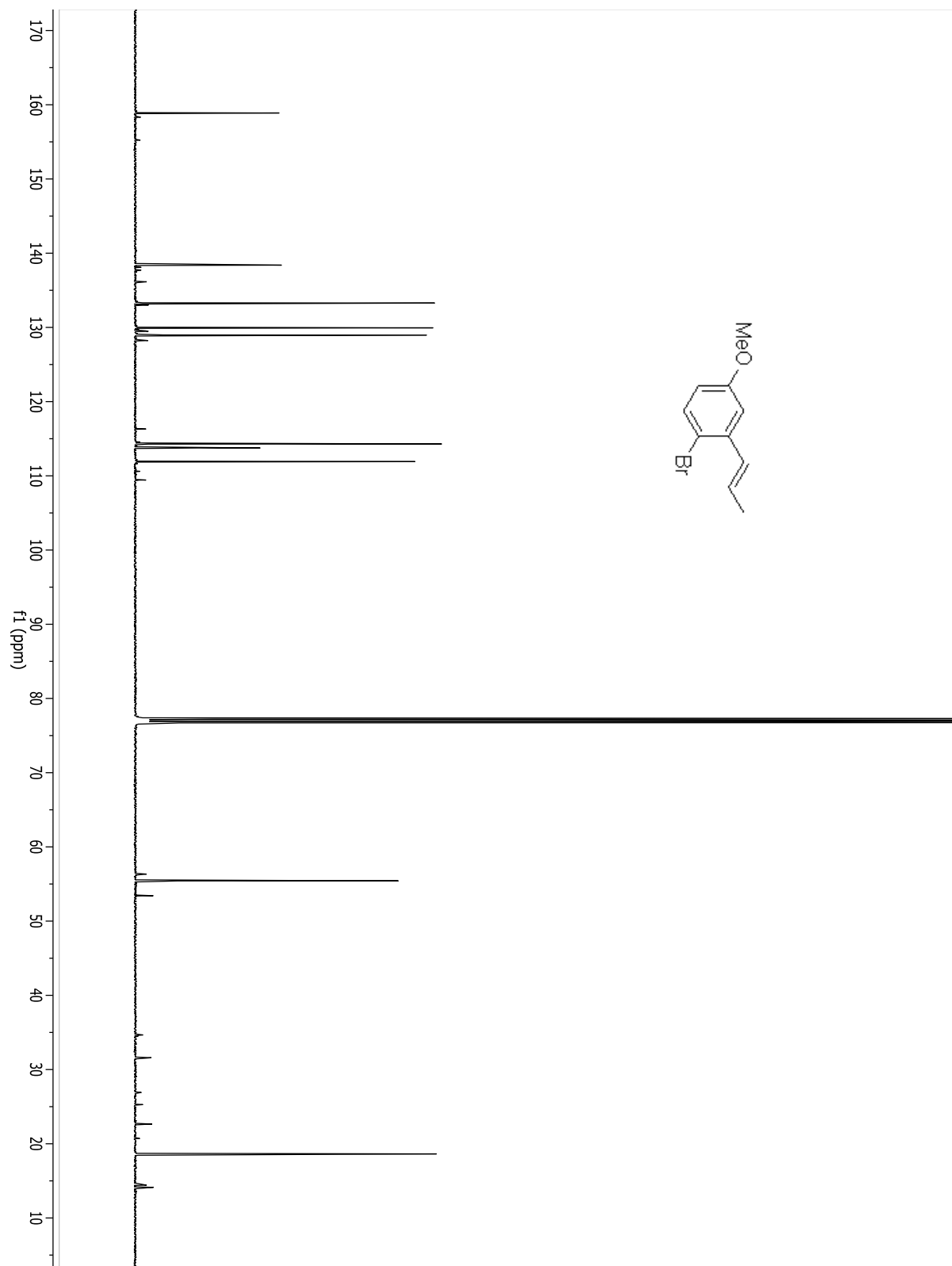
Compound 3.16.



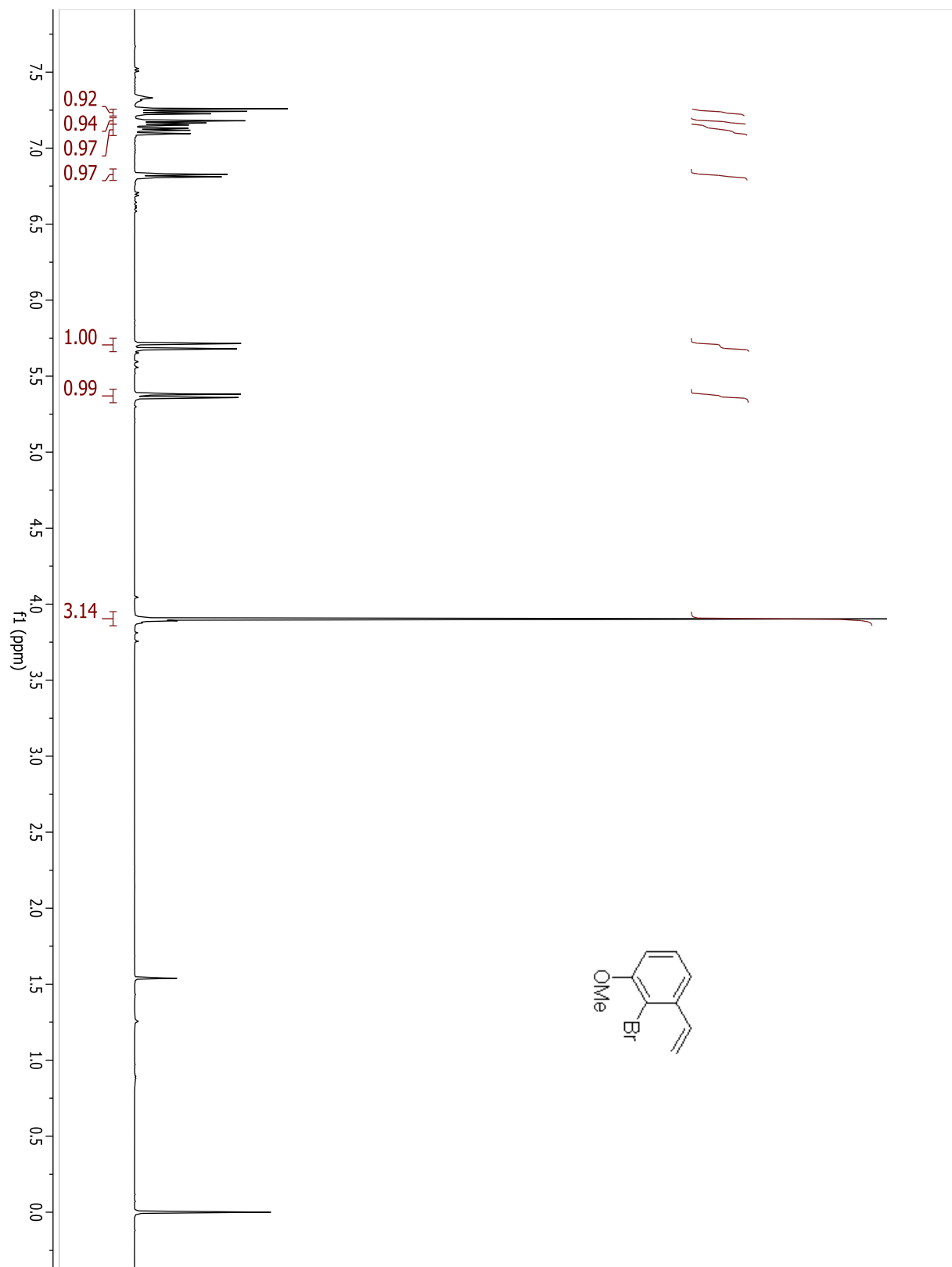
Compound 3.17.



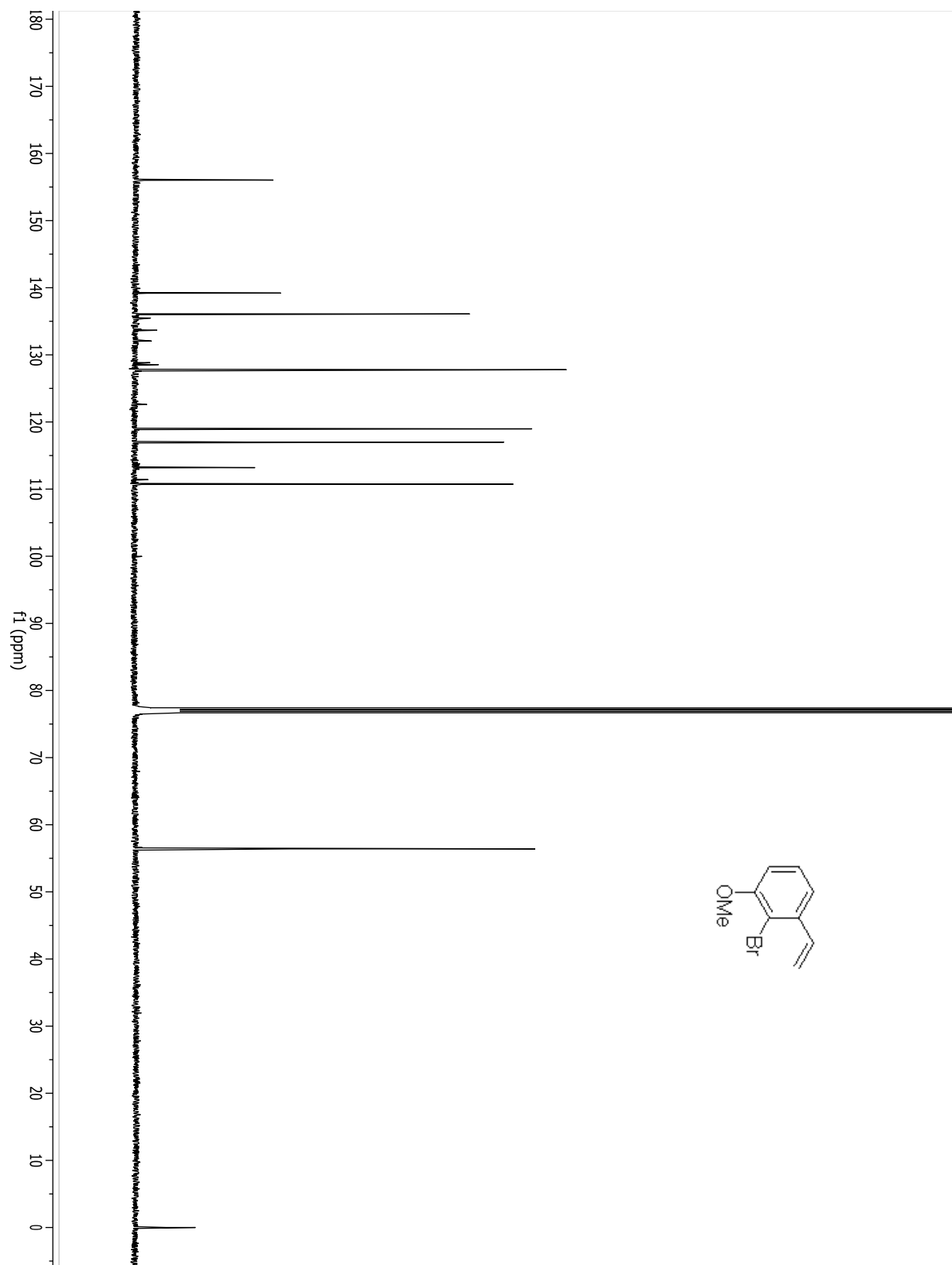
Compound 3.17.



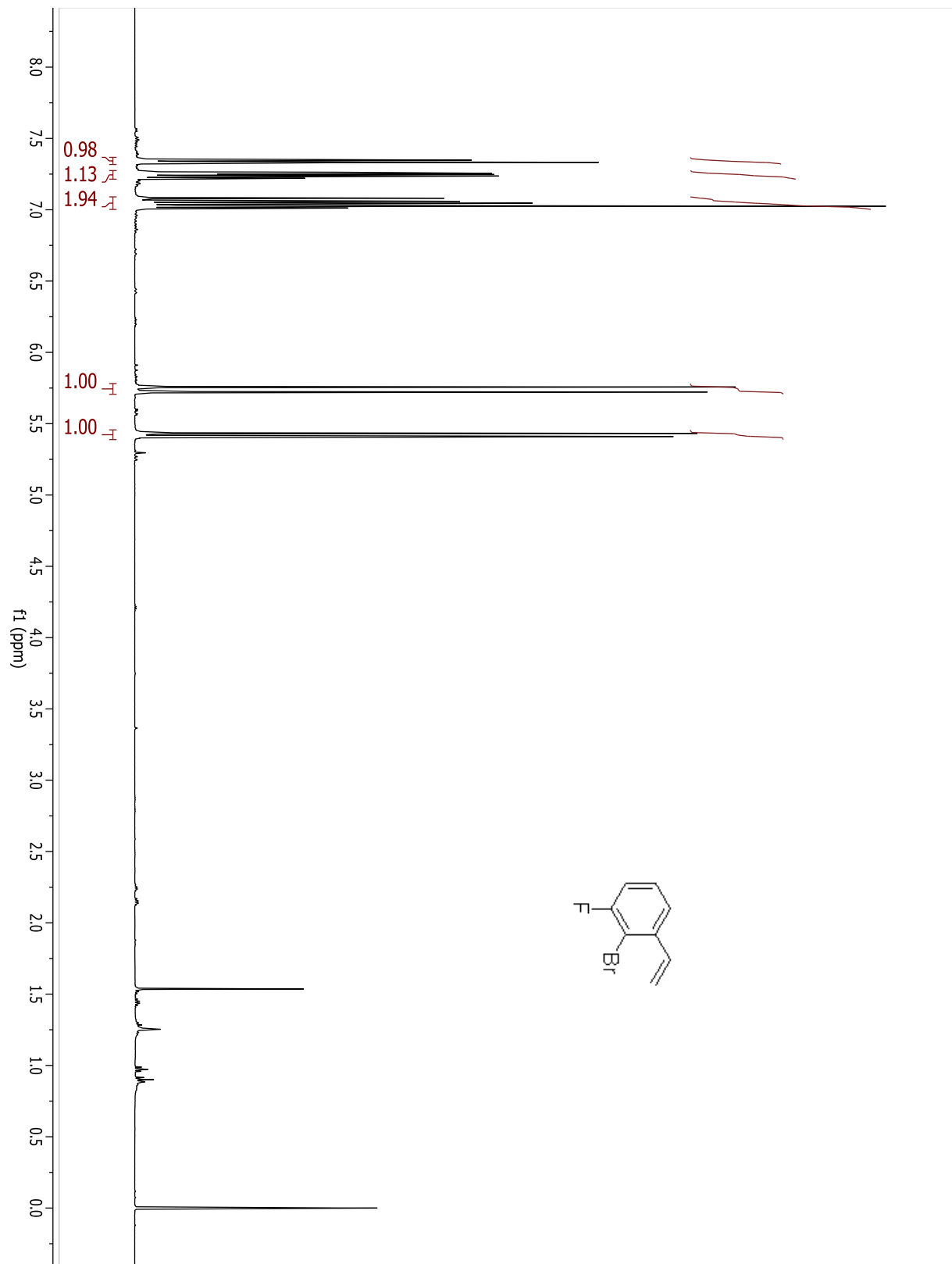
Compound 3.18.



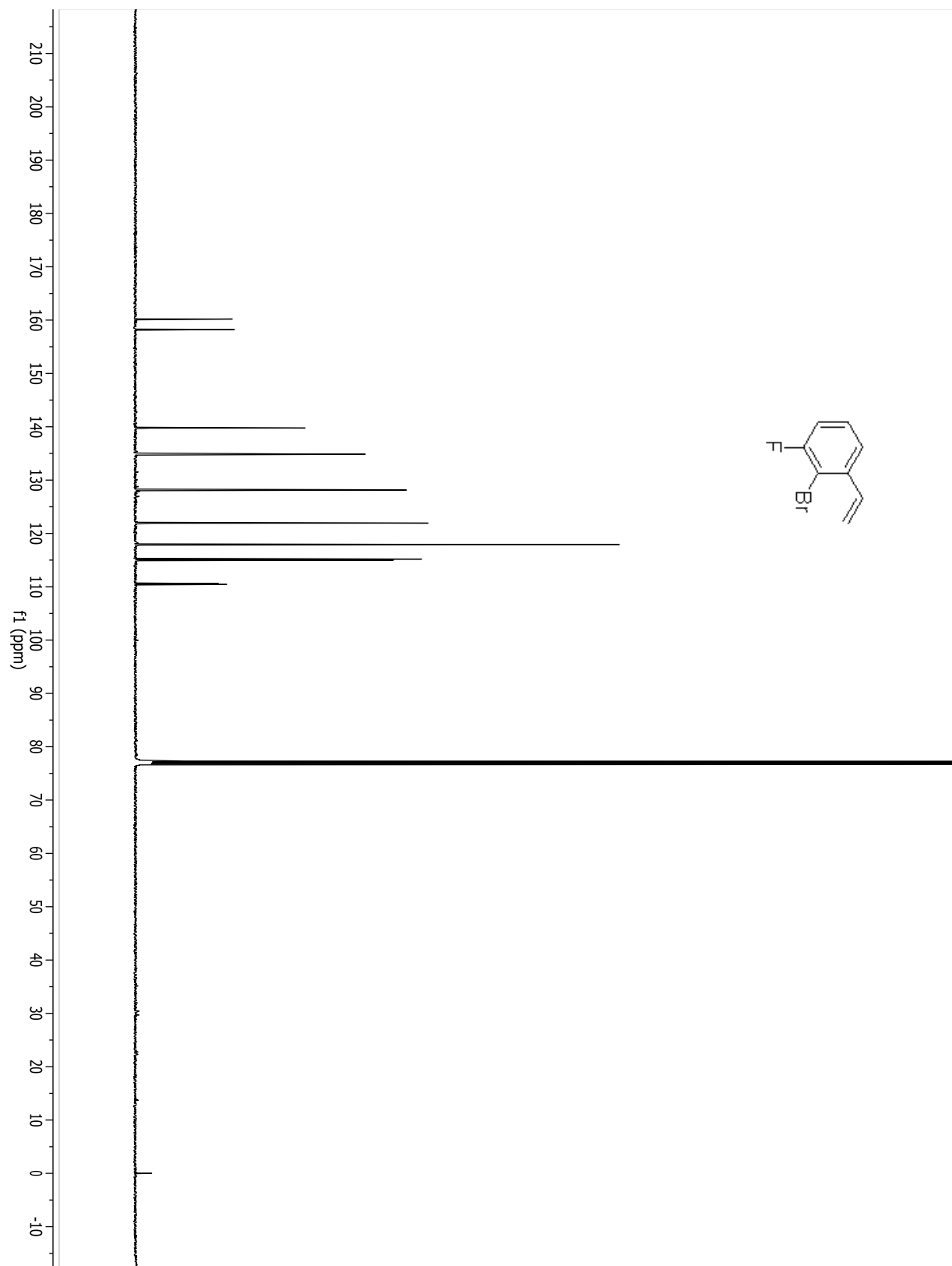
Compound 3.18.



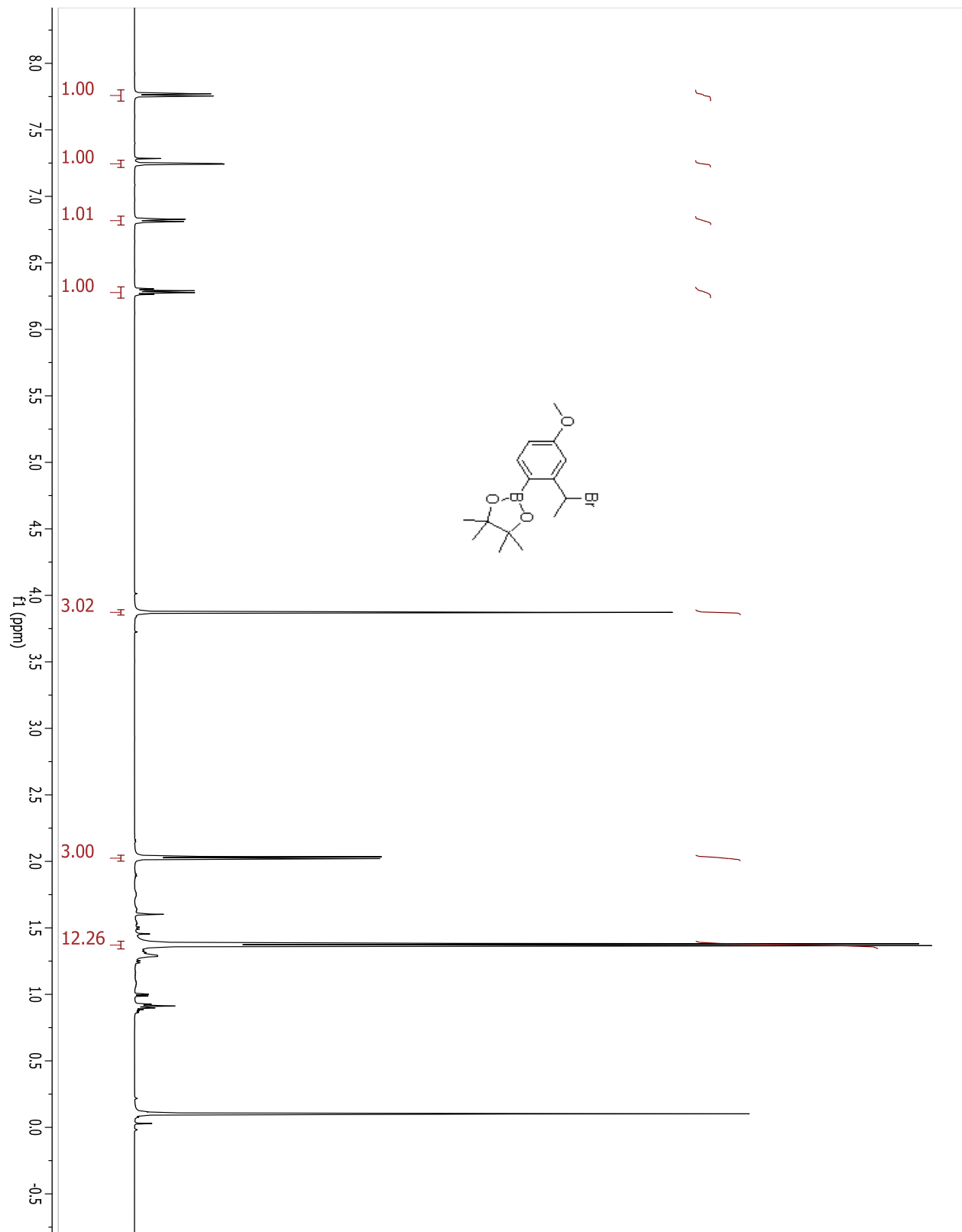
Compound 3.19.



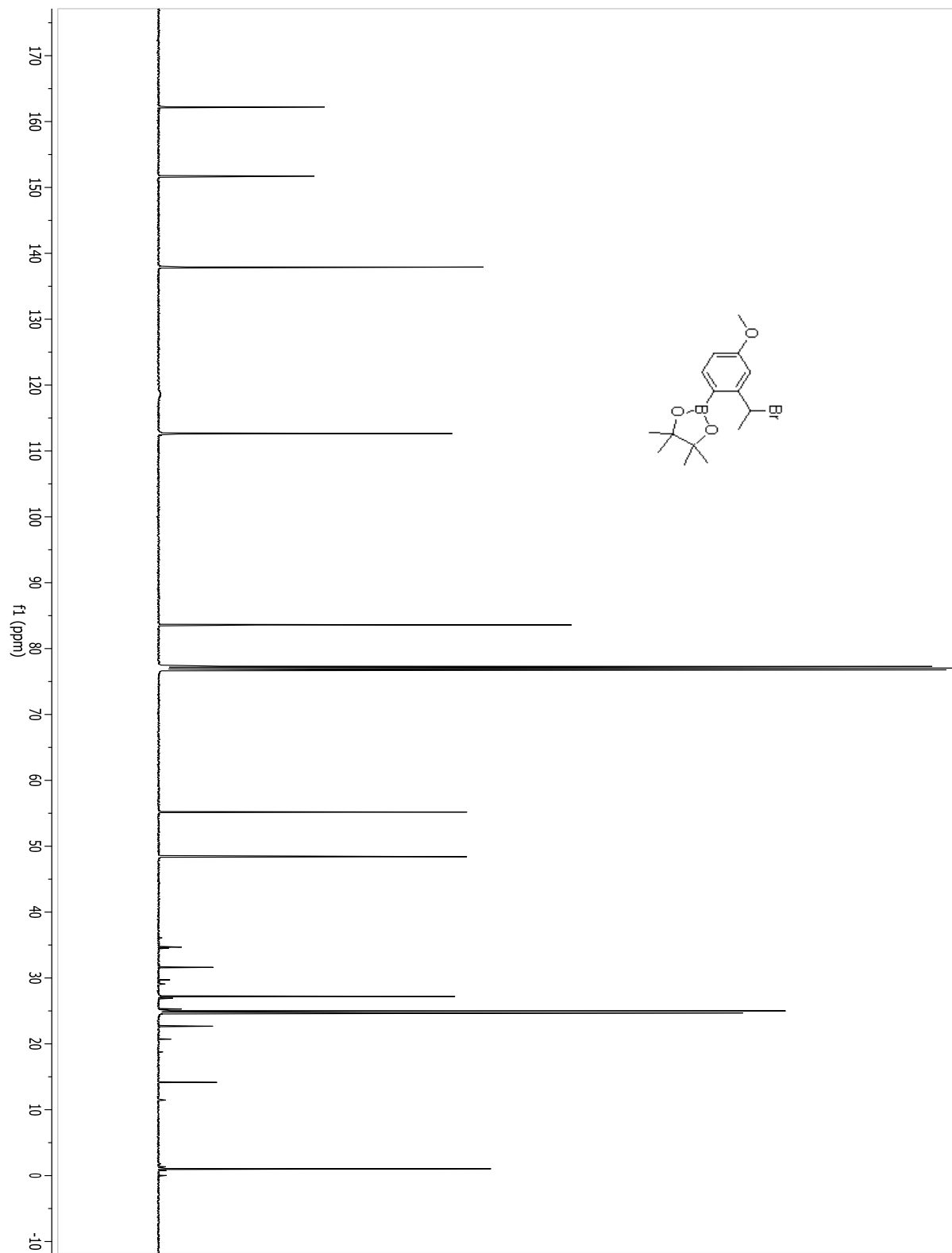
Compound 3.19.



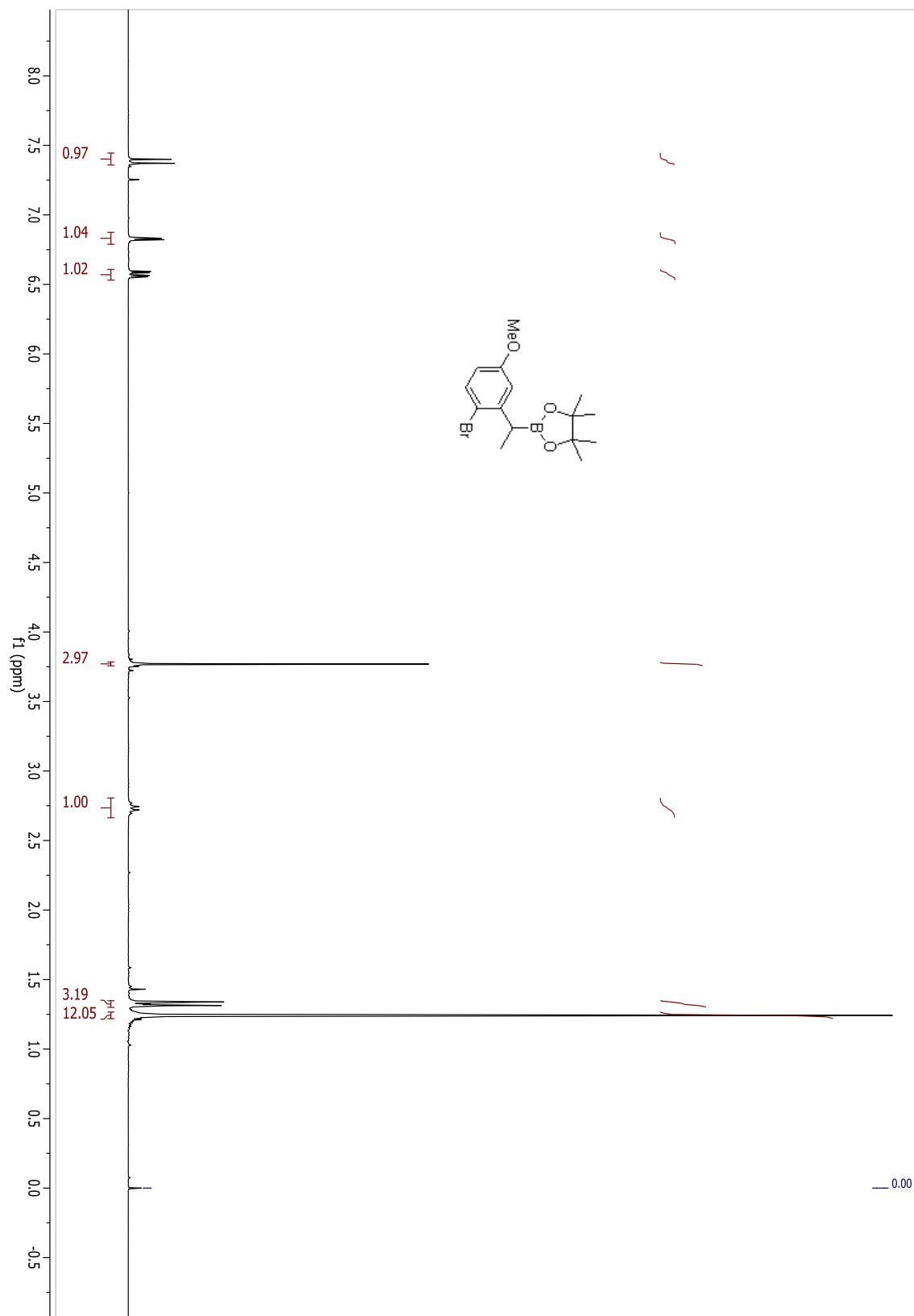
Compound 3.2.



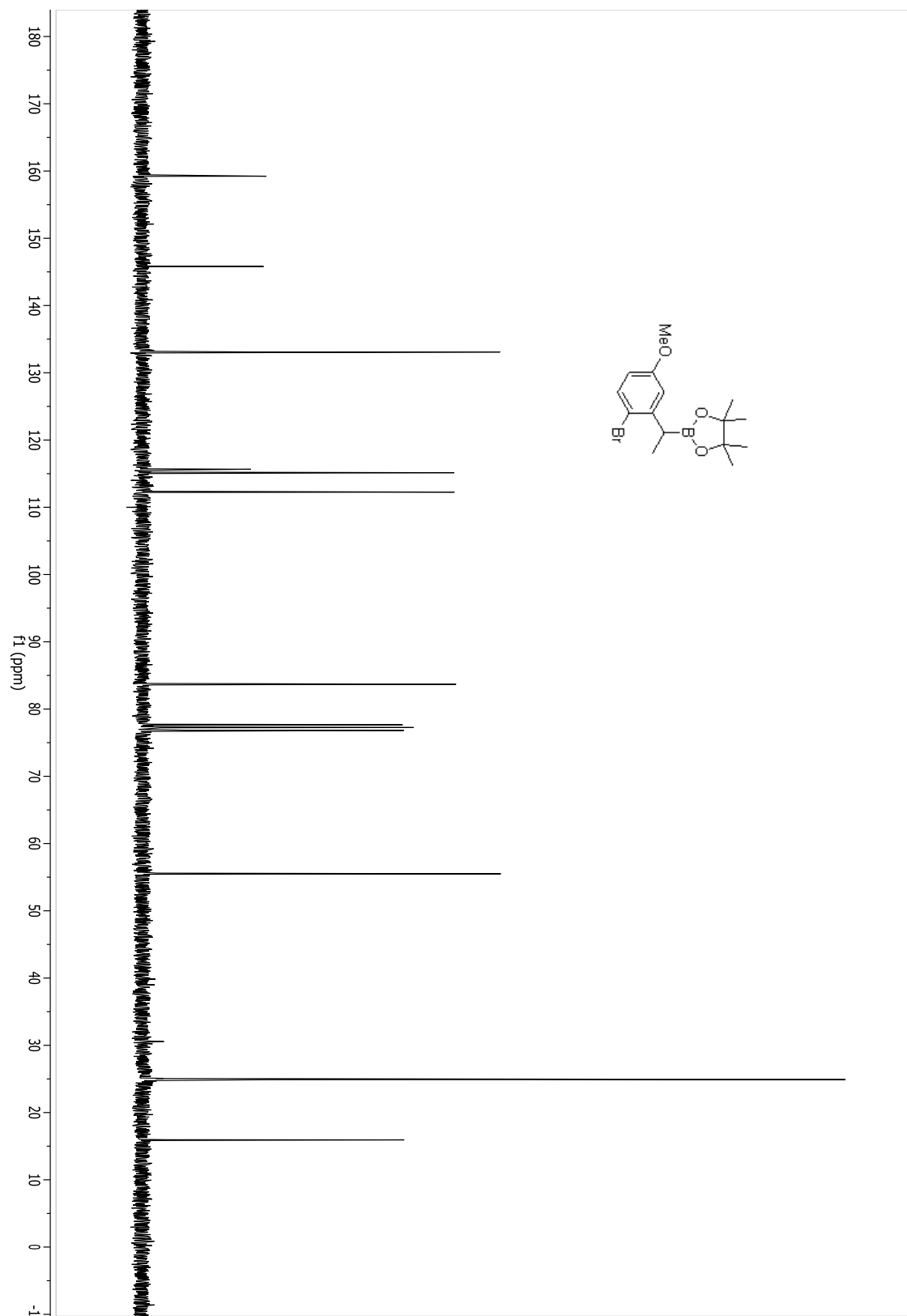
Compound 3.2.



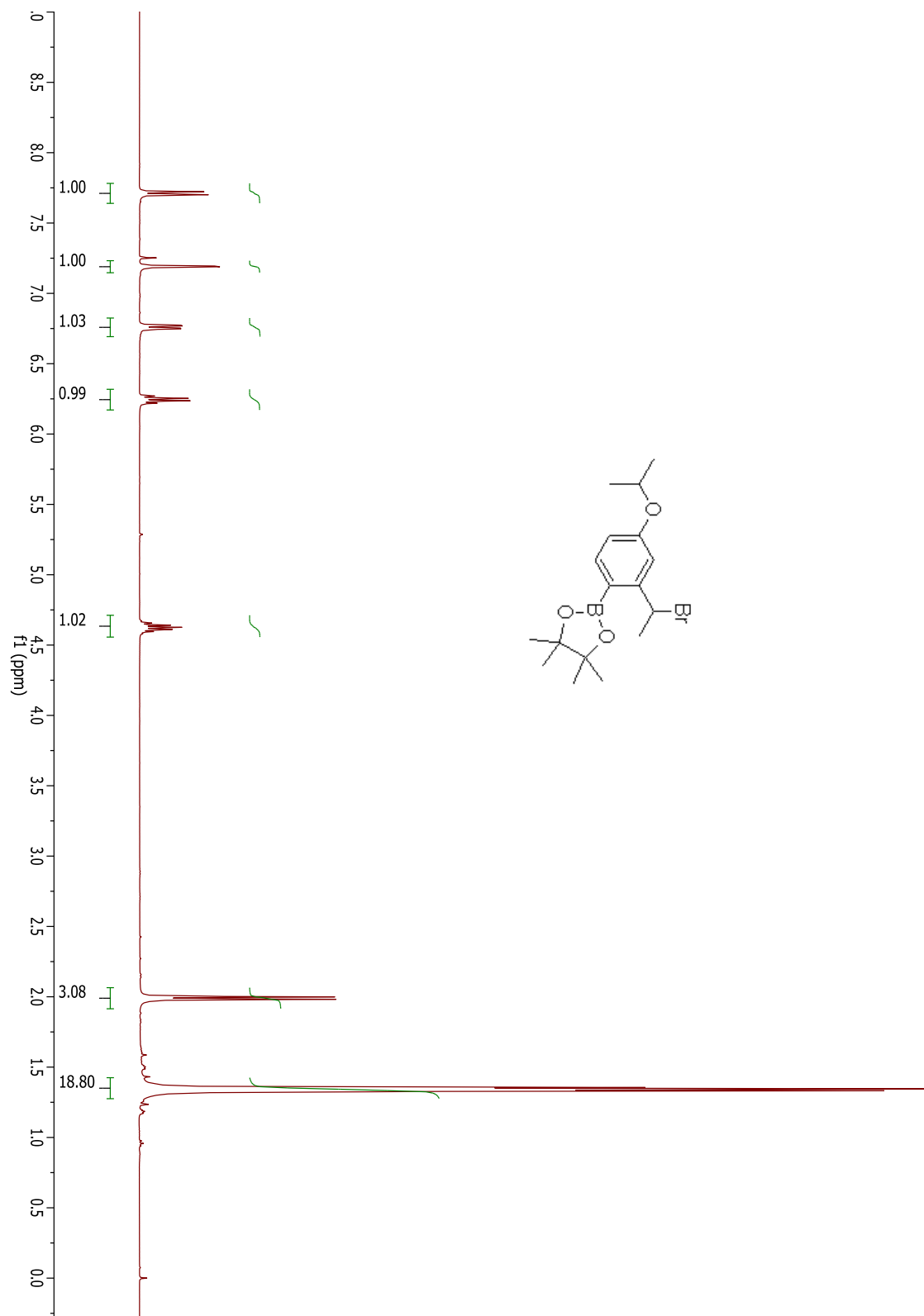
Compound 3.3.



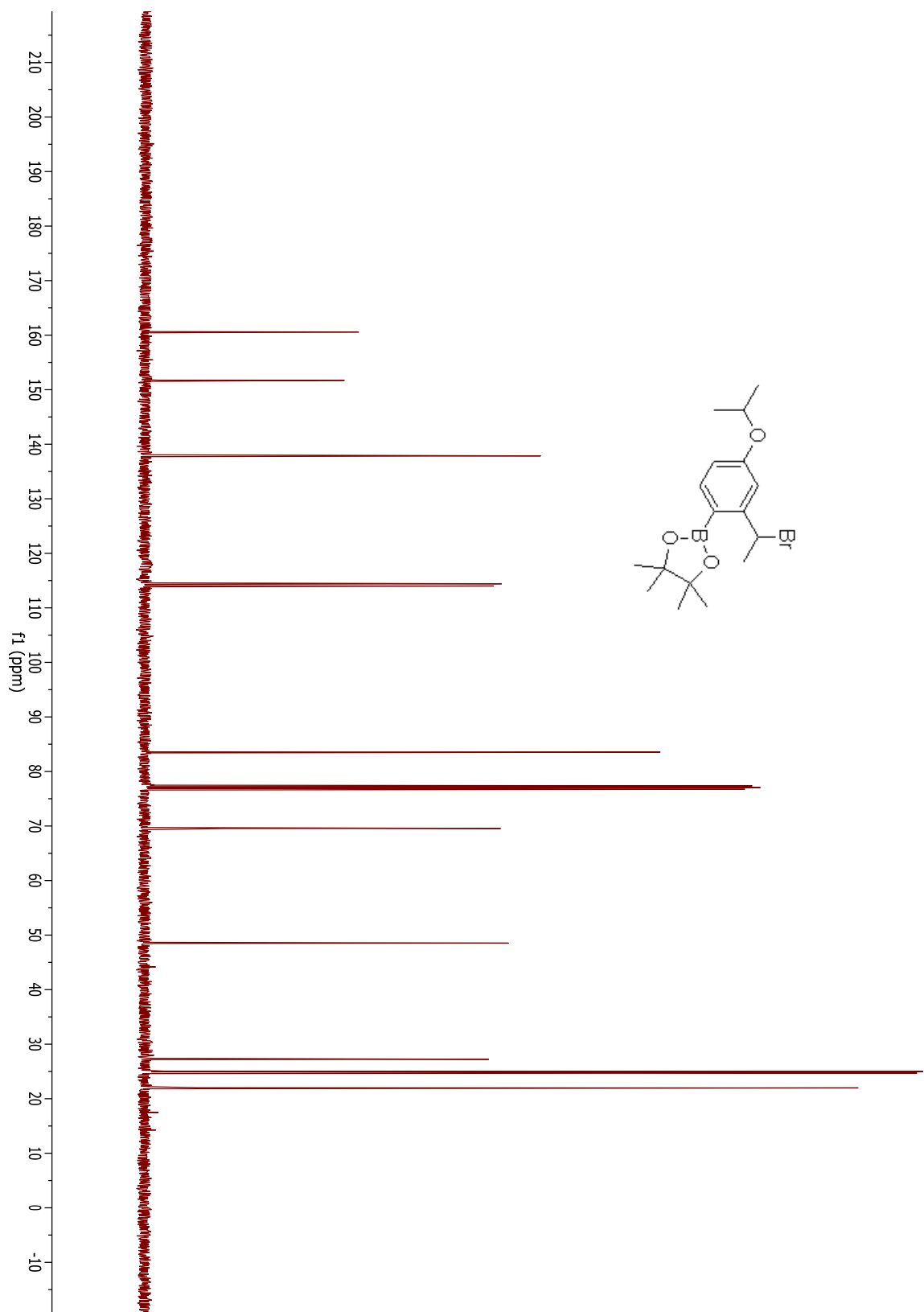
Compound 3.3.



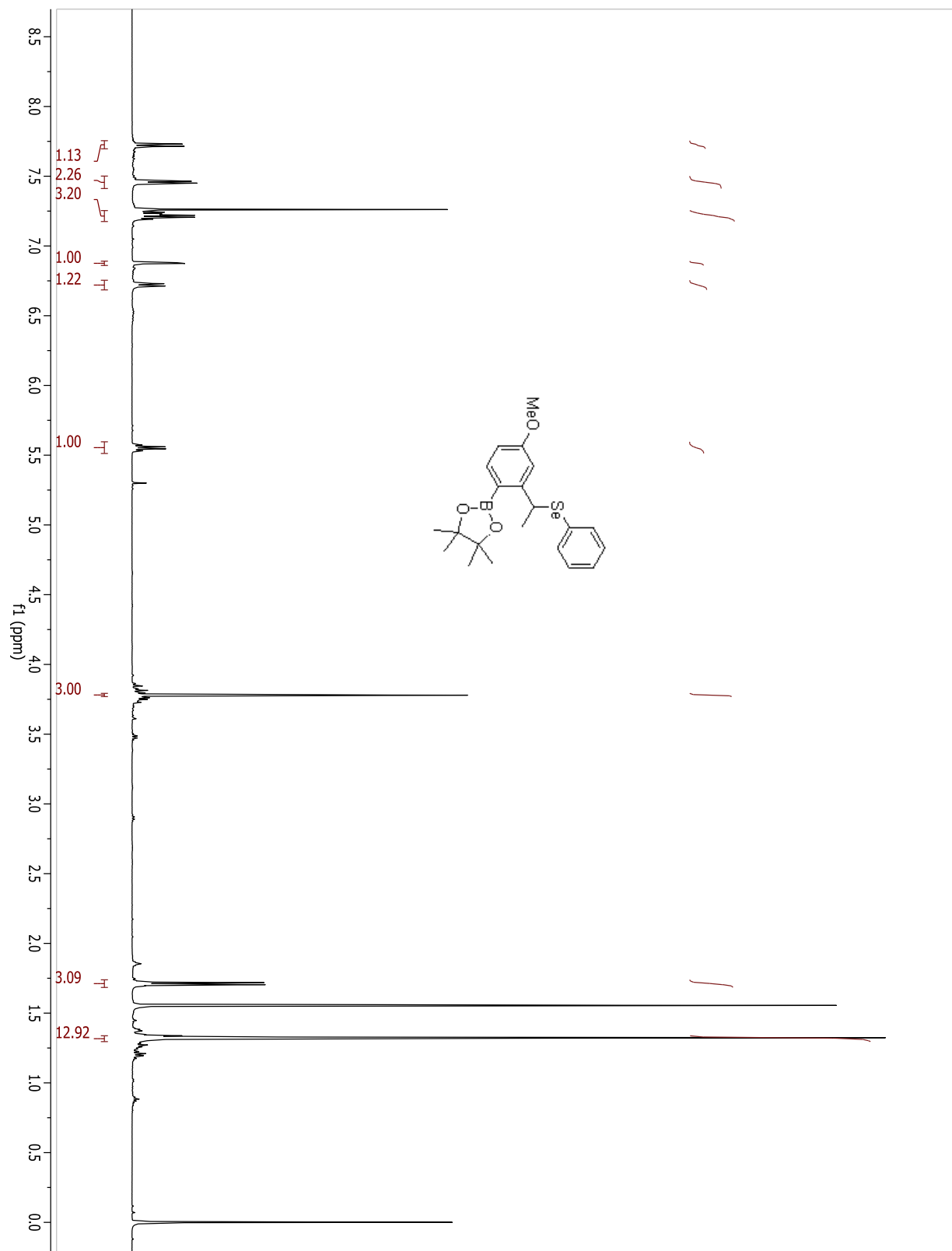
Compound 3.9.



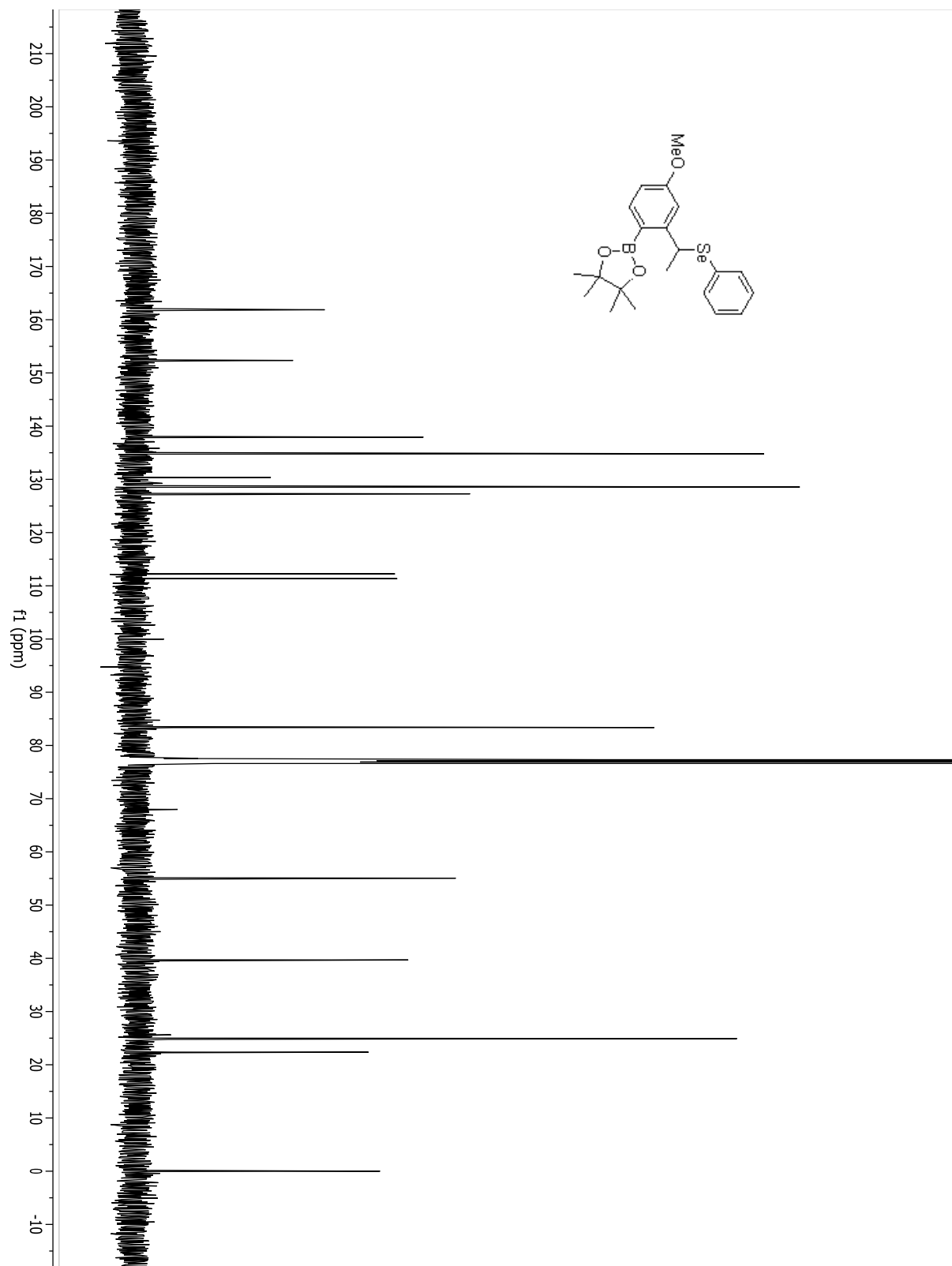
Compound 3.9.



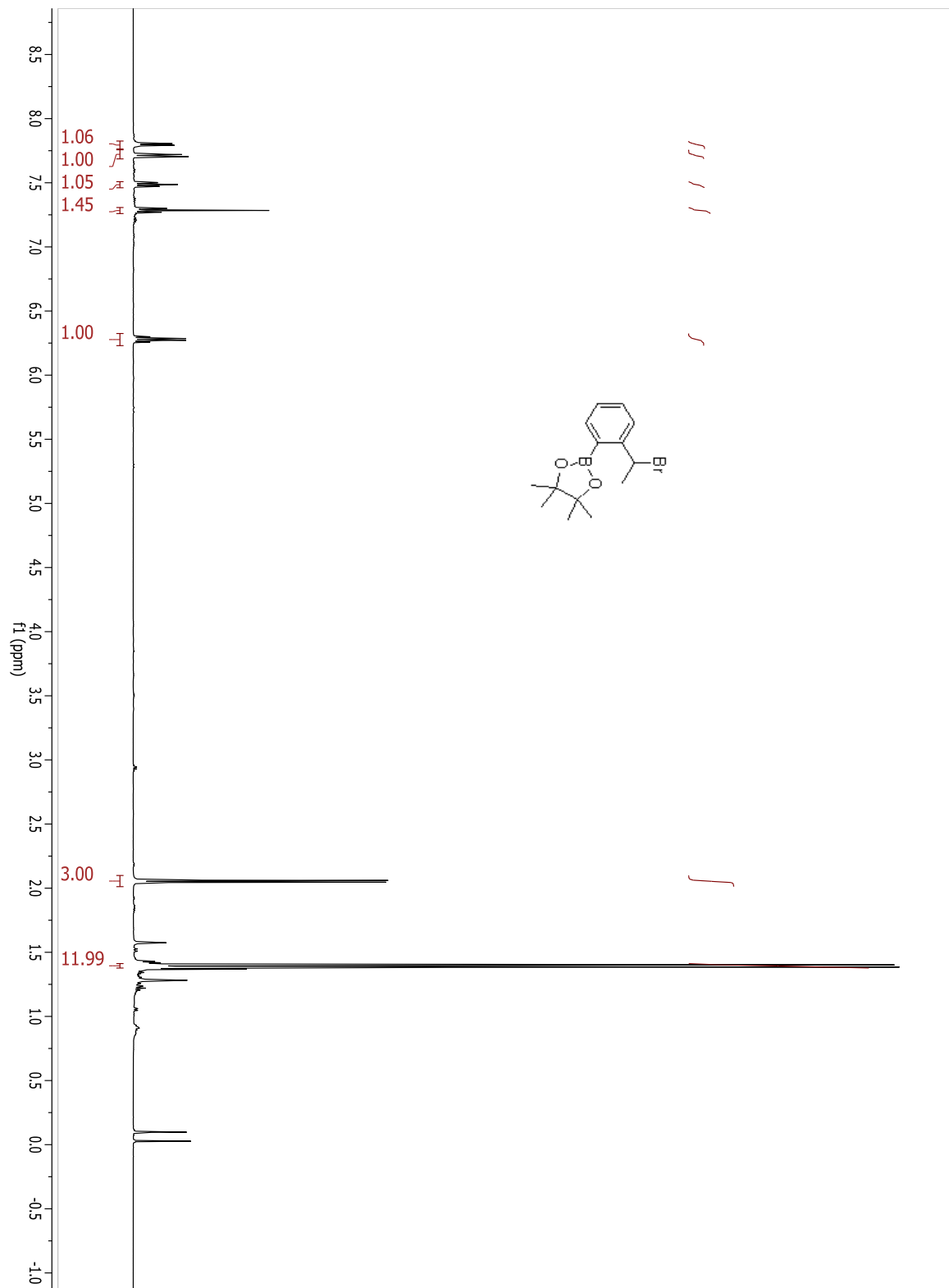
Selenide of Compound 3.10.



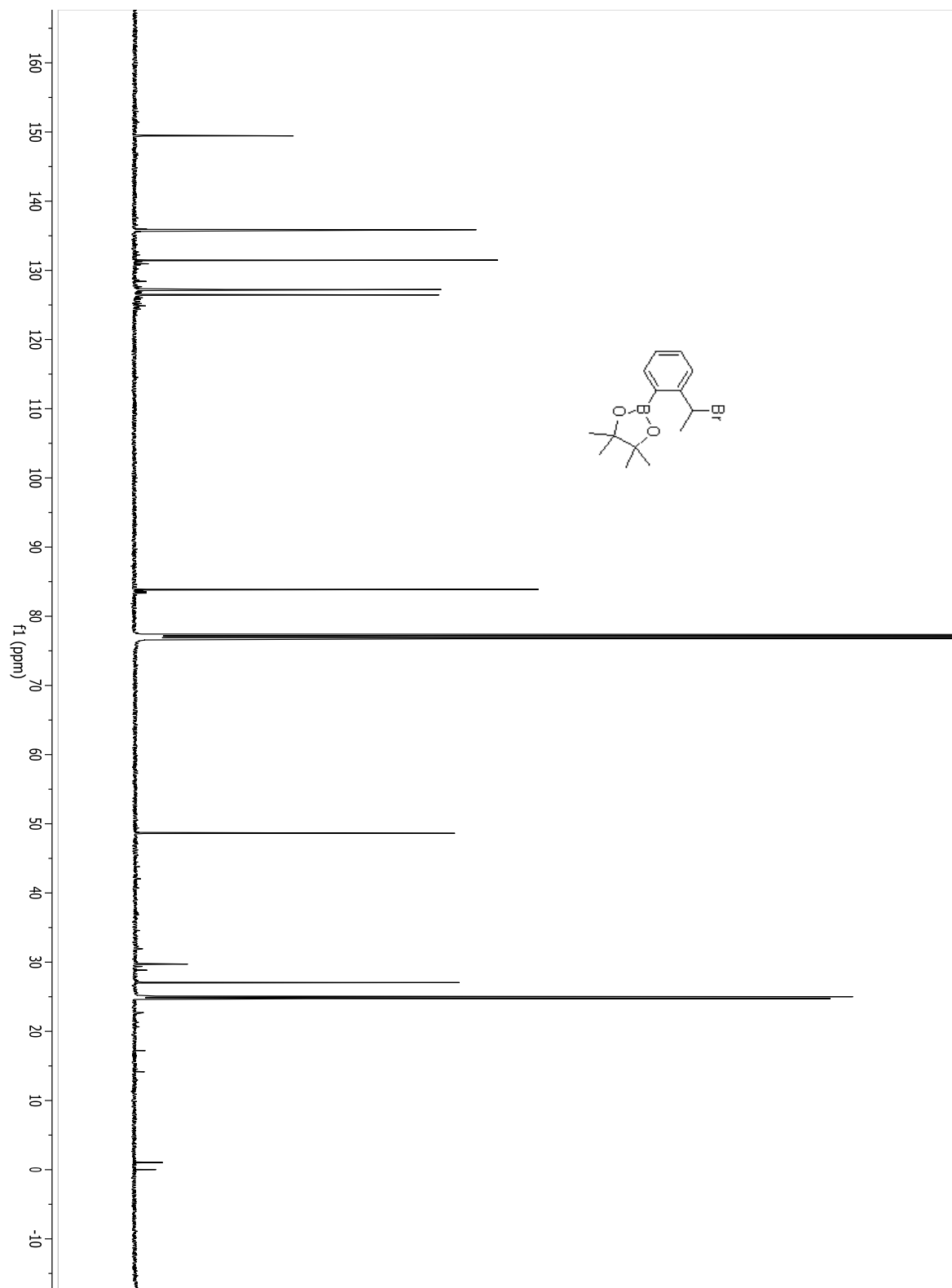
Selenide of Compound 3.10.



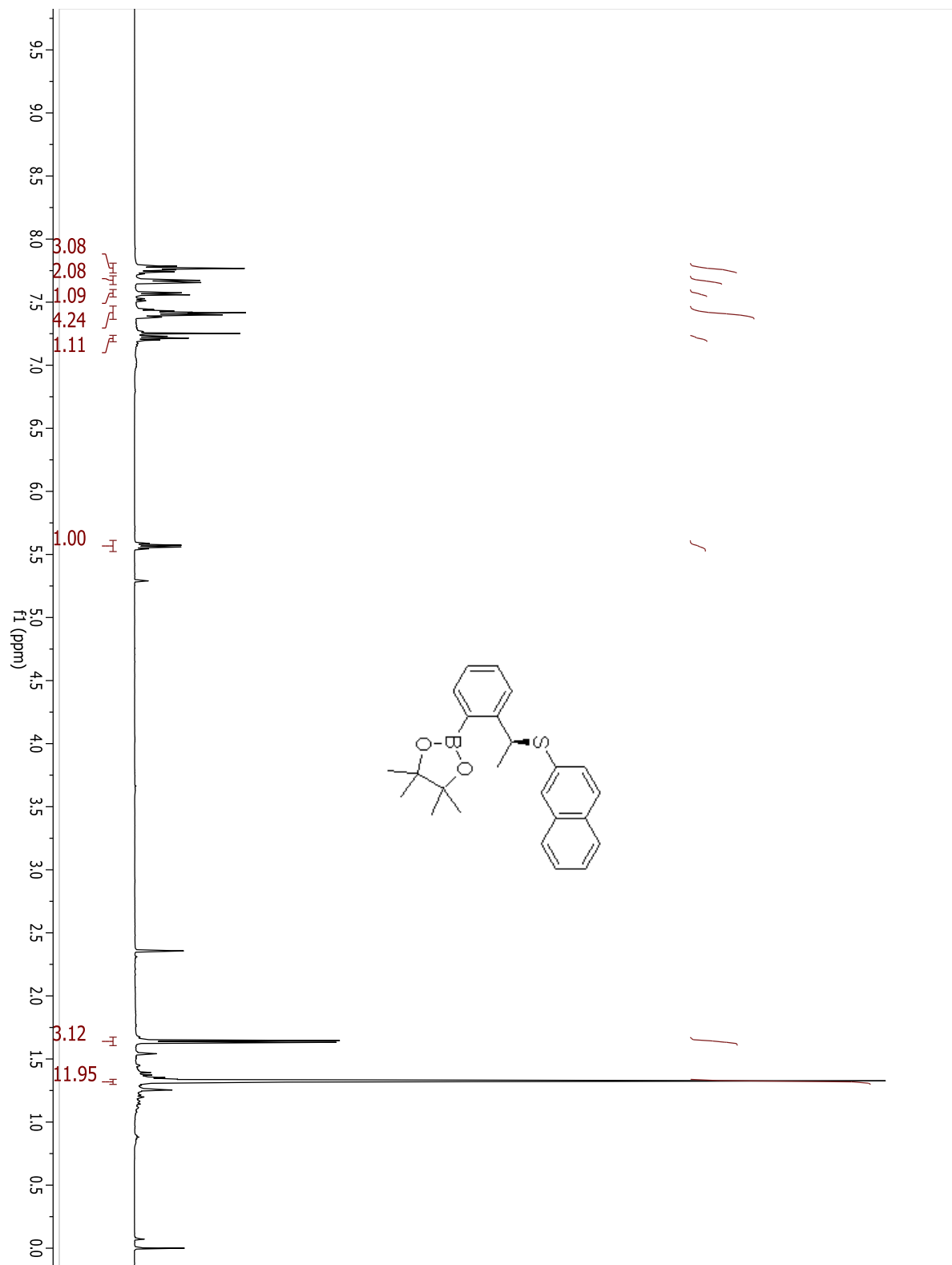
Compound 3.11.



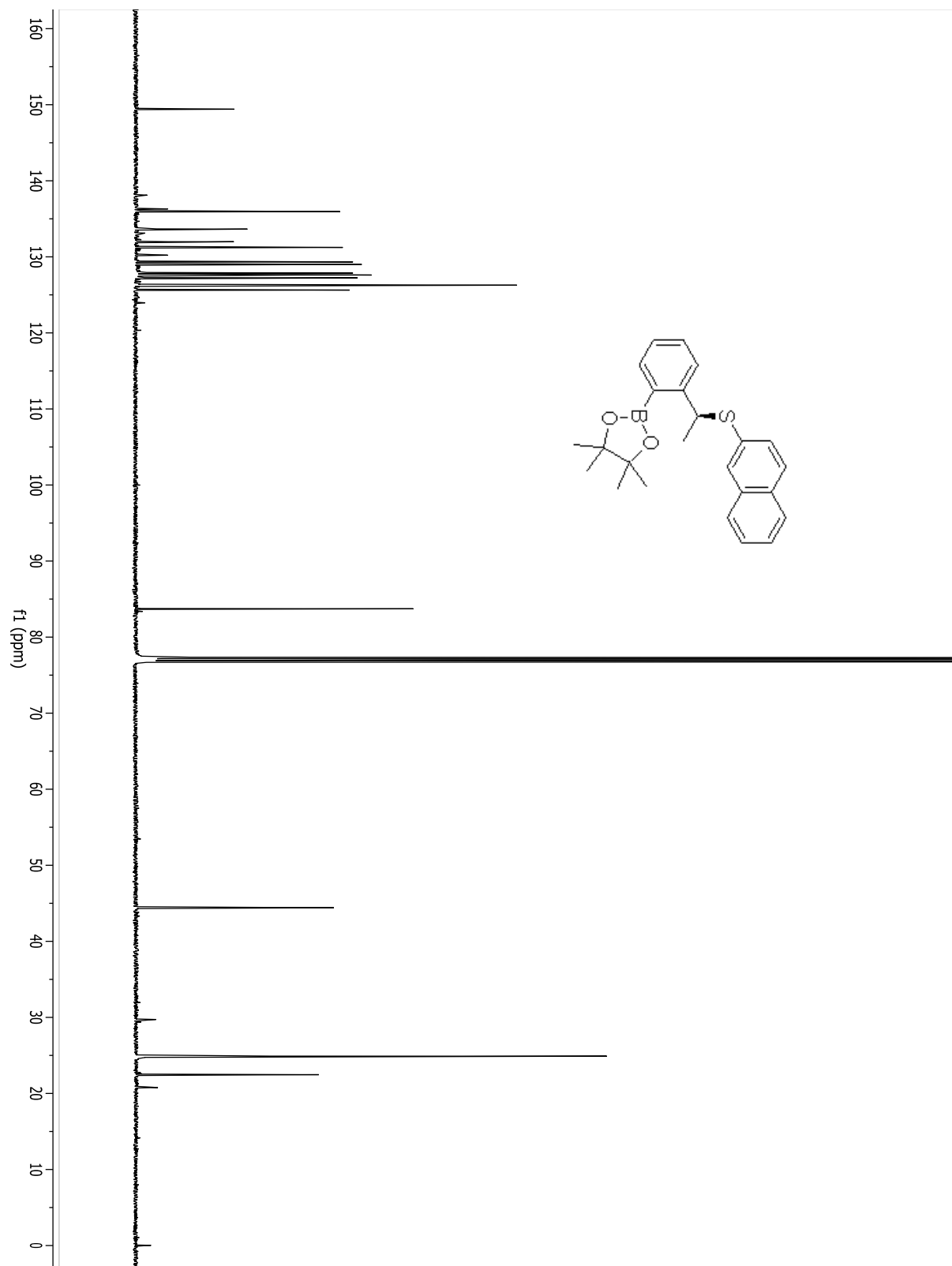
Compound 3.11.



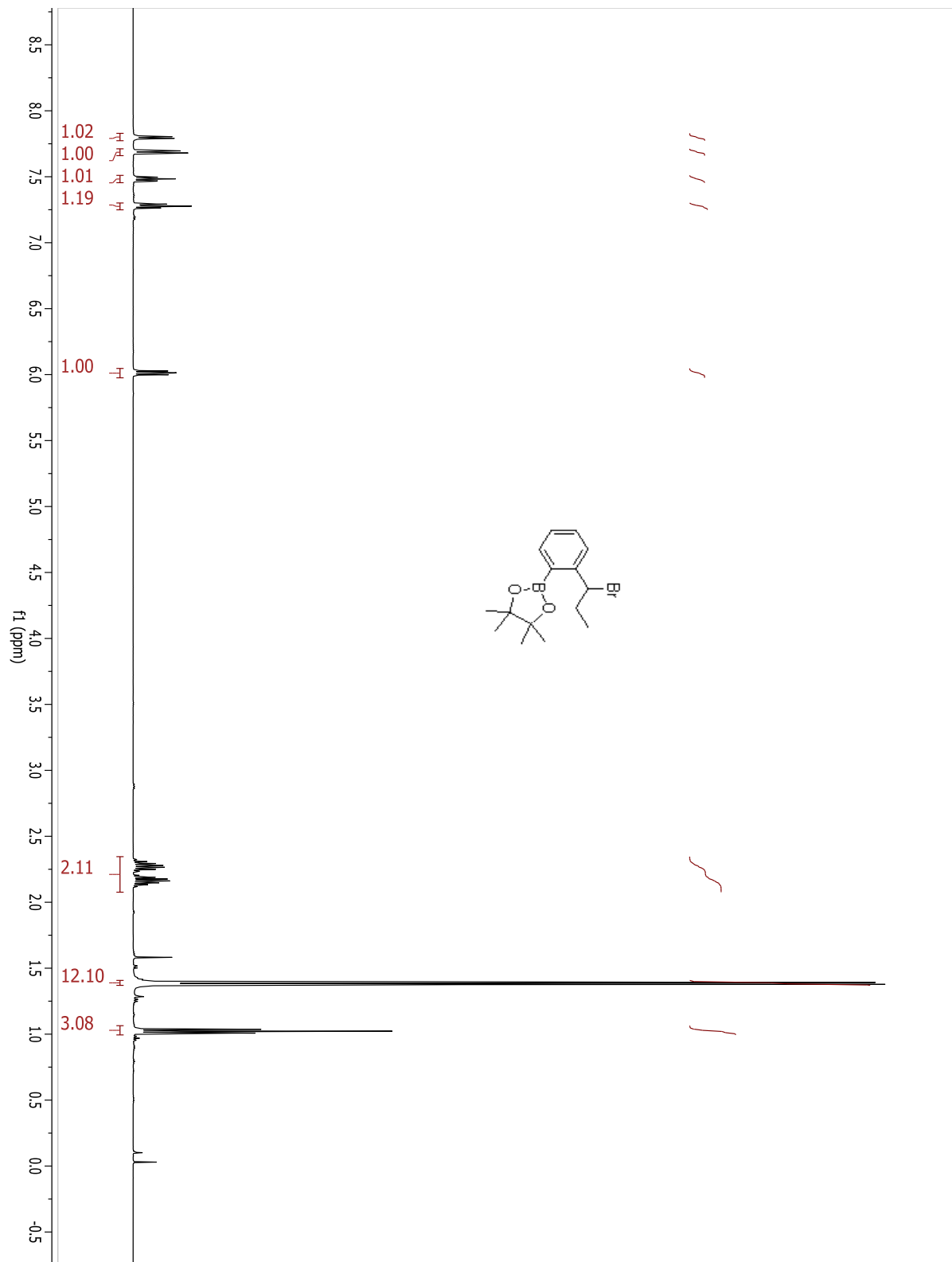
Sulfide of Compound 3.11.



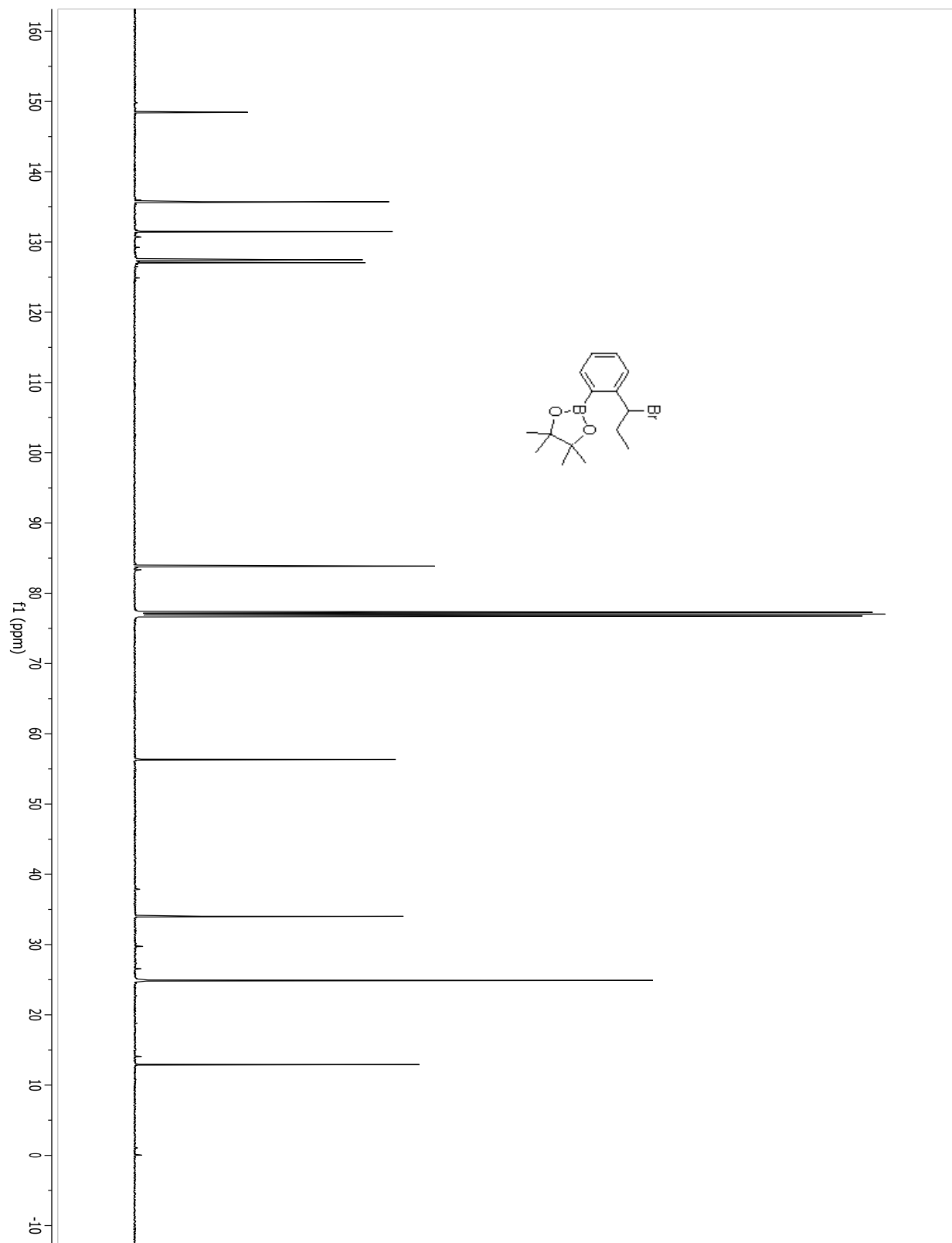
Sulfide of Compound 3.11.



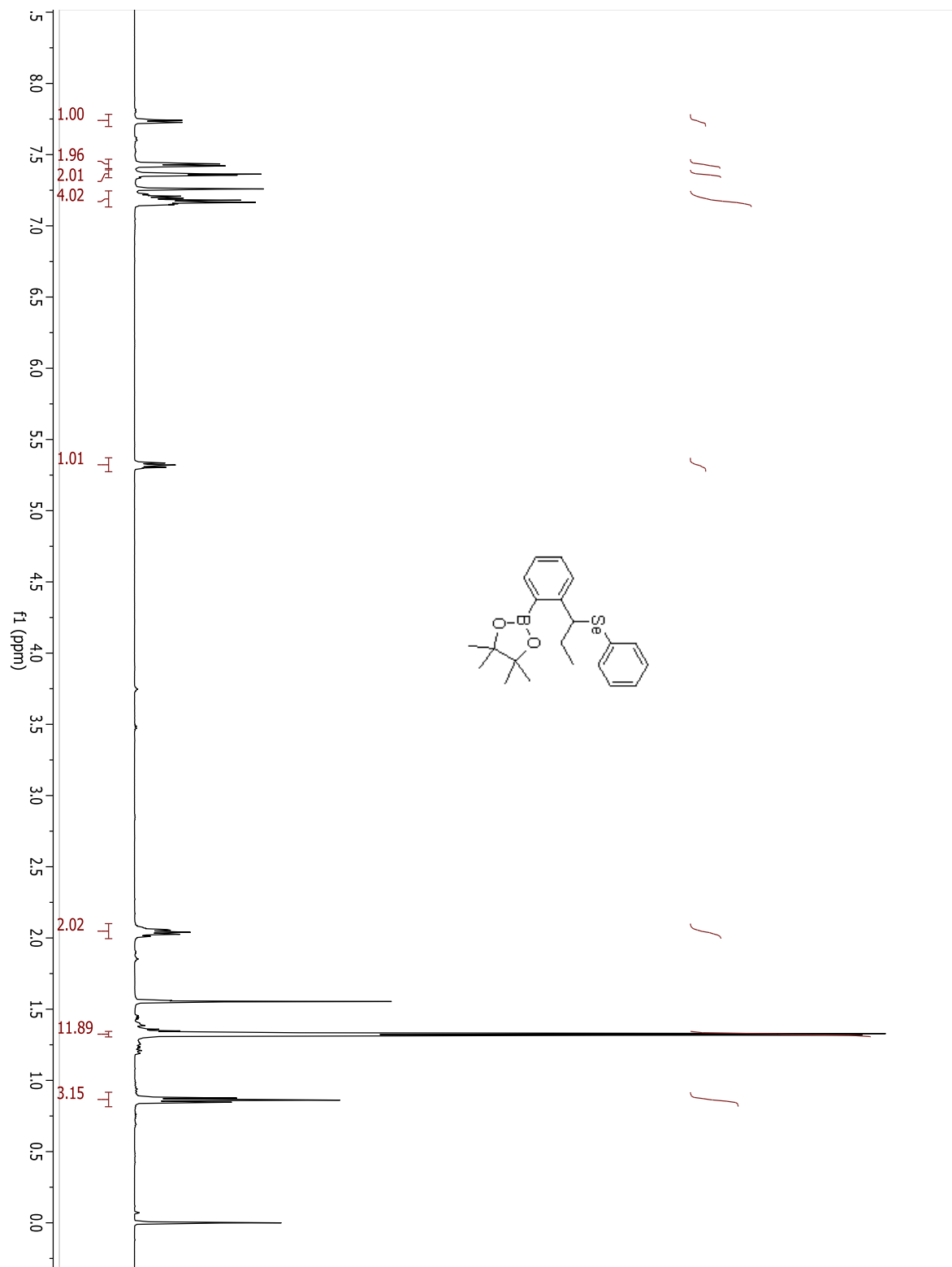
Compound 3.12.



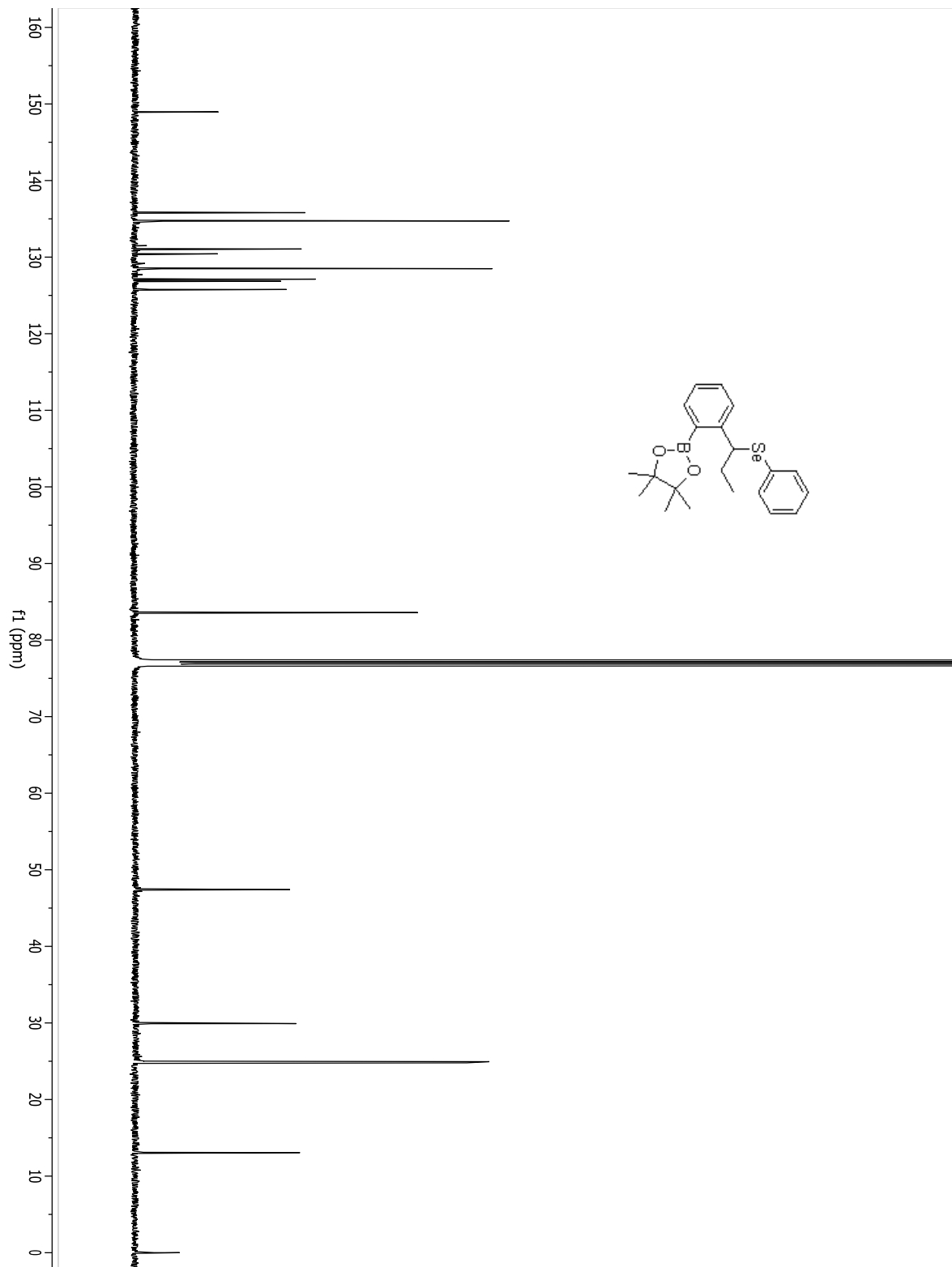
Compound 3.12.



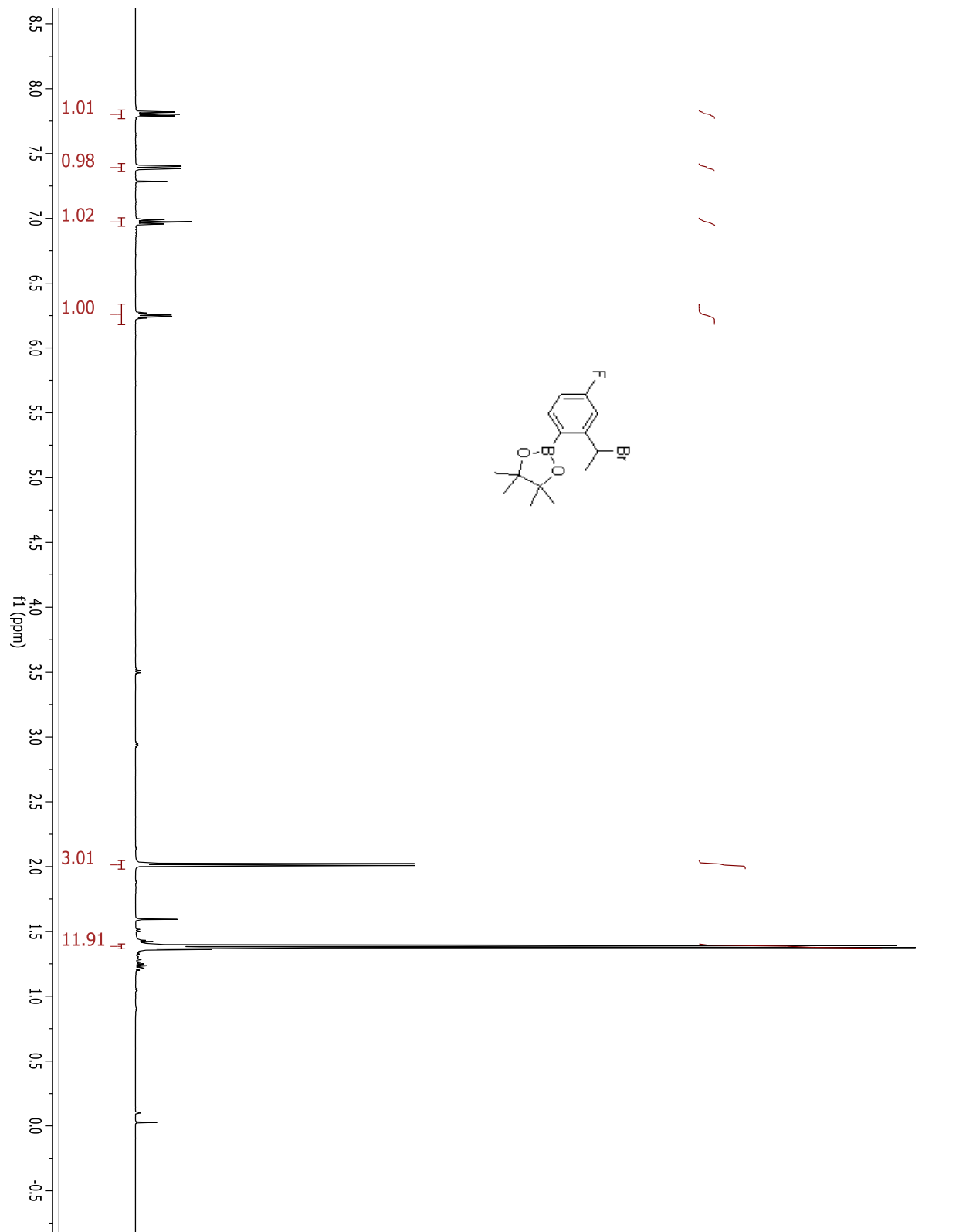
Selenide of Compound 3.12.



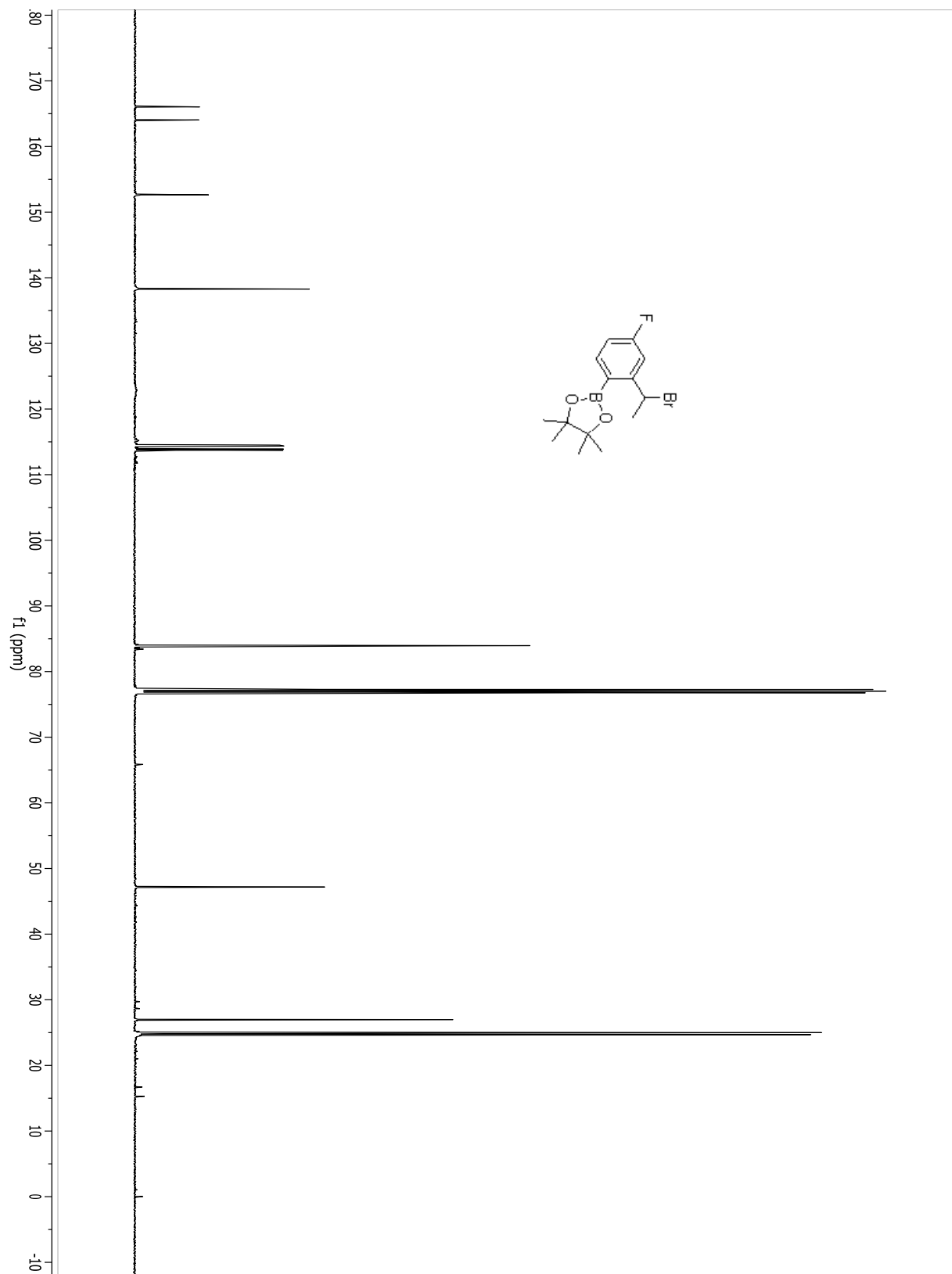
Selenide of Compound 3.12.



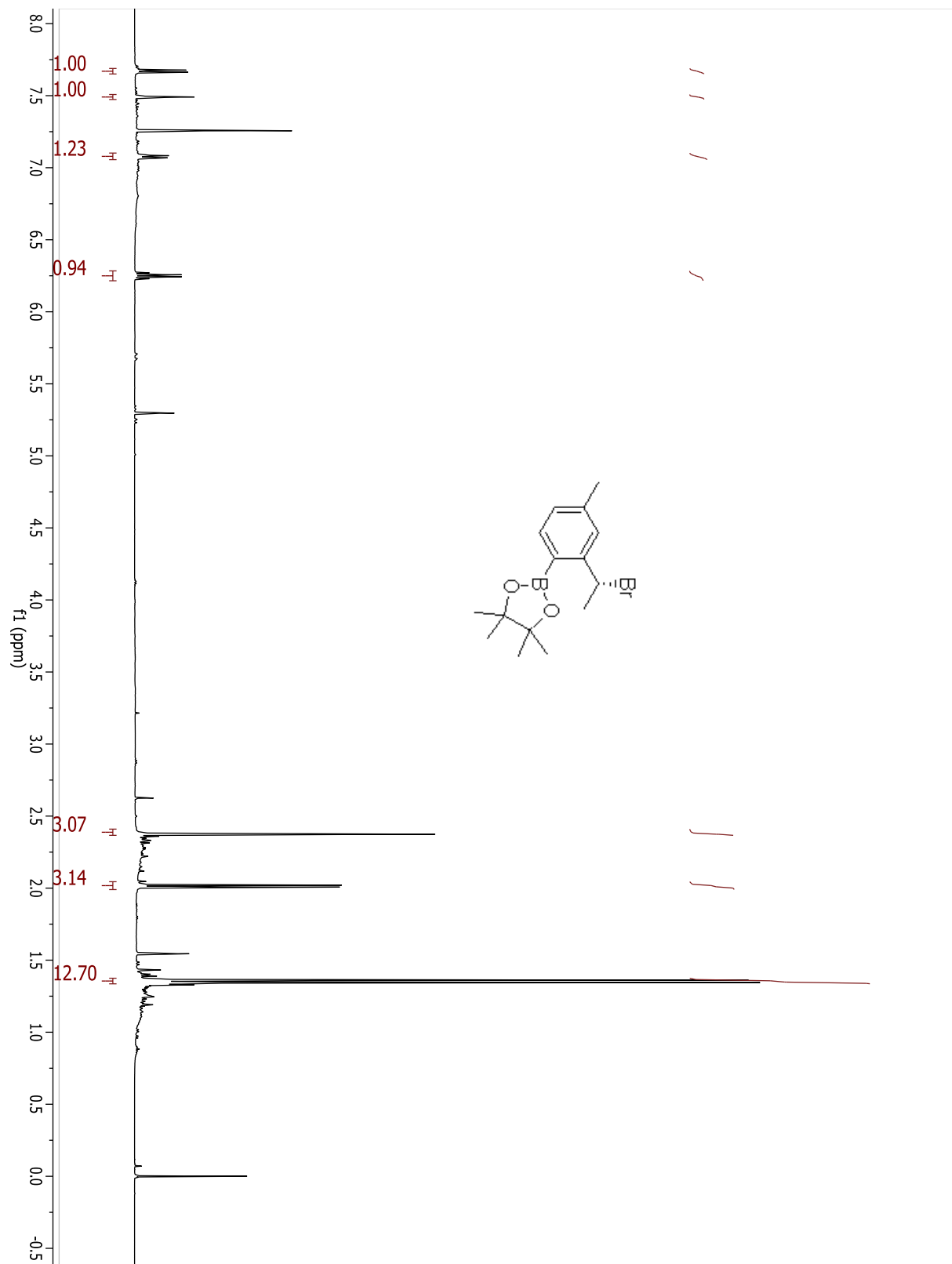
Compound 3.13.



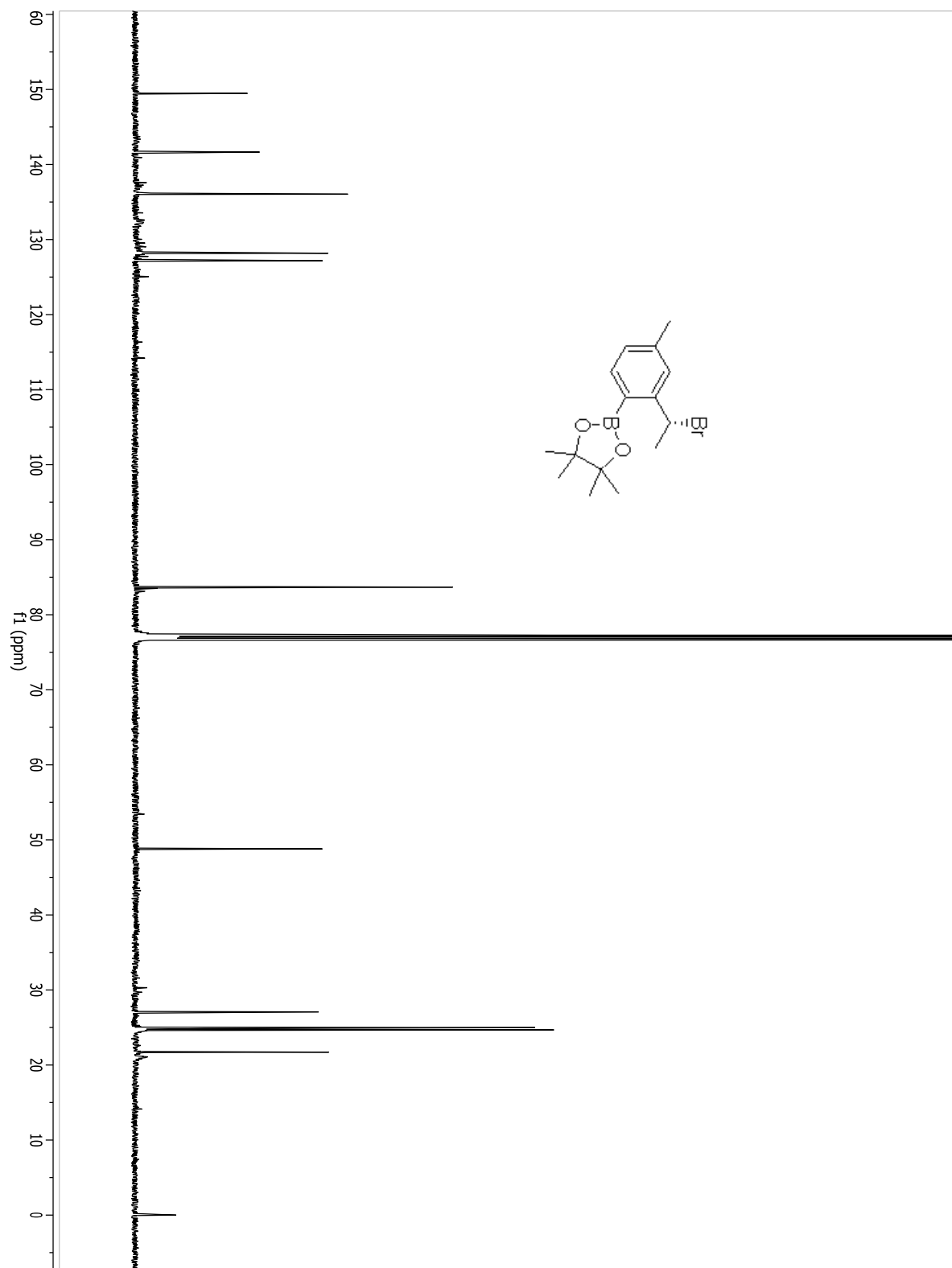
Compound 3.13.



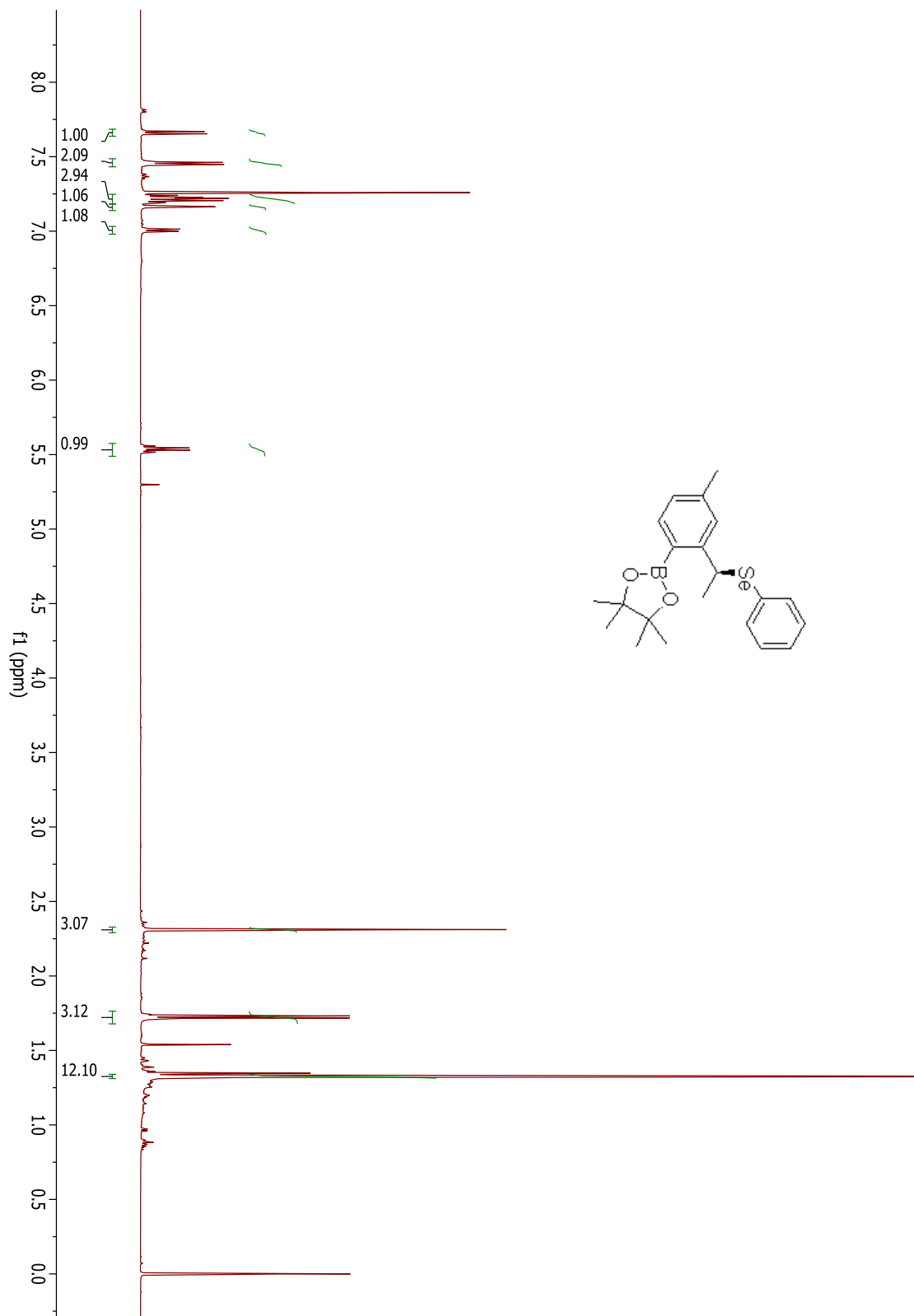
Compound 3.21.



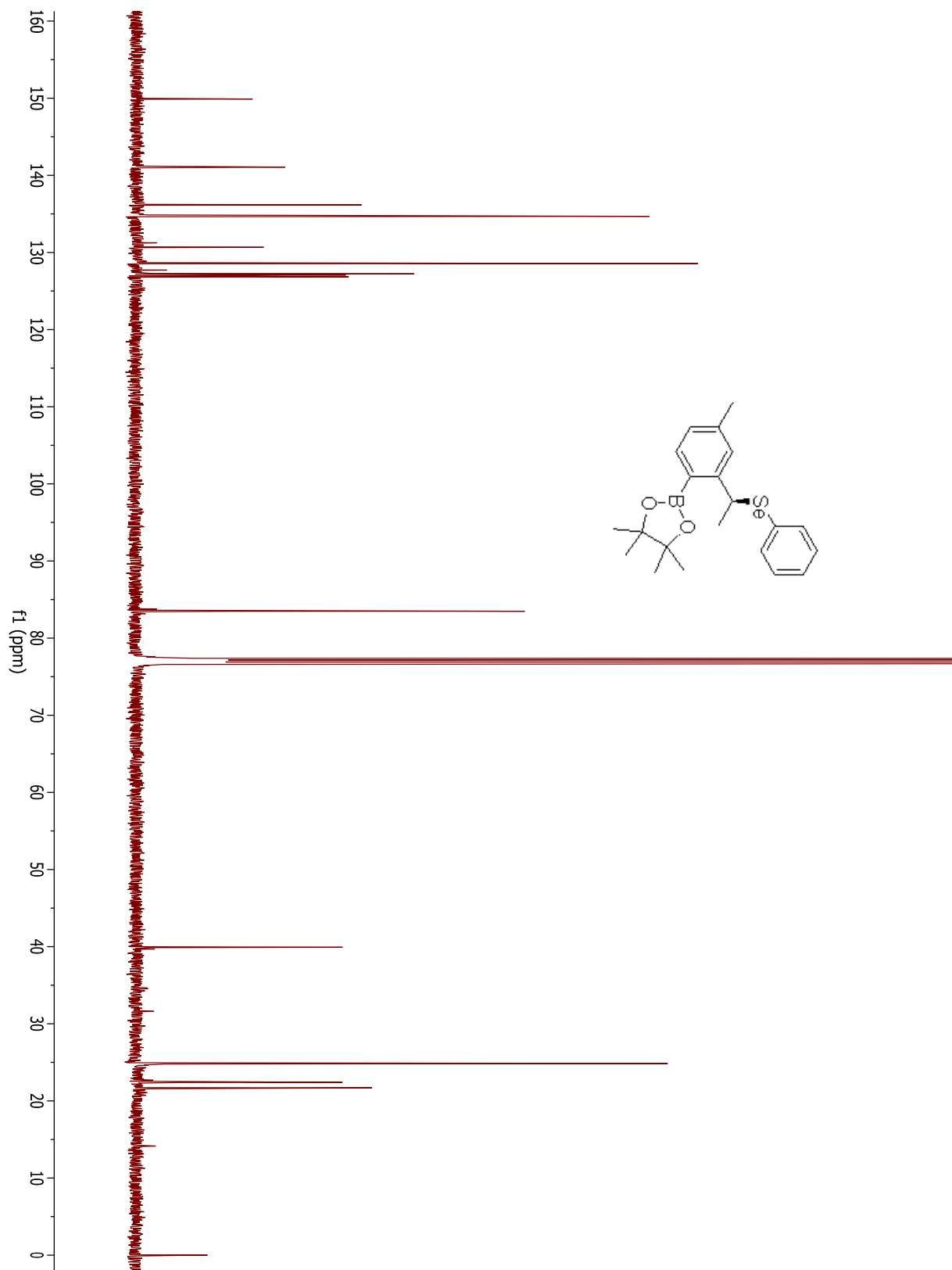
Compound 3.21.



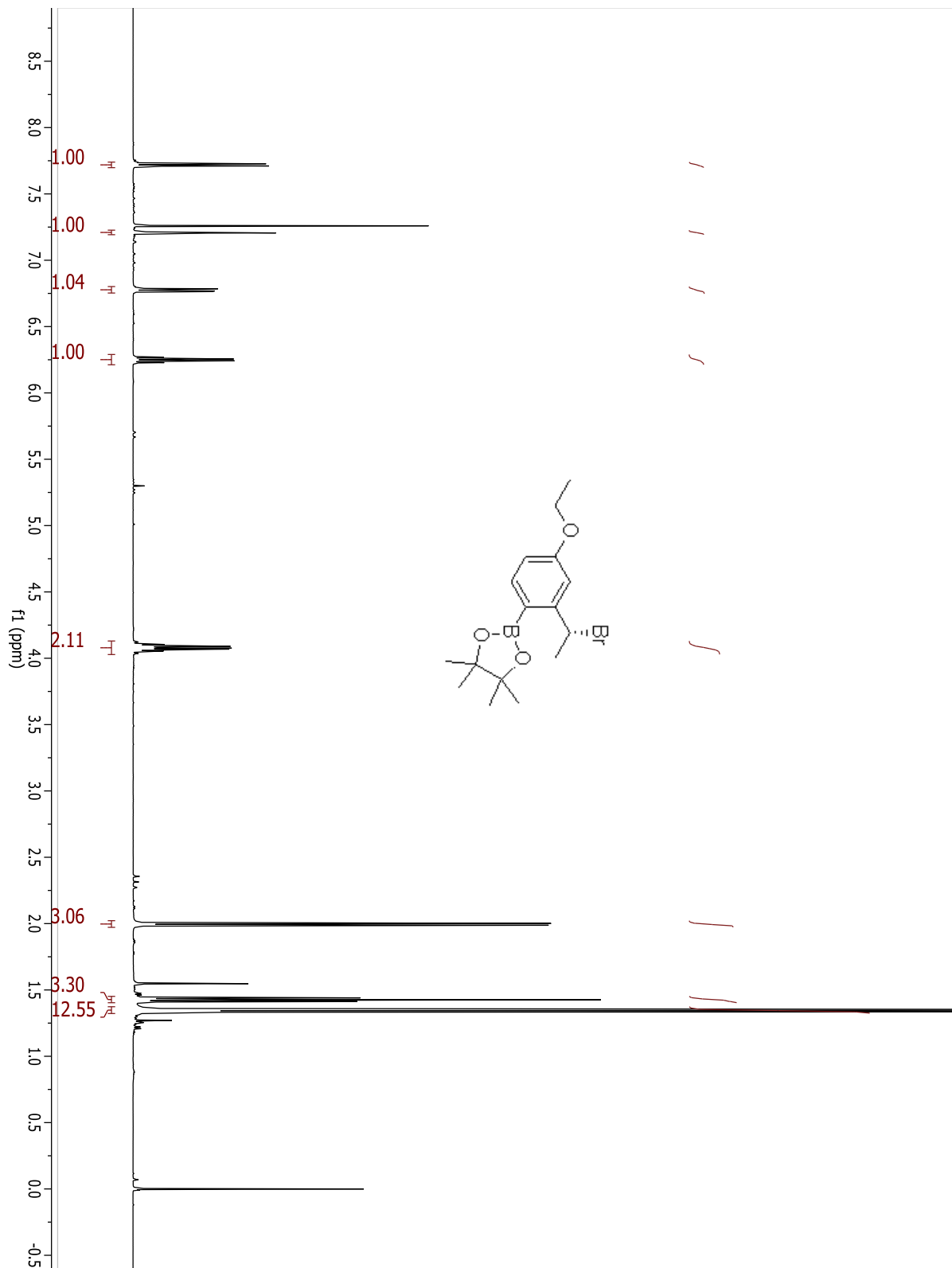
Selenide of 3.21.



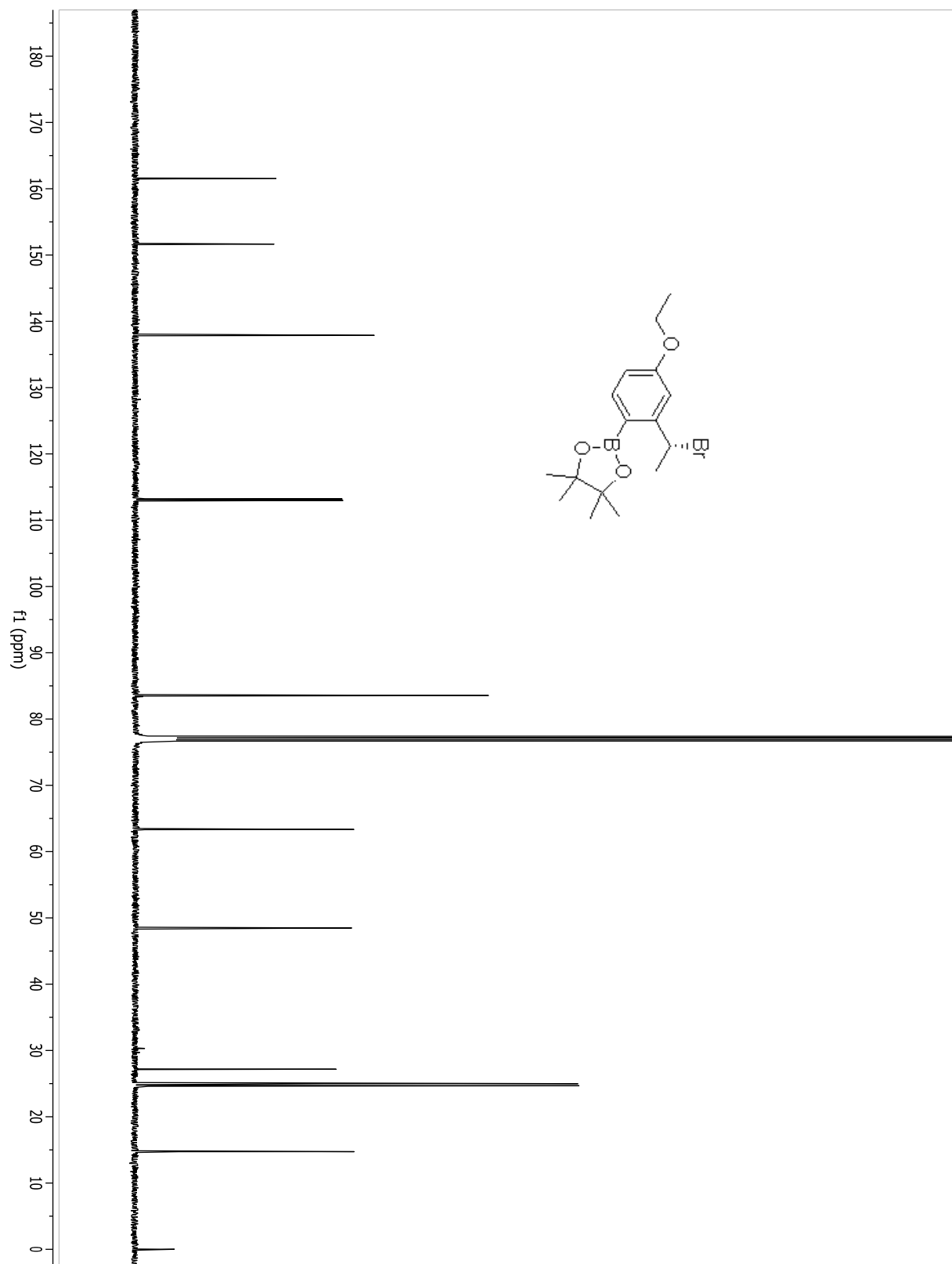
Selenide of 3.21.



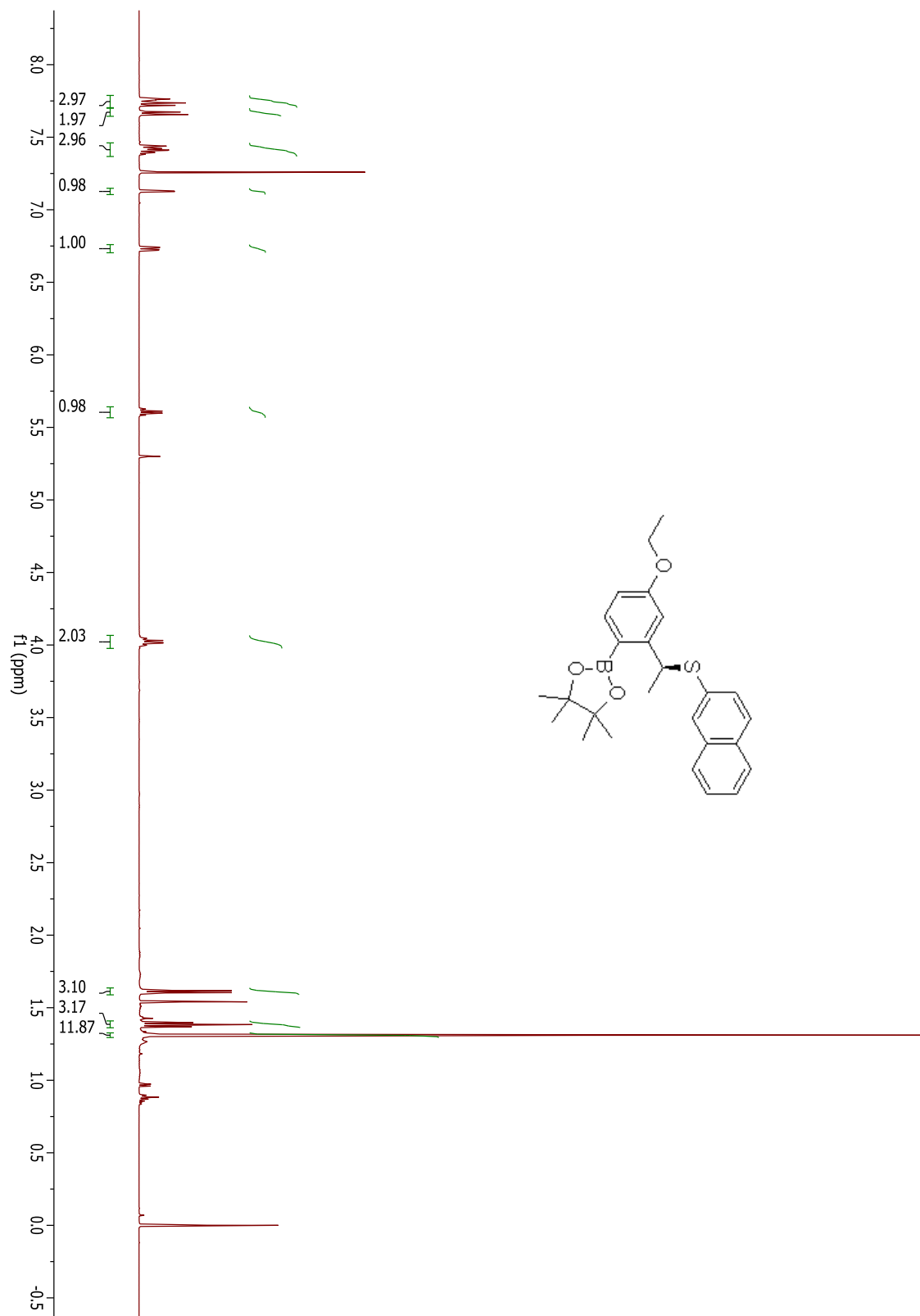
Compound 3.22.



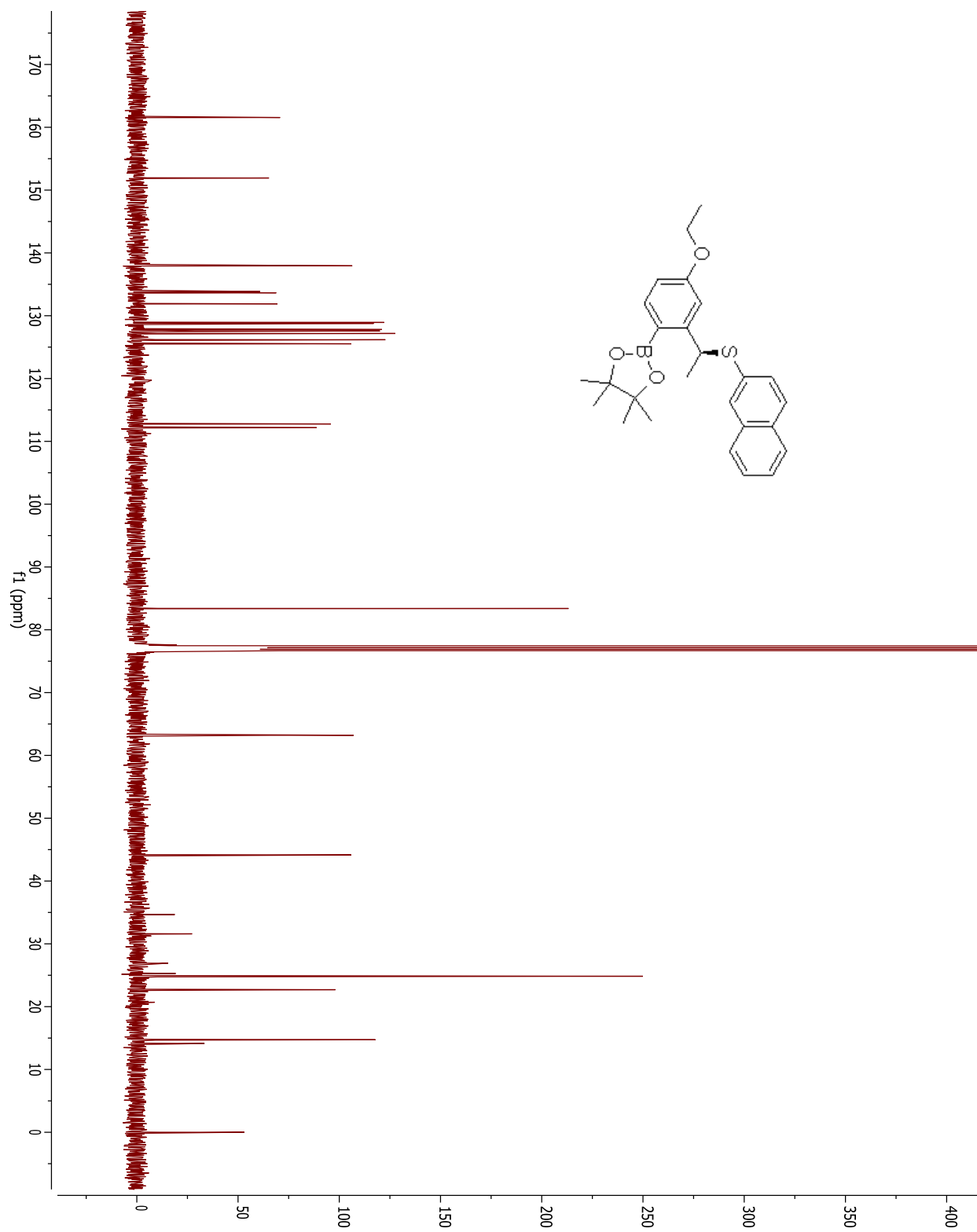
Compound 3.22.



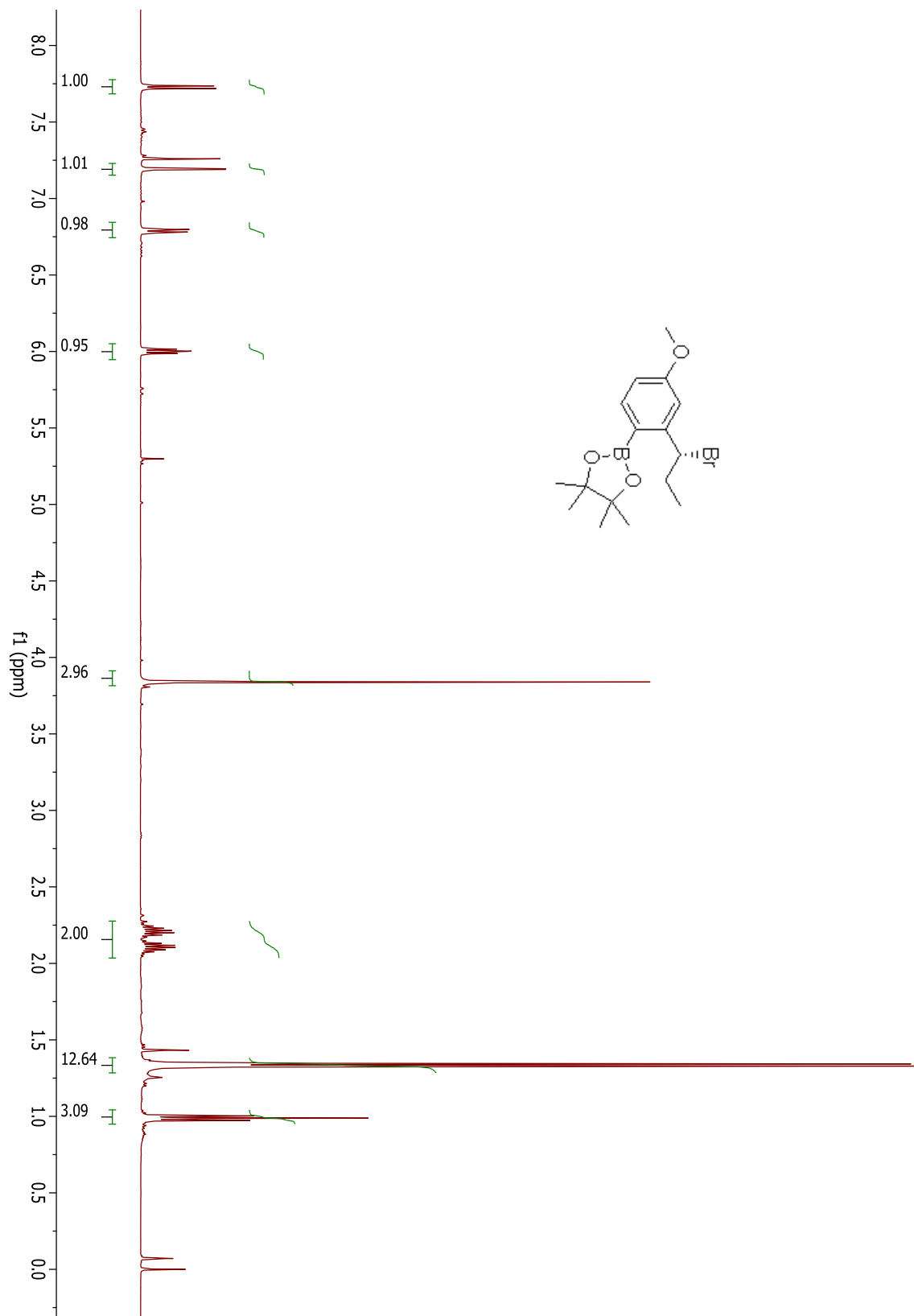
Sulfide for 3.22.



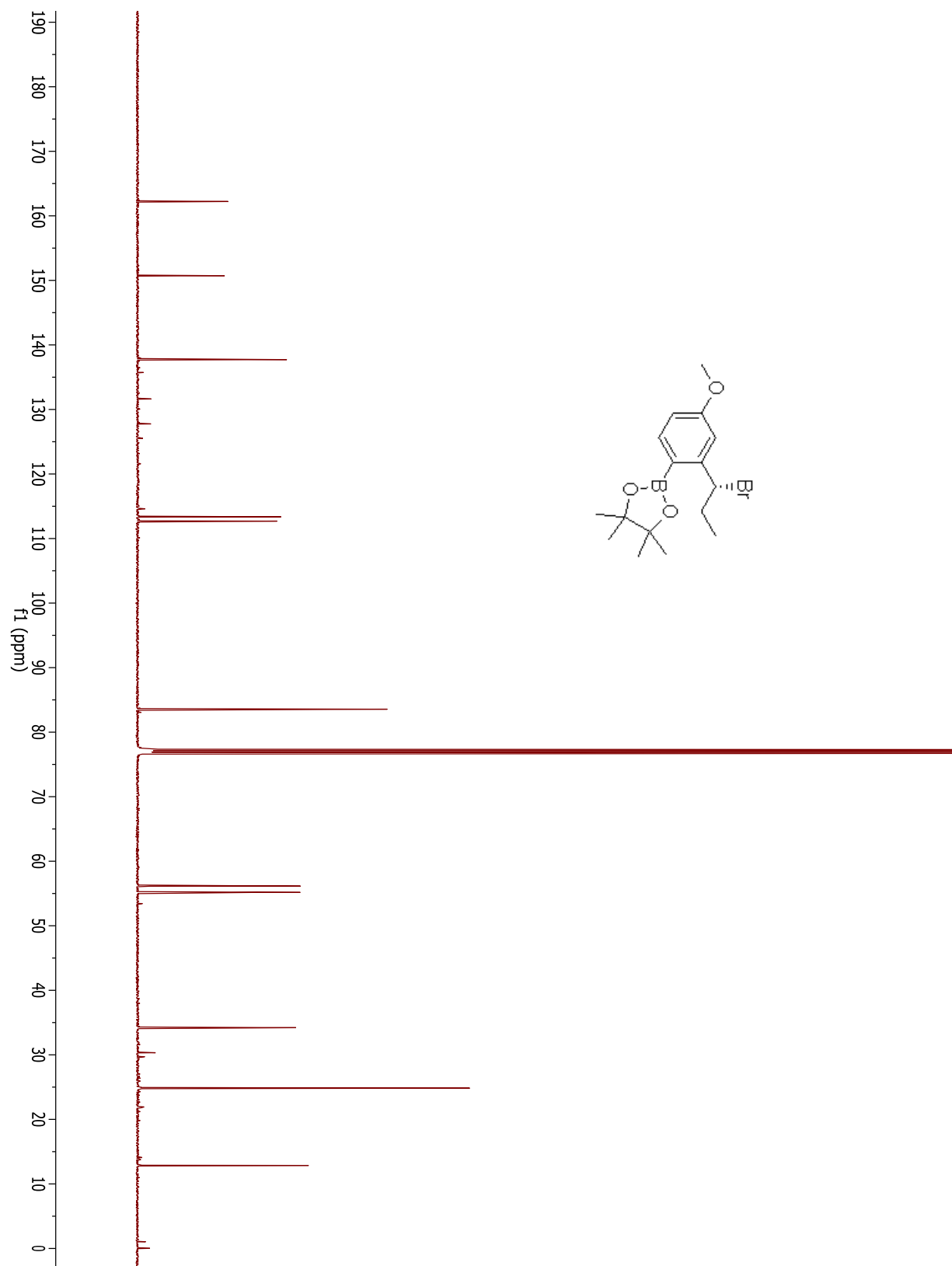
Sulfide for 3.22.



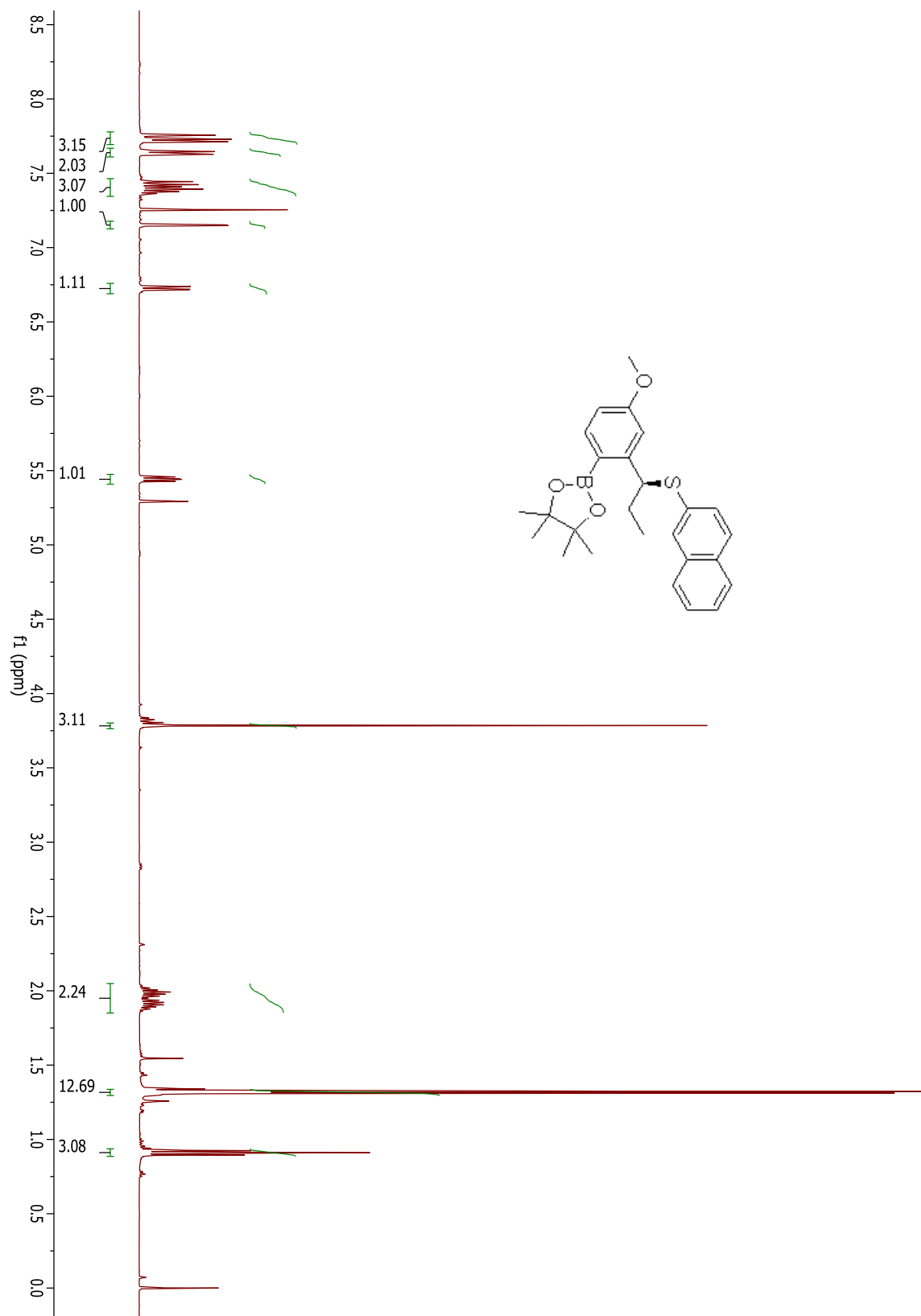
Compound 3.23.



Compound 3.23.

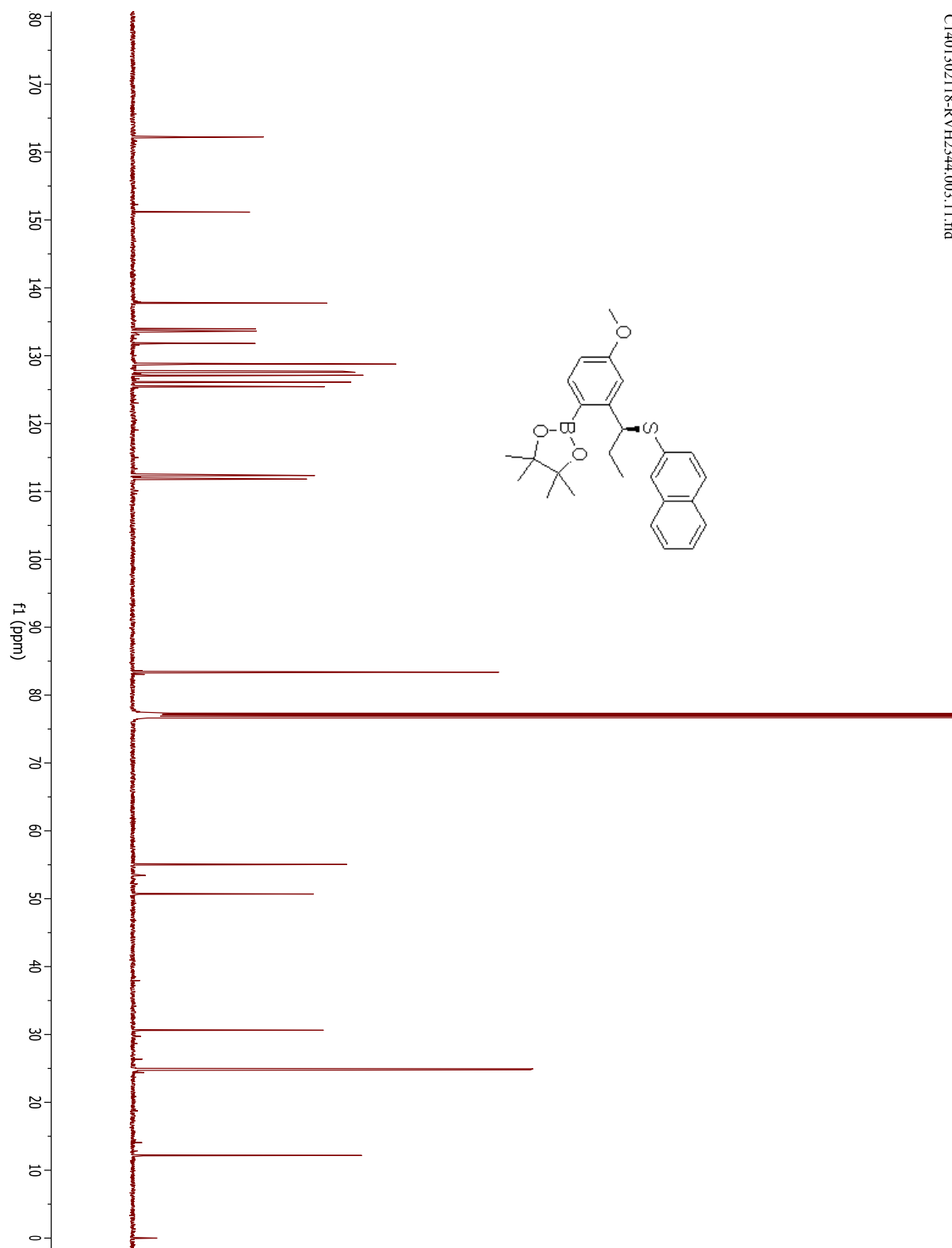


Sulfide of 3.23.

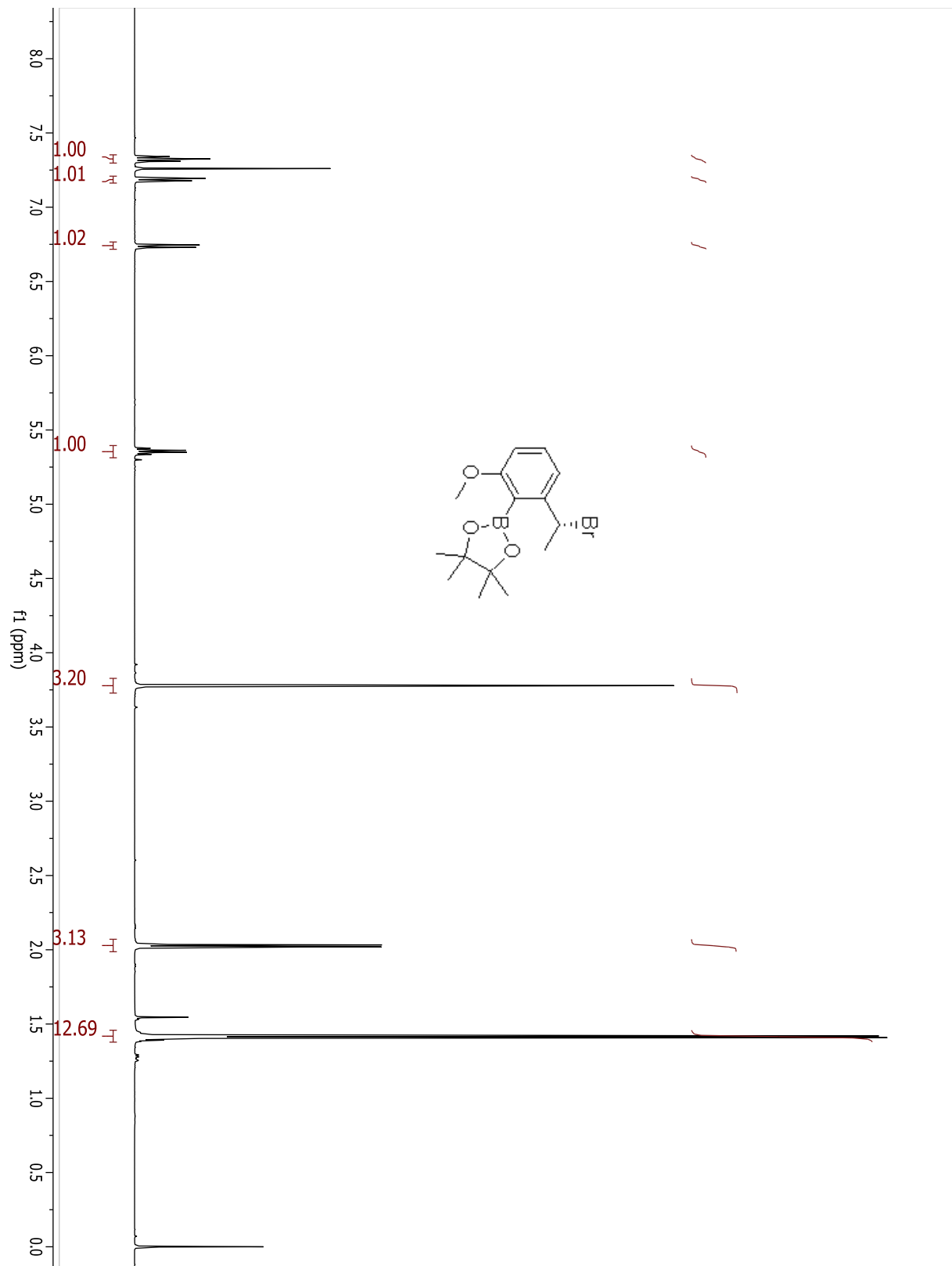


Sulfide of 3.23.

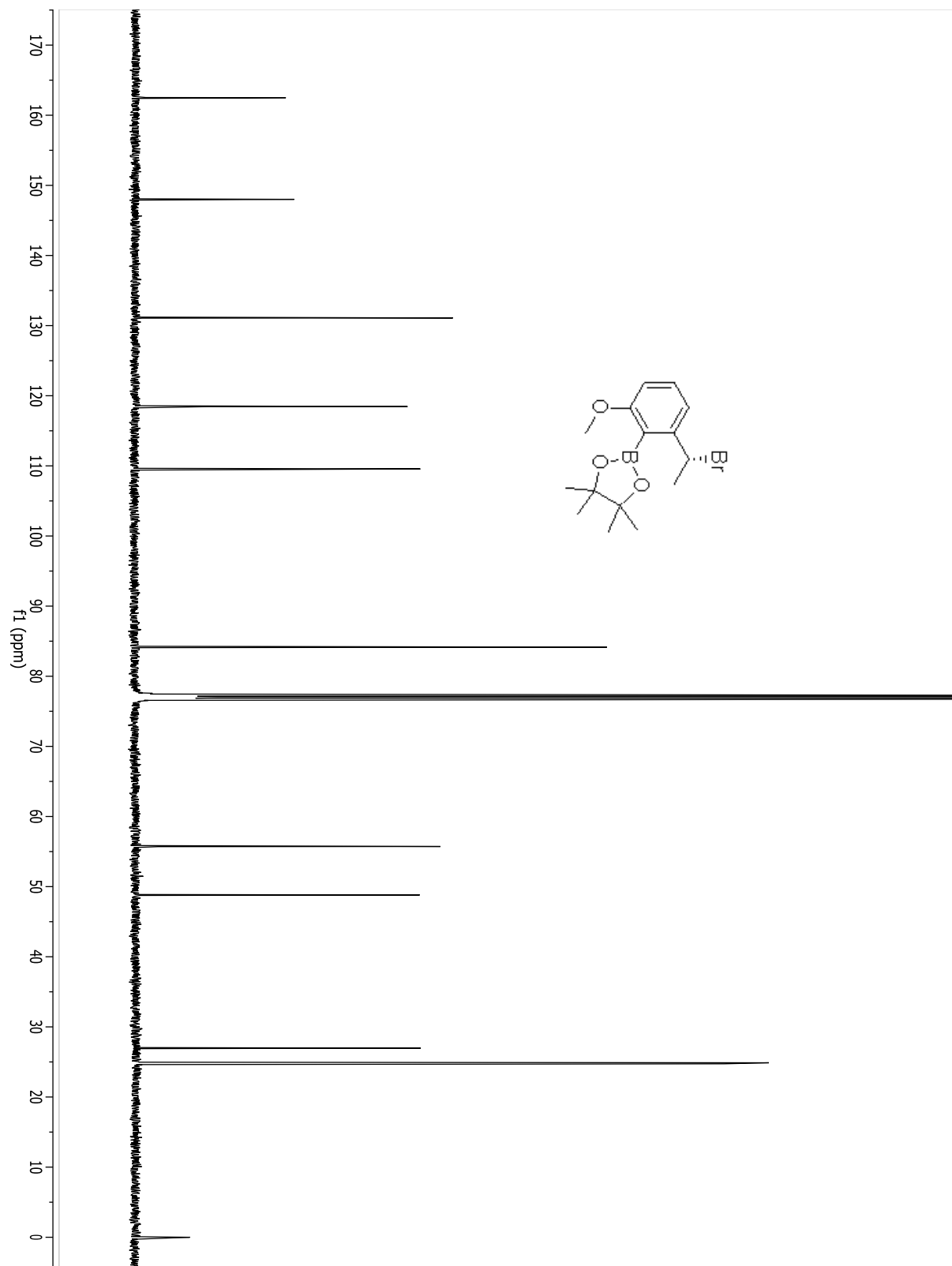
C1401302118-RV/H234;003;11.fid



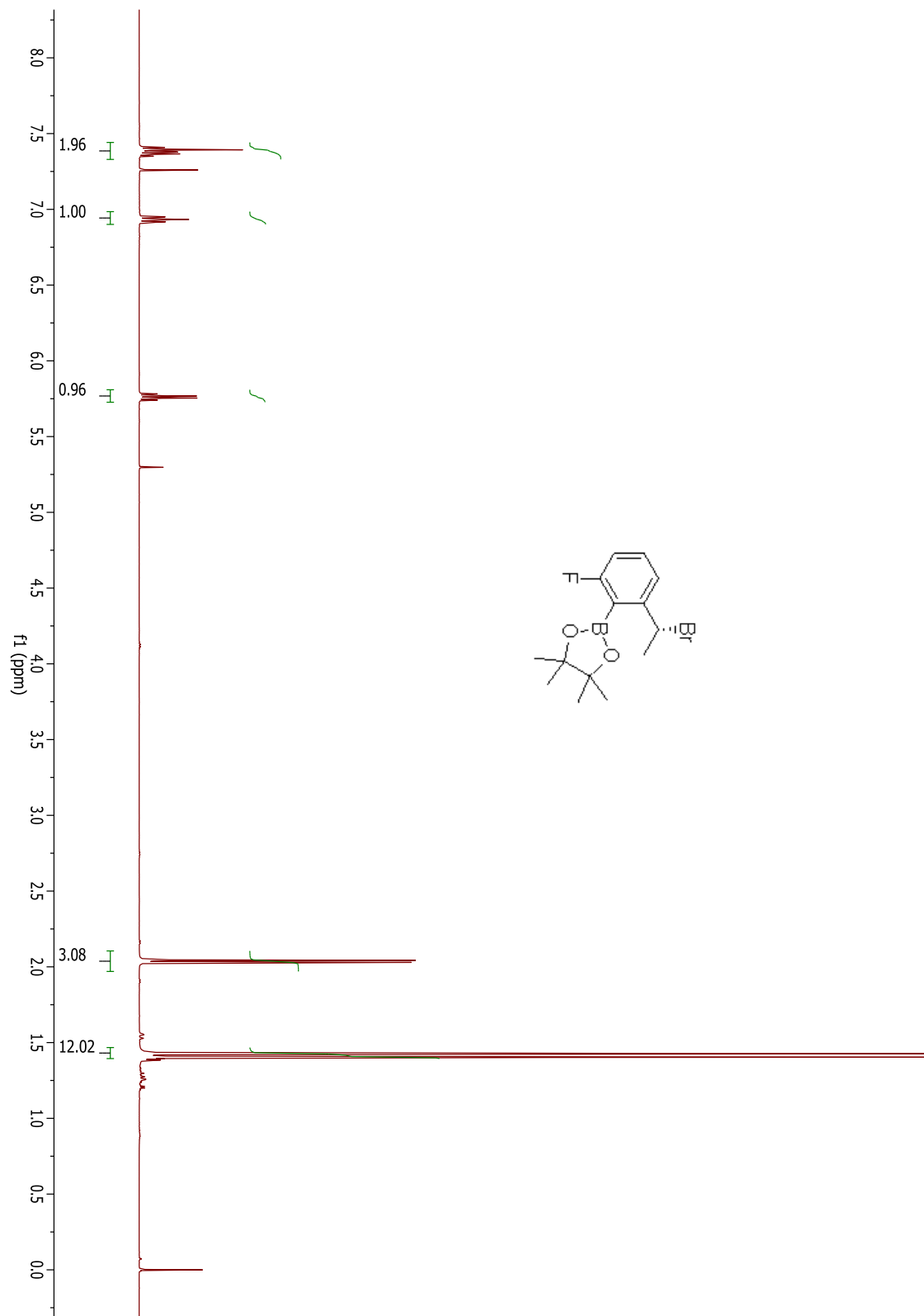
Compound 3.24.



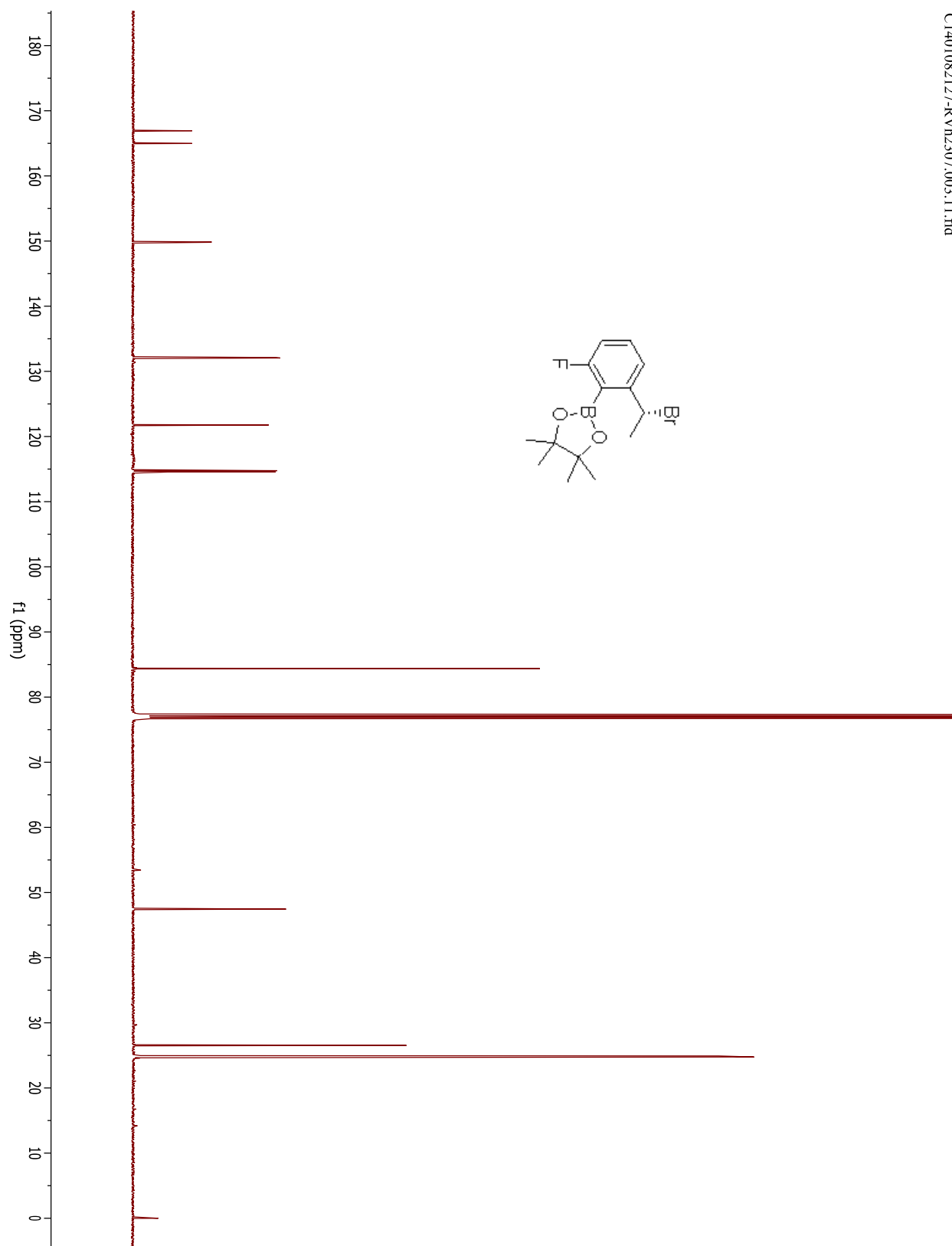
Compound 3.24.



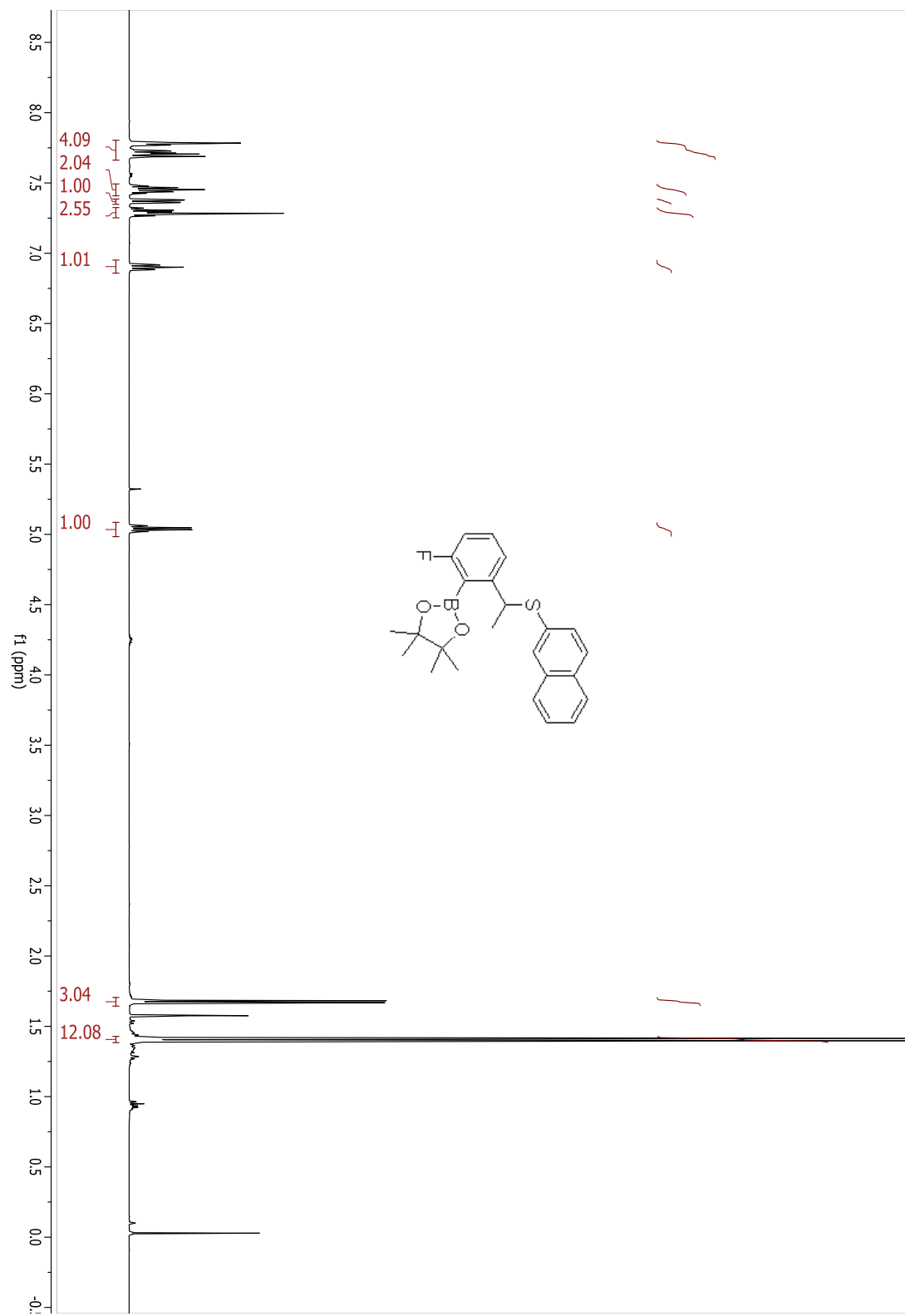
Compound 3.25.



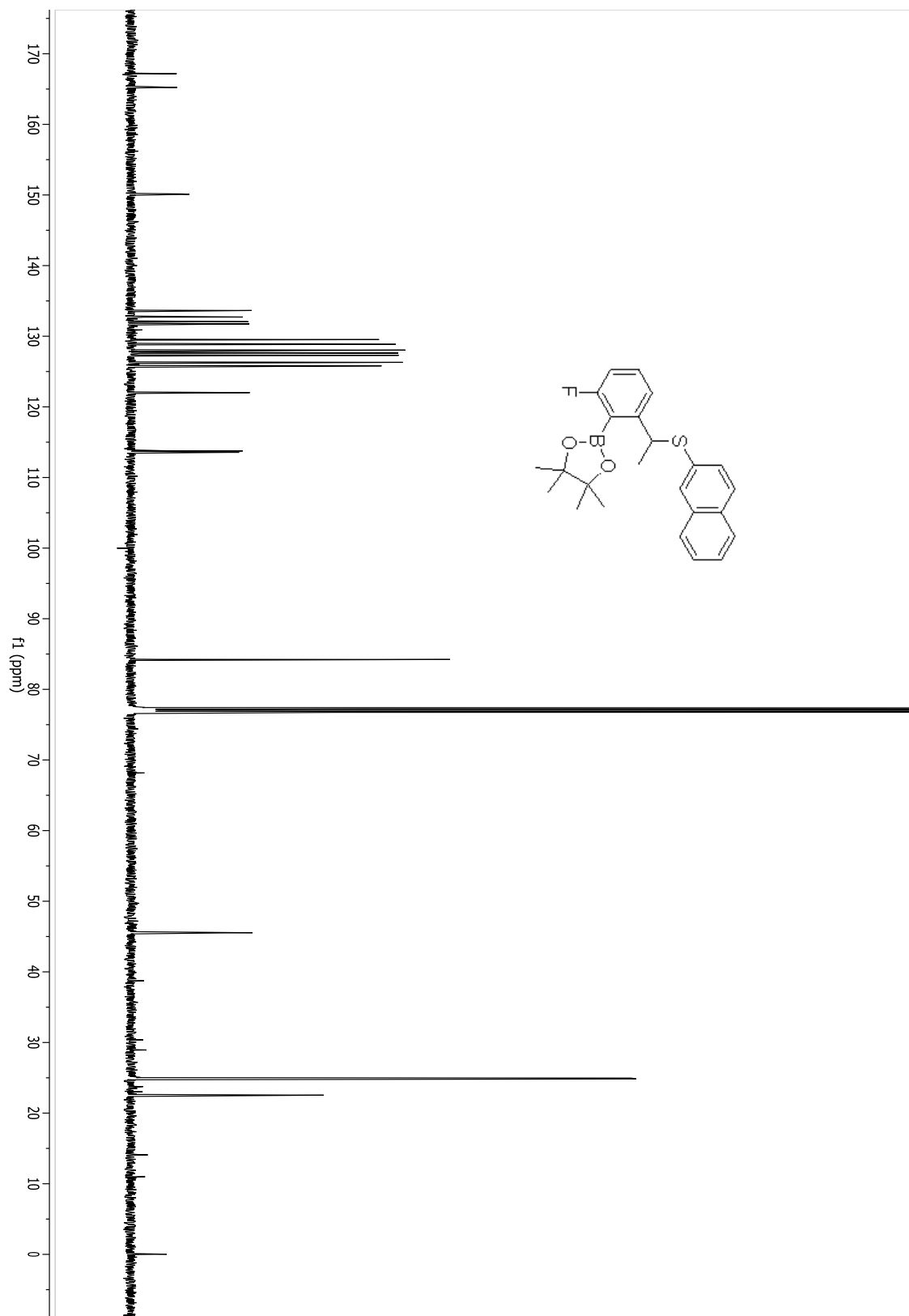
Compound 3.25.



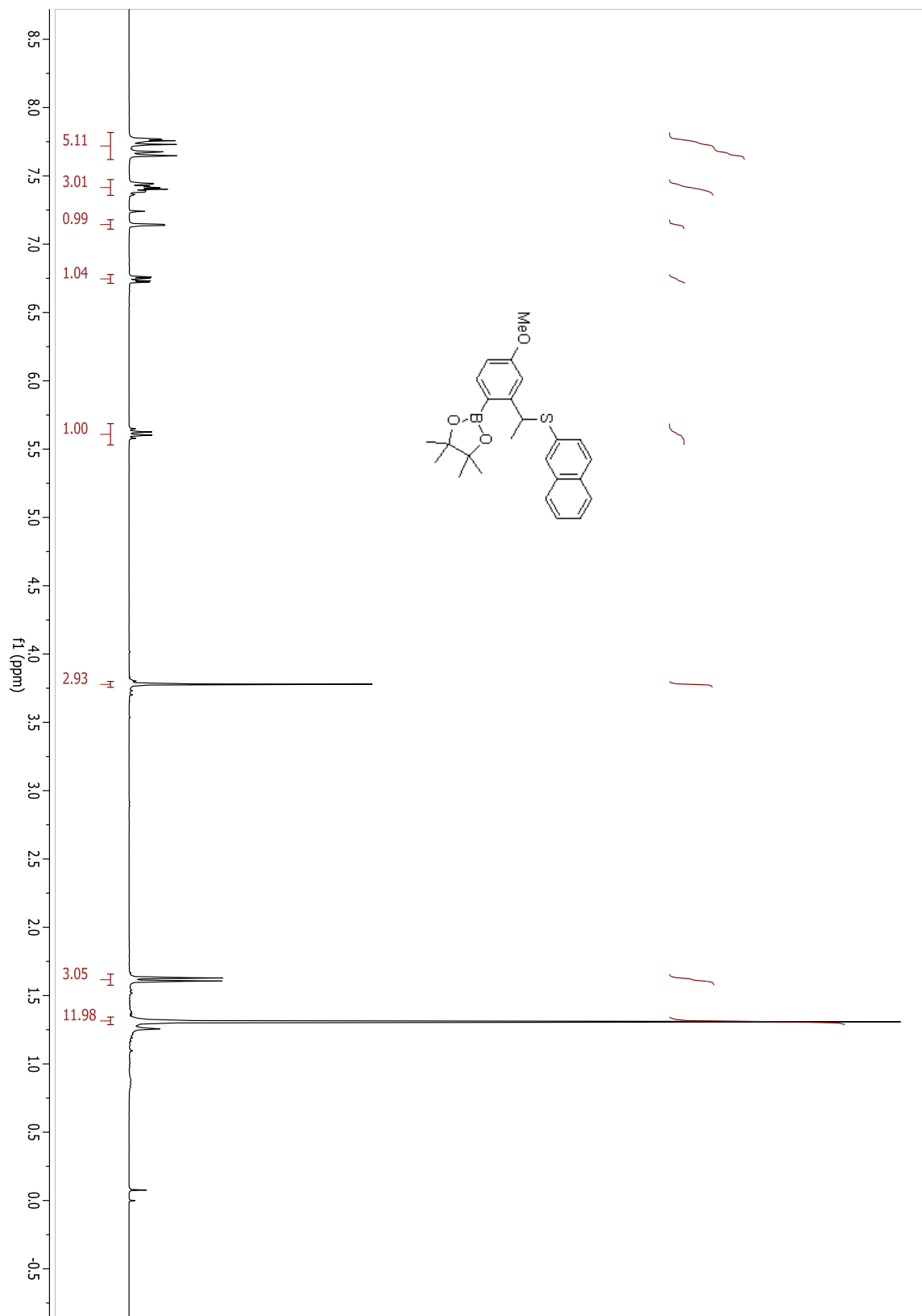
Sulfide of Compound 3.25.



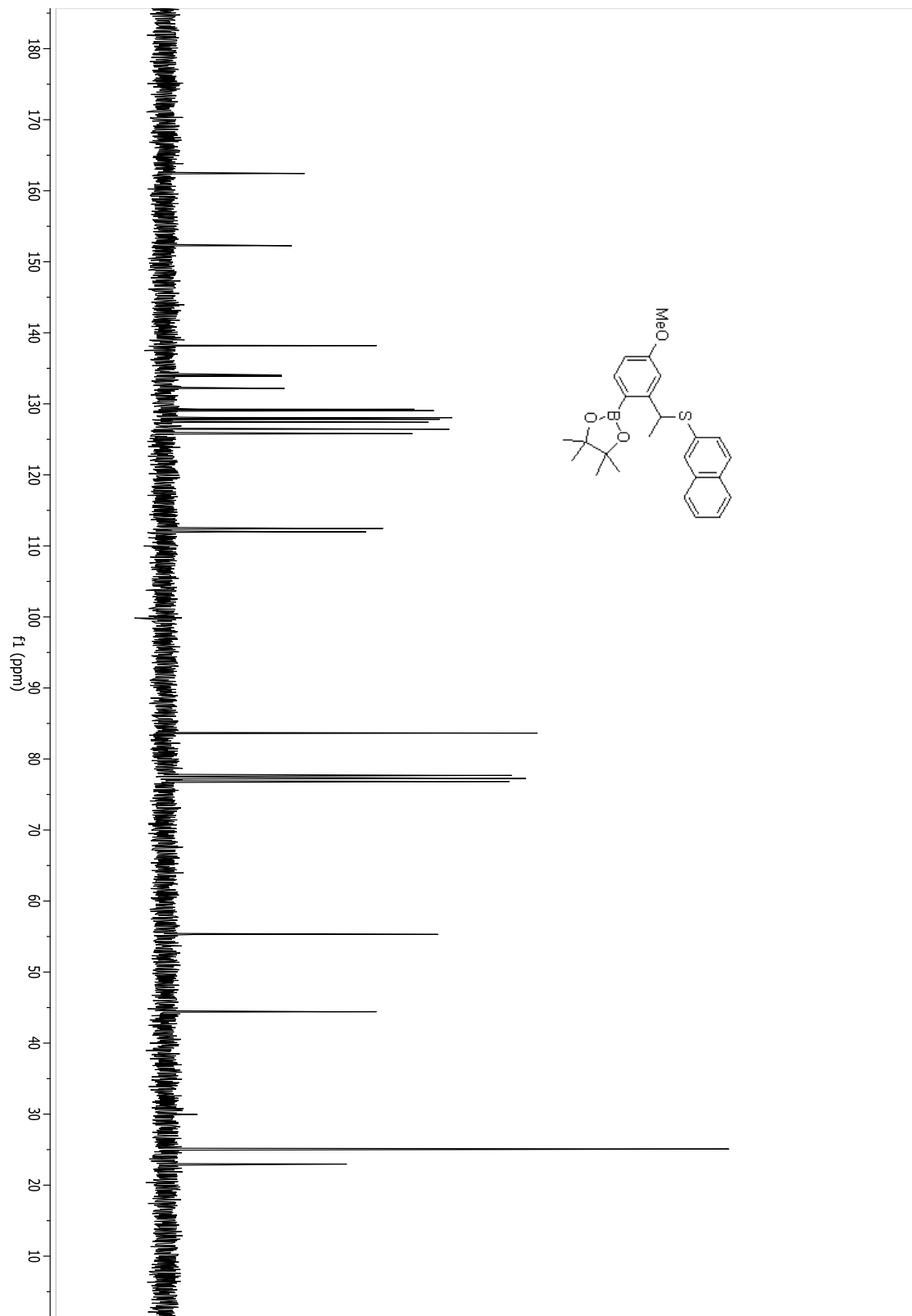
Sulfide of Compound 3.25.



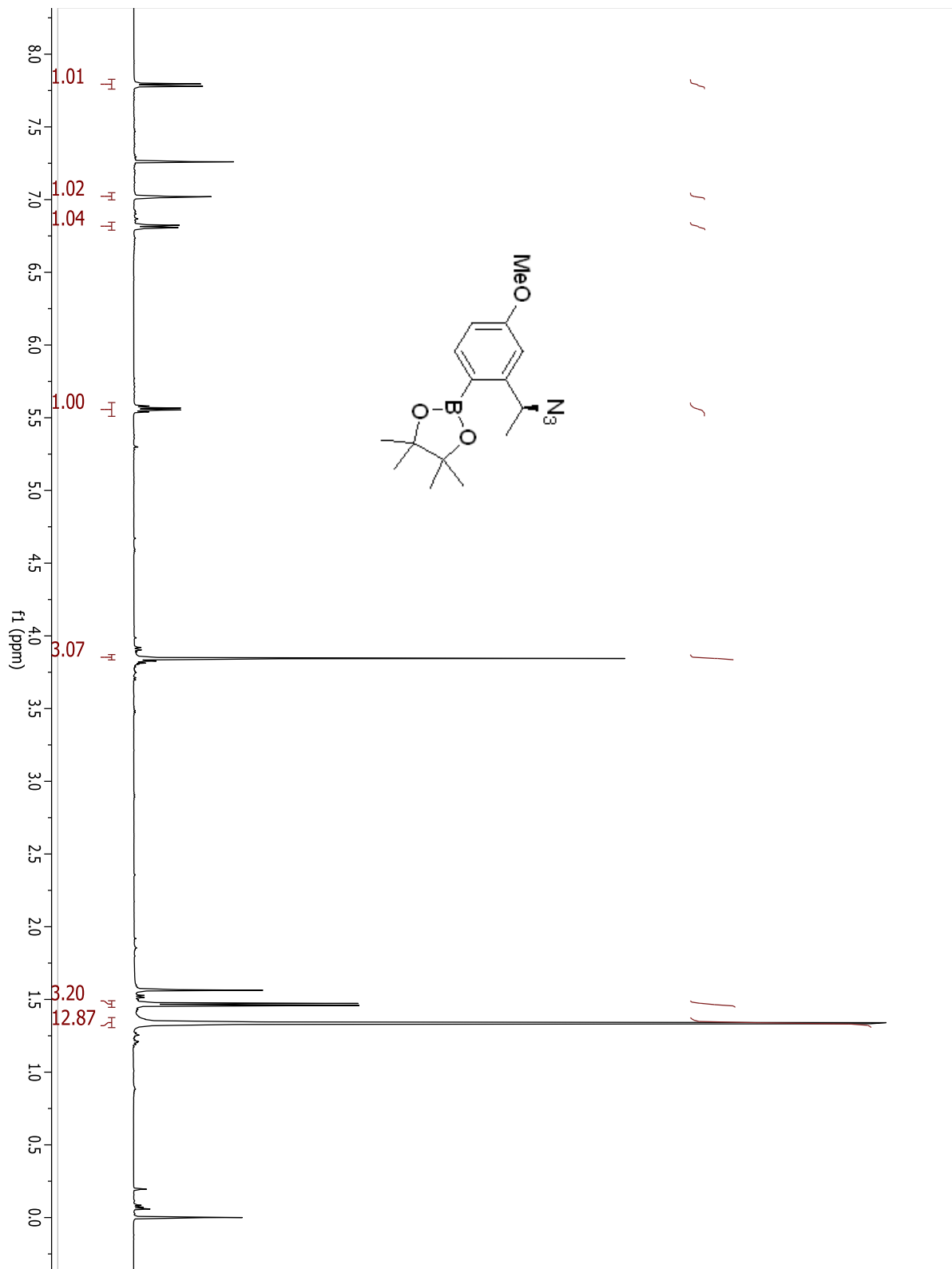
Compound 3.26.



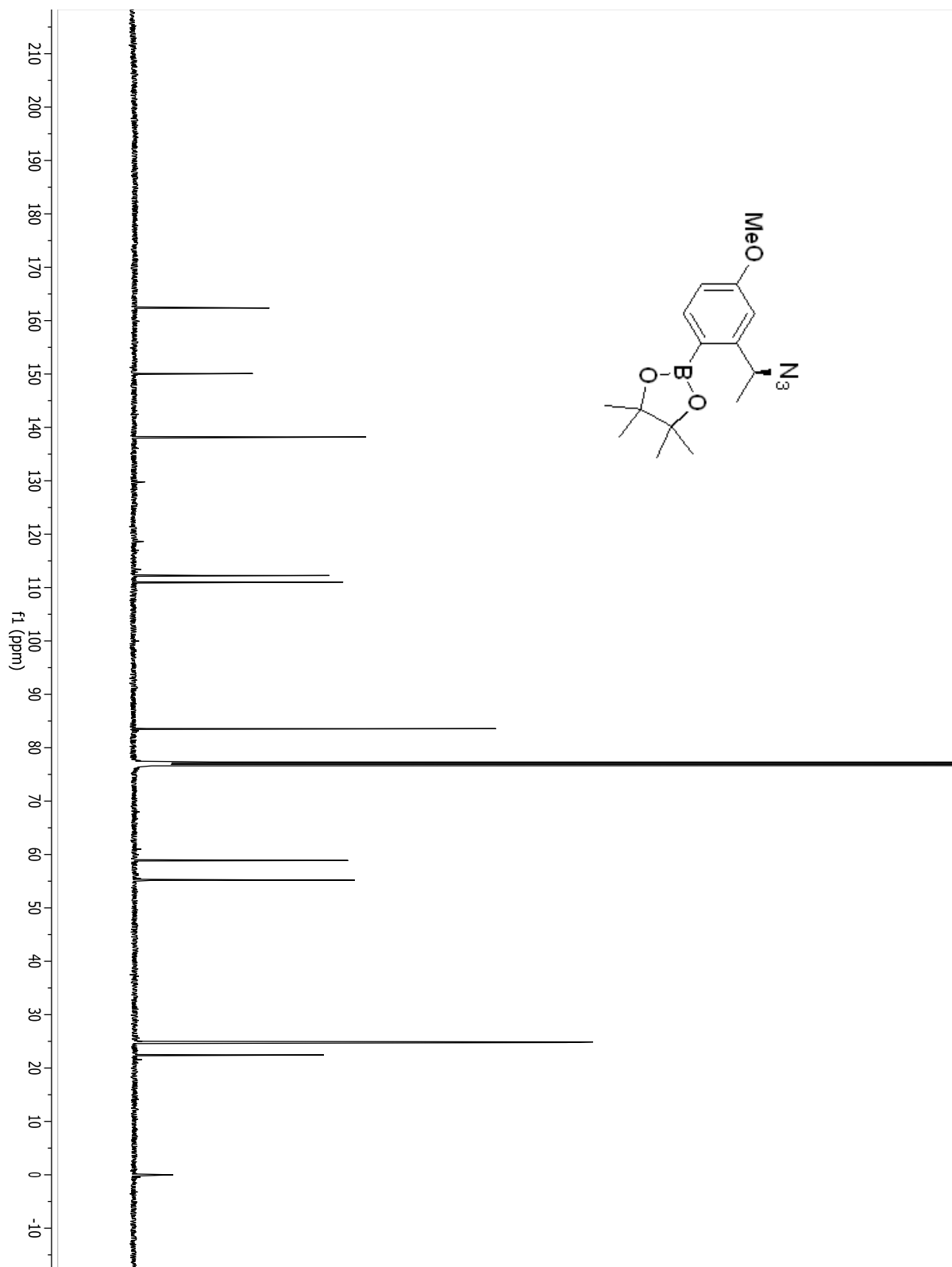
Compound 2.26.



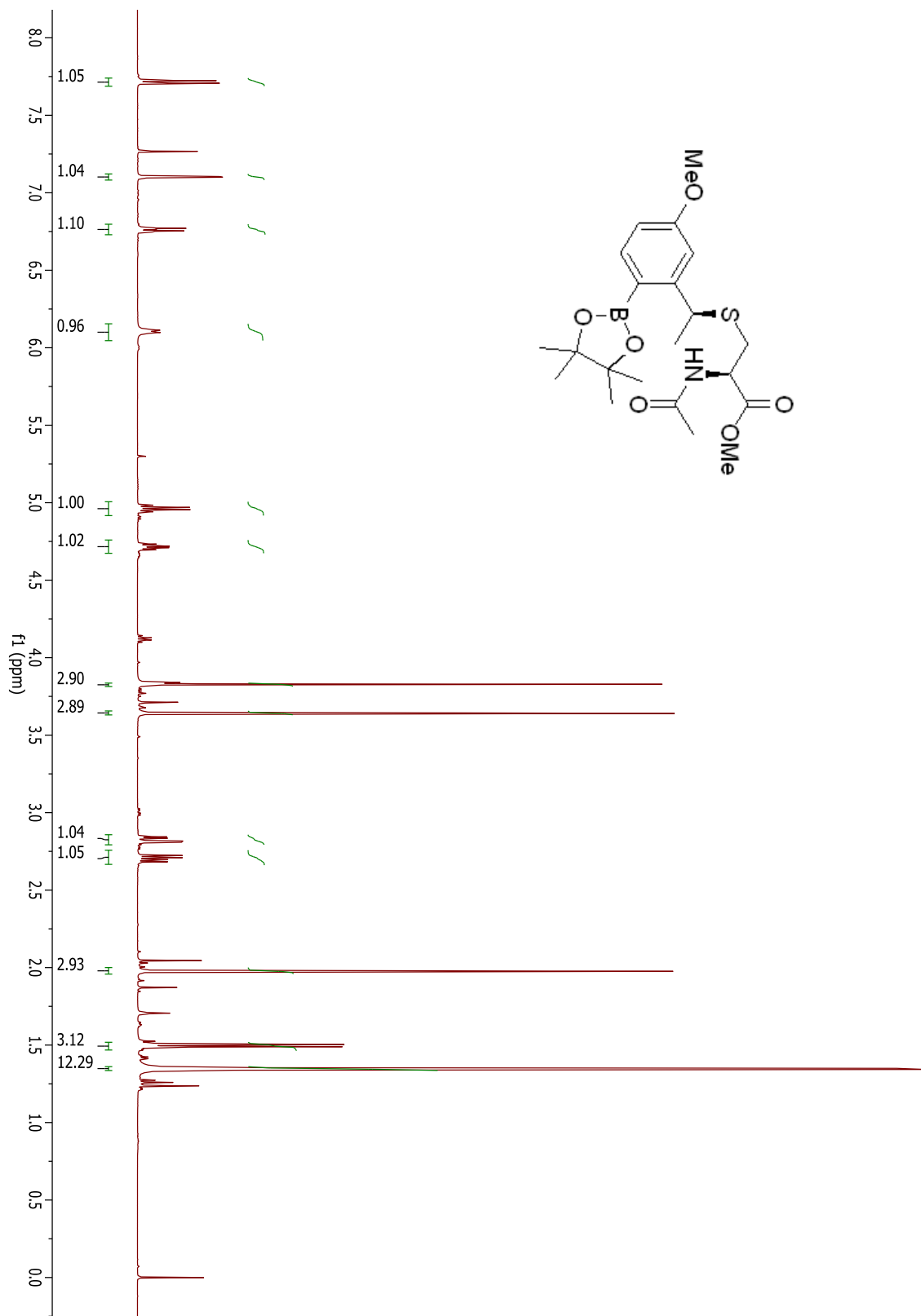
Compound 3.28.



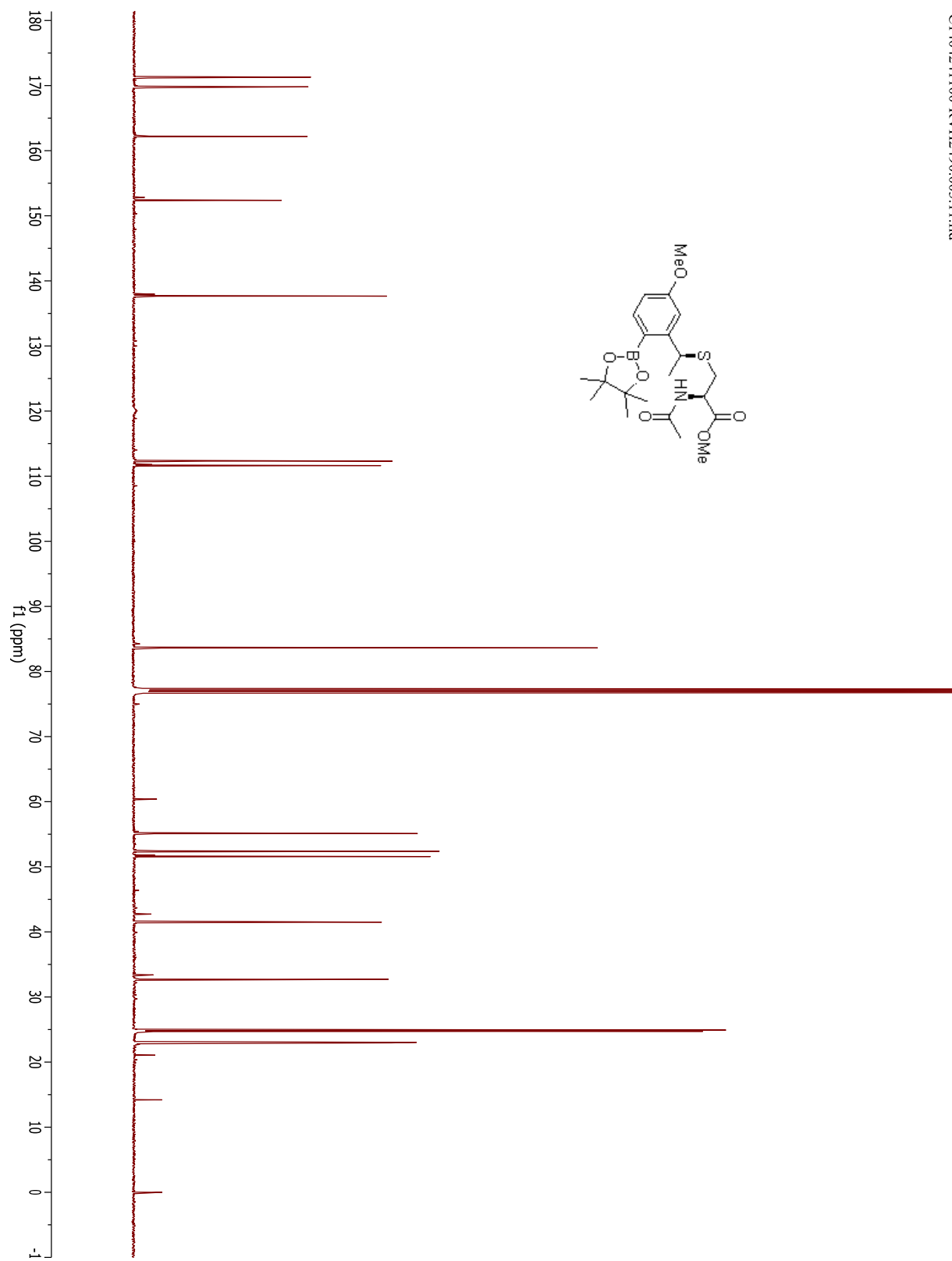
Compound 3.28.



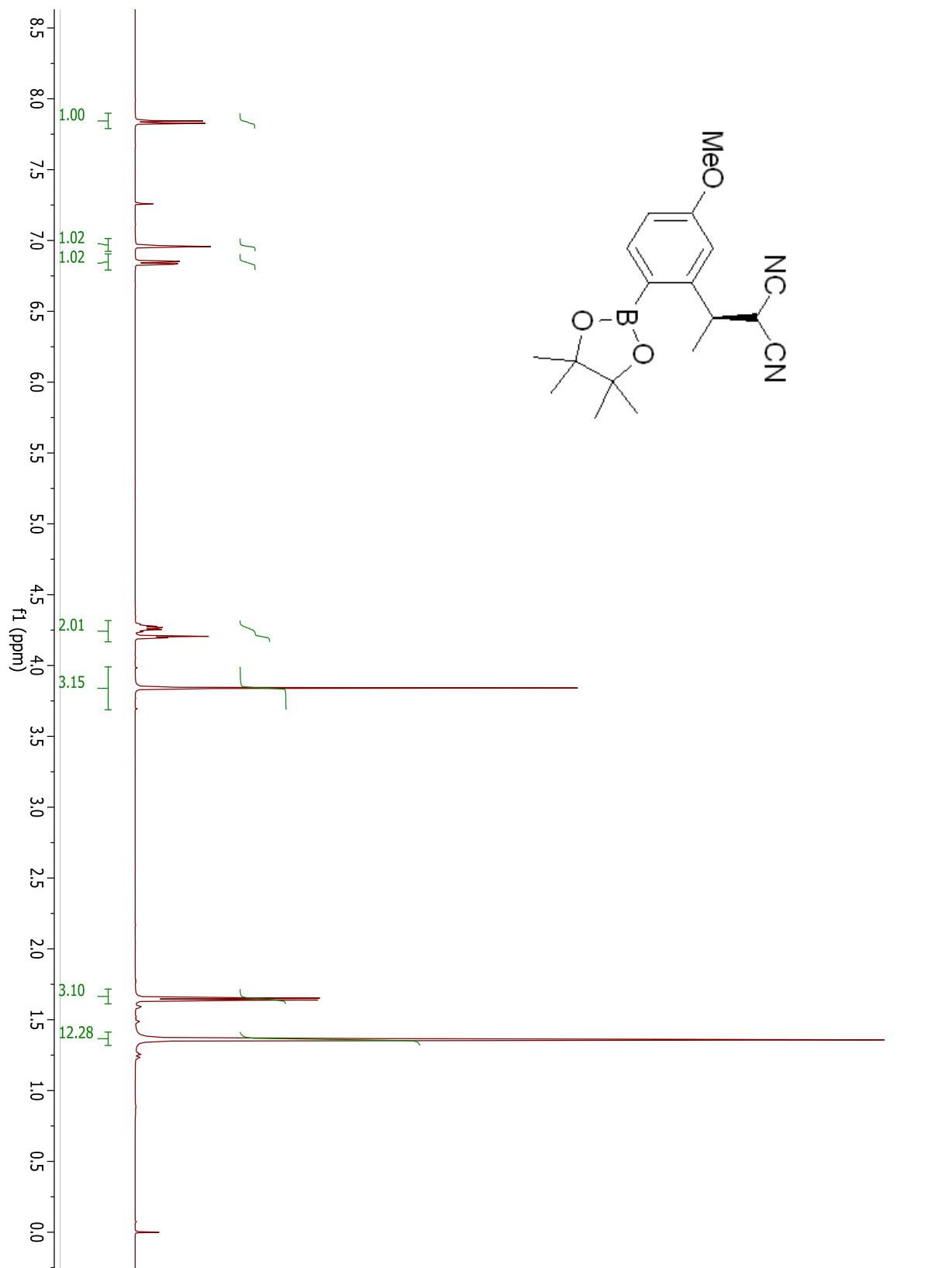
Compound 3.29.



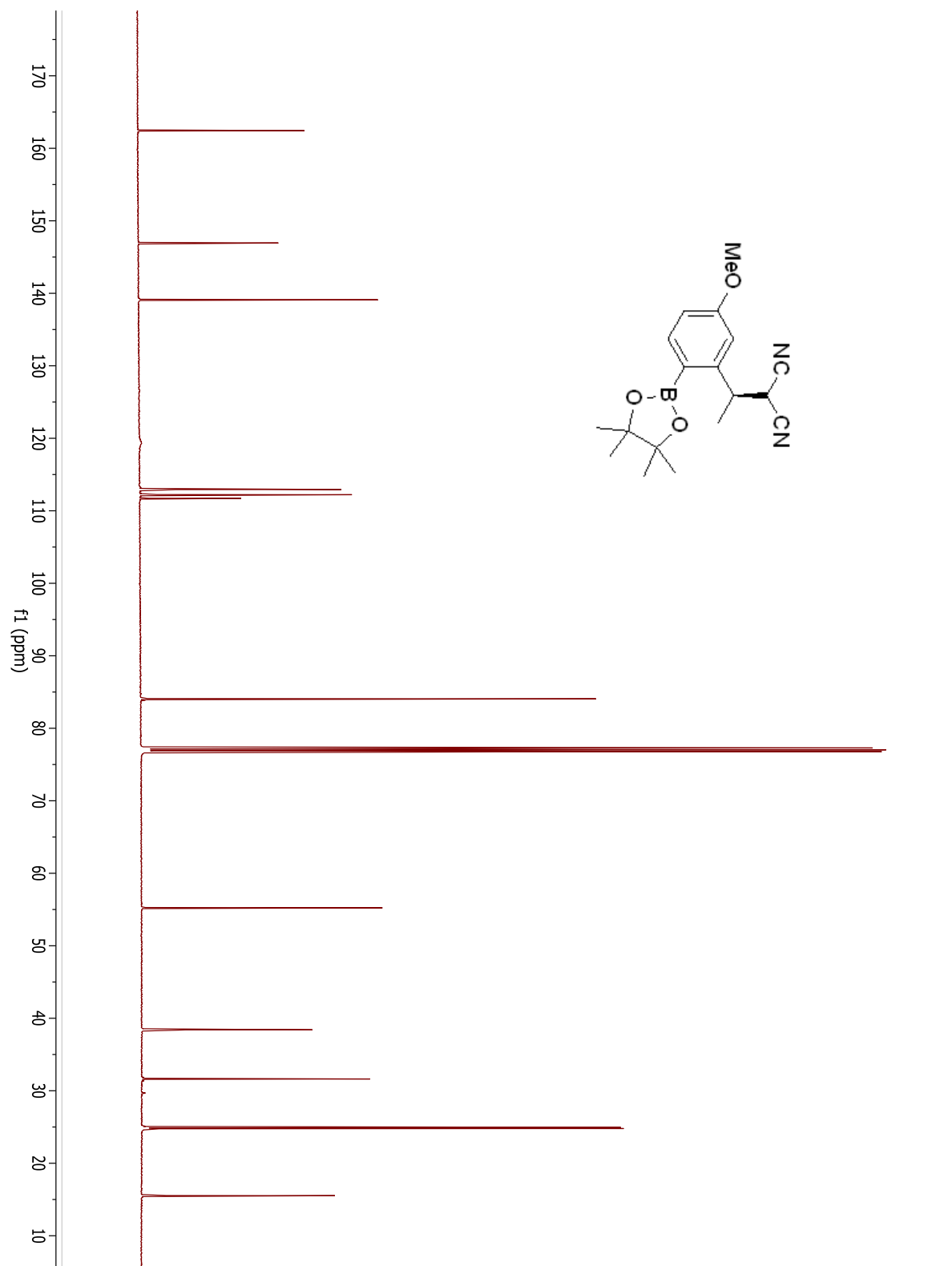
Compound 3.29.



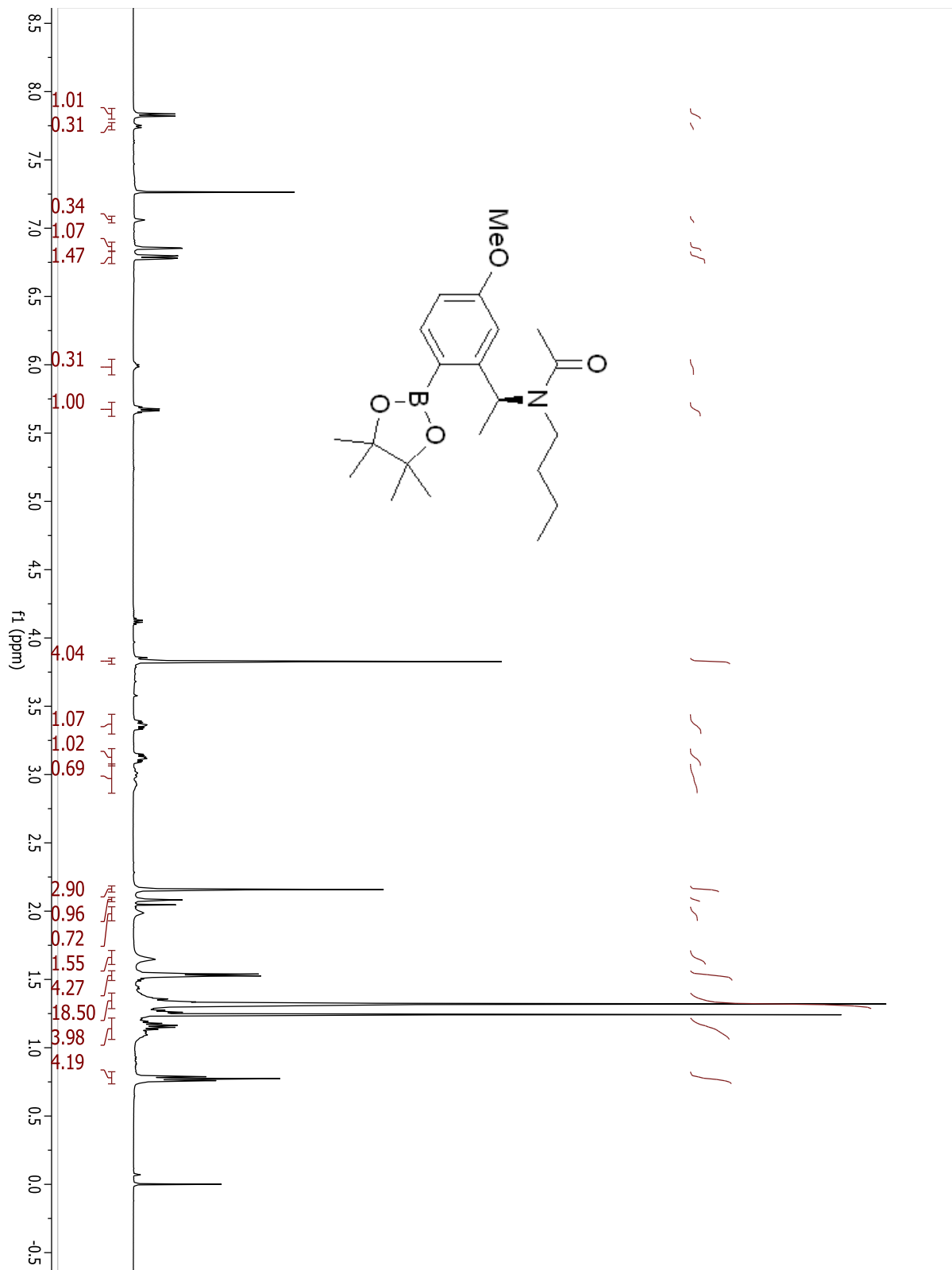
Compound 3.30.



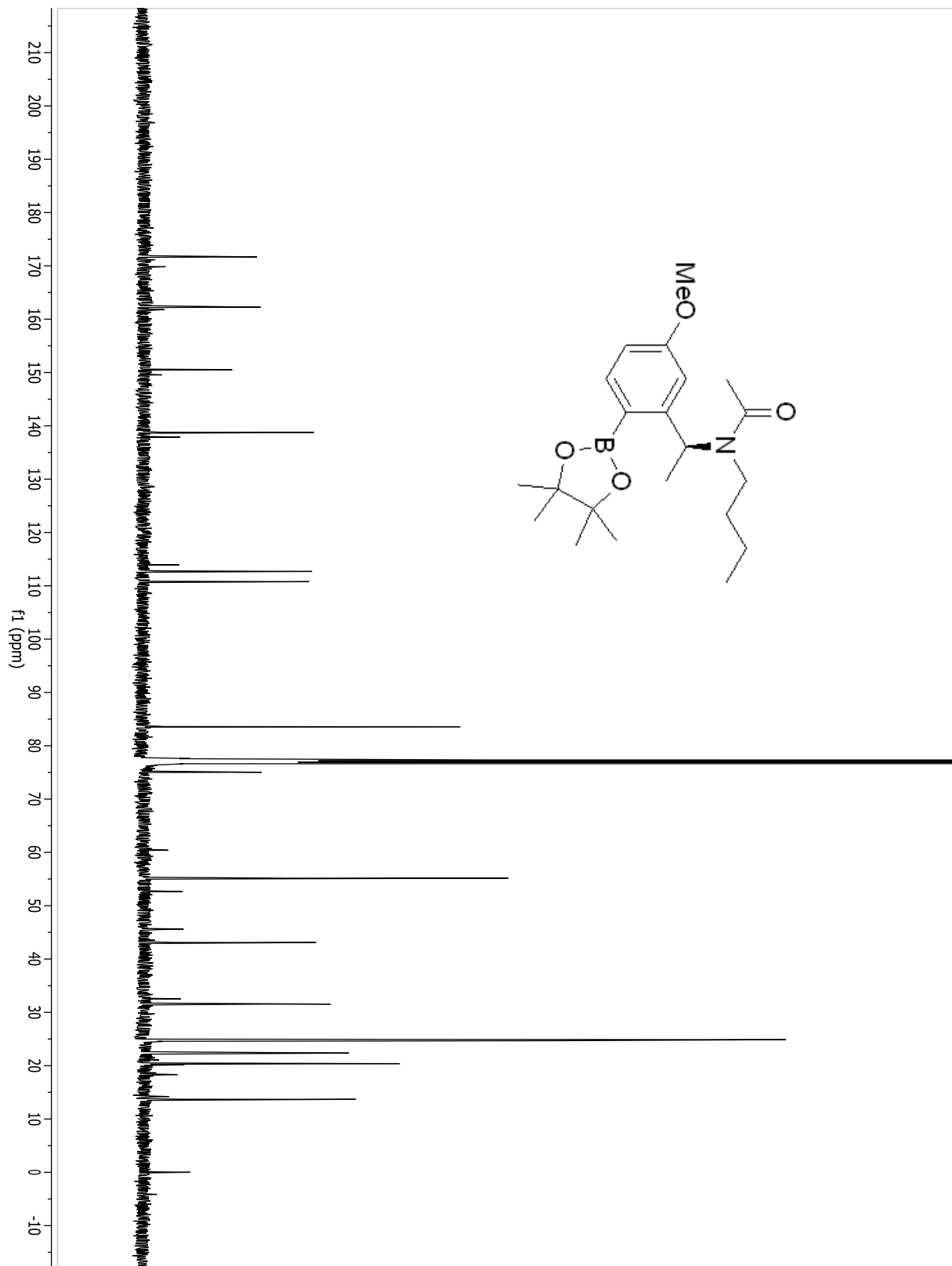
Compound 3.30



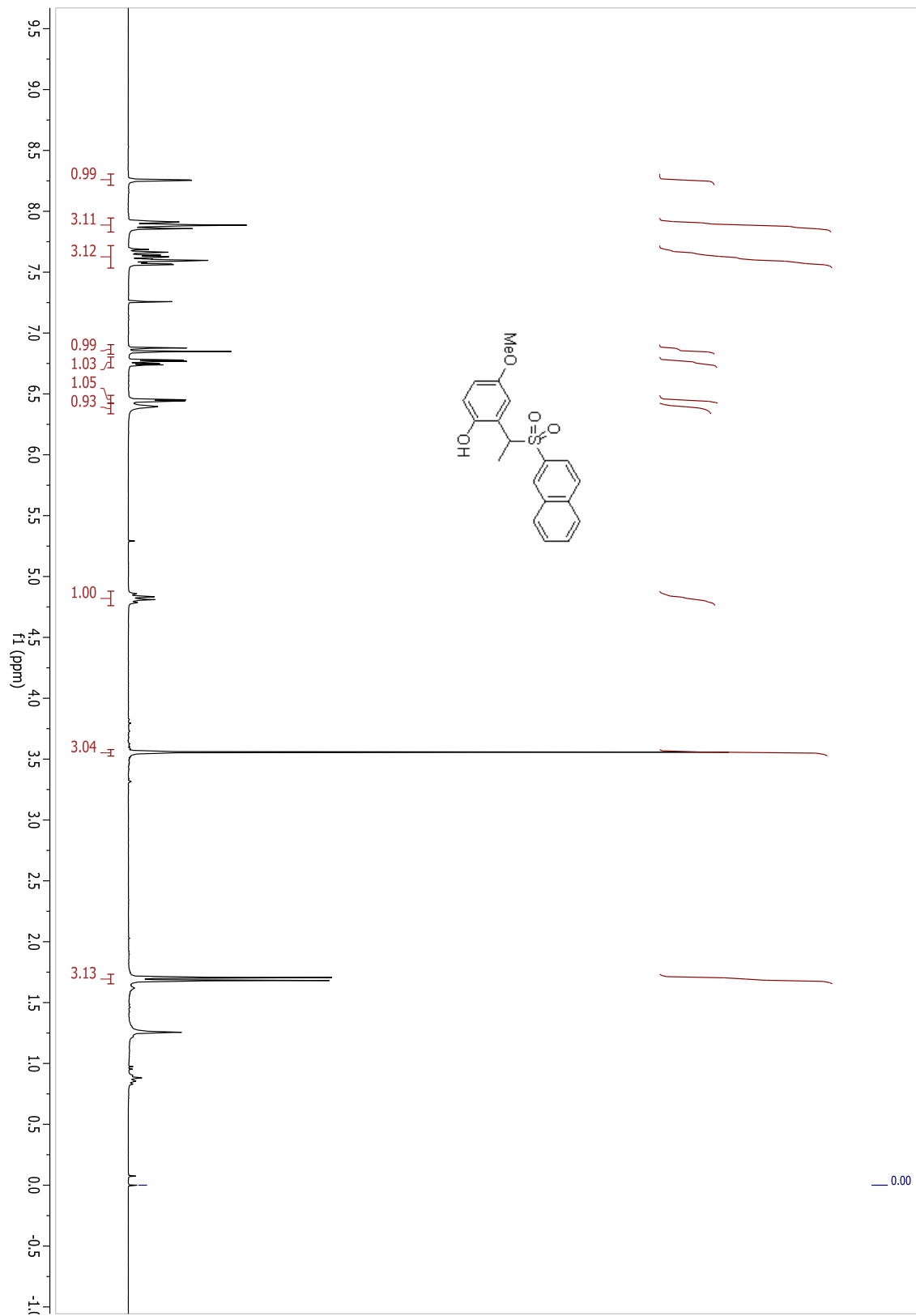
Compound 3.31.



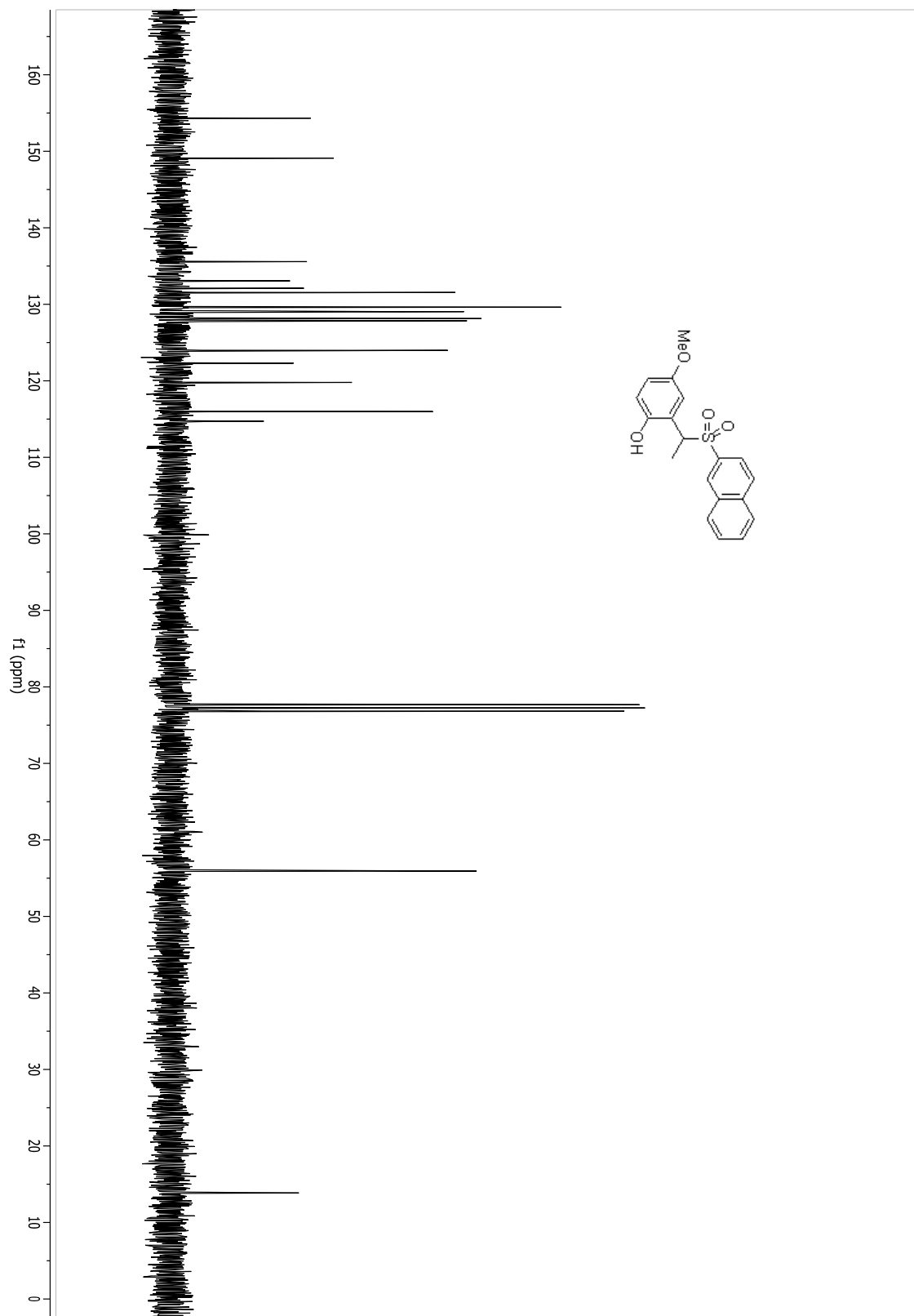
Compound 3.31



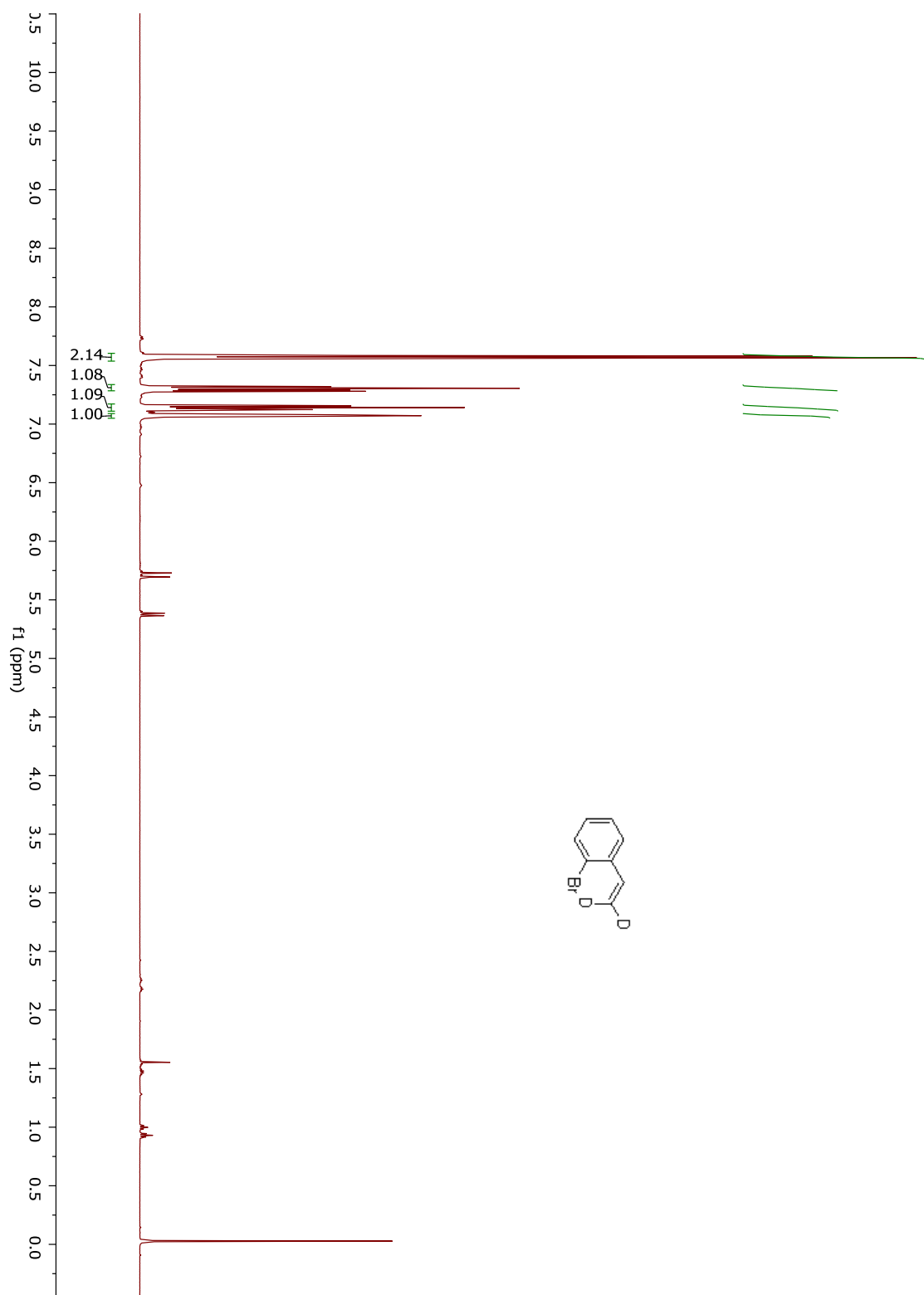
Compound C.1.



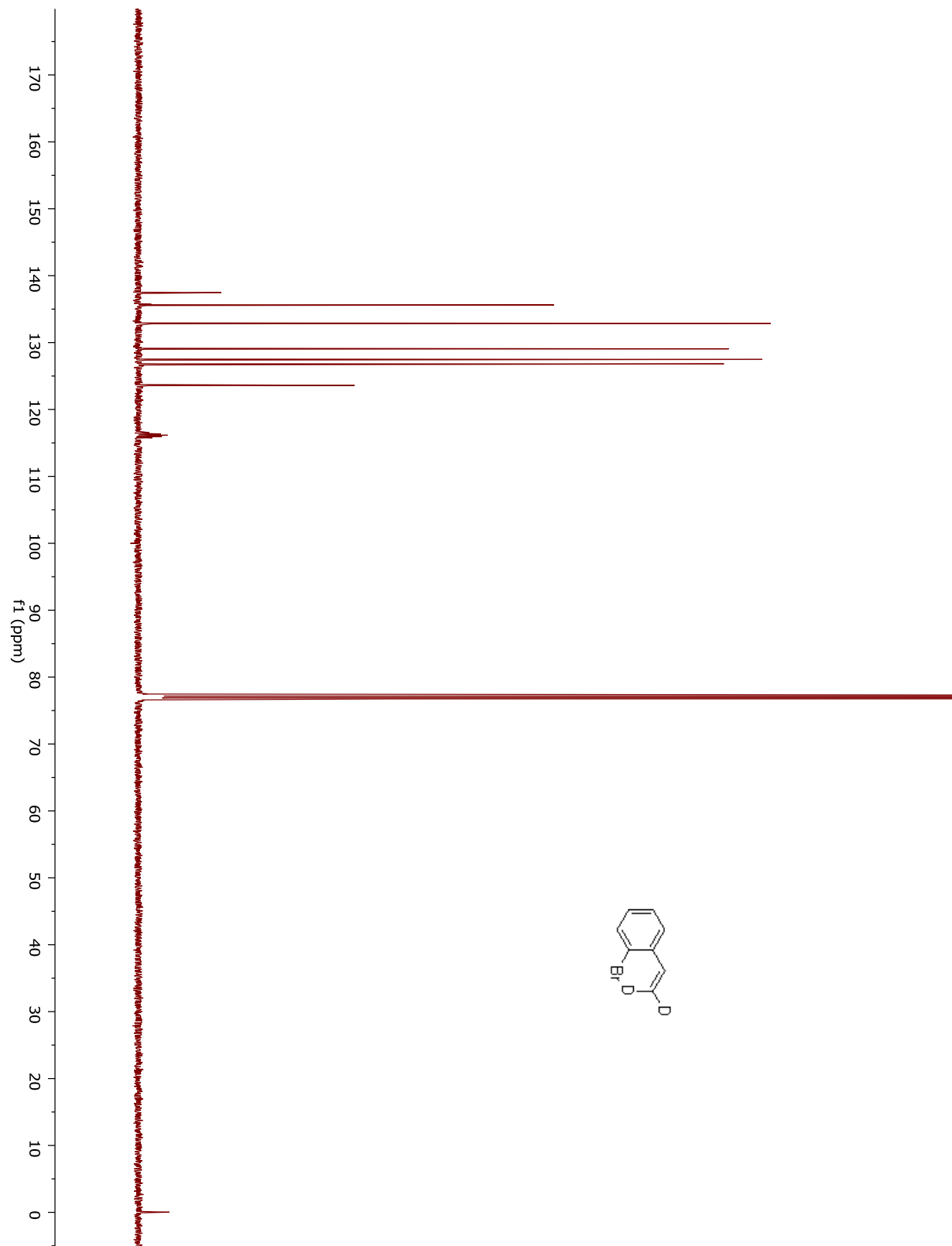
Compound C.1.



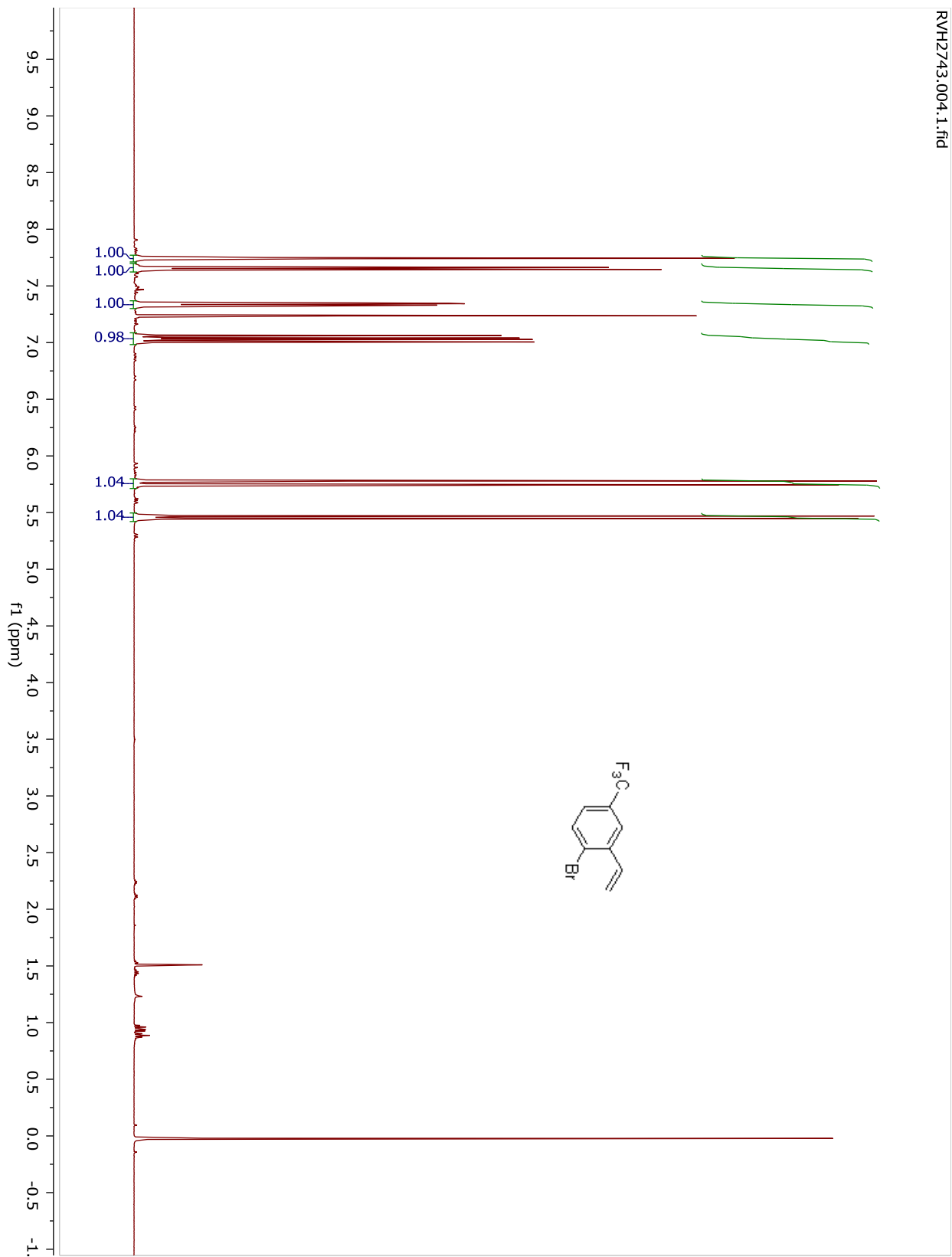
Compound 4.13.



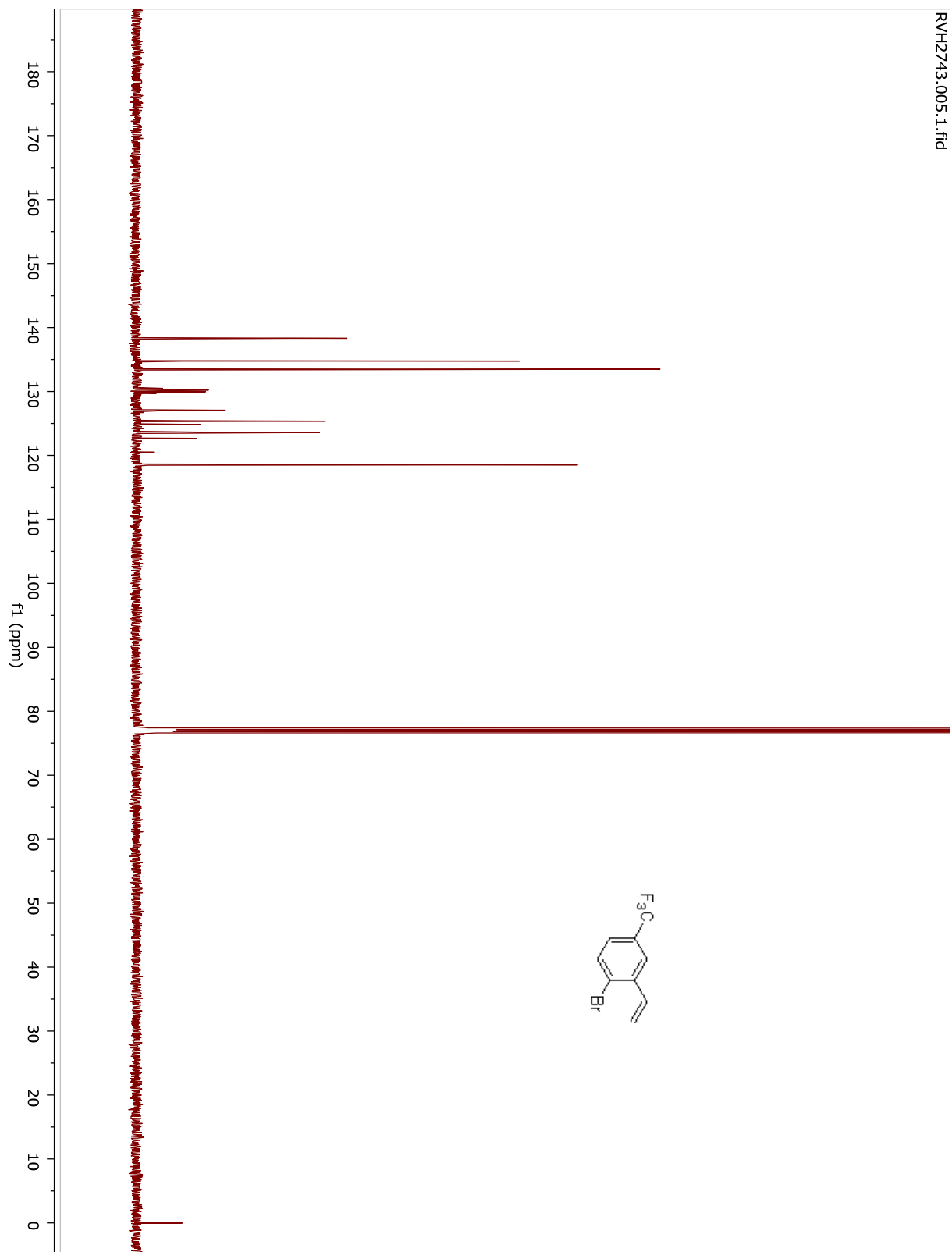
Compound 4.13.



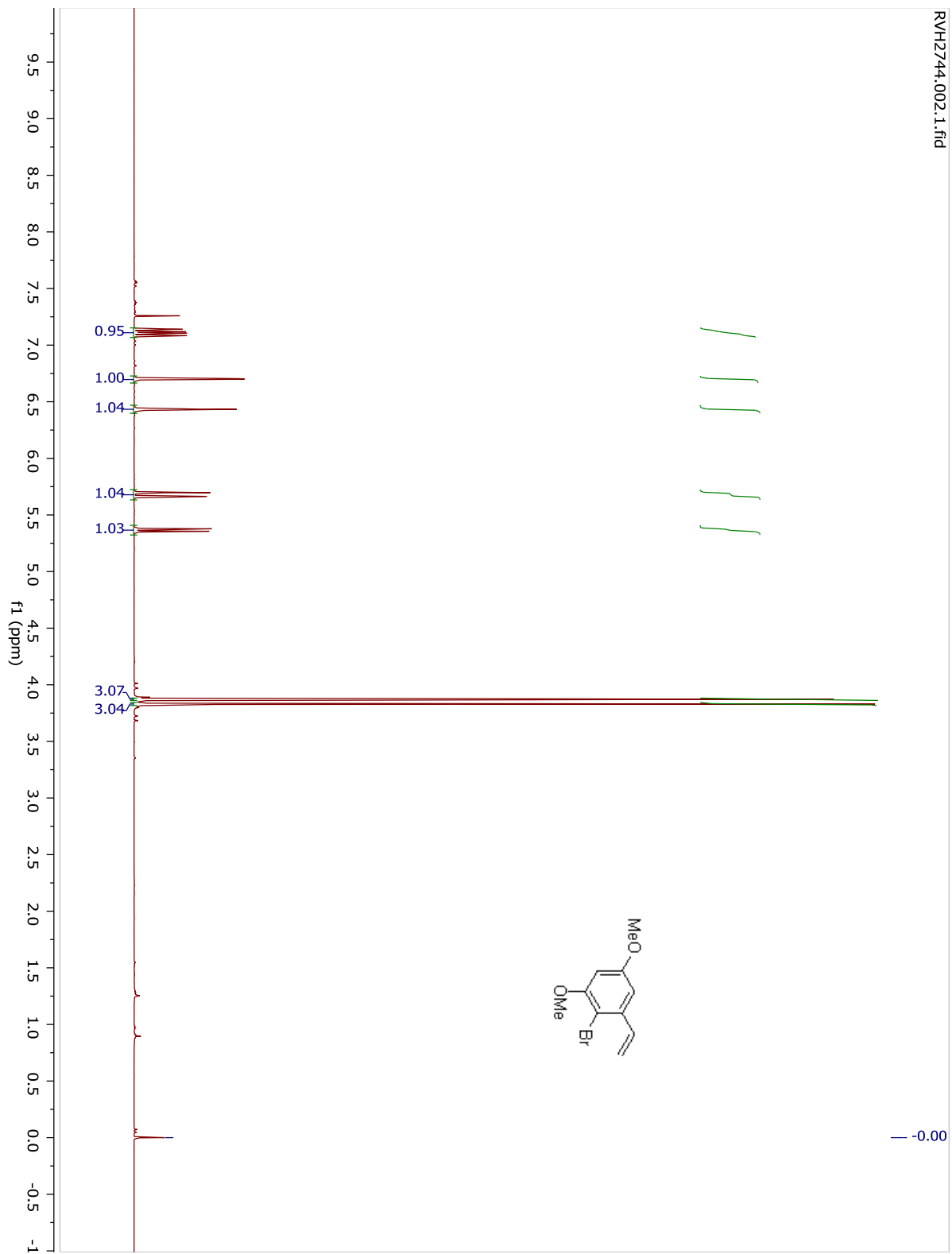
Compound 4.36.



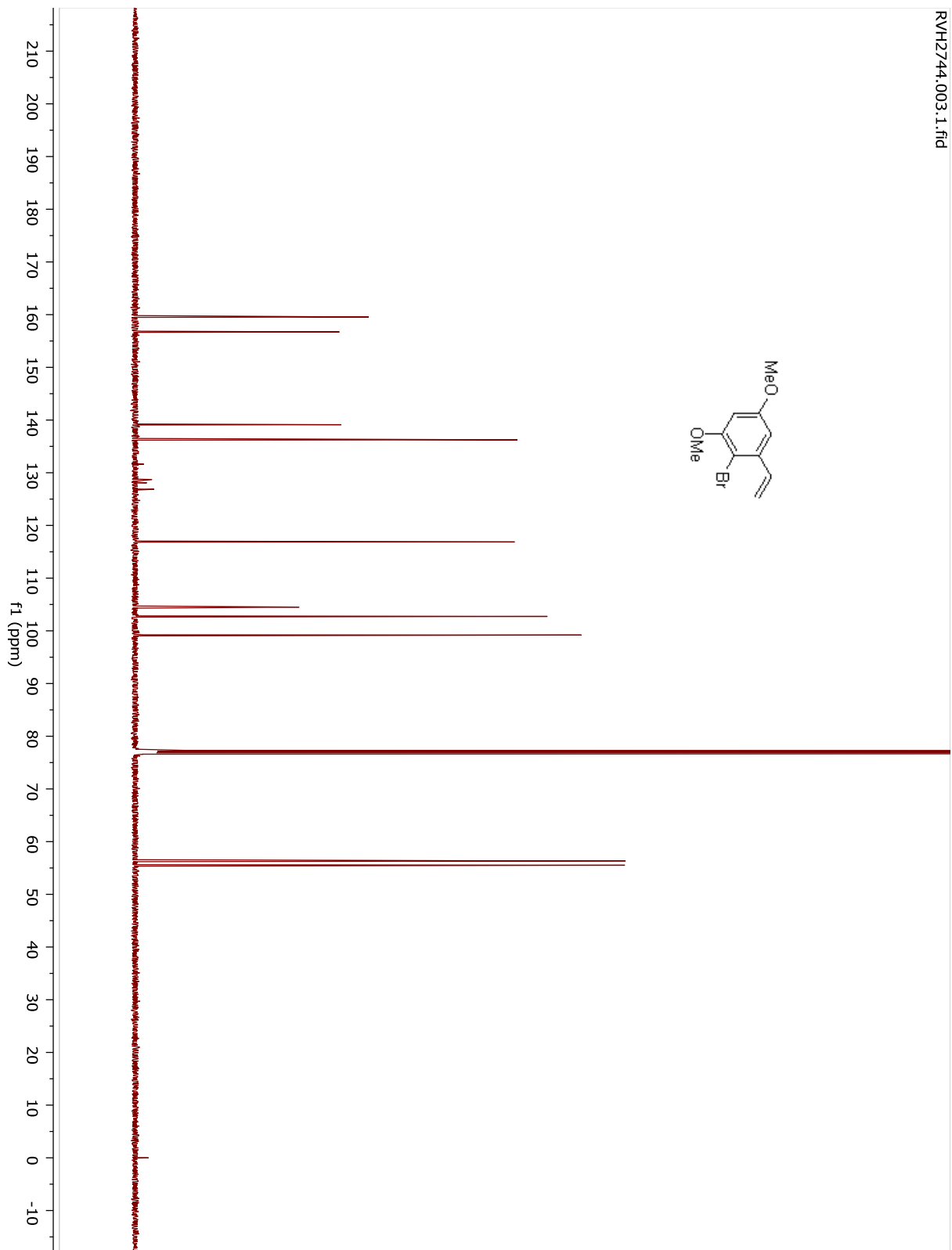
Compound 4.36.



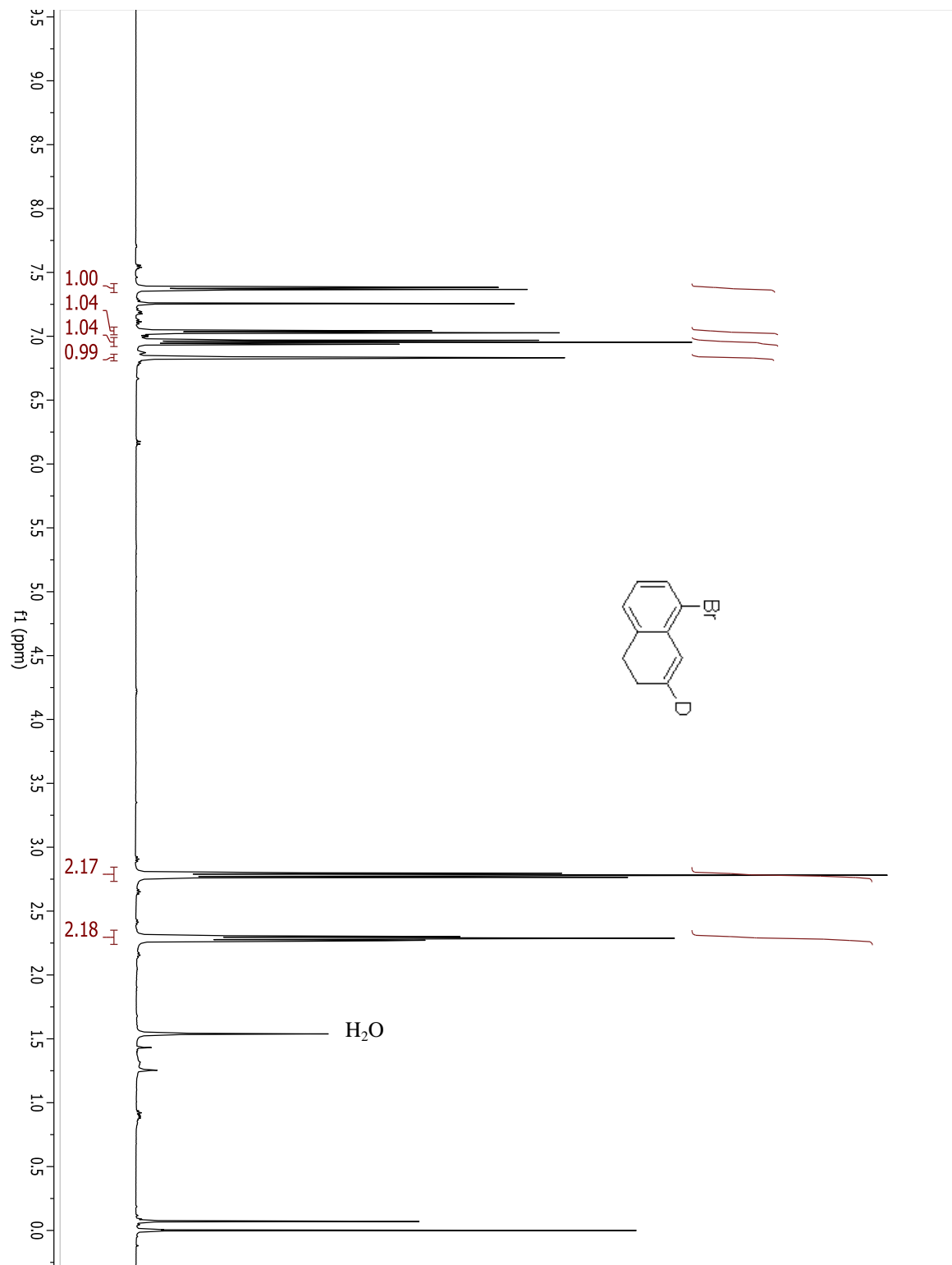
Compound 4.40.



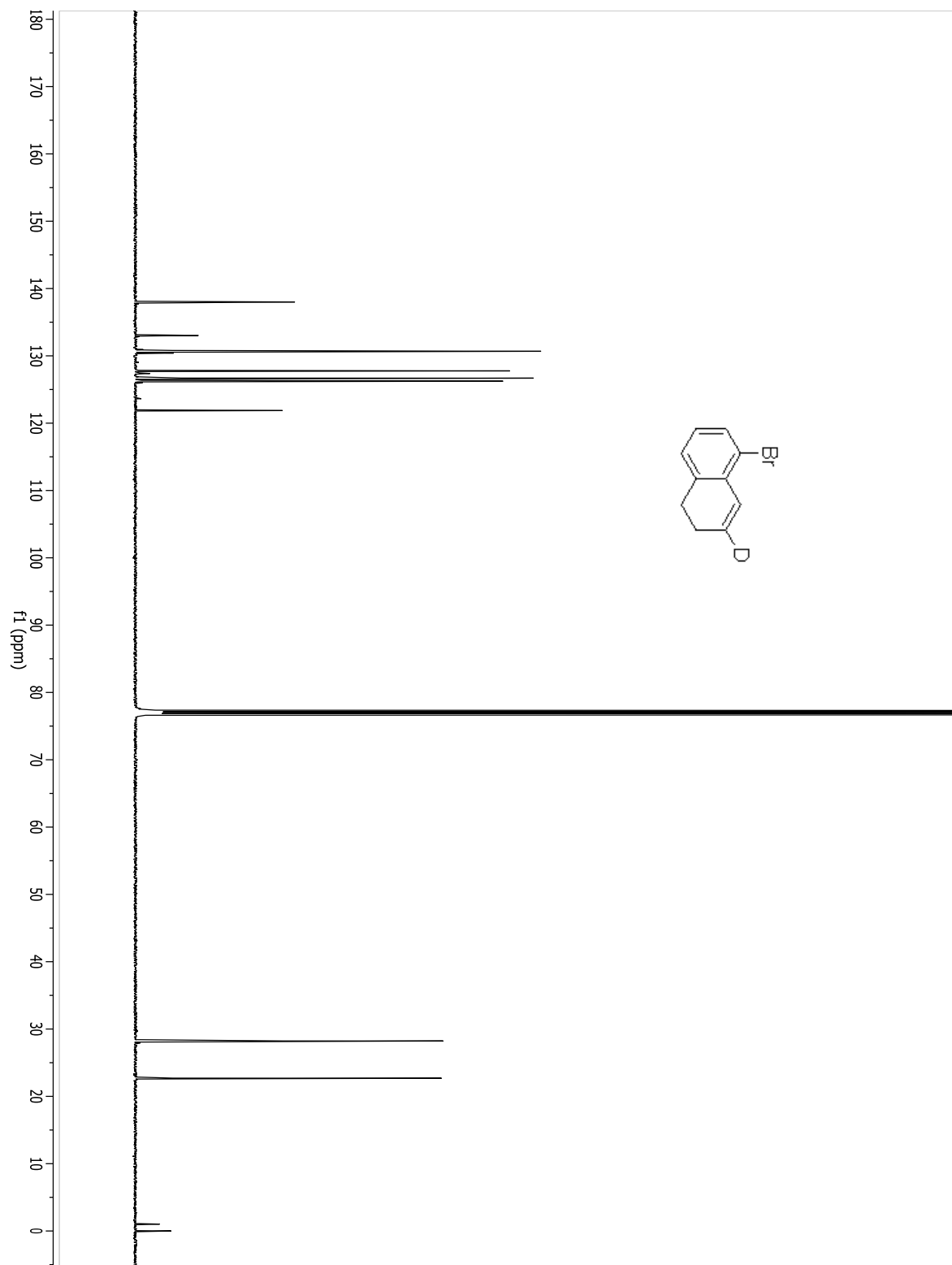
Compound 4.40.



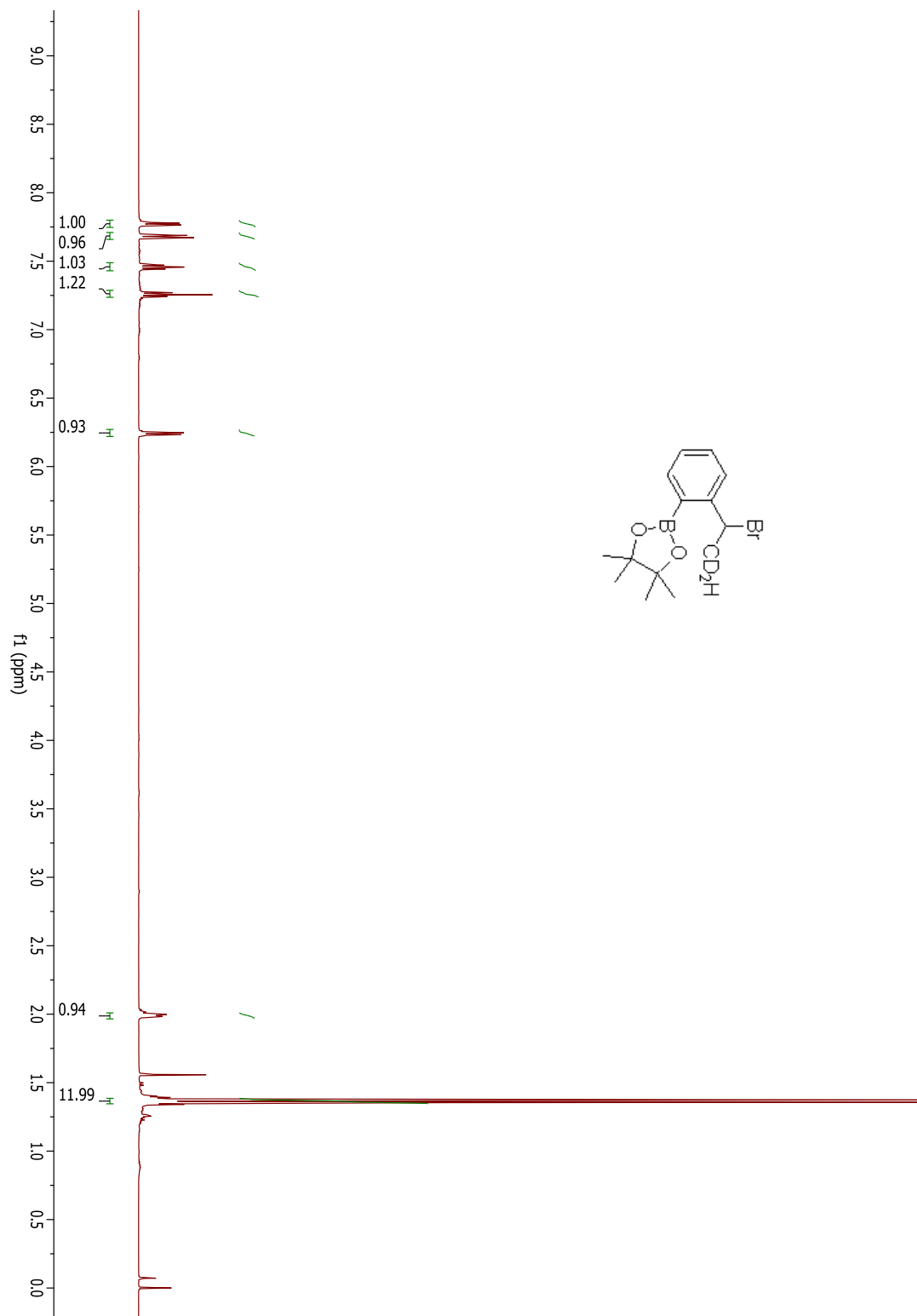
Compound 4.45.



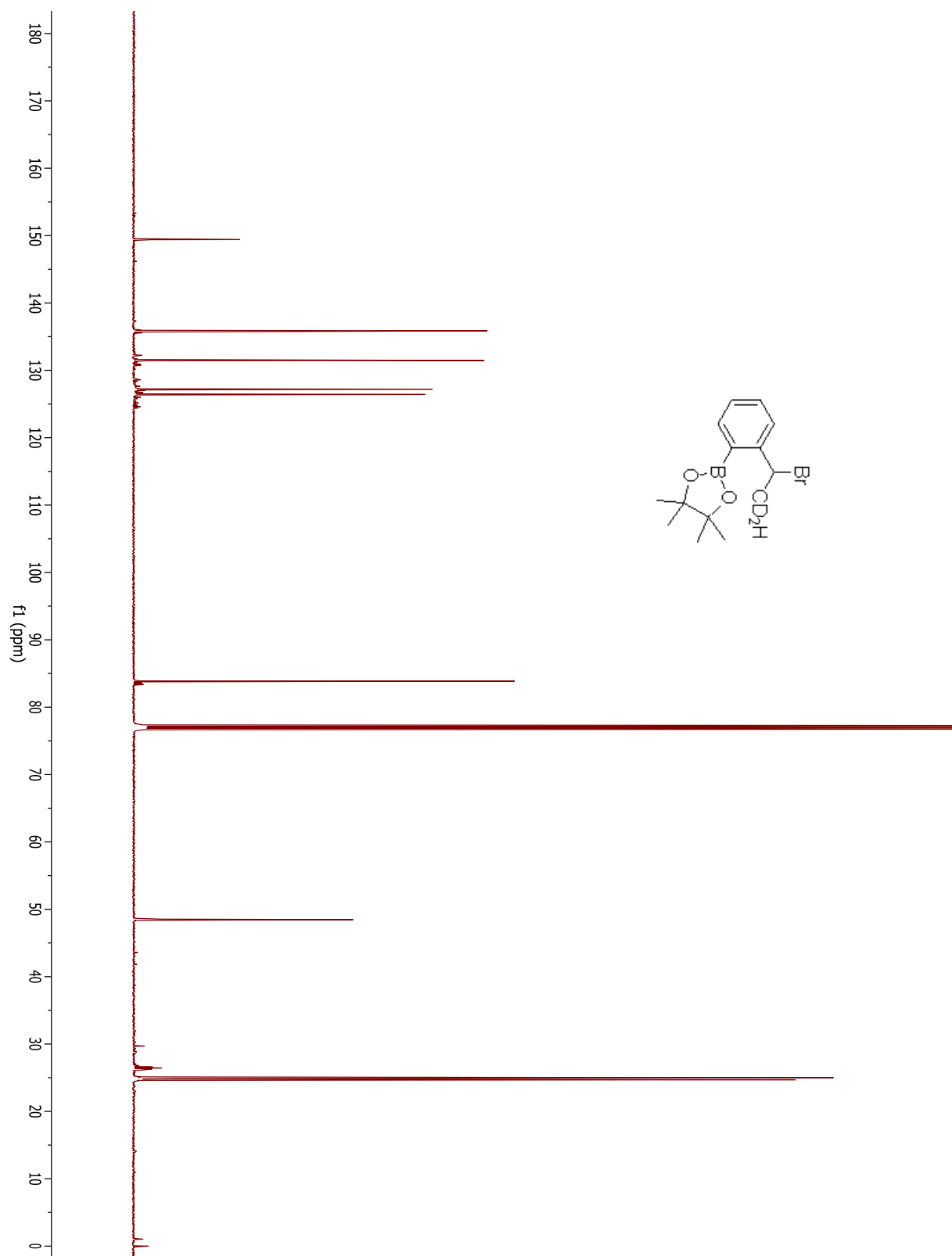
Compound 4.45.



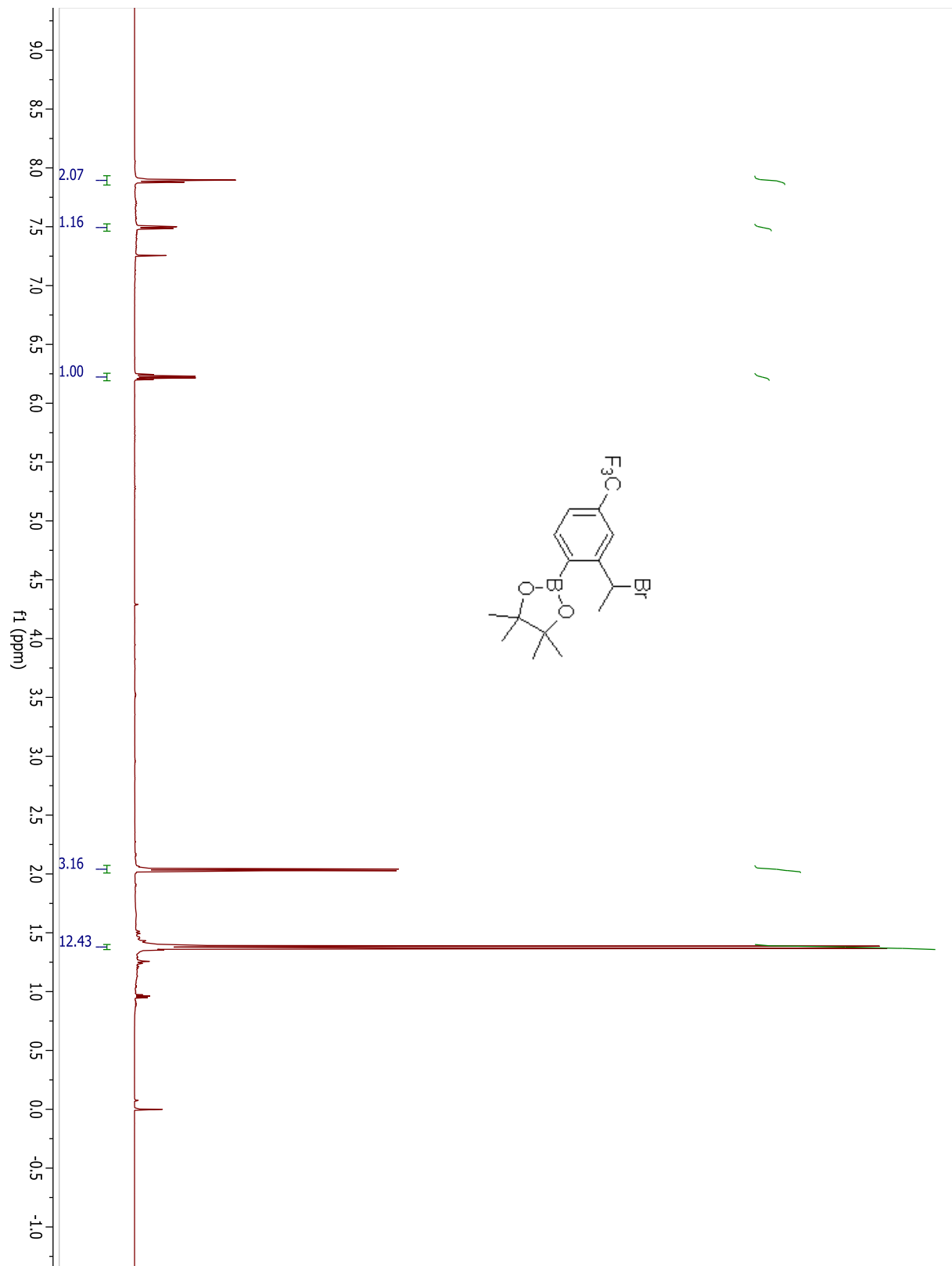
Compound 4.14



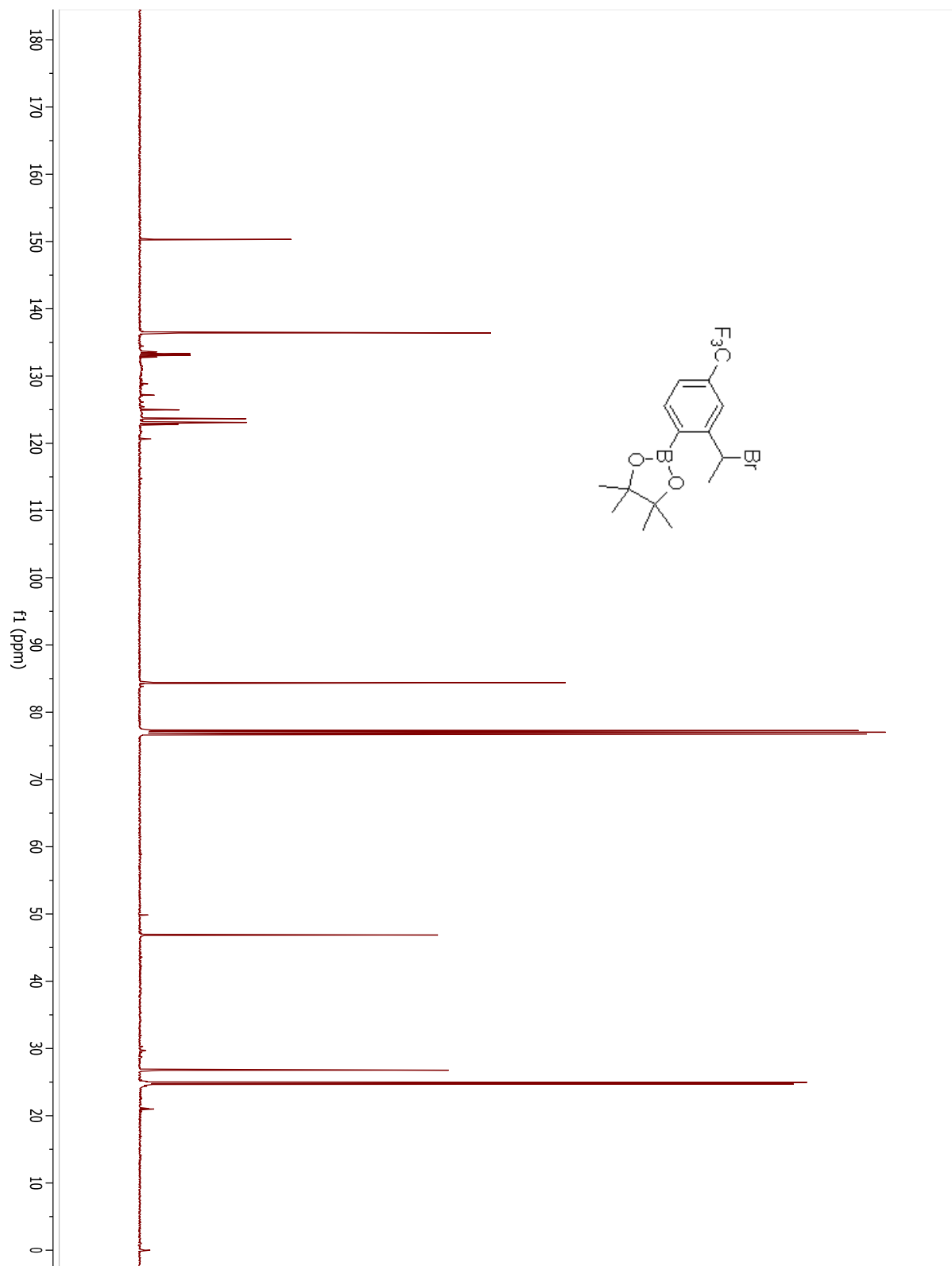
Compound 4.14



Compound 4.37.

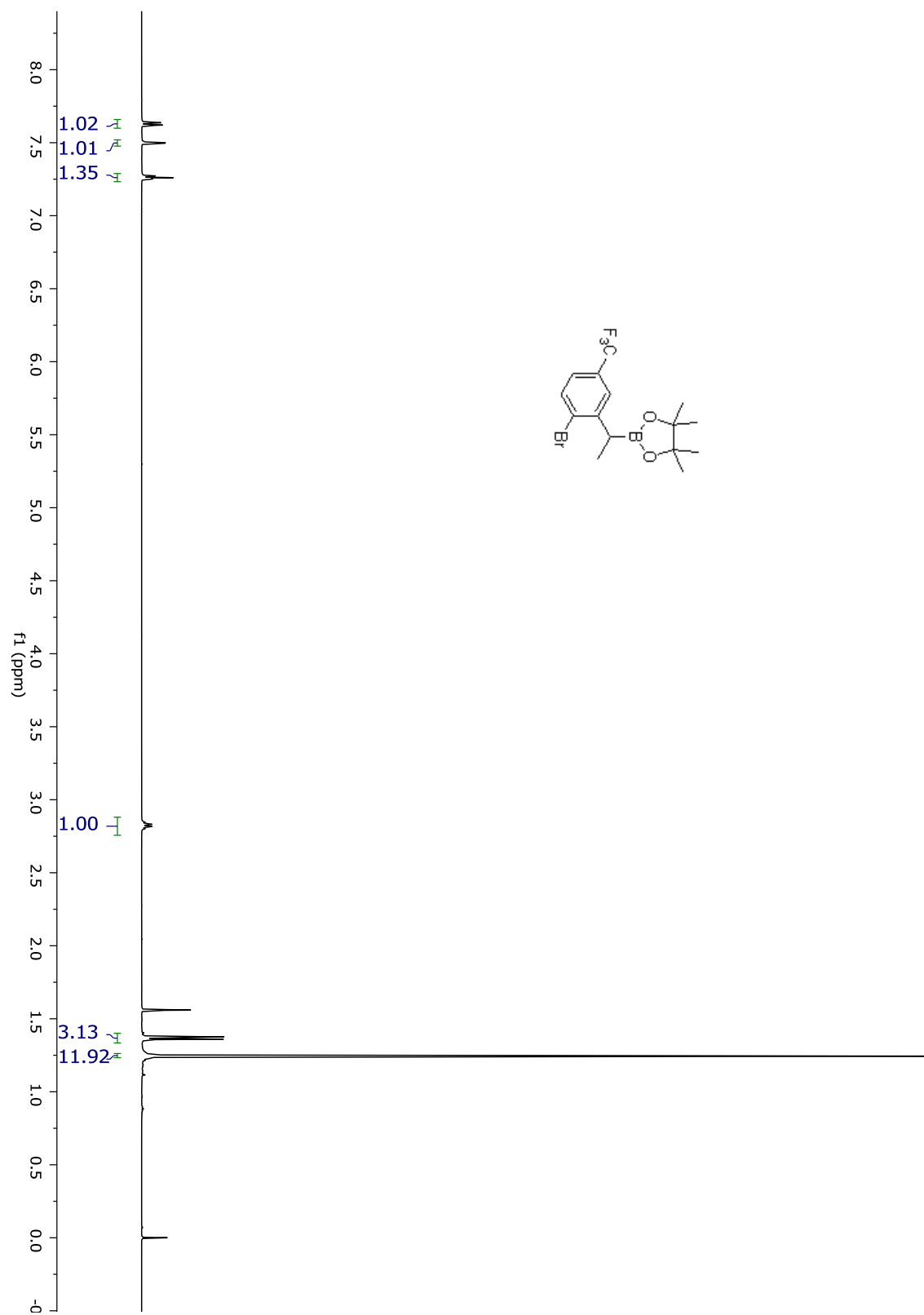


Compound 4.37.

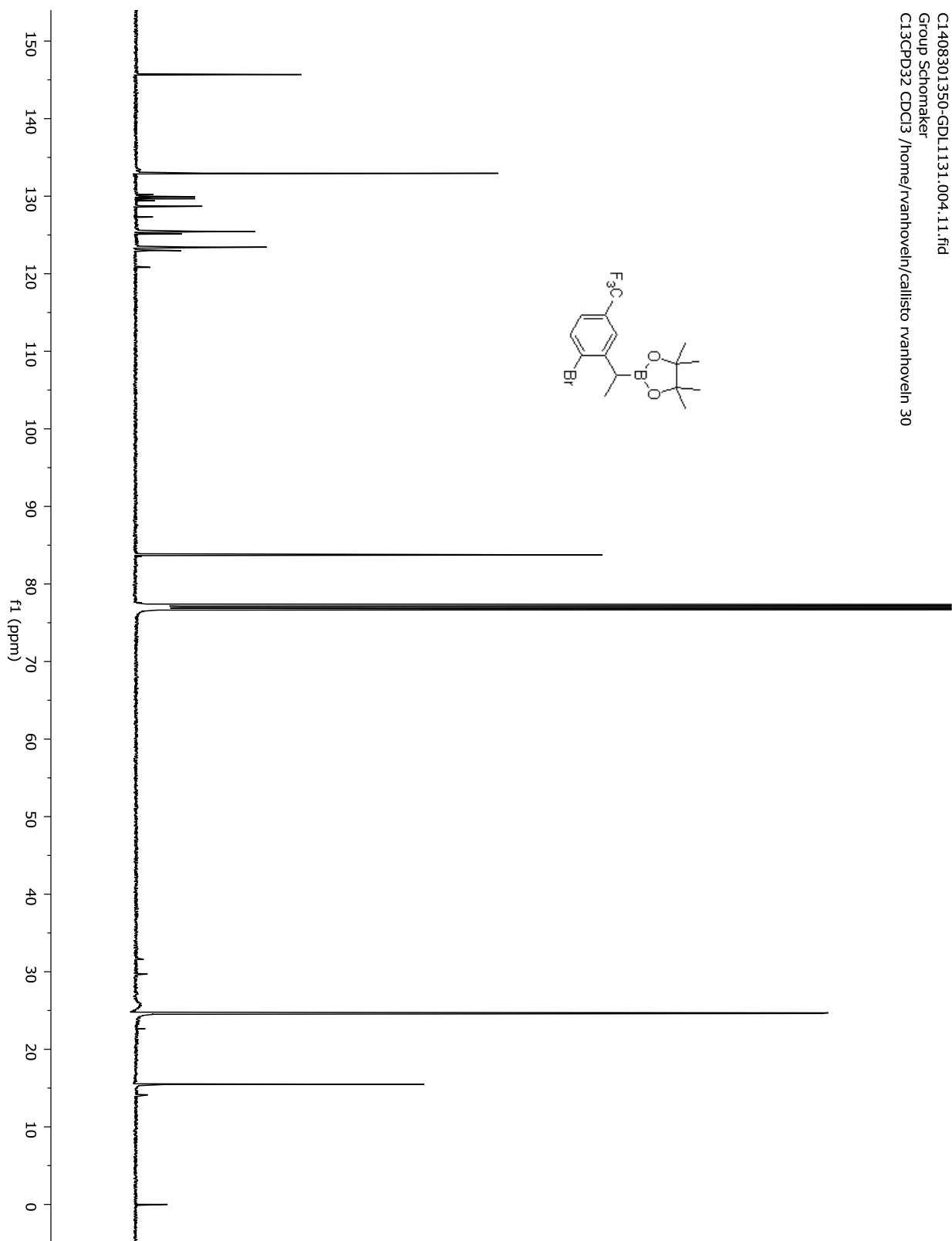


C1408301350-GDL1131.004.10.fid
Group Schomaker
PROTON CDCl3 /home/vanhoveln/callisto vanhoveln 30

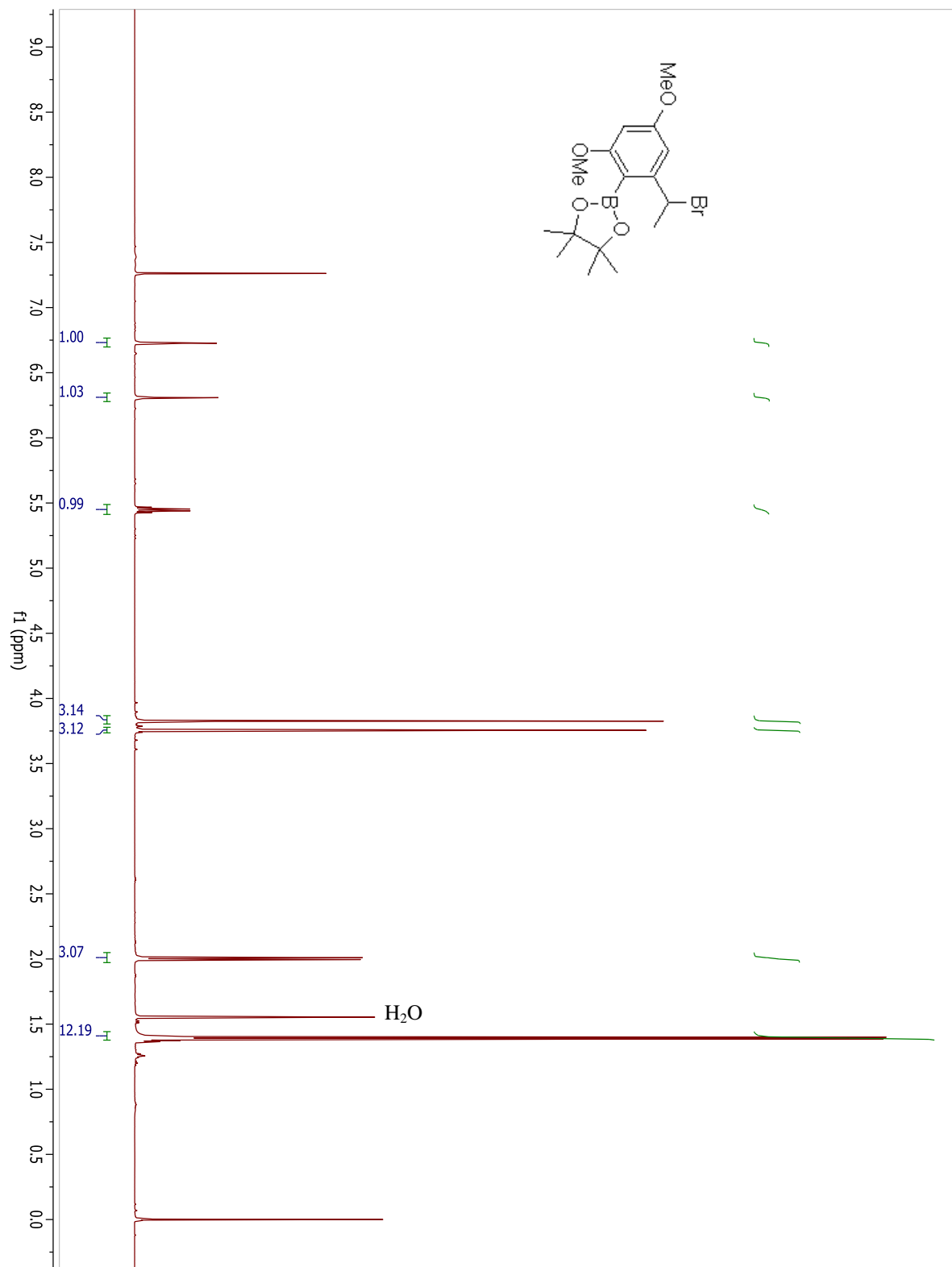
Compound 4.38.



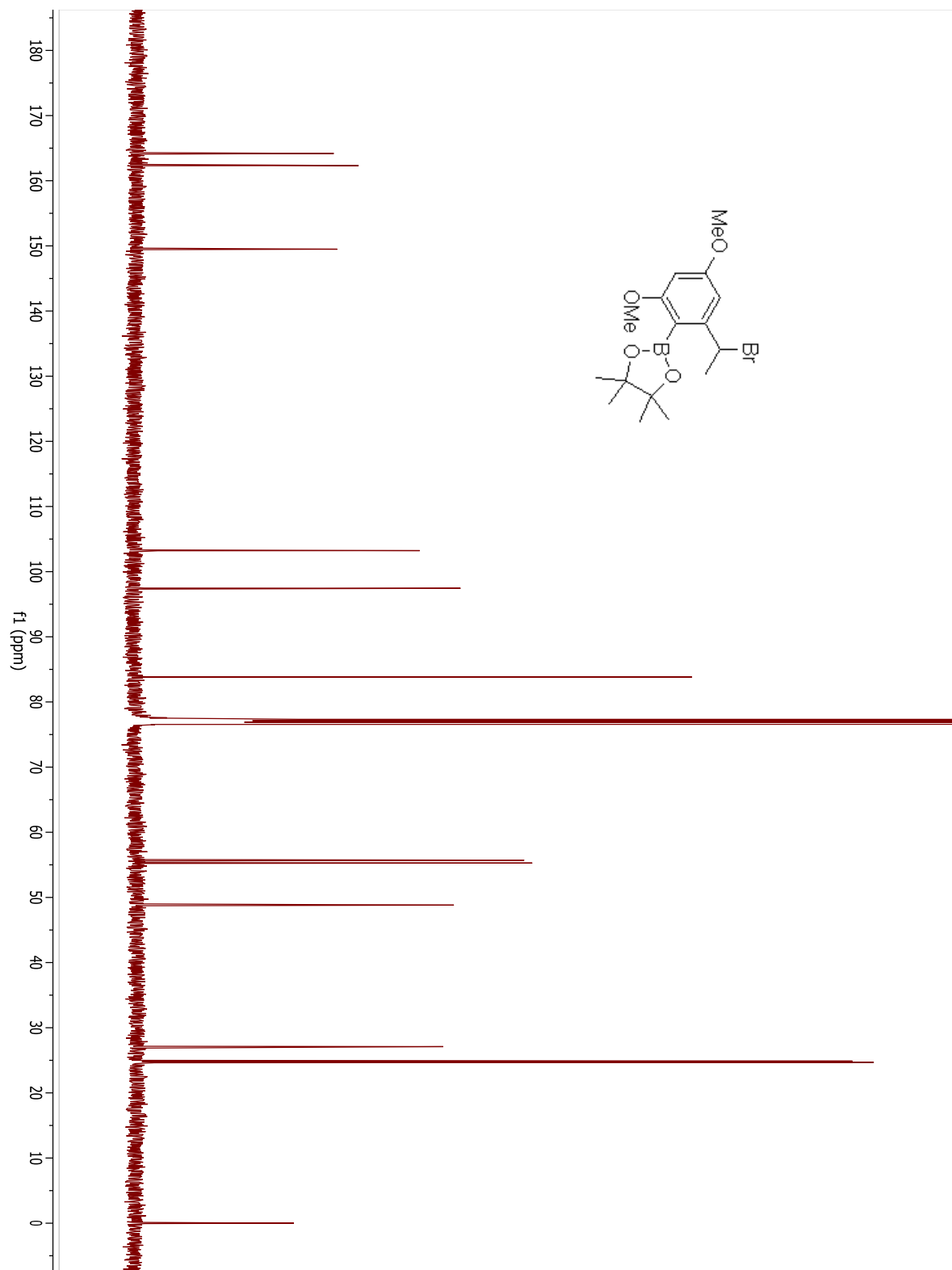
Compound 4.38.



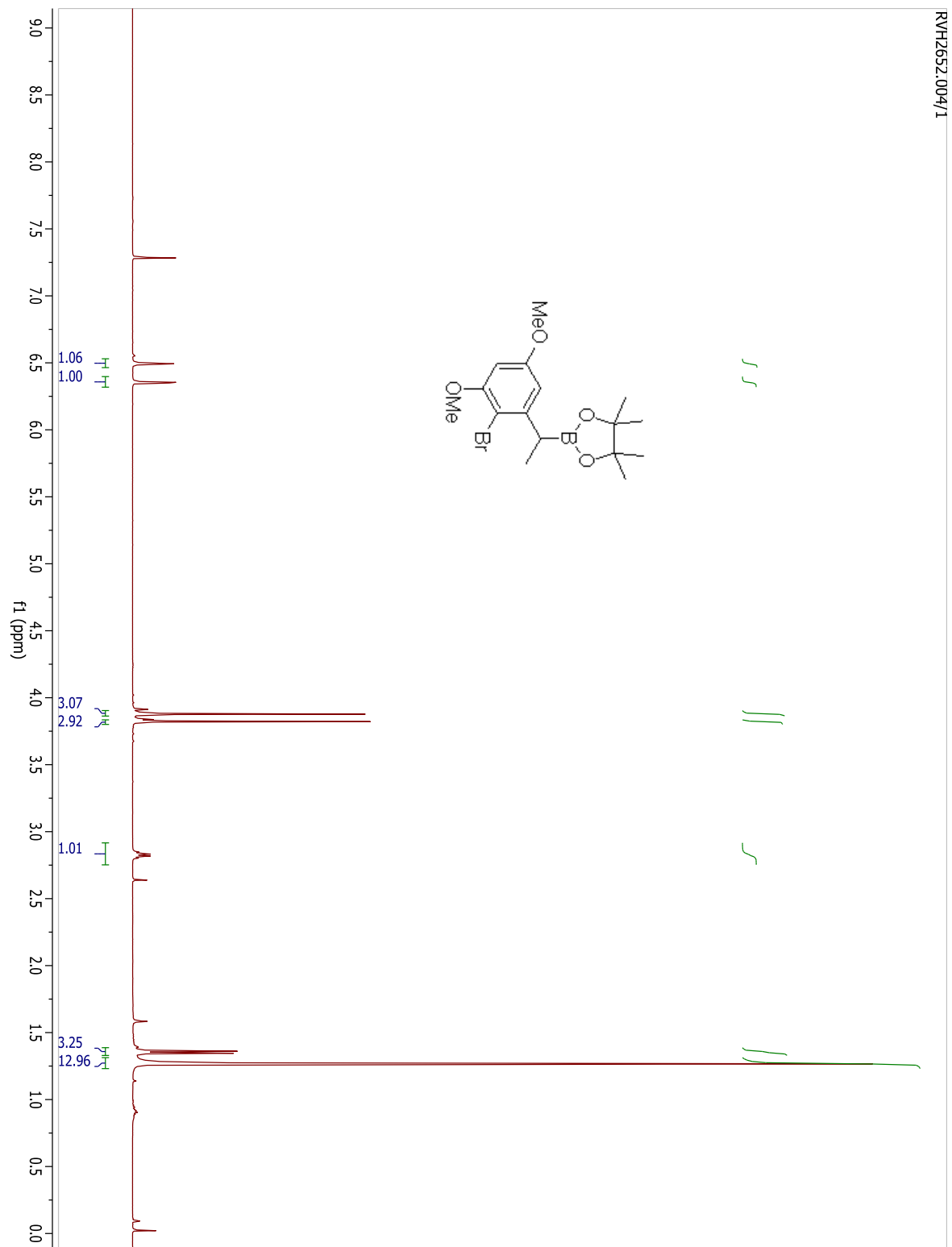
Compound 4.41.



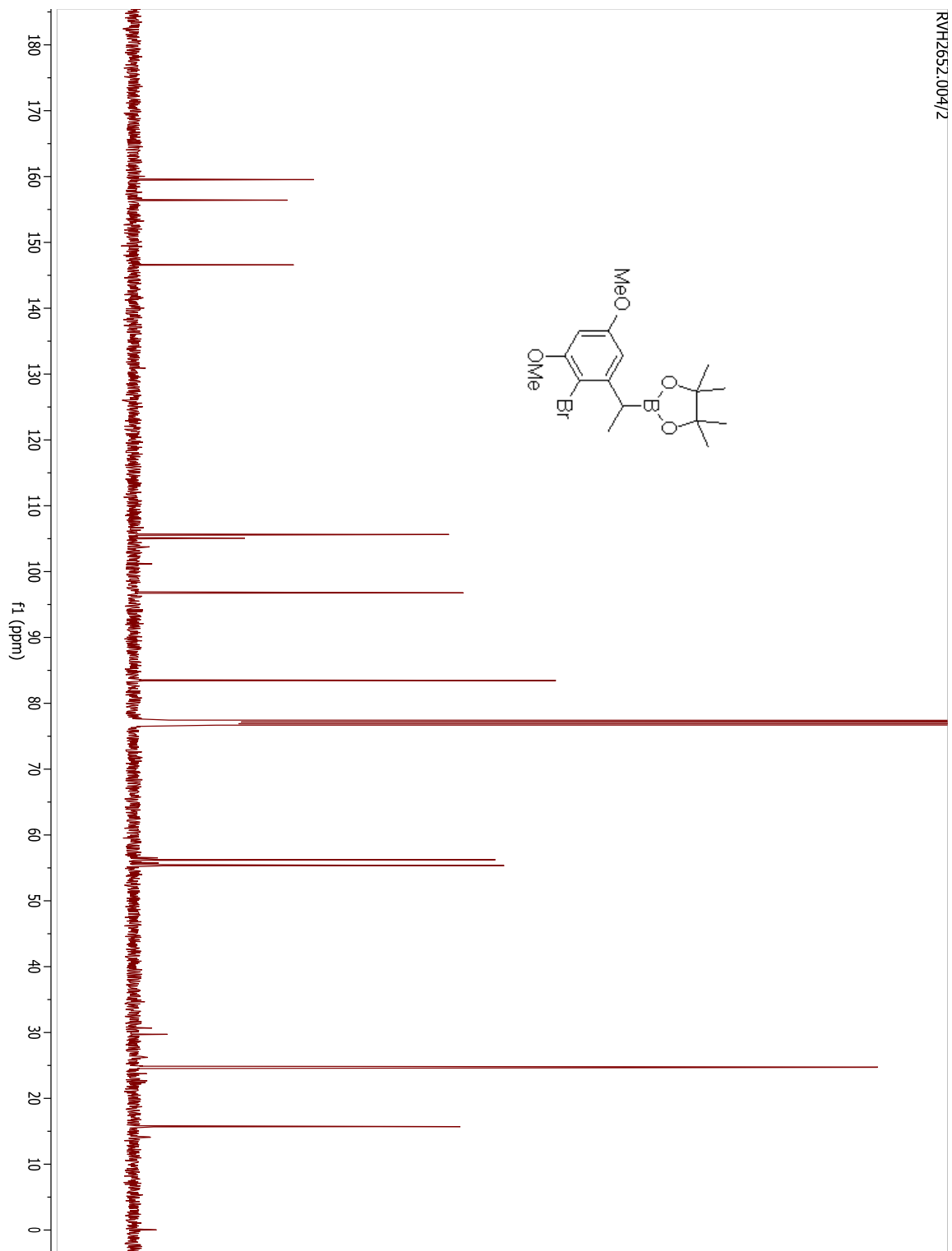
Compound 4.41.



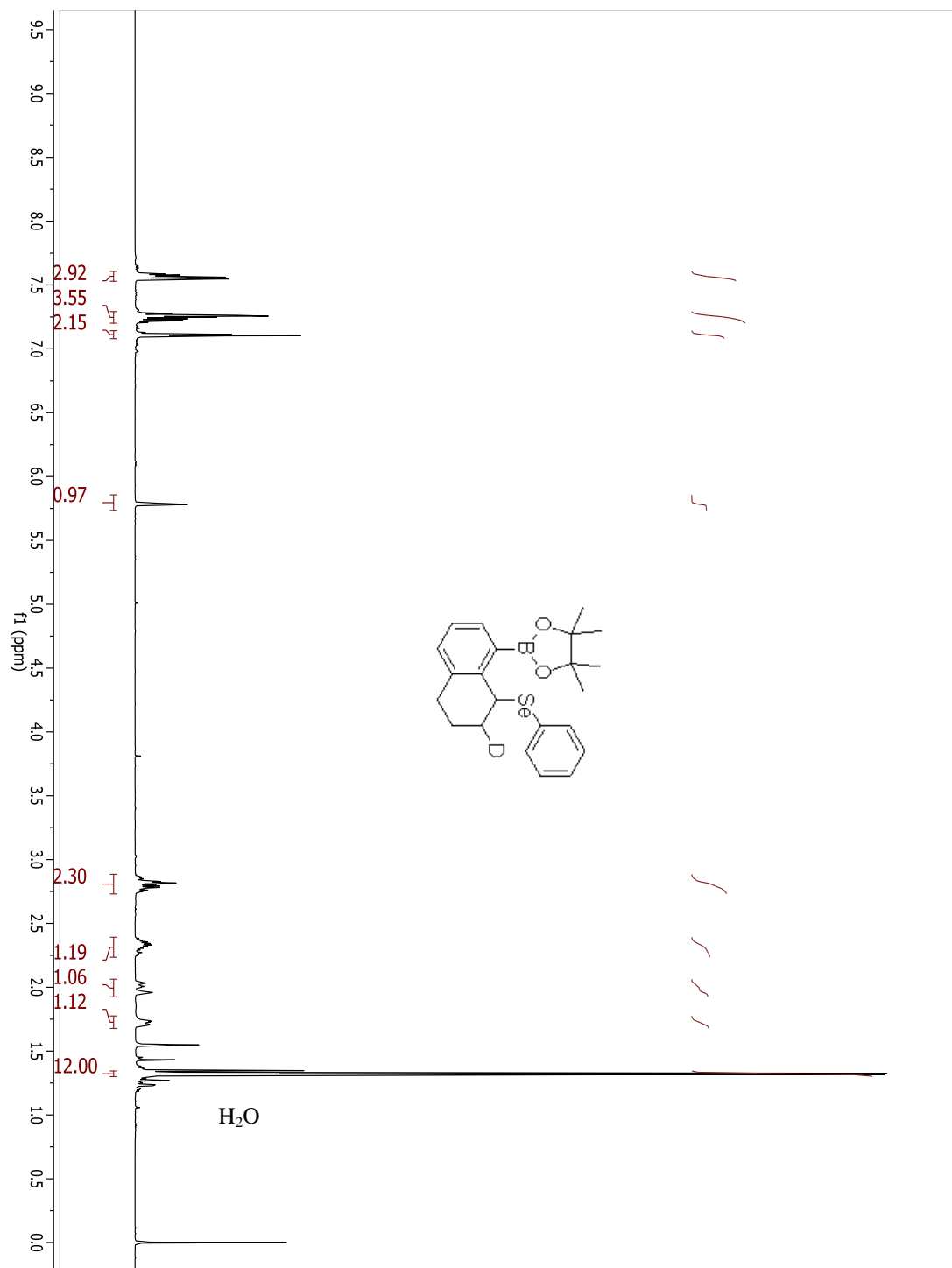
Compound 4.42.



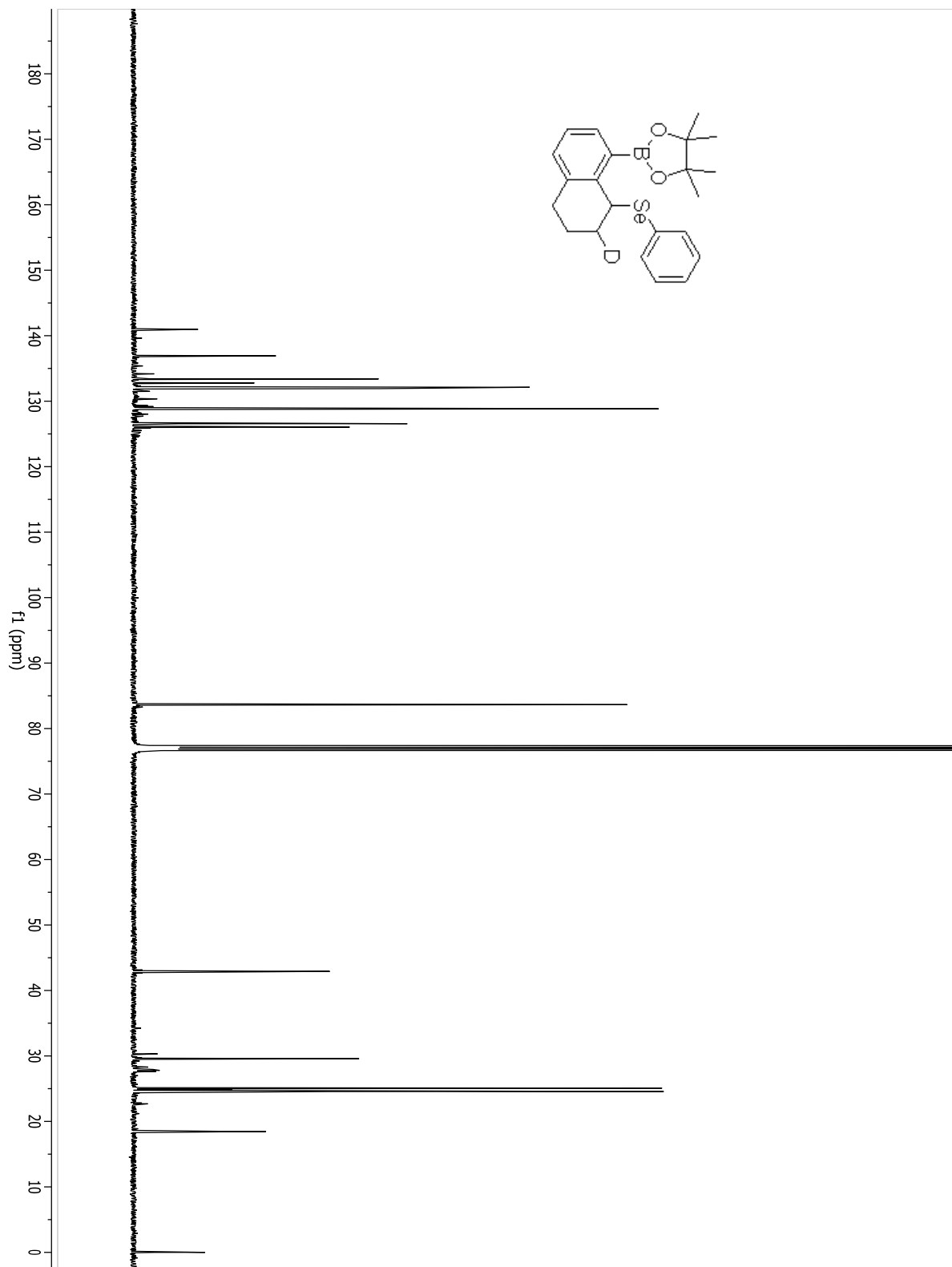
Compound 4.42.



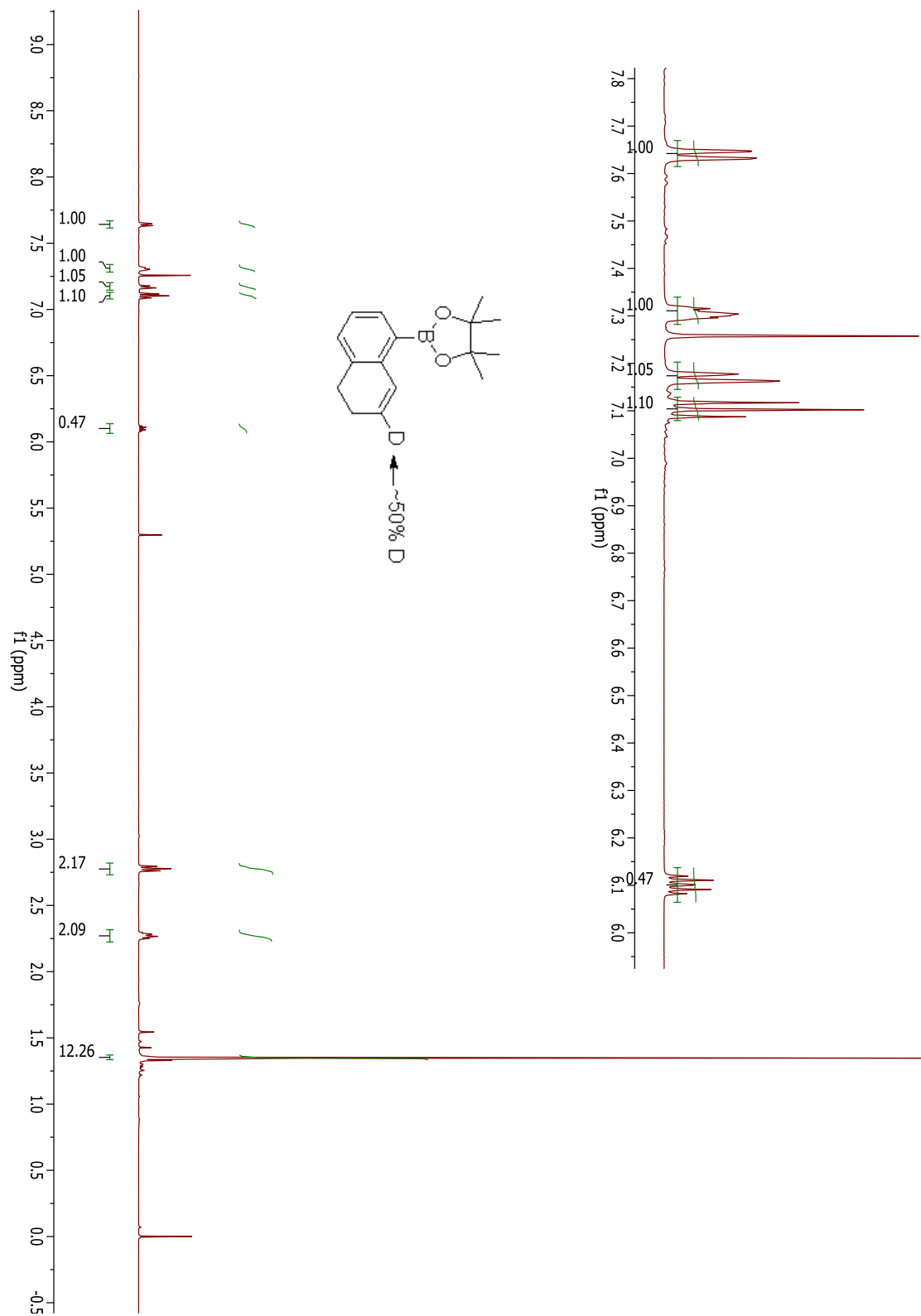
8-[2-(4,4,5,5-tetramethyl-1,3,2-dioxaborolane)]-1-(phenylselenenyl)(2-D)-1,2,3,4-tetrahydronaphthalene



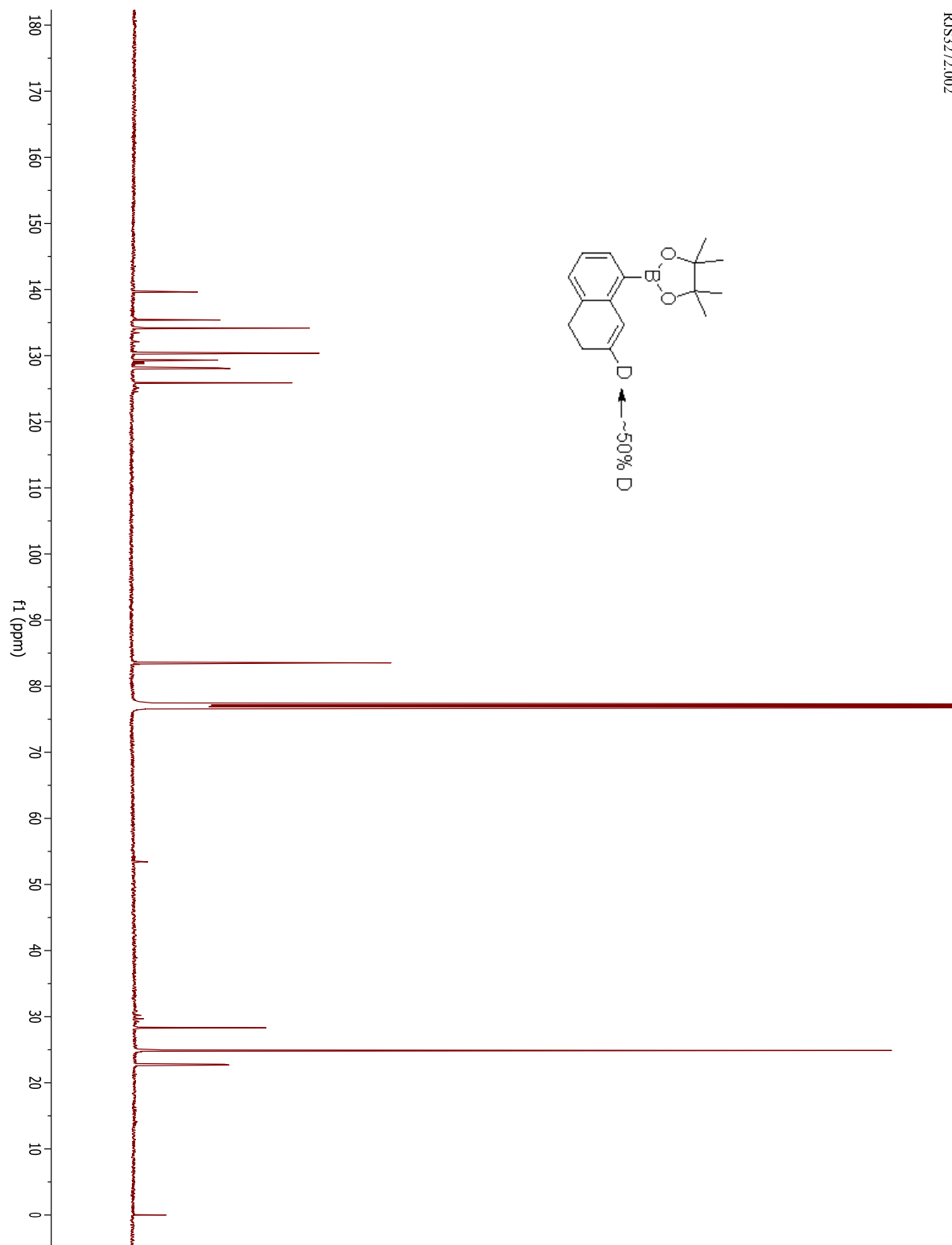
8-[2-(4,4,5,5-tetramethyl-1,3,2-dioxaborolane)]-1-(phenylselenenyl)(2-D)-1,2,3,4-tetrahydronaphthalene

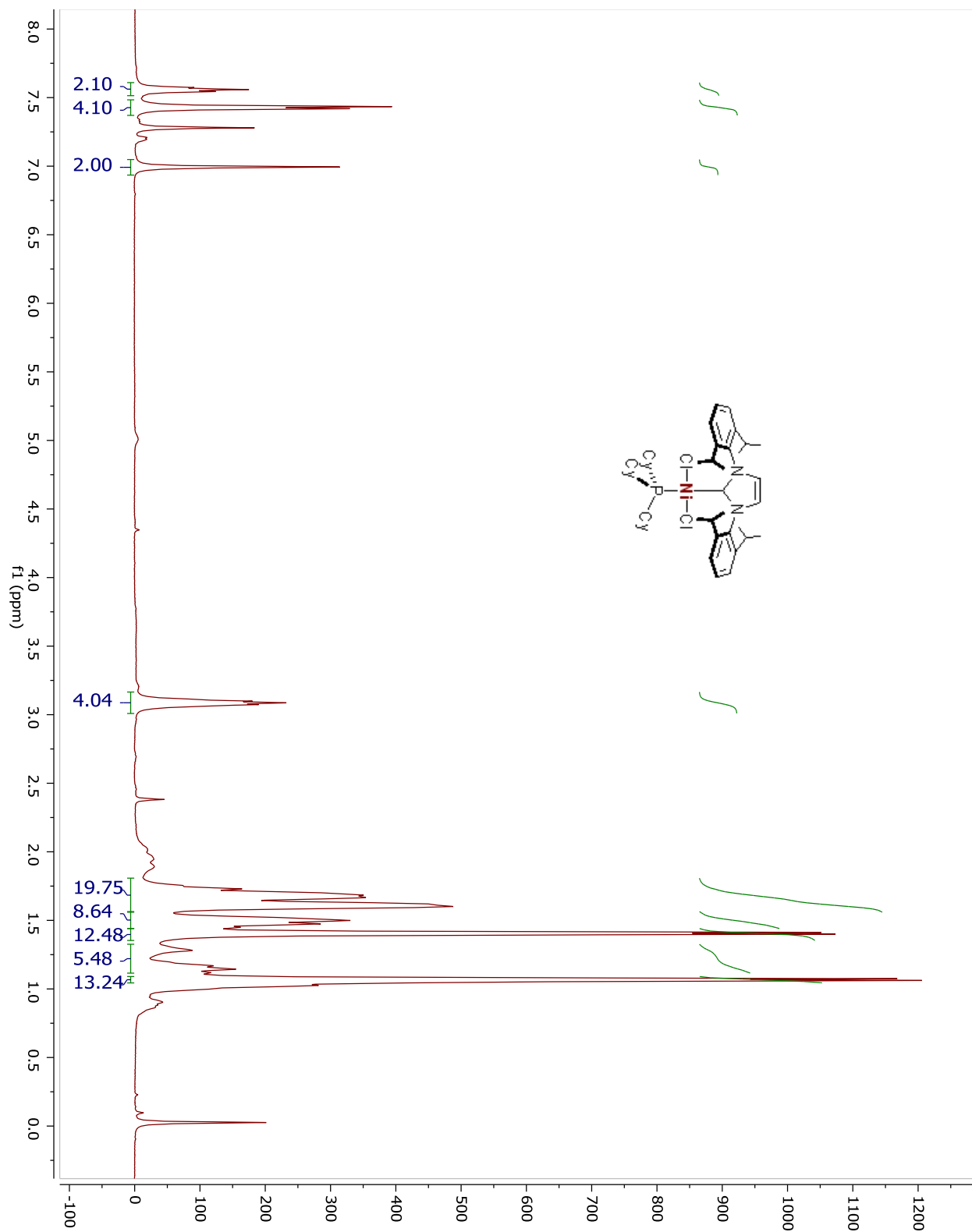


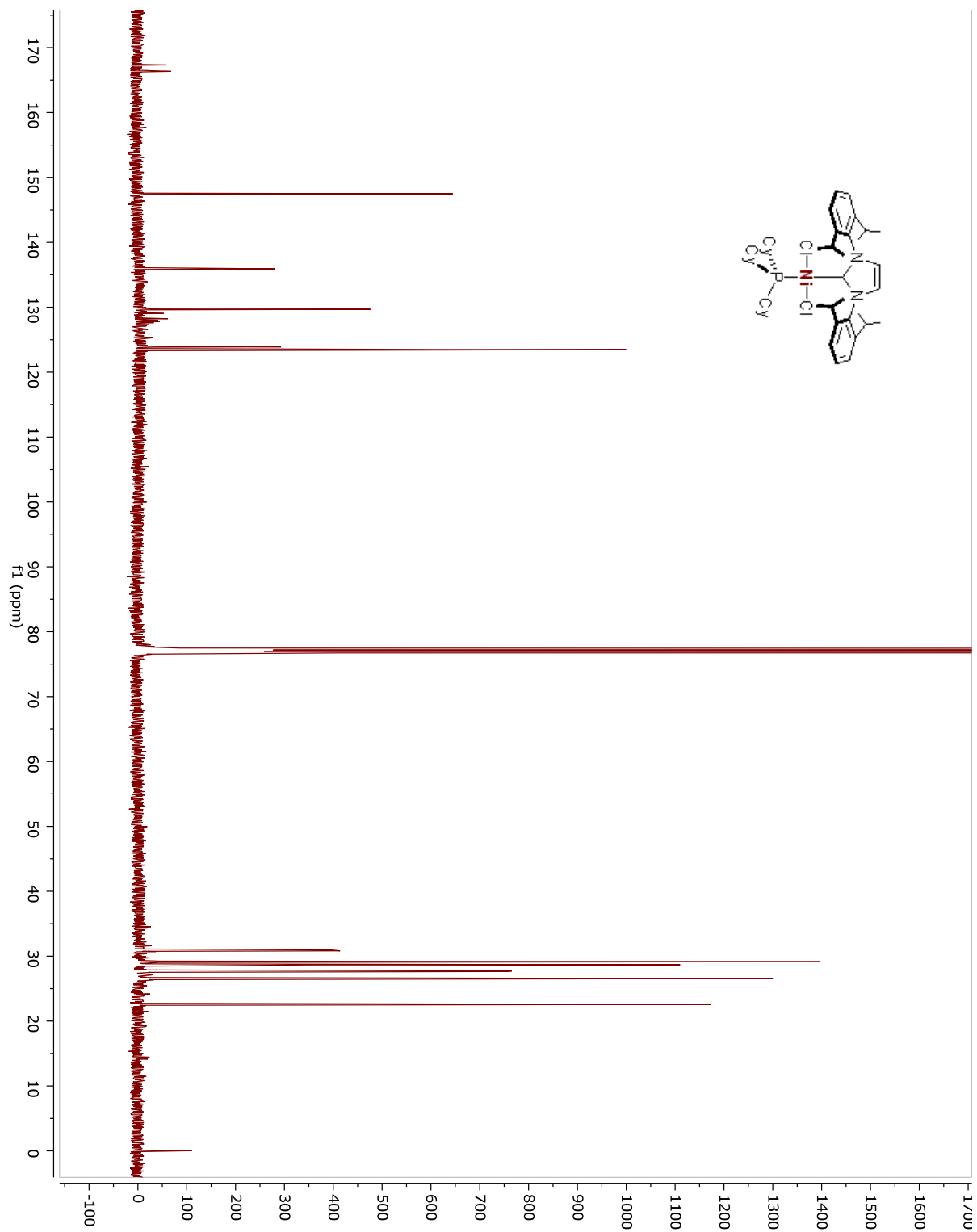
8-[2-(4,4,5,5-tetramethyl-1,3,2-dioxaborolane)]-2-deutero-3,4-dihydronaphthalene

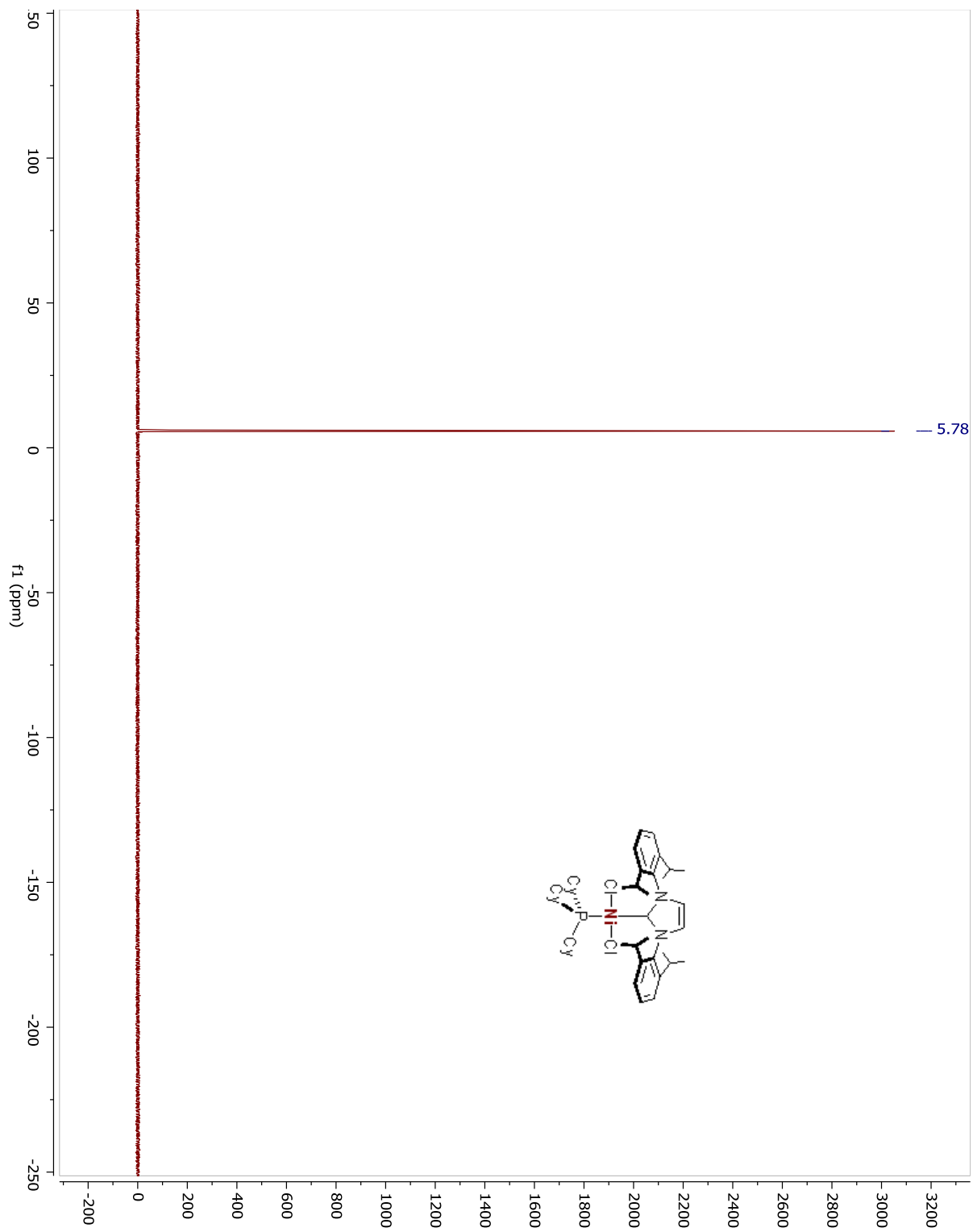


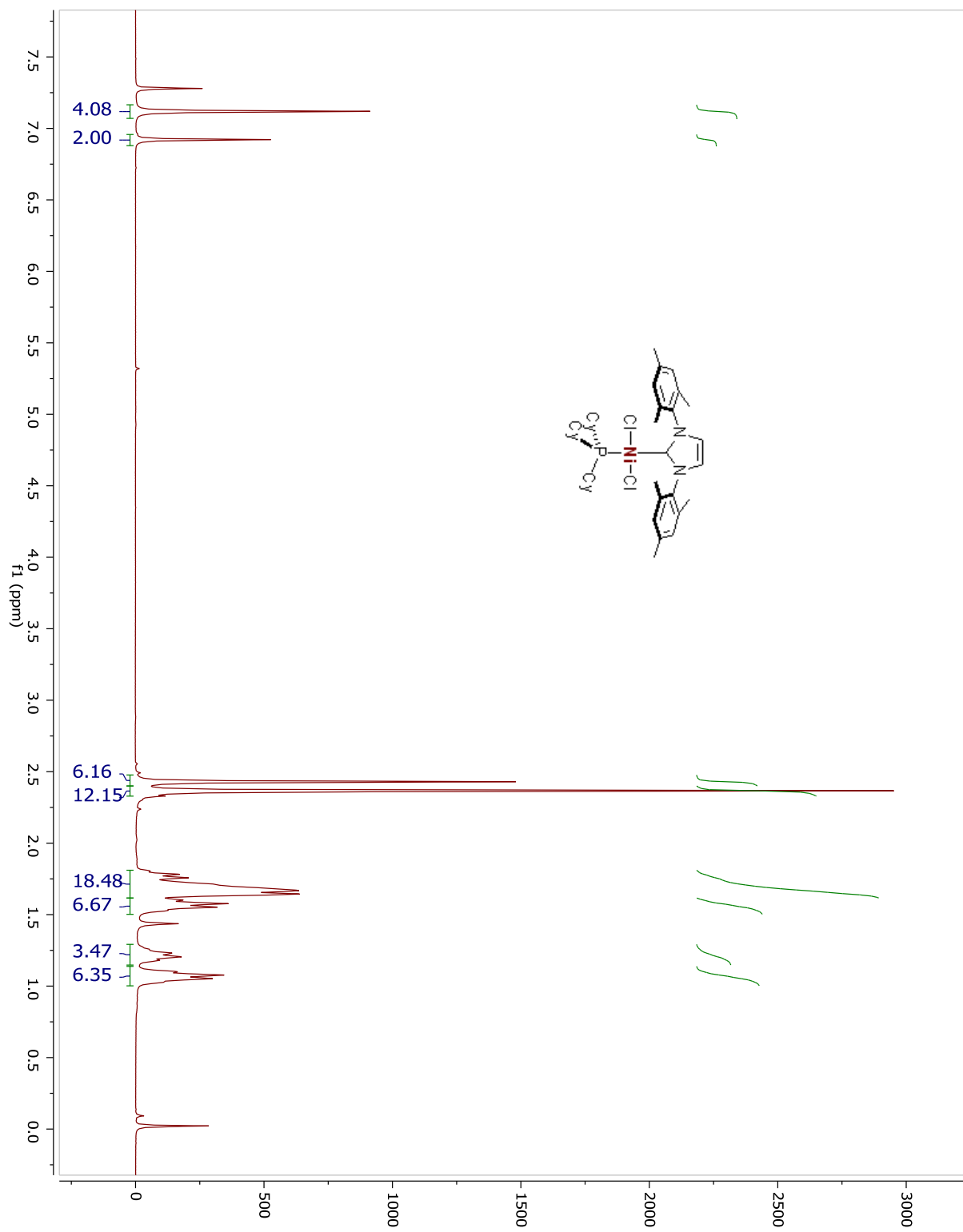
8-[2-(4,4,5,5-tetramethyl-1,3,2-dioxaborolane)]-2-deutero-3,4-dihydronaphthalene

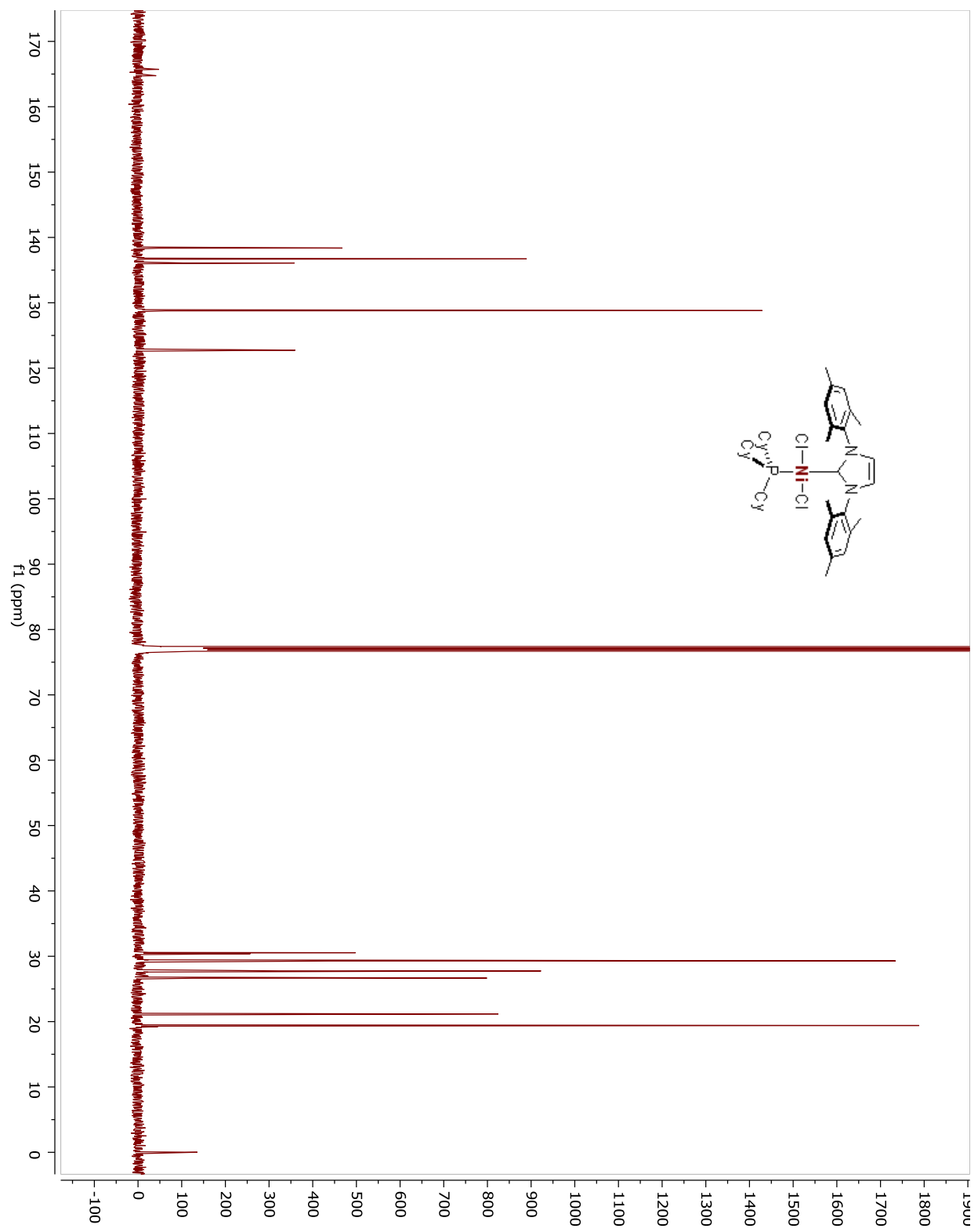


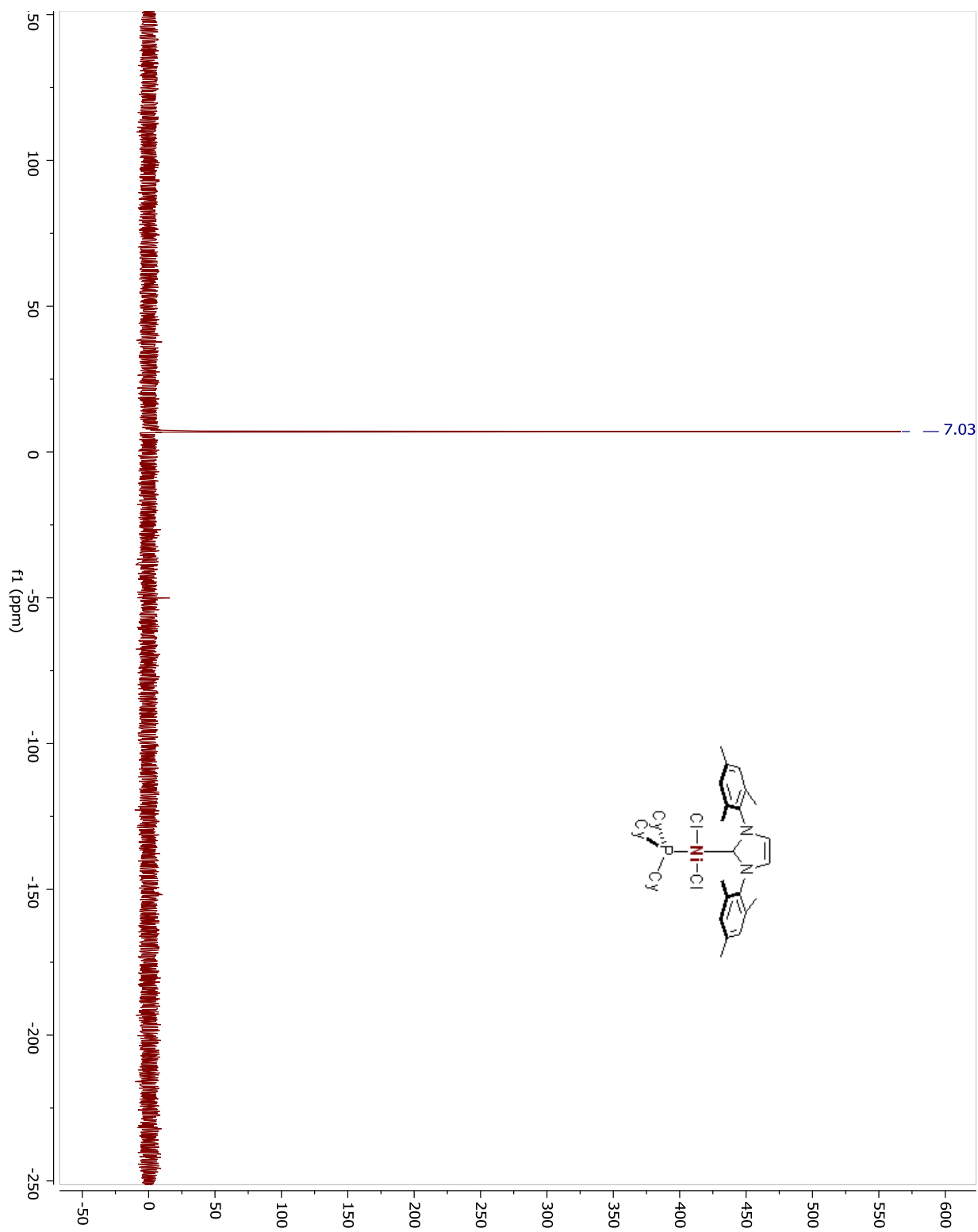
IPr(Cy₃P)NiCl₂

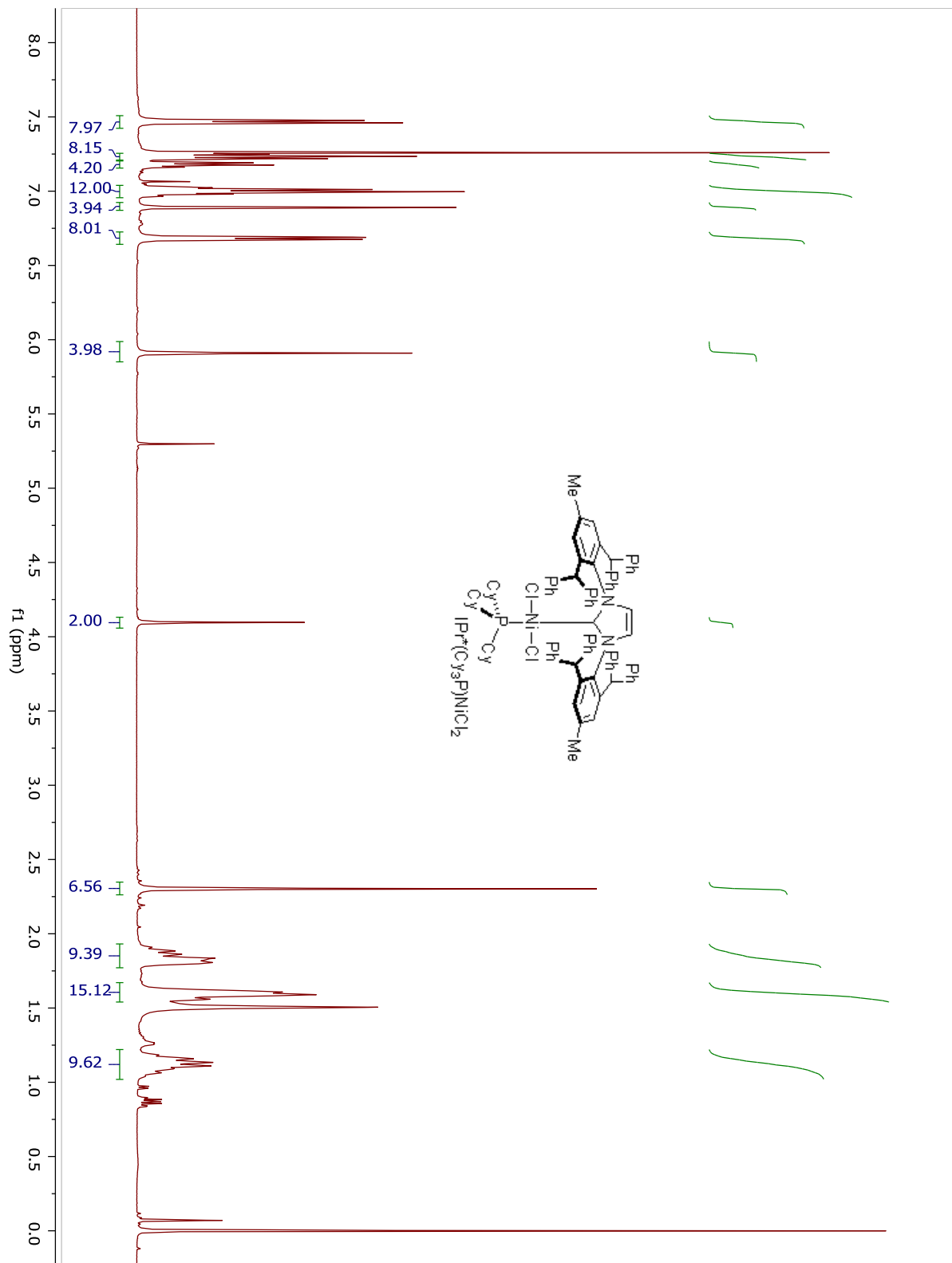
$\text{IPr}(\text{Cy}_3\text{P})\text{NiCl}_2$ 

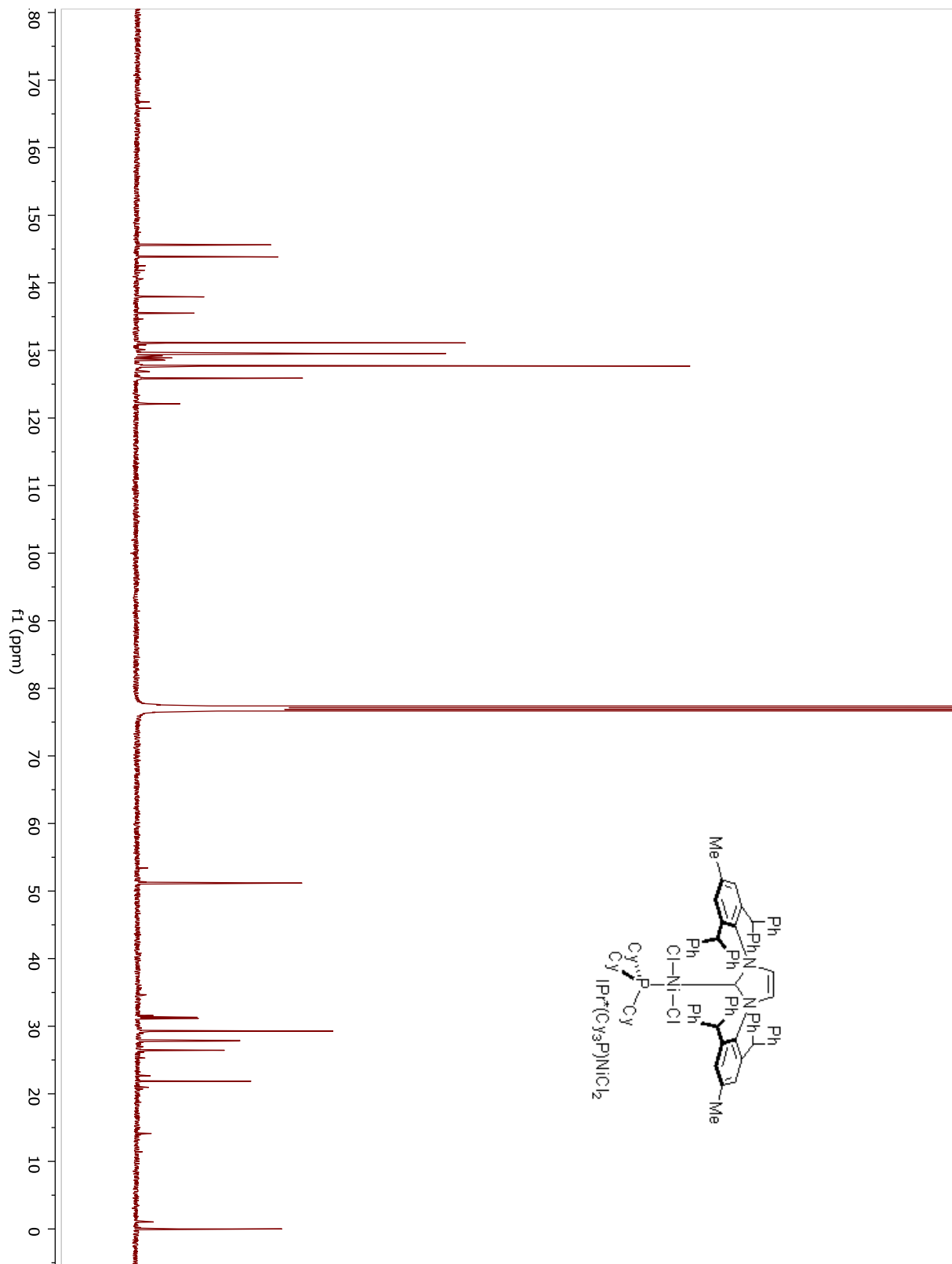
$\text{IPr}(\text{Cy}_3\text{P})\text{NiCl}_2$ 

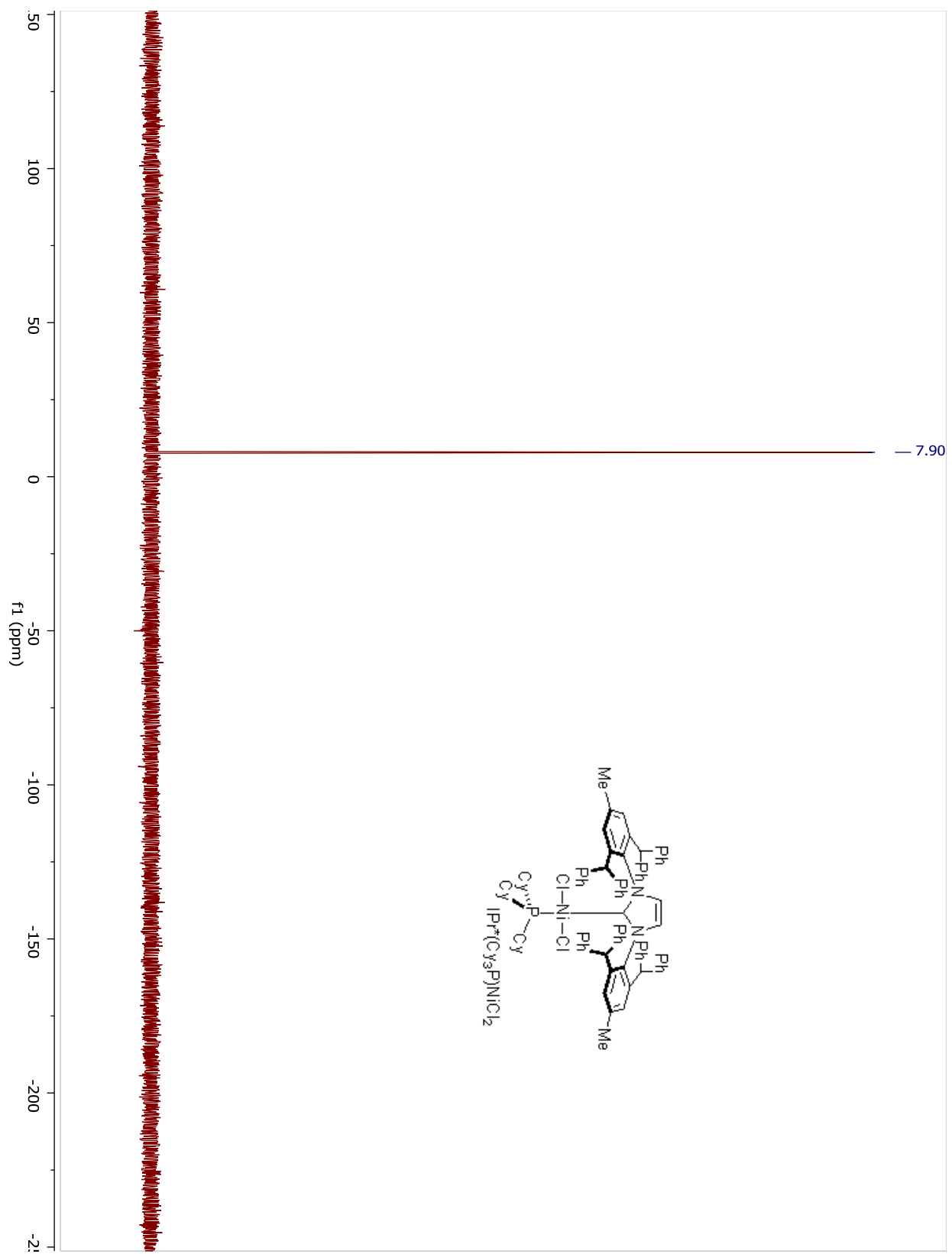
IMes(Cy₃P)NiCl₂

$\text{IMes}(\text{Cy}_3\text{P})\text{NiCl}_2$ 

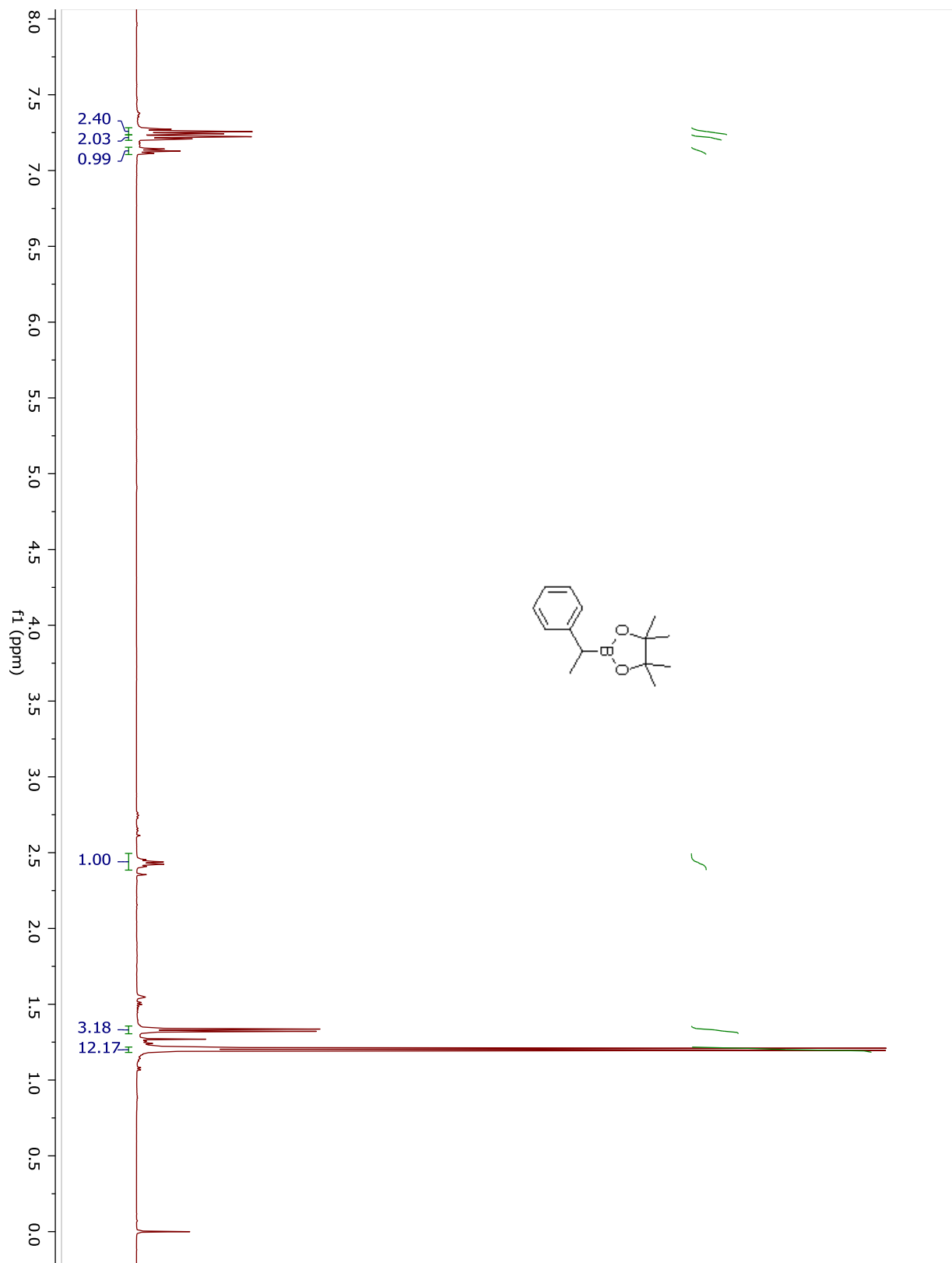
IMes(Cy₃P)NiCl₂

$\text{IPr}^*(\text{Cy}_3\text{P})\text{NiCl}_2$ 

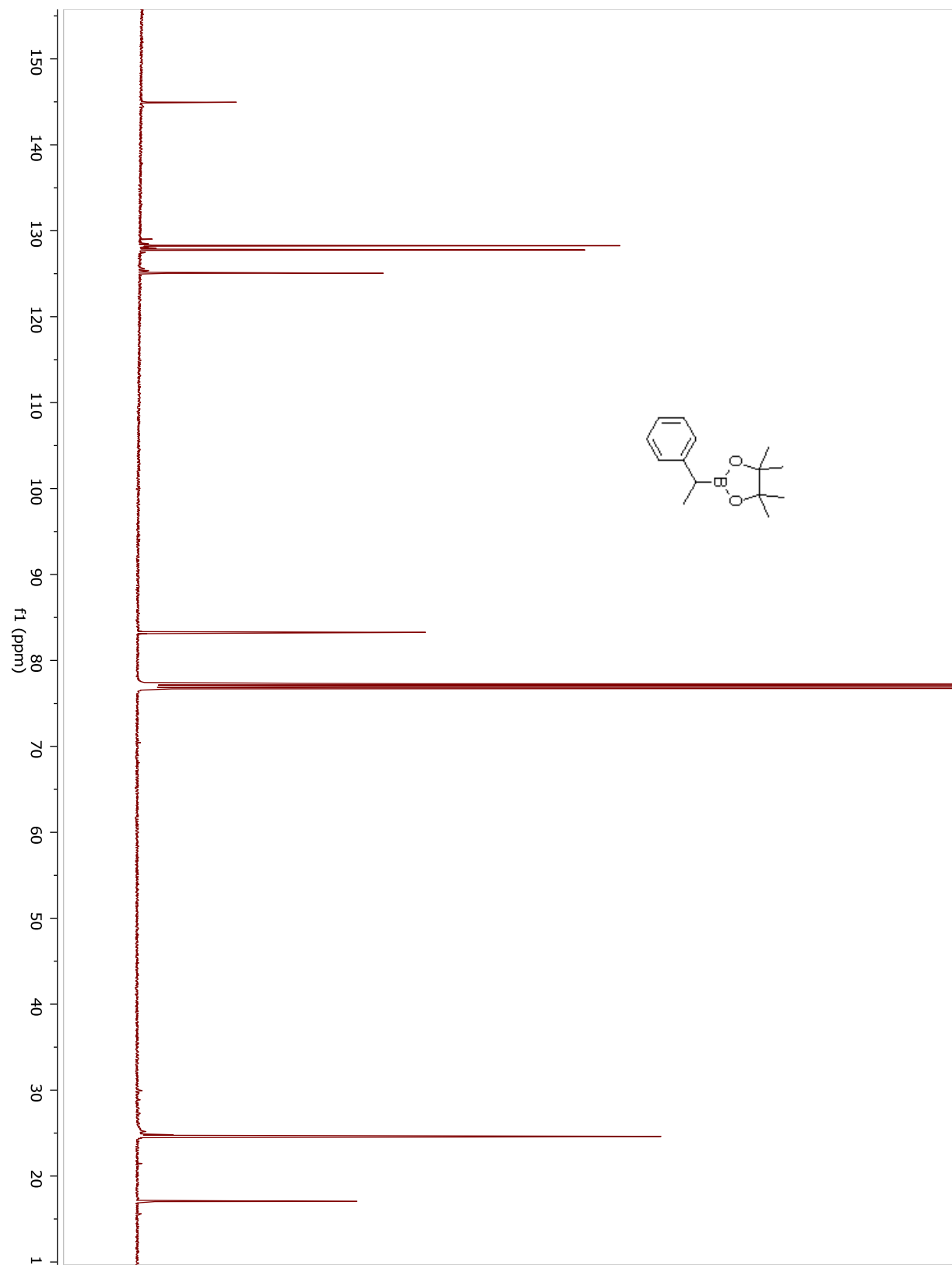
$\text{IPr}^*(\text{Cy}_3\text{P})\text{NiCl}_2$ 

$\text{IPr}^*(\text{Cy}_3\text{P})\text{NiCl}_2$ 

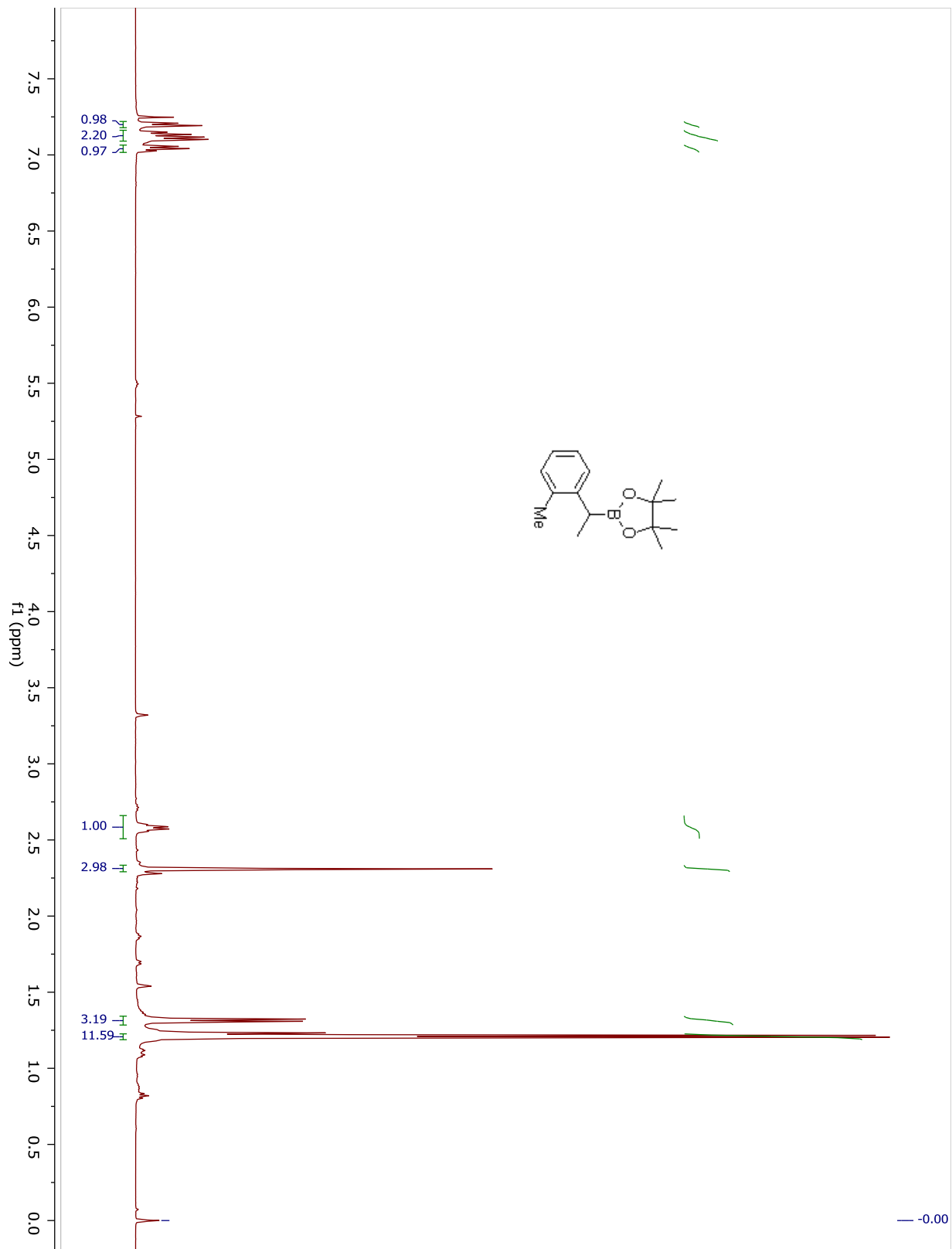
Compound 5.12.



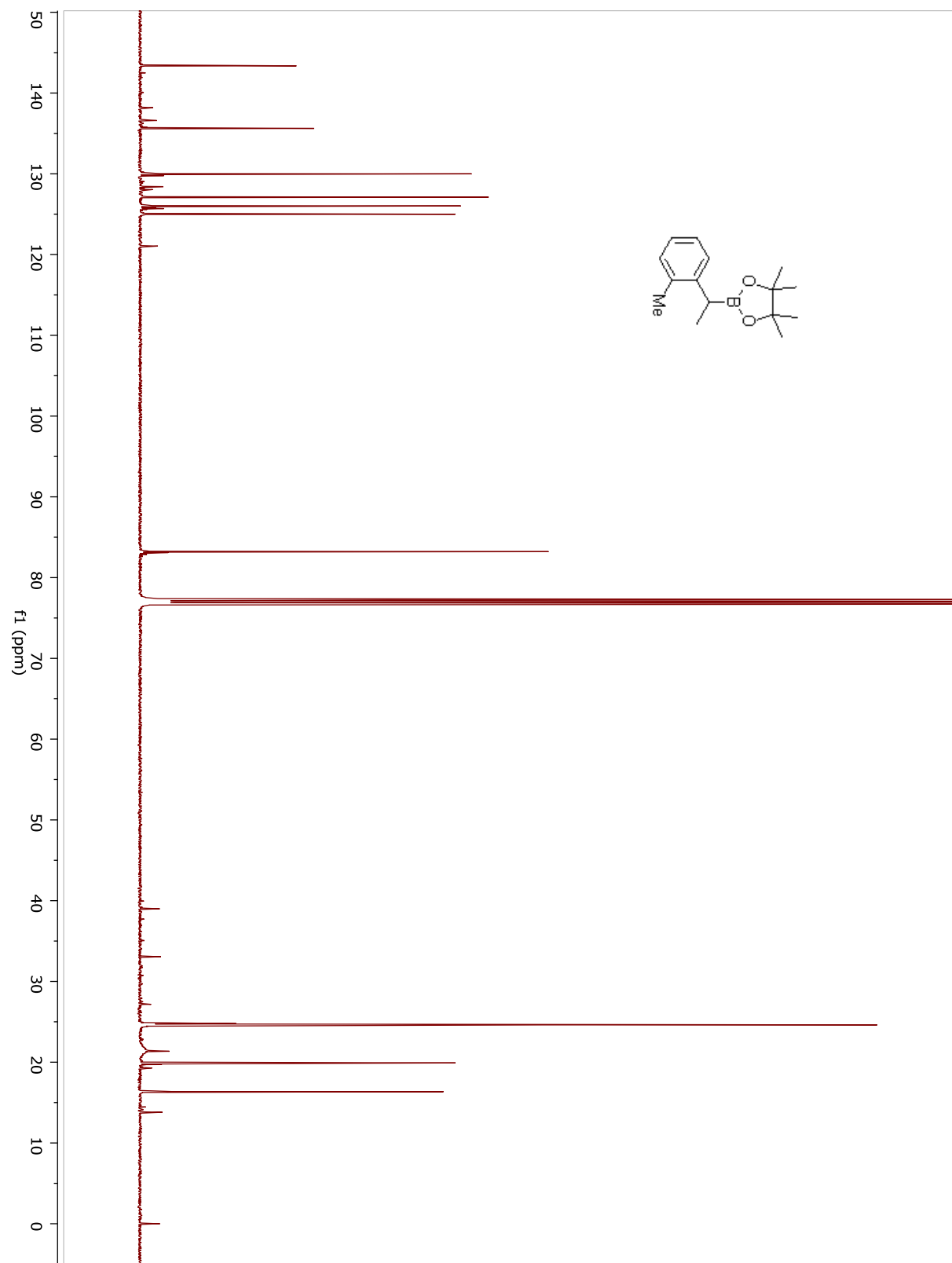
Compound 5.12.



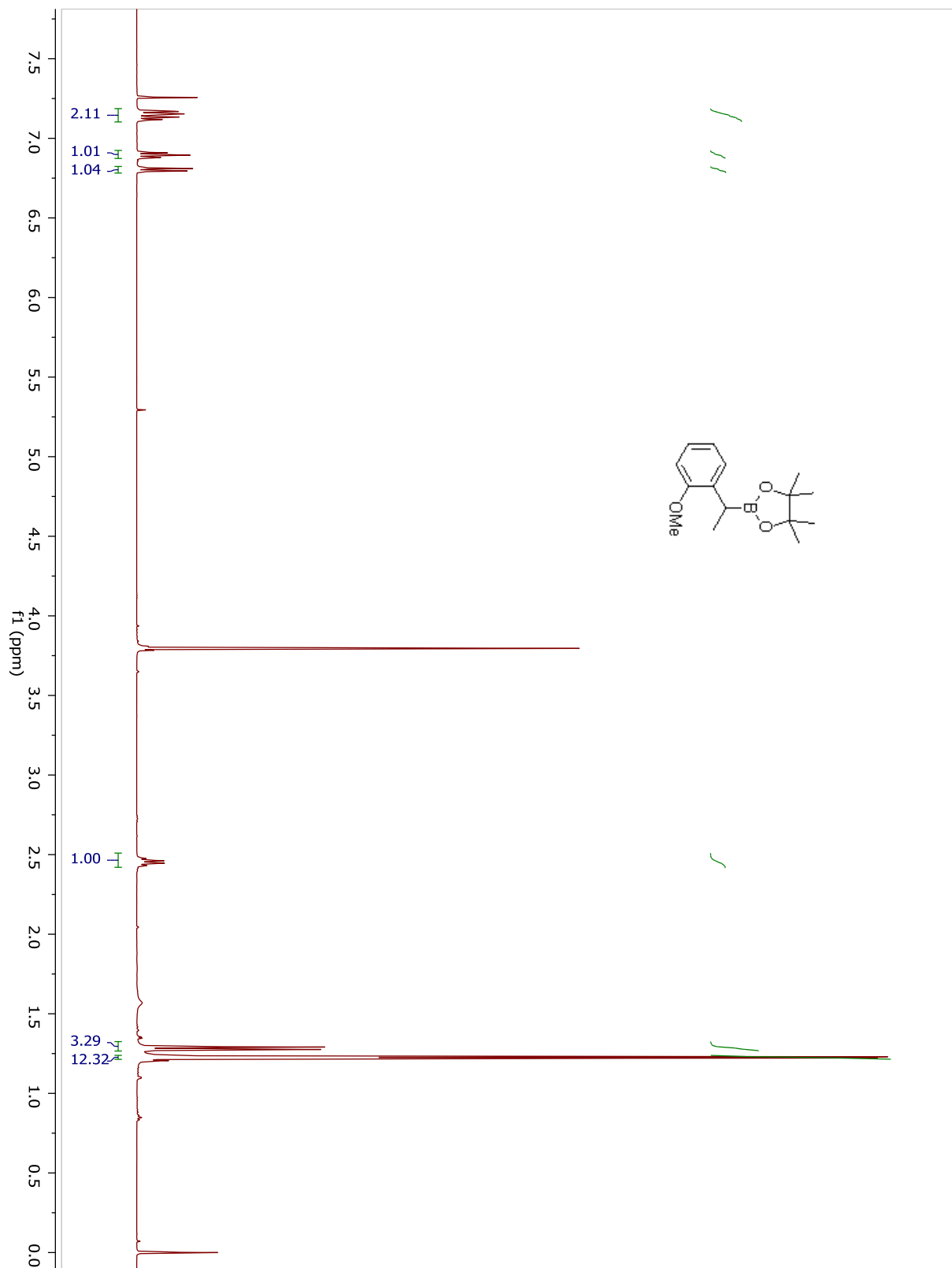
Compound 5.13.



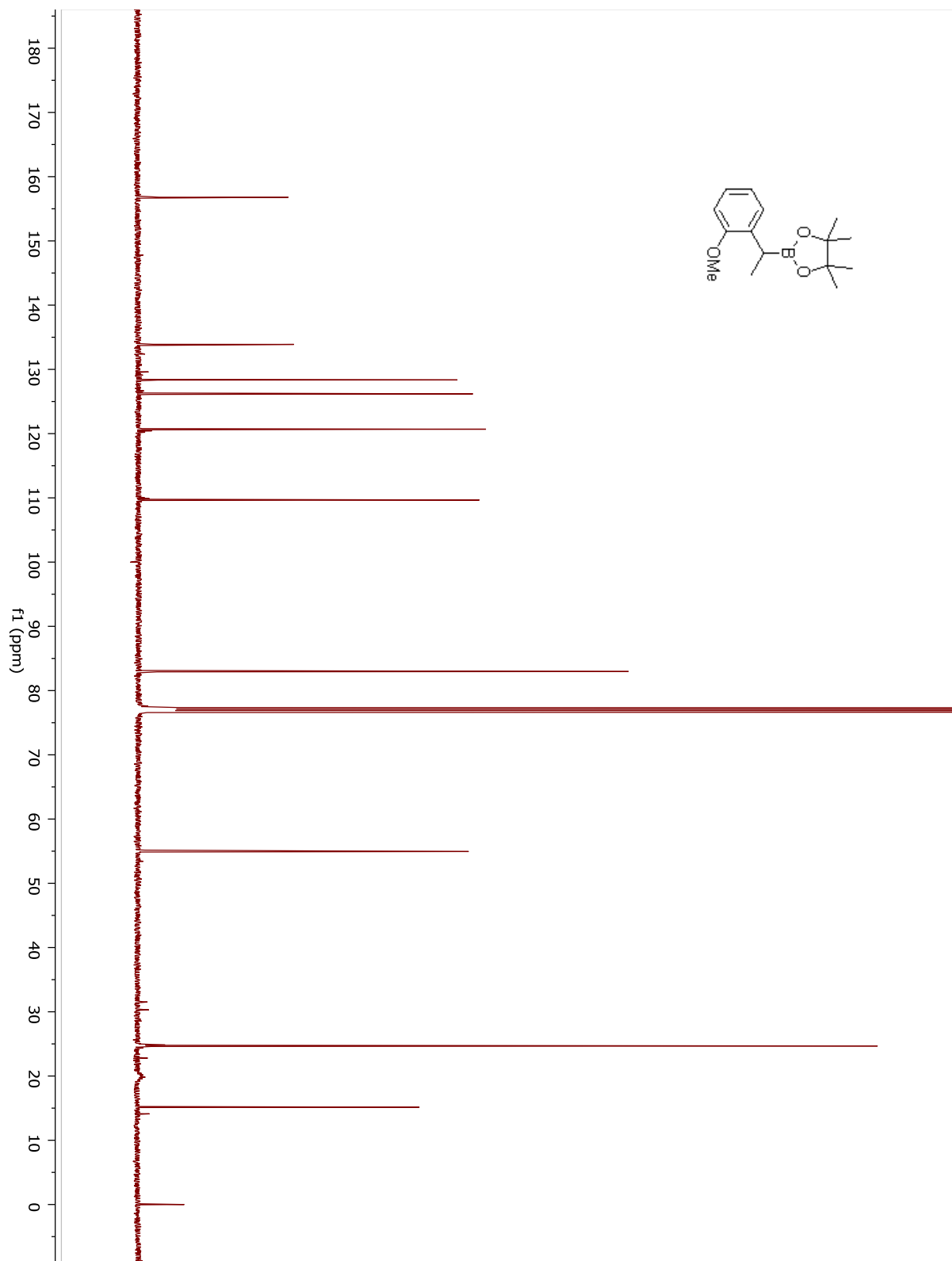
Compound 5.13.



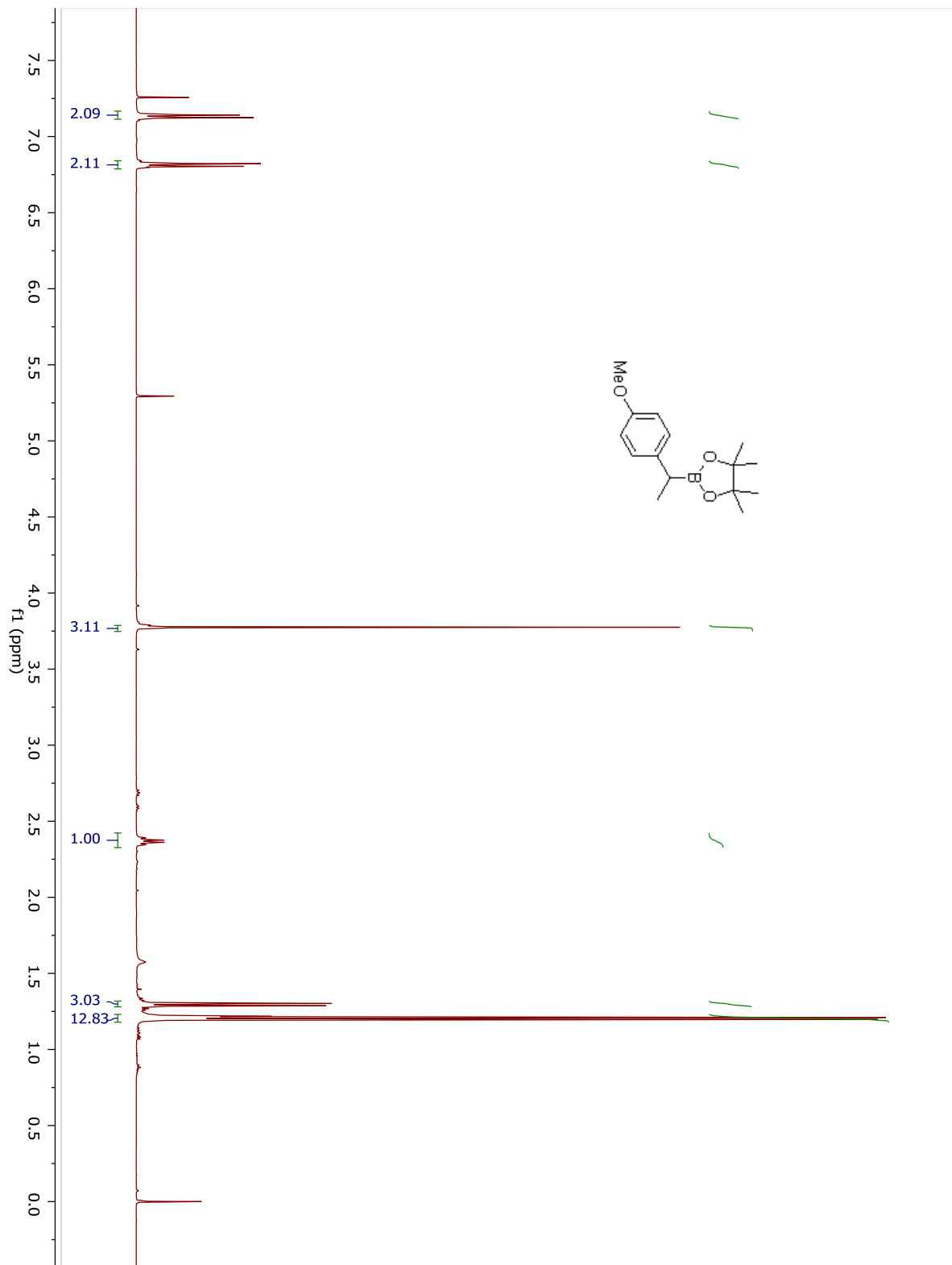
Compound 5.14.



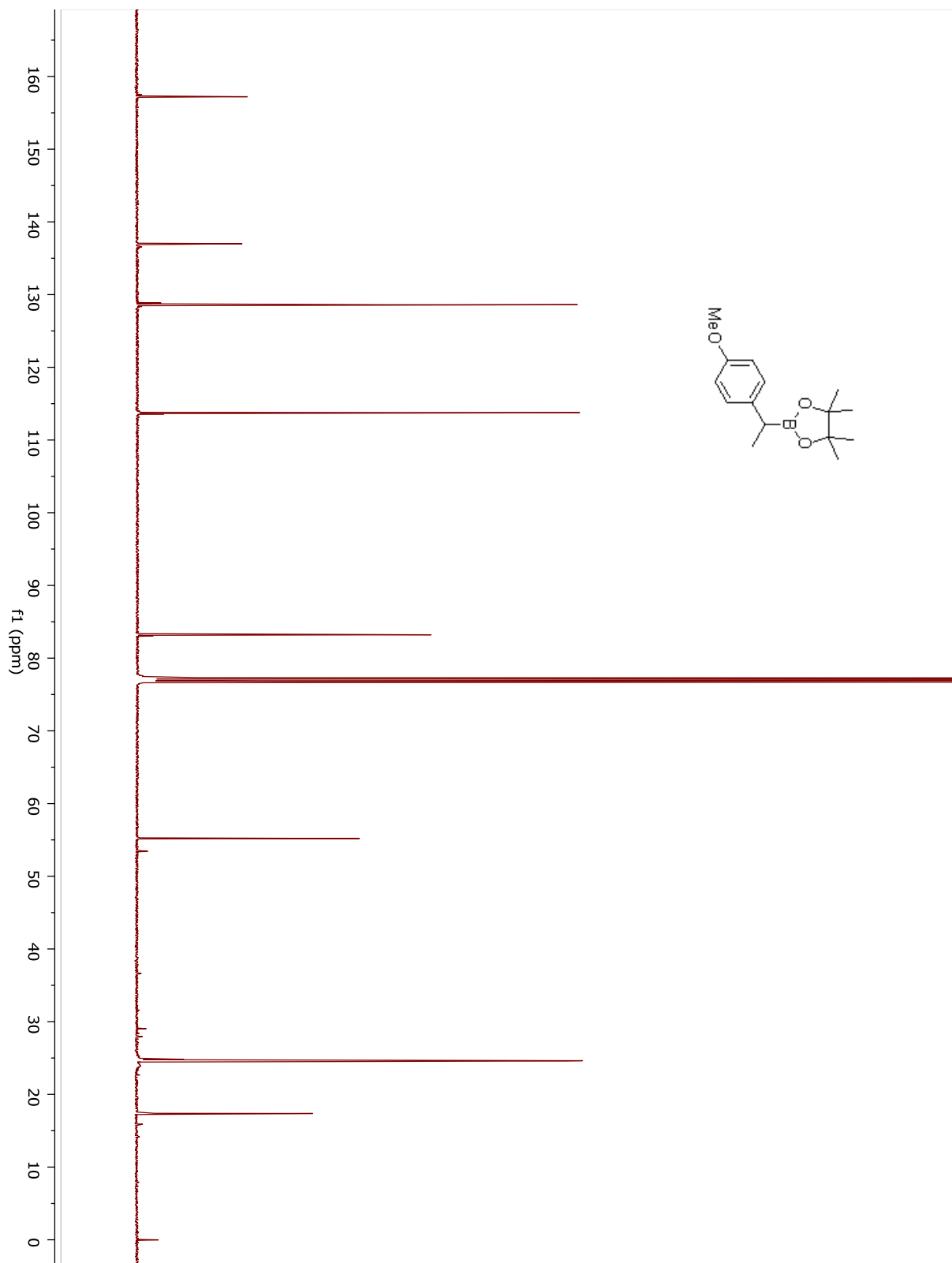
Compound 5.14.



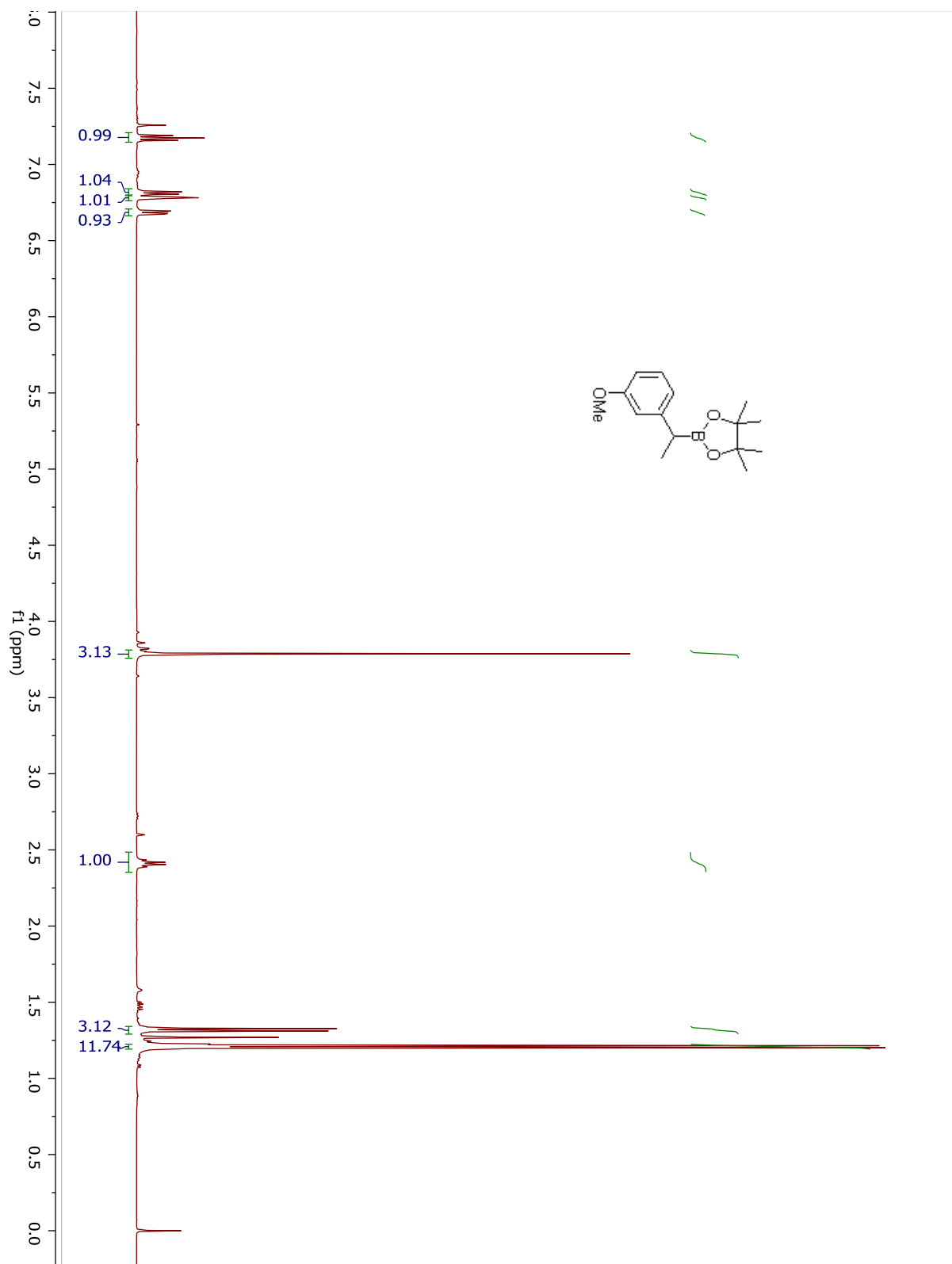
Compound 5.15.



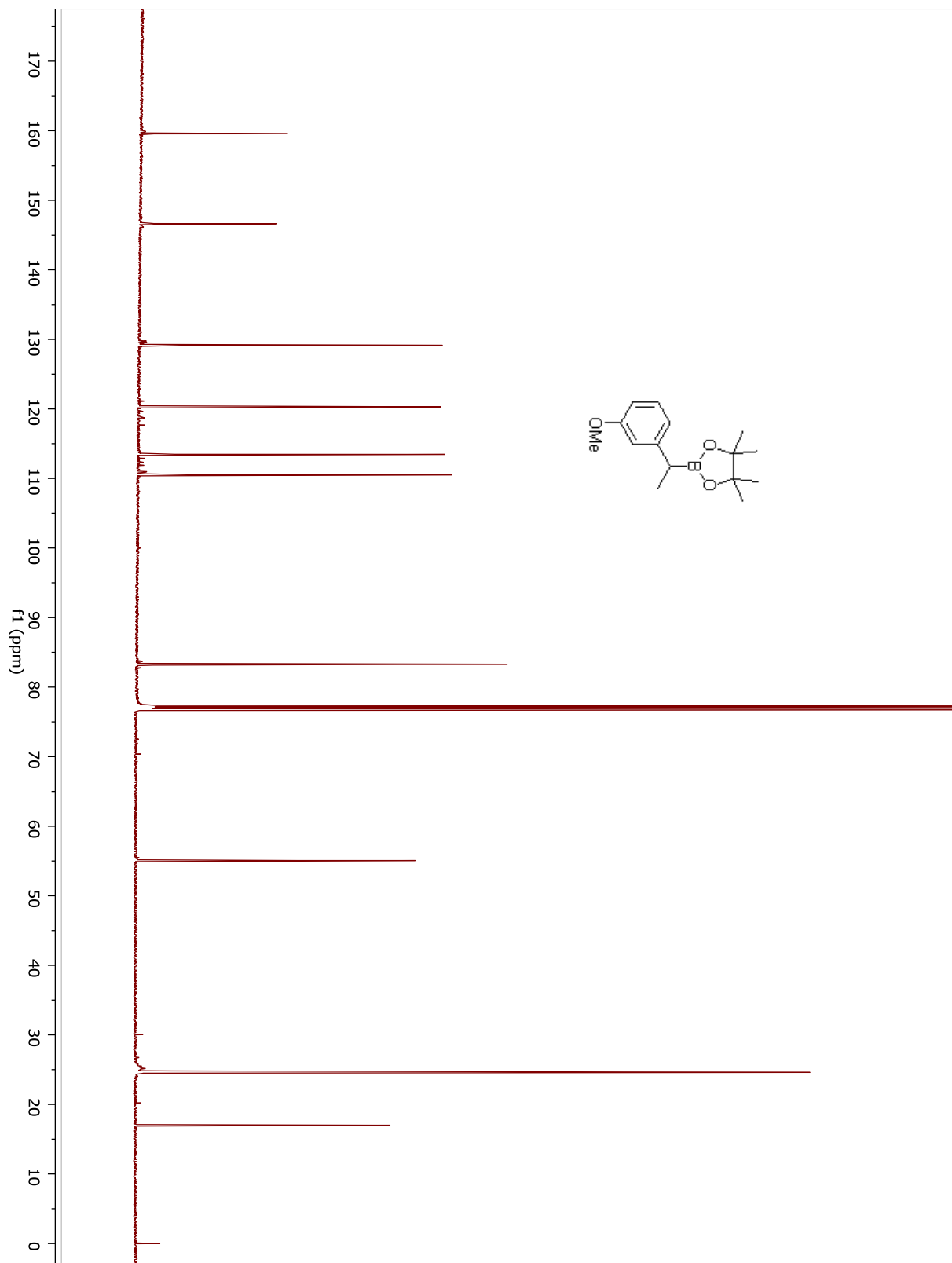
Compound 5.15.



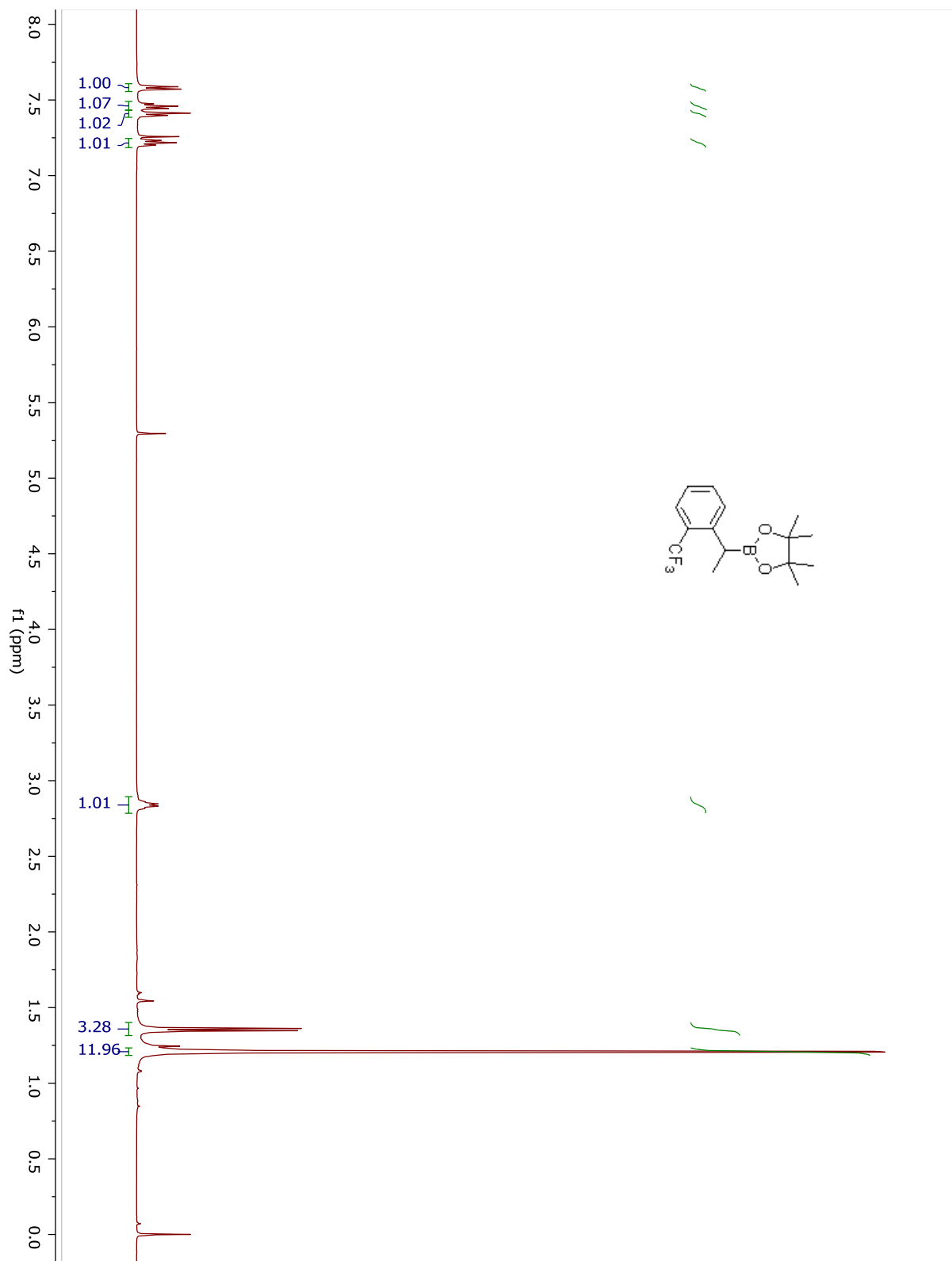
Compound 5.16.



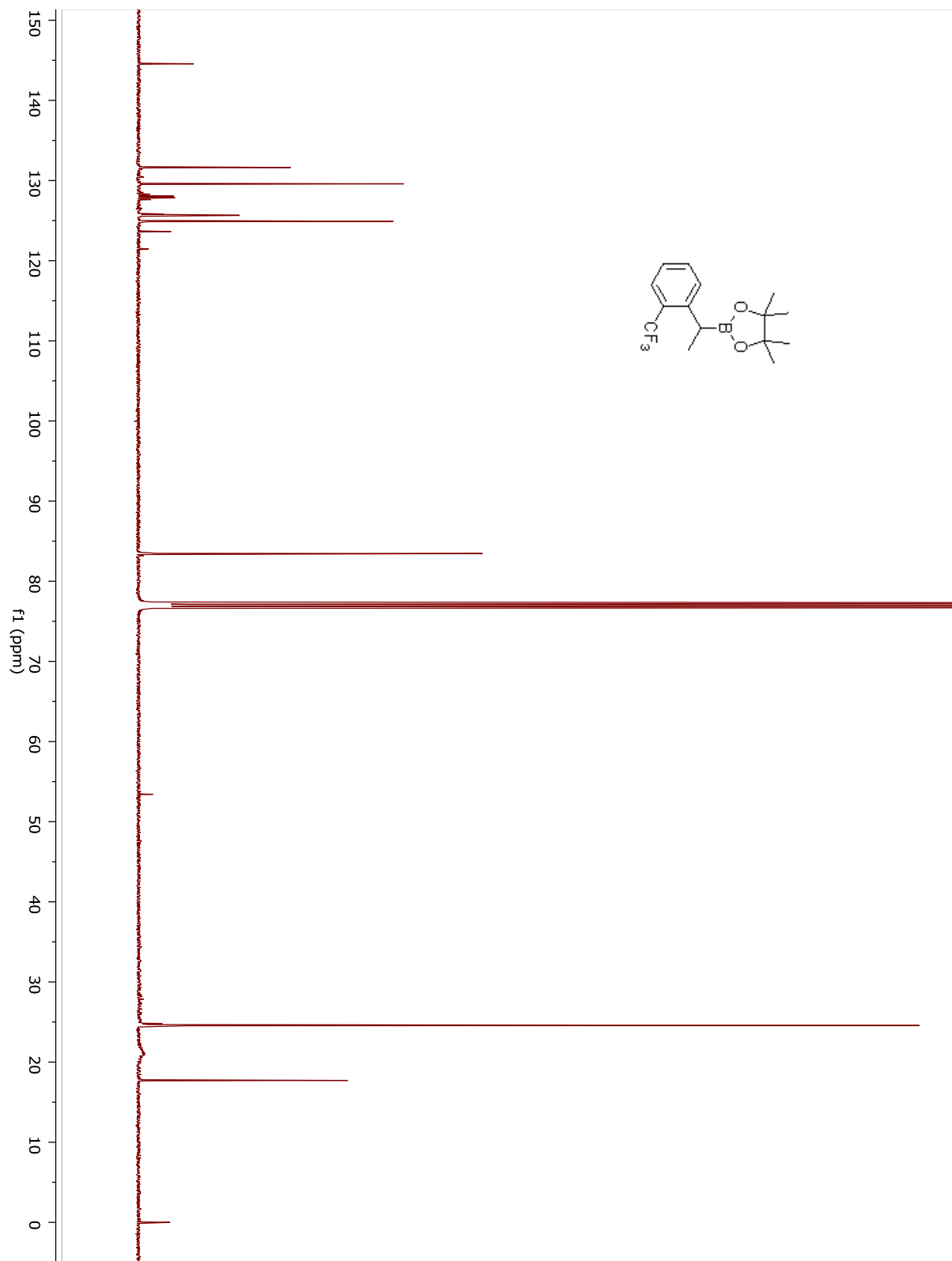
Compound 5.16.



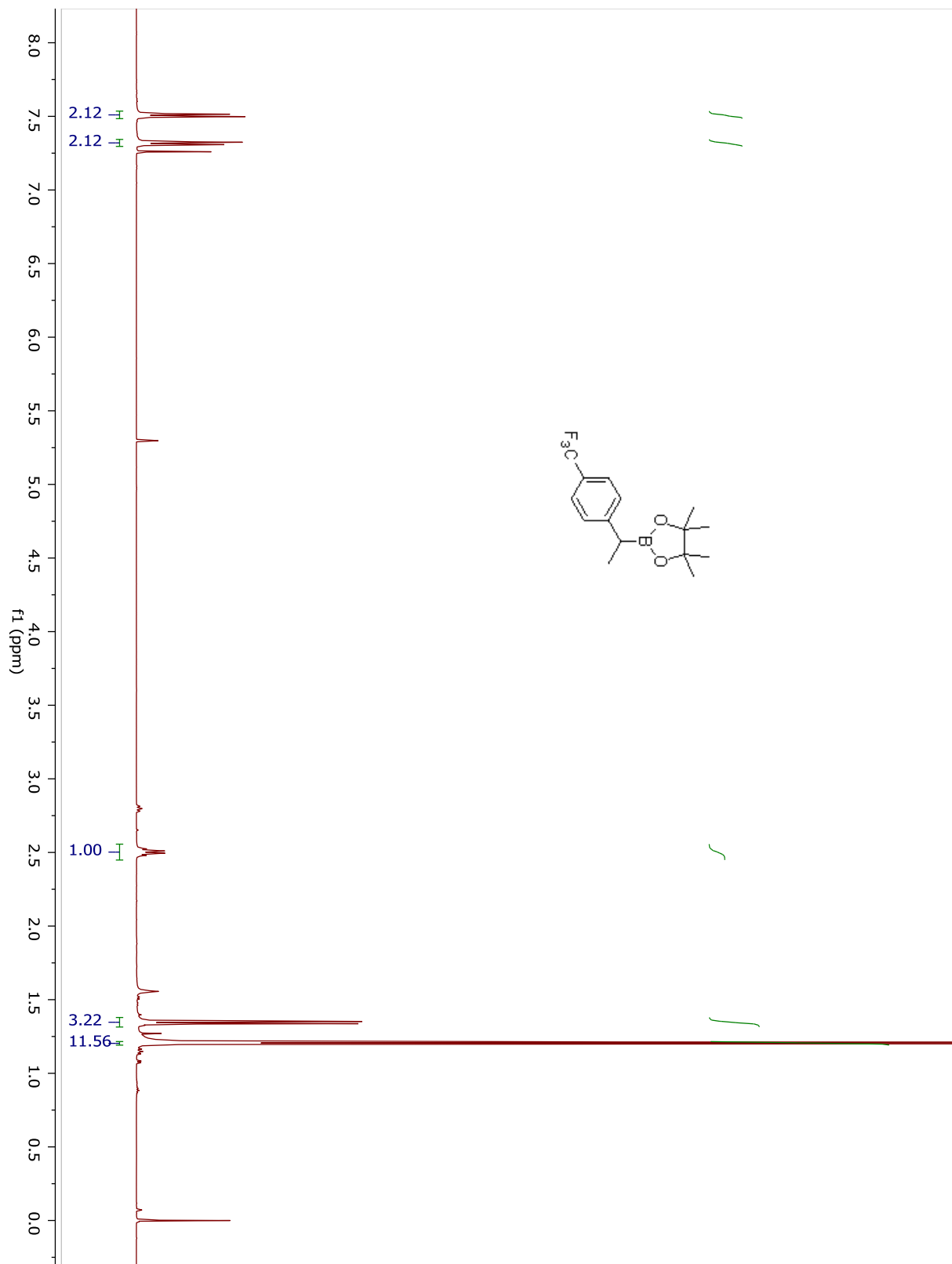
Compound 5.17.



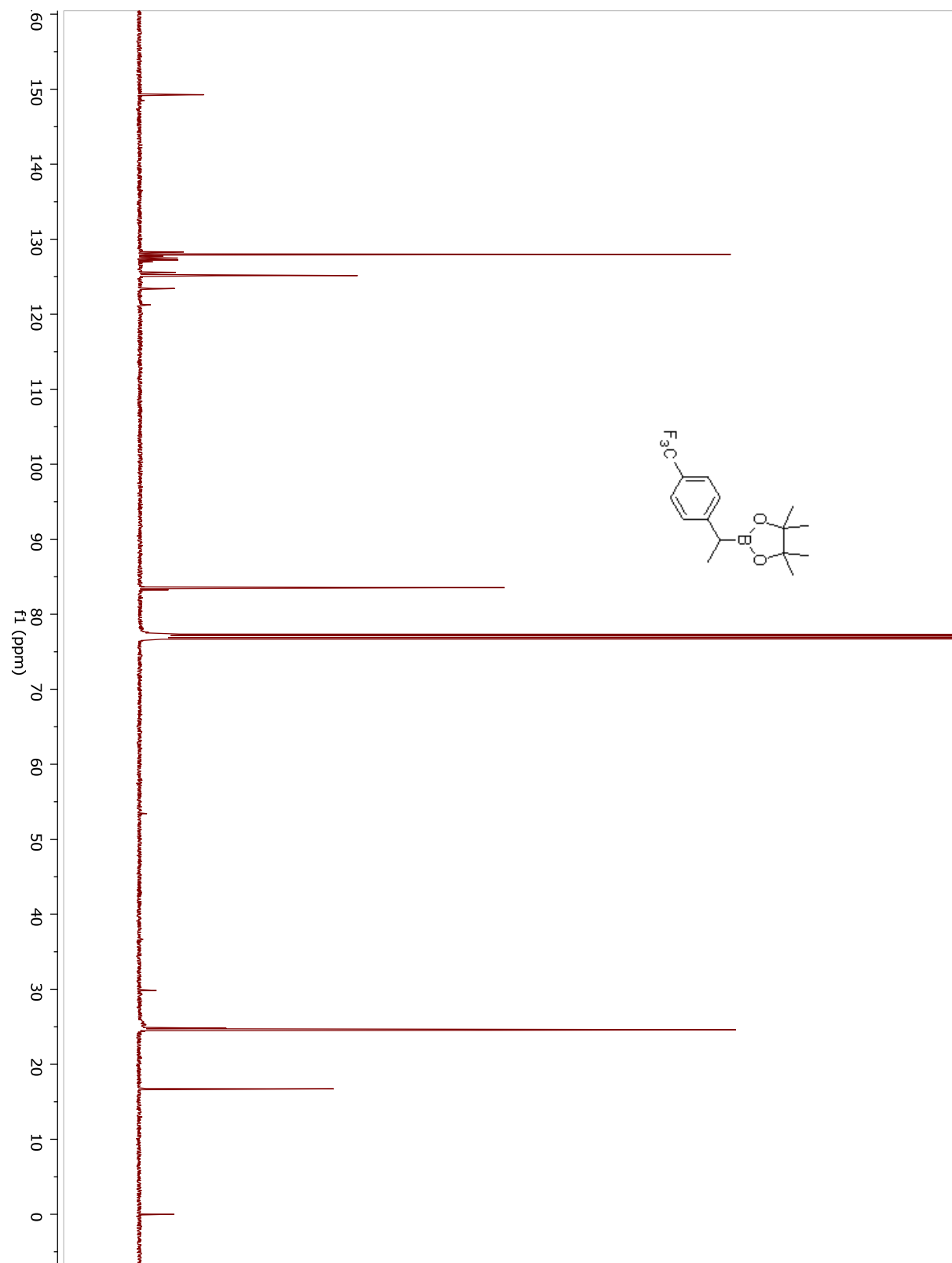
Compound 5.17.



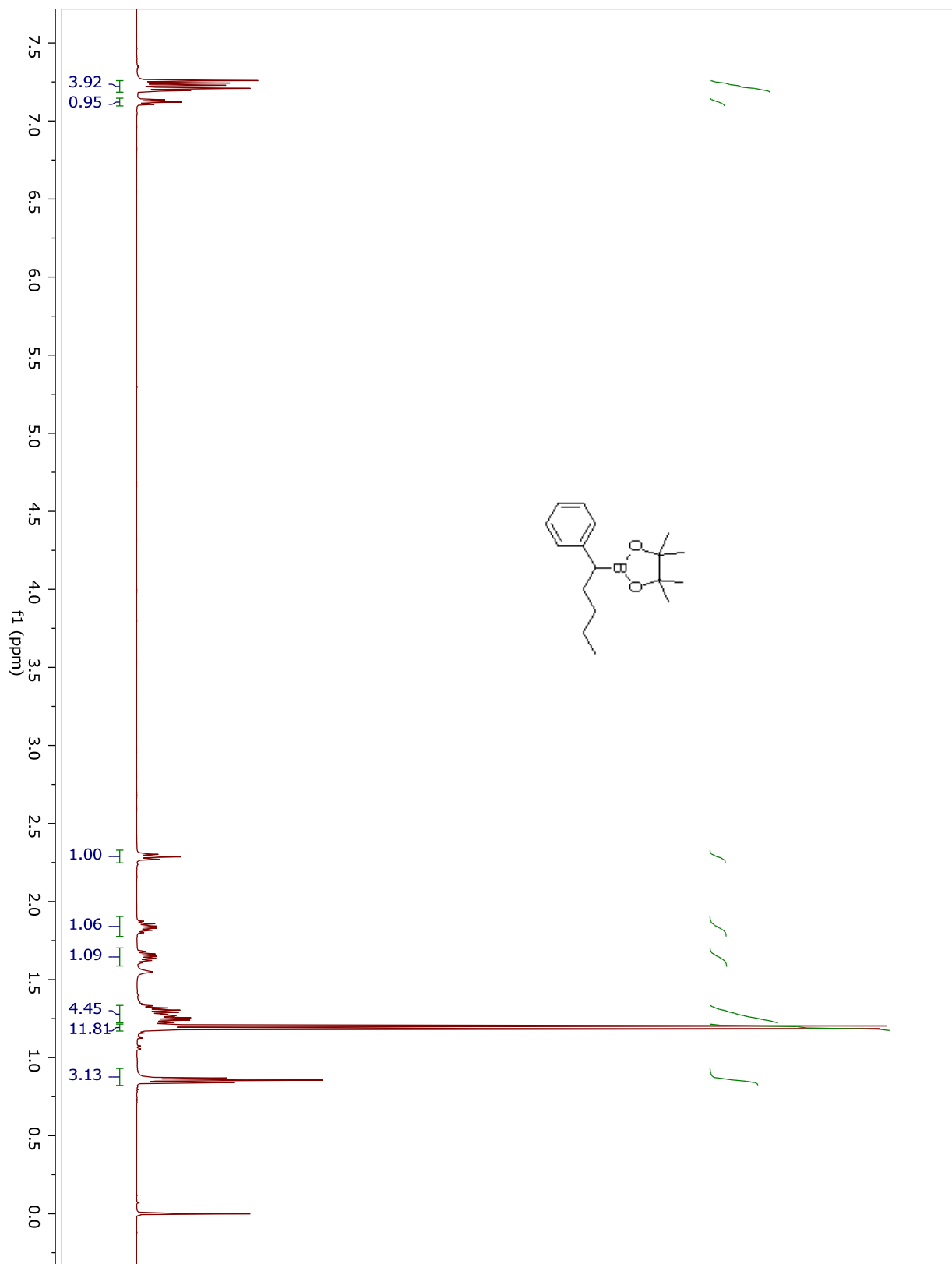
Compound 5.18.



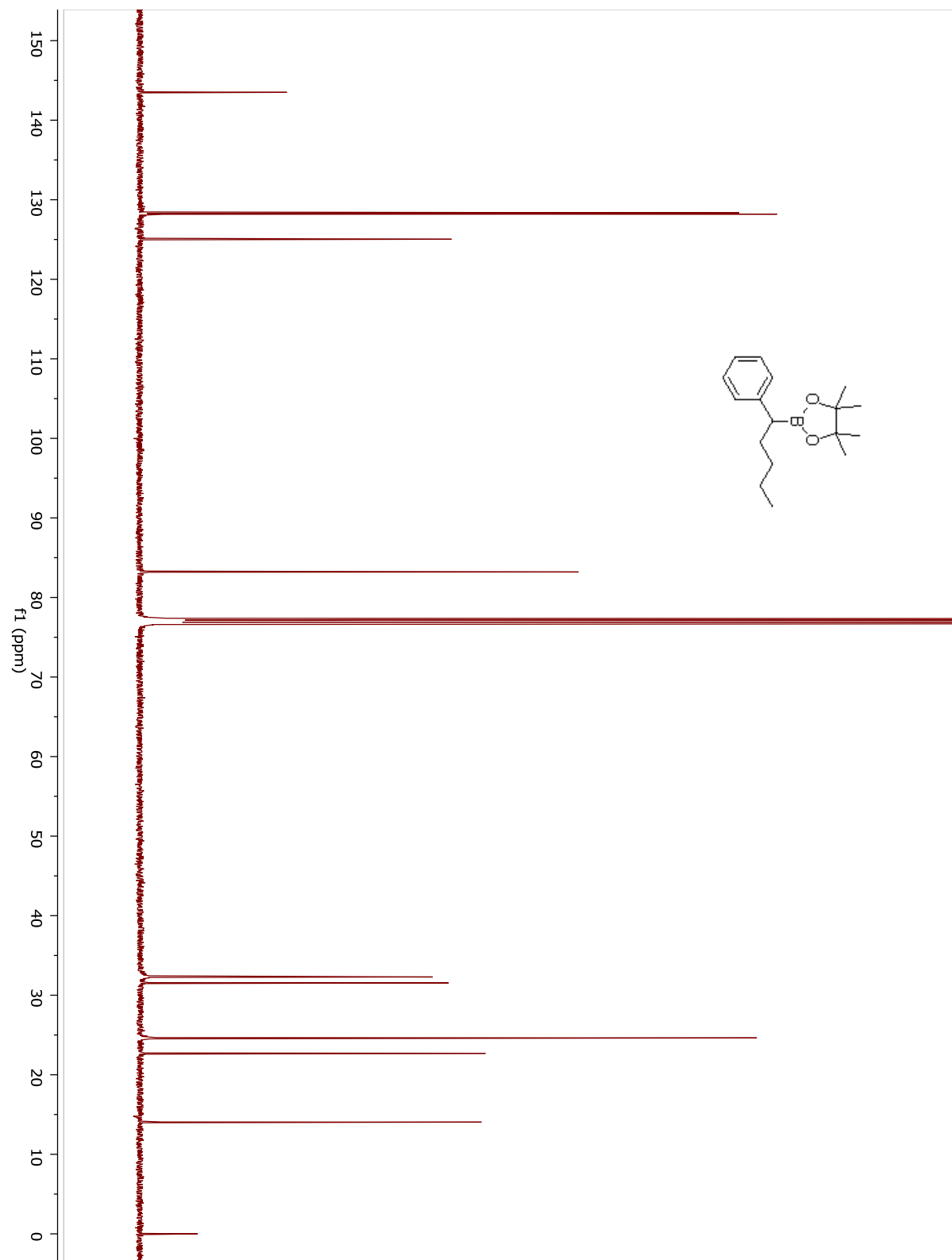
Compound 5.18.



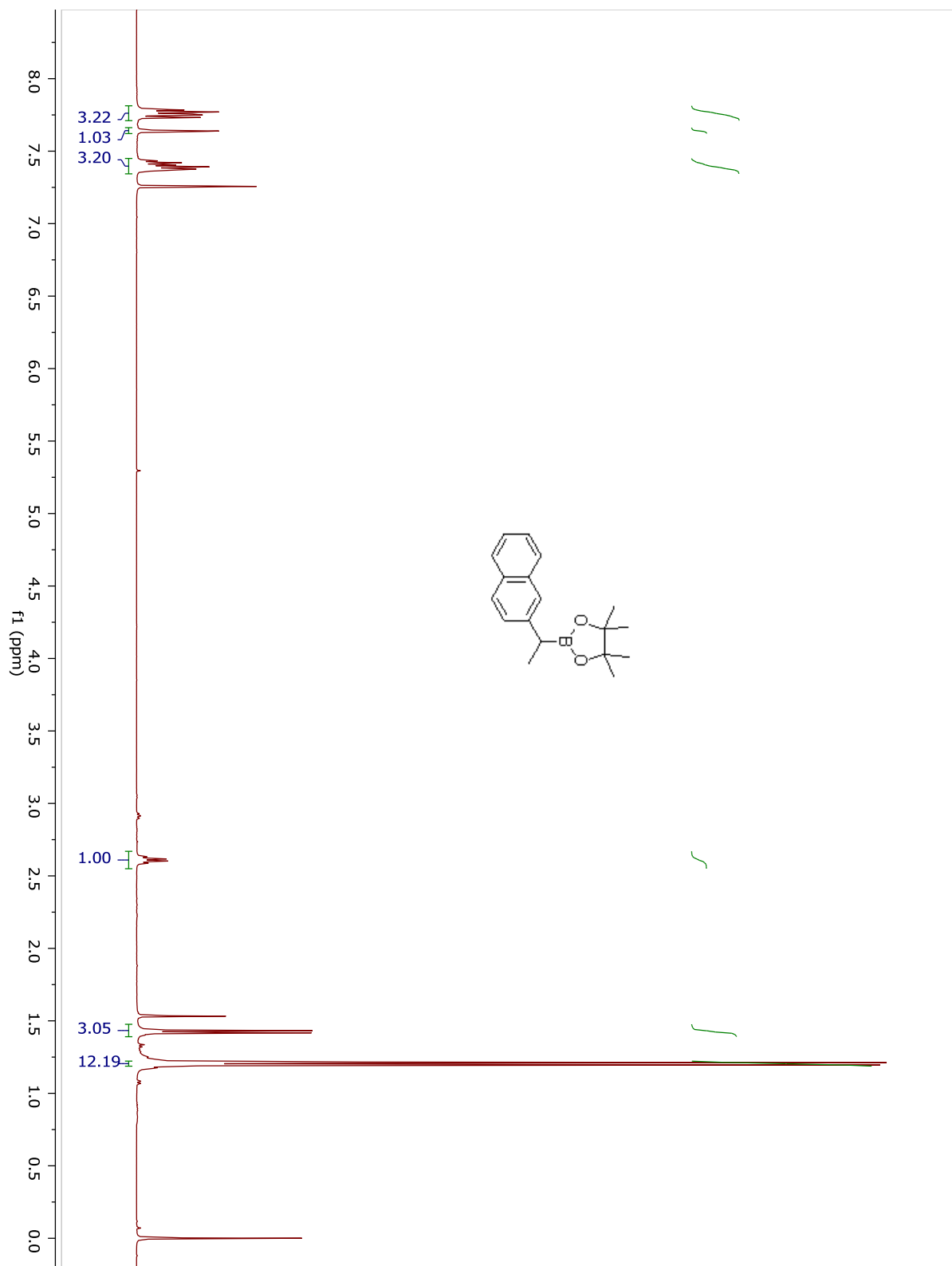
Compound 5.19.



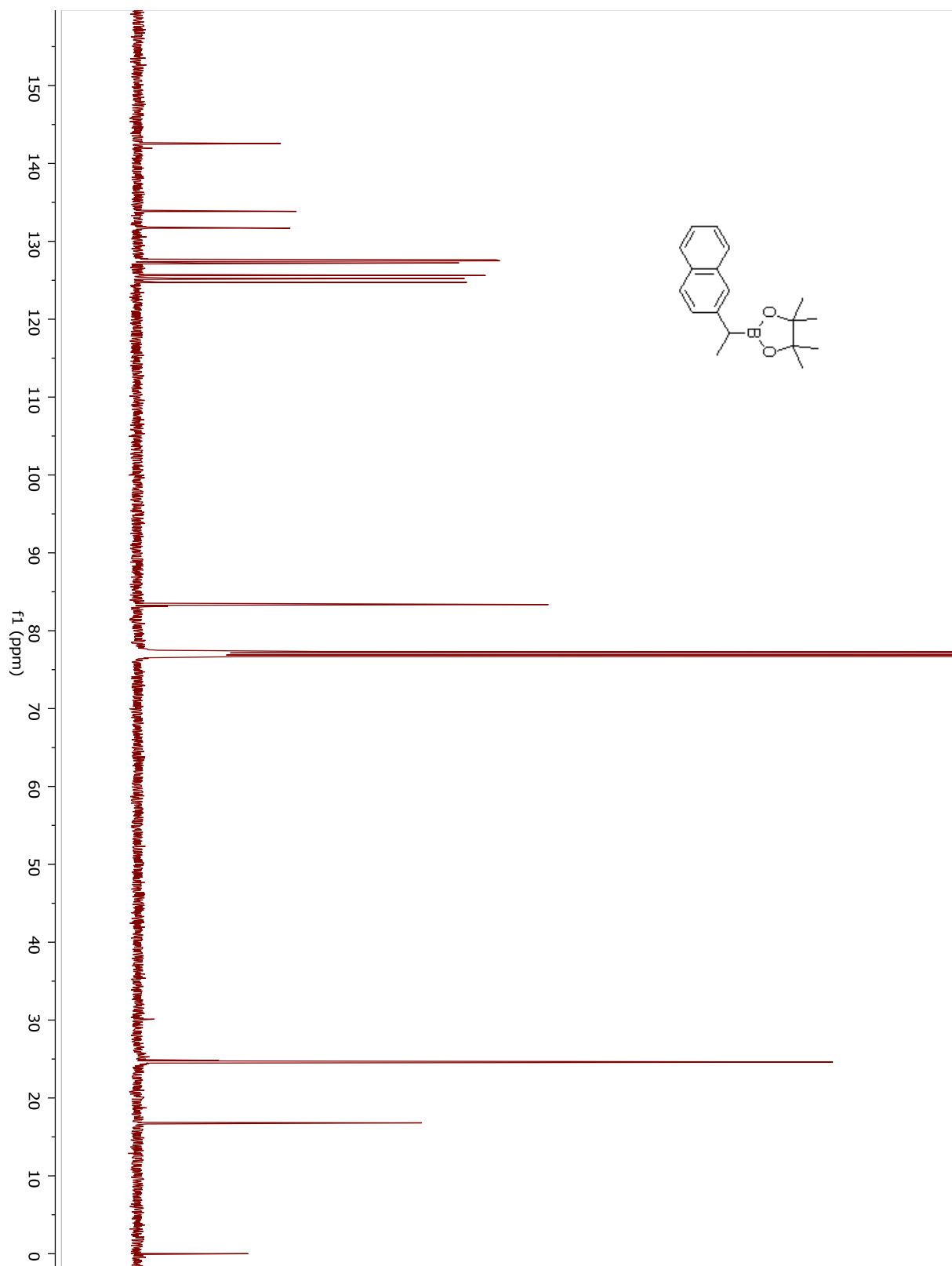
Compound 5.19.



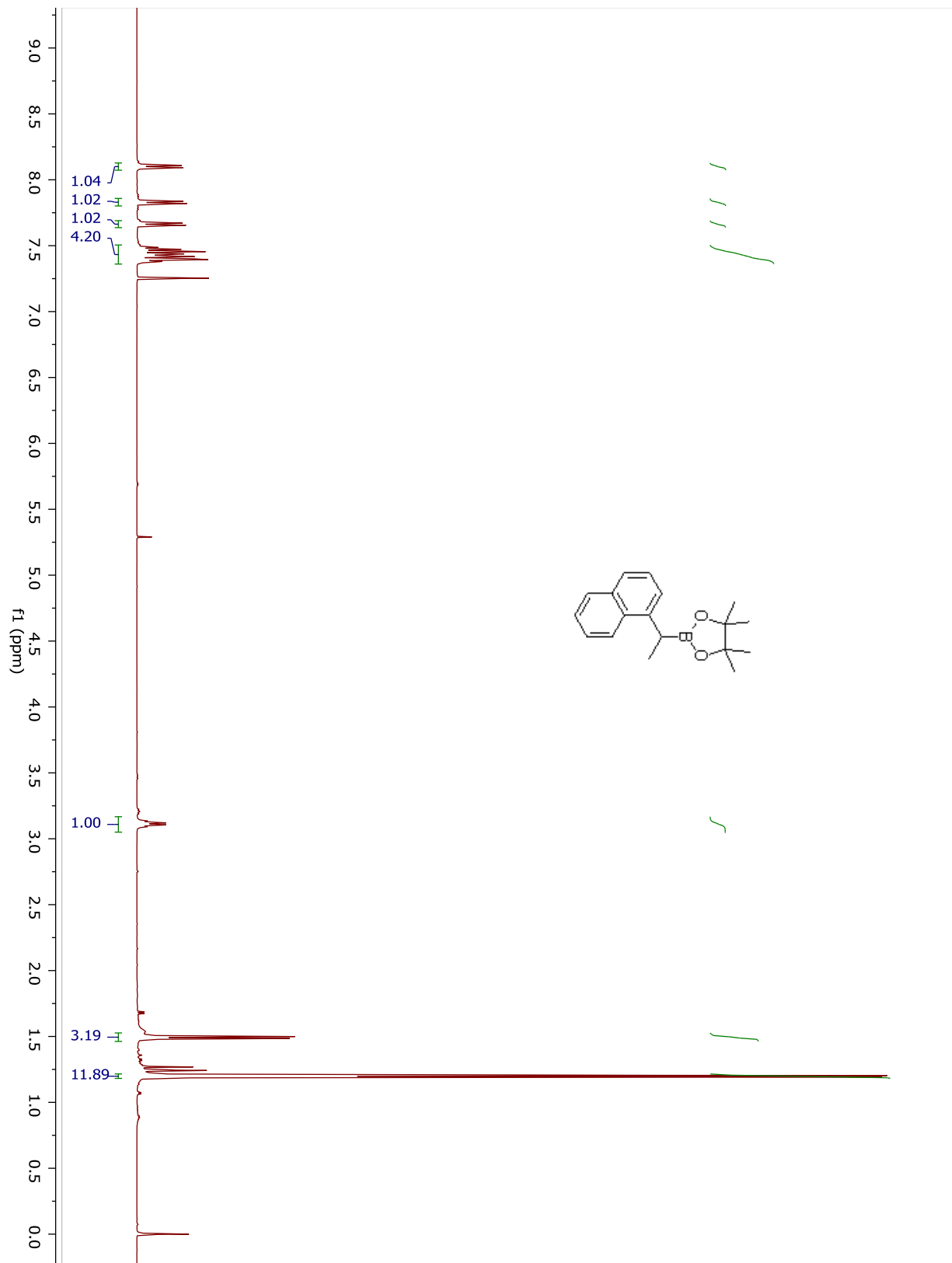
Compound 5.20.



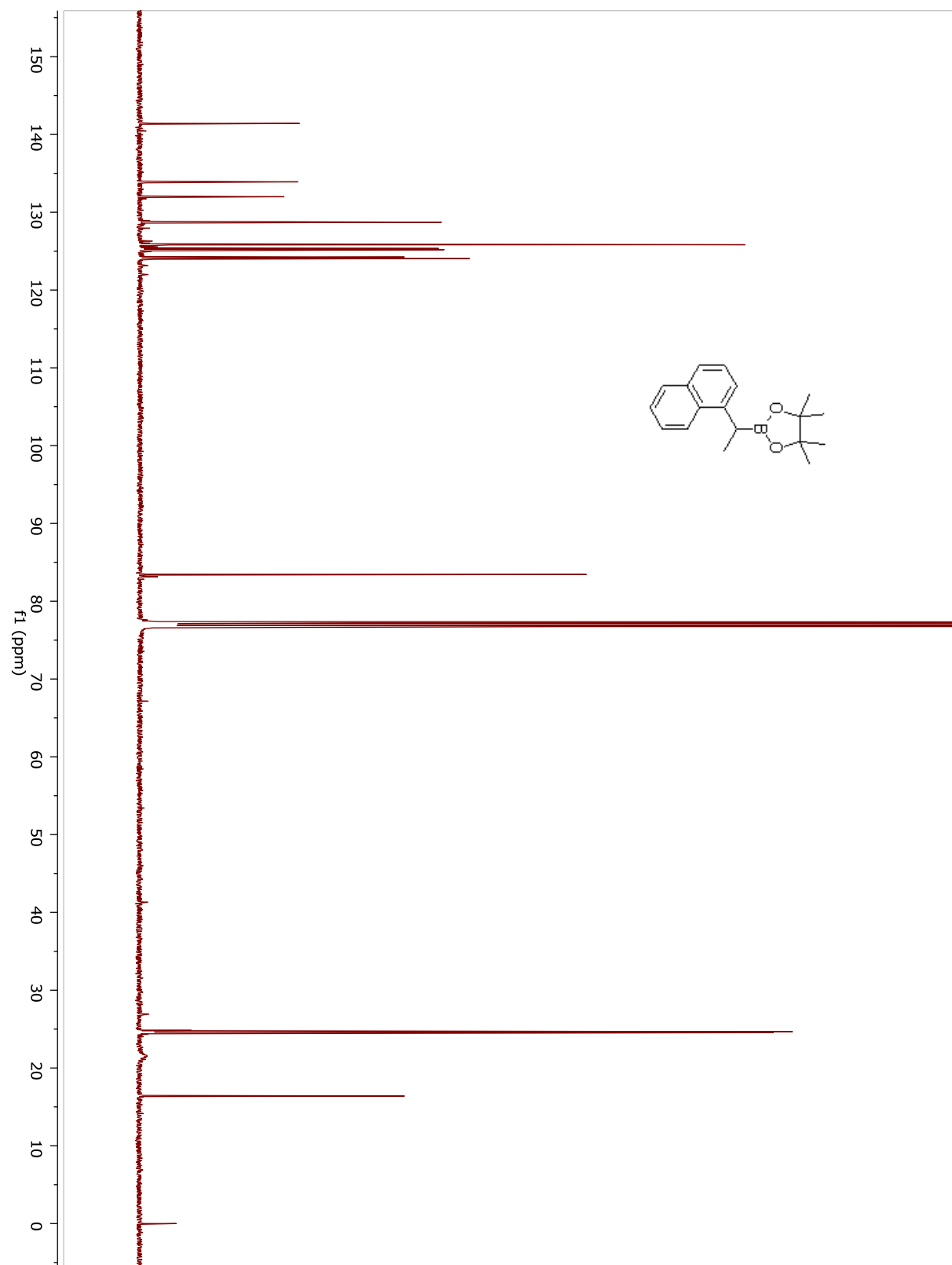
Compound 5.20.



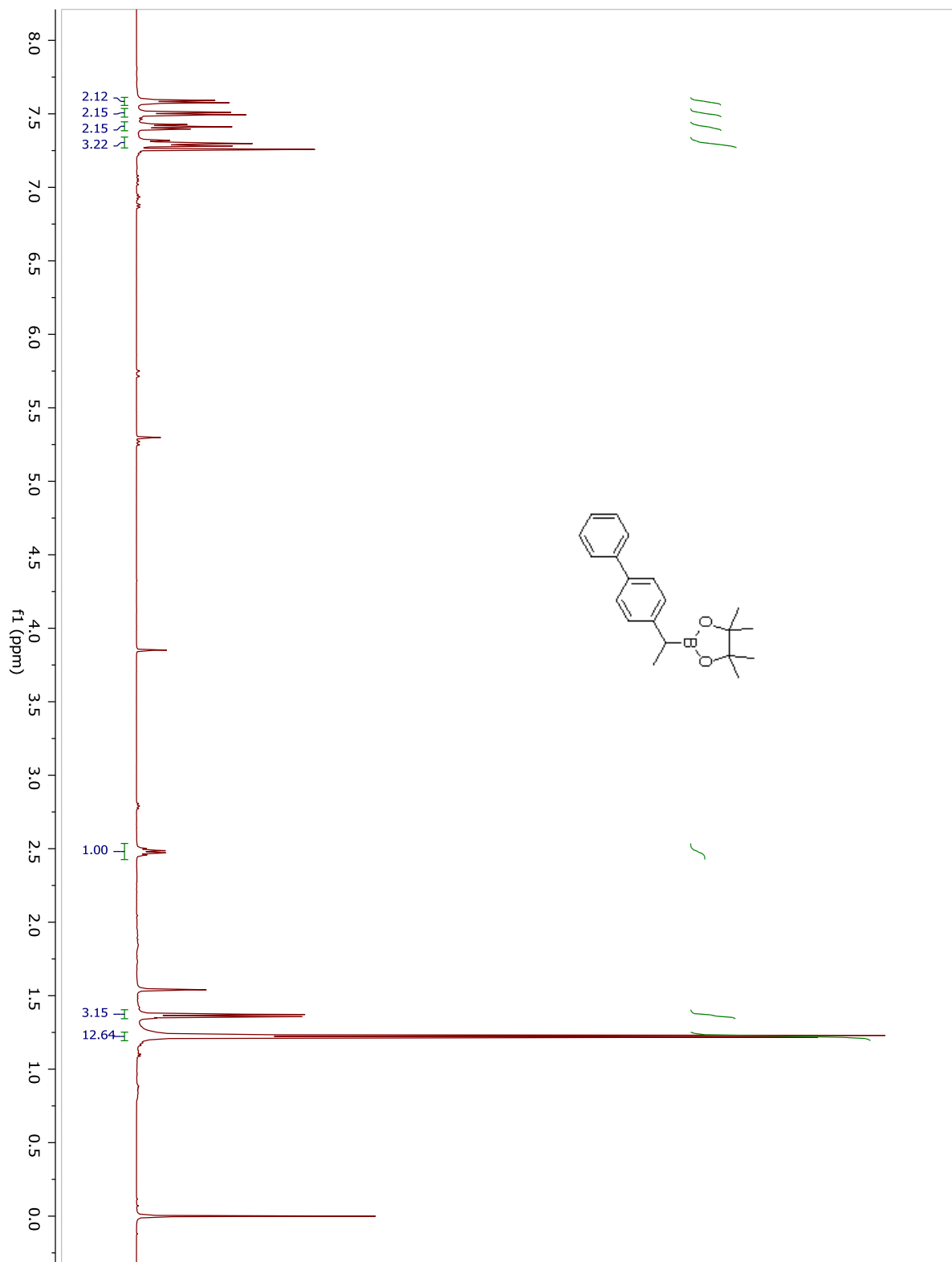
Compound 5.21.



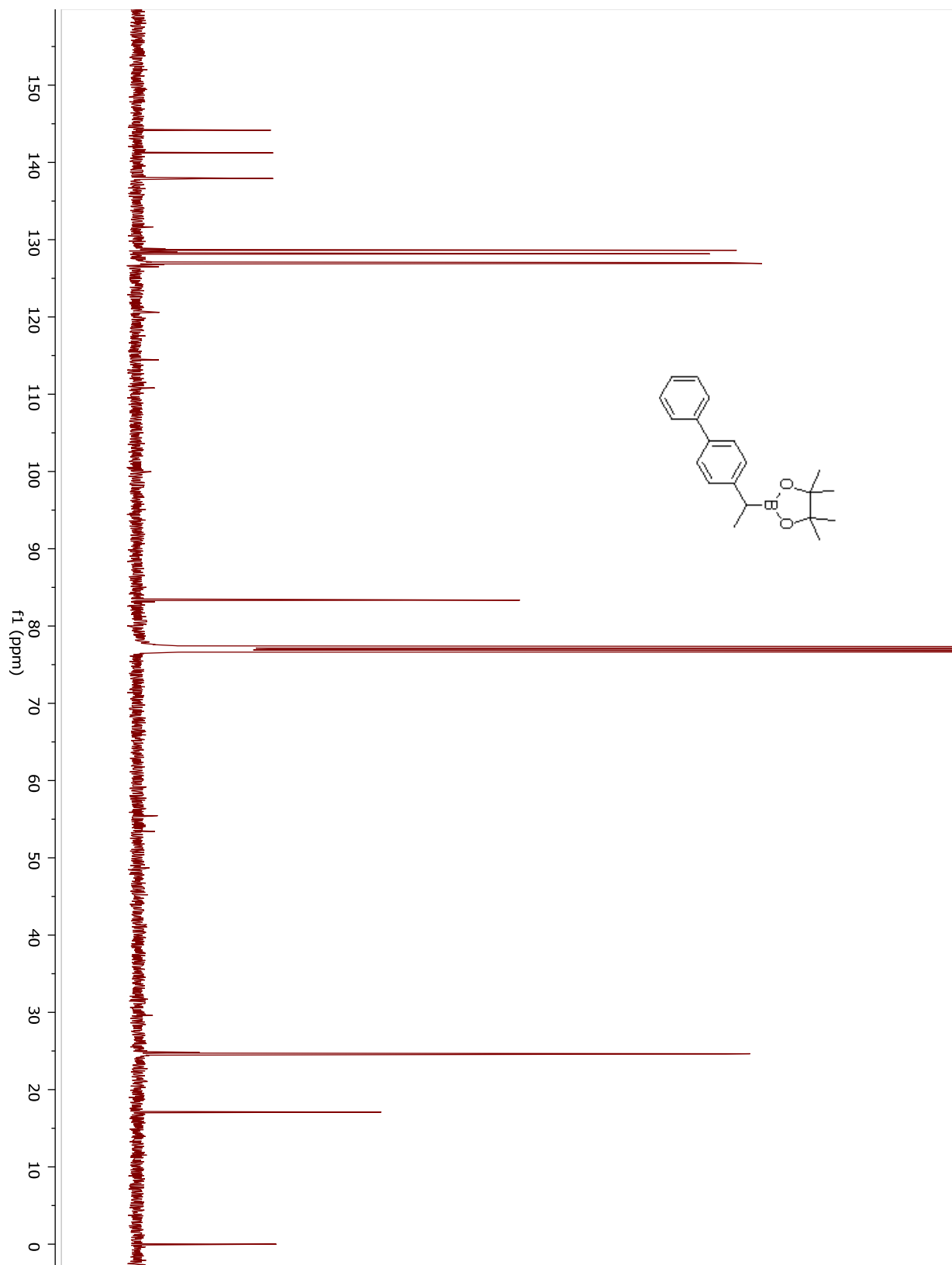
Compound 5.21



Compound 5.22.

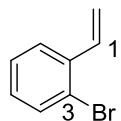


Compound 5.22.



Appendix B: Optimized Geometries

B.1 Optimized Geometries for the Predictive Model.



RB3LYP energy: -2883.2756824

Volume: 111.428 cm³/mol

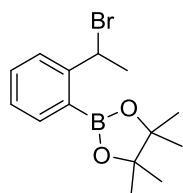
NPA at C1: -0.19540

NPA at C3: -0.06883

```

C  0.00000000  0.00000000  0.00000000
C  1.35297000  0.31294500 -0.00048300
C  1.75176500  1.64009500 -0.08500400
C  0.83030600  2.69275400 -0.16721500
C -0.52846800  2.33780700 -0.17606500
C -0.94334200  1.01901300 -0.08830600
H -2.00075200  0.78452300 -0.10277500
H -1.26573200  3.12437000 -0.27796100
C  1.24485500  4.10075400 -0.26076100
C  0.53329900  5.14765700  0.15498200
H -0.42904200  5.04196000  0.64239700
H  0.90881500  6.15564200  0.03275500
H  2.22198600  4.27698900 -0.69594300
Br  3.64585800  1.98511900 -0.05378000
H  2.09721000 -0.46879200  0.06721900
H -0.31051400 -1.03582900  0.06186400

```



RB3LYP energy: -3295.3249220

```

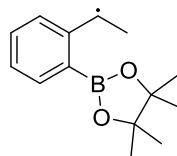
C  0.00000000  0.00000000  0.00000000
C -0.81643600  0.21268900 -1.26244500
C -0.95994000  1.63805600 -1.72093100
C -2.22012200  2.18403800 -2.05265400
C -2.27300800  3.53303000 -2.44553700
C -1.13642100  4.32354800 -2.51664000
C  0.09894500  3.77190000 -2.19291500

```

```

C  0.17932300  2.44456100 -1.80074100
H  1.14932600  2.02087800 -1.57196800
H  0.99909100  4.37297300 -2.24979400
H -1.21024700  5.35949000 -2.82593100
H -3.23548900  3.95837900 -2.70164200
B -3.58863800  1.42714100 -2.03902600
O -3.81907000  0.15136100 -1.58636000
C -5.17742100 -0.22734900 -1.96966900
C -5.86495600  1.17611300 -2.16428900
O -4.73289500  2.02781700 -2.50244200
C -6.47452200  1.74205800 -0.87928700
H -6.74886300  2.78417500 -1.04951900
H -7.37283400  1.19484400 -0.58746700
H -5.76457700  1.71073800 -0.05148300
C -6.87806200  1.24669100 -3.29967500
H -7.71049300  0.56240900 -3.11895600
H -7.28169700  2.25842200 -3.36621500
H -6.42614400  1.00040300 -4.25895600
C -5.05768700 -1.03500600 -3.26337500
H -4.40381500 -1.89016000 -3.08720700
H -6.02955000 -1.40787900 -3.59210800
H -4.62266000 -0.44083000 -4.06803400
C -5.76512600 -1.09194300 -0.86259600
H -5.72472500 -0.59369000  0.10455800
H -6.80510300 -1.34538200 -1.08175000
H -5.20096300 -2.02308800 -0.78851600
H -1.78319000 -0.26194400 -1.17346500
Br  0.02037700 -0.89082400 -2.75962600
H  1.02570500  0.35427900 -0.09952600
H -0.47169200  0.55039200  0.82051800
H  0.02791800 -1.05702600  0.26445700

```



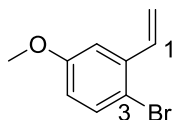
UB3LYP energy: -721.1363910

```

C  0.00000000  0.00000000  0.00000000
C  1.04565900 -1.06663800 -0.06139500

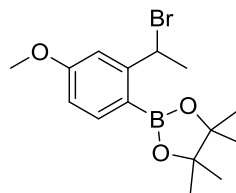
```

C 0.77381300 -2.44869800 -0.13091700
 C 1.82147600 -3.43781300 -0.18516200
 C 1.46090200 -4.78621400 -0.25096100
 C 0.13370000 -5.20663800 -0.26653200
 C -0.88415500 -4.25181400 -0.21415100
 C -0.57395400 -2.90931800 -0.14821400
 H -1.37823500 -2.18608900 -0.10827200
 H -1.92263300 -4.56379800 -0.22462900
 H -0.10510100 -6.26207600 -0.31814700
 H 2.24932400 -5.52837200 -0.29104100
 B 3.35015100 -3.14038100 -0.17753100
 O 3.95085100 -1.90911700 -0.05497000
 C 5.37872400 -2.07055600 -0.29994400
 C 5.59154500 -3.60454300 -0.01291700
 O 4.27537300 -4.15384500 -0.29312200
 C 5.89560400 -3.91304200 1.45558600
 H 5.83744500 -4.99191100 1.60706300
 H 6.89636400 -3.58031200 1.73746600
 H 5.17138700 -3.43979800 2.12023000
 C 6.60736000 -4.29641900 -0.91335700
 H 7.60157100 -3.86190000 -0.78333200
 H 6.66530500 -5.35430100 -0.65146100
 H 6.32984000 -4.22473000 -1.96369700
 C 5.62030900 -1.68408600 -1.76127500
 H 5.26547700 -0.66449500 -1.91939000
 H 6.68124500 -1.72092000 -2.01596000
 H 5.07652400 -2.33984600 -2.44269500
 C 6.13613400 -1.12525500 0.62359900
 H 5.86914100 -1.28012300 1.66764200
 H 7.21513200 -1.25930700 0.51467800
 H 5.89799100 -0.09229800 0.36387300
 H 2.07941500 -0.75471200 -0.05039900
 H -0.65160600 -0.10734700 0.87602900
 H 0.45724900 0.98854700 0.05162500
 H -0.65845500 -0.01253200 -0.87747200



RB3LYP energy: -2997.835000
 Volume: 133.585 cm³/mol
 NPA at C1: -0.19220
 NPA at C3: -0.09534

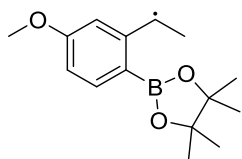
C 0.00000000 0.00000000 0.00000000
 O -0.86673900 -1.12328800 -0.07614900
 C -2.21210900 -0.90724500 -0.07017500
 C -3.01155900 -2.05225400 -0.14491800
 C -4.38743800 -1.92896000 -0.13014900
 C -4.97815400 -0.67188900 -0.04410000
 C -4.20813100 0.49165600 0.02382300
 C -2.80890400 0.34320800 0.01820700
 H -2.20439200 1.23314200 0.11193000
 C -4.81255300 1.82956500 0.11475400
 C -4.24940700 2.97070800 -0.28076800
 H -3.27259200 3.00998700 -0.74902300
 H -4.76850900 3.91325400 -0.16216500
 H -5.81343000 1.86371800 0.52954700
 Br -6.90170100 -0.60375300 -0.05895200
 H -5.00921100 -2.81216700 -0.18771800
 H -2.53854400 -3.02400600 -0.20433100
 H -0.14666200 0.55363400 0.93221800
 H 1.01031700 -0.40214400 -0.02542800
 H -0.14462300 0.67218300 -0.85117600



RB3LYP energy: -3409.8858775

C 0.00000000 0.00000000 0.00000000
 O 0.49171100 1.30044200 0.29563400
 C 1.83674900 1.50672700 0.27139800
 C 2.78469400 0.52542800 -0.01854400
 C 4.12832400 0.87237300 -0.01428100
 C 4.58251700 2.16761000 0.27341800
 C 3.60212100 3.14750600 0.56659900
 C 2.25584800 2.80423900 0.55946300
 H 1.49286100 3.54700200 0.75362000
 C 3.98800900 4.56142000 0.91166600
 C 3.36235600 5.12624300 2.17470800
 H 2.27374200 5.14740400 2.12785200
 H 3.71722600 6.14036500 2.35830000

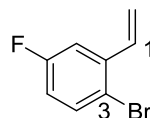
H 3.65347300 4.49745000 3.02237000
 H 5.06330400 4.66796400 0.93868100
 Br 3.51245800 5.78875300 -0.64270200
 B 6.12539000 2.37470000 0.24128800
 O 6.97455800 1.34695600 -0.09631000
 C 8.31335600 1.89419100 -0.25489100
 C 8.23277400 3.22217300 0.58974600
 O 6.80752000 3.53103400 0.53685800
 C 9.00245200 4.40510100 0.01715500
 H 8.86371700 5.27667400 0.65904700
 H 10.0721110 4.18624300 -0.02647600
 H 8.65781100 4.66515600 -0.98209000
 C 8.58436100 3.02946700 2.06660900
 H 8.31752100 3.93509300 2.61355300
 H 8.03347900 2.19538400 2.50362400
 H 9.65237800 2.85076300 2.20374200
 C 8.51618100 2.13677700 -1.75260300
 H 9.52367100 2.49785900 -1.96757800
 H 8.36868900 1.19552700 -2.28418900
 H 7.79766800 2.85972000 -2.14127800
 C 9.31839600 0.86639900 0.24967000
 H 10.3351070 1.26470500 0.20919800
 H 9.10403000 0.55996200 1.27218900
 H 9.27973500 -0.02152500 -0.38366400
 H 4.86085800 0.10795700 -0.24327100
 H 2.49345400 -0.48973800 -0.24869300
 H 0.36661200 -0.73759100 0.72000500
 H -1.08310300 0.06858100 0.07373100
 H 0.27576600 -0.30912700 -1.01242000



UB3LYP energy: -835.69700677

C 0.00000000 0.00000000 0.00000000
 O 0.65492500 1.25926300 -0.04416300
 C 2.01974100 1.28335400 -0.04495300
 C 2.82614200 0.14239400 0.00140900
 C 4.21139100 0.30138000 -0.00621600
 C 4.84150400 1.54302100 -0.05746600

C 4.00573100 2.71816700 -0.10547300
 C 2.60155900 2.54208700 -0.09685500
 H 1.93993800 3.39723100 -0.13200800
 C 4.55027300 4.02140600 -0.16076600
 C 3.73728800 5.27366400 -0.20987700
 H 3.09046500 5.38160200 0.66986100
 H 3.07452600 5.30288400 -1.08370900
 H 4.37984400 6.15346700 -0.25505400
 H 5.62581000 4.11743200 -0.16864500
 B 6.39364000 1.52543000 -0.05346800
 O 7.09557000 0.34472500 0.06854300
 C 8.49653500 0.61611300 -0.20050000
 C 8.59682900 2.16075500 0.08882400
 O 7.23481400 2.60927300 -0.16943400
 C 9.54037500 2.93285800 -0.82458900
 H 9.52630300 3.99045100 -0.55520600
 H 10.5661760 2.57167500 -0.71743300
 H 9.24814800 2.84804900 -1.86994100
 C 8.89659000 2.48918800 1.55363800
 H 8.75052900 3.55885800 1.71142500
 H 8.22571000 1.95420300 2.22726500
 H 9.92635600 2.24169700 1.81858700
 C 8.74439100 0.25379100 -1.66778300
 H 9.79488900 0.37193200 -1.94073100
 H 8.46564900 -0.78961500 -1.82285600
 H 8.14003600 0.86675000 -2.33810200
 C 9.34414700 -0.26897300 0.70493800
 H 10.4075510 -0.05300100 0.57562000
 H 9.08601000 -0.13776100 1.75442600
 H 9.17979700 -1.31644600 0.44625300
 H 4.82912100 -0.58815100 0.03011000
 H 2.40090200 -0.85015000 0.04224000
 H 0.24678000 -0.54773500 0.91449200
 H -1.06579300 0.21875900 -0.01138200
 H 0.25263000 -0.61286100 -0.87051500



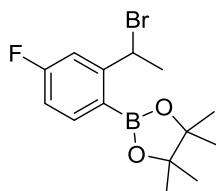
RB3LYP energy: -2982.5458369

Volume: 121.737 cm³/mol

NPA at C1: -0.19946

NPA at C3: -0.08679

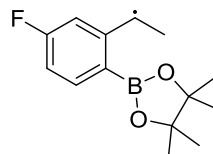
C 0.00000000 0.00000000 0.00000000
 C 1.38738900 0.04252500 -0.00528400
 C 2.04969900 1.26069500 -0.08762500
 C 1.35806300 2.47837200 -0.16353800
 C -0.04385900 2.41406200 -0.16712000
 C -0.68707800 1.19880000 -0.08058100
 F -2.03932200 1.17681500 -0.09101600
 H -0.63325200 3.31600500 -0.26214900
 C 2.04751200 3.77437600 -0.25222600
 C 1.54835300 4.94670100 0.13653500
 H 0.56986700 5.04389300 0.59253400
 H 2.12330500 5.85674600 0.02275500
 H 3.05227100 3.74530800 -0.65730000
 Br 3.97170500 1.21091200 -0.06144100
 H 1.95534600 -0.87548400 0.05743000
 H -0.53795500 -0.93682300 0.05759700



RB3LYP energy: -3394.5971078

C 0.00000000 0.00000000 0.00000000
 C 0.74452900 0.40950500 -1.25844000
 C 0.65097800 1.86623400 -1.62599300
 C 1.80161000 2.63281200 -1.91533300
 C 1.62623800 3.99235800 -2.23036300
 C 0.37884100 4.59467400 -2.26025400
 C -0.72116600 3.80613000 -1.97282700
 C -0.60963300 2.46774900 -1.66199500
 H -1.51022600 1.89861300 -1.47369500
 F -1.95209300 4.36561000 -2.00131200
 H 0.24992400 5.64129400 -2.50354000
 H 2.50154800 4.58713300 -2.45932400
 B 3.27634500 2.11843700 -1.92990200
 O 3.71384600 0.86946400 -1.56656800
 C 5.17507700 0.88721100 -1.53860400
 C 5.50709400 2.12356000 -2.45780100
 O 4.30487400 2.93610700 -2.32669200

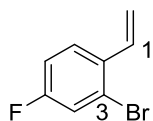
C 5.63545300 1.76460800 -3.94008000
 H 4.78010700 1.18338700 -4.28725700
 H 5.67553300 2.68592100 -4.52293700
 H 6.54557400 1.19500800 -4.13650200
 C 6.70275800 2.95704000 -2.01530700
 H 7.62059300 2.36497700 -2.04411500
 H 6.82651800 3.80223300 -2.69433500
 H 6.57232100 3.35007100 -1.00845300
 C 5.68116900 -0.45545100 -2.04839000
 H 5.27521900 -0.69305100 -3.02993200
 H 6.77205000 -0.45826300 -2.10985300
 H 5.38110800 -1.24576900 -1.35831300
 C 5.58076000 1.08406100 -0.07645000
 H 6.66492300 1.05086900 0.04517500
 H 5.21665100 2.03447900 0.31630400
 H 5.14620900 0.28156700 0.52149400
 H 1.77684200 0.09287900 -1.21063600
 Br 0.05626000 -0.71208200 -2.80964700
 H -1.07020200 0.19548900 -0.06518800
 H 0.14163700 -1.06192400 0.20015100
 H 0.39864400 0.56875300 0.84625800



UB3LYP energy: -820.40950926

C 0.00000000 0.00000000 0.00000000
 C 0.94755800 -1.15376700 -0.05255800
 C 0.55288200 -2.50629300 -0.11407800
 C 1.50785600 -3.58507400 -0.16460500
 C 1.02799000 -4.89578600 -0.22428500
 C -0.32931200 -5.20485400 -0.23650600
 C -1.22778400 -4.14759500 -0.18657400
 C -0.83161000 -2.83593500 -0.12719800
 H -1.58945100 -2.06564200 -0.09006400
 F -2.55428600 -4.42708000 -0.19651800
 H -0.68863900 -6.22425700 -0.28241700
 H 1.74554100 -5.70614500 -0.26250300
 B 3.05623400 -3.42574200 -0.16163400
 O 3.76451800 -2.25477000 -0.03094100

C 5.17126900 -2.54156800 -0.28669000
 C 5.24763100 -4.09177500 -0.01718300
 O 3.88412900 -4.51776800 -0.29128400
 C 5.53269400 -4.44432300 1.44504400
 H 4.86393600 -3.91093900 2.12216000
 H 5.37078700 -5.51406100 1.58548200
 H 6.56355800 -4.21505100 1.72172900
 C 6.18902700 -4.86234800 -0.93428700
 H 7.21886200 -4.51782900 -0.81240000
 H 6.15682700 -5.92344500 -0.68122000
 H 5.90752100 -4.75781300 -1.98077800
 C 6.01531400 -1.67888400 0.64245500
 H 5.73910200 -1.81905300 1.68615300
 H 7.07699900 -1.91014000 0.52739100
 H 5.87227500 -0.62586800 0.39385400
 C 5.43780700 -2.16101700 -1.74502300
 H 6.48978700 -2.28838900 -2.00730900
 H 4.83424100 -2.75741600 -2.43063800
 H 5.17437700 -1.11207100 -1.88895800
 H 2.00580100 -0.93965100 -0.04024000
 H 0.54063700 0.94605900 0.03319300
 H -0.66468300 0.02958200 -0.87211800
 H -0.65033400 -0.03917600 0.88272100



RB3LYP energy: -2982.5456217

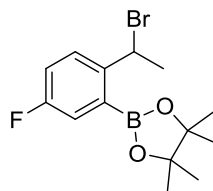
Volume: 120.435 cm³/mol

NPA at C1: -0.19547

NPA at C3: -0.05658

C 0.00000000 0.00000000 0.00000000
 C -0.05156700 -1.26330100 -0.42014100
 C -1.22775300 -2.14299800 -0.34908500
 C -1.12278100 -3.53894600 -0.27552000
 C -2.23607800 -4.36607200 -0.20896200
 C -3.48758200 -3.78094900 -0.22087700
 C -3.65869400 -2.41013600 -0.30196000
 C -2.52805800 -1.61313800 -0.37049100
 H -2.64724100 -0.54157900 -0.46614000
 H -4.65473800 -1.98840600 -0.32600600
 F -4.57506800 -4.57917400 -0.16020500

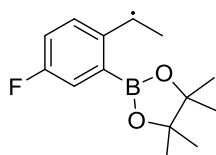
H -2.14115200 -5.44066300 -0.14586600
 Br 0.59322200 -4.40190200 -0.23059200
 H 0.84291700 -1.70557400 -0.84369200
 H 0.90630300 0.58194500 -0.10795000
 H -0.84027900 0.49199000 0.47631700



RB3LYP energy: -3394.5963625

C 0.00000000 0.00000000 0.00000000
 C 0.78493000 0.44359200 -1.22173000
 C 0.75294500 1.91466700 -1.52728000
 C 1.93258100 2.63847200 -1.80789800
 C 1.82809500 4.01379600 -2.07476000
 C 0.59835600 4.63479300 -2.05570700
 C -0.56837200 3.94121000 -1.78781900
 C -0.47580100 2.58301800 -1.52846000
 H -1.38624100 2.02744100 -1.34347100
 H -1.52004600 4.45697900 -1.79172000
 F 0.52465900 5.96250900 -2.31224800
 H 2.71283400 4.59505100 -2.29958400
 B 3.38628300 2.05823200 -1.85968500
 O 3.77679300 0.79521700 -1.49773300
 C 5.23880400 0.75123800 -1.50467800
 C 5.60054300 1.96781200 -2.43937900
 O 4.43537400 2.83044800 -2.28639400
 C 5.67924000 1.59603600 -3.92181100
 H 4.79222600 1.05020100 -4.24624800
 H 5.74559000 2.51150500 -4.51136500
 H 6.55936200 0.98666200 -4.13472700
 C 6.83910200 2.75362300 -2.02954400
 H 7.73072300 2.12393300 -2.07722800
 H 6.98099400 3.59008700 -2.71569500
 H 6.74914600 3.15576200 -1.02187400
 C 5.67458900 -0.61427100 -2.01844200
 H 5.23220800 -0.84091700 -2.98677900
 H 6.76226100 -0.66269300 -2.10989600
 H 5.36162700 -1.38730100 -1.31464700

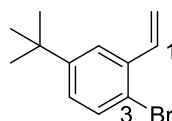
C 5.68539900 0.93835800 -0.05341200
 H 6.76976700 0.86139800 0.04428800
 H 5.36923700 1.90483800 0.34163800
 H 5.23179100 0.15742100 0.55871600
 H 1.80249500 0.08272100 -1.16948900
 Br 0.08805800 -0.58940000 -2.83807500
 H 0.10200900 -1.07444300 0.15168200
 H 0.39893900 0.51428300 0.88034700
 H -1.06179800 0.23340600 -0.07653100



UB3LYP energy: -820.40801555

C 0.00000000 0.00000000 0.00000000
 C -0.87469300 -1.21066900 0.06263700
 C -0.39782900 -2.53491300 0.13634600
 C -1.28425100 -3.67117700 0.18275600
 C -0.73384200 -4.95361300 0.24055000
 C 0.63633800 -5.13536000 0.26250800
 C 1.52026200 -4.06540600 0.22305000
 C 1.00504300 -2.78797900 0.15910100
 H 1.69293800 -1.95347200 0.12538200
 H 2.58761700 -4.24732700 0.24135300
 F 1.13654700 -6.39442000 0.32344500
 H -1.38003600 -5.82177600 0.27105200
 B -2.84193600 -3.60949000 0.18294800
 O -3.62135200 -2.47845600 0.19123800
 C -5.00488500 -2.88422200 0.41982000
 C -4.98628300 -4.39008400 -0.04104900
 O -3.59660900 -4.75948900 0.18253500
 C -5.25644000 -4.57210100 -1.53645100
 H -4.62456500 -3.91743600 -2.13840400
 H -5.03220000 -5.60372100 -1.81171700
 H -6.30057200 -4.37068200 -1.78308800
 C -5.87258900 -5.32717100 0.76942100
 H -6.92365200 -5.04237300 0.67863500
 H -5.76620000 -6.34560600 0.39202600
 H -5.60118400 -5.32883000 1.82382300
 C -5.91518700 -1.96810400 -0.38725000

H -5.64621600 -1.95846400 -1.44223500
 H -6.95813400 -2.28069200 -0.29504800
 H -5.83579700 -0.94767100 -0.00834200
 C -5.27150300 -2.70859000 1.91610700
 H -6.30945900 -2.93531400 2.16655700
 H -4.62183100 -3.34877700 2.51448600
 H -5.07126200 -1.67206200 2.19161500
 H -1.94368100 -1.05893700 0.05080200
 H -0.59942900 0.90834600 -0.06590300
 H 0.64304300 0.09443500 0.88409200
 H 0.66957400 -0.01588100 -0.86892600



RB3LYP energy: -3040.5750776

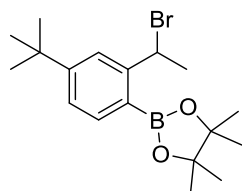
Volume: 160.309 cm**3/mol

NPA at C1: -0.19203

NPA at C3: -0.07463

C 0.00000000 0.00000000 0.00000000
 C -1.53541500 -0.06950600 0.00536000
 C -2.18000700 -1.31103400 0.09060000
 C -3.56168800 -1.40698100 0.08206000
 C -4.33472900 -0.25745800 -0.00727700
 C -3.74839000 1.00784100 -0.08514100
 C -2.34252500 1.05836200 -0.08613900
 H -1.88989700 2.03423800 -0.18622700
 C -4.54438700 2.24115200 -0.17990800
 C -4.15903400 3.45158000 0.22287300
 H -4.80966300 4.30818100 0.10068300
 H -3.20206100 3.63141600 0.69893400
 H -5.53594400 2.12882100 -0.60370100
 Br -6.24702800 -0.47761700 0.01443000
 H -4.04062200 -2.37463200 0.14808100
 H -1.60348800 -2.22530700 0.15736500
 C 0.54547000 -0.63099700 1.30029800
 H 1.63798000 -0.59243200 1.30907900
 H 0.17979500 -0.09386800 2.17854500
 H 0.24959600 -1.67658000 1.40131100
 C 0.52112300 1.44390600 -0.08536500
 H 1.61329800 1.43870700 -0.07926500

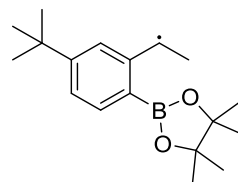
H 0.20050600 1.93975800 -1.00438400
 H 0.19048700 2.04689100 0.76350700
 C 0.54529500 -0.78162400 -1.21564600
 H 0.17748600 -0.35492700 -2.15166500
 H 1.63784700 -0.74340600 -1.23113000
 H 0.25032000 -1.83211500 -1.18885200



RB3LYP energy: -3452.6245112

C 0.00000000 0.00000000 0.00000000
 C -0.52228100 -0.56856900 -1.30785400
 C -0.01176400 -1.93773400 -1.66833800
 C -0.89295100 -2.99946000 -1.94911500
 C -0.31728000 -4.24909500 -2.24158300
 C 1.05072900 -4.44615800 -2.25626800
 C 1.93448200 -3.39297500 -1.98382800
 C 1.37088800 -2.15457900 -1.69440900
 H 2.01694200 -1.30964800 -1.50248600
 C 3.45180500 -3.63205500 -2.01499200
 C 3.82202600 -4.69617600 -0.95800000
 H 4.89885100 -4.88534500 -0.97304800
 H 3.55048900 -4.36080100 0.04577500
 H 3.31473700 -5.64490100 -1.14155600
 C 4.25523900 -2.35617300 -1.71455800
 H 5.32362500 -2.57980600 -1.75620400
 H 4.05427200 -1.56733300 -2.44275000
 H 4.04039100 -1.96483000 -0.71750300
 C 3.86218500 -4.13898500 -3.41556900
 H 3.61750000 -3.40234200 -4.18419600
 H 4.93969800 -4.32121900 -3.44995300
 H 3.35881100 -5.07191100 -3.67403500
 H 1.43313600 -5.43270300 -2.48934600
 H -0.97351900 -5.08202500 -2.46319800
 B -2.45253300 -2.93899600 -1.96693300
 O -3.23779300 -1.85831500 -1.64614800
 C -4.62843900 -2.29989300 -1.59608900
 C -4.58783000 -3.61829900 -2.45887600

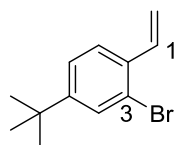
O -3.20060100 -4.03597100 -2.31869700
 C -4.82621400 -3.37820400 -3.95170300
 H -4.18360600 -2.58547100 -4.33730200
 H -4.59442500 -4.29459200 -4.49645000
 H -5.86547800 -3.11264000 -4.15396400
 C -5.48257800 -4.74637400 -1.96127000
 H -6.53433900 -4.45214700 -1.99522100
 H -5.35669500 -5.61937700 -2.60381400
 H -5.23460200 -5.03970800 -0.94257100
 C -5.50499100 -1.18490000 -2.15138700
 H -5.19172700 -0.88382100 -3.14945000
 H -6.55115400 -1.49776700 -2.19166000
 H -5.44028700 -0.31162300 -1.50012600
 C -4.95657400 -2.54357400 -0.12142300
 H -6.00101100 -2.83068500 0.01361500
 H -4.32431300 -3.32354200 0.30526200
 H -4.78093300 -1.62257500 0.43654500
 H -1.60253400 -0.54185500 -1.32918700
 Br -0.06929600 0.74482300 -2.80086700
 H -0.42734200 0.98429600 0.19159300
 H -0.29280000 -0.67045900 0.81454100
 H 1.08625200 0.08840400 0.00964800



UB3LYP energy: -878.43572094

C 0.00000000 0.00000000 0.00000000
 C -0.80495700 -1.25879400 0.05397400
 C -0.26066600 -2.55829700 0.11277100
 C -1.08974200 -3.73150700 0.16524300
 C -0.45033400 -4.97243500 0.22114700
 C 0.93151000 -5.10609400 0.22696000
 C 1.76626400 -3.97436300 0.17472000
 C 1.15493300 -2.73425200 0.12033400
 H 1.76717500 -1.84562600 0.08054100
 C 3.29277100 -4.15387300 0.17904200
 C 3.72005500 -4.87131800 1.47856600
 H 4.80376200 -5.01705900 1.49221000
 H 3.44551200 -4.28214900 2.35675200

H 3.25073800 -5.85183000 1.57458100
 C 4.04516700 -2.81531600 0.10327100
 H 5.12207200 -2.99961000 0.10883400
 H 3.80998300 -2.26679300 -0.81177900
 H 3.81743600 -2.17183600 0.95615200
 C 3.71114900 -5.00899100 -1.03775600
 H 3.42227800 -4.52363000 -1.97302600
 H 4.79573800 -5.14773800 -1.04764700
 H 3.24899000 -5.99738500 -1.01851800
 H 1.36031800 -6.09959200 0.27064000
 H -1.06156900 -5.86645500 0.26143500
 B -2.64417500 -3.75525900 0.16865300
 O -3.48874400 -2.67477700 0.05343400
 C -4.84968100 -3.12926600 0.30952900
 C -4.74247300 -4.67374700 0.02089000
 O -3.33965600 -4.93875600 0.28878700
 C -4.98940700 -5.03831300 -1.44594100
 H -4.38825500 -4.42320200 -2.11716800
 H -4.70604400 -6.08053600 -1.60040800
 H -6.04059500 -4.92503300 -1.71822800
 C -5.58508400 -5.56234700 0.92750200
 H -6.64960100 -5.35183700 0.79841900
 H -5.41547100 -6.60913500 0.66957000
 H -5.32721100 -5.42900600 1.97678400
 C -5.79478400 -2.36144700 -0.60582800
 H -5.50073200 -2.44587400 -1.65069800
 H -6.81928100 -2.72663600 -0.49995900
 H -5.78527400 -1.30364400 -0.33710000
 C -5.15298200 -2.80133600 1.77364300
 H -6.18181600 -3.05404100 2.03717700
 H -4.48038600 -3.33251600 2.44855400
 H -5.01269000 -1.73083600 1.93097300
 H -1.88082100 -1.16390300 0.04626900
 H -0.65040200 0.87422800 -0.04284500
 H 0.64948900 0.11605900 0.87664200
 H 0.65749600 0.03596900 -0.87755900



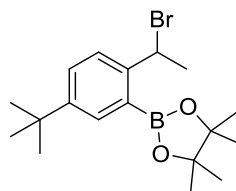
RB3LYP energy: -3040.5755169

Volume: 161.971 cm**3/mol

NPA at C1: -0.19292

NPA at C3: -0.06925

C 0.00000000 0.00000000 0.00000000
 C 1.45568600 0.48855400 -0.05221800
 C 2.50087600 -0.44015900 -0.02996600
 C 3.82439600 -0.03502600 -0.07344000
 C 4.19655000 1.31403300 -0.13566400
 C 3.13916900 2.23152500 -0.17005800
 C 1.81011700 1.83765300 -0.12492600
 H 1.04749500 2.60310400 -0.16071100
 H 3.37223700 3.28562100 -0.25804800
 C 5.59763800 1.75560200 -0.18154300
 C 6.05496000 2.93598400 0.23513000
 H 7.10487900 3.18486400 0.14768600
 H 5.41336300 3.68282500 0.68830900
 H 6.30511400 1.03795100 -0.58141800
 Br 5.16076200 -1.42406900 -0.01312100
 H 2.28852200 -1.49878000 0.02599800
 C -1.00348400 1.16356000 -0.05124300
 H -0.88050300 1.84581100 0.79300000
 H -0.91108600 1.74003500 -0.97452800
 H -2.02125000 0.76956800 -0.00991200
 C -0.27815600 -0.92888400 -1.20227300
 H 0.37286100 -1.80481900 -1.20060500
 H -1.31182900 -1.28368400 -1.17329300
 H -0.12667300 -0.40168500 -2.14701900
 C -0.23138600 -0.77952500 1.31355600
 H 0.42483200 -1.64792000 1.39201500
 H -0.04927700 -0.14325700 2.18273700
 H -1.26350000 -1.13652100 1.36399800

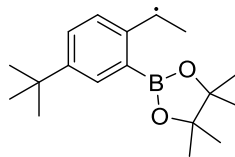


RB3LYP energy: -3452.6241910

C 0.00000000 0.00000000 0.00000000
 C -0.16306100 -0.89614700 -1.21491100
 C 0.93705500 -1.89142100 -1.45057200

C 0.66845400 -3.25427100 -1.70817900
 C 1.75535100 -4.11944800 -1.90094700
 C 3.08884500 -3.71000000 -1.85054100
 C 3.31871400 -2.35650100 -1.59830300
 C 2.26558000 -1.47274600 -1.40472900
 H 2.49039200 -0.42672600 -1.23583900
 H 4.32764500 -1.96896900 -1.55501400
 C 4.21886100 -4.72746400 -2.07277900
 C 5.61110800 -4.08026800 -1.98863500
 H 5.74717100 -3.30649600 -2.74787100
 H 5.79444300 -3.63380000 -1.00838600
 H 6.37882000 -4.83992500 -2.15231400
 C 4.13419200 -5.83102300 -0.99534400
 H 3.17999100 -6.35932900 -1.03184300
 H 4.92954200 -6.56713900 -1.14184100
 H 4.24402900 -5.40788100 0.00604600
 C 4.06851300 -5.36634800 -3.47115400
 H 3.11512600 -5.88628900 -3.57885000
 H 4.12558000 -4.60742900 -4.25497200
 H 4.86687900 -6.09348800 -3.64327700
 H 1.52876100 -5.15914200 -2.10065300
 B -0.74563300 -3.91474000 -1.80255100
 O -1.95305200 -3.30665300 -1.56224600
 C -2.99201000 -4.33249100 -1.56175500
 C -2.30587900 -5.49700600 -2.37184700
 O -0.89098600 -5.23710500 -2.14536900
 C -2.53164600 -5.40584200 -3.88310100
 H -2.29857400 -4.41012900 -4.26279100
 H -1.87225000 -6.11903600 -4.37985100
 H -3.56175100 -5.64778000 -4.15111400
 C -2.62417200 -6.90260600 -1.87847600
 H -3.69234300 -7.11332800 -1.97102300
 H -2.08387100 -7.63221700 -2.48402600
 H -2.32992900 -7.04298900 -0.83968900
 C -4.24439100 -3.74725800 -2.20049600
 H -4.04247200 -3.34876500 -3.19306200
 H -5.02863000 -4.50406500 -2.27880200
 H -4.62357700 -2.93290600 -1.58088900
 C -3.26037300 -4.68164500 -0.09629000
 H -4.06833600 -5.40913400 0.00003200
 H -2.37002100 -5.08487200 0.38826600
 H -3.55313000 -3.77450700 0.43464300
 H -1.12789400 -1.38306900 -1.20216600
 Br -0.35823900 0.29711700 -2.86199100

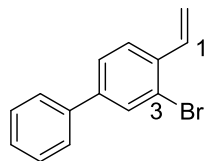
H -0.85304500 0.67110200 0.10001100
 H 0.05478700 -0.62841900 0.89493200
 H 0.90622900 0.60364400 -0.04488600



UB3LYP energy: -878.43560330

C 0.00000000 0.00000000 0.00000000
 C -0.37137300 -1.44811800 0.03225600
 C 0.55808900 -2.50673800 0.06669900
 C 0.16169000 -3.89190500 0.09384000
 C 1.15362900 -4.87062700 0.12060600
 C 2.52927200 -4.59731700 0.12890500
 C 2.89790800 -3.24593800 0.10306400
 C 1.95289700 -2.23893600 0.07234200
 H 2.29308300 -1.21128300 0.05228900
 H 3.94294500 -2.96495500 0.10633500
 C 3.54573000 -5.74656900 0.16815300
 C 4.99819700 -5.24153100 0.16259300
 H 5.22494500 -4.66523300 -0.73752100
 H 5.21471300 -4.61654000 1.03215600
 H 5.68302300 -6.09226900 0.19036800
 C 3.33106200 -6.57964500 1.45183400
 H 2.32494800 -6.99991600 1.49707900
 H 4.04258500 -7.40952400 1.49108800
 H 3.47673600 -5.96507000 2.34345900
 C 3.34805300 -6.65529800 -1.06594500
 H 2.34438800 -7.08264200 -1.09717900
 H 3.50139700 -6.09472200 -1.99120100
 H 4.06320700 -7.48264300 -1.04714600
 H 0.82541000 -5.90291500 0.13823900
 B -1.30645000 -4.41066000 0.10675300
 O -2.44997000 -3.64637400 0.08028800
 C -3.58914000 -4.51974000 0.33030900
 C -3.01729600 -5.93103400 -0.07235900
 O -1.59170700 -5.75809300 0.15248000
 C -3.19645300 -6.25721800 -1.55749400
 H -2.84198800 -5.44192200 -2.18985900
 H -2.61210800 -7.14734400 -1.79561500

H -4.24149300 -6.45771300 -1.80126100
 C -3.50507900 -7.09503300 0.78122600
 H -4.58735900 -7.21636200 0.69120500
 H -3.03357700 -8.01850500 0.44063800
 H -3.25540400 -6.95716900 1.83200600
 C -4.76444300 -4.03128600 -0.50646800
 H -4.50678600 -3.96121200 -1.56191800
 H -5.62148600 -4.70055300 -0.39874400
 H -5.06780400 -3.03950300 -0.16636400
 C -3.91700400 -4.39766200 1.82043000
 H -4.80223700 -4.97889600 2.08562500
 H -3.08326200 -4.73099200 2.43997400
 H -4.11289700 -3.34995800 2.05350800
 H -1.42239000 -1.69600000 0.02951200
 H -0.89058300 0.62843900 -0.03332700
 H 0.58104500 0.29965600 0.88130500
 H 0.61375100 0.25216100 -0.87372300



RB3LYP energy: -3114.3939510

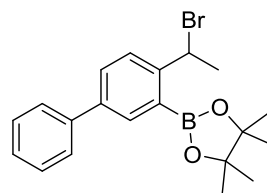
Volume: 168.433 cm**3/mol

NPA at C1: -0.19545

NPA at C3: -0.07227

C 0.00000000 0.00000000 0.00000000
 C -0.54464500 -1.10691700 -0.50506900
 C -1.97507300 -1.44130100 -0.49793700
 C -2.44728100 -2.75823600 -0.56935300
 C -3.79905000 -3.06568400 -0.56144400
 C -4.76110200 -2.05522600 -0.48485500
 C -4.30938000 -0.73106000 -0.42261300
 C -2.95784700 -0.44061800 -0.43381400
 H -2.64009400 0.59416700 -0.40490300
 H -5.02561200 0.07821000 -0.35266700
 C -6.20689300 -2.38037200 -0.47866500
 C -6.69278400 -3.49317600 0.21887900
 C -8.04911600 -3.79417400 0.22633100
 C -8.94970600 -2.99008100 -0.46488700
 C -8.48140400 -1.88197800 -1.16348800
 C -7.12530500 -1.58005200 -1.16949500

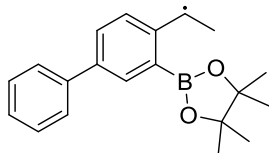
H -6.77099300 -0.72791300 -1.73703100
 H -9.17305700 -1.25418400 -1.71284300
 H -10.0072490 -3.22513600 -0.45926600
 H -8.40419500 -4.65498900 0.78057200
 H -6.00536800 -4.11403300 0.78095500
 H -4.10735100 -4.09934200 -0.63759700
 Br -1.22399500 -4.24321900 -0.66806200
 H 0.10899600 -1.84607400 -0.95390900
 H 1.06734200 0.16893300 -0.06375500
 H -0.58340200 0.76176800 0.50411800



RB3LYP energy: -3526.4428746

C 0.00000000 0.00000000 0.00000000
 C 0.12740800 -1.00209400 -1.13327100
 C 1.47846200 -1.63290000 -1.31438100
 C 1.62573400 -3.01997500 -1.53255300
 C 2.92082300 -3.53524900 -1.68963900
 C 4.06709700 -2.74162800 -1.63152900
 C 3.89082200 -1.36980900 -1.41887600
 C 2.62355000 -0.83332400 -1.26886900
 H 2.52329900 0.23730400 -1.14138000
 H 4.75183400 -0.71207400 -1.40031200
 C 5.41941600 -3.32770000 -1.79412700
 C 5.65533200 -4.34825600 -2.72362700
 C 6.92259400 -4.89730100 -2.87555300
 C 7.98334300 -4.43902100 -2.10063100
 C 7.76463300 -3.42571300 -1.17291900
 C 6.49725100 -2.87606500 -1.02248800
 H 6.33564500 -2.10316000 -0.28046200
 H 8.58176700 -3.06659600 -0.55818800
 H 8.97153700 -4.86719200 -2.21912300
 H 7.08369700 -5.68003600 -3.60762300
 H 4.84281900 -4.69855900 -3.34871600
 H 3.02958100 -4.60216800 -1.84018600
 B 0.46665400 -4.06792000 -1.60783200
 O -0.83857500 -3.87175100 -1.23123800

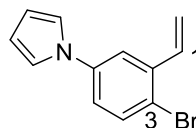
C -1.51776600 -5.16545500 -1.24979000
 C -0.59585500 -6.00723600 -2.21101800
 O 0.69238400 -5.34354800 -2.06050300
 C -0.98128800 -5.88650300 -3.68738700
 H -1.09034200 -4.84395000 -3.98938500
 H -0.19146000 -6.33170400 -4.29416500
 H -1.91461200 -6.41025200 -3.90232900
 C -0.43177800 -7.47295700 -1.83073200
 H -1.39212800 -7.99277700 -1.86955600
 H 0.24245800 -7.95885500 -2.53791100
 H -0.01279800 -7.58781200 -0.83247000
 C -2.94399100 -4.95189400 -1.73868800
 H -2.96928800 -4.44306700 -2.70061500
 H -3.46722100 -5.90639500 -1.83313600
 H -3.48934600 -4.33963000 -1.01846300
 C -1.52458000 -5.67550100 0.19274800
 H -2.06746800 -6.61838200 0.27947500
 H -0.51171100 -5.82169800 0.57062500
 H -2.01880700 -4.93725900 0.82606100
 H -0.64316900 -1.75677900 -1.06025400
 Br -0.40776500 -0.06876500 -2.87055900
 H -1.02056400 0.37731400 0.06375100
 H 0.24423700 -0.50113900 0.94223800
 H 0.67041900 0.85112400 -0.11543300



UB3LYP energy: -952.25568862

C 0.00000000 0.00000000 0.00000000
 C -0.07386700 -1.49163200 0.07771600
 C 1.04305500 -2.34260400 0.12742300
 C 0.92385200 -3.77832000 0.19629800
 C 2.08555200 -4.54565100 0.22932300
 C 3.37844700 -4.00057800 0.20966300
 C 3.48138700 -2.59857200 0.14552900
 C 2.36158900 -1.80159500 0.10316600
 H 2.48945100 -0.72862300 0.03816200
 H 4.46001800 -2.13518400 0.09929100
 C 4.57869700 -4.86027400 0.25367000

C 4.58766400 -6.12552000 -0.35252400
 C 5.71649300 -6.93332400 -0.31165400
 C 6.86897300 -6.49963400 0.33662200
 C 6.87819900 -5.24778800 0.94397600
 C 5.74924500 -4.43975800 0.90273000
 H 5.76674700 -3.47956000 1.40397100
 H 7.76596800 -4.90173100 1.46061800
 H 7.74956500 -7.13001500 0.36833700
 H 5.69887600 -7.90279100 -0.79603900
 H 3.70785800 -6.46983000 -0.88211200
 H 1.97700700 -5.62085800 0.30022200
 B -0.41585300 -4.57224400 0.25264400
 O -1.68594700 -4.04526800 0.25214700
 C -2.62601400 -5.12315600 0.53638100
 C -1.79985500 -6.39841900 0.12452100
 O -0.43005400 -5.94765400 0.31113900
 C -1.94553600 -6.76850900 -1.35402800
 H -1.77652700 -5.90587900 -2.00024300
 H -1.20019000 -7.52585200 -1.60146500
 H -2.93422900 -7.17736800 -1.57125000
 C -2.02767700 -7.62713400 0.99589100
 H -3.06796400 -7.95683800 0.93876700
 H -1.39560600 -8.44462300 0.64494300
 H -1.77949100 -7.43364300 2.03809300
 C -3.89510300 -4.88044600 -0.27060300
 H -3.68339400 -4.77045900 -1.33290700
 H -4.60251300 -5.70276700 -0.13822900
 H -4.37699900 -3.96412200 0.07462100
 C -2.93362300 -5.05325500 2.03412900
 H -3.68105400 -5.79386300 2.32482600
 H -2.03609700 -5.21137400 2.63365500
 H -3.32488500 -4.06196800 2.26775400
 H -1.05459100 -1.94362300 0.09571900
 H -0.99855900 0.43739700 -0.02085300
 H 0.53217000 0.43429800 0.85513900
 H 0.52785100 0.34236700 -0.89868700



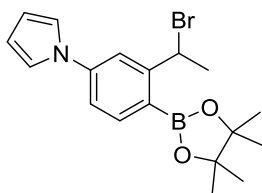
RB3LYP energy: -3092.3026437

Volume: 161.663 cm**3/mol

NPA at C1: -0.19699

NPA at C3: -0.08140

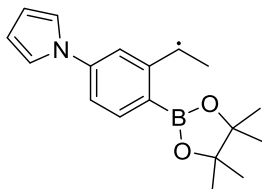
C 0.0000000 0.0000000 0.0000000
 C 0.39739000 -1.16442200 -0.51054200
 C -0.38618800 -2.40979600 -0.52098500
 C 0.21555400 -3.67488600 -0.54361100
 C -0.54102400 -4.83853100 -0.54665200
 C -1.92520100 -4.77162200 -0.54145700
 C -2.55742800 -3.52745000 -0.51730000
 C -1.78685100 -2.37126300 -0.50731200
 H -2.28055900 -1.40903800 -0.49103800
 N -3.96917400 -3.44396000 -0.51925000
 C -4.82713000 -4.30186000 0.14178800
 C -6.11355300 -3.89352000 -0.09613000
 C -6.04762500 -2.74873100 -0.93858100
 C -4.72292000 -2.49222000 -1.17895800
 H -4.25238800 -1.74662700 -1.79658800
 H -6.87794900 -2.18618400 -1.33429600
 H -7.00287200 -4.35708600 0.29970100
 H -4.44528600 -5.09851400 0.75699300
 H -2.51055000 -5.68039400 -0.58699500
 H -0.04802900 -5.80079500 -0.56829900
 Br 2.12776500 -3.86903800 -0.54049400
 H 1.38715500 -1.22970100 -0.94756000
 H 0.64026000 0.87152500 -0.04830900
 H -0.95580800 0.12577900 0.49549000



RB3LYP energy: -3504.3532618

C 0.0000000 0.0000000 0.0000000
 C -0.57328700 -0.68462800 -1.22806100
 C 0.00136100 -2.03817300 -1.55148900
 C -0.83054100 -3.14722800 -1.81805200
 C -0.20392800 -4.37281900 -2.10255200
 C 1.17101400 -4.52132900 -2.11469400
 C 1.98171300 -3.41440300 -1.85743300

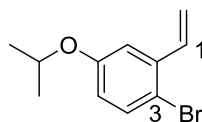
C 1.38809700 -2.18599800 -1.58593000
 H 2.02074900 -1.32012100 -1.44414900
 N 3.38896900 -3.53796900 -1.87520200
 C 4.11513900 -4.38144000 -2.69504800
 C 5.44611800 -4.21314400 -2.41817500
 C 5.54623500 -3.23785200 -1.38603600
 C 4.27329600 -2.83824800 -1.07556400
 H 3.91700200 -2.15147100 -0.32760700
 H 6.44874400 -2.88018900 -0.91689200
 H 6.25918200 -4.72221700 -2.91043700
 H 3.62434600 -4.99171300 -3.43329200
 H 1.61613900 -5.48988700 -2.30147800
 H -0.82537800 -5.23638300 -2.30446500
 B -2.39179800 -3.15847400 -1.82887100
 O -3.22390300 -2.11410500 -1.51044600
 C -4.59289900 -2.62094500 -1.45299700
 C -4.49318800 -3.94014200 -2.30972600
 O -3.08654200 -4.29201500 -2.17102300
 C -4.74479100 -3.71868200 -3.80311000
 H -4.14319400 -2.89651000 -4.19315200
 H -4.46820500 -4.62485700 -4.34399300
 H -5.79624400 -3.50677400 -4.00522000
 C -5.33380400 -5.10521300 -1.80381100
 H -6.39732200 -4.85643900 -1.83145300
 H -5.17475900 -5.97358500 -2.44521600
 H -5.06710400 -5.38465900 -0.78594900
 C -5.52373900 -1.55261500 -2.01111900
 H -5.22557500 -1.23855400 -3.00978300
 H -6.55230100 -1.91907700 -2.05129100
 H -5.50433600 -0.67551400 -1.36208700
 C -4.90293100 -2.87248900 0.02414200
 H -5.93273800 -3.20561600 0.16534600
 H -4.23451800 -3.62138500 0.45144800
 H -4.76657300 -1.94194500 0.57717500
 H -1.65153700 -0.73258500 -1.16902700
 Br -0.31949700 0.54608700 -2.82870400
 H -0.49651600 0.95462800 0.17348700
 H -0.16683900 -0.64123700 0.87152300
 H 1.07077500 0.18403000 -0.08588100



UB3LYP energy: -930.16540378

C 0.00000000 0.00000000 0.00000000
 C -0.79049700 -1.26228800 0.11910700
 C -0.22738700 -2.54931200 0.25419400
 C -1.04022900 -3.73295600 0.36292700
 C -0.39108200 -4.96378900 0.47942300
 C 0.99229300 -5.09024400 0.50830300
 C 1.78579200 -3.94178400 0.39770000
 C 1.18550600 -2.70218400 0.26611000
 H 1.81426800 -1.83137900 0.14368400
 N 3.19749100 -4.05269200 0.42093600
 C 3.93318100 -5.08352100 -0.13018400
 C 5.26307400 -4.82912500 0.08416600
 C 5.35061100 -3.60192900 0.79917200
 C 4.07151200 -3.14631800 0.98807200
 H 3.70413600 -2.28203700 1.51389500
 H 6.24820400 -3.11685100 1.14806800
 H 6.08222600 -5.44831700 -0.24488500
 H 3.44850500 -5.88367500 -0.66239300
 H 1.45336100 -6.05975700 0.64268400
 H -0.99498100 -5.85863900 0.56918600
 B -2.59566500 -3.77365200 0.37757800
 O -3.45139800 -2.70512800 0.24894200
 C -4.80418200 -3.16822600 0.53841600
 C -4.68492700 -4.71760900 0.28149400
 O -3.27371100 -4.96163400 0.53241400
 C -4.95099500 -5.11649500 -1.17254900
 H -4.36778600 -4.50972500 -1.86676500
 H -4.65929300 -6.15883700 -1.30950700
 H -6.00760000 -5.02002900 -1.42961600
 C -5.50213600 -5.59468500 1.22165500
 H -6.57066300 -5.39667400 1.10732100
 H -5.32731600 -6.64511100 0.98285000
 H -5.22716300 -5.43657400 2.26314700
 C -5.77255200 -2.43065900 -0.37712300
 H -5.49662000 -2.53616900 -1.42501200
 H -6.79109800 -2.80351000 -0.24447000

H -5.76941400 -1.36702400 -0.13242400
 C -5.08435600 -2.81089300 1.99981000
 H -6.10553500 -3.06773900 2.28775200
 H -4.39439200 -3.32014500 2.67403600
 H -4.95247700 -1.73580700 2.13076200
 H -1.86743000 -1.18488200 0.09974400
 H -0.65905100 0.86349400 -0.09233500
 H 0.64436300 0.16907400 0.87168600
 H 0.66067000 -0.00524800 -0.87582900



RB3LYP energy: -3076.4930119

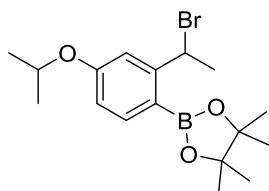
Volume: 167.219 cm³/mol

NPA at C1: -0.19114

NPA at C3: -0.09718

C 0.00000000 0.00000000 0.00000000
 O -0.94684300 -1.08796900 -0.01476900
 C -2.28636900 -0.84927000 0.03637600
 C -3.09748100 -1.98967000 0.05354400
 C -4.47223200 -1.85930700 0.10090900
 C -5.05574500 -0.59716500 0.13005800
 C -4.27757300 0.56282100 0.10766200
 C -2.88005100 0.40719600 0.07158600
 H -2.27499900 1.30055200 0.10261600
 C -4.87270800 1.90792300 0.13928800
 C -4.32146800 3.01813300 -0.35001600
 H -3.36504800 3.02017000 -0.86016100
 H -4.83078300 3.97006100 -0.26977500
 H -5.85580000 1.97464500 0.59123700
 Br -6.97873500 -0.51665900 0.17034700
 H -5.09777000 -2.74174700 0.11274500
 H -2.63133000 -2.96639400 0.03523500
 C 0.21293300 0.50998000 1.42135800
 H 0.92100100 1.34208000 1.42079700
 H -0.71754200 0.85705200 1.87215600
 H 0.61912100 -0.28704800 2.04796400
 C 1.27415900 -0.55346300 -0.61847500
 H 2.04333900 0.22074800 -0.65376100
 H 1.65236600 -1.38947800 -0.02632800

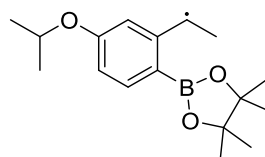
H 1.08849900 -0.90601600 -1.63391100
 H -0.38272300 0.80351000 -0.63769000



RB3LYP energy: -3488.5440976

C 0.00000000 0.00000000 0.00000000
 O 0.84721500 1.12843400 0.30088700
 C 2.20065400 1.02592700 0.21734700
 C 2.90999500 -0.14622500 -0.05343800
 C 4.29585600 -0.09964700 -0.08862300
 C 5.02951300 1.07458200 0.13531600
 C 4.29241400 2.25353800 0.40476200
 C 2.90417100 2.20959500 0.44034600
 H 2.32694000 3.10747300 0.61941400
 C 4.98428300 3.56329400 0.67247700
 C 4.53136100 4.31038000 1.91427700
 H 4.70221300 3.67376100 2.78851700
 H 3.47250200 4.56639700 1.88446800
 H 5.10319600 5.22993800 2.03891300
 H 6.05750400 3.43491900 0.67536200
 Br 4.74413700 4.79043700 -0.93708400
 B 6.57828000 0.94022000 0.06238600
 O 7.17521700 -0.25371700 -0.27098900
 C 8.59540400 -0.01202900 -0.47457600
 C 8.82804500 1.31353300 0.34318300
 O 7.50386500 1.92536500 0.31556100
 C 9.82285400 2.28975400 -0.27067000
 H 9.89493700 3.18059600 0.35559600
 H 10.8167490 1.84006400 -0.33269500
 H 9.51837100 2.60351300 -1.26755600
 C 9.16718900 1.07132500 1.81600100
 H 9.11798900 2.02163200 2.34976900
 H 8.45815700 0.38488900 2.28112800
 H 10.1732780 0.66469300 1.93426800
 C 8.80219400 0.15811800 -1.98197900
 H 9.85716500 0.28742700 -2.23115800
 H 8.43757600 -0.73629300 -2.48935600

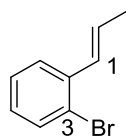
H 8.24626500 1.01402600 -2.36711200
 C 9.36948700 -1.22479000 0.02650200
 H 10.4464360 -1.05411600 -0.04401500
 H 9.12131800 -1.46407600 1.05925100
 H 9.12525200 -2.09223600 -0.58900900
 H 4.83807900 -1.01300800 -0.30151400
 H 2.40551300 -1.08296200 -0.24204100
 H 0.44072500 -0.89762200 0.44490700
 C -1.32668300 0.28679200 0.68533700
 H -2.02574900 -0.53421800 0.51297600
 H -1.18763200 0.40479100 1.76089300
 H -1.76785500 1.20499500 0.29171700
 C -0.14347900 -0.17489300 -1.50774500
 H -0.77493800 -1.03886100 -1.72841900
 H -0.60680400 0.71193600 -1.94555500
 H 0.82285300 -0.32771300 -1.98964500



UB3LYP energy: -914.35497688

C 0.00000000 0.00000000 0.00000000
 O -0.85175800 1.15859600 0.08479200
 C -2.20868200 1.02709900 0.13461900
 C -2.90294300 -0.18482400 0.04377400
 C -4.29609500 -0.16615900 0.08258500
 C -5.04761200 1.00060700 0.20968700
 C -4.33109700 2.24825500 0.31172800
 C -2.91700300 2.21370100 0.26995800
 H -2.34451500 3.12884000 0.33957100
 C -4.99916100 3.48602300 0.45246700
 C -4.31186600 4.80770400 0.56625500
 H -3.69593000 5.03109500 -0.31393900
 H -3.63826700 4.85088800 1.43116900
 H -5.03670500 5.61529400 0.67331200
 H -6.07855400 3.47500700 0.47905500
 B -6.58992500 0.83016700 0.21374400
 O -7.17534700 -0.41104100 0.07412200
 C -8.59791300 -0.27759000 0.33549400
 C -8.84197900 1.25415800 0.06293100

O -7.53240000 1.82617600 0.34283900
 C -9.86506400 1.92132900 0.97335800
 H -9.94263300 2.98051800 0.72147200
 H -10.8521680 1.47109900 0.84281500
 H -9.58265200 1.84413700 2.02202700
 C -9.15676300 1.56932800 -1.40157200
 H -9.11905800 2.65018300 -1.54559700
 H -8.42674200 1.11355800 -2.07191100
 H -10.1524890 1.22040100 -1.68167000
 C -8.82180700 -0.67719900 1.79676500
 H -9.88087800 -0.65857800 2.06147400
 H -8.44909800 -1.69194800 1.94475300
 H -8.28184700 -0.01747600 2.47757300
 C -9.35158300 -1.22788700 -0.58679700
 H -10.4315710 -1.11255700 -0.46587000
 H -9.09751500 -1.06152900 -1.63236000
 H -9.09322000 -2.25845500 -0.33710600
 H -4.82179700 -1.11094000 0.00906700
 H -2.38722800 -1.12902000 -0.05317200
 H -0.44748900 -0.71555600 -0.69692900
 C 1.31467300 0.49508800 -0.58305800
 H 2.01788500 -0.33391500 -0.68704600
 H 1.15624100 0.94256800 -1.56526900
 H 1.76139900 1.24749400 0.07055800
 C 0.17421100 -0.64219200 1.37241300
 H 0.80791800 -1.52928000 1.29711000
 H 0.64845700 0.06300600 2.05872300
 H -0.78287700 -0.94309800 1.80002500



RB3LYP energy: -2922.6066003

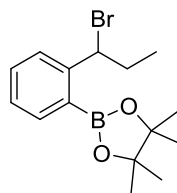
Volume: 120.487 cm³/mol

NPA at C1: -0.21533

NPA at C3: -0.07125

C 0.00000000 0.00000000 0.00000000
 C -1.24048100 0.82499000 0.14016300
 C -2.45081500 0.45172100 -0.28060300
 C -3.67851400 1.25245300 -0.17201700
 C -4.95086500 0.67184000 -0.07631100

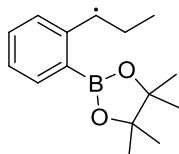
C -6.10847900 1.43190000 0.02273800
 C -6.02389100 2.81789200 0.02712800
 C -4.77872100 3.43043000 -0.07451200
 C -3.63420000 2.65687000 -0.17969300
 H -2.67262800 3.14136700 -0.29497100
 H -4.70135500 4.51087500 -0.08715300
 H -6.92727800 3.41069500 0.10167100
 H -7.06877500 0.94037300 0.09989100
 Br -5.16111100 -1.24295100 -0.04541500
 H -2.56288400 -0.53099600 -0.72673300
 H -1.12112000 1.78469600 0.63765800
 H -0.20325500 -0.95185500 -0.49351900
 H 0.76046700 0.53097500 -0.58247000
 H 0.44595800 -0.20852300 0.97795000



B3LYP energy: -3334.6495051

C 0.00000000 0.00000000 0.00000000
 C 0.85076000 0.40104600 -1.20015100
 C 1.11904800 1.87577400 -1.33004200
 C 2.43125400 2.37978800 -1.46730200
 C 2.59833500 3.77371100 -1.55196600
 C 1.52390200 4.64768500 -1.49861400
 C 0.23586200 4.13756400 -1.36963700
 C 0.04239300 2.76722000 -1.29049100
 H -0.96610600 2.37931200 -1.21883100
 H -0.61712200 4.80557700 -1.33803300
 H 1.68612600 5.71709700 -1.56447200
 H 3.60106900 4.16744200 -1.66411800
 B 3.74435400 1.53419300 -1.54359800
 O 3.86246300 0.17871100 -1.35881100
 C 5.28376200 -0.15550600 -1.31330200
 C 5.93697700 1.08105500 -2.03933700
 O 4.95292100 2.12916000 -1.80840300
 C 6.04907800 0.91008300 -3.55619900
 H 6.32621700 1.86830300 -3.99797000
 H 6.81291100 0.17683100 -3.82155100

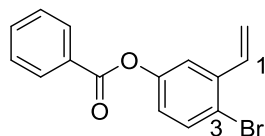
H 5.10052900 0.59888300 -3.99579800
 C 7.27182300 1.53810700 -1.46459300
 H 8.02479600 0.75188700 -1.55860200
 H 7.62524400 2.41046800 -2.01667700
 H 7.18632400 1.81528300 -0.41520600
 C 5.65809500 -0.26589700 0.16625800
 H 5.01987500 -1.01537000 0.63667700
 H 6.69744900 -0.57401100 0.29417300
 H 5.51029200 0.68036900 0.68866200
 C 5.48357300 -1.49614600 -2.00764600
 H 5.07711400 -1.49178400 -3.01740200
 H 6.54490500 -1.75092800 -2.05770800
 H 4.97580100 -2.27980800 -1.44285800
 H 1.77341500 -0.16353100 -1.21269500
 Br -0.03316100 -0.25560500 -2.91944900
 H -0.99677500 0.44008300 -0.07651000
 C -0.10505800 -1.50644600 0.22988100
 H 0.88455400 -1.95924400 0.33367500
 H -0.66493000 -1.71441900 1.14430700
 H -0.61462200 -1.99972600 -0.59870000
 H 0.47478800 0.46826500 0.87124800



UB3LYP energy: -760.46043077

C 0.00000000 0.00000000 0.00000000
 C 1.16299700 -0.93136800 0.13172500
 C 1.10039700 -2.33589300 0.23320000
 C 2.29017000 -3.14384500 0.36376600
 C 2.14773200 -4.52989200 0.46740500
 C 0.90647900 -5.15980700 0.44867200
 C -0.24794000 -4.38315800 0.32245700
 C -0.15524300 -3.01171100 0.21721500
 H -1.06554800 -2.43398000 0.12649100
 H -1.22290800 -4.85764000 0.30895600
 H 0.83800200 -6.23777100 0.53134900
 H 3.04287200 -5.13246600 0.56509700
 B 3.75331700 -2.61051200 0.38888700
 O 4.15743400 -1.29596600 0.34917600

C 5.60414000 -1.26842400 0.17315400
 C 6.02691200 -2.69213500 0.69487600
 O 4.82471400 -3.47369700 0.45770800
 C 6.29124600 -2.73477800 2.20249700
 H 6.37764000 -3.77676400 2.51420800
 H 7.21845200 -2.22108500 2.46390000
 H 5.47265600 -2.28211300 2.76399400
 C 7.18297900 -3.33972700 -0.05694200
 H 8.09175300 -2.74023600 0.03733000
 H 7.38471700 -4.32596900 0.36451300
 H 6.95601000 -3.46580600 -1.11426900
 C 5.86021900 -1.06466600 -1.32236600
 H 5.36306900 -0.14794400 -1.64308400
 H 6.92615700 -0.96912100 -1.53789400
 H 5.45886900 -1.89006300 -1.91196600
 C 6.16435100 -0.09368300 0.96466600
 H 5.86159100 -0.12971800 2.00983700
 H 7.25591600 -0.07971800 0.91700900
 H 5.79775600 0.84207800 0.53901700
 H 2.13936600 -0.47102200 0.19580700
 H -0.85048400 -0.48425000 -0.48571100
 C -0.45782600 0.58641700 1.35191800
 H -0.79884000 -0.20334500 2.02464800
 H 0.36109200 1.11346000 1.84681700
 H -1.27901800 1.29394700 1.20963000
 H 0.29122100 0.82962100 -0.65348500



RB3LYP energy: -3303.0018388

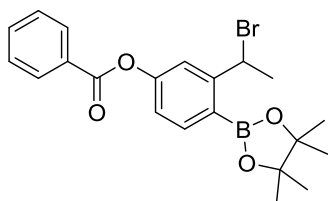
Volume: 183.864 cm**3/mol

NPA at C1: -0.19734

NPA at C3: -0.08595

C 0.00000000 0.00000000 0.00000000
 C -0.99340100 -0.48532200 -0.83868000
 C -2.20953900 0.17462700 -0.94112700
 C -2.41868000 1.31934900 -0.17894400
 C -1.41995200 1.81044700 0.64472500
 C -0.18375200 1.16146700 0.76448600
 C 0.86433900 1.69865400 1.64560000

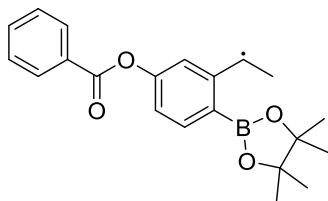
C 0.66501700 2.47289500 2.71127500
 H -0.32345200 2.76222700 3.04889100
 H 1.50166200 2.83469400 3.29514500
 H 1.87920300 1.41398100 1.39363600
 H -1.59946700 2.73328000 1.18040600
 O -3.57185100 2.07544500 -0.28294500
 C -4.81829900 1.50686900 -0.48424600
 O -5.55507200 2.01883600 -1.27891500
 C -5.20390900 0.35090100 0.37386000
 C -4.63697900 0.12174900 1.62983400
 C -5.09275600 -0.92765000 2.41741500
 C -6.10277400 -1.76328100 1.95088400
 C -6.67146300 -1.53841400 0.69975400
 C -6.23277900 -0.47898700 -0.08123900
 H -6.67998600 -0.27646600 -1.04585700
 H -7.46168100 -2.18470300 0.33758300
 H -6.44992100 -2.58666500 2.56373600
 H -4.65810700 -1.09394200 3.39545900
 H -3.85264300 0.76798800 1.99893200
 H -2.97189600 -0.19008200 -1.61696500
 H -0.81656000 -1.37885300 -1.42160900
 Br 1.63931200 -1.00103700 0.08598900



B3LYP energy: -3715.0525655

C 0.00000000 0.00000000 0.00000000
 C -0.93809000 -0.84886100 -0.81658400
 C -0.53441000 -2.09508400 -1.34646000
 C -1.47571700 -2.81990000 -2.09711100
 C -2.76475100 -2.36499700 -2.31884100
 C -3.14188400 -1.14527900 -1.76745600
 C -2.23758400 -0.39194200 -1.03597200
 H -2.55692800 0.57330100 -0.66501700
 O -4.38591500 -0.58619800 -1.98992300
 C -5.52797800 -1.35673200 -2.12357400
 O -6.28436300 -1.11150600 -3.02039200
 C -5.79636000 -2.37945900 -1.07291300

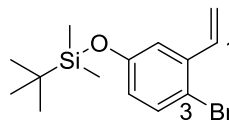
C -5.25554500 -2.29699200 0.21225300
 C -5.60085900 -3.23852300 1.17332900
 C -6.47209100 -4.27538400 0.85401400
 C -7.01423000 -4.36117200 -0.42592700
 C -6.68747000 -3.41101700 -1.38253800
 H -7.11677500 -3.45006000 -2.37534600
 H -7.69673700 -5.16475400 -0.67451200
 H -6.73244100 -5.01360400 1.60327300
 H -5.18901400 -3.16322300 2.17233800
 H -4.57948300 -1.49221600 0.46614800
 H -3.45863400 -2.93804400 -2.92059800
 H -1.17604200 -3.76831800 -2.52520300
 B 0.86809400 -2.76168300 -1.18605800
 O 1.17196400 -3.93412200 -1.83228800
 C 2.59692600 -4.18900000 -1.66807600
 C 2.94092500 -3.34163900 -0.38478100
 O 1.90971200 -2.30713500 -0.41555500
 C 4.30324700 -2.66164800 -0.40080900
 H 4.43223800 -2.07986100 0.51339200
 H 5.10444000 -3.40331200 -0.44345800
 H 4.40740800 -1.98590600 -1.24773800
 C 2.74958000 -4.10927300 0.92507800
 H 2.81780500 -3.40795600 1.75812200
 H 1.77195200 -4.59156300 0.96784400
 H 3.51901400 -4.87203700 1.05740300
 C 3.28351700 -3.68078600 -2.93799400
 H 4.35547000 -3.88597800 -2.92327800
 H 2.84929600 -4.18934800 -3.79992300
 H 3.13719500 -2.60803000 -3.07100400
 C 2.80466100 -5.69140600 -1.52603900
 H 3.85585800 -5.92160400 -1.33684800
 H 2.20523500 -6.10821500 -0.71844200
 H 2.51354600 -6.18776000 -2.45320900
 C -0.54354500 0.49297100 1.32967100
 H -1.43391500 1.11093100 1.21410300
 H 0.20996000 1.07642800 1.85857100
 H -0.80624900 -0.37309800 1.94588900
 H 0.94554600 -0.50442400 0.14038100
 Br 0.56671600 1.61162400 -1.10167800



UB3LYP energy: -1140.8651860

C	0.00000000	0.00000000	0.00000000
O	-1.44657300	0.08525900	-0.12512600
B	-1.85514000	1.28892200	0.40310000
C	-3.31874700	1.78897300	0.23090300
C	-4.17209700	0.95449700	-0.49315400
C	-5.51040100	1.25538300	-0.72708300
C	-6.02392200	2.44044600	-0.20067500
C	-5.22414800	3.31043800	0.50892700
C	-3.85328100	3.02356500	0.74778400
C	-3.06155200	3.94101000	1.47087700
C	-3.55893300	5.23948400	2.01720500
H	-3.96239000	5.89120800	1.23271400
H	-2.75704000	5.78365400	2.51650600
H	-4.36632600	5.10016800	2.74721400
H	-2.02569400	3.68696600	1.63969100
H	-5.66661500	4.22722400	0.87462900
O	-7.32747900	2.84417600	-0.44493300
C	-8.38399600	1.95966700	-0.51059300
O	-9.20631800	2.11479200	-1.37061600
C	-8.50158200	0.92334900	0.55620600
C	-7.92695000	1.07049400	1.82077500
C	-8.14152100	0.10708200	2.79846200
C	-8.91479200	-1.01463800	2.51656900
C	-9.48977400	-1.16559100	1.25720900
C	-9.29410800	-0.19565100	0.28476300
H	-9.75297400	-0.28592500	-0.69128600
H	-10.0964420	-2.03570300	1.03729200
H	-9.07306900	-1.76859700	3.27864500
H	-7.70316400	0.23211600	3.78109700
H	-7.32415700	1.93918900	2.04664700
H	-6.13402500	0.59344200	-1.31371500
H	-3.77178800	0.03272900	-0.89749400
O	-0.83666000	1.93347800	1.06467000
C	0.29151700	1.01482400	1.16874300
C	1.57924000	1.81631000	1.02849800

H	1.67583000	2.50308300	1.87122000
H	2.44891900	1.15482800	1.03232300
H	1.59173600	2.40353900	0.11181200
C	0.21484000	0.38191200	2.56017400
H	0.22787000	1.17470200	3.30960700
H	-0.70581000	-0.18901600	2.68866400
H	1.06289100	-0.27958000	2.74688200
C	0.58699100	0.43501500	-1.34534000
H	1.67486400	0.34543600	-1.35693300
H	0.18202400	-0.20624700	-2.12955000
H	0.32086800	1.46612800	-1.58235100
C	0.37574000	-1.44738700	0.29097800
H	1.45160900	-1.54356100	0.45621100
H	-0.14749800	-1.83234200	1.16469700
H	0.10949800	-2.07156500	-0.56374000



RB3LYP energy: -3485.2702716

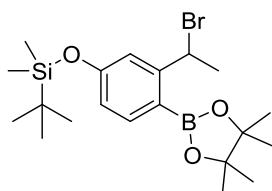
Volume: 234.378 cm**3/mol

NPA at C1: -0.19426

NPA at C3: -0.09471

Si	0.00000000	0.00000000	0.00000000
O	1.38324500	0.95967700	-0.03608300
C	2.71573000	0.70088900	-0.02472400
C	3.25800000	-0.58403100	-0.09847300
C	4.63619900	-0.75098500	-0.07267800
C	5.47560100	0.34753800	0.02269900
C	4.96528800	1.65206900	0.08967300
C	3.57311700	1.79272500	0.07336200
H	3.13318700	2.77720600	0.16303200
C	5.83720900	2.83305100	0.18961600
C	5.53073000	4.06307300	-0.22026000
H	4.59013100	4.29912700	-0.70433000
H	6.23207400	4.87832200	-0.09548300
H	6.81561400	2.65879200	0.62253400
Br	7.37149500	0.01237700	0.02442800
H	5.05672400	-1.74586700	-0.13102700
H	2.61947900	-1.45363700	-0.17154100
C	0.01306400	-1.07652100	1.53964100

H -0.91136500 -1.65576300 1.61213300
 H 0.84214500 -1.78736000 1.53167200
 H 0.10387000 -0.47440200 2.44629400
 C -1.41028200 1.27905700 0.04124500
 C -1.34902200 2.17129000 -1.21492100
 H -2.14805000 2.92086100 -1.18137700
 H -0.39787200 2.70312300 -1.28696100
 H -1.48358500 1.59583700 -2.13457500
 C -1.27862900 2.16981300 1.29269600
 H -2.07845700 2.91914600 1.30481600
 H -1.36132400 1.59328100 2.21771500
 H -0.32508400 2.70173900 1.31183600
 C -2.77089700 0.55411800 0.07947600
 H -3.58557500 1.28674900 0.10290500
 H -2.92852500 -0.07502000 -0.80075300
 H -2.87809900 -0.07570600 0.96684800
 C -0.08031100 -1.06722000 -1.54465300
 H -1.03244500 -1.60224900 -1.59373100
 H 0.01265900 -0.46404700 -2.45041100
 H 0.71356500 -1.81692200 -1.56421900

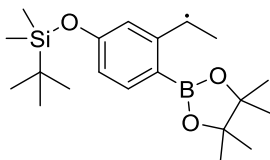


RB3LYP energy: -3897.3214523

Si 0.00000000 0.00000000 0.00000000
 O 1.30175300 0.89684000 0.58274900
 C 2.64808300 0.75115900 0.50161000
 C 3.27827000 -0.46405400 0.22545600
 C 4.66125000 -0.51371100 0.17269000
 C 5.47185500 0.61147200 0.39586700
 C 4.81878200 1.83386100 0.67759100
 C 3.42809700 1.88316700 0.72433800
 H 2.91483100 2.81757000 0.91055100
 C 5.59845600 3.09409800 0.94047000
 C 5.20509400 3.87095000 2.18414000
 H 5.33850000 3.22517200 3.05811600
 H 4.16592600 4.19832600 2.16068500
 H 5.83863000 4.74984600 2.30355000

H 6.66087500 2.89499800 0.93630300
 Br 5.42735200 4.33429000 -0.66914100
 B 7.00869100 0.37432800 0.31661100
 O 7.52247600 -0.83936700 -0.07610700
 C 8.95874900 -0.68888800 -0.25693600
 C 9.27528300 0.57078500 0.63380800
 O 7.99844100 1.27715700 0.62659600
 C 10.3453440 1.50424700 0.08332000
 H 10.4694670 2.35460400 0.75597300
 H 11.3067300 0.99008400 0.01009800
 H 10.0789900 1.88875700 -0.89961100
 C 9.57702300 0.22601200 2.09419800
 H 9.59167900 1.14741100 2.67834100
 H 8.81428400 -0.42993400 2.51637700
 H 10.5490360 -0.25971300 2.19793100
 C 9.19310300 -0.45266500 -1.75120200
 H 10.2573520 -0.38688600 -1.98537100
 H 8.77065400 -1.28937400 -2.30955300
 H 8.70457600 0.46104000 -2.09249300
 C 9.63865000 -1.97934000 0.18255700
 H 10.7258100 -1.88379400 0.12798100
 H 9.36340900 -2.25455800 1.19933100
 H 9.33876100 -2.79263700 -0.48041600
 H 5.14085200 -1.46005400 -0.04616000
 H 2.69665900 -1.36086000 0.05787100
 C -0.15538900 -1.61144100 0.95645100
 H -1.08418900 -2.12568600 0.69549300
 H 0.66665300 -2.29631600 0.73760100
 H -0.16104000 -1.43476700 2.03426000
 C -1.48729700 1.14433100 0.32719400
 C -1.30531200 2.47299000 -0.43304300
 H -2.14605800 3.14395400 -0.22213700
 H -0.38847700 2.98616300 -0.13584800
 H -1.27246800 2.32590500 -1.51578500
 C -1.59552600 1.44244800 1.83592600
 H -2.43661800 2.11954000 2.02541100
 H -1.77034600 0.53664400 2.42276600
 H -0.69139700 1.92144300 2.21779700
 C -2.78723500 0.46553900 -0.14941600
 H -3.64292200 1.12683700 0.02842800
 H -2.76809700 0.24412400 -1.22014300
 H -2.98620900 -0.46824200 0.38348500
 C 0.24630300 -0.34486100 -1.82887000
 H -0.60325400 -0.89911200 -2.23660500

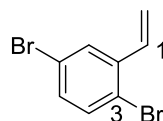
H 0.35061300 0.58037100 -2.39948000
 H 1.14298500 -0.94317400 -2.00452400



UB3LYP energy: -1323.1325047

Si 0.00000000 0.00000000 0.00000000
 O 1.25816700 1.09889800 -0.18290100
 C 2.61456200 1.00243800 -0.15346800
 C 3.29705100 -0.21993700 -0.12268400
 C 4.68817800 -0.21974200 -0.09998700
 C 5.45306200 0.94751800 -0.10830600
 C 4.75267300 2.20690600 -0.14488800
 C 3.33489100 2.18616500 -0.16549100
 H 2.77517300 3.11131700 -0.19290900
 C 5.43632100 3.44284100 -0.16042100
 C 4.76710600 4.77827300 -0.19667900
 H 4.11069400 4.93635100 0.66811100
 H 4.13803300 4.90225000 -1.08698200
 H 5.50371200 5.58229400 -0.20101600
 H 6.51581400 3.42067400 -0.14712600
 B 6.99370600 0.76048300 -0.07034600
 O 7.56023500 -0.49182700 0.04000100
 C 8.99023900 -0.36831300 -0.18331700
 C 9.24709500 1.15048400 0.14522500
 O 7.95007000 1.74865500 -0.13961100
 C 10.2949950 1.83465400 -0.72343500
 H 10.3815880 2.88339000 -0.43377700
 H 11.2737400 1.36699400 -0.59143700
 H 10.0304490 1.79757700 -1.77889200
 C 9.53848900 1.41266600 1.62506600
 H 9.51418500 2.48867000 1.80421600
 H 8.78971200 0.94654700 2.26704500
 H 10.5235790 1.03951700 1.91144700
 C 9.24251000 -0.72484700 -1.65122000
 H 10.3075640 -0.71543100 -1.89125000
 H 8.85770300 -1.72830000 -1.83944800
 H 8.72858900 -0.03585300 -2.32311100
 C 9.70972000 -1.35805600 0.72473100

H 10.7936050 -1.25138300 0.63505600
 H 9.43083100 -1.22370000 1.76850500
 H 9.44644600 -2.37654700 0.43401700
 H 5.20311400 -1.17287100 -0.07493300
 H 2.75590800 -1.15637100 -0.12086100
 C 0.16726400 -0.90598400 1.63786300
 H -0.68522500 -1.57101300 1.80066500
 H 1.07048000 -1.51904500 1.66721700
 H 0.21541100 -0.20926800 2.47750400
 C -1.54465800 1.11748300 -0.03728000
 C -1.61142800 1.87249700 -1.37944100
 H -2.48202100 2.53869300 -1.39347500
 H -0.72158600 2.48416800 -1.54255700
 H -1.71095500 1.19057400 -2.22807000
 C -1.47395600 2.14314400 1.11095400
 H -2.34758900 2.80477500 1.07910000
 H -1.46828600 1.66131600 2.09225400
 H -0.58100000 2.76742200 1.03856200
 C -2.81759700 0.26317300 0.12534200
 H -3.70640900 0.90411100 0.10163700
 H -2.92745400 -0.46985000 -0.67847800
 H -2.83391000 -0.27583000 1.07647100
 C -0.00234400 -1.22742600 -1.42451400
 H -0.88802500 -1.86733200 -1.38290000
 H -0.00219200 -0.71632800 -2.38981600
 H 0.87262300 -1.88041400 -1.39759100



RB3LYP energy: -5456.8134754

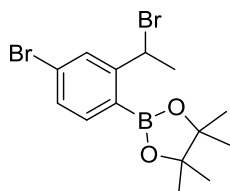
Volume: 136.627 cm**3/mol

NPA at C1: -0.19909

NPA at C3: -0.07572

C 0.00000000 0.00000000 0.00000000
 C 1.38644300 -0.07023100 -0.01013100
 C 2.14500800 1.08883200 -0.10072000
 C 1.55123800 2.35560700 -0.18049200
 C 0.14793800 2.40214100 -0.18182400
 C -0.60431300 1.24680900 -0.08590700
 Br -2.51698400 1.36833300 -0.09461400

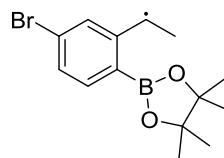
H -0.34522000 3.35869000 -0.28229500
 C 2.33868700 3.59427500 -0.27798600
 C 1.94457800 4.79696300 0.13726900
 H 0.99086900 4.96330100 0.62468700
 H 2.58490400 5.66109300 0.01482300
 H 3.32591700 3.49055300 -0.71326500
 Br 4.05539100 0.88958300 -0.08008000
 H 1.87643300 -1.03205000 0.05622500
 H -0.59206700 -0.90225900 0.06692200



RB3LYP energy: -5868.8643438

C 0.00000000 0.00000000 0.00000000
 C 0.55086900 -0.53366000 -1.31087700
 C 0.03202600 -1.88435900 -1.72870200
 C 0.90383000 -2.94695400 -2.04828100
 C 0.33134100 -4.18357700 -2.39298500
 C -1.03900600 -4.38556700 -2.42927000
 C -1.86935300 -3.31905600 -2.11410100
 C -1.35125300 -2.08485400 -1.76924100
 H -2.02221800 -1.26553000 -1.55099800
 Br -3.77078400 -3.56045100 -2.16044500
 H -1.45258400 -5.34764800 -2.69958300
 H 0.98811800 -5.00809700 -2.64126500
 B 2.46627200 -2.88960300 -2.06680100
 O 3.20584600 -3.95688300 -2.50910100
 C 4.60729800 -3.69782400 -2.20219800
 C 4.63074200 -2.12922400 -2.05717500
 O 3.25240600 -1.84088100 -1.66120500
 C 4.86755400 -1.39541300 -3.37805900
 H 4.66919300 -0.33259800 -3.23336500
 H 5.89883200 -1.50862400 -3.71700800
 H 4.20183900 -1.75738600 -4.16266300
 C 5.56151200 -1.58936000 -0.97986200
 H 6.60040100 -1.84160400 -1.20515300
 H 5.48152700 -0.50177600 -0.94016600
 H 5.31345600 -1.98303000 0.00451600

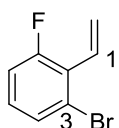
C 4.91482900 -4.43624400 -0.89765300
 H 4.68785400 -5.49504900 -1.03043900
 H 5.96725400 -4.34357000 -0.62369400
 H 4.30693600 -4.06156600 -0.07285700
 C 5.45969700 -4.25538700 -3.33452600
 H 5.15668300 -3.85802800 -4.30169700
 H 6.51535000 -4.02270600 -3.17559900
 H 5.35591300 -5.34117200 -3.36770000
 H 1.63164600 -0.52769900 -1.30044900
 Br 0.15737900 0.81842800 -2.77694100
 H -1.08412900 0.11079000 -0.01728900
 H 0.25730700 -0.70059400 0.80087900
 H 0.44016900 0.96908500 0.23436600



UB3LYP energy: -3294.6766686

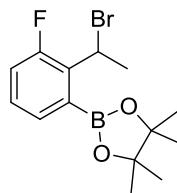
C 0.00000000 0.00000000 0.00000000
 C 0.80977600 -1.25445900 -0.05185800
 C 0.26714500 -2.55478400 -0.11131600
 C 1.09360600 -3.73293700 -0.16209000
 C 0.46634300 -4.97885500 -0.21633800
 C -0.91761100 -5.13140900 -0.22528500
 C -1.70325200 -3.98291600 -0.17718900
 C -1.14752600 -2.72655500 -0.12148400
 H -1.79282100 -1.86089300 -0.08470500
 Br -3.61650100 -4.16471200 -0.18815200
 H -1.37026000 -6.11218700 -0.26814800
 H 1.08409000 -5.86805000 -0.25390200
 B 2.65128900 -3.75134400 -0.16780700
 O 3.34606600 -4.93321200 -0.28011100
 C 4.75151400 -4.66206100 -0.02164000
 C 4.85249300 -3.11903900 -0.32153300
 O 3.48862100 -2.66688200 -0.06439600
 C 5.14872000 -2.79951600 -1.78861100
 H 5.00494400 -1.73051900 -1.95255500
 H 6.17735600 -3.05074500 -2.05386500
 H 4.47591800 -3.33718700 -2.45817500
 C 5.79656200 -2.34144200 0.58601000

H 6.82200500 -2.70342100 0.47922500
 H 5.78241900 -1.28561100 0.31012200
 H 5.50631500 -2.42015000 1.63233700
 C 5.00612600 -5.01698900 1.44586500
 H 4.72603700 -6.05881300 1.60830700
 H 6.05850900 -4.90012200 1.71152700
 H 4.40789700 -4.39896600 2.11704300
 C 5.59050900 -5.55417400 -0.92765200
 H 5.32559000 -5.42907100 -1.97613600
 H 6.65498700 -5.33910300 -0.80685900
 H 5.42638100 -6.59960800 -0.66116200
 H 1.88566700 -1.16048800 -0.04328300
 H -0.64430800 0.11321200 -0.88061500
 H -0.66273600 0.02952300 0.87352400
 H 0.64583000 0.87686400 0.04845400



RB3LYP energy: -2982.5437798
 Volume: 110.091 cm**3/mol
 NPA at C1: -0.21366
 NPA at C3: -0.05664

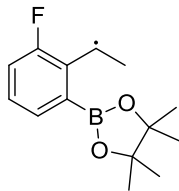
C 0.00000000 0.00000000 0.00000000
 C 0.89203900 -0.95883100 -0.25852000
 C 0.71620100 -2.41442900 -0.18963100
 C 1.81194000 -3.29867000 -0.15673000
 C 1.67083100 -4.67783400 -0.11435300
 C 0.40018700 -5.23753800 -0.10730700
 C -0.71768100 -4.41553500 -0.14214300
 C -0.53610200 -3.04806700 -0.17977200
 F -1.65264700 -2.28677300 -0.22340200
 H -1.72437300 -4.81194600 -0.14283300
 H 0.28410500 -6.31342200 -0.07497000
 H 2.54867500 -5.30775900 -0.08518800
 Br 3.61567300 -2.62924200 -0.14847400
 H 1.89050700 -0.65004700 -0.54230000
 H 0.29566600 1.03785900 -0.09194000
 H -1.01518100 -0.19552300 0.31037300



RB3LYP energy: -3394.5938014

C 0.00000000 0.00000000 0.00000000
 C -0.72923900 0.26203600 -1.30843300
 C -0.81599900 1.69247700 -1.76055800
 C -2.05559300 2.30251800 -2.07136800
 C -2.07156100 3.65063700 -2.46230100
 C -0.90840600 4.40045200 -2.55650900
 C 0.31189100 3.80889400 -2.26077600
 C 0.32834100 2.48286600 -1.87486300
 F 1.53985100 1.93657300 -1.61304100
 H 1.24741700 4.34960100 -2.32697700
 H -0.94670300 5.43882300 -2.86252000
 H -3.02305700 4.10867900 -2.69894800
 B -3.45580900 1.59961800 -2.03440200
 O -4.57655000 2.24545900 -2.49082600
 C -5.74144300 1.44441800 -2.13616500
 C -5.11191600 0.01494700 -1.93297600
 O -3.73350100 0.33993900 -1.56809400
 C -5.03909000 -0.81183600 -3.21795800
 H -4.41382100 -1.68761300 -3.03964800
 H -6.02813100 -1.15406300 -3.52816600
 H -4.59508700 -0.24394300 -4.03655400
 C -5.72257300 -0.81179600 -0.80960400
 H -6.77578500 -1.01960100 -1.01263800
 H -5.20037200 -1.76693000 -0.73386700
 H -5.64632100 -0.30729600 0.15213500
 C -6.31704700 2.04701200 -0.85250000
 H -6.55295000 3.09709300 -1.03105000
 H -7.23294800 1.53723900 -0.54831300
 H -5.60217600 1.99655700 -0.02990800
 C -6.75826200 1.54743900 -3.26558600
 H -6.32384500 1.27386100 -4.22552500
 H -7.61767700 0.90080200 -3.07341200
 H -7.11925000 2.57465500 -3.33871700
 H -1.72083900 -0.16401600 -1.26836700
 Br 0.10871400 -0.86564600 -2.77814500

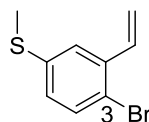
H 1.04730900 0.28842600 -0.03796600
 H -0.48968100 0.57585100 0.79246100
 H -0.06469700 -1.05703700 0.25848800



UB3LYP energy: -820.40531767

C 0.00000000 0.00000000 0.00000000
 C 1.01114200 -1.10116900 -0.05798200
 C 0.77544000 -2.48776100 -0.13015300
 C 1.85979000 -3.44535300 -0.18142200
 C 1.56886200 -4.80890500 -0.24968100
 C 0.26523100 -5.29603400 -0.27317400
 C -0.79791800 -4.39477400 -0.22510700
 C -0.53069300 -3.05048400 -0.15636700
 F -1.60305100 -2.21702100 -0.11031300
 H -1.82969500 -4.72318300 -0.23915600
 H 0.07372100 -6.36031700 -0.32718900
 H 2.39400900 -5.50894600 -0.28630700
 B 3.37831700 -3.08727400 -0.17143000
 O 3.93555300 -1.83513000 -0.07114500
 C 5.37008400 -1.95218400 -0.30948300
 C 5.63362300 -3.47250600 0.00681900
 O 4.33653200 -4.07081900 -0.26489500
 C 5.94578900 -3.74289200 1.48105300
 H 5.92599800 -4.82008000 1.65290200
 H 6.93378200 -3.36936600 1.75651100
 H 5.20492500 -3.28313800 2.13677200
 C 6.67287200 -4.14717400 -0.87964100
 H 7.65236000 -3.67916100 -0.75495900
 H 6.76371200 -5.19791800 -0.59917600
 H 6.39617900 -4.10240100 -1.93165800
 C 5.60212100 -1.58472000 -1.77705200
 H 5.21375800 -0.58080700 -1.95498300
 H 6.66447800 -1.59060100 -2.02815000
 H 5.08303500 -2.27102200 -2.44758000
 C 6.09075800 -0.96433100 0.59849500
 H 5.82342800 -1.10756100 1.64405800

H 7.17404600 -1.06533900 0.49739700
 H 5.82039700 0.05489600 0.31716200
 H 2.04813500 -0.80191400 -0.04173700
 H -0.64684900 -0.07416500 0.88018200
 H 0.50357300 0.96692000 0.03476100
 H -0.66946100 -0.00177700 -0.86568500

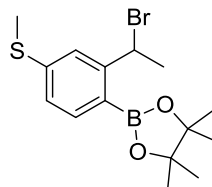


RB3LYP energy: -3320.8154515

Volume: 158.733 cm³/mol

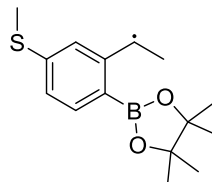
NPA at C3: -0.06643

C 0.00000000 0.00000000 0.00000000
 S 0.58223900 0.24951600 -1.72031500
 C 2.35725200 0.11022800 -1.50053300
 C 2.96991200 -1.14079600 -1.40744200
 C 4.34820500 -1.22878700 -1.28149500
 C 5.11702300 -0.07214500 -1.25912200
 C 4.54240000 1.20134400 -1.35577900
 C 3.14473600 1.25403900 -1.48339800
 H 2.66771600 2.21875800 -1.59628800
 C 5.34396100 2.43467000 -1.34298200
 C 4.91997300 3.63143900 -0.93958900
 H 5.57551800 4.49202300 -0.97849500
 H 3.92348100 3.79589000 -0.54638200
 H 6.36848700 2.33370200 -1.68240000
 Br 7.01759100 -0.28989900 -1.06583200
 H 4.82757300 -2.19555600 -1.20810000
 H 2.37317200 -2.04307800 -1.45030400
 H 0.38536200 0.78015600 0.65459300
 H -1.08745000 0.06423500 -0.03916300
 H 0.28788700 -0.98240100 0.37095400



RB3LYP energy: -3732.8673367

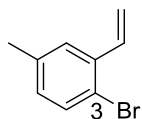
C	0.00000000	0.00000000	0.00000000
S	0.34319000	1.74640800	0.37488600
C	2.11447200	1.84773300	0.34771100
C	2.96705000	0.77682200	0.07563600
C	4.33788900	0.98031600	0.07676100
C	4.92142700	2.22763000	0.34910700
C	4.04705600	3.30433500	0.62636200
C	2.67045800	3.09860700	0.61784200
H	2.00867700	3.93628300	0.80438800
C	4.57251500	4.67518600	0.96288400
C	4.04074700	5.28072000	2.24997900
H	2.95655400	5.39129600	2.24101600
H	4.48463600	6.26042500	2.42668200
H	4.30731200	4.62294900	3.08355600
H	5.65335300	4.68198700	0.95704000
Br	4.16151000	5.95276000	-0.56724000
B	6.47926700	2.27652400	0.31802400
O	7.21676300	1.16710900	-0.01932100
C	8.60542100	1.57267300	-0.17901400
C	8.66263800	2.90526800	0.66077300
O	7.27517900	3.35695500	0.61286700
C	9.54430900	4.00304000	0.07988900
H	9.49436000	4.88707300	0.71779100
H	10.58689600	3.67912500	0.03458100
H	9.22441100	4.29149600	-0.91981500
C	8.99945700	2.68361800	2.13681900
H	8.83395600	3.61483500	2.68072800
H	8.36488900	1.91512500	2.58051400
H	10.04284300	2.39163200	2.26937700
C	8.83226200	1.78599600	-1.67764600
H	9.87180800	2.03912900	-1.89375900
H	8.58785800	0.86261200	-2.20480900
H	8.19277200	2.57761500	-2.07058700
C	9.49721000	0.44732400	0.32996500
H	10.55037500	0.73461100	0.28274200
H	9.25583800	0.17230900	1.35536100
H	9.36107000	-0.43537700	-0.29708600
H	4.98850200	0.14203200	-0.14123800
H	2.57754100	-0.20816900	-0.14086700
H	0.41854100	-0.65949700	0.75944100
H	-1.08584800	-0.08699600	0.01355800
H	0.36539500	-0.27400700	-0.98901900



UB3LYP energy: -1158.6787399

C	0.00000000	0.00000000	0.00000000
S	0.46883300	1.75663600	-0.06516900
C	2.24703700	1.72910000	-0.06656600
C	3.01665900	0.56190200	-0.02476100
C	4.40582800	0.66173900	-0.03146400
C	5.08470400	1.87885500	-0.07783700
C	4.29683900	3.08510300	-0.12173300
C	2.88403700	2.96218200	-0.11362200
H	2.27889600	3.85952100	-0.14581300
C	4.88933900	4.36652500	-0.17216200
C	4.12700300	5.65079100	-0.21697800
H	3.46939200	5.71238900	-1.09295800
H	4.80529300	6.50358200	-0.25569000
H	3.48293000	5.78137700	0.66157500
H	5.96783900	4.42111900	-0.17953500
B	6.63670800	1.80196300	-0.07115400
O	7.29170400	0.59535100	0.04709900
C	8.70404800	0.81501700	-0.21410300
C	8.86065800	2.35384900	0.08206400
O	7.51697400	2.85408200	-0.17964500
C	9.83574700	3.09389100	-0.82458200
H	9.85750300	4.15071500	-0.55277400
H	10.84749300	2.69645800	-0.71249700
H	9.54673900	3.02153700	-1.87175800
C	9.16668500	2.66456700	1.54930000
H	9.06535100	3.73883600	1.71073800
H	8.47082300	2.15562300	2.21772700
H	10.18375600	2.37249500	1.81747600
C	8.94518900	0.44936200	-1.68154700
H	10.00067100	0.52969300	-1.94881100
H	8.62885100	-0.58238700	-1.84228800
H	8.36744900	1.08698200	-2.35233100
C	9.51309800	-0.10459400	0.69202600
H	10.58440100	0.07236400	0.56882700
H	9.25472900	0.03215100	1.74074500
H	9.31139600	-1.14419700	0.42819800

H 4.98736100 -0.25211900 0.00178800
 H 2.55485400 -0.41453600 0.01239300
 H 0.35602500 -0.47450500 0.91373200
 H -1.08954000 -0.00478600 -0.00060600
 H 0.35727200 -0.54081400 -0.87559800

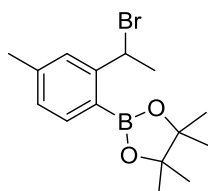


RB3LYP energy: -2922.6045069

Volume: 132.922 cm³/mol

NPA at C3: -0.07525

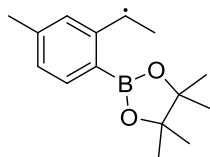
C 0.00000000 0.00000000 0.00000000
 C 1.50764900 0.01723600 -0.00158300
 C 2.23570100 -1.17307800 0.08235000
 C 3.62188000 -1.15769700 0.07959100
 C 4.29938100 0.05155800 -0.00342200
 C 3.61816600 1.27090600 -0.08227000
 C 2.21435500 1.20946200 -0.08917700
 H 1.66532900 2.13807500 -0.19187400
 C 4.31738900 2.56162600 -0.17419000
 C 3.83653200 3.73781300 0.22710600
 H 4.41839800 4.64288600 0.10759300
 H 2.86642500 3.84168200 0.69922200
 H 5.31619300 2.52707500 -0.59434100
 Br 6.22335600 -0.01722800 0.02381200
 H 4.17844100 -2.08306300 0.14289400
 H 1.71684400 -2.12353100 0.14144100
 H -0.38864700 -0.27859600 0.98394400
 H -0.40970300 0.97861300 -0.25330800
 H -0.38927800 -0.72510700 -0.71868800



RB3LYP energy: -3334.6543194

C 0.00000000 0.00000000 0.00000000

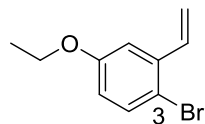
C 1.38004500 0.60207500 0.06111100
 C 2.50824900 -0.16247600 -0.24936200
 C 3.77105900 0.40031500 -0.19890600
 C 3.97909200 1.74236000 0.16794100
 C 2.84217800 2.51286000 0.48905900
 C 1.57288700 1.92978800 0.42409400
 H 0.70307700 2.53808100 0.64352400
 C 2.96383800 3.94858400 0.92076200
 C 2.21221100 4.32863800 2.18396000
 H 2.38080900 5.37700100 2.43009700
 H 2.58279900 3.71426400 3.01089200
 H 1.13821800 4.16631800 2.09647200
 H 4.00184400 4.24055500 0.99428800
 Br 2.32526100 5.16178100 -0.59157400
 B 5.46101800 2.23330500 0.16177400
 O 5.93518500 3.42180000 0.66188200
 C 7.32971700 3.56372500 0.25027400
 C 7.74108500 2.06917400 -0.03231900
 O 6.46302700 1.45623700 -0.36558100
 C 8.27109700 1.33756000 1.20318400
 H 8.34558800 0.27295900 0.97644400
 H 9.26165400 1.69655200 1.48877100
 H 7.60006700 1.45493000 2.05531300
 C 8.69114800 1.87112600 -1.20645400
 H 9.64296900 2.37628300 -1.02532300
 H 8.89407600 0.80659200 -1.33511100
 H 8.26749200 2.24772200 -2.13590400
 C 8.09552000 4.24691700 1.37525600
 H 7.71849000 5.26221400 1.50939500
 H 7.98452800 3.71761700 2.32029300
 H 9.15927600 4.31272100 1.13441800
 C 7.32872900 4.44580500 -0.99974300
 H 6.77481000 3.98220900 -1.81702400
 H 6.84465400 5.39411200 -0.76243900
 H 8.34402700 4.65527100 -1.34146600
 H 4.63259800 -0.20566000 -0.45171600
 H 2.39184900 -1.20188400 -0.53827000
 H -0.10072100 -0.82582300 0.71003700
 H -0.76861700 0.73812500 0.23232800
 H -0.20971500 -0.40312800 -0.99441700



UB3LYP energy: -760.46551804

C	0.00000000	0.00000000	0.00000000
C	1.47640100	0.30441600	0.01368300
C	2.41556000	-0.73756900	-0.03378800
C	3.77595400	-0.45491600	-0.02177500
C	4.27506900	0.84929500	0.03709400
C	3.32738700	1.93196000	0.08661400
C	1.94062600	1.60493900	0.07231600
H	1.21635800	2.40973900	0.10979600
C	3.73183700	3.28117100	0.14819000
C	2.79638000	4.44620600	0.20015700
H	3.34862300	5.38581500	0.23495900
H	2.14386100	4.41529000	1.08167400
H	2.13332300	4.48556300	-0.67292400
H	4.79150600	3.48894200	0.16120300
B	5.82352800	0.99345000	0.03919200
O	6.54514500	2.15799400	0.16923200
C	7.94731000	1.85848200	-0.08877100
C	8.01006500	0.30796500	0.18136500
O	6.64401300	-0.10584900	-0.09132900
C	8.29403700	-0.04581700	1.64380200
H	8.12193900	-1.11385400	1.78535500
H	9.32736200	0.17403700	1.91930100
H	7.63077400	0.49442400	2.32088100
C	8.94464900	-0.47145700	-0.73557600
H	9.97770000	-0.13626700	-0.61432500
H	8.90274500	-1.53216300	-0.48207900
H	8.66352500	-0.36492500	-1.78199600
C	8.80160400	2.71417400	0.83782200
H	8.66788600	3.76824800	0.58832000
H	8.52547900	2.57790000	1.88208400
H	9.86096500	2.47280100	0.72148400
C	8.21530100	2.23535600	-1.54807100
H	7.60532900	1.64329900	-2.23177500
H	7.95994400	3.28625200	-1.69252300
H	9.26580300	2.09906700	-1.81214400
H	4.48289100	-1.27532300	-0.05933500

H	2.07739200	-1.76723700	-0.07952100
H	-0.27923100	-0.63401100	0.84629600
H	-0.59644800	0.91196100	0.05149600
H	-0.28269500	-0.53652100	-0.91025200

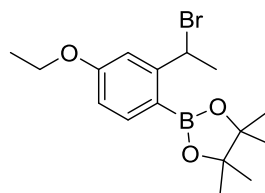


RB3LYP energy: -3037.1656602

Volume: 157.010 cm**3/mol

NPA at C3: -0.09408

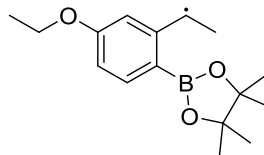
C	0.00000000	0.00000000	0.00000000
O	-0.85473800	-1.14362300	-0.07187500
C	-2.20384800	-0.95898900	-0.06468400
C	-2.97706500	-2.12245600	-0.13865700
C	-4.35554200	-2.03267700	-0.12326600
C	-4.97635700	-0.79037100	-0.03727700
C	-4.23423300	0.39118400	0.03029800
C	-2.83183600	0.27691100	0.02378900
H	-2.24971100	1.18145500	0.11723600
C	-4.87083600	1.71418400	0.12123900
C	-4.33484000	2.86911800	-0.27208200
H	-3.35832900	2.93258700	-0.73829000
H	-4.87691500	3.79865600	-0.15346000
H	-5.87299000	1.72389300	0.53426200
Br	-6.90131700	-0.76887200	-0.05122000
H	-4.95566800	-2.93078700	-0.18039600
H	-2.48120000	-3.08277100	-0.19826400
H	-0.20026000	0.54910200	0.92677800
C	1.43211300	-0.49072400	-0.03929900
H	2.11698300	0.35832800	0.01437200
H	1.63727000	-1.15349000	0.80294100
H	1.62924900	-1.03562000	-0.96393400
H	-0.20919500	0.66601900	-0.84456200



RB3LYP energy: -3449.2142778

C 0.00000000 0.00000000 0.00000000
 O -0.74852100 1.19195300 0.26727800
 C -2.10533000 1.18509500 0.16066900
 C -2.88470600 0.06660800 -0.13919300
 C -4.26370400 0.20570200 -0.19604200
 C -4.92030600 1.42423600 0.02945700
 C -4.11162500 2.54760500 0.32974300
 C -2.73011100 2.41049700 0.38943300
 H -2.09673900 3.26344000 0.59634700
 C -4.72110400 3.89494400 0.61020600
 C -4.21940200 4.60583200 1.85412800
 H -3.14778100 4.80073500 1.82103500
 H -4.42312900 3.97468400 2.72522700
 H -4.73633100 5.55613700 1.98746000
 H -5.80015000 3.83090500 0.61625900
 Br -4.41440200 5.11527500 -0.99392900
 B -6.47198800 1.40094800 -0.08959300
 O -7.13698500 0.27771800 -0.52362400
 C -8.56249700 0.48193400 -0.31396100
 C -8.66723600 2.05223200 -0.25572500
 O -7.33672600 2.42640500 0.21377700
 C -9.69487300 2.59949200 0.72598600
 H -9.66791400 3.69038500 0.71210000
 H -10.7029340 2.28445800 0.44591400
 H -9.49720100 2.26953200 1.74466800
 C -8.84849300 2.70392300 -1.62813000
 H -8.70751200 3.78109300 -1.52961400
 H -8.11523500 2.33437600 -2.34616000
 H -9.84860900 2.52312800 -2.02638900
 C -8.91776000 -0.20100400 1.00924100
 H -9.98854000 -0.14608500 1.21430000
 H -8.63373500 -1.25276500 0.95015300
 H -8.38028500 0.24737400 1.84610900
 C -9.31816400 -0.17456800 -1.46223300
 H -10.3915880 0.01166800 -1.37774400
 H -8.97609300 0.18868200 -2.42990600
 H -9.16047400 -1.25407100 -1.43194600
 H -4.86209300 -0.66636500 -0.43036900
 H -2.43874800 -0.89866600 -0.33230700
 C 0.23059000 -0.22463200 -1.48639100
 H 0.85883400 -1.10714300 -1.63308900
 H -0.70535000 -0.37963200 -2.02478900

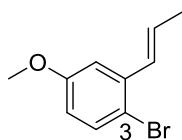
H 0.73910200 0.63536600 -1.92544500
 H 0.94944300 0.16285900 0.51097800
 H -0.48340800 -0.86028100 0.47132000



UB3LYP energy: -875.025023948

C 0.00000000 0.00000000 0.00000000
 O 0.80741400 1.18071600 0.02483600
 C 2.16753300 1.08139900 0.08933700
 C 2.88377500 -0.12037200 0.07441600
 C 4.27592800 -0.07322600 0.12439100
 C 5.00350800 1.11325300 0.19805000
 C 4.26334100 2.35115300 0.21326300
 C 2.85060300 2.28756000 0.15750800
 H 2.26044000 3.19402200 0.16236700
 C 4.90715400 3.60798900 0.27401400
 C 4.19497900 4.92129400 0.28694800
 H 3.51159700 5.01359400 1.14024400
 H 3.58477300 5.07002900 -0.61273500
 H 4.90414300 5.74775200 0.34270500
 H 5.98620600 3.61935300 0.31143300
 B 6.54719500 0.97200900 0.27260400
 O 7.15742300 -0.26472300 0.25361000
 C 8.58990200 -0.06630800 0.11749600
 C 8.77137400 1.40686500 0.64514500
 O 7.46698900 1.99232800 0.37012900
 C 9.83086100 2.23089600 -0.07559100
 H 9.85398600 3.23945400 0.34113100
 H 10.8219550 1.78977700 0.05598500
 H 9.62345000 2.31158200 -1.14133200
 C 8.98184600 1.48928300 2.15918000
 H 8.90168100 2.53200000 2.47012300
 H 8.22502500 0.91731600 2.69775400
 H 9.96793900 1.12021600 2.44762400
 C 8.92312000 -0.22442400 -1.36854100
 H 9.99689900 -0.14630600 -1.54959800
 H 8.59037900 -1.20891400 -1.70107400
 H 8.41272900 0.52584600 -1.97417700

C 9.30629100 -1.13816900 0.92988900
 H 10.3875580 -0.98076900 0.91429500
 H 8.97021800 -1.15056800 1.96545100
 H 9.10263500 -2.11946700 0.49767300
 H 4.81990100 -1.01039800 0.11104600
 H 2.38529100 -1.07782800 0.02798900
 C -0.22580600 -0.58534500 1.38604400
 H -0.90026300 -1.44331300 1.32044600
 H 0.70699400 -0.91920900 1.84258700
 H -0.68050900 0.15899900 2.04219600
 H -0.94623100 0.33289100 -0.42845700
 H 0.42856500 -0.73632700 -0.68568900



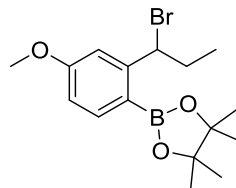
RB3LYP energy: -3037.16582354

Volume: 143.922 cm**3/mol

NPA at C3: -0.09651

C 0.00000000 0.00000000 0.00000000
 C 0.78368900 -1.26721000 0.14052500
 C 0.36390800 -2.46697900 -0.26675900
 C 1.11511100 -3.72581200 -0.15797800
 C 0.48096100 -4.96825800 -0.07508300
 C 1.20667300 -6.15098200 0.02534600
 C 2.58788000 -6.12217000 0.04297800
 C 3.25424800 -4.89622900 -0.04505600
 C 2.52297500 -3.72072100 -0.15142600
 H 3.02683500 -2.77182900 -0.26087600
 O 4.61618500 -4.96166700 -0.03514300
 C 5.35388300 -3.75093600 -0.11862100
 H 6.40231500 -4.03842800 -0.08025800
 H 5.15642300 -3.22713100 -1.05884200
 H 5.12837200 -3.08867900 0.72278000
 H 3.16535900 -7.03474200 0.11485200
 H 0.68582900 -7.09649300 0.09313200
 Br -1.43929000 -5.11411100 -0.05905500
 H -0.62723300 -2.54633800 -0.70085600
 H 1.75175400 -1.17633400 0.62786100
 H 0.54829800 0.73715500 -0.59633900
 H -0.96470100 -0.17483900 -0.47918800

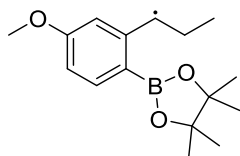
H -0.18049000 0.46124200 0.97645400



RB3LYP energy: -3449.2106232

C 0.00000000 0.00000000 0.00000000
 O 0.42611300 1.34827400 0.14410900
 C 1.76109400 1.61264300 0.12097900
 C 2.75839200 0.64683200 -0.01511500
 C 4.08473400 1.05399700 -0.03169100
 C 4.47397500 2.39625800 0.08763700
 C 3.44454100 3.35917200 0.22811000
 C 2.11492300 2.95519800 0.24041700
 H 1.31587800 3.68138900 0.31633900
 C 3.75804000 4.82261200 0.39664800
 C 3.12021500 5.48362900 1.61344400
 H 2.03143500 5.46094700 1.52996600
 C 3.59969700 6.90766500 1.88807600
 H 4.68665400 6.94287200 1.99957600
 H 3.32340000 7.58307500 1.07746200
 H 3.15691000 7.28771300 2.81139700
 H 3.37446600 4.84333000 2.46733700
 H 4.82694200 4.98952600 0.39231000
 Br 3.19953100 5.81014800 -1.29743200
 B 6.00614200 2.66966400 0.04402100
 O 6.90526900 1.64667300 -0.14782600
 C 8.21769800 2.22903200 -0.37932000
 C 8.06982900 3.65545000 0.27373000
 O 6.63175200 3.88597800 0.18400000
 C 8.78364600 4.78289400 -0.46047200
 H 8.60160000 5.72775000 0.05436400
 H 9.86259400 4.61097200 -0.47747400
 H 8.42958000 4.88464800 -1.48472000
 C 8.42783400 3.68594100 1.76161100
 H 8.12278300 4.64665100 2.17920500
 H 7.91255200 2.89801300 2.31290400
 H 9.50241500 3.57215400 1.91620600
 C 8.42049900 2.27057900 -1.89641300

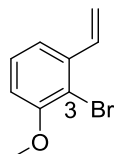
H 9.41109200 2.64684100 -2.15875200
 H 8.32284100 1.25831700 -2.29149900
 H 7.67083200 2.89588100 -2.38326400
 C 9.26587100 1.32905100 0.26281400
 H 10.2633880 1.76431400 0.16582000
 H 9.06049800 1.15861600 1.31833000
 H 9.27100800 0.36080400 -0.24058600
 H 4.85572400 0.30146800 -0.14387500
 H 2.51820700 -0.40248700 -0.11330500
 H 0.37743200 -0.62659500 0.81345000
 H -1.08674600 0.02640200 0.03970100
 H 0.31794800 -0.41671400 -0.96013100



UB3LYP energy: -875.021764880

C 0.00000000 0.00000000 0.00000000
 O 0.60668500 1.28323000 -0.04216400
 C 1.96960000 1.35874000 -0.06015500
 C 2.81865400 0.24829700 -0.04788200
 C 4.19669700 0.45989200 -0.06731100
 C 4.77883000 1.72554200 -0.09260700
 C 3.89921500 2.86907700 -0.11155700
 C 2.50268500 2.63937800 -0.09467800
 H 1.80866400 3.46899800 -0.10801200
 C 4.39452400 4.19255000 -0.15493200
 C 3.54258800 5.42202900 -0.19368500
 H 2.86299100 5.38125200 -1.05636100
 C 4.35755100 6.71625400 -0.25364700
 H 5.00783700 6.81188600 0.61950600
 H 4.99152700 6.74000000 -1.14358600
 H 3.70602200 7.59226800 -0.28339000
 H 2.88146000 5.44975800 0.68398100
 H 5.46707400 4.32945000 -0.16207500
 B 6.33058500 1.76709500 -0.08561800
 O 7.07894100 0.60862600 -0.10592600
 C 8.47011700 0.96911200 -0.31863300
 C 8.50290400 2.46255000 0.17830700
 O 7.12845300 2.88891500 -0.05116100

C 9.43147200 3.38702700 -0.59845800
 H 9.36195200 4.39859600 -0.19447500
 H 10.4698420 3.05901200 -0.50722800
 H 9.17004800 3.42699900 -1.65467400
 C 8.76158800 2.59697300 1.68072300
 H 8.57232700 3.62875700 1.98079200
 H 8.09864800 1.95053700 2.25746000
 H 9.79465500 2.35045700 1.93313800
 C 8.74341200 0.82298900 -1.81786800
 H 9.78951900 1.02319300 -2.05747900
 H 8.51204800 -0.19966900 -2.11974600
 H 8.11713300 1.49733600 -2.40370300
 C 9.34747700 0.00407600 0.46923100
 H 10.4012440 0.28235000 0.38903200
 H 9.07274300 -0.02274100 1.52250300
 H 9.23393800 -1.00348700 0.06528200
 H 4.84816400 -0.40599300 -0.05885300
 H 2.43126500 -0.76015700 -0.02417900
 H 0.28609300 -0.54814500 0.90273400
 H -1.07319400 0.17890400 0.01289200
 H 0.25691200 -0.59352300 -0.88259900



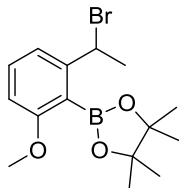
RB3LYP energy: -2997.8318188

Volume: 130.751 cm**3/mol

NPA at C3: -0.11791

C 0.00000000 0.00000000 0.00000000
 O 1.29333400 -0.58650800 -0.05218400
 C 2.37659400 0.22760400 -0.10585000
 C 2.30454300 1.61947500 -0.11026200
 C 3.47335700 2.37243500 -0.16925500
 C 4.70835700 1.75585300 -0.22277000
 C 4.81908600 0.35560400 -0.20839700
 C 3.63684100 -0.38930700 -0.15633200
 Br 3.68220800 -2.30571700 -0.11541000
 C 6.14177600 -0.28785500 -0.26816400
 C 7.27558400 0.23461400 0.19704300
 H 7.31136900 1.19250300 0.70299000
 H 8.21215100 -0.29940900 0.09791000

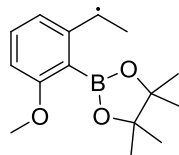
H 6.17063800 -1.27269500 -0.71972200
 H 5.60819900 2.35084000 -0.30392200
 H 3.40756200 3.45361600 -0.18670000
 H 1.34618100 2.11710300 -0.07545900
 H -0.69745000 -0.83367200 0.03727000
 H -0.12218100 0.61621400 0.89543700
 H -0.20061200 0.60211800 -0.89087600



RB3LYP energy: -3409.8801241

C 0.00000000 0.00000000 0.00000000
 C 0.01766600 1.46425700 -0.34133100
 C -1.18649300 2.14620500 -0.59112100
 C -1.12402400 3.52848400 -0.85513400
 C 0.09236200 4.20474400 -0.90767200
 C 1.27052300 3.49833200 -0.68786400
 C 1.23861700 2.14546100 -0.40251600
 H 2.16630300 1.61396000 -0.23960500
 H 2.21967600 4.01915100 -0.73603600
 H 0.13416000 5.26462100 -1.11349000
 O -2.32955600 4.14734800 -1.02478300
 C -2.35082300 5.52415700 -1.36577500
 H -3.40030300 5.78372900 -1.48849400
 H -1.91636500 6.14066800 -0.57257200
 H -1.82040400 5.71068400 -2.30442900
 B -2.58511900 1.42913600 -0.64118800
 O -3.43360900 1.50088400 -1.70841700
 C -4.49887800 0.52569100 -1.51262400
 C -4.44337900 0.27336000 0.04438600
 O -3.06344100 0.62868800 0.36678300
 C -4.68174400 -1.16750700 0.47669900
 H -4.58600300 -1.24314300 1.56132600
 H -5.68896800 -1.49227400 0.20446100
 H -3.96370800 -1.84954700 0.02448500
 C -5.33314000 1.21969400 0.85314800
 H -5.09758100 1.10562700 1.91243500
 H -5.15968600 2.26122100 0.57940100

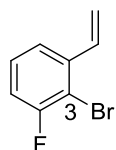
H -6.39146700 0.99290700 0.71139700
 C -4.12777900 -0.70176100 -2.34751300
 H -4.90419500 -1.46782400 -2.30022200
 H -4.01131100 -0.39517100 -3.38794800
 H -3.18282900 -1.13853100 -2.02232900
 C -5.80146800 1.13062000 -2.02146300
 H -6.64041100 0.45431900 -1.83987000
 H -6.01477800 2.08744200 -1.54805500
 H -5.72809300 1.29542700 -3.09766200
 C 0.99279400 -0.46777900 1.04759800
 H 0.82067100 0.09235400 1.97205400
 H 2.02760500 -0.31556300 0.74302500
 H 0.85407200 -1.52864700 1.25512100
 H -0.99986800 -0.31483800 0.26992500
 Br 0.31082300 -1.09254800 -1.70025700



UB3LYP energy: -835.690121648

C 0.00000000 0.00000000 0.00000000
 O 0.55373800 1.30440700 0.04751200
 C -0.29278600 2.38389000 0.01059200
 C -1.68414600 2.26145000 -0.01196800
 C -2.46374900 3.42126900 -0.02919400
 C -1.88243600 4.66938900 -0.01686600
 C -0.46709600 4.81081700 0.01043600
 C 0.33646700 3.63035100 0.01302200
 B 1.90455400 3.67783300 0.00551400
 O 2.66540400 3.36050000 -1.08713600
 C 4.05313000 3.68747500 -0.79134300
 C 4.05477800 3.76458700 0.78599500
 O 2.65882800 4.05916400 1.08517100
 C 4.91951700 4.86901800 1.38096300
 H 4.82058100 4.86159900 2.46773000
 H 5.97293600 4.71123800 1.13679500
 H 4.62375100 5.85394400 1.02293500
 C 4.37150300 2.42896400 1.46311600
 H 4.17504100 2.52215500 2.53231500
 H 3.74118600 1.62850800 1.07417400

H 5.41813800 2.14908600 1.32881000
 C 4.34509000 5.02656300 -1.47283000
 H 5.38915200 5.32058800 -1.34914300
 H 4.13924300 4.92975000 -2.53986800
 H 3.71187300 5.82340000 -1.08059800
 C 4.93946500 2.59940000 -1.38581300
 H 5.98928500 2.77303100 -1.13675700
 H 4.65505400 1.61011800 -1.03135200
 H 4.84461000 2.60806800 -2.47295800
 C 0.13230800 6.09121400 0.02964800
 C -0.61680400 7.38328000 0.01444100
 H -1.25842100 7.49787800 0.89742500
 H -1.27387300 7.47046300 -0.85913100
 H 0.06812500 8.23161300 -0.00286000
 H 1.21261600 6.14399600 0.08544700
 H -2.50954500 5.55097200 -0.02498900
 H -3.54379500 3.32943800 -0.04820400
 H -2.16387000 1.29354600 -0.01341300
 H 0.84587000 -0.68467300 0.01435100
 H -0.63774600 -0.19795400 0.86730400
 H -0.57507900 -0.15760100 -0.91767700



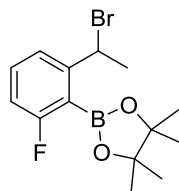
RB3LYP energy: -2982.5428433

Volume: 111.626 cm³/mol

NPA at C3: -0.15289

C 0.00000000 0.00000000 0.00000000
 C -1.01020700 0.74620400 -0.44388600
 C -1.08566800 2.21342500 -0.36423200
 C -2.31664900 2.88416100 -0.29581800
 C -2.35133500 4.27114600 -0.22616100
 C -1.19736000 5.03184200 -0.22513600
 C 0.02723300 4.37905900 -0.30097700
 C 0.07826700 2.99629600 -0.37473000
 H 1.03532600 2.50016500 -0.46804700
 H 0.94328400 4.95619500 -0.31622000
 H -1.27647700 6.10983600 -0.17345100
 F -3.53580000 4.90491800 -0.15422200
 Br -3.98072900 1.94670000 -0.26135300

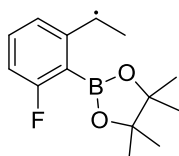
H -1.86506200 0.25221700 -0.89114100
 H -0.01706700 -1.07661200 -0.11207900
 H 0.86204200 0.42410900 0.50160800



RB3LYP energy: -3394.59389464

C 0.00000000 0.00000000 0.00000000
 C -1.00777300 0.44969000 -1.04117900
 C -1.00455100 1.90945000 -1.40293300
 C -2.21933400 2.57787300 -1.68176600
 C -2.12498000 3.93517200 -1.98095300
 C -0.93735400 4.64159700 -2.03375500
 C 0.24114100 3.95520400 -1.77760200
 C 0.20543600 2.60359500 -1.46458500
 H 1.13445000 2.08286300 -1.27669400
 H 1.18935500 4.47744500 -1.81912000
 H -0.95144700 5.69758300 -2.26936000
 F -3.26354100 4.63258900 -2.21337500
 B -3.62947600 1.88396800 -1.70714900
 O -4.54180500 2.09330000 -2.69788100
 C -5.79804000 1.47008800 -2.29692100
 C -5.32479700 0.42216000 -1.21529000
 O -4.06837800 1.00978500 -0.74661100
 C -4.97811200 -0.94785100 -1.79995700
 H -4.50067300 -1.55341300 -1.02798600
 H -5.87314000 -1.47327600 -2.13769100
 H -4.28571400 -0.86462600 -2.63824100
 C -6.25121900 0.26363000 -0.01729500
 H -7.22568300 -0.11818200 -0.33084200
 H -5.82040800 -0.45197100 0.68505800
 H -6.39884500 1.20553700 0.50804400
 C -6.67575900 2.58567200 -1.72601300
 H -6.79851500 3.35944700 -2.48478700
 H -7.66397600 2.21341600 -1.44948900
 H -6.21958100 3.04736100 -0.84923600
 C -6.45062100 0.86962400 -3.53478800
 H -5.78203400 0.18210300 -4.04999700

H -7.36654700 0.33611500 -3.26957400
 H -6.71418500 1.66850000 -4.22956200
 H -2.00357100 0.13486900 -0.75805200
 Br -0.70936000 -0.64939300 -2.73466100
 H 1.03088200 0.15031800 -0.31846900
 H -0.16278900 0.56941400 0.92033500
 H -0.13284200 -1.05871000 0.22133700

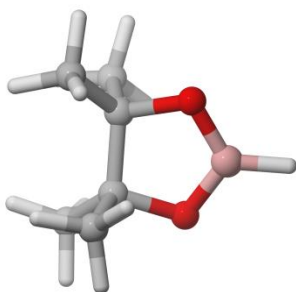


UB3LYP energy: -820.40529293

C 0.00000000 0.00000000 0.00000000
 C -0.93735400 -1.16097200 -0.07824400
 C -0.53498700 -2.51192000 -0.13259600
 C -1.50039400 -3.58301600 -0.18743200
 C -0.99602800 -4.87228000 -0.24213700
 C 0.35403600 -5.19746300 -0.24049700
 C 1.27670900 -4.15564500 -0.17259300
 C 0.84792700 -2.84485700 -0.11971600
 H 1.58160900 -2.05163000 -0.07043300
 H 2.33708500 -4.37915900 -0.16609500
 H 0.65541300 -6.23495900 -0.29429600

F -1.86106300 -5.91460600 -0.32996300
 B -3.05057000 -3.36352700 -0.17197500
 O -3.69548000 -2.36539400 -0.85985600
 C -5.09681900 -2.36662600 -0.45118200
 C -5.27064400 -3.81882200 0.13782000
 O -3.91163900 -4.15310100 0.53926600
 C -5.68636600 -4.85753500 -0.90710200
 H -5.58793600 -5.85213500 -0.47047800
 H -6.72313900 -4.71875000 -1.21989300
 H -5.04737200 -4.81532400 -1.79018900
 C -6.17214500 -3.91992400 1.36150100
 H -7.19383200 -3.61848300 1.11784000
 H -6.19899100 -4.95451600 1.70728900
 H -5.81146700 -3.30157500 2.18184800
 C -5.25092900 -1.25970200 0.59459700
 H -4.93826800 -0.31114200 0.15475800
 H -6.28801500 -1.15799900 0.91937800
 H -4.63024500 -1.44807400 1.47176700
 C -5.95203400 -2.05457400 -1.67221600
 H -5.75356300 -2.74447300 -2.49046300
 H -7.01496200 -2.10339900 -1.42348000
 H -5.73376300 -1.04409500 -2.02197300
 H -1.99523400 -0.94712200 -0.12363200
 H 0.65859500 0.05861000 -0.87560900
 H -0.55025300 0.93944700 0.05753600
 H 0.65534700 -0.05389800 0.87748100

B.2 Optimized Geometries for the Calculated Pathway



pinacol borane (HBpin)

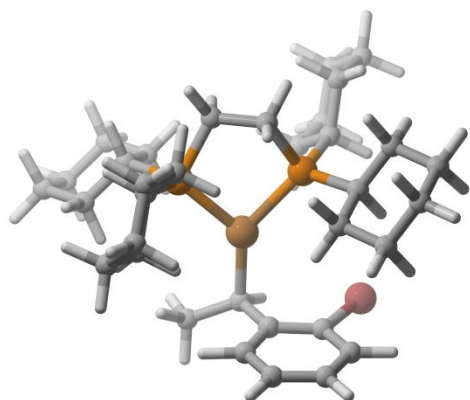
RM06 energy: -411.6949742

Sum of electronic and thermal Free Energies: -

411.53869

6 -0.777774 -0.188563 0.054067
 8 -1.065963 1.191305 0.407590
 5 -0.000002 1.928162 0.000002
 8 1.065962 1.191309 -0.407584
 6 0.777774 -0.188562 -0.054067
 6 1.472695 -0.446512 1.269144
 1 1.379804 -1.492214 1.581852
 1 2.539302 -0.221746 1.159936

1 1.079216 0.190231 2.069403
 6 1.341781 -1.095676 -1.120875
 1 2.435189 -1.024740 -1.126912
 1 1.078151 -2.141385 -0.921025
 1 0.984050 -0.833537 -2.120512
 1 -0.000002 3.114082 0.000009
 6 -1.472695 -0.446506 -1.269146
 1 -1.079218 0.190242 -2.069402
 1 -1.379803 -1.492207 -1.581859
 1 -2.539302 -0.221743 -1.159936
 6 -1.341778 -1.095684 1.120869
 1 -2.435187 -1.024749 1.126908
 1 -1.078148 -2.141391 0.921014
 1 -0.984047 -0.833551 2.120508



benzyl copper (dCype)

Compound 4.17

RM06 energy: -4781.6101141

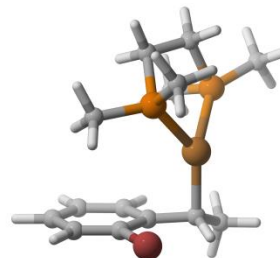
Sum of electronic and thermal Free Energies: -
 4780.849906

6 0.005603 0.788502 2.453552
 6 -1.463952 1.080488 2.154490
 15 -2.126424 0.070605 0.739439
 6 -2.811384 -1.484297 1.514505

1 -3.844916 -1.256138 1.830206
 6 -2.041506 -1.967758 2.741485
 6 -2.665458 -3.237553 3.307585
 6 -2.736595 -4.341855 2.264151
 6 -3.466496 -3.869233 1.015892
 6 -2.837532 -2.598523 0.465636
 1 -3.357433 -2.277093 -0.446021
 1 -1.796825 -2.805521 0.160982
 1 -4.523863 -3.674401 1.259384
 1 -3.464760 -4.653614 0.247664
 1 -3.220561 -5.234377 2.682183
 1 -1.713146 -4.643367 1.988553
 1 -3.681747 -3.007743 3.665959
 1 -2.097518 -3.572666 4.185594
 1 -0.996961 -2.176444 2.455276
 1 -2.008863 -1.192901 3.517407
 6 -3.639584 1.049942 0.276196
 1 -4.156020 1.323068 1.214608
 6 -3.212766 2.325855 -0.451476
 6 -4.410359 3.154938 -0.892460
 6 -5.352279 2.339147 -1.762438
 6 -5.792654 1.076009 -1.040483
 6 -4.598017 0.242372 -0.596990
 1 -4.950548 -0.651393 -0.066338
 1 -4.054299 -0.115241 -1.487580
 1 -6.389730 1.351790 -0.156204
 1 -6.449293 0.472049 -1.680489
 1 -6.223378 2.939260 -2.056077
 1 -4.835246 2.062989 -2.695951
 1 -4.953605 3.510935 -0.002243
 1 -4.068384 4.051549 -1.425622
 1 -2.552773 2.933375 0.181340
 1 -2.615370 2.044289 -1.336183
 29 -0.336394 0.064735 -0.758431
 15 1.051288 0.869539 0.917830
 6 2.572206 -0.100555 1.350891
 6 3.305677 0.313334 2.622724
 6 4.546601 -0.542523 2.850028
 6 4.210927 -2.025769 2.863983
 6 3.493011 -2.432924 1.586119
 6 2.241779 -1.594274 1.368020
 1 1.531356 -1.805973 2.183889
 1 1.740028 -1.881487 0.431889
 1 4.171766 -2.298833 0.727912

1	3.231759	-3.499322	1.609165
1	3.563084	-2.244093	3.728845
1	5.121775	-2.623267	3.001533
1	5.271217	-0.344367	2.043846
1	5.038930	-0.247953	3.786323
1	3.591988	1.372002	2.577232
1	2.627330	0.208272	3.485251
1	3.236306	0.079297	0.486382
6	1.610724	2.642195	0.760178
6	1.629553	3.469886	2.042580
6	2.161150	4.874028	1.782201
6	1.348696	5.582027	0.709025
6	1.301379	4.761847	-0.571193
6	0.781205	3.355557	-0.310698
1	0.769911	2.765816	-1.237168
1	-0.268639	3.413384	0.025585
1	0.680477	5.260315	-1.327337
1	2.315291	4.694698	-0.998078
1	0.321656	5.736509	1.078173
1	1.759403	6.580941	0.512271
1	2.158551	5.455021	2.714298
1	3.213259	4.809052	1.460852
1	0.603735	3.547884	2.437694
1	2.222766	2.978438	2.823413
1	2.646158	2.556862	0.382955
6	-0.197901	-0.477476	-2.709392
6	-1.546594	-0.781825	-3.330399
1	-1.480338	-1.318880	-4.295672
1	-2.199147	-1.386830	-2.685009
1	-2.097828	0.148072	-3.524731
6	0.690868	-1.604338	-2.475614
6	0.190618	-2.916085	-2.267577
6	1.001632	-3.994629	-1.961779
6	2.380411	-3.843663	-1.860621
6	2.922150	-2.582460	-2.081456
6	2.099776	-1.510332	-2.378325
35	2.968710	0.179066	-2.654365
1	3.998902	-2.432938	-2.024604
1	3.027258	-4.685759	-1.626086
1	0.548133	-4.973319	-1.808865
1	-0.883587	-3.073500	-2.348244
1	0.314916	0.331860	-3.240605
1	-2.085256	0.944611	3.050233
1	-1.580155	2.133305	1.862455

1	0.116016	-0.232144	2.840218
1	0.380497	1.456792	3.237769



benzyl copper (dMepe)

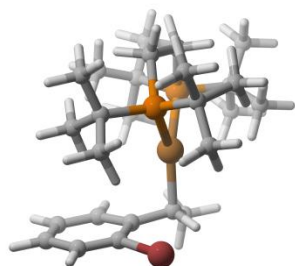
Compound 4.30

RM06 energy: -4000.5973263

Sum of electronic and thermal Free Energies: -
4000.30738

6	-2.345235	1.670202	1.334663
6	-3.460983	1.030160	0.521344
15	-2.919571	-0.571402	-0.236522
6	-2.823427	-1.651164	1.245010
1	-3.706453	-1.534632	1.886804
1	-2.758303	-2.698123	0.928950
1	-1.924936	-1.426656	1.830486
6	-4.491654	-1.142130	-0.985158
1	-5.303123	-1.149603	-0.246562
1	-4.776275	-0.486740	-1.814639
1	-4.369578	-2.154394	-1.383886
29	-0.655152	-0.172280	-0.834138
15	-0.777527	1.804830	0.358551
6	0.408333	2.303742	1.656993
1	1.359817	2.598702	1.202555
1	0.020864	3.147583	2.242077
1	0.601796	1.461628	2.330955
6	-1.028826	3.370864	-0.554172
1	-0.119673	3.621669	-1.111565
1	-1.843159	3.261139	-1.278090
1	-1.264905	4.197964	0.127181
6	0.762528	-1.535971	-1.294469

6	0.169721	-2.887092	-1.639289
1	0.895110	-3.719724	-1.578020
1	-0.681506	-3.170674	-1.003844
1	-0.217796	-2.880095	-2.665646
6	1.430349	-1.408264	-0.007875
6	1.081200	-2.223869	1.098967
6	1.640015	-2.069808	2.355294
6	2.607033	-1.098272	2.592293
6	2.996586	-0.285683	1.533670
6	2.423686	-0.442446	0.284825
35	3.010023	0.764124	-1.085067
1	3.755771	0.480110	1.682251
1	3.059408	-0.977527	3.573588
1	1.322537	-2.729307	3.162125
1	0.331354	-2.999331	0.950628
1	1.380395	-1.144729	-2.108695
1	-4.354869	0.860775	1.138547
1	-3.764275	1.688626	-0.305628
1	-2.115698	1.059193	2.219460
1	-2.637391	2.662879	1.705317



benzyl copper (dtBupe)

Compound 4.27

RM06 energy: -4472.0714495

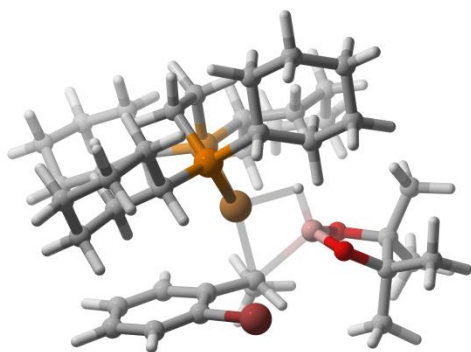
Sum of electronic and thermal Free Energies: -

4471.456222

6	-1.430885	2.148981	1.238630
6	-2.667975	1.555534	0.558961
15	-2.507872	-0.223075	0.021793

6	-3.221742	-1.233080	1.460105
6	-4.713112	-1.055638	1.704382
1	-5.324934	-1.470598	0.897203
1	-4.996018	-1.588885	2.623849
1	-4.995902	-0.005105	1.844992
6	-2.904784	-2.708776	1.231459
1	-1.827305	-2.871583	1.101633
1	-3.220125	-3.288830	2.110364
1	-3.415867	-3.131727	0.361881
6	-2.465540	-0.801426	2.712941
1	-1.381969	-0.927571	2.597446
1	-2.671312	0.236595	2.997772
1	-2.774640	-1.434642	3.556077
6	-3.673486	-0.293811	-1.475630
6	-4.992392	0.453618	-1.317373
1	-4.853350	1.520303	-1.108597
1	-5.557122	0.386887	-2.258857
1	-5.628573	0.037031	-0.531751
6	-2.895671	0.332829	-2.631678
1	-1.921093	-0.150333	-2.785686
1	-3.472326	0.225462	-3.561035
1	-2.724203	1.404875	-2.486911
6	-3.953674	-1.747405	-1.838409
1	-3.031643	-2.335500	-1.924739
1	-4.613224	-2.242593	-1.118595
1	-4.458570	-1.785429	-2.813875
29	-0.188864	-0.351535	-0.535314
15	0.199386	1.762739	0.419323
6	1.398360	1.804398	1.892022
6	2.837632	1.888755	1.395980
1	3.518273	1.699017	2.238363
1	3.061358	1.139577	0.626729
1	3.087845	2.877733	0.997919
6	1.147615	2.917856	2.902724
1	1.863911	2.814695	3.730846
1	1.287864	3.916705	2.482125
1	0.145763	2.873881	3.344167
6	1.222702	0.460499	2.596102
1	1.952491	0.376152	3.413905
1	0.228391	0.350893	3.042452
1	1.389831	-0.384378	1.917081
6	0.524730	3.224729	-0.744595
6	1.707930	2.874613	-1.642077
1	1.556101	1.917044	-2.155589

1	1.825120	3.652646	-2.410137
1	2.654382	2.809159	-1.098478
6	-0.703259	3.347319	-1.640291
1	-0.922561	2.405701	-2.157468
1	-1.598736	3.665996	-1.094637
1	-0.512162	4.103808	-2.414078
6	0.766497	4.563190	-0.062308
1	1.709504	4.590756	0.493042
1	0.822682	5.352814	-0.825815
1	-0.044375	4.837965	0.623326
6	0.798945	-1.929508	-1.381627
6	-0.144162	-3.057718	-1.756926
1	0.377236	-4.005474	-1.988572
1	-0.884611	-3.294910	-0.981078
1	-0.722554	-2.790725	-2.651047
6	1.721293	-2.195801	-0.286602
6	1.361465	-3.038406	0.796461
6	2.173418	-3.242174	1.896804
6	3.416832	-2.624413	1.989334
6	3.831287	-1.819204	0.935583
6	3.011649	-1.631495	-0.164522
35	3.718998	-0.548986	-1.583238
1	4.809249	-1.341836	0.963096
1	4.061400	-2.776617	2.851571
1	1.830898	-3.897469	2.696757
1	0.394895	-3.539073	0.756985
1	1.334437	-1.567424	-2.265640
1	-3.543755	1.687852	1.208775
1	-2.887854	2.119072	-0.353493
1	-1.351314	1.747476	2.254654
1	-1.558187	3.233891	1.357069



Hydroboration for benzyl copper (dCype) – TS

Compound 4.25

RM06 energy: -5193.2978242

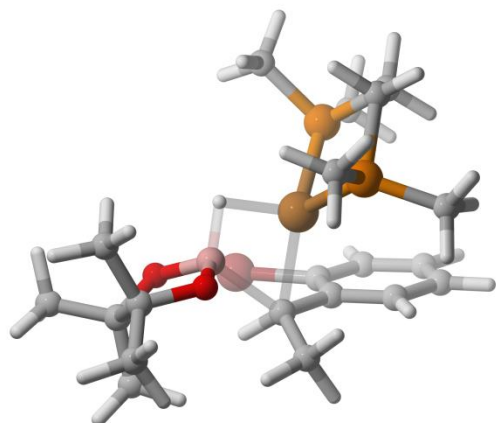
Sum of electronic and thermal Free Energies: -

5192.352459

Imaginary frequency: -100.2408

6	-1.860942	0.873112	2.194737
6	-0.732831	1.898639	2.259853
15	0.035485	2.271108	0.610304
6	-1.006075	3.614178	-0.141394
1	-0.482512	3.828855	-1.089683
6	-1.120071	4.919157	0.641910
6	-1.877224	5.964773	-0.170606
6	-3.246282	5.462882	-0.606942
6	-3.141736	4.137028	-1.347695
6	-2.399180	3.106482	-0.510508
1	-2.335244	2.146951	-1.040833
1	-2.973776	2.920188	0.410693
1	-2.602643	4.283982	-2.298636
1	-4.140021	3.762924	-1.612360
1	-3.748690	6.215149	-1.229003
1	-3.880674	5.324218	0.283623
1	-1.282222	6.219318	-1.062668
1	-1.975904	6.892799	0.408136
1	-1.655714	4.732839	1.586621
1	-0.131933	5.310567	0.916396
6	1.599502	3.146930	1.102669
1	1.331358	3.898278	1.866491
6	2.613298	2.174346	1.709110
6	3.888393	2.897644	2.122848
6	4.512775	3.627148	0.943383
6	3.514431	4.575708	0.299476
6	2.232322	3.854766	-0.095584
1	1.535378	4.569525	-0.552548
1	2.458933	3.100345	-0.868193
1	3.268751	5.384613	1.007068
1	3.956255	5.060480	-0.581274
1	5.413388	4.171553	1.257045
1	4.839848	2.888362	0.194406

1	3.659498	3.622378	2.921096	6	3.750617	-2.396499	-1.053516
1	4.601216	2.180253	2.552735	8	2.408443	-2.185389	-0.620036
1	2.188814	1.643903	2.573072	6	4.321811	-3.583251	-0.305748
1	2.858789	1.408307	0.958264	1	3.807889	-4.500973	-0.616127
29	0.161733	0.115675	-0.277744	1	5.390534	-3.714195	-0.519499
15	-1.385783	-0.691920	1.310089	1	4.194114	-3.482503	0.776482
6	-3.033717	-1.454462	0.888971	6	3.753690	-2.703513	-2.545518
6	-3.920759	-1.849543	2.067351	1	3.060554	-3.530469	-2.738614
6	-5.198458	-2.531404	1.589340	1	3.427974	-1.849907	-3.149603
6	-5.965720	-1.663096	0.604324	1	4.746325	-3.008468	-2.899554
6	-5.081228	-1.267000	-0.566795	6	5.592336	-0.665741	-1.609880
6	-3.813949	-0.573984	-0.085286	1	5.292453	-0.572741	-2.658118
1	-4.103121	0.363701	0.415863	1	6.010474	0.298486	-1.296978
1	-3.185132	-0.293395	-0.939153	1	6.394515	-1.411811	-1.544221
1	-4.809480	-2.168976	-1.139227	6	4.854147	-0.936915	0.740778
1	-5.623015	-0.611912	-1.262671	1	5.721807	-1.568305	0.965459
1	-6.864746	-2.185403	0.251730	1	5.129911	0.101916	0.962442
1	-6.316581	-0.753446	1.118505	1	4.040713	-1.214919	1.422530
1	-4.935189	-3.484253	1.102408	1	-1.081327	2.822873	2.741312
1	-5.828488	-2.789460	2.451160	1	0.080896	1.513985	2.890773
1	-3.387341	-2.515944	2.756719	1	-2.708857	1.284104	1.636087
1	-4.188152	-0.947885	2.642378	1	-2.236966	0.661366	3.201824
1	-2.745254	-2.374586	0.347712	6	0.942312	-0.342807	-2.270770
6	-0.724598	-1.857047	2.626645	6	1.642656	0.805196	-2.986223
6	-1.093649	-1.504772	4.066616	1	1.382080	0.845740	-4.056121
6	-0.617648	-2.579991	5.035566	1	1.402007	1.788417	-2.560352
6	0.881381	-2.806723	4.920505	1	2.726469	0.701373	-2.908017
6	1.269734	-3.132629	3.487396	6	-0.512337	-0.405926	-2.622461
6	0.784876	-2.066411	2.514891	6	-1.211221	0.745574	-3.047970
1	1.065842	-2.334734	1.489520	6	-2.518755	0.713082	-3.502173
1	1.298841	-1.113834	2.730248	6	-3.209908	-0.488619	-3.574855
1	2.358057	-3.251661	3.398144	6	-2.570223	-1.645861	-3.154327
1	0.829456	-4.102444	3.203576	6	-1.268748	-1.595579	-2.679631
1	1.409969	-1.894224	5.240886	35	-0.513591	-3.255681	-2.111573
1	1.203974	-3.605815	5.601104	1	-3.087844	-2.602066	-3.193518
1	-0.889368	-2.303832	6.063319	1	-4.231531	-0.531730	-3.945072
1	-1.148552	-3.521267	4.817269	1	-2.996688	1.641753	-3.811767
1	-0.617413	-0.547622	4.335724	1	-0.697073	1.704144	-3.030014
1	-2.173642	-1.354317	4.181423	1	1.372346	-1.294849	-2.601678
1	-1.203642	-2.818750	2.369115				
5	2.154788	-0.791018	-0.616944				
1	1.667696	-0.416651	0.470102				
8	3.363414	-0.107445	-0.929093				
6	4.426426	-1.034229	-0.718899				



hydroboration of benzyl copper (dMepe) – TS

Compound 4.31

RM06 energy: -4412.2883274

Sum of electronic and thermal Free Energies: -

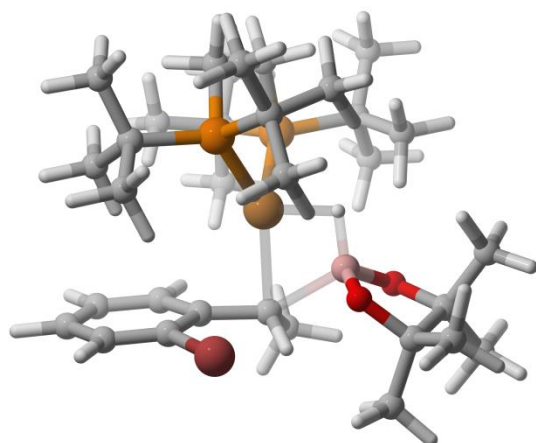
4411.815599

Imaginary frequency: -105.5431

29	0.496483	-0.585916	0.117355
15	1.288127	-2.690624	-0.471593
6	2.508625	-3.012378	0.881564
6	3.337050	-1.771225	1.190311
15	2.260754	-0.328029	1.616501
6	3.504493	0.985870	1.885616
1	3.011888	1.903827	2.223150
1	4.238586	0.682740	2.643125
1	4.028740	1.206531	0.950084
6	1.751416	-0.713336	3.331475
1	1.053633	-1.557393	3.338890
1	2.608646	-0.949566	3.974781
1	1.221569	0.149892	3.749989
1	3.926740	-1.470344	0.310549
1	4.050573	-1.961845	2.004466
1	3.149498	-3.863720	0.612010
1	1.932938	-3.319663	1.766282
6	2.292175	-3.029716	-1.964920
1	1.677088	-2.938722	-2.866416

1	3.116559	-2.312819	-2.041722
1	2.711453	-4.043213	-1.930205
6	0.215608	-4.166631	-0.397675
1	0.797866	-5.096905	-0.390156
1	-0.407125	-4.125648	0.502617
1	-0.452539	-4.174930	-1.265890
5	-1.667378	-0.275018	0.224212
8	-2.479640	-1.253029	-0.415563
6	-3.816998	-1.056886	0.038091
6	-3.844820	0.464906	0.373296
8	-2.511390	0.707303	0.808408
6	-4.798169	0.845724	1.487748
1	-4.768794	1.930536	1.647004
1	-5.832630	0.575494	1.238910
1	-4.533036	0.366826	2.434531
6	-4.141000	1.340911	-0.838707
1	-3.902548	2.381056	-0.584406
1	-3.541326	1.070869	-1.714072
1	-5.198729	1.302692	-1.127469
6	-4.783505	-1.484787	-1.045063
1	-4.583556	-0.984176	-1.996898
1	-4.700022	-2.565204	-1.214791
1	-5.821739	-1.274484	-0.757399
6	-4.025631	-1.929986	1.269444
1	-5.056788	-1.894098	1.640971
1	-3.800163	-2.970595	1.007039
1	-3.356358	-1.642922	2.088633
1	-0.911745	-0.753420	1.135692
6	-0.649082	0.626520	-1.320517
6	-1.075940	-0.086387	-2.593476
1	-0.844623	0.503152	-3.494899
1	-0.601254	-1.069484	-2.717319
1	-2.151165	-0.277044	-2.592650
6	0.729935	1.200118	-1.426609
6	1.688483	0.656414	-2.309481
6	2.969517	1.166448	-2.433812
6	3.356362	2.282200	-1.702537
6	2.435180	2.870131	-0.845887
6	1.164205	2.336918	-0.714132
35	-0.004641	3.189287	0.531973
1	2.710924	3.748233	-0.266071
1	4.354547	2.702190	-1.801904
1	3.667255	0.694905	-3.124108
1	1.410092	-0.207333	-2.908367

1 -1.315520 1.472821 -1.122111



Hydroboration of benzyl copper (dtBupe) – TS

Compound 4.28

RM06 energy: -4883.7540547

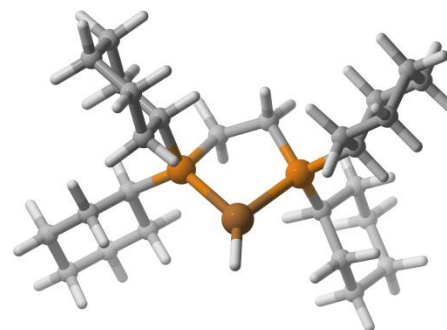
Sum of electronic and thermal Free Energies: -
4882.956181

Imaginary frequency: -118.9103

29 -0.333110 0.129105 -0.169449
 15 -2.460375 1.240908 -0.239896
 6 -3.189326 0.560887 1.337337
 6 -2.848145 -0.879603 1.718836
 15 -1.069391 -1.392319 1.507543
 6 -1.246079 -3.263291 1.225259
 6 0.125431 -3.920107 1.339937
 1 0.068572 -4.951336 0.962854
 1 0.885958 -3.398085 0.746931
 1 0.480406 -3.974434 2.374619
 6 -2.234716 -3.987569 2.133240
 1 -3.245833 -3.569407 2.076670
 1 -2.308706 -5.034996 1.805835
 1 -1.933452 -4.002716 3.182926
 6 -1.727408 -3.421311 -0.214846
 1 -2.754330 -3.066066 -0.358252
 1 -1.081245 -2.895716 -0.923422

1 -1.718868 -4.486625 -0.485335
 6 -0.266344 -1.072758 3.201849
 6 1.250264 -1.187479 3.060458
 1 1.580530 -2.198643 2.804006
 1 1.657685 -0.506491 2.303521
 1 1.718572 -0.928666 4.021619
 6 -0.589353 0.365795 3.599427
 1 -1.656415 0.520599 3.797687
 1 -0.053321 0.605375 4.528428
 1 -0.262025 1.087811 2.843516
 6 -0.747221 -1.987411 4.319997
 1 -0.404624 -3.019339 4.197596
 1 -0.338704 -1.629113 5.276129
 1 -1.839298 -1.995255 4.422137
 1 -3.429653 -1.570074 1.099253
 1 -3.176385 -1.063608 2.751260
 1 -4.280841 0.680914 1.326469
 1 -2.828834 1.234739 2.121834
 6 -3.742147 0.816770 -1.580893
 6 -3.202167 1.204653 -2.955194
 1 -3.898580 0.847709 -3.727226
 1 -3.093228 2.283054 -3.094862
 1 -2.231032 0.741782 -3.158582
 6 -3.892364 -0.702227 -1.567506
 1 -4.511699 -1.011493 -2.420995
 1 -2.927240 -1.213573 -1.665952
 1 -4.390609 -1.067600 -0.662855
 6 -5.116365 1.441555 -1.392536
 1 -5.812396 1.003931 -2.122830
 1 -5.539713 1.255233 -0.398561
 1 -5.112309 2.521963 -1.568212
 6 -2.524077 3.109710 0.130853
 6 -3.790323 3.580653 0.839430
 1 -4.703167 3.417989 0.261309
 1 -3.924327 3.111730 1.820480
 1 -3.712858 4.663146 1.016818
 6 -1.329532 3.424518 1.028934
 1 -1.351584 2.879396 1.980599
 1 -0.376200 3.216244 0.533508
 1 -1.349414 4.495652 1.277610
 6 -2.344814 3.900199 -1.159751
 1 -3.237154 3.879967 -1.794685
 1 -2.151939 4.953427 -0.912082
 1 -1.489462 3.545735 -1.749862

5	1.542770	1.339325	0.085582
1	0.607636	1.178177	0.895079
8	1.659316	2.674107	-0.396047
6	2.805981	3.249709	0.227181
6	3.722356	2.009987	0.444881
8	2.776949	0.968515	0.676864
6	4.639711	2.105264	1.645927
1	5.251793	1.198005	1.717076
1	5.322889	2.960288	1.562037
1	4.078506	2.199741	2.580409
6	4.554912	1.673640	-0.785530
1	4.979143	0.670347	-0.663025
1	3.962453	1.672154	-1.707049
1	5.385820	2.377093	-0.920268
6	3.380503	4.314722	-0.681630
1	3.587868	3.928739	-1.684288
1	2.665501	5.139784	-0.785261
1	4.309779	4.731274	-0.272001
6	2.358629	3.890781	1.535248
1	3.176595	4.411916	2.046440
1	1.578401	4.630615	1.320044
1	1.934236	3.153499	2.227984
6	1.297125	0.262654	-1.691341
6	0.959831	1.262208	-2.793279
1	1.330523	0.932926	-3.777772
1	-0.115990	1.446171	-2.905202
1	1.412704	2.231863	-2.574561
6	0.945394	-1.139359	-2.083948
6	-0.104896	-1.397374	-2.990195
6	-0.396825	-2.657817	-3.479979
6	0.359478	-3.755106	-3.089870
6	1.400616	-3.554981	-2.197091
6	1.678378	-2.283281	-1.713561
35	3.169283	-2.145458	-0.524830
1	2.015312	-4.393538	-1.876484
1	0.148154	-4.751404	-3.470838
1	-1.220330	-2.779198	-4.181898
1	-0.702955	-0.559689	-3.336263
1	2.384450	0.254439	-1.559967



Copper-Hydride (dCType)

Compound 4.26

RM06 energy: -1898.6704047

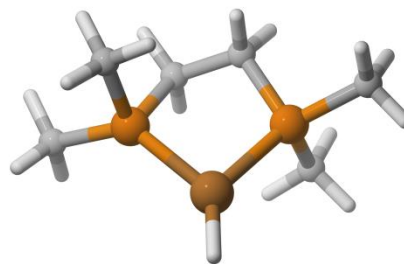
Sum of electronic and thermal Free Energies: -

1898.030668

6	-0.549247	0.274726	1.684626
15	-1.595267	0.073050	0.163103
6	-2.184727	-1.678993	0.372747
1	-1.254798	-2.202978	0.661950
6	-3.213131	-1.913122	1.474342
6	-3.534884	-3.396212	1.616871
6	-3.998915	-3.987561	0.293863
6	-2.962671	-3.766165	-0.797849
6	-2.629619	-2.289343	-0.956510
1	-3.513959	-1.755355	-1.336196
1	-1.842129	-2.144981	-1.710353
1	-2.043663	-4.318510	-0.542181
1	-3.314162	-4.177380	-1.753184
1	-4.946454	-3.509275	-0.003418
1	-4.215678	-5.058020	0.406945
1	-2.635187	-3.932697	1.958966
1	-4.297222	-3.542186	2.393850
1	-2.857347	-1.509847	2.432550
1	-4.141530	-1.372633	1.234704
6	-3.010454	1.230786	0.479182
1	-3.403317	1.045707	1.493995
29	-0.105853	0.148796	-1.626981
1	-0.211540	0.262910	-3.216296

15	1.622038	0.020853	-0.065553
6	0.804506	-0.415184	1.541278
1	1.443194	-0.182874	2.402216
1	0.680981	-1.506950	1.538971
6	2.268945	1.737428	0.210027
1	1.353174	2.302416	0.469253
6	3.288579	1.932694	1.326581
6	3.674254	3.400705	1.466899
6	4.204627	3.957775	0.154329
6	3.195763	3.764370	-0.967327
6	2.793504	2.303155	-1.110325
1	3.668566	1.715043	-1.433770
1	2.034283	2.184200	-1.895617
1	2.296719	4.364726	-0.754368
1	3.597861	4.138333	-1.918027
1	5.140882	3.438159	-0.106306
1	4.460568	5.020002	0.262564
1	4.418681	3.519143	2.265557
1	2.789692	3.980060	1.777158
1	4.194067	1.350145	1.094256
1	2.905827	1.550432	2.282665
6	3.064887	-1.142519	-0.197989
1	3.820119	-0.586671	-0.780977
6	3.694780	-1.603146	1.116254
6	4.847623	-2.568512	0.869160
6	4.399653	-3.767988	0.048563
6	3.770234	-3.324091	-1.262686
6	2.625278	-2.348551	-1.033785
1	1.798845	-2.865776	-0.513163
1	2.213366	-2.005586	-1.992263
1	4.536508	-2.833817	-1.884499
1	3.416621	-4.191006	-1.835990
1	3.662169	-4.347184	0.627778
1	5.244398	-4.443428	-0.139761
1	5.654917	-2.041967	0.335069
1	5.273046	-2.894420	1.827733
1	4.041157	-0.747448	1.708567
1	2.932564	-2.113258	1.725853
1	-1.080320	-0.100411	2.570211
1	-0.401713	1.349679	1.848325
6	-5.246862	2.043510	-0.364658
6	-4.720534	3.467593	-0.437214
6	-3.613880	3.684386	0.581983
6	-2.492675	2.670345	0.402215

1	-2.018488	2.822258	-0.582664
1	-1.710481	2.846093	1.152043
1	-4.030177	3.589338	1.597882
1	-3.210430	4.702708	0.506184
1	-4.324026	3.656481	-1.447658
1	-5.534064	4.188693	-0.282906
6	-4.129098	1.024700	-0.542176
1	-4.541062	0.010262	-0.470862
1	-3.704604	1.116376	-1.556241
1	-5.729597	1.883656	0.613261
1	-6.023695	1.879488	-1.123021



Copper-hydride (dMepe)

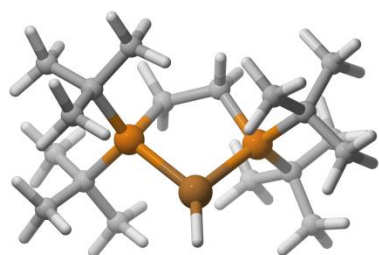
Compound 4.32

RM06 energy: -1117.6625474

Sum of electronic and thermal Free Energies: -
1117.491407

6	-0.665206	-1.704445	0.370213
6	0.665305	-1.704618	-0.369319
15	1.602976	-0.136381	-0.068587
6	2.173506	-0.386729	1.653772
1	2.610322	-1.383458	1.796475
1	2.928226	0.367331	1.900115
1	1.340600	-0.256174	2.352550
6	3.137168	-0.450309	-1.014752
1	3.591888	-1.406784	-0.727811
1	2.921676	-0.468999	-2.087756
1	3.857847	0.352372	-0.830347
29	-0.000159	1.576557	-0.000142

15	-1.602939	-0.136434	0.068541
6	-3.137317	-0.450002	1.014499
1	-3.857914	0.352673	0.829751
1	-3.592036	-1.406524	0.727720
1	-2.922022	-0.468418	2.087547
6	-2.173049	-0.387594	-1.653839
1	-2.927490	0.366527	-1.900839
1	-1.339902	-0.257680	-2.352449
1	-2.610086	-1.384290	-1.796100
1	0.000297	3.166011	0.000168
1	1.283876	-2.565160	-0.076931
1	0.503472	-1.784406	-1.453466
1	-0.503400	-1.783583	1.454414
1	-1.283732	-2.565183	0.078310



Copper hydride (dtBupe)

Compound 4.29

RM06 energy: -1589.1361155

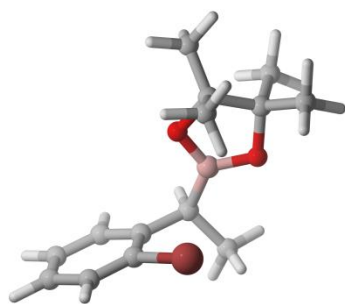
Sum of electronic and thermal Free Energies: -

1588.636059

6	0.304676	-0.703869	-1.628812
6	-0.304676	0.703869	-1.628812
15	0.000000	1.668386	-0.059676
6	1.515591	2.741334	-0.423903
6	1.289053	3.873995	-1.414165
1	0.626182	4.649883	-1.018446
1	2.251108	4.358277	-1.637222
1	0.876184	3.523552	-2.368623
6	2.030987	3.302053	0.899819
1	2.203081	2.506974	1.636675
1	2.988561	3.815247	0.731888

1	1.348856	4.028782	1.350574
6	2.593049	1.814221	-0.978421
1	2.808502	0.984899	-0.294834
1	2.336641	1.401980	-1.960929
1	3.525822	2.381771	-1.100505
6	-1.557725	2.726305	0.106748
6	-2.022772	3.435621	-1.158286
1	-2.144166	2.751404	-2.005766
1	-3.006638	3.892009	-0.975427
1	-1.351862	4.240744	-1.469108
6	-2.655014	1.758160	0.550936
1	-2.347748	1.148862	1.413255
1	-3.547271	2.327367	0.846779
1	-2.962524	1.082884	-0.254373
6	-1.350512	3.742371	1.223910
1	-1.003257	3.266751	2.150216
1	-0.637157	4.526333	0.950260
1	-2.305823	4.238309	1.445681
29	0.000000	0.000000	1.588633
15	0.000000	-1.668386	-0.059676
6	1.557725	-2.726305	0.106748
6	1.350512	-3.742371	1.223910
1	2.305823	-4.238309	1.445681
1	1.003257	-3.266751	2.150216
1	0.637157	-4.526333	0.950260
6	2.022772	-3.435621	-1.158286
1	3.006638	-3.892009	-0.975427
1	1.351862	-4.240744	-1.469108
1	2.144166	-2.751404	-2.005766
6	2.655014	-1.758160	0.550936
1	3.547271	-2.327367	0.846779
1	2.962524	-1.082884	-0.254373
1	2.347748	-1.148862	1.413255
6	-1.515591	-2.741334	-0.423903
6	-2.030987	-3.302053	0.899819
1	-2.203081	-2.506974	1.636675
1	-2.988561	-3.815247	0.731888
1	-1.348856	-4.028782	1.350574
6	-2.593049	-1.814221	-0.978421
1	-2.808502	-0.984899	-0.294834
1	-2.336641	-1.401980	-1.960929
1	-3.525822	-2.381771	-1.100505
6	-1.289053	-3.873995	-1.414165
1	-0.626182	-4.649883	-1.018446

1	-2.251108	-4.358277	-1.637222
1	-0.876184	-3.523552	-2.368623
1	0.000000	0.000000	3.190624
1	0.046094	1.265175	-2.505842
1	-1.392431	0.629816	-1.736561
1	1.392431	-0.629816	-1.736561
1	-0.046094	-1.265175	-2.505842



Hydroboration product

Compound 4.24

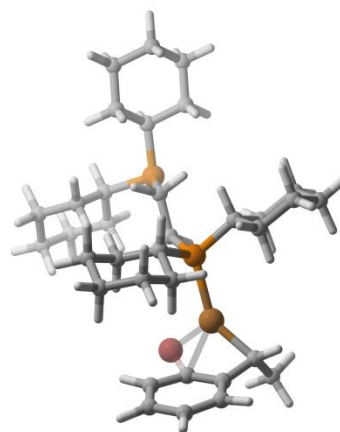
RM06 energy: -3294.6307469

Sum of electronic and thermal Free Energies: -

3294.36006

6	-0.525407	-1.128257	1.191725
6	-0.710529	-0.624410	2.623127
1	-0.832501	0.462609	2.668496
1	-1.592751	-1.078374	3.091485
1	0.160859	-0.876349	3.237088
6	-1.768266	-0.965701	0.355742
6	-2.236185	0.258447	-0.126941
6	-3.407024	0.373263	-0.862766
6	-4.153825	-0.760105	-1.144620
6	-3.719434	-1.994683	-0.685793
6	-2.548976	-2.084563	0.050734
1	-2.215999	-3.057242	0.411164
1	-4.293736	-2.892878	-0.900765
1	-5.070754	-0.672098	-1.722307
1	-3.732436	1.347629	-1.218600

35	-1.266080	1.875804	0.197047
5	0.802241	-0.634428	0.506918
8	1.078863	-0.841037	-0.814770
6	2.360404	-0.223984	-1.088122
6	3.006197	-0.151709	0.329935
8	1.848595	-0.093291	1.198671
6	3.868487	1.062856	0.579224
1	3.306084	1.995849	0.485721
1	4.279437	1.022151	1.594284
1	4.712191	1.094790	-0.121108
6	3.768035	-1.410193	0.703655
1	4.023269	-1.371500	1.768265
1	3.172511	-2.314970	0.536768
1	4.700782	-1.503286	0.136574
6	3.108646	-1.077696	-2.084922
1	2.584577	-1.066606	-3.047235
1	4.119862	-0.687062	-2.251950
1	3.188754	-2.118930	-1.761166
6	2.080312	1.139681	-1.691237
1	1.429601	1.015172	-2.563792
1	1.565763	1.801783	-0.987966
1	3.001103	1.633361	-2.021914
1	-0.359306	-2.218095	1.266058



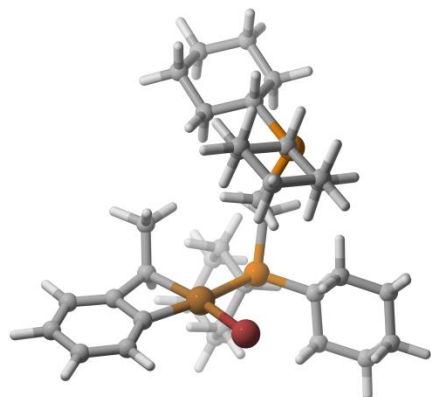
Oxidative insertion from benzyl copper to
cupracyclobutane – TS – dCype

Compound 4.53

RM06 energy: -4781.5217209

Sum of electronic and thermal Free Energies: -	6	4.544880	0.834633	-2.870721
4780.769833	1	5.592169	0.996995	-3.183802
	1	4.294479	-0.199719	-3.137806
Imaginary frequency: -278.1170	1	3.921008	1.482029	-3.499877
	6	4.940100	0.146418	-0.460738
6 -2.247489	6	5.944951	0.335859	0.493594
6 -0.870954	6	6.186418	-0.643855	1.452205
15 0.573033	6	5.406558	-1.790165	1.516114
6 0.023744	6	4.328543	-1.968138	0.636541
1 -0.915271	6	4.181157	-1.011709	-0.334381
6 -0.248828	1	3.668373	-2.825133	0.731369
6 -0.673697	1	5.622198	-2.564400	2.249696
6 0.352035	1	6.986444	-0.503019	2.176400
6 0.601534	1	6.483648	1.284250	0.510668
6 1.036136	1	4.557680	2.153753	-1.128618
1 1.173630	35	2.366382	-2.027872	-1.763079
1 2.016909	1	-0.636457	-1.178090	-0.307290
1 -0.322978	1	-0.832331	-0.010932	-1.577818
1 1.360241	15	-3.592800	-0.326686	-1.102980
1 0.023923	6	-5.125209	0.425155	-0.339880
1 1.297232	6	-5.387299	0.152488	1.137611
1 -1.645641	6	-6.701122	0.777090	1.593975
1 -0.835402	6	-6.737195	2.269647	1.305235
1 0.671147	6	-6.483765	2.545928	-0.168956
1 -1.018575	6	-5.170825	1.926323	-0.629482
6 0.704573	1	-4.339098	2.428943	-0.107574
1 -0.008164	1	-5.015720	2.109490	-1.702123
6 0.375675	1	-7.309009	2.123234	-0.764084
6 0.597985	1	-6.481822	3.626400	-0.365455
6 2.016807	1	-5.962947	2.773730	1.906545
6 2.353209	1	-7.698202	2.698974	1.617783
6 2.133998	1	-7.535888	0.285382	1.068756
1 2.399473	1	-6.856358	0.587504	2.664681
1 2.821393	1	-5.401260	-0.927274	1.335155
1 1.721667	1	-4.565104	0.572382	1.739158
1 3.394008	1	-5.939884	-0.044620	-0.921116
1 2.148513	6	-3.810347	-2.153063	-0.716417
1 2.722368	6	-3.218598	-2.666849	0.593192
1 -0.111330	6	-3.521447	-4.146119	0.797148
1 0.365498	6	-3.010686	-4.976813	-0.369889
1 -0.659904	6	-3.580519	-4.474358	-1.687436
1 1.018330	6	-3.296616	-2.992304	-1.889031
29 2.567914	1	-3.745646	-2.639947	-2.827564
6 4.333075	1	-2.209162	-2.838368	-1.997623

1 -3.178188 -5.054900 -2.528205
 1 -4.671204 -4.633910 -1.694526
 1 -1.910692 -4.912959 -0.403467
 1 -3.254277 -6.037562 -0.224480
 1 -3.079391 -4.494057 1.740571
 1 -4.610466 -4.283953 0.895931
 1 -2.125301 -2.536123 0.571615
 1 -3.581874 -2.085879 1.449866
 1 -4.906506 -2.285598 -0.673516
 1 -2.367951 1.339367 0.082414
 1 -2.385364 -0.106556 1.077625



Cupracyclobutane – dCype

Compound 4.54

RM06 energy: -4781.5722064

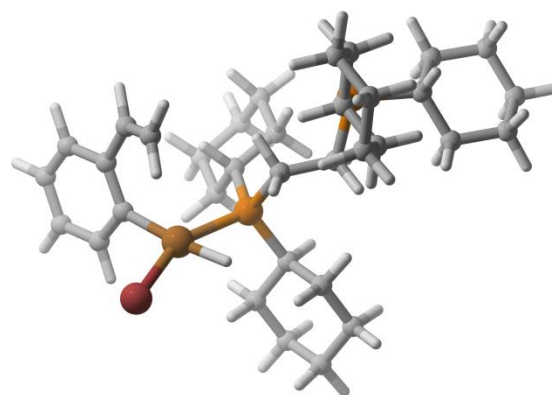
Sum of electronic and thermal Free Energies: -

4780.81397

6 1.516403 0.153170 -0.462048
 6 0.579098 1.087878 -1.224903
 15 -1.153303 0.446557 -1.180505
 6 -2.293735 1.850628 -1.645879
 1 -2.329398 1.846349 -2.748910
 6 -1.809055 3.232100 -1.206110
 6 -2.794908 4.317706 -1.620801
 6 -4.195927 4.038797 -1.099288
 6 -4.678267 2.671983 -1.555874

6 -3.709748 1.581914 -1.122244
 1 -4.071403 0.599399 -1.449305
 1 -3.690694 1.536971 -0.023738
 1 -4.770389 2.664054 -2.653793
 1 -5.679368 2.460606 -1.158706
 1 -4.889897 4.823709 -1.426881
 1 -4.188466 4.070790 0.002717
 1 -2.823506 4.374782 -2.720736
 1 -2.437134 5.294816 -1.270409
 1 -1.680969 3.258202 -0.112765
 1 -0.825432 3.448366 -1.641020
 6 -1.192875 -0.579561 -2.743738
 1 -1.055368 0.178848 -3.537741
 6 -0.041735 -1.579093 -2.857915
 6 -0.106702 -2.355476 -4.166414
 6 -1.442628 -3.061268 -4.323155
 6 -2.579594 -2.056506 -4.253582
 6 -2.545974 -1.255869 -2.958267
 1 -3.348307 -0.508821 -2.982716
 1 -2.753698 -1.918819 -2.105253
 1 -2.502923 -1.365166 -5.108823
 1 -3.551109 -2.558805 -4.349428
 1 -1.478652 -3.619367 -5.268016
 1 -1.559845 -3.802429 -3.515868
 1 0.041330 -1.664361 -5.012375
 1 0.722319 -3.074364 -4.205561
 1 0.924308 -1.062603 -2.793737
 1 -0.086371 -2.284998 -2.018045
 29 -1.636428 -0.476855 0.934838
 6 -1.720854 1.280200 2.036322
 6 -0.362959 1.892509 2.178051
 1 -0.416216 2.719309 2.906678
 1 0.363621 1.173682 2.576713
 1 0.028398 2.304546 1.243372
 6 -2.249864 0.580680 3.234547
 6 -2.608419 0.906433 4.533240
 6 -2.989453 -0.155434 5.349948
 6 -2.983543 -1.468699 4.876895
 6 -2.596595 -1.772306 3.571818
 6 -2.239676 -0.704228 2.762276
 1 -2.578265 -2.800671 3.216121
 1 -3.285117 -2.273889 5.545809
 1 -3.292061 0.036114 6.377902
 1 -2.598940 1.929304 4.907999

1	-2.447246	1.873568	1.473308
35	-1.398581	-2.824257	0.426999
1	0.607049	2.090747	-0.785861
1	0.874174	1.205598	-2.278330
15	3.270908	0.208431	-1.072758
6	4.023343	-1.219746	-0.129641
6	3.826246	-1.251752	1.383327
6	4.522610	-2.453053	2.012100
6	4.057357	-3.755582	1.380926
6	4.272167	-3.734921	-0.124372
6	3.576725	-2.539959	-0.762374
1	2.487788	-2.660413	-0.636276
1	3.760490	-2.521063	-1.846061
1	5.352192	-3.683175	-0.338242
1	3.910347	-4.666808	-0.578703
1	2.984199	-3.896642	1.590913
1	4.576599	-4.610855	1.833360
1	5.611796	-2.352017	1.876680
1	4.345275	-2.463775	3.095939
1	4.200566	-0.326597	1.840431
1	2.749904	-1.306719	1.616062
1	5.104930	-1.108043	-0.329406
6	4.015592	1.715012	-0.230043
6	3.275274	2.279112	0.980452
6	4.016080	3.467574	1.580696
6	4.229956	4.562180	0.547161
6	4.953029	4.021656	-0.677248
6	4.229971	2.819314	-1.268000
1	4.787182	2.424636	-2.128234
1	3.249219	3.137490	-1.662962
1	5.067366	4.806563	-1.436916
1	5.973153	3.718863	-0.390219
1	3.250645	4.965308	0.241096
1	4.786133	5.402403	0.983503
1	3.462321	3.856958	2.445786
1	4.992399	3.130137	1.964568
1	2.273408	2.613857	0.666279
1	3.113356	1.510226	1.745870
1	5.012262	1.371453	0.101580
1	1.210871	-0.893409	-0.581591
1	1.451804	0.356776	0.612453



Copper-hydride oxidative insertion into Ar-Br bond

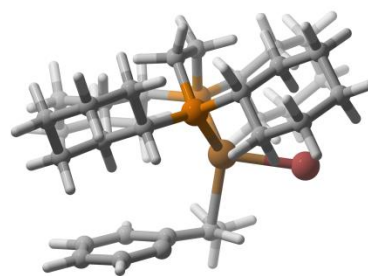
RB3LYP energy: -4782.7628464

Sum of electronic and thermal Free Energies: -

4782.008426

6	0.665830	0.330206	-0.080771
15	-0.895274	-0.579334	0.370733
6	-1.184869	-1.794600	-1.038852
1	-1.516674	-1.130219	-1.843891
6	0.092661	-2.519861	-1.511379
6	-0.200918	-3.399491	-2.739907
6	-1.339483	-4.391879	-2.487494
6	-2.597941	-3.668592	-1.999084
6	-2.310051	-2.807285	-0.759613
1	-2.014892	-3.467695	0.063435
1	-3.221702	-2.291485	-0.453285
1	-2.991830	-3.030093	-2.799171
1	-3.386736	-4.389948	-1.760573
1	-1.024091	-5.124034	-1.732247
1	-1.554959	-4.959523	-3.399155
1	-0.463484	-2.751675	-3.585698
1	0.714276	-3.928457	-3.026964
1	0.871908	-1.803900	-1.777665
1	0.489776	-3.146432	-0.703519
6	-0.754986	-1.529253	1.970728
1	-0.267454	-2.475940	1.707385

6	0.093572	-0.811493	3.038444	1	4.412632	-2.597154	-1.298214
6	0.172359	-1.634961	4.334760	1	5.203453	-1.546800	-2.458386
6	-1.213720	-1.976331	4.889942	1	7.369639	-1.801129	-1.309752
6	-2.079089	-2.660798	3.827782	1	6.716865	-3.385891	-1.692090
6	-2.161512	-1.828188	2.540230	1	5.932506	-3.678524	0.635860
1	-2.658331	-0.875691	2.759168	1	7.644478	-3.284735	0.647516
1	-2.783749	-2.343818	1.808946	1	7.145015	-0.922082	1.197282
1	-3.090875	-2.830884	4.210729	1	6.366858	-1.970868	2.371706
1	-1.664603	-3.650226	3.595049	1	4.825379	-0.170929	1.625867
1	-1.709579	-1.054787	5.220554	1	4.202494	-1.757805	1.212772
1	-1.120182	-2.614727	5.775014	1	0.602346	1.297537	0.416546
1	0.725859	-2.562212	4.137448	1	0.528915	0.533276	-1.147901
1	0.754583	-1.078855	5.077097	6	-2.425346	1.489163	-2.881682
1	-0.352290	0.166516	3.256794	6	-1.605443	2.322121	-2.230497
1	1.103163	-0.624385	2.672846	1	-1.769496	2.611218	-1.196273
29	-2.574453	0.947373	0.478875	1	-0.758617	2.780863	-2.731632
15	3.306033	0.192959	-1.094596	1	-2.227351	1.312098	-3.938882
6	2.039465	-0.314536	0.197645	6	-3.619394	0.803572	-2.351171
1	2.374790	-0.046579	1.198686	6	-3.825161	0.538138	-0.975984
1	1.996246	-1.403675	0.163114	6	-5.035683	-0.071400	-0.613576
6	3.547963	2.027500	-0.729964	6	-6.008592	-0.429310	-1.549641
1	2.536993	2.438793	-0.862814	6	-5.782866	-0.187339	-2.904087
6	4.040747	2.425500	0.672424	6	-4.595560	0.421885	-3.293535
6	4.134963	3.952505	0.827685	1	-4.419482	0.622684	-4.347926
6	5.022750	4.577262	-0.254997	1	-6.523906	-0.466955	-3.647026
6	4.549099	4.183218	-1.659090	1	-6.931428	-0.901915	-1.223684
6	4.438880	2.659385	-1.819810	1	-5.236845	-0.277882	0.435354
1	5.444037	2.220681	-1.770750	35	-3.610456	2.817585	1.604561
1	4.044852	2.416651	-2.812296	1	-1.497643	1.029208	1.540954
1	3.567539	4.636401	-1.850371				
1	5.229264	4.587249	-2.417441				
1	6.058127	4.239512	-0.113254				
1	5.036656	5.667941	-0.152098				
1	4.518772	4.200149	1.823937				
1	3.128245	4.386564	0.767329				
1	5.032188	1.991957	0.848284				
1	3.380215	2.018312	1.444564				
6	4.905182	-0.635701	-0.505603				
1	5.678581	0.119270	-0.700507				
6	4.994278	-1.035650	0.979703				
6	6.352446	-1.672593	1.317017				
6	6.652952	-2.878224	0.419398				
6	6.560709	-2.501827	-1.063635				
6	5.212303	-1.851580	-1.407024				



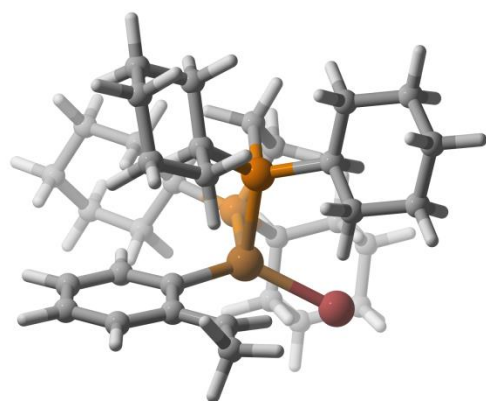
Benzyl copper bromide/aryl radical (triplet)

Compound 4.56

UM06 energy: -4781.5688977

Sum of electronic and thermal Free Energies:	-	6	-3.967799	1.048666	-1.845891
4780.812989		6	-5.408724	0.555318	-1.773899
		6	-5.480674	-0.962356	-1.736902
6	-0.716844	0.490610	-2.321180		
6	0.788850	0.221130	-2.362715		
15	1.492663	-0.758055	-0.943948		
6	1.327650	-2.525911	-1.527087		
1	1.775207	-2.556659	-2.537259		
6	-0.138250	-2.941749	-1.624557		
6	-0.301827	-4.393889	-2.051698		
6	0.460947	-5.333620	-1.133476		
6	1.926879	-4.939750	-1.068989		
6	2.095469	-3.492853	-0.626181		
1	3.162846	-3.240584	-0.601842		
1	1.726137	-3.388559	0.408386		
1	2.382644	-5.069811	-2.063945		
1	2.478617	-5.601828	-0.388779		
1	0.353408	-6.373571	-1.468433		
1	0.026037	-5.286562	-0.121235		
1	0.069758	-4.513426	-3.082254		
1	-1.368812	-4.653627	-2.075636		
1	-0.619801	-2.795001	-0.642811		
1	-0.673646	-2.295448	-2.329483		
6	3.342975	-0.490027	-1.087075		
1	3.719059	-1.275052	-1.767082		
6	3.746671	0.864935	-1.668899		
6	5.262393	1.022952	-1.706429		
6	5.888475	0.823042	-0.337008		
6	5.497482	-0.529774	0.236317		
6	3.983965	-0.674428	0.291914		
1	3.710460	-1.646621	0.721896		
1	3.567880	0.088900	0.967479		
1	5.924015	-1.330766	-0.390453		
1	5.923058	-0.662569	1.239867		
1	6.980690	0.921167	-0.395169		
1	5.538443	1.616810	0.342631		
1	5.682843	0.283549	-2.407978		
1	5.519993	2.011202	-2.109843		
1	3.351685	0.985487	-2.684957		
1	3.308917	1.670844	-1.056735		
29	0.361187	0.346299	0.809462		
15	-1.349185	1.054484	-0.662826		
6	-3.128422	0.492436	-0.696234		
				6	-3.967799
				6	-5.408724
				6	-5.480674
				6	-4.657562
				6	-3.213562
				1	-2.761338
				1	-2.631284
				1	-5.099130
				1	-4.688319
				1	-5.093509
				1	-6.523750
				1	-5.882047
				1	-5.980370
				1	-3.960169
				1	-3.528419
				1	-3.546220
				6	-1.472838
				6	-0.139392
				6	-0.247396
				6	-0.736118
				6	-2.072964
				6	-1.984397
				1	-2.965908
				1	-1.294689
				1	-2.413644
				1	-2.835710
				1	0.005345
				1	-0.815657
				1	0.725253
				1	-0.948784
				1	0.632368
				1	0.187124
				1	-2.199764
				6	0.220872
				6	1.527912
				1	1.572561
				1	1.723125
				1	2.349414
				6	-1.001946
				6	-1.100245
				6	-2.328311
				6	-3.517265
				6	-3.470170
				6	-2.238755
					1.048666
					0.555318
					-0.962356
					-1.508948
					-1.033260
					-1.452912
					0.182833
					0.369892
					-0.564299
					-2.685624
					-1.660356
					-0.865909
					-2.623935
					2.145748
					-2.806341
					0.254169
					-0.845157
					-1.252100
					-1.330100
					-0.015470
					0.381536
					0.461653
					0.721619
					1.273081
					1.343250
					-0.362913
					0.771294
					-0.086388
					-1.605921
					-2.134424
					-0.515907
					-2.223445
					-1.646768
					2.903016
					3.042186
					3.985740
					2.235339
					3.055015
					2.676918
					2.302866
					2.209289
					2.472320
					2.808882
					2.875906

1 -4.384957 -0.858770 3.004429
 1 -4.475210 -3.288295 2.408454
 1 -2.368740 -4.515352 1.937808
 1 -0.188427 -3.400494 2.110722
 1 0.135913 0.207592 3.341089
 35 1.699433 2.126592 1.832539
 1 1.067126 -0.250891 -3.316457
 1 1.311441 1.183050 -2.331840
 1 -1.278758 -0.410025 -2.589307
 1 -0.973536 1.239570 -3.083299



Aryl copper bromide/benzyl radical (triplet)

Compound 4.58

UM06 energy: -4781.5787403

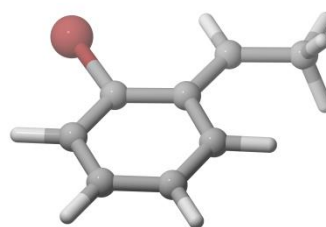
Sum of electronic and thermal Free Energies: -

4780.825517

6 0.190172 0.060376 -2.294520
 15 1.289894 -0.274444 -0.845528
 6 2.023016 -1.935685 -1.215889
 6 2.921662 -2.022437 -2.447564
 6 3.294695 -3.473010 -2.731265
 6 3.960983 -4.119898 -1.526271
 6 3.087834 -4.004716 -0.285659
 6 2.712800 -2.557354 -0.000543
 1 3.621279 -1.985573 0.248261
 1 2.049650 -2.503858 0.870737
 1 2.163266 -4.587776 -0.429131
 1 3.595148 -4.440633 0.585022

1 4.195357 -5.171588 -1.737377
 1 4.924932 -3.620174 -1.336455
 1 2.383901 -4.035948 -2.991140
 1 3.951664 -3.525025 -3.609676
 1 3.841383 -1.445246 -2.267834
 1 2.438320 -1.578715 -3.328007
 1 1.114427 -2.534396 -1.414720
 6 2.561000 1.073136 -0.957421
 1 2.013945 1.929674 -0.521243
 6 3.026478 1.492657 -2.353393
 6 3.908686 2.733436 -2.259745
 6 5.098515 2.514185 -1.336415
 6 4.649213 2.043006 0.038531
 6 3.773107 0.803075 -0.065898
 1 4.362250 -0.019810 -0.500053
 1 3.459583 0.472501 0.931464
 1 4.078884 2.844183 0.536745
 1 5.517180 1.836321 0.679267
 1 5.692504 3.433861 -1.254310
 1 5.764273 1.754609 -1.777736
 1 3.304135 3.573159 -1.880989
 1 4.248850 3.025214 -3.262221
 1 3.595822 0.674863 -2.818496
 1 2.175668 1.696675 -3.014719
 29 -0.288719 -0.256244 0.925664
 6 0.473923 1.306681 1.879179
 6 1.608026 1.148243 2.726973
 6 2.168803 2.324768 3.297041
 6 1.618897 3.570158 3.067340
 6 0.485869 3.699609 2.265405
 6 -0.071901 2.560599 1.677544
 1 -0.951062 2.674968 1.043611
 1 0.041115 4.678269 2.090702
 1 2.068544 4.451647 3.521296
 1 3.040165 2.238102 3.945438
 6 2.166779 -0.121768 2.977649
 1 1.617530 -0.988221 2.609286
 6 3.424975 -0.350789 3.729048
 1 3.746532 -1.394530 3.655805
 1 4.250992 0.277474 3.361622
 1 3.324711 -0.121900 4.801955
 15 -2.134430 0.198745 -0.672893
 6 -1.234764 -0.475102 -2.152321
 1 -1.803566 -0.275731 -3.072266

1	-1.204154	-1.565550	-2.035988
6	-2.862865	1.804998	-1.305763
6	-1.818153	2.773869	-1.858015
6	-2.418035	4.123725	-2.231522
6	-3.179911	4.740157	-1.071442
6	-4.277583	3.798048	-0.611221
6	-3.708982	2.446760	-0.202628
1	-3.094449	2.574242	0.703595
1	-4.530229	1.776244	0.080118
1	-5.001323	3.658365	-1.430289
1	-4.839163	4.230002	0.227244
1	-2.484970	4.930387	-0.236177
1	-3.597252	5.714351	-1.357215
1	-1.622149	4.794858	-2.580176
1	-3.105976	3.991403	-3.082269
1	-1.014537	2.926699	-1.119042
1	-1.345137	2.341521	-2.747515
1	-3.533710	1.520901	-2.136500
6	-3.692782	-0.834553	-0.534908
6	-3.589686	-2.237320	-1.131948
6	-4.899099	-3.000080	-0.964409
6	-5.332213	-3.063464	0.491755
6	-5.442258	-1.667067	1.082341
6	-4.129913	-0.911961	0.931899
1	-3.342865	-1.427490	1.502488
1	-4.216097	0.091838	1.369184
1	-6.247907	-1.115165	0.569662
1	-5.726562	-1.716604	2.141808
1	-4.589892	-3.640142	1.066949
1	-6.285480	-3.600812	0.585849
1	-5.685846	-2.500601	-1.553490
1	-4.795719	-4.010407	-1.382409
1	-2.778799	-2.788679	-0.631013
1	-3.332373	-2.187308	-2.197999
1	-4.466070	-0.286964	-1.102242
35	-0.736159	-2.535226	1.585094
1	0.650792	-0.345545	-3.205198
1	0.185243	1.147819	-2.416122



Benzyl radical (doublet)

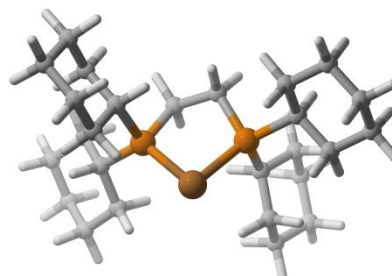
Compound 4.57

UM06 energy: -2883.4665678

Sum of electronic and thermal Free Energies: -

2883.371259

6	1.916405	2.754636	0.000192
6	0.774073	1.809571	-0.000259
6	0.915901	0.411494	-0.000117
6	-0.181750	-0.495589	-0.000021
6	-0.008352	-1.864221	0.000080
6	1.274348	-2.405908	0.000066
6	2.378891	-1.556252	-0.000028
6	2.205416	-0.190301	-0.000101
1	3.079204	0.457409	-0.000182
1	3.383972	-1.971768	-0.000058
1	1.402972	-3.485170	0.000120
1	-0.875688	-2.519916	0.000182
35	-1.974662	0.156429	0.000010
1	-0.230509	2.225134	-0.000480
1	2.564384	2.623663	0.879422
1	2.566072	2.622843	-0.877646
1	1.573182	3.792228	-0.000577



Copper(0) – dCype

Compound 4.57

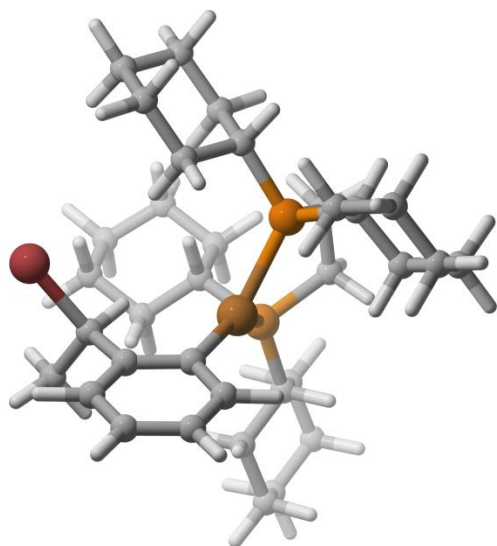
UM06 energy: -1898.0253665

Sum of electronic and thermal Free Energies: -

1897.391555

6 0.591449 -0.447884 1.678737
 15 1.603128 -0.169880 0.139635
 6 1.953958 1.653975 0.276218
 1 0.966297 2.064698 0.551293
 6 2.940482 2.071703 1.362165
 6 3.039698 3.590182 1.449839
 6 3.404738 4.199349 0.104343
 6 2.413439 3.786385 -0.974067
 6 2.306150 2.271660 -1.077329
 1 3.260282 1.861032 -1.444070
 1 1.546751 1.981802 -1.821288
 1 1.421044 4.201972 -0.733020
 1 2.699289 4.212722 -1.944606
 1 4.413865 3.861506 -0.183603
 1 3.456555 5.293499 0.180777
 1 2.071075 3.997260 1.782795
 1 3.774215 3.876588 2.214382
 1 2.644875 1.656069 2.335601
 1 3.938070 1.662521 1.137819
 6 3.177226 -1.077549 0.525796
 1 3.554390 -0.741729 1.507715
 6 2.886550 -2.578507 0.598520
 6 4.155392 -3.387839 0.830918
 6 5.202431 -3.098628 -0.232542
 6 5.503509 -1.610131 -0.301970
 6 4.236788 -0.799360 -0.540287
 1 4.480630 0.270037 -0.574531
 1 3.819443 -1.051318 -1.529969
 1 5.967070 -1.287546 0.644464
 1 6.236186 -1.400037 -1.092227
 1 4.827776 -3.437980 -1.211502
 1 6.119364 -3.669586 -0.035314
 1 4.565780 -3.138196 1.822671
 1 3.915244 -4.458970 0.856651
 1 2.417901 -2.894653 -0.349470
 1 2.160029 -2.796831 1.391600
 29 0.118191 -0.389338 -1.695623

15 -1.583735 -0.107827 -0.058913
 6 -0.780699 0.216534 1.591387
 1 -1.414964 -0.101181 2.429624
 1 -0.682050 1.306815 1.680720
 6 -2.292112 -1.816380 0.136562
 1 -1.396076 -2.417214 0.385962
 6 -3.331674 -2.030308 1.231050
 6 -3.737839 -3.496878 1.320088
 6 -4.260513 -4.004203 -0.015605
 6 -3.239048 -3.784332 -1.121008
 6 -2.813793 -2.325328 -1.207527
 1 -3.674871 -1.710578 -1.519990
 1 -2.039948 -2.186812 -1.978871
 1 -2.350377 -4.404604 -0.922018
 1 -3.638057 -4.118805 -2.087781
 1 -5.188610 -3.465770 -0.267478
 1 -4.529342 -5.066598 0.054558
 1 -4.493209 -3.631446 2.106022
 1 -2.864414 -4.097313 1.621727
 1 -4.226097 -1.430581 0.999944
 1 -2.961317 -1.679722 2.203864
 6 -2.988514 1.104443 -0.154065
 1 -3.725896 0.619431 -0.817772
 6 -3.676749 1.479896 1.157549
 6 -4.794129 2.489772 0.924280
 6 -4.280742 3.736375 0.220247
 6 -3.585987 3.377497 -1.084516
 6 -2.475651 2.361420 -0.863659
 1 -1.679580 2.819806 -0.250546
 1 -2.004410 2.085029 -1.818044
 1 -4.323855 2.953947 -1.784786
 1 -3.182777 4.277313 -1.567791
 1 -3.567483 4.256863 0.880014
 1 -5.102428 4.441313 0.037280
 1 -5.580645 2.023164 0.309564
 1 -5.265803 2.753184 1.880476
 1 -4.074508 0.591753 1.662369
 1 -2.936697 1.919602 1.844914
 1 1.133559 -0.102952 2.570844
 1 0.469114 -1.532280 1.792536



Aryl copper/benzyl bromide

Compound 4.18

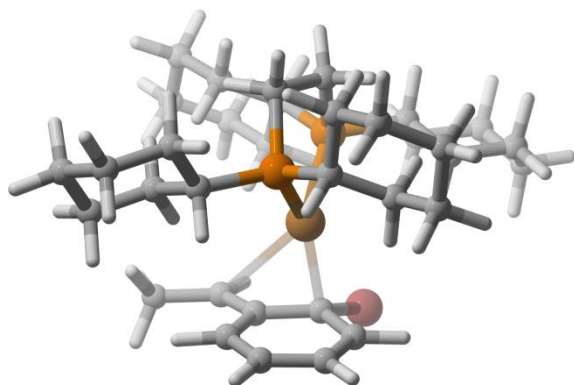
RM06 energy: -4781.6125195

Sum of electronic and thermal Free Energies: -

4780.851193

6	3.528039	1.361469	0.545330
1	3.320534	2.413031	0.819186
6	4.782392	1.343082	-0.323113
6	5.981547	1.893342	0.441058
6	6.206451	1.130597	1.738176
6	4.956571	1.142391	2.605034
6	3.754618	0.593717	1.848962
1	3.926200	-0.470903	1.624343
1	2.850780	0.633562	2.472444
1	4.742594	2.176458	2.920085
1	5.119396	0.565961	3.525205
1	7.059598	1.550857	2.286716
1	6.473283	0.087576	1.501914
1	5.807761	2.957103	0.669891
1	6.879330	1.855506	-0.190149
1	4.998717	0.306795	-0.624955
1	4.625579	1.912723	-1.249187
29	-0.161353	0.574977	0.762570
6	-1.006469	-0.134750	2.396214
6	-1.153813	-1.518430	2.619347
6	-1.775604	-2.023124	3.764084
6	-2.281151	-1.166366	4.728422
6	-2.152807	0.206766	4.545810
6	-1.528703	0.696655	3.405256
1	-1.450898	1.782201	3.296632
1	-2.546596	0.894643	5.294399
1	-2.771570	-1.564728	5.615083
1	-1.881411	-3.100937	3.899284
6	-0.532084	-2.463434	1.634480
35	-1.877018	-3.730144	0.845234
1	-0.209672	-1.893925	0.754348
6	0.611911	-3.275763	2.188120
1	1.373807	-2.588292	2.584061
1	0.292493	-3.921232	3.014071
1	1.080603	-3.904680	1.422415
15	-1.069318	1.459416	-1.209284
6	0.350249	2.044470	-2.264124
1	0.076067	2.968407	-2.791417
1	0.519288	1.291565	-3.041215
6	-2.063726	3.005268	-0.948862
6	-1.238691	4.022943	-0.163116
6	-2.038824	5.276633	0.163405
6	-3.324660	4.937307	0.899081
6	-4.159556	3.955101	0.093928
6	1.637405	2.235275	-1.461448
15	1.926353	0.861289	-0.248804
6	2.145196	-0.634884	-1.334447
6	2.929779	-0.505354	-2.636705
6	2.773240	-1.773751	-3.469517
6	3.195555	-3.012097	-2.691757
6	2.455603	-3.119523	-1.365696
6	2.624687	-1.850009	-0.543291
1	3.688107	-1.724083	-0.286073
1	2.083927	-1.928111	0.408747
1	1.380301	-3.283885	-1.555619
1	2.805033	-3.991958	-0.797334
1	3.035925	-3.915536	-3.294611
1	4.278399	-2.960236	-2.492987
1	1.718124	-1.876335	-3.772816
1	3.352667	-1.689925	-4.398495
1	3.994676	-0.344696	-2.415161
1	2.601207	0.365181	-3.219336
1	1.093444	-0.842552	-1.611074

6	-3.371648	2.691604	-0.224047
1	-3.143347	2.159624	0.714894
1	-3.989267	2.008560	-0.822266
1	-4.478984	4.433596	-0.846031
1	-5.078046	3.692783	0.634913
1	-3.076941	4.487601	1.874305
1	-3.898357	5.848523	1.113501
1	-1.423004	5.966965	0.754799
1	-2.283556	5.804033	-0.772907
1	-0.895835	3.552435	0.775094
1	-0.334287	4.296879	-0.722501
1	-2.295295	3.422712	-1.945195
6	-2.170247	0.409844	-2.302158
6	-1.461695	-0.240828	-3.487836
6	-2.402413	-1.144756	-4.275453
6	-3.046723	-2.199742	-3.390249
6	-3.765185	-1.552554	-2.218036
6	-2.818468	-0.666373	-1.425633
1	-2.020479	-1.292964	-0.992756
1	-3.333998	-0.217520	-0.566194
1	-4.607831	-0.948588	-2.592306
1	-4.198149	-2.315682	-1.558004
1	-2.267259	-2.878894	-3.005542
1	-3.736816	-2.821817	-3.975371
1	-3.190825	-0.526603	-4.734133
1	-1.856913	-1.614043	-5.105042
1	-0.609316	-0.840645	-3.124179
1	-1.045743	0.521397	-4.158663
1	-2.957689	1.074361	-2.697639
1	2.492311	2.361037	-2.138388
1	1.586628	3.148452	-0.852495



κ -2 dearomative transition state

Compound 4.59

RM06 energy: -4781.5858654

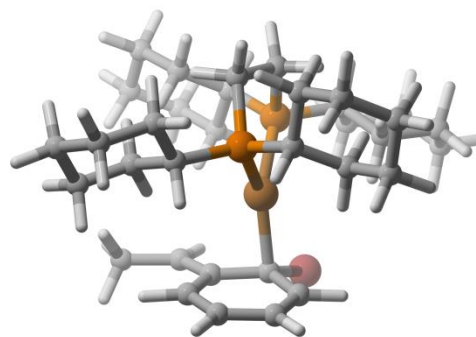
Sum of electronic and thermal Free Energies: -
4780.824178

Imaginary frequency: -27.3185

6	-1.404219	0.044602	-2.261837
6	0.002918	0.566270	-2.555456
15	1.311390	0.022707	-1.341173
6	2.019314	-1.531472	-2.088768
1	2.612183	-1.230925	-2.971585
6	0.910129	-2.479393	-2.545917
6	1.468100	-3.784060	-3.098877
6	2.372353	-4.476588	-2.092807
6	3.484076	-3.544016	-1.644310
6	2.919817	-2.248661	-1.079811
1	3.733849	-1.599685	-0.740709
1	2.321711	-2.471096	-0.181046
1	4.139832	-3.316697	-2.500794
1	4.117690	-4.031350	-0.891709
1	2.786133	-5.400839	-2.517390
1	1.776386	-4.775678	-1.214790
1	2.040612	-3.570831	-4.016295
1	0.641573	-4.442627	-3.397290
1	0.255466	-2.702014	-1.684771
1	0.280813	-2.002894	-3.307758
6	2.576983	1.361375	-1.632482
1	2.547747	1.590886	-2.713386
6	2.152651	2.605188	-0.848234
6	3.127210	3.758606	-1.037624
6	4.540552	3.347515	-0.659193
6	4.972572	2.126449	-1.454483
6	4.005099	0.964581	-1.266383
1	4.334688	0.113621	-1.875689
1	4.033965	0.634497	-0.214990
1	5.020692	2.388597	-2.523850
1	5.985400	1.814340	-1.167279
1	5.241229	4.178028	-0.816081
1	4.573222	3.110558	0.416805

1	3.111182	4.082810	-2.090830
1	2.802316	4.622579	-0.443018
1	1.140753	2.919264	-1.135962
1	2.099078	2.342915	0.221823
29	0.087770	0.046017	0.614949
15	-1.914332	0.339679	-0.502328
6	-3.232708	-0.912021	-0.156043
6	-4.481453	-0.896515	-1.030913
6	-5.482247	-1.948143	-0.562679
6	-4.862202	-3.336246	-0.505485
6	-3.612440	-3.344284	0.362086
6	-2.610052	-2.307136	-0.120544
1	-2.268272	-2.585802	-1.131061
1	-1.716878	-2.299466	0.519054
1	-3.885265	-3.121976	1.406885
1	-3.151467	-4.341027	0.367143
1	-4.594247	-3.655821	-1.525811
1	-5.593714	-4.066635	-0.135567
1	-5.843024	-1.671996	0.441097
1	-6.363289	-1.946008	-1.218044
1	-4.956279	0.092406	-1.013412
1	-4.202161	-1.095994	-2.078622
1	-3.530676	-0.660084	0.878039
6	-2.761556	1.995594	-0.440313
6	-3.440979	2.463671	-1.725742
6	-4.160066	3.790015	-1.510761
6	-3.207299	4.859322	-0.998468
6	-2.498770	4.400732	0.267088
6	-1.792303	3.069929	0.056091
1	-1.300436	2.740063	0.981355
1	-0.991775	3.199447	-0.691691
1	-1.780952	5.159720	0.604875
1	-3.236504	4.289217	1.078116
1	-2.456138	5.074871	-1.775815
1	-3.744965	5.799805	-0.819975
1	-4.635690	4.114162	-2.445854
1	-4.973658	3.646423	-0.781753
1	-2.677439	2.599259	-2.508922
1	-4.141192	1.710181	-2.106802
1	-3.533672	1.854504	0.338462
6	0.805220	-2.398866	2.256906
6	0.176822	-3.755342	2.300356
1	-0.076714	-4.096433	3.319291
1	-0.759404	-3.832340	1.722729

1	0.856185	-4.509051	1.884036
6	0.170933	-1.243033	2.636334
6	-1.208107	-1.237863	3.111461
6	-1.833677	-0.122892	3.580731
6	-1.197075	1.144229	3.593260
6	0.092548	1.221670	3.123475
6	0.764732	0.099751	2.583953
35	2.709826	0.234919	2.576616
1	0.626224	2.172252	3.146884
1	-1.713942	2.032465	3.948240
1	-2.850172	-0.213093	3.965254
1	-1.717569	-2.199231	3.177021
1	1.861425	-2.342509	2.003363
1	0.314300	0.295553	-3.574560
1	0.002534	1.664661	-2.522680
1	-1.444334	-1.042177	-2.403775
1	-2.123734	0.470918	-2.971123



κ -2 dearomatized intermediate

Compound 4.60

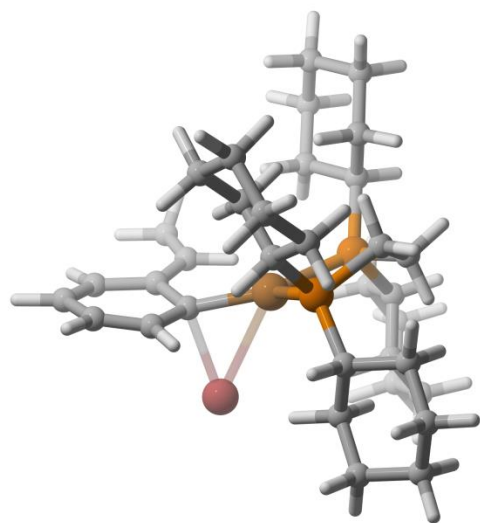
RM06 energy: -4781.586216

Sum of electronic and thermal Free Energies: -
4780.825867

6	-0.925679	0.077780	-2.660864
6	0.479971	0.669243	-2.654197
15	1.536173	0.156555	-1.205250
6	2.515428	-1.282110	-1.868196

1	3.220509	-0.876543	-2.616526	1	-6.038926	-2.050595	0.293872
6	1.599886	-2.294770	-2.557734	1	-4.115805	-3.467754	0.980096
6	2.376494	-3.499504	-3.072561	1	-5.135875	-4.338010	-0.163404
6	3.161141	-4.175019	-1.960375	1	-3.589517	-3.767549	-2.020926
6	4.076790	-3.177958	-1.270709	1	-2.698159	-4.568913	-0.729292
6	3.292272	-1.981458	-0.751165	1	-1.452998	-2.591112	-1.540765
1	3.963785	-1.287529	-0.235075	1	-1.916598	-2.390679	0.144361
1	2.569270	-2.322984	0.006907	1	-3.382774	-1.143344	-2.233938
1	4.844167	-2.831178	-1.982214	6	-2.830394	1.807947	-1.213718
1	4.616095	-3.656221	-0.442570	6	-2.085288	2.934547	-1.927407
1	3.735565	-5.023501	-2.354459	6	-2.952633	4.182093	-2.040515
1	2.457984	-4.591175	-1.219945	6	-3.442700	4.652794	-0.680228
1	3.073318	-3.169309	-3.860109	6	-4.166038	3.534017	0.052304
1	1.686657	-4.209416	-3.547848	6	-3.289001	2.295313	0.162940
1	0.842414	-2.637994	-1.830937	1	-3.813352	1.504405	0.713614
1	1.055110	-1.828917	-3.388307	1	-2.394111	2.532753	0.762756
6	2.696113	1.617477	-1.182891	1	-4.476038	3.863856	1.052572
1	2.834266	1.916134	-2.238206	1	-5.090612	3.277703	-0.490271
6	2.010172	2.758569	-0.427860	1	-2.580344	4.979307	-0.077013
6	2.867072	4.015283	-0.396901	1	-4.093997	5.529744	-0.789503
6	4.235625	3.725676	0.199172	1	-2.393768	4.979836	-2.547482
6	4.925438	2.602993	-0.558728	1	-3.820454	3.957165	-2.681403
6	4.073784	1.340038	-0.588123	1	-1.172777	3.179075	-1.357800
1	4.591289	0.561047	-1.162461	1	-1.758718	2.622328	-2.927319
1	3.957353	0.956097	0.437752	1	-3.714672	1.541790	-1.820141
1	5.123555	2.930732	-1.592234	6	0.552974	-2.516304	2.147305
1	5.903654	2.379754	-0.113007	6	0.004379	-3.903920	2.046113
1	4.857556	4.630435	0.198307	1	-0.313834	-4.331487	3.012926
1	4.115505	3.431577	1.254894	1	-0.875116	-3.983983	1.385183
1	2.989520	4.401046	-1.421989	1	0.757208	-4.590939	1.640194
1	2.355138	4.803108	0.171268	6	-0.192203	-1.416593	2.480069
1	1.028180	2.984086	-0.866888	6	-1.612954	-1.515259	2.792494
1	1.813491	2.424339	0.604118	6	-2.363384	-0.461066	3.214983
29	-0.083530	0.070885	0.483584	6	-1.823072	0.845562	3.334048
15	-1.814938	0.257631	-1.039789	6	-0.500811	1.023662	3.016190
6	-3.037748	-1.137191	-1.183687	6	0.308744	-0.032995	2.522277
6	-2.318860	-2.451830	-0.879089	35	2.219565	0.219723	2.843550
6	-3.248384	-3.651676	-0.979414	1	-0.038827	2.004795	3.128277
6	-4.454598	-3.482406	-0.069120	1	-2.441198	1.684898	3.642900
6	-5.182280	-2.184464	-0.379747	1	-3.407866	-0.632102	3.478331
6	-4.253858	-0.981366	-0.273660	1	-2.061328	-2.508550	2.783184
1	-3.912443	-0.878550	0.769390	1	1.625163	-2.388305	2.014624
1	-4.808043	-0.065635	-0.517673	1	1.010287	0.437083	-3.588827
1	-5.595650	-2.235643	-1.400209	1	0.421922	1.763635	-2.606356

1 -0.883661 -0.999892 -2.859317
 1 -1.530847 0.509738 -3.469783



κ -2 1,2-bromide shift

Compound 4.61

RM06 energy: -4781.5714587

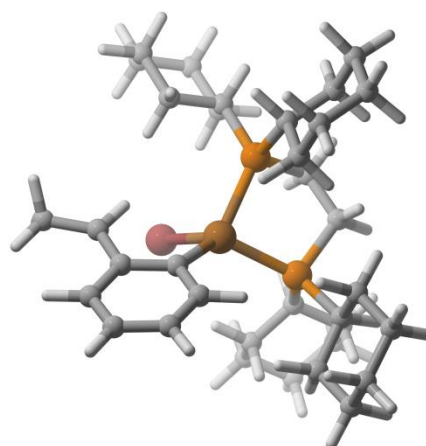
Sum of electronic and thermal Free Energies: -
 4780.814047

Imaginary frequency: -109.1455

6 -1.625992 -0.048725 -2.258448
 6 -0.369941 0.737045 -2.624848
 15 1.099244 0.319580 -1.559633
 6 2.001693 -0.992863 -2.537869
 1 2.522421 -0.475216 -3.363995
 6 1.040097 -2.017826 -3.138706
 6 1.782175 -3.088864 -3.927328
 6 2.832686 -3.787890 -3.079819
 6 3.786455 -2.778316 -2.463377
 6 3.028555 -1.724464 -1.668240
 1 3.732935 -1.024879 -1.202202
 1 2.494741 -2.214144 -0.836204
 1 4.366829 -2.285831 -3.260428

1 4.516062 -3.281600 -1.815059
 1 3.381999 -4.525767 -3.679078
 1 2.333752 -4.350136 -2.274140
 1 2.269543 -2.618730 -4.797163
 1 1.065040 -3.815650 -4.331713
 1 0.470330 -2.494909 -2.322080
 1 0.306636 -1.532459 -3.792889
 6 2.111929 1.867022 -1.776020
 1 2.079117 2.124353 -2.850687
 6 1.477602 3.000307 -0.966768
 6 2.277955 4.290962 -1.068312
 6 3.718528 4.076481 -0.634286
 6 4.362837 2.970773 -1.453339
 6 3.569683 1.673700 -1.362422
 1 4.047550 0.908140 -1.986152
 1 3.602666 1.302018 -0.323614
 1 4.420357 3.286116 -2.507844
 1 5.396342 2.796096 -1.126617
 1 4.292337 5.008264 -0.724079
 1 3.737769 3.798681 0.432268
 1 2.261278 4.654756 -2.108679
 1 1.801957 5.071050 -0.459805
 1 0.442474 3.179865 -1.286884
 1 1.419536 2.690206 0.089565
 29 0.162389 -0.151114 0.505675
 15 -1.992325 0.040826 -0.438895
 6 -3.084867 -1.425581 -0.132490
 6 -4.335968 -1.542003 -0.998736
 6 -5.165815 -2.756142 -0.597104
 6 -4.344492 -4.035892 -0.640474
 6 -3.094910 -3.917250 0.220245
 6 -2.260777 -2.712031 -0.187188
 1 -1.887657 -2.867572 -1.213346
 1 -1.371676 -2.618137 0.452801
 1 -3.385810 -3.812187 1.277912
 1 -2.492927 -4.833050 0.155204
 1 -4.047030 -4.239833 -1.682258
 1 -4.952744 -4.892360 -0.320695
 1 -5.549081 -2.605634 0.424977
 1 -6.046576 -2.841037 -1.247458
 1 -4.947171 -0.632510 -0.923190
 1 -4.041323 -1.636534 -2.056560
 1 -3.405313 -1.282333 0.915440
 6 -3.113162 1.512997 -0.179634

6	-3.777023	2.079552	-1.431586
6	-4.688716	3.251411	-1.089000
6	-3.932886	4.342810	-0.346492
6	-3.264669	3.787834	0.901988
6	-2.358610	2.611586	0.570521
1	-1.896513	2.204537	1.480154
1	-1.518320	2.959589	-0.053954
1	-2.692303	4.570888	1.416501
1	-4.040078	3.455523	1.611124
1	-3.162275	4.764501	-1.012322
1	-4.606118	5.171282	-0.089463
1	-5.143777	3.651437	-2.005113
1	-5.519821	2.891710	-0.461327
1	-2.998387	2.428815	-2.129356
1	-4.342996	1.303939	-1.963769
1	-3.904708	1.132344	0.490352
6	2.927287	-1.349677	1.904419
6	4.299012	-1.875798	2.087534
1	4.448718	-2.426106	3.020649
1	4.571529	-2.545808	1.258565
1	5.034666	-1.059074	2.059832
6	1.859836	-1.442994	2.733128
6	1.908891	-2.184243	3.981150
6	0.780940	-2.465831	4.664857
6	-0.489729	-1.962087	4.220433
6	-0.553891	-1.098046	3.180212
6	0.585978	-0.790409	2.342007
35	0.838840	1.455730	2.853577
1	-1.506554	-0.629048	2.926380
1	-1.392555	-2.246068	4.759549
1	0.825772	-3.052808	5.580815
1	2.869033	-2.527907	4.362388
1	2.756587	-0.781951	0.988178
1	-0.114136	0.608168	-3.685900
1	-0.552994	1.811388	-2.490087
1	-1.487258	-1.113922	-2.481655
1	-2.478464	0.281902	-2.862793



κ -2 aryl copper with bromine on copper

Compound 4.58

RM06 energy: -4781.590401

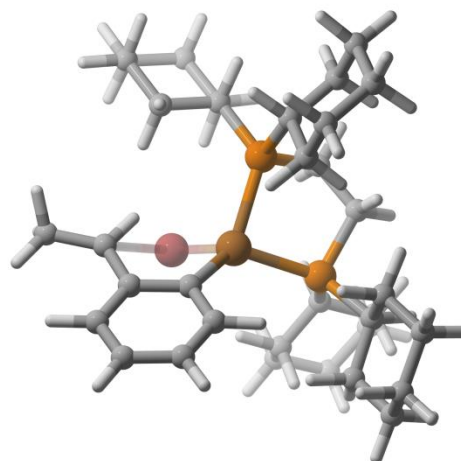
Sum of electronic and thermal Free Energies: -

4780.832421

6	-0.648658	0.494479	-2.470057
6	-0.607159	0.427409	-2.504032
6	0.854725	0.832411	-2.361724
15	1.665768	-0.023053	-0.919833
6	2.146894	-1.645769	-1.698296
1	1.198456	-1.961775	-2.170331
6	2.492291	-2.715479	-0.661818
6	2.651694	-4.073671	-1.329257
6	3.701240	-4.031021	-2.430698
6	3.389612	-2.944722	-3.450166
6	3.216642	-1.583214	-2.785317
1	2.972657	-0.828372	-3.545300
1	4.175882	-1.276644	-2.338433
1	2.460967	-3.203165	-3.984310
1	4.179550	-2.893635	-4.211808
1	3.783866	-5.007530	-2.926648
1	4.687012	-3.829736	-1.979972
1	1.681095	-4.377992	-1.754637
1	2.910935	-4.834731	-0.581158
1	3.431958	-2.456043	-0.151416
1	1.707632	-2.754345	0.103307
6	3.245504	0.949723	-0.731867

1	3.745133	0.980270	-1.715584
6	2.940902	2.385122	-0.299760
6	4.208610	3.188496	-0.047441
6	5.097653	2.511690	0.982014
6	5.433424	1.097026	0.542163
6	4.177460	0.277746	0.277900
1	4.464516	-0.720846	-0.071522
1	3.630931	0.126080	1.224302
1	6.038479	1.138947	-0.378235
1	6.052467	0.591457	1.294928
1	6.013882	3.093873	1.146659
1	4.571526	2.477510	1.950328
1	4.764821	3.295038	-0.993045
1	3.946050	4.205609	0.272783
1	2.330734	2.897384	-1.053833
1	2.335886	2.362206	0.622292
29	-0.067673	-0.085629	0.704411
15	-1.551408	0.708759	-0.935082
6	-3.259444	0.051084	-1.305897
6	-3.277901	-1.220670	-2.150420
6	-4.703305	-1.712012	-2.375310
6	-5.442485	-1.920360	-1.062238
6	-5.431083	-0.649552	-0.226565
6	-4.004127	-0.178080	0.011474
1	-3.464153	-0.955098	0.575635
1	-3.994451	0.731170	0.630877
1	-6.000399	0.137637	-0.747504
1	-5.937676	-0.814623	0.734389
1	-4.951579	-2.728851	-0.496430
1	-6.472483	-2.251927	-1.249695
1	-5.250442	-0.972937	-2.983851
1	-4.687865	-2.641679	-2.959855
1	-2.798647	-1.043655	-3.121780
1	-2.690892	-1.999827	-1.639202
1	-3.783952	0.842953	-1.869603
6	-1.900711	2.541954	-0.876176
6	-2.147064	3.213960	-2.223773
6	-2.549510	4.672655	-2.041591
6	-1.504356	5.437746	-1.243630
6	-1.236652	4.766986	0.095651
6	-0.843750	3.306967	-0.082017
1	-0.682824	2.826017	0.893112
1	0.121664	3.254952	-0.610511
1	-0.453289	5.304762	0.646351

1	-2.144940	4.821783	0.717294
1	-0.567117	5.477971	-1.822791
1	-1.819715	6.479197	-1.096336
1	-2.708371	5.145352	-3.020206
1	-3.516118	4.717952	-1.514529
1	-1.225349	3.172831	-2.826159
1	-2.915749	2.678765	-2.798240
1	-2.840606	2.588914	-0.295888
6	-1.830349	-1.041688	3.135481
6	-2.841420	-1.816902	3.858619
1	-3.151175	-2.664808	3.234907
1	-2.532280	-2.185896	4.838818
1	-3.745950	-1.200271	3.978169
6	-0.640582	-0.502638	3.603376
6	-0.300965	-0.571384	4.989057
6	0.772227	0.128252	5.460374
6	1.528760	0.905649	4.561177
6	1.223927	0.951207	3.214167
6	0.163856	0.217534	2.647490
35	-0.966756	-2.717579	0.634960
1	1.861548	1.557223	2.566956
1	2.381477	1.468257	4.941063
1	1.034732	0.104327	6.514882
1	-0.917732	-1.144532	5.678162
1	-2.082650	-0.762302	2.114846
1	1.406019	0.618374	-3.287285
1	0.932615	1.914000	-2.198371
1	-0.673847	-0.651590	-2.696067
1	-1.075984	0.926155	-3.362991



κ -2 1,4-bromide shift

Compound 4.62

RM06 energy: -4781.5901184

Sum of electronic and thermal Free Energies: -

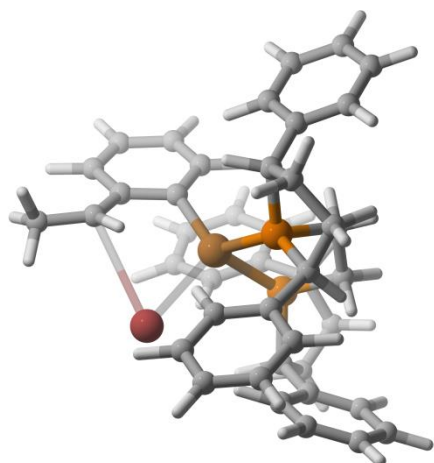
4780.830862

Imaginary frequency: -10.8903

6 -0.570848 0.207979 -2.499086
 6 0.890231 0.620777 -2.372591
 15 1.687982 -0.120898 -0.861383
 6 2.188020 -1.794765 -1.510329
 1 1.239416 -2.156978 -1.947498
 6 2.550887 -2.778213 -0.397236
 6 2.726947 -4.181261 -0.960630
 6 3.768250 -4.209134 -2.070342
 6 3.434277 -3.209481 -3.167694
 6 3.252319 -1.804272 -2.604332
 1 3.001091 -1.108153 -3.416079
 1 4.211795 -1.461730 -2.185462
 1 2.503881 -3.518643 -3.670503
 1 4.217215 -3.208464 -3.938226
 1 3.861082 -5.220107 -2.489546
 1 4.754444 -3.959764 -1.645314
 1 1.757879 -4.530044 -1.353188
 1 3.002522 -4.878661 -0.158009
 1 3.488006 -2.468572 0.088263
 1 1.767448 -2.770135 0.369659
 6 3.259566 0.877849 -0.732497
 1 3.771875 0.837859 -1.709659
 6 2.938038 2.338611 -0.411819
 6 4.192063 3.170479 -0.181688
 6 5.064938 2.572093 0.908184
 6 5.424490 1.136652 0.566576
 6 4.181742 0.287861 0.335511
 1 4.484804 -0.728113 0.058163
 1 3.620988 0.191904 1.281259
 1 6.044930 1.126934 -0.344478
 1 6.036056 0.687714 1.360246
 1 5.970827 3.175074 1.053808
 1 4.518167 2.593570 1.865357

1 4.768820 3.224849 -1.119400
 1 3.910875 4.202519 0.067126
 1 2.348400 2.792467 -1.217925
 1 2.304370 2.377327 0.490224
 29 -0.085070 -0.098528 0.734603
 15 -1.528786 0.640758 -0.972062
 6 -3.255126 0.009462 -1.310953
 6 -3.318665 -1.272106 -2.137195
 6 -4.760824 -1.721158 -2.342135
 6 -5.491653 -1.890629 -1.019099
 6 -5.433834 -0.610305 -0.199443
 6 -3.991299 -0.177965 0.017432
 1 -3.466809 -0.960743 0.588389
 1 -3.947002 0.741154 0.621344
 1 -5.985265 0.186543 -0.724827
 1 -5.935627 -0.748320 0.768198
 1 -5.018512 -2.705794 -0.447942
 1 -6.533096 -2.193895 -1.190780
 1 -5.290963 -0.972739 -2.954139
 1 -4.780820 -2.657963 -2.914916
 1 -2.842154 -1.123308 -3.114843
 1 -2.751973 -2.061268 -1.619744
 1 -3.766110 0.805817 -1.881007
 6 -1.832156 2.482373 -1.079366
 6 -1.973184 3.036027 -2.493444
 6 -2.321605 4.519318 -2.476570
 6 -1.296089 5.314744 -1.683173
 6 -1.157789 4.769232 -0.269689
 6 -0.809751 3.287002 -0.280103
 1 -0.741039 2.894550 0.744250
 1 0.190010 3.154796 -0.722078
 1 -0.397685 5.331942 0.288652
 1 -2.108393 4.913477 0.269194
 1 -0.319564 5.251285 -2.191028
 1 -1.565728 6.378880 -1.662078
 1 -2.394453 4.900331 -3.504075
 1 -3.317274 4.654634 -2.024318
 1 -1.021615 2.903600 -3.032787
 1 -2.729910 2.475739 -3.060122
 1 -2.806416 2.600268 -0.570073
 6 -1.923758 -0.842231 3.231011
 6 -2.986235 -1.488042 4.002813
 1 -3.179477 -2.479159 3.569618
 1 -2.796073 -1.592747 5.072755

1 -3.924479 -0.931277 3.856891
 6 -0.764059 -0.234046 3.669427
 6 -0.482383 -0.106854 5.068208
 6 0.577407 0.641105 5.482232
 6 1.376638 1.287050 4.513573
 6 1.125053 1.155238 3.163654
 6 0.083374 0.351685 2.654181
 35 -0.983453 -2.688836 0.624816
 1 1.792530 1.667463 2.468017
 1 2.220556 1.890544 4.847786
 1 0.802651 0.756991 6.539369
 1 -1.129695 -0.584298 5.800853
 1 -2.079479 -0.799307 2.154092
 1 1.450340 0.340290 -3.274724
 1 0.965379 1.711986 -2.290192
 1 -0.642892 -0.883448 -2.594074
 1 -1.023832 0.631349 -3.405185



Transfer of bromine from copper to benzyl copper
 with (*S,S*)-Ph-BPE ligand setting the *R* stereocenter –
 TS

Compound 4.63

RB3LYP energy: -5079.019292

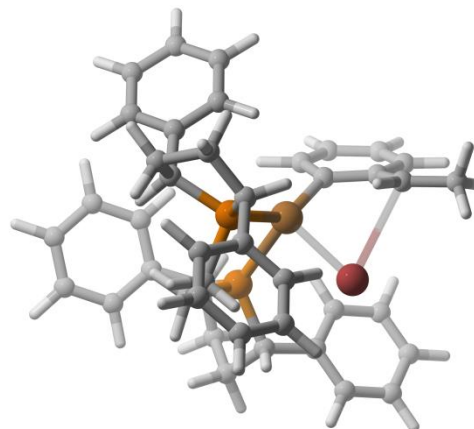
Sum of electronic and thermal Free Energies: -
 5078.357036

Imaginary frequency: -37.7769

6 0.664227 -0.515679 -2.387095
 6 0.763429 0.991737 -2.159884
 15 1.292634 1.313028 -0.406304
 6 3.150959 1.124274 -0.610684
 6 3.598167 2.509579 -1.102387
 6 2.862204 3.551085 -0.272125
 6 1.370157 3.198938 -0.220519
 1 0.977517 3.381643 0.787985
 6 0.457131 3.879701 -1.196657
 6 -0.909266 3.935198 -0.913359
 6 -1.807939 4.472674 -1.821411
 6 -1.356504 4.980518 -3.033051
 6 0.000462 4.948542 -3.319710
 6 0.897834 4.402038 -2.411373
 1 1.956750 4.382873 -2.662404
 1 0.367939 5.351171 -4.261634
 1 -2.058541 5.405275 -3.747159
 1 -2.868471 4.498356 -1.576851
 1 -1.271885 3.526650 0.030478
 1 3.024062 4.570282 -0.644712
 1 3.264233 3.528612 0.749603
 1 4.686297 2.628284 -1.024107
 1 3.345929 2.617658 -2.166014
 1 3.307840 0.379806 -1.405231
 6 3.909618 0.659837 0.612239
 6 5.282236 0.425221 0.485860
 6 6.038641 -0.012355 1.560422
 6 5.434034 -0.235368 2.792625
 6 4.072748 -0.018301 2.929685
 6 3.318539 0.429259 1.850432
 1 2.243224 0.546244 1.979041
 1 3.576710 -0.210777 3.878950
 1 6.023164 -0.586287 3.637188
 1 7.105021 -0.190386 1.435049
 1 5.761997 0.575205 -0.481986
 1 1.453978 1.447570 -2.881785
 1 -0.212894 1.475669 -2.307780
 15 -0.488203 -1.281964 -1.137738
 29 -0.446053 0.195619 0.686115
 6 -2.167056 1.054742 1.163856
 6 -2.609639 1.090947 2.533479
 6 -3.991483 1.223742 2.877105
 6 -4.921183 1.401030 1.895470
 6 -4.499762 1.446017 0.550460

6	-3.171183	1.299074	0.208722
1	-2.908343	1.307194	-0.851759
1	-5.248508	1.569965	-0.232265
1	-5.974272	1.517474	2.140118
1	-4.301212	1.226968	3.920376
6	-1.629597	1.062814	3.514523
6	-1.803759	1.033326	4.971769
1	-1.069323	0.345900	5.406409
1	-1.565675	2.023795	5.388282
1	-2.802134	0.745663	5.307156
1	-0.607678	1.170148	3.156738
35	0.067856	-1.388412	2.662786
6	-1.951433	-1.723821	-2.214878
6	-1.531998	-3.049327	-2.868998
6	-0.891394	-3.922924	-1.795946
6	0.064816	-3.081723	-0.933808
1	-0.119548	-3.276458	0.131794
6	1.539466	-3.220628	-1.167146
6	2.076051	-3.600867	-2.396432
6	3.449593	-3.603540	-2.601481
6	4.311133	-3.219891	-1.582625
6	3.788554	-2.852299	-0.348388
6	2.417121	-2.857194	-0.142566
1	2.009739	-2.555744	0.824723
1	4.452154	-2.556725	0.462604
1	5.386829	-3.215660	-1.746371
1	3.848849	-3.904823	-3.568224
1	1.415166	-3.885406	-3.214362
1	-0.381381	-4.789345	-2.233902
1	-1.679591	-4.331612	-1.151408
1	-2.388950	-3.546844	-3.344027
1	-0.805851	-2.837696	-3.666865
1	-2.042070	-0.935486	-2.976722
6	-3.256373	-1.807323	-1.465264
6	-4.441375	-1.528700	-2.147132
6	-5.669500	-1.581371	-1.504673
6	-5.734914	-1.916076	-0.158359
6	-4.565913	-2.202172	0.531307
6	-3.338838	-2.148739	-0.115526
1	-2.435451	-2.343092	0.462112
1	-4.600697	-2.455094	1.589169
1	-6.695311	-1.950057	0.352113
1	-6.579595	-1.355314	-2.057243
1	-4.394437	-1.258138	-3.202595

1	0.338141	-0.734739	-3.412631
1	1.652337	-0.979194	-2.274912



Transfer of bromine from copper to benzyl copper
with (S,S)-Ph-BPE ligand setting the S stereocenter –
TS

Compound 4.64

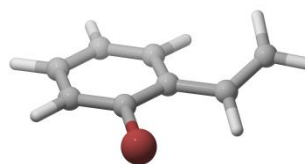
RM06 energy: -5079.0159294

Sum of electronic and thermal Free Energies: -
5078.352705

Imaginary frequency: -4.2147

6	1.668074	1.036731	-1.497599
6	1.052978	-0.184163	-2.176624
15	-0.571422	-0.674074	-1.405593
6	-1.804552	0.036025	-2.616238
6	-1.789094	-0.968533	-3.777493
6	-1.858866	-2.362148	-3.169230
6	-0.865075	-2.463975	-1.999438
1	-1.356261	-2.948066	-1.144410
6	0.418699	-3.192223	-2.253452
6	1.104923	-3.758840	-1.177919
6	2.328455	-4.385999	-1.360308
6	2.895373	-4.456590	-2.626036
6	2.223589	-3.897093	-3.704539
6	0.998205	-3.272931	-3.519632

1	0.492011	-2.831973	-4.376904	6	3.870141	1.738916	1.678864
1	2.656993	-3.947368	-4.701422	6	2.607451	2.330608	1.042130
1	3.853078	-4.951247	-2.772568	1	1.932892	2.709508	1.820908
1	2.836567	-4.829489	-0.506207	6	2.816740	3.435362	0.039975
1	0.669553	-3.702070	-0.178660	6	4.038988	3.677779	-0.585933
1	-1.684288	-3.146353	-3.915535	6	4.172812	4.694561	-1.523663
1	-2.873044	-2.526880	-2.784842	6	3.085860	5.487821	-1.856931
1	-2.621828	-0.784429	-4.469398	6	1.864877	5.262876	-1.233879
1	-0.863204	-0.848876	-4.357360	6	1.734120	4.251915	-0.295525
1	-1.418086	1.013261	-2.937397	1	0.765745	4.068887	0.171763
6	-3.192034	0.228055	-2.056782	1	1.002733	5.879641	-1.479744
6	-4.044873	1.131365	-2.690045	1	3.190286	6.281170	-2.594023
6	-5.336531	1.339219	-2.233698	1	5.138554	4.864918	-1.995807
6	-5.806879	0.636739	-1.131740	1	4.912719	3.078260	-0.338869
6	-4.975451	-0.275324	-0.500277	1	4.638448	2.507277	1.830964
6	-3.680961	-0.476666	-0.960544	1	3.621626	1.355691	2.677734
1	-3.034893	-1.169399	-0.421607	1	5.189710	0.039211	1.302904
1	-5.325275	-0.828797	0.369607	1	4.757528	0.962076	-0.136064
1	-6.818117	0.803422	-0.766428	1	3.329238	-0.848201	-0.427868
1	-5.977569	2.061903	-2.734692	6	3.008972	-1.410842	1.589774
1	-3.675852	1.697401	-3.545793	6	3.642253	-2.640289	1.400984
1	0.949211	-0.006186	-3.255336	6	3.559480	-3.646845	2.351000
1	1.727420	-1.044371	-2.072952	6	2.841378	-3.440390	3.521800
15	1.710227	0.810040	0.340862	6	2.211469	-2.221981	3.727877
29	-0.436494	0.107609	0.834525	6	2.294917	-1.217661	2.771952
6	-1.570327	-0.776716	2.162733	1	1.763882	-0.282314	2.941627
6	-2.602653	-0.070266	2.881376	1	1.639284	-2.048750	4.637103
6	-3.733197	-0.748712	3.438739	1	2.770455	-4.227897	4.268990
6	-3.811121	-2.107667	3.374197	1	4.058258	-4.598819	2.176265
6	-2.765821	-2.827254	2.755189	1	4.205712	-2.808922	0.482729
6	-1.686787	-2.182770	2.189394	1	2.673107	1.227952	-1.898035
1	-0.916059	-2.786112	1.705003	1	1.070243	1.937419	-1.687150
1	-2.829983	-3.914560	2.714459				
1	-4.653701	-2.638616	3.810228				
1	-4.512332	-0.187970	3.951055				
6	-2.414878	1.286022	3.086061				
6	-3.314467	2.241417	3.741134				
1	-2.881387	2.552779	4.703579				
1	-3.361058	3.153567	3.133858				
1	-4.328883	1.876977	3.914245				
1	-1.448353	1.676943	2.773797				
35	-1.545398	2.473786	0.254453				
6	3.177974	-0.345421	0.537895				
6	4.369188	0.585350	0.819140				



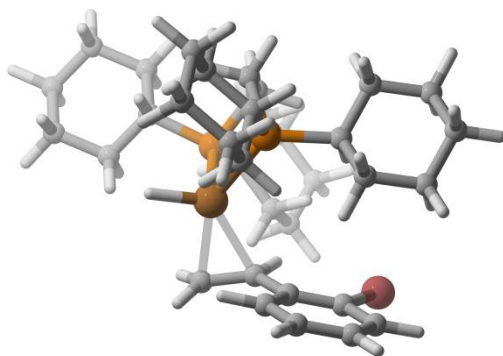
2-bromostyrene

Compound 4.3

RM06 energy: -2882.881315

Sum of electronic and thermal Free Energies: -
2882.792882

6 -2.653897 -1.080356 -0.023764
6 -1.720826 -2.104393 0.071642
6 -0.367800 -1.803615 0.070051
6 0.040759 -0.481561 -0.024571
6 -0.872611 0.574420 -0.117262
6 -2.230825 0.233028 -0.121168
1 -2.965768 1.028374 -0.229276
6 -0.457157 1.977099 -0.222253
6 -1.148943 3.009548 0.249803
1 -2.083780 2.884559 0.794216
1 -0.793083 4.028685 0.123363
1 0.492271 2.168392 -0.722567
35 1.920127 -0.143108 0.013889
1 0.371356 -2.596704 0.146315
1 -2.040699 -3.141125 0.141325
1 -3.716946 -1.308421 -0.034370



π -acid complex between (dCype)CuH and 2-
bromostyrene

Compound 4.16

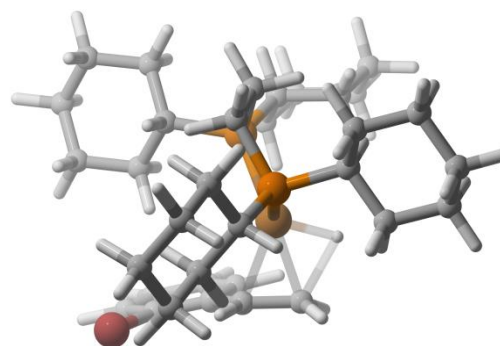
RM06 energy: -4781.5718157

Sum of electronic and thermal Free Energies: -
4780.817536

6 0.861220 1.655967 1.716481
15 -0.659036 1.368299 0.705079
6 -1.656694 0.206626 1.775349
1 -1.170716 -0.772008 1.604130
6 -1.640885 0.487270 3.275379
6 -2.436628 -0.566118 4.039422
6 -3.862900 -0.683241 3.524974
6 -3.879256 -0.957336 2.029410
6 -3.096876 0.106225 1.272928
1 -3.598834 1.077042 1.415076
1 -3.114800 -0.099099 0.196597
1 -3.436207 -1.947195 1.829175
1 -4.910069 -0.999957 1.651608
1 -4.399242 0.258726 3.725369
1 -4.403566 -1.468802 4.069244
1 -1.932579 -1.540464 3.930524
1 -2.430420 -0.333613 5.112708
1 -0.614322 0.513437 3.660612
1 -2.072268 1.483380 3.468578
6 -1.580596 2.988749 0.774114
1 -2.196438 2.974661 1.690072
6 -0.657128 4.204522 0.847179
6 -1.455171 5.502402 0.862506
6 -2.384170 5.610255 -0.335902
6 -3.304122 4.402237 -0.414677
6 -2.502637 3.109385 -0.441975
1 -1.880376 3.082797 -1.351081
1 -3.175478 2.245288 -0.509967
1 -3.947952 4.462495 -1.302231
1 -3.978175 4.397239 0.457859
1 -1.782378 5.665070 -1.257205
1 -2.966597 6.540083 -0.288687
1 -2.051896 5.545335 1.788463
1 -0.769462 6.359375 0.897709
1 0.019907 4.198988 -0.022909
1 -0.021694 4.157580 1.740185
29 0.276272 0.682753 -1.313336
1 0.748424 2.004203 -2.139017
15 2.295186 -0.050391 0.040601
6 1.743848 0.414841 1.751456
1 2.594862 0.575117 2.424966
1 1.187984 -0.444674 2.151861
6 3.681725 1.147222 -0.293734
1 3.174983 2.127692 -0.243125

6	4.856951	1.168178	0.677308
6	5.852453	2.260940	0.304416
6	6.347248	2.088454	-1.123423
6	5.185366	2.049188	-2.104479
6	4.173669	0.973335	-1.730814
1	4.643694	-0.018393	-1.841594
1	3.319527	0.996446	-2.421601
1	4.678195	3.027213	-2.109374
1	5.549955	1.885530	-3.127418
1	6.915566	1.146734	-1.196473
1	7.046852	2.892217	-1.388448
1	6.695851	2.259180	1.007973
1	5.365571	3.244237	0.405731
1	5.375887	0.196900	0.649776
1	4.512260	1.312756	1.710126
6	3.130317	-1.711171	0.285809
1	3.979741	-1.700569	-0.419326
6	3.668467	-2.003140	1.686108
6	4.335407	-3.371218	1.752594
6	3.374314	-4.470891	1.330025
6	2.820028	-4.200517	-0.059462
6	2.176877	-2.824034	-0.152251
1	1.275825	-2.794540	0.486904
1	1.832062	-2.641892	-1.179407
1	3.640151	-4.259671	-0.793343
1	2.094307	-4.973926	-0.345341
1	2.541912	-4.520312	2.051068
1	3.868927	-5.450542	1.362481
1	5.216775	-3.381471	1.091073
1	4.710097	-3.555132	2.768524
1	4.368538	-1.224797	2.010754
1	2.835395	-1.988231	2.405945
1	0.608519	1.987698	2.731820
1	1.402758	2.485996	1.245438
6	-0.641808	-1.202163	-2.078995
6	0.143243	-0.585182	-3.014215
1	-0.278108	-0.024936	-3.844820
1	1.194136	-0.848212	-3.108332
1	-0.177963	-1.925092	-1.412931
6	-2.105395	-1.142406	-2.061913
6	-2.893753	-2.112288	-1.429974
6	-4.280983	-2.064346	-1.438557
6	-4.928048	-1.024800	-2.086469
6	-4.176344	-0.041983	-2.721430

6	-2.796218	-0.104367	-2.706003
1	-2.220986	0.687101	-3.183169
1	-4.671460	0.784272	-3.226561
1	-6.014457	-0.984378	-2.092495
1	-4.853196	-2.838195	-0.932672
35	-2.094637	-3.579163	-0.496297



Hydrometallation

Compound 4.67

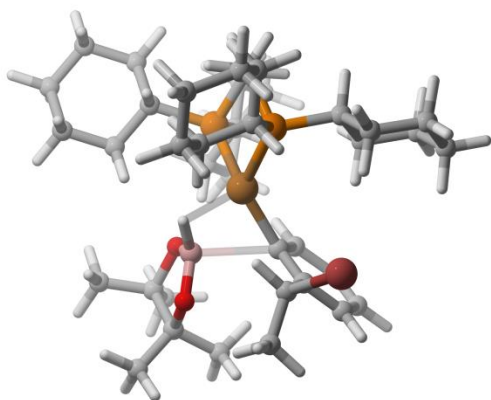
RM06 energy: -4781.557306

Sum of electronic and thermal Free Energies: -
4780.801848

Imaginary frequency: -869.8164

6	0.880692	1.709272	1.871005
15	-0.628295	1.432485	0.829952
6	-1.710101	0.527966	2.047378
1	-1.004902	-0.203581	2.484117
6	-2.273759	1.369532	3.189229
6	-3.026089	0.495829	4.186588
6	-4.123025	-0.307086	3.503311
6	-3.558381	-1.146510	2.366773
6	-2.805920	-0.284972	1.363445
1	-3.517331	0.386748	0.857636
1	-2.364963	-0.907863	0.575899
1	-2.871124	-1.903373	2.779532
1	-4.359552	-1.701334	1.859243
1	-4.879113	0.386689	3.100370
1	-4.643658	-0.942511	4.231830

1	-2.316296	-0.195051	4.669664	6	3.455762	-4.414023	1.536476
1	-3.445758	1.118049	4.988223	6	2.875357	-4.179220	0.150863
1	-1.476185	1.923240	3.703541	6	2.206561	-2.816780	0.045355
1	-2.965406	2.124803	2.785061	1	1.311309	-2.791381	0.691862
6	-1.331294	3.143822	0.649505	1	1.841551	-2.650781	-0.977787
6	-2.701167	3.090349	-0.026541	1	3.684657	-4.239404	-0.594967
6	-3.281414	4.481817	-0.235960	1	2.157537	-4.969293	-0.108411
6	-2.332224	5.362177	-1.032032	1	2.635382	-4.463257	2.271043
6	-0.969577	5.427922	-0.361474	1	3.967231	-5.384625	1.579860
6	-0.384860	4.036840	-0.153891	1	5.275602	-3.299690	1.246897
1	-0.197215	3.565869	-1.132698	1	4.801294	-3.452106	2.935711
1	0.592435	4.116973	0.339856	1	4.413305	-1.139003	2.138231
1	-1.068579	5.930612	0.614329	1	2.899324	-1.916145	2.582557
1	-0.275898	6.038227	-0.954816	1	2.641607	0.650846	2.553544
1	-2.217073	4.945916	-2.045851	1	1.230197	-0.375104	2.345259
1	-2.751054	6.369689	-1.155290	1	0.588200	2.001047	2.888904
1	-3.472136	4.946363	0.745445	1	1.432609	2.559325	1.452358
1	-4.255493	4.408373	-0.737390	29	0.235959	0.358277	-1.005008
1	-2.592250	2.587355	-1.002224	1	0.577494	1.269525	-2.325082
1	-3.401819	2.478648	0.555509	6	-0.650730	-1.213233	-2.209656
1	-1.444180	3.571023	1.660779	6	0.060222	-0.283324	-3.003144
6	1.773266	0.474371	1.907506	1	-0.468399	0.302582	-3.750863
15	2.267043	-0.052029	0.201283	1	1.067314	-0.557569	-3.310697
6	3.575145	1.175792	-0.282105	1	-0.113900	-2.084330	-1.846756
1	3.015912	2.129913	-0.299433	6	-2.091001	-1.219246	-2.093666
6	4.771004	1.336044	0.650300	6	-2.821429	-2.279375	-1.522982
6	5.708887	2.429211	0.151300	6	-4.203433	-2.277267	-1.421410
6	6.170393	2.156849	-1.272083	6	-4.934329	-1.193450	-1.886512
6	4.983833	1.986145	-2.208836	6	-4.251600	-0.118897	-2.448847
6	4.037064	0.902005	-1.713043	6	-2.874283	-0.135012	-2.547121
1	4.553236	-0.071461	-1.754188	1	-2.366239	0.729952	-2.970424
1	3.165248	0.823184	-2.376810	1	-4.801830	0.748683	-2.809356
1	4.433126	2.938026	-2.278002	1	-6.018563	-1.191184	-1.807175
1	5.325204	1.751881	-3.225875	1	-4.710382	-3.126225	-0.968040
1	6.776599	1.236239	-1.284555	35	-1.908832	-3.792068	-0.778891
1	6.826761	2.963626	-1.624401				
1	6.571246	2.520873	0.825007				
1	5.184605	3.397835	0.185343				
1	5.327602	0.386040	0.702158				
1	4.443017	1.563941	1.673503				
6	3.146793	-1.681129	0.451468				
1	3.983412	-1.661222	-0.268144				
6	3.717311	-1.934795	1.845773				
6	4.405883	-3.291635	1.923672				



Hydroboration of aryl copper

Compound 4.75

RM06 energy: -5193.3131562

Sum of electronic and thermal Free Energies: -

5192.369021

Imaginary frequency: -120.0498

6 -0.735927 -2.874707 1.301367
 15 -1.693312 -1.454401 0.597537
 6 -2.726276 -2.305561 -0.703193
 6 -3.738072 -3.341733 -0.222415
 6 -4.384025 -4.064247 -1.398986
 6 -5.036690 -3.080907 -2.358644
 6 -4.037244 -2.037560 -2.833440
 6 -3.387118 -1.315752 -1.661793
 1 -4.154088 -0.738631 -1.121826
 1 -2.656688 -0.578597 -2.013618
 1 -3.254690 -2.529907 -3.433724
 1 -4.524339 -1.311276 -3.498923
 1 -5.477980 -3.611428 -3.212776
 1 -5.870115 -2.574864 -1.844191
 1 -3.614452 -4.641728 -1.936320
 1 -5.119393 -4.793683 -1.033621
 1 -4.524904 -2.836242 0.358345
 1 -3.269624 -4.069697 0.453009
 1 -1.947636 -2.837355 -1.284105
 6 -2.743999 -0.913655 2.037908
 1 -1.986633 -0.383446 2.647920

6 -3.370776 -1.968967 2.948464
 6 -3.994475 -1.302241 4.170736
 6 -5.020152 -0.249295 3.773878
 6 -4.417146 0.784687 2.834581
 6 -3.788104 0.122417 1.617132
 1 -4.579444 -0.382055 1.037899
 1 -3.347867 0.870268 0.944702
 1 -3.646577 1.363201 3.371071
 1 -5.180812 1.508716 2.518516
 1 -5.436799 0.234483 4.667340
 1 -5.865394 -0.743901 3.267534
 1 -3.197893 -0.827649 4.766249
 1 -4.454285 -2.060348 4.818941
 1 -4.150827 -2.524961 2.408465
 1 -2.624162 -2.707720 3.267918
 29 0.081574 -0.000443 -0.098773
 6 0.360896 1.889489 0.580484
 6 1.515641 2.667663 0.373150
 6 1.869543 3.690964 1.257663
 6 1.101046 3.962286 2.377670
 6 -0.053723 3.219485 2.604057
 6 -0.408475 2.219886 1.708563
 1 -1.339209 1.677158 1.889083
 1 -0.675599 3.427215 3.474914
 1 1.395650 4.753265 3.065311
 1 2.772407 4.277136 1.079497
 6 2.343868 2.452283 -0.858189
 35 4.216961 1.890905 -0.371194
 1 1.973102 1.578746 -1.401386
 6 2.467256 3.646673 -1.771620
 1 1.467568 3.908098 -2.136492
 1 2.888604 4.515908 -1.254790
 1 3.098639 3.426529 -2.638679
 15 1.576962 -1.772552 0.125635
 6 0.461281 -3.226794 0.424779
 1 1.031950 -4.052426 0.870112
 1 0.118067 -3.578264 -0.558175
 6 2.635413 -1.797221 1.672619
 6 2.091564 -0.762208 2.662194
 6 2.887960 -0.740681 3.957835
 6 4.359939 -0.479139 3.682818
 6 4.915699 -1.509708 2.713511
 6 4.118986 -1.545889 1.414904
 1 4.232217 -0.584126 0.894443

1	4.537653	-2.312611	0.750953
1	4.885843	-2.505366	3.185606
1	5.971905	-1.304415	2.493316
1	4.470270	0.527099	3.246222
1	4.936048	-0.478202	4.617668
1	2.478315	0.023160	4.632364
1	2.778037	-1.707619	4.476049
1	2.138610	0.233077	2.192429
1	1.027637	-0.943428	2.870941
1	2.522527	-2.803338	2.113394
6	2.641783	-2.349422	-1.281485
6	3.101582	-3.803635	-1.213169
6	3.995192	-4.147657	-2.397728
6	3.278232	-3.883080	-3.713469
6	2.798146	-2.442078	-3.795918
6	1.927017	-2.068117	-2.604458
1	0.983018	-2.639242	-2.642877
1	1.644951	-1.007496	-2.659577
1	3.671636	-1.770803	-3.821190
1	2.249703	-2.270086	-4.731451
1	2.412325	-4.560370	-3.793468
1	3.932597	-4.117663	-4.563226
1	4.912630	-3.538761	-2.351995
1	4.315346	-5.196311	-2.337474
1	2.222618	-4.465991	-1.232618
1	3.618249	-4.007858	-0.265499
1	3.529382	-1.696043	-1.245100
1	-1.370948	-3.758231	1.443578
1	-0.400886	-2.570108	2.302767
1	-0.476821	0.499330	-1.830084
5	-0.943000	1.569343	-1.420503
8	-2.246751	1.659230	-0.948921
6	-2.857647	2.806658	-1.558645
6	-1.629602	3.685704	-1.953141
8	-0.597952	2.699193	-2.149190
6	-1.790051	4.459508	-3.243983
1	-0.883527	5.046304	-3.436213
1	-1.948209	3.803466	-4.104481
1	-2.630863	5.161777	-3.181796
6	-1.199973	4.642160	-0.852558
1	-0.231840	5.084903	-1.112950
1	-1.919113	5.461726	-0.736669
1	-1.087795	4.141465	0.112880
6	-3.805649	3.441150	-0.563926

1	-4.217033	4.382387	-0.950134
1	-4.649969	2.766432	-0.374367
1	-3.318600	3.643097	0.395958
6	-3.641401	2.307067	-2.762470
1	-2.990027	1.816519	-3.495730
1	-4.379166	1.569276	-2.426212
1	-4.181827	3.115906	-3.268110



Benzyl bromide product

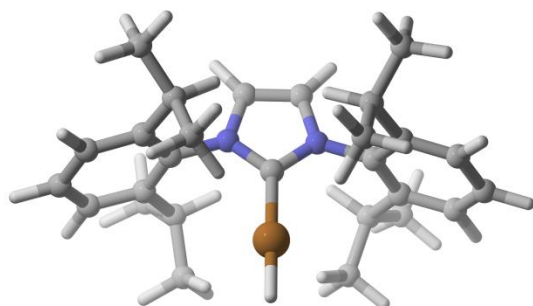
Compound 4.4

RM06 energy: -3294.6411658

Sum of electronic and thermal Free Energies: -
3294.368892

6	1.824469	-0.699921	0.853291
6	1.800762	0.734079	0.416232
6	0.590109	1.360324	0.057351
6	0.636075	2.691353	-0.370698
6	1.825886	3.399667	-0.438908
6	3.009986	2.772269	-0.083066
6	2.992976	1.450317	0.335895
1	3.933999	0.972524	0.598806
1	3.954270	3.310450	-0.133511
1	1.828990	4.435382	-0.770989
1	-0.292633	3.182883	-0.654385
5	-0.817370	0.687916	0.081260
8	-1.163380	-0.436244	0.780201
6	-2.491443	-0.821610	0.341491
6	-3.064834	0.527516	-0.182150
8	-1.868670	1.224526	-0.608742
6	-3.698850	1.372489	0.907301
1	-4.652925	0.953069	1.245006
1	-3.041705	1.477892	1.777946

1 -3.893541 2.375849 0.512971
 6 -4.004039 0.404212 -1.357965
 1 -4.356338 1.397541 -1.657668
 1 -3.521117 -0.054660 -2.225373
 1 -3.259542 -2.262278 -1.096870
 6 -3.237831 -1.422407 1.508099
 1 -4.275514 -1.646160 1.232130
 1 -2.763365 -2.363750 1.806820
 1 -3.247643 -0.760184 2.378126
 6 -2.302145 -1.860771 -0.747035
 1 -4.883996 -0.195042 -1.093957
 1 -1.758688 -1.457577 -1.609025
 1 -1.715859 -2.693835 -0.344803
 6 2.916147 -1.102304 1.810755
 1 2.784873 -2.140944 2.128258
 1 3.919244 -1.012108 1.382822
 1 2.871362 -0.468638 2.706002
 35 1.973710 -1.846692 -0.785882
 1 0.849918 -0.993314 1.242026



IPrCuH

Compound 4.65

RM06 energy: -1356.2579274

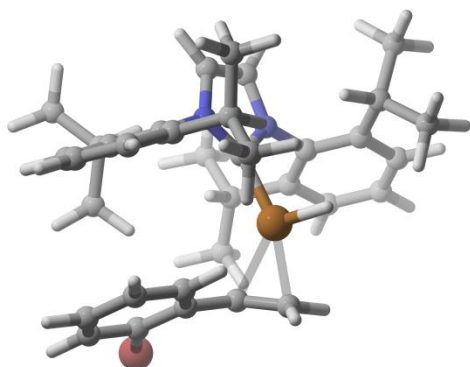
Sum of electronic and thermal Free Energies: -

1355.743382

6 -2.329301 2.531423 -0.385583
 6 -3.059027 1.217724 -0.216553
 6 -4.376683 1.190291 0.231448
 6 -5.025276 -0.012908 0.461719
 6 -4.366629 -1.214574 0.259021

6 -3.046981 -1.239979 -0.185965
 6 -2.424731 -0.011402 -0.424952
 7 -1.064843 -0.011509 -0.877359
 6 -0.673066 -0.021417 -2.205423
 6 0.677047 -0.028092 -2.204542
 7 1.067491 -0.029468 -0.875999
 6 0.000682 -0.016136 -0.043980
 29 -0.001496 0.006271 1.884024
 1 -0.003150 0.031417 3.444268
 6 2.427174 -0.000219 -0.423503
 6 3.019239 1.242864 -0.183935
 6 4.340977 1.249915 0.256662
 6 5.028668 0.064919 0.457942
 6 4.408825 -1.154082 0.228954
 6 3.092367 -1.214010 -0.218285
 6 2.390903 -2.542639 -0.388240
 6 1.920824 -3.051280 0.972224
 1 1.367100 -3.992511 0.867831
 1 2.777794 -3.241738 1.632035
 1 1.271492 -2.323162 1.479014
 6 3.247467 -3.588499 -1.086727
 1 2.652696 -4.486191 -1.292973
 1 3.642019 -3.223887 -2.042560
 1 4.098726 -3.906140 -0.472268
 1 1.500067 -2.383262 -1.011504
 1 4.958441 -2.075300 0.412359
 1 6.058930 0.089703 0.806444
 1 4.835142 2.198981 0.457785
 6 2.260574 2.542262 -0.336966
 6 2.053546 3.197681 1.024084
 1 1.543174 2.520342 1.722359
 1 3.009682 3.485286 1.479592
 1 1.448447 4.107565 0.929543
 6 2.949376 3.489858 -1.309236
 1 3.081752 3.029356 -2.296231
 1 2.356537 4.402626 -1.443217
 1 3.939672 3.795589 -0.949325
 1 1.264997 2.320455 -0.746619
 1 1.396970 -0.034220 -3.011182
 1 -1.391957 -0.021228 -3.013001
 6 -2.317899 -2.555801 -0.340340
 6 -3.050995 -3.509100 -1.273694
 1 -3.204726 -3.064678 -2.264852
 1 -2.476899 -4.433767 -1.407566
 1 -4.034647 -3.792405 -0.879451
 6 -2.079355 -3.191125 1.025291
 1 -3.025867 -3.459174 1.512126
 1 -1.487223 -4.109443 0.929004
 1 -1.542405 -2.509216 1.698647
 1 -1.332927 -2.357895 -0.785293
 1 -4.883620 -2.150706 0.463576
 1 -6.054989 -0.013170 0.812664
 1 -4.901794 2.125544 0.416296
 6 -3.145149 3.568605 -1.143871
 1 -3.499813 3.185487 -2.108126

1	-4.021078	3.901285	-0.573619
1	-2.536897	4.459017	-1.341970
6	-1.912025	3.065902	0.981908
1	-1.275662	2.350973	1.523344
1	-1.362759	4.009980	0.881536
1	-2.792294	3.262064	1.608336
1	-1.413391	2.346301	-0.964947



IPrCuH---2-bromostyrene

Compound 4.66

RM06 energy: -4239.1516096

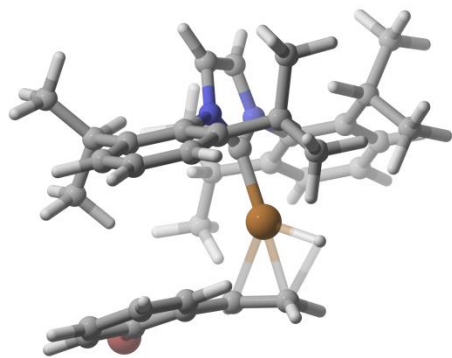
Sum of electronic and thermal Free Energies: -

4238.524983

6	-0.091361	3.778588	-0.723941
6	1.009117	3.210740	0.142466
6	2.296809	3.739970	0.118616
6	3.293142	3.227437	0.935752
6	3.025428	2.173255	1.793503
6	1.750762	1.615208	1.862278
6	0.764925	2.159935	1.031043
7	-0.552775	1.603053	1.115252
6	-1.426463	1.850559	2.166281
6	-2.452839	0.989541	2.022420
7	-2.181059	0.243932	0.884640
6	-1.013622	0.619056	0.305574
29	-0.597398	0.106376	-1.551436
1	-1.469399	1.030603	-2.556849
6	-3.002262	-0.817650	0.385819
6	-4.152520	-0.496913	-0.340992
6	-4.955032	-1.552701	-0.771004
6	-4.607902	-2.865190	-0.502391
6	-3.443145	-3.155373	0.193324
6	-2.610346	-2.138522	0.650325
6	-1.360082	-2.453029	1.444749
6	-0.690652	-3.752900	1.024777

1	0.294337	-3.837467	1.499804
1	-1.270226	-4.635177	1.325027
1	-0.538281	-3.808754	-0.060319
6	-1.673494	-2.479624	2.937934
1	-0.766281	-2.671310	3.525312
1	-2.103549	-1.533715	3.288647
1	-2.393084	-3.276839	3.169144
1	-0.631866	-1.648190	1.266965
1	-3.179632	-4.193389	0.383136
1	-5.247343	-3.675345	-0.846893
1	-5.864311	-1.342825	-1.331459
6	-4.538479	0.932851	-0.647261
6	-4.884013	1.135841	-2.116251
1	-4.081968	0.779898	-2.772187
1	-5.810423	0.618892	-2.397276
1	-5.034411	2.202024	-2.323410
6	-5.696876	1.381247	0.237216
1	-5.465126	1.284791	1.304540
1	-5.948715	2.430901	0.043361
1	-6.597061	0.784041	0.039182
1	-3.674203	1.575054	-0.426344
1	-3.340474	0.824567	2.616475
1	-1.214090	2.596550	2.919562
6	1.473227	0.448958	2.788806
6	1.864815	0.759664	4.226357
1	1.362794	1.662862	4.596692
1	1.588302	-0.071377	4.887219
1	2.946399	0.913174	4.332453
6	2.152921	-0.819416	2.290096
1	3.245766	-0.714691	2.262563
1	1.919964	-1.669574	2.945015
1	1.820025	-1.072370	1.277602
1	0.393165	0.248177	2.783707
1	3.822441	1.772881	2.418486
1	4.294969	3.650964	0.896226
1	2.527284	4.565096	-0.552491
6	-0.709128	4.998648	-0.048083
1	-1.104465	4.750469	0.945550
1	0.034698	5.797520	0.078291
1	-1.535026	5.402110	-0.647240
6	0.373467	4.109730	-2.133804
1	0.864585	3.250369	-2.609497
1	-0.485982	4.380213	-2.758868
1	1.070854	4.957104	-2.157938
1	-0.874308	3.014542	-0.822011
6	3.725819	1.092296	-1.852666
6	4.735016	0.384026	-1.210986
6	4.496283	-0.914851	-0.792510
6	3.254449	-1.493650	-1.016262
6	2.213751	-0.808901	-1.653147
6	2.494221	0.503405	-2.064366
1	1.699151	1.073386	-2.545292
6	0.894631	-1.400110	-1.906350
6	0.140660	-1.095584	-3.021627
1	0.529412	-0.477250	-3.827279

1	-0.723043	-1.709506	-3.271173
1	0.606510	-2.254723	-1.295643
35	3.028792	-3.304525	-0.446750
1	5.278302	-1.483936	-0.295464
1	5.706684	0.839068	-1.033819
1	3.893912	2.116525	-2.179004



IPrCuH hydrocupration TS

Compound 4.68

RM06 energy: -4239.1374913

Sum of electronic and thermal Free Energies: -

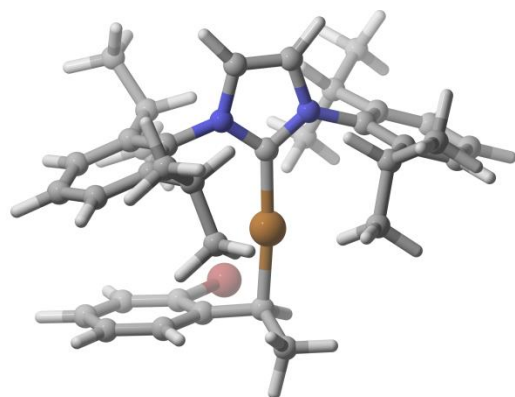
4238.510352

Imaginary Frequency: -778.5422

6	-0.915120	3.582226	-0.723503
6	0.383693	3.302678	0.001339
6	1.523038	4.070627	-0.218941
6	2.695704	3.825219	0.482280
6	2.755095	2.808621	1.418867
6	1.638843	2.016712	1.684400
6	0.474454	2.283430	0.960379
7	-0.676403	1.464769	1.201660
6	-1.530747	1.585266	2.288334
6	-2.452655	0.609197	2.162392
7	-2.136891	-0.081805	1.001912
6	-1.042527	0.438116	0.396394
29	-0.317725	-0.051807	-1.304239
1	-0.760805	0.505917	-2.756940
6	-2.952606	-1.090086	0.397248
6	-4.021840	-0.671753	-0.400944
6	-4.814283	-1.660251	-0.980743
6	-4.537971	-3.001971	-0.775427
6	-3.459386	-3.386239	0.007448
6	-2.637929	-2.437118	0.609559
6	-1.488138	-2.847237	1.502192

6	-0.745496	-4.074269	0.997273
1	0.141613	-4.255404	1.615078
1	-1.359348	-4.982380	1.046581
1	-0.408659	-3.950285	-0.038684
6	-1.990450	-3.078928	2.924237
1	-1.161627	-3.337777	3.594572
1	-2.488085	-2.192205	3.334925
1	-2.713019	-3.905889	2.949941
1	-0.763103	-2.021127	1.529472
1	-3.254003	-4.444898	0.152115
1	-5.167599	-3.760360	-1.236151
1	-5.658505	-1.373548	-1.605320
6	-4.331280	0.790456	-0.638240
6	-4.308459	1.140532	-2.119869
1	-3.347042	0.876250	-2.577236
1	-5.100802	0.623744	-2.676365
1	-4.462895	2.217973	-2.260396
6	-5.661921	1.175236	-0.002788
1	-5.677584	0.952495	1.071146
1	-5.853415	2.248515	-0.124695
1	-6.498649	0.636444	-0.466015
1	-3.551054	1.394535	-0.155831
1	-3.304057	0.341686	2.772557
1	-1.385957	2.344858	3.044210
6	1.715064	0.911521	2.714814
6	2.104759	1.454752	4.083484
1	1.422596	2.246094	4.418596
1	2.084997	0.655760	4.834479
1	3.119844	1.871690	4.078802
6	2.663826	-0.192465	2.270668
1	3.694869	0.172864	2.178266
1	2.665713	-1.016211	2.995834
1	2.370004	-0.601376	1.297421
1	0.720154	0.457071	2.812060
1	3.686012	2.621258	1.951964
1	3.577340	4.432541	0.286693
1	1.499653	4.874131	-0.951415
6	-1.795121	4.513638	0.105241
1	-1.987602	4.118334	1.109771
1	-1.320405	5.497554	0.222437
1	-2.766397	4.668129	-0.382412
6	-0.726284	4.143797	-2.122753
1	-0.059995	3.519805	-2.730319
1	-1.692959	4.191315	-2.637870
1	-0.321252	5.163741	-2.111170
1	-1.445357	2.626674	-0.835673
6	4.077701	1.202456	-1.560170
6	5.030189	0.443249	-0.887678
6	4.728274	-0.873790	-0.572017
6	3.503585	-1.412845	-0.929663
6	2.518119	-0.688552	-1.628569
6	2.861990	0.652293	-1.916423
1	2.134096	1.275382	-2.434449
6	1.254843	-1.249340	-2.050826
6	0.460342	-0.654871	-3.079531

1	0.918976	0.069040	-3.750497
1	-0.238639	-1.313224	-3.591594
1	1.037229	-2.277566	-1.777182
35	3.171164	-3.221421	-0.392301
1	5.449225	-1.488360	-0.036967
1	5.992643	0.865681	-0.609297
1	4.286343	2.240645	-1.812763



Benzyl Copper

Compound 4.69

RM06 energy: -4239.1971545

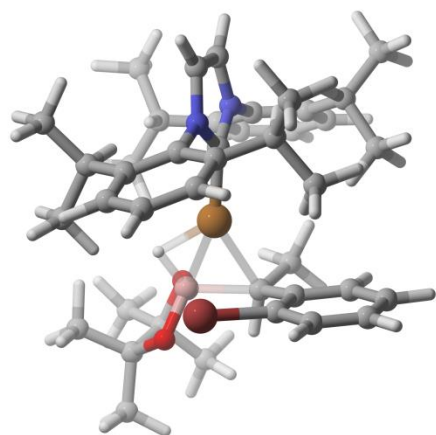
Sum of electronic and thermal Free Energies: -

4238.565074

6	0.529215	3.717140	-0.160750
6	1.480021	2.891078	0.675249
6	2.847093	3.153719	0.653545
6	3.735982	2.358876	1.359462
6	3.277564	1.282335	2.100259
6	1.920583	0.972987	2.147201
6	1.047090	1.796189	1.429798
7	-0.352740	1.489036	1.460513
6	-1.245121	1.948255	2.414317
6	-2.439685	1.393711	2.117074
7	-2.238864	0.607916	0.993400
6	-0.953117	0.660480	0.574873
29	-0.122365	-0.144469	-0.972889
1	0.673049	1.014605	-3.673377
6	-3.255107	-0.166753	0.341454
6	-3.943724	0.402735	-0.732802
6	-4.906984	-0.381441	-1.364694
6	-5.168545	-1.671001	-0.933324
6	-4.473217	-2.207351	0.139527
6	-3.499657	-1.465893	0.802712
6	-2.690934	-2.071465	1.929328

6	-1.494593	-2.831698	1.361010
1	-0.856236	-3.219463	2.165475
1	-1.830794	-3.687792	0.759909
1	-0.872616	-2.203609	0.710412
6	-3.512182	-2.974433	2.837310
1	-2.917348	-3.274270	3.708022
1	-4.415832	-2.475080	3.206077
1	-3.821031	-3.897411	2.331719
1	-2.302999	-1.251807	2.550162
1	-4.688149	-3.223854	0.462385
1	-5.924159	-2.267588	-1.440153
1	-5.457585	0.024004	-2.211020
6	-3.633441	1.792505	-1.243838
6	-2.771149	1.708759	-2.500156
1	-1.827810	1.178772	-2.305689
1	-3.294987	1.170383	-3.301410
1	-2.529313	2.710587	-2.876378
6	-4.888542	2.613023	-1.507641
1	-5.549451	2.644459	-0.633423
1	-4.620203	3.645637	-1.760408
1	-5.468261	2.218630	-2.351044
1	-3.052385	2.321503	-0.474555
1	-3.408559	1.476436	2.589270
1	-0.939653	2.619857	3.204566
6	1.438051	-0.204899	2.964321
6	1.662830	0.037279	4.451802
1	1.172919	0.958013	4.792056
1	1.262218	-0.793582	5.045143
1	2.731619	0.123662	4.686105
6	2.093596	-1.502082	2.511728
1	3.180207	-1.485159	2.666433
1	1.696672	-2.354180	3.077345
1	1.912165	-1.693253	1.447355
1	0.356142	-0.317746	2.806363
1	3.989353	0.664164	2.644802
1	4.801554	2.577705	1.325901
1	3.224587	3.985798	0.062237
6	0.741358	5.214375	0.010527
1	0.694409	5.515866	1.063646
1	1.710586	5.541133	-0.385680
1	-0.031196	5.773184	-0.531073
6	0.655039	3.312187	-1.626065
1	0.483464	2.233689	-1.753857
1	-0.066304	3.854983	-2.249421
1	1.660033	3.538176	-2.006913
1	-0.498332	3.492097	0.158151
6	4.340037	0.397400	-1.658498
6	4.863092	-0.631051	-0.882698
6	4.086194	-1.762237	-0.673304
6	2.817366	-1.847542	-1.223851
6	2.233694	-0.823449	-1.997864
6	3.071864	0.296812	-2.201099
1	2.690948	1.120946	-2.802070
6	0.865624	-0.864943	-2.526553
6	0.616496	-0.074984	-3.801355

1	1.323842	-0.327423	-4.612215
1	-0.391023	-0.279533	-4.184841
1	0.537930	-1.902631	-2.658843
35	1.840335	-3.462627	-0.873112
1	4.470617	-2.589838	-0.080117
1	5.859200	-0.562600	-0.451464
1	4.930082	1.293678	-1.846305



Borylation of Benzyl Copper TS

Compound 4.77

RM06 energy: -4650.868771

Sum of electronic and thermal Free Energies: -

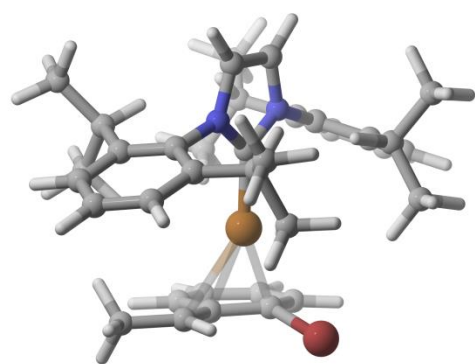
4650.052012

Imaginary Frequency: -81.6358

6	-1.332848	2.814407	2.276105
6	-1.012485	3.394063	0.915072
6	-1.931590	4.199541	0.248315
6	-1.613947	4.785267	-0.967821
6	-0.364503	4.594015	-1.535219
6	0.591709	3.797994	-0.907791
6	0.232361	3.200455	0.304130
7	1.173226	2.323377	0.934854
6	2.167957	2.716018	1.813279
6	2.804881	1.588827	2.194040
7	2.178723	0.541674	1.538721
6	1.162310	0.978971	0.756878
29	-0.299074	0.001618	-0.032851
6	-1.434290	-0.405730	-1.901595
6	-1.748938	1.026651	-2.345415
1	-0.867233	1.679717	-2.305183
1	-2.143360	1.083234	-3.371320

1	-2.508206	1.462934	-1.693800
6	-0.225473	-0.978247	-2.630363
6	0.451901	-2.167250	-2.313848
6	1.445977	-2.711949	-3.116750
6	1.845796	-2.066603	-4.274803
6	1.239073	-0.865533	-4.604768
6	0.231062	-0.351127	-3.804969
1	-0.235879	0.577129	-4.117902
1	1.536730	-0.324020	-5.500777
1	2.630671	-2.492458	-4.895538
1	1.929080	-3.637592	-2.812230
35	0.119341	-3.109567	-0.687421
1	-2.250831	-1.047318	-2.267003
5	-2.303622	-0.792244	-0.262718
1	-1.609558	-0.696869	0.819871
8	-3.387824	0.151619	-0.167003
6	-4.623009	-0.547352	-0.250540
6	-4.212724	-1.986930	0.174830
8	-2.895839	-2.098787	-0.347011
6	-4.157195	-2.144210	1.691178
1	-3.656775	-3.089860	1.932078
1	-3.588011	-1.334831	2.163837
1	-5.155653	-2.167259	2.144891
6	-5.069024	-3.089963	-0.408394
1	-4.719638	-4.063857	-0.044294
1	-6.120078	-2.981817	-0.110625
1	-5.018793	-3.109460	-1.501121
6	-5.135610	-0.475511	-1.683565
1	-6.140647	-0.903000	-1.787790
1	-5.190391	0.576135	-1.989779
1	-4.473249	-0.991213	-2.387505
6	-5.624983	0.129292	0.663869
1	-5.245701	0.231798	1.685264
1	-5.842624	1.138504	0.291902
1	-6.572973	-0.422993	0.699054
6	2.575295	-0.829431	1.663521
6	1.912195	-1.641372	2.589511
6	2.332666	-2.964879	2.693928
6	3.354362	-3.451931	1.895220
6	3.984115	-2.626076	0.978303
6	3.613052	-1.290553	0.847354
6	4.292968	-0.398682	-0.168581
6	3.872772	-0.784636	-1.580668
1	4.315033	-0.107668	-2.322973
1	4.197073	-1.804445	-1.827640
1	2.783267	-0.749618	-1.700497
6	5.808058	-0.411888	-0.021379
1	6.265165	0.307613	-0.711237
1	6.119271	-0.144528	0.996071
1	6.233737	-1.396182	-0.252709
1	3.959315	0.634500	-0.001559
1	4.779678	-3.027365	0.352966
1	3.662447	-4.491549	1.986646
1	1.847049	-3.627793	3.407832
6	0.792692	-1.123317	3.464100

6	-0.448120	-2.005104	3.394390
1	-0.770192	-2.173414	2.358712
1	-0.283707	-2.983950	3.862719
1	-1.282120	-1.527991	3.924905
6	1.268703	-0.957941	4.902605
1	2.126768	-0.277057	4.967756
1	0.469312	-0.550461	5.533748
1	1.574364	-1.919606	5.335186
1	0.502568	-0.129405	3.098749
1	3.648344	1.423625	2.850065
1	2.329142	3.755168	2.064955
6	1.954788	3.597350	-1.535964
6	2.641982	4.928907	-1.811147
1	2.703070	5.548277	-0.907860
1	3.663930	4.765359	-2.173509
1	2.116015	5.510199	-2.578593
6	1.868815	2.753492	-2.801512
1	1.215113	3.216402	-3.553151
1	2.861107	2.633558	-3.254840
1	1.479108	1.750986	-2.591732
1	2.585594	3.047239	-0.824537
1	-0.131048	5.066318	-2.488011
1	-2.349225	5.405055	-1.476730
1	-2.912073	4.371654	0.688162
6	-1.196028	3.895746	3.343512
1	-0.196802	4.348336	3.348077
1	-1.923083	4.702551	3.180438
1	-1.379742	3.481171	4.342453
6	-2.706619	2.160909	2.342221
1	-2.860056	1.431071	1.538146
1	-2.829290	1.643223	3.303105
1	-3.513439	2.903677	2.274900
1	-0.591195	2.035111	2.497424



1,3-Copper Shift TS

Compound 4.70

RM06 energy: -3294.6411658

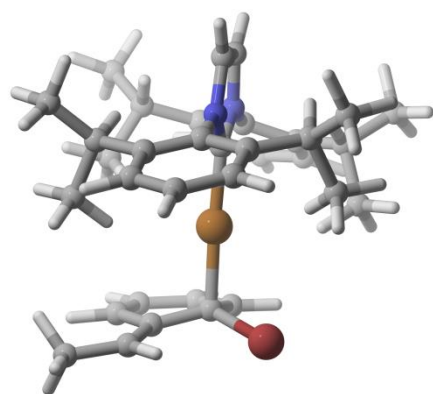
Sum of electronic and thermal Free Energies: -

3294.368892

Imaginary Frequency: -76.2026

6	-2.197204	3.064894	0.908643
6	-2.932237	2.011953	0.109239
6	-4.249110	1.680235	0.415869
6	-4.916899	0.690445	-0.287321
6	-4.282279	0.013823	-1.315868
6	-2.962050	0.300249	-1.654389
6	-2.312587	1.299455	-0.922905
7	-0.938953	1.581073	-1.226059
6	-0.494054	2.522327	-2.138350
6	0.853636	2.429524	-2.158314
7	1.190913	1.426942	-1.265796
6	0.093248	0.896884	-0.680663
29	-0.012753	-0.531881	0.590407
1	3.028609	-0.445090	2.772716
6	2.526328	1.028562	-0.926210
6	3.144470	1.653694	0.159412
6	4.418411	1.212277	0.511487
6	5.038346	0.196115	-0.196206
6	4.400977	-0.400283	-1.274193
6	3.128716	0.004744	-1.665518
6	2.397078	-0.692906	-2.790314
6	1.691992	-1.936587	-2.254321
1	1.070446	-2.406306	-3.027732
1	2.423848	-2.680943	-1.911314
1	1.047319	-1.704210	-1.397410
6	3.298758	-1.054476	-3.960849
1	2.699703	-1.449431	-4.789685
1	3.856572	-0.187973	-4.334959
1	4.025168	-1.831855	-3.694760
1	1.625600	-0.007730	-3.170542
1	4.900572	-1.201923	-1.813899
1	6.031361	-0.138548	0.096994
1	4.930748	1.670084	1.356177
6	2.479818	2.768128	0.937538
6	2.221516	2.366296	2.383928
1	1.584056	1.474634	2.449401
1	3.156836	2.150250	2.916447
1	1.718864	3.177969	2.924249
6	3.296620	4.051777	0.862094
1	3.474935	4.356269	-0.176795
1	2.773682	4.872883	1.367156
1	4.274120	3.938502	1.347597
1	1.503412	2.977150	0.479479
1	1.604242	2.974433	-2.713727
1	-1.178025	3.166309	-2.673002
6	-2.292689	-0.430731	-2.797244
6	-2.835252	0.064130	-4.133141
1	-2.701690	1.146189	-4.253071
1	-2.324115	-0.430742	-4.968096

1	-3.907950	-0.149328	-4.228506
6	-2.439262	-1.940922	-2.680070
1	-3.481849	-2.262257	-2.797378
1	-1.859347	-2.443680	-3.463706
1	-2.081054	-2.309386	-1.710835
1	-1.216769	-0.205294	-2.773275
1	-4.821762	-0.755407	-1.864773
1	-5.945623	0.445134	-0.031742
1	-4.759114	2.201563	1.223311
6	-3.038477	4.307075	1.164825
1	-3.441033	4.729490	0.236583
1	-3.883845	4.101010	1.832758
1	-2.431111	5.081294	1.648201
6	-1.700459	2.471273	2.222958
1	-1.056696	1.598367	2.055437
1	-1.129501	3.212261	2.796792
1	-2.544199	2.144942	2.845721
1	-1.316089	3.380308	0.332227
6	-1.144039	-0.651454	3.827240
6	-2.262989	-1.170632	3.133240
6	-2.025835	-1.967917	2.038069
6	-0.717735	-2.232131	1.584902
6	0.472083	-1.774215	2.309094
6	0.137461	-0.912013	3.440247
1	0.962637	-0.521700	4.034090
6	1.777784	-2.038371	1.946653
6	2.959836	-1.544146	2.718860
1	2.980068	-1.898587	3.764449
1	3.893874	-1.884607	2.257669
1	1.956311	-2.756373	1.149419
35	-0.531397	-3.745916	0.387356
1	-2.856810	-2.419937	1.497956
1	-3.277751	-0.931748	3.440520
1	-1.307157	-0.022905	4.703057



Dearomatized Intermediate

Compound 4.71

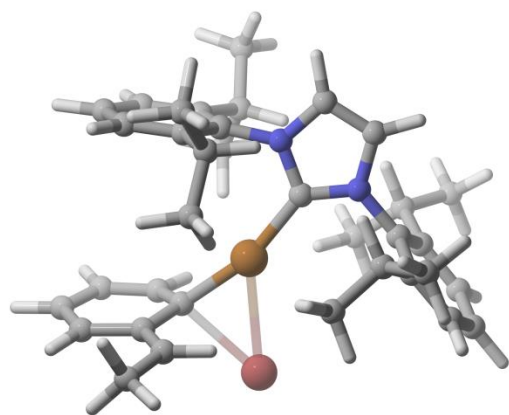
RM06 energy: -4239.1670608

Sum of electronic and thermal Free Energies: -

4238.538492

6	-2.865307	0.081512	2.692244
6	-3.427752	0.314754	1.307868
6	-4.610901	-0.295125	0.902947
6	-5.080285	-0.145817	-0.393515
6	-4.376668	0.615648	-1.311806
6	-3.185640	1.246546	-0.956273
6	-2.736646	1.073494	0.355951
7	-1.489860	1.671033	0.734821
6	-1.345547	2.896682	1.362958
6	-0.018488	3.092369	1.517729
7	0.608066	1.985945	0.968561
6	-0.290308	1.099625	0.486415
29	0.024930	-0.602912	-0.353878
1	2.429612	-3.947040	2.046990
6	2.024962	1.771479	0.923253
6	2.607693	0.963216	1.902868
6	3.978806	0.731024	1.806300
6	4.723891	1.287814	0.781241
6	4.117791	2.091784	-0.172635
6	2.751866	2.352339	-0.122892
6	2.071736	3.155770	-1.209503
6	1.726097	2.241663	-2.381109
1	1.180182	2.790495	-3.159324
1	2.639117	1.832894	-2.835088
1	1.110981	1.389250	-2.065703
6	2.896051	4.343930	-1.681165
1	2.313784	4.951605	-2.383552
1	3.196686	4.991551	-0.849148
1	3.805875	4.031981	-2.208101
1	1.128238	3.553061	-0.809117
1	4.717870	2.513729	-0.975775
1	5.792188	1.090718	0.721198
1	4.470297	0.098304	2.543034
6	1.807588	0.321908	3.015666
6	1.759366	-1.189253	2.821712
1	1.296443	-1.450695	1.860836
1	2.767907	-1.623002	2.831685
1	1.182891	-1.673984	3.619939
6	2.357936	0.684858	4.388872
1	2.408770	1.771070	4.532854
1	1.718431	0.272568	5.178522
1	3.366122	0.280589	4.543181
1	0.773616	0.694538	2.967227
1	0.542077	3.905154	1.957574
1	-2.199873	3.499135	1.638006
6	-2.411546	2.049632	-1.979673
6	-3.275959	3.121414	-2.631743
1	-3.736785	3.780620	-1.885607
1	-2.671310	3.745207	-3.300936
1	-4.081810	2.685315	-3.235167
6	-1.796891	1.131070	-3.031150

1	-2.570583	0.573164	-3.575041
1	-1.224923	1.706784	-3.769405
1	-1.114671	0.400434	-2.575176
1	-1.582716	2.562080	-1.468432
1	-4.758286	0.719627	-2.325933
1	-6.005937	-0.633438	-0.691952
1	-5.170850	-0.905413	1.608429
6	-3.924716	0.093637	3.783142
1	-4.521181	1.013565	3.766388
1	-4.615306	-0.754384	3.700471
1	-3.450709	0.021490	4.769066
6	-2.086242	-1.230175	2.705354
1	-1.295687	-1.233084	1.943537
1	-1.621133	-1.402257	3.684344
1	-2.749450	-2.079561	2.492012
1	-2.154096	0.888290	2.918991
6	-1.439457	-3.817974	0.272526
6	-1.938660	-3.168895	-0.898343
6	-1.052340	-2.483467	-1.678210
6	0.327569	-2.333579	-1.301301
6	0.905129	-3.228017	-0.278807
6	-0.117683	-3.827342	0.576315
1	0.219736	-4.390274	1.445855
6	2.225480	-3.464418	-0.072180
6	2.760624	-4.293459	1.053604
1	2.470293	-5.354714	0.994013
1	3.856618	-4.274155	1.067225
1	2.949172	-3.011096	-0.747378
35	1.508511	-1.867062	-2.805033
1	-1.392919	-1.983804	-2.584703
1	-2.998388	-3.186665	-1.142023
1	-2.137886	-4.334766	0.931190



1,2-bromide shift TS

Compound 4.72

RM06 energy: -4239.1521863

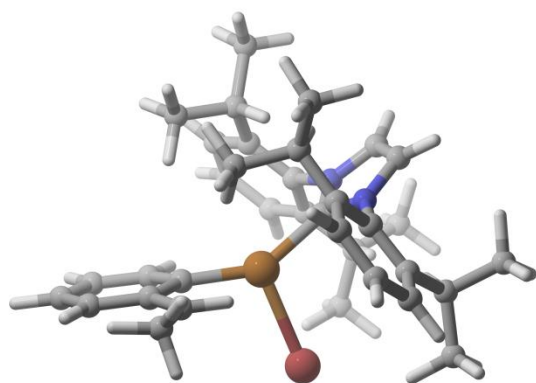
Sum of electronic and thermal Free Energies: -

4238.525913

Imaginary Frequency: -136.5455

6	-1.817315	0.916280	3.001188
6	-2.290340	1.657045	1.770128
6	-3.649970	1.745457	1.481475
6	-4.092689	2.357948	0.320094
6	-3.186039	2.901470	-0.575675
6	-1.815553	2.831663	-0.337156
6	-1.399409	2.202148	0.840559
7	0.007953	2.020888	1.048441
6	0.866518	2.899021	1.683874
6	2.100286	2.355818	1.591850
7	1.956311	1.165583	0.897090
6	0.668020	0.944785	0.557354
29	-0.281240	-0.480293	-0.334462
1	-3.524807	-3.634240	2.157974
6	3.032155	0.284861	0.547926
6	3.323836	-0.784528	1.399032
6	4.364671	-1.632352	1.026786
6	5.070197	-1.417941	-0.145370
6	4.750831	-0.354196	-0.974742
6	3.721767	0.523489	-0.646045
6	3.312133	1.632900	-1.590589
6	2.373953	1.078385	-2.661010
1	2.026584	1.878281	-3.327510
1	2.888269	0.327683	-3.276129
1	1.494759	0.586210	-2.223904
6	4.495064	2.342121	-2.233575
1	4.148030	3.211830	-2.803682
1	5.216357	2.697530	-1.488028
1	5.032004	1.694878	-2.937468
1	2.753475	2.388117	-1.018069
1	5.306368	-0.213037	-1.899519
1	5.876198	-2.094359	-0.422292
1	4.619184	-2.482808	1.656357
6	2.499437	-1.074661	2.633432
6	1.509077	-2.194978	2.327873
1	0.867458	-1.933465	1.475640
1	2.035235	-3.122918	2.067004
1	0.867762	-2.405397	3.193195
6	3.347465	-1.421705	3.848103
1	4.100634	-0.652594	4.055847
1	2.713395	-1.517931	4.737331
1	3.870519	-2.377923	3.724447
1	1.916694	-0.175010	2.883128
1	3.063886	2.695288	1.944788
1	0.515944	3.817280	2.134220
6	-0.837953	3.411975	-1.336084
6	-0.952731	4.930576	-1.385528
1	-0.796738	5.382064	-0.397687
1	-0.207334	5.354542	-2.069370

1	-1.942010	5.246836	-1.740664
6	-1.019957	2.801224	-2.719097
1	-2.016004	3.006896	-3.130628
1	-0.286074	3.211649	-3.423420
1	-0.888033	1.712499	-2.691658
1	0.182759	3.166116	-1.010581
1	-3.550861	3.376870	-1.484519
1	-5.158713	2.407980	0.108105
1	-4.374230	1.314811	2.170224
6	-2.541713	1.358616	4.264672
1	-2.476707	2.442371	4.417320
1	-3.604702	1.088387	4.241643
1	-2.105806	0.869783	5.144164
6	-1.972364	-0.585443	2.785243
1	-1.410016	-0.913733	1.901387
1	-1.617665	-1.151338	3.656515
1	-3.026584	-0.847599	2.620419
1	-0.746180	1.123264	3.141406
6	-4.384249	-1.863873	-1.884433
6	-3.494823	-1.049084	-2.660005
6	-2.170107	-1.001800	-2.358561
6	-1.656591	-1.564205	-1.145769
6	-2.528073	-2.499704	-0.425448
6	-3.913926	-2.594818	-0.851623
1	-4.573845	-3.288560	-0.332927
6	-2.072722	-3.224320	0.631364
6	-2.867380	-4.170908	1.455722
1	-3.519554	-4.821582	0.859208
1	-2.219469	-4.815044	2.057429
1	-1.015385	-3.123850	0.880669
35	0.404430	-2.726575	-2.006681
1	-1.491530	-0.426507	-2.987712
1	-3.889306	-0.466674	-3.491288
1	-5.431901	-1.930835	-2.172650



Copper Bromide Intermediate

Compound 4.73

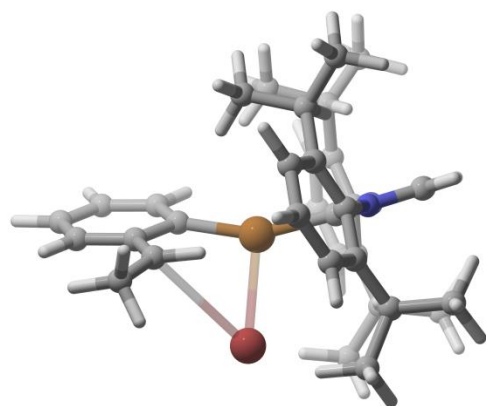
RM06 energy: -4239.1682248

Sum of electronic and thermal Free Energies: -

4238.5399

6	2.348349	0.191679	2.742847
6	2.979066	-0.571215	1.597747
6	4.333627	-0.414457	1.312564
6	4.924691	-1.102948	0.265282
6	4.170905	-1.953540	-0.527606
6	2.812997	-2.145604	-0.283493
6	2.248963	-1.456220	0.795648
7	0.859667	-1.648090	1.085231
6	0.348991	-2.586414	1.968734
6	-0.983297	-2.376758	2.016797
7	-1.246932	-1.318437	1.158826
6	-0.113672	-0.854709	0.576377
29	0.215759	0.589289	-0.698040
1	-1.697253	5.595461	-0.959629
6	-2.525110	-0.702051	0.956778
6	-2.840765	0.430049	1.715961
6	-4.043187	1.077600	1.436048
6	-4.899741	0.594276	0.461251
6	-4.580641	-0.554808	-0.245919
6	-3.384731	-1.228900	-0.014975
6	-3.063588	-2.515891	-0.739870
6	-3.501334	-2.520918	-2.195458
1	-3.130519	-3.426153	-2.691507
1	-4.593853	-2.527208	-2.299586
1	-3.095585	-1.658221	-2.734341
6	-3.696288	-3.690119	0.003762
1	-3.432221	-4.642670	-0.471927
1	-3.379333	-3.739669	1.052095
1	-4.791667	-3.606655	-0.004603
1	-1.972027	-2.647478	-0.727264
1	-5.275468	-0.930089	-0.994238
1	-5.834278	1.112953	0.256165
1	-4.316389	1.971611	1.994264
6	-1.929263	0.956370	2.803790
6	-1.254714	2.254773	2.379017
1	-0.671792	2.111324	1.460768
1	-1.992919	3.048123	2.197401
1	-0.570510	2.613639	3.158645
6	-2.670998	1.131906	4.122664
1	-3.173461	0.207626	4.432267
1	-1.972760	1.415636	4.919200
1	-3.432068	1.920062	4.063046
1	-1.134323	0.216905	2.973175
1	-1.765292	-2.867308	2.578844
1	0.981249	-3.304642	2.472086
6	2.003904	-3.097047	-1.135263
6	2.283648	-4.538140	-0.723502
1	2.070130	-4.710273	0.338741
1	1.669918	-5.235797	-1.306390
1	3.336758	-4.798561	-0.896027
6	2.251902	-2.900040	-2.623258

1 3.275099 -3.171593 -2.913256
 1 1.571422 -3.533097 -3.205763
 1 2.064500 -1.863090 -2.923932
 1 0.938373 -2.893299 -0.959264
 1 4.648838 -2.480068 -1.351187
 1 5.984774 -0.969149 0.059106
 1 4.937261 0.258770 1.919010
 6 2.854685 -0.328994 4.082506
 1 2.668962 -1.404546 4.193411
 1 3.934243 -0.164807 4.195697
 1 2.354814 0.183673 4.913734
 6 2.570624 1.693737 2.618844
 1 2.192910 2.078860 1.662528
 1 2.049221 2.224879 3.425022
 1 3.632953 1.959304 2.691365
 1 1.262867 0.025508 2.713812
 6 2.266199 4.864819 -1.438235
 6 2.995555 3.646910 -1.436538
 6 2.373403 2.438023 -1.242225
 6 0.985228 2.330205 -0.985094
 6 0.253729 3.580867 -1.034274
 6 0.921953 4.836457 -1.254619
 1 0.350332 5.761113 -1.289005
 6 -1.113881 3.508713 -0.914720
 6 -2.107708 4.584165 -0.987025
 1 -2.683910 4.468715 -1.918088
 1 -2.844284 4.464244 -0.181482
 1 -1.519454 2.500007 -0.788077
 35 -0.552769 -0.182740 -2.986240
 1 2.977662 1.528666 -1.256841
 1 4.073928 3.684032 -1.588780
 1 2.786922 5.804842 -1.603290



1,4-Bromide Shift TS

Compound 4.74

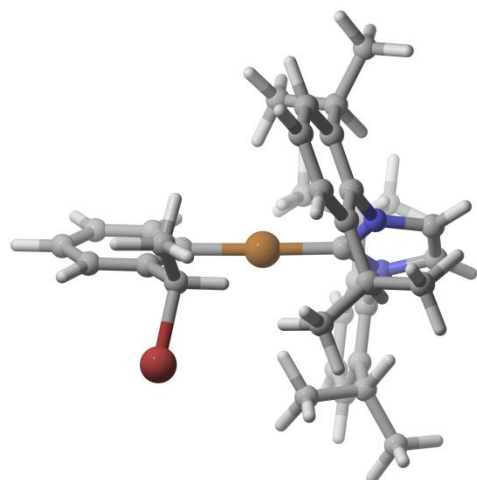
RM06 energy: -4239.1677249

Sum of electronic and thermal Free Energies: -
4238.539388

Imaginary Frequency: -37.2780

6 2.897553 -0.278188 2.529183
 6 3.429847 -0.334099 1.114058
 6 4.617793 0.316322 0.785504
 6 5.103887 0.292479 -0.511276
 6 4.410480 -0.373920 -1.510069
 6 3.213930 -1.031183 -1.234849
 6 2.755618 -1.001345 0.086866
 7 1.516267 -1.645846 0.399629
 6 1.374190 -2.934057 0.890072
 6 0.056734 -3.104207 1.131465
 7 -0.566290 -1.918257 0.771741
 6 0.328070 -1.001066 0.329595
 29 0.070220 0.843459 -0.227013
 1 -3.727790 4.387541 -0.954455
 6 -1.959050 -1.627112 0.941071
 6 -2.350479 -0.922046 2.084493
 6 -3.702499 -0.609232 2.216214
 6 -4.617355 -0.991815 1.249981
 6 -4.201622 -1.696240 0.130127
 6 -2.861417 -2.026357 -0.053152
 6 -2.414554 -2.821213 -1.259503
 6 -3.142067 -2.433178 -2.537434
 1 -2.683455 -2.941744 -3.394404
 1 -4.198382 -2.730884 -2.519734
 1 -3.074584 -1.355350 -2.721503
 6 -2.583781 -4.314942 -0.993405
 1 -2.238484 -4.905440 -1.850939
 1 -2.025256 -4.649615 -0.111548
 1 -3.641492 -4.559844 -0.825634
 1 -1.345973 -2.615273 -1.418814
 1 -4.934609 -1.988557 -0.618639
 1 -5.669214 -0.739383 1.369629
 1 -4.042497 -0.060105 3.092849
 6 -1.377189 -0.517460 3.170513
 6 -1.371878 0.989876 3.389319
 1 -1.114840 1.523296 2.464737
 1 -2.347765 1.356171 3.733359
 1 -0.633116 1.267319 4.151313
 6 -1.681268 -1.259504 4.466489
 1 -1.663253 -2.347265 4.323068
 1 -0.942128 -1.011731 5.238169
 1 -2.670450 -0.992731 4.859953
 1 -0.363749 -0.804095 2.858206
 1 -0.496832 -3.944632 1.526243
 1 2.221315 -3.591635 1.028013
 6 2.469210 -1.782283 -2.315546
 6 3.076754 -3.169551 -2.496352
 1 3.060162 -3.750159 -1.565696
 1 2.528888 -3.740345 -3.256273

1	4.122870	-3.097710	-2.824084
6	2.429193	-1.035087	-3.639561
1	3.420802	-0.956148	-4.103194
1	1.783541	-1.566727	-4.348617
1	2.017958	-0.026293	-3.520519
1	1.427247	-1.906968	-1.988704
1	4.807557	-0.376966	-2.522965
1	6.033637	0.805185	-0.749813
1	5.168321	0.852840	1.556352
6	3.900121	-0.843199	3.526449
1	4.189882	-1.869529	3.268466
1	4.816124	-0.240582	3.572092
1	3.471619	-0.860955	4.535851
6	2.483436	1.139887	2.904470
1	1.723778	1.531965	2.214929
1	2.062953	1.163066	3.918147
1	3.339110	1.827886	2.888186
1	1.996215	-0.903205	2.585098
6	0.046550	5.647712	-0.213448
6	1.235057	4.921461	0.007241
6	1.235423	3.542703	0.094305
6	0.063345	2.776704	-0.052899
6	-1.140256	3.542005	-0.275133
6	-1.127325	4.968919	-0.358586
1	-2.053522	5.516305	-0.520543
6	-2.316566	2.827534	-0.428840
6	-3.659557	3.320691	-0.735544
1	-4.058866	2.750602	-1.584926
1	-4.326516	3.078724	0.105734
1	-2.238235	1.751350	-0.269979
35	-1.101260	0.768525	-2.683775
1	2.188121	3.036572	0.262500
1	2.172478	5.468025	0.108463
1	0.074327	6.733014	-0.265350



Aryl Copper Intermediate

Compound 4.20

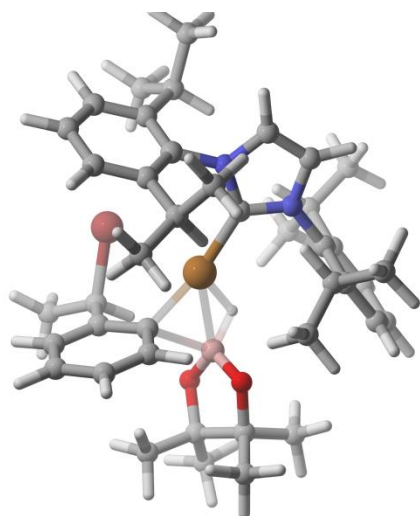
RM06 energy: -4239.2037776

Sum of electronic and thermal Free Energies: -

4238.569977

6	4.058871	0.006578	-1.465881
6	3.869415	-1.014795	-0.366508
6	4.465516	-2.271089	-0.447760
6	4.226129	-3.235561	0.518083
6	3.377419	-2.969672	1.580405
6	2.755187	-1.730161	1.705913
6	3.028301	-0.772427	0.723292
7	2.384871	0.504977	0.823334
6	2.895282	1.604762	1.493174
6	1.966423	2.580064	1.388880
7	0.918800	2.043915	0.660573
6	1.165332	0.764142	0.300076
29	0.054619	-0.380172	-0.786153
1	-4.978881	-0.432851	-0.983580
6	-0.318772	2.703531	0.369454
6	-0.481300	3.305616	-0.882013
6	-1.711275	3.903251	-1.148411
6	-2.724765	3.899840	-0.203278
6	-2.534518	3.292169	1.027817
6	-1.326336	2.673550	1.340203
6	-1.128774	2.019446	2.690767
6	-2.193681	0.971811	2.983493
1	-2.003210	0.492911	3.951946
1	-3.199286	1.407886	3.033255
1	-2.208975	0.181443	2.223336
6	-1.083542	3.069338	3.794793
1	-0.888877	2.602214	4.767813
1	-0.299010	3.815110	3.617847
1	-2.037889	3.606230	3.872564
1	-0.159853	1.500288	2.686091
1	-3.340873	3.296055	1.759345
1	-3.677360	4.373955	-0.430674
1	-1.880172	4.375882	-2.114287
6	0.606862	3.289527	-1.933397
6	0.231490	2.360775	-3.083465
1	0.053414	1.334080	-2.731738
1	-0.681645	2.702050	-3.588390
1	1.031504	2.329282	-3.833409
6	0.922489	4.688118	-2.445888
1	1.187028	5.370733	-1.629481
1	1.767331	4.656679	-3.144246
1	0.074566	5.127037	-2.985985
1	1.524602	2.893126	-1.474987
1	1.946531	3.595667	1.758364
1	3.863551	1.582181	1.972974
6	1.755898	-1.480526	2.814740

6	2.222570	-2.006058	4.164328
1	3.210791	-1.617894	4.437674
1	1.517724	-1.707740	4.949212
1	2.275465	-3.101206	4.183703
6	0.405684	-2.091825	2.443515
1	0.490502	-3.180744	2.327983
1	-0.339102	-1.902193	3.226422
1	0.013960	-1.695008	1.495549
1	1.614343	-0.395132	2.919234
1	3.184896	-3.744634	2.319530
1	4.699274	-4.211801	0.435628
1	5.117896	-2.503988	-1.286769
6	5.502582	0.117409	-1.933160
1	6.188546	0.312285	-1.100507
1	5.842093	-0.794084	-2.440366
1	5.606953	0.939557	-2.650859
6	3.136753	-0.324418	-2.637200
1	2.083237	-0.363157	-2.323844
1	3.228097	0.426862	-3.431806
1	3.390278	-1.301917	-3.068883
1	3.760330	0.991661	-1.078513
6	-2.892140	-2.986787	-3.496714
6	-1.565226	-2.815202	-3.877145
6	-0.710706	-2.064907	-3.078816
6	-1.121941	-1.465642	-1.874587
6	-2.472602	-1.656201	-1.524712
6	-3.342032	-2.401256	-2.324884
1	-4.381362	-2.539633	-2.022777
6	-2.993435	-0.979055	-0.293095
6	-4.091885	0.025113	-0.530857
1	-4.397091	0.526904	0.394324
1	-3.720621	0.791763	-1.226249
1	-2.153059	-0.506210	0.227996
35	-3.628143	-2.323372	1.056252
1	0.324866	-1.946232	-3.408003
1	-1.199389	-3.269093	-4.798042
1	-3.571405	-3.574312	-4.112103



Hydroboration of aryl copper (IPr)

Compound 4.76

RM06 energy: -4650.888767

Sum of electronic and thermal Free Energies: -

4650.075188

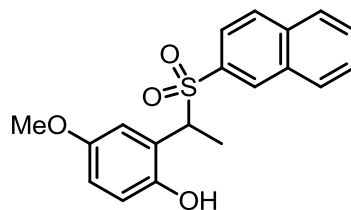
Imaginary Frequency: -155.6621

6	-2.020261	-0.329827	2.975141
6	-2.981025	-0.787045	1.895151
6	-3.692687	-1.976388	2.017777
6	-4.618742	-2.361242	1.058906
6	-4.850214	-1.567093	-0.048685
6	-4.150146	-0.375546	-0.233077
6	-3.229457	-0.009363	0.754041
7	-2.487198	1.206245	0.577887
6	-3.008441	2.483307	0.716675
6	-2.003774	3.341261	0.443709
7	-0.898570	2.563243	0.146044
6	-1.177487	1.242078	0.229907
29	0.109102	-0.194758	0.028025
6	1.035801	-1.896563	0.520892
6	1.377785	-2.012044	1.871726
6	1.389410	-3.230078	2.542198
6	1.054981	-4.388044	1.856069
6	0.725834	-4.315269	0.507857
6	0.718875	-3.090304	-0.159647
6	0.447798	-3.036644	-1.633079
6	0.487448	-4.332329	-2.399154
1	-0.277974	-5.042621	-2.069392
1	0.340429	-4.155572	-3.468641
1	1.469411	-4.807121	-2.271837
1	1.124256	-2.310534	-2.088841
35	-1.346342	-2.189020	-1.962199
1	0.486040	-5.235805	-0.021507
1	1.058242	-5.351862	2.362146
1	1.650455	-3.273621	3.599379
1	1.668415	-1.114363	2.420952
6	0.408226	3.080093	-0.127191
6	1.265107	3.303019	0.953821
6	2.529265	3.816090	0.671964
6	2.914553	4.074251	-0.633049
6	2.048685	3.821442	-1.686782
6	0.772441	3.315781	-1.456496
6	-0.184199	3.058634	-2.599843
6	0.483906	2.382810	-3.787760
1	-0.269835	2.102440	-4.533112
1	1.201353	3.044167	-4.289133
1	1.015027	1.470878	-3.489462
6	-0.855878	4.359660	-3.025851

1	-1.575791	4.183411	-3.834544	1	4.553589	1.210231	-1.385156
1	-1.394778	4.831487	-2.195048	1	4.912735	1.821557	0.233103
1	-0.113924	5.081680	-3.392633	1	6.133610	0.868605	-0.637823
1	-0.972147	2.379533	-2.243501	6	5.188328	-0.561666	1.504962
1	2.374746	4.018330	-2.706184	1	4.702560	-1.357013	2.078535
1	3.909279	4.467154	-0.834930	1	6.229829	-0.854598	1.320485
1	3.227732	4.001323	1.486422	1	5.202646	0.339084	2.131485
6	0.867483	2.977922	2.377035	1	1.566506	0.331502	-1.149071
6	1.814136	1.954781	2.993672				
1	1.922123	1.070757	2.354069				
1	2.820612	2.371172	3.138455				
1	1.447999	1.635613	3.978417				
6	0.776353	4.235062	3.231891				
1	0.060827	4.956831	2.818400				
1	0.450074	3.987006	4.249605				
1	1.747846	4.739423	3.313427				
1	-0.132327	2.521251	2.361264				
1	-1.959017	4.421234	0.446107				
1	-4.037318	2.654287	0.999912				
6	-4.436579	0.493532	-1.439906				
6	-5.746523	1.251592	-1.240171				
1	-5.750353	1.842110	-0.317254				
1	-5.936206	1.934264	-2.077427				
1	-6.592508	0.553880	-1.183397				
6	-4.494496	-0.286704	-2.745675				
1	-5.330304	-0.996272	-2.767609				
1	-4.635485	0.401288	-3.587691				
1	-3.573636	-0.850039	-2.932937				
1	-3.627236	1.231580	-1.539383				
1	-5.580998	-1.882261	-0.790703				
1	-5.164972	-3.294289	1.181246				
1	-3.528013	-2.615649	2.880648				
6	-2.656358	0.762490	3.832333				
1	-2.971382	1.633843	3.247522				
1	-3.542947	0.375413	4.352936				
1	-1.952091	1.116167	4.596304				
6	-1.531586	-1.455266	3.871582				
1	-1.137919	-2.301978	3.298715				
1	-0.725405	-1.091493	4.520648				
1	-2.326253	-1.829048	4.530408				
1	-1.134617	0.095855	2.478383				
5	2.313414	-0.448506	-0.553168				
8	3.097367	0.037852	0.502424				
6	4.462265	-0.269480	0.210372				
6	4.351042	-1.485116	-0.766814				
8	3.086355	-1.255704	-1.402678				
6	5.419317	-1.529364	-1.839882				
1	5.262922	-2.407567	-2.477392				
1	5.397514	-0.645352	-2.483544				
1	6.421047	-1.614634	-1.399719				
6	4.309121	-2.832831	-0.063318				
1	3.574420	-2.857530	0.745747				
1	4.027163	-3.602257	-0.792596				
1	5.288239	-3.108503	0.346586				
6	5.059247	0.969267	-0.442338				

Appendix C: Crystallographic Details and Structures

C.1 Determination of absolute configuration for asymmetric 1,3-halogen migration



Compound C.1. A stirred solution of the sulfide **3.26** synthesized above (22.8 mg, 0.052 mmol, 1.0 equiv) in CH_2Cl_2 (0.65 mL) at 0 °C was treated with *m*CPBA (44.0 mg, 0.255 mmol, 4.9 equiv). The reaction mixture was stirred at 0 °C until complete as judged by TLC (generally 1-1.5 h), then quenched with saturated sodium thiosulfate (2 mL) and saturated sodium bicarbonate (2 mL). The biphasic mixture was separated and the aqueous layers extracted with CH_2Cl_2 (3 x 10 mL). The combined organics were dried over Na_2SO_4 and concentrated *in vacuo*. The residue was purified by column chromatography (0-50% EtOAc/hexane gradient, 10% increments) and isolated as a white solid (16 mg, 90%). ^1H NMR (300 MHz, CDCl_3) δ 8.26 (d, $J = 1.7$ Hz, 1H), 7.89 (m, 3H), 7.62 (m, 3H), 6.86 (d, $J = 8.8$ Hz, 1H), 6.76 (dd, $J = 8.8, 3.0$ Hz, 1H), 6.45 (d, $J = 3.0$ Hz, 1H), 6.40 (s, 1H), 4.82 (q, $J = 7.2$ Hz, 1H), 3.56 (s, 3H), 1.69 (d, $J = 7.2$ Hz, 3H). ^{13}C NMR (75 MHz, CDCl_3) δ 154.33, 149.11, 135.58, 133.06, 132.10, 131.55, 129.64, 126.92, 129.04, 128.14, 127.85, 123.98, 122.31, 119.79, 115.98, 114.72, 55.92, 13.86. HRMS (ESI) m/z calculated for $\text{C}_{19}\text{H}_{22}\text{O}_4\text{N}$ [$\text{M}+\text{NH}_4$] $^+$ calculated 360.1265, found 360.1269.

Preparation of Crystals of C.1. A sample consisting of 16.0 mg of the enantiopure **2a** was dissolved in deuterated chloroform and crystallized at 7 °C slowly overnight. The air-stable crystals were selected using a microscope to choose the best sample for X-ray crystallography.

Data Collection: A colorless crystal with approximate dimensions 0.110 x 0.205 x 0.785 mm³ (block) was selected under oil under ambient conditions and attached to the tip of a X-ray capillary (MiTeGenMicroMount[®]). The crystal was mounted in a stream of cold nitrogen at 100.0(15) K and centered in the X-ray beam by using a video camera. The crystal evaluation and data collection were performed on a three-circle Bruker Quazar SMART APEXII diffractometer with Molybdenum Cu K_α ($\alpha = 1.54184$ Å) radiation and the diffractometer to crystal distance of 4.96 cm. The initial cell constants were obtained from three series of ω scans at different starting angles. Each series consisted of 12 frames collected at intervals of 0.5° in 6° range about ω with the exposure time of 10 seconds per frame. The reflections were successfully indexed by an automated indexing routine built in the APEXII program suite. The final cell constants were calculated from a set of 9893 strong from the actual data collection. The data were collected by using the full sphere data

collection routine to survey the reciprocal space to the extent of a full sphere to a high-resolution of 1.54 Å. A total of 25291 reflection data were harvested by collecting 6 sets of frames with 0.6° scans in ω and ϕ with exposure times of 5/10 sec per frame. These highly redundant datasets were corrected for Lorentz and polarization effects. The absorption correction was based on fitting a function to the empirical transmission surface as sampled by multiple equivalent measurements.^[5,6]

Structure Solution and Refinement: The systematic absences in the diffraction data were consistent for the orthorhombic space groups $P2_12_12_1$. The E-statistics strongly suggested the chiral space group that yielded chemically reasonable and computationally stable results of refinement.^[7,8] The systematic absences in the diffraction data were uniquely consistent for the space group $P2_12_12_1$. A successful solution by the direct methods by using SHELX-2013 provided most non-hydrogen atoms from the E-map. Using Olex2, all non-hydrogen atoms were refined with anisotropic displacement coefficients. All hydrogen atoms were included in the structure factor calculation at idealized positions and were allowed to ride on the neighboring atoms with relative isotropic displacement coefficients.

Table C.1. Crystal data collection and structure solution refinement for Schomaker34 [SCS2037]

Parameter	SCS2037	Parameter	SCS2037
empiric formula	C ₁₉ H ₃₇ O ₄ S	$\rho_{\text{calc.}}$ [g · cm ⁻³]	1.27
MW [g · mol ⁻¹]	342.41	crystal size [mm]	0.158 x 0.437 x 0.437
X-ray lab code	Schomaker34	T [K]	100.0(15)
a [Å]	5.5066(1)	radiation type / λ [nm]	Mo K α / 0.71072
b [Å]	14.1867(2)	μ [mm ⁻¹]	0.227
c [Å]	20.9510(4)	F(000)	945.3
α [°]	90.000(0)°	Reflections collected	25180
β [°]	90.000(0)	Independent reflections	3198 [R _{int} = 0.0534]
γ [°]	90.000(0)°	Data/restraints/parameters	3198/0/221
V [Å ³]	1633(2)	Goof on F ²	0.446
Z	4	Largest diff. peak/hole [eÅ ⁻³]	0.49 / -0.27
crystal system	orthorhombic	Flack <i>x</i> parameter	0.0143(160)
crystal color	colorless	Final $R_I^{[a]}/wR_2^{[b]}$ all data	0.0282/ 0.0757
space group	P2 ₁ 2 ₁ 2 ₁	Final $R_I^{[a]}/wR_2^{[b]}$ I>2s(I)	0.0278/ 0.0731

$$^{[a]} R_I = \frac{\sum |F_o| - |F_c|}{\sum |F_o|}; ^{[b]} wR_2 = \left[\frac{\sum \{w(F_o^2 - F_c^2)^2\}}{\sum \{w(F_o^2)^2\}} \right]^{1/2}$$

The final least-squares refinement of 221 parameters against 3198 data resulted in $R = 0.0278$ (based on F^2 for I>2s) and $wR_2 = 0.0757$ (based on F^2 for all data), respectively. The final structure was visualized using Interactive Molecular Graphics.^[9]

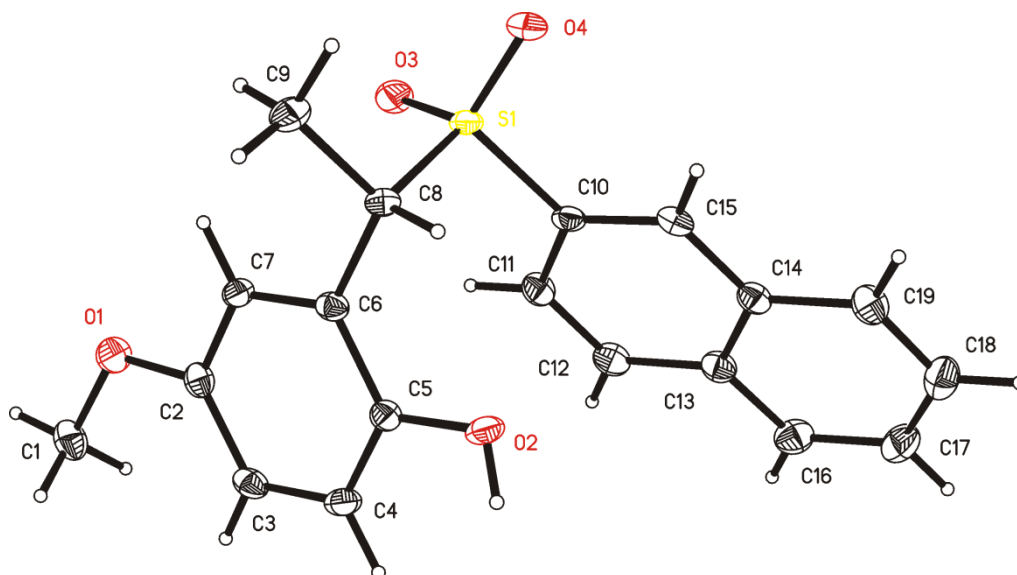
Figure C.1. Thermal-ellipsoid of Schomaker34 [SCS2037] are set with 50 % probability.

Table C.2. Fractional Atomic Coordinates ($\times 10^4$) and Equivalent Isotropic Displacement Parameters ($\text{\AA}^2 \times 10^3$) for Schomaker34 [SCS2037]. U_{eq} is defined as 1/3 of the trace of the orthogonalised U_{ij} tensor.

Atom	x	y	z	U(eq)
C2	4283(3)	3034.9(11)	6049.8(7)	15.9(3)
C3	4794(3)	3957.7(10)	6233.7(7)	16.7(3)
C4	6733(3)	4130.6(10)	6643.7(7)	17.5(3)
C5	8168(3)	3398(1)	6869.9(7)	14.5(3)
C6	7643(3)	2470.2(9)	6691.2(6)	13.6(3)
C7	5694(3)	2303.8(10)	6281.8(7)	14.6(3)
C9	9702(3)	865.0(11)	6493.6(7)	19.3(3)
C8	9100(3)	1662.3(10)	6962.5(7)	13.6(3)
C10	7036(3)	2093.9(10)	8169.9(7)	14.3(3)
C11	5054(3)	2721.2(11)	8095.7(7)	16.9(3)
C12	4828(3)	3456.9(11)	8511.3(7)	19.0(3)
C13	6512(3)	3595.2(10)	9015.2(7)	17.3(3)
C14	8497(3)	2958.7(10)	9081.1(7)	15.9(3)
C15	8724(3)	2202.4(10)	8643.9(7)	15.4(3)
C16	6280(3)	4344.4(11)	9459.0(8)	22.1(3)
C17	7943(3)	4457.6(12)	9941.1(8)	24.3(4)
C18	9918(3)	3826.5(13)	10002.5(8)	24.2(3)
C19	10190(3)	3095.4(11)	9584.6(7)	20.0(3)
C1	1058(3)	3517.7(12)	5365.1(8)	22.9(3)
O1	2409(2)	2777.5(7)	5652.9(5)	20.7(2)
O2	10082(2)	3546.1(8)	7277.0(5)	18.8(2)
O3	5010(2)	885.1(7)	7391.3(5)	19.7(2)
O4	8886(2)	446.8(7)	7919.9(5)	20.0(2)
S1	7383.6(6)	1159.9(2)	7617.45(16)	14.0(1)

Table C.3. Anisotropic Displacement Parameters ($\text{\AA}^2 \times 10^3$) for Schomaker34 [SCS2037]. The Anisotropic displacement factor exponent takes the form: $-2\pi^2[h^2a^2U_{11} + \dots + 2hka \times b \times U_{12}]$

Atom	U ₁₁	U ₂₂	U ₃₃	U ₂₃	U ₁₃	U ₁₂
C2	15.7(7)	19.1(7)	12.9(6)	0.5(5)	2.1(6)	0.6(6)
C3	18.8(7)	14.0(7)	17.4(6)	3.2(6)	2.7(6)	5.2(6)
C4	22.6(7)	10.7(6)	19.1(7)	-0.1(6)	3.6(6)	-1.4(6)
C5	16.6(7)	13.9(6)	13.0(6)	0.8(5)	1.7(5)	-1.6(6)
C6	14.9(7)	11.9(6)	13.9(6)	1.2(5)	3.1(6)	0.6(6)
C7	17.4(7)	11.5(6)	15.0(6)	-1.3(6)	0.8(6)	-0.8(5)
C9	21.5(8)	14.2(7)	22.2(7)	-3.6(6)	1.2(6)	3.3(6)
C8	13.3(6)	10.4(6)	16.9(6)	0.7(6)	0.9(5)	-1.4(5)

C10	17.3(7)	10.0(6)	15.6(6)	2.7(5)	2.1(5)	-1.7(5)
C11	13.9(7)	18.5(7)	18.2(7)	2.3(6)	-1.4(6)	1.2(6)
C12	16.4(7)	17.9(7)	22.8(7)	2.5(6)	0.2(6)	4.7(6)
C13	17.8(7)	16.8(7)	17.2(7)	2.6(6)	2.9(6)	0.2(6)
C14	15.5(7)	16.1(7)	16.1(7)	3.8(6)	1.2(6)	-0.7(6)
C15	15.2(7)	13.4(7)	17.5(7)	4.4(6)	1.5(6)	2.4(6)
C16	21.2(8)	18.2(8)	26.7(8)	-2.2(6)	1.0(7)	2.9(7)
C17	28.2(9)	21.2(7)	23.6(8)	-6.9(6)	1.5(7)	-1.2(7)
C18	22.7(8)	28.1(8)	21.8(7)	-3.0(7)	-2.7(6)	-4.3(7)
C19	17.0(7)	22.9(8)	20.2(7)	1.7(6)	-0.6(6)	2.9(7)
C1	22.6(8)	27.2(8)	18.8(7)	3.6(6)	-3.7(6)	4.3(7)
O1	19.9(5)	20.0(5)	22.1(5)	0.1(4)	-6.2(5)	2.1(5)
O2	22.1(5)	10.3(5)	24.0(5)	0.0(4)	-5.3(5)	-3.5(4)
O3	19.2(5)	16.7(5)	23.2(5)	2.2(4)	-2.2(5)	-6.6(4)
O4	25.6(6)	11.0(5)	23.4(6)	2.2(4)	-2.3(5)	2.8(4)
S1	16.59(17)	8.40(16)	17.01(17)	1.47(12)	-0.90(14)	-0.80(13)

Table C.4. Bond Lengths for Schomaker34 [SCS2037].

Atom	Atom	Length/Å	Atom	Atom	Length/Å
C2	C3	1.393(2)	C10	S1	1.7699(15)
C2	C7	1.384(2)	C11	C12	1.365(2)
C2	O1	1.3745(19)	C12	C13	1.419(2)
C3	C4	1.392(2)	C13	C14	1.425(2)
C4	C5	1.389(2)	C13	C16	1.418(2)
C5	C6	1.399(2)	C14	C15	1.416(2)
C5	O2	1.3719(18)	C14	C19	1.421(2)
C6	C7	1.394(2)	C16	C17	1.373(2)
C6	C8	1.5102(19)	C17	C18	1.415(3)
C9	C8	1.5345(19)	C18	C19	1.366(2)
C8	S1	1.8123(15)	C1	O1	1.4211(19)
C10	C11	1.417(2)	O3	S1	1.4439(11)
C10	C15	1.369(2)	O4	S1	1.4525(11)

Table C.5. Bond Angles for Schomaker34 [SCS2037].

Atom	Atom	Atom	Angle/°	Atom	Atom	Atom	Angle/°
C7	C2	C3	119.57(14)	C11	C12	C13	121.37(14)
O1	C2	C3	124.64(14)	C12	C13	C14	119.08(14)
O1	C2	C7	115.78(13)	C16	C13	C12	122.18(15)

C4	C3	C2	119.40(14)	C16	C13	C14	118.74(14)
C5	C4	C3	121.00(14)	C15	C14	C13	119.02(14)
C4	C5	C6	119.69(14)	C15	C14	C19	121.73(14)
O2	C5	C4	122.31(13)	C19	C14	C13	119.25(14)
O2	C5	C6	117.99(13)	C10	C15	C14	119.64(13)
C5	C6	C8	120.24(13)	C17	C16	C13	120.66(15)
C7	C6	C5	118.89(13)	C16	C17	C18	120.39(15)
C7	C6	C8	120.81(13)	C19	C18	C17	120.43(15)
C2	C7	C6	121.43(13)	C18	C19	C14	120.53(15)
C6	C8	C9	115.67(12)	C2	O1	C1	116.96(12)
C6	C8	S1	107.83(10)	C10	S1	C8	104.90(6)
C9	C8	S1	107.91(10)	O3	S1	C8	109.26(7)
C11	C10	S1	118.81(11)	O3	S1	C10	108.60(7)
C15	C10	C11	122.14(14)	O3	S1	O4	118.08(7)
C15	C10	S1	119.02(11)	O4	S1	C8	107.89(7)
C12	C11	C10	118.74(14)	O4	S1	C10	107.32(7)

Table C.6. Torsion Angles Schomaker34 [SCS2037]

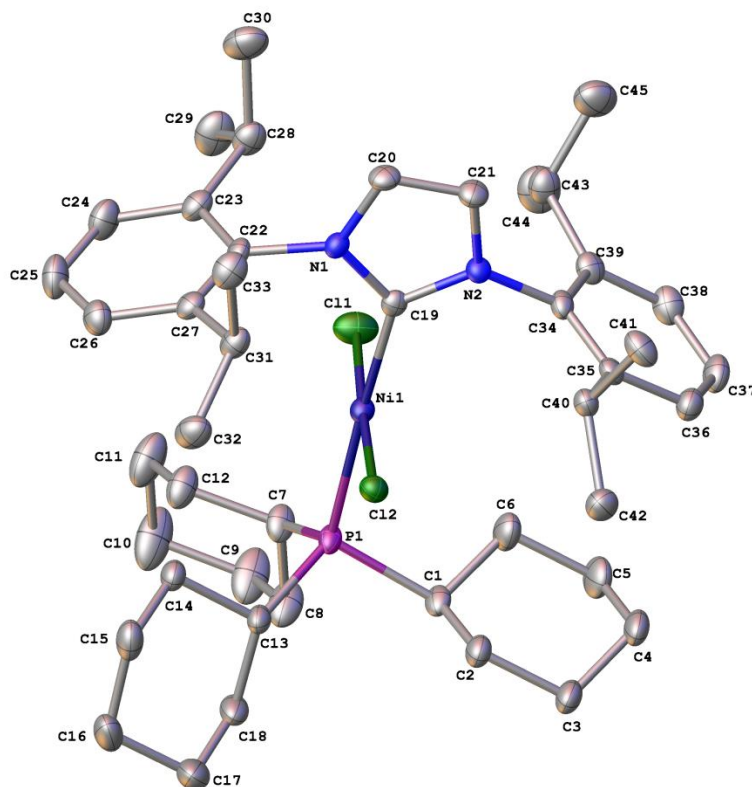
A	B	C	D	Angle/°	A	B	C	D	Angle/°
C2	C3	C4	C5	0.2(2)	C11	C12	C13	C14	0.9(2)
C3	C2	C7	C6	-0.8(2)	C11	C12	C13	C16	-178.74(15)
C3	C2	O1	C1	6.3(2)	C12	C13	C14	C15	-0.4(2)
C3	C4	C5	C6	-0.9(2)	C12	C13	C14	C19	179.93(14)
C3	C4	C5	O2	-179.63(13)	C12	C13	C16	C17	180.00(15)
C4	C5	C6	C7	0.7(2)	C13	C14	C15	C10	-0.3(2)
C4	C5	C6	C8	-176.58(13)	C13	C14	C19	C18	0.2(2)
C5	C6	C7	C2	0.1(2)	C13	C16	C17	C18	0.0(3)
C5	C6	C8	C9	-140.67(14)	C14	C13	C16	C17	0.3(2)
C5	C6	C8	S1	98.46(14)	C15	C10	C11	C12	0.0(2)
C6	C8	S1	C10	-60.13(11)	C15	C10	S1	C8	-91.77(12)
C6	C8	S1	O3	56.14(11)	C15	C10	S1	O3	151.50(11)
C6	C8	S1	O4	-174.31(9)	C15	C10	S1	O4	22.81(14)
C7	C2	C3	C4	0.6(2)	C15	C14	C19	C18	-179.50(15)
C7	C2	O1	C1	-174.85(13)	C16	C13	C14	C15	179.26(14)
C7	C6	C8	C9	42.10(19)	C16	C13	C14	C19	-0.4(2)
C7	C6	C8	S1	-78.77(15)	C16	C17	C18	C19	-0.2(3)
C9	C8	S1	C10	174.27(10)	C17	C18	C19	C14	0.2(3)

C9	C8	S1	O3	-69.47(12)	C19	C14	C15	C10	179.39(14)
C9	C8	S1	O4	60.09(11)	O1	C2	C3	C4	179.42(13)
C8	C6	C7	C2	177.39(13)	O1	C2	C7	C6	-179.70(13)
C10	C11	C12	C13	-0.7(2)	O2	C5	C6	C7	179.50(13)
C11	C10	C15	C14	0.5(2)	O2	C5	C6	C8	2.2(2)
C11	C10	S1	C8	86.46(12)	S1	C10	C11	C12	-178.16(12)
C11	C10	S1	O3	-30.27(13)	S1	C10	C15	C14	178.65(11)
C11	C10	S1	O4	-158.96(11)					

Table C.7. Hydrogen Atom Coordinates ($\text{\AA}\times 10^4$) and Isotropic Displacement Parameters ($\text{\AA}^2\times 10^3$) for Schomaker34 [SCS2037]

Atom	x	y	z	U(eq)
H20	10430(40)	4104(15)	7261(9)	17(5)
H3	3848	4454	6084	20
H4	7073	4746	6768	21
H7	5335	1688	6162	18
H9C	10630	388	6709	29
H9A	10630	1113	6144	29
H9B	8223	595	6335	29
H8	10626	1914	7132	16
H11	3929	2633	7770	20
H12	3543	3876	8463	23
H15	10012	1782	8679	18
H16	4988	4763	9423	26
H17	7770	4952	10229	29
H18	11039	3910	10330	29
H19	11492	2684	9630	24
H1A	-193	3254	5101	34
H1C	2121	3898	5109	34
H1B	335	3901	5691	34

C.2. IPr(Cy₃P)NiCl₂



Crystallographic Experimental Section

Data Collection

A red crystal with approximate dimensions 0.174 x 0.162 x 0.137 mm³ was selected under oil under ambient conditions and attached to the tip of a MiTeGen MicroMount©. The crystal was mounted in a stream of cold nitrogen at 100(1) K and centered in the X-ray beam by using a video camera.

The crystal evaluation and data collection were performed on a Bruker Quazar SMART APEXII diffractometer with Mo K_α ($\lambda = 0.71073 \text{ \AA}$) radiation and the diffractometer to crystal distance of 4.96 cm.

The initial cell constants were obtained from three series of ω scans at different starting angles. Each series consisted of 12 frames collected at intervals of 0.5° in a 6° range about ω with the exposure time of 10 seconds per frame. The reflections were successfully indexed by an automated indexing routine built in the APEXII program suite. The final cell constants were calculated from a set of 9749 strong reflections from the actual data collection.

The data were collected by using the full sphere data collection routine to survey the reciprocal space to the extent of a full sphere to a resolution of 0.70 Å. A total of 221546 data were harvested by collecting 6 sets of frames with 0.5° scans in ω and ϕ with exposure times of 20 sec per frame. These highly redundant datasets were corrected for Lorentz and polarization effects. The absorption correction was based on fitting a function to the empirical transmission surface as sampled by multiple equivalent measurements. [1]

Structure Solution and Refinement

The systematic absences in the diffraction data were consistent for the space groups $P1$ and $P\bar{1}$. The E -statistics strongly suggested the centrosymmetric space group $P\bar{1}$ that yielded chemically reasonable and computationally stable results of refinement [2-8].

A successful solution by the direct methods provided most non-hydrogen atoms from the E -map. The remaining non-hydrogen atoms were located in an alternating series of least-squares cycles and difference Fourier maps. All non-hydrogen atoms except those of toluene molecules C25S and C32S were refined with anisotropic displacement coefficients. All hydrogen atoms were included in the structure factor calculation at idealized positions and were allowed to ride on the neighboring atoms with relative isotropic displacement coefficients.

The asymmetric unit consists of four molecules of the Ni complex shown in Figure 1, 0.69 molecules of PCy₃, and 1.26 molecules of toluene. The PCy₃ and toluene are located in two solvent accessible voids. The first void is filled with one partially occupied molecule of toluene. The second void is occupied by either free PCy₃ or toluene.

Within the four Ni complexes, cyclohexyl rings C1B, C1C, and C13C are each disordered over two positions (major components: 54.9(18)%, 67.5(11)%, 63.2(6)%).

Complex Ni1 can be overlaid with complexes Ni1A and Ni1C with inversion (RMSD: 0.197 Å, 0.222 Å) and with complex Ni1B without inversion (RMSD = 0.430 Å). The four complexes mostly differ in the conformation of the Cy rings of the PCy₃ ligand.

The first solvent accessible void contains toluene. The toluene molecule is disordered over two positions (occupancies: 51.7(4)%, 39.4(4)%).

The second solvent accessible void is occupied by either free PCy₃ or toluene.that is compositionally disordered with two toluene molecules (PCy₃ occupancy: 69.27(16)%.) Cyclohexyl ring C13S of the free PCy₃ is

disordered over two positions (occupancies: 56.6(2)%, 12.7(2)%). The two toluene positions were refined with idealized geometries. (occupancies: 18.4(3)%, 16.7(3)%). [9]

All of the toluene molecules were refined with idealized geometries. [9] All disordered components were refined with bond distance and thermal parameter restraints in order to ensure a chemically reasonable and computationally stable refinement.

The final least-squares refinement of 2392 parameters against 41461 data resulted in residuals R (based on F^2 for $I \geq 2\sigma$) and wR (based on F^2 for all data) of 0.0402 and 0.1062, respectively. The final difference Fourier map was featureless.

Summary

Crystal Data for $C_{45}H_{69}N_2PNiCl_2$, 0.173($C_{18}H_{33}P$), 0.315 (C_7H_8) ($M = 876.07$ g/mol): triclinic, space group $P\bar{1}$ (no. 2), $a = 21.649(6)$ Å, $b = 21.671(6)$ Å, $c = 22.852(7)$ Å, $\alpha = 71.100(7)^\circ$, $\beta = 79.041(5)^\circ$, $\gamma = 88.030(17)^\circ$, $V = 9954(5)$ Å³, $Z = 8$, $T = 100.0$ K, $\mu(\text{MoK}\alpha) = 0.568$ mm⁻¹, $D_{\text{calc}} = 1.169$ g/cm³, 221546 reflections measured ($2.272^\circ \leq 2\theta \leq 53.152^\circ$), 41461 unique ($R_{\text{int}} = 0.0532$, $R_{\text{sigma}} = 0.0396$) which were used in all calculations. The final R_1 was 0.0402 ($I > 2\sigma(I)$) and wR_2 was 0.1062 (all data).

References

1. Bruker-AXS (2014). *APEX2*. Version 2014.11-0. Madison, Wisconsin, USA.
2. Krause, L., Herbst-Irmer, R., Sheldrick, G. M. & Stalke, D. (2015). *J. Appl. Cryst.* 48. *in print*.
3. Sheldrick, G. M. (2013b). *XPREP*. Version 2013/1. Georg-August-Universität Göttingen, Göttingen, Germany.
4. Sheldrick, G. M. (2013a). The *SHELX* homepage, <http://shelx.uni-ac.gwdg.de/SHELX/>.
5. Sheldrick, G. M. (2015a). *Acta Cryst. A*, 71, 3-8.
6. Sheldrick, G. M. (2015b). *Acta Cryst. C*, 71, 3-8.
7. Dolomanov, O. V., Bourhis, L. J., Gildea, R. J., Howard, J. A. K. & Puschmann, H. (2009). *J. Appl. Crystallogr.* 42, 339-341.
8. Guzei, I. A. (2007-2013). Programs *Gn*. University of Wisconsin-Madison, Madison, Wisconsin, USA.
9. Guzei, I. A. (2014). *J. Appl. Cryst.* 47, 806-809.

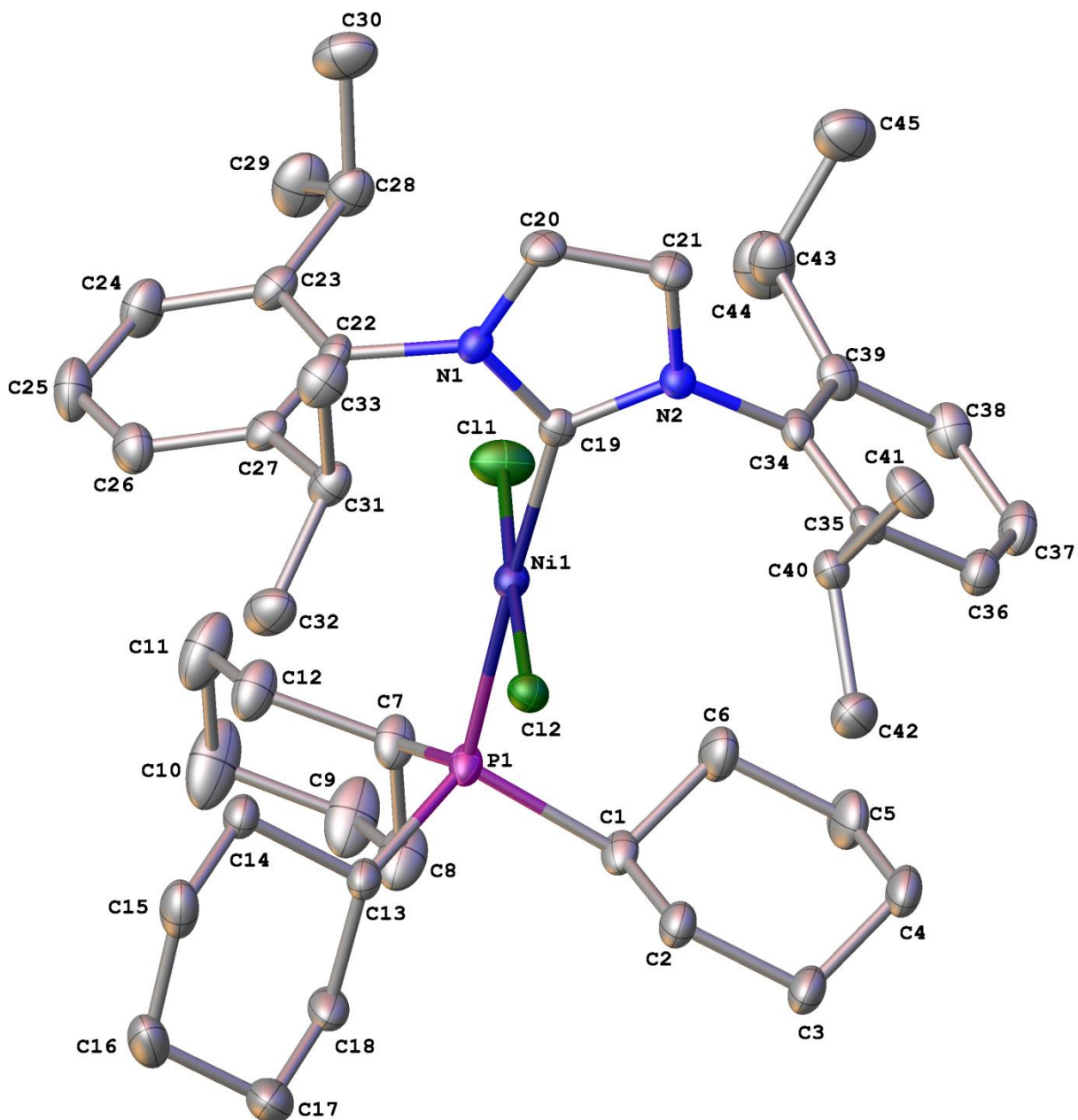


Figure 1. A molecular drawing of the nickel complex of Schomaker52. All atoms are drawn as 50% thermal probability ellipsoids. All H atoms are omitted for clarity.

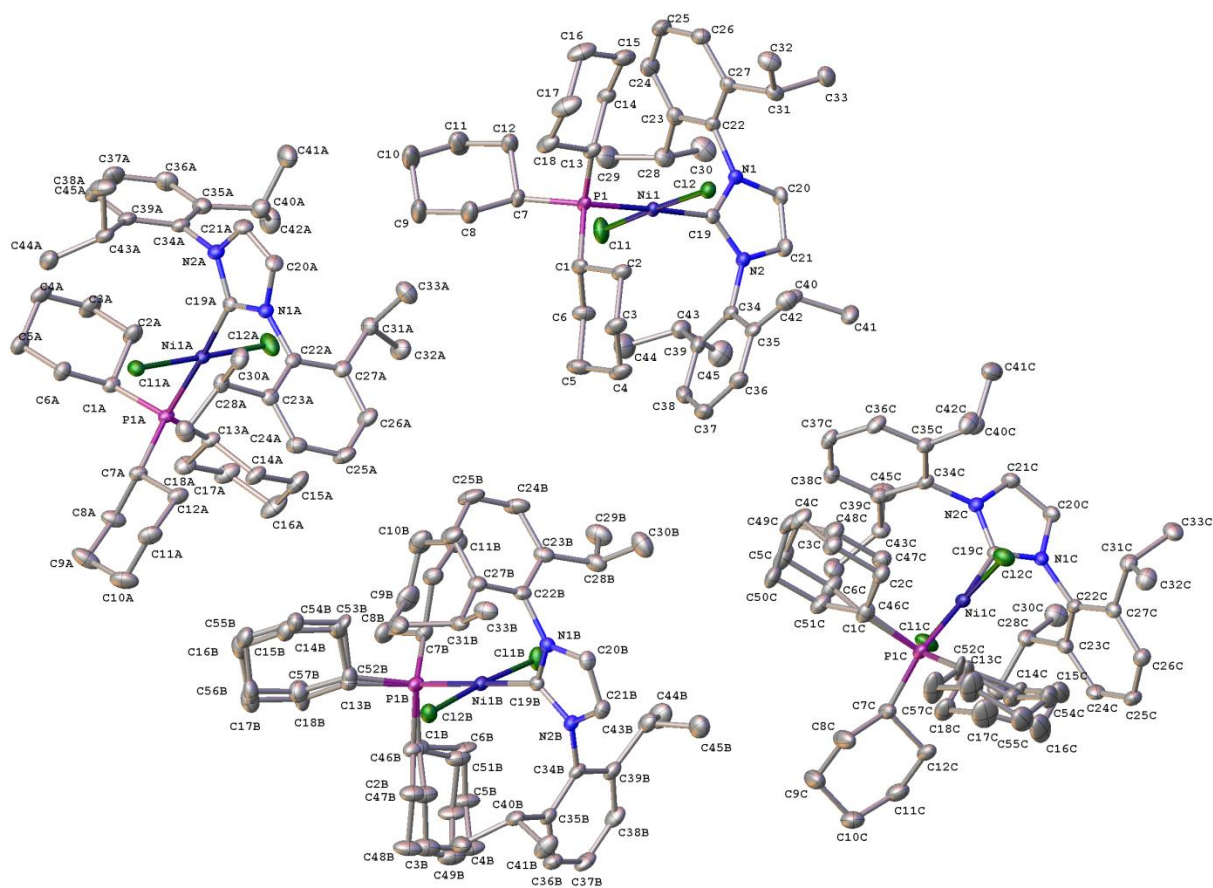


Figure 2. The four symmetry independent Ni molecules of Schomaker52, including all disordered components. All atoms are drawn as 50% thermal probability ellipsoids. All H atoms are omitted for clarity.

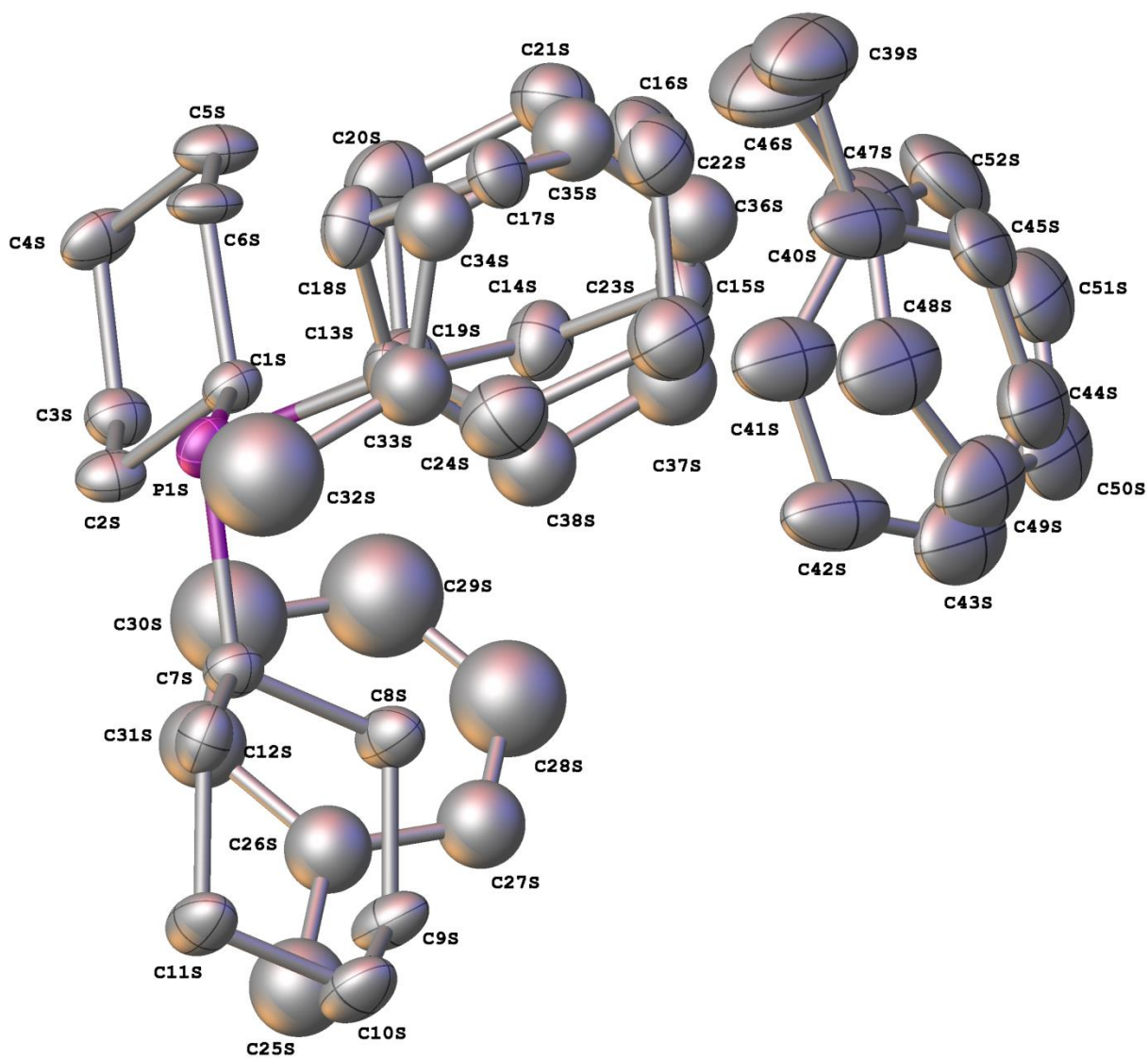


Figure 3. The solvent molecules of Schomaker52, including all disordered components. All atoms are drawn as thermal probability ellipsoids. All H atoms are omitted for clarity.

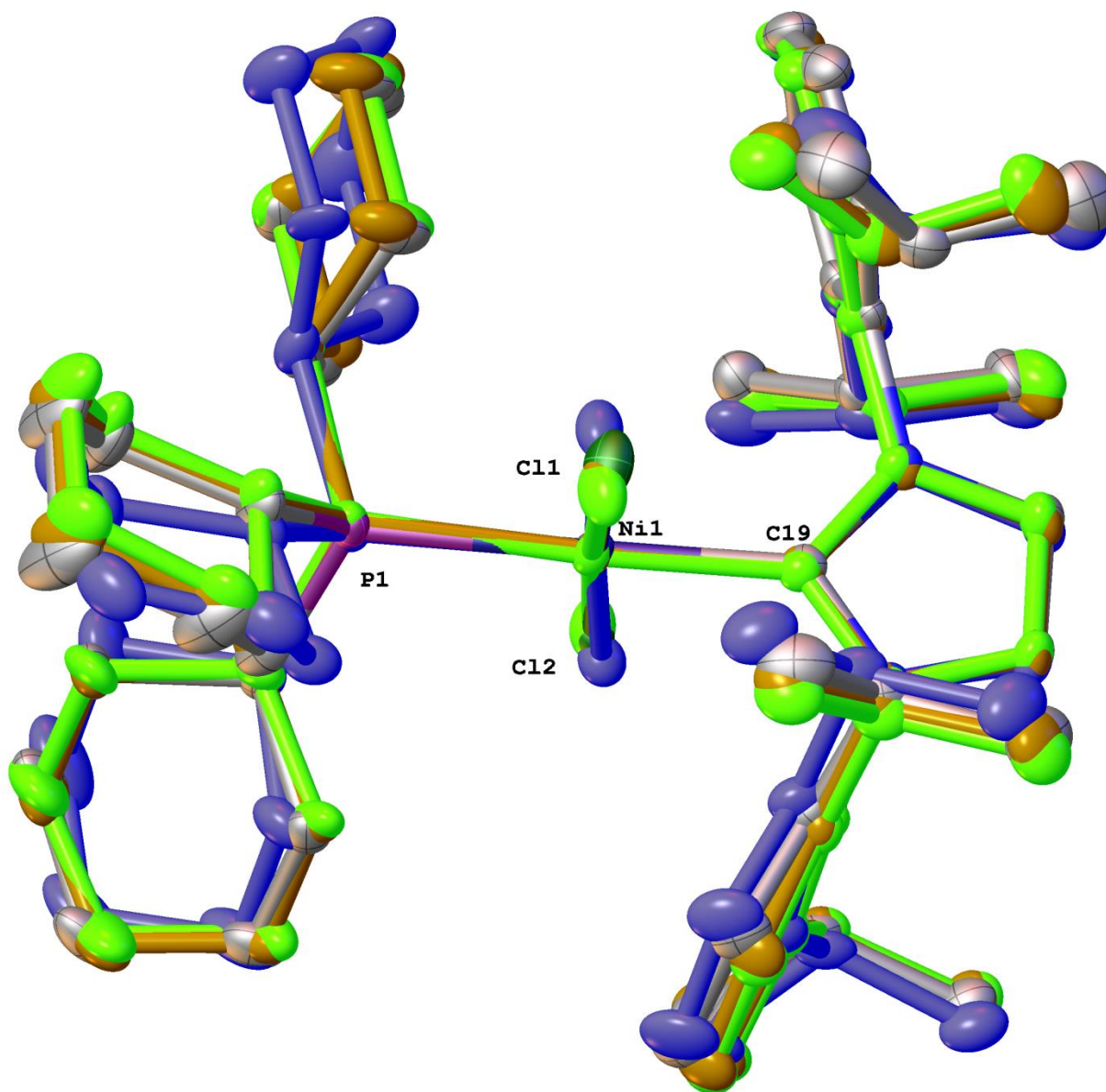


Figure 4. The overlay diagram of Schomaker52. Ni1 is shown in gray, Ni1A is shown in orange, Ni1B is shown in purple, Ni1C is shown in light green. All atoms are drawn as 50% thermal probability ellipsoids. All H atoms are omitted for clarity.

Table 1. Crystal data and structure refinement for Schomaker52.

Identification code	Schomaker52
Empirical formula	C ₄₅ H ₆₉ N ₂ PNiCl ₂ , 0.173(C ₁₈ H ₃₃ P), 0.315 (C ₇ H ₈)
Formula weight	876.07
Temperature/K	100.0
Crystal system	triclinic
Space group	$P\bar{1}$
a/Å	21.649(6)
b/Å	21.671(6)
c/Å	22.852(7)
α /°	71.100(7)
β /°	79.041(5)
γ /°	88.030(17)
Volume/Å ³	9954(5)
Z	8
$\rho_{\text{calc}}/\text{cm}^3$	1.169
μ/mm^{-1}	0.568
F(000)	3782.0
Crystal size/mm ³	0.174 × 0.162 × 0.137
Radiation	MoK α ($\lambda = 0.71073$)
2 θ range for data collection/°	2.272 to 53.152
Index ranges	-27 ≤ h ≤ 27, -27 ≤ k ≤ 27, -28 ≤ l ≤ 28
Reflections collected	221546
Independent reflections	41461 [R _{int} = 0.0532, R _{sigma} = 0.0396]
Data/restraints/parameters	41461/1740/2392
Goodness-of-fit on F ²	1.024
Final R indexes [I ≥ 2 σ (I)]	R ₁ = 0.0402, wR ₂ = 0.0972
Final R indexes [all data]	R ₁ = 0.0570, wR ₂ = 0.1062
Largest diff. peak/hole / e Å ⁻³	0.81/-0.55

Table 2 Fractional Atomic Coordinates ($\times 10^4$) and Equivalent Isotropic Displacement Parameters ($\text{\AA}^2 \times 10^3$) for Schomaker52. U_{eq} is defined as 1/3 of the trace of the orthogonalised U_{ij} tensor.

Atom	x	y	z	U(eq)
Ni1	3425.1(2)	3133.7(2)	7503.1(2)	15.03(6)

C11	3674.1(3)	2122.1(3)	7700.2(3)	30.47(13)
C12	3150.6(2)	4153.2(2)	7270.4(2)	18.74(10)
N1	2098.0(8)	2757.9(8)	7658.0(8)	15.5(4)
N2	2570.8(8)	2957.7(9)	6700.4(8)	16.2(4)
P1	4328.4(3)	3403.3(3)	7728.8(2)	17.90(11)
C1	4898.8(9)	3756.6(10)	6982.5(8)	21.5(5)
C2	4775(1)	4457.8(10)	6607.7(9)	24.7(5)
C3	5257.7(11)	4696.5(11)	5990.6(9)	28.4(5)
C4	5252.6(12)	4255.3(11)	5595.2(10)	30.6(6)
C5	5380.7(12)	3555.7(12)	5960.8(10)	34.4(6)
C6	4908.1(12)	3308.4(11)	6579.2(10)	29.7(5)
C7	4752.2(10)	2718.6(12)	8181(1)	25.0(5)
C8	5453.4(11)	2833.1(15)	8167.0(12)	37.8(7)
C9	5743.5(13)	2202.7(16)	8504.0(13)	46.0(8)
C10	5391.0(14)	1903.6(18)	9180.1(13)	52.7(9)
C11	4697.6(13)	1797.0(15)	9195.9(13)	44.7(7)
C12	4400.2(11)	2425.8(13)	8864.4(11)	30.4(6)
C13	4230(1)	4034.4(11)	8115.7(10)	20.8(5)
C14	3685.3(10)	3883.6(11)	8686.6(10)	22.2(5)
C15	3548.4(12)	4486.6(12)	8887.9(11)	30.8(6)
C16	4131.9(14)	4743.5(14)	9027.3(12)	37.9(6)
C17	4674.4(14)	4871.6(14)	8466.0(12)	41.0(7)
C18	4816.6(11)	4261.6(13)	8282.2(11)	30.0(6)
C19	2670.1(10)	2932(1)	7276.7(9)	15.4(4)
C20	1648.7(10)	2683.7(11)	7323.8(10)	20.0(4)
C21	1946.3(10)	2812.4(11)	6724(1)	21.3(5)
C22	2004.7(10)	2622.0(11)	8334.9(9)	17.4(4)
C23	2098.4(10)	1983.3(11)	8706.8(10)	21.9(5)
C24	2065.0(12)	1876.9(12)	9345.7(11)	29.4(5)
C25	1943.8(12)	2377.9(13)	9598.6(11)	31.1(6)
C26	1822.5(11)	2995.3(12)	9222.8(10)	25.3(5)
C27	1842.6(10)	3131.4(11)	8579.6(10)	19.1(4)
C28	2191.0(11)	1421.8(11)	8439.1(11)	26.3(5)
C29	2606.7(14)	890.9(13)	8766.4(13)	37.6(6)
C30	1546.6(13)	1124.4(13)	8469.5(14)	37.3(6)
C31	1647.4(10)	3787.7(11)	8178.3(10)	21.6(5)

C32	1801.2(12)	4356.5(12)	8389.1(12)	29.9(5)
C33	937.8(11)	3759.8(12)	8180.0(11)	27.7(5)
C34	3064.8(10)	3064.1(11)	6148.8(9)	17.9(4)
C35	3201.4(10)	3698.8(11)	5736.1(9)	18.4(4)
C36	3691.8(11)	3779.5(12)	5222.2(10)	24.0(5)
C37	4030.3(11)	3253.8(12)	5134.5(10)	26.8(5)
C38	3869.2(11)	2630.0(12)	5536.5(11)	26.3(5)
C39	3375.7(10)	2516.1(11)	6051(1)	21.1(5)
C40	2813.6(10)	4279.4(11)	5806.3(10)	19.6(4)
C41	2310.8(11)	4399.6(12)	5393.6(11)	27.6(5)
C42	3210.5(12)	4904.7(12)	5633.9(11)	27.8(5)
C43	3154.0(12)	1821.2(11)	6445.4(11)	27.0(5)
C44	3688.6(14)	1347.2(14)	6574.4(14)	41.1(7)
C45	2713.1(14)	1569.6(13)	6115.3(13)	39.0(6)
Ni1A	8998.5(2)	1981.2(2)	7735.1(2)	14.53(6)
Cl1A	9956.7(2)	2228.7(2)	7777.0(2)	18.39(10)
Cl2A	8042.6(3)	1779.7(3)	7687.8(3)	29.56(13)
PIA	9348.5(3)	1114.9(3)	7437.0(2)	15.09(11)
N1A	8622.4(8)	3316.9(8)	7685.2(8)	16.1(4)
N2A	8578.1(8)	2688.5(9)	8637.0(8)	17.7(4)
C1A	9492.1(10)	431.4(10)	8128.0(9)	18.6(4)
C2A	8883.5(11)	282.3(12)	8631.4(10)	28.7(5)
C3A	8957.1(13)	-295.3(13)	9210.9(11)	33.6(6)
C4A	9516.2(12)	-182.5(12)	9482.3(10)	28.1(5)
C5A	10112.6(12)	-42.6(12)	8984.4(10)	27.3(5)
C6A	10042.9(11)	542.2(11)	8411.8(10)	23.3(5)
C7A	10095.9(10)	1318.2(10)	6867.7(10)	19.0(4)
C8A	10394.0(12)	794.1(12)	6595.8(11)	28.0(5)
C9A	11050.4(13)	1028.7(13)	6206.4(14)	39.3(7)
C10A	11030.2(13)	1673.0(13)	5686.9(12)	36.8(6)
C11A	10718.5(12)	2189.8(12)	5951.1(11)	28.5(5)
C12A	10062.6(11)	1964.0(11)	6333.3(10)	22.9(5)
C13A	8786.3(10)	744(1)	7125.4(10)	18.8(4)
C14A	8666.2(11)	1184.0(11)	6482.5(10)	24.4(5)
C15A	8094.7(13)	924.5(13)	6329.8(12)	34.0(6)
C16A	8180.3(14)	230.4(13)	6323.7(12)	37.5(7)

C17A	8329.2(13)	-216.0(12)	6947.6(11)	31.2(6)
C18A	8897.6(12)	43.2(11)	7111.8(11)	25.4(5)
C19A	8713.6(9)	2691.5(10)	8029.6(9)	16.1(4)
C20A	8434.5(11)	3697.1(11)	8071.6(10)	20.7(5)
C21A	8406.6(11)	3303.3(11)	8662.7(10)	22.3(5)
C22A	8686.8(10)	3540.5(10)	7005.4(9)	16.5(4)
C23A	9275.8(10)	3775.8(10)	6633(1)	19.2(4)
C24A	9326.3(11)	3959.0(11)	5982.3(10)	24.4(5)
C25A	8808.4(12)	3926.7(12)	5719.6(11)	28.5(5)
C26A	8226.1(11)	3721.9(12)	6098.2(11)	26.7(5)
C27A	8150.4(10)	3523.3(11)	6751.5(10)	20.6(5)
C28A	9824.2(10)	3890.3(11)	6917.6(10)	20.7(5)
C29A	10465.6(11)	3779.3(12)	6556.3(12)	28.8(5)
C30A	9800.4(11)	4590.2(11)	6946.9(11)	26.7(5)
C31A	7500.6(10)	3328.5(12)	7162.2(11)	23.3(5)
C32A	7093.5(11)	2957.4(13)	6902.3(12)	30.6(6)
C33A	7159.8(12)	3933.4(13)	7249.2(13)	34.1(6)
C34A	8571.3(10)	2114.3(11)	9184.4(9)	19.4(4)
C35A	8024.7(11)	1714.2(12)	9416.9(10)	23.6(5)
C36A	8037.4(12)	1156.6(12)	9937.8(11)	29.7(5)
C37A	8557.6(12)	1012.3(13)	10211.1(11)	32.6(6)
C38A	9079.6(11)	1422.1(12)	9985.5(10)	28.1(5)
C39A	9101.9(11)	1985.5(11)	9465.9(10)	21.8(5)
C40A	7431.1(11)	1882.3(12)	9150.3(11)	27.4(5)
C41A	6992.9(12)	2245.9(15)	9529.0(13)	37.7(6)
C42A	7099.8(13)	1270.3(13)	9138.1(14)	36.2(6)
C43A	9676.2(11)	2442.3(12)	9250.2(10)	23.3(5)
C44A	10292.1(11)	2070.5(13)	9268.8(11)	30.3(6)
C45A	9631.3(12)	2884.4(14)	9661.9(12)	34.7(6)
Ni1B	7707.6(2)	2267.2(2)	3224.7(2)	15.54(6)
Cl1B	6745.3(3)	1917.8(3)	3385.1(3)	26.42(12)
Cl2B	8674.0(2)	2653.3(3)	2988.3(2)	21.89(11)
P1B	7997.5(3)	1244.3(3)	3691.2(2)	18.22(11)
C13B	8747.5(10)	1220.7(11)	3966.2(10)	24.7(5)
C14B	8677.6(10)	1509.4(12)	4504(1)	27.7(5)
C15B	9322.3(11)	1622.3(13)	4638.1(12)	41.4(7)

C16B	9679.2(12)	993.2(15)	4789.2(12)	49.4(8)
C17B	9743.1(12)	696.5(15)	4262.4(13)	50.4(8)
C18B	9098.9(11)	583.3(12)	4123.1(13)	39.6(7)
N1B	7353.7(8)	3620.7(8)	3080.9(8)	16.2(4)
N2B	7421.5(8)	3420.9(8)	2212.8(8)	16.2(4)
C1B	8099(4)	783(4)	3125(3)	23.7(15)
C2B	8496(5)	1198(5)	2496(3)	32.4(16)
C3B	8605(5)	837(5)	2013(3)	40.1(18)
C4B	7990(6)	620(4)	1909(3)	33.6(17)
C5B	7590(5)	208(4)	2527(3)	35.6(17)
C6B	7479(4)	570(5)	3011(4)	26.9(14)
C46B	8187(3)	802(4)	3112(3)	24.6(19)
C47B	8644(5)	1216(6)	2528(4)	32.1(18)
C48B	8833(5)	852(5)	2052(4)	36.2(19)
C49B	8264(6)	630(5)	1871(3)	35.0(19)
C50B	7807(6)	219(5)	2449(4)	34.2(19)
C51B	7612(4)	592(6)	2918(5)	32.3(19)
C7B	7381.2(11)	757.7(11)	4329.5(10)	21.4(5)
C8B	7499.3(12)	36.6(12)	4648.0(11)	30.8(6)
C9B	6875.9(14)	-308.0(13)	5018.1(12)	38.4(6)
C10B	6557.6(13)	6.3(14)	5499.0(12)	39.6(7)
C11B	6482.9(12)	739.4(14)	5195.6(12)	35.2(6)
C12B	7109.8(11)	1080.3(12)	4826.3(11)	26.4(5)
C19B	7466.8(9)	3134(1)	2822.8(9)	15.8(4)
C20B	7248.6(10)	4205.9(10)	2632.5(10)	20.2(4)
C21B	7294.2(10)	4078.4(11)	2090.1(10)	21.3(5)
C22B	7305.2(10)	3513.3(10)	3747(1)	18.2(4)
C23B	6725.2(11)	3281.8(11)	4141.8(10)	22.6(5)
C24B	6700.7(12)	3135.1(13)	4785.6(11)	32.4(6)
C25B	7220.7(13)	3214.7(14)	5019.1(11)	37.3(6)
C26B	7780.7(12)	3468.9(13)	4614.7(11)	30.2(6)
C27B	7835(1)	3630.7(11)	3966.3(10)	21.3(5)
C28B	6138.9(11)	3233.1(12)	3886.9(11)	26.6(5)
C29B	5684.2(12)	2673.8(14)	4314.2(13)	37.1(6)
C30B	5799.9(12)	3885.4(14)	3765.0(14)	38.5(6)
C31B	8430.1(10)	3967.9(11)	3522.7(10)	22.3(5)

C32B	9030.9(11)	3719.8(13)	3772.2(11)	29.9(5)
C33B	8392.1(12)	4706.7(12)	3386.0(12)	29.5(5)
C34B	7462.2(10)	3077.4(10)	1759.3(9)	18.9(4)
C35B	8046.5(11)	3057.6(11)	1381.1(10)	21.0(5)
C36B	8076.5(11)	2693.6(12)	972.1(10)	26.0(5)
C37B	7548.1(12)	2374.9(12)	940.7(11)	29.6(5)
C38B	6972.5(12)	2428.1(12)	1301.6(11)	27.3(5)
C39B	6911.9(11)	2783.6(11)	1718.8(10)	22.7(5)
C40B	8623.2(11)	3435.1(12)	1380.5(10)	23.9(5)
C41B	8718.9(13)	4063.8(14)	814.6(12)	36.3(6)
C42B	9215.3(11)	3028.3(13)	1381.7(12)	30.9(6)
C43B	6271.2(11)	2878.8(13)	2087.4(11)	28.0(5)
C44B	5812.2(13)	2298.6(14)	2263.7(13)	39.9(7)
C45B	5975.6(12)	3494.4(14)	1721.1(13)	36.4(6)
Ni1C	2215.8(2)	3582.1(2)	2154.9(2)	17.38(6)
Cl1C	2430.3(3)	2632.4(3)	2060.9(3)	30.60(13)
Cl2C	1936.8(3)	4529.8(3)	2245.7(3)	25.53(12)
P1C	3191.8(3)	3988.6(3)	1653.6(2)	20.53(12)
C52C	3204(3)	4853(2)	1147(4)	34.5(15)
C53C	2842(4)	4990(3)	609(4)	35.9(14)
C54C	2762(4)	5722(3)	297(4)	44.0(15)
C55C	3384(4)	6099(4)	66(3)	48.2(16)
C56C	3740(3)	5977(3)	606(4)	50.8(18)
C57C	3824(3)	5245(3)	915(4)	47.8(15)
N1C	870.3(8)	3179.7(9)	2437.1(8)	16.4(4)
N2C	1248.4(8)	3006.2(8)	3277.0(8)	16.0(4)
C1C	3665(2)	4044.9(18)	2231.0(17)	18.3(13)
C2C	3511(2)	4626(2)	2466(2)	24.9(11)
C3C	3933(3)	4643(2)	2930(2)	25.5(11)
C4C	3867(3)	4015(3)	3477(2)	32.0(12)
C5C	4008(3)	3425(2)	3255(2)	36.7(13)
C6C	3597(3)	3405(2)	2785(2)	28.7(11)
C46C	3667(4)	4060(4)	2225(3)	23(3)
C47C	3356(5)	4460(5)	2639(4)	28.1(19)
C48C	3778(5)	4520(5)	3087(5)	32(2)
C49C	3952(6)	3859(6)	3491(4)	29(2)

C50C	4259(5)	3458(5)	3083(4)	31(2)
C51C	3827(5)	3389(4)	2649(4)	29(2)
C7C	3671.2(10)	3462.9(13)	1256.2(11)	26.2(5)
C8C	4388.8(12)	3576.6(16)	1068.5(13)	41.5(7)
C9C	4689.5(13)	3003.3(17)	885.2(13)	43.9(7)
C10C	4424.7(13)	2896.7(15)	350.7(12)	38.8(6)
C11C	3708.7(12)	2827.8(14)	509.5(12)	34.7(6)
C12C	3411.5(11)	3399.0(13)	697.7(10)	27.2(5)
C13C	3150(2)	4801.9(19)	1086(2)	33.1(10)
C14C	2641(2)	4828(2)	695(2)	30.9(10)
C15C	2521(2)	5546(2)	364(2)	42.1(11)
C16C	3121(2)	5899(3)	-44(2)	52.8(13)
C17C	3656(2)	5834(2)	316(2)	51.9(12)
C18C	3767.7(18)	5116.3(19)	668.0(19)	37.2(10)
C19C	1410.3(10)	3236.6(10)	2639.4(9)	15.9(4)
C20C	378.4(10)	2923.3(11)	2940.9(10)	20.4(5)
C21C	615.6(10)	2815.6(11)	3464.9(10)	21.0(5)
C22C	829.2(10)	3338.9(11)	1778.1(9)	17.9(4)
C23C	921.2(10)	2838.2(11)	1508.1(10)	20.1(5)
C24C	905.8(11)	3009.8(12)	866.4(10)	24.6(5)
C25C	803.0(11)	3643.4(12)	520.2(10)	25.0(5)
C26C	690.9(11)	4120.5(12)	805.8(10)	23.5(5)
C27C	689.5(10)	3976.7(11)	1446.6(10)	18.8(4)
C28C	994.1(11)	2132.9(11)	1892.6(11)	24.1(5)
C29C	1452.8(13)	1770.6(13)	1529.6(12)	33.4(6)
C30C	351.0(13)	1774.2(13)	2124.7(13)	34.6(6)
C31C	480.4(11)	4478.2(11)	1773.4(10)	22.0(5)
C32C	694.2(12)	5176.8(12)	1369.7(12)	30.5(5)
C33C	-240.2(11)	4429.9(12)	1970.5(11)	26.7(5)
C34C	1677.2(10)	2939.2(10)	3707.6(9)	17.5(4)
C35C	1704.6(10)	3428.6(10)	3979.3(9)	18.3(4)
C36C	2125.2(11)	3350.2(11)	4387.8(10)	22.8(5)
C37C	2500.5(11)	2812.1(11)	4523.1(10)	23.5(5)
C38C	2448.6(11)	2327.9(11)	4261.4(10)	21.7(5)
C39C	2031.8(10)	2374.9(10)	3853.9(9)	18.3(4)
C40C	1282.0(11)	4012.6(11)	3872.9(10)	22.6(5)

C41C	729.0(13)	3895.4(13)	4429.1(11)	33.4(6)
C42C	1645.6(13)	4644.5(11)	3771.1(12)	29.5(5)
C43C	1938.9(11)	1806.3(11)	3625.3(10)	21.4(5)
C44C	2557.4(12)	1484.5(12)	3453.1(12)	31.2(6)
C45C	1474.3(13)	1308.7(12)	4140.3(12)	32.5(6)
P1S	4376.3(5)	-468.9(5)	1565.5(5)	32.0(3)
C19S	5011(4)	105(5)	1524(6)	50(3)
C20S	5595(5)	-247(6)	1738(9)	66(4)
C21S	6094(6)	225(8)	1753(8)	54(3)
C22S	6264(6)	780(9)	1143(9)	55(3)
C23S	5684(7)	1119(6)	920(10)	66(3)
C24S	5211(7)	630(7)	882(7)	61(3)
C1S	4206.5(17)	-761.1(17)	2442.4(16)	28.6(8)
C2S	3571.9(17)	-1136.5(19)	2694.6(17)	32.4(8)
C3S	3448.3(18)	-1435.5(19)	3407.7(18)	34.7(9)
C4S	3970.3(18)	-1851.8(19)	3639.0(19)	37.2(9)
C5S	4598.1(18)	-1491(2)	3392.6(19)	40.7(10)
C6S	4723.9(17)	-1219(2)	2697.2(19)	36.4(9)
C7S	3685.4(18)	27.9(18)	1358.5(17)	30.3(8)
C8S	3534(2)	595(2)	1618.9(19)	37.9(9)
C9S	2946(2)	936(2)	1426.4(18)	39.4(9)
C10S	2990(2)	1157(2)	719(2)	44.3(10)
C11S	3137(2)	598(2)	455.0(19)	40.5(10)
C12S	3736.5(19)	265.0(18)	644.8(17)	33.3(8)
C13S	5031.5(16)	145.9(18)	1322.1(19)	37.4(11)
C14S	5137(2)	454(2)	1809(2)	43.7(12)
C15S	5681(2)	966(2)	1548(3)	50.8(13)
C16S	6293.4(19)	677(3)	1326(3)	49.0(14)
C17S	6188(2)	381(2)	826(2)	37.9(11)
C18S	5655.7(17)	-130(2)	1078(2)	40.0(11)
C25S	2814(8)	874(8)	894(6)	70(5)
C26S	3087(5)	582(5)	1482(4)	54(3)
C27S	3237(6)	973(5)	1821(6)	53(3)
C28S	3476(7)	702(7)	2373(6)	87(6)
C29S	3570(7)	32(7)	2595(5)	98(6)
C30S	3425(7)	-364(5)	2261(6)	87(6)

C31S	3186(6)	-90(5)	1710(6)	52(3)
C32S	4907(8)	121(9)	470(8)	96(8)
C33S	5276(5)	391(5)	834(5)	50(3)
C34S	5895(5)	203(6)	884(6)	42(3)
C35S	6243(5)	463(8)	1209(7)	51(3)
C36S	5976(7)	917(7)	1491(7)	57(3)
C37S	5359(7)	1108(6)	1447(7)	59(3)
C38S	5014(5)	845(6)	1122(6)	56(2)
C39S	5728(3)	375(4)	3563(5)	87(4)
C40S	5169(2)	811(3)	3576(3)	66(2)
C41S	4771(3)	904(3)	3139(3)	69(3)
C42S	4261(3)	1320(3)	3141(3)	70(2)
C43S	4141(2)	1649(3)	3584(4)	75(2)
C44S	4532(3)	1559(3)	4024(3)	69(2)
C45S	5040(3)	1144(3)	4019(3)	60.0(19)
C46S	5547(3)	294(3)	3631(4)	104(4)
C47S	5092(2)	746(2)	3862(2)	73(2)
C48S	4740(2)	1179(2)	3459(2)	79(2)
C49S	4328(2)	1609(2)	3667(2)	73(2)
C50S	4261(2)	1614(2)	4286(3)	66.7(19)
C51S	4607(2)	1185(2)	4695(2)	69.7(18)
C52S	5017(2)	755(2)	4484(2)	75(2)

Table 3 Anisotropic Displacement Parameters ($\text{\AA}^2 \times 10^3$) for Schomaker52. The Anisotropic displacement factor exponent takes the form: $-2\pi^2[h^2a^2U_{11}+2hka*b*U_{12}+\dots]$.

Atom	U_{11}	U_{22}	U_{33}	U_{23}	U_{13}	U_{12}
Ni1	11.94(13)	18.50(14)	13.94(12)	-3.81(10)	-3.25(10)	0.22(10)
Cl1	25.1(3)	22.1(3)	45.8(4)	-8.5(3)	-15.7(3)	5.2(2)
Cl2	18.6(3)	19.3(3)	19.5(2)	-6.7(2)	-5.67(19)	0.4(2)
N1	14.2(9)	16.1(9)	14.5(8)	-3.2(7)	-1.6(7)	-0.5(7)
N2	14.5(9)	19.3(9)	14.8(8)	-4.9(7)	-4.0(7)	-0.3(7)
P1	13.0(3)	26.7(3)	12.4(2)	-3.9(2)	-2.9(2)	-0.6(2)
C1	12(1)	34.7(13)	16.4(10)	-7.4(9)	-0.3(8)	-2.6(9)
C2	23.2(12)	32.2(13)	16.1(10)	-5.9(9)	-0.1(9)	-4.7(10)
C3	26.6(13)	37.8(14)	16.1(11)	-3.9(10)	0.2(9)	-8.7(11)

C4	27.4(13)	45.4(16)	15.8(11)	-7.7(10)	1.3(9)	-8.8(11)
C5	32.5(14)	46.4(16)	23.0(12)	-15.5(12)	6.4(10)	-1.3(12)
C6	32.6(14)	33.4(14)	20.2(11)	-9.6(10)	3.6(10)	-1.1(11)
C7	18.3(11)	36.2(14)	18.2(11)	-4.3(10)	-6.4(9)	5.4(10)
C8	20.0(13)	58.9(19)	27.7(13)	-4.4(12)	-5.8(10)	4.2(12)
C9	24.3(14)	72(2)	31.2(14)	-1.6(14)	-8.4(11)	15.5(14)
C10	36.1(16)	75(2)	30.0(15)	4.3(15)	-6.6(12)	23.2(16)
C11	37.5(16)	50.4(18)	28.9(14)	6.6(13)	-0.5(12)	12.0(14)
C12	23.1(12)	38.7(15)	21.8(12)	-0.6(10)	-3.3(10)	6.3(11)
C13	19.8(11)	28.0(12)	13.2(10)	-4.7(9)	-2.7(8)	-4.7(9)
C14	21.2(12)	28.6(13)	15(1)	-5.4(9)	-1.1(9)	-3.8(9)
C15	39.6(15)	32.9(14)	17.7(11)	-7.8(10)	-0.7(10)	1.9(11)
C16	58.4(18)	35.5(15)	21.0(12)	-11.5(11)	-4.3(12)	-10.7(13)
C17	49.8(18)	48.4(17)	26.3(13)	-13.2(12)	-4.4(12)	-23.1(14)
C18	25.0(13)	45.3(16)	19.8(11)	-9.8(11)	-3.4(9)	-13.0(11)
C19	17.2(10)	12.5(10)	15.5(10)	-3.0(8)	-3.4(8)	2.1(8)
C20	12.8(10)	23.2(12)	24.0(11)	-6.6(9)	-4.7(8)	-2.3(9)
C21	16.1(11)	27.1(12)	21.6(11)	-7.4(9)	-6.4(9)	-1.8(9)
C22	12.8(10)	23.0(11)	13.2(10)	-3.1(8)	0.5(8)	-1.5(8)
C23	17.7(11)	21.6(12)	21.6(11)	-2.2(9)	-0.9(9)	-0.3(9)
C24	32.2(14)	27.5(13)	21.7(12)	-0.3(10)	-2.9(10)	5.6(11)
C25	32.1(14)	41.8(15)	16.2(11)	-5.9(10)	-4.1(10)	7.3(11)
C26	24.5(12)	30.9(13)	20.9(11)	-10.4(10)	-1.6(9)	2.3(10)
C27	14(1)	21.1(11)	19.5(10)	-4.8(9)	0.7(8)	-1.6(9)
C28	29.7(13)	19.4(12)	26.6(12)	-5(1)	-2.3(10)	1.8(10)
C29	47.2(17)	24.2(14)	35.4(14)	-4.4(11)	-4.5(12)	9.8(12)
C30	37.8(15)	24.1(14)	48.1(16)	-12.1(12)	-2.2(12)	-3.9(11)
C31	20.6(11)	19.4(11)	21.6(11)	-5.3(9)	1.1(9)	1.7(9)
C32	32.0(14)	23.4(13)	32.9(13)	-11.1(10)	1.2(11)	-1.9(10)
C33	25.2(13)	25.7(13)	28.5(12)	-4.6(10)	-4.1(10)	5.5(10)
C34	14.2(10)	26.9(12)	13.2(10)	-7.0(9)	-3.3(8)	-0.1(9)
C35	18.4(11)	24.3(12)	15.3(10)	-8.5(9)	-5.7(8)	-1.5(9)
C36	23.5(12)	28.6(13)	17.1(10)	-4.2(9)	-2.0(9)	-2.6(10)
C37	20.0(12)	40.1(15)	17.7(11)	-8.5(10)	0.6(9)	1.2(10)
C38	22.8(12)	33.4(14)	24.8(12)	-12.1(10)	-6.3(9)	9.1(10)
C39	20.5(11)	25.1(12)	19.5(11)	-7.3(9)	-8.2(9)	4.2(9)

C40	23.0(11)	21.3(11)	15.4(10)	-7.2(9)	-3.2(8)	-1.7(9)
C41	29.9(13)	33.0(14)	27.4(12)	-16.2(11)	-12.4(10)	6.2(11)
C42	32.8(14)	24.7(13)	24.0(12)	-5(1)	-4.7(10)	-4.3(10)
C43	31.8(13)	24.3(13)	23.1(12)	-5.7(10)	-5.1(10)	4.2(10)
C44	47.1(17)	33.6(15)	41.6(16)	-9.9(12)	-12.7(13)	14.3(13)
C45	47.5(17)	26.6(14)	41.3(15)	-6.3(12)	-12.0(13)	-3.4(12)
Ni1A	16.87(14)	14.11(13)	14.42(12)	-6.56(10)	-3.74(10)	-0.26(10)
Cl1A	17.9(3)	19.2(3)	20.8(2)	-10.2(2)	-3.48(19)	-0.8(2)
Cl2A	20.3(3)	31.4(3)	48.1(4)	-25.9(3)	-10.7(2)	3.1(2)
P1A	19.8(3)	13.9(3)	12.5(2)	-5.3(2)	-3.2(2)	-1.0(2)
N1A	18.1(9)	16.4(9)	16.1(8)	-7.7(7)	-4.5(7)	1.4(7)
N2A	20.2(9)	19.0(9)	16.1(8)	-8.2(7)	-3.8(7)	-0.9(7)
C1A	25.4(12)	14.4(11)	16(1)	-4.8(8)	-3.9(9)	-0.6(9)
C2A	27.3(13)	34.1(14)	17.8(11)	0.9(10)	-3.4(9)	-3.7(11)
C3A	36.6(15)	35.6(15)	19.5(12)	3.9(10)	-4.9(10)	-7.2(12)
C4A	41.5(15)	25.7(13)	15.7(11)	-3.4(9)	-8.3(10)	2.6(11)
C5A	35.0(14)	24.5(13)	20.5(11)	-2.4(9)	-10.5(10)	3.9(10)
C6A	26.2(12)	22.7(12)	19.8(11)	-3.1(9)	-7.9(9)	-0.6(10)
C7A	21.4(11)	20.0(11)	15.4(10)	-6.7(9)	-0.5(8)	-2.0(9)
C8A	31.6(13)	22.0(12)	28.1(12)	-11.2(10)	6.2(10)	-2.8(10)
C9A	32.9(15)	33.4(15)	47.9(16)	-19.4(13)	12.7(12)	-0.2(12)
C10A	33.9(15)	44.5(16)	29.6(13)	-17.3(12)	11.5(11)	-12.3(12)
C11A	34.9(14)	26.9(13)	20.1(11)	-5(1)	1(1)	-10.7(11)
C12A	30.1(13)	20.2(12)	16.7(10)	-4.6(9)	-2.0(9)	-4.1(10)
C13A	23.9(12)	18.8(11)	15.4(10)	-7.2(8)	-4.2(8)	-4.4(9)
C14A	33.2(13)	23.0(12)	17.1(10)	-4.3(9)	-8.3(9)	-4.8(10)
C15A	41.9(16)	37.9(15)	23.2(12)	-5.5(11)	-14.8(11)	-7.1(12)
C16A	51.3(17)	38.6(15)	24.7(12)	-7.4(11)	-14.1(12)	-19.2(13)
C17A	44.8(16)	27.5(13)	22.2(12)	-7.4(10)	-6.9(11)	-14.0(11)
C18A	34.4(14)	20.2(12)	24.8(12)	-10.6(10)	-6.4(10)	-3.2(10)
C19A	12.9(10)	20.4(11)	17.3(10)	-8.4(8)	-4.2(8)	-1.1(8)
C20A	25.7(12)	17.3(11)	23.6(11)	-12.5(9)	-6.0(9)	3.7(9)
C21A	27.1(12)	24.1(12)	20.4(11)	-13.8(9)	-3.8(9)	1.4(10)
C22A	22.1(11)	13.5(10)	15.7(10)	-6.3(8)	-5.2(8)	2.2(8)
C23A	23.5(12)	14.4(11)	20.8(11)	-6.8(8)	-5.2(9)	1.3(9)
C24A	24.5(12)	27.8(13)	21.0(11)	-10(1)	0.1(9)	-4.1(10)

C25A	34.2(14)	35.6(14)	17.6(11)	-10.7(10)	-4.5(10)	-7.3(11)
C26A	28.5(13)	33.3(14)	22.5(11)	-11.6(10)	-9.1(10)	-5(1)
C27A	23.4(12)	19.8(11)	21.1(11)	-9.6(9)	-5.0(9)	-1.1(9)
C28A	20.6(11)	18.7(11)	22.3(11)	-4.5(9)	-7.2(9)	0.4(9)
C29A	24.2(13)	27.4(13)	32.2(13)	-6.9(10)	-4.1(10)	-0.3(10)
C30A	27.1(13)	26.3(13)	31.9(13)	-11.9(10)	-13.4(10)	-0.6(10)
C31A	19.4(11)	28.7(13)	23.5(11)	-10(1)	-5.3(9)	-0.7(10)
C32A	22.8(13)	42.4(15)	29.4(13)	-14.1(11)	-6.2(10)	-5.4(11)
C33A	25.3(13)	34.8(15)	41.7(15)	-14.4(12)	-1.9(11)	3.9(11)
C34A	24.9(12)	20.2(11)	13.3(10)	-6.8(8)	-1.9(8)	-0.3(9)
C35A	21.3(12)	29.8(13)	22.0(11)	-12.1(10)	-2.4(9)	-1.9(10)
C36A	27.5(13)	29.8(14)	26.0(12)	-4.9(10)	3.2(10)	-6.6(11)
C37A	35.0(14)	34.5(14)	17.7(11)	2.4(10)	1.1(10)	0.3(11)
C38A	25.7(13)	39.1(15)	16.1(11)	-5.2(10)	-2.8(9)	2.4(11)
C39A	23.6(12)	28.2(12)	14.2(10)	-8.9(9)	-1.3(8)	0.2(10)
C40A	25.2(13)	32.5(14)	25.1(12)	-9.1(10)	-5.5(10)	-3.5(10)
C41A	27.0(14)	51.1(18)	42.5(15)	-22.7(14)	-12.1(12)	5.6(12)
C42A	30.0(14)	34.5(15)	46.7(16)	-13.3(12)	-12.3(12)	-3.0(11)
C43A	24.0(12)	32.4(13)	14.4(10)	-8.6(9)	-3.4(9)	-1.3(10)
C44A	23.0(12)	42.6(15)	23.3(12)	-7.4(11)	-5.1(10)	-0.5(11)
C45A	31.6(14)	50.5(17)	27.1(13)	-22.5(12)	1.9(10)	-10.2(12)
Ni1B	17.95(14)	15.26(14)	14.22(13)	-5.18(10)	-4.36(10)	1.05(11)
Cl1B	22.0(3)	20.7(3)	34.2(3)	-3.1(2)	-9.7(2)	-1.4(2)
Cl2B	18.9(3)	21.9(3)	23.3(3)	-4.7(2)	-4.7(2)	-0.5(2)
P1B	22.5(3)	17.4(3)	15.1(3)	-5.3(2)	-4.7(2)	2.5(2)
C13B	22.3(12)	26.2(13)	22.6(11)	-2.9(9)	-6.5(9)	2.6(10)
C14B	26.6(13)	33.9(14)	19.6(11)	-2.1(10)	-8.1(9)	-5.1(10)
C15B	34.3(15)	59.6(19)	24.3(13)	-1.7(12)	-9.2(11)	-17.9(14)
C16B	21.9(14)	81(2)	31.4(15)	4.9(15)	-10.5(11)	-5.0(14)
C17B	26.7(15)	62(2)	46.2(17)	5.3(15)	-9.8(13)	12.1(14)
C18B	32.9(15)	35.7(16)	44.4(16)	-4.0(13)	-11.2(12)	12.6(12)
N1B	15.1(9)	17.0(9)	17.3(9)	-7.0(7)	-2.6(7)	-0.3(7)
N2B	17.5(9)	16.9(9)	15.7(8)	-5.9(7)	-5.5(7)	0.3(7)
C1B	34(3)	16(3)	18(3)	-6(2)	1(2)	2(2)
C2B	37(3)	32(3)	26(2)	-12(2)	6(2)	-5(3)
C3B	45(4)	39(3)	31(3)	-13(2)	11(3)	-1(3)

C4B	54(5)	25(2)	21(2)	-12.8(19)	5(3)	-6(3)
C5B	53(4)	31(3)	20(3)	-11(2)	7(3)	-7(3)
C6B	42(3)	29(3)	13(3)	-13(2)	1(2)	-6(3)
C46B	33(3)	22(3)	22(3)	-11(3)	-7(3)	5(3)
C47B	40(4)	32(3)	25(3)	-14(2)	3(3)	-4(3)
C48B	46(5)	32(3)	29(3)	-18(2)	12(3)	-4(4)
C49B	50(5)	30(3)	21(3)	-9(2)	5(3)	-5(4)
C50B	50(5)	32(3)	25(3)	-20(2)	3(3)	-8(3)
C51B	42(4)	32(3)	20(3)	-10(3)	2(3)	-2(3)
C7B	25.0(12)	21.4(12)	16.1(10)	-2.5(9)	-5.6(9)	-1.4(9)
C8B	39.7(15)	25.1(13)	23.3(12)	-0.5(10)	-9.1(11)	3.0(11)
C9B	48.2(17)	27.9(14)	30.4(14)	5.4(11)	-11.7(12)	-5.9(12)
C10B	34.6(15)	47.9(17)	26.8(13)	1.3(12)	-4.4(11)	-10.9(13)
C11B	27.4(14)	48.0(17)	27.8(13)	-10.3(12)	-2.5(10)	-3.7(12)
C12B	25.2(12)	32.9(14)	21.0(11)	-8.9(10)	-2.5(9)	-4.2(10)
C19B	12.3(10)	19.8(11)	16.2(10)	-6.8(8)	-2.8(8)	-1.5(8)
C20B	21.4(11)	13.8(11)	24.8(11)	-4.5(9)	-6.2(9)	0.7(9)
C21B	23.2(12)	19.1(11)	20.1(11)	-2.4(9)	-7.5(9)	0.6(9)
C22B	21.1(11)	18.1(11)	16.4(10)	-8.7(8)	-0.6(8)	-0.7(9)
C23B	22.3(12)	24.3(12)	22.9(11)	-12.6(9)	0.9(9)	-3.2(9)
C24B	30.3(14)	43.8(16)	21.7(12)	-14.4(11)	7.8(10)	-12.6(12)
C25B	42.5(16)	53.3(18)	16.2(11)	-13.6(11)	0.4(11)	-12.1(13)
C26B	29.2(13)	44.4(16)	21.4(12)	-15.5(11)	-5.7(10)	-6.2(11)
C27B	22.0(12)	24.4(12)	19.9(11)	-10.9(9)	-2.6(9)	-1.5(9)
C28B	20.1(12)	32.5(14)	29.5(12)	-15.8(11)	1.4(9)	-4.4(10)
C29B	26.7(14)	42.9(16)	41.8(15)	-19.1(13)	5.0(11)	-10.3(12)
C30B	24.0(14)	40.1(16)	54.6(17)	-20.3(14)	-6.4(12)	1.9(12)
C31B	18.3(11)	33.1(13)	19.4(11)	-14.9(10)	-0.8(9)	-4.4(9)
C32B	22.7(12)	44.8(16)	28.7(12)	-20.0(12)	-5.8(10)	0.0(11)
C33B	26.0(13)	34.0(14)	30.3(13)	-16.0(11)	1.9(10)	-9.1(11)
C34B	26.1(12)	19.1(11)	12.9(10)	-4.8(8)	-7.7(8)	0.1(9)
C35B	25.1(12)	23.2(12)	15(1)	-4.7(9)	-6.9(9)	0.7(9)
C36B	28.4(13)	33.7(14)	18.2(11)	-11(1)	-5.2(9)	1.9(10)
C37B	43.4(15)	30.9(14)	21.6(11)	-13.3(10)	-14.4(11)	1.2(11)
C38B	32.1(13)	29.2(13)	23.6(12)	-7.8(10)	-12.3(10)	-6.8(10)
C39B	27.3(12)	24.4(12)	16.5(10)	-3.9(9)	-8.7(9)	-2.6(10)

C40B	23.8(12)	34.3(13)	16.4(10)	-11.6(10)	-4.0(9)	-2.7(10)
C41B	36.4(15)	43.2(16)	25.3(13)	-2.5(11)	-8.8(11)	-14.7(12)
C42B	24.3(13)	48.3(16)	27.3(12)	-22.4(12)	-4.4(10)	3.1(11)
C43B	22.5(12)	39.6(15)	22.3(11)	-8.3(10)	-6.8(9)	-5.3(11)
C44B	30.9(15)	49.2(18)	36.7(15)	-8.2(13)	-7.2(12)	-14.4(13)
C45B	25.2(13)	46.5(17)	35.5(14)	-10.2(12)	-5.7(11)	-1.6(12)
Ni1C	13.23(13)	25.77(15)	13.99(13)	-7.61(11)	-2.39(10)	-0.18(11)
Cl1C	27.2(3)	28.5(3)	31.0(3)	-10.1(2)	7.1(2)	2.4(2)
Cl2C	21.5(3)	26.8(3)	29.4(3)	-13.6(2)	1.2(2)	-4.1(2)
P1C	15.1(3)	32.1(3)	12.4(2)	-4.2(2)	-3.1(2)	-0.1(2)
C52C	26(2)	49(2)	16(2)	8(2)	-8(2)	7(2)
C53C	30(2)	51(2)	19(2)	-2(2)	-5(2)	12(2)
C54C	37(3)	55(3)	27(2)	3(2)	-6(2)	17(3)
C55C	43(3)	53(3)	29(2)	10(2)	-4(2)	11(2)
C56C	44(3)	53(3)	30(3)	20(3)	-5(3)	2(3)
C57C	37(2)	55(2)	27(2)	19(2)	-3(2)	3(2)
N1C	14.9(9)	21.4(9)	15.7(8)	-9.4(7)	-3.9(7)	1.8(7)
N2C	15.0(9)	19.0(9)	15.6(8)	-7.4(7)	-3.5(7)	-0.9(7)
C1C	16(2)	23(2)	16(2)	-4.7(19)	-4.5(19)	-5(2)
C2C	24(2)	24(2)	28(2)	-6.9(17)	-11.2(17)	-2.5(16)
C3C	23(2)	28(2)	28(2)	-9.3(18)	-8.5(18)	-5.9(17)
C4C	37(3)	38(3)	23(2)	-8.6(18)	-10.0(17)	-12(2)
C5C	47(3)	33(2)	30(2)	-0.7(19)	-23(2)	-2(2)
C6C	39(3)	23.5(19)	23(2)	-0.8(16)	-15.4(19)	-4.3(18)
C46C	23(4)	24(4)	20(4)	-2(4)	-7(4)	-3(4)
C47C	25(4)	30(4)	30(3)	-9(3)	-10(3)	-4(3)
C48C	30(4)	36(4)	32(4)	-11(3)	-10(3)	-5(3)
C49C	32(4)	41(4)	16(3)	-6(3)	-12(3)	0(4)
C50C	34(5)	36(4)	24(4)	-5(3)	-17(3)	7(4)
C51C	37(4)	30(3)	21(3)	-8(3)	-11(3)	0(3)
C7C	18.2(11)	43.1(15)	19.4(11)	-13.2(10)	-2.9(9)	1.2(10)
C8C	18.6(13)	78(2)	37.6(15)	-32.4(15)	-3.3(11)	0.4(13)
C9C	24.8(14)	77(2)	36.4(15)	-28.6(15)	-5.4(11)	11.6(14)
C10C	38.4(15)	54.0(18)	25.4(13)	-17.8(12)	-2.1(11)	7.6(13)
C11C	38.4(15)	45.9(16)	20.6(12)	-12.0(11)	-5.0(11)	-0.8(12)
C12C	22.2(12)	42.3(15)	15.9(11)	-8.3(10)	-2.7(9)	-2.6(11)

C13C	26.1(17)	46.8(18)	15.9(15)	3.5(15)	-4.2(14)	6.9(15)
C14C	23(2)	50(2)	14.3(17)	-2.9(15)	-4.7(15)	10.2(17)
C15C	32(2)	55(2)	23.7(17)	3.7(17)	0.7(18)	16.8(19)
C16C	43(2)	57(2)	34.4(19)	14.2(18)	-4.1(18)	16(2)
C17C	46(2)	54(2)	30(2)	17.6(18)	-0.6(18)	0.5(18)
C18C	33.1(18)	49(2)	15.1(17)	7.8(15)	-1.1(15)	0.4(16)
C19C	16.6(10)	17.1(11)	15.9(10)	-7.8(8)	-3.4(8)	1.8(8)
C20C	14.6(11)	26.3(12)	21.5(11)	-9.9(9)	-1.9(8)	-2.7(9)
C21C	17.3(11)	26.2(12)	18.4(10)	-7.9(9)	1.1(8)	-3.0(9)
C22C	14.3(10)	26.5(12)	14.5(10)	-8.3(9)	-3.2(8)	0.5(9)
C23C	17.3(11)	24.8(12)	21.0(11)	-11.7(9)	-3.5(8)	3.0(9)
C24C	26.4(12)	30.6(13)	22.3(11)	-16.2(10)	-5.1(9)	5.4(10)
C25C	25.7(12)	34.6(14)	15.4(10)	-8.8(10)	-4.5(9)	3.5(10)
C26C	23.8(12)	25.8(12)	20.5(11)	-6.2(9)	-5.6(9)	1.4(10)
C27C	15.3(10)	23.0(12)	20.4(10)	-10.0(9)	-3.8(8)	-0.5(9)
C28C	29.0(13)	23.8(12)	23.0(11)	-11.6(10)	-6.8(9)	6.2(10)
C29C	41.2(15)	29.0(14)	33.1(13)	-14.8(11)	-8.1(11)	10.9(12)
C30C	38.3(15)	26.2(14)	37.4(14)	-9.4(11)	-4.3(12)	0.6(11)
C31C	25.5(12)	22.3(12)	22.6(11)	-11.3(9)	-8.3(9)	1.8(9)
C32C	35.1(14)	25.8(13)	33.3(13)	-10.6(11)	-10.7(11)	-0.5(11)
C33C	26.3(13)	28.5(13)	31.9(13)	-18.8(11)	-5.5(10)	3.6(10)
C34C	19.2(11)	20.4(11)	12.9(9)	-4.7(8)	-3.8(8)	-2.2(9)
C35C	22.4(11)	16.9(11)	14.9(10)	-4.4(8)	-3.1(8)	-1.0(9)
C36C	32.3(13)	20.6(12)	18.2(10)	-6.7(9)	-9.7(9)	-2.7(10)
C37C	27.3(12)	24.4(12)	18.4(11)	-2.3(9)	-10.6(9)	-2.2(10)
C38C	22.6(12)	20.6(12)	21.3(11)	-4.3(9)	-7.1(9)	2.5(9)
C39C	20.4(11)	18.6(11)	15.4(10)	-5.7(8)	-1.2(8)	-2.0(9)
C40C	30.2(13)	20.8(12)	18.3(10)	-6.7(9)	-7.8(9)	3.9(10)
C41C	39.5(15)	33.0(14)	25.1(12)	-8.6(11)	-3.3(11)	12.4(12)
C42C	43.8(15)	19.5(12)	29.9(13)	-9.1(10)	-16.9(11)	5.2(11)
C43C	26.2(12)	19.0(11)	21.6(11)	-9.8(9)	-5.0(9)	1.3(9)
C44C	36.8(15)	28.5(14)	33.3(13)	-15.7(11)	-10.1(11)	9.4(11)
C45C	43.0(16)	25.2(13)	31.1(13)	-14.9(11)	0.4(11)	-6.3(11)
P1S	33.5(6)	25.6(5)	32.2(5)	-3.7(4)	-4.3(4)	-0.3(4)
C19S	57(4)	45(4)	45(4)	-11(4)	-12(4)	-2(4)
C20S	62(6)	59(6)	60(6)	-1(6)	-3(6)	0(6)

C21S	47(5)	58(5)	51(5)	-7(4)	-12(4)	3(4)
C22S	49(4)	50(4)	59(4)	-14(4)	-4(4)	-4(4)
C23S	59(4)	56(4)	68(4)	-7(4)	-2(4)	6(4)
C24S	65(5)	57(5)	54(5)	-12(4)	-8(5)	6(5)
C1S	28.7(18)	24.5(18)	29.9(18)	-5.7(14)	-4.9(14)	3.2(14)
C2S	25.3(18)	36(2)	32.5(19)	-8.2(16)	-2.2(15)	5.9(15)
C3S	29.5(19)	33(2)	37(2)	-6.5(16)	-4.5(16)	-0.7(16)
C4S	38(2)	26.8(19)	36(2)	1.5(16)	-2.0(16)	5.3(16)
C5S	27(2)	44(2)	44(2)	-4.2(18)	-6.8(17)	9.6(17)
C6S	22.6(18)	37(2)	46(2)	-5.5(17)	-11.4(16)	9.7(16)
C7S	31.2(19)	28.1(18)	30.2(18)	-6.6(15)	-7.8(15)	3.0(15)
C8S	45(2)	39(2)	33.6(18)	-14.8(16)	-12.6(16)	8.6(17)
C9S	46(2)	37(2)	34.1(19)	-10.8(16)	-9.8(17)	16.0(18)
C10S	54(3)	37(2)	42(2)	-9.9(19)	-16(2)	15(2)
C11S	52(3)	39(2)	36(2)	-13.6(17)	-20.6(18)	12.7(19)
C12S	41(2)	27.3(19)	30.7(18)	-10.0(15)	-3.8(16)	0.2(16)
C13S	52(2)	24(2)	37(2)	-1.2(18)	-26(2)	-6.1(19)
C14S	43(3)	38(2)	48(3)	-15(2)	1(2)	-6(2)
C15S	45(3)	45(3)	73(3)	-34(2)	-9(2)	-8(2)
C16S	38(2)	48(3)	56(3)	-10(2)	-7(2)	-11(2)
C17S	33(2)	33(2)	43(2)	-7(2)	-3(2)	-7(2)
C18S	42(2)	34(2)	37(2)	-9.5(19)	7(2)	-9(2)
C39S	42(6)	70(7)	138(9)	-22(7)	-13(6)	6(5)
C40S	29(3)	45(4)	98(5)	9(4)	-7(4)	-10(3)
C41S	40(4)	52(4)	88(5)	9(4)	3(4)	-8(4)
C42S	34(4)	52(4)	92(5)	16(4)	-9(4)	-4(3)
C43S	50(4)	42(4)	111(5)	1(4)	-3(4)	-15(3)
C44S	48(4)	42(3)	115(5)	-20(4)	-17(4)	-14(3)
C45S	39(3)	46(4)	98(4)	-20(3)	-24(3)	-12(3)
C46S	57(6)	102(7)	140(8)	-32(6)	-4(5)	27(5)
C47S	36(3)	63(4)	109(5)	-16(4)	-5(3)	-10(3)
C48S	48(3)	57(3)	104(4)	4(3)	6(3)	-16(3)
C49S	56(4)	41(3)	102(4)	-4(3)	1(4)	-12(3)
C50S	50(4)	42(3)	95(4)	-10(3)	1(3)	-25(3)
C51S	46(3)	54(3)	108(4)	-26(3)	-11(3)	-19(3)
C52S	49(3)	78(4)	104(5)	-23(4)	-34(4)	-16(3)

Table 4 Bond Lengths for Schomaker52.

Atom	Atom	Length/Å	Atom	Atom	Length/Å
Ni1	C11	2.1613(9)	C22B	C23B	1.401(3)
Ni1	C12	2.1877(9)	C22B	C27B	1.397(3)
Ni1	P1	2.2558(8)	C23B	C24B	1.392(3)
Ni1	C19	1.910(2)	C23B	C28B	1.514(3)
N1	C19	1.358(3)	C24B	C25B	1.372(4)
N1	C20	1.389(3)	C25B	C26B	1.385(3)
N1	C22	1.453(3)	C26B	C27B	1.390(3)
N2	C19	1.357(3)	C27B	C31B	1.520(3)
N2	C21	1.386(3)	C28B	C29B	1.530(3)
N2	C34	1.450(3)	C28B	C30B	1.538(4)
P1	C1	1.8542(19)	C31B	C32B	1.530(3)
P1	C7	1.840(2)	C31B	C33B	1.531(3)
P1	C13	1.841(2)	C34B	C35B	1.398(3)
C1	C2	1.527(3)	C34B	C39B	1.402(3)
C1	C6	1.538(3)	C35B	C36B	1.397(3)
C2	C3	1.534(2)	C35B	C40B	1.515(3)
C3	C4	1.515(3)	C36B	C37B	1.381(3)
C4	C5	1.521(3)	C37B	C38B	1.381(4)
C5	C6	1.526(3)	C38B	C39B	1.393(3)
C7	C8	1.539(3)	C39B	C43B	1.525(3)
C7	C12	1.536(3)	C40B	C41B	1.532(3)
C8	C9	1.516(4)	C40B	C42B	1.530(3)
C9	C10	1.525(4)	C43B	C44B	1.528(3)
C10	C11	1.519(4)	C43B	C45B	1.520(4)
C11	C12	1.517(4)	Ni1C	Cl1C	2.1635(9)
C13	C14	1.538(3)	Ni1C	Cl2C	2.1838(9)
C13	C18	1.532(3)	Ni1C	P1C	2.2598(8)
C14	C15	1.523(3)	Ni1C	C19C	1.909(2)
C15	C16	1.524(4)	P1C	C52C	1.854(3)
C16	C17	1.523(4)	P1C	C1C	1.853(2)
C17	C18	1.517(4)	P1C	C46C	1.855(3)
C20	C21	1.342(3)	P1C	C7C	1.852(2)

C22	C23	1.401(3)	P1C	C13C	1.830(3)
C22	C27	1.398(3)	C52C	C53C	1.526(4)
C23	C24	1.390(3)	C52C	C57C	1.523(4)
C23	C28	1.521(3)	C53C	C54C	1.533(4)
C24	C25	1.382(4)	C54C	C55C	1.511(4)
C25	C26	1.383(3)	C55C	C56C	1.524(4)
C26	C27	1.395(3)	C56C	C57C	1.534(4)
C27	C31	1.518(3)	N1C	C19C	1.359(3)
C28	C29	1.523(3)	N1C	C20C	1.389(3)
C28	C30	1.537(4)	N1C	C22C	1.451(3)
C31	C32	1.528(3)	N2C	C19C	1.357(3)
C31	C33	1.539(3)	N2C	C21C	1.390(3)
C34	C35	1.397(3)	N2C	C34C	1.448(3)
C34	C39	1.405(3)	C1C	C2C	1.526(3)
C35	C36	1.394(3)	C1C	C6C	1.534(3)
C35	C40	1.523(3)	C2C	C3C	1.534(3)
C36	C37	1.382(3)	C3C	C4C	1.510(4)
C37	C38	1.378(3)	C4C	C5C	1.522(4)
C38	C39	1.392(3)	C5C	C6C	1.529(3)
C39	C43	1.522(3)	C46C	C47C	1.532(4)
C40	C41	1.534(3)	C46C	C51C	1.534(4)
C40	C42	1.528(3)	C47C	C48C	1.533(4)
C43	C44	1.528(3)	C48C	C49C	1.512(4)
C43	C45	1.534(4)	C49C	C50C	1.523(4)
Ni1A	C11A	2.1875(8)	C50C	C51C	1.530(4)
Ni1A	C12A	2.1593(8)	C7C	C8C	1.537(3)
Ni1A	P1A	2.2579(8)	C7C	C12C	1.535(3)
Ni1A	C19A	1.911(2)	C8C	C9C	1.523(4)
P1A	C1A	1.850(2)	C9C	C10C	1.527(4)
P1A	C7A	1.839(2)	C10C	C11C	1.524(4)
P1A	C13A	1.845(2)	C11C	C12C	1.522(4)
N1A	C19A	1.358(3)	C13C	C14C	1.534(3)
N1A	C20A	1.391(3)	C13C	C18C	1.524(3)
N1A	C22A	1.450(3)	C14C	C15C	1.532(3)
N2A	C19A	1.361(3)	C15C	C16C	1.514(4)
N2A	C21A	1.388(3)	C16C	C17C	1.522(4)

N2A C34A 1.449(3)	C17C C18C 1.537(3)
C1A C2A 1.541(3)	C20C C21C 1.340(3)
C1A C6A 1.521(3)	C22C C23C 1.404(3)
C2A C3A 1.529(3)	C22C C27C 1.399(3)
C3A C4A 1.521(3)	C23C C24C 1.398(3)
C4A C5A 1.516(3)	C23C C28C 1.516(3)
C5A C6A 1.526(3)	C24C C25C 1.379(3)
C7A C8A 1.532(3)	C25C C26C 1.383(3)
C7A C12A 1.541(3)	C26C C27C 1.394(3)
C8A C9A 1.532(3)	C27C C31C 1.519(3)
C9A C10A 1.517(4)	C28C C29C 1.532(3)
C10A C11A 1.518(4)	C28C C30C 1.533(4)
C11A C12A 1.522(3)	C31C C32C 1.529(3)
C13A C14A 1.535(3)	C31C C33C 1.536(3)
C13A C18A 1.539(3)	C34C C35C 1.400(3)
C14A C15A 1.519(3)	C34C C39C 1.402(3)
C15A C16A 1.513(4)	C35C C36C 1.393(3)
C16A C17A 1.527(3)	C35C C40C 1.518(3)
C17A C18A 1.526(3)	C36C C37C 1.383(3)
C20A C21A 1.335(3)	C37C C38C 1.382(3)
C22A C23A 1.401(3)	C38C C39C 1.394(3)
C22A C27A 1.400(3)	C39C C43C 1.518(3)
C23A C24A 1.393(3)	C40C C41C 1.532(3)
C23A C28A 1.521(3)	C40C C42C 1.532(3)
C24A C25A 1.383(3)	C43C C44C 1.532(3)
C25A C26A 1.382(3)	C43C C45C 1.537(3)
C26A C27A 1.391(3)	P1S C19S 1.854(4)
C27A C31A 1.523(3)	P1S C1S 1.861(4)
C28A C29A 1.529(3)	P1S C7S 1.857(4)
C28A C30A 1.539(3)	P1S C13S 1.856(3)
C31A C32A 1.528(3)	C19S C20S 1.532(4)
C31A C33A 1.533(3)	C19S C24S 1.531(4)
C34A C35A 1.403(3)	C20S C21S 1.526(4)
C34A C39A 1.398(3)	C21S C22S 1.509(4)
C35A C36A 1.399(3)	C22S C23S 1.522(4)
C35A C40A 1.509(3)	C23S C24S 1.532(4)

C36A C37A 1.369(4)	C1S C2S 1.534(5)
C37A C38A 1.372(4)	C1S C6S 1.541(5)
C38A C39A 1.395(3)	C2S C3S 1.520(5)
C39A C43A 1.518(3)	C3S C4S 1.489(5)
C40A C41A 1.532(3)	C4S C5S 1.508(5)
C40A C42A 1.540(3)	C5S C6S 1.479(6)
C43A C44A 1.534(3)	C7S C8S 1.532(5)
C43A C45A 1.535(3)	C7S C12S 1.526(5)
Ni1B Cl1B 2.1646(8)	C8S C9S 1.516(5)
Ni1B Cl2B 2.1834(8)	C9S C10S 1.515(6)
Ni1B P1B 2.2522(8)	C10S C11S 1.520(6)
Ni1B C19B 1.908(2)	C11S C12S 1.529(5)
P1B C13B 1.843(2)	C13S C14S 1.523(3)
P1B C1B 1.855(3)	C13S C18S 1.539(4)
P1B C46B 1.851(3)	C14S C15S 1.539(4)
P1B C7B 1.839(2)	C15S C16S 1.517(4)
C13B C14B 1.531(3)	C16S C17S 1.535(4)
C13B C18B 1.525(3)	C17S C18S 1.519(3)
C14B C15B 1.528(3)	C25S C26S 1.5082
C15B C16B 1.516(3)	C26S C27S 1.4019
C16B C17B 1.521(3)	C26S C31S 1.4021
C17B C18B 1.533(3)	C27S C28S 1.3980
N1B C19B 1.360(3)	C28S C29S 1.3959
N1B C20B 1.392(3)	C29S C30S 1.3963
N1B C22B 1.447(3)	C30S C31S 1.3964
N2B C19B 1.351(3)	C32S C33S 1.5071
N2B C21B 1.389(3)	C33S C34S 1.4026
N2B C34B 1.448(3)	C33S C38S 1.4023
C1B C2B 1.535(4)	C34S C35S 1.3959
C1B C6B 1.529(4)	C35S C36S 1.3955
C2B C3B 1.530(4)	C36S C37S 1.3963
C3B C4B 1.510(4)	C37S C38S 1.3978
C4B C5B 1.521(4)	C39S C40S 1.5098
C5B C6B 1.530(4)	C40S C41S 1.4026
C46B C47B 1.533(4)	C40S C45S 1.4038
C46B C51B 1.528(4)	C41S C42S 1.4008

C47B	C48B	1.529(4)	C42S	C43S	1.3981
C48B	C49B	1.512(4)	C43S	C44S	1.3969
C49B	C50B	1.522(4)	C44S	C45S	1.3981
C50B	C51B	1.531(4)	C46S	C47S	1.5103
C7B	C8B	1.531(3)	C47S	C48S	1.4028
C7B	C12B	1.535(3)	C47S	C52S	1.4050
C8B	C9B	1.523(4)	C48S	C49S	1.4002
C9B	C10B	1.520(4)	C49S	C50S	1.3986
C10B	C11B	1.531(4)	C50S	C51S	1.3981
C11B	C12B	1.526(3)	C51S	C52S	1.3999
C20B	C21B	1.340(3)			

Table 5 Bond Angles for Schomaker52.

Atom	Atom	Atom	Angle/°	Atom	Atom	Atom	Angle/°
C11	Ni1	C12	177.37(2)	C9B	C10B	C11B	111.7(2)
C11	Ni1	P1	92.25(3)	C12B	C11B	C10B	111.5(2)
C12	Ni1	P1	89.96(3)	C11B	C12B	C7B	108.8(2)
C19	Ni1	C11	89.03(7)	N1B	C19B	Ni1B	127.00(15)
C19	Ni1	C12	88.71(6)	N2B	C19B	Ni1B	128.46(15)
C19	Ni1	P1	177.54(6)	N2B	C19B	N1B	104.33(18)
C19	N1	C20	111.33(17)	C21B	C20B	N1B	106.20(19)
C19	N1	C22	122.31(17)	C20B	C21B	N2B	107.30(19)
C20	N1	C22	126.19(17)	C23B	C22B	N1B	117.54(19)
C19	N2	C21	110.97(17)	C27B	C22B	N1B	119.08(18)
C19	N2	C34	124.19(17)	C27B	C22B	C23B	123.37(19)
C21	N2	C34	124.62(17)	C22B	C23B	C28B	122.3(2)
C1	P1	Ni1	108.85(7)	C24B	C23B	C22B	116.7(2)
C7	P1	Ni1	115.72(8)	C24B	C23B	C28B	120.9(2)
C7	P1	C1	103.27(10)	C25B	C24B	C23B	121.4(2)
C7	P1	C13	109.16(11)	C24B	C25B	C26B	120.5(2)
C13	P1	Ni1	113.11(7)	C25B	C26B	C27B	121.0(2)
C13	P1	C1	105.83(10)	C22B	C27B	C31B	122.23(19)
C2	C1	P1	114.74(14)	C26B	C27B	C22B	117.0(2)
C2	C1	C6	110.50(17)	C26B	C27B	C31B	120.6(2)

C6	C1	P1	108.34(14)	C23B	C28B	C29B	113.8(2)
C1	C2	C3	110.70(17)	C23B	C28B	C30B	109.5(2)
C4	C3	C2	111.24(18)	C29B	C28B	C30B	110.1(2)
C3	C4	C5	110.83(18)	C27B	C31B	C32B	113.2(2)
C4	C5	C6	110.96(19)	C27B	C31B	C33B	109.83(18)
C5	C6	C1	111.72(18)	C32B	C31B	C33B	110.19(19)
C8	C7	P1	117.62(18)	C35B	C34B	N2B	118.50(19)
C12	C7	P1	111.47(16)	C35B	C34B	C39B	123.2(2)
C12	C7	C8	110.19(19)	C39B	C34B	N2B	118.31(19)
C9	C8	C7	110.5(2)	C34B	C35B	C40B	122.71(19)
C8	C9	C10	111.5(2)	C36B	C35B	C34B	117.0(2)
C11	C10	C9	110.8(2)	C36B	C35B	C40B	120.2(2)
C12	C11	C10	111.5(3)	C37B	C36B	C35B	121.1(2)
C11	C12	C7	110.5(2)	C38B	C37B	C36B	120.3(2)
C14	C13	P1	113.70(15)	C37B	C38B	C39B	121.3(2)
C18	C13	P1	117.51(17)	C34B	C39B	C43B	121.6(2)
C18	C13	C14	109.82(17)	C38B	C39B	C34B	116.9(2)
C15	C14	C13	109.98(19)	C38B	C39B	C43B	121.4(2)
C14	C15	C16	111.8(2)	C35B	C40B	C41B	109.86(19)
C17	C16	C15	110.8(2)	C35B	C40B	C42B	112.3(2)
C18	C17	C16	110.9(2)	C42B	C40B	C41B	110.7(2)
C17	C18	C13	109.6(2)	C39B	C43B	C44B	113.5(2)
N1	C19	Ni1	127.22(15)	C45B	C43B	C39B	110.6(2)
N2	C19	Ni1	128.56(15)	C45B	C43B	C44B	109.4(2)
N2	C19	N1	104.16(17)	Cl1C	Ni1C	Cl2C	176.30(3)
C21	C20	N1	106.35(19)	Cl1C	Ni1C	P1C	92.42(3)
C20	C21	N2	107.19(19)	Cl2C	Ni1C	P1C	90.72(3)
C23	C22	N1	117.54(19)	C19C	Ni1C	Cl1C	88.77(7)
C27	C22	N1	118.92(19)	C19C	Ni1C	Cl2C	88.24(7)
C27	C22	C23	123.53(19)	C19C	Ni1C	P1C	175.46(6)
C22	C23	C28	122.2(2)	C52C	P1C	Ni1C	113.6(2)
C24	C23	C22	116.7(2)	C52C	P1C	C46C	100.3(3)
C24	C23	C28	121.1(2)	C1C	P1C	Ni1C	110.10(15)
C25	C24	C23	121.4(2)	C46C	P1C	Ni1C	110.6(3)
C24	C25	C26	120.3(2)	C7C	P1C	Ni1C	114.73(8)
C25	C26	C27	120.9(2)	C7C	P1C	C52C	113.1(3)

C22	C27	C31	121.82(19)	C7C	P1C	C1C	102.60(15)
C26	C27	C22	116.9(2)	C7C	P1C	C46C	103.1(3)
C26	C27	C31	121.1(2)	C13C	P1C	Ni1C	110.46(14)
C23	C28	C29	113.8(2)	C13C	P1C	C1C	109.0(2)
C23	C28	C30	109.5(2)	C13C	P1C	C7C	109.6(2)
C29	C28	C30	109.9(2)	C53C	C52C	P1C	115.5(4)
C27	C31	C32	113.57(19)	C57C	C52C	P1C	119.5(4)
C27	C31	C33	109.32(18)	C57C	C52C	C53C	109.7(4)
C32	C31	C33	109.85(19)	C52C	C53C	C54C	112.2(4)
C35	C34	N2	118.96(19)	C55C	C54C	C53C	112.5(4)
C35	C34	C39	123.19(19)	C54C	C55C	C56C	110.0(4)
C39	C34	N2	117.84(19)	C55C	C56C	C57C	111.1(4)
C34	C35	C40	122.74(19)	C52C	C57C	C56C	113.1(4)
C36	C35	C34	116.9(2)	C19C	N1C	C20C	111.21(17)
C36	C35	C40	120.2(2)	C19C	N1C	C22C	123.71(17)
C37	C36	C35	121.1(2)	C20C	N1C	C22C	125.02(17)
C38	C37	C36	120.6(2)	C19C	N2C	C21C	110.74(17)
C37	C38	C39	120.9(2)	C19C	N2C	C34C	125.13(17)
C34	C39	C43	122.4(2)	C21C	N2C	C34C	124.08(17)
C38	C39	C34	117.1(2)	C2C	C1C	P1C	113.9(2)
C38	C39	C43	120.3(2)	C2C	C1C	C6C	110.7(3)
C35	C40	C41	109.56(17)	C6C	C1C	P1C	110.0(2)
C35	C40	C42	113.21(19)	C1C	C2C	C3C	110.4(3)
C42	C40	C41	109.26(19)	C4C	C3C	C2C	111.1(3)
C39	C43	C44	113.9(2)	C3C	C4C	C5C	111.7(3)
C39	C43	C45	109.31(19)	C4C	C5C	C6C	111.2(3)
C44	C43	C45	109.3(2)	C5C	C6C	C1C	111.2(3)
Cl1A	Ni1A	P1A	90.60(3)	C47C	C46C	P1C	113.6(4)
Cl2A	Ni1A	Cl1A	177.57(2)	C47C	C46C	C51C	109.0(5)
Cl2A	Ni1A	P1A	91.62(3)	C51C	C46C	P1C	111.8(4)
C19A	Ni1A	Cl1A	88.25(6)	C46C	C47C	C48C	111.3(4)
C19A	Ni1A	Cl2A	89.59(6)	C49C	C48C	C47C	111.7(5)
C19A	Ni1A	P1A	176.99(6)	C48C	C49C	C50C	110.7(5)
C1A	P1A	Ni1A	110.10(7)	C49C	C50C	C51C	110.7(5)
C7A	P1A	Ni1A	111.02(7)	C50C	C51C	C46C	111.0(4)
C7A	P1A	C1A	107.50(10)	C8C	C7C	P1C	119.51(18)

C7A P1A C13A 109.66(10) C12C C7C P1C 112.92(16)
 C13A P1A Ni1A 115.53(8) C12C C7C C8C 109.46(19)
 C13A P1A C1A 102.45(10) C9C C8C C7C 109.6(2)
 C19A N1A C20A 111.18(17) C8C C9C C10C 111.7(2)
 C19A N1A C22A 123.51(17) C11C C10C C9C 111.4(2)
 C20A N1A C22A 125.25(17) C12C C11C C10C 111.7(2)
 C19A N2A C21A 110.66(18) C11C C12C C7C 110.0(2)
 C19A N2A C34A 124.81(18) C14C C13C P1C 111.9(3)
 C21A N2A C34A 124.41(17) C18C C13C P1C 116.7(3)
 C2A C1A P1A 108.49(15) C18C C13C C14C 111.2(3)
 C6A C1A P1A 114.98(15) C15C C14C C13C 108.1(3)
 C6A C1A C2A 110.12(18) C16C C15C C14C 110.8(3)
 C3A C2A C1A 111.7(2) C15C C16C C17C 113.0(3)
 C4A C3A C2A 111.0(2) C16C C17C C18C 111.6(3)
 C5A C4A C3A 110.72(19) C13C C18C C17C 108.7(3)
 C4A C5A C6A 111.5(2) N1C C19C Ni1C 128.95(15)
 C1A C6A C5A 110.80(19) N2C C19C Ni1C 126.67(15)
 C8A C7A P1A 118.35(16) N2C C19C N1C 104.35(17)
 C8A C7A C12A 110.24(18) C21C C20C N1C 106.47(19)
 C12A C7A P1A 111.61(15) C20C C21C N2C 107.23(19)
 C9A C8A C7A 109.83(19) C23C C22C N1C 118.00(19)
 C10A C9A C8A 111.7(2) C27C C22C N1C 118.79(18)
 C9A C10A C11A 111.2(2) C27C C22C C23C 123.20(19)
 C10A C11A C12A 111.3(2) C22C C23C C28C 122.48(19)
 C11A C12A C7A 110.18(19) C24C C23C C22C 116.9(2)
 C14A C13A P1A 112.89(15) C24C C23C C28C 120.5(2)
 C14A C13A C18A 109.71(17) C25C C24C C23C 121.0(2)
 C18A C13A P1A 118.16(16) C24C C25C C26C 120.6(2)
 C15A C14A C13A 109.67(19) C25C C26C C27C 121.0(2)
 C16A C15A C14A 111.6(2) C22C C27C C31C 122.14(19)
 C15A C16A C17A 111.1(2) C26C C27C C22C 117.1(2)
 C18A C17A C16A 111.4(2) C26C C27C C31C 120.5(2)
 C17A C18A C13A 110.1(2) C23C C28C C29C 112.79(19)
 N1A C19A Ni1A 128.32(15) C23C C28C C30C 110.21(19)
 N1A C19A N2A 104.23(17) C29C C28C C30C 110.1(2)
 N2A C19A Ni1A 127.41(16) C27C C31C C32C 113.52(19)

C21A C20A N1A	106.46(19)	C27C C31C C33C	108.62(18)
C20A C21A N2A	107.47(18)	C32C C31C C33C	110.3(2)
C23A C22A N1A	118.89(18)	C35C C34C N2C	118.77(19)
C27A C22A N1A	118.14(19)	C35C C34C C39C	122.53(19)
C27A C22A C23A	122.95(19)	C39C C34C N2C	118.66(18)
C22A C23A C28A	121.84(19)	C34C C35C C40C	123.30(19)
C24A C23A C22A	117.3(2)	C36C C35C C34C	117.2(2)
C24A C23A C28A	120.7(2)	C36C C35C C40C	119.43(19)
C25A C24A C23A	120.9(2)	C37C C36C C35C	121.7(2)
C26A C25A C24A	120.5(2)	C38C C37C C36C	119.6(2)
C25A C26A C27A	121.0(2)	C37C C38C C39C	121.4(2)
C22A C27A C31A	122.29(19)	C34C C39C C43C	122.32(19)
C26A C27A C22A	117.2(2)	C38C C39C C34C	117.47(19)
C26A C27A C31A	120.4(2)	C38C C39C C43C	120.0(2)
C23A C28A C29A	113.37(19)	C35C C40C C41C	110.02(19)
C23A C28A C30A	108.80(18)	C35C C40C C42C	111.74(19)
C29A C28A C30A	109.99(19)	C41C C40C C42C	110.5(2)
C27A C31A C32A	113.07(19)	C39C C43C C44C	112.78(19)
C27A C31A C33A	110.2(2)	C39C C43C C45C	108.34(18)
C32A C31A C33A	109.9(2)	C44C C43C C45C	110.8(2)
C35A C34A N2A	118.30(19)	C7S P1S C1S	103.41(16)
C39A C34A N2A	119.11(19)	C13S P1S C1S	106.30(18)
C39A C34A C35A	122.6(2)	C13S P1S C7S	103.55(18)
C34A C35A C40A	122.8(2)	C20S C19S P1S	112.4(5)
C36A C35A C34A	116.9(2)	C24S C19S P1S	115.1(5)
C36A C35A C40A	120.2(2)	C24S C19S C20S	109.2(6)
C37A C36A C35A	121.4(2)	C21S C20S C19S	112.1(6)
C36A C37A C38A	120.4(2)	C22S C21S C20S	113.1(6)
C37A C38A C39A	121.3(2)	C21S C22S C23S	111.9(6)
C34A C39A C43A	123.0(2)	C22S C23S C24S	111.3(6)
C38A C39A C34A	117.3(2)	C19S C24S C23S	110.7(5)
C38A C39A C43A	119.6(2)	C2S C1S P1S	110.6(2)
C35A C40A C41A	109.63(19)	C2S C1S C6S	108.5(3)
C35A C40A C42A	111.5(2)	C6S C1S P1S	110.3(3)
C41A C40A C42A	111.3(2)	C3S C2S C1S	111.8(3)
C39A C43A C44A	112.1(2)	C4S C3S C2S	112.4(3)

C39A	C43A	C45A	109.60(18)	C3S	C4S	C5S	111.8(3)
C44A	C43A	C45A	110.1(2)	C6S	C5S	C4S	111.3(4)
C11B	Ni1B	C12B	175.70(2)	C5S	C6S	C1S	112.6(3)
C11B	Ni1B	P1B	89.99(3)	C8S	C7S	P1S	118.1(3)
C12B	Ni1B	P1B	92.59(3)	C12S	C7S	P1S	109.4(3)
C19B	Ni1B	C11B	90.26(7)	C12S	C7S	C8S	110.3(3)
C19B	Ni1B	C12B	87.14(7)	C9S	C8S	C7S	111.5(3)
C19B	Ni1B	P1B	179.50(7)	C10S	C9S	C8S	111.8(4)
C13B	P1B	Ni1B	112.87(8)	C9S	C10S	C11S	111.8(4)
C13B	P1B	C1B	107.3(3)	C10S	C11S	C12S	110.5(3)
C13B	P1B	C46B	101.9(2)	C7S	C12S	C11S	111.5(3)
C1B	P1B	Ni1B	109.7(3)	C14S	C13S	P1S	116.7(3)
C46B	P1B	Ni1B	110.6(3)	C14S	C13S	C18S	108.9(3)
C7B	P1B	Ni1B	113.13(8)	C18S	C13S	P1S	111.3(2)
C7B	P1B	C13B	110.75(10)	C13S	C14S	C15S	112.0(3)
C7B	P1B	C1B	102.4(2)	C16S	C15S	C14S	111.9(3)
C7B	P1B	C46B	106.9(3)	C15S	C16S	C17S	108.1(3)
C14B	C13B	P1B	110.71(14)	C18S	C17S	C16S	111.7(3)
C18B	C13B	P1B	119.11(16)	C17S	C18S	C13S	112.3(3)
C18B	C13B	C14B	110.68(18)	C27S	C26S	C25S	120.9
C15B	C14B	C13B	110.61(18)	C27S	C26S	C31S	118.2
C16B	C15B	C14B	110.7(2)	C31S	C26S	C25S	120.9
C15B	C16B	C17B	111.3(2)	C28S	C27S	C26S	121.1
C16B	C17B	C18B	111.4(2)	C29S	C28S	C27S	120.0
C13B	C18B	C17B	110.1(2)	C28S	C29S	C30S	119.6
C19B	N1B	C20B	111.19(17)	C29S	C30S	C31S	120.1
C19B	N1B	C22B	122.90(17)	C30S	C31S	C26S	121.1
C20B	N1B	C22B	125.75(17)	C34S	C33S	C32S	120.9
C19B	N2B	C21B	110.96(17)	C38S	C33S	C32S	121.0
C19B	N2B	C34B	124.25(18)	C38S	C33S	C34S	118.1
C21B	N2B	C34B	124.69(17)	C35S	C34S	C33S	121.1
C2B	C1B	P1B	109.3(3)	C36S	C35S	C34S	120.1
C6B	C1B	P1B	113.7(3)	C35S	C36S	C37S	119.6
C6B	C1B	C2B	109.6(4)	C36S	C37S	C38S	120.0
C3B	C2B	C1B	111.6(4)	C37S	C38S	C33S	121.1
C4B	C3B	C2B	111.5(4)	C41S	C40S	C39S	120.9

C3B	C4B	C5B	111.1(4)	C41S	C40S	C45S	118.1
C4B	C5B	C6B	111.3(4)	C45S	C40S	C39S	121.0
C1B	C6B	C5B	111.5(4)	C42S	C41S	C40S	121.0
C47B	C46B	P1B	110.0(4)	C43S	C42S	C41S	120.2
C51B	C46B	P1B	114.2(4)	C44S	C43S	C42S	119.4
C51B	C46B	C47B	110.0(4)	C43S	C44S	C45S	120.1
C48B	C47B	C46B	111.3(4)	C44S	C45S	C40S	121.2
C49B	C48B	C47B	111.5(4)	C48S	C47S	C46S	121.0
C48B	C49B	C50B	111.3(4)	C48S	C47S	C52S	118.0
C49B	C50B	C51B	110.8(4)	C52S	C47S	C46S	121.0
C46B	C51B	C50B	111.0(4)	C49S	C48S	C47S	121.1
C8B	C7B	P1B	118.21(17)	C50S	C49S	C48S	120.2
C8B	C7B	C12B	110.30(19)	C51S	C50S	C49S	119.4
C12B	C7B	P1B	114.80(16)	C50S	C51S	C52S	120.0
C9B	C8B	C7B	108.9(2)	C51S	C52S	C47S	121.2
C10B	C9B	C8B	111.9(2)				

Table 6 Torsion Angles for Schomaker52.

A	B	C	D	Angle/°	A	B	C	D	Angle/°
Ni1	P1	C1	C2	76.32(16)	C7B	C8B	C9B	C10B	-56.9(3)
Ni1	P1	C1	C6	-47.67(16)	C8B	C7B	C12B	C11B	-61.2(3)
Ni1	P1	C7	C8	160.83(16)	C8B	C9B	C10B	C11B	53.7(3)
Ni1	P1	C7	C12	-70.54(19)	C9B	C10B	C11B	C12B	-53.7(3)
Ni1	P1	C13	C14	50.58(17)	C10B	C11B	C12B	C7B	56.9(3)
Ni1	P1	C13	C18	-179.17(14)	C12B	C7B	C8B	C9B	61.0(3)
N1	C20	C21	N2	0.5(2)	C19B	N1B	C20B	C21B	0.3(2)
N1	C22	C23	C24	174.1(2)	C19B	N1B	C22B	C23B	-82.7(3)
N1	C22	C23	C28	-9.6(3)	C19B	N1B	C22B	C27B	96.0(2)
N1	C22	C27	C26	-173.45(19)	C19B	N2B	C21B	C20B	-1.0(2)
N1	C22	C27	C31	11.2(3)	C19B	N2B	C34B	C35B	-94.2(3)
N2	C34	C35	C36	178.22(18)	C19B	N2B	C34B	C39B	86.2(3)
N2	C34	C35	C40	-5.8(3)	C20B	N1B	C19B	Ni1B	174.16(15)
N2	C34	C39	C38	-176.94(18)	C20B	N1B	C19B	N2B	-0.9(2)
N2	C34	C39	C43	8.7(3)	C20B	N1B	C22B	C23B	92.3(3)

P1	C1	C2	C3	-178.14(15)	C20B N1B	C22B C27B	-89.0(3)
P1	C1	C6	C5	-178.49(17)	C21B N2B	C19B Ni1B	-173.82(16)
P1	C7	C8	C9	-173.96(19)	C21B N2B	C19B N1B	1.1(2)
P1	C7	C12	C11	170.6(2)	C21B N2B	C34B C35B	89.8(3)
P1	C13	C14	C15	-167.86(16)	C21B N2B	C34B C39B	-89.9(3)
P1	C13	C18	C17	168.13(16)	C22B N1B	C19B Ni1B	-10.2(3)
C1	P1	C7	C8	42.0(2)	C22B N1B	C19B N2B	174.79(18)
C1	P1	C7	C12	170.65(17)	C22B N1B	C20B C21B	-175.21(19)
C1	P1	C13	C14	169.66(15)	C22B C23B	C24B C25B	0.0(4)
C1	P1	C13	C18	-60.09(19)	C22B C23B	C28B C29B	148.8(2)
C1	C2	C3	C4	57.1(3)	C22B C23B	C28B C30B	-87.6(3)
C2	C1	C6	C5	55.0(3)	C22B C27B	C31B C32B	-146.7(2)
C2	C3	C4	C5	-57.3(3)	C22B C27B	C31B C33B	89.7(2)
C3	C4	C5	C6	56.2(3)	C23B C22B	C27B C26B	3.9(3)
C4	C5	C6	C1	-55.4(3)	C23B C22B	C27B C31B	-171.4(2)
C6	C1	C2	C3	-55.3(2)	C23B C24B	C25B C26B	2.5(4)
C7	P1	C1	C2	-160.21(16)	C24B C23B	C28B C29B	-35.4(3)
C7	P1	C1	C6	75.81(17)	C24B C23B	C28B C30B	88.3(3)
C7	P1	C13	C14	-79.79(18)	C24B C25B	C26B C27B	-1.9(4)
C7	P1	C13	C18	50.46(19)	C25B C26B	C27B C22B	-1.2(4)
C7	C8	C9	C10	-56.5(3)	C25B C26B	C27B C31B	174.2(2)
C8	C7	C12	C11	-56.9(3)	C26B C27B	C31B C32B	38.1(3)
C8	C9	C10	C11	56.0(4)	C26B C27B	C31B C33B	-85.5(3)
C9	C10	C11	C12	-56.1(4)	C27B C22B	C23B C24B	-3.3(3)
C10	C11	C12	C7	57.0(3)	C27B C22B	C23B C28B	172.7(2)
C12	C7	C8	C9	56.8(3)	C28B C23B	C24B C25B	-176.1(2)
C13	P1	C1	C2	-45.54(18)	C34B N2B	C19B Ni1B	9.7(3)
C13	P1	C1	C6	-169.52(15)	C34B N2B	C19B N1B	-175.37(18)
C13	P1	C7	C8	-70.2(2)	C34B N2B	C21B C20B	175.49(19)
C13	P1	C7	C12	58.4(2)	C34B C35B	C36B C37B	0.7(3)
C13	C14	C15	C16	-55.9(2)	C34B C35B	C40B C41B	-99.5(3)
C14	C13	C18	C17	-59.8(3)	C34B C35B	C40B C42B	136.9(2)
C14	C15	C16	C17	54.9(3)	C34B C39B	C43B C44B	-150.3(2)
C15	C16	C17	C18	-56.3(3)	C34B C39B	C43B C45B	86.3(3)
C16	C17	C18	C13	59.0(3)	C35B C34B	C39B C38B	3.6(3)
C18	C13	C14	C15	58.2(3)	C35B C34B	C39B C43B	-173.2(2)

C19	N1	C20	C21	0.1(2)	C35B C36B C37B C38B	2.1(4)
C19	N1	C22	C23	-87.4(2)	C36B C35B C40B C41B	77.5(3)
C19	N1	C22	C27	91.1(2)	C36B C35B C40B C42B	-46.1(3)
C19	N2	C21	C20	-0.9(3)	C36B C37B C38B C39B	-2.1(4)
C19	N2	C34	C35	-93.8(2)	C37B C38B C39B C34B	-0.7(3)
C19	N2	C34	C39	87.4(3)	C37B C38B C39B C43B	176.1(2)
C20	N1	C19	Ni1	176.60(15)	C38B C39B C43B C44B	33.1(3)
C20	N1	C19	N2	-0.7(2)	C38B C39B C43B C45B	-90.3(3)
C20	N1	C22	C23	87.4(3)	C39B C34B C35B C36B	-3.6(3)
C20	N1	C22	C27	-94.1(3)	C39B C34B C35B C40B	173.4(2)
C21	N2	C19	Ni1	-176.26(16)	C40B C35B C36B C37B	-176.4(2)
C21	N2	C19	N1	0.9(2)	Ni1C P1C C52C C53C	-61.4(7)
C21	N2	C34	C35	92.2(3)	Ni1C P1C C52C C57C	164.3(6)
C21	N2	C34	C39	-86.7(3)	Ni1C P1C C1C C2C	-77.6(4)
C22	N1	C19	Ni1	-7.9(3)	Ni1C P1C C1C C6C	47.2(4)
C22	N1	C19	N2	174.84(18)	Ni1C P1C C46C C47C	-54.8(7)
C22	N1	C20	C21	-175.2(2)	Ni1C P1C C46C C51C	69.1(7)
C22	C23	C24	C25	0.2(4)	Ni1C P1C C7C C8C	-162.30(18)
C22	C23	C28	C29	149.4(2)	Ni1C P1C C7C C12C	66.80(19)
C22	C23	C28	C30	-87.2(3)	Ni1C P1C C13C C14C	-45.1(4)
C22	C27	C31	C32	-151.3(2)	Ni1C P1C C13C C18C	-174.7(3)
C22	C27	C31	C33	85.6(2)	P1C C52C C53C C54C	168.5(6)
C23	C22	C27	C26	5.0(3)	P1C C52C C57C C56C	-169.5(6)
C23	C22	C27	C31	-170.4(2)	P1C C1C C2C C3C	-178.8(3)
C23	C24	C25	C26	3.1(4)	P1C C1C C6C C5C	177.3(3)
C24	C23	C28	C29	-34.5(3)	P1C C46C C47C C48C	-178.2(6)
C24	C23	C28	C30	88.9(3)	P1C C46C C51C C50C	175.7(6)
C24	C25	C26	C27	-2.4(4)	P1C C7C C8C C9C	167.70(19)
C25	C26	C27	C22	-1.5(3)	P1C C7C C12C C11C	-164.47(17)
C25	C26	C27	C31	173.9(2)	P1C C13C C14C C15C	165.5(3)
C26	C27	C31	C32	33.5(3)	P1C C13C C18C C17C	-169.8(4)
C26	C27	C31	C33	-89.5(3)	C52C P1C C46C C47C	65.4(7)
C27	C22	C23	C24	-4.3(3)	C52C P1C C46C C51C	-170.8(7)
C27	C22	C23	C28	171.9(2)	C52C P1C C7C C8C	65.3(3)
C28	C23	C24	C25	-176.1(2)	C52C P1C C7C C12C	-65.6(3)
C34	N2	C19	Ni1	9.0(3)	C52C C53C C54C C55C	55.5(8)

C34	N2	C19	N1	-173.80(18)	C53C	C52C	C57C	C56C	53.8(8)
C34	N2	C21	C20	173.8(2)	C53C	C54C	C55C	C56C	-55.6(8)
C34	C35	C36	C37	-0.9(3)	C54C	C55C	C56C	C57C	55.2(8)
C34	C35	C40	C41	-94.4(2)	C55C	C56C	C57C	C52C	-55.9(8)
C34	C35	C40	C42	143.3(2)	C57C	C52C	C53C	C54C	-52.9(8)
C34	C39	C43	C44	-144.3(2)	N1C	C20C	C21C	N2C	0.0(2)
C34	C39	C43	C45	93.1(3)	N1C	C22C	C23C	C24C	-177.37(19)
C35	C34	C39	C38	4.3(3)	N1C	C22C	C23C	C28C	6.4(3)
C35	C34	C39	C43	-170.1(2)	N1C	C22C	C27C	C26C	176.29(19)
C35	C36	C37	C38	3.4(3)	N1C	C22C	C27C	C31C	-9.7(3)
C36	C35	C40	C41	81.4(2)	N2C	C34C	C35C	C36C	-179.58(19)
C36	C35	C40	C42	-40.8(3)	N2C	C34C	C35C	C40C	3.3(3)
C36	C37	C38	C39	-2.1(4)	N2C	C34C	C39C	C38C	178.95(18)
C37	C38	C39	C34	-1.7(3)	N2C	C34C	C39C	C43C	-5.7(3)
C37	C38	C39	C43	172.8(2)	C1C	P1C	C7C	C8C	-42.9(3)
C38	C39	C43	C44	41.5(3)	C1C	P1C	C7C	C12C	-173.8(2)
C38	C39	C43	C45	-81.1(3)	C1C	P1C	C13C	C14C	-166.1(3)
C39	C34	C35	C36	-3.0(3)	C1C	P1C	C13C	C18C	64.2(5)
C39	C34	C35	C40	172.95(19)	C1C	C2C	C3C	C4C	-57.0(5)
C40	C35	C36	C37	-177.0(2)	C2C	C1C	C6C	C5C	-56.0(5)
Ni1A	P1A	C1A	C2A	55.17(16)	C2C	C3C	C4C	C5C	56.1(6)
Ni1A	P1A	C1A	C6A	-68.60(17)	C3C	C4C	C5C	C6C	-55.0(6)
Ni1A	P1A	C7A	C8A	-178.03(15)	C4C	C5C	C6C	C1C	54.7(5)
Ni1A	P1A	C7A	C12A	-48.49(16)	C6C	C1C	C2C	C3C	56.7(4)
Ni1A	P1A	C13A	C14A	69.24(17)	C46C	P1C	C52C	C53C	-179.3(6)
Ni1A	P1A	C13A	C18A	-160.87(14)	C46C	P1C	C52C	C57C	46.4(8)
P1A	C1A	C2A	C3A	178.00(17)	C46C	P1C	C7C	C8C	-42.0(4)
P1A	C1A	C6A	C5A	178.89(16)	C46C	P1C	C7C	C12C	-172.9(3)
P1A	C7A	C8A	C9A	-172.29(18)	C46C	C47C	C48C	C49C	-56.2(9)
P1A	C7A	C12A	C11A	168.21(15)	C47C	C46C	C51C	C50C	-57.9(8)
P1A	C13A	C14A	C15A	-166.74(17)	C47C	C48C	C49C	C50C	55.4(10)
P1A	C13A	C18A	C17A	170.30(15)	C48C	C49C	C50C	C51C	-56.4(10)
N1A	C20A	C21A	N2A	0.2(2)	C49C	C50C	C51C	C46C	58.4(8)
N1A	C22A	C23A	C24A	177.21(19)	C51C	C46C	C47C	C48C	56.4(8)
N1A	C22A	C23A	C28A	-8.5(3)	C7C	P1C	C52C	C53C	71.6(6)
N1A	C22A	C27A	C26A	-178.15(19)	C7C	P1C	C52C	C57C	-62.7(7)

N1A	C22A	C27A	C31A	4.7(3)	C7C	P1C	C1C	C2C	159.8(4)
N2A	C34A	C35A	C36A	178.73(19)	C7C	P1C	C1C	C6C	-75.3(4)
N2A	C34A	C35A	C40A	-4.5(3)	C7C	P1C	C46C	C47C	-177.9(6)
N2A	C34A	C39A	C38A	-178.98(19)	C7C	P1C	C46C	C51C	-54.0(7)
N2A	C34A	C39A	C43A	3.9(3)	C7C	P1C	C13C	C14C	82.3(3)
C1A	P1A	C7A	C8A	61.5(2)	C7C	P1C	C13C	C18C	-47.3(4)
C1A	P1A	C7A	C12A	-168.96(14)	C7C	C8C	C9C	C10C	57.2(3)
C1A	P1A	C13A	C14A	-171.05(16)	C8C	C7C	C12C	C11C	59.8(3)
C1A	P1A	C13A	C18A	-41.17(18)	C8C	C9C	C10C	C11C	-53.9(3)
C1A	C2A	C3A	C4A	55.2(3)	C9C	C10C	C11C	C12C	53.5(3)
C2A	C1A	C6A	C5A	56.0(2)	C10C	C11C	C12C	C7C	-56.8(3)
C2A	C3A	C4A	C5A	-55.5(3)	C12C	C7C	C8C	C9C	-59.9(3)
C3A	C4A	C5A	C6A	56.9(3)	C13C	P1C	C1C	C2C	43.7(4)
C4A	C5A	C6A	C1A	-57.6(3)	C13C	P1C	C1C	C6C	168.5(4)
C6A	C1A	C2A	C3A	-55.4(3)	C13C	P1C	C7C	C8C	72.8(3)
C7A	P1A	C1A	C2A	176.23(15)	C13C	P1C	C7C	C12C	-58.1(2)
C7A	P1A	C1A	C6A	52.46(18)	C13C	C14C	C15C	C16C	57.7(5)
C7A	P1A	C13A	C14A	-57.11(19)	C14C	C13C	C18C	C17C	60.3(5)
C7A	P1A	C13A	C18A	72.78(18)	C14C	C15C	C16C	C17C	-54.6(6)
C7A	C8A	C9A	C10A	-56.5(3)	C15C	C16C	C17C	C18C	53.0(6)
C8A	C7A	C12A	C11A	-58.1(2)	C16C	C17C	C18C	C13C	-54.5(5)
C8A	C9A	C10A	C11A	55.5(3)	C18C	C13C	C14C	C15C	-62.0(5)
C9A	C10A	C11A	C12A	-55.6(3)	C19C	N1C	C20C	C21C	-0.3(2)
C10A	C11A	C12A	C7A	56.9(3)	C19C	N1C	C22C	C23C	91.6(3)
C12A	C7A	C8A	C9A	57.5(3)	C19C	N1C	C22C	C27C	-89.6(3)
C13A	P1A	C1A	C2A	-68.25(17)	C19C	N2C	C21C	C20C	0.4(2)
C13A	P1A	C1A	C6A	167.98(16)	C19C	N2C	C34C	C35C	98.0(2)
C13A	P1A	C7A	C8A	-49.2(2)	C19C	N2C	C34C	C39C	-84.3(3)
C13A	P1A	C7A	C12A	80.38(17)	C20C	N1C	C19C	Ni1C	-177.81(16)
C13A	C14A	C15A	C16A	-58.3(3)	C20C	N1C	C19C	N2C	0.5(2)
C14A	C13A	C18A	C17A	-58.4(2)	C20C	N1C	C22C	C23C	-85.3(3)
C14A	C15A	C16A	C17A	55.8(3)	C20C	N1C	C22C	C27C	93.6(3)
C15A	C16A	C17A	C18A	-54.6(3)	C21C	N2C	C19C	Ni1C	177.84(15)
C16A	C17A	C18A	C13A	56.1(3)	C21C	N2C	C19C	N1C	-0.5(2)
C18A	C13A	C14A	C15A	59.2(3)	C21C	N2C	C34C	C35C	-84.8(3)
C19A	N1A	C20A	C21A	-0.2(3)	C21C	N2C	C34C	C39C	92.9(2)

C19A N1A C22A C23A -89.8(2)	C22C N1C C19C Ni1C 5.0(3)
C19A N1A C22A C27A 91.5(2)	C22C N1C C19C N2C -176.70(18)
C19A N2A C21A C20A -0.1(3)	C22C N1C C20C C21C 176.9(2)
C19A N2A C34A C35A -83.8(3)	C22C C23C C24C C25C -0.2(3)
C19A N2A C34A C39A 97.2(2)	C22C C23C C28C C29C -145.2(2)
C20A N1A C19A Ni1A -177.68(15)	C22C C23C C28C C30C 91.3(3)
C20A N1A C19A N2A 0.1(2)	C22C C27C C31C C32C 147.8(2)
C20A N1A C22A C23A 93.3(3)	C22C C27C C31C C33C -89.1(2)
C20A N1A C22A C27A -85.4(3)	C23C C22C C27C C26C -4.9(3)
C21A N2A C19A Ni1A 177.83(15)	C23C C22C C27C C31C 169.1(2)
C21A N2A C19A N1A 0.0(2)	C23C C24C C25C C26C -2.2(4)
C21A N2A C34A C35A 91.8(3)	C24C C23C C28C C29C 38.7(3)
C21A N2A C34A C39A -87.2(3)	C24C C23C C28C C30C -84.8(3)
C22A N1A C19A Ni1A 5.0(3)	C24C C25C C26C C27C 1.1(4)
C22A N1A C19A N2A -177.20(18)	C25C C26C C27C C22C 2.4(3)
C22A N1A C20A C21A 177.07(19)	C25C C26C C27C C31C -171.7(2)
C22A C23A C24A C25A 1.9(3)	C26C C27C C31C C32C -38.4(3)
C22A C23A C28A C29A 148.4(2)	C26C C27C C31C C33C 84.7(3)
C22A C23A C28A C30A -88.9(2)	C27C C22C C23C C24C 3.8(3)
C22A C27A C31A C32A -145.5(2)	C27C C22C C23C C28C -172.4(2)
C22A C27A C31A C33A 91.2(3)	C28C C23C C24C C25C 176.2(2)
C23A C22A C27A C26A 3.2(3)	C34C N2C C19C Ni1C -4.6(3)
C23A C22A C27A C31A -173.9(2)	C34C N2C C19C N1C 176.99(18)
C23A C24A C25A C26A 1.1(4)	C34C N2C C21C C20C -177.19(19)
C24A C23A C28A C29A -37.6(3)	C34C C35C C36C C37C -0.2(3)
C24A C23A C28A C30A 85.1(3)	C34C C35C C40C C41C 98.9(2)
C24A C25A C26A C27A -2.1(4)	C34C C35C C40C C42C -137.9(2)
C25A C26A C27A C22A 0.0(3)	C34C C39C C43C C44C 143.1(2)
C25A C26A C27A C31A 177.2(2)	C34C C39C C43C C45C -93.9(2)
C26A C27A C31A C32A 37.5(3)	C35C C34C C39C C38C -3.5(3)
C26A C27A C31A C33A -85.9(3)	C35C C34C C39C C43C 171.9(2)
C27A C22A C23A C24A -4.2(3)	C35C C36C C37C C38C -1.7(3)
C27A C22A C23A C28A 170.1(2)	C36C C35C C40C C41C -78.1(3)
C28A C23A C24A C25A -172.4(2)	C36C C35C C40C C42C 45.0(3)
C34A N2A C19A Ni1A -6.1(3)	C36C C37C C38C C39C 1.1(3)
C34A N2A C19A N1A 176.08(18)	C37C C38C C39C C34C 1.4(3)

C34A N2A C21A C20A -176.2(2)	C37C C38C C39C C43C -174.0(2)
C34A C35A C36A C37A 0.6(3)	C38C C39C C43C C44C -41.7(3)
C34A C35A C40A C41A -93.6(3)	C38C C39C C43C C45C 81.3(3)
C34A C35A C40A C42A 142.7(2)	C39C C34C C35C C36C 2.8(3)
C34A C39A C43A C44A -141.3(2)	C39C C34C C35C C40C -174.3(2)
C34A C39A C43A C45A 96.1(2)	C40C C35C C36C C37C 177.1(2)
C35A C34A C39A C38A 2.1(3)	P1S C19S C20S C21S -175.3(11)
C35A C34A C39A C43A -175.1(2)	P1S C19S C24S C23S 173.9(10)
C35A C36A C37A C38A 1.3(4)	P1S C1S C2S C3S 174.7(3)
C36A C35A C40A C41A 83.1(3)	P1S C1S C6S C5S -177.4(3)
C36A C35A C40A C42A -40.6(3)	P1S C7S C8S C9S -178.0(3)
C36A C37A C38A C39A -1.5(4)	P1S C7S C12S C11S 172.3(3)
C37A C38A C39A C34A -0.1(3)	P1S C13S C14S C15S -178.6(3)
C37A C38A C39A C43A 177.1(2)	P1S C13S C18S C17S 175.3(3)
C38A C39A C43A C44A 41.6(3)	C19S C20S C21S C22S -52.4(14)
C38A C39A C43A C45A -81.0(3)	C20S C19S C24S C23S -58.6(11)
C39A C34A C35A C36A -2.3(3)	C20S C21S C22S C23S 50.6(14)
C39A C34A C35A C40A 174.5(2)	C21S C22S C23S C24S -53.4(13)
C40A C35A C36A C37A -176.3(2)	C22S C23S C24S C19S 58.1(12)
Ni1B P1B C13B C14B 66.79(17)	C24S C19S C20S C21S 55.7(12)
Ni1B P1B C13B C18B -163.21(16)	C1S P1S C7S C8S 56.6(3)
Ni1B P1B C1B C2B 47.5(5)	C1S P1S C7S C12S -176.1(3)
Ni1B P1B C1B C6B -75.4(5)	C1S P1S C13S C14S -20.3(4)
Ni1B P1B C46B C47B 50.0(6)	C1S P1S C13S C18S 105.5(3)
Ni1B P1B C46B C51B -74.2(7)	C1S C2S C3S C4S -54.1(4)
Ni1B P1B C7B C8B 175.02(15)	C2S C1S C6S C5S -56.1(4)
Ni1B P1B C7B C12B -52.03(18)	C2S C3S C4S C5S 53.5(5)
P1B C13B C14B C15B -168.10(16)	C3S C4S C5S C6S -54.9(5)
P1B C13B C18B C17B 173.09(18)	C4S C5S C6S C1S 57.1(5)
P1B C1B C2B C3B 179.0(5)	C6S C1S C2S C3S 53.6(4)
P1B C1B C6B C5B 178.5(5)	C7S P1S C1S C2S 56.9(3)
P1B C46B C47B C48B 177.4(7)	C7S P1S C1S C6S 176.9(3)
P1B C46B C51B C50B -179.0(7)	C7S P1S C13S C14S 88.3(4)
P1B C7B C8B C9B -164.13(17)	C7S P1S C13S C18S -145.9(3)
P1B C7B C12B C11B 162.29(17)	C7S C8S C9S C10S -54.6(5)
C13B P1B C1B C2B -75.5(5)	C8S C7S C12S C11S -56.2(4)

C13B P1B C1B C6B 161.7(5)	C8S C9S C10S C11S 54.8(5)
C13B P1B C46B C47B -70.2(6)	C9S C10S C11S C12S -55.2(5)
C13B P1B C46B C51B 165.6(6)	C10S C11S C12S C7S 56.3(5)
C13B P1B C7B C8B -57.1(2)	C12S C7S C8S C9S 55.1(4)
C13B P1B C7B C12B 75.83(18)	C13S P1S C1S C2S 165.6(3)
C13B C14B C15B C16B -56.8(3)	C13S P1S C1S C6S -74.4(3)
C14B C13B C18B C17B -56.9(3)	C13S P1S C7S C8S -54.1(3)
C14B C15B C16B C17B 56.0(3)	C13S P1S C7S C12S 73.2(3)
C15B C16B C17B C18B -56.0(3)	C13S C14S C15S C16S -58.1(6)
C16B C17B C18B C13B 56.2(3)	C14S C13S C18S C17S -54.7(5)
C18B C13B C14B C15B 57.6(3)	C14S C15S C16S C17S 57.3(6)
N1B C20B C21B N2B 0.4(2)	C15S C16S C17S C18S -57.3(5)
N1B C22B C23B C24B 175.3(2)	C16S C17S C18S C13S 57.7(5)
N1B C22B C23B C28B -8.6(3)	C18S C13S C14S C15S 54.4(5)
N1B C22B C27B C26B -174.8(2)	C25S C26S C27S C28S 178.6
N1B C22B C27B C31B 9.9(3)	C25S C26S C31S C30S -178.6
N2B C34B C35B C36B 176.72(19)	C26S C27S C28S C29S 0.0
N2B C34B C35B C40B -6.2(3)	C27S C26S C31S C30S 0.3
N2B C34B C39B C38B -176.74(19)	C27S C28S C29S C30S 0.2
N2B C34B C39B C43B 6.5(3)	C28S C29S C30S C31S -0.2
C1B P1B C13B C14B -172.2(3)	C29S C30S C31S C26S -0.1
C1B P1B C13B C18B -42.2(3)	C31S C26S C27S C28S -0.2
C1B P1B C7B C8B 57.0(3)	C32S C33S C34S C35S 178.5
C1B P1B C7B C12B -170.0(3)	C32S C33S C38S C37S -178.5
C1B C2B C3B C4B 56.2(7)	C33S C34S C35S C36S 0.1
C2B C1B C6B C5B 55.8(6)	C34S C33S C38S C37S 0.3
C2B C3B C4B C5B -55.3(7)	C34S C35S C36S C37S 0.1
C3B C4B C5B C6B 55.4(6)	C35S C36S C37S C38S -0.1
C4B C5B C6B C1B -56.2(7)	C36S C37S C38S C33S -0.1
C6B C1B C2B C3B -55.7(6)	C38S C33S C34S C35S -0.3
C46B P1B C13B C14B -174.6(3)	C39S C40S C41S C42S -178.5
C46B P1B C13B C18B -44.6(4)	C39S C40S C45S C44S 178.6
C46B P1B C7B C8B 53.1(3)	C40S C41S C42S C43S -0.1
C46B P1B C7B C12B -173.9(3)	C41S C40S C45S C44S -0.3
C46B C47B C48B C49B 55.4(8)	C41S C42S C43S C44S -0.1
C47B C46B C51B C50B 56.8(8)	C42S C43S C44S C45S 0.2

C47B C48B C49B C50B -55.2(8)	C43S C44S C45S C40S 0.0
C48B C49B C50B C51B 55.9(8)	C45S C40S C41S C42S 0.3
C49B C50B C51B C46B -57.0(9)	C46S C47S C48S C49S -178.5
C51B C46B C47B C48B -55.9(8)	C46S C47S C52S C51S 178.3
C7B P1B C13B C14B -61.20(18)	C47S C48S C49S C50S 0.0
C7B P1B C13B C18B 68.8(2)	C48S C47S C52S C51S -0.4
C7B P1B C1B C2B 167.9(4)	C48S C49S C50S C51S -0.2
C7B P1B C1B C6B 45.0(5)	C49S C50S C51S C52S 0.1
C7B P1B C46B C47B 173.5(5)	C50S C51S C52S C47S 0.2
C7B P1B C46B C51B 49.3(7)	C52S C47S C48S C49S 0.3

Table 7 Hydrogen Atom Coordinates ($\text{\AA} \times 10^4$) and Isotropic Displacement Parameters ($\text{\AA}^2 \times 10^3$) for Schomaker52.

Atom	<i>x</i>	<i>y</i>	<i>z</i>	U(eq)
H1	5326	3753	7090	26
H2A	4799	4745	6863	30
H2B	4346	4481	6513	30
H3A	5160	5146	5748	34
H3B	5683	4708	6087	34
H4A	5578	4412	5207	37
H4B	4838	4271	5469	37
H5A	5812	3533	6050	41
H5B	5354	3273	5702	41
H6A	5018	2863	6819	36
H6B	4483	3283	6487	36
H7	4740	2369	7985	30
H8A	5679	3004	7725	45
H8B	5497	3162	8373	45
H9A	6189	2290	8507	55
H9B	5735	1888	8273	55
H10E	5576	1481	9379	63
H10F	5437	2197	9424	63
H11E	4651	1469	8989	54
H11F	4475	1624	9639	54
H12E	4413	2743	9092	36

H12F	3954	2337	8868	36
H13	4098	4429	7797	25
H14E	3304	3746	8575	27
H14F	3799	3521	9040	27
H15E	3213	4377	9269	37
H15F	3393	4832	8549	37
H16E	4034	5153	9125	45
H16F	4258	4420	9401	45
H17E	4564	5225	8104	49
H17F	5054	5017	8574	49
H18E	4945	3912	8636	36
H18F	5168	4355	7915	36
H20	1216	2565	7487	24
H21	1763	2805	6380	26
H24	2127	1451	9614	35
H25	1944	2298	10033	37
H26	1724	3331	9406	30
H28	2397	1604	7986	32
H29G	3005	1088	8772	56
H29H	2690	575	8538	56
H29I	2392	668	9200	56
H30G	1337	937	8910	56
H30H	1605	781	8272	56
H30I	1287	1465	8245	56
H31	1877	3870	7736	26
H32G	1539	4316	8800	45
H32H	1717	4769	8080	45
H32I	2246	4349	8422	45
H33G	845	3405	8028	42
H33H	815	4175	7903	42
H33I	702	3681	8609	42
H36	3795	4203	4927	29
H37	4377	3323	4794	32
H38	4098	2273	5461	32
H40	2595	4170	6256	24
H41G	2515	4488	4952	41

H41H	2064	4776	5436	41
H41I	2032	4012	5528	41
H42G	3561	4817	5862	42
H42H	2949	5241	5749	42
H42I	3377	5058	5180	42
H43	2908	1831	6860	32
H44G	3915	1302	6177	62
H44H	3515	920	6858	62
H44I	3980	1515	6771	62
H45G	2364	1867	6042	58
H45H	2547	1134	6382	58
H45I	2947	1547	5711	58
H1A	9581	38	7991	22
H2AA	8773	673	8760	34
H2AB	8535	183	8448	34
H3AA	8569	-358	9535	40
H3AB	9017	-697	9093	40
H4AA	9435	190	9644	34
H4AB	9571	-574	9839	34
H5AA	10213	-431	8850	33
H5AB	10467	45	9167	33
H6AA	9974	939	8539	28
H6AB	10435	613	8092	28
H7A	10406	1408	7106	23
H8AA	10426	385	6943	34
H8AB	10125	703	6326	34
H9AA	11328	1080	6487	47
H9AB	11232	695	6018	47
H10G	10794	1610	5379	44
H10H	11464	1823	5463	44
H11G	10689	2596	5600	34
H11H	10981	2288	6223	34
H12G	9788	1901	6055	28
H12H	9878	2302	6514	28
H13A	8376	717	7421	23
H14G	8593	1635	6491	29

H14H	9039	1195	6153	29
H15G	7719	940	6647	41
H15H	8023	1207	5912	41
H16G	8528	222	5976	45
H16H	7791	68	6248	45
H17G	7959	-252	7287	37
H17H	8415	-658	6919	37
H18G	9278	38	6795	31
H18H	8968	-242	7529	31
H20A	8344	4148	7941	25
H21A	8291	3422	9033	27
H24A	9722	4108	5715	29
H25A	8853	4046	5275	34
H26A	7872	3717	5910	32
H28A	9771	3581	7358	25
H29J	10465	3346	6508	43
H29K	10794	3808	6790	43
H29L	10550	4113	6139	43
H30J	9853	4902	6519	40
H30K	10140	4662	7149	40
H30L	9394	4653	7192	40
H31A	7559	3036	7586	28
H32J	6967	3257	6523	46
H32K	6717	2773	7221	46
H32L	7335	2604	6797	46
H33J	7408	4150	7447	51
H33K	6745	3802	7518	51
H33L	7109	4235	6838	51
H36A	7677	872	10106	36
H37A	8557	626	10559	39
H38A	9433	1320	10187	34
H40A	7550	2182	8707	33
H41J	6867	1959	9965	57
H41K	6618	2375	9341	57
H41L	7214	2636	9523	57
H42J	7406	1017	8943	54

H42K	6764	1402	8893	54
H42L	6919	1003	9570	54
H43A	9680	2724	8806	28
H44J	10330	1849	9708	45
H44K	10649	2378	9058	45
H44L	10291	1747	9052	45
H45J	9253	3144	9621	52
H45K	10004	3176	9524	52
H45L	9608	2615	10103	52
H13B	9037	1533	3607	30
H14C	8460	1929	4389	33
H14D	8418	1207	4888	33
H15C	9568	1953	4266	50
H15D	9267	1791	4998	50
H16C	9454	678	5186	59
H16D	10103	1082	4852	59
H17C	9957	276	4384	60
H17D	10006	992	3877	60
H18C	9156	413	3764	48
H18D	8849	255	4495	48
H1B	8337	382	3297	28
H2BA	8278	1609	2327	39
H2BB	8907	1313	2569	39
H3BA	8843	1127	1608	48
H3BB	8861	450	2162	48
H4BA	8077	363	1617	40
H4BB	7755	1008	1713	40
H5BA	7803	-204	2698	43
H5BB	7180	98	2450	43
H6BA	7227	959	2858	32
H6BB	7235	282	3413	32
H46B	8408	397	3311	29
H47C	8442	1627	2327	39
H47D	9025	1329	2656	39
H48C	9106	1142	1670	43
H48D	9078	467	2236	43

H49C	8401	371	1586	42
H49D	8047	1017	1641	42
H50C	8009	-190	2655	41
H50D	7429	103	2318	41
H51C	7378	982	2724	39
H51D	7327	310	3296	39
H7B	7022	747	4115	26
H8BA	7684	-166	4326	37
H8BB	7799	-5	4935	37
H9BA	6592	-295	4722	46
H9BB	6951	-771	5238	46
H10C	6811	-65	5832	48
H10D	6138	-205	5700	48
H11C	6179	810	4909	42
H11D	6312	934	5528	42
H12C	7407	1043	5116	32
H12D	7046	1549	4618	32
H20B	7162	4614	2698	24
H21B	7248	4382	1695	26
H24B	6316	2976	5069	39
H25B	7196	3095	5461	45
H26B	8133	3534	4783	36
H28B	6274	3157	3473	32
H29D	5913	2266	4419	56
H29E	5349	2630	4095	56
H29F	5500	2767	4702	56
H30D	5654	3968	4165	58
H30E	5438	3865	3570	58
H30F	6091	4239	3482	58
H31B	8453	3879	3116	27
H32D	9050	3859	4136	45
H32E	9399	3900	3441	45
H32F	9029	3242	3900	45
H33D	8011	4862	3216	44
H33E	8764	4924	3078	44
H33F	8377	4808	3777	44

H36B	8467	2665	711	31
H37B	7581	2118	670	36
H38B	6611	2218	1265	33
H40B	8546	3560	1772	29
H41D	8776	3954	424	54
H41E	9093	4305	816	54
H41F	8349	4334	841	54
H42D	9129	2607	1717	46
H42E	9558	3261	1454	46
H42F	9338	2956	974	46
H43B	6340	2937	2487	34
H44D	5692	2266	1882	60
H44E	5435	2361	2551	60
H44F	6014	1897	2471	60
H45D	6261	3870	1626	55
H45E	5575	3560	1974	55
H45F	5900	3450	1327	55
H52C	2952	5072	1433	41
H53A	2421	4770	774	43
H53B	3069	4804	289	43
H54A	2547	5786	-63	53
H54B	2491	5897	604	53
H55A	3308	6571	-106	58
H55B	3639	5962	-276	58
H56A	3505	6161	925	61
H56B	4158	6202	444	61
H57A	4100	5075	607	57
H57B	4038	5182	1276	57
H1C	4117	4098	2015	22
H2CA	3064	4593	2677	30
H2CB	3576	5036	2104	30
H3CA	4377	4714	2708	31
H3CB	3817	5013	3090	31
H4CA	3433	3968	3724	38
H4CB	4160	4031	3756	38
H5CA	3930	3021	3623	44

H5CB	4457	3443	3054	44
H6CA	3152	3331	3002	34
H6CB	3722	3037	2625	34
H46C	4073	4290	1977	28
H47A	2949	4246	2888	34
H47B	3269	4901	2368	34
H48A	4166	4774	2838	39
H48B	3555	4761	3362	39
H49A	3569	3624	3777	35
H49B	4246	3917	3754	35
H50A	4351	3020	3356	37
H50B	4663	3673	2826	37
H51A	3434	3151	2907	34
H51B	4037	3132	2384	34
H7C	3612	3016	1575	31
H8CA	4491	3985	709	50
H8CB	4558	3622	1426	50
H9CA	4614	2603	1257	53
H9CB	5150	3086	752	53
H10A	4553	3270	-39	47
H10B	4602	2498	272	47
H11A	3550	2802	139	42
H11B	3582	2417	860	42
H12A	2949	3329	816	33
H12B	3505	3807	336	33
H13C	3001	5090	1346	40
H14A	2783	4605	379	37
H14B	2249	4606	972	37
H15A	2201	5575	99	51
H15B	2354	5759	683	51
H16A	3037	6368	-228	63
H16B	3254	5723	-396	63
H17A	3555	6074	623	62
H17B	4047	6033	18	62
H18A	3920	4884	362	45
H18B	4091	5090	929	45

H20C	-43	2841	2919	24
H21C	393	2641	3886	25
H24C	967	2685	666	30
H25C	809	3753	81	30
H26C	614	4553	562	28
H28C	1164	2130	2271	29
H29A	1270	1714	1189	50
H29B	1533	1342	1816	50
H29C	1850	2024	1351	50
H30A	66	2000	2371	52
H30B	401	1325	2389	52
H30C	174	1768	1762	52
H31C	664	4365	2164	26
H32A	1150	5194	1218	46
H32B	590	5467	1623	46
H32C	480	5317	1009	46
H33A	-430	4563	1594	40
H33B	-378	4717	2222	40
H33C	-372	3979	2222	40
H36C	2155	3675	4579	27
H37C	2792	2775	4794	28
H38C	2702	1956	4361	26
H40C	1109	4061	3485	27
H41A	486	3505	4471	50
H41B	458	4274	4356	50
H41C	890	3832	4817	50
H42A	1772	4630	4165	44
H42B	1376	5018	3641	44
H42C	2021	4690	3442	44
H43C	1746	1974	3241	26
H44A	2865	1819	3165	47
H44B	2481	1168	3248	47
H44C	2722	1260	3836	47
H45A	1658	1135	4520	49
H45B	1388	951	3990	49
H45C	1081	1523	4240	49

H19S	4842	340	1829	60
H20D	5469	-569	2163	79
H20E	5777	-488	1447	79
H21D	5937	406	2098	65
H21E	6478	-19	1848	65
H22A	6503	610	816	66
H22B	6540	1101	1203	66
H23A	5812	1450	499	79
H23B	5481	1348	1214	79
H24D	4836	862	743	73
H24E	5404	422	567	73
H1S	4193	-377	2596	34
H2SA	3231	-836	2568	39
H2SB	3568	-1487	2505	39
H3SA	3391	-1082	3598	42
H3SB	3053	-1702	3547	42
H4SA	3985	-2243	3504	45
H4SB	3887	-2000	4105	45
H5SA	4603	-1132	3571	49
H5SB	4935	-1792	3530	49
H6SA	4758	-1582	2520	44
H6SB	5133	-975	2553	44
H7S	3311	-278	1533	36
H8SA	3473	428	2084	45
H8SB	3893	913	1461	45
H9SA	2577	634	1632	47
H9SB	2881	1319	1574	47
H10I	3323	1502	517	53
H10J	2586	1347	616	53
H11I	3193	766	-10	49
H11J	2781	276	617	49
H12I	3814	-111	487	40
H12J	4099	576	448	40
H13S	4929	510	957	45
H14I	5232	108	2184	52
H14J	4746	663	1942	52

H15I	5572	1328	1191	61
H15J	5737	1148	1880	61
H16I	6423	335	1685	59
H16J	6630	1021	1144	59
H17I	6088	732	456	45
H17J	6580	178	684	45
H18I	5772	-498	1425	48
H18J	5597	-301	739	48
H25D	2355	877	1009	106
H25E	2931	613	613	106
H25F	2980	1322	679	106
H27S	3174	1429	1673	64
H28S	3575	974	2598	105
H29S	3731	-154	2971	117
H30S	3489	-820	2409	104
H31S	3089	-363	1486	62
H32M	5153	184	47	144
H32N	4510	349	437	144
H32O	4818	-346	689	144
H34S	6081	-106	694	50
H35S	6662	331	1238	61
H36S	6213	1095	1712	69
H37S	5175	1416	1639	71
H38S	4594	978	1095	67
H39A	5641	-29	3921	130
H39B	6101	600	3591	130
H39C	5804	272	3169	130
H41S	4848	682	2837	83
H42S	3997	1378	2841	84
H43S	3795	1932	3586	90
H44S	4453	1780	4327	83
H45S	5303	1086	4320	72
H46A	5408	199	3285	156
H46D	5562	-113	3977	156
H46E	5968	504	3482	156
H48S	4781	1180	3037	95

H49S	4093	1898	3387	88
H50S	3983	1907	4428	80
H51S	4564	1185	5117	84
H52S	5249	465	4766	90

Table 8 Atomic Occupancy for Schomaker52.

<i>Atom Occupancy</i>	<i>Atom Occupancy</i>	<i>Atom Occupancy</i>
C1B 0.549(18)	H1B 0.549(18)	C2B 0.549(18)
H2BA 0.549(18)	H2BB 0.549(18)	C3B 0.549(18)
H3BA 0.549(18)	H3BB 0.549(18)	C4B 0.549(18)
H4BA 0.549(18)	H4BB 0.549(18)	C5B 0.549(18)
H5BA 0.549(18)	H5BB 0.549(18)	C6B 0.549(18)
H6BA 0.549(18)	H6BB 0.549(18)	C46B 0.451(18)
H46B 0.451(18)	C47B 0.451(18)	H47C 0.451(18)
H47D 0.451(18)	C48B 0.451(18)	H48C 0.451(18)
H48D 0.451(18)	C49B 0.451(18)	H49C 0.451(18)
H49D 0.451(18)	C50B 0.451(18)	H50C 0.451(18)
H50D 0.451(18)	C51B 0.451(18)	H51C 0.451(18)
H51D 0.451(18)	C52C 0.368(6)	H52C 0.368(6)
C53C 0.368(6)	H53A 0.368(6)	H53B 0.368(6)
C54C 0.368(6)	H54A 0.368(6)	H54B 0.368(6)
C55C 0.368(6)	H55A 0.368(6)	H55B 0.368(6)
C56C 0.368(6)	H56A 0.368(6)	H56B 0.368(6)
C57C 0.368(6)	H57A 0.368(6)	H57B 0.368(6)
C1C 0.675(11)	H1C 0.675(11)	C2C 0.675(11)
H2CA 0.675(11)	H2CB 0.675(11)	C3C 0.675(11)
H3CA 0.675(11)	H3CB 0.675(11)	C4C 0.675(11)
H4CA 0.675(11)	H4CB 0.675(11)	C5C 0.675(11)
H5CA 0.675(11)	H5CB 0.675(11)	C6C 0.675(11)
H6CA 0.675(11)	H6CB 0.675(11)	C46C 0.325(11)
H46C 0.325(11)	C47C 0.325(11)	H47A 0.325(11)
H47B 0.325(11)	C48C 0.325(11)	H48A 0.325(11)
H48B 0.325(11)	C49C 0.325(11)	H49A 0.325(11)
H49B 0.325(11)	C50C 0.325(11)	H50A 0.325(11)

H50B	0.325(11)	C51C	0.325(11)	H51A	0.325(11)
H51B	0.325(11)	C13C	0.632(6)	H13C	0.632(6)
C14C	0.632(6)	H14A	0.632(6)	H14B	0.632(6)
C15C	0.632(6)	H15A	0.632(6)	H15B	0.632(6)
C16C	0.632(6)	H16A	0.632(6)	H16B	0.632(6)
C17C	0.632(6)	H17A	0.632(6)	H17B	0.632(6)
C18C	0.632(6)	H18A	0.632(6)	H18B	0.632(6)
P1S	0.6927(16)	C19S	0.127(2)	H19S	0.127(2)
C20S	0.127(2)	H20D	0.127(2)	H20E	0.127(2)
C21S	0.127(2)	H21D	0.127(2)	H21E	0.127(2)
C22S	0.127(2)	H22A	0.127(2)	H22B	0.127(2)
C23S	0.127(2)	H23A	0.127(2)	H23B	0.127(2)
C24S	0.127(2)	H24D	0.127(2)	H24E	0.127(2)
C1S	0.6927(16)	H1S	0.6927(16)	C2S	0.6927(16)
H2SA	0.6927(16)	H2SB	0.6927(16)	C3S	0.6927(16)
H3SA	0.6927(16)	H3SB	0.6927(16)	C4S	0.6927(16)
H4SA	0.6927(16)	H4SB	0.6927(16)	C5S	0.6927(16)
H5SA	0.6927(16)	H5SB	0.6927(16)	C6S	0.6927(16)
H6SA	0.6927(16)	H6SB	0.6927(16)	C7S	0.6927(16)
H7S	0.6927(16)	C8S	0.6927(16)	H8SA	0.6927(16)
H8SB	0.6927(16)	C9S	0.6927(16)	H9SA	0.6927(16)
H9SB	0.6927(16)	C10S	0.6927(16)	H10I	0.6927(16)
H10J	0.6927(16)	C11S	0.6927(16)	H11I	0.6927(16)
H11J	0.6927(16)	C12S	0.6927(16)	H12I	0.6927(16)
H12J	0.6927(16)	C13S	0.566(2)	H13S	0.566(2)
C14S	0.566(2)	H14I	0.566(2)	H14J	0.566(2)
C15S	0.566(2)	H15I	0.566(2)	H15J	0.566(2)
C16S	0.566(2)	H16I	0.566(2)	H16J	0.566(2)
C17S	0.566(2)	H17I	0.566(2)	H17J	0.566(2)
C18S	0.566(2)	H18I	0.566(2)	H18J	0.566(2)
C25S	0.184(3)	H25D	0.184(3)	H25E	0.184(3)
H25F	0.184(3)	C26S	0.184(3)	C27S	0.184(3)
H27S	0.184(3)	C28S	0.184(3)	H28S	0.184(3)
C29S	0.184(3)	H29S	0.184(3)	C30S	0.184(3)
H30S	0.184(3)	C31S	0.184(3)	H31S	0.184(3)
C32S	0.167(3)	H32M	0.167(3)	H32N	0.167(3)

H32O 0.167(3)	C33S 0.167(3)	C34S 0.167(3)
H34S 0.167(3)	C35S 0.167(3)	H35S 0.167(3)
C36S 0.167(3)	H36S 0.167(3)	C37S 0.167(3)
H37S 0.167(3)	C38S 0.167(3)	H38S 0.167(3)
C39S 0.394(4)	H39A 0.394(4)	H39B 0.394(4)
H39C 0.394(4)	C40S 0.394(4)	C41S 0.394(4)
H41S 0.394(4)	C42S 0.394(4)	H42S 0.394(4)
C43S 0.394(4)	H43S 0.394(4)	C44S 0.394(4)
H44S 0.394(4)	C45S 0.394(4)	H45S 0.394(4)
C46S 0.517(4)	H46A 0.517(4)	H46D 0.517(4)
H46E 0.517(4)	C47S 0.517(4)	C48S 0.517(4)
H48S 0.517(4)	C49S 0.517(4)	H49S 0.517(4)
C50S 0.517(4)	H50S 0.517(4)	C51S 0.517(4)
H51S 0.517(4)	C52S 0.517(4)	H52S 0.517(4)

C.3 IMes(Cy₃P)NiCl₂

Data Collection

A colorless crystal with approximate dimensions 0.050 x 0.193 x 0.226 mm³ was selected under oil under ambient conditions and attached to the tip of a MiTeGen MicroMount©. The crystal was mounted in a stream of cold nitrogen at 100(1) K and centered in the X-ray beam by using a video camera.

The crystal evaluation and data collection were performed on a Bruker SMART APEXII diffractometer with Cu K_α ($\lambda = 1.54178 \text{ \AA}$) radiation and the diffractometer to crystal distance of 4.03 cm [1].

The initial cell constants were obtained from three series of ω scans at different starting angles. Each series consisted of 41 frames collected at intervals of 0.8° in a 25° range about ω with the exposure time of 10 seconds per frame. The reflections were successfully indexed by an automated indexing routine built in the APEXII program. The final cell constants were calculated from a set of 9543 strong reflections from the actual data collection.

The data were collected by using the full sphere data collection routine to survey the reciprocal space to the extent of a full sphere to a resolution of 0.80 Å. A total of 88354 data were harvested by collecting 32 sets of frames with 0.8° scans in ω and φ with an exposure time 20-40 sec per frame. These highly redundant datasets were corrected for Lorentz and polarization effects. The absorption correction was based on fitting a function to the empirical transmission surface as sampled by multiple equivalent measurements. [2]

Structure Solution and Refinement

The systematic absences in the diffraction data were consistent for the space group $P2_1/c$ that yielded a chemically reasonable and computationally stable results of refinement [3-8].

A successful solution by the direct methods provided most non-hydrogen atoms from the E -map. The remaining non-hydrogen atoms were located in an alternating series of least-squares cycles and difference Fourier maps. All non-hydrogen atoms were refined with anisotropic displacement coefficients. All hydrogen atoms were included in the structure factor calculation at idealized positions and were allowed to ride on the neighboring atoms with relative isotropic displacement coefficients (Figure 1).

One cyclohexyl group (C22 – C27) on the tricyclohexylphosphine ligand is disordered over two positions with the major component present 87.1(3)% of the time. The disordered parts were refined with constraints and restraints (Figure 2).

The final least-squares refinement of 446 parameters against 7602 data resulted in residuals R (based on F^2 for $I \geq 2\sigma$) and wR (based on F^2 for all data) of 0.0335 and 0.0919, respectively. The final difference Fourier map was featureless.

Summary

Crystal Data for $C_{39}H_{57}Cl_2N_2NiP$ ($M = 714.44$ g/mol): monoclinic, space group $P2_1/c$ (no. 14), $a = 19.050(3)$ Å, $b = 14.103(3)$ Å, $c = 14.527(3)$ Å, $\beta = 103.505(5)^\circ$, $V = 3794.8(12)$ Å³, $Z = 4$, $T = 100.46$ K, $\mu(\text{CuK}\alpha) = 2.636$ mm⁻¹, $D_{\text{calc}} = 1.251$ g/cm³, 85883 reflections measured ($4.77^\circ \leq 2\Theta \leq 147.276^\circ$), 7602 unique ($R_{\text{int}} = 0.0341$, $R_{\text{sigma}} = 0.0156$) which were used in all calculations. The final R_1 was 0.0335 ($I > 2\sigma(I)$) and wR_2 was 0.0919 (all data).

References

10. Bruker-AXS (2014). *APEX2*. Version 2014.11-0. Madison, Wisconsin, USA.
11. Krause, L., Herbst-Irmer, R., Sheldrick, G. M. & Stalke, D. (2015). *J. Appl. Cryst.* 48, 3-10.
12. Sheldrick, G. M. (2013b). *XPREF*. Version 2013/1. Georg-August-Universität Göttingen, Göttingen, Germany.
13. Sheldrick, G. M. (2013a). The *SHELX* homepage, <http://shelx.uni-ac.gwdg.de/SHELX/>.
14. Sheldrick, G. M. (2015a). *Acta Cryst. A*, 71, 3-8.
15. Sheldrick, G. M. (2015b). *Acta Cryst. C*, 71, 3-8.
16. Dolomanov, O. V., Bourhis, L. J., Gildea, R. J., Howard, J. A. K. & Puschmann, H. (2009). *J. Appl. Crystallogr.* 42, 339-341.
17. Guzei, I. A. (2007-2013). Programs *Gn*. University of Wisconsin-Madison, Madison, Wisconsin, USA.

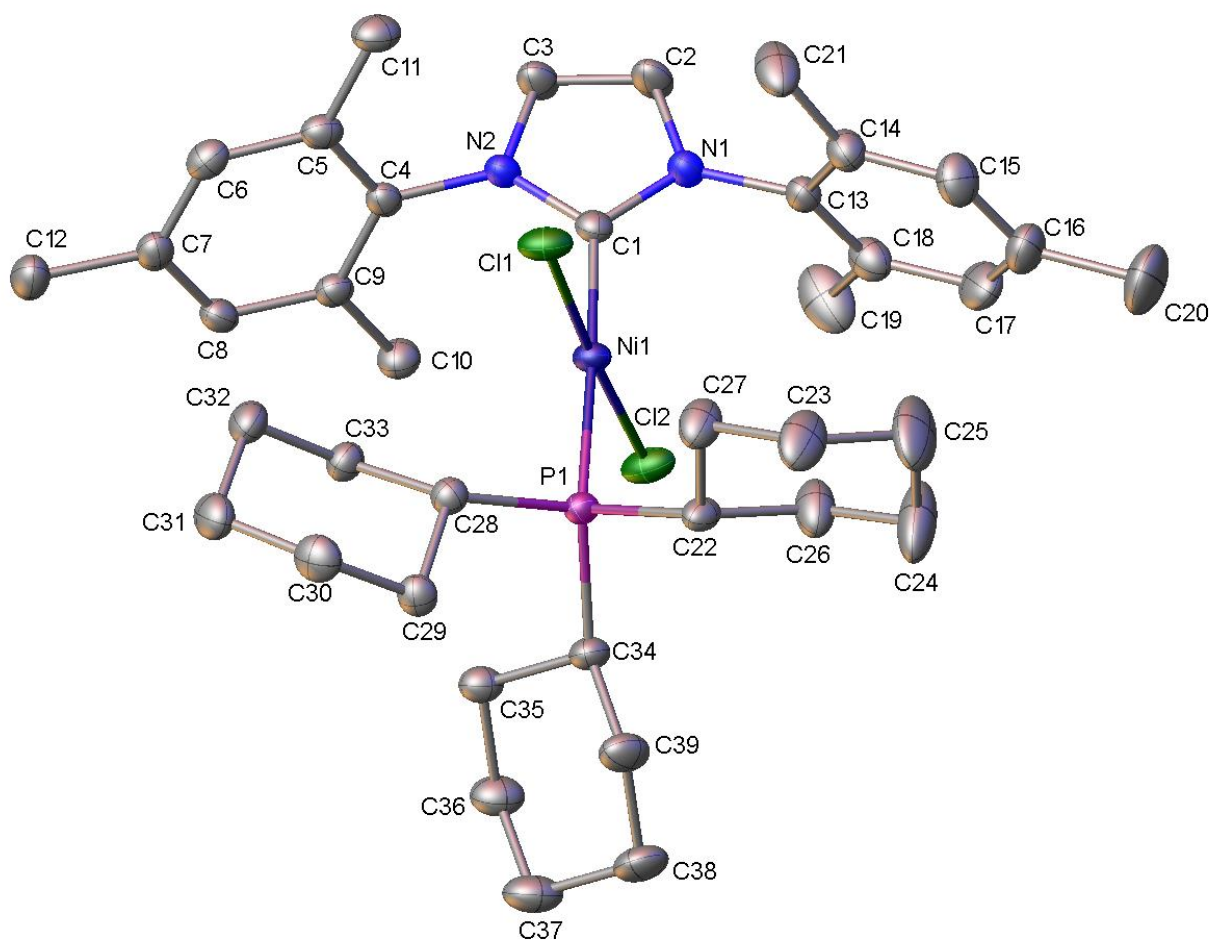


Figure 1. A molecular drawing of Schomaker58 shown with 50% probability ellipsoids. All H atoms and minor disordered components are omitted.

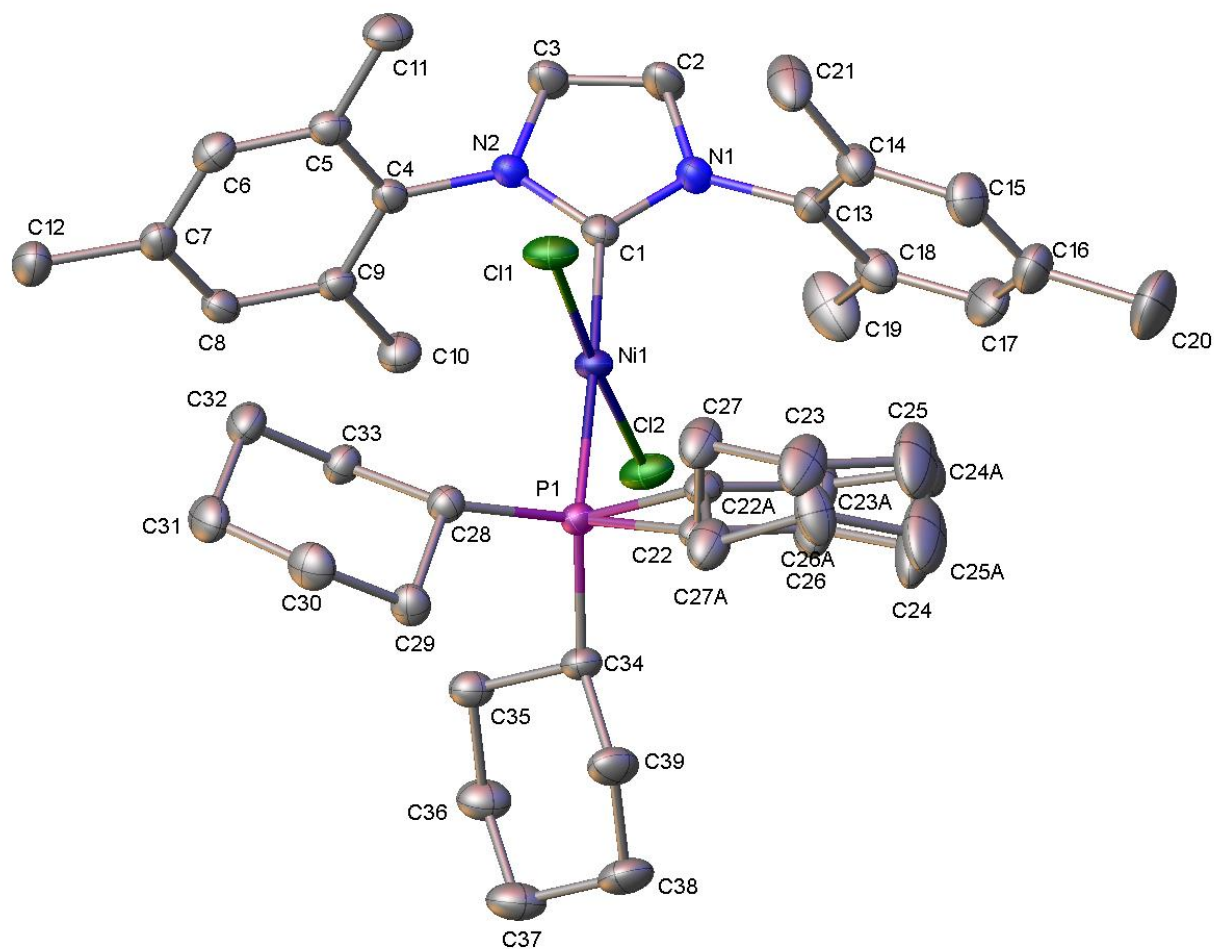


Figure 2. A molecular drawing of Schomaker58 shown with 50% probability ellipsoids. All H atoms are omitted. All disordered components are shown.

Table 1 Crystal data and structure refinement for Schomaker58.

Identification code	Schomaker58
Empirical formula	NiCl ₂ (N ₂ C ₂₁ H ₂₄)[P(C ₆ H ₁₁) ₃]
Formula weight	714.44
Temperature/K	100.46
Crystal system	monoclinic
Space group	P2 ₁ /c
a/Å	19.050(3)
b/Å	14.103(3)
c/Å	14.527(3)
α/°	90
β/°	103.505(5)
γ/°	90
Volume/Å ³	3794.8(12)
Z	4
ρ _{calc} /cm ³	1.251
μ/mm ⁻¹	2.636
F(000)	1528.0
Crystal size/mm ³	0.226 × 0.193 × 0.05
Radiation	CuKα (λ = 1.54178)
2θ range for data collection/°	4.77 to 147.276
Index ranges	-23 ≤ h ≤ 23, -17 ≤ k ≤ 17, -18 ≤ l ≤ 17
Reflections collected	85883
Independent reflections	7602 [R _{int} = 0.0341, R _{sigma} = 0.0156]
Data/restraints/parameters	7602/72/443
Goodness-of-fit on F ²	1.025
Final R indexes [I ≥ 2σ (I)]	R ₁ = 0.0335, wR ₂ = 0.0873
Final R indexes [all data]	R ₁ = 0.0395, wR ₂ = 0.0919
Largest diff. peak/hole / e Å ⁻³	0.45/-0.28

Table 2 Fractional Atomic Coordinates (×10⁴) and Equivalent Isotropic Displacement Parameters (Å²×10³) for Schomaker58. U_{eq} is defined as 1/3 of the trace of the orthogonalised U_{ij} tensor.

Atom	x	y	z	U(eq)
Ni1	7313.8(2)	4833.8(2)	3264.0(2)	18.89(8)
Cl1	6803.0(2)	3913.5(3)	2079.5(3)	28.86(10)

C12	7870.8(2)	5689.3(3)	4450.8(3)	29.80(11)
N1	7518.6(7)	3288.6(10)	4678.4(10)	22.5(3)
N2	6425.9(7)	3780.2(9)	4331(1)	20.8(3)
C1	7078.0(9)	3925.9(11)	4131.5(11)	20.0(3)
C2	7146.7(10)	2755.7(13)	5215.9(13)	28.2(4)
C3	6464.6(10)	3063.8(12)	4998.7(13)	27.0(4)
C4	5769.0(9)	4280.8(11)	3901.7(11)	20.1(3)
C5	5260.9(9)	3827.5(12)	3185.9(12)	22.9(3)
C6	4629.8(9)	4313.8(13)	2788.6(12)	24.8(3)
C7	4497.4(9)	5223.4(12)	3075.5(12)	24.0(3)
C8	5012.9(9)	5643.7(12)	3795.0(12)	23.0(3)
C9	5652.4(9)	5180.3(11)	4229.9(12)	21.0(3)
C10	6178.9(9)	5644.7(13)	5035.3(13)	27.2(4)
C11	5389.3(10)	2852.2(13)	2844.2(14)	30.2(4)
C12	3799.7(10)	5719.5(14)	2627.7(15)	33.0(4)
C13	8268.7(9)	3152.5(11)	4671.2(12)	21.7(3)
C14	8432.3(9)	2587.7(13)	3962.9(13)	27.1(4)
C15	9154.5(10)	2498.5(15)	3940.8(14)	34.3(4)
C16	9698.6(10)	2936.9(15)	4605.3(16)	38.0(5)
C17	9513.8(10)	3455.0(15)	5316.4(15)	38.6(5)
C18	8799.8(10)	3570.4(13)	5373.5(13)	29.1(4)
C19	8625.4(14)	4116.9(18)	6177.2(15)	49.4(6)
C20	10479.8(12)	2829(2)	4556(2)	65.3(8)
C21	7855.2(11)	2050.7(15)	3280.9(17)	43.4(5)
P1	7537.2(2)	5899.9(3)	2211.6(3)	17.99(9)
C22	8257.3(11)	5521.8(17)	1636.9(16)	24.1(5)
C23	8932.4(13)	5263(2)	2417(2)	42.0(7)
C24	9565.5(14)	5018(3)	1986(3)	68.1(11)
C25	9371.1(16)	4232(3)	1240(3)	64.6(10)
C26	8710.1(16)	4500(2)	493(3)	47.3(9)
C27	8069.5(12)	4718.4(17)	926.3(18)	36.1(5)
C22A	8193(8)	5163(11)	1683(10)	24.1(5)
C23A	8868(9)	4915(15)	2432(14)	42.0(7)
C24A	9462(8)	4421(13)	2125(12)	38(3)
C25A	9590(9)	4785(17)	1188(13)	64.6(10)
C26A	8892(9)	4834(15)	439(11)	34(5)

C27A	8336(7)	5449(11)	771(10)	36.1(5)
C28	6717.2(9)	6045.4(12)	1259.9(11)	20.8(3)
C29	6714.4(9)	6811.1(12)	514.3(12)	24.3(3)
C30	6041.7(10)	6690.9(14)	-296.0(13)	31.2(4)
C31	5343.6(10)	6707.0(14)	57.1(13)	32.1(4)
C32	5369.2(9)	5982.9(13)	840.9(14)	29.0(4)
C33	6031.8(9)	6129.3(12)	1649.9(12)	23.5(3)
C34	7873.8(9)	7081.5(12)	2676.8(13)	24.1(3)
C35	7289.3(9)	7676.1(12)	2977.7(13)	25.5(4)
C36	7608.8(11)	8575.0(13)	3498.0(15)	34.7(4)
C37	8006.7(12)	9158.7(14)	2903.9(16)	39.5(5)
C38	8589.8(11)	8573.0(14)	2620.5(16)	39.1(5)
C39	8269.8(11)	7676.6(13)	2083.0(15)	33.2(4)

Table 3 Anisotropic Displacement Parameters ($\text{\AA}^2 \times 10^3$) for Schomaker58. The Anisotropic displacement factor exponent takes the form: $-2\pi^2[h^2a^2U_{11}+2hka*b*U_{12}+\dots]$.

Atom	U_{11}	U_{22}	U_{33}	U_{23}	U_{13}	U_{12}
Ni1	20.87(15)	15.23(14)	20.30(15)	1.07(10)	4.29(11)	-2.96(10)
Cl1	41.3(2)	20.7(2)	24.6(2)	-2.77(16)	7.75(17)	-10.48(16)
Cl2	36.3(2)	27.5(2)	22.8(2)	0.65(16)	1.39(16)	-13.66(17)
N1	21.6(7)	20.1(7)	26.8(7)	5.0(6)	7.6(6)	2.1(5)
N2	20.8(7)	16.5(6)	26.1(7)	3.8(5)	7.6(5)	1.1(5)
C1	21.7(8)	15.0(7)	22.8(8)	-1.7(6)	4.3(6)	-0.6(6)
C2	29.5(9)	23.8(8)	34.0(9)	12.9(7)	12.9(7)	4.2(7)
C3	27.9(9)	22.7(8)	33.9(9)	8.9(7)	14.3(7)	2.8(7)
C4	20.4(7)	18.0(8)	23.6(8)	3.9(6)	8.3(6)	0.7(6)
C5	25.7(8)	19.9(8)	25.3(8)	0.2(7)	10.0(7)	-2.9(6)
C6	23.4(8)	28.3(9)	22.4(8)	0.1(7)	4.6(6)	-5.3(7)
C7	20.9(8)	24.6(8)	27.4(8)	6.4(7)	7.5(7)	0.1(6)
C8	23.9(8)	16.8(8)	29.8(9)	1.6(7)	9.5(7)	1.1(6)
C9	21.1(8)	18.7(8)	24.2(8)	1.5(6)	7.6(6)	-2.6(6)
C10	26.7(9)	24.1(9)	30.0(9)	-4.4(7)	5.2(7)	-2.2(7)
C11	34.3(9)	22.0(9)	36.2(10)	-5.6(8)	12.0(8)	-5.1(7)
C12	23.0(9)	32.9(10)	41.6(11)	9.0(8)	4.6(8)	1.1(7)
C13	19.9(8)	19.6(8)	25.3(8)	3.8(7)	5.0(6)	1.2(6)

C14	25.2(8)	24.3(9)	30.4(9)	-2.1(7)	3.5(7)	2.6(7)
C15	30.8(10)	38.5(11)	35.9(10)	-2.8(8)	12.1(8)	7.6(8)
C16	22.0(9)	41.6(11)	51.5(12)	5.6(10)	10.8(8)	0.3(8)
C17	26.4(9)	36.5(11)	45.4(11)	-3.1(9)	-7.0(8)	-4.4(8)
C18	31.5(9)	26.6(9)	26.4(9)	-0.6(7)	0.7(7)	3.0(7)
C19	60.1(14)	54.2(14)	26(1)	-11(1)	-5.9(9)	17.2(11)
C20	24.5(11)	79.3(19)	95(2)	5.4(17)	19.4(12)	1.0(11)
C21	35.3(11)	34.2(11)	52.8(13)	-20.5(10)	-5.9(9)	7.0(8)
P1	17.53(18)	16.60(19)	20.55(19)	0.59(15)	5.85(15)	-1.10(14)
C22	21.3(9)	18.9(11)	34.1(9)	-5.8(9)	10.5(7)	-1.8(8)
C23	26.5(10)	43.9(17)	49.8(12)	-17.0(13)	-2.6(9)	6.9(11)
C24	25.2(12)	87(3)	85(2)	-42(2)	-1.1(13)	14.4(14)
C25	38.0(14)	65(2)	87(2)	-35.9(18)	7.9(13)	21.4(14)
C26	34.5(14)	48.5(19)	61.0(18)	-29.8(15)	15.5(12)	2.7(13)
C27	27.3(10)	36.5(12)	44.8(12)	-17(1)	9.0(9)	-0.2(8)
C22A	21.3(9)	18.9(11)	34.1(9)	-5.8(9)	10.5(7)	-1.8(8)
C23A	26.5(10)	43.9(17)	49.8(12)	-17.0(13)	-2.6(9)	6.9(11)
C24A	31(5)	28(7)	57(8)	9(6)	13(5)	9(5)
C25A	38.0(14)	65(2)	87(2)	-35.9(18)	7.9(13)	21.4(14)
C26A	34(7)	43(9)	24(6)	-5(6)	6(6)	16(7)
C27A	27.3(10)	36.5(12)	44.8(12)	-17(1)	9.0(9)	-0.2(8)
C28	20.5(8)	21.2(8)	21.0(8)	-0.2(6)	5.5(6)	-0.5(6)
C29	24.8(8)	26.4(9)	22.4(8)	3.8(7)	6.8(7)	1.7(7)
C30	34.9(10)	33.2(10)	23.2(8)	3.0(8)	2.0(7)	1.0(8)
C31	25.6(9)	31.8(10)	33.9(10)	0.2(8)	-3.4(7)	0.9(7)
C32	21.3(8)	27.6(9)	36.6(10)	-4.2(8)	3.5(7)	-2.0(7)
C33	19.5(8)	25.0(8)	26.9(8)	-0.4(7)	6.9(7)	-1.5(6)
C34	23.3(8)	18.2(8)	31.4(9)	1.0(7)	7.5(7)	-3.8(6)
C35	28.7(9)	20.5(8)	28.5(9)	-1.0(7)	9.4(7)	-2.7(7)
C36	42.4(11)	24.8(9)	38.6(10)	-4.6(8)	12.9(9)	-4.9(8)
C37	51.6(12)	22.8(9)	46.7(12)	-0.8(9)	16.9(10)	-7.8(8)
C38	38.6(11)	28.3(10)	53.3(12)	3.9(9)	16.1(9)	-12.2(8)
C39	35.8(10)	25.8(9)	43.9(11)	2.3(8)	21.3(9)	-4.4(8)

Table 4 Bond Lengths for Schomaker58.

Atom	Atom	Length/Å	Atom	Atom	Length/Å
Ni1	C11	2.1932(5)	P1	C22	1.843(2)
Ni1	C12	2.1678(5)	P1	C22A	1.918(12)
Ni1	C1	1.9219(16)	P1	C28	1.8399(17)
Ni1	P1	2.2545(5)	P1	C34	1.8554(17)
N1	C1	1.354(2)	C22	C23	1.546(3)
N1	C2	1.391(2)	C22	C27	1.518(3)
N1	C13	1.444(2)	C23	C24	1.523(4)
N2	C1	1.356(2)	C24	C25	1.534(4)
N2	C3	1.391(2)	C25	C26	1.506(4)
N2	C4	1.445(2)	C26	C27	1.530(3)
C2	C3	1.336(2)	C22A	C23A	1.518(15)
C4	C5	1.399(2)	C22A	C27A	1.469(15)
C4	C9	1.391(2)	C23A	C24A	1.484(15)
C5	C6	1.387(2)	C24A	C25A	1.526(17)
C5	C11	1.502(2)	C25A	C26A	1.511(16)
C6	C7	1.390(3)	C26A	C27A	1.531(15)
C7	C8	1.389(2)	C28	C29	1.529(2)
C7	C12	1.508(2)	C28	C33	1.544(2)
C8	C9	1.397(2)	C29	C30	1.534(2)
C9	C10	1.502(2)	C30	C31	1.533(3)
C13	C14	1.393(2)	C31	C32	1.522(3)
C13	C18	1.389(2)	C32	C33	1.525(2)
C14	C15	1.389(3)	C34	C35	1.537(2)
C14	C21	1.502(3)	C34	C39	1.524(2)
C15	C16	1.386(3)	C35	C36	1.528(2)
C16	C17	1.376(3)	C36	C37	1.517(3)
C16	C20	1.514(3)	C37	C38	1.516(3)
C17	C18	1.391(3)	C38	C39	1.535(3)
C18	C19	1.500(3)			

Table 5 Bond Angles for Schomaker58.

Atom	Atom	Atom	Angle/°	Atom	Atom	Atom	Angle/°
------	------	------	---------	------	------	------	---------

C11	Ni1	P1	88.97(2)	C13	C18	C19	122.28(18)
C12	Ni1	C11	176.75(2)	C17	C18	C19	120.26(18)
C12	Ni1	P1	91.90(2)	C22	P1	Ni1	113.11(8)
C1	Ni1	C11	89.50(5)	C22	P1	C34	101.20(9)
C1	Ni1	C12	89.73(5)	C22A	P1	Ni1	98.9(5)
C1	Ni1	P1	177.40(5)	C28	P1	Ni1	108.80(5)
C1	N1	C2	111.15(14)	C28	P1	C22	106.44(9)
C1	N1	C13	124.27(14)	C28	P1	C22A	106.1(5)
C2	N1	C13	124.53(14)	C28	P1	C34	109.52(8)
C1	N2	C3	110.93(14)	C34	P1	Ni1	117.13(6)
C1	N2	C4	125.32(13)	C34	P1	C22A	115.5(5)
C3	N2	C4	123.74(14)	C23	C22	P1	108.41(16)
N1	C1	Ni1	128.27(12)	C27	C22	P1	116.21(15)
N1	C1	N2	104.34(13)	C27	C22	C23	110.22(18)
N2	C1	Ni1	127.39(12)	C24	C23	C22	110.8(2)
C3	C2	N1	106.65(15)	C23	C24	C25	111.8(3)
C2	C3	N2	106.93(15)	C26	C25	C24	110.5(2)
C5	C4	N2	118.47(14)	C25	C26	C27	111.5(3)
C9	C4	N2	119.27(15)	C22	C27	C26	110.3(2)
C9	C4	C5	122.23(15)	C23A	C22A	P1	111.1(10)
C4	C5	C11	121.76(16)	C27A	C22A	P1	119.2(10)
C6	C5	C4	117.74(15)	C27A	C22A	C23A	113.9(12)
C6	C5	C11	120.50(16)	C24A	C23A	C22A	118.0(14)
C5	C6	C7	122.12(16)	C23A	C24A	C25A	113.7(13)
C6	C7	C12	120.13(16)	C26A	C25A	C24A	111.1(15)
C8	C7	C6	118.27(15)	C25A	C26A	C27A	110.9(13)
C8	C7	C12	121.58(16)	C22A	C27A	C26A	114.6(12)
C7	C8	C9	121.98(15)	C29	C28	P1	118.23(11)
C4	C9	C8	117.63(15)	C29	C28	C33	110.03(13)
C4	C9	C10	122.25(15)	C33	C28	P1	112.03(11)
C8	C9	C10	120.11(15)	C28	C29	C30	109.25(14)
C14	C13	N1	118.29(15)	C31	C30	C29	112.10(15)
C18	C13	N1	119.37(15)	C32	C31	C30	111.21(15)
C18	C13	C14	122.33(16)	C31	C32	C33	111.22(15)
C13	C14	C21	121.34(16)	C32	C33	C28	109.00(14)
C15	C14	C13	117.55(16)	C35	C34	P1	112.45(11)

C15	C14	C21	121.03(17)	C39	C34	P1	117.60(13)
C16	C15	C14	121.81(18)	C39	C34	C35	110.37(14)
C15	C16	C20	120.4(2)	C36	C35	C34	111.23(15)
C17	C16	C15	118.60(17)	C37	C36	C35	111.29(16)
C17	C16	C20	121.0(2)	C38	C37	C36	110.73(17)
C16	C17	C18	122.12(18)	C37	C38	C39	110.95(17)
C13	C18	C17	117.46(17)	C34	C39	C38	110.85(16)

Table 6 Torsion Angles for Schomaker58.

A	B	C	D	Angle/°	A	B	C	D	Angle/°
Ni1	P1	C22	C23	-53.24(17)	C16	C17	C18	C19	178.2(2)
Ni1	P1	C22	C27	71.50(19)	C18	C13	C14	C15	-4.0(3)
Ni1	P1	C28	C29	173.83(11)	C18	C13	C14	C21	172.65(18)
Ni1	P1	C28	C33	44.28(12)	C20	C16	C17	C18	179.5(2)
Ni1	P1	C34	C35	-71.04(13)	C21	C14	C15	C16	-175.5(2)
Ni1	P1	C34	C39	159.10(12)	P1	C22	C23	C24	-175.6(2)
N1	C2	C3	N2	0.1(2)	P1	C22	C27	C26	178.6(2)
N1	C13	C14	C15	177.18(16)	P1	C22A	C23A	C24A	-174.5(15)
N1	C13	C14	C21	-6.2(3)	P1	C22A	C27A	C26A	177.5(12)
N1	C13	C18	C17	-177.28(16)	P1	C28	C29	C30	169.98(12)
N1	C13	C18	C19	3.5(3)	P1	C28	C33	C32	-165.07(12)
N2	C4	C5	C6	179.30(14)	P1	C34	C35	C36	171.08(13)
N2	C4	C5	C11	-1.3(2)	P1	C34	C39	C38	-173.17(13)
N2	C4	C9	C8	179.73(14)	C22	P1	C28	C29	-63.98(15)
N2	C4	C9	C10	-1.5(2)	C22	P1	C28	C33	166.48(13)
C1	N1	C2	C3	0.2(2)	C22	P1	C34	C35	165.52(13)
C1	N1	C13	C14	-81.7(2)	C22	P1	C34	C39	35.66(16)
C1	N1	C13	C18	99.5(2)	C22	C23	C24	C25	-54.8(4)
C1	N2	C3	C2	-0.3(2)	C23	C22	C27	C26	-57.6(3)
C1	N2	C4	C5	101.62(19)	C23	C24	C25	C26	54.9(5)
C1	N2	C4	C9	-80.3(2)	C24	C25	C26	C27	-56.5(4)
C2	N1	C1	Ni1	179.80(13)	C25	C26	C27	C22	58.6(3)
C2	N1	C1	N2	-0.31(18)	C27	C22	C23	C24	56.2(3)
C2	N1	C13	C14	95.4(2)	C22A	P1	C28	C29	-80.6(5)

C2	N1	C13	C18	-83.4(2)	C22A	P1	C28	C33	149.8(5)
C3	N2	C1	Ni1	-179.76(12)	C22A	P1	C34	C35	173.1(5)
C3	N2	C1	N1	0.34(18)	C22A	P1	C34	C39	43.3(5)
C3	N2	C4	C5	-77.1(2)	C22A	C23A	C24A	C25A	40(3)
C3	N2	C4	C9	101.01(19)	C23A	C22A	C27A	C26A	43(2)
C4	N2	C1	Ni1	1.4(2)	C23A	C24A	C25A	C26A	-50(2)
C4	N2	C1	N1	-178.49(15)	C24A	C25A	C26A	C27A	56(2)
C4	N2	C3	C2	178.59(16)	C25A	C26A	C27A	C22A	-54(2)
C4	C5	C6	C7	0.5(2)	C27A	C22A	C23A	C24A	-37(2)
C5	C4	C9	C8	-2.3(2)	C28	P1	C22	C23	-172.67(15)
C5	C4	C9	C10	176.47(15)	C28	P1	C22	C27	-47.9(2)
C5	C6	C7	C8	-1.1(3)	C28	P1	C34	C35	53.42(14)
C5	C6	C7	C12	-179.45(16)	C28	P1	C34	C39	-76.44(15)
C6	C7	C8	C9	0.1(2)	C28	C29	C30	C31	55.9(2)
C7	C8	C9	C4	1.6(2)	C29	C28	C33	C32	61.25(18)
C7	C8	C9	C10	-177.20(16)	C29	C30	C31	C32	-53.7(2)
C9	C4	C5	C6	1.3(2)	C30	C31	C32	C33	55.1(2)
C9	C4	C5	C11	-179.35(15)	C31	C32	C33	C28	-58.63(19)
C11	C5	C6	C7	-178.91(16)	C33	C28	C29	C30	-59.56(18)
C12	C7	C8	C9	178.38(16)	C34	P1	C22	C23	72.91(17)
C13	N1	C1	Ni1	-2.8(2)	C34	P1	C22	C27	-162.35(18)
C13	N1	C1	N2	177.09(15)	C34	P1	C28	C29	44.65(15)
C13	N1	C2	C3	-177.23(16)	C34	P1	C28	C33	-84.89(13)
C13	C14	C15	C16	1.2(3)	C34	C35	C36	C37	55.8(2)
C14	C13	C18	C17	3.9(3)	C35	C34	C39	C38	56.0(2)
C14	C13	C18	C19	-175.25(18)	C35	C36	C37	C38	-56.4(2)
C14	C15	C16	C17	1.5(3)	C36	C37	C38	C39	57.0(2)
C14	C15	C16	C20	-179.6(2)	C37	C38	C39	C34	-57.3(2)
C15	C16	C17	C18	-1.6(3)	C39	C34	C35	C36	-55.4(2)
C16	C17	C18	C13	-1.0(3)					

Table 7 Hydrogen Atom Coordinates ($\text{\AA}\times 10^4$) and Isotropic Displacement Parameters ($\text{\AA}^2\times 10^3$) for Schomaker58.

Atom	x	y	z	U(eq)
H2	7340	2268	5652	34

H3	6079	2837	5252	32
H6	4277	4016	2305	30
H8	4928	6265	3997	28
H10A	6444	5156	5457	41
H10B	5917	6050	5389	41
H10C	6520	6031	4785	41
H11A	5806	2866	2557	45
H11B	4961	2643	2372	45
H11C	5484	2411	3380	45
H12A	3778	5834	1956	49
H12B	3776	6326	2948	49
H12C	3391	5321	2687	49
H15	9279	2127	3457	41
H17	9886	3743	5783	46
H19A	9012	4574	6419	74
H19B	8583	3678	6684	74
H19C	8168	4455	5953	74
H20A	10774	3305	4964	98
H20B	10520	2920	3902	98
H20C	10651	2193	4771	98
H21A	7572	1678	3634	65
H21B	8079	1625	2900	65
H21C	7538	2499	2864	65
H22	8387	6084	1290	29
H23A	9065	5804	2857	50
H23B	8821	4714	2784	50
H24A	9979	4809	2494	82
H24B	9715	5592	1689	82
H25A	9781	4126	941	78
H25B	9280	3634	1549	78
H26A	8581	3973	34	57
H26B	8819	5064	144	57
H27A	7646	4899	420	43
H27B	7942	4145	1245	43
H22A	7940	4540	1539	29
H23C	9065	5510	2751	50

H23D	8720	4513	2913	50
H24C	9349	3735	2061	46
H24D	9912	4495	2622	46
H25C	9810	5424	1284	78
H25D	9931	4359	972	78
H26C	8696	4187	297	41
H26D	8986	5104	-150	41
H27C	8507	6114	822	43
H27D	7876	5428	283	43
H28	6662	5433	903	25
H29A	7155	6756	266	29
H29B	6712	7447	803	29
H30A	6027	7208	-762	37
H30B	6074	6082	-622	37
H31A	5273	7348	298	39
H31B	4928	6567	-477	39
H32A	5380	5336	580	35
H32B	4928	6041	1086	35
H33A	6042	5645	2146	28
H33B	6013	6763	1935	28
H34	8241	6948	3277	29
H35A	6913	7852	2410	31
H35B	7059	7293	3396	31
H36A	7216	8961	3649	42
H36B	7946	8399	4101	42
H37A	7660	9387	2328	47
H37B	8228	9719	3270	47
H38A	8958	8390	3194	47
H38B	8830	8958	2214	47
H39A	7930	7859	1483	40
H39B	8662	7296	1924	40

C.4. $\text{IPr}^*(\text{Cy}_3\text{P})\text{NiCl}_2$

Crystallographic Experimental Section

Data Collection

A red crystal with approximate dimensions $0.13 \times 0.07 \times 0.07 \text{ mm}^3$ was selected under oil under ambient conditions and attached to the tip of a MiTeGen MicroMount©. The crystal was mounted in a stream of cold nitrogen at 100(1) K and centered in the X-ray beam by using a video camera.

The crystal evaluation and data collection were performed on a Bruker Quazar SMART APEXII diffractometer with Mo K_α ($\lambda = 0.71073 \text{ \AA}$) radiation and the diffractometer to crystal distance of 5.00 cm [1].

The initial cell constants were obtained from three series of ω scans at different starting angles. Each series consisted of 12 frames collected at intervals of 0.5° in a 6° range about ω with the exposure time of 10 seconds per frame. The reflections were successfully indexed by an automated indexing routine built in the APEXII program suite. The final cell constants were calculated from a set of 9833 strong reflections from the actual data collection.

The data were collected by using the full sphere data collection routine to survey the reciprocal space to the extent of a full sphere to a resolution of 0.80 \AA . A total of 160626 data were harvested by collecting 6 sets of frames with 0.5° scans in ω and ϕ with exposure times of 40 sec per frame. These highly redundant datasets were corrected for Lorentz and polarization effects. The absorption correction was based on fitting a function to the empirical transmission surface as sampled by multiple equivalent measurements. [2]

Structure Solution and Refinement

The systematic absences in the diffraction data were consistent for the space groups $P\bar{1}$ and $P1$. The E -statistics strongly suggested the centrosymmetric space group $P\bar{1}$ that yielded chemically reasonable and computationally stable results of refinement [3-8].

A successful solution by the direct methods provided most non-hydrogen atoms from the E -map. The remaining non-hydrogen atoms were located in an alternating series of least-squares cycles and difference Fourier maps. All non-hydrogen atoms were refined with anisotropic displacement coefficients. All hydrogen atoms were included in the structure factor calculation at idealized positions and were allowed to ride on the neighboring atoms with relative isotropic displacement coefficients.

There is also 1.5 molecules of solvent p-xylene per two Ni complexes molecules of carbene in the asymmetric unit. One molecule (C88) was fully occupied and refined well. The other, molecule of p-xylene (that contributes the 0.5 molecule) was disordered over a crystallographic inversion center and could not be reasonably refined. A significant amount of time was invested in identifying and refining the disordered molecule. Bond length restraints were applied to model the molecule but the resulting isotropic displacement coefficients suggested the molecule was mobile [9]. In addition, the refinement was computationally unstable. Option SQUEEZE of program PLATON [10] was used to correct the diffraction data for diffuse scattering effects and to identify the solvate molecule. PLATON calculated the upper limit of volume that can be occupied by the solvent molecule to be 195 \AA^3 , or 2.6% of the unit cell volume. The program calculated 60 electrons in the unit cell for the diffuse species. This corresponds well to one molecule of p-xylene at the inversion center (165 \AA^3 , 58 electrons). Please note that all derived results in the following tables are based on the known contents. No data are given for the diffusely scattering species.

The final least-squares refinement of 1753 parameters against 29504 data resulted in residuals R (based on F^2 for $I \geq 2\sigma$) and wR (based on F^2 for all data) of 0.0444 and 0.1000, respectively. The final difference Fourier map was featureless.

Summary

Crystal Data for $\text{C}_{93}\text{H}_{96.5}\text{Cl}_2\text{N}_2\text{NiP}$ ($M = 1402.80 \text{ g/mol}$): triclinic, space group P-1 (no. 2), $a = 13.613(4) \text{ \AA}$, $b = 23.589(7) \text{ \AA}$, $c = 24.661(7) \text{ \AA}$, $\alpha = 106.004(16)^\circ$, $\beta = 95.015(18)^\circ$, $\gamma = 96.289(15)^\circ$, $V = 7509(4) \text{ \AA}^3$, $Z = 4$, $T = 100 \text{ K}$, $\mu(\text{MoK}\alpha) = 0.400 \text{ mm}^{-1}$, $D_{\text{calc}} = 1.241 \text{ g/cm}^3$, 160626 reflections measured ($1.732^\circ \leq 2\theta \leq 52^\circ$), 29504 unique ($R_{\text{int}} = 0.0855$, $R_{\text{sigma}} = 0.0656$) which were used in all calculations. The final R_1 was 0.0444 ($I > 2\sigma(I)$) and wR_2 was 0.1000 (all data).

References

18. Bruker-AXS (2014). *APEX2*. Version 2014.11-0. Madison, Wisconsin, USA.
19. Krause, L., Herbst-Irmer, R., Sheldrick, G. M. & Stalke, D. (2015). *J. Appl. Cryst.* 48, 3-10.
20. Sheldrick, G. M. (2013b). *XPREP*. Version 2013/1. Georg-August-Universität Göttingen, Göttingen, Germany.
21. Sheldrick, G. M. (2013a). The *SHELX* homepage, <http://shelx.uni-ac.gwdg.de/SHELX/>.
22. Sheldrick, G. M. (2015a). *Acta Cryst. A*, 71, 3-8.

23. Sheldrick, G. M. (2015b). *Acta Cryst. C*, 71, 3-8.
24. Dolomanov, O. V., Bourhis, L. J., Gildea, R. J., Howard, J. A. K. & Puschmann, H. (2009). *J. Appl. Crystallogr.* 42, 339-341.
25. Guzei, I. A. (2007-2013). Programs *Gn*. University of Wisconsin-Madison, Madison, Wisconsin, USA.
26. Guzei, I. A. (2014). *J. Appl. Cryst.* 47, 806-809.
27. Spek, A. L. (2015). *Acta Cryst. C*, 71, 9-18.

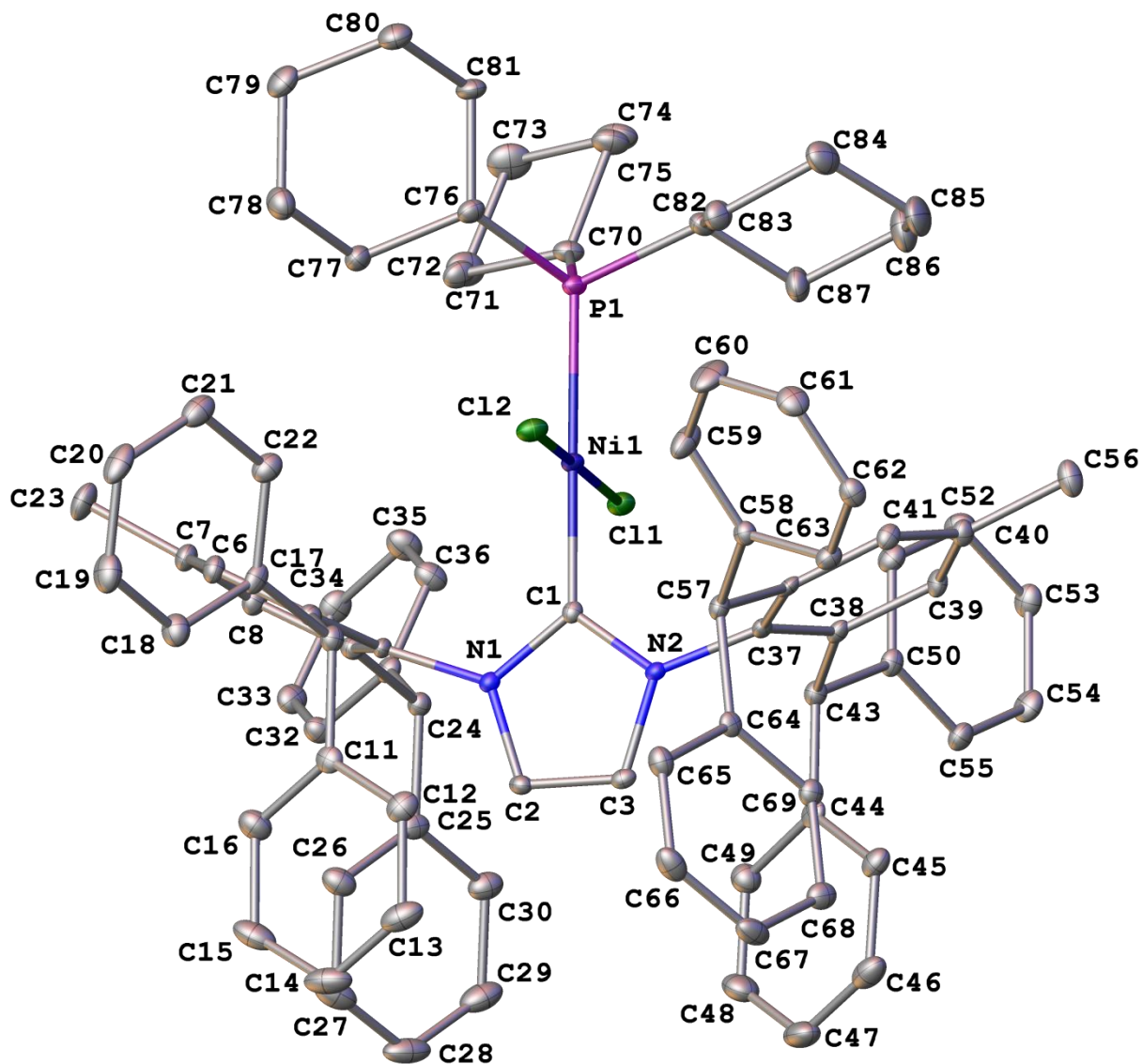


Figure 1. A molecular drawing of the first Ni complex shown with 30% probability ellipsoids. All H atoms are omitted.

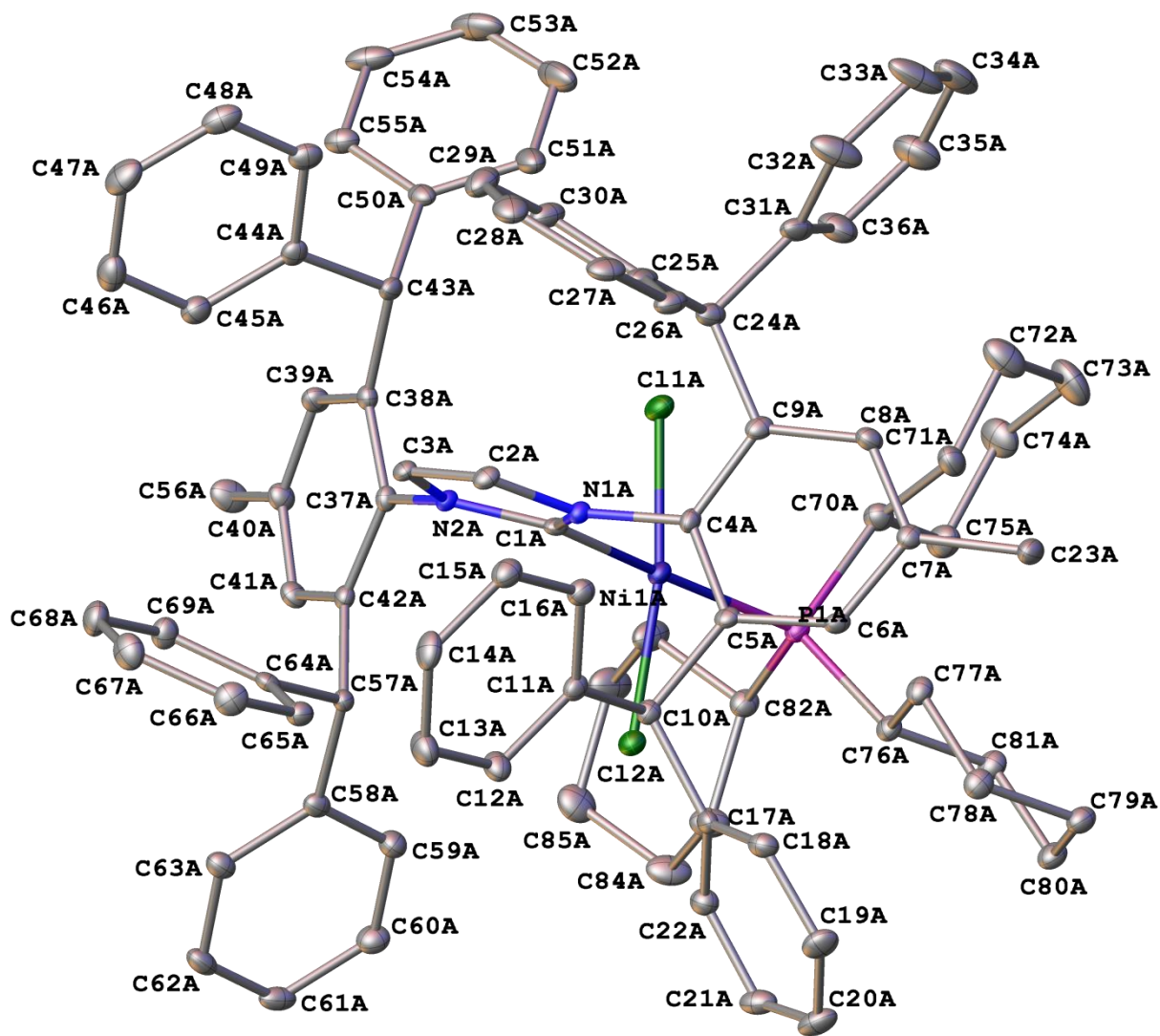


Figure 2. A molecular drawing of the second Ni complex shown with 30% probability ellipsoids. All H atoms are omitted.

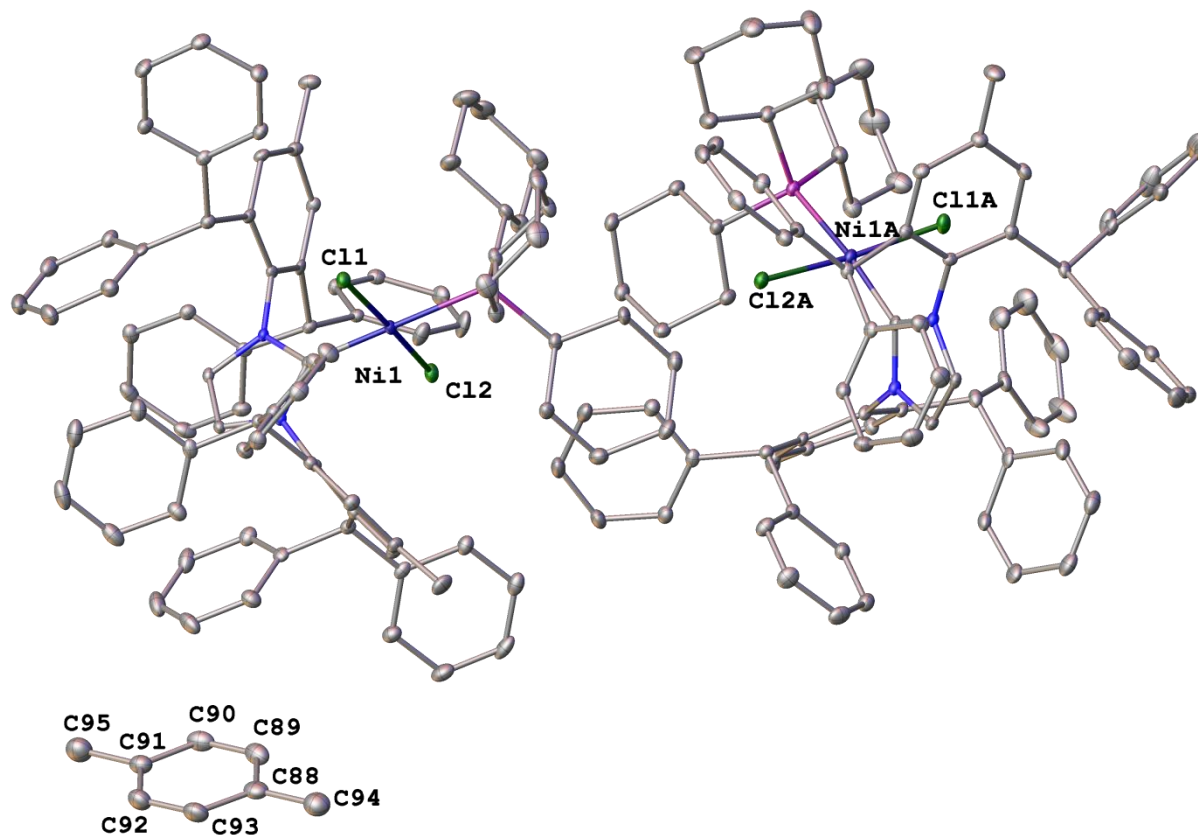


Figure 3. A molecular drawing of the asymmetric unit content. Note the presence of a solvent p-xylene molecule; there is also $\frac{1}{2}$ of another p-xylene molecule in the asymmetric unit, but this second molecules was “squeezed out” as described in the experimental. There is $\frac{3}{4}$ of -xylene per Ni complex in the structure. All H atoms are omitted.

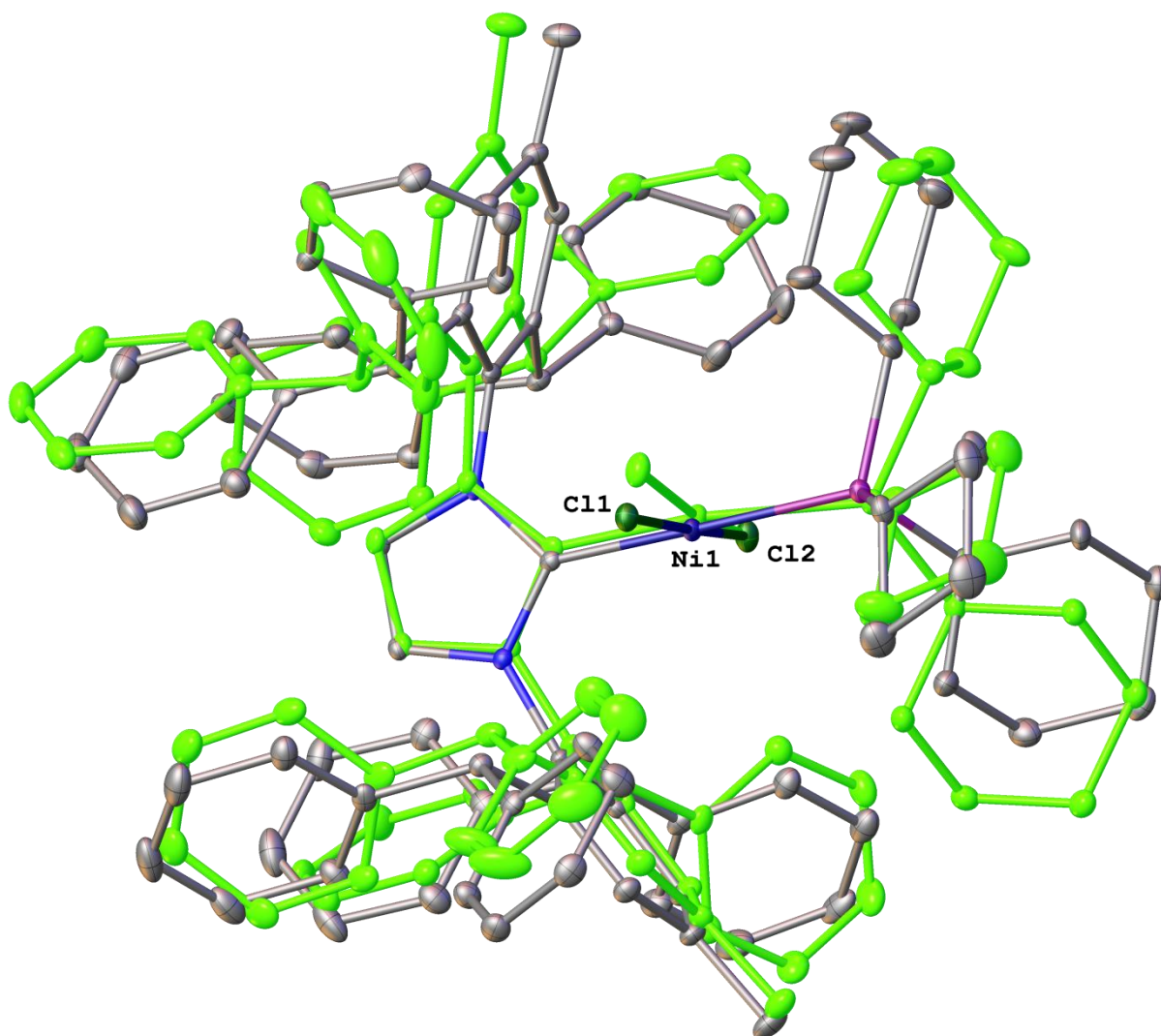


Figure 4. The two Ni complexes superimposed. All H atoms are omitted.

Table 1 Crystal data and structure refinement for Schomaker59_sq.

Identification code	Schomaker59_sq
Empirical formula	C ₈₇ H ₈₉ Cl ₂ N ₂ NiP · ¾ p-xylene
Formula weight	1402.80
Temperature/K	100
Crystal system	triclinic
Space group	P $\bar{1}$
a/Å	13.613(4)
b/Å	23.589(7)
c/Å	24.661(7)
α /°	106.004(16)
β /°	95.015(18)
γ /°	96.289(15)
Volume/Å ³	7509(4)
Z	4
ρ_{calc} /cm ³	1.241
μ /mm ⁻¹	0.400
F(000)	2982.0
Crystal size/mm ³	0.13 × 0.069 × 0.065
Radiation	MoK α (λ = 0.71073)
2 θ range for data collection/°	1.732 to 52
Index ranges	-16 ≤ h ≤ 16, -29 ≤ k ≤ 29, -30 ≤ l ≤ 30
Reflections collected	160626
Independent reflections	29504 [R _{int} = 0.0855, R _{sigma} = 0.0656]
Data/restraints/parameters	29504/0/1753
Goodness-of-fit on F ²	1.006
Final R indexes [I ≥ 2 σ (I)]	R ₁ = 0.0444, wR ₂ = 0.0874
Final R indexes [all data]	R ₁ = 0.0796, wR ₂ = 0.1000
Largest diff. peak/hole / e Å ⁻³	0.41/-0.32

Table 2 Fractional Atomic Coordinates (×10⁴) and Equivalent Isotropic Displacement Parameters (Å²×10³) for Schomaker59_sq. U_{eq} is defined as 1/3 of the trace of the orthogonalised U_{ij} tensor.

Atom	x	y	z	U(eq)
Ni1	1331.7 (2)	7872.0 (2)	6548.0 (2)	14.07 (7)
Cl1	1.0 (4)	8159.6 (3)	6897.2 (3)	19.24 (13)
Cl2	2648.9 (5)	7530.9 (3)	6223.2 (3)	20.97 (14)

P1	889.9 (5)	8074.5 (3)	5726.7 (3)	16.31 (14)
N1	2258.0 (14)	8054.0 (8)	7715.1 (8)	13.0 (4)
N2	1497.0 (14)	7157.4 (8)	7349.7 (8)	12.3 (4)
C1	1717.6 (17)	7685.2 (10)	7233.8 (10)	12.5 (5)
C2	2373.2 (17)	7759.1 (10)	8129.3 (10)	14.0 (5)
C3	1903.8 (17)	7204.3 (11)	7905.2 (10)	14.1 (5)
C4	2710.4 (17)	8652.6 (10)	7748.7 (9)	12.7 (5)
C5	3669.6 (17)	8728.6 (10)	7585 (1)	14.9 (5)
C6	4034.9 (18)	9288.5 (11)	7547 (1)	18.3 (5)
C7	3499.4 (19)	9765.1 (11)	7675.8 (11)	19.8 (6)
C8	2606.1 (18)	9684.5 (11)	7891.1 (10)	19.0 (6)
C9	2196.8 (17)	9137.6 (11)	7941.2 (10)	15.7 (5)
C10	4334.3 (18)	8234.8 (11)	7508.6 (10)	17.0 (5)
C11	4606.3 (17)	8123.1 (11)	8077.9 (10)	18.3 (5)
C12	4643.8 (19)	7546.1 (12)	8107.4 (12)	24.1 (6)
C13	4880 (2)	7434.4 (14)	8622.5 (13)	34.1 (7)
C14	5088 (2)	7898.5 (16)	9116.5 (13)	39.3 (8)
C15	5066 (2)	8473.0 (15)	9093.6 (12)	34.7 (7)
C16	4826 (2)	8585.0 (13)	8577.9 (11)	26.8 (6)
C17	5256.0 (18)	8361 (1)	7225.1 (11)	18.3 (5)
C18	6204.0 (19)	8508.3 (12)	7518.2 (12)	25.5 (6)
C19	7028 (2)	8622.6 (12)	7247.0 (13)	31.9 (7)
C20	6906 (2)	8595.5 (12)	6681.1 (13)	31.6 (7)
C21	5966 (2)	8451.8 (12)	6382.5 (12)	28.0 (6)
C22	5143 (2)	8331.0 (11)	6648.6 (11)	23.6 (6)
C23	3894 (2)	10354.7 (11)	7595.8 (13)	28.9 (7)
C24	1255.8 (18)	9088.5 (11)	8233.2 (10)	16.1 (5)
C25	1475.2 (19)	9018.2 (11)	8827.9 (10)	19.4 (6)
C26	2421 (2)	9131.0 (12)	9127.9 (11)	25.6 (6)
C27	2555 (2)	9094.5 (13)	9686.2 (12)	35.1 (7)
C28	1737 (3)	8953.1 (13)	9943.7 (12)	38.4 (8)
C29	798 (3)	8845.8 (13)	9653.2 (12)	37.2 (8)
C30	668 (2)	8875.4 (12)	9099.0 (11)	27.4 (6)
C31	668.4 (18)	9613.8 (11)	8263.9 (10)	17.0 (5)
C32	782.9 (19)	10100.1 (11)	8748.1 (11)	20.9 (6)
C33	241 (2)	10567.6 (12)	8773.9 (11)	24.1 (6)
C34	-422.3 (19)	10562.0 (12)	8317.4 (12)	25.7 (6)

C35	-532 (2)	10086.9 (12)	7828.9 (12)	28.9 (7)
C36	8.9 (19)	9616.2 (12)	7803.9 (11)	24.1 (6)
C37	888.9 (17)	6640.5 (10)	6953.1 (10)	13.5 (5)
C38	-147.9 (17)	6570.8 (10)	6970.9 (10)	14.5 (5)
C39	-730.4 (18)	6096.7 (10)	6564.3 (10)	16.8 (5)
C40	-320.9 (18)	5697.9 (11)	6150.4 (10)	17.3 (5)
C41	705.9 (18)	5760.5 (10)	6167.3 (10)	16.2 (5)
C42	1331.3 (17)	6215.3 (10)	6574.3 (10)	14.4 (5)
C43	-615.0 (17)	6974.8 (11)	7446.6 (10)	16.3 (5)
C44	-332.2 (17)	6854.1 (11)	8012.3 (11)	18.5 (6)
C45	-172.2 (19)	6295.9 (12)	8052.7 (12)	23.5 (6)
C46	110 (2)	6210.8 (14)	8577.2 (13)	32.6 (7)
C47	211 (2)	6677.1 (15)	9063.2 (13)	38.4 (8)
C48	37 (2)	7233.4 (14)	9032.4 (12)	34.8 (7)
C49	-226.3 (19)	7319.4 (12)	8511.6 (11)	25.7 (6)
C50	-1737.8 (18)	6944.6 (10)	7307.4 (10)	16.4 (5)
C51	-2100.5 (19)	7123.4 (11)	6847.8 (11)	20.8 (6)
C52	-3114.8 (19)	7101.3 (12)	6705.2 (11)	24.3 (6)
C53	-3780.7 (19)	6908.4 (11)	7027.8 (11)	23.6 (6)
C54	-3435.1 (19)	6738.7 (12)	7495.0 (12)	25.3 (6)
C55	-2417.8 (18)	6754.1 (11)	7632.3 (11)	20.3 (6)
C56	-981.6 (19)	5200.5 (12)	5705.0 (11)	26.3 (6)
C57	2451.0 (17)	6195.6 (11)	6644 (1)	15.3 (5)
C58	2827.1 (17)	5812.4 (11)	6116 (1)	15.6 (5)
C59	3245 (2)	6059.1 (12)	5727.2 (12)	29.4 (7)
C60	3593 (2)	5704.5 (13)	5253.9 (12)	36.1 (8)
C61	3527 (2)	5097.5 (12)	5160.7 (11)	26.1 (6)
C62	3112.5 (18)	4845.5 (11)	5545.4 (10)	20.4 (6)
C63	2770.1 (18)	5197.4 (11)	6015 (1)	18.5 (5)
C64	2749.1 (18)	5963.8 (10)	7150.6 (10)	15.2 (5)
C65	3757.9 (19)	5999.6 (11)	7332.6 (11)	21.8 (6)
C66	4071 (2)	5766.6 (12)	7762.5 (11)	27.0 (6)
C67	3384 (2)	5485.8 (11)	8020.3 (11)	27.0 (6)
C68	2384 (2)	5450.8 (11)	7849.3 (11)	22.8 (6)
C69	2064.4 (19)	5687.3 (10)	7416.7 (10)	18.2 (5)
C70	-57.8 (19)	8587.1 (11)	5765.1 (10)	21.0 (6)
C71	347 (2)	9229.6 (11)	6107.9 (11)	23.8 (6)

C72	-507 (2)	9601.1 (13)	6237.9 (12)	34.1 (7)
C73	-1154 (2)	9581.7 (14)	5697.4 (13)	39.2 (8)
C74	-1534 (2)	8948.2 (13)	5348.6 (12)	33.4 (7)
C75	-692 (2)	8577.6 (13)	5216.3 (11)	28.1 (7)
C76	1970.1 (19)	8331.5 (11)	5414.7 (10)	19.3 (6)
C77	2675.2 (19)	8851.4 (11)	5828.5 (11)	22.2 (6)
C78	3628 (2)	8970.4 (13)	5567.4 (12)	28.5 (6)
C79	3393 (2)	9070.5 (12)	4987.4 (11)	27.4 (6)
C80	2696 (2)	8553.4 (13)	4584.2 (11)	27.4 (6)
C81	1732.6 (19)	8447.3 (12)	4838.8 (10)	23.1 (6)
C82	277.7 (19)	7392.8 (11)	5177.7 (10)	20.6 (6)
C83	965 (2)	6938.1 (11)	4948.9 (11)	25.8 (6)
C84	390 (2)	6414.9 (12)	4476.6 (12)	34.1 (7)
C85	-490 (2)	6120.3 (13)	4689.0 (13)	39.2 (8)
C86	-1170 (2)	6566.1 (13)	4937.6 (14)	42.3 (8)
C87	-598 (2)	7098.8 (12)	5400.0 (12)	30.0 (7)
Ni1A	3447.0 (2)	6617.5 (2)	2285.6 (2)	16.40 (8)
Cl1A	3523.6 (5)	6379.8 (3)	1381.8 (3)	24.57 (15)
Cl2A	3141.1 (5)	6936.0 (3)	3160.0 (3)	20.52 (14)
PIA	2800.3 (5)	5684.1 (3)	2268.0 (3)	17.78 (14)
N1A	5104.7 (14)	7587.6 (9)	2579.2 (8)	15.1 (4)
N2A	3830.5 (14)	7857.6 (9)	2188.0 (8)	14.3 (4)
C1A	4136.8 (17)	7389.1 (11)	2347.3 (10)	14.9 (5)
C2A	5386.8 (18)	8167.5 (11)	2559.1 (10)	16.8 (5)
C3A	4595.6 (17)	8331.8 (11)	2317.5 (10)	15.8 (5)
C4A	5750.0 (17)	7202.6 (11)	2752.3 (10)	15.8 (5)
C5A	5912.9 (17)	7208.6 (11)	3322.9 (10)	15.6 (5)
C6A	6465.9 (17)	6790.5 (11)	3449.6 (10)	16.3 (5)
C7A	6851.4 (18)	6379.9 (11)	3035.1 (10)	17.6 (5)
C8A	6737.6 (18)	6411.1 (11)	2480.8 (10)	19.7 (6)
C9A	6214.8 (18)	6829.4 (11)	2330.8 (10)	18.4 (5)
C10A	5543.8 (18)	7674.0 (11)	3794.4 (10)	16.6 (5)
C11A	6172.1 (18)	8284.4 (11)	3934.2 (10)	18.3 (5)
C12A	5885 (2)	8754.0 (11)	4344.6 (11)	24.8 (6)
C13A	6382 (2)	9322.4 (12)	4476.4 (13)	30.6 (7)
C14A	7194 (2)	9437.5 (12)	4198.8 (12)	28.9 (7)
C15A	7506 (2)	8982.4 (12)	3803.7 (11)	25.2 (6)

C16A	7004.0 (19)	8404.9 (12)	3677.2 (11)	21.2 (6)
C17A	5464.6 (19)	7485.8 (11)	4337.3 (10)	18.0 (5)
C18A	6311 (2)	7515.1 (11)	4710.2 (10)	22.1 (6)
C19A	6238 (2)	7322.4 (12)	5191.5 (11)	28.7 (7)
C20A	5312 (2)	7123.7 (13)	5317.4 (11)	31.9 (7)
C21A	4467 (2)	7119.9 (12)	4965.8 (11)	27.5 (6)
C22A	4544.3 (19)	7295.0 (11)	4474.1 (11)	21.9 (6)
C23A	7366 (2)	5900.5 (12)	3191.7 (11)	25.5 (6)
C24A	6265.6 (19)	6943.6 (12)	1751.6 (10)	21.8 (6)
C25A	6946.7 (19)	7525.1 (12)	1830.2 (11)	23.3 (6)
C26A	7784.4 (19)	7711.2 (13)	2236.7 (11)	25.6 (6)
C27A	8377 (2)	8245.6 (13)	2306.6 (12)	29.1 (7)
C28A	8148 (2)	8610.5 (13)	1971.6 (12)	32.7 (7)
C29A	7335 (2)	8429.3 (14)	1564.7 (13)	34.5 (7)
C30A	6738 (2)	7890.7 (13)	1492.0 (11)	28.4 (7)
C31A	6574 (2)	6426.9 (13)	1305.1 (11)	26.2 (6)
C32A	7539 (2)	6429.6 (17)	1163.6 (13)	44.4 (9)
C33A	7797 (3)	5948.2 (18)	759.7 (13)	53.7 (10)
C34A	7108 (3)	5466.5 (17)	493.9 (13)	49.7 (9)
C35A	6145 (3)	5458.1 (16)	623.8 (14)	49.0 (9)
C36A	5883 (2)	5936.6 (14)	1025.3 (13)	37.5 (8)
C37A	2857.0 (17)	7843.7 (10)	1895.3 (10)	14.7 (5)
C38A	2755.8 (18)	7751.2 (10)	1307.7 (10)	15.9 (5)
C39A	1790.5 (18)	7696.9 (11)	1034.3 (11)	20.2 (6)
C40A	966.4 (18)	7746.6 (11)	1327.5 (11)	20.4 (6)
C41A	1111.7 (18)	7887.8 (11)	1916.9 (11)	19.2 (6)
C42A	2055.6 (18)	7947 (1)	2210.7 (10)	15.4 (5)
C43A	3658.1 (18)	7773.1 (11)	984.1 (10)	17.7 (5)
C44A	4058.3 (18)	8414.6 (11)	998.9 (10)	18.6 (6)
C45A	3612 (2)	8904.0 (12)	1251.9 (11)	25.3 (6)
C46A	4012 (2)	9473.7 (13)	1248.9 (12)	33.4 (7)
C47A	4852 (2)	9558.8 (13)	989.4 (12)	35.2 (7)
C48A	5299 (2)	9070.0 (13)	734.6 (11)	29.7 (7)
C49A	4907.4 (19)	8506.8 (12)	739.9 (11)	23.7 (6)
C50A	3484.8 (19)	7380.1 (11)	371.0 (11)	19.6 (6)
C51A	3863 (2)	6843.2 (12)	216.3 (12)	32.8 (7)
C52A	3679 (3)	6485.1 (14)	-344.5 (15)	48.3 (9)

C53A	3118 (3)	6655.7 (15)	-747.4 (14)	48.0 (9)
C54A	2757 (2)	7190.7 (14)	-602.5 (12)	36.4 (8)
C55A	2950 (2)	7553.9 (12)	-49.6 (11)	24.6 (6)
C56A	-66.9 (19)	7661.8 (14)	1011.9 (12)	30.6 (7)
C57A	2248.9 (18)	8190.8 (10)	2859.4 (10)	15.6 (5)
C58A	1300.3 (18)	8163.7 (11)	3146.3 (10)	18.3 (5)
C59A	810.6 (19)	7612.3 (12)	3133.8 (11)	24.3 (6)
C60A	-46 (2)	7563.5 (13)	3393.4 (11)	26.8 (6)
C61A	-416 (2)	8070.4 (13)	3681.3 (11)	26.7 (6)
C62A	72 (2)	8622.4 (13)	3704.0 (11)	25.5 (6)
C63A	920.1 (19)	8670.1 (12)	3435.2 (10)	21.8 (6)
C64A	2843.6 (18)	8812.5 (11)	3023.3 (10)	16.8 (5)
C65A	3644.8 (18)	8974.8 (11)	3448.7 (10)	20.2 (6)
C66A	4179 (2)	9539.9 (12)	3605.4 (12)	27.2 (6)
C67A	3921 (2)	9953.1 (12)	3337.3 (12)	30.1 (7)
C68A	3131 (2)	9798.5 (12)	2908.7 (12)	28.9 (7)
C69A	2597 (2)	9231.3 (12)	2750.3 (11)	24.0 (6)
C70A	2967.2 (19)	5097.2 (12)	1620.5 (11)	23.5 (6)
C71A	4055 (2)	4988.4 (12)	1615.7 (11)	26.8 (6)
C72A	4215 (2)	4579.7 (15)	1046.5 (13)	42.2 (8)
C73A	3549 (3)	3995.6 (14)	899.9 (15)	50.2 (9)
C74A	2460 (2)	4091.0 (13)	900.1 (13)	38.2 (8)
C75A	2275 (2)	4511.3 (12)	1466.5 (12)	33.2 (7)
C76A	3287.9 (18)	5496.1 (11)	2910.4 (11)	18.4 (5)
C77A	4420.4 (18)	5677.2 (11)	3061.4 (11)	20.9 (6)
C78A	4748.1 (19)	5610.3 (12)	3647.6 (11)	22.5 (6)
C79A	4451.9 (19)	4974.5 (12)	3663.1 (11)	23.2 (6)
C80A	3336.9 (19)	4786.7 (12)	3507.0 (11)	23.3 (6)
C81A	2982.7 (19)	4853.9 (11)	2925.5 (11)	21.5 (6)
C82A	1433.4 (18)	5602.0 (12)	2257.2 (11)	22.2 (6)
C83A	1037 (2)	5848.7 (14)	2822.7 (12)	30.0 (7)
C84A	-97 (2)	5742.1 (15)	2737.3 (12)	34.8 (7)
C85A	-539 (2)	5999.1 (14)	2288.0 (13)	36.6 (7)
C86A	-132 (2)	5765.9 (16)	1730.9 (13)	41.9 (8)
C87A	1001 (2)	5869.8 (15)	1808.1 (13)	35.3 (7)
C88	7897 (2)	8965.3 (14)	9147.1 (13)	36.4 (7)
C89	7810 (2)	8362.7 (15)	8851.5 (13)	38.7 (8)

C90	7706 (2)	7922.9 (14)	9125.8 (13)	38.9 (8)
C91	7696 (2)	8070.7 (13)	9711.1 (13)	33.3 (7)
C92	7774 (2)	8668.0 (14)	10004.0 (13)	39.1 (8)
C93	7872 (2)	9108.1 (15)	9730.8 (13)	39.4 (8)
C94	8015 (2)	9437.8 (15)	8850.6 (15)	48.5 (9)
C95	7572 (3)	7592.7 (15)	10010.9 (14)	50.3 (9)

Table 3 Anisotropic Displacement Parameters ($\text{\AA}^2 \times 10^3$) for Schomaker59_sq. The Anisotropic displacement factor exponent takes the form: $-2\pi^2[h^2a^*U_{11}+2hka^*b^*U_{12}+\dots]$.

Atom	U_{11}	U_{22}	U_{33}	U_{23}	U_{13}	U_{12}
Ni1	17.49 (17)	13.47 (16)	12.09 (16)	5.35 (13)	1.10 (13)	1.93 (13)
Cl1	19.6 (3)	22.2 (3)	18.2 (3)	9.0 (3)	2.5 (2)	4.1 (3)
Cl2	25.6 (3)	22.8 (3)	18.7 (3)	9.9 (3)	5.9 (3)	8.8 (3)
P1	21.6 (4)	14.5 (3)	13.1 (3)	5.1 (3)	0.7 (3)	1.9 (3)
N1	14 (1)	13.1 (10)	12.5 (10)	4.6 (8)	3.0 (8)	0.9 (8)
N2	12.7 (10)	13.9 (10)	11.5 (10)	5.7 (8)	2.5 (8)	0.7 (8)
C1	11.9 (12)	12.0 (12)	13.8 (12)	3.4 (10)	4 (1)	1.9 (10)
C2	13.8 (12)	17.4 (13)	11.3 (12)	5 (1)	1.3 (10)	1.7 (10)
C3	14.0 (12)	17.4 (13)	13.8 (12)	7.3 (10)	4.6 (10)	4.7 (10)
C4	14.7 (12)	11.0 (12)	12.0 (12)	4 (1)	0.9 (10)	-1.3 (10)
C5	16.1 (13)	15.0 (13)	12.9 (12)	3.3 (10)	0.4 (10)	1.3 (10)
C6	16.6 (13)	16.1 (13)	21.9 (14)	5.2 (11)	4.5 (11)	-0.5 (11)
C7	21.1 (14)	15.9 (13)	22.2 (14)	7.0 (11)	2.9 (11)	-1.6 (11)
C8	20.1 (14)	14.5 (13)	23.0 (14)	5.4 (11)	4.8 (11)	3.2 (11)
C9	15.1 (13)	17.3 (13)	14.5 (13)	4.5 (11)	0.5 (10)	2.3 (10)
C10	16.5 (13)	14.7 (13)	19.5 (13)	3.9 (11)	3.4 (10)	2.4 (10)
C11	11.4 (12)	23.7 (14)	20.7 (14)	5.8 (11)	5.4 (10)	4.6 (11)
C12	21.2 (14)	25.8 (15)	28.5 (15)	9.7 (12)	9.6 (12)	8.0 (12)
C13	32.2 (17)	46 (2)	37.3 (18)	26.2 (16)	15.5 (14)	17.2 (15)
C14	32.6 (18)	68 (2)	28.3 (17)	26.4 (17)	8.3 (14)	19.6 (17)
C15	30.1 (17)	53 (2)	17.6 (15)	1.6 (14)	1.1 (12)	14.6 (15)
C16	24.4 (15)	30.3 (16)	24.3 (15)	4.9 (13)	-0.4 (12)	7.3 (13)
C17	19.6 (14)	11.1 (13)	26.0 (14)	5.1 (11)	10.2 (11)	4.4 (11)
C18	20.5 (15)	26.0 (15)	28.4 (15)	4.7 (12)	6.3 (12)	1.9 (12)
C19	21.1 (15)	29.8 (17)	42.2 (18)	5.8 (14)	9.7 (13)	-0.3 (13)
C20	32.4 (17)	22.5 (15)	43.8 (19)	9.3 (14)	25.3 (15)	4.6 (13)

C21	36.5 (17)	21.9 (15)	29.6 (16)	8.6 (13)	16.6 (13)	8.0 (13)
C22	24.9 (15)	22.8 (15)	25.9 (15)	8.5 (12)	10.1 (12)	6.2 (12)
C23	28.6 (16)	17.6 (14)	43.9 (18)	13.4 (13)	11.0 (13)	0.8 (12)
C24	16.2 (13)	15.2 (13)	17.3 (13)	5.1 (11)	2.2 (10)	2.3 (10)
C25	28.8 (15)	13.3 (13)	17.5 (13)	3.6 (11)	6.3 (11)	8.5 (11)
C26	26.9 (15)	27.6 (16)	20.8 (14)	3.1 (12)	0.9 (12)	9.4 (12)
C27	42.6 (19)	37.1 (18)	23.4 (16)	2.8 (14)	-4.0 (14)	17.6 (15)
C28	64 (2)	38.2 (19)	19.9 (15)	12.1 (14)	11.3 (15)	24.0 (17)
C29	53 (2)	36.5 (18)	31.8 (17)	17.6 (15)	21.0 (16)	15.5 (16)
C30	35.4 (17)	26.4 (16)	24.0 (15)	9.6 (13)	9.3 (13)	9.4 (13)
C31	14.1 (13)	18.6 (14)	20.2 (13)	6.9 (11)	6.4 (10)	2.7 (11)
C32	22.4 (14)	20.5 (14)	19.3 (14)	5.0 (11)	0.0 (11)	4.9 (11)
C33	30.4 (16)	18.8 (14)	21.6 (14)	1.9 (12)	6.5 (12)	5.1 (12)
C34	23.8 (15)	22.9 (15)	34.8 (16)	11.5 (13)	7.3 (12)	10.5 (12)
C35	28.8 (16)	29.7 (16)	28.2 (16)	7.5 (13)	-2.7 (12)	11.5 (13)
C36	25.4 (15)	24.3 (15)	21.0 (14)	2.3 (12)	0.7 (11)	9.4 (12)
C37	15.3 (13)	12.4 (12)	13.8 (12)	6.5 (10)	0.1 (10)	0 (1)
C38	14.0 (13)	13.5 (13)	19.0 (13)	8.8 (11)	4 (1)	2.3 (10)
C39	12.4 (13)	15.2 (13)	22.5 (14)	5.3 (11)	3.6 (10)	-0.3 (10)
C40	16.4 (13)	13.9 (13)	21.3 (14)	5.1 (11)	1.4 (11)	1.3 (10)
C41	18.1 (13)	12.9 (13)	18.2 (13)	3.4 (11)	6.6 (10)	3.4 (10)
C42	17.0 (13)	13.9 (13)	16.4 (13)	9.6 (10)	5.9 (10)	2.2 (10)
C43	15.5 (13)	14.7 (13)	19.0 (13)	4.9 (11)	3.2 (10)	2.1 (10)
C44	9.2 (12)	23.8 (14)	24.3 (14)	10.0 (12)	5.1 (10)	0.6 (11)
C45	20.0 (14)	24.9 (15)	29.2 (15)	13.1 (12)	6.4 (12)	2.5 (12)
C46	24.1 (16)	40.4 (18)	42.5 (19)	27.2 (16)	3.7 (13)	3.9 (14)
C47	34.7 (18)	56 (2)	28.9 (17)	24.7 (17)	-1.3 (14)	-3.3 (16)
C48	37.6 (18)	45 (2)	19.1 (15)	6.3 (14)	1.7 (13)	2.0 (15)
C49	25.4 (15)	27.0 (16)	23.4 (15)	5.1 (12)	3.8 (12)	3.1 (12)
C50	16.1 (13)	12.1 (13)	21.1 (13)	3.5 (11)	5.4 (10)	3.5 (10)
C51	19.3 (14)	21.9 (14)	23.6 (14)	8.6 (12)	7.8 (11)	3.6 (11)
C52	21.1 (14)	28.7 (16)	26.4 (15)	12.5 (13)	2.0 (12)	6.9 (12)
C53	15.0 (13)	23.4 (15)	33.4 (16)	8.9 (12)	4.4 (12)	4.2 (11)
C54	19.5 (14)	28.1 (16)	31.5 (16)	11.2 (13)	11.3 (12)	3.8 (12)
C55	21.0 (14)	17.0 (14)	24.9 (14)	9.1 (11)	5.0 (11)	2.2 (11)
C56	19.6 (14)	20.7 (15)	32.1 (16)	-1.7 (12)	1.9 (12)	0.7 (12)
C57	14.3 (13)	12.8 (12)	18.9 (13)	4.7 (10)	3.7 (10)	0.7 (10)

C58	13.1 (12)	16.3 (13)	17.0 (13)	4.3 (11)	1.8 (10)	2 (1)
C59	39.6 (18)	17.8 (14)	33.7 (17)	7.9 (13)	19.3 (14)	3.0 (13)
C60	52 (2)	32.3 (17)	29.6 (17)	10.7 (14)	26.7 (15)	6.0 (15)
C61	26.8 (15)	29.0 (16)	20.6 (14)	1.5 (12)	8.7 (12)	7.0 (13)
C62	18.4 (14)	18.8 (14)	22.6 (14)	3.7 (11)	-0.3 (11)	4.5 (11)
C63	20.3 (14)	18.0 (14)	19.0 (13)	7.5 (11)	4.8 (11)	3.3 (11)
C64	17.2 (13)	10.4 (12)	16.3 (13)	0.4 (10)	2.1 (10)	3.3 (10)
C65	17.6 (14)	19.9 (14)	25.3 (15)	2.7 (12)	1.2 (11)	2.1 (11)
C66	24.2 (15)	23.0 (15)	30.0 (16)	2.9 (13)	-6.9 (12)	7.3 (12)
C67	39.5 (17)	19.2 (14)	20.7 (14)	4.1 (12)	-5.6 (13)	8.6 (13)
C68	31.1 (16)	17.1 (14)	20.4 (14)	4.3 (11)	4.6 (12)	5.7 (12)
C69	19.1 (14)	14.4 (13)	20.7 (14)	3.8 (11)	3.3 (11)	3.1 (11)
C70	25.0 (15)	24.4 (15)	15.2 (13)	7.4 (11)	1.9 (11)	6.4 (12)
C71	30.9 (16)	19.5 (14)	24.6 (15)	9.8 (12)	6.0 (12)	7.6 (12)
C72	46.1 (19)	24.6 (16)	33.1 (17)	7.0 (13)	5.0 (14)	14.7 (14)
C73	41.4 (19)	41.2 (19)	43.3 (19)	18.6 (16)	7.1 (15)	23.4 (16)
C74	31.7 (17)	48 (2)	27.1 (16)	18.4 (15)	2.5 (13)	16.0 (15)
C75	33.0 (16)	33.5 (17)	21.0 (14)	11.0 (13)	0.4 (12)	12.7 (13)
C76	23.9 (14)	17.9 (13)	18.6 (13)	8.3 (11)	4.1 (11)	3.9 (11)
C77	25.9 (15)	20.5 (14)	20.6 (14)	8.1 (12)	2.0 (11)	-0.7 (12)
C78	23.2 (15)	31.1 (16)	27.9 (16)	5.3 (13)	2.3 (12)	-1.0 (13)
C79	25.4 (15)	29.2 (16)	32.4 (16)	13.9 (13)	12.8 (13)	3.9 (13)
C80	31.3 (16)	32.6 (17)	22.2 (15)	12.2 (13)	8.3 (12)	5.7 (13)
C81	26.8 (15)	29.0 (15)	16.1 (13)	11.6 (12)	2.9 (11)	1.9 (12)
C82	26.5 (15)	18.9 (14)	14.4 (13)	3.6 (11)	-1.1 (11)	0.9 (11)
C83	31.9 (16)	19.6 (14)	23.9 (15)	3.5 (12)	3.7 (12)	2.3 (12)
C84	49 (2)	21.6 (16)	26.3 (16)	-0.2 (13)	-0.7 (14)	4.1 (14)
C85	48 (2)	21.0 (16)	37.3 (18)	-2.1 (14)	-3.7 (15)	-9.4 (14)
C86	35.5 (19)	31.2 (18)	48 (2)	-1.6 (15)	0.5 (15)	-9.5 (15)
C87	30.5 (16)	23.0 (15)	29.8 (16)	1.3 (13)	1.9 (13)	-7.2 (13)
Ni1A	17.11 (17)	16.67 (17)	18.30 (17)	8.88 (14)	4.59 (13)	2.84 (13)
Cl1A	33.7 (4)	21.8 (3)	20.9 (3)	9.8 (3)	7.3 (3)	2.9 (3)
Cl2A	21.8 (3)	20.8 (3)	21.3 (3)	9.2 (3)	5.7 (3)	2.7 (3)
P1A	17.6 (3)	18.5 (4)	19.6 (3)	8.8 (3)	4.0 (3)	2.4 (3)
N1A	14.4 (11)	16.9 (11)	16.8 (11)	8.5 (9)	4.2 (8)	3.4 (9)
N2A	14.9 (11)	15.6 (11)	15.3 (11)	8.3 (9)	4.0 (8)	3.2 (9)
C1A	13.8 (13)	20.4 (13)	13.4 (12)	7.1 (11)	6.4 (10)	5 (1)

C2A	14.8 (13)	19.2 (14)	18.0 (13)	8.8 (11)	3.3 (10)	-0.8 (11)
C3A	18.7 (13)	15.7 (13)	15.9 (13)	8.1 (11)	5.9 (10)	2.1 (11)
C4A	13.5 (12)	17.7 (13)	20.0 (13)	10.5 (11)	3.4 (10)	4.9 (10)
C5A	14.1 (13)	17.8 (13)	17.1 (13)	8.4 (11)	5.1 (10)	0.5 (10)
C6A	15.9 (13)	21.5 (14)	13.3 (12)	7.3 (11)	2.8 (10)	3.4 (11)
C7A	14.0 (13)	20.8 (14)	20.4 (13)	8.7 (11)	4.2 (10)	3.3 (11)
C8A	19.1 (14)	23.4 (14)	17.9 (13)	5.0 (11)	6.1 (11)	7.6 (11)
C9A	13.5 (13)	25.2 (14)	19.7 (13)	11.1 (11)	4.5 (10)	2.3 (11)
C10A	14.0 (13)	18.0 (13)	18.7 (13)	6.8 (11)	2.4 (10)	2.3 (10)
C11A	16.4 (13)	21.6 (14)	19.8 (13)	10.6 (11)	1.3 (11)	4.3 (11)
C12A	21.8 (15)	21.7 (15)	33.2 (16)	9.3 (13)	10.2 (12)	4.8 (12)
C13A	32.7 (17)	20.0 (15)	39.8 (18)	6.6 (13)	10.4 (14)	6.9 (13)
C14A	26.2 (16)	18.0 (15)	44.6 (18)	13.8 (13)	2.2 (13)	1.1 (12)
C15A	22.5 (15)	28.8 (16)	28.1 (15)	13.8 (13)	5.2 (12)	3.4 (12)
C16A	21.6 (14)	23.5 (15)	20.8 (14)	9.2 (12)	3.3 (11)	4.0 (12)
C17A	24.6 (14)	13.2 (13)	18.1 (13)	4.9 (11)	7.5 (11)	6.3 (11)
C18A	23.7 (14)	23.2 (15)	19.0 (14)	4.5 (12)	6.3 (11)	2.7 (12)
C19A	34.6 (17)	34.0 (17)	16.9 (14)	9.1 (13)	-1.2 (12)	0.9 (13)
C20A	42.5 (19)	34.1 (17)	19.0 (15)	11.5 (13)	3.8 (13)	-4.3 (14)
C21A	31.5 (16)	28.3 (16)	21.1 (15)	5.6 (12)	9.6 (12)	-3.3 (13)
C22A	22.7 (14)	21.7 (14)	21.8 (14)	6.0 (12)	5.7 (11)	3.4 (12)
C23A	29.0 (16)	30.9 (16)	24.3 (15)	14.9 (13)	9.8 (12)	14.4 (13)
C24A	18.2 (14)	32.7 (16)	18.8 (14)	11.3 (12)	6.1 (11)	9.1 (12)
C25A	21.7 (14)	36.6 (17)	19.3 (14)	14.1 (12)	13.7 (11)	12.1 (12)
C26A	21.2 (15)	39.6 (17)	22.7 (15)	17.2 (13)	8.4 (12)	7.9 (13)
C27A	21.0 (15)	43.9 (19)	25.9 (15)	12.7 (14)	12.0 (12)	4.8 (13)
C28A	30.3 (17)	35.2 (18)	38.9 (18)	15.8 (15)	19.3 (14)	5.7 (14)
C29A	32.4 (17)	44.3 (19)	39.3 (18)	27.4 (16)	14.2 (14)	10.7 (15)
C30A	22.6 (15)	45.9 (19)	25.3 (15)	20.3 (14)	8.5 (12)	10.7 (14)
C31A	26.6 (15)	40.6 (18)	16.0 (14)	12.1 (13)	6.1 (12)	12.1 (14)
C32A	23.4 (17)	75 (3)	27.1 (17)	-1.1 (17)	4.3 (13)	11.7 (16)
C33A	31.1 (19)	93 (3)	27.9 (18)	-5.3 (19)	6.6 (15)	26 (2)
C34A	57 (2)	64 (2)	26.7 (18)	-0.4 (17)	12.6 (17)	32 (2)
C35A	55 (2)	49 (2)	36.9 (19)	-1.6 (17)	17.7 (17)	9.4 (18)
C36A	37.9 (18)	41.2 (19)	34.0 (18)	5.9 (15)	17.4 (15)	10.3 (16)
C37A	12.6 (12)	13.5 (13)	18.5 (13)	5.6 (10)	0.6 (10)	2.3 (10)
C38A	18.0 (13)	12.9 (13)	17.6 (13)	4.8 (10)	3.2 (10)	4.1 (10)

C39A	22.1 (14)	24.3 (14)	14.4 (13)	5.1 (11)	1.1 (11)	6.2 (12)
C40A	17.2 (13)	22.5 (14)	21.6 (14)	5.7 (12)	2.0 (11)	5.4 (11)
C41A	14.9 (13)	20.3 (14)	22.5 (14)	4.9 (11)	4.8 (11)	4.8 (11)
C42A	16.9 (13)	13.2 (13)	18.0 (13)	6.8 (10)	3.6 (10)	3.5 (10)
C43A	18.7 (13)	22.3 (14)	16.5 (13)	10.4 (11)	4.2 (10)	8.0 (11)
C44A	21.1 (14)	21.0 (14)	13.5 (13)	5.8 (11)	-1.7 (10)	2.9 (11)
C45A	27.3 (15)	28.4 (16)	22.6 (15)	10.6 (12)	4.5 (12)	5.3 (13)
C46A	44.1 (19)	23.4 (16)	31.7 (17)	6.7 (13)	-0.4 (14)	8.0 (14)
C47A	46 (2)	26.0 (17)	32.6 (17)	13.0 (14)	1.1 (15)	-7.5 (14)
C48A	28.9 (16)	37.0 (18)	21.6 (15)	11.9 (13)	-0.8 (12)	-7.7 (14)
C49A	22.7 (15)	31.5 (16)	16.4 (13)	7.8 (12)	0.2 (11)	0.9 (12)
C50A	22.3 (14)	16.8 (13)	21.1 (14)	5.8 (11)	11.2 (11)	1.0 (11)
C51A	47.0 (19)	25.4 (16)	34.3 (17)	13.7 (14)	24.5 (15)	11.6 (14)
C52A	76 (3)	22.1 (17)	48 (2)	3.0 (16)	40 (2)	7.5 (17)
C53A	70 (3)	38 (2)	24.7 (17)	-5.4 (15)	19.7 (17)	-14.6 (18)
C54A	39.6 (19)	46 (2)	19.0 (15)	7.1 (14)	7.8 (13)	-12.3 (15)
C55A	26.9 (15)	26.4 (15)	18.9 (14)	5.4 (12)	5.5 (12)	-2.4 (12)
C56A	17.2 (14)	44.1 (19)	27.8 (16)	6.1 (14)	-0.6 (12)	6.6 (13)
C57A	17.7 (13)	15.2 (13)	16.4 (13)	6.2 (10)	5.3 (10)	6.1 (10)
C58A	17.0 (13)	24.2 (14)	14.4 (13)	5.7 (11)	1 (1)	6.0 (11)
C59A	25.1 (15)	25.0 (15)	26.1 (15)	8.9 (12)	9.1 (12)	8.5 (12)
C60A	23.8 (15)	31.3 (16)	27.9 (15)	12.3 (13)	6.6 (12)	2.3 (13)
C61A	19.6 (14)	45.1 (19)	18.7 (14)	12.1 (13)	5.8 (11)	8.1 (13)
C62A	26.0 (15)	31.9 (16)	19.3 (14)	3.7 (12)	6.7 (12)	14.0 (13)
C63A	20.4 (14)	25.8 (15)	18.9 (14)	4.4 (12)	3.2 (11)	6.5 (12)
C64A	17.0 (13)	19.0 (13)	15.5 (13)	3.4 (11)	8 (1)	6.4 (11)
C65A	20.8 (14)	23.3 (15)	19.0 (14)	8.3 (11)	5.3 (11)	5.5 (12)
C66A	21.9 (15)	29.0 (16)	27.6 (15)	6.5 (13)	-2.1 (12)	-1.2 (12)
C67A	30.0 (16)	19.9 (15)	37.4 (17)	4.9 (13)	3.4 (13)	0.0 (13)
C68A	33.7 (17)	21.4 (15)	34.9 (17)	12.4 (13)	4.2 (13)	7.1 (13)
C69A	25.2 (15)	22.8 (15)	24.4 (15)	7.8 (12)	-0.1 (12)	5.1 (12)
C70A	24.7 (15)	25.6 (15)	20.4 (14)	6.5 (12)	3.2 (11)	4.3 (12)
C71A	28.7 (16)	28.1 (16)	25.6 (15)	7.0 (13)	5.5 (12)	12.9 (13)
C72A	29.7 (18)	52 (2)	38.6 (19)	-0.4 (16)	4.1 (14)	13.5 (16)
C73A	54 (2)	33.7 (19)	55 (2)	-6.7 (17)	11.4 (18)	16.0 (17)
C74A	41.7 (19)	23.9 (16)	41.7 (19)	-1.3 (14)	7.3 (15)	-0.9 (14)
C75A	43.9 (19)	25.2 (16)	30.0 (16)	7.6 (13)	7.1 (14)	2.2 (14)

C76A	19.3 (14)	17.0 (13)	20.4 (14)	7.8 (11)	3.6 (11)	1.1 (11)
C77A	18.2 (14)	20.7 (14)	26.3 (15)	11.0 (12)	4.0 (11)	1.5 (11)
C78A	17.1 (14)	25.5 (15)	25.2 (15)	8.9 (12)	0.8 (11)	1.4 (11)
C79A	22.1 (14)	28.0 (15)	24.0 (14)	13.3 (12)	5.3 (11)	5.0 (12)
C80A	23.2 (15)	25.9 (15)	25.0 (15)	13.4 (12)	6.2 (12)	2.7 (12)
C81A	18.6 (14)	21.8 (14)	25.2 (14)	10.1 (12)	2.6 (11)	0.0 (11)
C82A	18.1 (14)	26.4 (15)	24.6 (14)	10.8 (12)	3.5 (11)	3.6 (12)
C83A	21.1 (15)	40.9 (18)	26.0 (15)	7.7 (14)	3.9 (12)	-0.4 (13)
C84A	16.9 (15)	54 (2)	31.3 (17)	9.8 (15)	6.7 (12)	-0.5 (14)
C85A	20.8 (16)	45 (2)	43.5 (19)	10.5 (16)	4.5 (14)	8.2 (14)
C86A	28.0 (17)	70 (2)	34.9 (18)	22.9 (17)	3.8 (14)	18.0 (16)
C87A	23.5 (16)	58 (2)	36.2 (17)	27.3 (16)	8.3 (13)	16.9 (15)
C88	20.7 (16)	45 (2)	39.1 (19)	4.9 (16)	1.9 (13)	5.1 (14)
C89	30.0 (17)	50 (2)	31.8 (17)	1.6 (16)	5.6 (14)	13.6 (15)
C90	30.5 (17)	36.3 (19)	40.4 (19)	-6.1 (15)	3.1 (14)	9.3 (14)
C91	27.4 (16)	34.4 (18)	32.9 (17)	2.3 (14)	2.5 (13)	3.3 (14)
C92	38.2 (19)	43 (2)	30.0 (17)	2.5 (15)	-0.6 (14)	4.1 (15)
C93	36.0 (18)	39.0 (19)	33.9 (18)	-2.2 (15)	-1.9 (14)	2.7 (15)
C94	40 (2)	53 (2)	51 (2)	12.4 (18)	3.9 (17)	8.8 (17)
C95	53 (2)	47 (2)	45 (2)	5.1 (17)	2.8 (17)	3.7 (18)

Table 4 Bond Lengths for Schomaker59_sq.

Atom	Atom	Length/Å	Atom	Atom	Length/Å
Ni1	Cl1	2.1685 (9)	P1A	C70A	1.853 (3)
Ni1	Cl2	2.1717 (9)	P1A	C76A	1.848 (2)
Ni1	P1	2.2530 (9)	P1A	C82A	1.847 (3)
Ni1	C1	1.907 (2)	N1A	C1A	1.367 (3)
P1	C70	1.853 (3)	N1A	C2A	1.395 (3)
P1	C76	1.839 (3)	N1A	C4A	1.450 (3)
P1	C82	1.850 (3)	N2A	C1A	1.364 (3)
N1	C1	1.358 (3)	N2A	C3A	1.388 (3)
N1	C2	1.393 (3)	N2A	C37A	1.445 (3)
N1	C4	1.454 (3)	C2A	C3A	1.331 (3)
N2	C1	1.360 (3)	C4A	C5A	1.401 (3)
N2	C3	1.402 (3)	C4A	C9A	1.410 (3)

N2	C37	1.452 (3)	C5A C6A	1.389 (3)
C2	C3	1.335 (3)	C5A C10A	1.526 (3)
C4	C5	1.407 (3)	C6A C7A	1.385 (3)
C4	C9	1.399 (3)	C7A C8A	1.385 (3)
C5	C6	1.390 (3)	C7A C23A	1.512 (3)
C5	C10	1.533 (3)	C8A C9A	1.388 (3)
C6	C7	1.385 (3)	C9A C24A	1.531 (3)
C7	C8	1.384 (3)	C10A C11A	1.526 (3)
C7	C23	1.506 (3)	C10A C17A	1.531 (3)
C8	C9	1.390 (3)	C11A C12A	1.397 (4)
C9	C24	1.532 (3)	C11A C16A	1.385 (3)
C10	C11	1.521 (3)	C12A C13A	1.372 (4)
C10	C17	1.529 (3)	C13A C14A	1.391 (4)
C11	C12	1.389 (3)	C14A C15A	1.370 (4)
C11	C16	1.386 (4)	C15A C16A	1.394 (4)
C12	C13	1.385 (4)	C17A C18A	1.393 (3)
C13	C14	1.378 (4)	C17A C22A	1.386 (4)
C14	C15	1.375 (4)	C18A C19A	1.390 (3)
C15	C16	1.388 (4)	C19A C20A	1.388 (4)
C17	C18	1.382 (4)	C20A C21A	1.376 (4)
C17	C22	1.398 (3)	C21A C22A	1.393 (3)
C18	C19	1.394 (4)	C24A C25A	1.524 (4)
C19	C20	1.374 (4)	C24A C31A	1.525 (4)
C20	C21	1.377 (4)	C25A C26A	1.395 (4)
C21	C22	1.389 (4)	C25A C30A	1.389 (3)
C24	C25	1.528 (3)	C26A C27A	1.380 (4)
C24	C31	1.535 (3)	C27A C28A	1.388 (4)
C25	C26	1.388 (4)	C28A C29A	1.372 (4)
C25	C30	1.393 (4)	C29A C30A	1.389 (4)
C26	C27	1.400 (4)	C31A C32A	1.388 (4)
C27	C28	1.384 (4)	C31A C36A	1.380 (4)
C28	C29	1.371 (4)	C32A C33A	1.389 (4)
C29	C30	1.384 (4)	C33A C34A	1.360 (5)
C31	C32	1.393 (4)	C34A C35A	1.376 (5)
C31	C36	1.385 (3)	C35A C36A	1.384 (4)
C32	C33	1.383 (3)	C37A C38A	1.397 (3)
C33	C34	1.376 (4)	C37A C42A	1.399 (3)

C34	C35	1.385 (4)	C38A C39A	1.399 (3)
C35	C36	1.388 (3)	C38A C43A	1.526 (3)
C37	C38	1.409 (3)	C39A C40A	1.385 (3)
C37	C42	1.398 (3)	C40A C41A	1.390 (3)
C38	C39	1.390 (3)	C40A C56A	1.512 (3)
C38	C43	1.528 (3)	C41A C42A	1.392 (3)
C39	C40	1.387 (3)	C42A C57A	1.531 (3)
C40	C41	1.385 (3)	C43A C44A	1.540 (3)
C40	C56	1.509 (3)	C43A C50A	1.523 (3)
C41	C42	1.393 (3)	C44A C45A	1.384 (4)
C42	C57	1.526 (3)	C44A C49A	1.393 (4)
C43	C44	1.525 (3)	C45A C46A	1.396 (4)
C43	C50	1.526 (3)	C46A C47A	1.381 (4)
C44	C45	1.387 (3)	C47A C48A	1.384 (4)
C44	C49	1.390 (4)	C48A C49A	1.380 (4)
C45	C46	1.391 (4)	C50A C51A	1.387 (4)
C46	C47	1.370 (4)	C50A C55A	1.393 (4)
C47	C48	1.380 (4)	C51A C52A	1.392 (4)
C48	C49	1.378 (4)	C52A C53A	1.374 (5)
C50	C51	1.385 (3)	C53A C54A	1.371 (5)
C50	C55	1.392 (3)	C54A C55A	1.381 (4)
C51	C52	1.386 (3)	C57A C58A	1.529 (3)
C52	C53	1.377 (4)	C57A C64A	1.525 (3)
C53	C54	1.382 (4)	C58A C59A	1.386 (4)
C54	C55	1.391 (4)	C58A C63A	1.390 (3)
C57	C58	1.531 (3)	C59A C60A	1.387 (4)
C57	C64	1.537 (3)	C60A C61A	1.383 (4)
C58	C59	1.382 (3)	C61A C62A	1.380 (4)
C58	C63	1.395 (3)	C62A C63A	1.390 (4)
C59	C60	1.390 (4)	C64A C65A	1.387 (3)
C60	C61	1.378 (4)	C64A C69A	1.394 (3)
C61	C62	1.380 (4)	C65A C66A	1.382 (4)
C62	C63	1.377 (3)	C66A C67A	1.378 (4)
C64	C65	1.393 (3)	C67A C68A	1.381 (4)
C64	C69	1.391 (3)	C68A C69A	1.386 (4)
C65	C66	1.379 (4)	C70A C71A	1.530 (4)
C66	C67	1.385 (4)	C70A C75A	1.518 (4)

C67	C68	1.376 (4)	C71A C72A	1.517 (4)
C68	C69	1.393 (3)	C72A C73A	1.499 (5)
C70	C71	1.531 (4)	C73A C74A	1.522 (4)
C70	C75	1.534 (3)	C74A C75A	1.533 (4)
C71	C72	1.535 (4)	C76A C77A	1.538 (3)
C72	C73	1.519 (4)	C76A C81A	1.538 (3)
C73	C74	1.511 (4)	C77A C78A	1.530 (3)
C74	C75	1.520 (4)	C78A C79A	1.522 (3)
C76	C77	1.532 (4)	C79A C80A	1.518 (4)
C76	C81	1.533 (3)	C80A C81A	1.528 (3)
C77	C78	1.530 (4)	C82A C83A	1.525 (4)
C78	C79	1.525 (4)	C82A C87A	1.525 (3)
C79	C80	1.513 (4)	C83A C84A	1.524 (4)
C80	C81	1.528 (4)	C84A C85A	1.514 (4)
C82	C83	1.524 (4)	C85A C86A	1.509 (4)
C82	C87	1.531 (4)	C86A C87A	1.522 (4)
C83	C84	1.526 (4)	C88 C89	1.394 (4)
C84	C85	1.523 (4)	C88 C93	1.390 (4)
C85	C86	1.515 (4)	C88 C94	1.494 (4)
C86	C87	1.525 (4)	C89 C90	1.388 (4)
Ni1A	Cl1A	2.1583 (9)	C90 C91	1.390 (4)
Ni1A	Cl2A	2.1726 (9)	C91 C92	1.382 (4)
Ni1A	P1A	2.2674 (10)	C91 C95	1.512 (4)
Ni1A	C1A	1.915 (2)	C92 C93	1.386 (4)

Table 5 Bond Angles for Schomaker59_sq.

Atom Atom Atom	Angle/°	Atom Atom Atom	Angle/°
Cl1 Ni1 Cl2	175.93 (3)	C1A Ni1A P1A	173.08 (7)
Cl1 Ni1 P1	92.36 (3)	C70A P1A Ni1A	114.33 (9)
Cl2 Ni1 P1	90.65 (3)	C76A P1A Ni1A	111.29 (8)
C1 Ni1 Cl1	88.67 (7)	C76A P1A C70A	110.21 (12)
C1 Ni1 Cl2	88.28 (7)	C82A P1A Ni1A	112.03 (9)
C1 Ni1 P1	178.71 (7)	C82A P1A C70A	102.56 (12)
C70 P1 Ni1	114.74 (8)	C82A P1A C76A	105.77 (11)
C76 P1 Ni1	112.51 (8)	C1A N1A C2A	110.83 (19)

C76	P1	C70	110.69 (12)	C1A	N1A	C4A	122.3 (2)
C76	P1	C82	104.32 (12)	C2A	N1A	C4A	126.5 (2)
C82	P1	Ni1	110.72 (8)	C1A	N2A	C3A	110.80 (19)
C82	P1	C70	102.92 (12)	C1A	N2A	C37A	124.0 (2)
C1	N1	C2	110.55 (19)	C3A	N2A	C37A	125.08 (19)
C1	N1	C4	122.32 (18)	N1A	C1A	Ni1A	124.83 (16)
C2	N1	C4	126.90 (19)	N2A	C1A	Ni1A	131.13 (18)
C1	N2	C3	109.93 (19)	N2A	C1A	N1A	104.0 (2)
C1	N2	C37	123.47 (18)	C3A	C2A	N1A	106.8 (2)
C3	N2	C37	126.54 (18)	C2A	C3A	N2A	107.5 (2)
N1	C1	Ni1	127.34 (17)	C5A	C4A	N1A	120.7 (2)
N1	C1	N2	105.20 (19)	C5A	C4A	C9A	121.3 (2)
N2	C1	Ni1	127.46 (17)	C9A	C4A	N1A	118.0 (2)
C3	C2	N1	107.1 (2)	C4A	C5A	C10A	121.7 (2)
C2	C3	N2	107.2 (2)	C6A	C5A	C4A	117.5 (2)
C5	C4	N1	118.4 (2)	C6A	C5A	C10A	120.8 (2)
C9	C4	N1	120.2 (2)	C7A	C6A	C5A	122.2 (2)
C9	C4	C5	121.3 (2)	C6A	C7A	C8A	118.9 (2)
C4	C5	C10	121.6 (2)	C6A	C7A	C23A	119.7 (2)
C6	C5	C4	117.6 (2)	C8A	C7A	C23A	121.3 (2)
C6	C5	C10	120.6 (2)	C7A	C8A	C9A	121.4 (2)
C7	C6	C5	122.3 (2)	C4A	C9A	C24A	120.5 (2)
C6	C7	C23	120.7 (2)	C8A	C9A	C4A	118.1 (2)
C8	C7	C6	117.8 (2)	C8A	C9A	C24A	120.8 (2)
C8	C7	C23	121.4 (2)	C5A	C10A	C17A	113.17 (19)
C7	C8	C9	122.7 (2)	C11A	C10A	C5A	112.5 (2)
C4	C9	C24	122.2 (2)	C11A	C10A	C17A	110.0 (2)
C8	C9	C4	117.4 (2)	C12A	C11A	C10A	117.9 (2)
C8	C9	C24	120.3 (2)	C16A	C11A	C10A	124.3 (2)
C11	C10	C5	109.62 (19)	C16A	C11A	C12A	117.8 (2)
C11	C10	C17	111.9 (2)	C13A	C12A	C11A	121.6 (3)
C17	C10	C5	113.05 (19)	C12A	C13A	C14A	119.7 (3)
C12	C11	C10	120.1 (2)	C15A	C14A	C13A	120.0 (3)
C16	C11	C10	121.8 (2)	C14A	C15A	C16A	120.0 (3)
C16	C11	C12	118.1 (2)	C11A	C16A	C15A	121.0 (2)
C13	C12	C11	121.0 (3)	C18A	C17A	C10A	120.9 (2)
C14	C13	C12	120.2 (3)	C22A	C17A	C10A	120.5 (2)

C15	C14	C13	119.5 (3)	C22A C17A C18A	118.6 (2)
C14	C15	C16	120.3 (3)	C19A C18A C17A	120.5 (2)
C11	C16	C15	120.9 (3)	C20A C19A C18A	120.0 (3)
C18	C17	C10	122.5 (2)	C21A C20A C19A	119.8 (3)
C18	C17	C22	118.2 (2)	C20A C21A C22A	120.1 (3)
C22	C17	C10	119.3 (2)	C17A C22A C21A	120.8 (2)
C17	C18	C19	121.0 (3)	C25A C24A C9A	109.0 (2)
C20	C19	C18	120.1 (3)	C25A C24A C31A	112.0 (2)
C19	C20	C21	119.7 (3)	C31A C24A C9A	113.5 (2)
C20	C21	C22	120.5 (3)	C26A C25A C24A	122.3 (2)
C21	C22	C17	120.5 (3)	C30A C25A C24A	119.9 (2)
C9	C24	C31	112.87 (19)	C30A C25A C26A	117.9 (3)
C25	C24	C9	112.6 (2)	C27A C26A C25A	121.1 (2)
C25	C24	C31	109.56 (19)	C26A C27A C28A	120.4 (3)
C26	C25	C24	123.9 (2)	C29A C28A C27A	119.2 (3)
C26	C25	C30	118.3 (2)	C28A C29A C30A	120.6 (3)
C30	C25	C24	117.7 (2)	C25A C30A C29A	120.9 (3)
C25	C26	C27	120.5 (3)	C32A C31A C24A	122.1 (3)
C28	C27	C26	119.8 (3)	C36A C31A C24A	120.1 (2)
C29	C28	C27	120.2 (3)	C36A C31A C32A	117.8 (3)
C28	C29	C30	120.0 (3)	C31A C32A C33A	120.6 (3)
C29	C30	C25	121.3 (3)	C34A C33A C32A	120.6 (3)
C32	C31	C24	121.5 (2)	C33A C34A C35A	119.7 (3)
C36	C31	C24	120.4 (2)	C34A C35A C36A	120.0 (3)
C36	C31	C32	118.1 (2)	C31A C36A C35A	121.3 (3)
C33	C32	C31	121.0 (2)	C38A C37A N2A	118.7 (2)
C34	C33	C32	120.4 (2)	C38A C37A C42A	122.1 (2)
C33	C34	C35	119.3 (2)	C42A C37A N2A	119.1 (2)
C34	C35	C36	120.3 (2)	C37A C38A C39A	117.0 (2)
C31	C36	C35	120.8 (2)	C37A C38A C43A	121.8 (2)
C38	C37	N2	118.5 (2)	C39A C38A C43A	120.9 (2)
C42	C37	N2	120.4 (2)	C40A C39A C38A	122.3 (2)
C42	C37	C38	121.1 (2)	C39A C40A C41A	118.7 (2)
C37	C38	C43	121.3 (2)	C39A C40A C56A	120.5 (2)
C39	C38	C37	118.0 (2)	C41A C40A C56A	120.8 (2)
C39	C38	C43	120.6 (2)	C40A C41A C42A	121.3 (2)
C40	C39	C38	122.1 (2)	C37A C42A C57A	119.7 (2)

C39	C40	C56	120.5 (2)	C41A C42A C37A	118.2 (2)
C41	C40	C39	118.2 (2)	C41A C42A C57A	121.7 (2)
C41	C40	C56	121.3 (2)	C38A C43A C44A	111.9 (2)
C40	C41	C42	122.4 (2)	C50A C43A C38A	114.4 (2)
C37	C42	C57	121.8 (2)	C50A C43A C44A	109.41 (19)
C41	C42	C37	117.8 (2)	C45A C44A C43A	123.3 (2)
C41	C42	C57	119.9 (2)	C45A C44A C49A	118.2 (2)
C44	C43	C38	110.71 (19)	C49A C44A C43A	118.4 (2)
C44	C43	C50	112.6 (2)	C44A C45A C46A	120.4 (3)
C50	C43	C38	112.9 (2)	C47A C46A C45A	120.8 (3)
C45	C44	C43	122.8 (2)	C46A C47A C48A	119.0 (3)
C45	C44	C49	118.0 (2)	C49A C48A C47A	120.3 (3)
C49	C44	C43	119.2 (2)	C48A C49A C44A	121.3 (3)
C44	C45	C46	120.7 (3)	C51A C50A C43A	120.9 (2)
C47	C46	C45	120.2 (3)	C51A C50A C55A	118.4 (2)
C46	C47	C48	119.9 (3)	C55A C50A C43A	120.7 (2)
C49	C48	C47	119.8 (3)	C50A C51A C52A	119.9 (3)
C48	C49	C44	121.3 (3)	C53A C52A C51A	120.6 (3)
C51	C50	C43	119.2 (2)	C54A C53A C52A	120.0 (3)
C51	C50	C55	118.3 (2)	C53A C54A C55A	119.8 (3)
C55	C50	C43	122.5 (2)	C54A C55A C50A	121.2 (3)
C50	C51	C52	121.1 (2)	C58A C57A C42A	113.1 (2)
C53	C52	C51	120.1 (2)	C64A C57A C42A	109.42 (19)
C52	C53	C54	119.8 (2)	C64A C57A C58A	113.3 (2)
C53	C54	C55	119.9 (2)	C59A C58A C57A	118.9 (2)
C54	C55	C50	120.8 (2)	C59A C58A C63A	118.2 (2)
C42	C57	C58	113.8 (2)	C63A C58A C57A	122.9 (2)
C42	C57	C64	110.50 (19)	C58A C59A C60A	121.2 (3)
C58	C57	C64	108.55 (19)	C61A C60A C59A	120.1 (3)
C59	C58	C57	121.8 (2)	C62A C61A C60A	119.3 (3)
C59	C58	C63	117.6 (2)	C61A C62A C63A	120.5 (3)
C63	C58	C57	120.7 (2)	C62A C63A C58A	120.7 (3)
C58	C59	C60	120.9 (3)	C65A C64A C57A	120.7 (2)
C61	C60	C59	120.6 (3)	C65A C64A C69A	118.4 (2)
C60	C61	C62	119.0 (2)	C69A C64A C57A	120.9 (2)
C63	C62	C61	120.3 (2)	C66A C65A C64A	121.1 (2)
C62	C63	C58	121.6 (2)	C67A C66A C65A	120.1 (3)

C65 C64 C57	118.5 (2)	C66A C67A C68A	119.7 (3)
C69 C64 C57	123.3 (2)	C67A C68A C69A	120.2 (2)
C69 C64 C65	118.0 (2)	C68A C69A C64A	120.5 (2)
C66 C65 C64	121.1 (3)	C71A C70A P1A	111.31 (18)
C65 C66 C67	120.4 (3)	C75A C70A P1A	118.00 (19)
C68 C67 C66	119.3 (2)	C75A C70A C71A	110.7 (2)
C67 C68 C69	120.5 (3)	C72A C71A C70A	110.9 (2)
C64 C69 C68	120.7 (2)	C73A C72A C71A	111.7 (3)
C71 C70 P1	113.09 (18)	C72A C73A C74A	110.8 (3)
C71 C70 C75	110.2 (2)	C73A C74A C75A	111.6 (3)
C75 C70 P1	118.96 (18)	C70A C75A C74A	111.6 (2)
C70 C71 C72	110.7 (2)	C77A C76A P1A	112.59 (17)
C73 C72 C71	111.4 (2)	C81A C76A P1A	116.47 (17)
C74 C73 C72	111.4 (2)	C81A C76A C77A	110.8 (2)
C73 C74 C75	112.1 (2)	C78A C77A C76A	109.9 (2)
C74 C75 C70	110.7 (2)	C79A C78A C77A	110.8 (2)
C77 C76 P1	113.68 (17)	C80A C79A C78A	111.1 (2)
C77 C76 C81	111.4 (2)	C79A C80A C81A	111.5 (2)
C81 C76 P1	115.57 (18)	C80A C81A C76A	110.4 (2)
C78 C77 C76	110.1 (2)	C83A C82A P1A	116.67 (18)
C79 C78 C77	111.2 (2)	C87A C82A P1A	108.28 (18)
C80 C79 C78	111.8 (2)	C87A C82A C83A	110.9 (2)
C79 C80 C81	110.4 (2)	C84A C83A C82A	109.7 (2)
C80 C81 C76	109.9 (2)	C85A C84A C83A	112.8 (2)
C83 C82 P1	115.06 (18)	C86A C85A C84A	111.2 (2)
C83 C82 C87	110.0 (2)	C85A C86A C87A	111.2 (3)
C87 C82 P1	110.15 (18)	C86A C87A C82A	111.6 (2)
C82 C83 C84	110.2 (2)	C89 C88 C94	121.6 (3)
C85 C84 C83	111.0 (2)	C93 C88 C89	117.0 (3)
C86 C85 C84	111.3 (2)	C93 C88 C94	121.4 (3)
C85 C86 C87	111.4 (3)	C90 C89 C88	121.7 (3)
C86 C87 C82	111.1 (2)	C89 C90 C91	120.8 (3)
Cl1A Ni1A Cl2A	169.55 (3)	C90 C91 C95	121.0 (3)
Cl1A Ni1A P1A	93.75 (3)	C92 C91 C90	117.5 (3)
Cl2A Ni1A P1A	89.15 (3)	C92 C91 C95	121.5 (3)
C1A Ni1A Cl1A	88.63 (7)	C91 C92 C93	121.8 (3)
C1A Ni1A Cl2A	89.65 (7)	C92 C93 C88	121.1 (3)

Table 6 Torsion Angles for Schomaker59_sq.

A	B	C	D	Angle/°	A	B	C	D	Angle/°
Ni1	P1	C70	C71	71.01 (19)	Ni1A	P1A	C82A	C87A	47.3 (2)
Ni1	P1	C70	C75	-157.38 (18)	P1A	C70A	C71A	C72A	-171.2 (2)
Ni1	P1	C76	C77	-52.33 (19)	P1A	C70A	C75A	C74A	176.0 (2)
Ni1	P1	C76	C81	176.94 (16)	P1A	C76A	C77A	C78A	170.23 (17)
Ni1	P1	C82	C83	-70.82 (19)	P1A	C76A	C81A	C80A	-173.29 (17)
Ni1	P1	C82	C87	54.23 (19)	P1A	C82A	C83A	C84A	-179.8 (2)
P1	C70	C71	C72	-167.43 (18)	P1A	C82A	C87A	C86A	174.4 (2)
P1	C70	C75	C74	170.4 (2)	N1A	C2A	C3A	N2A	-0.1 (3)
P1	C76	C77	C78	171.01 (17)	N1A	C4A	C5A	C6A	174.3 (2)
P1	C76	C81	C80	-170.38 (18)	N1A	C4A	C5A	C10A	-8.6 (4)
P1	C82	C83	C84	-176.68 (18)	N1A	C4A	C9A	C8A	-172.6 (2)
P1	C82	C87	C86	175.1 (2)	N1A	C4A	C9A	C24A	16.0 (3)
N1	C2	C3	N2	0.0 (3)	N2A	C37A	C38A	C39A	175.4 (2)
N1	C4	C5	C6	171.6 (2)	N2A	C37A	C38A	C43A	-10.9 (3)
N1	C4	C5	C10	-14.4 (3)	N2A	C37A	C42A	C41A	-175.3 (2)
N1	C4	C9	C8	-171.4 (2)	N2A	C37A	C42A	C57A	11.9 (3)
N1	C4	C9	C24	12.5 (3)	C1A	N1A	C2A	C3A	0.3 (3)
N2	C37	C38	C39	175.69 (19)	C1A	N1A	C4A	C5A	-98.7 (3)
N2	C37	C38	C43	-8.7 (3)	C1A	N1A	C4A	C9A	82.0 (3)
N2	C37	C42	C41	-173.86 (19)	C1A	N2A	C3A	C2A	-0.1 (3)
N2	C37	C42	C57	13.9 (3)	C1A	N2A	C37A	C38A	-100.0 (3)
C1	N1	C2	C3	0.1 (3)	C1A	N2A	C37A	C42A	82.6 (3)
C1	N1	C4	C5	-87.6 (3)	C2A	N1A	C1A	Ni1A	179.82 (16)
C1	N1	C4	C9	92.5 (3)	C2A	N1A	C1A	N2A	-0.3 (3)
C1	N2	C3	C2	0.0 (3)	C2A	N1A	C4A	C5A	89.2 (3)
C1	N2	C37	C38	-90.1 (3)	C2A	N1A	C4A	C9A	-90.0 (3)
C1	N2	C37	C42	91.6 (3)	C3A	N2A	C1A	Ni1A	-179.90 (18)
C2	N1	C1	Ni1	178.92 (16)	C3A	N2A	C1A	N1A	0.2 (3)
C2	N1	C1	N2	-0.1 (2)	C3A	N2A	C37A	C38A	76.3 (3)
C2	N1	C4	C5	86.4 (3)	C3A	N2A	C37A	C42A	-101.1 (3)
C2	N1	C4	C9	-93.4 (3)	C4A	N1A	C1A	Ni1A	6.7 (3)
C3	N2	C1	Ni1	-178.92 (16)	C4A	N1A	C1A	N2A	-173.5 (2)
C3	N2	C1	N1	0.1 (2)	C4A	N1A	C2A	C3A	173.1 (2)

C3	N2	C37	C38	86.9 (3)	C4A	C5A	C6A	C7A	0.2 (4)
C3	N2	C37	C42	-91.4 (3)	C4A	C5A	C10A	C11A	-74.7 (3)
C4	N1	C1	Ni1	-6.2 (3)	C4A	C5A	C10A	C17A	159.9 (2)
C4	N1	C1	N2	174.82 (19)	C4A	C9A	C24A	C25A	67.5 (3)
C4	N1	C2	C3	-174.6 (2)	C4A	C9A	C24A	C31A	-166.9 (2)
C4	C5	C6	C7	1.5 (4)	C5A	C4A	C9A	C8A	8.2 (4)
C4	C5	C10	C11	-65.1 (3)	C5A	C4A	C9A	C24A	-163.2 (2)
C4	C5	C10	C17	169.2 (2)	C5A	C6A	C7A	C8A	4.3 (4)
C4	C9	C24	C25	70.7 (3)	C5A	C6A	C7A	C23A	-174.4 (2)
C4	C9	C24	C31	-164.7 (2)	C5A	C10A	C11A	C12A	177.6 (2)
C5	C4	C9	C8	8.7 (3)	C5A	C10A	C11A	C16A	-1.8 (3)
C5	C4	C9	C24	-167.3 (2)	C5A	C10A	C17A	C18A	77.1 (3)
C5	C6	C7	C8	5.1 (4)	C5A	C10A	C17A	C22A	-104.3 (3)
C5	C6	C7	C23	-176.3 (2)	C6A	C5A	C10A	C11A	102.2 (3)
C5	C10	C11	C12	141.0 (2)	C6A	C5A	C10A	C17A	-23.1 (3)
C5	C10	C11	C16	-39.3 (3)	C6A	C7A	C8A	C9A	-2.5 (4)
C5	C10	C17	C18	108.6 (3)	C7A	C8A	C9A	C4A	-3.6 (4)
C5	C10	C17	C22	-71.0 (3)	C7A	C8A	C9A	C24A	167.8 (2)
C6	C5	C10	C11	108.7 (3)	C8A	C9A	C24A	C25A	-103.6 (3)
C6	C5	C10	C17	-16.9 (3)	C8A	C9A	C24A	C31A	22.0 (3)
C6	C7	C8	C9	-5.0 (4)	C9A	C4A	C5A	C6A	-6.5 (4)
C7	C8	C9	C4	-1.8 (4)	C9A	C4A	C5A	C10A	170.6 (2)
C7	C8	C9	C24	174.3 (2)	C9A	C24A	C25A	C26A	34.4 (3)
C8	C9	C24	C25	-105.2 (3)	C9A	C24A	C25A	C30A	-145.3 (2)
C8	C9	C24	C31	19.4 (3)	C9A	C24A	C31A	C32A	-100.3 (3)
C9	C4	C5	C6	-8.6 (3)	C9A	C24A	C31A	C36A	79.9 (3)
C9	C4	C5	C10	165.4 (2)	C10A	C5A	C6A	C7A	-176.9 (2)
C9	C24	C25	C26	14.9 (3)	C10A	C11A	C12A	C13A	-177.0 (2)
C9	C24	C25	C30	-170.1 (2)	C10A	C11A	C16A	C15A	176.2 (2)
C9	C24	C31	C32	-96.6 (3)	C10A	C17A	C18A	C19A	-177.6 (2)
C9	C24	C31	C36	83.1 (3)	C10A	C17A	C22A	C21A	179.6 (2)
C10	C5	C6	C7	-172.6 (2)	C11A	C10A	C17A	C18A	-49.6 (3)
C10	C11	C12	C13	-179.3 (2)	C11A	C10A	C17A	C22A	128.9 (2)
C10	C11	C16	C15	179.5 (2)	C11A	C12A	C13A	C14A	-0.3 (4)
C10	C17	C18	C19	-179.8 (2)	C12A	C11A	C16A	C15A	-3.2 (4)
C10	C17	C22	C21	179.1 (2)	C12A	C13A	C14A	C15A	-1.2 (4)
C11	C10	C17	C18	-15.7 (3)	C13A	C14A	C15A	C16A	0.5 (4)

C11 C10 C17 C22	164.7 (2)	C14A C15A	C16A C11A	1.8 (4)
C11 C12 C13 C14	-0.4 (4)	C16A C11A	C12A C13A	2.5 (4)
C12 C11 C16 C15	-0.7 (4)	C17A C10A	C11A C12A	-55.3 (3)
C12 C13 C14 C15	-0.3 (4)	C17A C10A	C11A C16A	125.3 (2)
C13 C14 C15 C16	0.5 (4)	C17A C18A	C19A C20A	-2.9 (4)
C14 C15 C16 C11	0.0 (4)	C18A C17A	C22A C21A	-1.8 (4)
C16 C11 C12 C13	0.9 (4)	C18A C19A	C20A C21A	-0.2 (4)
C17 C10 C11 C12	-92.7 (3)	C19A C20A	C21A C22A	2.3 (4)
C17 C10 C11 C16	87.0 (3)	C20A C21A	C22A C17A	-1.3 (4)
C17 C18 C19 C20	0.6 (4)	C22A C17A	C18A C19A	3.8 (4)
C18 C17 C22 C21	-0.5 (4)	C23A C7A	C8A C9A	176.2 (2)
C18 C19 C20 C21	-0.4 (4)	C24A C25A	C26A C27A	-178.7 (2)
C19 C20 C21 C22	-0.3 (4)	C24A C25A	C30A C29A	178.5 (2)
C20 C21 C22 C17	0.8 (4)	C24A C31A	C32A C33A	179.2 (3)
C22 C17 C18 C19	-0.2 (4)	C24A C31A	C36A C35A	-179.1 (3)
C23 C7 C8 C9	176.5 (2)	C25A C24A	C31A C32A	23.7 (3)
C24 C25 C26 C27	175.8 (2)	C25A C24A	C31A C36A	-156.1 (2)
C24 C25 C30 C29	-175.3 (2)	C25A C26A	C27A C28A	0.1 (4)
C24 C31 C32 C33	-179.2 (2)	C26A C25A	C30A C29A	-1.2 (4)
C24 C31 C36 C35	179.5 (2)	C26A C27A	C28A C29A	-1.0 (4)
C25 C24 C31 C32	29.7 (3)	C27A C28A	C29A C30A	0.8 (4)
C25 C24 C31 C36	-150.6 (2)	C28A C29A	C30A C25A	0.3 (4)
C25 C26 C27 C28	-0.9 (4)	C30A C25A	C26A C27A	1.0 (4)
C26 C25 C30 C29	0.0 (4)	C31A C24A	C25A C26A	-92.0 (3)
C26 C27 C28 C29	0.4 (4)	C31A C24A	C25A C30A	88.3 (3)
C27 C28 C29 C30	0.4 (4)	C31A C32A	C33A C34A	0.3 (5)
C28 C29 C30 C25	-0.6 (4)	C32A C31A	C36A C35A	1.1 (4)
C30 C25 C26 C27	0.7 (4)	C32A C33A	C34A C35A	0.4 (5)
C31 C24 C25 C26	-111.6 (3)	C33A C34A	C35A C36A	-0.4 (5)
C31 C24 C25 C30	63.5 (3)	C34A C35A	C36A C31A	-0.4 (5)
C31 C32 C33 C34	-0.3 (4)	C36A C31A	C32A C33A	-1.0 (5)
C32 C31 C36 C35	-0.9 (4)	C37A N2A	C1A Ni1A	-3.1 (3)
C32 C33 C34 C35	-0.8 (4)	C37A N2A	C1A N1A	177.0 (2)
C33 C34 C35 C36	1.1 (4)	C37A N2A	C3A C2A	-176.8 (2)
C34 C35 C36 C31	-0.3 (4)	C37A C38A	C39A C40A	1.6 (4)
C36 C31 C32 C33	1.2 (4)	C37A C38A	C43A C44A	-84.2 (3)
C37 N2 C1 Ni1	-1.5 (3)	C37A C38A	C43A C50A	150.6 (2)

C37 N2 C1 N1	177.54 (19)	C37A C42A	C57A C58A	-168.7 (2)
C37 N2 C3 C2	-177.4 (2)	C37A C42A	C57A C64A	63.9 (3)
C37 C38 C39 C40	0.1 (3)	C38A C37A	C42A C41A	7.4 (4)
C37 C38 C43 C44	-68.5 (3)	C38A C37A	C42A C57A	-165.4 (2)
C37 C38 C43 C50	164.3 (2)	C38A C39A	C40A C41A	3.6 (4)
C37 C42 C57 C58	-165.2 (2)	C38A C39A	C40A C56A	-177.7 (2)
C37 C42 C57 C64	72.3 (3)	C38A C43A	C44A C45A	-3.2 (3)
C38 C37 C42 C41	7.9 (3)	C38A C43A	C44A C49A	177.5 (2)
C38 C37 C42 C57	-164.4 (2)	C38A C43A	C50A C51A	-103.8 (3)
C38 C39 C40 C41	3.6 (4)	C38A C43A	C50A C55A	76.8 (3)
C38 C39 C40 C56	-178.0 (2)	C39A C38A	C43A C44A	89.2 (3)
C38 C43 C44 C45	-32.0 (3)	C39A C38A	C43A C50A	-35.9 (3)
C38 C43 C44 C49	147.9 (2)	C39A C40A	C41A C42A	-3.5 (4)
C38 C43 C50 C51	-62.5 (3)	C40A C41A	C42A C37A	-1.8 (4)
C38 C43 C50 C55	118.8 (3)	C40A C41A	C42A C57A	170.8 (2)
C39 C38 C43 C44	107.0 (2)	C41A C42A	C57A C58A	18.8 (3)
C39 C38 C43 C50	-20.2 (3)	C41A C42A	C57A C64A	-108.6 (2)
C39 C40 C41 C42	-1.6 (3)	C42A C37A	C38A C39A	-7.2 (3)
C40 C41 C42 C37	-4.0 (3)	C42A C37A	C38A C43A	166.5 (2)
C40 C41 C42 C57	168.4 (2)	C42A C57A	C58A C59A	68.6 (3)
C41 C42 C57 C58	22.7 (3)	C42A C57A	C58A C63A	-113.3 (3)
C41 C42 C57 C64	-99.8 (2)	C42A C57A	C64A C65A	-135.7 (2)
C42 C37 C38 C39	-6.0 (3)	C42A C57A	C64A C69A	44.3 (3)
C42 C37 C38 C43	169.6 (2)	C43A C38A	C39A C40A	-172.1 (2)
C42 C57 C58 C59	97.4 (3)	C43A C44A	C45A C46A	-179.8 (2)
C42 C57 C58 C63	-83.5 (3)	C43A C44A	C49A C48A	179.5 (2)
C42 C57 C64 C65	-170.4 (2)	C43A C50A	C51A C52A	178.7 (3)
C42 C57 C64 C69	13.5 (3)	C43A C50A	C55A C54A	-177.6 (2)
C43 C38 C39 C40	-175.5 (2)	C44A C43A	C50A C51A	129.7 (2)
C43 C44 C45 C46	178.3 (2)	C44A C43A	C50A C55A	-49.6 (3)
C43 C44 C49 C48	-179.4 (2)	C44A C45A	C46A C47A	0.6 (4)
C43 C50 C51 C52	179.8 (2)	C45A C44A	C49A C48A	0.1 (4)
C43 C50 C55 C54	179.3 (2)	C45A C46A	C47A C48A	-0.5 (4)
C44 C43 C50 C51	171.3 (2)	C46A C47A	C48A C49A	0.1 (4)
C44 C43 C50 C55	-7.5 (3)	C47A C48A	C49A C44A	0.0 (4)
C44 C45 C46 C47	1.5 (4)	C49A C44A	C45A C46A	-0.5 (4)
C45 C44 C49 C48	0.5 (4)	C50A C43A	C44A C45A	124.7 (2)

C45 C46 C47 C48	-0.3 (4)	C50A C43A	C44A C49A	-54.7 (3)
C46 C47 C48 C49	-0.8 (5)	C50A C51A	C52A C53A	-0.5 (5)
C47 C48 C49 C44	0.7 (4)	C51A C50A	C55A C54A	3.0 (4)
C49 C44 C45 C46	-1.6 (4)	C51A C52A	C53A C54A	1.8 (5)
C50 C43 C44 C45	95.4 (3)	C52A C53A	C54A C55A	-0.7 (5)
C50 C43 C44 C49	-84.7 (3)	C53A C54A	C55A C50A	-1.8 (4)
C50 C51 C52 C53	1.1 (4)	C55A C50A	C51A C52A	-1.9 (4)
C51 C50 C55 C54	0.6 (4)	C56A C40A	C41A C42A	177.8 (2)
C51 C52 C53 C54	0.2 (4)	C57A C58A	C59A C60A	179.2 (2)
C52 C53 C54 C55	-1.1 (4)	C57A C58A	C63A C62A	-178.0 (2)
C53 C54 C55 C50	0.6 (4)	C57A C64A	C65A C66A	-179.1 (2)
C55 C50 C51 C52	-1.4 (4)	C57A C64A	C69A C68A	178.9 (2)
C56 C40 C41 C42	-179.9 (2)	C58A C57A	C64A C65A	97.0 (3)
C57 C58 C59 C60	179.2 (3)	C58A C57A	C64A C69A	-83.0 (3)
C57 C58 C63 C62	-179.4 (2)	C58A C59A	C60A C61A	-1.3 (4)
C57 C64 C65 C66	-176.1 (2)	C59A C58A	C63A C62A	0.0 (4)
C57 C64 C69 C68	175.7 (2)	C59A C60A	C61A C62A	0.4 (4)
C58 C57 C64 C65	64.1 (3)	C60A C61A	C62A C63A	0.8 (4)
C58 C57 C64 C69	-112.0 (2)	C61A C62A	C63A C58A	-1.0 (4)
C58 C59 C60 C61	0.2 (5)	C63A C58A	C59A C60A	1.1 (4)
C59 C58 C63 C62	-0.2 (4)	C64A C57A	C58A C59A	-166.1 (2)
C59 C60 C61 C62	-0.2 (4)	C64A C57A	C58A C63A	11.9 (3)
C60 C61 C62 C63	0.0 (4)	C64A C65A	C66A C67A	-0.2 (4)
C61 C62 C63 C58	0.2 (4)	C65A C64A	C69A C68A	-1.1 (4)
C63 C58 C59 C60	0.0 (4)	C65A C66A	C67A C68A	-0.4 (4)
C64 C57 C58 C59	-139.1 (2)	C66A C67A	C68A C69A	0.3 (4)
C64 C57 C58 C63	40.0 (3)	C67A C68A	C69A C64A	0.5 (4)
C64 C65 C66 C67	0.6 (4)	C69A C64A	C65A C66A	0.9 (4)
C65 C64 C69 C68	-0.4 (4)	C70A P1A	C76A C77A	82.9 (2)
C65 C66 C67 C68	-1.1 (4)	C70A P1A	C76A C81A	-46.6 (2)
C66 C67 C68 C69	0.9 (4)	C70A P1A	C82A C83A	158.3 (2)
C67 C68 C69 C64	-0.1 (4)	C70A P1A	C82A C87A	-75.8 (2)
C69 C64 C65 C66	0.2 (4)	C70A C71A	C72A C73A	-57.3 (3)
C70 P1 C76 C77	77.5 (2)	C71A C70A	C75A C74A	-54.1 (3)
C70 P1 C76 C81	-53.2 (2)	C71A C72A	C73A C74A	56.7 (4)
C70 P1 C82 C83	166.09 (19)	C72A C73A	C74A C75A	-54.9 (4)
C70 P1 C82 C87	-68.9 (2)	C73A C74A	C75A C70A	54.2 (3)

C70 C71 C72 C73	-55.9 (3)	C75A C70A	C71A C72A	55.5 (3)
C71 C70 C75 C74	-56.7 (3)	C76A P1A	C70A C71A	-54.7 (2)
C71 C72 C73 C74	54.5 (3)	C76A P1A	C70A C75A	74.9 (2)
C72 C73 C74 C75	-54.9 (3)	C76A P1A	C82A C83A	42.8 (2)
C73 C74 C75 C70	56.1 (3)	C76A P1A	C82A C87A	168.7 (2)
C75 C70 C71 C72	56.7 (3)	C76A C77A	C78A C79A	57.6 (3)
C76 P1 C70 C71	-57.7 (2)	C77A C76A	C81A C80A	56.3 (3)
C76 P1 C70 C75	74.0 (2)	C77A C78A	C79A C80A	-57.2 (3)
C76 P1 C82 C83	50.4 (2)	C78A C79A	C80A C81A	56.3 (3)
C76 P1 C82 C87	175.50 (18)	C79A C80A	C81A C76A	-55.7 (3)
C76 C77 C78 C79	54.6 (3)	C81A C76A	C77A C78A	-57.4 (3)
C77 C76 C81 C80	57.8 (3)	C82A P1A	C70A C71A	-166.92 (18)
C77 C78 C79 C80	-56.0 (3)	C82A P1A	C70A C75A	-37.4 (2)
C78 C79 C80 C81	57.2 (3)	C82A P1A	C76A C77A	-166.90 (18)
C79 C80 C81 C76	-57.6 (3)	C82A P1A	C76A C81A	63.6 (2)
C81 C76 C77 C78	-56.2 (3)	C82A C83A	C84A C85A	-55.7 (3)
C82 P1 C70 C71	-168.63 (18)	C83A C82A	C87A C86A	-56.4 (3)
C82 P1 C70 C75	-37.0 (2)	C83A C84A	C85A C86A	55.2 (4)
C82 P1 C76 C77	-172.40 (17)	C84A C85A	C86A C87A	-54.0 (4)
C82 P1 C76 C81	56.9 (2)	C85A C86A	C87A C82A	55.3 (4)
C82 C83 C84 C85	-57.8 (3)	C87A C82A	C83A C84A	55.6 (3)
C83 C82 C87 C86	-57.0 (3)	C88 C89	C90 C91	-0.7 (5)
C83 C84 C85 C86	55.9 (3)	C89 C88	C93 C92	0.7 (4)
C84 C85 C86 C87	-54.4 (3)	C89 C90	C91 C92	1.2 (4)
C85 C86 C87 C82	55.2 (3)	C89 C90	C91 C95	179.3 (3)
C87 C82 C83 C84	58.2 (3)	C90 C91	C92 C93	-0.8 (5)
Ni1AP1AC70AC71A	71.58 (19)	C91 C92	C93 C88	-0.2 (5)
Ni1AP1AC70AC75A	-158.86 (18)	C93 C88	C89 C90	-0.3 (4)
Ni1AP1AC76AC77A	-45.00 (19)	C94 C88	C89 C90	179.7 (3)
Ni1AP1AC76AC81A	-174.50 (16)	C94 C88	C93 C92	-179.2 (3)
Ni1AP1AC82AC83A	-78.6 (2)	C95 C91	C92 C93	-178.9 (3)

Table 7 Hydrogen Atom Coordinates ($\text{\AA}\times 10^4$) and Isotropic Displacement Parameters ($\text{\AA}^2\times 10^3$) for Schomaker59_sq.

Atom	x	y	z	U(eq)
------	---	---	---	-------

H2	2720	7922	8501	17
H3	1855	6898	8088	17
H6	4674	9346	7429	22
H8	2258	10017	8010	23
H10	3931	7862	7253	20
H12	4506	7223	7769	29
H13	4897	7037	8635	41
H14	5247	7822	9470	47
H15	5215	8795	9432	42
H16	4812	8984	8567	32
H18	6296	8532	7911	31
H19	7676	8719	7454	38
H20	7467	8676	6497	38
H21	5880	8435	5992	34
H22	4499	8227	6437	28
H23A	4044	10656	7967	43
H23B	3392	10476	7357	43
H23C	4502	10316	7411	43
H24	813	8720	7998	19
H26	2982	9234	8953	31
H27	3205	9167	9887	42
H28	1826	8930	10323	46
H29	238	8751	9832	45
H30	15	8797	8900	33
H32	1241	10111	9066	25
H33	326	10894	9109	29
H34	-801	10881	8337	31
H35	-979	10083	7509	35
H36	-74	9292	7467	29
H39	-1431	6044	6570	20
H41	994	5483	5891	19
H43	-315	7393	7487	20
H45	-256	5968	7719	28
H46	233	5828	8598	39
H47	401	6618	9421	46
H48	98	7556	9369	42
H49	-338	7705	8494	31

H51	-1647	7263	6626	25
H52	-3351	7219	6385	29
H53	-4476	6892	6929	28
H54	-3892	6612	7722	30
H55	-2184	6633	7952	24
H56A	-580	4993	5423	39
H56B	-1495	5366	5517	39
H56C	-1299	4919	5886	39
H57	2798	6612	6726	18
H59	3294	6477	5784	35
H60	3879	5883	4992	43
H61	3763	4856	4836	31
H62	3063	4427	5486	24
H63	2488	5017	6276	22
H65	4238	6188	7158	26
H66	4762	5799	7883	32
H67	3600	5319	8312	32
H68	1908	5264	8028	27
H69	1372	5660	7302	22
H70	-547	8452	5999	25
H71A	802	9409	5890	29
H71B	731	9232	6469	29
H72A	-921	9446	6490	41
H72B	-228	10019	6441	41
H73A	-1727	9798	5798	47
H73B	-762	9785	5468	47
H74A	-1911	8951	4988	40
H74B	-1995	8762	5559	40
H75A	-268	8738	4971	34
H75B	-974	8162	5006	34
H76	2366	7991	5335	23
H77A	2342	9213	5915	27
H77B	2844	8755	6189	27
H78A	4054	9327	5825	34
H78B	4002	8627	5526	34
H79A	3084	9439	5035	33
H79B	4020	9125	4821	33

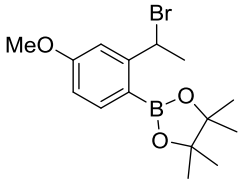
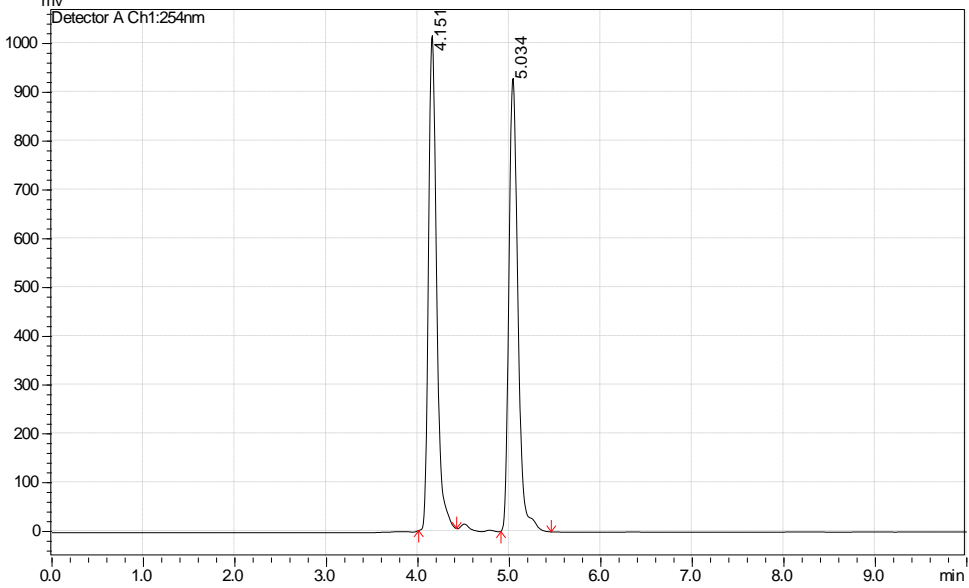
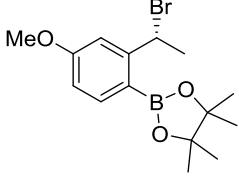
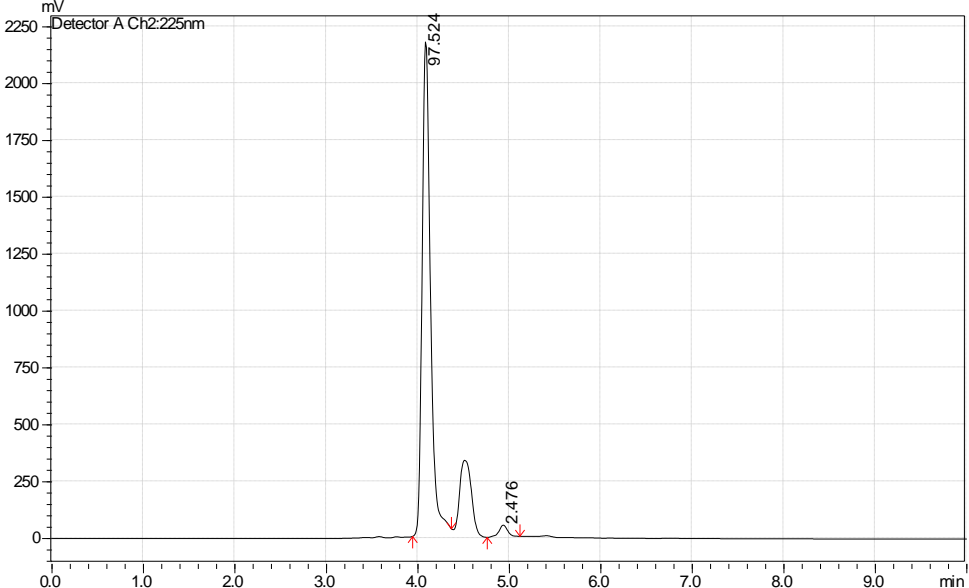
H80A	3024	8190	4510	33
H80B	2541	8640	4218	33
H81A	1291	8100	4577	28
H81B	1380	8800	4889	28
H82	-5	7520	4849	25
H83A	1249	6792	5260	31
H83B	1523	7129	4799	31
H84A	146	6558	4155	41
H84B	840	6119	4337	41
H85A	-872	5798	4370	47
H85B	-241	5940	4983	47
H86A	-1702	6369	5100	51
H86B	-1490	6706	4632	51
H87A	-345	6966	5727	36
H87B	-1053	7394	5535	36
H2A	6021	8400	2692	20
H3A	4561	8705	2247	19
H6A	6584	6786	3834	20
H8A	7023	6141	2198	24
H10A	4856	7720	3650	20
H12A	5332	8678	4537	30
H13A	6172	9636	4756	37
H14A	7533	9832	4283	35
H15A	8064	9060	3616	30
H16A	7236	8090	3411	25
H18A	6944	7668	4635	26
H19A	6822	7327	5434	34
H20A	5261	6991	5645	38
H21A	3830	6998	5058	33
H22A	3959	7283	4229	26
H23D	7909	5812	2959	38
H23E	6886	5539	3123	38
H23F	7638	6039	3595	38
H24A	5582	7000	1611	26
H26A	7949	7466	2469	31
H27A	8945	8364	2585	35
H28A	8551	8981	2023	39

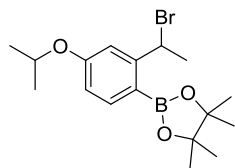
H29A	7178	8674	1331	41
H30A	6179	7771	1207	34
H32A	8027	6764	1345	53
H33A	8461	5956	668	64
H34A	7290	5138	220	60
H35A	5659	5124	438	59
H36A	5215	5928	1110	45
H39A	1697	7623	633	24
H41A	556	7945	2123	23
H43A	4197	7623	1185	21
H45A	3030	8852	1429	30
H46A	3703	9807	1427	40
H47A	5119	9947	986	42
H48A	5879	9122	555	36
H49A	5223	8176	564	28
H51A	4247	6720	493	39
H52A	3943	6119	-450	58
H53A	2980	6403	-1127	58
H54A	2375	7311	-882	44
H55A	2714	7929	46	30
H56D	-350	7240	908	46
H56E	-29	7788	667	46
H56F	-491	7902	1256	46
H57A	2683	7929	2995	19
H59A	1066	7262	2944	29
H60A	-378	7181	3374	32
H61A	-1000	8039	3861	32
H62A	-174	8972	3905	31
H63A	1243	9053	3449	26
H65A	3830	8693	3635	24
H66A	4724	9644	3899	33
H67A	4285	10343	3447	36
H68A	2954	10082	2722	35
H69A	2058	9127	2453	29
H70A	2827	5270	1299	28
H71C	4490	5373	1693	32
H71D	4239	4807	1921	32

H72C	4083	4777	747	51
H72D	4919	4507	1059	51
H73C	3721	3781	1180	60
H73D	3652	3748	520	60
H74C	2039	3702	830	46
H74D	2267	4261	588	46
H75C	1576	4590	1440	40
H75D	2378	4317	1771	40
H76A	2989	5753	3230	22
H77C	4768	5422	2772	25
H77D	4601	6096	3063	25
H78C	5480	5717	3738	27
H78D	4435	5887	3939	27
H79C	4808	4702	3393	28
H79D	4650	4945	4049	28
H80C	2984	5034	3799	28
H80D	3170	4366	3502	28
H81C	2249	4753	2847	26
H81D	3279	4575	2627	26
H82A	1188	5165	2124	27
H83C	1291	5650	3101	36
H83D	1274	6281	2975	36
H84C	-325	5308	2626	42
H84D	-346	5923	3102	42
H85C	-1272	5894	2231	44
H85D	-383	6439	2419	44
H86C	-387	5968	1456	50
H86D	-368	5334	1573	50
H87C	1235	6303	1922	42
H87D	1244	5689	1442	42
H89	7822	8250	8452	46
H90	7641	7516	8911	47
H92	7761	8780	10404	47
H93	7921	9514	9946	47
H94A	7415	9399	8585	73
H94B	8594	9393	8640	73
H94C	8113	9831	9132	73

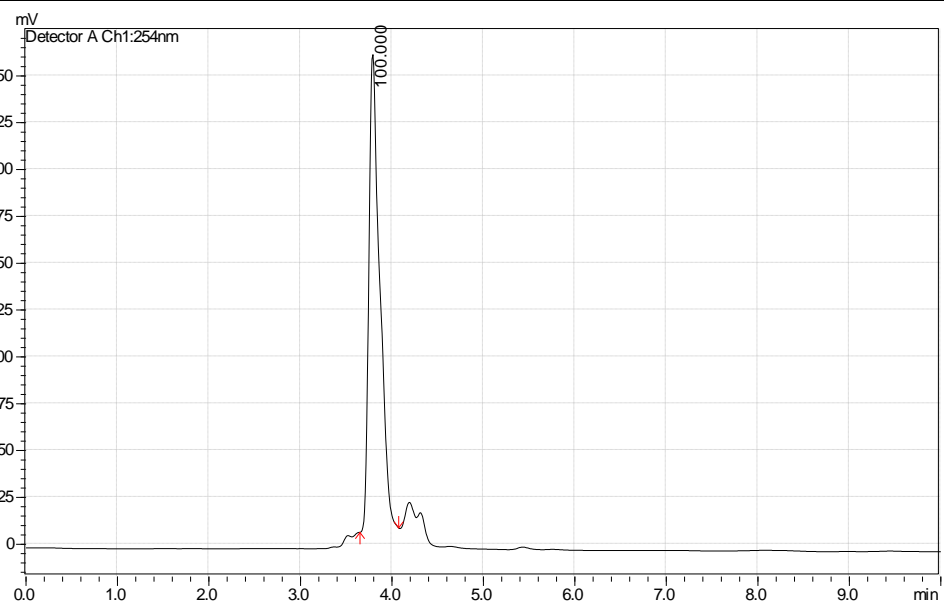
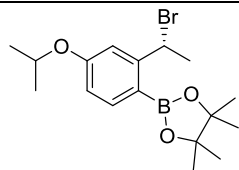
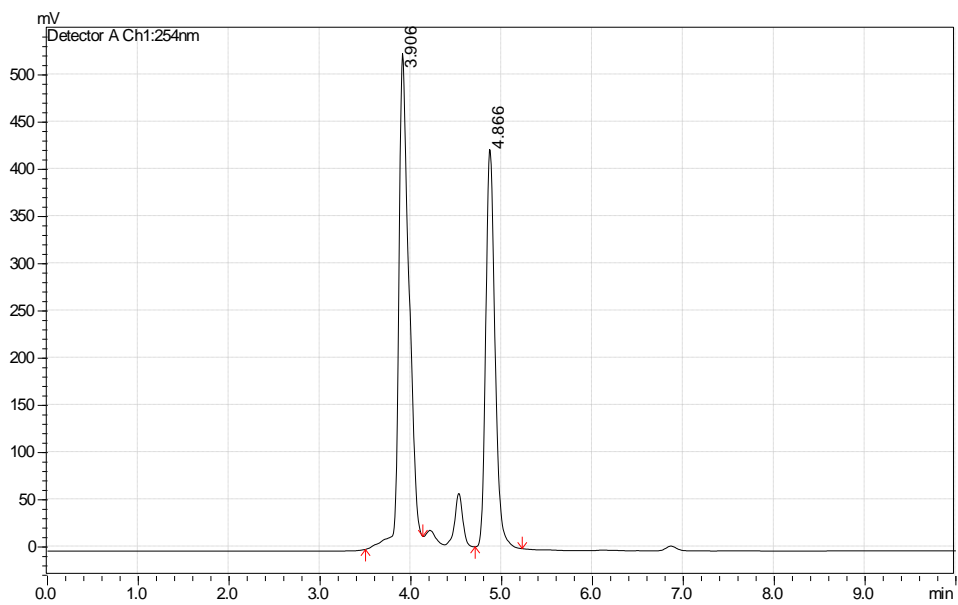
H95A	7772	7770	10420	75
H95B	7991	7287	9862	75
H95C	6873	7411	9945	75

Appendix D: HPLC Chromatograms

Structure	Chromatogram
<p data-bbox="191 306 365 331">Compound 3.2:</p>  <p data-bbox="191 594 292 619">(racemic)</p>	 <p data-bbox="479 321 1442 905">Chromatogram showing detector response (mV) versus time (min) for Compound 3.2 (racemic). The plot displays two major peaks at retention times 4.151 and 5.034 minutes. The y-axis ranges from 0 to 1000 mV, and the x-axis ranges from 0.0 to 9.0 minutes.</p>
	 <p data-bbox="479 1024 1442 1608">Chromatogram showing detector response (mV) versus time (min) for Compound 3.2 (chiral). The plot displays two major peaks at retention times 97.524 and 2.476 minutes. The y-axis ranges from 0 to 2250 mV, and the x-axis ranges from 0.0 to 9.0 minutes.</p>
<p data-bbox="191 1654 1507 1680">Conditions: Chromatograms were acquired on a Shimadzu Prominence HPLC equipped with a Chiralcel AD-H column.</p> <p data-bbox="191 1711 1448 1736">Flow rate: 1.00 mL/min.; Oven temp: 40.0 °C; Solvent: isocratic 1.00% <i>i</i>PrOH in hexanes; Detector: UV @ 254 nm</p>	

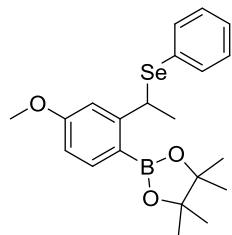
3.9:

(racemic)

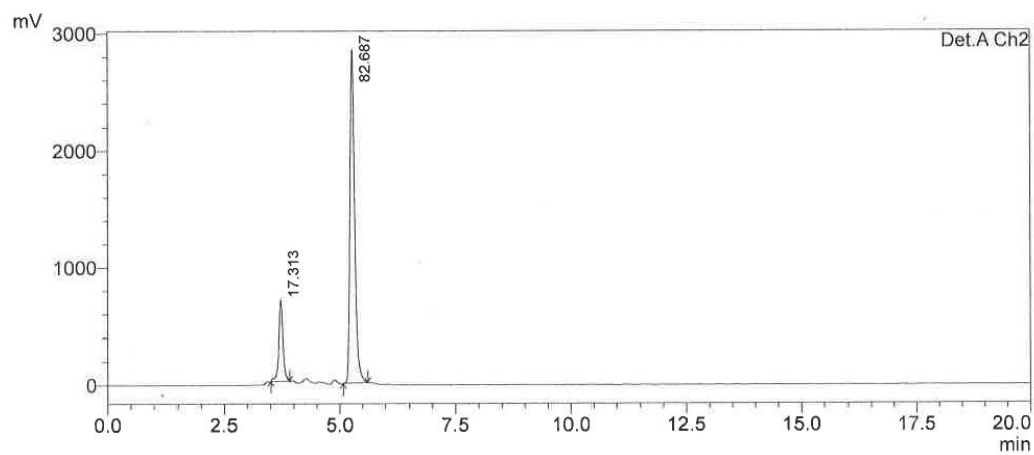
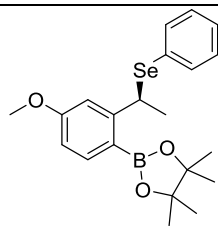
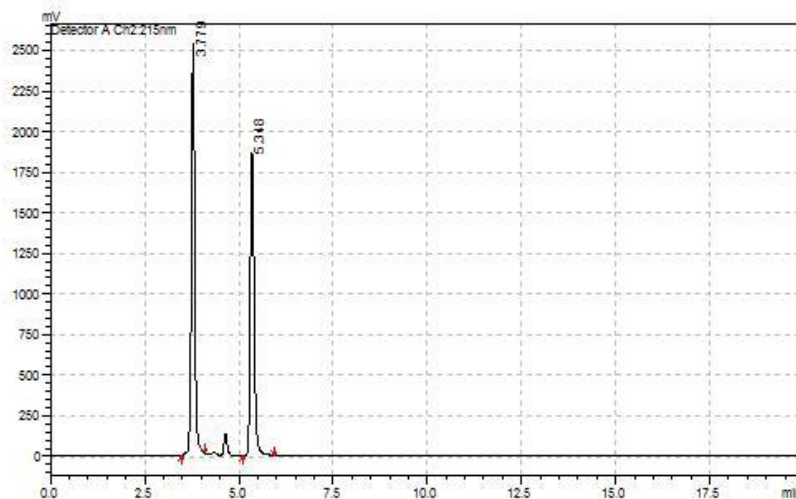


Conditions: Chromatograms were acquired on a Shimadzu Prominence HPLC equipped with a Chiracel AD-H column.

Flow rate: 1.00 mL/min.; Oven temp: 40.0 °C; Solvent: isocratic 0.50% *i*PrOH in hexanes; Detector: UV @ 254 nm

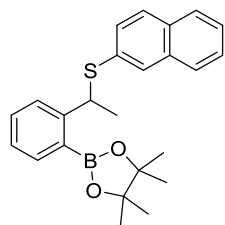
selenide of **3.10**:

(racemic)

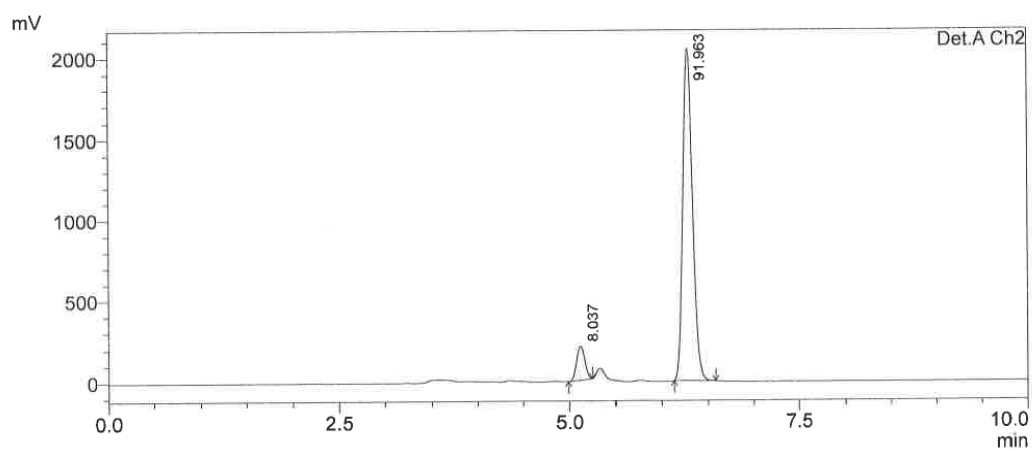
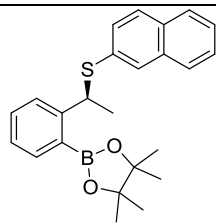
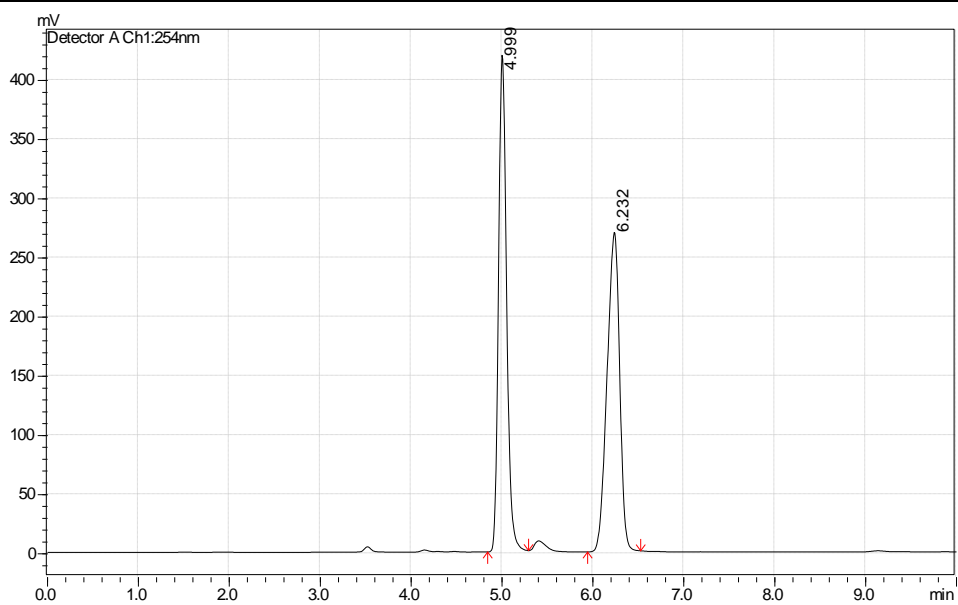


Conditions: Chromatograms were acquired on a Shimadzu Prominence HPLC equipped with a Chiralcel AD-H column.

Flow rate: 1.00 mL/min.; Oven temp: 40.0 °C; Solvent: isocratic 5.00% *i*PrOH in hexanes; Detector: UV @ 215 nm

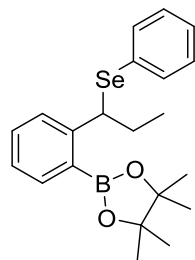
Thioether of **3.11**:

(racemic)

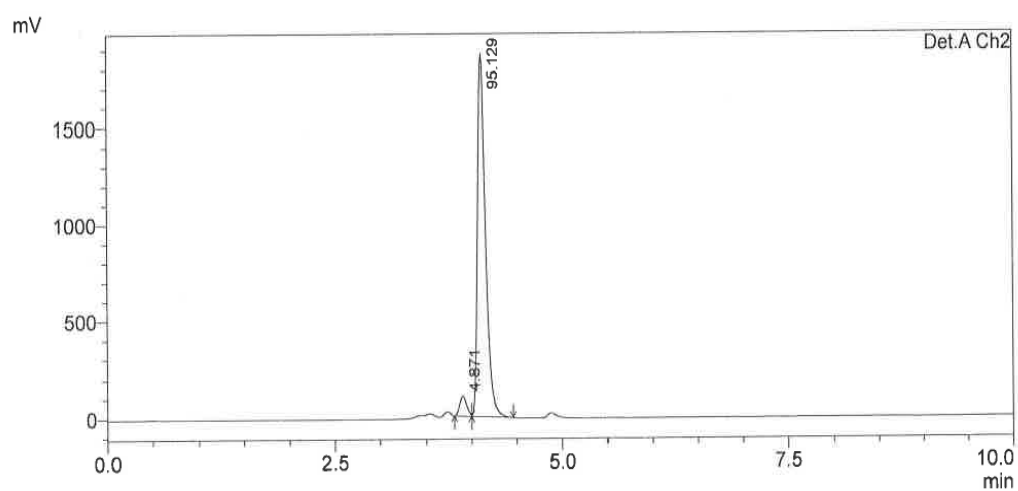
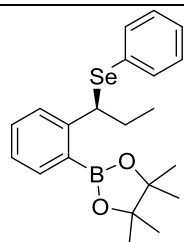
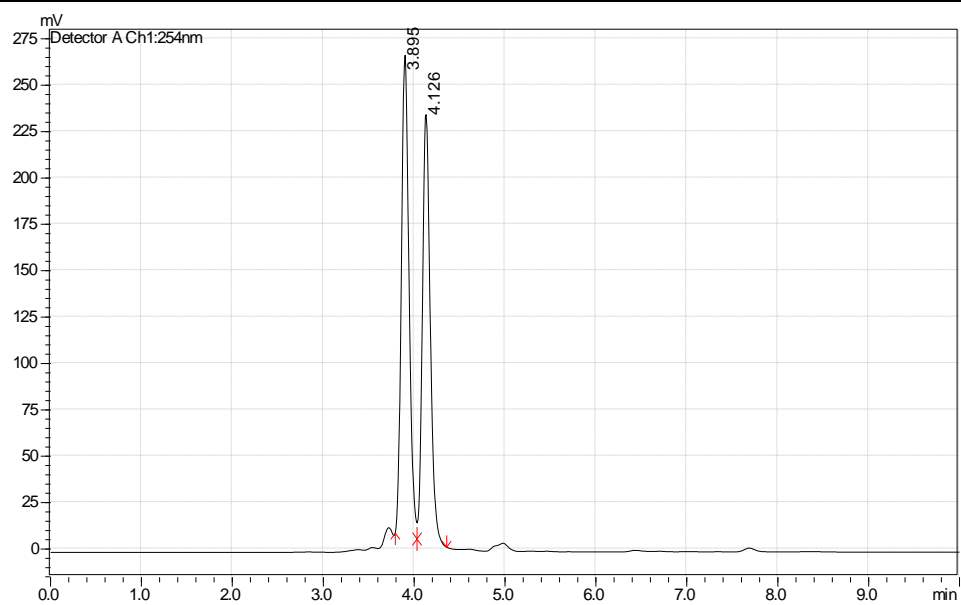


Conditions: Chromatograms were acquired on a Shimadzu Prominence HPLC equipped with a Chiralcel AD-H column.

Flow rate: 1.00 mL/min.; Oven temp: 40.0 °C; Solvent: isocratic 1.00% *i*PrOH in hexanes; Detector: UV @ 225 nm and 254 nm

Selenide of **3.12**:

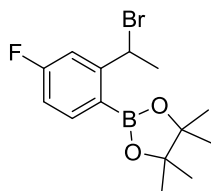
(racemic)



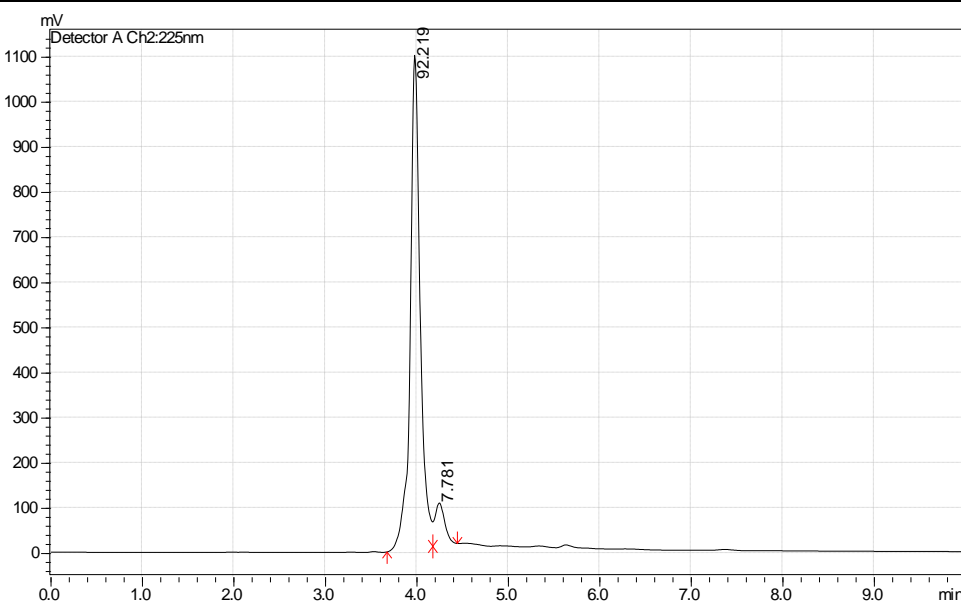
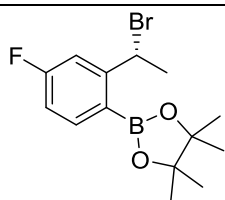
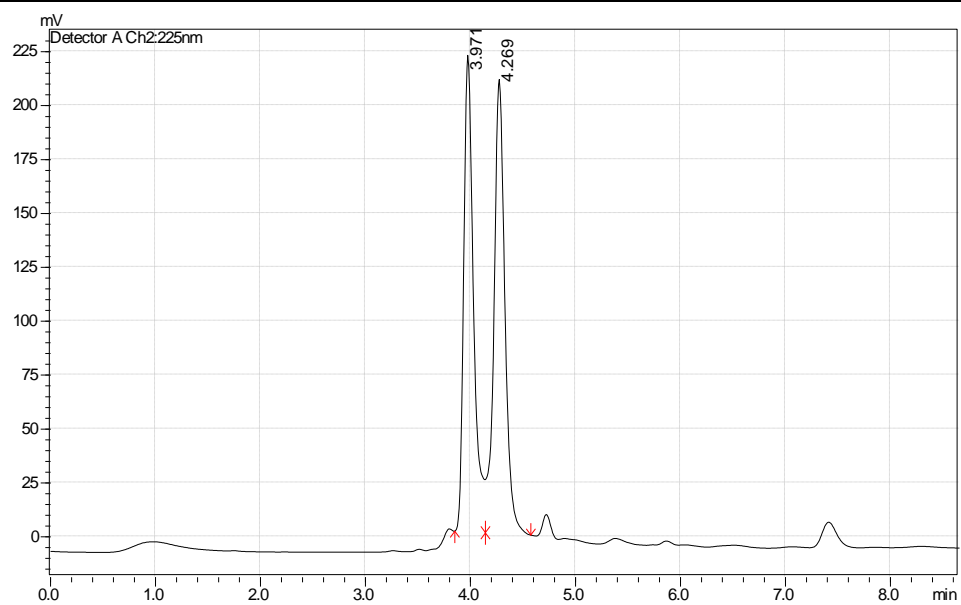
Conditions: Chromatograms were acquired on a Shimadzu Prominence HPLC equipped with a Chiracel AD-H column.

Flow rate: 1.00 mL/min.; Oven temp: 40.0 °C; Solvent: isocratic 0.50% *i*PrOH in hexanes; Detector: UV @ 225 nm

Compound 3.13:



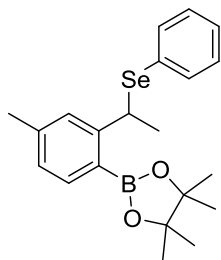
(racemic)



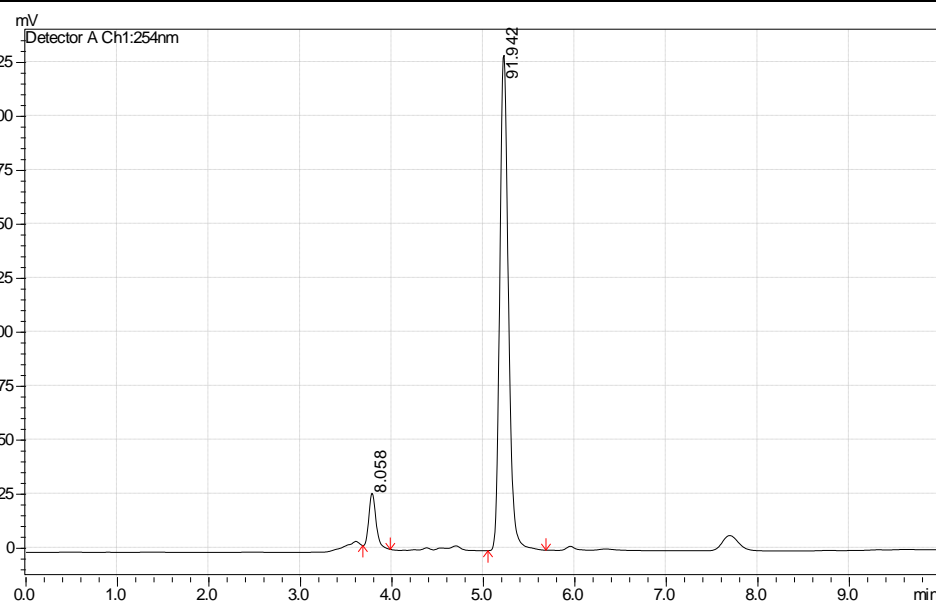
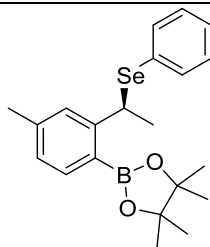
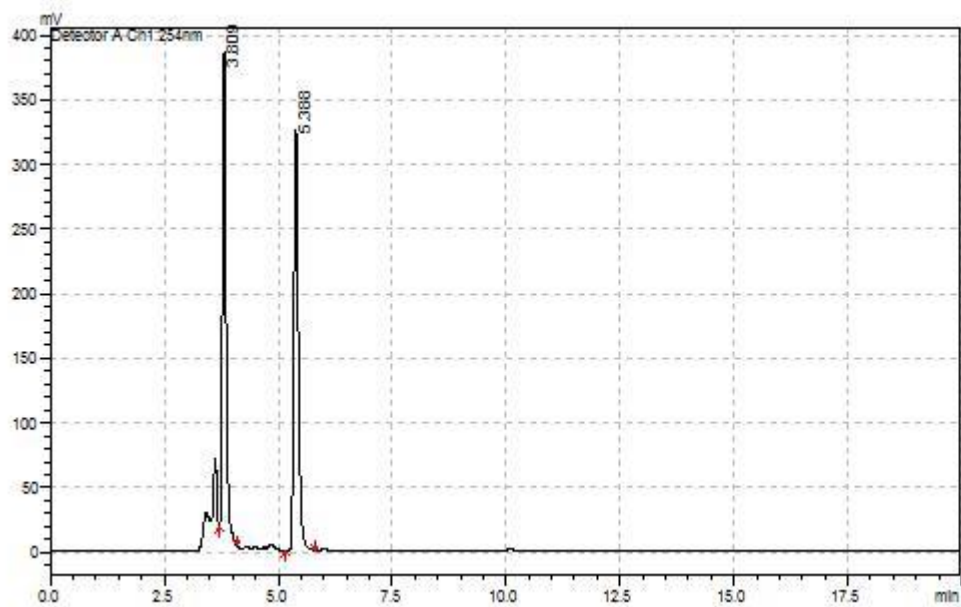
Conditions: Chromatograms were acquired on a Shimadzu Prominence HPLC equipped with a Chiralcel AD-H column.

Flow rate: 1.00 mL/min.; Oven temp: 40.0 °C; Solvent: isocratic 0.10% *i*PrOH in hexanes; Detector: UV @ 254 nm

Selenide of **3.21**:



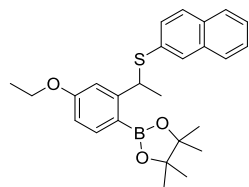
(racemic)



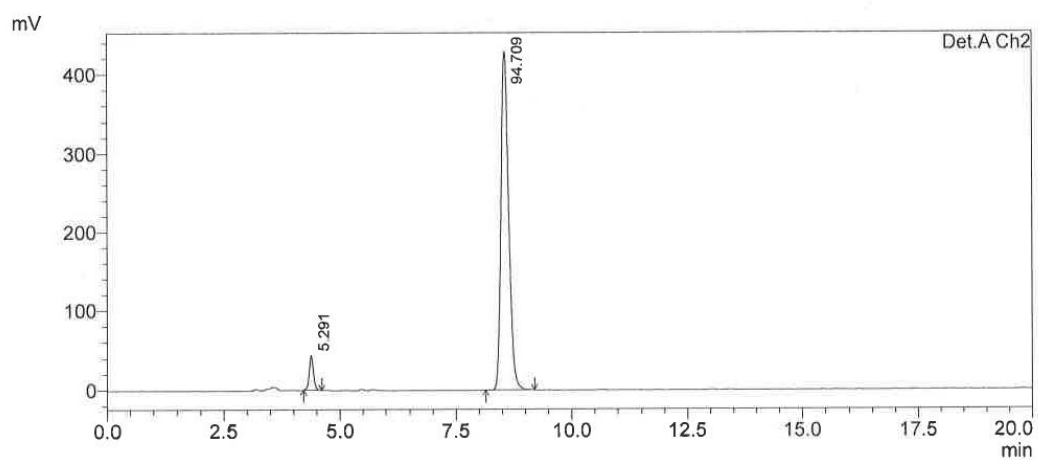
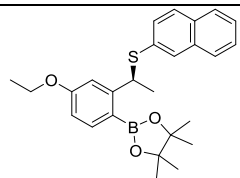
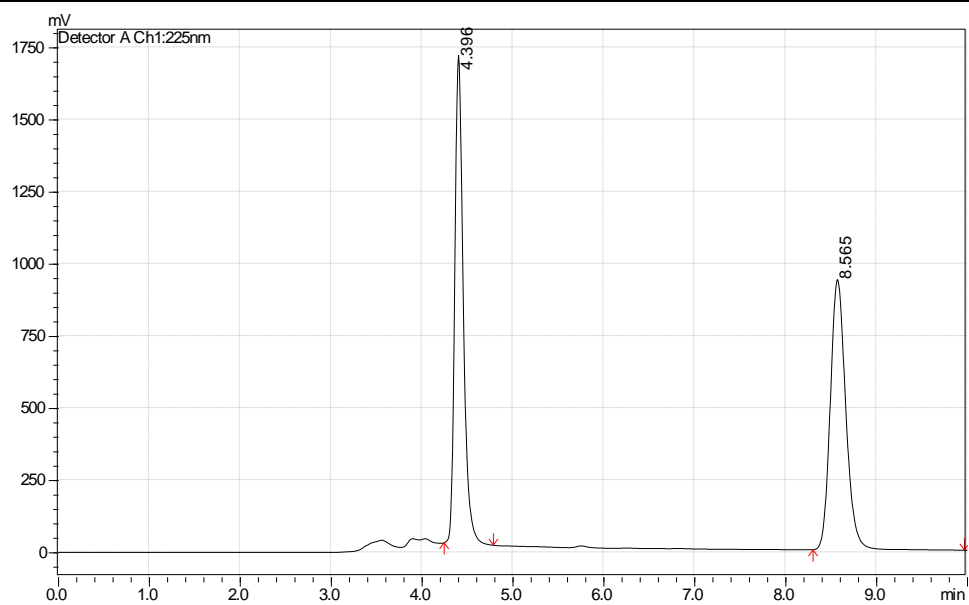
Conditions: Chromatograms were acquired on a Shimadzu Prominence HPLC equipped with a Chiralcel AD-H column.

Flow rate: 1.00 mL/min.; Oven temp: 40.0 °C; Solvent: isocratic 5.00% *i*PrOH in hexanes; Detector: UV @ 254 nm

Thioether of **3.22**:



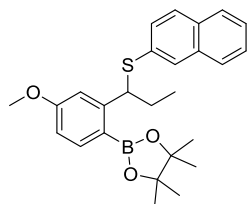
(racemic)



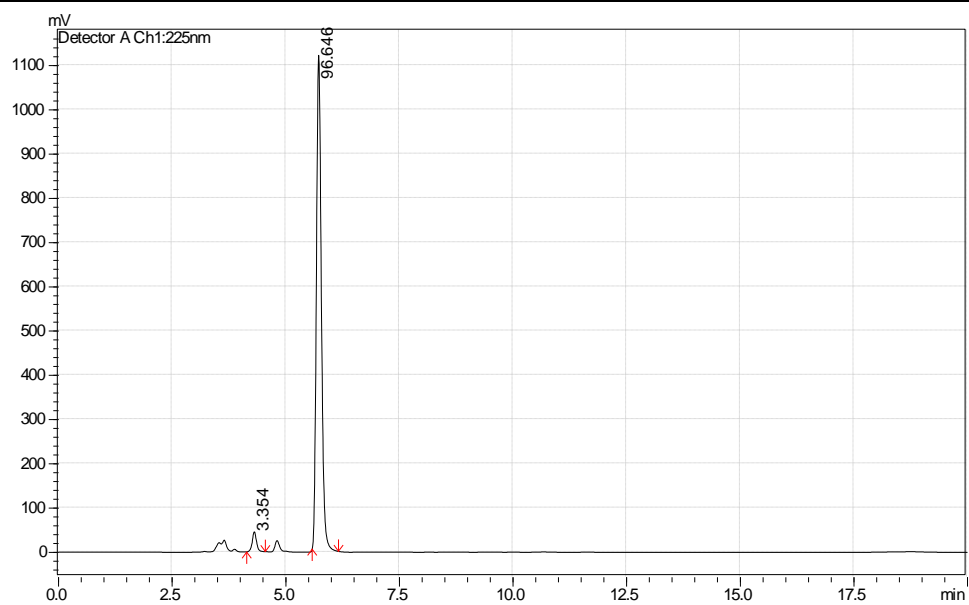
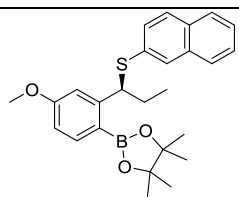
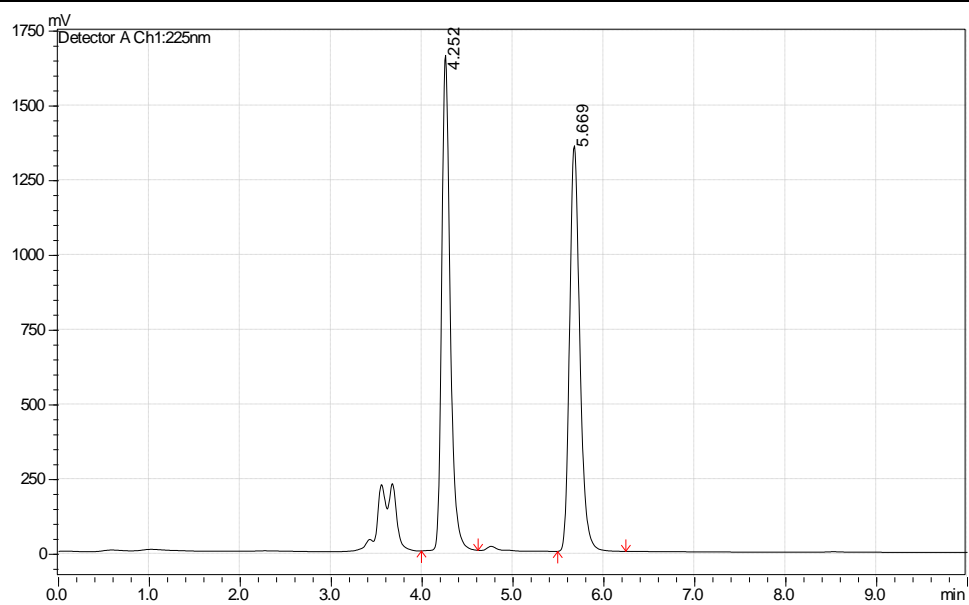
Conditions: Chromatograms were acquired on a Shimadzu Prominence HPLC equipped with a Chiralcel AD-H column.

Flow rate: 1.00 mL/min.; Oven temp: 40.0 °C; Solvent: isocratic 5.00% *i*PrOH in hexanes; Detector: UV @ 215 nm and 225 nm

Thioether of **3.23**:



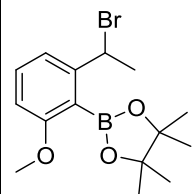
(racemic)



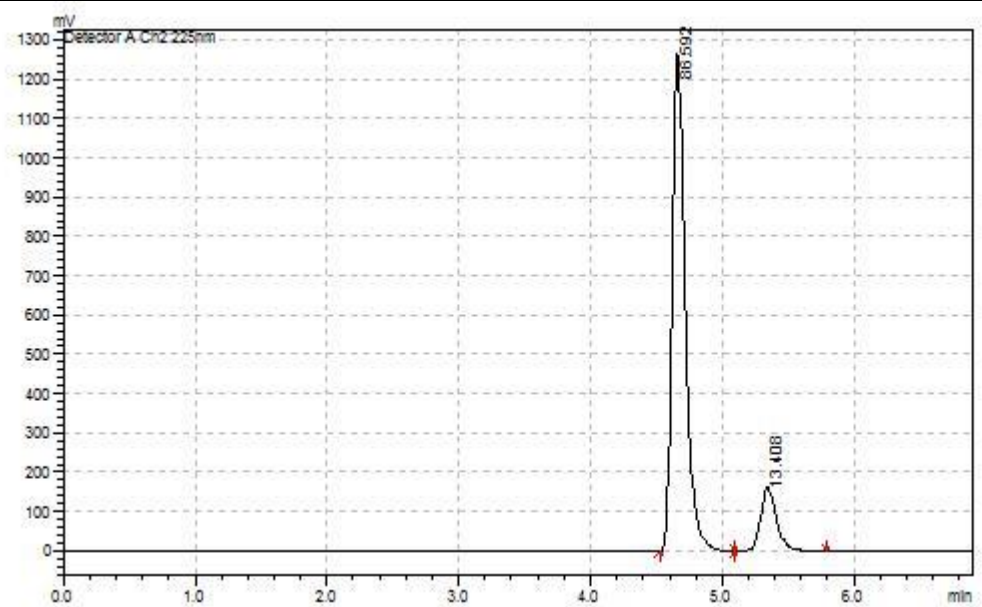
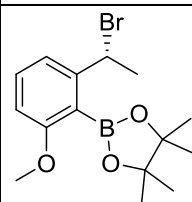
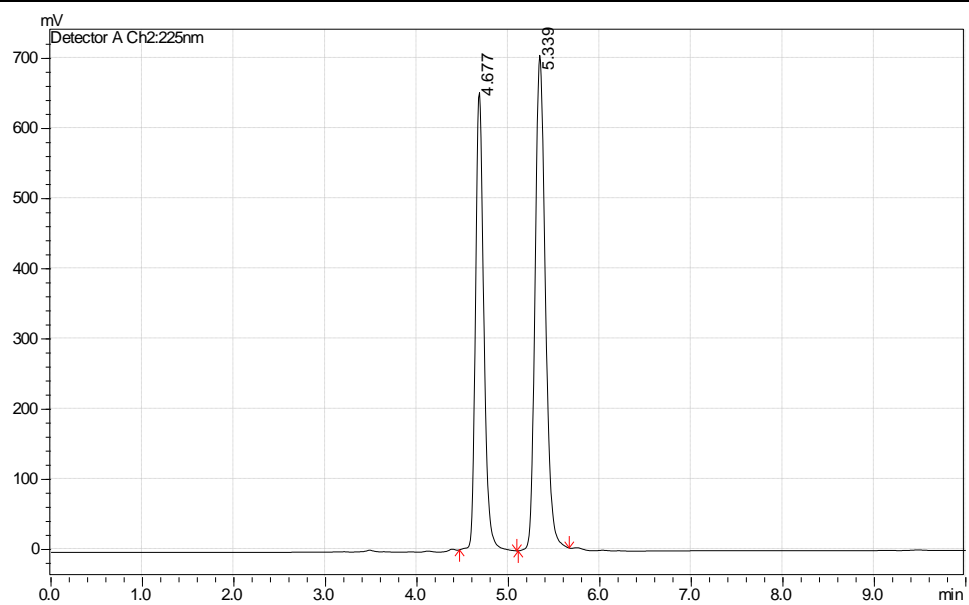
Conditions: Chromatograms were acquired on a Shimadzu Prominence HPLC equipped with a Chiralcel AD-H column.

Flow rate: 1.00 mL/min.; Oven temp: 40.0 °C; Solvent: isocratic 5.00% *i*PrOH in hexanes; Detector: UV @ 225 nm

Compound 3.24:

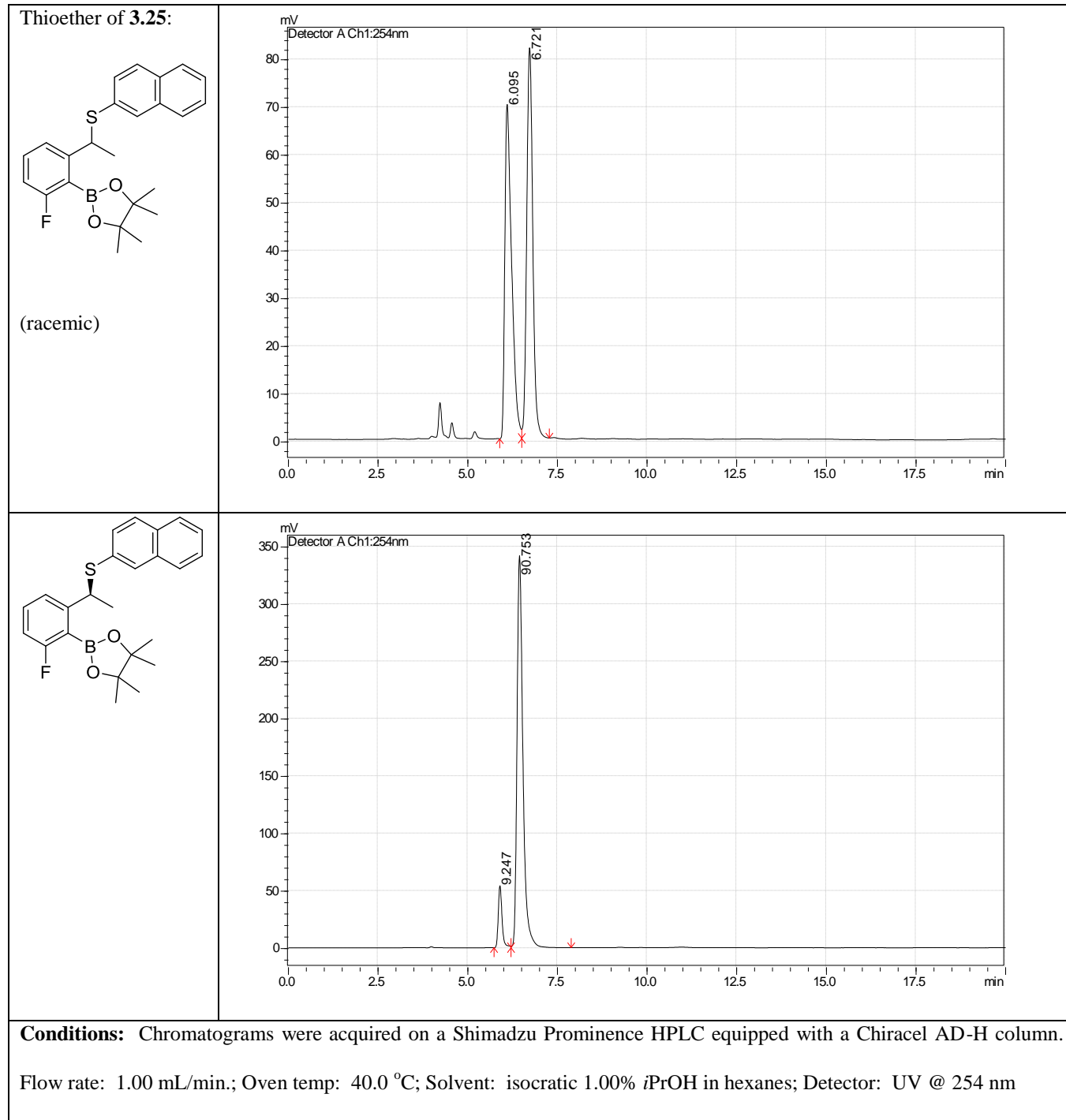


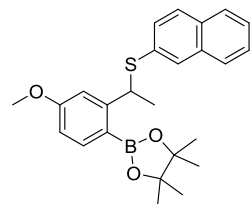
(racemic)



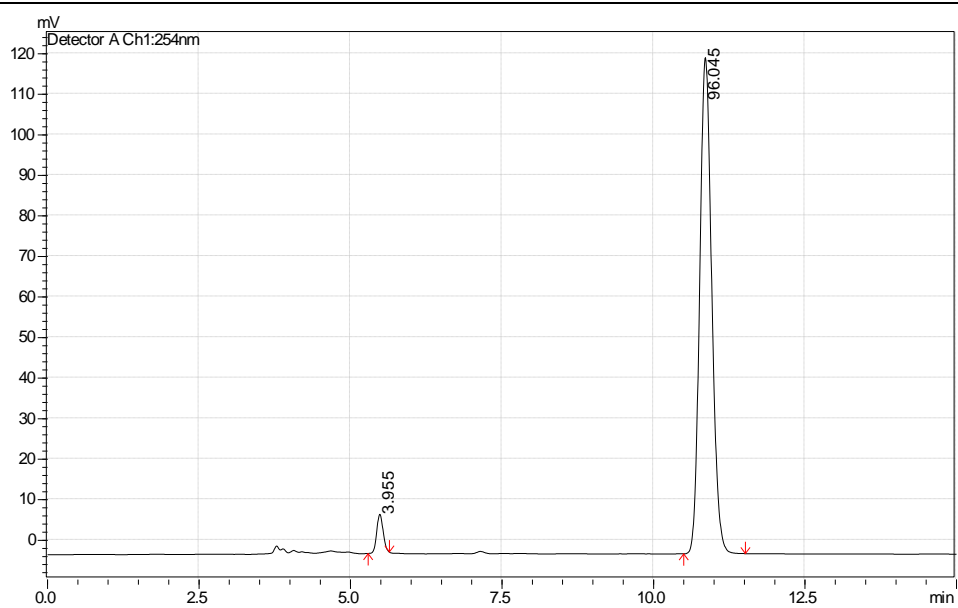
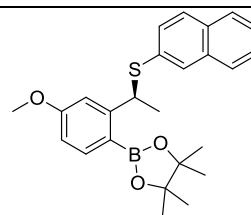
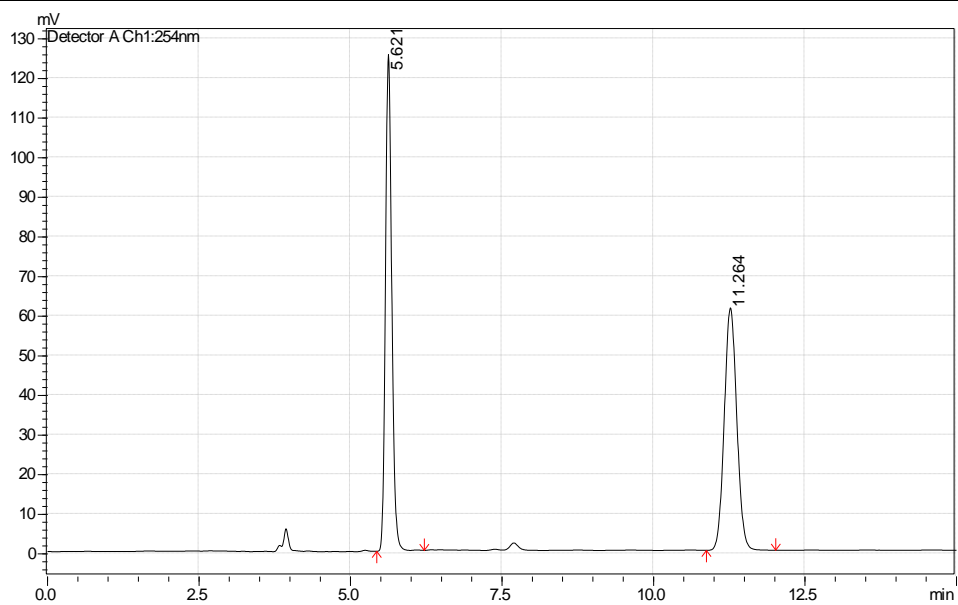
Conditions: Chromatograms were acquired on a Shimadzu Prominence HPLC equipped with a Chiralcel AD-H column.

Flow rate: 1.00 mL/min.; Oven temp: 40.0 °C; Solvent: isocratic 1.00% *i*PrOH in hexanes; Detector: UV @ 225 nm



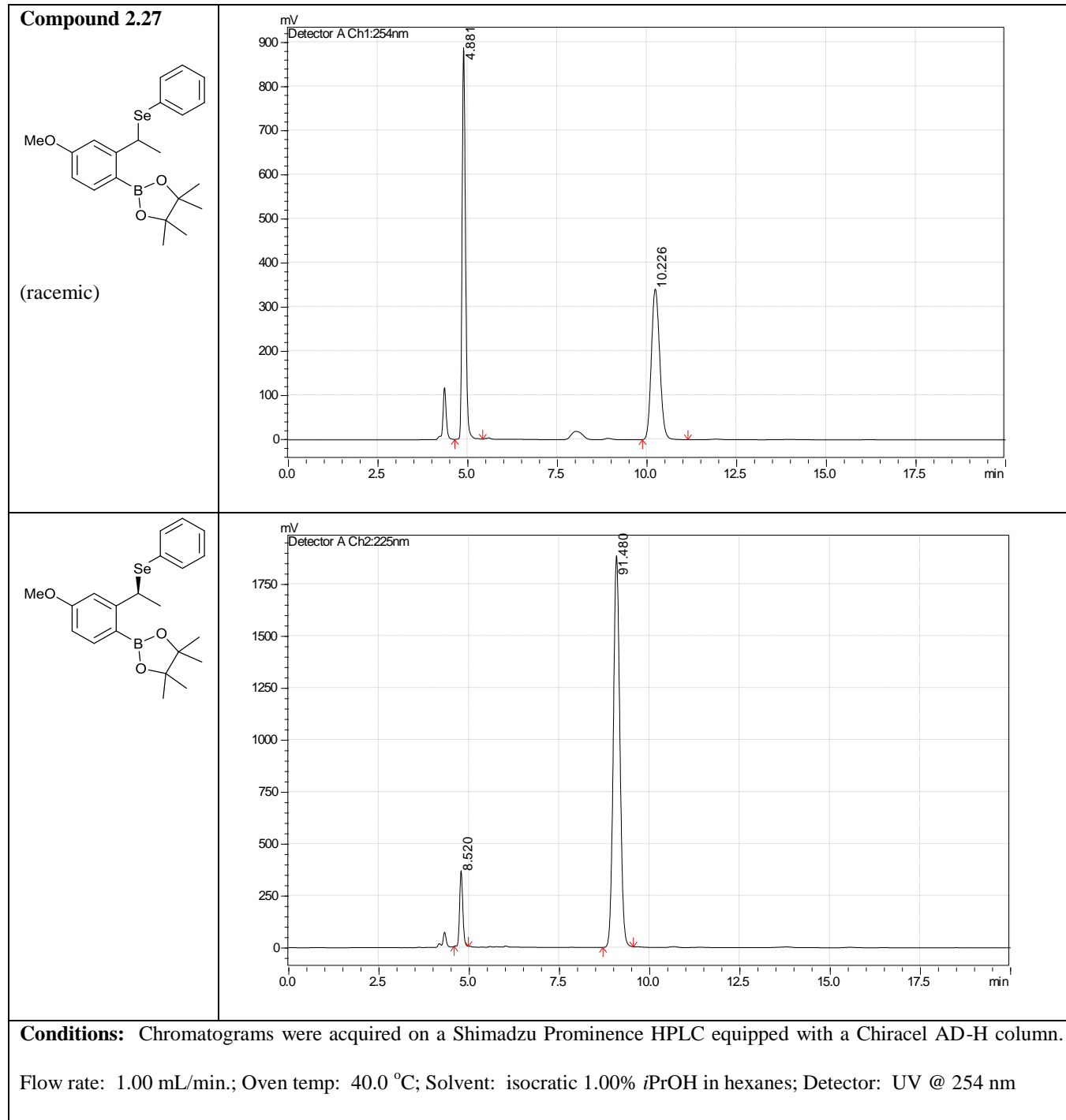
Compound 2.26

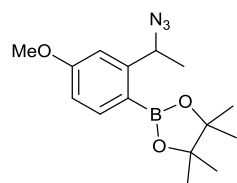
(racemic)



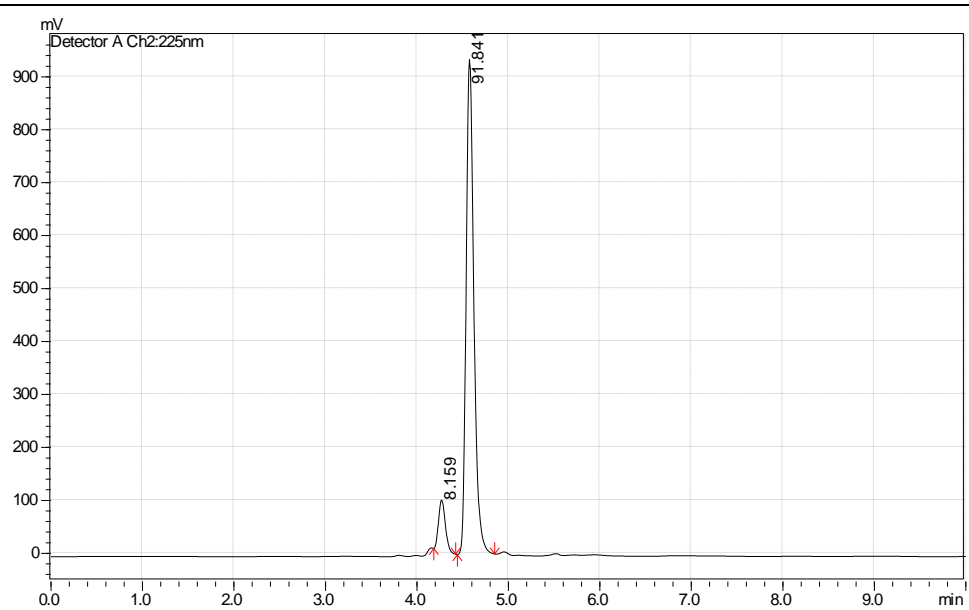
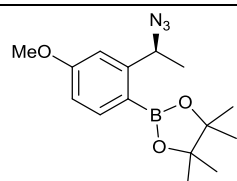
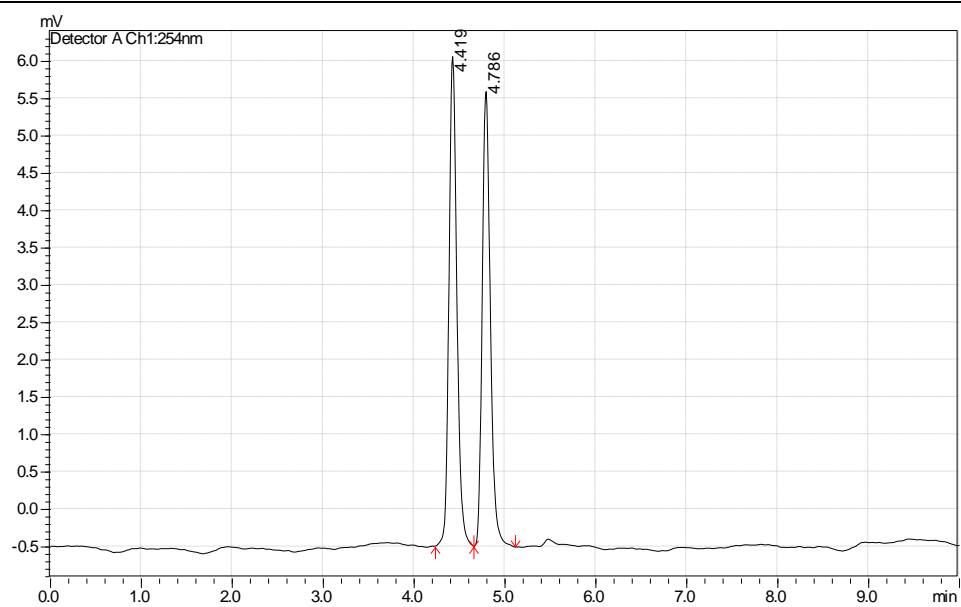
Conditions: Chromatograms were acquired on a Shimadzu Prominence HPLC equipped with a Chiracel AD-H column.

Flow rate: 1.00 mL/min.; Oven temp: 40.0 °C; Solvent: isocratic 2.00% *i*PrOH in hexanes; Detector: UV @ 254 nm



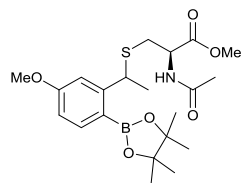
Compound 3.28

(racemic)

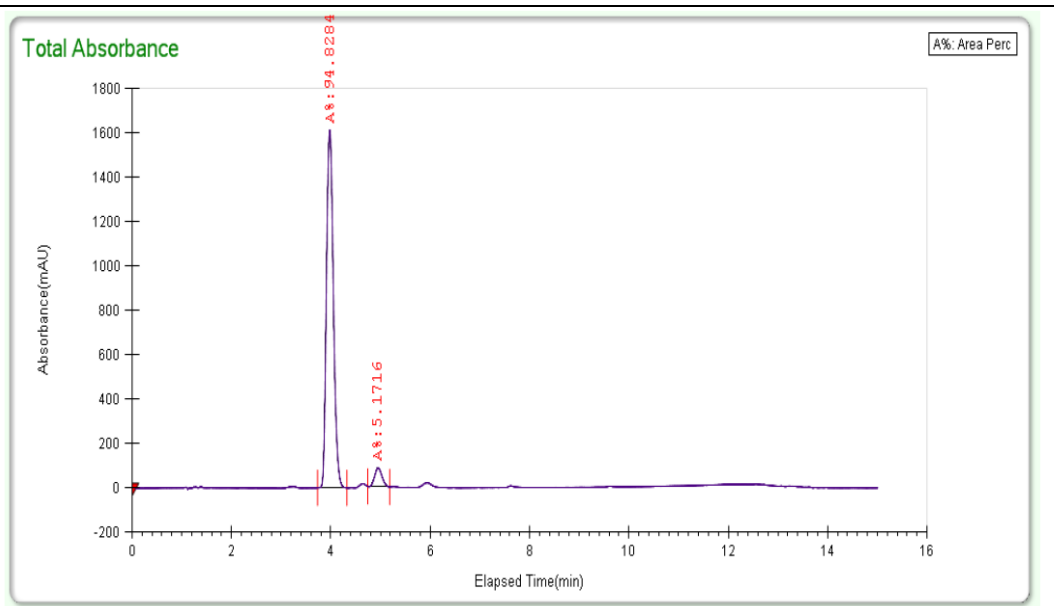
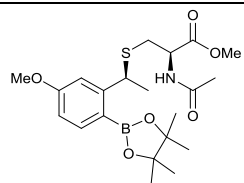
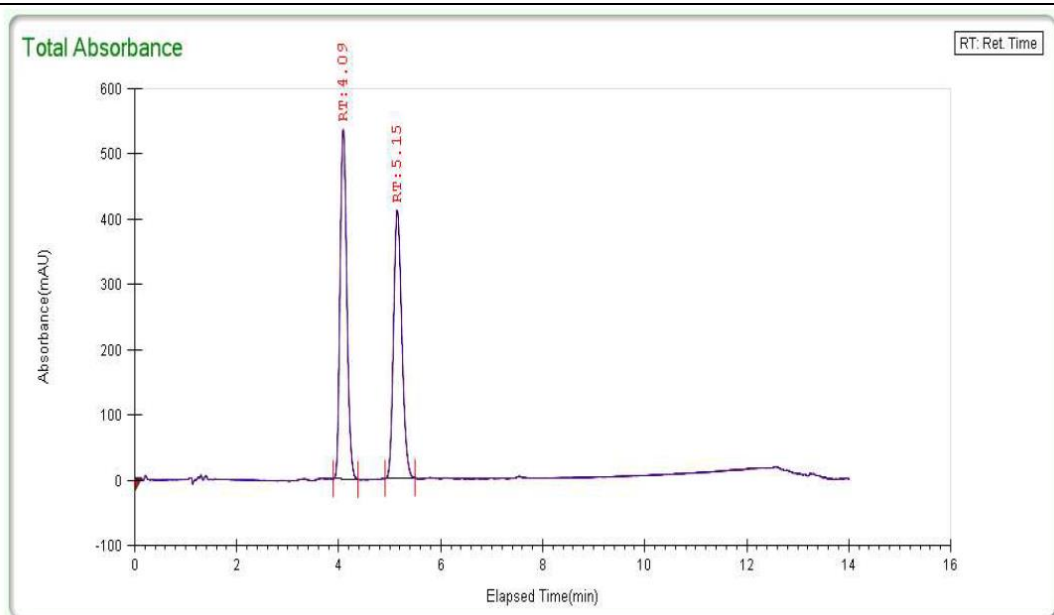


Conditions: Chromatograms were acquired on a Shimadzu Prominence HPLC equipped with a Chiracel AD-H column.

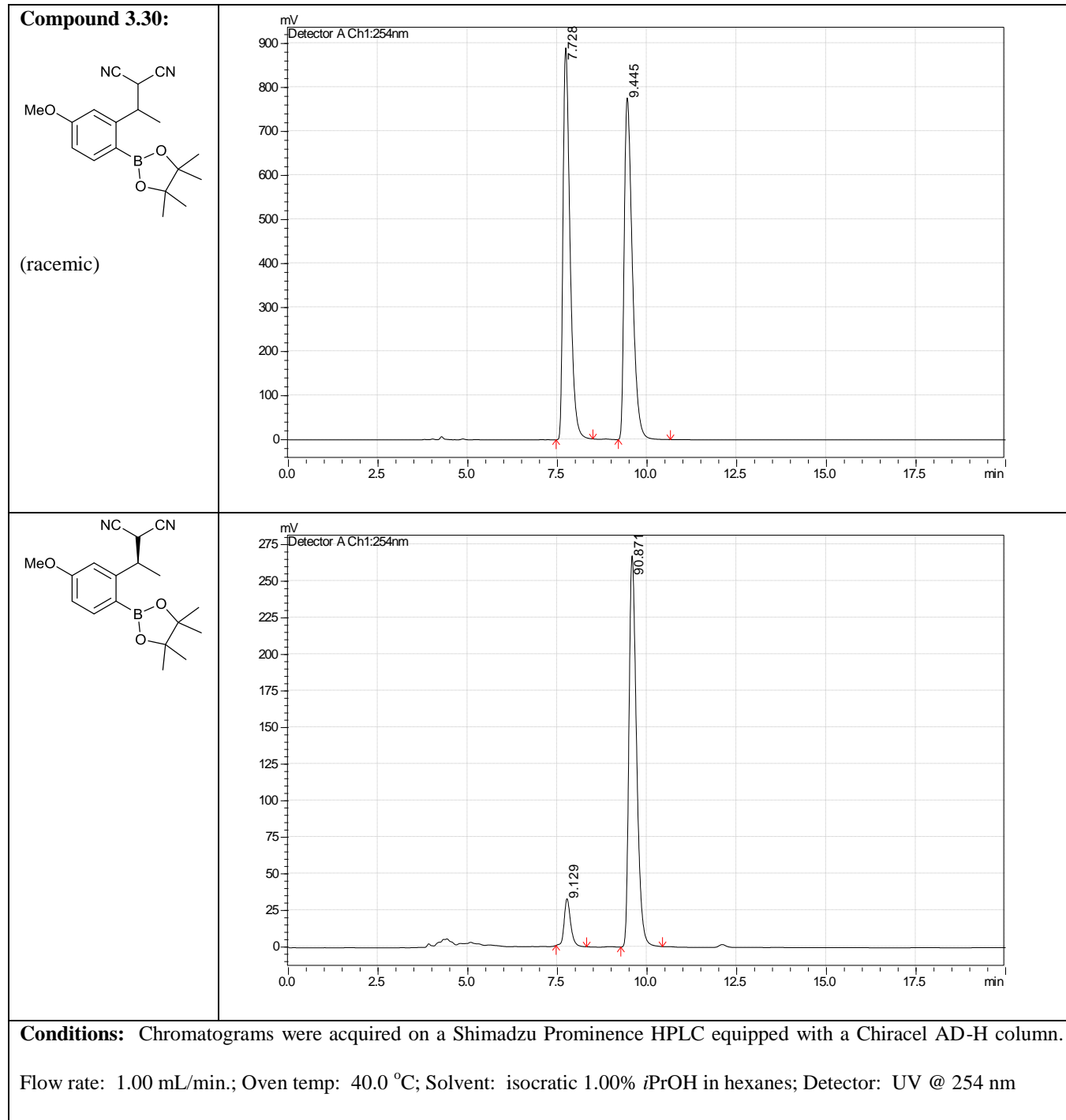
Flow rate: 1.00 mL/min.; Oven temp: 40.0 °C; Solvent: isocratic 1.00% *i*PrOH in hexanes; Detector: UV @ 254 nm

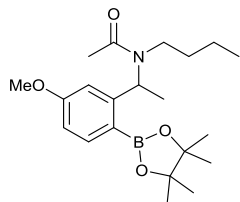
Compound 3.29:

(mixture of diastereomers)

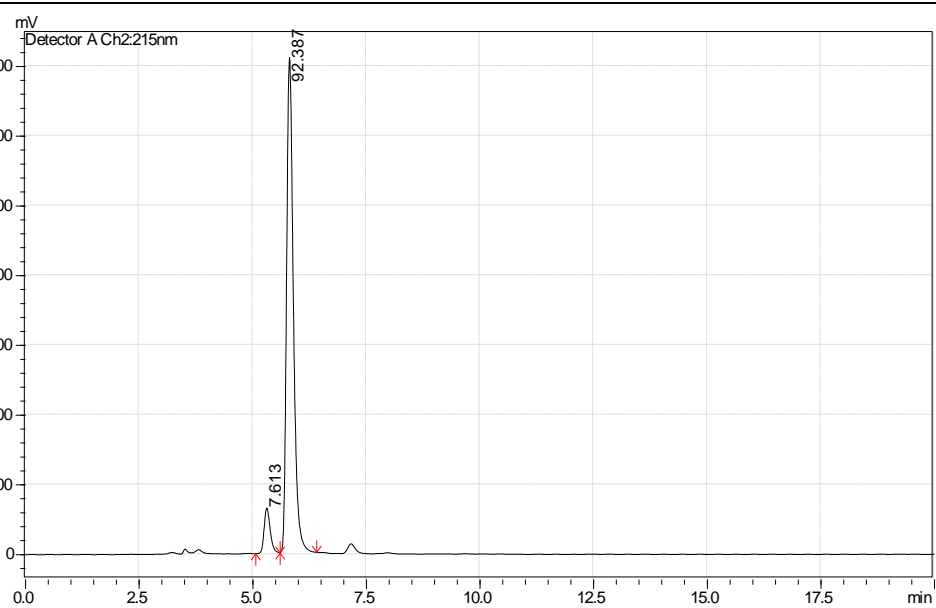
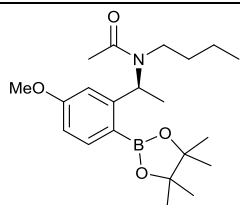
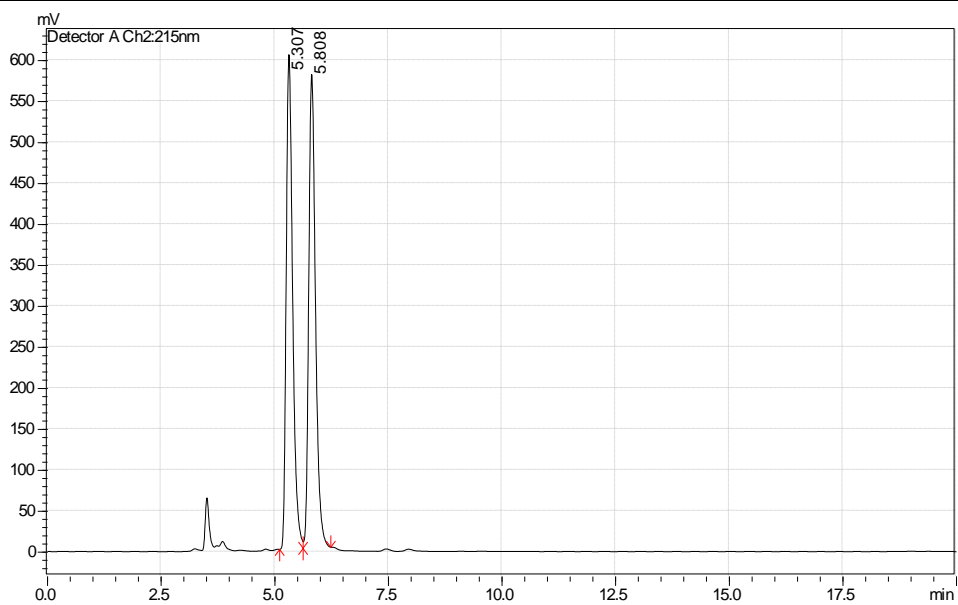


Conditions: Chromatograms were acquired on a Thar SFC equipped with a Chiralcel AD-H column. Flow rate: 3.00 mL/min.; Oven temp: 30.0 °C; Solvent: ramp 5-50% MeOH in CO₂ over 10 min; Detector: UV @ 220-300 nm



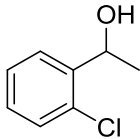
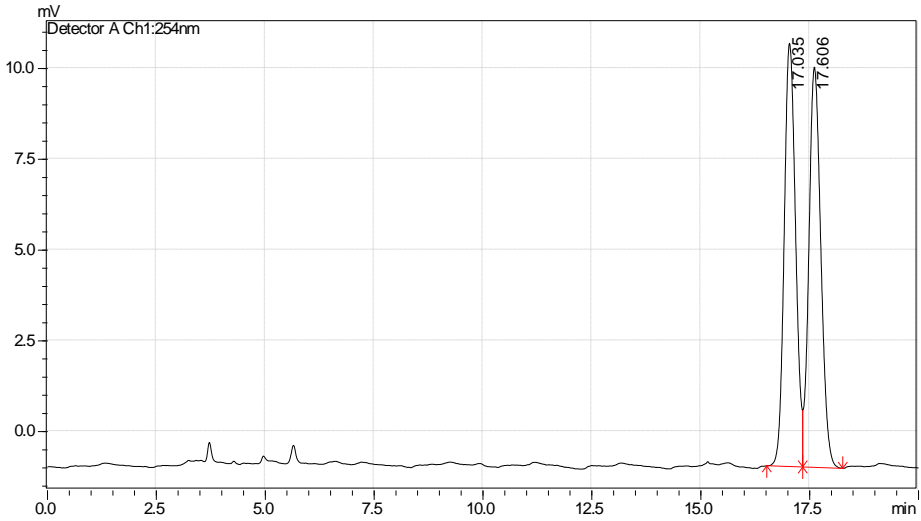
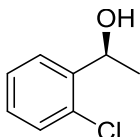
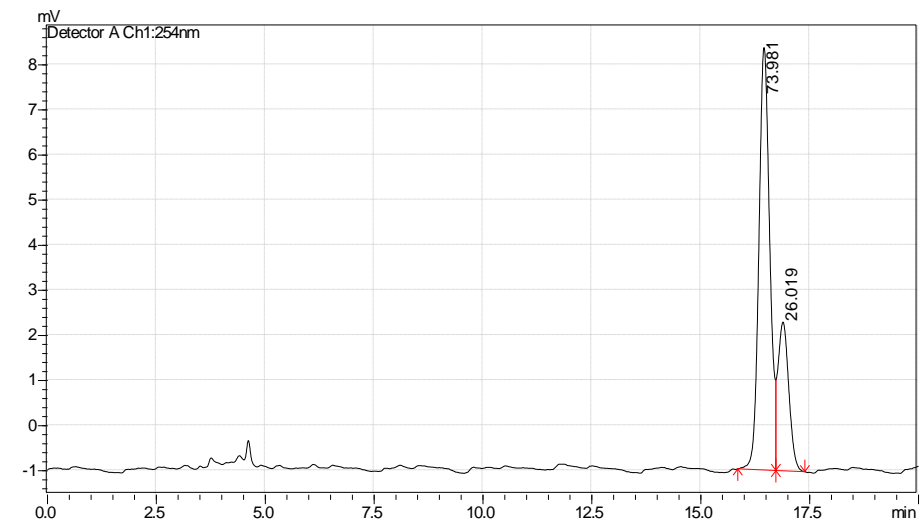
Compound 3.31:

(racemic)



Conditions: Chromatograms were acquired on a Shimadzu Prominence HPLC equipped with a Chiracel AD-H column.

Flow rate: 1.00 mL/min.; Oven temp: 40.0 °C; Solvent: isocratic 5.00% *i*PrOH in hexanes; Detector: UV @ 215 nm

<p>2-chloro-α-methylbenzylalcohol</p>  <p>(racemic)</p>	 <p>Chromatogram showing two peaks at retention times 17.035 min and 17.606 min. The y-axis is mV (0.0 to 10.0) and the x-axis is min (0.0 to 17.5).</p>
<p>2-chloro-α-methylbenzylalcohol</p> 	 <p>Chromatogram showing two peaks at retention times 73.981 min and 26.019 min. The y-axis is mV (-1 to 8) and the x-axis is min (0.0 to 17.5).</p>
<p>Conditions: Chromatograms were acquired on a Shimadzu Prominence HPLC equipped with a Chiralcel OJ-H column. Flow rate: 1.00 mL/min.; Oven temp: 40.0 °C; Solvent: isocratic 5.00% <i>i</i>PrOH in hexanes; Detector: UV @ 254 nm</p>	